

Dissertation zur Erlangung des Doktorgrades
der Fakultät für Chemie und Pharmazie
der Ludwig-Maximilians-Universität München

Size-Induced Selective Acylation of 1,2-Ethanedionols

Stefanie Mayr
aus Starnberg, Deutschland

2022

Erklärung

Diese Dissertation wurde im Sinne von § 7 der Promotionsordnung vom 28. November 2011 von Herrn Prof. Dr. Hendrik Zipse betreut.

Eidesstattliche Versicherung

Diese Dissertation wurde eigenständig und ohne unerlaubte Hilfe erarbeitet.

München, 07.01.2022

.....
Stefanie Mayr

Dissertation eingereicht am 26.04.2021

1. Gutachter: Prof. Dr Hendrik Zipse

2. Gutachter: Prof. Dr. Oliver Trapp

Mündliche Prüfung am 07.06 2021

Acknowledgment

Zu aller erst möchte ich mich bei meinem Doktorvater Prof. Dr. Hendrik Zipse bedanken, dass er mich in seiner Arbeitsgruppe aufgenommen hat. Er hat mich nicht nur mit viel Geduld an die Computerchemie herangeführt, sondern mich auch gelehrt, alles so oft zu überprüfen, dass man wissenschaftliche Ergebnisse produziert. Trotz seines stetigen Interesses hat er mir stets immer große Freiheiten gelassen, eigene Ideen und Vorstellungen zu verfolgen. Vielen Dank für die vielen wertvollen Tipps und Förderungen, die mich nicht nur beruflich, sondern auch charakterlich weitergebracht haben.

Mein zweiter Dank gilt Prof. Dr. Oliver Trapp, der sich bereit erklärt hat, als Zweitgutachter dieser Arbeit zu agieren. Des Weiteren möchte ich mich bei den zusätzlichen Mitgliedern der Prüfungskommission bedanken, dass sie Zeit und Arbeit in meine Prüfung investieren.

Meinen Kollegen möchte ich für die gute Zusammenarbeit und der schönen und doch immer auch lustigen Zeit in den letzten 4.5 Jahren danken. Dr. Marta Marin-Luna, die mir nicht nur in unserer Zusammenarbeit im Anhydrid-Projekt immer mit gutem und hilfreichen Rat zur Seite stand, sondern auch eine zielgerichtete Arbeitsweise und wissenschaftliche Projektplanung beigebracht hat. Nicht nur hat sie mir gezeigt, auch in „schwereren“ Zeiten die eigene Arbeit nicht abzuschreiben, sondern auch, dass sich viel Geduld und Fleiß irgendwann doch auszahlen können. Dr. Benjamin Pölloth, für seine freundliche und hilfsbereite Art, den intensiven Diskussionen und Austausch nicht nur über unsere Projekte, sondern auch über das Berufliche hinaus. Unvergessen werden immer die Britney-, Scooter- und ABBA-Labortage bleiben. Dr. Julian Helberg, für seine vielen hilfreichen Projekt-bezogenen Tipps als auch sein offenes Ohr, wenn es mal nicht so gut lief. Dr. Harish Jangra, für seine geduldige und immer freundliche Art, sowie den hilfreichen Tipps, besonders bei Computerproblemen. Veronika Burger, für die entspannte Zusammenarbeit und intensiven Gespräche, als auch den vielen gemeinsamen Lach-Momenten. Fabian Zott und Salavat Ashirbaev, für die gute Zusammenarbeit und den vielen humorvollen Gesprächen. Heena Ugale, für die vielen interessanten Gesprächsthemen und den intensiven Einblick in andere Kulturen. Ieva Teikmane, für die gute Abzugsnachbarschaft und vielen wertvollen Tipps auch über das Leben. Jutta Tumpach, für die zwar kurze, aber dennoch schöne gemeinsame Zeit im Labor. Vasily Korotenko, Sandiya Lakshmanan und Florian Barth für die gute Zusammenarbeit im Labor. Ein weiteres Dankeschön geht an meine Studentin Ana Mateos Calbet, für die Zusammenarbeit an meinem Katalysator-Thema.

Ein großes Dankeschön geht an die Analytikabteilung, die immer alles gemessen hat, egal wie viele Proben ich Ihnen auch gegeben habe. Hervorzuheben sind hierbei Sonja Kosak aus der Massenspektrometrie, die unermüdlich jeden Ester gemessen hat, den ich ihr gebracht habe, die NMR-Abteilung mit Claudia Ober und Dr. Stephenson, die hunderte von NMR-Proben gemessen haben, und Dr. Peter Mayer, für die guten Kristallstrukturmessungen.

Auch muss ich mich bei Eva Mayr und Silvia Tölscher für ihren Einsatz bedanken, meine sprachlichen Schwächen auszugleichen, und bei Prof. Hendrik Zipse, Dr. Benjamin Pölloth, Veronika Burger und Dr. Harish Jangra, für das Korrekturlesen dieser Arbeit. Vielen herzlichen Dank!

Auch neben der Uni gab es viele Personen, die mich während meiner Zeit der Promotion als auch schon davor begleitet haben und mich immer wieder mit tollen Gesprächen, tollen Ausflügen und Unternehmungen unterstützt haben und gezeigt haben, was das Leben lebenswert macht. Vielen Dank dafür, an meine langjährigen Freundinnen Almut, Laura, Claudia; meine Stallmädeln Franzi, Katharina, Helena, Gitti und natürlich Caro und ihre Luna, für die vielen schönen gemeinsamen Momente am Stall, sowie im Privaten als auch deren Vertrauen. Gerade die viele Zeit, die ich mit Luna verbringe, haben mich immer wieder geerdet und für den nötigen Ausgleich gesorgt. Sie hat mir immer auf ihrer Art gezeigt, was im jeweiligen Moment wirklich wichtig ist.

Mein größtes Dankeschön geht jedoch an meine Familie, besonders an meine Eltern, Siglinde und Reiner, sowie meinen Bruder und meiner Schwägerin, Wolfgang und Eva. Danke, dass ihr immer an mich geglaubt habt und mich immer best möglichst unterstützt habt, soweit es in euren Möglichkeiten lag. Ohne euch wäre diese Arbeit nicht möglich gewesen!

"Being a Scientist is like
being an explorer. You have this
immense curiosity, this
stubbornness, this resolute will
that you will go forward no
matter what other people say."

Sara Seager
(Astrophysicist)

*„Mut brüllt nicht immer nur. Mut
kann auch die leise Stimme am
Ende des Tages sein, die sagt:
Morgen versuche ich es nochmal.“*

Mary Anne Radmacher
(Schriftstellerin)

List of Publications

Parts of this thesis have been published as follows:

Stefanie Mayr, Marta Marin-Luna, Hendrik Zipse* **“Size-Driven Inversion of Selectivity in Esterification Reactions: Secondary Beat Primary Alcohols”** *J. Org. Chem.*, **2021**, *86*, 3456-3489.

Stefanie Mayr, Hendrik Zipse* **“Size-Induced Inversion of Selectivity in the Acylation of 1,2-Diols”** *Chem. Eur. J.*, **2021**, *27*, 18084-18092.

Stefanie Mayr, Hendrik Zipse* **“Annulated Pyridine Bases for the Selective Acylation of 1,2-Diols”** *Eur. J. Org. Chem.*, **2021**, submitted. Manuscript ID: *ejoc.202101521*

Table of Contents

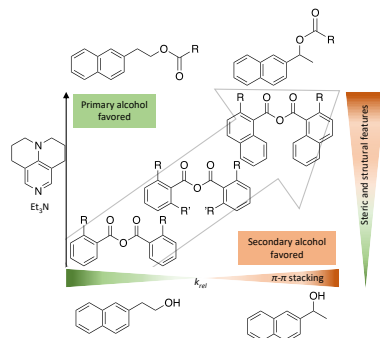
Summary	1
Chapter 1. Introduction.....	2
1.1 Protection Strategies of Mixed 1,2-Diols and Polyols	2
1.1.1 Role of Acylation Agent	2
1.1.2 Role of Auxiliary Base	4
1.1.3 Role of Catalyst	5
1.1.4 Extrinsic Methods.....	7
1.2 Lewis Base Catalysis	7
1.3 Non-Covalent Interactions.....	9
1.3.1 London Dispersion	10
1.3.2 π -Effects.....	11
1.3.3 Non-Covalent Interactions in Organocatalysis	13
1.4 Aim of this Thesis	15
1.5 References	16
Chapter 2. Acylation Reagents in Size-Dependent Esterification Reactions.....	20
2.1 Introduction	21
2.2 Results and Discussion	22
2.3 Conclusion.....	25
2.4 Experimental Part.....	26
2.4.1 Turnover-limited Competition Experiments	26
2.4.2 Synthesis of Reagent	37
2.5 References	39
Chapter 3. Size-Driven Inversion of Selectivity in Esterification Reactions: Secondary Beat Primary Alcohols.....	40
3.1 Experimental Part.....	75
3.1.1 Turnover-limited Competition Experiments of Aryl-Substituted Ethanols.....	75
3.1.2 Investigation of Size Effects of the Alcohol Starting Materials	100
3.1.3 Effects of Reaction Conditions.....	103
3.2 Computational Data	111
3.2.1 Reaction Path Calculations	112

3.2.2	NCI Analysis.....	127
3.2.3	Computational Study about Acid Anhydride Structures	128
3.3	References	145
Chapter 4.	Size-Induced Inversion of Selectivity in the Acylation of 1,2-Diols	146
4.1	Experimental Part.....	156
4.1.1	Turnover-limited Competition Experiments of Aryl Substituted 1,2-Ethanediods	156
4.1.2	Absolute Kinetic Studies of Aryl Substituted 1,2-Ethanediods.....	175
4.1.3	Turnover-limited Competition vs. Absolute Kinetic Experiments	201
4.1.4	Influence of Alcohol Size	201
4.1.5	Transesterification	202
4.1.6	Investigation of Reaction Conditions	207
4.1.7	Turnover-limited Competition Experiments with Aryl Substituted Propanols	217
4.1.8	Analytical Data	224
4.2	Computational Data	246
4.3	References	254
Chapter 5.	Annelated Pyridine Bases for the Selective Acylation of 1,2-Diols.....	255
5.1	Experimental Part.....	265
5.1.1	Turnover-limited Competition Experiments of 2-Naphthyl Substituted Ethanol265	265
5.1.2	Absolute Kinetic Study with 2-Naphthyl-1,2-ethanediol	280
5.1.3	INT1 Analytics via ¹ H NMR and UV/VIS Spectroscopy	303
5.1.4	Analytic Data of Synthesised Catalysts.....	304
5.2	Computational Study.....	356
5.2.1	Cation Affinities Values	356
5.2.2	Computational Data of INT1	373
5.3	References	377
Chapter 6.	Conclusion	379
6.1	References	382
Abbreviation		383

SUMMARY

Selective acylation of hydroxyl groups in natural products are most commonly based on repulsive steric or hydrogen bond effects. Attractive size effects could influence the direction of organocatalyzed reactions, too. Thereby transition states are stabilized by size effects which results in an acceleration of defined reaction rates. In this work size effects induced through reagents, catalysts and substrates in the selective acylation of 1,2-ethanediols are investigated

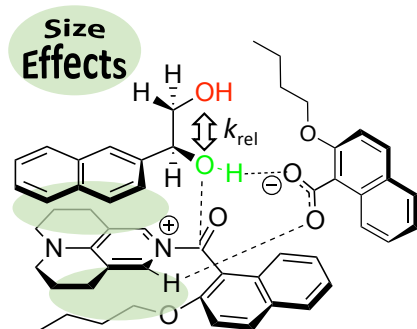
Chapter 2 und 3. Size-Driven Inversion of Selectivity in Esterification Reactions: Secondary Beat Primary Alcohols¹



Relative rates for the Lewis base-mediated acylation of secondary and primary alcohols carrying large aromatic side chains with anhydrides differing in size and electronic structure have been measured. While primary alcohols react faster than secondary ones in transformations with monosubstituted benzoic anhydride derivatives, relative reactivities are inverted in reactions with sterically biased 1-naphthyl anhydrides. Further analysis of reaction rates shows that increasing substrate size leads to an actual acceleration of the acylation process, the effect being larger for secondary as compared to primary alcohols. Computational results

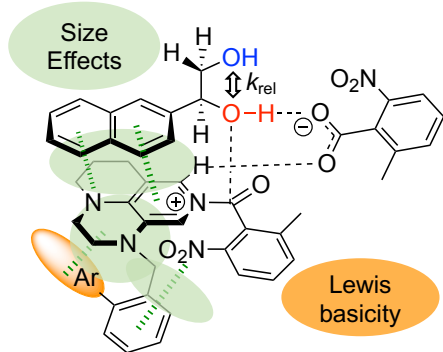
indicate that acylation rates are guided by non-covalent interactions (NCI) between the catalyst ring system and the DED-substituents in the alcohol and anhydride reactants. Thereby stronger NCI are formed for secondary alcohols than for the primary alcohols.

Chapter 4. Size-Induced Inversion of Selectivity in the Acylation of 1,2-Diols²



Relative rates for the Lewis base-catalyzed acylation of aryl-substituted 1,2-diols with anhydrides differing in size have been determined by turnover-limited competition experiments and absolute kinetics measurements. Depending on the structure of the anhydride reagent, the secondary hydroxyl group of the 1,2-diol reacts faster than the primary one. This preference towards the secondary hydroxyl group is boosted in the second acylation step from the monoesters to the diester through size and additional steric effects. In absolute terms the first acylation step is found to be up to 35 times faster than the second one for the primary alcohols due to neighboring group effects.

Chapter 5. Annelated Pyridine Bases for the Selective Acylation of 1,2-Diols³



A set of 24 annelated derivatives of 4-diaminopyridine (DMAP) has been synthesized and tested with respect to its catalytic potential in the regioselective acylation of 1,2-diol substrates. The Lewis basicities of the catalysts as quantified through quantum chemical calculations vary due to inductive substituent effects and intramolecular stacking interactions between side chain π -systems and the pyridinium core ring system. The primary over secondary hydroxyl group selectivities in catalytic acylations of 1,2-diol substrates depend on the size and the steric demand of the Lewis base and the anhydride reagent.

¹Reprinted with permission from *The Journal of Organic Chemistry*, **2021**, *86*, 3456-3489. -Copyright 2021 American Chemical Society.

²Reprinted with permission from *Chemistry – A European Journal*, **2021**, *27*, 18084-18092. - Copyright © 2021 Wiley VCH GmbH & Co. KGaA.

³Submitted to *European Journal of Organic Chemistry* with Manuscript ID ejoc.202101521 - © 2021 Wiley VCH GmbH & Co. KGaA.

Chapter 1. Introduction

1.1 Protection Strategies of Mixed 1,2-Diols and Polyols

The site-selective protection of functional groups in polyol systems or natural products is still a hot topic in organic and pharmaceutical chemistry.^[1] Hydroxyl groups play a major role due to their high incidence in biological chemistry.^[2] Well-known representatives of these compounds are carbohydrates as well as simpler diols,^[3] and several strategies about their selective protection of hydroxyl groups were developed in the last decades.^[1b,3c,4] In addition to silyl ether^[5] or alkyl protection groups (PG),^[3c,4b,6] acylation is a common way to protect hydroxyl groups.^[1c,4a,6b,7] Since in most studies^[8] on the selective acylation of carbohydrates examples with 1,2-diols are presented and common approaches could be deduced, an overview of protection strategies for 1,2-diols and (oligo)saccharides will be provided in the following. Further PGs for regioselective functionalizations like thiocarbonylations,^[4e,9] or phosphorylations^[1b,10] are presented in the literature.

Different approaches to site selective acylations are reported in the literature whereby most strategies are affected by the intrinsic network of intra- and intermolecular hydrogen (H) - bonds in carbohydrate systems.^[4b,11] The strategies may be roughly divided up into four groups influencing each another:

1. Auxiliary base, 2. Acylation agent, 3. Catalyst, 4. Pre-activation by extrinsic methods.

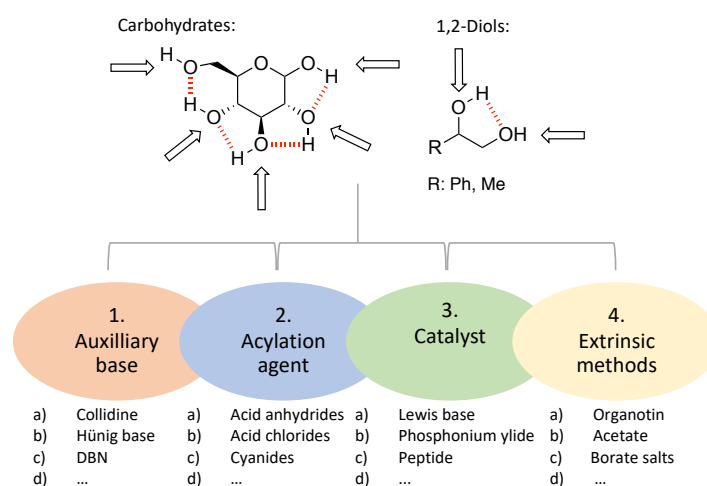


Figure 1.1. Strategies for site selective protection of polyol systems.

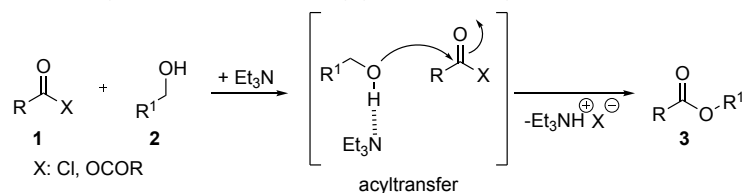
Before the different protection strategies will be discussed in the following, a short statement about the H-bond network is necessary. Defined by spectroscopic methods e.g. UV^[12] or IR^[13] the intramolecular non-covalent interactions (NCI) between the hydroxyl groups -O-H...O- were identified as H-bonds. However, this definition is in contrast to some computational studies about aliphatical (*n,n+1*)-diols and carbohydrates, where no H-bonds was found for vicinal hydroxyl groups. Klein *et al.*^[14] studied the electron density topology of several aliphatical (*n,n+1*)-diols and glucopyranose^[14a,15] on several high level of theories. Corresponding to studies by Silla *et al.*^[16] no H-bonds were quantified as the NCI between adjacent hydroxyl groups in *D*-glucose explored by natural bond orbital (NBO), NCI and the quantum theory of atom in molecules (QTAIM) analysis. In 2004, Corachado *et al.*^[17] already called these interactions “hydroxyl-interactions” referring to the work of Klein. Nevertheless, these intramolecular interaction networks are influencing the intrinsic reactivity by effecting the acidity of the OH-groups in carbohydrates in a way that selective PG strategies are challenging and dependent from the reaction conditions. This in turn means, that under neutral conditions the most acidic hydroxyl group is the least reactive one, because of intramolecular H-bonds interactions. In contrast under basic conditions, which is mostly the case, the most acidic hydroxyl group is the most reactive one, because of transformation in an alkoxide group.^[4b,11a]

1.1.1 Role of Acylation Agent

The formation of esters has been studied extensively in organic chemistry and biochemistry over decades,^[1a,4a] and preferentially starting from carboxylic acids as substrates.^[18] These latter substrates are

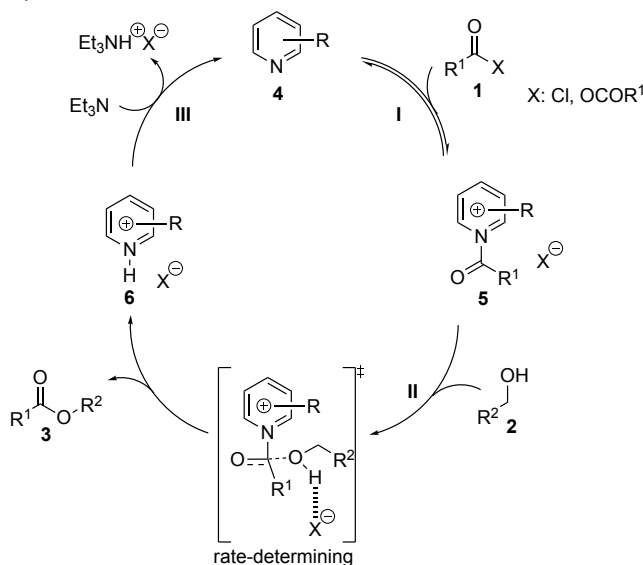
normally require activation through acid-catalysis in the Fischer-esterification^[18-19] or through reagents like dicyclohexylcarbodiimid (DCC, Steglich).^[18,20] In contrast, the Mitsunobu reaction is activating the alcohol by a combination of triphenylphosphine and diethylazodicarboxylate (DEAD)^[20] and converts them to an ester.^[18] However, activated carboxylic acid derivatives like acid chlorides or anhydrides, are nowadays a more prominent reagent to form esters and will be discussed in the following in more detail.^[1c,4a,6b,18a]

The acyltransfer from acylation reagent **1** to alcohol **2** already takes place in the presence of an organic base like sterically hindered amines (Et₃N, DIPEA or DBU) (Scheme 1.1).^[18b,21]



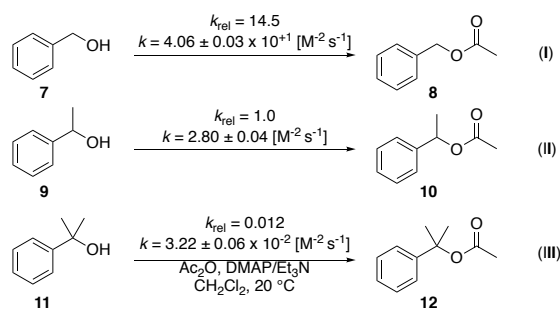
Scheme 1.1. Acylation of a primary alcohol in the presence of a non-nucleophilic base.^[18b,21b]

The acylation is significantly accelerated if a nucleophilic catalyst, like the Lewis base 4-(dimethylamino)pyridine (DMAP) is added.^[22] In numerous mechanistic studies, for example from Zipse,^[23] Spivey^[24] or Jencks,^[25] a mechanism with Lewis base catalysts is proposed (Scheme 1.2). First of all, the nucleophilic catalyst **4** and activated carboxylic acid derivative **1** react to an acylpyridinium cation intermediate **5** (step I, Scheme 1.2), which subsequently undergoes the rate determining acyl transfer step with alcohol **2** to yield the corresponding ester **3** (step II, Scheme 1.2). This step is dominated by two processes: deprotonation by the counterion of the carboxylic acid derivative and nucleophilic attack of the alcohol. The catalyst **4** is recovered by adding a base like Et₃N, which deprotonates the protonated catalyst **6** (step III, Scheme 1.2). In chapter 1.2 Lewis-base catalysis will be discussed in more detail.



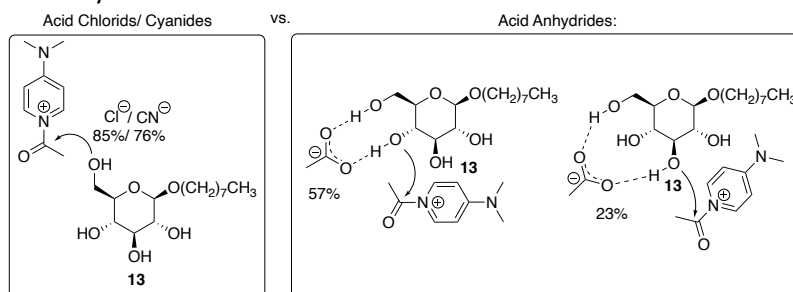
Scheme 1.2. Acylation of a primary alcohol in the presence of a nucleophilic catalyst.^[23b,23d,23e,24,26]

Focusing now on the site selective acylation of OH-groups, primary hydroxyl groups are usually more favoured than secondary and tertiary ones. Steric hindrance around the reactive OH-site might be responsible for this reactivity.^[4a] This reactivity trend is easily exemplified with the acylation rate constants of primary (**7**), secondary (**9**) and tertiary benzyl (**11**) alcohols catalysed by DMAP (Scheme 1.3).^[23a] Thus, the acylation of the primary alcohol **7** with acetic anhydride is almost 15 times faster than the secondary one **9** and even 10³ times faster than the tertiary benzyl alcohol **11**. For this purpose, a selective protection of primary or secondary OH group in the presence of tertiary OH group is trivial, whereas the selective protection between primary or secondary OH groups is challenging.^[4a,6b,27]



Scheme 1.3. Rate constants of the acylation of primary (I), secondary (II) and tertiary alcohol (III) with acetic anhydride catalyzed by DMAP in the presence of Et₃N.^[23a]

In spite of the large number of studies about selective acylation reactions by Lewis base catalysis (see Chapter 1.1.3), there are only few studies about the reactivity behaviour of the acylation reagents towards different OH-groups.^[22a,28] Although the equilibrium between DMAP and acid chloride is shifted completely to the acylpyridinium cation intermediate **5** (Step I, Scheme 1.2) and consequently supposed to act faster in contrast to acid anhydrides, which is only forming 5-10 % of **5**,^[28b] some groups observed that acetic anhydrides react faster than acetic chlorides in a DMAP-catalysed acylation.^[22a,29] This effect is caused by the more basic and mesomeric stabilized counterion.^[22c,28b] Generally, it is assumed that the acylation rate is based on the basicity of the counterion in the order CN⁻ >> OAc⁻ > Cl⁻ due to the deprotonation of the OH-group.^[22c,30] Even though the regioselective acylation of sugars as polyol systems are challenging, Albert *et al.*^[28b] discovered that octyl β-D-glucopyranoside (**13**) could acylate selectively on the C-6 or C-3/4 depending on the acylation reagent catalysed by DMAP under basic conditions. Due to the acetate anion induced formation of hydrogen bonds to the OH groups at C-6 and C-3/4 position via a cyclic intermediate, which favoured the deprotonation of the secondary OH groups at C-3 (23%) and C-4 (57%) position in the presence of pyridine (Scheme 1.4). In contrast, neither the chloride nor the cyanide anion is able to form these NCI and acylation occurs at the C-6 position with 85% or 76% yield.



Scheme 1.4. Counterion effects in the DMAP-catalysed acylation of β-D-glucopyranoside (**13**) with acid chlorides/cyanides vs. acid anhydrides in the presence of pyridine.^[28b]

2016, Schmidt *et al.*^[30] reported that at -78 °C the axial, thermodynamically unfavourable C-4 position instead of the equatorial C-3 position of galactopyranoside could be selective acylated (90%) with benzoic cyanide catalysed by DMAP. This cyanide effect is working, too, during the benzoylation of 3,4,6-O-protected galactopyranosides at the C-4 position with 61% yield. Again H-bonds with the counterion CN⁻ is the key to this effect.

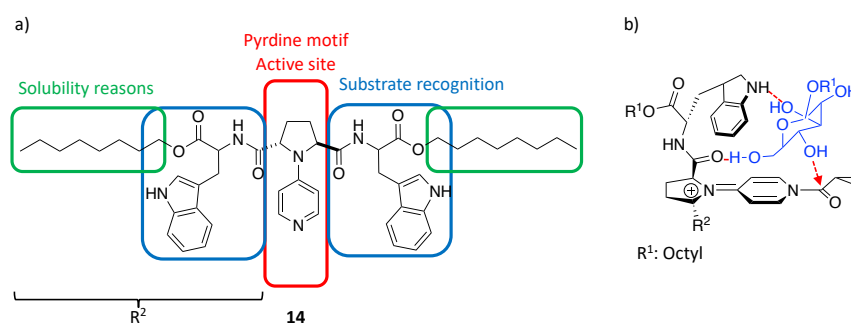
1.1.2 Role of Auxiliary Base

In addition to the acylation reagents the used auxiliary bases influence the selective acylation of OH-groups, too. In 1993, Yamamoto *et al.*^[21a] studied the selective acylation of the primary hydroxyl functionality in primary-secondary alcohols by using acetyl chloride and a sterically hindered amine as a base, e.g. collidine, DABCO, Et₃N or Hünig base. Thereby, the stronger sterically hindered amine collidine preferred the primary alcohol with a regioselectivity > 99. Albert *et al.*^[28b] were not only investigating the role of the counterion, but also the impact of a heterogeneous base like potassium carbonate (K₂CO₃) in contrast to a homogeneous base like pyridine to the regioselective acylation on primary and secondary alcohols. Acetyl chloride

performed as a much faster acylation reagent than acetic anhydride in pyridine. However, the reaction rates are inverted by changing the base to K_2CO_3 . This phenomenon is caused by the basicity of the counterion in the acylpyridinium cation intermediate **5**. If the base is homogeneous, the deprotonation of the OH-group in the transition state (TS) is done even by the counterion or by the base. In contrast, using a heterogeneous base the deprotonation in the TS has to be done by the counterion (Scheme 1.2). For this purpose, the selective acylation of octyl β -D-glucopyranoside (**13**) is influenced by the base, too. As mentioned in chapter 1.1.1 acetyl chloride or cyanide are favouring the primary C-6 OH-group of **13**, whereby acetic anhydride acylates **13** in a 1:1 mixture in the presence of K_2CO_3 and in a 2.5:1 mixture the C-3 and C-4 position in the presence of pyridine. In the late 2010s the Dong group demonstrated further the impact of organobases like DBU,^[31] Hünig base^[8a] or DBN^[32] in the acylation of primary OH groups in 1,2-diols or carbohydrates like α -D-glucopyranoside. Again H-bonds play the major part for the site selective acylation. The organobases are forming H-bonds with the OH-groups whereby at the least sterically hindered side the acylation takes place.

1.1.3 Role of Catalyst

A lot of studies about selective catalysis with polyol systems were performed in the last decades.^[3c,4b,33] One big catalyst group is based on the DMAP motif discovered in the 1960s by Steglich^[22a,22b] and Litvinenko,^[34] a highly active Lewis base catalyst to transfer the acyl group of carboxylic acid derivatives. (In chapter 1.2 Lewis-base catalysis will be discussed in detail.) Kurahashi *et al.*^[35] functionalized the dimethylamino group of DMAP with an aliphatic side chain ($n = 10$) and an acid motif - e.g. $-COOH$ or $-OSO_3H$ - by which the C-6 position of octyl α - octyl β -D-glucopyranoside and galactopyranosides was selectively acylated. The acidic element of the modified catalysts is the key component which promotes the regioselective esterification. The zwitterionic acetyl pyridinium intermediate, in which the acidic part is stacked on top of the pyridinium ring, is assumed to be the reason for the shown selectivity. Due to H-bonds between the primary alcohol at C-6 and $-COO^-/-OSO_3^-$ anions the primary OH-group is acylated with high selectivity, because the acylation of the further OH-groups is sterically unfavoured. A famous DMAP derivate is catalyst **14** developed by Kawabata *et al.*^[36] (Scheme 1.5a). Catalyst **14** catalyzed the site-selective monoacylation of monosaccharides like octyl β -D-glucopyranoside at the C-4 position with isobutyric anhydride. The advantage here is that the secondary OH group at C-4 is acylated with 98% yield in the presence of the more active primary OH group at C-6 and the two further secondary OH groups at C-2 and C-3. The OH groups of β -D-glucopyranoside are fixed in a kind of cage by H-bonds to **14**, so that the C-4 position is preferentially acylated (Scheme 1.5b). However, analoges of **14** are acylating the primary OH group at C-6 if acid chlorides are used instead of isobutyric anhydride. Remarkable is that catalyst **14** and its variants can be flexibly applied in natural product synthesis. The monoacylation in the synthesis of digitoxin,^[37] lanatoside C,^[38] stricotine as well as euginiin^[39] or multifidosides A-C^[3b] are a few examples where the site-selective monoacylation of glucose derivatives in a natural product synthesis takes place.

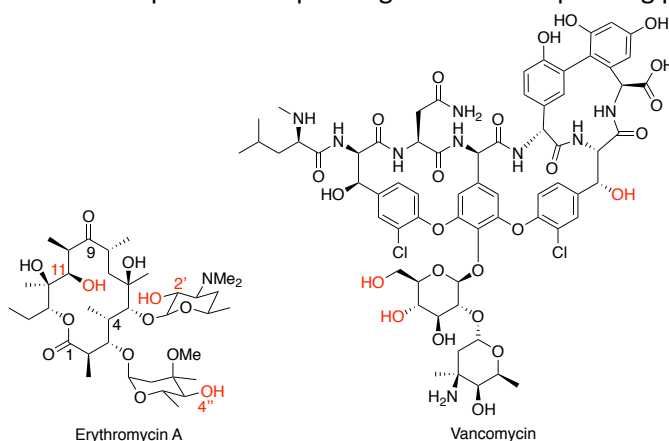


Scheme 1.5. a) Structure of catalyst **14** designed by Kawabata *et al.*^[36a] b) H-bonded cage of β -D-glucopyranoside with catalyst **14**.

Another class of acylation catalysts are peptide-based as pioneered by Miller *et al.*^[40] The Miller group was screening hundreds of peptide-based catalysts, which are not only able to acylate carbohydrates site selective at C-3 or C-4 position, but also for example the polyol erythromycin A,^[2c] where three of the

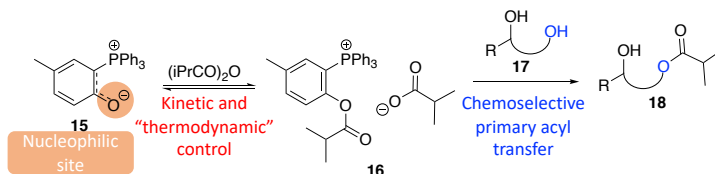
Introduction

attendant unprotected OH groups (C-2', C-4'' or C-11) could selective functionalized, or vancomycin (Scheme 1.6).^[1b] Vancomycin has a variety of functional groups, but it could be site selectively acylated with decanoic anhydride at three different positions depending on the corresponding peptide catalyst.



Scheme 1.6. Natural product polyols erythromycin A and vancomycin.^[1b,2c,4b]

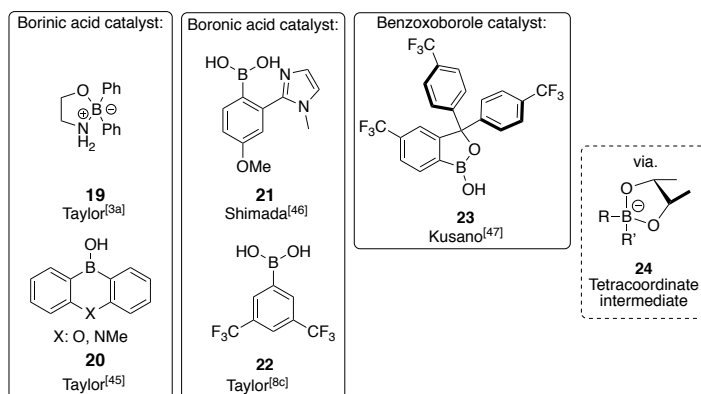
In 2017, Suga *et al.*^[8b] discovered the zwitter ionic phosphonium ylide **15** as catalyst for the selective acylation of primary alcohols. The phosphonium ylide **15** contains an aryl group whereby *O*-acylation is favored because of kinetic and thermodynamic control. Competition studies with 1- vs. 2-heptanol and mixed 1,*n*-diols (**17**) acylated by isobutyric anhydride demonstrates its high quality as nucleophilic catalyst to functionalized primary OH-groups in high yields. Unfortunately, the Suga group did not comment why **15** shows this kind of site selectivity and how high the catalytic activity of **15** in terms of rate constants is in comparison to commonly available acylation catalysts like DMAP.



Scheme 1.7. Acylation of primary OH groups in mixed 1,*n*-diols catalyzed by phosphonium ylide **15**.^[8b]

In 2018, *N*-heterocyclic carbenes were used as chemo- and enantioselective organocatalysts for the asymmetric acylation of aryl-1,2-ethanediols. Simultaneously, the chiral 1,2-diol and the corresponding monoester at the primary position were obtained with good yields and enantioselectivity supported by non-covalent interactions.^[41]

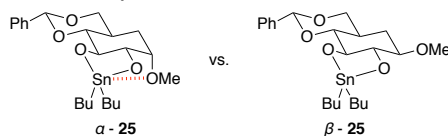
A further large group of catalysts for acylation reactions are based on pre-activating the polyols via an in-situ formation of cyclic intermediates. Already in the 70s synthetic methods using organotin compounds were described for the selective monoacylation of diols.^[42] In 1998, Matsumura *et al.*^[43] developed a one-pot procedure for the site-selective monobenzoylation of 1,2-diols using dimethyltin dichloride in catalytical amounts and the inorganic base potassium carbonate. Thereby, the less substituted site is preferred by benzoyl chloride and the primary ester was formed with a yield of 90%. 10 years later the Matsumura group^[44] described the catalytic acylation process of sugars with dimethyltin dichloride. Even if a high selectivity was predicted, it has to be remembered that the site-selective benzoylation was based on the intrinsic character of the carbohydrates caused by the H-bond network of the OH groups. Based on the organotin-mediated acylation catalysts, organoboron motifs as borinic acids,^[3a,8c,45] boronic acid,^[8c,46] or benzoxaborate^[47] catalysts pioneered by Taylor^[48] and Aoyama^[49] are well-known in the PG chemistry, too (Scheme 1.8). Focussing on the acylation of 1,*n*-diols, the borinic acid catalyst **19**^[3a] and benzoxaborate catalysts **23**^[47] are acylating with high yields selectively the primary alcohol via formation of a tetracoordinate borinate respectively boronate intermediate **24**. Thereby, the organoboron compound is connected via a two-point covalent binding to the diol so that the acylation takes place at the primary nucleophilic oxygen.



Scheme 1.8. Organoboron catalysts for the selective functionalization of 1,*n*-diols.

1.1.4 Extrinsic Methods

Instead of developing a site-selective catalyst, many studies on the pre-activation of carbohydrates or diols exist despite the high toxicity of some reagents e.g. organostannylene reagents. First studies about pre-activation by forming stannyl ethers between bis(tributyltin)oxide and methyl α -D-glucopyranoside at C-6 and C-2 were reported by Ogawa and Matsui.^[42b,50] In a second synthetic step the benzylation proceeds at C-6 and C-2 with good yields (82%). Furthermore, pre-activation via stannylene acetals is also a well-known acylation strategy of carbohydrates. At the the same time, Munavu and Szmant studied the selective acylation of α/β -D-hexopyranoside sugars (**25**) via dibutylstannylene acetals and detected that the α - and β -anomer of D-glucopyranoside were chemoselectively benzyloated differently due to the stabilization of the stannylene acetals (Scheme 1.9).^[51] The stannylene acetal is stabilized by NCI between the C-2 oxygen and the tin, which is only possible in the α -conformer. Due to that the C-2 of the α -anomer was benzyloated with a ratio of 94:1 corresponding to C-3, whereby the β -anomer exhibits a ration of 30:20 (C-2:C-3).



Scheme 1.9. Stannylene acetals for α/β -D-hexopyranosides (**25**).^[51]

Further investigations about the selective benzylation of axial C-4 vs. equatorial C-3 OH groups via stannylene acetals were reported by Nashed and Anderson, whereby the equatorial alcohol was more reactive.^[52] Roelens *et al.*^[53] studied the monoesterification of unsymmetrical diols by obtaining first a dioxastannane, which is subsequently transformed by benzoyl chloride and subsequently phenyldimethylsilyl chloride to the 1-silylated-2-benzoylated monoester as main product. In the last years Dong *et al.*^[54] have been exploring many strategies about site-selective acylation (see Chapter 1.1.2) and reviewing some of the organostannylene chemistry, too. Because of the toxicity of stannylene or other reagents, the Dong group is searching for mild and green protection strategies based on H-bond activation. Tetrabutylammonium acetate^[55] or - benzoate^[56] are able to protect diols and sugars selective without any organic amine bases. The acetate or benzoate anion forms the dual H-bond complex to the OH groups of 1,*n*-diols so that the less sterically hindered primary OH group is acylated with good yields.

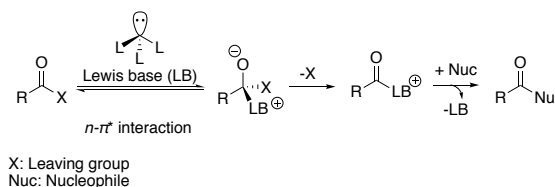
Organoborone compounds could not only be used as catalysts but also as effective *O*-acylation reagents as demonstrated by Bull *et al.*^[57] The air-stable and crystalline *N*-acyl DBN tetraphenylborate salts reacted with mono primary alcohols as well as with mono secondary alcohols to the corresponding esters in good yields. By using 1,2-diols instead of monoalcohols, the primary alcohol was selective acylated with good yield and only traces of secondary protected ester.

1.2 Lewis Base Catalysis

Even though the concept of an organocatalyst is known since the 19th century, the catalysis with organic compounds was approached systematically in organic chemistry only in the last 20 years.^[58] Lewis base catalysis is one kind of organocatalysis defined by Denmark as a “process by which an electronpair donor

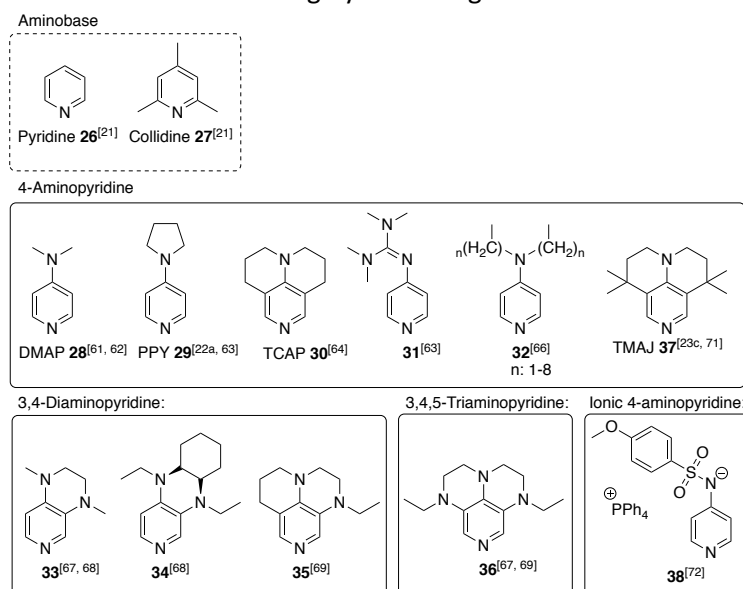
Introduction

increases the rate of a given chemical reaction by interacting with an acceptor atom in one of the reagents or substrates. The binding event may enhance either the electrophilic or nucleophilic character of the bound species."^[22c] More generally, a Lewis base interacts with a Lewis acid, which "lead to a transfer of electron density to the acceptor fragment of a newly formed adduct."^[22c] Jensen was describing the Lewis base interactions by an orbital analysis,^[59] of which the $n-\pi^*$ interaction is reflecting a Lewis base, or also called nucleophilic catalysis, the best (Scheme 1.10).^[22c] $n-\pi^*$ interactions are defined as interactions "between nonbonding electron pairs and antibonding orbitals with π -character."^[22c]



Scheme 1.10. General mechanism of a nucleophilic catalysis with carbonyl compounds based on $n-\pi^*$ interactions.^[22c]

Lewis base catalysts could affect a broad range of reactions like *O*-acylation, aldol reaction, Morita-Baylis-Hillman reaction, silylation, cycloaddition and many more.^[60] Since catalyzed reactions discussed in this work are based on acylation by activated carboxylic acid derivatives, the focus will be on this kind of reaction. Acylation could take place already in the presence of bases like pyridine (**26**) or collidine (**27**).^[21] Modifying the basic pyridine structure through donor substituents like a dimethylamino group by Steglich and Höfle^[22b,61] or by Litvinenko and Kirichenko^[62] leads to the development of DMAP (**28**). This modification leads not only to an acceleration of reaction rates, but also facilitates the protection chemistry of secondary - and especially of tertiary alcohols, which were not acylated by pyridine.^[22a] Steglich^[22a,29] and Hassner^[63] improved the catalytic potential by installing a better electron donating group like pyrrolidine in *para* position to create 4-(pyrrolidinyl)pyridine (PPY, **29**), caused by the better stabilization of intermediate **5** in the catalytic cycle (Scheme 1.2). Conformational fixation of the 4-amino nitrogen atom leads to the tricyclic 4-aminopyridine derivative 9-azajulolidine (TCAP, **30**), which results in an increased catalytic activity by a factor of six in comparison to DMAP.^[24,64] Studies by Mayr and coworkers showed that for TCAP the $n-\pi^*$ interaction in the acylation intermediate **5** is highly stabilizing.^[64-65] Further variation of the 4-amino group



Scheme 1.11. Common pyridine-based Lewis base catalysts. Dotted lines are Lewis bases, solid lines are Lewis base catalysts.

can be seen in catalyst **31**^[63] carrying a tetramethylated guanidine part or the (*n*-alkylamino)pyridine **32** ($n = 1-8$).^[66] Even though **31/32** have a higher catalytic potential as DMAP, **31** has still a similar potential as PPY. Based on the reported stabilization idea of the 4-amino nitrogen atom, in 2007 Han was publishing a synthetic entry to the 3,4-diaminopyridine **33** and 3,4,5-triaminopyridine **36**.^[67] At the same time Zipse *et al.*^[68] were

also presenting the 3,4-diaminopyridine catalyst type **33** and simultaneously the tricyclic catalyst **34**, too, based on theoretical prediction.^[23c,68] Although **33** seems to be more active than DMAP, the catalytic activity of TCAP was not attained. In contrast, **34** has a similar catalytic activity as TCAP.^[67-68] In 2013, further improvements of the TCAP structure was done again by the Zipse group^[69] by studying the tricyclic 3,4-diaminopyridine catalyst **35** and other types of 3,4,5-triaminopyridine catalysts such as **36**, which both should be stronger Lewis base catalysts predicted by methyl cation affinity analysis. Again **35/36** are more active catalysts than DMAP and PPY, however, the kinetic studies by Han^[67] or by Zipse^[69] produce similar rate constants as TCAP, also depending on the solvent used in the reaction. Surprisingly, these findings are in contradiction to what quantum chemical studies about affinity values of the methyl-/ acetyl group transfer predicted for these two catalyst systems. The 6-membered ring system of TCAP was modified by exploring a 5- or 7 membered ring due to the stabilization scale of the cyclic benzhydryl cations predicted by the Mayr group.^[70] However, the ring modified TCAP catalysts (n = 5, 7) showed the same catalytic effectiveness as DMAP which is in line with computed affinity numbers.^[23c,70b] Further predictions about the catalytic activity of Lewis bases by quantum chemical studies were done by Zipse *et al.*^[23c] who predicted that catalyst 1,1,7,7-tetramethyl-9-azajulolidine (TMAJ, **37**) should be stabilized the best in the acylpyridinium cation intermediate **5**. In 2020, Namba *et al.*^[71] reported a reaction pathway to synthesize **37** and demonstrated the catalytic potential of TMAJ, which is slightly higher than that of TCAP. Also in 2020 a new type of ion-pair catalyst, like e.g. **38** was developed by Zipse *et al.*^[72] For the first time since years a DMAP based catalyst illustrates a much stronger catalytic potential than TCAP in an urethan as well as in an *aza*-Morita-Baylis-Hillman reaction.

1.3 Non-Covalent Interactions

In organic chemistry there are several driving forces, which have significant impacts on reactivity or selectivity of a reaction.^[73] One of them are non-covalent interactions. Even in literature there is not a clear categorization of NCI,^[74] a broad classification is still feasible into electrostatic forces, Van der Waals (VdW) interactions and hydrophobic interactions (Figure 1.2). VdW interactions result from dipole-dipole forces found by Keesom,^[75] dipole-induced dipole forces described by Debye^[76] and induced-dipole-induced-dipole forces called London dispersion (LD).^[77] H-bonds or ionic interactions could be considered as electrostatic interactions.^[78] Some effects are existing of electrostatic and VdW interactions like for example the π -effects^[79] or some repulsion effects.^[73b,74a]

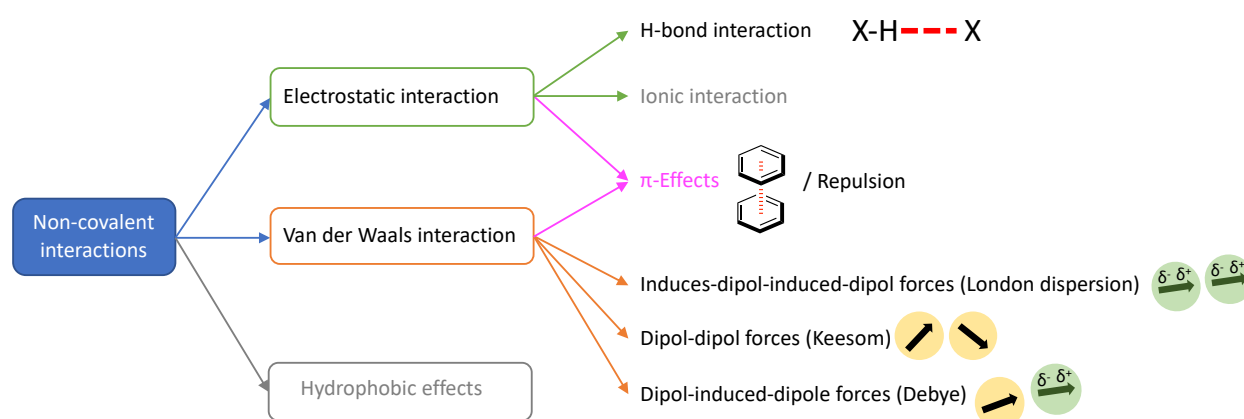


Figure 1.2. Devision of NCI by their origin.^[16,78]

Despite the great significance of NCI in nature – structure and stability of DNA, RNA, or proteins or the molecular recognition process^[80] - and early definition of the attractive part of VdW forces like the London dispersion by F. London in 1930,^[77] the VdW forces have become more prominent in research in the last years. In contrast, hydrogen bonds are well recognized in organic chemistry^[81] and are the interaction between a “H atom bonded covalently to either F, O or N and an unshared pair of electrons on a neighbouring F, O or N”.^[74b] The characteristics of this kind of NCI are short-range, directional and specific.^[82]

1.3.1 London Dispersion

With the definition of the ideal gas law (Eq. 1.1) the basic building block was set to define VdW interactions. Advancements of Eq. 1.1 to the Van der Waals equation of state (Eq. 1.2) by Johannes D. Van der Waals in 1873, gases could be described over a wide range of conditions, because now an interaction between the particles is allowed.

$$p = \frac{NRT}{V} \quad \text{Eq. 1.1}$$

$$\left(p + \frac{a}{V^2}\right)(V - b) = NRT \quad \text{Eq. 1.2}$$

p = pressure of a gas
R = gas constant

N = number of moles
b = co-volume

T = absolute temperature
a = cohesion pressure

Described by Eq. 1.2 especially by the term a/V^2 , all species, even for particles owning no permanent charges, - dipole or multiple electric moments - could perceive forces, which could attract the particles to each other.^[83] Almost 40 years later Keesom^[75,84] described the interaction between a permanent dipol and a further permanent dipol which is caused in the assumption of permanent electric moments in molecules. Further assumptions were made by Debye,^[76] who predicted that a permanent electric dipol could induce polarizable species. These are always attractive forces in contrast to the Keesom interactions which could be attractive or repulsive. With the development of quantum mechanics in 1920s, Fritz London was able to characterize attractive VdW forces for species (molecules, atoms or ions), which do not contain permanent dipoles.^[74b,77] This attractive VdW force is called dispersion force and results from a temporary fluctuation caused in an electron distribution in the electron charge cloud of a molecule or atom (Eq. 1.3).^[74b,77,85] Again a momentary dipol moment is formed which leads to an electric field generation. In addition, the induced dipoles induce themselves further dipoles, so that attractive interactions between induced-dipoles/induced-dipoles arise.^[86]

$$E_{Disp}^{AB} = -\frac{1}{2} \sum_{A,B} \frac{C_6^{AB}}{R_{AB}^6} = -\frac{3}{2} \frac{\alpha_A \alpha_B R^{-6} I_1 I_2}{I_1 + I_2} \quad \text{Eq. 1.3}$$

C_6 = empirical polarization coefficients
 α = polarizability

R = distance between particles A and B
I = ionization energy

Still nowadays this formulation by London is corresponding to the London dispersion forces studied by Schreiner *et al.*^[87] A good historical overview on the further conceptual developments until today is given by Ángyán, Dobson, Jansen and Gould.^[83a]

The counterparts of attractive VdW interactions are repulsive interactions which occur when two molecules come too close to each other and result in a repulsion (Figure 1.3a). Unfortunately, it is more common in organic chemistry that steric effects are taken to be synonymous with repulsive effects.^[73b] The big drawback of LD forces is that this force is weak in comparison to other interactions, like H-bonds or ionic interactions. But in contrast to the other forces, the impact of LD increases strongly with the size of the molecules,^[85,87-88] which was identified by the successful synthesis of stable molecules with, for example, a long C-C distance (171 pm) like in tetramantane-dimantyl adduct **39**, or the highly crowded all-*meta* tert-butylhexaphenylethane **40** (Figure 1.3b/c).^[89] An important consideration of LD forces is, that they are temperature independent, which is not the case for most other forces.^[77,90] Because most organic reactions are performed in solution, the main question is, how strong are the LD forces in solution? Cockroft^[91] and Shimizu^[92] both declare that in solution solvent effects have a key role and LD has a minor role.

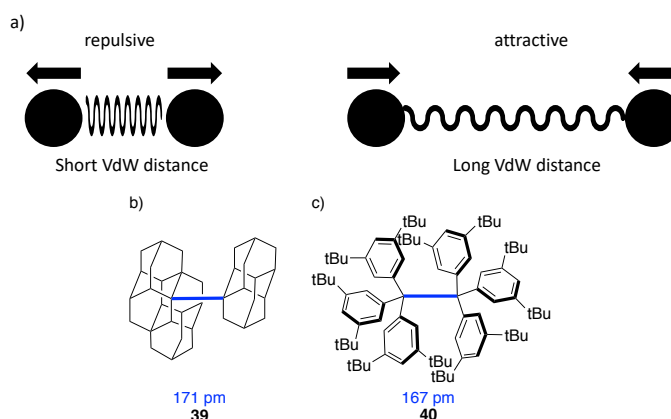


Figure 1.3. a) Attractive and repulsive VdW forces,^[73b] and stable compounds with long C-C distances like b) tetramantane-dimantyl adduct **39** and c) in the highly crowded all-*meta tert*-butylhexaphenylethane **40**.^[89]

However, in 2017 the Chen group reported that proton-bound dimers in dichloromethane are less influenced (~70%) by LD than in gas phase, but still present.^[93] The Zipse group found a correlation between VdW interactions and solvophobic effects experimentally as well as theoretically.^[5c] Depending on the solvent and its H-bond donor ability defined by Hunter,^[94] size effects of the studied aromatic surfaces can have a minor or major role with changes in selectivity of around a factor of 4.5. The Schreiner group^[90] was studying the intramolecular dispersion interaction of di-*tert*-butyl substituted cyclooctatetraene in 16 common solvents. Independent from the used solvent the sterically more challenging folded 1,6- cyclooctatetraene conformer was found to be stabilized by intramolecular LD forces.

1.3.2 π -Effects

Further NCI occur through regions of negative charge contained in π -systems – aromatic compounds or alkenes –, because of attractive electrostatic interactions between regions of positive and negative charges. This so called π -effect could be separated in three subcategories: cation- π , polar- π and π -donor-acceptor.^[74a]

1.3.2.1 Aromatic π - π Stacking Interactions

Aromatic π - π stacking interactions are one major part of this effect and are widespread in nature - DNA, proteins, solid state of benzene or in the high melting point of a benzene-perfluorobenzene mixture.^[95] Although a growing area of research is existing to understand π - π stacking interactions, until today the nature of NCI is not fully elucidated.^[95b] One challenge is, that stacking interactions result from several forces such as electrostatic, London dispersion and also solvophobic forces (Eq. 1.4).^[95]

$$\Delta E_{\text{stacking}} = \Delta E_{\text{electrostatic}} + \Delta E_{\text{dispersion}} + \Delta E_{\text{solvophobic}} \quad \text{Eq. 1.4}$$

A second challenge in quantifying this stacking interaction is the geometrical diversity of aryl rings orientations, which is shown in Figure 1.4 for benzene. Hunter and Sanders defined an electrostatic model (HS) based on the quadrupole moment of aromatic rings, which explains the sandwich, off-set, tilted and edge-to-face benzene dimer configurations.^[79,95b,96] The quadrupole moments in arene systems arise by the arrangement of electron density, so that the ring is partially negatively charged at the face and partially positively charged at the edge.^[74a] The HS model claims that between opposite electronic charge clouds the interaction is maximized, while between same electronic charge clouds the interaction is minimized. This explains why edge-to-face and off-set benzene dimers are more stable (~4 kJ mol⁻¹) than the sandwich conformer studied by quantum chemical methods.^[97] The sandwich geometry is favoured, when one of the aromatic rings holds strong electron-withdrawing groups like in a benzene-perfluorobenzene mixture. The F substituents invert the quadrupole moment so that the ring is partially positively charged at the face, which can easily interact with the negatively charged face of a benzene ring.^[98] It should be added that the edge-to-face conformation could be, in addition to the π -stacking NCI, regarded as CH- π interaction, which is nothing else as a weak hydrogen-bond interaction.^[73b,95a,99] With this in mind, it is evident that substituents,

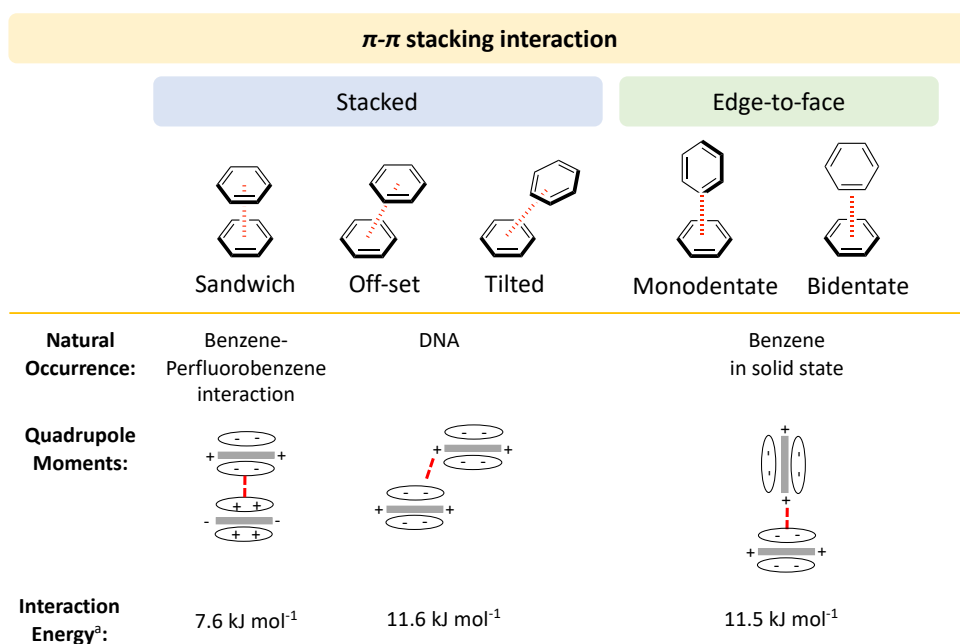


Figure 1.4. Aromatic π - π stacking interaction geometrical arrangement illustrated with benzene dimers. ^aLevel of theory CBS CCDD(T).^[97]

either electron-withdrawing or electron-donating, affecting the electron clouds can thus strengthen or weaken the stacking interaction.^[79,95b,98] Experimental control of this hypothesis was obtained by several groups, thus the kinetic model system reported by Cozzi and Siegel should be debated in more detail.^[100] The Hammett σ_m electronic parameter could correlate with the unimolecular bond rotation rate, which is an experimental value for stacking forces induced by substituent effects.^[95b] Cozzi and Siegel were observing the rotational barriers of 1,8-diaryl-naphthalene and discovered a flipping of the Hammett plot when a perfluorinated phenyl ring was present in the π -cofacial system.^[100] Getting away from the electrostatic HS model, quantum chemical studies of Grimme^[101] or the Sherrill group^[97,102] indicate an increase in stacking interaction for all kinds of substituents. Based on these studies, Wheeler and Houk (WH) defined a further model for stacking interactions with substituted aryl rings.^[103] Now the substituent itself interacts electrostatically with the stacked aromatic surface. Correlating again the Hammett σ_m electronic parameters against the computed substituent effects for the π - π stacking interactions results in the same plots if the aromatic ring of the substituted benzene is exchanged by a proton. Sherrill and coworkers verified the WH model by computational methods like functional-group SAPT, electrostatic potential and density analysis of stacking interactions between substituted benzene dimers against substituted benzene-benzene dimers in situ.^[104] Comparing the HS with the WH model, Sherrill *et al.*^[104] found that the WH model shows stronger electrostatic and dispersion terms and thus the WH is the more dominant model with a broadly accurate picture.

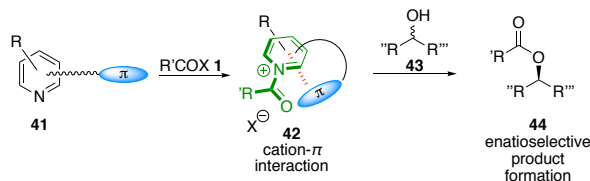
Even though the electrostatic terms of aromatic stacking interactions are well recognized, there exist two further forces affecting the stacking interactions (Eq. 1.4). The huge challenge in both quantum chemical and experimental studies is to distinguish between the dispersion and solvophobic forces as both are strengthened by increasing size of the system. Nonetheless, quantum chemical and experimental studies by Santos and coworkers predict,^[105] that dispersion forces are a main part in the sandwich conformer of 1,8-diarylnaphthalenes and that aromatic stacking interactions are not exclusively determined by electrostatic models.^[97,102b] Grimme suggested that a “stronger interaction for stacked aromatic dimers (...) becomes very significant for more than 10-15 carbon atoms”^[106] and that this interaction is dominated by LD forces. Further high level *ab initio* studies^[87] showed that “dispersion plays a major role in the attractive nature of π - π interactions.”^[99]

1.3.2.2 Cation- π Interactions

Cation- π interactions are a much stronger forces than the just discussed aromatic π - π -interactions, which are comparable with hydrogen bonds^[74a] and are to be found in aromatic boxes of proteins.^[107] These aromatic boxes consist of various combinations of three to four amino acids – tryptophan, tyrosine and phenylalanine – which are stabilizing cations in these kinds of binding pockets. A further example in nature is localized in the nicotine receptor, where acetylcholine is bound by a cation- π interaction to the receptor in the brain.^[74a,107b,108] Simplified, a cation- π interaction is an electrostatic interaction between a cation and the electronic cloud in the face of an aromatic ring.^[74a,107b] Thereby electrostatic and induction interaction play the major part in cation- π interactions whereby other forces like LD have contributing values.^[109] Even though in the 80s the NCI between alkali metal cations and aromatic compounds were defined by Kebarle as cation- π interactions,^[110] also organic cations like pyridinium could be applied.^[109b] Hence cation- π interactions gain access in the organic chemistry as special control elements in regio-, chemo- or stereoselective reactions (see Chapter 1.3.3).^[109b]

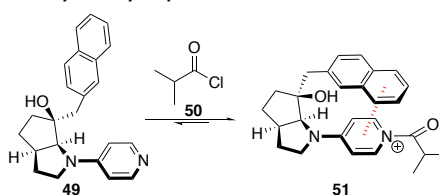
1.3.3 Non-Covalent Interactions in Organocatalysis

As mentioned in 1.3.2. π -effects are an important control element in organic synthesis, like nucleophilic addition, cycloaddition or rearrangements.^[111] Thereby “cation- π interactions can control the conformation of the substrates or the transition state to give the desired products.”^[109b] In the following the focus is on heterocyclic organocatalysts containing nitrogen like pyridine-based structures as in *O*-acylation reactions (Scheme 1.12). Thereby, in the *N*-acylpyridinium cation intermediat **42** the acylpyridinium face (green) interacts with the aromatic face of the substituent (blue) via cation- π forces. The supplied chiral settings in the TS favours stereoselective acylation of a racemic secondary alcohol **43** to an enatio enriched ester **44**. In the literature numerous examples exist about chiral organocatalysts.



Scheme 1.12. Asymmetric *O*-acylation promoted by cation- π interaction.^[109b]

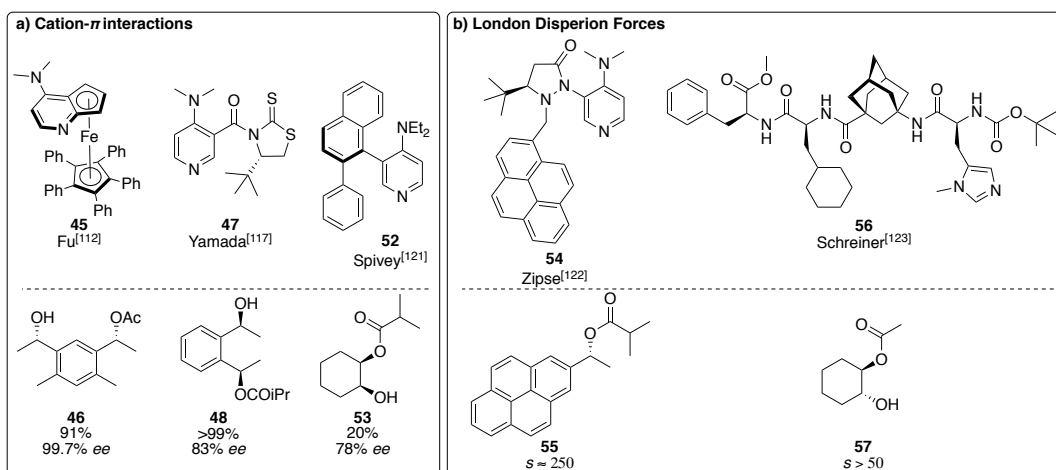
One is the planar-chiral DMAP-ferrocene hybrid catalyst **45** developed by Fu *et al.*^[112], which forms with 91% yield and 99.7% *ee* the monoester **46** out of the corresponding *meso*-diol. Bressy^[113] and Diner^[114] validated the high quality of catalyst **45** in asymmetric acylation and desymmetrization reactions. Additional, in 2015 Diner^[115] was proving cation- π interactions between the *N*-acylpyridinium cation and the aromatic size of the alcohol through quantum chemical analysis. Yamada and coworkers reported with catalyst **47** – a DMAP-based catalyst modified at *meta* position with a thiazolidine-2-thione – high kinetic resolution of secondary 2-naphthylethanol^[116] and desymmetrization of aromatic *meso* diol to monoester **48** (>99% yield, 83% *ee*).^[117] X-ray crystal structures and quantum chemical analysis demonstrate that already in the *N*-acyl pyridinium cation intermediat **42** the N-C=S component is stacking over the pyridinium ring via intramolecular cation- π interactions. In the TS a triple sandwich motif is predicted by additional intermolecular cation- π interactions between the organic cation **42** and aromatic ring of the alcohol motif. That NCI influence the geometry of the *N*-acylpyridinium intermediat **42**, too, was demonstrated in a ¹H NMR analysis by Fujii^[118] and subsequently in quantum chemical analysis by Zipse.^[119] Both demonstrated that the configuration of the



Scheme 1.13. Non-stacked and stacked geometry of catalyst **49** during the activation by acid chloride **50** to *N*-acylpyridinium cation intermediate **51**.^[111b,118]

Introduction

2-naphthyl element of catalyst **49** is switching from non-stacked to face-to-face stacked interaction during the activation with acid chloride **50** to *N*-acylpyridinium cation intermediate **51**. It is presumed that the well stereoselectivity of **49** in the kinetic resolution *cis*-2-hydroxycyclohexyl-benzoate derivatives is promoted by the open and closed conformation in the catalyst which is induced by attractive NCI. A further DMAP-based catalyst **52**, again modified at the pyridine ring, was developed by Spivey.^[120] Instead of a thione motif an aryl substituted 1-naphthyl is the axially-chiral motif of **52**, which is performing well as a chiral acyl transfer catalyst for secondary alcohols. 1,2-cyclohexandiol is desymmetrized by **52** with 78% *ee* and 20% yield to the corresponding monoester **53**.^[121] Schreiner *et al.*^[87] suggested that TS could simply be affected by LD forces, too, because the looser bonds in a TS lead to a simplified polarization, which lead to a stereoselective controlled reaction. The Zipse group^[122] demonstrated recently the big influence of LD forces in the enantioselective acylation of secondary aromatic ethanols catalyzed by 1-pyrene-modified DMAP based catalyst **54** (Scheme 1.14b). The corresponding stereoselective (*R*)-ester **55** was obtained by an enantioselectivity of around $s \approx 250$. Attractive NCI between the aromatic surface of the alcohol and the catalyst structure speed up the major enantiomer of the bigger pyrene alcohol by a factor of 40 in comparison to the smaller phenyl alcohol. A further example for LD forces during an acyl transfer was reported for the tetrapeptide catalyst **56** by Schreiner and Thiele (Scheme 1.14b),^[123] where the histidine element is the catalytic center of the peptide and the (*S*)-cyclohexylalanine component should promote dispersion interaction. Via NMR spectroscopic and density functional theory computational studies, intermolecular dispersion interactions were characterized in the enantiodiscrimination of *meso*-1,2-cyclohexandiol to monoester **57**.



Scheme 1.14. Chiral organocatalysts used in asymmetric *O*-acylation.

1.4 Aim of this Thesis

The short literature overview about site-selective protection strategies in polyol systems, organocatalysis and NCI forces are illustrating the focus of this work well. Many strategies to protect site-selective polyol systems are presented in literature. However, most of them are based on influencing the H-bond network of the polyol or installing steric effects to cause high selectivity. Excluding the carbohydrates, the focus in literature is more or less on selective protection of the already more reactive primary alcohol group. From stereoselective catalysis in *O*-acylation it is already known, that NCI could have an attractive effect on the selectivity in *meso*-diols. Studies about catalysis processes influencing the site-selectivity of a reaction mechanism by attractive VdW forces are rare, although it is known that transition state structures could be stabilize by LD and consequently influence the reaction rates. The main goal of this work is to influence the reaction rates of primary and secondary alcohols in an 1,2-ethanediol system by London dispersion forces. The aim is to accelerate the reaction rate of secondary alcohols in a way to flip the regioselectivity from primary towards secondary alcohols, although it is reported that the primary alcohol is about an order or two more reactive. To induced LD forces, as polyols aryl substituted 1,2-ethanediols were acylated by a set of acylation reagents carrying dispersion-energy donor (DED) groups. The site-selective acylation is catalyzed with catalysts containing big faces to increase π - effects. Due to the high complexity in the reaction pathway of acylation 1,2-diols (around 6 reaction rates influencing each other, is discussed in chapter 4), the relative rates of primary vs. secondary were detected first with a separated aromatic ethanol system. The corresponding primary and secondary alcohols having the structural motif of the 1,2-diol system. These first benchmarking reaction conditions were further applied to the Lewis-based catalyzed acylation of origin 1,2-diols, while ensuring a model to detect the reaction rates for the first and second acylation steps and size effects. Finally, LD forces were provoked in the Lewis base catalysts by synthesizing catalysts with DED-substituents. The impact of the DED-substituents on the Lewis basicity was defined by a quantum chemical study. How Lewis basicity and LD forces are affecting the site-selectivity of the acylation and catalytic potential was studied.

1.5 References

- [1] a) G. Sartori, R. Ballini, F. Bigi, G. Bosica, R. Maggi, P. Righi, *Chem. Rev.* **2004**, *104*, 199-250; b) S. Yoganathan, S. J. Miller, *J. Med. Chem.* **2015**, *58*, 2367-2377; c) N. A. Afagh, A. K. Yudin, *Angew. Chem. Int. Ed.* **2010**, *49*, 262-310; d) O. Robles, D. Romo, *Nat. Prod. Rep.* **2014**, *31*, 318-334; e) K. C. Nicolaou, J. S. Chen, *Classics in Total Synthesis III*, Wiley-VCH, Weinheim, **2011**.
- [2] a) G. Zong, E. Barber, H. Aljewari, J. Zhou, Z. Hu, Y. Du, W. Q. Shi, *J. Org. Chem.* **2015**, *80*, 9279-9291; b) M. Koshimizu, M. Nagatomo, M. Inoue, *Angew. Chem. Int. Ed.* **2016**, *55*, 2493-2497; c) C. A. Lewis, S. J. Miller, *Angew. Chem. Int. Ed.* **2006**, *45*, 5616-5619.
- [3] a) D. Lee, C. L. Williamson, L. Chan, M. S. Taylor, *J. Am. Chem. Soc.* **2012**, *134*, 8260-8267; b) Y. Ueda, T. Furuta, T. Kawabata, *Angew. Chem.* **2015**, *127*, 12134-12138; c) V. Dimakos, M. S. Taylor, *Chem. Rev.* **2018**, *118*, 11457-11517; d) T. M. Beale, M. S. Taylor, *Org. Lett.* **2013**, *15*, 1358-1361.
- [4] a) M. Nahmany, A. Melman, *Org. Biomol. Chem.* **2004**, *2*, 1563-1572; b) J. Lawandi, S. Rocheleau, N. Moitessier, *Tetrahedron* **2016**, *72*, 6283-6319; c) S. M. Polyakova, A. V. Nizovtsev, R. A. Kunetskiy, N. V. Bovin, *Russ. Chem. Bull.* **2015**, *64*, 973-989; d) C.-C. Wang, J.-C. Lee, S.-Y. Luo, S. S. Kulkarni, Y.-W. Huang, C.-C. Lee, K.-L. Chang, S.-C. Hung, *Nature* **2007**, *446*, 896-899; e) B. S. Fowler, K. M. Laemmerhold, S. J. Miller, *J. Am. Chem. Soc.* **2012**, *134*, 9755-9761.
- [5] a) S. K. Chaudhary, O. Hernandez, *Tetrahedron Lett.* **1979**, *20*, 99-102; b) K. Yoshida, H. Suzuki, H. Inoue, K. Matsui, Y. Fujino, Y. Kanoko, Y. Itatsu, K.-i. Takao, *Adv. Synth. Catal.* **2016**, *358*, 1886-1891; c) M. Marin-Luna, B. Pölloth, F. Zott, H. Zipse, *Chem. Sci.* **2018**, *9*, 6509-6515; d) D. Lee, M. S. Taylor, *Org. Biomol. Chem.* **2013**, *11*, 5409-5412.
- [6] a) B. Ren, O. Ramström, Q. Zhang, J. Ge, H. Dong, *Chem. Eur. J.* **2016**, *22*, 2481-2486; b) P. G. M. Wuts, *Greene's Protective Groups in Organic Synthesis*, 5 ed., John Wiley & Sons, Hoboken, New Jersey, **2014**; c) L. Chan, M. S. Taylor, *Org. Lett.* **2011**, *13*, 3090-3093.
- [7] A. H. Haines, *Adv. Carbohydr. Chem. Biochem.* **1976**, *33*, 11-109.
- [8] a) B. Ren, L. Gan, L. Zhang, N. Yan, H. Dong, *Org. Biomol. Chem.* **2018**, *16*, 5591-5597; b) Y. Toda, T. Sakamoto, Y. Komiyama, A. Kikuchi, H. Suga, *ACS Catal.* **2017**, *7*, 6150-6154; c) M. S. Taylor, *Acc. Chem. Res.* **2015**, *48*, 295-305.
- [9] A. S. Nagle, R. N. Salvatore, R. M. Cross, E. A. Kapxhiu, S. Sahab, C. H. Yoon, K. W. Jung, *Tetrahedron Lett.* **2003**, *44*, 5695-5698.
- [10] a) B. R. Sculimbrene, A. J. Morgan, S. J. Miller, *Chem. Comm.* **2003**, 1781-1785; b) S. Han, S. J. Miller, *J. Am. Chem. Soc.* **2013**, *135*, 12414-12421.
- [11] a) T. Kurahashi, T. Mizutani, J.-i. Yoshida, *J. Chem. Soc., Perkin Trans. 1* **1999**, 465-474; b) N. Moitessier, Y. Chapleur, *Tetrahedron Lett.* **2003**, *44*, 1731-1735.
- [12] P. Çarçabal, R. A. Jockusch, I. Hünig, L. C. Snoek, R. T. Kroemer, B. G. Davis, D. P. Gamblin, I. Compagnon, J. Oomens, J. P. Simons, *J. Am. Chem. Soc.* **2005**, *127*, 11414-11425.
- [13] V. Crupi, G. Maisano, D. Majolino, P. Migliardo, V. Venuti, *J. Phys. Chem. A* **2000**, *104*, 3933-3939.
- [14] a) R. A. Klein, *J. Am. Chem. Soc.* **2002**, *124*, 13931-13937; b) R. A. Klein, *J. Comput. Chem.* **2002**, *23*, 585-599.
- [15] R. A. Klein, *Chem. Phys. Lett.* **2006**, *433*, 165-169.
- [16] J. M. Silla, R. A. Cormanich, R. Rittner, M. P. Freitas, *Carbohydr. Res.* **2014**, *396*, 9-13.
- [17] J. C. Corchado, M. L. Sánchez, M. A. Aguilar, *J. Am. Chem. Soc.* **2004**, *126*, 7311-7319.
- [18] a) F. A. Carey, R. J. Sundberg, *Advanced Organic Chemistry Part B: Reactions and Synthesis*, 5 ed., Springer Science+Business Media, New York, **2007**; b) J. Clayden, N. Greeves, S. Warren, *Organische Chemie*, 2 ed., Springer Spektrum, Berlin Heidelberg, **2013**.
- [19] H. G. O. Becker, W. Berger, G. Domschke, E. Fanghänel, J. Faust, M. Fischer, F. Gentz, K. Gewalt, R. Gluch, R. Mayer, K. Müller, D. Pavel, H. Schmidt, K. Schollberg, K. Schwetlick, E. Seiler, G. Zeppenfeld, *Organikum*, 23 ed., Wiley-VCH, Weinheim, **2009**.
- [20] J. Xiang, A. Orita, J. Otera, *Angew. Chem. Int. Ed.* **2002**, *41*, 4117-4119.
- [21] a) K. Ishihara, H. Kurihara, H. Yamamoto, *J. Org. Chem.* **1993**, *58*, 3791-3793; b) G. H. Schenk, P. Wines, C. Mojzis, *Anal. Chem.* **1964**, *36*, 914-919.
- [22] a) G. Höfle, W. Steglich, H. Vorbrüggen, *Angew. Chem. Int. Ed.* **1978**, *17*, 569-583; b) W. Steglich, G. Höfle, *Angew. Chem. Int. Ed.* **1969**, *8*, 981-981; c) S. E. Denmark, G. L. Beutner, *Angew. Chem. Int. Ed.* **2008**, *47*, 1560-1638.
- [23] a) C. B. Fischer, S. Xu, H. Zipse, *Chem. Eur. J.* **2006**, *12*, 5779-5784; b) S. Xu, I. Held, B. Kempf, H. Mayr, W. Steglich, H. Zipse, *Chem. Eur. J.* **2005**, *11*, 4751-4757; c) I. Held, A. Villinger, H. Zipse, *Synthesis* **2005**, *2005*, 1425-1430; d) E. Larionov, M. Mahesh, A. C. Spivey, Y. Wei, H. Zipse, *J. Am. Chem. Soc.* **2012**, *134*, 9390-9399; e) E. Larionov, H. Zipse, *WIREs Computational Molecular Science* **2011**, *1*, 601-619.
- [24] A. C. Spivey, S. Arseniyadis, *Angew. Chem. Int. Ed.* **2004**, *43*, 5436-5441.
- [25] a) A. R. Fersht, W. P. Jencks, *J. Am. Chem. Soc.* **1970**, *92*, 5432-5442; b) A. R. Fersht, W. P. Jencks, *J. Am. Chem. Soc.* **1970**, *92*, 5442-5452.
- [26] H. Mandai, K. Fujii, S. Suga, *Tetrahedron Lett.* **2018**, *59*, 1787-1803.

- [27] a) S. Araki, S. Kambe, K. Kameda, T. Hirashita, *Synthesis* **2003**, 2003, 0751-0754; b) K. Ishihara, M. Nakayama, S. Ohara, H. Yamamoto, *Synlett* **2001**, 2001, 1117-1120.
- [28] a) E. Guibe-Jampel, G. Le Corre, M. Wakselman, *Tetrahedron Lett.* **1979**, 20, 1157-1160; b) E. Kattinig, M. Albert, *Org. Lett.* **2004**, 6, 945-948.
- [29] W. Steglich, G. Höfle, *Tetrahedron Lett.* **1970**, 11, 4727-4730.
- [30] P. Peng, M. Linseis, R. F. Winter, R. R. Schmidt, *J. Am. Chem. Soc.* **2016**, 138, 6002-6009.
- [31] Y. Lu, C. Hou, J. Ren, X. Xin, H. Xu, Y. Pei, H. Dong, Z. Pei, *Molecules* **2016**, 21, 641-649.
- [32] B. Ren, M. Zhang, S. Xu, L. Gan, L. Zhang, L. Tang, *Eur. J. Org. Chem.* **2019**, 2019, 4757-4762.
- [33] T. Kawabata, *Site-Selective Catalysis*, Springer, Berlin, **2018**.
- [34] L. M. Litvinenko, A. I. Kirichenko, *Dokl. Akad. Nauk. SSSR Ser. Khim.* **1967**, 176, 97-100.
- [35] T. Kurahashi, T. Mizutani, J.-i. Yoshida, *Tetrahedron* **2002**, 58, 8669-8677.
- [36] a) T. Kawabata, W. Muramatsu, T. Nishio, T. Shibata, H. Schedel, *J. Am. Chem. Soc.* **2007**, 129, 12890-12895; b) T. Kawabata, W. Muramatsu, T. Nishio, T. Shibata, Y. Uruno, R. Stragies, *Synthesis* **2008**, 2008, 747-753; c) Y. Ueda, W. Muramatsu, K. Mishiro, T. Furuta, T. Kawabata, *J. Org. Chem.* **2009**, 74, 8802-8805.
- [37] K. Yoshida, T. Furuta, T. Kawabata, *Tetrahedron Lett.* **2010**, 51, 4830-4832.
- [38] Y. Ueda, K. Mishiro, K. Yoshida, T. Furuta, T. Kawabata, *J. Org. Chem.* **2012**, 77, 7850-7857.
- [39] H. Takeuchi, K. Mishiro, Y. Ueda, Y. Fujimori, T. Furuta, T. Kawabata, *Angew. Chem. Int. Ed.* **2015**, 54, 6177-6180.
- [40] K. S. Griswold, S. J. Miller, *Tetrahedron* **2003**, 59, 8869-8875.
- [41] B. Liu, J. Yan, R. Huang, W. Wang, Z. Jin, G. Zanon, P. Zheng, S. Yang, Y. R. Chi, *Org. Lett.* **2018**, 20, 3447-3450.
- [42] a) D. Wagner, J. P. H. Verheyden, J. G. Moffatt, *J. Org. Chem.* **1974**, 39, 24-30; b) T. Ogawa, M. Matsui, *Carbohydr. Res.* **1977**, 56, c1-c6.
- [43] a) T. Maki, F. Iwasaki, Y. Matsumura, *Tetrahedron Lett.* **1998**, 39, 5601-5604; b) F. Iwasaki, T. Maki, O. Onomura, W. Nakashima, Y. Matsumura, *J. Org. Chem.* **2000**, 65, 996-1002.
- [44] Y. Demizu, Y. Kubo, H. Miyoshi, T. Maki, Y. Matsumura, N. Moriyama, O. Onomura, *Org. Lett.* **2008**, 10, 5075-5077.
- [45] E. Dimitrijević, M. S. Taylor, *Chem. Sci.* **2013**, 4, 3298-3303.
- [46] N. Shimada, Y. Nakamura, T. Ochiai, K. Makino, *Org. Lett.* **2019**, 21, 3789-3794.
- [47] S. Kusano, S. Miyamoto, A. Matsuoka, Y. Yamada, R. Ishikawa, O. Hayashida, *Eur. J. Org. Chem.* **2020**, 2020, 1598-1602.
- [48] E. Dimitrijević, M. S. Taylor, *ACS Catal.* **2013**, 3, 945-962.
- [49] a) K. Oshima, Y. Aoyama, *J. Am. Chem. Soc.* **1999**, 121, 2315-2316; b) K. Oshima, E.-i. Kitazono, Y. Aoyama, *Tetrahedron Lett.* **1997**, 38, 5001-5004.
- [50] T. Ogawa, M. Matsui, *Tetrahedron* **1981**, 37, 2363-2369.
- [51] R. M. Munavu, H. H. Szmant, *J. Org. Chem.* **1976**, 41, 1832-1836.
- [52] M. A. Nashed, L. Anderson, *Tetrahedron Lett.* **1976**, 17, 3503-3506.
- [53] G. Reginato, A. Ricci, S. Roelens, S. Scapecchi, *J. Org. Chem.* **1990**, 55, 5132-5139.
- [54] a) H. Dong, Z. Pei, S. Byström, O. Ramström, *J. Org. Chem.* **2007**, 72, 1499-1502; b) H. Dong, Y. Zhou, X. Pan, F. Cui, W. Liu, J. Liu, O. Ramström, *J. Org. Chem.* **2012**, 77, 1457-1467.
- [55] a) Y. Zhou, M. Rahm, B. Wu, X. Zhang, B. Ren, H. Dong, *J. Org. Chem.* **2013**, 78, 11618-11622; b) B. Ren, M. Rahm, X. Zhang, Y. Zhou, H. Dong, *J. Org. Chem.* **2014**, 79, 8134-8142.
- [56] X. Zhang, B. Ren, J. Ge, Z. Pei, H. Dong, *Tetrahedron* **2016**, 72, 1005-1010.
- [57] J. E. Taylor, J. M. J. Williams, S. D. Bull, *Tetrahedron Lett.* **2012**, 53, 4074-4076.
- [58] a) P. I. Dalko, L. Moisan, *Angew. Chem. Int. Ed.* **2004**, 43, 5138-5175; b) K. A. Ahrendt, C. J. Borths, D. W. C. MacMillan, *J. Am. Chem. Soc.* **2000**, 122, 4243-4244.
- [59] a) W. Linert, in *Facets of Coordination Chemistry*, pp. 81-110; b) W. B. Jensen, *Chem. Rev.* **1978**, 78, 1-22.
- [60] E. Vedejs, S. E. Denmark, *Lewis Base Catalysis in Organic Synthesis*, 1 ed., Wiley-VCH, Weinheim, **2016**.
- [61] G. Höfle, W. Steglich, *Synthesis* **1972**, 619-621.
- [62] L. M. Litvinenko, A. I. Kirichenko, *Dokl. Akad. Nauk. SSSR Ser. Khim.* **1967**, 176, 97-100.
- [63] A. Hassner, L. R. Krepski, V. Alexanian, *Tetrahedron* **1978**, 34, 2069-2076.
- [64] M. R. Heinrich, H. S. Klisa, H. Mayr, W. Steglich, H. Zipse, *Angew. Chem. Int. Ed.* **2003**, 42, 4826-4828.
- [65] H. Mayr, T. Bug, M. F. Gotta, N. Hering, B. Irrgang, B. Janker, B. Kempf, R. Loos, A. R. Ofial, G. Remennikov, H. Schimmel, *J. Am. Chem. Soc.* **2001**, 123, 9500-9512.
- [66] R. Tandon, T. A. Nigst, H. Zipse, *Eur. J. Org. Chem.* **2013**, 2013, 5423-5430.
- [67] S. Singh, G. Das, O. V. Singh, H. Han, *Org. Lett.* **2007**, 9, 401-404.
- [68] I. Held, S. Xu, H. Zipse, *Synthesis* **2007**, 2007, 1185-1196.
- [69] R. Tandon, T. Unzner, T. A. Nigst, N. De Rycke, P. Mayer, B. Wendt, O. R. P. David, H. Zipse, *Chem. Eur. J.* **2013**, 19, 6435-6442.
- [70] a) H. Mayr, B. Kempf, A. R. Ofial, *Acc. Chem. Res.* **2003**, 36, 66-77; b) S. Singh, G. Das, O. V. Singh, H. Han, *Tetrahedron Lett.* **2007**, 48, 1983-1986.

Introduction

- [71] T. Tsutsumi, A. Saitoh, T. Kasai, M. Chu, S. Karanjit, A. Nakayama, K. Namba, *Tetrahedron Lett.* **2020**, *61*, 152047.
- [72] J. Helberg, T. Ampßler, H. Zipse, *J. Org. Chem.* **2020**, *85*, 5390-5402.
- [73] a) F. A. Carey, R. J. Sundberg, *Advanced Organic Chemistry Part A: Structure and Mechanisms*, 5 ed., Springer Science+Business Media, New York, **2007**; b) O. Takahashi, Y. Kohno, M. Nishio, *Chem. Rev.* **2010**, *110*, 6049-6076.
- [74] a) E. V. Anslyn, D. A. Dougherty, *Modern Physical Organic Chemistry*, University Science Books, Sausalito, California, **2006**; b) B. Linder, *Elementary Physical Chemistry*, World Scientific Publishing Co. Pte. Ltd., 5 Toh Tuck Link, Singapore, **2011**; c) P. Hobza, *Non-covalent interactions : Theory and experiment* Royal Society of Chemistry, Cambridge, **2009**.
- [75] W. H. Keesom, *Proc. R. Acad. Sci.* **1915**, *18*, 636-646.
- [76] P. Debye, *Phys. Z.* **1920**, *21*, 178-187.
- [77] F. London, *Zeitschrift für Physik A Hadrons Nuclei* **1930**, *63*, 245-279.
- [78] a) F. L. Leite, C. C. Bueno, A. L. Da Róz, E. C. Ziemath, O. N. Oliveira, *Int. J. Mol. Sci.* **2012**, *13*, 12773-12856; b) P. Muller, *Pure Appl. Chem.* **1994**, *66*, 1077-1184.
- [79] C. A. Hunter, J. K. M. Sanders, *J. Am. Chem. Soc.* **1990**, *112*, 5525-5534.
- [80] J. Černý, P. Hobza, *Phys. Chem. Chem. Phys.* **2007**, *9*, 5291-5303.
- [81] E. Arunan, G. R. Desiraju, R. A. Klein, J. Sadlej, S. Scheiner, I. Alkorta, D. C. Clary, R. H. Crabtree, J. J. Dannenberg, P. Hobza, H. G. Kjaergaard, A. C. Legon, B. Mennucci, D. J. Nesbitt, *Pure Appl. Chem.* **2011**, *83*, 1619-1636.
- [82] L. Schaeffer, in *The Practice of Medicinal Chemistry (Fourth Edition)* (Eds.: C. G. Wermuth, D. Aldous, P. Raboisson, D. Rognan), Academic Press, San Diego, **2008**, pp. 359-378.
- [83] a) J. Ángyán, J. Dobson, G. Jansen, T. Gould, *London Dispersion Forces in Molecules, Solids and Nano-structures: An Introduction to Physical Models and Computational Methods*, Royal Society of Chemistry, Cambridge, **2020**; b) J. D. van der Waals, *Nobel Lectures, Physics 1901-1921*, Elsevier, Amsterdam, **1967**.
- [84] W. H. Keesom, *Leiden Comm. Suppl.* **1912**, *248*, 24-26.
- [85] M. A. Strauss, H. A. Wegner, *Eur. J. Org. Chem.* **2019**, *2019*, 295-302.
- [86] J. W. Gooch, *Encyclopedic Dictionary of Polymers*, Springer New York, New York, **2007**.
- [87] J. P. Wagner, P. R. Schreiner, *Angew. Chem. Int. Ed.* **2015**, *54*, 12274-12296.
- [88] M. M. Quesada Moreno, P. Pinacho, C. Pérez, M. Šekutor, P. R. Schreiner, M. Schnell, *Chem. Eur. J.* **2020**, *26*, 10817-10825.
- [89] S. Rösel, J. Becker, W. D. Allen, P. R. Schreiner, *J. Am. Chem. Soc.* **2018**, *140*, 14421-14432.
- [90] J. M. Schümann, J. P. Wagner, A. K. Eckhardt, H. Quanz, P. R. Schreiner, *J. Am. Chem. Soc.* **2021**, *143*, 41-45.
- [91] L. Yang, C. Adam, G. S. Nichol, S. L. Cockroft, *Nat. Chem.* **2013**, *5*, 1006-1010.
- [92] J. Hwang, B. E. Dial, P. Li, M. E. Kozik, M. D. Smith, K. D. Shimizu, *Chem. Sci.* **2015**, *6*, 4358-4364.
- [93] R. Pollice, M. Bot, I. J. Kobylanskii, I. Shenderovich, P. Chen, *J. Am. Chem. Soc.* **2017**, *139*, 13126-13140.
- [94] C. A. Hunter, *Angew. Chem. Int. Ed.* **2004**, *43*, 5310-5324.
- [95] a) M. L. Waters, *Curr Opin Chem Biol* **2002**, *6*, 736-741; b) J. w. Hwang, P. Li, K. D. Shimizu, *Org. Biomol. Chem.* **2017**, *15*, 1554-1564.
- [96] S. Tsuzuki, K. Honda, T. Uchamaru, M. Mikami, K. Tanabe, *J. Am. Chem. Soc.* **2002**, *124*, 104-112.
- [97] M. O. Sinnokrot, C. D. Sherrill, *J. Phys. Chem. A* **2006**, *110*, 10656-10668.
- [98] C. A. Hunter, K. R. Lawson, J. Perkins, C. J. Urch, *J. Chem. Soc., Perkin Trans. 2* **2001**, 651-669.
- [99] A. J. Neel, M. J. Hilton, M. S. Sigman, F. D. Toste, *Nature* **2017**, *543*, 637-646.
- [100] F. Cozzi, F. Ponzini, R. Annunziata, M. Cinquini, J. S. Siegel, *Angew. Chem. Int. Ed.* **1995**, *34*, 1019-1020.
- [101] S. Grimme, J. Antony, T. Schwabe, C. Mück-Lichtenfeld, *Org. Biomol. Chem.* **2007**, *5*, 741-758.
- [102] a) A. L. Ringer, M. O. Sinnokrot, R. P. Lively, C. D. Sherrill, *Chem. Eur. J.* **2006**, *12*, 3821-3828; b) M. O. Sinnokrot, C. D. Sherrill, *J. Am. Chem. Soc.* **2004**, *126*, 7690-7697.
- [103] S. E. Wheeler, K. N. Houk, *J. Am. Chem. Soc.* **2008**, *130*, 10854-10855.
- [104] R. M. Parrish, C. D. Sherrill, *J. Am. Chem. Soc.* **2014**, *136*, 17386-17389.
- [105] C. F. R. A. C. Lima, M. A. A. Rocha, L. R. Gomes, J. N. Low, A. M. S. Silva, L. M. N. B. F. Santos, *Chem. Eur. J.* **2012**, *18*, 8934-8943.
- [106] S. Grimme, *Angew. Chem. Int. Ed.* **2008**, *47*, 3430-3434.
- [107] a) K. D. Daze, F. Hof, *Acc. Chem. Res.* **2013**, *46*, 937-945; b) D. A. Dougherty, *Acc. Chem. Res.* **2013**, *46*, 885-893.
- [108] W. Zhong, J. P. Gallivan, Y. Zhang, L. Li, H. A. Lester, D. A. Dougherty, *Proceedings of the National Academy of Sciences USA* **1998**, *95*, 12088-12093.
- [109] a) C. R. Kennedy, S. Lin, E. N. Jacobsen, *Angew. Chem. Int. Ed.* **2016**, *55*, 12596-12624; b) S. Yamada, *Chem. Rev.* **2018**, *118*, 11353-11432.
- [110] J. Sunner, K. Nishizawa, P. Kebarle, *J. Phys. Chem.* **1981**, *85*, 1814-1820.
- [111] a) R. P. Wurz, *Chem. Rev.* **2007**, *107*, 5570-5595; b) C. E. Müller, P. R. Schreiner, *Angew. Chem. Int. Ed.* **2011**, *50*, 6012-6042.
- [112] a) J. C. Ruble, H. A. Latham, G. C. Fu, *J. Am. Chem. Soc.* **1997**, *119*, 1492-1493; b) J. C. Ruble, J. Tweddell, G. C. Fu, *J. Org. Chem.* **1998**, *63*, 2794-2795.

- [113] C. Roux, M. Candy, J.-M. Pons, O. Chuzel, C. Bressy, *Angew. Chem. Int. Ed.* **2014**, *53*, 766-770.
- [114] A. E. Díazlvarez, L. Mesas-Sánchez, P. Dinér, *Molecules* **2014**, *19*, 14273-14291.
- [115] L. Mesas-Sánchez, P. Dinér, *Chem. Eur. J.* **2015**, *21*, 5623-5631.
- [116] S. Yamada, T. Misono, Y. Iwai, *Tetrahedron Lett.* **2005**, *46*, 2239-2242.
- [117] S. Yamada, T. Misono, Y. Iwai, A. Masumizu, Y. Akiyama, *J. Org. Chem.* **2006**, *71*, 6872-6880.
- [118] T. Kawabata, M. Nagato, K. Takasu, K. Fuji, *J. Am. Chem. Soc.* **1997**, *119*, 3169-3170.
- [119] Y. Wei, I. Held, H. Zipse, *Org. Biomol. Chem.* **2006**, *4*, 4223-4230.
- [120] A. C. Spivey, T. Fekner, S. E. Spey, *J. Org. Chem.* **2000**, *65*, 3154-3159.
- [121] A. C. Spivey, F. Zhu, M. B. Mitchell, S. G. Davey, R. L. Jarvest, *J. Org. Chem.* **2003**, *68*, 7379-7385.
- [122] B. Pölloth, M. P. Sibi, H. Zipse, *Angew. Chem. Int. Ed.* **2021**, *60*, 774-778.
- [123] E. Procházková, A. Kolmer, J. Ilgen, M. Schwab, L. Kaltschnee, M. Fredersdorf, V. Schmidts, R. C. Wende, P. R. Schreiner, C. M. Thiele, *Angew. Chem. Int. Ed.* **2016**, *55*, 15754-15759.

Chapter 2. Acylation Reagents in Size-Dependent Esterification Reactions

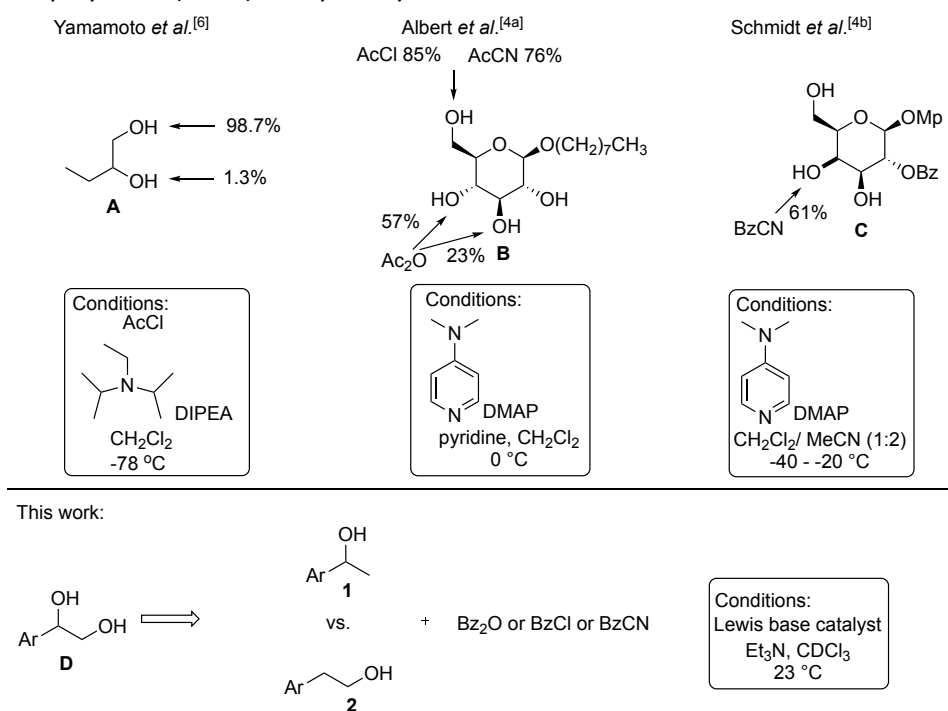
Stefanie Mayr and Hendrik Zipse*

Unpublished Results

Author contributions: S.M. and H.Z. conceived the study. The experimental study was performed by S.M.

2.1 Introduction

Since decades esterification strategies are a hot topic in organic chemistry.^[1] Well studied protocols for the formation of esters are acid-catalysed Fischer- esterification,^[2] use of the Steglich reagent DCC,^[2-3] or the Mitsunobu reaction.^[2-3] However, nowadays activated carboxylic acid derivatives like acid chlorides, acid anhydrides or acid cyanides are the most common choice to protect OH groups in polyol systems like mixed 1,*n*-diols or carbohydrates.^[1c, 2a, 4] Based on their counterions (CN⁻, Cl⁻ or OAc⁻) and the reaction conditions, the activated carboxylic acid derivatives are performing in different ways with respect to reaction rate and selectivity.^[4a, 5] Already in the 70s, Lewis base-catalysed acylation reactions demonstrate that acid anhydride and acid chloride are reacting in a different way.^[5b, 5c] Focusing on the selective reaction behaviour in diols, acetyl chloride (AcCl) is protecting the primary OH group of 1,2-diol **A** with 98% yield supported by sterically hindered aminobase diisopropylethylamin (DIPEA, Scheme 2.1).^[6] In 2004, Albert *et al.*^[4a] studied the reaction behaviour of different acylation reagents – acetyl chloride, acetic anhydride and acetyl cyanide – dependent on their counterion in the regioselective acylation of octyl β-D-glucopyranoside (**B**). They defined the so-called counterion effect, which is the possibility to form H-bonds between the OH-groups and the counterion like the acetate anion. Because of these H-bonds, **B** is acylated at the C-3 (57%) and C-4 (23%) position with acetic anhydride, however, the C-6 position is preferred by AcCl (85%) and AcCN (76%). In contrast to the prediction of Albert about acetic cyanides,^[4a] in 2016 Schmidt *et al.*^[4b] reported a cyanide effect, whereby the thermodynamically unfavourable C-4 position of galactopyranoside (**C**) is favoured. **C** is protected with benzoic cyanide at –40 °C with 61% yield. In the last two examples, the Lewis base dimethylaminopyridine (DMAP) was catalysing the protection of the polyols **B** and **C**. In the 1960s Steglich and Höfle,^[7] and at the same time Litvinenko and Kirichenko,^[8] were developing the donor substituted pyridine motif of DMAP, which leads to a strong acceleration of reaction rates and thus allows to protect the more sterically challenging tertiary and also secondary alcohols which is not possible with pyridine. Installing stronger electron donating groups as in 4-(pyrrolidinyl)pyridine (PPY)^[5b, 9] or conformational fixation of the 4-amino nitrogen as in 9-azajulodine (TCAP), increase the efficiency of the catalyst by a factor of 6 in comparison to DMAP.^[10] In this chapter, we are studying the counterion effect by analyzing the selectivity for the acylation of primary vs. secondary alcohols (**1** vs. **2**) with benzoyl chloride (BzCl), benzoic anhydride (Bz₂O) and benzoyl cyanide (BzCN) catalysed by a Lewis base.



Scheme 2.1. Selective acylation of 1,2-diols and carbohydrates.

Acylation Reagents for Size-Dependent Esterification Reaction

As alcohol instead of the 1,2-diol **D**, a 1:1 mixture of aromatic secondary **1** and primary ethanol **2** system with the same structure motif as **D** was chosen. Thus, attractive intramolecular H-bonding interactions changing the reactivity of the two OH groups are inhibited. The Zipse group^[11] demonstrated that the pyridinium motif of the TCAP (red) and the aromatic part of the alcohol system (green) could stabilize each other by attractive forces and accelerate the acylation of secondary alcohol **1** with acid chloride (Figure 2.1a). Based on the familiar transition state (TS) of DMAP-based esterification reactions with acetic anhydride,^[12] three TS are predicted for the TCAP-based acylation with different kinds of acylation reagents (Figure 2.1). We are assuming that the aromatic face of the alcohol is stacked on the pyridinium motif of the catalyst. Depending on the counterion (blue), the benzoate anion could bracket the TS (Figure 2.1b) whereby the chloride or cyanide anion is only interacting with the *ortho*-hydrogen of the catalyst. Based on these suggestions the acylation rates should be tuned differently depending on the counterion. To boost the difference in size effects, both the alcohols and the catalyst surface were varied in size.

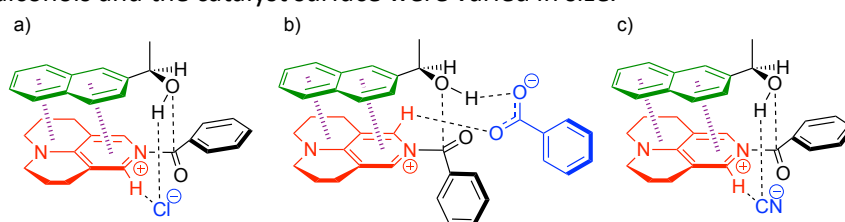
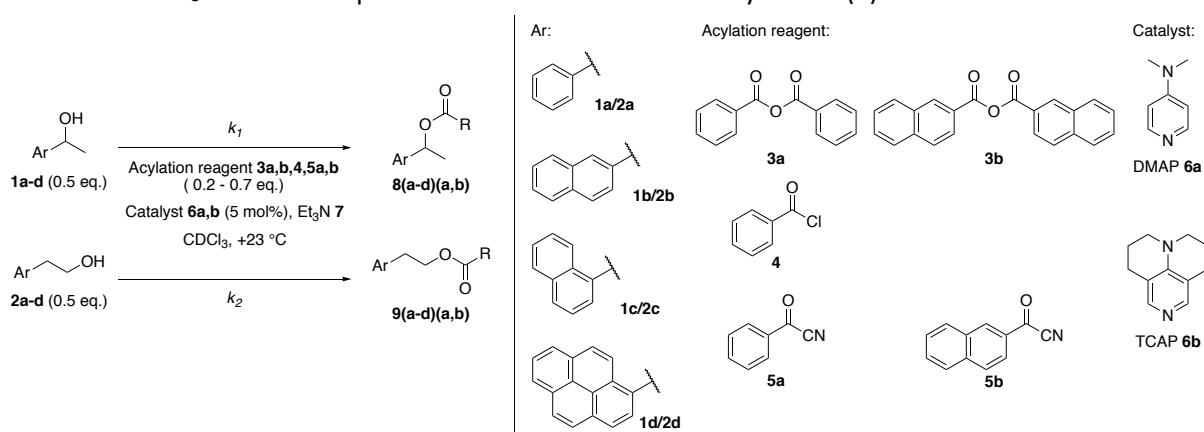


Figure 2.1. Proposed transition state structures for the acylation of 2-naphthalene-ethan-1-ol (**1b**, green) with a) benzoyl chloride (blue), b) benzoic anhydride (blue), and c) benzoyl cyanide (blue) catalysed by TCAP (red).

2.2 Results and Discussion

A simple reaction protocol was developed to explore the influence of common aryl acylation reagents like acid anhydride **3a,b**, acid chloride **4** or cyanide **5a,b** to their relative reactivity between secondary (**1a-d**) vs. primary (**2a-d**) alcohols as shown in Scheme 2.2. Thereby a 1:1 mixture of secondary and primary alcohols was acylated by a pre-defined amount of acylation reagent which was specified to achieved 20-70% conversion. As alcohol systems in this reaction model, aryl ethanols varying in size and surface, beginning from the small phenyl (**a**) via 2-naphthyl (**b**) or 1-naphthyl (**c**) to the big 1-pyrene (**d**) aryl system were used. The aromatic surface of the acylation reagents **3-5** was varied as well between Ph (**a**) and 2-Np (**b**). The benefit of a Lewis base catalyst was studied by adding 5 mol% of DMAP (**6a**) or TCAP (**6b**). The reaction was carried out in CDCl₃ at room temperature with an excess of triethylamine (**7**).



Scheme 2.2. Model turnover-limited competition reaction for the acylation of primary (**1a-d**) vs. secondary alcohol (**2a-d**) with acid anhydride **3a,b**, acid chloride **4** or cyanide **5a,b** catalysed by Lewis base catalysts DMAP (**6a**) or TCAP (**6b**).

The reactivity between secondary (**1a-d**) vs. primary (**2a-d**) alcohols is quantified by the relative rate constant k_{rel} defined as the ratio between the acylation of **1a-d** over **2a-d** (Eq. 2.1, Figure 2.2). Defined by the Kagan equation^[13] (Eq. 2.2, Figure 2.2) the relative rate can easily be detected by the defined combination of chemoselectivity (Eq. 2.3) and conversion values (Eq. 2.5, Figure 2.2). Eq. 2.3 implied the correction factor f (Eq. 2.4). f is defined as the exact ratio of both reactants presented in the reaction medium and should be

closed to 1:1 in the ideal case. This factor was included to avoid human error during the preparation of the 1:1 alcohol stock solution (for more details see Chapter 2.4.2.1). Because the analysis was performed via ^1H NMR spectroscopy, the integrals of the particular reagents correspond to the relative concentrations.

$$k_{\text{rel}} = \frac{k_2}{k_1} = \frac{k(2a-d)}{k(1a-d)} \quad \text{Eq. 2.1}$$

$$k_{\text{rel}} = \frac{\ln[1-\text{conv}(1+C)]}{\ln[1-\text{conv}(1-C)]} \quad \text{Eq. 2.2}$$

$$\text{Chem.}_{(C)} = \frac{[9(a-d)(a,b)] \cdot f - [8(a-d)(a,b)]}{[9(a-d)(a,b)] \cdot f + [8(a-d)(a,b)]} \quad \text{mit} \quad f = \frac{[1a-d] + [8(a-d)(a,b)]}{[2a-d] + [9(a-d)(a,b)]} \quad \text{Eq. 2.3 und 2.4}$$

$$\text{Conv.}_{(\%)} = \frac{[8(a-d)(a,b)] + [9(a-d)(a,b)]}{[1a-d] + [2a-d] + [9(a-d)(a,b)] + [8(a-d)(a,b)]} \quad \text{Eq. 2.5}$$

Figure 2.2. Relative rates (Eq. 2.1 and 2.2), chemoselectivity (Eq. 2.3) and conversion (Eq. 2.5) for the turnover-limited competition reaction of the acylation of primary (**1a-d**) vs. secondary alcohol (**2a-d**).

First of all, the influence of the Lewis base catalyst in the acylation of primary and secondary alcohol was explored by performing turnover-limited competition experiments between phenyl alcohols **1a** vs. **2a** uncatalysed as well as catalysed by DMAP (**6a**) and TCAP (**6b**) (Figure 2.3). As acylation reagents, benzoic anhydride (**3a**), benzoyl chloride (**4**) and cyanide (**5a**) were selected. In the background reactions, the benzylation of the primary alcohol **1a** is 26 times as fast as the secondary alcohol **2a** with **3a** and 45 times as fast as with **4** (green bar, Figure 2.3). With **5a** the uncatalysed acylation reaction was not explored. These findings suggest that the acylation of secondary alcohol **1** is affected by addition of the catalyst. Likewise, the role of acylation reagent and hence the counterion is noted, because a difference in selectivity of around $\Delta k_{\text{rel}} \approx 10$ between the different reagents **3a** and **4** were detected. Focusing on the acylation reaction catalysed by DMAP (**6a**) (blue bars, Figure 2.3), **4** shows with $k_{\text{rel}} = 17.8$ the higher preference for the acylation of primary alcohol **2a**. This preference is already reduced in the acylation with **5a** with a selectivity of $k_{\text{rel}} = 13.5$. In contrast, benzoic anhydride (**3a**) is acylating **2a** only 8 times as fast as **1a**. The size and Lewis basicity of the catalysts did not affect the selective acylation of Ph substituted alcohols, because only small differences in selectivity were determined by catalysing the acylation with TCAP (**6b**, red bars).

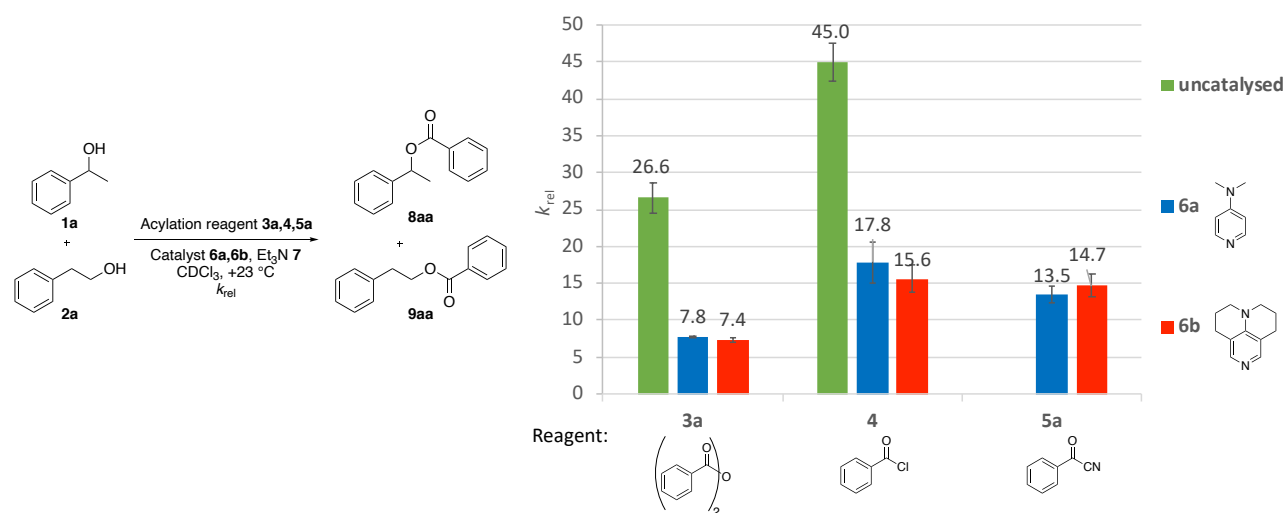


Figure 2.3. Relative rate constants k_{rel} for the acylation reaction of **1a** vs. **2a** under uncatalysed and catalysed condition with different acylation reagents.

Now the size effects between alcohol and acylation reagents (Ph vs. 2-Np) catalysed by TCAP were explored. The acylation of primary alcohols **2a,b** is in all cases favored, but differences in selectivities between acid anhydrides and acid chlorides/cyanides are clearly visible. Selectivity values between primary vs. secondary alcohols are similar for the cyanides **5a,b** irrespective of the size of the alcohols and are in a range of $k_{\text{rel}} = 12.3 - 14.5$. In contrast to this, for the acylation with **3a,b** or **4** a dependency on the size of the alcohols was determined. It can be generally identified with acylation reagent **3** and **4** that by increasing the size of the alcohols from Ph to Np, the selectivities decrease around $\Delta k_{\text{rel}} \approx 4-5$. The less preference for acylation primary

Acylation Reagents for Size-Dependent Esterification Reaction

alcohol with a selectivity of $k_{rel} = 3.7$ was achieved during the acylation of **1b** vs. **2b** with **3a**, whereby the highest preference for acylating the primary alcohol $k_{rel} = 15.6$ was obtained during the acylation of **1a** vs. **2a** with **4**. By increasing the size of anhydride from benzoic- to 2-naphthoic anhydride, the selectivities are increasing. Both **1a** vs. **2a** [$k_{rel} = 7.4$ (**3a**) to $k_{rel} = 9.1$ (**3b**)] and **1b** vs. **2b** [$k_{rel} = 3.7$ (**3a**) and $k_{rel} = 4.3$ (**3b**)] the acylation of primary alcohol is preferred. We may thus conclude at this point that the different counterions - benzoate, chloride or cyanide - could have a large impact on the selectivity in separated primary/secondary ethanol systems, too. Based on the studies of Albert *et al.*,^[4a] we are assuming that the benzoate anion is forming a H-bonded cage between hydroxyl groups of the alcohol and *ortho*-hydrogen of the catalysts, in contrast to chloride and cyanide.

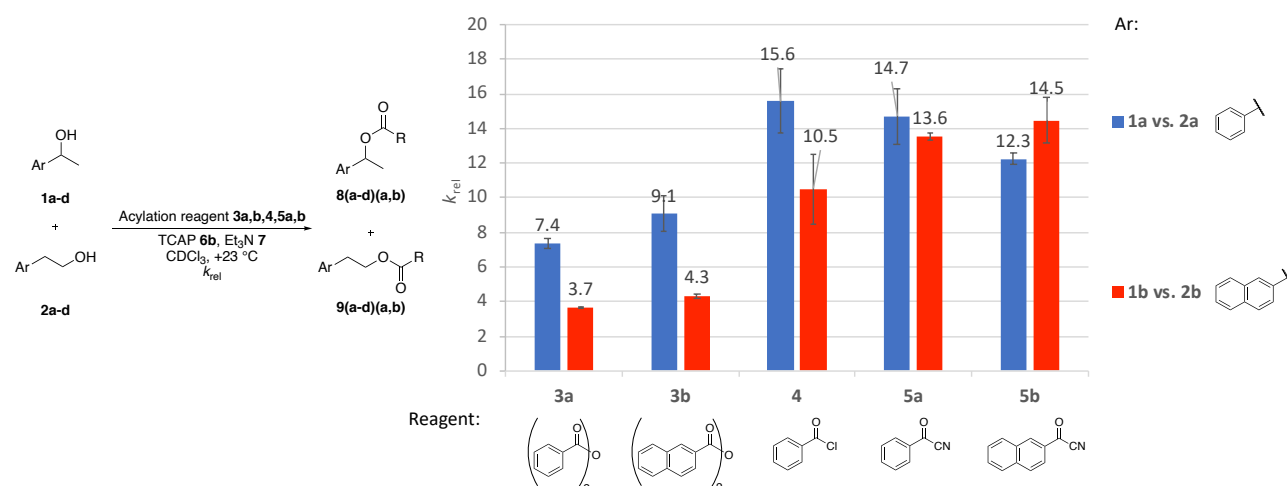


Figure 2.4. Relative rate constants k_{rel} for the acylation reaction of **1a,b** vs. **2a,b** with different acylation reagents **3-5** catalysed by TCAP.

Because the final aim of this thesis is to regioselectively acylate a secondary hydroxyl group in the presence of a primary hydroxyl group by size effects, the acylation with **3a** was now investigated further. One aspect is still a possible impact of the size and the Lewis basicity of the used catalysts **6a,b**. In addition, the aromatic size of the alcohols can still be increased by exploring 1-pyrenyl alcohols (**1d/2d**). Because there could be some repulsive 1,5-interactions between the hydrogen and oxygen atoms of **1d** in contrast to **1b** (marked in green, Figure 2.5), which could have as well some influence on the selectivity like detected in silylation reactions,^[14] 1-naphthyl alcohol system (**1c** vs. **2c**) was also studied. Comparing catalyst **6a** (blue bars, Figure 2.5) vs. **6b** (red bars) it can be established that only with the smallest alcohol system **1a/2a** the selectivities are similar [$k_{rel} = 7.8$ (**6a**), 7.4 (**6b**)]. For the further alcohol systems **1b/2b**, **1c/2c** or **1d/2d**, the selective acylation of primary alcohol catalysed with TCAP (**6b**) is around $\Delta k_{rel} \approx 2-3$ less preferred than with DMAP

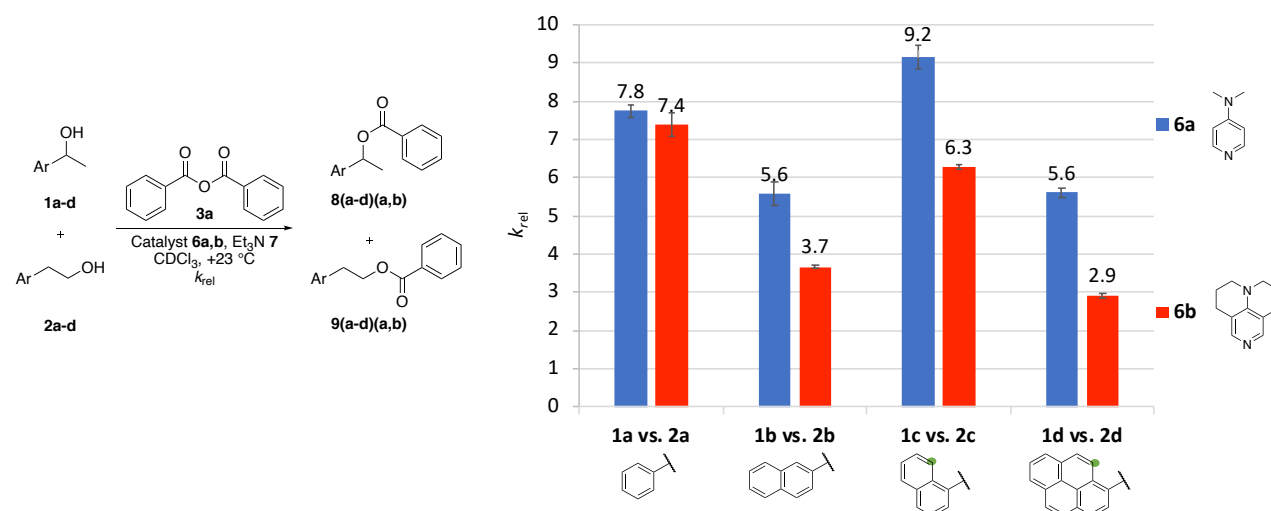


Figure 2.5. Relative rate constants k_{rel} for the acylation reaction of **1a-d** vs. **2a-d** with **3a** catalysed by Lewis base catalyst.

(6a). Comparing the acylation catalysed by TCAP, increasing the size of the alcohols indicates a decrease in selectivity [$k_{\text{rel}} = 7.4$ (Ph), 3.7 (2-Np) and 2.9 (1-Py)], except for the 1-Np side chain **1c/2c** ($k_{\text{rel}} = 6.3$). These last results imply that the acylation of secondary alcohol is accelerated due to a change in selectivities of around $\Delta k_{\text{rel}} = 4.5$ only by size effects. Referring to the proposed transition state structure (Figure 2.1), we suggested that the aromatic motif of the secondary alcohol is overlapping better with the catalyst surface than the primary alcohol. However, these size effects are only becoming significant with a specified aromatic size (**1b-d/2b-d**) and are without impact for **1a/2a**.

2.3 Conclusion

We are demonstrating here that attractive size effects between the different components (alcohol, catalysts, acylation reagent) could have an impact on the selective acylation of secondary and primary alcohol, by performing turnover-limited competition experiments. Thereby background reactions and catalysed reactions by DMAP or TCAP were explored. While in the uncatalysed esterification, the primary alcohol is favoured for both benzoyl chloride and benzoic anhydride, the acylation of secondary alcohol is more affected in a catalysed reaction, visible in the reduced selectivity. The counterion of the reagent is influencing the selectivity between secondary and primary alcohol, too. Bridging the rate determining transition state by an acetate anion, a decrease in selectivity of around a factor of 8 in comparison to chloride or a factor of 10 in comparison to cyanide was obtained. Further investigation of size effects of the alcohols (Ph, Np, Py) or the catalyst (DMAP, PPY) demonstrate that size effects and π - π stacking interactions are the main forces to accelerate the secondary alcohol more than the primary alcohol. The strongest preference for acylation of the secondary alcohol was obtained with a selectivity of $k_{\text{rel}} = 2.9$ for the alcohol-catalyst combination with the biggest size, TCAP and 1-pyrene ethanol. Further studies to optimize the acid anhydride structure or to increase the size of the catalyst system in order to raise the attractive stacking interactions and finally to invert the selectivity to the less reactive secondary alcohol are described in the following chapters.

2.4 Experimental Part

General Information

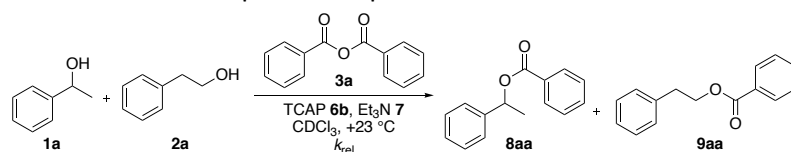
All reactions sensitive to air and moisture were performed under a nitrogen atmosphere and the glassware as well as magnetic stir bars were dried overnight in a dry oven at 110 °C. As heat source for temperature depending reactions an oil bath was used. CDCl_3 and Et_3N were freshly distilled over calcium hydride (CaH_2) under a nitrogen atmosphere. The aryl alcohols **1a-c**, **2a-c**, the reagents **3a**, **4**, **5a** and the catalysts **6a,b** have been obtained from commercial sources. All air- or water-sensitive reagents were stored under nitrogen. If not further specified, solvents were obtained from the companies Acros Organics, Sigma Aldrich or Merck and purified by distillation in a rotary evaporator. Silica gel for column chromatography was purchased from Acros Organics (mesh 35-70). Thin-layer chromatography was performed by using TLC plates purchased from Merck (silica gel 60 F254, thickness 0.2 mm). All ^1H NMR spectra were recorded by Varian INOVA 400, 600 and Bruker 400 machines in CDCl_3 at 400 MHz or 600 MHz at 23 °C. All ^{13}C NMR spectra were recorded respectively at 101 MHz. The chemical shifts are reported in ppm (δ), relative to the resonance of CDCl_3 at $\delta = 7.26$ ppm for ^1H and for ^{13}C relative to the resonance of CDCl_3 $\delta = 77.16$ ppm. Spectra were imported and processed in the MestreNova 10.0.2 program. HRMS spectra were obtained by using a Thermo Finnigan LTQ FT machine of the MAT 95 type with a direct exposure probe (DEP) and electron impact ionization (EI, 70 eV). The analytic data of aryl alcohols **1d**, **2d**, the reagent **3b** and corresponding esters **8(a-d)(a,b)** and **9(a-d)(a,b)** are reported by Zipse *et al.*^[15] and in chapter 3 of this work.

2.4.1 Turnover-limited Competition Experiments

The used techniques and instructions for determination the relative rate constants in turnover-limited competition experiments are the same as in the reported work of Zipse *et al.*^[15] and in chapter 3 of this work. Technical details: NMR tubes were dried in the oven for at least 12 h. CDCl_3 and Et_3N were freshly distilled under N_2 over CaH_2 before use. Hamilton syringes were cleaned with acetone, dried under vacuum, and flushed with nitrogen prior to use. A GC vial holder (Shimadzu 221-44998-91) was connected to the coolant circuit of a cryostat maintaining +23 °C constantly and placed on a magnetic stirrer. The speed of stirring was fixed at 750 rpm for all the experiments described here.

2.4.1.1 Experimental Design

Preparation of stock solutions for the catalysed reactions (Method A): A guideline for the preparation of stock solutions for turnover-limited competition experiments is described in the following:



Temperature control: +23 °C

Three CDCl_3 stock solutions are prepared under nitrogen (Table 2.1). Stock solution A contains the secondary alcohol **1a** and the primary alcohol **2a**, each at a concentration of 0.2 M. Stock solution B contains benzoic anhydride **3a** (0.4 M), while stock solution C consists of a 0.4 M Et_3N and catalyst TCAP at a concentration of 0.02 M.

Table 2.1. Preparation of initial CDCl_3 stock solutions for catalysed acylation (Method A).

Stock solution	Compound	Concentration (mol L ⁻¹)	Volume (mL)	n (mol)	M.W. (g mol ⁻¹)	Mass (mg)
Stock A	1a	0.2	2	4.00·10 ⁻⁴	122.16	48.9
	2a	0.2	2	4.00·10 ⁻⁴	122.16	48.9
Stock B	3a	0.4	2	8.00·10 ⁻⁴	226.23	181
Stock C	TCAP	0.02	2	4.00·10 ⁻⁵	174.24	7.00
	Et_3N	0.5	2	1.00·10 ⁻³	101.19	101

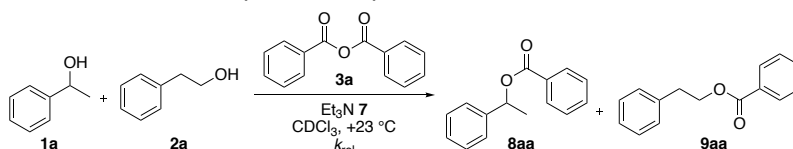
Following these initial preparations, stock solution B was diluted in four discrete steps as shown in Table 2.3. The concentrations of the new solutions have been fixed at 20, 35, 50, and 70% of the initial stock solution B.

Table 2.2. Dilution of stock solution B.

Stock solution	Concentration (mol L ⁻¹)	Vol. B ^b (mL)	Volume (mL)
Stock B1 (20%)^a	0.08	0.20	1
Stock B2 (35%)^a	0.14	0.35	1
Stock B3 (50%)^a	0.20	0.50	1
Stock B4 (70%)^a	0.28	0.70	1

^aConcentration relative to stock solution B; ^bInitial volume of stock solution B.

Preparation of stock solutions for the background reaction (Method B): A guideline for the preparation of stock solutions for turnover-limited competition experiments is described in the following:



Temperature control: +23 °C

For the turnover-limited competition experiments without catalysts three stock solutions are prepared under nitrogen (Table 2.2). Stock solution A contains the secondary alcohol **1a** and the primary alcohol **2a**, each at a concentration of 0.1 M. Stock solution B contains benzoic anhydride **3a** (0.2 M), while stock solution C consists only of 0.3 M Et₃N.

Table 2.3. Preparation of initial CDCl₃ stock solutions for background reaction (Method B).

Stock solution	Compound	Concentration (mol L ⁻¹)	Volume (mL)	n (mol)	M.W. (g mol ⁻¹)	Mass (mg)
Stock A	1a	0.1	5	5.00·10 ⁻⁴	122.16	61.1
	2a	0.1	5	5.00·10 ⁻⁴	122.16	61.1
Stock B	3a	0.2	5	1.00·10 ⁻³	226.23	226
Stock C	Et₃N	0.3	5	1.50·10 ⁻³	101.19	152

The further procedure is similar to Method A.

Methodology: Under nitrogen 0.4 mL of stock solution A, 0.4 mL of stock solution C, and 0.4 mL of stock solution B1 are transferred to a GC vial by use of a Hamilton syringe. The GC vial is then capped under nitrogen and placed in the GC vial holder with stirring.

Composition of each prepared GC vial for one turnover-limited competition experiment:

GC vial 1: 0.4 mL Stock A; 0.4 mL Stock C; 0.4 mL Stock B1

GC vial 2: 0.4 mL Stock A; 0.4 mL Stock C; 0.4 mL Stock B2

GC vial 3: 0.4 mL Stock A; 0.4 mL Stock C; 0.4 mL Stock B3

GC vial 4: 0.4 mL Stock A; 0.4 mL Stock C; 0.4 mL Stock B4

In terms of the actual starting concentrations (mol/L) for all components in the catalysed reaction:

GC vial 1: **1a** and **2a:** 0.0667, **3a:** 0.0267, **Et₃N:** 0.1667, **TCAP:** 0.0067

GC vial 2: **1a** and **2a:** 0.0667, **3a:** 0.0467, **Et₃N:** 0.1667, **TCAP:** 0.0067

GC vial 3: **1a** and **2a:** 0.0667, **3a:** 0.0667, **Et₃N:** 0.1667, **TCAP:** 0.0067

GC vial 4: **1a** and **2a:** 0.0667, **3a:** 0.0933, **Et₃N:** 0.1667, **TCAP:** 0.0067

In terms of the actual starting concentrations (mol/L) for all components in the background reaction:

GC vial 1: **1a** and **2a:** 0.0333, **3a:** 0.0133, **Et₃N:** 0.1000

GC vial 2: **1a** and **2a:** 0.0333, **3a:** 0.0233, **Et₃N:** 0.1000

GC vial 3: **1a** and **2a:** 0.0333, **3a:** 0.0333, **Et₃N:** 0.1000

GC vial 4: **1a** and **2a**: 0.0333, **3a**: 0.0467, **Et₃N**: 0.1000

Preparation of NMR samples: The turnover-limited competition experiment is considered finished when the reaction with the highest anhydride concentration (GC vial 4) is completed. The reaction is monitored by ¹H NMR. NMR tubes are dried under vacuum using a Schlenk-based glassware and flushed with nitrogen three times to eliminate moisture. The GC vials are placed in a Schlenk flask and flushed with nitrogen three times as well. Then, 0.6 mL of the solution contained in the GC vial is transferred to the NMR tube under nitrogen. The NMR tube is then capped and the relative concentrations of all reactants/products determined by ¹H NMR spectroscopy.

2.4.1.2 ¹H NMR Analysis

The ¹H NMR spectra of the turnover-limited competition experiments were edited by *MestReNova* 10.0. The spectra were corrected by using automatic phase correction and Bernstein polynomial fit with polynomial order 3 and referenced by the solvent signal of CDCl₃ ($\delta = 7.26$ ppm). For the secondary alcohol **1** and ester **8** the hydrogen signal of the methyl group was integrated as a measure of the evolution of the reaction. If there was an overlap with other signals, the corresponding CH signal was used instead. For the primary alcohol **2** and ester **9** the hydrogen signal of one of the two CH₂ groups was integrated as a measure of turnover.

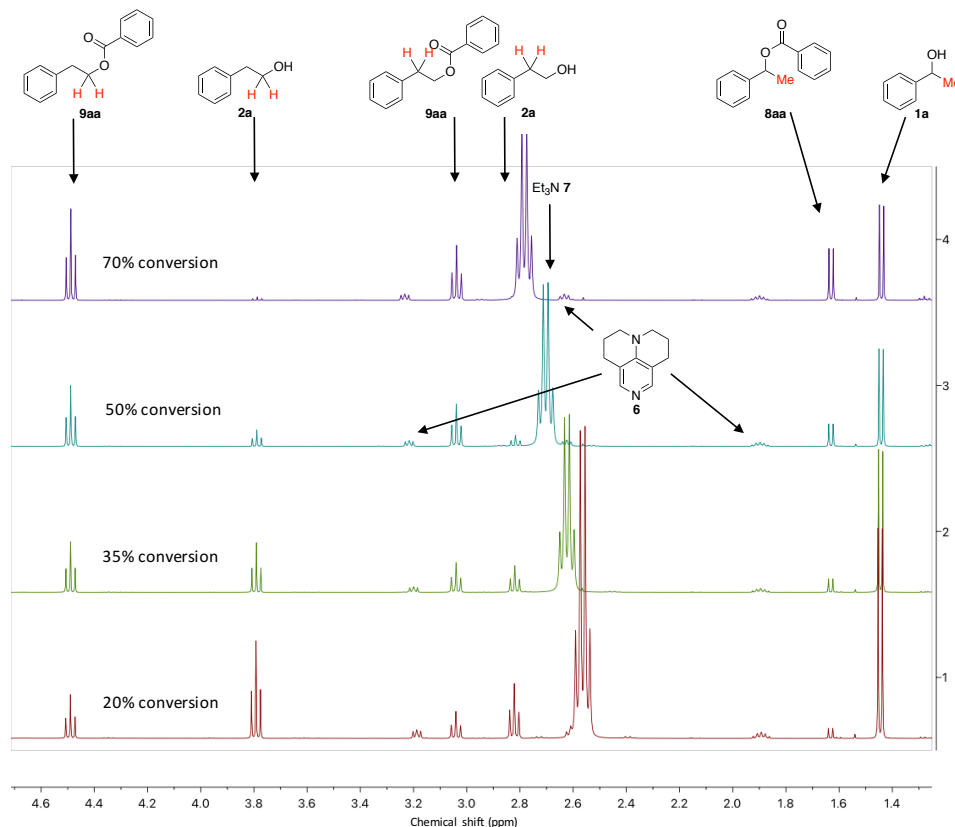
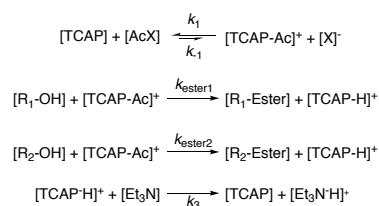


Figure 2.6. Example of ¹H NMR spectra for the turnover-limited competition experiments for **1a** vs. **2a** with **3a**.

2.4.1.3 Simulation of Turnover-Limited Competition Experiments

With the help of the CoPaSi^[16] and Pro Fit7 programs the k_{rel} values for the turnover-limited competition experiments have been simulated. Scheme 2.3 shows the reactions used in Copasi, in which the k values have been modified in order to achieve the k_{rel} values. The values k_1 , k_{-1} and k_3 have been used as constants: $k_1 = 1 \text{ l}\cdot\text{mol}^{-1}\cdot\text{s}^{-1}$; $k_{-1} = 100 \text{ l}\cdot\text{mol}^{-1}\cdot\text{s}^{-1}$; $k_3 = 0.1 \text{ l}\cdot\text{mol}^{-1}\cdot\text{s}^{-1}$, while k_{ester1} and k_{ester2} have been allowed to vary.



Scheme 2.3. The model reaction used in CoPaSi for the simulation of the rate constants.

The rate constants of the different turnover-limited competition experiments were simulated by CoPaSi by using the starting concentrations of the experiments. The simulated concentrations over the time were used to calculate the conversion by Eq. 2.5 and chemoselectivity by Eq. 2.3. In figures 2.9 to 2.15 conversion was plotted over the chemoselectivity to be able to validate the experimental and numerical simulated relative rate constants.

2.4.1.4 Results of Turnover-Limited Competition Experiments

Table 2.4. Integral limits (ppm), and relative and absolute integral values turnover-limited competition experiments of alcohol **1** vs. **2** using acylation reagents **3**, **4**, **5**. Conversion, corrected chemoselectivity, relative rate and natural logarithm of relative rate with standard derivations calculated from corresponding ¹H NMR measurements of the turnover-limited competition experiments.

Background reaction for 1a vs. 2a										
Reagent	Conv		integral limits (ppm)		integral	absolute	Conv.	Chem.	k_{rel}	$\ln k_{rel}$
3a	20%	1a	1.39	1.45	1.00	158348.88	9.78	0.92	25.79	3.25
		2a	3.73	3.83	0.53	84422.28				
		8aa	1.59	1.62	0.01	1292.96				
		9aa	4.43	4.50	0.12	19726.19				
	35%	1a	1.39	1.45	1.00	135009.22	18.35	0.92	30.12	3.41
		2a	3.73	3.82	0.43	57667.62				
		8aa	1.58	1.62	0.01	1982.36				
		9aa	4.42	4.50	0.24	31875.87				
	50%	1a	1.38	1.45	1.00	136224.18	27.56	0.90	25.59	3.24
		2a	3.74	3.82	0.31	42186.42				
		8aa	1.58	1.62	0.03	4064.25				
		9aa	4.39	4.50	0.35	47883.43				
70%	1a	1.38	1.46	1.00	125879.70	38.10	0.87	24.99	3.22	
	2a	3.73	3.82	0.19	23442.36					
	8aa	1.58	1.63	0.05	6561.33			Mean k_{rel}	Mean $\ln k_{rel}$	
	9aa	4.41	4.49	0.49	61714.37			26.62 ± 2.04	3.28 ± 0.07	
4	20%	1a	1.42	1.49	1.00	106940.99	15.92	1.00	/	/
		2a	3.77	3.84	0.43	45867.25				
		8aa								
		9aa	4.47	4.51	0.21	22187.51				
	35%	1a	1.41	1.48	1.00	106588.77	32.70	0.94	47.56	3.86
		2a	3.77	3.84	0.24	25144.23				
		8aa	1.60	1.67	0.02	2305.50				
		9aa	4.44	4.54	0.42	45197.87				
	50%	1a	1.42	1.48	1.00	105291.36	45.35	0.90	42.41	3.75
		2a	3.75	3.85	0.09	9155.92				
		8aa	1.61	1.66	0.05	5089.22				
		9aa	4.45	4.52	0.59	62461.66				
70%	1a	1.43	1.48	1.00	82876.94	63.84	0.55	14.04	2.64	
	2a									
	8aa	1.60	1.67	0.40	33552.49			Mean k_{rel}^a	Mean $\ln k_{rel}^a$	
	9aa	4.45	4.54	0.91	75163.98			44.99 ± 2.57	3.80 ± 0.06	
1a vs. 2a catalysed by TCAP (6b)										
Reagent	Conv		integral limits (ppm)		integral	absolute	Conv.	Chem.	k_{rel}	$\ln k_{rel}$
3a	20%	1a	3.76	3.82	1.00	73180.18	18.80	0.74	7.88	2.06
		2a	1.42	1.47	2.17	158753.89				
		8aa	4.46	4.52	0.49	35952.43				
		9aa	1.62	1.65	0.11	8242.69				
	35%	1a	3.76	3.82	1.00	33087.98	30.78	0.69	7.39	2.00
		2a	1.42	1.47	2.95	97652.12				
		8aa	4.46	4.52	1.11	36771.00				
		9aa	1.61	1.66	0.31	10342.68				

Acylation Reagents for Size-Dependent Esterification Reaction

	50%	1a	3.76	3.83	1.00	13514.12	49.79	0.60	7.18	1.97
		2a	1.41	1.47	6.26	84552.47				
		8aa	4.45	4.53	4.08	55148.32				
		9aa	1.61	1.65	1.57	21208.82				
	70%	1a	3.76	3.82	0.03	1857.27	67.42	0.43	7.11	1.96
		2a	1.42	1.47	1.00	65566.60				
		8aa	4.46	4.52	1.02	67088.56			<i>Mean k_{rel}</i>	<i>Mean ln k_{rel}</i>
		9aa	1.61	1.65	0.62	40818.83			7.39 ± 0.30	2.00 ± 0.01
3b	20%	2a	3.76	3.83	1.00	83172.16	18.24	0.77	9.15	2.21
		1a	1.42	1.47	2.15	178823.71				
		9ab	4.52	4.59	0.48	39924.06				
		8ab	1.66	1.71	0.09	7824.08				
	35%	2a	3.76	3.83	1.00	37681.03	35.77	0.70	8.22	2.11
		1a	1.42	1.47	3.51	132382.53				
		9ab	4.52	4.59	1.58	59417.12				
		8ab	1.66	1.71	0.43	16090.96				
	50%	2a	3.76	3.83	1.00	12870.24	48.02	0.64	8.20	2.10
		1a	1.42	1.47	6.24	80271.37				
		9ab	4.52	4.58	3.89	50050.14				
		8ab	1.66	1.70	1.31	16906.37				
	70%	2a					70.14	0.42	10.71	2.37
		1a	1.42	1.46	1.00	58510.61				
		9ab	4.52	4.58	1.11	64742.91			<i>Mean k_{rel}</i>	<i>Mean ln k_{rel}</i>
		8ab	1.66	1.70	0.69	40349.64			9.07 ± 1.02	2.20 ± 0.11
4	20%	2a	3.77	3.83	0.97	48869.74	16.00	0.83	12.35	2.51
		1a	1.43	1.47	2.09	105282.75				
		9aa	4.46	4.52	0.41	20651.93				
		8aa	1.62	1.65	0.06	3038.15				
	35%	2a	3.77	3.83	1.00	28642.09	32.17	0.84	16.71	2.82
		1a	1.43	1.47	3.62	103765.27				
		9aa	4.47	4.52	1.49	42540.58				
		8aa	1.62	1.65	0.20	5772.23				
	50%	2a	3.78	3.83	1.00	12354.45	46.06	0.79	16.60	2.81
		1a	1.43	1.48	8.10	100067.02				
		9aa	4.45	4.54	4.87	60131.81				
		8aa	1.62	1.65	0.90	11087.86				
	70%	2a					63.94	0.56	16.64	2.81
		1a	1.43	1.48	1.00	78892.81				
		9aa	4.45	4.53	0.92	72399.88			<i>Mean k_{rel}</i>	<i>Mean ln k_{rel}</i>
		8aa	1.62	1.65	0.40	31265.98			15.57 ± 1.86	2.74 ± 0.13
5a	20%	2a	3.82	3.90	0.92	78822.67	17.86	0.87	16.69	2.81
		1a	1.49	1.54	2.15	184685.35				
		9aa	4.52	4.58	0.48	40810.90				
		8aa	1.67	1.71	0.05	4649.52				
	35%	2a	3.83	3.89	0.98	49200.83	32.12	0.83	15.70	2.75
		1a	1.48	1.53	3.67	183782.01				
		9aa	4.52	4.58	1.48	73970.65				
		8aa	1.68	1.71	0.22	10914.44				
	50%	2a	3.82	3.90	1.30	24475.25	45.68	0.75	13.57	2.61
		1a	1.49	1.54	8.50	160494.82				
		9aa	4.52	4.58	5.14	97088.81				
		8aa	1.68	1.72	1.07	20220.80				
	70%	2a					69.50	0.44	12.78	2.55
		1a	1.48	1.54	1.00	108935.72				
		9aa	4.52	4.58	1.09	118561.47			<i>Mean k_{rel}</i>	<i>Mean ln k_{rel}</i>
		8aa	1.67	1.72	0.65	70330.89			14.69 ± 1.57	2.68 ± 0.11

5b	20%	2a	3.79	3.85	1.00	6752.05	19.72	0.83	12.74	2.54
		1a	1.45	1.49	2.34	15808.00				
		9ab	4.54	4.61	0.57	3866.28				
		8ab	1.68	1.72	0.08	570.39				
	35%	2a	3.78	3.85	1.01	3655.37	34.23	0.78	11.92	2.48
		1a	1.45	1.48	3.54	12756.37				
		9ab	4.54	4.61	1.56	5634.37				
		8ab	1.68	1.72	0.29	1040.44				
	50%	2a	2.82	2.88	1.00	2356.63	45.86	0.73	12.07	2.49
		1a	1.45	1.49	6.38	15040.44				
		9ab	4.54	4.61	3.86	9087.01				
		8ab	1.68	1.73	0.89	2104.24				
	70%	2a					66.02	0.52	/	/
		1a	1.45	1.49	1.00	9593.01				
		9ab	4.55	4.61	0.98	9422.40			<i>Mean k_{rel}</i>	<i>Mean ln k_{rel}</i>
		8ab	1.68	1.73	0.47	4506.84			12.25 ± 0.35	2.50 ± 0.03
1b vs. 2b catalysed by TCAP (6b)										
Reagent	Conv		integral limits (ppm)		integral	absolute	Conv.	Chem.	k_{rel}	ln k_{rel}
3a	20%	1b	3.82	3.88	0.52	71373.77	19.24	0.53	3.72	1.31
		2b	1.48	1.52	1.00	138189.24				
		8ba	4.54	4.60	0.22	29864.59				
		9ba	1.69	1.73	0.10	13625.29				
	35%	1b	3.82	3.88	0.39	48237.88	34.27	0.49	3.66	1.30
		2b	1.48	1.52	1.00	122625.93				
		8ba	4.54	4.60	0.41	50202.31				
		9ba	1.69	1.73	0.21	26336.08				
	50%	1b	3.82	3.88	0.28	31032.07	48.22	0.43	3.64	1.29
		2b	1.48	1.52	1.00	109698.27				
		8ba	4.54	4.60	0.63	69212.08				
		9ba	1.69	1.73	0.38	41658.85				
	65%	1b	3.82	3.88	0.17	15446.50	62.15	0.36	3.62	1.29
		2b	1.48	1.52	1.00	89339.01				
		8ba	4.54	4.60	0.93	83388.82			<i>Mean k_{rel}</i>	<i>Mean ln k_{rel}</i>
		9ba	1.69	1.73	0.67	59666.94			3.66 ± 0.04	1.30 ± 0.01
3b	20%	1b	3.87	3.93	1.00	6505.07	20.20	0.59	4.48	1.50
		2b	1.52	1.57	2.01	13124.35				
		8bb	4.63	4.69	0.47	3072.24				
		9bb	1.77	1.82	0.18	1183.26				
	35%	1b	3.87	3.93	0.99	4484.97	34.31	0.53	4.27	1.45
		2b	1.52	1.57	2.67	12141.23				
		8bb	4.63	4.69	1.10	5016.74				
		9bb	1.77	1.83	0.51	2330.48				
	50%	1b	3.87	3.93	1.00	2561.39	50.04	0.47	4.24	1.45
		2b	1.53	1.57	4.09	10480.92				
		8bb	4.63	4.69	2.73	7014.06				
		9bb	1.77	1.83	1.49	3823.99				
	70%	1b	3.87	3.93	1.00	735.76	68.63	0.34	4.29	1.46
		2b	1.52	1.57	10.70	7876.14				
		8bb	4.63	4.70	11.96	8802.32			<i>Mean k_{rel}</i>	<i>Mean ln k_{rel}</i>
		9bb	1.78	1.83	8.75	6438.67			4.32 ± 0.09	1.46 ± 0.02
4	20%	2b	3.92	3.97	1.00	60413.03	17.87	0.72	7.20	1.97
		1b	1.55	1.60	2.14	129042.44				
		9ba	4.59	4.66	0.45	27293.37				
		8ba	1.74	1.77	0.11	6839.33				
	35%	2b	3.92	3.97	1.00	35704.95	32.43	0.77	10.86	2.39
		1b	1.55	1.60	3.32	118603.38				

Acylation Reagents for Size-Dependent Esterification Reaction

		9ba	4.58	4.65	1.36	48606.19				
		8ba	1.74	1.77	0.27	9734.20				
	50%	2b	3.92	3.97	1.00	18693.91	43.64	0.73	11.47	2.44
		1b	1.55	1.60	5.68	106232.16				
		9ba	4.58	4.66	3.21	59952.42				
		8ba	1.74	1.77	0.75	14056.19				
	70%	2b	3.92	3.97	1.00	1432.77	62.80	0.56	12.46	2.52
		1b	1.55	1.59	65.37	93653.17				
		9ba	4.58	4.65	58.75	84169.91			<i>Mean k_{rel}</i>	<i>Mean ln k_{rel}</i>
		8ba	1.74	1.77	24.78	35507.53			10.50 ± 1.99	2.33 ± 0.21
5a	20%	2b	3.91	3.97	1.00	76695.96	18.10	0.84	13.77	2.62
		1b	1.57	1.62	2.27	174305.89				
		9ba	4.62	4.68	0.51	39116.07				
		8ba	1.77	1.81	0.07	5279.48				
	35%	2b	3.91	3.98	0.99	47047.41	32.48	0.81	13.70	2.62
		1b	1.57	1.63	3.55	168152.23				
		9ba	4.61	4.68	1.45	68992.05				
		8ba	1.77	1.81	0.24	11366.48				
	50%	2b	3.92	3.97	1.05	20980.47	46.71	0.74	13.29	2.59
		1b	1.57	1.62	7.92	158369.01				
		9ba	4.62	4.68	4.82	96488.63				
		8ba	1.77	1.81	1.08	21632.89				
	70%	2b					69.50	0.44	13.43	2.60
		1b	1.57	1.61	1.00	108858.93				
		9ba	4.62	4.68	1.09	118624.61			<i>Mean k_{rel}</i>	<i>Mean ln k_{rel}</i>
		8ba	1.76	1.83	0.64	70116.99			13.55 ± 0.20	2.61 ± 0.01
5b	20%	2b	3.91	3.97	1.00	78128.43	16.85	0.85	15.01	2.71
		1b	1.56	1.62	2.17	169708.97				
		9bb	4.68	4.74	0.46	35875.87				
		8bb	1.81	1.86	0.06	4319.31				
	35%	2b	3.92	3.97	1.01	47252.04	32.22	0.81	13.89	2.63
		1b	1.57	1.62	3.41	160339.58				
		9bb	4.67	4.74	1.41	66311.77				
		8bb	1.82	1.86	0.22	10442.67				
	50%	2b	3.92	3.97	1.18	28594.98	43.38	0.75	12.72	2.54
		1b	1.57	1.62	6.26	151891.29				
		9bb	4.67	4.75	3.61	87556.90				
		8bb	1.82	1.86	0.74	17898.27				
	70%	2b					64.36	0.55	16.24	2.79
		1b	1.57	1.62	1.00	109712.33				
		9bb	4.69	4.74	0.93	101919.34			<i>Mean k_{rel}</i>	<i>Mean ln k_{rel}</i>
		8bb	1.82	1.87	0.41	45274.47			14.47 ± 1.31	2.67 ± 0.09
1a vs. 2a catalysed by DMAP (6a)										
Reagent	Conv		integral limits (ppm)		integral	absolute	Conv.	Chem.	k_{rel}	ln k_{rel}
3a	20%	1a	3.75	3.81	0.46	70513.18	17.88	0.74	7.95	2.07
		2a	1.40	1.45	1.00	152004.89				
		8aa	3.01	3.06	0.21	32476.18				
		9aa	1.61	1.65	0.05	7399.55				
	35%	1a	3.74	3.81	0.32	43612.35	32.93	0.70	7.74	2.05
		2a	1.41	1.46	1.00	137424.76				
		8aa	3.00	3.06	0.41	56121.32				
		9aa	1.61	1.65	0.11	15430.83				
	50%	1a	3.75	3.80	0.17	20845.48	48.67	0.62	7.53	2.02
		2a	1.41	1.46	1.00	125173.20				
		8aa	3.01	3.07	0.64	79683.73				
		9aa	1.60	1.66	0.23	28830.11				

	65%	1a	3.74	3.80	0.04	3713.50	65.58	0.47	7.78	2.05
		2a	1.40	1.45	1.00	99841.02				
		8aa	3.00	3.07	0.99	98438.04			<i>Mean k_{rel}</i>	<i>Mean ln k_{rel}</i>
		9aa	1.60	1.66	0.53	53168.89			7.75 ± 0.15	2.05 ± 0.02
4	20%	2a	3.77	3.84	0.95	46688.53	17.05	0.86	16.38	2.80
		1a	1.43	1.47	2.15	105619.69				
		9aa	4.45	4.52	0.45	22373.14				
		8aa	1.62	1.66	0.05	2544.76				
	35%	2a	3.77	3.83	1.00	31276.40	30.38	0.87	21.54	3.07
		1a	1.43	1.48	3.43	107262.74				
		9aa	4.46	4.52	1.34	41985.74				
		8aa	1.62	1.65	0.14	4306.92				
	50%	2a	3.78	3.84	1.00	12068.65	45.72	0.81	18.98	2.94
		1a	1.43	1.48	8.65	104405.49				
		9aa	4.46	4.52	5.13	61967.21				
		8aa	1.61	1.65	0.85	10229.83				
	70%	2a					64.18	0.55	14.36	2.66
		1a	1.43	1.48	1.00	79831.26				
		9aa	4.46	4.51	0.92	73319.96			<i>Mean k_{rel}</i>	<i>Mean ln k_{rel}</i>
		8aa	1.61	1.66	0.41	33076.12			17.82 ± 2.70	2.87 ± 0.15
5a	20%	2a	3.83	3.89	0.96	77956.69	18.07	0.85	14.72	2.69
		1a	1.48	1.54	2.28	184527.92				
		9aa	4.51	4.58	0.50	40792.06				
		8aa	1.68	1.71	0.07	5319.59				
	35%	2a	3.82	3.89	0.99	48353.09	30.98	0.82	14.18	2.65
		1a	1.49	1.53	3.46	168909.96				
		9aa	4.52	4.59	1.34	65325.80				
		8aa	1.68	1.72	0.21	10377.04				
	50%	2a	3.83	3.89	1.14	23563.86	45.43	0.75	13.30	2.59
		1a	1.48	1.54	7.69	159157.21				
		9aa	4.51	4.58	4.56	94407.19				
		8aa	1.68	1.72	0.98	20334.08				
	70%	2a					68.84	0.45	11.68	2.46
		1a	1.48	1.53	1.00	110778.59				
		9aa	4.52	4.58	1.06	117534.09			<i>Mean</i>	<i>Mean</i>
		8aa	1.66	1.72	0.62	68476.70			13.47 ± 1.15	2.60 ± 0.09
1b vs. 2b catalysed by DMAP (6a)										
Reagent	Conv		integral limits (ppm)		integral	absolute	Conv.	Chem.	k_{rel}	ln k_{rel}
3a	20%	1b	3.82	3.88	0.48	67884.48	19.31	0.65	5.51	1.71
		2b	1.49	1.53	1.00	140803.85				
		8ba	3.14	3.23	0.23	31912.02				
		9ba	1.68	1.73	0.07	10184.25				
	35%	1b	3.82	3.88	0.35	46916.07	33.75	0.60	5.38	1.68
		2b	1.48	1.53	1.00	134656.80				
		8ba	3.15	3.23	0.41	55608.20				
		9ba	1.68	1.74	0.16	21031.35				
	50%	1b	3.82	3.88	0.23	26956.64	48.25	0.53	5.30	1.67
		2b	1.49	1.52	1.00	119193.19				
		8ba	3.15	3.22	0.64	76262.23				
		9ba	1.68	1.74	0.29	34454.63				
	65%	1b	3.81	3.90	0.11	10863.51	60.84	0.48	6.09	1.81
		2b	1.47	1.53	1.00	102447.75				
		8ba	3.13	3.22	0.90	91773.61			<i>Mean k_{rel}</i>	<i>Mean ln k_{rel}</i>
		9ba	1.70	1.73	0.46	46798.39			5.57 ± 0.31	1.72 ± 0.05
3b	20%	1b	3.87	3.93	1.00	6852.07	18.53	0.68	6.08	1.80
		2b	1.51	1.58	2.04	13971.09				

Acylation Reagents for Size-Dependent Esterification Reaction

		8bb	4.64	4.70	0.45	3088.66				
		9bb	1.78	1.82	0.13	882.53				
	35%	1b	3.87	3.93	1.04	4109.54	34.65	0.64	6.25	1.83
		2b	1.52	1.57	3.10	12268.71				
		8bb	4.63	4.69	1.35	5345.93				
		9bb	1.78	1.83	0.44	1752.68				
	50%	1b	3.87	3.93	0.99	2145.99	49.47	0.56	6.01	1.79
		2b	1.52	1.57	5.11	11028.96				
		8bb	4.63	4.69	3.36	7249.09				
		9bb	1.78	1.82	1.42	3073.04				
	70%	1b	3.87	3.93	1.00	520.78	66.97	0.42	/	/
		2b	1.52	1.58	16.81	8753.23				
		8bb	4.63	4.70	17.58	9152.77			Mean k_{rel}	Mean $\ln k_{rel}$
		9bb	1.78	1.83	10.76	5603.93			6.11 ± 0.10	1.81 ± 0.02
5a	20%	2b	3.91	3.97	1.00	81803.61	18.30	0.85	14.52	2.68
		1b	1.57	1.61	2.29	187264.77				
		9ba	4.61	4.68	0.52	42637.39				
		8ba	1.76	1.80	0.07	5473.52				
	35%	2b	3.91	3.98	0.99	47446.71	32.15	0.81	13.75	2.62
		1b	1.57	1.61	3.46	166299.38				
		9ba	4.61	4.68	1.41	67671.25				
		8ba	1.77	1.81	0.23	11006.72				
	50%	2b	3.91	3.97	1.04	18828.66	48.19	0.74	13.35	2.59
		1b	1.58	1.61	8.46	152601.85				
		9ba	4.61	4.68	5.40	97337.40				
		8ba	1.77	1.82	1.23	22235.89				
	70%	2b					70.42	0.42	12.48	2.52
		1b	1.57	1.63	1.00	105071.12				
		9ba	4.62	4.69	1.12	118001.92			Mean k_{rel}	Mean $\ln k_{rel}$
		8ba	1.76	1.81	0.70	73114.10			13.52 ± 0.74	2.60 ± 0.05
5b	20%	2b	3.91	3.97	1.00	85685.70	16.34	0.85	14.79	2.69
		1b	1.57	1.62	2.14	183674.44				
		9bb	4.68	4.73	0.44	37612.73				
		8bb	1.82	1.86	0.05	4568.57				
	35%	2b	3.91	3.98	0.99	49516.91	31.66	0.81	13.97	2.64
		1b	1.57	1.62	3.28	164694.39				
		9bb	4.67	4.73	1.33	66894.07				
		8bb	1.82	1.86	0.21	10383.09				
	50%	2b	3.91	3.98	1.15	28935.13	43.78	0.76	13.07	2.57
		1b	1.58	1.62	6.15	154113.45				
		9bb	4.68	4.75	3.61	90551.56				
		8bb	1.82	1.86	0.72	18008.16				
	70%	2b					64.61	0.55	/	
		1b	1.57	1.62	1.00	122906.70				
		9bb	4.67	4.74	0.94	115668.87			Mean k_{rel}	Mean $\ln k_{rel}$
		8bb	1.82	1.87	0.41	50927.01			13.94 ± 0.70	2.63 ± 0.05
1c vs. 2c acylated with 3a										
Catalyst	Conv		integral limits (ppm)		integral	absolute	Conv.	Chem.	k_{rel}	$\ln k_{rel}$
DMAP	20%	2c	3.95	4.02	1.01	89057.60	15.78	0.78	9.41	2.24
		1c	1.65	1.70	1.88	166726.96				
		9ca	4.63	4.71	0.38	33636.81				
		8ca	1.84	1.88	0.07	5799.90				
	35%	2c	3.94	4.01	0.99	57872.50	29.65	0.73	8.79	2.17
		1c	1.64	1.70	2.73	159326.54				
		9ca	4.64	4.71	1.03	60147.28				
		8ca	1.84	1.89	0.23	13509.32				

	50%	2c	3.95	4.01	0.98	28626.66	45.73	0.67	8.89	2.19
		1c	1.64	1.70	4.95	144858.28				
		9ca	4.64	4.71	3.03	88682.14				
		8ca	1.85	1.89	0.86	25252.08				
	70%	2c	3.93	4.03	0.85	6999.96	59.77	0.57	9.51	2.25
		1c	1.63	1.70	13.51	111305.95				
		9ca	4.64	4.71	11.59	95462.83			Mean k_{rel}	Mean $\ln k_{rel}$
		8ca	1.83	1.88	4.59	37802.73			9.15 ± 0.31	2.21 ± 0.03
TCAP	20%	1c	1.54	1.63	1.00	123312.54	19.53	0.69	6.36	1.85
		2c	3.87	3.94	0.39	48622.41				
		8ca	1.73	1.79	0.07	8507.97				
		9ca	3.43	3.54	0.21	26074.15				
	35%	1c	1.57	1.61	1.00	112699.98	34.34	0.64	6.18	1.82
		2c	3.87	3.93	0.26	29462.98				
		8ca	1.74	1.78	0.15	17193.72				
		9ca	3.45	3.53	0.38	43240.51				
	50%	1c	1.55	1.60	1.00	98979.00	44.29	0.60	6.34	1.85
		2c	3.86	3.95	0.22	22124.08				
		8ca	1.74	1.79	0.22	21507.05				
		9ca	3.44	3.53	0.56	55710.01				
	70%	1c	1.55	1.62	1.00	82539.83	60.90	0.49	6.26	1.83
		2c	3.85	3.93	0.08	6550.57				
		8ca	1.72	1.80	0.46	38274.06			Mean k_{rel}	Mean $\ln k_{rel}$
		9ca	3.43	3.54	0.85	70410.59			6.28 ± 0.07	1.84 ± 0.01
1d vs. 2d acylated with 3a										
Catalyst	Conv		integral limits (ppm)		integral	absolute	Conv.	Chem.	k_{rel}	$\ln k_{rel}$
DMAP	20%	2d	3.92	4.01	1.01	54166.03	18.65	0.67	5.82	1.76
		1d	1.64	1.71	2.09	112448.67				
		9da	3.68	3.76	0.46	24627.38				
		8da	1.87	1.93	0.14	7472.20				
	35%	2d	3.94	4.01	1.00	37352.98	33.85	0.61	5.60	1.72
		1d	1.64	1.70	2.93	109932.73				
		9da	3.68	3.75	1.21	45458.76				
		8da	1.86	1.91	0.45	16731.47				
	50%	2d	3.94	4.00	0.31	17764.18	49.49	0.54	5.52	1.71
		1d	1.65	1.71	1.54	89036.02				
		9da	3.68	3.76	1.00	57879.76				
		8da	1.86	1.91	0.46	26547.94				
	70%	2d	3.95	4.01	0.92	3528.16	69.00	0.38	5.51	1.71
		1d	1.64	1.70	19.33	74057.54				
		9da	3.69	3.76	21.05	80655.16			Mean k_{rel}	Mean $\ln k_{rel}$
		8da	1.86	1.92	14.51	55607.88			5.61 ± 0.13	1.72 ± 0.02
TCAP	20%	2d	3.93	4.01	1.00	49896.19	19.30	0.45	2.92	1.07
		1d	1.65	1.70	1.89	93956.13				
		9da	3.68	3.76	0.39	19444.11				
		8da	1.87	1.91	0.23	11205.39				
	35%	2d	3.94	4.01	1.01	42795.47	33.89	0.40	2.84	1.04
		1d	1.65	1.69	2.34	99088.14				
		9da	3.69	3.75	0.92	38905.98				
		8da	1.87	1.92	0.60	25343.29				
	50%	2d	3.94	4.01	0.99	29457.82	47.65	0.36	2.91	1.07
		1d	1.65	1.69	2.99	88861.92				
		9da	3.68	3.76	1.85	54931.48				
		8da	1.87	1.92	1.30	38699.59				
	70%	2d	3.94	4.00	0.98	11183.81	67.07	0.28	3.01	1.10
		1d	1.65	1.70	5.92	67568.01				

Acylation Reagents for Size-Dependent Esterification Reaction

	9da	3.68	3.75	6.34	72357.62			Mean k_{rel}	Mean $\ln k_{rel}$
	8da	1.87	1.92	5.54	63264.98			2.92 ± 0.06	1.07 ± 0.02

^aOnly the 35% and 50% conversion point was considered for the mean and st. deviation.

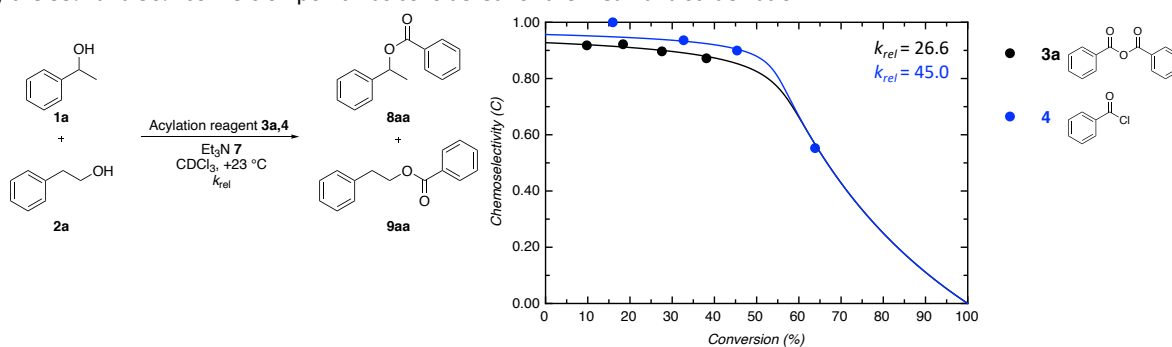


Figure 2.7. Plot of conversion (%) vs. corrected chemoselectivity for uncatalysed turnover-limited competition experiment 1a vs. 2a with 3a,4.

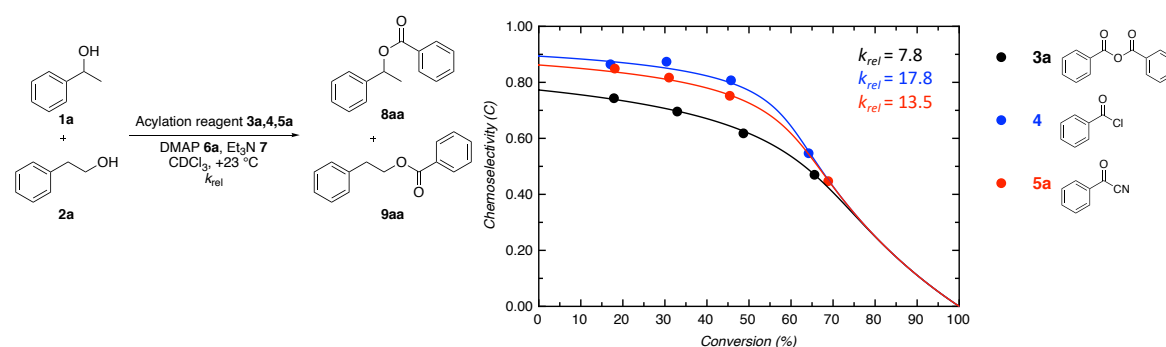


Figure 2.8. Plot of conversion (%) vs. corrected chemoselectivity for turnover-limited competition experiment 1a vs. 2a with 3a,4,5a catalysed by DMAP.

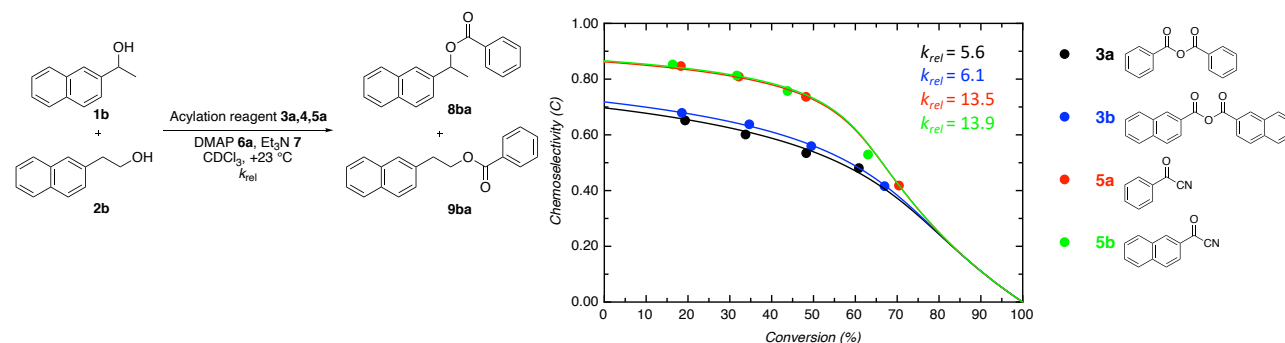


Figure 2.9. Plot of conversion (%) vs. corrected chemoselectivity for turnover-limited competition experiment 1b vs. 2b with 3a,4,5a catalysed by DMAP.

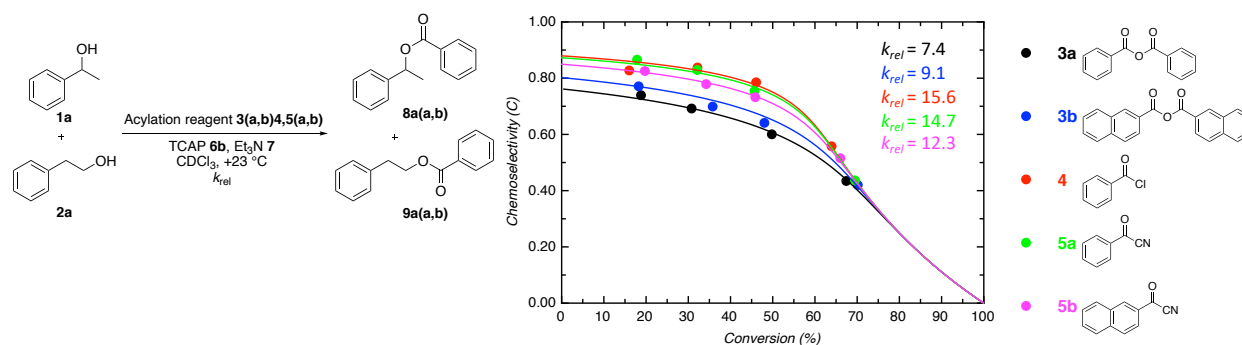


Figure 2.10. Plot of conversion (%) vs. corrected chemoselectivity for turnover-limited competition experiment 1a vs. 2a with 3,4,5 catalysed by TCAP.

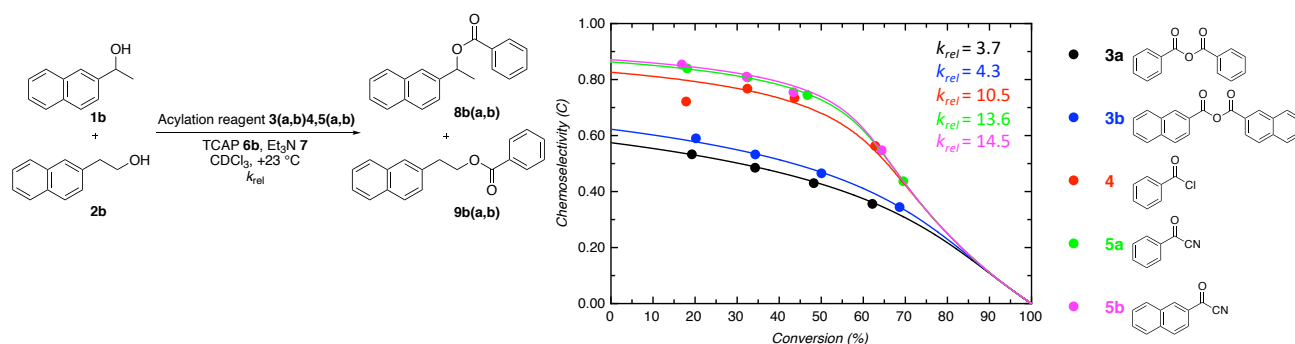


Figure 2.11. Plot of *conversion (%)* vs. *corrected chemoselectivity* for turnover-limited competition experiment **1b** vs. **2b** with **3,4,5** catalysed by TCAP.

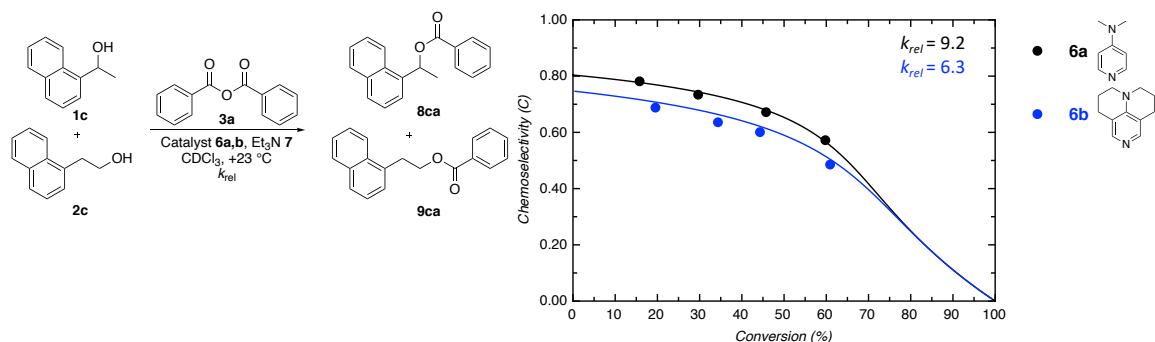


Figure 2.12. Plot of *conversion (%)* vs. *corrected chemoselectivity* for turnover-limited competition experiment **1c** vs. **2c** with **3a** catalysed by TCAP.

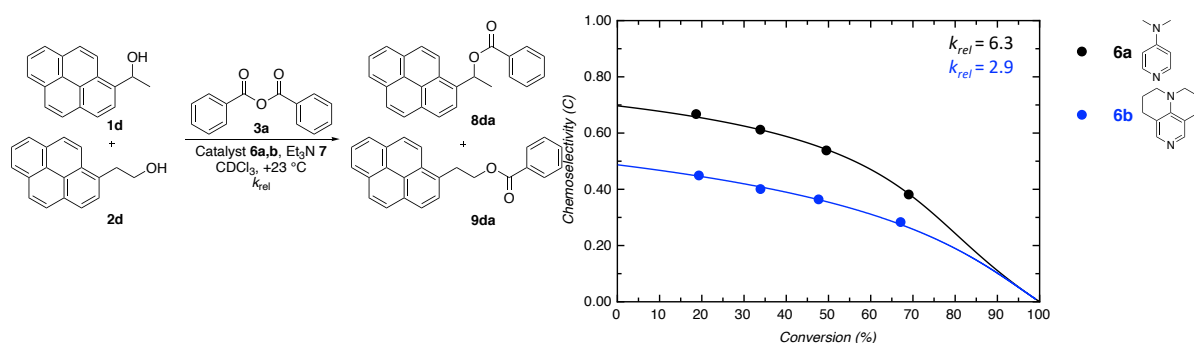


Figure 2.13. Plot of *conversion (%)* vs. *corrected chemoselectivity* for turnover-limited competition experiment **1d** vs. **2d** with **3a** catalysed by TCAP.

2.4.2 Synthesis of Reagent

2-Naphthoyl cyanide 5b (Based on the procedure reported by Hou *et al.*^[17])

Cu(I)CN (939 mg, 10.5 mmol, 2.0 eq) was stirred in dry MeCN (20 mL) and 2-naphthoyl chloride (1.00 g, 5.25 mmol, 1.0 eq) was added carefully at room temperature. The reaction mixture was stirring under reflux for 4 h. After cooling down to room temperature, the mixture was concentrated and washed with hot ether. The mixture was filtered and again concentrated. **5b** (900 mg, 95%) was obtained as a yellow solid.

¹H NMR (400 MHz, CDCl₃) δ = 8.75 (d, J = 1.8 Hz, 1H, Ar), 8.07 (td, J = 8.8, 8.3, 1.5 Hz, 2H, Ar), 8.00 – 7.92 (m, 2H, Ar), 7.75 (ddd, J = 8.2, 6.9, 1.3 Hz, 1H, Ar), 7.67 (ddd, J = 8.2, 6.9, 1.3 Hz, 1H, Ar) ppm; ¹³C NMR (101 MHz, CDCl₃) δ = 167.86, 137.32, 135.79, 132.38, 131.21, 130.99, 130.47, 129.87, 128.30, 128.08, 122.92, 113.10 ppm; HRMS (EI): m/z calcd for C₁₂H₇ON⁺ [M]⁺: 181.0522; found: 181.0520. The ¹H/¹³C spectra are in full agreement with literature reports.^[18]

Acylation Reagents for Size-Dependent Esterification Reaction

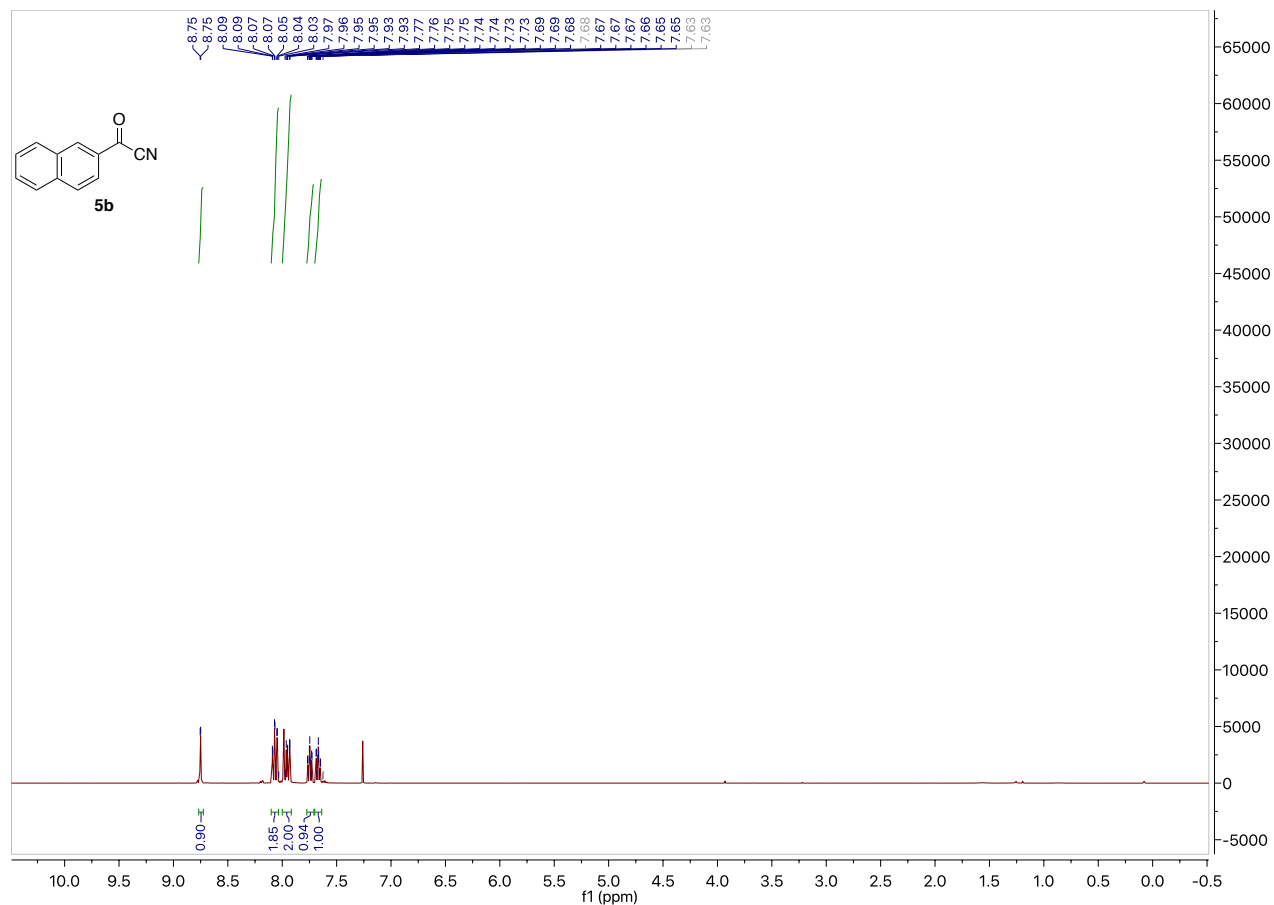


Figure 2.14. ^1H NMR spectrum of **5b** (400 MHz, CDCl_3).

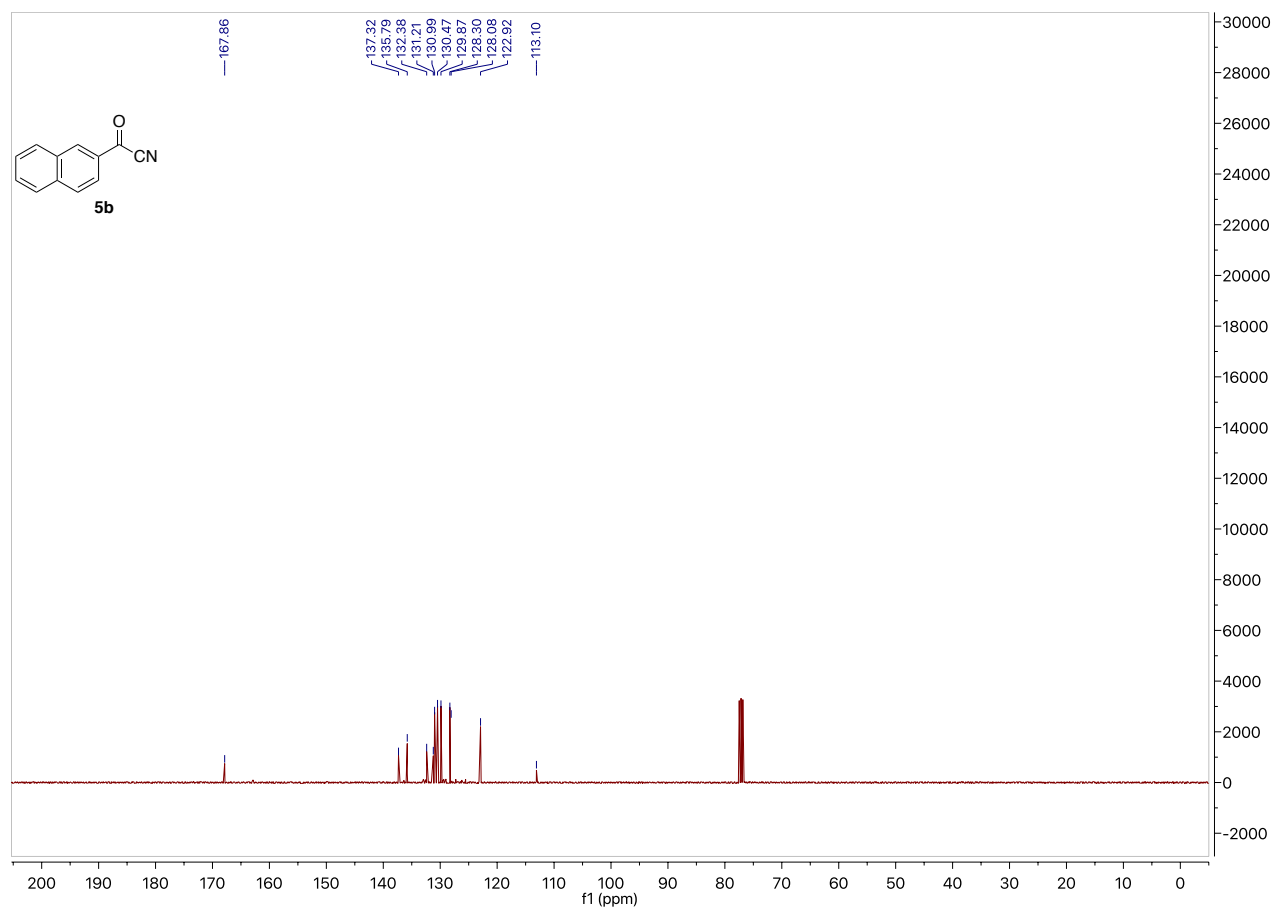


Figure 2.15. ^{13}C NMR spectrum of **5b** (101 MHz, CDCl_3).

2.5 References

- [1] a) O. Robles, D. Romo, *Nat. Prod. Rep.* **2014**, *31*, 318-334; b) K. C. Nicolaou, J. S. Chen, *Classics in Total Synthesis III*, Wiley-VCH, Weinheim, **2011**; c) P. G. M. Wuts, *Greene's Protective Groups in Organic Synthesis*, 5 ed., John Wiley & Sons, Hoboken, New Jersey, **2014**.
- [2] a) F. A. Carey, R. J. Sundberg, *Advanced Organic Chemistry Part B: Reactions and Synthesis*, 5 ed., Springer Science+Business Media, New York, **2007**; b) H. G. O. Becker, W. Berger, G. Domschke, E. Fanghänel, J. Faust, M. Fischer, F. Gentz, K. Gewalt, R. Gluch, R. Mayer, K. Müller, D. Pavel, H. Schmidt, K. Schollberg, K. Schwetlick, E. Seiler, G. Zeppenfeld, *Organikum*, 23 ed., Wiley-VCH, Weinheim, **2009**; c) J. Clayden, N. Greeves, S. Warren, *Organische Chemie*, 2 ed., Springer Spektrum, Berlin Heidelberg, **2013**.
- [3] J. Xiang, A. Orita, J. Otera, *Angew. Chem. Int. Ed.* **2002**, *41*, 4117-4119.
- [4] a) E. Kattnig, M. Albert, *Org. Lett.* **2004**, *6*, 945-948; b) P. Peng, M. Linseis, R. F. Winter, R. R. Schmidt, *J. Am. Chem. Soc.* **2016**, *138*, 6002-6009; c) M. Nahmany, A. Melman, *Org. Biomol. Chem.* **2004**, *2*, 1563-1572; d) N. A. Afagh, A. K. Yudin, *Angew. Chem. Int. Ed.* **2010**, *49*, 262-310; e) A. H. Haines, *Adv. Carbohydr. Chem. Biochem.* **1976**, *33*, 11-109.
- [5] a) S. E. Denmark, G. L. Beutner, *Angew. Chem. Int. Ed.* **2008**, *47*, 1560-1638; b) G. Höfle, W. Steglich, H. Vorbrüggen, *Angew. Chem. Int. Ed.* **1978**, *17*, 569-583; c) E. Guibe-Jampel, G. Le Corre, M. Wakselman, *Tetrahedron Lett.* **1979**, *20*, 1157-1160.
- [6] K. Ishihara, H. Kurihara, H. Yamamoto, *J. Org. Chem.* **1993**, *58*, 3791-3793.
- [7] a) W. Steglich, G. Höfle, *Angew. Chem. Int. Ed.* **1969**, *8*, 981-981; b) G. Höfle, W. Steglich, *Synthesis* **1972**, 619-621.
- [8] L. M. Litvinenko, A. I. Kirichenko, *Dokl. Akad. Nauk. SSSR Ser. Khim.* **1967**, *176*, 97-100.
- [9] a) W. Steglich, G. Höfle, *Tetrahedron Lett.* **1970**, *11*, 4727-4730; b) A. Hassner, L. R. Krepski, V. Alexanian, *Tetrahedron* **1978**, *34*, 2069-2076.
- [10] a) A. C. Spivey, S. Arseniyadis, *Angew. Chem. Int. Ed.* **2004**, *43*, 5436-5441; b) M. R. Heinrich, H. S. Klisa, H. Mayr, W. Steglich, H. Zipse, *Angew. Chem. Int. Ed.* **2003**, *42*, 4826-4828.
- [11] J. Helberg, M. Marin-Luna, H. Zipse, *Synthesis* **2017**, *49*, 3460-3470.
- [12] a) S. Xu, I. Held, B. Kempf, H. Mayr, W. Steglich, H. Zipse, *Chem. Eur. J.* **2005**, *11*, 4751-4757; b) Y. Wei, I. Held, H. Zipse, *Org. Biomol. Chem.* **2006**, *4*, 4223-4230; c) E. Larionov, M. Mahesh, A. C. Spivey, Y. Wei, H. Zipse, *J. Am. Chem. Soc.* **2012**, *134*, 9390-9399; d) I. Held, A. Villinger, H. Zipse, *Synthesis* **2005**, *2005*, 1425-1430.
- [13] H. B. Kagan, J. C. Fiaud, *Top. Stereochem.* **1988**, *18*, 249-330.
- [14] M. Marin-Luna, B. Pölloth, F. Zott, H. Zipse, *Chem. Sci.* **2018**, *9*, 6509-6515.
- [15] S. Mayr, M. Marin-Luna, H. Zipse, *J. Org. Chem.* **2021**, *86*, 3456-3489.
- [16] S. Hoops, S. Sahle, R. Gauges, C. Lee, J. Pahle, N. Simus, M. Singhal, L. Xu, P. Mendes, U. Kummer, *Bioinformatics* **2006**, *22*, 3067-3074.
- [17] M. Li, D. Kong, G. Zi, G. Hou, *J. Org. Chem.* **2017**, *82*, 680-687.
- [18] C. Zhou, J. Wang, J. Jin, P. Lu, Y. Wang, *Eur. J. Org. Chem.* **2014**, *2014*, 1832-1835.

Chapter 3. Size-Driven Inversion of Selectivity in Esterfication Reactions: Secondary Beat Primary Alcohols.

Stefanie Mayr, Marta Marin-Luna and Hendrik Zipse*

J. Org. Chem., **2021**, *86*, 3456-3489. - Published by American Chemical Society.

DOI: [10.1021/acs.joc.0c02848](https://doi.org/10.1021/acs.joc.0c02848)

Author contributions: The project was conceived by S.M. and H.Z. The experimental study was performed by S.M. The computational studies were performed by S.M., M.M.-L. and H.Z. The manuscript was jointly written by S.M., M.M.-L. and H.Z. The supporting information was prepared by S.M. Computational part of the mechanistic study was jointly prepared by S.M. and M.M.-L.

Copyright: Reprinted with permission from *The Journal of Organic Chemistry*, **2021**, *86*, 3456-3489. - Copyright 2021 American Chemical Society.

Additional information: The herein printed Supporting Information (SI) is an altered version of the published SI. NMR spectra, integral tables for turnover-limited competition experiments, crystal structures, tables of energies, enthalpies and free energies for all conformers, and Cartesian coordinates and number of imaginary frequencies of the best conformers can be accessed online in the original version of the SI free of charge (<https://pubs.acs.org/doi/10.1021/acs.joc.0c02848>).

Size-Driven Inversion of Selectivity in Esterification Reactions: Secondary Beat Primary Alcohols

Stefanie Mayr, Marta Marin-Luna, and Hendrik Zipse*



Cite This: *J. Org. Chem.* 2021, 86, 3456–3489



Read Online

ACCESS |



Metrics & More

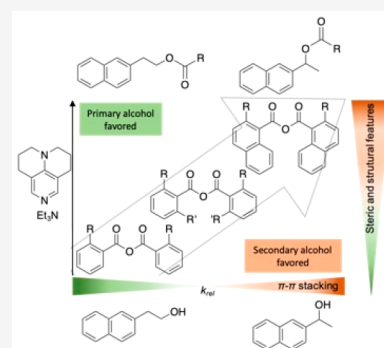


Article Recommendations



Supporting Information

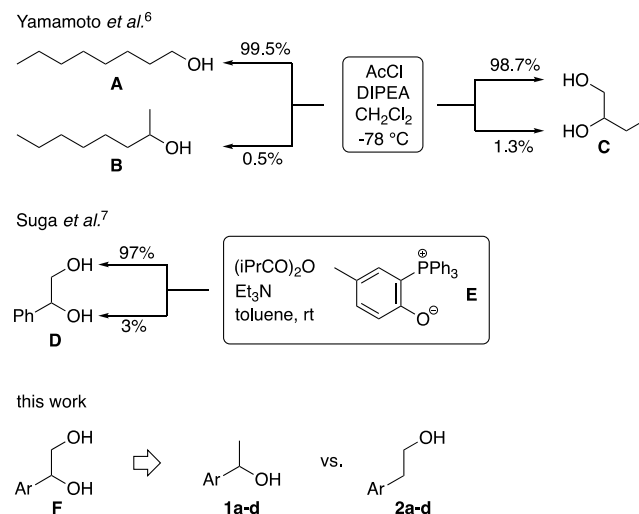
ABSTRACT: Relative rates for the Lewis base-mediated acylation of secondary and primary alcohols carrying large aromatic side chains with anhydrides differing in size and electronic structure have been measured. While primary alcohols react faster than secondary ones in transformations with monosubstituted benzoic anhydride derivatives, relative reactivities are inverted in reactions with sterically biased 1-naphthyl anhydrides. Further analysis of reaction rates shows that increasing substrate size leads to an actual acceleration of the acylation process, the effect being larger for secondary as compared to primary alcohols. Computational results indicate that acylation rates are guided by noncovalent interactions (NCIs) between the catalyst ring system and the DED substituents in the alcohol and anhydride reactants. Thereby stronger NCIs are formed for secondary alcohols than for primary alcohols.



INTRODUCTION

The selective manipulation of functional groups is of key importance in the synthesis of complex organic molecules.¹ Hydroxyl groups are particularly prevalent in molecules with biological or pharmaceutical activity,² and the synthesis of, for example, (oligo)saccharides is thus dominated by hydroxyl group protection/deprotection strategies.³ During the last decades, many efforts have been undertaken to develop regio- and chemoselective processes for protecting selected alcohol functionalities in polyol substrates.⁴ In the protecting chemistry toolbox, acylation reactions are among the most useful and typically employ either carboxylic acids or their activated derivatives (anhydrides, halides, or cyanides) as reagents.⁵ In acylation reactions, primary hydroxyl groups are usually more reactive as compared to secondary ones. This trend is commonly found in intermolecular competition experiments such as the acetylation of octanol substrates **A** and **B** with acetyl chloride, where acetylation of primary alcohol **A** is preferred by more than 2 orders of magnitude (Scheme 1).⁶ The same preference is also found in the acetylation of diol **C**, where acetylation of the primary hydroxyl terminus is strongly preferred.⁶ Repulsive steric interactions around the reacting OH group are commonly assumed to be responsible for this reactivity difference, and similarly, large preferences for the primary hydroxyl group are often observed for substrates carrying aliphatic (as in **C**) or aromatic (as in **D**) substituents.⁷ The attachment of sizable groups at the acylation reagent⁸ and/or the catalyst,⁹ or even at the auxiliary base⁶ is thus a common strategy in highly regio- and stereoselective esterification reactions. In this study, we demonstrate how the use of size effects in substrates and acylation reagents can be utilized to invert the primary/secondary selectivity such that the acylation of secondary

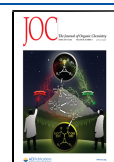
Scheme 1. Selective Acylation of Primary and Secondary Alcohols (DIPEA = *N,N*-Diisopropylethylamine)



alcohols is preferred. In rare cases, the preferred transformation of secondary alcohols rather than primary ones has been reported in carbohydrate derivatives, where intrinsic reactivities

Received: November 30, 2020

Published: February 8, 2021



are modified through hydrogen bonding effects within an array of hydroxyl substituents.^{9a,10} In order to avoid this type of interference and also eliminate the risk of competing intramolecular acyl transfer reactions, we formally dissect diol substrate **F** into a set of secondary alcohols of general structure **1** and associated primary alcohols **2** (Scheme 1, bottom). We have recently reported that stabilizing interactions between two dispersion energy donor (DED) groups such as the pyrenyl substituent (green) and the pyridinium ion surface (red) notably accelerate the reaction rate in esterification reactions of secondary alcohols using acyl chlorides as reagents and 9-azajulolidine (TCAP) as the catalyst (Figure 1a).¹¹ The size of

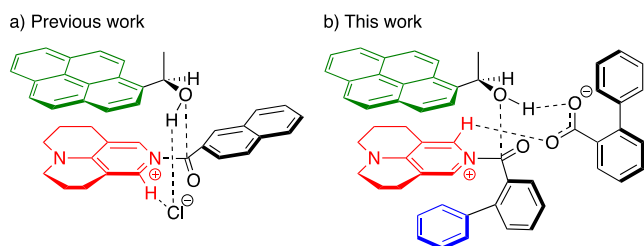


Figure 1. Proposed transition structures for the acylation of 1-(pyren-1-yl)ethanol (green) with (a) acyl chlorides (left) and with (b) acid anhydrides (right).

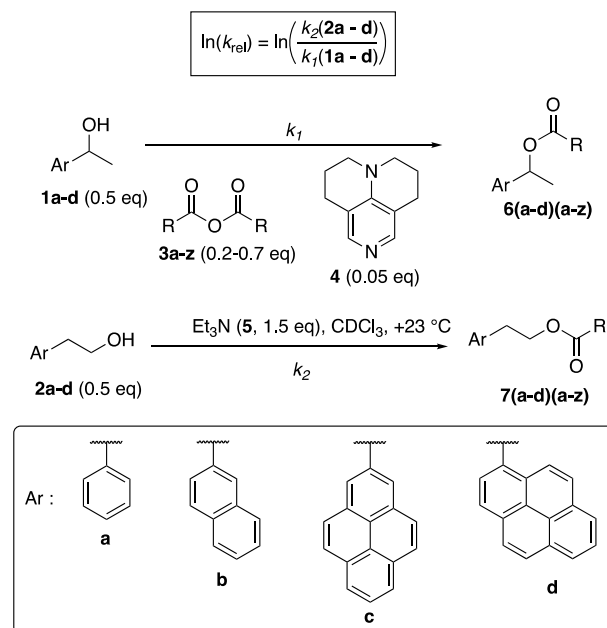
the acyl halide substituent (black) had, in this case, a limited effect on the reaction rates, which is in line with the transition state structure shown in Figure 1a. Related transition structures have been proposed for DMAP-catalyzed acylation reactions with acid anhydrides.¹² We, therefore, reasoned that acylation rates might be tuned by decorating the anhydrides with DED-groups large enough to interact with the pyridinium ion surface as illustrated in Figure 1b. We report herein the analysis of relative reaction rates for the acylation of primary vs secondary alcohols with acid anhydrides, where both the alcohol substrates and the acid anhydride reagents carry sizable aromatic surfaces.

RESULTS AND DISCUSSION

How the Choice of Anhydride Influences Selectivity.

Relative reactivities of secondary (**1a–d**) vs primary (**2a–d**) alcohols toward anhydrides **3** have been determined following the general outline shown in Scheme 2 and are expressed through the relative rate constant, k_{rel} , defined as the ratio between the acylation rate of primary over secondary alcohols; 1- and 2-substituted ethanol substrates, **1** and **2**, both carrying sizable aryl groups such as phenyl (**a**), 2-naphthyl (**b**), and 2- and 1-pyrenyl (**c** and **d**), were chosen as substrate alcohols. We employ the library of 26 anhydrides shown in Figure 2 carrying smaller (as in **3a–p** and **3x**) or larger (as in **3q–w** and **3z**) aromatic side chains in order to probe the influence of electronic and steric effects on relative reaction rates. As an example for a heterocyclic system, we include the anhydride of 2-thiophenecarboxylic acid (**3y**). The competition experiments employ 1:1 mixtures of secondary and primary alcohols **1** and **2**, 0.05 equiv of TCAP (**4**), a small excess of Et₃N (**5**), and anhydrides **3** as the limiting reagents such that the final conversion of alcohols reaches 20–70%. The competition experiments are performed in CDCl₃ at +23 °C (for details, see Supporting Information). Relative reaction rates can be easily calculated through chemoselectivity and conversion factors, which reflect the relative distribution of reactant alcohols **1** and **2** and the corresponding ester products **6** and **7**. We demonstrated

Scheme 2. Competition Experiments between Primary Alcohols **2a–d** and the Corresponding Secondary Ones **1a–d** with Anhydrides **3a–z** Catalyzed by TCAP (**4**) in the Presence of Et₃N (**5**)



previously that, for TCAP-mediated acylation reactions, 2-naphthyl-substituted secondary alcohols react faster than phenyl- and slower than pyrenyl-substituted derivatives.¹¹

Based on these earlier findings, competition experiments were initially performed for naphthyl-substituted alcohols **1b** and **2b** in order to test the influence of anhydrides **3** on acylation selectivity values (Figure 3). Benzoic anhydride (**3a**) represents an important reference system with a selectivity value of $\ln(k_{rel}) = 1.30$ (purple bar in Figure 3), which implies that primary alcohol **2b** reacts 3.7 times as fast as secondary alcohol **1b**. Similar k_{rel} values are obtained for benzoic anhydrides decorated with electron-donating (as in **3b**) or withdrawing (as in **3d–e**) substituents. *ortho*-Substituted benzoic anhydrides **3f–j** bearing substituents of various sizes provide lower selectivities than **3a**, the lowest value being that for *ortho*-(1-naphthyl)benzoic anhydride (**3h**) with $\ln(k_{rel}) = 0.68$. The actual size of the *ortho*-substituent appears to be less relevant here because the *ortho*-methyl substituted anhydride **3c** gives similar values with $\ln(k_{rel}) = 0.82$. Moving substituents to the *meta*-position changes selectivity values back to that found for the benzoic anhydride parent system as can be seen from the results for *meta*-phenylbenzoic anhydride **3x** with $\ln(k_{rel}) = 1.29$. The value found for 2-naphthoic anhydride **3z** is also quite similar at $\ln(k_{rel}) = 1.46$. The largest preference for primary alcohol **2b** of $\ln(k_{rel}) = 1.74$ is actually found for the heterocyclic anhydride **3y**. A much larger range of selectivity values is observed for 2,6-disubstituted benzoic anhydride derivatives **3k–p**. While anhydrides **3l,k** carrying electron-donating methoxy groups show the same selectivity as reference compound **3a**, a large reduction or even inversion of selectivity toward the preferred transformation of secondary alcohol **1b** is observed for 2,6-disubstituted benzoic anhydrides with trifluoromethyl- (as in **3p**) or methyl substituents (as in **3m–o**). Whether the methyl substituents present in these latter systems can also be replaced by annulated ring systems has been explored for anhydrides derived from 2-substituted 1-naphthoic acids. The actual parent

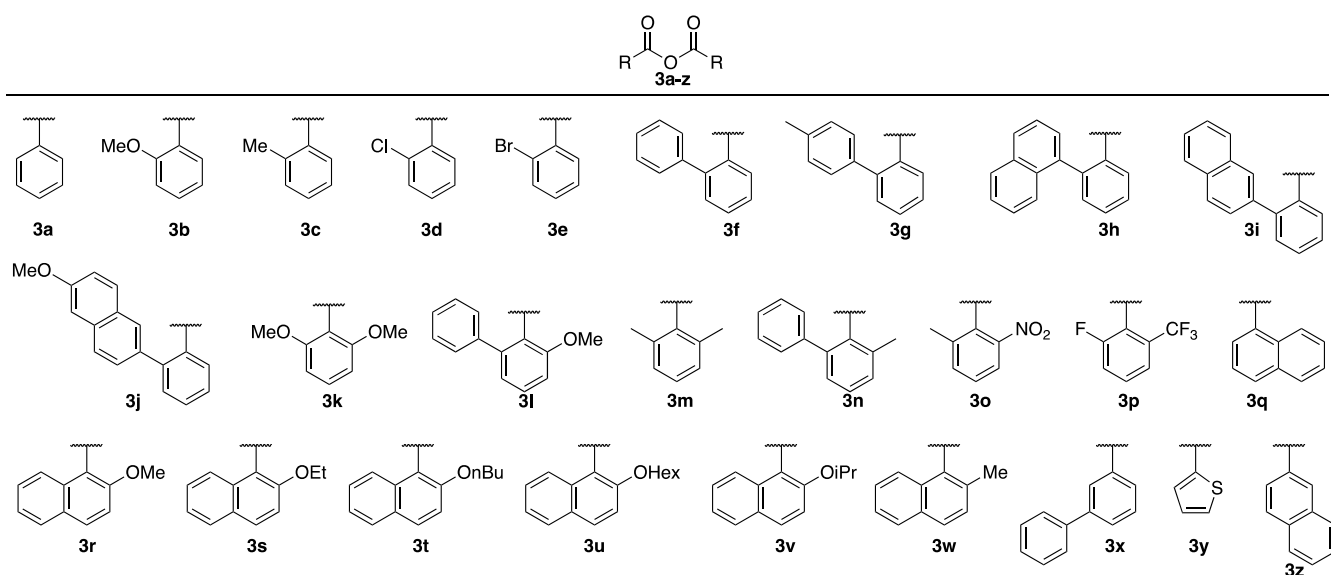


Figure 2. Structures of anhydrides **3** used in the competition experiments.

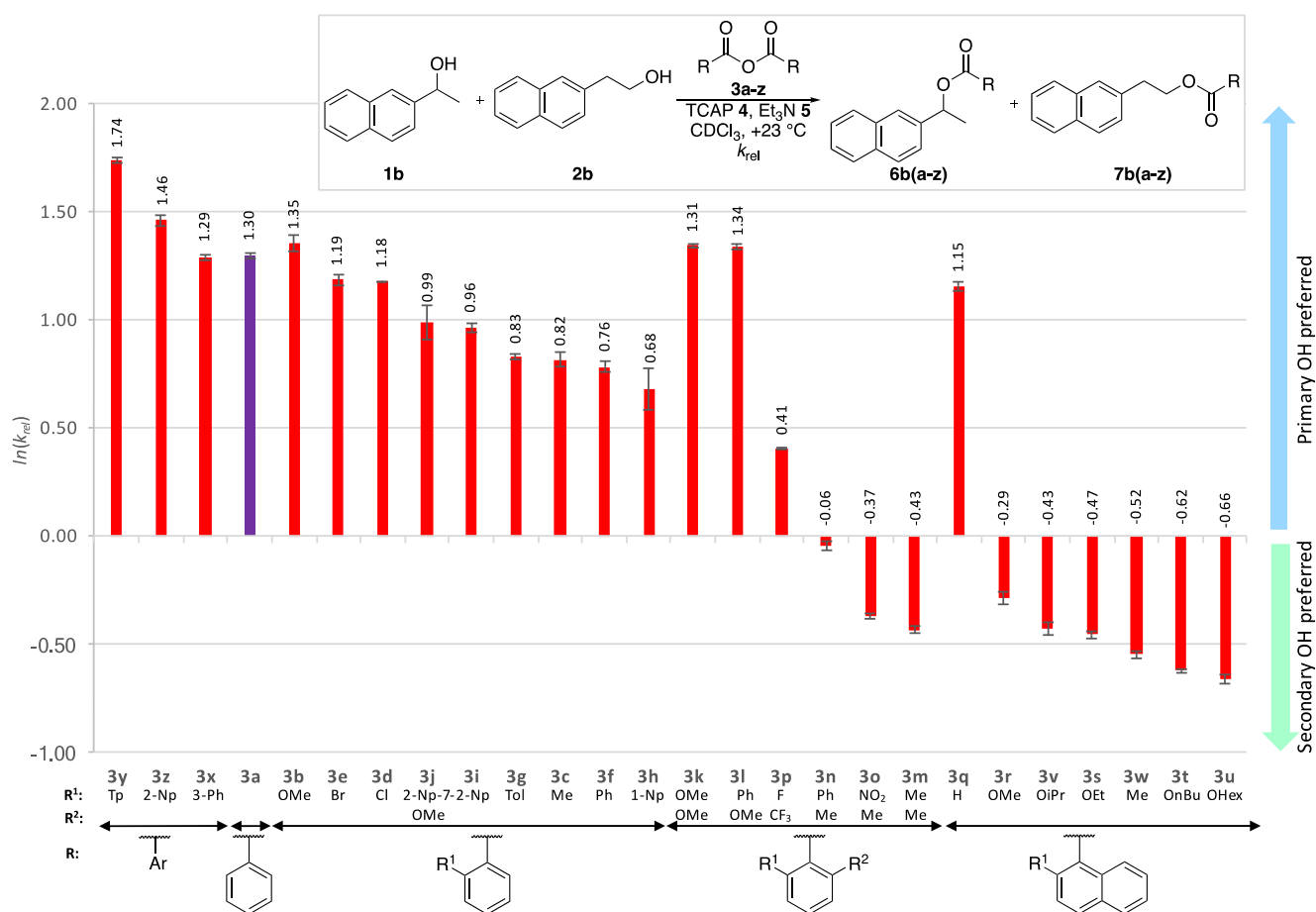


Figure 3. Relative rate constants $\ln(k_{\text{rel}})$ for secondary alcohol **1b** and the corresponding primary alcohol **2b** with anhydride derivatives **3a–z** catalyzed by TCAP (**4**).

system for this class of anhydrides is 1-naphthoic anhydride (**3q**) with $\ln(k_{\text{rel}}) = 1.15$. Introduction of alkoxy substituents at C2-position leads to an inversion of selectivity as demonstrated for the methoxy-substituted anhydride **3r** with $\ln(k_{\text{rel}}) = -0.29$. The actual preference for the conversion of secondary alcohol **1b** shows a systematic dependence on alkyl group length and

reaches a maximum for *n*-hexyloxy-substituted anhydride **3u** with $\ln(k_{\text{rel}}) = -0.66$. This latter value implies that anhydride **3u** reacts 1.9 times faster with secondary alcohol **1b** than primary alcohol **2b**. The chain length dependence observed here is reminiscent of similar effects observed in the kinetic resolution of secondary alcohols catalyzed with Lewis base catalysts of

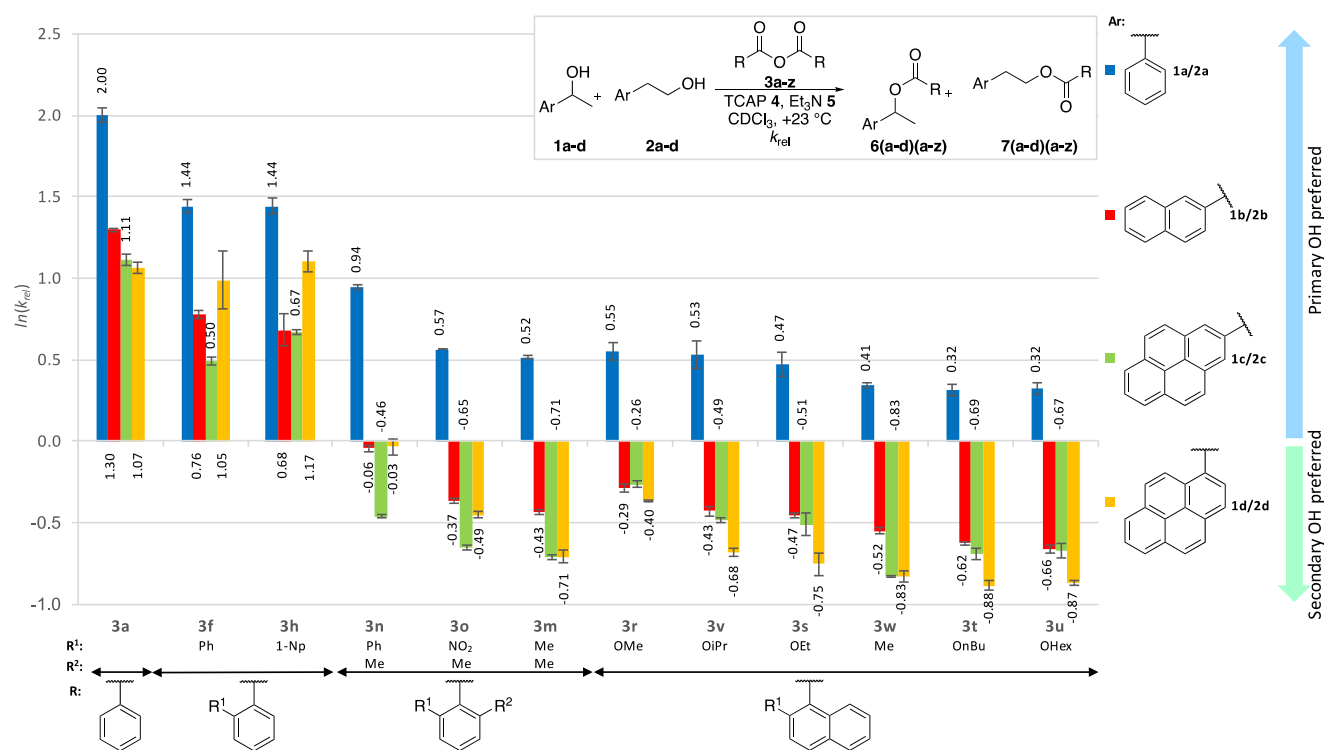


Figure 4. Relative rate constant $\ln(k_{rel})$ between secondary alcohols **1a–d** and the corresponding primary alcohol **2a–d** with selected anhydride reagents **3** catalyzed by TCAP (**4**).

different sizes.¹³ The linear or branched shape of the alkoxy substituent has an insignificant influence on the selectivity trend, as the k_{rel} value obtained for isopropoxy-substituted anhydride **3v** is closely similar to those for anhydrides **3s** and **3t**. It should be added that similar selectivities are also found for anhydrides with simple alkyl substituents as in methyl-substituted anhydride **3w** with $\ln(k_{rel}) = -0.52$. We may thus conclude at this point that “inverted” selectivities signaling a preference for secondary alcohol **1b** are obtained for a larger set of 1-naphthoic acid anhydrides carrying alkyl or alkoxy substituents at C2 position and for 2,6-disubstituted benzoic anhydride derivatives holding at least one methyl group (**3m–o**).

How the selectivity pattern observed for the alcohol substrate pair **1b/2b** shown in Figure 3 responds to changes in the size of the attached π -system was subsequently explored for the phenyl-substituted alcohols **1a/2a**, the 2-pyrenyl-substituted alcohols **1c/2c**, and the 1-pyrenyl-substituted alcohols **1d/2d**.¹⁴ The relative rates obtained for these substrate pairs are shown in Figure 4 together with those for the naphthyl-substituted alcohols **1b/2b** studied before as a reference. The competition experiments for the three new substrate pairs focus on anhydrides favoring the acylation of secondary alcohols in the earlier reactions but also include benzoic anhydride **3a** as the reference. For this comparatively small anhydride, we find a systematic influence of the alcohol size on the measured selectivity values in that the smallest alcohol pair **1a/2a** shows the largest preference for the reaction of the primary alcohol. In quantitative terms, primary alcohol **2a** reacts 7.2 times faster with anhydride **3a** than secondary alcohol **1a**, which equates to $\ln(k_{rel}) = 2.0$ in Figure 4. This preference drops to $\ln(k_{rel}) = 1.07$ for the larger alcohol substrate pair **1d/2d** carrying the 1-pyrenyl side chain. Moving from left to right in Figure 4 from smaller to larger anhydrides, we see that the preference for the reaction of the primary alcohol is reduced for all alcohols. For the smallest

alcohol substrate pair **1a/2a**, the effects are, however, not significant enough to reach the inverted reactivity regime. This is clearly the case for the pyrenyl-substituted alcohol pairs, where all anhydrides based on the 2,6-disubstituted benzoate or the 2-substituted 1-naphthoate substructure produce inverted selectivities. The preference for the reaction of the secondary alcohol is largest for the reaction of anhydride **3t** with substrate pair **1d/2d**, where the reaction of secondary alcohol **1d** is 2.4 times faster than that of primary alcohol **2d** (shown as $\ln(k_{rel}) = -0.88$ in Figure 4). Note that the point of attachment to the pyrenyl π -system in alcohol pairs **1c/2c** and **1d/2d** does not have the same consequences in all reactions. For anhydrides **3r–3w** based on the 2-naphthoate substructure, the most negative selectivity values $\ln(k_{rel})$ are observed for the 1-pyrenyl alcohols **1d/2d**, but this is not so for the other anhydrides studied here.

How Alcohol Size Influences Selectivity. Why selectivity inversion occurs in reactions combining larger substrates with larger anhydride reagents is not immediately obvious from the selectivity values presented in Figures 3 and 4. One possible reason for the observed effects rests on the assumption that the transition states for reactions of secondary alcohols allow for a better alignment of alcohol and anhydride side chains, either among each other or with the catalyst-derived pyridinium unit. Should this alignment result in increased attractive London dispersion interactions in the respective transition states, then we must expect an actual acceleration of acylation reactions with increasing substrate size. This latter assumption was first tested for anhydride **3f**, whose reactions always prefer the primary over the secondary alcohol. Relative reaction rates for this anhydride are shown in Figure 5a, where the reaction rate for the smallest secondary alcohol **1a** is set to 1.0 as the reference for all alcohol substrates. Increasing the side chain in secondary alcohol **1a** to 2-naphthyl (**1b**) and 2-pyrenyl (**1c**) accelerates the reaction rate to $k_{rel}(\mathbf{1b}) = 3.8$ and $k_{rel}(\mathbf{1c}) = 10.3$

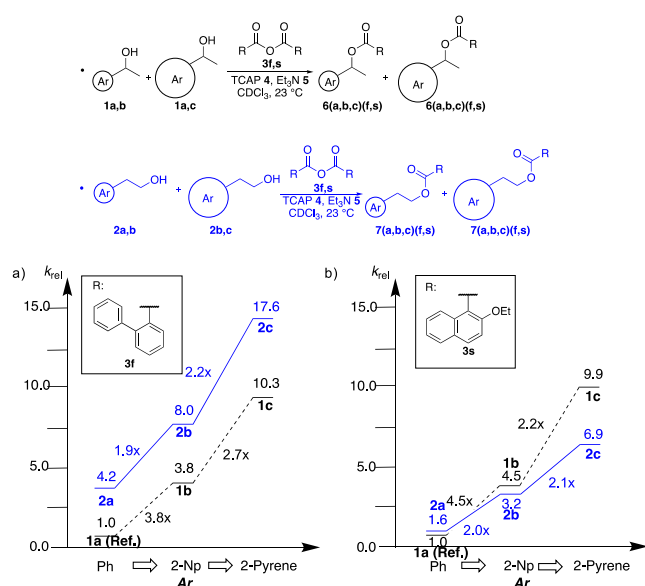


Figure 5. Relative rate constant k_{rel} for competition experiments between secondary alcohols **1a–c** (black, dashed line) and primary alcohols **2a–c** (blue, plain line) with (a) anhydride **3f**, and (b) anhydride **3s**.

(dashed line in Figure 5a). Reactions of the respective primary alcohols are faster in all cases (solid line in Figure 5a), as is already apparent from $k_{rel}(\mathbf{2a}) = 4.2$ for 2-phenylethanol (**2a**). However, the speedup achieved through the increase of the side chain is systematically smaller now with $k_{rel}(\mathbf{2b}) = 8.0$ and $k_{rel}(\mathbf{2c}) = 17.6$. Even if we accept that the rate accelerations observed here for alcohols carrying larger π -system are not solely due to increased attractive London dispersion interactions in the acylation transition states, we nevertheless note that these factors benefit secondary alcohols more than primary ones. What, then, is the situation for anhydrides where inverted selectivities are observed? This was explored for anhydride **3s**, for which reaction rates for the same alcohols as before are assembled in Figure 5b. The reaction rate for secondary alcohol **1a** is again set to $k_{rel}(\mathbf{1a}) = 1.0$ and chosen as the reference for all other alcohols. Increasing the side-chain size from phenyl to 2-naphthyl and 2-pyrenyl, we again note an increase in the reaction rate to $k_{rel}(\mathbf{1b}) = 4.5$ and $k_{rel}(\mathbf{1c}) = 9.9$ (dashed line in Figure 5b). Comparison of these results to those obtained for anhydride **3f** in Figure 5a shows that size effects in secondary alcohols are more or less comparable for both anhydrides. In contrast, a rather different behavior is observed for the respective primary alcohols, the smallest member of this group **2a** reacting only 1.6 times faster than **1a**. Increasing side-chain size again leads to an increase in reaction rate and $k_{rel}(\mathbf{2c}) = 6.9$ (solid line in Figure 5b). But the small selectivity difference between the phenyl substituted alcohols **1a/2a** and the smaller rate accelerations for the primary as compared to the secondary alcohols now lead to the inversion of selectivity already observed in Figures 3 and 4. In qualitative terms, this finding can be rationalized by the spatial disposition and alignment of the alcohol substituents with the pyridinium surface as shown in the schematic transition structure in Figure 1b.

The Influence of Reaction Conditions on Selectivity.

How the experimentally determined selectivities react to changes in the reaction conditions such as catalyst concentration, choice of auxiliary base, choice of solvent, and the reaction temperature was studied for the 2-naphthyl alcohols

1b/2b with *ortho*-phenylbenzoic anhydride **3f** and/or the 1-(2-butoxy)naphthoic anhydride **3t**. In contrast to the recently studied DMAP-mediated silylation reactions,¹⁵ the k_{rel} values are here found to be almost independent of solvent polarity. A similar k_{rel} was also observed when using different concentrations of catalyst TCAP (from 1 to 20 mol %) or replacing the Et_3N auxiliary base with the sterically more demanding Hünig base (see Supporting Information). Variations of the catalyst concentration and possible background reactivity were also studied for alcohol system **1a/2a** in its reaction with benzoic anhydride (**3a**). Similar values of $\ln(k_{rel}) = 2.0$ were observed for different concentrations of **4**, while the much slower background reaction proceeds with $\ln(k_{rel}) = 3.28$. Temperature effects were explored for the reaction of alcohols **1b/2b** with anhydride **3f** in the temperature range from $-10\text{ }^\circ\text{C}$ to $+40\text{ }^\circ\text{C}$. The relative rate $k_{rel}(\mathbf{2b}/\mathbf{1b})$ shows very little variation in this temperature range, and analysis through the Eyring equation indicates a difference in activation enthalpy and entropy of -0.3 kJ mol^{-1} and $-7.4\text{ J K}^{-1}\text{ mol}^{-1}$, respectively. Slightly larger temperature effects were found for anhydride **3t**, where the differences in activation enthalpy and entropy amount to -4.5 kJ mol^{-1} and of $-10.3\text{ J K}^{-1}\text{ mol}^{-1}$ (see Supporting Information).

Theoretical Analysis of Reaction Pathways. In how far the qualitative picture of side-chain/catalyst alignment shown in Figure 1 and supported by the rate studies presented in Figures 3–5 is also reinforced by quantum chemical calculations was explored for the TCAP-mediated reaction of **1a/2a** with anhydride **3f** in chloroform as the solvent. The free energy surface calculated for secondary alcohol **1a** at the SMD-(CHCl_3)/DLPNO-CCSD(T)/def2-TZVPP//SMD-(CHCl_3)/B3LYP-D3/6-31+G(d) level of theory¹⁶ is shown in Figure 6 (for details, see Supporting Information). In line with earlier theoretical studies, catalyst **4** is here assumed to act as a Lewis rather than a Brønsted base.^{12d,17} It is furthermore assumed that the role of the auxiliary base Et_3N is restricted to the out-of-cycle regeneration of protonated catalysts. This assumption has been confirmed in earlier related studies.^{12d} Initial reaction of anhydride **3f** with catalyst **4** and formation of the acylpyridinium intermediate **INT1** proceeds through transition state **TS1** with a free energy barrier of $\Delta G_{298}^\ddagger = +79.3\text{ kJ mol}^{-1}$. After incorporation of alcohol **1a** through intermediate **INT2**, the actual acyl transfer step occurs in transition state **TS2·1a** located $+88.7\text{ kJ mol}^{-1}$ above the separate reactants. Transition state **TS2·1a** is characterized by a combined carboxylate-assisted deprotonation and nucleophilic attack of the alcohol to the carboxylic center and represents the highest free energy point along the reaction coordinate. The tetrahedral intermediate **INT3** encountered when following down the reaction pathway from **TS2·1a** is almost isoenergetic with **TS3·1a** ($+62.6\text{ kJ mol}^{-1}$), which describes cleavage of the C–N bond and thus the departure of the TCAP moiety from the ester product **6af**. Formation of this latter species together with free catalyst **4** and acid **8f** is calculated to be exergonic by -24.7 kJ mol^{-1} . We also computed the related rate-determining benzyl transfer step of the TCAP-catalyzed esterification reaction of primary alcohol **2a** with anhydride **3f** (see Supporting Information for details). The free energy barrier for the acylation of primary alcohol **2a** through transition state **TS2·2a** is found to be $+13.9\text{ kJ mol}^{-1}$ lower than the barrier for acylation of secondary alcohol **1a** through state **TS2·1a**. This difference is in qualitative agreement with the experimentally found faster acylation of primary alcohol **2a** as compared to secondary alcohol **1a**. The structures of transition states **TS2·1a**

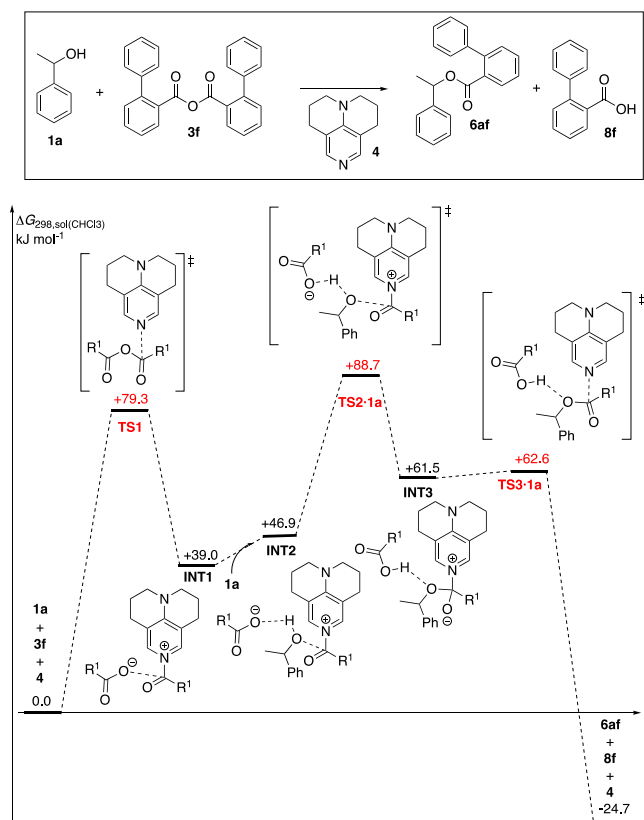


Figure 6. Free energy profile for the Lewis base-catalyzed reaction of alcohol **1a** with benzoic anhydride derivative **3f** and TCAP (**4**) as the catalyst.

and **TS2-2a** (Figure 7a) are both characterized by a triple “sandwich” conformation between the catalyst-derived pyridinium ring system (red), the phenyl groups of the alcohol moiety (green), and the *ortho*-substituent of the anhydride (blue). The carboxylate counterion acts as a clamp through hydrogen bonding interactions with the alcohol hydroxyl group and with one of the *ortho*-hydrogen atoms of the pyridinium ring system. In structural terms, the transition state **TS2-2a** for the reaction of primary alcohol **2a** is slightly more compact as compared to transition state **TS2-1a** as can be seen in the lengths of the forming C–O bond (196.3 vs 200.4 pm) as well as the distances for the cleaving O–H bond (134.4 vs 138.6 pm). The contact between the alcohol phenyl substituent and the TCAP ring system is clearly tighter in **TS2-1a** than in **TS2-2a** as is visible in the distances N1–C (325.4 vs 376.8 pm) and N–C (414.6 vs 486.3 pm). The rate-determining benzyl transfer step of the TCAP-catalyzed esterification reaction of primary naphthyl alcohol **2b** and secondary naphthyl alcohol **1b** with anhydride **3w** was also computed as an example for reactions with inverted selectivity (see Supporting Information for full details). Transition state **TS2-1b** for the reaction of secondary alcohol **1b** is located +77.1 kJ mol⁻¹ above the separate reactants and thus +12.0 kJ mol⁻¹ lower than transition state **TS2-2b** for the reaction of primary alcohol **2b** ($\Delta G_{298}^{\ddagger} = +89.1$ kJ mol⁻¹, Figure 7b). This is in qualitative agreement with the relative rate data shown in Figure 4. Again a “triple sandwich” conformation between the catalyst-derived pyridinium ring system (red), the naphthyl group of the alcohol (green), and the *ortho*-substituent of the anhydride (blue) is dominating the structures of **TS2-1b** and **TS2-2b**. As illustrated through the selected C–C and N–N

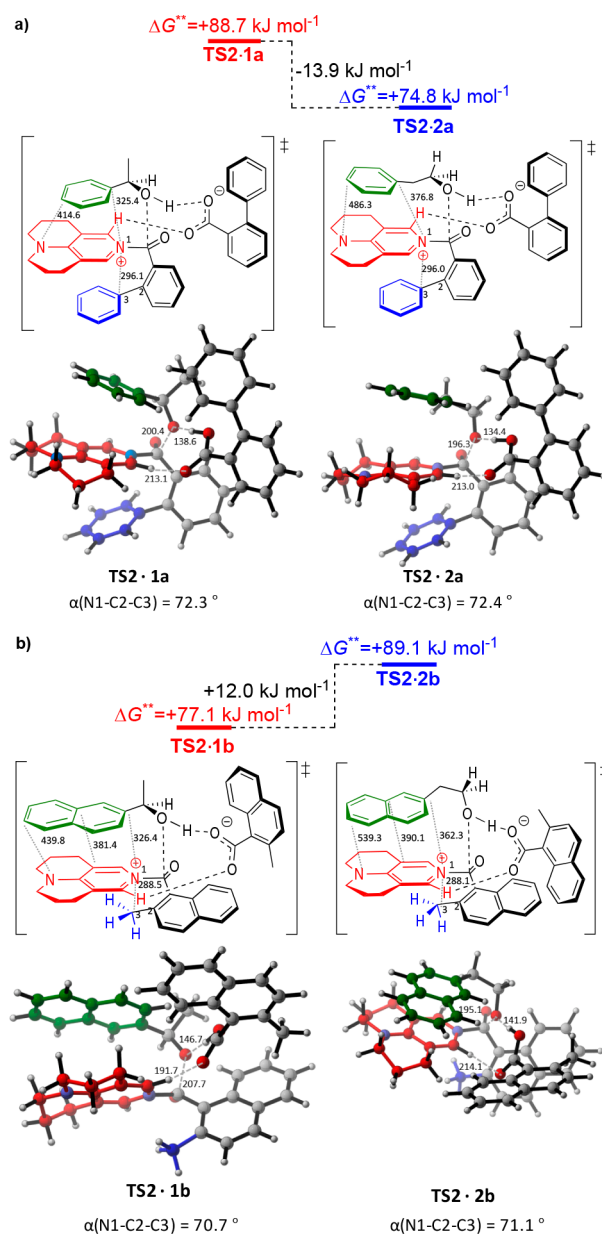


Figure 7. Computed transition structures involving (a) the secondary alcohol **1a** (**TS2-1a**) and the primary alcohol **2a** (**TS2-2a**) with anhydride **3f** and (b) the secondary alcohol **1b** (**TS2-1b**) and the primary alcohol **2b** (**TS2-2b**) with anhydride **3w**. Distances are given in pm.¹⁸

bond distances shown in Figure 7b, the contact between the naphthyl side chain and the TCAP ring system is tighter in **TS2-1b** than in **TS2-2b**. That substantial noncovalent interactions (NCIs) exist between these fragments is easily visible in the respective NCIs plots based on analysis of the reduced energy gradients (see Supporting Information for details).¹⁹ What makes the above transition states triple sandwich structures is the anhydride-derived methyl substituent as indicated by the comparatively short pyridine N1, methyl C3 distances of 288.5 pm in **TS2-1b** and 288.1 pm in **TS2-2b**. A final comment should be made on the calculated barriers for alcohols **1b/2b**, which are slightly higher as compared to those for **1a/2a**, despite the more favorable stacking interactions in the former. This implies that the more highly substituted anhydride **3w** leads to intrinsically higher reaction barriers than anhydride **3f**.

Structure-Selectivity Relationships. The anhydride reagents employed here play the dual role of Brønsted base and acylation donor, as is readily seen from the transition state structures in Figure 7. We, therefore, wondered whether a quantitative relationship can be identified between anhydride properties and the observed chemoselectivities. To this end, the conformational space of all anhydrides shown in Figure 2 was explored at the SMD(CHCl₃)/B3LYP-D3/6-31+G(d) level of theory.^{16a,d,e,gh} From the experimental data presented in Figure 3, it is apparent that the electronic nature and size of the *ortho*-substituents present in the acid anhydrides modulate the experimental k_{rel} values. We have therefore selected several electronic and geometrical parameters such as Charton values of the anhydride side chains and characteristics of the anhydride core region (NPA atomic charges, vibrational frequencies and bond lengths of the C–O double bonds, dihedral angles) and explored their ability to predict the experimentally observed selectivity values in multiparameter models without finding a strict guideline (for full details, see Supporting Information). Analyzing the computed structures of the energetically best conformations, we find that anhydrides favoring the acylation of the secondary alcohols are characterized by a twisted conformation, where both pendant aromatic surfaces are interacting with each other (for full details, see Supporting Information). This implies that anhydrides with DED *ortho*-substituents and more strongly deformed anhydride core structures lead to preferential transformation of the secondary alcohol **1b**.

How Various Factors Contribute to Overall Results.

The most relevant factor leading to faster acylation rates for secondary as compared to primary alcohols is substrate size. This is easily seen from the kinetic data in Figure 5, where growing the alcohol side chain from phenyl to pyrenyl leads to much larger rate increases for secondary alcohols than for primary ones. Why acylation rates respond so favorably to system size is readily understood from the calculated transition states shown in Figure 7 or, more simply, from the corresponding cartoon in Figure 1b: alcohol side chains are stacked directly on top of the catalyst-derived pyridinium π -system due to favorable electrostatic and London dispersion interactions. More detailed structural analysis indicates that alignment is better for secondary than for primary alcohols, providing a logical basis for the observed size effects. How the choice of anhydrides impacts the balance between acylation rates of primary and secondary alcohols is easily rationalized on the basis of reaction kinetics but more difficult to understand in structural terms. The kinetic data shown in Figure 5 for the smallest alcohol substrates (where size effects are not yet dominant) simply show that “noninverting” anhydrides are those that preserve the intrinsic kinetic advantage of primary alcohols over secondary ones. Once this difference becomes small (e.g., for highly substituted anhydride **3s**), a systematic increase in substrate size will lead to inverted reactivities. What, then, is it in the anhydride structure that leads to a reduction of the intrinsic reactivity benefit of primary over secondary alcohols? Results from our structure-selectivity study point to absolute steric bulk and deformation (or twisting) of the anhydride core structure are important parameters. Both factors seem to increase the reaction barriers for alcohol acylation by burdening the respective transition states with (repulsive) steric bulk. This burden appears to impact reactions of primary alcohols more than those of secondary ones.

CONCLUSION

In summary, we have determined the relative acylation rates between primary and secondary alcohols bearing sizable aromatic surfaces with acid anhydride derivatives by performing 1:1 competition experiments in the presence of catalytic amounts of TCAP (**4**). Among the twenty-six acid anhydrides tested in the competition reaction between 2- and 1-(1-naphthyl)ethanol substrates **2b/1b**, a preference for acylation of the secondary alcohol **1b** was found for 2,6-disubstituted benzoic anhydrides carrying at least one methyl group and for all 2-substituted 1-naphthyl anhydrides. Compared to the reaction with benzoic anhydride **3a**, this represents a selective acceleration of the acylation of secondary alcohol **1b** of up to seven times. For alcohols **1a/2a** carrying a smaller phenyl substituent, most of this selective acceleration cannot be detected, while for alcohol pairs **1c/2c** and **1d/2d** carrying larger 2- or 1-pyrenyl substituents, the selective acylation of secondary alcohols becomes even more pronounced. An important finding of this study is that acylation rates of alcohols increase together with the size of the attached π -systems and that this increase is actually larger for secondary as compared to primary alcohols. Further work is currently underway in our laboratories to explore the utility of these catalyst/anhydride combinations in transformations of structurally extended polyol substrates.

EXPERIMENTAL SECTION

General Information. All reactions sensitive to air and moisture were performed under a nitrogen atmosphere, and the glassware as well as magnetic stir bars were dried overnight in a dry oven at 110 °C. An oil bath was used for reactions that require heating. CDCl₃, Et₃N, and CH₂Cl₂ were freshly distilled from calcium hydride (CaH₂) under a nitrogen atmosphere. All reagents were purchased from the companies TCI, Sigma-Aldrich, ABCR, or Acros and used without further purification, if not mentioned otherwise. The aromatic alcohols **1a,b,e** and **2a,e**, the acid anhydrides **3a,o**, and TCAP (**4**) have been obtained from commercial sources. All air- or water-sensitive reagents were stored under nitrogen. If not further specified, solvents were obtained from the companies Acros Organics, Sigma-Aldrich, or Merck and purified by distillation in a rotary evaporator. THF and MeCN for solvent competition experiments were purchased “extra-dry” and used without further purification. Trifluorotoluene was stored over a molecular sieve (4 Å). Silica gel for column chromatography was purchased from Acros Organics (mesh 35–70). Thin-layer chromatography was performed by using TLC plates purchased from Merck (silica gel 60 F254, thickness 0.2 mm). Preparative layer chromatography (PLC) was carried out using Merck TLC glass plates (silica gel 60 F254, thickness 2 mm). All ¹H NMR spectra were recorded by Varian Mercury 200, Varian INOVA 400, and 600 machines in CDCl₃ or DMSO-*d*₆ at 400 or 600 MHz at 23 °C. All ¹³C{¹H} NMR spectra were recorded, respectively, at 101 and 151 MHz. All ¹⁹F NMR spectra were recorded at 377 MHz. The chemical shifts are reported in ppm (δ), relative to the resonance of CDCl₃ at δ = 7.26 ppm and DMSO-*d*₆ at δ = 2.50 ppm for ¹H and for ¹³C{¹H} relative to the resonance of CDCl₃ δ = 77.16 ppm. Spectra were imported and processed in the MestreNova 10.0.2 program. HRMS spectra were obtained by using a Thermo Finnigan LTQ FT machine of the MAT 95 type with a direct exposure probe (DEP) and electron impact ionization (EI, 70 eV). For ESI measurements, a Thermo Finnigan LTQ FT Ultra Fourier Transform Ion Cyclotron Resonance machine was used. IR spectra were measured on a PerkinElmer FT-IR BX spectrometer mounting an ATR technology module. Melting points were measured at a Stuart SMP10 and are stated uncorrected. Crystallographic measurements were done using an Oxford Diffraction XCalibur with Saphir CCD detector and a molybdenum-K α source (λ = 0.71073) with a concentric circle kappa-device. Structures were resolved using SHELXS or SIR97

and refined with SHELXS. Crystals obtained from compounds **3f**, **1l**–**p**, **r**–**w**, **6aw**, **7ar**, **7aw**, **7bv**, **7ca**, **7cs**, **6da**, **6dr**, and **6du** were grown from a CDCl_3 solution in an NMR tube at an ambient temperature.

Competition Experiments. Three different CDCl_3 stock solutions were prepared under nitrogen. Stock solution A contained the secondary alcohol **1a** and primary alcohol **2a** each at a concentration of 0.05 M. Stock B contained anhydride **3a**–**z** (0.1 M), while stock solution C consisted of a 0.15 M Et_3N and catalyst TCAP (**4**) at a concentration of 0.005 M. Stock solution B was diluted in four discrete steps. The concentrations of the new solutions were fixed at 20, 35, 50, and 70% of the initial stock solution B. Under nitrogen, 0.4 mL of stock solution A, 0.4 mL of stock solution C, and 0.4 mL of stock solution B1–4 were transferred to a GC vial by using a Hamilton syringe. The GC vial was then capped under nitrogen and placed in the GC vial holder with stirring. The competition experiment was considered finished when the reaction with the highest anhydride concentration (GC vial 4) was over. The reaction was monitored by ^1H NMR spectroscopy.

Synthesis of Aryl Alcohols 1 and 2. 2-(Naphthalen-2-yl)ethan-1-ol **2b**. In a Schlenk flask, 2-(naphthalen-2-yl)acetic acid (1.00 g, 5.35 mmol, 1.0 equiv) was dissolved in THF (25 mL) and cooled down to 0 °C. LiAlH_4 (1.02 g, 26.8 mmol, 5.0 equiv) was carefully added and the reaction mixture was stirred at room temperature for 12 h. The reaction mixture was quenched by adding 2 M NaOH solution and water. The water phase was extracted by EtOAc (3×15 mL) and CH_2Cl_2 (3×15 mL). The combined organic phase was dried over MgSO_4 , filtered, and concentrated in a vacuum. After purification by column chromatography on silica (isohexane/EtOAc 8:2), **2b** (782 mg, 85%) was obtained as a white solid: mp 68–69 °C; ^1H NMR (400 MHz, CDCl_3) δ 7.85–7.77 (m, 3H, Ar), 7.69 (s, 1H, Ar), 7.51–7.41 (m, 2H, Ar), 7.37 (dd, $J = 8.4, 1.7$ Hz, 1H, Ar), 3.96 (q, $J = 6.0$ Hz, 2H, CH_2), 3.04 (t, $J = 6.5$ Hz, 2H, CH_2), 1.43 (s, 1H, OH) ppm; $^{13}\text{C}\{^1\text{H}\}$ NMR (101 MHz, CDCl_3) δ 136.08, 133.72, 132.44, 128.42, 127.79, 127.63, 127.62, 127.52, 126.25, 125.62, 63.70, 39.51 ppm; HRMS (EI) m/z [M] $^+$ calcd for $\text{C}_{12}\text{H}_{12}\text{O}$ 172.0888, found 172.0880. The $^1\text{H}/^{13}\text{C}\{^1\text{H}\}$ NMR spectra are in full agreement with them reported in literature.²⁰

1-(Pyren-1-yl)ethan-1-ol **1d**. In a Schlenk flask, pyrene-1-carbaldehyde (2.00 g, 8.69 mmol, 1.0 equiv) was dissolved in THF (11 mL). After cooling to 0 °C, MeMgCl (3 M in THF, 5.80 mL, 17.4 mmol, 2.0 equiv) was added dropwise, and the reaction mixture was stirred at room temperature for 12 h. The mixture was then quenched with saturated aqueous solution of NH_4Cl and extracted with CH_2Cl_2 (3×30 mL). The combined organic phase was washed with brine, dried over MgSO_4 , filtered, and concentrated in a vacuum. After purification by column chromatography on silica (isohexane/EtOAc 8:2), **1d** (1.82 g, 85%) was obtained as a brown solid: mp 108–110 °C; ^1H NMR (400 MHz, CDCl_3) δ 8.32 (d, $J = 9.3$ Hz, 1H, Ar), 8.24–8.16 (m, 4H, Ar), 8.09 (d, $J = 9.3$ Hz, 1H, Ar), 8.04 (s, 2H, Ar), 8.01 (t, $J = 7.6$ Hz, 1H, Ar), 5.97 (q, $J = 6.4$ Hz, 1H, CH), 2.15 (s, 1H, OH), 1.77 (d, $J = 6.5$ Hz, 3H, Me) ppm; $^{13}\text{C}\{^1\text{H}\}$ NMR (101 MHz, CDCl_3) δ 139.17, 131.48, 130.74, 130.70, 127.66, 127.56, 127.32, 127.25, 126.01, 125.31, 125.18, 125.10, 125.01, 124.92, 122.55, 122.48, 67.40, 25.16; HRMS (EI) m/z [M] $^+$ calcd for $\text{C}_{18}\text{H}_{14}\text{O}$ 246.1045, found 246.1039. The $^1\text{H}/^{13}\text{C}\{^1\text{H}\}$ NMR spectra are in full agreement with them reported in literature.¹¹

2-(Pyren-1-yl)ethan-1-ol **2d**. In a Schlenk flask, 2-(pyren-1-yl)acetic acid (200 mg, 762 μmol , 1.0 equiv) was dissolved in THF (4 mL) and cooled down to 0 °C. LiAlH_4 (144 mg, 3.81 mmol, 5.0 equiv) was carefully added and the reaction mixture was stirred at room temperature for 48 h. The reaction mixture was then quenched by adding 2 M NaOH solution and water. The water phase was extracted with EtOAc (3×10 mL) and CH_2Cl_2 (3×30 mL). The combined organic phase was dried over MgSO_4 , filtered, and concentrated in a vacuum. After purification by column chromatography on silica (isohexane/EtOAc 8:2), **2d** (180 mg, 95%) was obtained as a brown solid: mp 100–102 °C; ^1H NMR (400 MHz, CDCl_3) δ 8.32 (d, $J = 9.3$ Hz, 1H, Ar), 8.21–8.17 (m, 2H, Ar), 8.14 (dd, $J = 8.5, 5.3$ Hz, 2H, Ar), 8.05 (s, 2H, Ar), 8.01 (t, $J = 7.6$ Hz, 1H, Ar), 7.92 (d, $J = 7.8$ Hz, 1H, Ar), 4.11 (q, $J = 6.5$ Hz, 2H, CH_2), 3.64 (t, $J = 6.7$ Hz, 2H, CH_2), 1.43 (t, $J = 5.8$ Hz, 1H, OH) ppm; $^{13}\text{C}\{^1\text{H}\}$ NMR (101 MHz, CDCl_3) δ 132.54,

131.56, 131.01, 130.47, 129.41, 128.10, 127.74, 127.60, 127.13, 126.09, 125.30, 125.22, 125.08, 125.03, 125.01, 123.33, 64.02, 36.83 ppm; HRMS (EI) m/z [M] $^+$ calcd for $\text{C}_{18}\text{H}_{14}\text{O}$ 246.1045, found 246.1047. The $^1\text{H}/^{13}\text{C}\{^1\text{H}\}$ NMR spectra are in full agreement with them reported in literature.²¹

Pyrene-2-carboxylic Acid 11. The synthesis of **11** is based on the procedure reported by Davis et al.²² 1-(*o*-Carboxybenzoyl)pyrene **9**. In a round-bottom flask, pyrene (5.00 g, 24.7 mmol, 1.0 equiv) and phthalic anhydride (3.66 g, 24.7 mmol, 1.0 equiv) were suspended in CH_2Cl_2 (150 mL). AlCl_3 (8.34 g, 61.8 mmol, 1.0 equiv) was added to the reaction mixture under a N_2 atmosphere. The reaction mixture was heated under reflux for 3 h. After concentration of the mixture, the residue was cooled to 0 °C and suspended in H_2O (250 mL). Conc. HCl was added to the suspension until the pH value of 0–1 was reached. The solid was isolated by filtration, washed with water, and dried in a vacuum. The solid was suspended in glacial acetic acid (250 mL) and heated to 130 °C for 5 min. After the insoluble material was removed by hot filtration, ice water (500 mL) was added to the filtrate. The resulting solid was isolated by filtration, washed with ice water several times, and dried in a vacuum. Compound **9** (7.50 g, 87%) was isolated as a yellow solid and used in the next step without any further purification or characterization.

1,2-Phthaloylpyrene **10**. In a round-bottom flask, **9** (7.5 g, 21.4 mmol, 1.0 equiv), PCl_5 (6.70 g, 32.1 mmol, 1.5 equiv), and AlCl_3 (4.30 g, 32.1 mmol, 1.5 equiv) were suspended in chlorobenzene (140 mL) under N_2 atmosphere and heated under reflux for 2.5 h. After concentration of the reaction mixture, the residue was cooled to 0 °C and suspended in H_2O (200 mL). The precipitate was isolated by filtration and dried in a vacuum. Compound **10** (7.30 g, quant.) was obtained as a red solid and used in the next step without any further purification or characterization.

Pyrene-2-carboxylic Acid 11. In a round-bottom flask, **10** (5.00 g, 15.0 mmol, 1.0 equiv) and potassium *tert*-butoxide (34.0 g, 300 mmol, 20.0 equiv) were suspended in 1,2-dimethoxyethane (72 mL), and H_2O (1.62 mL, 90.3 mmol, 6.0 equiv) was added to the suspension. After heating under reflux for 6 h, the reaction mixture was concentrated in a vacuum. The residue was cooled to 0 °C, suspended in H_2O (250 mL), and acidified to a pH 1–2 with conc. HCl. The resulting solid was isolated by filtration and dried in a vacuum. Compound **11** (4.00 g, 87%) was obtained as a light gray solid and used in the next step without any further purification or characterization.

1-(Pyren-2-yl)ethan-1-ol **12**. In a Schlenk flask, **11** (1.00 g, 4.06 mmol, 1.0 equiv) was dissolved in THF (20 mL) and cooled to 0 °C. MeLi (1.6 M in Et_2O , 10.0 mL, 16.2 mmol, 4.0 equiv) was dropwise added, and the mixture was stirred at room temperature for 48 h. After cooling to 0 °C, TMSCl (10.3 mL, 81.2 mmol, 20.0 equiv) and 1 M HCl solution (30 mL) was added. The mixture was extracted with CH_2Cl_2 (3×40 mL). The combined organic phase was washed with brine, dried over MgSO_4 , filtered, and concentrated in a vacuum. After purification by column chromatography on silica (isohexane/EtOAc 8:2), **12** (510 mg, 56%) was obtained as a brown solid: mp 139–141 °C; ^1H NMR (400 MHz, CDCl_3) δ 8.75 (s, 2H, Ar), 8.22 (d, $J = 7.6$ Hz, 2H, Ar), 8.17–8.10 (m, 4H, Ar), 8.07 (t, $J = 7.6$ Hz, 1H, Ar), 2.91 (s, 3H, Me) ppm. The ^1H NMR spectrum is in full agreement with that reported in literature.²³

1-(Pyren-2-yl)ethan-1-ol **1c**. In a Schlenk flask, **12** (320 mg, 1.31 mmol, 1.0 equiv) was dissolved in MeOH (16 mL) and CH_2Cl_2 (until obtaining a clear solution). The reaction mixture was cooled to 0 °C, and NaBH_4 (317 mg, 8.38 mmol, 6.4 equiv) was added. After stirring at room temperature for 12 h, the mixture was quenched by adding 2 M HCl solution and extracted with CH_2Cl_2 (3×20 mL). The combined organic phase was dried over MgSO_4 , filtered, and concentrated in a vacuum. After purification by column chromatography on silica (isohexane/EtOAc 8:2), **1c** (291 mg, 90%) was obtained as a brown solid: mp 138–139 °C; ^1H NMR (400 MHz, CDCl_3) δ 8.20–8.14 (m, 4H, Ar), 8.09–8.02 (m, 4H, Ar), 8.02–7.97 (m, 1H, Ar), 5.33 (q, $J = 6.4$ Hz, 1H, CH), 2.18 (s, 1H, OH), 1.72 (d, $J = 6.5$ Hz, 3H, Me) ppm; $^{13}\text{C}\{^1\text{H}\}$ NMR (101 MHz, CDCl_3) δ 143.66, 131.39, 131.12, 127.77, 127.48, 125.93, 125.16, 124.64, 124.23, 121.95, 71.04, 26.10 ppm; HRMS (EI) m/z [M] $^+$ calcd for $\text{C}_{18}\text{H}_{14}\text{O}$ 246.1045, found 246.1040.

The ^1H NMR spectrum is in full agreement with that reported in literature.²⁴

2-(Pyren-2-yl)acetic Acid 14. The synthesis of **14** is based on the Willgerodt reaction after Daub et al.²⁵ A mixture of **12** (510 mg, 2.09 mmol, 1.0 equiv), sulfur (167 mg, 5.22 mmol, 2.5 equiv), and morpholine (2.60 mL) were heated at 125 °C for 6 h. After cooling down to room temperature, the product was precipitated by adding MeOH. After filtration, the mixture was recrystallized in ethanol. 1-Morpholino-3-(pyren-2-yl)ethane-1-thione **13** (600 mg, 83%) was obtained as a brown solid and used in the next step without any further purification or characterization.

2-(Pyren-2-yl)acetic Acid 14. A mixture of **13** (600 mg, 1.73 mmol, 1.0 equiv), glacial acetic acid (8.6 mL), and conc. HCl (4.3 mL) was heated under reflux for 8 h. After cooling down to room temperature, conc. HCl was added again, and the precipitate was filtered. Compound **14** (200 mg, 43%) was obtained as a brown solid and used in the next step without any further purification or characterization.

2-(Pyren-2-yl)ethan-1-ol 2c. In a Schlenk flask, **14** (200 mg, 768 μmol , 1.0 equiv) was dissolved in THF (4 mL) and was cooled down to 0 °C. LiAlH_4 (145 mg, 3.84 mmol, 5.0 equiv) was carefully added and the reaction mixture was stirred at room temperature for 48 h. The reaction mixture was quenched by adding 2 M NaOH solution and water. The water phase was extracted by EtOAc (3 \times 10 mL) and CH_2Cl_2 (3 \times 30 mL). The combined organic phase was dried over MgSO_4 , filtered, and concentrated in a vacuum. After purification by column chromatography on silica (isohexane/EtOAc 8:2), **2c** (130 mg, 69%) was obtained as a brown solid: mp 141–142 °C; ^1H NMR (400 MHz, CDCl_3) δ 8.18 (d, J = 7.6 Hz, 2H, Ar), 8.10–7.96 (m, 7H, Ar), 4.09 (t, J = 6.5 Hz, 2H, CH_2), 3.31 (t, J = 6.5 Hz, 2H, CH_2), 1.51 (s, 1H, OH) ppm; $^{13}\text{C}\{^1\text{H}\}$ NMR (101 MHz, CDCl_3) δ 136.40, 131.54, 131.04, 127.80, 127.23, 125.84, 125.65, 125.18, 124.67, 123.64, 64.22, 39.86 ppm; IR (ATR) ν (cm^{-1}) 3307, 2949, 1599, 1423, 1282, 1173, 1045, 878, 840, 815, 700; HRMS (EI) m/z [M] $^+$ calcd for $\text{C}_{18}\text{H}_{14}\text{O}$ 246.1045, found 246.1045.

1-(Anthracen-2-yl)ethan-1-ol 1f. In a Schlenk flask, 1-(anthracen-2-yl)ethan-1-one (1.30 g, 5.90 mmol, 1.0 equiv) was dissolved in MeOH (74 mL) and CH_2Cl_2 (until obtaining a clear solution). The reaction mixture was cooled to 0 °C and NaBH_4 (2.23 g, 59.0 mmol, 10.0 equiv) was added. After stirring at room temperature for 12 h, the mixture was quenched by adding 2 M HCl solution and extracted with CH_2Cl_2 (3 \times 20 mL). The combined organic phase was dried over MgSO_4 , filtered, and concentrated in a vacuum. After purification by column chromatography on silica (isohexane/EtOAc 8:2), **1f** (588 mg, 45%) was obtained as a brown solid: mp 163–165 °C; ^1H NMR (400 MHz, CDCl_3) δ 8.41 (s, 2H, Ar), 8.03–7.97 (m, 3H, Ar), 7.95 (s, 1H, Ar), 7.53–7.43 (m, 3H, Ar), 5.11 (qd, J = 6.5, 3.4 Hz, 1H, CH), 1.93 (d, J = 3.4 Hz, 1H, OH), 1.62 (d, J = 6.5 Hz, 3H, Me) ppm; $^{13}\text{C}\{^1\text{H}\}$ NMR (101 MHz, CDCl_3) δ 142.56, 132.07, 131.84, 131.60, 131.37, 128.86, 128.32, 128.24, 126.39, 126.21, 125.57, 125.46, 123.88, 123.75, 70.78, 24.96 ppm. IR (ATR) ν (cm^{-1}) 3273, 2967, 1625, 1533, 1291, 1152, 1067, 998, 955, 906, 891, 720; HRMS (EI) m/z [M] $^+$ calcd for $\text{C}_{16}\text{H}_{14}\text{O}$ 222.1045, found 222.1031.

2-(Anthracen-2-yl)acetic Acid 16 (Synthesis of 16 is Based on the Procedure Reported by Daub et al.²⁵) Morpholino-3-(anthracen-2-yl)ethane-1-thione 15. A mixture of 1-(anthracen-2-yl)ethan-1-one (2.00 g, 9.08 mmol, 1.0 equiv), sulfur (727 mg, 22.7 mmol, 2.5 equiv), and morpholine (12 mL) was heated to 125 °C for 6 h. After cooling down to room temperature, the product was precipitated through the addition of MeOH. After filtration, the mixture was recrystallized from ethanol. Compound **15** (1.90 g, 65%) was obtained as a brown solid and used in the next step without any further purification or characterization.

2-(Anthracen-2-yl)acetic Acid 16. A mixture of **15** (1.90 g, 5.91 mmol, 1.0 equiv), glacial acetic acid (30 mL), and conc. HCl (15 mL) was heated under reflux for 8 h. After cooling down to room temperature, conc. HCl was added again, and the precipitate was filtered. Compound **16** (652 mg, 47%) was obtained as a brown solid and used in the next step without any further purification or characterization.

2-(Anthracen-2-yl)ethan-1-ol 2f. In a Schlenk flask, **16** (650 mg, 2.75 mmol, 1.0 equiv) was dissolved in THF (14 mL) and cooled down to 0 °C. LiAlH_4 (522 mg, 13.8 mmol, 5.0 equiv) was carefully added and the reaction mixture was stirred at room temperature for 48 h. The reaction mixture was quenched by adding 2 M NaOH solution and water. The water phase was extracted with EtOAc (3 \times 10 mL) and CH_2Cl_2 (3 \times 30 mL). The combined organic phase was dried over MgSO_4 , filtered, and concentrated in a vacuum. After purification by column chromatography on silica (isohexane/EtOAc 8:2), **2f** (100 mg, 16%) was obtained as a brown solid: mp 175–177 °C; ^1H NMR (400 MHz, CDCl_3) δ 8.39 (d, J = 14.7 Hz, 2H, Ar), 8.04–7.94 (m, 3H, Ar), 7.84 (s, 1H, Ar), 7.47 (t, J = 4.8 Hz, 2H, Ar), 7.36 (dd, J = 8.7, 1.3 Hz, 1H, Ar), 4.00 (t, J = 6.4 Hz, 2H, CH_2), 3.08 (t, J = 6.4 Hz, 2H, CH_2), 1.50 (bs, 1H, OH) ppm; $^{13}\text{C}\{^1\text{H}\}$ NMR (101 MHz, CDCl_3) δ 135.47, 132.05, 131.88, 131.64, 130.83, 128.78, 128.32, 128.24, 127.41, 127.37, 126.19, 125.76, 125.55, 125.34, 63.41, 39.67 ppm; IR (ATR) ν (cm^{-1}) 3322, 1626, 1455, 1039, 892, 700; HRMS (EI) m/z [M] $^+$ calcd for $\text{C}_{16}\text{H}_{14}\text{O}$ 222.1045, found 222.1037.

General Procedure A (GP A, Synthesis of Acid Anhydrides 3): Synthesis of Acetic Anhydride Derivatives 3. In a round-bottom flask, the corresponding carboxylic acid (1.0 equiv), TsCl (0.5 equiv), and K_2CO_3 (1.5 equiv) were dissolved in a 1:1 mixture of MeCN and CH_2Cl_2 and stirred at room temperature for 48 h. The mixture was filtered and washed well with CH_2Cl_2 . After concentration under a vacuum, the anhydride was triturated in *n*-hexane, filtered, and washed in *n*-hexane to obtain the pure anhydride **3**.

2-Methoxybenzoic Anhydride 3b. 2-Methoxybenzoic acid (2.00 g, 13.2 mmol, 1.0 equiv), TsCl (1.25 g, 6.57 mmol, 0.5 equiv), and K_2CO_3 (2.73 g, 19.7 mmol, 1.5 equiv) were dissolved in MeCN (65 mL) and CH_2Cl_2 (65 mL) and synthesized according to GP A. Compound **3b** (788 mg, 42%) was obtained as a white solid: mp 71–73 °C; ^1H NMR (400 MHz, CDCl_3) δ 8.02 (dd, J = 7.8, 1.8 Hz, 1H, Ar), 7.56 (ddd, J = 9.0, 7.5, 1.8 Hz, 1H, Ar), 7.08–6.96 (m, 2H, Ar), 3.86 (s, 3H, Me) ppm; $^{13}\text{C}\{^1\text{H}\}$ NMR (101 MHz, CDCl_3) δ 161.99, 160.28, 135.32, 133.25, 120.48, 118.38, 112.25, 56.03 ppm; HRMS (EI) m/z [M] $^+$ calcd for $\text{C}_{16}\text{H}_{14}\text{O}_5$ 286.0841, found 286.0831. The $^1\text{H}/^{13}\text{C}\{^1\text{H}\}$ NMR spectra are in full agreement with them reported in literature.²⁶

2-Methylbenzoic Anhydride 3c. 2-Methylbenzoic acid (1.00 g, 7.34 mmol, 1.0 equiv), TsCl (700 mg, 3.67 mmol, 0.5 equiv), and K_2CO_3 (1.52 g, 11.0 mmol, 1.5 equiv) were dissolved in MeCN (40 mL) and CH_2Cl_2 (40 mL) and synthesized according to GP A. Compound **3c** (777 mg, 83%) was obtained as a white solid: mp 38–39 °C; ^1H NMR (400 MHz, CDCl_3) δ 8.06 (d, J = 7.7 Hz, 1H, Ar), 7.51 (t, J = 7.0 Hz, 1H, Ar), 7.36–7.28 (m, 2H, Ar), 2.71 (s, 3H, Me) ppm; $^{13}\text{C}\{^1\text{H}\}$ NMR (101 MHz, CDCl_3) δ 163.06, 142.71, 133.71, 132.37, 131.55, 127.94, 126.22, 22.12 ppm; HRMS (EI) m/z [M] $^+$ calcd for $\text{C}_{16}\text{H}_{14}\text{O}_3$ 254.0943, found 254.0943. The $^1\text{H}/^{13}\text{C}\{^1\text{H}\}$ NMR spectra are in full agreement with them reported in literature.²⁶

2-Chlorobenzoic Anhydride 3d. 2-Chlorobenzoic acid (1.50 g, 9.58 mmol, 1.0 equiv), TsCl (913 mg, 4.79 mmol, 0.5 equiv), and K_2CO_3 (1.99 g, 14.4 mmol, 1.5 equiv) were dissolved in MeCN (50 mL) and CH_2Cl_2 (50 mL) and synthesized according to GP A. Compound **3d** (624 mg, 44%) was obtained as a white solid: mp 70–72 °C; ^1H NMR (600 MHz, CDCl_3) δ 8.03 (dt, J = 8.0, 1.1 Hz, 1H, Ar), 7.56–7.50 (m, 2H, Ar), 7.43–7.37 (m, 1H, Ar) ppm; $^{13}\text{C}\{^1\text{H}\}$ NMR (151 MHz, CDCl_3) δ 160.53, 135.28, 134.33, 132.75, 131.81, 128.07, 127.08 ppm; HRMS (EI) m/z [$\text{M} - \text{Cl}$] $^+$ calcd for $\text{C}_{14}\text{H}_9\text{O}_3\text{Cl}$ 259.0162, found 259.0157. The ^1H NMR spectrum is in full agreement with that reported in literature.²⁷

2-Bromobenzoic Anhydride 3e. 2-Bromobenzoic acid (2.00 g, 9.85 mmol, 1.0 equiv), TsCl (938 mg, 4.93 mmol, 0.5 equiv), and K_2CO_3 (2.04 g, 4.93 mmol, 1.5 equiv) were dissolved in MeCN (50 mL) and CH_2Cl_2 (50 mL) and synthesized according to GP A. Compound **3e** (620 mg, 33%) was obtained as a white solid: mp 70–73 °C; ^1H NMR (600 MHz, CDCl_3) δ 8.04–7.98 (m, 1H, Ar), 7.77–7.72 (m, 1H, Ar), 7.47–7.41 (m, 2H, Ar) ppm; $^{13}\text{C}\{^1\text{H}\}$ NMR (151 MHz, CDCl_3) δ 160.93, 135.18, 134.27, 132.76, 129.99, 127.63, 123.18 ppm; HRMS (EI) m/z [$\text{M} - \text{Br}$] $^+$ calcd for $\text{C}_{14}\text{H}_9\text{O}_3\text{Br}$ 302.9657, found 302.9654. The ^1H NMR spectrum is in full agreement with that reported in literature.²⁸

2-Phenylbenzoic Anhydride 3f. 2-Phenylbenzoic acid (2.00 g, 10.1 mmol, 1.0 equiv), TsCl (961 mg, 5.04 mmol, 0.5 equiv), and K_2CO_3 (2.09 g, 15.1 mmol, 1.5 equiv) were dissolved in MeCN (50 mL) and CH_2Cl_2 (50 mL) and synthesized according to GP A. Compound **3f** (1.3 g, 68%) was obtained as a white solid: mp 71–73 °C; 1H NMR (400 MHz, $CDCl_3$) δ 7.54 (td, $J = 7.6, 1.4$ Hz, 1H, Ar), 7.47 (dd, $J = 7.8, 1.3$ Hz, 1H, Ar), 7.40–7.27 (m, 7H, Ar) ppm; $^{13}C\{^1H\}$ NMR (101 MHz, $CDCl_3$) δ 163.32, 143.72, 140.65, 132.62, 131.21, 131.16, 128.69, 128.34, 127.59, 127.26 ppm (one signal is overlapping); IR (ATR) ν (cm^{-1}) 3057, 1789, 1593, 1474, 1199, 1065, 1018, 981, 699; HRMS (EI) m/z $[M]^+$ calcd for $C_{26}H_{18}O_3$ 378.1256, found 378.1237.

2-(4-Methylphenyl)benzoic Anhydride 3g. 2-(4-Methylphenyl)benzoic acid (2.00 g, 9.42 mmol, 1.0 equiv), TsCl (898 mg, 4.71 mmol, 0.5 equiv), and K_2CO_3 (1.95 g, 14.1 mmol, 1.5 equiv) were dissolved in MeCN (50 mL) and CH_2Cl_2 (50 mL) and synthesized according to GP A. Compound **3g** (1.50 g, 78%) was obtained as a white solid: mp 93–95 °C; 1H NMR (400 MHz, $CDCl_3$) δ 7.53 (td, $J = 7.6, 1.4$ Hz, 1H, Ar), 7.47 (dd, $J = 7.8, 1.4$ Hz, 1H, Ar), 7.35–7.27 (m, 2H, Ar), 7.22–7.15 (m, 4H, Ar), 2.36 (s, 3H, Me) ppm; $^{13}C\{^1H\}$ NMR (101 MHz, $CDCl_3$) δ 163.44, 143.79, 137.84, 137.38, 132.53, 131.20, 131.17, 129.08, 128.80, 128.61, 126.98, 21.32 ppm; IR (ATR) ν (cm^{-1}) 2916, 1774, 1598, 1476, 1207, 1057, 1001, 819, 773, 692; HRMS (EI) m/z $[M]^+$ calcd for $C_{28}H_{22}O_3$ 406.1569, found 406.1572.

2,6-Dimethoxybenzoic Anhydride 3k. 2,6-Dimethoxybenzoic acid (2.00 g, 11.0 mmol, 1.0 equiv), TsCl (1.05 g, 5.49 mmol, 0.5 equiv), K_2CO_3 (2.28 g, 16.5 mmol, 1.5 equiv) were dissolved in MeCN (55 mL) and CH_2Cl_2 (55 mL) and synthesized according to GP A. Compound **3k** (998 mg, 52%) was obtained as a white solid: mp 160–161 °C; 1H NMR (400 MHz, $CDCl_3$) δ 7.30 (t, $J = 8.4$ Hz, 1H, Ar), 6.53 (d, $J = 8.4$ Hz, 2H, Ar), 3.83 (s, 6H, Me₂) ppm; $^{13}C\{^1H\}$ NMR (101 MHz, $CDCl_3$) δ 160.94, 158.46, 132.35, 111.76, 104.02, 56.21 ppm; HRMS (EI) m/z $[M]^+$ calcd for $C_{18}H_{18}O_7$ 346.1053, found 346.1043. The $^1H/^{13}C\{^1H\}$ NMR spectra are in full agreement with them reported in literature.²⁹

2,6-Dimethylbenzoic Anhydride 3m. 2,6-Dimethylbenzoic acid (1.00 g, 6.66 mmol, 1.0 equiv), TsCl (634 mg, 3.33 mmol, 0.5 equiv), and K_2CO_3 (1.38 g, 9.99 mmol, 1.5 equiv) were dissolved in MeCN (35 mL) and CH_2Cl_2 (35 mL) and synthesized according to GP A. Compound **3m** (882 mg, 94%) was obtained as a white solid: mp 77–80 °C; 1H NMR (400 MHz, $CDCl_3$) δ 7.23 (t, $J = 7.7$ Hz, 1H, Ar), 7.06 (d, $J = 7.4$ Hz, 2H, Ar), 2.43 (s, 6H, Me₂) ppm; $^{13}C\{^1H\}$ NMR (101 MHz, $CDCl_3$) δ 165.32, 136.00, 131.92, 130.61, 128.12, 20.10 ppm; HRMS (EI) m/z $[M]^+$ calcd for $C_{18}H_{18}O_3$ 282.1256, found 282.1245. The $^1H/^{13}C\{^1H\}$ NMR spectra are in full agreement with them reported in literature.³⁰

2-Fluoro-6-(trifluoromethyl)benzoic Anhydride 3p. 2-Fluoro-6-(trifluoromethyl)benzoic acid (500 mg, 2.40 mmol, 1.0 equiv), TsCl (229 mg, 1.20 mmol, 0.5 equiv), and K_2CO_3 (498 mg, 3.60 mmol, 1.5 equiv) were dissolved in MeCN (12 mL) and CH_2Cl_2 (12 mL) and synthesized according to GP A. Compound **3p** (480 mg, quant.) was obtained as a white solid: mp 76–78 °C; 1H NMR (400 MHz, $CDCl_3$) δ 7.64 (td, $J = 8.1, 4.8$ Hz, 1H, Ar), 7.56 (d, $J = 7.8$ Hz, 1H, Ar), 7.40 (t, $J = 8.4$ Hz, 1H, Ar) ppm; $^{13}C\{^1H\}$ NMR (101 MHz, $CDCl_3$) δ 159.78 (d, $J = 255.1$ Hz), 156.84, 133.18 (d, $J = 8.7$ Hz), 130.08 (q, $J = 33.5$ Hz), 123.85 (q, $J = 273.7$ Hz), 122.45, 120.18 (d, $J = 21.4$ Hz), 118.73 (d, $J = 20.0$ Hz) ppm; ^{19}F NMR (188 MHz, $CDCl_3$) δ -59.59, -111.48 ppm; HRMS (EI) m/z $[M]^+$ calcd for $C_{16}H_6O_3F_3$ 398.0189, found 398.0180. The $^1H/^{13}C\{^1H\}/^{19}F$ NMR spectra are in full agreement with them reported in literature.³¹

1-Naphthoic Anhydride 3q. 1-Naphthoic acid (2.00 g, 11.6 mmol, 1.0 equiv), TsCl (1.11 g, 5.81 mmol, 0.5 equiv), and K_2CO_3 (2.41 g, 17.4 mmol, 1.5 equiv) were dissolved in MeCN (60 mL) and CH_2Cl_2 (60 mL) and synthesized according to GP A. Compound **3q** (1.50 g, 79%) was obtained as a white solid: mp 137–139 °C; 1H NMR (400 MHz, $CDCl_3$) δ 9.15 (d, $J = 8.6$ Hz, 1H, Ar), 8.44 (dd, $J = 7.3, 1.2$ Hz, 1H, Ar), 8.16 (d, $J = 8.1$ Hz, 1H, Ar), 7.95 (dd, $J = 8.2, 1.3$ Hz, 1H, Ar), 7.72 (ddd, $J = 8.6, 6.8, 1.4$ Hz, 1H, Ar), 7.65–7.54 (m, 2H, Ar) ppm; $^{13}C\{^1H\}$ NMR (101 MHz, $CDCl_3$) δ 163.09, 135.68, 134.11, 132.26, 132.05, 128.98, 128.95, 126.93, 125.82, 125.06, 124.62 ppm; HRMS (EI) m/z $[M]^+$ calcd for $C_{22}H_{14}O_3$ 326.0943, found 326.0941. The

$^1H/^{13}C\{^1H\}$ NMR spectra are in full agreement with them reported in literature.²⁶

2-Methoxy-1-naphthoic Anhydride 3r. 2-Methoxy-1-naphthoic acid (500 mg, 2.48 mmol, 1.0 equiv), TsCl (235 mg, 1.24 mmol, 0.5 equiv), and K_2CO_3 (512 mg, 3.71 mmol, 1.5 equiv) were dissolved in MeCN (13 mL) and CH_2Cl_2 (13 mL) and synthesized according to GP A. Compound **3r** (324 mg, 68%) was obtained as a white solid: mp 138–140 °C; 1H NMR (400 MHz, $CDCl_3$) δ 8.11 (dq, $J = 8.6, 0.9$ Hz, 1H, Ar), 7.93 (dt, $J = 9.1, 0.6$ Hz, 1H, Ar), 7.78 (ddd, $J = 8.2, 1.4, 0.7$ Hz, 1H, Ar), 7.54 (ddd, $J = 8.5, 6.9, 1.4$ Hz, 1H, Ar), 7.39 (ddd, $J = 8.1, 6.9, 1.1$ Hz, 1H, Ar), 7.27 (s, 1H, Ar), 3.97 (s, 3H, Me) ppm; $^{13}C\{^1H\}$ NMR (101 MHz, $CDCl_3$) δ 163.23, 156.19, 133.41, 131.43, 128.59, 128.32, 128.29, 124.48, 123.98, 115.36, 112.97, 56.84 ppm; IR (ATR) ν (cm^{-1}) 3055, 2946, 2847, 1766, 1707, 1593, 1509, 1431, 1349, 1280, 1179, 1095, 1063, 993, 788, 751; HRMS (EI) m/z $[M]^+$ calcd for $C_{24}H_{18}O_5$ 386.1154, found 386.1156.

2-Ethoxy-1-naphthoic Anhydride 3s. 2-Ethoxy-1-naphthoic acid (500 mg, 2.31 mmol, 1.0 equiv), TsCl (220 mg, 1.16 mmol, 0.5 equiv), and K_2CO_3 (479 mg, 3.47 mmol, 1.5 equiv) were dissolved in MeCN (12 mL) and CH_2Cl_2 (12 mL) and synthesized according to GP A. Compound **3s** (354 mg, 74%) was obtained as a white solid: mp 127–128 °C; 1H NMR (600 MHz, $CDCl_3$) δ 8.13–8.08 (m, 1H, Ar), 7.89 (d, $J = 9.1$ Hz, 1H, Ar), 7.78 (d, $J = 8.2$ Hz, 1H, Ar), 7.53 (ddd, $J = 8.4, 6.9, 1.3$ Hz, 1H, Ar), 7.38 (ddd, $J = 8.0, 6.9, 1.0$ Hz, 1H, Ar), 7.23 (d, $J = 9.1$ Hz, 1H, Ar), 4.21 (q, $J = 7.0$ Hz, 2H, CH₂), 1.38 (t, $J = 7.0$ Hz, 3H, Me) ppm; $^{13}C\{^1H\}$ NMR (151 MHz, $CDCl_3$) δ 163.30, 155.63, 133.17, 131.51, 128.61, 128.28, 128.18, 124.43, 123.95, 115.96, 114.22, 65.62, 15.00 ppm; IR (ATR) ν (cm^{-1}) 2979, 1769, 1709, 1620, 1513, 1434, 1277, 1149, 1086, 1051, 1004, 996, 801, 729; HRMS (ESI) m/z $[M + Na]^+$ calcd for $C_{26}H_{22}O_5Na$ 437.1365, found 437.1358.

2-Methyl-1-naphthoic Anhydride 3w. 2-Methyl-1-naphthoic acid (1.00 g, 5.37 mmol, 1.0 equiv), TsCl (511 mg, 2.69 mmol, 0.5 equiv), K_2CO_3 (1.11 g, 8.06 mmol, 1.5 equiv) were dissolved in MeCN (30 mL) and CH_2Cl_2 (30 mL) and synthesized according to GP A. Compound **3w** (655 mg, 69%) was obtained as a white solid: mp 105–108 °C; 1H NMR (400 MHz, $CDCl_3$) δ 8.05 (d, $J = 8.3$ Hz, 1H, Ar), 7.85 (t, $J = 8.8$ Hz, 2H, Ar), 7.56–7.44 (m, 2H, Ar), 7.33 (d, $J = 8.4$ Hz, 1H, Ar), 2.61 (s, 3H, Me) ppm; $^{13}C\{^1H\}$ NMR (101 MHz, $CDCl_3$) δ 165.48, 135.17, 131.73, 131.12, 130.13, 128.56, 128.35, 128.09, 127.74, 125.98, 124.41, 20.49 ppm; IR (ATR) ν (cm^{-1}) 2942, 1805, 1572, 1467, 1259, 1200, 1122, 988, 745, 699; HRMS (EI) m/z $[M]^+$ calcd for $C_{24}H_{18}O_3$ 354.1256, Found 354.1252.

3-Phenylbenzoic Anhydride 3x. 3-Phenylbenzoic acid (1.50 g, 7.57 mmol, 1.0 equiv), TsCl (721 mg, 3.78 mmol, 0.5 equiv), and K_2CO_3 (1.57 g, 11.3 mmol, 1.5 equiv) were dissolved in MeCN (80 mL) and CH_2Cl_2 (80 mL) and synthesized according to GP A. Compound **3x** (1.40 g, 98%) was obtained as a white solid: mp 90–92 °C; 1H NMR (400 MHz, $CDCl_3$) δ 8.40 (t, $J = 1.8$ Hz, 1H, Ar), 8.15 (ddd, $J = 7.8, 1.8, 1.2$ Hz, 1H, Ar), 7.91 (ddd, $J = 7.8, 1.9, 1.1$ Hz, 1H, Ar), 7.66–7.59 (m, 3H, Ar), 7.52–7.45 (m, 2H, Ar), 7.44–7.38 (m, 1H, Ar) ppm; $^{13}C\{^1H\}$ NMR (101 MHz, $CDCl_3$) δ 162.54, 142.31, 139.79, 133.37, 129.55, 129.54, 129.41, 129.37, 129.18, 128.21, 127.35 ppm; IR (ATR) ν (cm^{-1}) 3032, 1783, 1723, 1573, 1451, 1287, 1187, 1086, 1016, 905, 765, 695; HRMS (EI) m/z $[M]^+$ calcd for $C_{26}H_{18}O_3$ 378.1256, found 378.1248.

Thiophene-2-carboxylic Anhydride 3y. Thiophene-2-carboxylic acid (1.50 g, 11.7 mmol, 1.0 equiv), TsCl (1.12 g, 5.85 mmol, 0.5 equiv), K_2CO_3 (2.43 g, 17.6 mmol, 1.5 equiv) were dissolved in MeCN (60 mL) and CH_2Cl_2 (60 mL) and synthesized according to GP A. Compound **3y** (1.12 g, 80%) was obtained as a white solid: mp 59–60 °C; 1H NMR (400 MHz, $CDCl_3$) δ 7.98 (dd, $J = 3.8, 1.2$ Hz, 1H, Ar), 7.74 (dd, $J = 5.0, 1.2$ Hz, 1H, Ar), 7.20 (dd, $J = 5.0, 3.8$ Hz, 1H, Ar) ppm; $^{13}C\{^1H\}$ NMR (101 MHz, $CDCl_3$) δ 156.77, 136.16, 135.42, 132.22, 128.59 ppm; HRMS (EI) m/z $[M]^+$ calcd for $C_{10}H_6O_3S_2$ 237.9758, found 237.9739. The $^1H/^{13}C\{^1H\}$ NMR spectra are in full agreement with them reported in literature.²⁶

2-Naphthoic Anhydride 3z. 2-Naphthoic acid (500 mg, 2.90 mmol, 1.0 equiv), TsCl (277 mg, 1.45 mmol, 0.5 equiv), K_2CO_3 (602 mg, 4.36 mmol, 1.5 equiv) were dissolved in MeCN (15 mL) and CH_2Cl_2 (15 mL) and synthesized according to GP A. Compound **3z** (284 mg, 60%)

was obtained as a white solid: mp 137–139 °C; ^1H NMR (400 MHz, CDCl_3) δ 8.79 (d, $J = 1.7$ Hz, 1H, Ar), 8.20 (dd, $J = 8.6, 1.8$ Hz, 1H, Ar), 8.05–7.93 (m, 3H, Ar), 7.68 (ddd, $J = 8.2, 6.9, 1.4$ Hz, 1H, Ar), 7.61 (ddd, $J = 8.2, 6.9, 1.3$ Hz, 1H, Ar) ppm; $^{13}\text{C}\{^1\text{H}\}$ NMR (101 MHz, CDCl_3) δ 162.90, 136.39, 132.97, 132.60, 129.82, 129.39, 129.01, 128.08, 127.29, 126.25, 125.56; HRMS (EI) m/z [M] calcd for $\text{C}_{22}\text{H}_{14}\text{O}_3$ 326.0943, found 326.0954. The $^1\text{H}/^{13}\text{C}\{^1\text{H}\}$ NMR spectra are in full agreement with them reported in literature.²⁶

General Procedure B (GP B, Synthesis of Acid Anhydride Precursors 17h–j). This method is based on the procedure reported by Glorius et al.³² In a Schlenk flask, equipped with a low-temperature thermometer, the corresponding bromonaphthalene (1.0 equiv) was dissolved in dry THF and cooled down to -78 °C. $n\text{-BuLi}$ (2.5 M in hexane, 1.0 equiv) was added dropwise to the solution, and the mixture was stirring for 2 h at -78 °C. Trimethylborate (1.5 equiv) dissolved in THF was added carefully, and the reaction mixture was stirring overnight and allowed to warm up to room temperature. The reaction mixture was quenched with 2 M HCl, and water was added. The mixture was extracted with EtOAc (3 \times). The combined organic phase was washed with water (1 \times), dried over MgSO_4 , filtered and concentrated in a vacuum. Ethyl 2-bromobenzoate (1.0 equiv), the corresponding naphthaleneboronic acid (1.5 equiv), and Na_2CO_3 (2.0 equiv) were dissolved in a 2:1 mixture of THF and water. After the reaction mixture was degassed with N_2 , $(\text{PPh}_3)_2\text{PdCl}_2$ was added, and the mixture was stirred overnight at 60 °C. After cooling down to room temperature, water was added to the reaction mixture and extracted with CH_2Cl_2 (3 \times). The combined organic phase was dried over MgSO_4 , filtered, and concentrated in a vacuum. The pure product was obtained by column chromatography on silica (isohexane/EtOAc 8:2).

General Procedure C (GP C, Synthesis of Acetic Acids 8). In a round flask, the corresponding esters (1.0 equiv) and NaOH (15.0 equiv) were dissolved in a 1:1 mixture of water and MeOH. The reaction mixture was stirred for 24 h at 100 °C. After adding 2 M HCl until a pH value of 2 was reached, the mixture was extracted with EtOAc (3 \times), dried over MgSO_4 , filtered, and concentrated in a vacuum to obtain the pure product.

Ethyl 2-(Naphthalen-1-yl)benzoate 17h. 1-Bromonaphthalene (5.00 g, 24.1 mmol, 1.0 equiv) and $n\text{-BuLi}$ (2.5 M in hexane, 9.64 mL, 24.1 mmol, 1.0 equiv) were dissolved in THF (60 mL). Trimethylborate (4.04 mL, 36.2 mmol, 1.5 equiv) dissolved in THF (6 mL) was added to the mixture and synthesized according to GP B. Ethyl-2-Bromobenzoate (2.50 mL, 15.7 mmol, 1.0 equiv), naphthalene-1-ylboronic acid (4.05 g, 23.6 mmol, 1.5 equiv), Na_2CO_3 (3.33 g, 31.4 mmol, 2.0 equiv), and $(\text{PPh}_3)_2\text{PdCl}_2$ (275 mg, 393 μmol , 2.5 mol %) were dissolved in THF (63 mL) and water (31 mL) and synthesized according to GP B. After purification by column chromatography on silica (isohexane/EtOAc 8:2), **17h** (3.60 g, 83%) was obtained as an oil: ^1H NMR (400 MHz, CDCl_3) δ 8.04 (dd, $J = 7.8, 1.5$ Hz, 1H, Ar), 7.87 (ddt, $J = 10.5, 8.1, 1.0$ Hz, 2H, Ar), 7.61 (td, $J = 7.5, 1.5$ Hz, 1H, Ar), 7.55–7.34 (m, 7H, Ar), 7.32 (dd, $J = 7.0, 1.2$ Hz, 1H, Ar), 3.77 (qq, $J = 10.8, 7.1$ Hz, 2H, CH_2), 0.52 (t, $J = 7.1$ Hz, 3H, Me) ppm. The ^1H NMR spectrum is in full agreement with that reported in literature.³²

2-(Naphthalen-1-yl)benzoic Acid 8h. Compound **17h** (3.60 g, 13.0 mmol, 1.0 equiv) and NaOH (7.82 g, 195 mmol, 15 equiv) were dissolved in MeOH (60 mL) and water (60 mL) and synthesized according to GP C. Compound **8h** (3.20 g, 99%) was obtained as a white solid: mp 160–162 °C; ^1H NMR (400 MHz, $\text{DMSO}-d_6$) δ 12.46 (bs, 1H, COOH), 7.99–7.89 (m, 3H, Ar), 7.66 (td, $J = 7.5, 1.5$ Hz, 1H, Ar), 7.60–7.46 (m, 3H, Ar), 7.44–7.37 (m, 2H, Ar), 7.36 (dd, $J = 7.6, 1.3$ Hz, 1H, Ar), 7.31 (dd, $J = 7.0, 1.2$ Hz, 1H, Ar). The ^1H NMR spectrum is in full agreement with that reported in literature.^{32,33}

2-(Naphthalen-1-yl)benzoic Anhydride 3h. Compound **8h** (1.00 g, 4.03 mmol, 1.0 equiv), TsCl (384 mg, 2.01 mmol, 0.5 equiv), K_2CO_3 (835 mg, 6.04 mmol, 1.5 equiv) were dissolved in MeCN (20 mL) and CH_2Cl_2 (20 mL) and synthesized according to GP A. Compound **3h** (790 mg, 82%) was obtained as a white solid (1:1 diastomeric mixture): mp 130–132 °C; ^1H NMR (400 MHz, CDCl_3) δ 7.82 (t, $J = 7.6$ Hz, 1H, Ar), 7.80–7.74 (m, 1H, Ar), 7.56–7.50 (m, 1H, Ar), 7.49–7.42 (m, 1.5H, Ar), 7.42–7.38 (m, 1H, Ar), 7.38–7.33 (m, 1H, Ar), 7.31 (ddt, $J = 3.5, 1.6, 0.9$ Hz, 0.5H, Ar), 7.30–7.28 (m, 1H, Ar), 7.28–

7.26 (m, 1H, Ar), 7.24 (dt, $J = 7.9, 1.6$ Hz, 1H, Ar), 7.21 (dd, $J = 7.0, 1.2$ Hz, 0.5H, Ar), 7.12 (dd, $J = 7.0, 1.2$ Hz, 0.5H, Ar) ppm; $^{13}\text{C}\{^1\text{H}\}$ NMR (101 MHz, CDCl_3) δ 162.08, 162.00, 142.33, 142.25, 138.87, 138.86, 133.53, 133.52, 132.68, 132.60, 132.15, 132.14, 131.97, 131.96, 131.31, 131.20, 129.27, 129.14, 128.36, 128.30, 127.92, 127.82, 127.59, 126.28, 126.25, 126.21, 125.86, 125.85, 125.74, 125.73, 125.29, 125.23 ppm (two signals are overlapping); IR (ATR) ν (cm^{-1}) 3052, 1781, 1591, 1392, 1205, 1000, 801, 761, 696; HRMS (EI) m/z [M]⁺ calcd for $\text{C}_{34}\text{H}_{22}\text{O}_3$ 478.1569, found 478.1567.

Ethyl 2-(Naphthalen-2-yl)benzoate 17i. 2-Bromonaphthalene (2.00 g, 9.66 mmol, 1.0 equiv) and $n\text{-BuLi}$ (2.5 M in hexane, 3.86 mL, 9.66 mmol, 1.0 equiv) were dissolved in THF (24 mL). Trimethylborate (1.62 mL, 14.5 mmol, 1.5 equiv) dissolved in THF (2.4 mL) was added to the mixture and reacted according to GP B. Ethyl 2-bromobenzoate (312 μL , 1.96 mmol, 1.0 equiv), naphthalene-2-ylboronic acid (506 mg, 2.95 mmol, 1.5 equiv), Na_2CO_3 (416 mg, 3.93 mmol, 2.0 equiv), and $(\text{PPh}_3)_2\text{PdCl}_2$ (68.0 mg, 98.2 μmol , 5.0 mol %) were dissolved in THF (8 mL) and water (4 mL) and reacted according to GP B. After purification by column chromatography on silica (isohexane/EtOAc 8:2), **17i** (540 mg, 99%) was obtained as an oil: ^1H NMR (200 MHz, CDCl_3) δ 7.95–7.72 (m, 5H, Ar), 7.49 (dtt, $J = 7.0, 5.2, 3.6$ Hz, 6H, Ar), 4.06 (q, $J = 7.1$ Hz, 2H, CH_2), 0.89 (t, $J = 7.1$ Hz, 3H, Me) ppm. The ^1H NMR spectrum is in full agreement with that reported in literature.³²

2-(Naphthalen-2-yl)benzoic Acid 8i. Compound **17i** (549 mg, 1.95 mmol, 1.0 equiv) and NaOH (1.09 g, 27.3 mmol, 14 equiv) were dissolved in MeOH (10 mL) and water (10 mL), and reacted according to GP C. Compound **8i** (338 mg, 70%) was obtained as a white solid: mp 192–193 °C; ^1H NMR (400 MHz, $\text{DMSO}-d_6$) δ 12.80 (bs, 1H, COOH), 7.99–7.91 (m, 3H, Ar), 7.87 (d, $J = 1.8$ Hz, 1H, Ar), 7.80 (dd, $J = 7.9, 1.4$ Hz, 1H, Ar), 7.63 (td, $J = 7.6, 1.4$ Hz, 1H, Ar), 7.57–7.45 (m, 5H, Ar) ppm. The ^1H NMR spectrum is in full agreement with that reported in literature.³²

2-(Naphthalen-2-yl)benzoic Anhydride 3i. Compound **8i** (1.70 g, 6.85 mmol, 1.0 equiv), TsCl (652 mg, 3.42 mmol, 0.5 equiv), K_2CO_3 (1.42 g, 10.3 mmol, 1.5 equiv) were dissolved in MeCN (34 mL) and CH_2Cl_2 (34 mL) and reacted according to GP A. Compound **3i** (733 mg, 45%) was optimized as a white solid: mp 75–77 °C; ^1H NMR (400 MHz, CDCl_3) δ 7.85–7.80 (m, 2H, Ar), 7.77 (d, $J = 8.4$ Hz, 1H, Ar), 7.72 (d, $J = 1.7$ Hz, 1H, Ar), 7.47 (ddd, $J = 17.9, 6.9, 2.3$ Hz, 3H, Ar), 7.37i–7.31 (m, 2H, Ar), 7.30–7.24 (m, 1H, Ar), 7.03 (td, $J = 7.7, 1.3$ Hz, 1H, Ar) ppm; $^{13}\text{C}\{^1\text{H}\}$ NMR (101 MHz, CDCl_3) δ 163.25, 143.51, 138.28, 133.26, 132.62, 131.34, 131.12, 128.48, 128.23, 127.77, 127.75, 127.23, 127.18, 127.08, 126.38, 126.21 ppm (one signal is overlapping); IR (ATR) ν (cm^{-1}) 3048, 1765, 1707, 1600, 1484, 1266, 1202, 1059, 1017, 851, 816, 775, 704; HRMS (EI) m/z [M]⁺ calcd for $\text{C}_{34}\text{H}_{22}\text{O}_3$ 478.1569, found 478.1564.

Ethyl 2-(6-Methoxynaphthalen-2-yl)benzoate 17j. 2-Bromo-6-methoxynaphthalene (2.00 g, 8.44 mmol, 1.0 equiv) and $n\text{-BuLi}$ (2.5 M in hexane, 3.37 mL, 8.44 mmol, 1.0 equiv) was dissolved in THF (21 mL). Trimethylborate (1.41 mL, 12.6 mmol, 1.5 equiv) dissolved in THF (2.1 mL) was added to the mixture and reacted according to GP B. Ethyl 2-bromobenzoate (416 μL , 2.62 mmol, 1.0 equiv), 2-bromo-6-methoxynaphthalene-2-ylboronic acid (793 mg, 3.93 mmol, 1.5 equiv), Na_2CO_3 (555 mg, 5.24 mmol, 2.0 equiv), and $(\text{PPh}_3)_2\text{PdCl}_2$ (92.0 mg, 131 μmol , 5.0 mol %) were dissolved in THF (10 mL) and water (5 mL) and reacted according to GP B. After purification by column chromatography on silica (isohexane/EtOAc 8:2), **17j** (750 mg, 94%) was obtained as an oil: ^1H NMR (400 MHz, CDCl_3) δ 7.86 (dd, $J = 7.7, 1.4$ Hz, 1H, Ar), 7.77–7.70 (m, 3H, Ar), 7.55 (td, $J = 7.5, 1.5$ Hz, 1H, Ar), 7.49–7.39 (m, 3H, Ar), 7.20–7.14 (m, 2H, Ar), 4.06 (q, $J = 7.1$ Hz, 2H, CH_2), 3.95 (s, 3H, Me), 0.90 (t, $J = 7.1$ Hz, 3H, Me) ppm. Compound **17j** is used in the next step without any further characterization.

2-(6-Methoxynaphthalen-2-yl)benzoic Acid 8j. Compound **17j** (1.80 g, 5.88 mmol, 1.0 equiv) and NaOH (3.30 g, 82.3 mmol, 14 equiv) were dissolved in MeOH (30 mL) and water (30 mL), and reacted according to GP C. Compound **8j** (1.60 g, 98%) was obtained as a white solid: mp 179–180 °C; ^1H NMR (400 MHz, $\text{DMSO}-d_6$) δ 12.77 (bs, 1H, COOH), 7.89–7.74 (m, 4H, Ar), 7.60 (td, $J = 7.5, 1.4$

Hz, 1H, Ar), 7.52–7.45 (m, 2H, Ar), 7.42 (dd, $J = 8.4, 1.7$ Hz, 1H, Ar), 7.35 (d, $J = 2.4$ Hz, 1H, Ar), 7.19 (dd, $J = 8.9, 2.5$ Hz, 1H, Ar), 3.89 (s, 3H, Me) ppm. Compound **8j** is used in the next step without any further characterization.

2-(6-Methoxynaphthalen-2-yl)benzoic Anhydride 3j. Compound **8j** (300 mg, 1.08 mmol, 1.0 equiv), TsCl (102 mg, 539 μ mol, 0.5 equiv), and K_2CO_3 (223 mg, 1.62 mmol, 1.5 equiv) were dissolved in MeCN (5 mL) and CH_2Cl_2 (5 mL), and reacted according to GP A. Compound **3j** (256 mg, 88%) was obtained as a white solid: mp 145–147 °C; 1H NMR (400 MHz, $CDCl_3$) δ 7.72 (d, $J = 8.9$ Hz, 1H, Ar), 7.69–7.64 (m, 2H, Ar), 7.46 (td, $J = 7.5, 1.4$ Hz, 1H, Ar), 7.35 (dd, $J = 7.8, 1.3$ Hz, 1H, Ar), 7.30 (ddd, $J = 9.2, 8.1, 1.6$ Hz, 2H, Ar), 7.16 (dd, $J = 8.9, 2.5$ Hz, 1H, Ar), 7.12 (d, $J = 2.5$ Hz, 1H, Ar), 7.05 (td, $J = 7.6, 1.3$ Hz, 1H, Ar), 3.84 (s, 3H, Me) ppm; $^{13}C\{^1H\}$ NMR (101 MHz, $CDCl_3$) δ 163.48, 157.97, 143.61, 136.02, 133.89, 132.56, 131.37, 131.14, 129.79, 128.82, 128.64, 127.62, 127.15, 127.01, 126.71, 119.24, 105.70, 55.50 ppm; IR (ATR) ν (cm^{-1}) 3051, 2959, 1766m 1710, 1594, 1489, 1386, 1266, 1202, 1009, 902, 847, 811, 760, 703, 668; HRMS (EI) m/z [M] $^+$ calcd for $C_{28}H_{26}O_5$, 538.1780, found 538.1783.

Methyl 2-Methoxy-6-phenylbenzoate 17l. In a Schlenk flask, 2-methoxybenzoic acid (1.00 g, 6.57 mmol, 1.0 equiv), $[Ru(p-cym)Cl_2]_2$ (160 mg, 263 μ mol, 0.04 equiv), $HPeEt_3BF_4$ (108 mg, 526 μ mol, 0.08 equiv), and K_2CO_3 (1.00 g, 7.23 mmol, 1.1 equiv) were dissolved in NMP (33 mL) and stirred for 18 h at 100 °C. After cooling down to room temperature, MeI (2.03 mL, 32.9 mmol, 5.0 equiv), K_2CO_3 (2.73 g, 19.7 mmol, 3.0 equiv), and NMP (25 mL) were added to the reaction mixture and stirred for 2 h at 60 °C. After the addition of EtOAc (50 mL), the mixture was washed with water, aqueous LiCl solution (20%), and brine, dried over $MgSO_4$, filtered, and concentrated in a vacuum. After purification by column chromatography on silica (isohexane/EtOAc 8:2), **17l** (1.09 g, 70%) was obtained as a clear liquid: 1H NMR (400 MHz, $CDCl_3$) δ 7.44–7.30 (m, 6H, Ar), 7.00 (d, $J = 7.7$ Hz, 1H, Ar), 6.95 (d, $J = 8.4$ Hz, 1H, Ar), 3.89 (s, 3H, Me), 3.63 (s, 3H, Me) ppm. The 1H NMR spectrum is in full agreement with that reported in literature.³⁴

2-Methoxy-6-phenylbenzoic Acid 8l. Compound **17l** (580 mg, 2.54 mmol, 1.0 equiv) and NaOH (1.42 g, 35.6 mmol, 14 equiv) were dissolved in MeOH (11 mL) and water (11 mL) and reacted according to GP C. Compound **8l** (542 mg, 99%) was obtained as a white solid: mp 112–113 °C; 1H NMR (200 MHz, $DMSO-d_6$) δ 12.88 (bs, 1H, COOH), 7.52–7.29 (m, 6H, Ar), 7.11 (d, $J = 8.3$ Hz, 1H, Ar), 6.96 (d, $J = 7.6$ Hz, 1H, Ar), 3.83 (s, 3H, Me) ppm. The 1H NMR spectrum is in full agreement with that reported in literature.³⁵

2-Methoxy-6-phenylbenzoic Anhydride 3l. Compound **8l** (1.00 g, 4.38 mmol, 1.0 equiv), TsCl (417 mg, 2.19 mmol, 0.5 equiv), and K_2CO_3 (908 mg, 6.57 mmol, 1.5 equiv) were dissolved in MeCN (20 mL) and CH_2Cl_2 (20 mL) and reacted according to GP A. Compound **3l** (950 mg, 99%) was obtained as a white solid: mp 168–170 °C; 1H NMR (400 MHz, $CDCl_3$) δ 7.43–7.38 (m, 1H, Ar), 7.36 (s, 5H, Ar), 6.96 (d, $J = 8.4$ Hz, 1H, Ar), 6.89 (d, $J = 8.4$ Hz, 1H, Ar), 3.81 (s, 3H, Me) ppm; $^{13}C\{^1H\}$ NMR (101 MHz, $CDCl_3$) δ 162.00, 157.26, 141.88, 139.28, 131.35, 128.70, 128.50, 127.81, 122.28, 121.67, 109.98, 56.15 ppm; IR (ATR) ν (cm^{-1}) 2942, 1805, 1572, 1467, 1259, 1200, 1122, 988, 745, 699; HRMS (EI) m/z [M] $^+$ calcd for $C_{28}H_{22}O_5$, 438.1467, found 438.1454.

Methyl 2-Methyl-6-phenylbenzoate 17n. In a Schlenk flask, 2-methylbenzoic acid (3.00 g, 22.0 mmol, 1.0 equiv), $[Ru(p-cym)Cl_2]_2$ (537 mg, 881 μ mol, 0.04 equiv), $HPeEt_3BF_4$ (363 mg, 1.76 mmol, 0.08 equiv), and K_2CO_3 (3.05 g, 24.2 mmol, 1.1 equiv) were dissolved in NMP (110 mL) and stirred for 18 h at 100 °C. After cooling down to room temperature, MeI (6.80 mL, 110 mmol, 5.0 equiv), K_2CO_3 (9.14 g, 66.1 mmol, 3.0 equiv), and NMP (88 mL) were added to the reaction mixture and stirred for 2 h at 60 °C. After the addition of EtOAc (50 mL), the mixture was washed with water, aqueous LiCl solution (20%) and brine, dried over $MgSO_4$, filtered, and concentrated in a vacuum. After purification by column chromatography on silica (isohexane/EtOAc 8:2), **17n** (4.26 g, 85%) was obtained as a clear solution: 1H NMR (400 MHz, $CDCl_3$) δ 7.43–7.32 (m, 6H, Ar), 7.23 (d, $J = 7.6$ Hz, 2H, Ar), 3.59 (s, 3H, Me), 2.41 (s, 3H, Me) ppm. The 1H NMR spectrum is in full agreement with that reported in literature.³⁴

2-Methyl-6-phenylbenzoic Acid 8n. Compound **17n** (4.26 g, 18.8 mmol, 1.0 equiv) and NaOH (10.0 g, 263 mmol, 14 equiv) were dissolved in MeOH (82 mL) and water (82 mL) and reacted according to GP C. Compound **8n** (3.50 g, 88%) was obtained as a white solid: mp 135–137 °C; 1H NMR (400 MHz, $DMSO-d_6$) δ 13.02 (bs, 1H, COOH), 7.48–7.32 (m, 6H, Ar), 7.28 (d, $J = 7.5$ Hz, 1H, Ar), 7.20 (d, $J = 7.6$ Hz, 1H, Ar), 2.34 (s, 3H, Me) ppm. The 1H NMR spectrum is in full agreement with that reported in literature.³³

2-Methyl-6-phenylbenzoic Anhydride 3n. Compound **8n** (430 mg, 2.03 mmol, 1.0 equiv), TsCl (193 mg, 1.02 mmol, 0.5 equiv), and K_2CO_3 (419 mg, 3.05 mmol, 1.5 equiv) were dissolved in MeCN (10 mL) and CH_2Cl_2 (10 mL) and reacted according to GP A. Compound **3n** (218 mg, 53%) was obtained as a white solid: mp 138–140 °C; 1H NMR (400 MHz, $CDCl_3$) δ 7.42–7.28 (m, 6H, Ar), 7.12 (dd, $J = 17.2, 7.7$ Hz, 2H, Ar), 1.95 (s, 3H, Me) ppm; $^{13}C\{^1H\}$ NMR (101 MHz, $CDCl_3$) δ 163.86, 140.54, 140.01, 136.76, 131.03, 130.26, 129.28, 128.71, 128.68, 127.81, 127.53, 19.44 ppm; IR (ATR) ν (cm^{-1}) 3055, 1790, 1588, 1459, 1201, 983, 792, 750, 694; HRMS (EI) m/z [M] $^+$ calcd for $C_{28}H_{22}O_3$, 406.1569, found 406.1566.

General Procedure D (GP D): Syntheses of Acid Anhydride Precursors 17t–v. This method is based on the procedure reported by Ruzicka et al.³⁶ In a round-bottom flask, methyl 2-hydroxy-1-naphthoate (1.0 equiv), the corresponding halogenated compound (1.0 equiv), and K_2CO_3 (1.0 equiv) were dissolved in DMF and stirred for 24 h at 90 °C. After full conversion, the reaction mixture was quenched by adding water, extracted with ether (3 \times), dried over $MgSO_4$, filtered, and concentrated in a vacuum. The pure product was obtained by column chromatography on silica (isohexane/EtOAc 8:2).

Methyl 2-Hydroxy-1-naphthoate 18. In a round-bottom flask, 2-hydroxy-1-naphthoic acid (4.00 g, 21.3 mmol, 1.0 equiv), MeI (2.91 mL, 46.8 mmol, 2.2 equiv), and $KHCO_3$ (2.55 g, 25.5 mmol, 1.2 equiv) were dissolved in DMF (54 mL) and stirred at room temperature for 24 h. The reaction mixture was quenched with 1 M HCl and extracted with ether (3 \times 40 mL). The combined organic phase was washed with brine, dried over $MgSO_4$, filtered, and concentrated in a vacuum. After purification by column chromatography on silica (isohexane/EtOAc 8:2), **18** (4.12 g, 96%) was obtained as a white solid: mp 79–81 °C; 1H NMR (400 MHz, $CDCl_3$) δ 12.29 (s, 1H, OH), 8.75 (d, $J = 8.8$ Hz, 1H, Ar), 7.90 (d, $J = 9.0$ Hz, 1H, Ar), 7.76 (d, $J = 8.7$ Hz, 1H, Ar), 7.56 (ddd, $J = 8.6, 6.9, 1.4$ Hz, 1H, Ar), 7.38 (t, $J = 7.5$ Hz, 1H, Ar), 7.17 (d, $J = 9.0$ Hz, 1H, Ar), 4.11 (s, 3H, Me) ppm. The 1H NMR spectrum is in full agreement with that reported in literature.³⁷

Methyl 2-Butoxy-1-naphthoate 17t. Compound **18** (2.00 g, 9.89 mmol, 1.0 equiv), 1-bromobutane (1.06 mL, 9.89 mmol, 1.0 equiv), and K_2CO_3 (1.38 g, 9.99 mmol, 1.0 equiv) were dissolved in DMF (60 mL) and reacted according to GP D. After purification by column chromatography on silica (isohexane/EtOAc 8:2), **17t** (2.50 g, 98%) was obtained as an oil: 1H NMR (400 MHz, $CDCl_3$) δ 7.87 (d, $J = 9.0$ Hz, 1H, Ar), 7.78 (d, $J = 8.2$ Hz, 1H, Ar), 7.74 (dd, $J = 8.5, 0.9$ Hz, 1H, Ar), 7.49 (ddd, $J = 8.4, 6.8, 1.3$ Hz, 1H, Ar), 7.36 (ddd, $J = 8.1, 6.8, 1.1$ Hz, 1H, Ar), 7.27 (d, $J = 9.1$ Hz, 1H, Ar), 4.15 (t, $J = 6.4$ Hz, 2H, CH_2), 4.02 (s, 3H, Me), 1.85–1.73 (m, 2H, CH_2), 1.51 (dq, $J = 14.7, 7.4$ Hz, 2H, CH_2), 0.98 (t, $J = 7.4$ Hz, 3H, Me) ppm. Compound **17t** is used in the next step without any further characterization.

2-Butoxy-1-naphthoic Acid 8t. Compound **17t** (2.50 g, 9.69 mmol, 1.0 equiv) and NaOH (4.30 g, 106 mmol, 11 equiv) were dissolved in MeOH (42 mL) and water (42 mL) and synthesized according to GP C. Compound **8t** (2.27 g, 96%) was obtained as a white solid: mp 91–93 °C; 1H NMR (400 MHz, $DMSO-d_6$) δ 13.16 (s, 1H, COOH), 8.00 (d, $J = 9.1$ Hz, 1H, Ar), 7.92 (d, $J = 8.1$ Hz, 1H, Ar), 7.68 (d, $J = 8.4$ Hz, 1H, Ar), 7.53 (ddd, $J = 8.4, 6.9, 1.2$ Hz, 1H, Ar), 7.49 (d, $J = 9.1$ Hz, 1H, Ar), 7.44–7.37 (m, 1H, Ar), 4.17 (t, $J = 6.3$ Hz, 2H, CH_2), 1.70 (p, 2H, $J = 6.3, 7.4$ Hz CH_2), 1.47 (h, $J = 7.4$ Hz, 2H, CH_2), 0.94 (t, $J = 7.4$ Hz, 3H, Me) ppm. Compound **8t** is used in the next step without any further characterization.

2-Butoxy-1-naphthoic Anhydride 3t. Compound **8t** (500 mg, 2.05 mmol, 1.0 equiv), TsCl (195 mg, 1.03 mmol, 0.5 equiv), and K_2CO_3 (424 mg, 3.08 mmol, 1.5 equiv) were dissolved in MeCN (10 mL) and CH_2Cl_2 (10 mL) and reacted according to GP A. Compound **3t** (450 mg, 93%) was obtained as a white solid: mp 117–119 °C; 1H NMR

(400 MHz, CDCl₃) δ 8.10 (d, *J* = 8.6 Hz, 1H, Ar), 7.89 (d, *J* = 9.1 Hz, 1H, Ar), 7.78 (d, *J* = 8.1 Hz, 1H, Ar), 7.52 (ddd, *J* = 8.3, 7.0, 1.1 Hz, 1H, Ar), 7.38 (t, *J* = 7.5 Hz, 1H, Ar), 7.23 (d, *J* = 9.1 Hz, 1H, Ar), 4.11 (t, *J* = 6.6 Hz, 2H, CH₂), 1.71 (dq, *J* = 8.9, 6.7 Hz, 2H, CH₂), 1.39 (dt, *J* = 14.8, 7.5 Hz, 2H, CH₂), 0.86 (t, *J* = 7.4 Hz, 3H, Me) ppm; ¹³C{¹H} NMR (101 MHz, CDCl₃) δ 163.34, 155.75, 133.13, 131.51, 128.49, 128.27, 128.16, 124.35, 123.91, 115.63, 114.01, 69.57, 31.47, 19.17, 13.93 ppm; IR (ATR) ν (cm⁻¹) 2948, 1772, 1593, 1507, 1432, 1340, 1277, 1246, 1180, 1088, 1057, 983, 793, 749; HRMS (EI) *m/z* [M]⁺ calcd for C₃₀H₃₀O₅ 470.2093, found 470.2091.

Methyl 2-(Hexanoyloxy)-1-naphthoate 17u. Compound **18** (2.00 g, 9.89 mmol, 1.0 equiv), 1-bromohexane (1.38 mL, 9.89 mmol, 1.0 equiv), and K₂CO₃ (1.38 g, 9.99 mmol, 1.0 equiv) were dissolved in DMF (60 mL) and reacted according to GP D. After purification by column chromatography on silica (isohexane/EtOAc 8:2), **17u** (2.73 g, 92%) was obtained as an oil: ¹H NMR (400 MHz, CDCl₃) δ 7.87 (d, *J* = 9.1 Hz, 1H, Ar), 7.78 (d, *J* = 8.2 Hz, 1H, Ar), 7.74 (d, *J* = 9.2 Hz, 1H, Ar), 7.49 (ddd, *J* = 8.4, 6.8, 1.3 Hz, 1H, Ar), 7.36 (ddd, *J* = 8.1, 6.9, 1.1 Hz, 1H, Ar), 7.26 (d, *J* = 9.1 Hz, 1H, Ar), 4.14 (t, *J* = 6.5 Hz, 2H, CH₂), 4.02 (s, 3H, Me), 1.86–1.74 (m, 2H, CH₂), 1.51–1.42 (m, 2H, CH₂), 1.37–1.30 (m, 4H, 2 × CH₂), 0.93–0.89 (m, 3H, Me) ppm. Compound **17u** is used in the next step without any further characterization.

2-(Hexanoyloxy)-1-naphthoic Acid 8u. Compound **17u** (2.00 g, 6.67 mmol, 1.0 equiv) and NaOH (3.74 g, 93.4 mmol, 11 equiv) were dissolved in MeOH (31 mL) and water (31 mL) and reacted according to GP C. Compound **8u** (1.66 g, 87%) was obtained as a white solid: mp 100–103 °C; ¹H NMR (400 MHz, DMSO-*d*₆) δ 13.18 (s, 1H, COOH), 7.99 (d, *J* = 9.1 Hz, 1H, Ar), 7.91 (d, *J* = 8.1 Hz, 1H, Ar), 7.67 (d, *J* = 8.4 Hz, 1H, Ar, Ar), 7.54–7.50 (m, 1H), 7.48 (d, *J* = 9.1 Hz, 1H, Ar), 7.40 (ddd, *J* = 8.0, 6.9, 1.0 Hz, 1H, Ar), 4.15 (t, *J* = 6.4 Hz, 2H, CH₂), 1.76–1.65 (m, 2H, CH₂), 1.44 (p, *J* = 7.2 Hz, 2H, CH₂), 1.35–1.24 (m, 4, 2 × CH₂), 0.88 (m, 3H, Me) ppm. Compound **8u** is used in the next step without any further characterization.

2-(Hexanoyloxy)-1-naphthoic Anhydride 3u. Compound **8u** (550 mg, 2.02 mmol, 1.0 equiv), TsCl (192 mg, 1.01 mmol, 0.5 equiv), and K₂CO₃ (418 mg, 3.03 mmol, 1.5 equiv) were dissolved in MeCN (10 mL) and CH₂Cl₂ (10 mL) and reacted according to GP A. Compound **3u** (430 mg, 81%) was obtained as a white solid: mp 100–102 °C; ¹H NMR (400 MHz, CDCl₃) δ 8.10 (d, *J* = 8.5 Hz, 1H, Ar), 7.89 (d, *J* = 9.1 Hz, 1H, Ar), 7.77 (d, *J* = 8.1 Hz, 1H, Ar), 7.52 (t, *J* = 8.1 Hz, 1H, Ar), 7.38 (t, *J* = 7.5 Hz, 1H, Ar), 7.22 (d, *J* = 9.1 Hz, 1H, Ar), 4.08 (s, 2H, CH₂), 1.78–1.65 (m, 2H, CH₂), 1.42–1.30 (m, 2H, CH₂), 1.24–1.15 (m, 4H, 2 × CH₂), 0.87–0.79 (m, 3H, Me) ppm; ¹³C{¹H} NMR (101 MHz, CDCl₃) δ 163.34, 155.78, 133.13, 131.56, 128.55, 128.26, 128.15, 124.36, 123.98, 115.74, 114.11, 69.97, 31.65, 29.39, 25.58, 22.63, 14.17 ppm; IR (ATR) ν (cm⁻¹) 2950, 1766, 1706, 1595, 1512, 1432, 1240, 1277, 1147, 1093, 991, 808, 735; HRMS (EI) *m/z* [M]⁺ calcd for C₃₄H₃₈O₅ 526.2719, found 526.2707.

Methyl 2-Isopropoxy-1-naphthoate 17v. Compound **18** (1.00 g, 4.95 mmol, 1.0 equiv), 2-bromobutane (464 μL, 4.95 mmol, 1.0 equiv), and K₂CO₃ (690 mg, 4.99 mmol, 1.0 equiv) were dissolved in DMF (30 mL) and reacted according to GP D. After purification by column chromatography on silica (isohexane/EtOAc 8:2), **17v** (1.00 g, 83%) was obtained as an oil: ¹H NMR (400 MHz, CDCl₃) δ 7.86 (d, *J* = 9.1 Hz, 1H, Ar), 7.78 (d, *J* = 8.2 Hz, 1H, Ar), 7.72 (d, *J* = 8.5 Hz, 1H, Ar), 7.48 (t, *J* = 7.7 Hz, 1H, Ar), 7.37 (t, *J* = 7.5 Hz, 1H, Ar), 7.26 (d, *J* = 9.1 Hz, 1H, Ar), 4.68 (hept, *J* = 6.1 Hz, 1H, CH), 4.02 (s, 3H, Me), 1.36 (d, *J* = 6.1 Hz, 6H, Me₂) ppm. Compound **17v** is used in the next step without any further characterization.

2-Isopropoxy-1-naphthoic Acid 8v. Compound **17v** (1.00 g, 4.10 mmol, 1.0 equiv) and NaOH (2.30 g, 57.4 mmol, 14 equiv) were dissolved in MeOH (20 mL) and water (20 mL) and reacted according to GP C. Compound **8v** (800 mg, 85%) was obtained as a white solid: mp 152–153 °C; ¹H NMR (400 MHz, DMSO-*d*₆) δ 13.12 (s, 1H, COOH), 7.97 (d, *J* = 9.1 Hz, 1H, Ar), 7.90 (d, *J* = 8.1 Hz, 1H, Ar), 7.65 (d, *J* = 8.4 Hz, 1H, Ar), 7.56–7.46 (m, 2H, Ar), 7.41 (ddd, *J* = 8.1, 6.8, 1.2 Hz, 1H, Ar), 4.79 (hept, *J* = 6.1 Hz, 1H, CH), 1.28 (d, *J* = 6.1 Hz, 6H, Me₂) ppm. Compound **8v** is used in the next step without any further characterization.

2-Isopropoxy-1-naphthoic Anhydride 3v. Compound **8v** (335 mg, 1.46 mmol, 1.0 equiv), TsCl (138 mg, 726 μmol, 0.5 equiv), and K₂CO₃ (301 mg, 3.03 mmol, 1.5 equiv) were dissolved in MeCN (10 mL) and CH₂Cl₂ (10 mL) and reacted according to GP A. Compound **3v** (273 mg, 85%) was obtained as a white solid: mp 135–137 °C; ¹H NMR (400 MHz, CDCl₃) δ 8.11 (dd, *J* = 8.5, 0.8 Hz, 1H, Ar), 7.90 (d, *J* = 9.1 Hz, 1H, Ar), 7.80 (d, *J* = 8.2 Hz, 1H, Ar), 7.55 (ddd, *J* = 8.4, 6.9, 1.3 Hz, 1H, Ar), 7.41 (ddd, *J* = 8.1, 6.9, 1.1 Hz, 1H, Ar), 7.26 (d, *J* = 9.2 Hz, 1H, Ar), 4.74 (hept, *J* = 6.1 Hz, 1H, CH), 1.36 (d, *J* = 6.1 Hz, 6H, Me₂) ppm; ¹³C{¹H} NMR (101 MHz, CDCl₃) δ 163.37, 154.64, 132.77, 131.50, 128.64, 128.22, 128.04, 124.51, 123.95, 117.52, 115.90, 72.78, 22.40 ppm; HRMS (EI) *m/z* [M]⁺ calcd for C₂₈H₂₆O₅ 442.1780, found 442.1773.

General Procedure E (GPE): Synthesis of Product Esters 6 and 7. In a round-bottom flask, the corresponding alcohol (1.0 equiv), anhydride (1.1 or 1.2 equiv), DMAP (0.05 equiv), and Et₃N (1.5 or 2.0 equiv) were dissolved in CH₂Cl₂, and the mixture was stirred at room temperature for 24 h. After full conversion, the reaction mixture was concentrated in a vacuum. The mixture was purified by column chromatography on silica (isohexane/CH₂Cl₂ 6:4).

1-Phenylethyl Benzoate 6aa. Compound **1a** (30.0 mg, 246 μmol, 1.0 equiv), **3a** (61.1 mg, 270 μmol, 1.1 equiv), DMAP (1.50 mg, 12.3 μmol, 0.05 equiv), and Et₃N (70.0 μL, 491 μmol, 1.5 equiv) were dissolved in CH₂Cl₂ (1.23 mL) and reacted according to GP E. After purification by column chromatography on silica (isohexane/CH₂Cl₂ 6:4), **6aa** (50.0 mg, 90%) was obtained as an oil: ¹H NMR (400 MHz, CDCl₃) δ 8.11–8.05 (m, 2H, Ar), 7.60–7.51 (m, 1H, Ar), 7.44 (ddt, *J* = 8.2, 6.4, 1.4 Hz, 4H, Ar), 7.39–7.34 (m, 2H, Ar), 7.32–7.27 (m, 1H, Ar), 6.14 (q, *J* = 6.6 Hz, 1H, CH), 1.67 (d, *J* = 6.6 Hz, 3H, Me) ppm; ¹³C{¹H} NMR (151 MHz, CDCl₃) δ 165.93, 141.92, 133.04, 130.67, 129.78, 128.68, 128.47, 128.02, 126.18, 73.05, 22.56 ppm; HRMS (EI) *m/z* [M]⁺ calcd for C₁₅H₁₄O₂ 226.0994, found 226.0991. The ¹H/¹³C{¹H} NMR spectra are in full agreement with those reported in literature.³⁸

1-Phenylethyl 2-Methoxybenzoate 6ab. Compound **1a** (20.0 mg, 164 μmol, 1.0 equiv), **3f** (51.5 mg, 180 μmol, 1.1 equiv), DMAP (1.00 mg, 8.19 μmol, 0.05 equiv), and Et₃N (45.6 μL, 246 μmol, 2.0 equiv) were dissolved in CH₂Cl₂ (800 μL) and reacted according to GP E. After purification by column chromatography on silica (isohexane/CH₂Cl₂ 6:4), **6ab** (40.0 mg, 96%) was obtained as an oil: ¹H NMR (600 MHz, CDCl₃) δ 7.84 (dd, *J* = 8.0, 1.9 Hz, 1H, Ar), 7.49–7.44 (m, 3H, Ar), 7.36 (t, *J* = 7.6 Hz, 2H, Ar), 7.31–7.27 (m, 1H, Ar), 7.00–6.95 (m, 2H, Ar), 6.14 (q, *J* = 6.6 Hz, 1H, CH), 3.90 (s, 3H, Me), 1.66 (d, *J* = 6.7 Hz, 3H, Me) ppm; ¹³C{¹H} NMR (151 MHz, CDCl₃) δ 165.42, 159.49, 142.10, 133.60, 131.78, 128.57, 127.84, 126.28, 120.48, 120.21, 112.20, 72.78, 56.08, 22.60 ppm; IR (ATR) ν (cm⁻¹) 2938, 1721, 1599, 1490, 1295, 1245, 1130, 1061, 710, 697; HRMS (EI) *m/z* [M]⁺ calcd for C₁₆H₁₆O₃ 256.1099, found 256.1097.

1-Phenylethyl 2-Phenylbenzoate 6af. Compound **1a** (20.0 mg, 164 μmol, 1.0 equiv), **3f** (68.1 mg, 180 μmol, 1.1 equiv), DMAP (1.00 mg, 8.19 μmol, 0.05 equiv), and Et₃N (34.2 μL, 246 μmol, 1.5 equiv) were dissolved in CH₂Cl₂ (800 μL) and reacted according to GP E. After purification by column chromatography on silica (isohexane/CH₂Cl₂ 6:4), **6af** (49.0 mg, 99%) was obtained as an oil: ¹H NMR (400 MHz, CDCl₃) δ 7.84 (ddd, *J* = 7.7, 1.4, 0.5 Hz, 1H, Ar), 7.52 (td, *J* = 7.5, 1.4 Hz, 1H, Ar), 7.41 (td, *J* = 7.6, 1.3 Hz, 1H, Ar), 7.38–7.29 (m, 6H, Ar), 7.26–7.23 (m, 3H, Ar), 7.11–7.07 (m, 2H, Ar), 5.88 (q, *J* = 6.6 Hz, 1H, CH), 1.31 (d, *J* = 6.6 Hz, 3H, Me) ppm; ¹³C{¹H} NMR (101 MHz, CDCl₃) δ 168.14, 142.56, 141.63, 141.44, 131.48, 131.23, 130.88, 130.03, 128.69, 128.46, 128.19, 127.82, 127.32, 127.27, 126.23, 73.44, 22.01 ppm; IR (ATR) ν (cm⁻¹) 2929, 1709, 1597, 1450, 1275, 1125, 1046, 744; HRMS (EI) *m/z* [M]⁺ calcd for C₂₁H₁₈O₂ 302.1307, found 302.1301.

1-Phenylethyl 2-(4-Methylphenyl)benzoate 6ag. Compound **1a** (20.0 mg, 164 μmol, 1.0 equiv), **3g** (73.2 mg, 180 μmol, 1.1 equiv), DMAP (1.00 mg, 8.19 μmol, 0.05 equiv), and Et₃N (34.2 μL, 246 μmol, 1.5 equiv) were dissolved in CH₂Cl₂ (800 μL) and reacted according to GP E. After purification by column chromatography on silica (isohexane/CH₂Cl₂ 6:4), **6ag** (51.0 mg, 99%) was obtained as an oil: ¹H NMR (400 MHz, CDCl₃) δ 7.90 (dd, *J* = 7.8, 1.4 Hz, 1H, Ar), 7.58

CH₂Cl₂ 6:4), **6at** (51.0 mg, 89%) was obtained as an oil: ¹H NMR (400 MHz, CDCl₃) δ 7.86 (d, *J* = 9.1 Hz, 1H, Ar), 7.77 (d, *J* = 8.1 Hz, 1H, Ar), 7.64 (d, *J* = 8.4 Hz, 1H, Ar), 7.52–7.47 (m, 2H, Ar), 7.43 (ddd, *J* = 8.4, 6.9, 1.2 Hz, 1H, Ar), 7.41–7.29 (m, 4H, Ar), 7.26 (d, *J* = 9.1 Hz, 1H, Ar), 6.33 (q, *J* = 6.6 Hz, 1H, CH), 4.11 (t, *J* = 6.5 Hz, 2H, CH₂), 1.78–1.67 (m, 5H, CH₂ and Me), 1.42 (dq, *J* = 14.8, 7.4 Hz, 2H, CH₂), 0.92 (t, *J* = 7.4 Hz, 3H, Me) ppm; ¹³C{¹H} NMR (101 MHz, CDCl₃) δ 167.65, 153.98, 141.66, 131.42, 131.18, 128.61, 128.57, 128.15, 127.99, 127.57, 126.53, 124.10, 123.79, 118.26, 114.41, 73.44, 69.46, 31.56, 22.42, 19.24, 13.97 ppm; IR (ATR) ν (cm⁻¹) 2958, 1721, 1595, 1511, 1463, 1342, 1280, 1208, 1136, 1060, 1023, 807, 745, 697; HRMS (EI) *m/z* [M]⁺ calcd for C₂₃H₂₄O₃ 348.1725, found 348.1729.

1-Phenylethyl 2-(Hexanoxyloxy)-1-naphthoate 6au. Compound **1a** (10.0 mg, 81.9 μmol, 1.0 equiv), **3u** (47.4 mg, 90.4 μmol, 1.1 equiv), DMAP (500 μg, 4.09 μmol, 0.05 equiv), and Et₃N (17.1 μL, 123 μmol, 1.5 equiv) were dissolved in CH₂Cl₂ (400 μL) and reacted according to GP E. After purification by column chromatography on silica (isohexane/CH₂Cl₂ 6:4), **6au** (20.0 mg, 65%) was obtained as an oil: ¹H NMR (400 MHz, CDCl₃) δ 7.86 (d, *J* = 9.0 Hz, 1H, Ar), 7.77 (d, *J* = 8.1 Hz, 1H, Ar), 7.63 (d, *J* = 8.5 Hz, 1H, Ar), 7.51–7.47 (m, 2H, Ar), 7.42 (ddd, *J* = 8.4, 6.8, 1.4 Hz, 1H, Ar), 7.39–7.29 (m, 4H, Ar), 7.25 (d, *J* = 9.1 Hz, 1H, Ar), 6.33 (q, *J* = 6.6 Hz, 1H, CH), 4.10 (t, *J* = 6.6 Hz, 2H, CH₂), 1.78–1.67 (m, 5H, Me and CH₂), 1.46–1.34 (m, 2H, CH₂), 1.33–1.25 (m, 4H, 2xCH₂), 0.93–0.86 (m, 3H, Me) ppm; ¹³C{¹H} NMR (101 MHz, CDCl₃) δ 167.64, 154.01, 141.68, 131.43, 131.19, 128.62, 128.57, 128.15, 127.99, 127.57, 126.52, 124.11, 123.81, 118.27, 114.46, 73.42, 69.83, 31.71, 29.51, 25.71, 22.73, 22.45, 14.20 ppm; IR (ATR) ν (cm⁻¹) 2930, 1723, 1595, 1511, 1464, 1341, 1281, 1208, 1136, 1024, 910, 807, 746, 697; HRMS (EI) *m/z* [M]⁺ calcd for C₂₅H₂₈O₃ 376.2038, found 376.2032.

1-Phenylethyl 2-Isopropoxy-1-naphthoate 6av. Compound **1a** (10.0 mg, 81.9 μmol, 1.0 equiv), **3v** (39.8 mg, 90.4 μmol, 1.1 equiv), DMAP (500 μg, 4.09 μmol, 0.05 equiv), and Et₃N (17.1 μL, 123 μmol, 1.5 equiv) were dissolved in CH₂Cl₂ (400 μL) and reacted according to GP E. After purification by column chromatography on silica (isohexane/CH₂Cl₂ 6:4), **6av** (25.0 mg, 92%) was obtained as an oil: ¹H NMR (400 MHz, CDCl₃) δ 7.84 (d, *J* = 9.1 Hz, 1H, Ar), 7.77 (d, *J* = 8.1 Hz, 1H, Ar), 7.64 (d, *J* = 8.6 Hz, 1H, Ar), 7.52–7.48 (m, 2H, Ar), 7.43 (ddd, *J* = 8.4, 6.8, 1.4 Hz, 1H, Ar), 7.40–7.29 (m, 4H, Ar), 7.25 (d, *J* = 7.2 Hz, 1H, Ar), 6.34 (q, *J* = 6.6 Hz, 1H, CH), 4.68 (hept, *J* = 6.2 Hz, 1H, CH), 1.73 (d, *J* = 6.6 Hz, 3H, Me), 1.28 (d, *J* = 6.1 Hz, 6H, Me₂) ppm; ¹³C{¹H} NMR (101 MHz, CDCl₃) δ 167.71, 152.85, 141.67, 131.24, 131.21, 128.73, 128.56, 128.11, 127.98, 127.51, 126.58, 124.26, 123.85, 119.82, 116.07, 73.30, 72.18, 22.40, 22.38 ppm; IR (ATR) ν (cm⁻¹) 2918, 1718, 1594, 1508, 1465, 1374, 1279, 1227, 1135, 1107, 1042, 994, 907, 806, 747, 700; HRMS (EI) *m/z* [M]⁺ calcd for C₂₂H₂₂O₃ 334.1569, found 334.1558.

1-Phenylethyl 2-Methyl-1-naphthoate 6aw. Compound **1a** (15.0 mg, 123 μmol, 1.0 equiv), **3w** (47.9 mg, 135 μmol, 1.1 equiv), DMAP (750 μg, 6.14 μmol, 0.05 equiv), and Et₃N (25.7 μL, 184.2 μmol, 1.5 equiv) were dissolved in CH₂Cl₂ (600 μL) and reacted according to GP E. After purification by column chromatography on silica (isohexane/CH₂Cl₂ 6:4), **6aw** (15.0 mg, 43%) was obtained as an oil: ¹H NMR (400 MHz, CDCl₃) δ 7.83–7.76 (m, 2H, Ar), 7.73–7.68 (m, 1H, Ar), 7.51–7.28 (m, 8H, Ar), 6.35 (q, *J* = 6.6 Hz, 1H, CH), 2.44 (s, 3H, Me), 1.76 (d, *J* = 6.6 Hz, 3H, Me) ppm; ¹³C{¹H} NMR (101 MHz, CDCl₃) δ 169.17, 141.35, 133.22, 131.76, 130.41, 130.13, 129.65, 128.71, 128.50, 128.26, 128.14, 127.07, 126.61, 125.55, 124.54, 73.65, 22.45, 20.11 ppm; IR (ATR) ν (cm⁻¹) 2928, 1716, 1509, 1454, 1378, 1276, 1217, 1207, 1137, 1045, 1006, 993, 812, 741, 700; HRMS (EI) *m/z* [M]⁺ calcd for C₂₀H₁₈O₂ 290.1307, found 290.1298.

1-Phenylethyl 2-Naphthoate 6az. Compound **1a** (50.0 mg, 409 μmol, 1.0 equiv), **3z** (160 mg, 491 μmol, 1.2 equiv), DMAP (2.50 mg, 20.5 μmol, 0.05 equiv), and Et₃N (850 μL, 613 μmol, 1.5 equiv) were dissolved in CH₂Cl₂ (2 mL) and reacted according to GP E. After purification by column chromatography on silica (isohexane/CH₂Cl₂ 6:4), **6az** (110 mg, 97%) was obtained as an oil: ¹H NMR (400 MHz, CDCl₃) δ 8.65 (s, 1H, Ar), 8.10 (dd, *J* = 8.6, 1.7 Hz, 1H, Ar), 7.97 (d, *J* = 7.9 Hz, 1H, Ar), 7.89 (d, *J* = 8.5 Hz, 2H, Ar), 7.62–7.48 (m, 4H, Ar), 7.40 (t, *J* = 7.4 Hz, 2H, Ar), 7.36–7.29 (m, 1H, Ar), 6.21 (q, *J* = 6.6 Hz,

1H, CH), 1.74 (d, *J* = 6.6 Hz, 3H, Me) ppm; ¹³C{¹H} NMR (101 MHz, CDCl₃) δ 166.11, 141.95, 135.66, 132.62, 131.20, 129.49, 128.71, 128.34, 128.24, 128.05, 127.90, 127.89, 126.74, 126.24, 125.45, 73.19, 22.59 ppm; IR (ATR) ν (cm⁻¹) 2932, 1709, 1630, 1452, 1353, 1274, 1225, 1194, 1129, 1088, 1059, 954, 864, 777, 696; HRMS (EI) *m/z* [M]⁺ calcd for C₁₉H₁₆O₂ 276.1150, found 276.1155.

Phenylethyl Benzoate 7aa. Compound **2a** (30.0 mg, 246 μmol, 1.0 equiv), **3a** (61.1 mg, 270 μmol, 1.1 equiv), DMAP (1.50 mg, 12.3 μmol, 0.05 equiv), and Et₃N (850 μL, 613 μmol, 1.5 equiv) were dissolved in CH₂Cl₂ (2 mL) and reacted according to GP E. After purification by column chromatography on silica (isohexane/CH₂Cl₂ 6:4), **7aa** (50 mg, 90%) was obtained as an oil: ¹H NMR (400 MHz, CDCl₃) δ 8.05–8.00 (m, 2H, Ar), 7.59–7.52 (m, 1H, Ar), 7.45 (s, 2H, Ar), 7.36–7.27 (m, 4H, Ar), 7.26–7.22 (m, 1H, Ar), 4.54 (t, *J* = 7.0 Hz, 2H, CH₂), 3.09 (t, *J* = 7.0 Hz, 2H, CH₂) ppm; ¹³C{¹H} NMR (101 MHz, CDCl₃) δ 166.66, 138.05, 133.04, 130.43, 129.70, 129.11, 128.68, 128.49, 126.73, 65.62, 35.40 ppm; HRMS (EI) *m/z* [M - H₂]⁺ calcd for C₁₅H₁₂O₂ 224.0837, found 224.0831. The ¹H/¹³C{¹H} NMR spectra are in full agreement with them reported in literature.⁴⁰

Phenylethyl 2-Methoxybenzoate 7ab. Compound **2a** (20.0 mg, 164 μmol, 1.0 equiv), **3b** (51.5 mg, 180 μmol, 1.1 equiv), DMAP (1.00 mg, 8.19 μmol, 0.05 equiv), and Et₃N (45.6 μL, 246 μmol, 2.0 equiv) were dissolved in CH₂Cl₂ (800 μL) and reacted according to GP E. After purification by column chromatography on silica (isohexane/CH₂Cl₂ 6:4), **7ab** (40.0 mg, 96%) was obtained as an oil: ¹H NMR (600 MHz, CDCl₃) δ 7.74 (dd, *J* = 7.9, 1.8 Hz, 1H, Ar), 7.46 (ddd, *J* = 8.4, 7.4, 1.8 Hz, 1H, Ar), 7.34–7.28 (m, 4H, Ar), 7.26–7.22 (m, 1H, Ar), 6.99–6.94 (m, 2H, Ar), 4.52 (t, *J* = 7.0 Hz, 2H, CH₂), 3.88 (s, 3H, Me), 3.07 (t, *J* = 7.0 Hz, 2H, CH₂) ppm; ¹³C{¹H} NMR (151 MHz, CDCl₃) δ 166.21, 159.38, 138.21, 133.63, 131.77, 129.15, 128.61, 126.64, 120.24, 120.22, 112.12, 65.47, 56.05, 35.33 ppm; IR (ATR) ν (cm⁻¹) 2955, 1722, 1600, 1490, 1455, 1297, 1250, 1129, 1076, 750, 697; HRMS (EI) *m/z* [M]⁺ calcd for C₁₆H₁₆O₃ 256.1099, found 256.1088.

Phenylethyl 2-Phenylbenzoate 7af. Compound **2a** (20.0 mg, 164 μmol, 1.0 equiv), **3f** (68.1 mg, 180 μmol, 1.1 equiv), DMAP (1.00 mg, 8.19 μmol, 0.05 equiv), and Et₃N (34.2 μL, 246 μmol, 1.5 equiv) were dissolved in CH₂Cl₂ (800 μL) and reacted according to GP E. After purification by column chromatography on silica (isohexane/CH₂Cl₂ 6:4), **7af** (49.0 mg, 99%) was obtained as an oil: ¹H NMR (400 MHz, CDCl₃) δ 7.79 (dd, *J* = 7.7, 1.4 Hz, 1H, Ar), 7.53 (td, *J* = 7.5, 1.4 Hz, 1H, Ar), 7.43–7.36 (m, 5H, Ar), 7.34–7.30 (m, 2H, Ar), 7.29–7.26 (m, 1H, Ar), 7.25–7.24 (m, 1H, Ar), 7.23–7.17 (m, 1H, Ar), 7.11–7.06 (m, 2H, Ar), 4.26 (t, *J* = 7.2 Hz, 2H, CH₂), 2.66 (t, *J* = 7.2 Hz, 2H, CH₂) ppm; ¹³C{¹H} NMR (101 MHz, CDCl₃) δ 168.81, 142.63, 141.63, 137.82, 131.33, 131.22, 130.79, 129.93, 128.98, 128.56, 128.19, 127.37, 127.29, 126.60, 65.59, 34.77 ppm (one signal is overlapping); IR (ATR) ν (cm⁻¹) 2918, 1714, 1598, 1452, 1277, 1084, 1047, 743, 700; HRMS (EI) *m/z* [M]⁺ calcd for C₂₁H₁₈O₂ 302.1307, found 302.1287.

Phenylethyl 2-(4-Methylphenyl)benzoate 7ag. Compound **2a** (20.0 mg, 164 μmol, 1.0 equiv), **3g** (73.2 mg, 180 μmol, 1.1 equiv), DMAP (1.00 mg, 8.19 μmol, 0.05 equiv), and Et₃N (34.2 μL, 246 μmol, 1.5 equiv) were dissolved in CH₂Cl₂ (800 μL) and reacted according to GP E. After purification by column chromatography on silica (isohexane/CH₂Cl₂ 6:4), **7ag** (51.0 mg, 98%) was obtained as an oil: ¹H NMR (400 MHz, CDCl₃) δ 7.81 (d, *J* = 7.6 Hz, 1H, Ar), 7.59–7.54 (m, 1H, Ar), 7.43 (t, *J* = 7.5 Hz, 2H, Ar), 7.35–7.23 (m, 7H, Ar), 7.18–7.13 (m, 2H, Ar), 4.34 (t, *J* = 7.2 Hz, 2H, CH₂), 2.77 (t, *J* = 7.2 Hz, 2H, CH₂), 2.45 (s, 3H, Me) ppm; ¹³C{¹H} NMR (101 MHz, CDCl₃) δ 168.89, 142.61, 138.62, 137.90, 137.07, 131.28, 131.20, 130.82, 129.84, 128.98, 128.94, 128.56, 128.44, 127.06, 126.60, 65.56, 34.85, 21.37 ppm; IR (ATR) ν (cm⁻¹) 3026, 1715, 1599, 1445, 1240, 1124, 1082, 1046, 819, 757; HRMS (EI) *m/z* [M]⁺ calcd for C₂₂H₂₀O₂ 316.1463, found 316.1455.

Phenylethyl 2-(Naphthalene-1-yl)benzoate 7ah. Compound **2a** (20.0 mg, 164 μmol, 1.0 equiv), **3h** (86.2 mg, 180 μmol, 1.1 equiv), DMAP (1.00 mg, 8.19 μmol, 0.05 equiv), and Et₃N (34.2 μL, 246 μmol, 1.5 equiv) were dissolved in CH₂Cl₂ (800 μL) and reacted according to GP E. After purification by column chromatography on silica (isohexane/CH₂Cl₂ 6:4), **7ah** (50.0 mg, 87%) was obtained as an oil: ¹H NMR (400 MHz, CDCl₃) δ 7.99 (dd, *J* = 7.8, 1.2 Hz, 1H, Ar), 7.89

(dd, $J = 11.5, 8.2$ Hz, 2H, Ar), 7.61 (td, $J = 7.5, 1.4$ Hz, 1H, Ar), 7.54–7.49 (m, 3H, Ar), 7.48–7.45 (m, 1H, Ar), 7.42 (dd, $J = 7.6, 1.0$ Hz, 1H, Ar), 7.40–7.36 (m, 1H, Ar), 7.33 (dd, $J = 7.0, 1.1$ Hz, 1H, Ar), 7.21–7.12 (m, 3H, Ar), 6.86 (dd, $J = 7.7, 1.6$ Hz, 2H, Ar), 4.01–3.83 (m, 2H, CH₂), 2.24–2.06 (m, 2H, CH₂) ppm; ¹³C{¹H} NMR (101 MHz, CDCl₃) δ 167.87, 141.27, 139.98, 137.70, 133.42, 132.31, 131.96, 131.93, 131.71, 130.32, 128.82, 128.43, 128.34, 127.74, 127.67, 126.47, 126.22, 126.16, 125.85, 125.79, 125.32, 65.36, 34.26 ppm; IR (ATR) ν (cm⁻¹) 3028, 1709, 1594, 1496, 1453, 1394, 1280, 1243, 1119, 1076, 962, 800, 778, 760, 700; HRMS (EI) m/z [M]⁺ calcd for C₂₅H₂₀O₂ 352.1463, found 352.1457.

Phenylethyl 2,6-Dimethylbenzoate 7am. Compound **2a** (15.0 mg, 123 μ mol, 1.0 equiv), **3m** (38.1 mg, 135 μ mol, 1.1 equiv), DMAP (750 μ g, 6.14 μ mol, 0.05 equiv), and Et₃N (25.7 μ L, 184.2 μ mol, 1.5 equiv) were dissolved in CH₂Cl₂ (600 μ L) and reacted according to GP E. After purification by column chromatography on silica (isohexane/CH₂Cl₂ 6:4), **7am** (10.0 mg, 34%) was obtained as an oil: ¹H NMR (400 MHz, CDCl₃) δ 7.34–7.21 (m, 5H, Ar), 7.20–7.15 (m, 1H, Ar), 7.01 (d, $J = 7.6$ Hz, 2H, Ar), 4.57 (t, $J = 7.1$ Hz, 2H, CH₂), 3.07 (t, $J = 7.0$ Hz, 2H, CH₂), 2.22 (s, 6H, Me₂) ppm; ¹³C{¹H} NMR (101 MHz, CDCl₃) δ 170.12, 137.76, 135.05, 134.04, 129.38, 129.05, 128.68, 127.65, 126.78, 65.47, 35.23, 19.75 ppm; IR (ATR) ν (cm⁻¹) 2956, 1721, 1596, 11455, 1263, 1112, 1090, 770, 739, 697; HRMS (EI) m/z [M]⁺ calcd for C₁₇H₁₈O₂ 254.1307, found 254.1297.

Phenylethyl 2-Methyl-6-phenylbenzoate 7an. Compound **2a** (15.0 mg, 123 μ mol, 1.0 equiv), **3n** (54.9 mg, 135 μ mol, 1.1 equiv), DMAP (750 μ g, 6.14 μ mol, 0.05 equiv), and Et₃N (25.7 μ L, 184.2 μ mol, 1.5 equiv) were dissolved in CH₂Cl₂ (600 μ L) and reacted according to GP E. After purification by column chromatography on silica (isohexane/CH₂Cl₂ 6:4), **7an** (25.0 mg, 65%) was obtained as an oil: ¹H NMR (400 MHz, CDCl₃) δ 7.39–7.33 (m, 6H, Ar), 7.28–7.18 (m, 5H, Ar), 7.11–7.04 (m, 2H, Ar), 4.22 (t, $J = 7.3$ Hz, 2H, CH₂), 2.62 (t, $J = 7.3$ Hz, 2H, CH₂), 2.36 (s, 3H, Me) ppm; ¹³C{¹H} NMR (101 MHz, CDCl₃) δ 169.87, 141.17, 140.36, 137.72, 135.65, 133.35, 129.49, 129.26, 128.93, 128.57, 128.51, 128.41, 127.49, 127.34, 126.61, 65.53, 34.70, 19.80 ppm; IR (ATR) ν (cm⁻¹) 2954, 1721, 1461, 1260, 1122, 1091, 1065, 757, 700; HRMS (EI) m/z [M]⁺ calcd for C₂₂H₂₀O₂ 316.1463, found 316.1456.

Phenylethyl 2-Methyl-6-nitrobenzoate 7ao. Compound **2a** (20.0 mg, 164 μ mol, 1.0 equiv), **3o** (62.0 mg, 180 μ mol, 1.1 equiv), DMAP (1.00 mg, 8.19 μ mol, 0.05 equiv), and Et₃N (34.2 μ L, 245.6 μ mol, 1.5 equiv) were dissolved in CH₂Cl₂ (800 μ L) and reacted according to GP E. After purification by column chromatography on silica (isohexane/CH₂Cl₂ 6:4), **7ao** (40.0 mg, 86%) was obtained as a white solid: mp 55–58 °C; ¹H NMR (400 MHz, CDCl₃) δ 7.98 (d, $J = 8.1$ Hz, 1H, Ar), 7.53–7.49 (m, 1H, Ar), 7.45 (t, $J = 7.9$ Hz, 1H, Ar), 7.33–7.28 (m, 2H, Ar), 7.27–7.21 (m, 3H, Ar), 4.62 (t, $J = 7.1$ Hz, 2H, CH₂), 3.08 (t, $J = 7.1$ Hz, 2H, CH₂), 2.34–2.26 (m, 3H, Me) ppm; ¹³C{¹H} NMR (101 MHz, CDCl₃) δ 166.34, 137.53, 137.33, 135.89, 129.62, 129.47, 128.84, 128.51, 126.61, 121.73, 66.45, 34.64, 18.94 ppm (one signal is overlapping); IR (ATR) ν (cm⁻¹) 2917, 1721, 1529, 1454, 1343, 21270, 1121, 1077, 991, 920, 804, 740, 700; HRMS (EI) m/z [M]⁺ calcd for C₁₆H₁₅NO₄ 285.1001, found 285.0992.

Phenylethyl 2-Fluoro-6-(trifluoromethyl)benzoate 7ap. Compound **2a** (15.0 mg, 123 μ mol, 1.0 equiv), **3p** (53.8 mg, 135 μ mol, 1.1 equiv), DMAP (750 μ g, 6.14 μ mol, 0.05 equiv), and Et₃N (25.7 μ L, 184.2 μ mol, 1.5 equiv) were dissolved in CH₂Cl₂ (600 μ L) and reacted according to GP E. After purification by column chromatography on silica (isohexane/CH₂Cl₂ 6:4), **7ap** (15.0 mg, 39%) was obtained as an oil: ¹H NMR (400 MHz, CDCl₃) δ 7.58–7.48 (m, 2H, Ar), 7.37–7.28 (m, 3H, Ar), 7.29–7.22 (m, 3H, Ar), 4.59 (t, $J = 7.3$ Hz, 2H, CH₂), 3.08 (t, $J = 7.3$ Hz, 2H, CH₂) ppm; ¹³C{¹H} NMR (101 MHz, CDCl₃) δ 163.44, 160.75, 158.24, 137.28, 131.74, 131.65, 129.01, 128.70, 126.83, 122.11 (qd, $J = 4.7, 3.5$ Hz), 119.95 (q, $J = 1.0$ Hz), 119.73 (q, $J = 1.0$ Hz), 67.05, 34.91 ppm; ¹⁹F NMR (377 MHz, CDCl₃) δ –59.78, –113.07 ppm; IR (ATR) ν (cm⁻¹) 2961, 1739, 1464, 1218, 1269, 1171, 1061, 913, 803, 747, 698; HRMS (EI) m/z [M]⁺ calcd for C₁₆H₁₂O₂F₄ 312.0773, found 312.0761.

Phenylethyl 1-Naphthoate 7aq. Compound **2a** (50.0 mg, 409 μ mol, 1.0 equiv), **3q** (160 mg, 491 μ mol, 1.2 equiv), DMAP (2.50 mg,

20.5 μ mol, 0.05 equiv), and Et₃N (850 μ L, 613 μ mol, 1.5 equiv) were dissolved in CH₂Cl₂ (2 mL) and reacted according to GP E. After purification by column chromatography on silica (isohexane/CH₂Cl₂ 6:4), **7aq** (112 mg, 99%) was obtained as an oil: ¹H NMR (400 MHz, CDCl₃) δ 8.80 (d, $J = 8.4$ Hz, 1H, Ar), 8.12 (d, $J = 7.3$ Hz, 1H, Ar), 8.01 (d, $J = 8.2$ Hz, 1H, Ar), 7.88 (d, $J = 7.9$ Hz, 1H, Ar), 7.60–7.45 (m, 3H, Ar), 7.39–7.31 (m, 4H, Ar), 7.31–7.27 (m, 1H, Ar), 4.65 (t, $J = 7.0$ Hz, 2H, CH₂), 3.15 (t, $J = 6.9$ Hz, 2H, CH₂); ¹³C{¹H} NMR (101 MHz, CDCl₃) δ 167.68, 138.10, 133.94, 133.43, 131.43, 130.30, 129.16, 128.73, 128.63, 127.82, 127.42, 126.78, 126.31, 125.97, 124.63, 65.77, 35.40 ppm; HRMS (EI) m/z [M]⁺ calcd for C₁₉H₁₆O₂ 276.1150, found 276.1132. The ¹H/¹³C{¹H} NMR spectra are in full agreement with them reported in literature.⁴¹

Phenylethyl 2-Methoxy-1-naphthoate 7ar. Compound **2a** (20.0 mg, 164 μ mol, 1.0 equiv), **3r** (75.9 mg, 196 μ mol, 1.2 equiv), DMAP (1.00 mg, 8.19 μ mol, 0.05 equiv), and Et₃N (45.6 μ L, 327 μ mol, 2.0 equiv) were dissolved in CH₂Cl₂ (800 μ L) and reacted according to GP E. After purification by column chromatography on silica (isohexane/CH₂Cl₂ 6:4), **7ar** (45.0 mg, 90%) was obtained as a white solid: mp 48–50 °C; ¹H NMR (400 MHz, CDCl₃) δ 7.89 (d, $J = 9.1$ Hz, 1H, Ar), 7.78 (d, $J = 7.5$ Hz, 1H, Ar), 7.56 (d, $J = 8.6$ Hz, 1H, Ar), 7.41 (ddd, $J = 8.4, 6.8, 1.4$ Hz, 1H, Ar), 7.37–7.34 (m, 1H, Ar), 7.34–7.29 (m, 4H, Ar), 7.29–7.26 (m, 2H, Ar), 4.70 (t, $J = 7.0$ Hz, 2H, CH₂), 3.92 (s, 3H, Me), 3.14 (t, $J = 7.0$ Hz, 2H, CH₂) ppm; ¹³C{¹H} NMR (101 MHz, CDCl₃) δ 168.14, 154.57, 137.98, 131.75, 131.07, 129.19, 128.67, 128.65, 128.15, 127.70, 126.70, 124.22, 123.97, 117.74, 113.26, 65.97, 56.87, 35.30 ppm; IR (ATR) ν (cm⁻¹) 2913, 1718, 1624, 1594, 1511, 1473, 1371, 1339, 1289, 1258, 1233, 1137, 1080, 1017, 813, 738, 697; HRMS (EI) m/z [M]⁺ calcd for C₂₀H₁₈O₃ 306.1256, found 306.1251.

Phenylethyl 2-Ethoxy-1-naphthoate 7as. Compound **2a** (20.0 mg, 164 μ mol, 1.0 equiv), **3s** (81.4 mg, 196 μ mol, 1.2 equiv), DMAP (1.00 mg, 8.19 μ mol, 0.05 equiv), and Et₃N (45.6 μ L, 327 μ mol, 2.0 equiv) were dissolved in CH₂Cl₂ (800 μ L) and reacted according to GP E. After purification by column chromatography on silica (isohexane/CH₂Cl₂ 6:4), **7as** (50.0 mg, 95%) was obtained as an oil: ¹H NMR (400 MHz, CDCl₃) δ 7.88 (d, $J = 9.1$ Hz, 1H, Ar), 7.79 (d, $J = 7.6$ Hz, 1H, Ar), 7.60 (d, $J = 9.1$ Hz, 1H, Ar), 7.43 (ddd, $J = 8.4, 6.8, 1.4$ Hz, 1H, Ar), 7.39–7.35 (m, 1H, Ar), 7.35–7.30 (m, 4H, Ar), 7.29–7.26 (m, 2H, Ar), 4.70 (t, $J = 7.1$ Hz, 2H, CH₂), 4.21 (q, $J = 7.0$ Hz, 2H, CH₂), 3.16 (t, $J = 7.2$ Hz, 2H, CH₂), 1.41 (t, $J = 7.0$ Hz, 3H, Me) ppm; ¹³C{¹H} NMR (101 MHz, CDCl₃) δ 168.21, 153.95, 137.94, 131.57, 131.10, 129.17, 128.68, 128.12, 127.61, 126.72, 124.22, 123.99, 118.38, 114.62, 65.90, 65.54, 35.37, 15.13 ppm (one signal is overlapping); IR (ATR) ν (cm⁻¹) 2980, 1720, 1594, 1511, 1466, 1435, 1372, 1281, 1212, 1134, 1063, 1023, 806, 744, 697; HRMS (EI) m/z [M]⁺ calcd for C₂₁H₂₀O₃ 320.1412, found 320.1403.

Phenylethyl 2-Butoxy-1-naphthoate 7at. Compound **2a** (20.0 mg, 164 μ mol, 1.0 equiv), **3t** (84.7 mg, 180 μ mol, 1.1 equiv), DMAP (1.00 mg, 8.19 μ mol, 0.05 equiv), and Et₃N (45.6 μ L, 327 μ mol, 2.0 equiv) were dissolved in CH₂Cl₂ (800 μ L) and reacted according to GP E. After purification by column chromatography on silica (isohexane/CH₂Cl₂ 6:4), **7at** (49.0 mg, 86%) was obtained as an oil: ¹H NMR (400 MHz, CDCl₃) δ 7.86 (d, $J = 9.1$ Hz, 1H, Ar), 7.77 (d, $J = 8.0$ Hz, 1H, Ar), 7.57 (d, $J = 8.4$ Hz, 1H, Ar), 7.41 (ddd, $J = 8.4, 6.9, 1.3$ Hz, 1H, Ar), 7.37–7.28 (m, 5H, Ar), 7.26 (d, $J = 9.0$ Hz, 2H, Ar), 4.67 (t, $J = 7.3$ Hz, 2H, CH₂), 4.13 (t, $J = 6.5$ Hz, 2H, CH₂), 3.13 (t, $J = 7.2$ Hz, 2H, CH₂), 1.82–1.70 (m, 2H, CH₂), 1.48 (dt, $J = 14.7, 7.5$ Hz, 2H, CH₂), 0.97 (t, $J = 7.4$ Hz, 3H, Me) ppm; ¹³C{¹H} NMR (101 MHz, CDCl₃) δ 168.19, 154.09, 137.87, 131.52, 131.08, 129.13, 128.67, 128.60, 128.10, 127.57, 126.70, 124.13, 123.91, 118.17, 114.47, 69.52, 65.87, 35.35, 31.55, 19.25, 13.97 ppm; IR (ATR) ν (cm⁻¹) 2957, 1722, 1625, 1594, 1511, 1463, 1341, 1281, 1212, 1134, 1070, 1021, 807, 744, 697; HRMS (EI) m/z [M]⁺ calcd for C₂₃H₂₄O₃ 348.1725, found 348.1716.

Phenylethyl 2-(Hexanoyloxy)-1-naphthoate 7au. Compound **2a** (10.0 mg, 81.9 μ mol, 1.0 equiv), **3u** (47.4 mg, 90.4 μ mol, 1.1 equiv), DMAP (500 μ g, 4.09 μ mol, 0.05 equiv), and Et₃N (17.1 μ L, 123 μ mol, 1.5 equiv) were dissolved in CH₂Cl₂ (400 μ L) and reacted according to GP E. After purification by column chromatography on silica (isohexane/CH₂Cl₂ 6:4), **7au** (10.0 mg, 33%) was obtained as an oil:

^1H NMR (400 MHz, CDCl_3) δ 7.86 (d, $J = 9.0$ Hz, 1H, Ar), 7.79–7.75 (m, 1H, Ar), 7.58 (dq, $J = 8.5, 0.9$ Hz, 1H, Ar), 7.41 (ddd, $J = 8.4, 6.8, 1.4$ Hz, 1H, Ar), 7.37–7.29 (m, 5H, Ar), 7.27 (d, $J = 2.3$ Hz, 1H, Ar), 7.26–7.23 (m, 1H, Ar), 4.68 (t, $J = 7.3$ Hz, 2H, CH_2), 4.12 (t, $J = 6.5$ Hz, 2H, CH_2), 3.14 (t, $J = 7.2$ Hz, 2H, CH_2), 1.84–1.72 (m, 2H, CH_2), 1.52–1.41 (m, 2H, CH_2), 1.38–1.28 (m, 4H, $2 \times \text{CH}_2$), 0.93–0.87 (m, 3H, Me) ppm; $^{13}\text{C}\{^1\text{H}\}$ NMR (101 MHz, CDCl_3) δ 168.20, 154.12, 137.89, 131.54, 131.11, 129.16, 128.69, 128.62, 128.12, 127.60, 126.73, 124.16, 123.95, 118.19, 114.52, 69.89, 65.89, 35.39, 31.69, 29.51, 25.74, 22.78, 14.19 ppm; IR (ATR) ν (cm^{-1}) 2925, 1723, 1594, 1511, 1463, 1341, 1282, 1213, 1135, 1066, 1018, 807, 744, 698; HRMS (EI) m/z $[\text{M}]^+$ calcd for $\text{C}_{25}\text{H}_{28}\text{O}_3$ 376.2038, found 376.2032.

Phenylethyl 2-Isopropoxy-1-naphthoate 7av. Compound **2a** (10.0 mg, 81.9 μmol , 1.0 equiv), **3v** (39.8 mg, 90.4 μmol , 1.1 equiv), DMAP (500 μg , 4.09 μmol , 0.05 equiv), and Et_3N (17.1 μL , 123 μmol , 1.5 equiv) were dissolved in CH_2Cl_2 (400 μL) and reacted according to GP E. After purification by column chromatography on silica (isohexane/ CH_2Cl_2 6:4), **7av** (25.0 mg, 92%) was obtained as an oil: ^1H NMR (400 MHz, CDCl_3) δ = 7.84 (d, $J = 9.0$ Hz, 1H, Ar), 7.80–7.74 (m, 1H, Ar), 7.61–7.55 (m, 1H, Ar), 7.41 (ddd, $J = 8.4, 6.8, 1.4$ Hz, 1H, Ar), 7.35 (ddd, $J = 8.0, 6.8, 1.2$ Hz, 1H, Ar), 7.33–7.29 (m, 4H, Ar), 7.28–7.22 (m, 2H, Ar), 4.75–4.60 (m, 3H, CH_2 and CH), 3.14 (t, $J = 7.2$ Hz, 2H, CH_2), 1.33 (d, $J = 6.1$ Hz, 6H, Me_2) ppm; $^{13}\text{C}\{^1\text{H}\}$ NMR (101 MHz, CDCl_3) δ 168.30, 153.05, 137.94, 131.32, 131.16, 129.16, 128.78, 128.70, 128.08, 127.52, 126.72, 124.33, 124.00, 119.86, 116.35, 72.59, 65.84, 35.39, 22.49 ppm; IR (ATR) ν (cm^{-1}) 2976, 1721, 1593, 1509, 1455, 1434, 1372, 1334, 1280, 1200, 1107, 1024, 998, 905, 807, 745, 697; HRMS (EI) m/z $[\text{M}]^+$ calcd for $\text{C}_{22}\text{H}_{22}\text{O}_3$ 334.1569, found 334.1560.

Phenylethyl 2-Methyl-1-naphthoate 7aw. Compound **2a** (15.0 mg, 123 μmol , 1.0 equiv), **3w** (47.9 mg, 135 μmol , 1.1 equiv), DMAP (750 μg , 6.14 μmol , 0.05 equiv), and Et_3N (25.7 μL , 184.2 μmol , 1.5 equiv) were dissolved in CH_2Cl_2 (600 μL) and reacted according to GP E. After purification by column chromatography on silica (isohexane/ CH_2Cl_2 6:4), **7aw** (15.0 mg, 43%) was obtained as an oil: ^1H NMR (400 MHz, CDCl_3) δ 7.83–7.77 (m, 2H, Ar), 7.66 (ddt, $J = 6.1, 3.3, 0.8$ Hz, 1H, Ar), 7.49–7.39 (m, 2H, Ar), 7.36–7.23 (m, 6H, Ar), 4.72 (t, $J = 7.0$ Hz, 2H, CH_2), 3.14 (t, $J = 7.0$ Hz, 2H, CH_2), 2.41 (s, 3H, Me) ppm; $^{13}\text{C}\{^1\text{H}\}$ NMR (101 MHz, CDCl_3) δ 169.81, 137.77, 133.53, 131.73, 130.23, 130.13, 129.74, 129.14, 128.73, 128.48, 128.10, 127.10, 126.82, 125.55, 124.68, 65.85, 35.30, 20.18 ppm; IR (ATR) ν (cm^{-1}) 2912, 1707, 1508, 1454, 1386, 1285, 1245, 1207, 1137, 1053, 989, 819, 740, 694; HRMS (EI) m/z $[\text{M}]^+$ calcd for $\text{C}_{20}\text{H}_{18}\text{O}_2$ 290.1307, found 290.1303.

Phenylethyl 2-Naphthoate 7az. Compound **2a** (50.0 mg, 409 μmol , 1.0 equiv), **3z** (160 mg, 491 μmol , 1.2 equiv), DMAP (2.50 mg, 20.5 μmol , 0.05 equiv), and Et_3N (850 μL , 613 μmol , 1.5 equiv) were dissolved in CH_2Cl_2 (2 mL) and reacted according to GP E. After purification by column chromatography on silica (isohexane/ CH_2Cl_2 6:4), **7az** (110 mg, 97%) was obtained as a white solid: mp 65–67 °C; ^1H NMR (400 MHz, CDCl_3) δ 8.59 (s, 1H, Ar), 8.04 (dd, $J = 8.6, 1.6$ Hz, 1H, Ar), 7.95 (d, $J = 8.0$ Hz, 1H, Ar), 7.88 (d, $J = 8.4$ Hz, 2H, Ar), 7.62–7.52 (m, 2H, Ar), 7.39–7.31 (m, 4H, Ar), 7.26 (m, 1H, Ar), 4.61 (t, $J = 7.1$ Hz, 2H, CH_2), 3.15 (t, $J = 7.0$ Hz, 2H, CH_2) ppm; $^{13}\text{C}\{^1\text{H}\}$ NMR (101 MHz, CDCl_3) δ 166.80, 138.05, 135.65, 132.61, 131.21, 129.50, 129.15, 128.70, 128.36, 128.27, 127.89, 127.67, 126.76, 126.76, 125.35, 65.74, 35.46; HRMS (EI) m/z $[\text{M}]^+$ calcd for $\text{C}_{19}\text{H}_{16}\text{O}_2$ 276.1150, found 276.1151. The $^1\text{H}/^{13}\text{C}\{^1\text{H}\}$ NMR spectra are in full agreement with them reported in literature.⁴¹

1-(Naphthalen-2-yl)ethyl Benzoate 6ba. Compound **1b** (60.0 mg, 348 μmol , 1.0 equiv), **3a** (118 mg, 522 μmol , 1.5 equiv), DMAP (2.13 mg, 17.4 μmol , 0.05 equiv), and Et_3N (100 μL , 696 μmol , 1.5 equiv) were dissolved in CH_2Cl_2 (2 mL) and reacted according to GP E. After purification by column chromatography on silica (isohexane/ CH_2Cl_2 6:4), **6ba** (95.0 mg, 99%) was obtained as a white solid: mp 52–53 °C; ^1H NMR (400 MHz, CDCl_3) δ 8.16–8.06 (m, 2H, Ar), 7.92–7.79 (m, 4H, Ar), 7.60–7.52 (m, 2H, Ar), 7.52–7.39 (m, 4H, Ar), 6.31 (q, $J = 6.6, 1.6$ Hz, 1H, CH), 1.77 (dd, $J = 6.7, 1.4$ Hz, 3H, Me) ppm; $^{13}\text{C}\{^1\text{H}\}$ NMR (101 MHz, CDCl_3) δ 165.99, 139.25, 133.35, 133.19, 133.08,

130.67, 129.81, 128.57, 128.50, 128.20, 127.81, 126.37, 126.21, 125.15, 124.22, 73.21, 22.50 ppm; HRMS (EI) m/z $[\text{M}]^+$ calcd for $\text{C}_{19}\text{H}_{16}\text{O}_2$ 276.1150, found 276.1157. The $^1\text{H}/^{13}\text{C}\{^1\text{H}\}$ NMR spectra are in full agreement with them reported in literature.⁴²

1-(Naphthalen-2-yl)ethyl 2-Methoxybenzoate 6bb. Compound **1b** (20.0 mg, 116 μmol , 1.0 equiv), **3b** (39.9 mg, 139 μmol , 1.2 equiv), DMAP (709 μg , 5.81 μmol , 0.05 equiv), and Et_3N (32.4 μL , 232 μmol , 2.0 equiv) were dissolved in CH_2Cl_2 (580 μL) and reacted according to GP E. After purification by column chromatography on silica (isohexane/ CH_2Cl_2 6:4), **6bb** (30.0 mg, quant.) was obtained as an oil: ^1H NMR (400 MHz, CDCl_3) δ 7.93 (s, 1H, Ar), 7.86 (tq, $J = 7.7, 6.7, 3.3, 2.6$ Hz, 4H, Ar), 7.60 (dd, $J = 8.5, 1.7$ Hz, 1H, Ar), 7.47 (ddd, $J = 9.1, 5.9, 1.9$ Hz, 3H, Ar), 7.05–6.94 (m, 2H, Ar), 6.31 (q, $J = 6.6$ Hz, 1H, CH), 3.91 (s, 3H, Me), 1.75 (d, $J = 6.6$ Hz, 3H, Me) ppm; $^{13}\text{C}\{^1\text{H}\}$ NMR (101 MHz, CDCl_3) δ 165.50, 159.46, 139.42, 133.61, 133.35, 133.10, 131.78, 128.38, 128.17, 127.77, 126.25, 126.07, 125.20, 124.37, 120.48, 120.22, 112.19, 72.91, 56.06, 22.52 ppm; IR (ATR) ν (cm^{-1}) 2977, 1721, 1599, 1490, 1435, 1294, 1200, 1178, 1126, 1060, 858, 819, 750; HRMS (EI) m/z $[\text{M}]^+$ calcd for $\text{C}_{20}\text{H}_{18}\text{O}_3$ 306.1256, found 306.1253.

1-(Naphthalen-2-yl)ethyl 2-Methylbenzoate 6bc. Compound **1b** (20.0 mg, 116 μmol , 1.0 equiv), **3c** (32.5 mg, 128 μmol , 1.1 equiv), DMAP (709 μg , 5.81 μmol , 0.05 equiv), and Et_3N (32.4 μL , 232 μmol , 2.0 equiv) were dissolved in CH_2Cl_2 (580 μL) and reacted according to GP E. After purification by column chromatography on silica (isohexane/ CH_2Cl_2 6:4), **6bc** (20.0 mg, 59%) was obtained as an oil: ^1H NMR (400 MHz, CDCl_3) δ 8.00 (dd, $J = 7.8, 1.4$ Hz, 1H, Ar), 7.90 (s, 1H, Ar), 7.89–7.82 (m, 3H, Ar), 7.59 (dd, $J = 8.5, 1.8$ Hz, 1H, Ar), 7.53–7.45 (m, 2H, Ar), 7.41 (td, $J = 7.5, 1.5$ Hz, 1H, Ar), 7.30–7.23 (m, 2H, Ar), 6.30 (q, $J = 6.6$ Hz, 1H, CH), 2.61 (s, 3H, Me), 1.77 (d, $J = 6.6$ Hz, 3H, Me) ppm; $^{13}\text{C}\{^1\text{H}\}$ NMR (101 MHz, CDCl_3) δ 166.98, 140.34, 139.31, 133.35, 133.17, 132.07, 131.82, 130.73, 130.04, 128.56, 128.19, 127.81, 126.36, 126.19, 125.85, 125.22, 124.27, 73.08, 22.56, 21.96 ppm; IR (ATR) ν (cm^{-1}) 2929, 1713, 1456, 1249, 1126, 1073, 855, 817, 750; HRMS (EI) m/z $[\text{M}]^+$ calcd for $\text{C}_{20}\text{H}_{18}\text{O}_2$ 290.1307, found 290.1298.

1-(Naphthalen-2-yl)ethyl 2-Chlorobenzoate 6bd. Compound **1b** (20.0 mg, 116 μmol , 1.0 equiv), **3d** (37.7 mg, 128 μmol , 1.1 equiv), DMAP (709 μg , 5.81 μmol , 0.05 equiv), and Et_3N (24.3 μL , 174 μmol , 1.5 equiv) were dissolved in CH_2Cl_2 (580 μL) and reacted according to GP E. After purification by column chromatography on silica (isohexane/ CH_2Cl_2 6:4), **6bd** (24.0 mg, 67%) was obtained as an oil: ^1H NMR (600 MHz, CDCl_3) δ 7.91 (s, 1H, Ar), 7.88–7.82 (m, 4H, Ar), 7.59 (dd, $J = 8.5, 1.7$ Hz, 1H, Ar), 7.51–7.44 (m, 3H, Ar), 7.41 (td, $J = 7.7, 1.7$ Hz, 1H, Ar), 7.31 (td, $J = 7.6, 1.3$ Hz, 1H, Ar), 6.32 (q, $J = 6.6$ Hz, 1H, CH), 1.78 (d, $J = 6.6$ Hz, 3H, Me) ppm; $^{13}\text{C}\{^1\text{H}\}$ NMR (101 MHz, CDCl_3) δ 165.18, 138.72, 133.87, 133.32, 133.24, 132.62, 131.58, 131.21, 130.58, 128.59, 128.23, 127.82, 126.71, 126.40, 126.28, 125.48, 124.31, 74.17, 22.42 ppm; IR (ATR) ν (cm^{-1}) 2980, 1724, 1591, 1435, 1286, 1246, 1122, 1046, 817, 710; HRMS (EI) m/z $[\text{M}]^+$ calcd for $\text{C}_{19}\text{H}_{15}\text{O}_2\text{Cl}$ 310.0761, found 310.0752.

1-(Naphthalen-2-yl)ethyl 2-Bromobenzoate 6be. Compound **1b** (20.0 mg, 116 μmol , 1.0 equiv), **3e** (49.0 mg, 128 μmol , 1.1 equiv), DMAP (709 μg , 5.81 μmol , 0.05 equiv), and Et_3N (24.3 μL , 174 μmol , 1.5 equiv) were dissolved in CH_2Cl_2 (580 μL) and reacted according to GP E. After purification by column chromatography on silica (isohexane/ CH_2Cl_2 6:4), **6be** (28.0 mg, 68%) was obtained as an oil: ^1H NMR (400 MHz, CDCl_3) δ 7.91 (s, 1H, Ar), 7.89–7.77 (m, 4H, Ar), 7.66 (dd, $J = 7.7, 1.3$ Hz, 1H, Ar), 7.60 (dd, $J = 8.5, 1.6$ Hz, 1H, Ar), 7.49 (p, $J = 5.6$ Hz, 2H, Ar), 7.40–7.29 (m, 2H, Ar), 6.32 (q, $J = 6.6$ Hz, 1H, CH), 1.78 (d, $J = 6.6$ Hz, 3H, Me) ppm; $^{13}\text{C}\{^1\text{H}\}$ NMR (101 MHz, CDCl_3) δ 165.65, 138.62, 134.48, 133.29, 133.22, 132.65, 132.59, 131.50, 128.59, 128.23, 127.82, 127.31, 126.40, 126.30, 125.53, 124.33, 121.80, 74.31, 22.38 ppm; IR (ATR) ν (cm^{-1}) 2929, 1724, 1589, 1432, 1246, 1124, 1026, 816, 700; HRMS (EI) m/z $[\text{M}]^+$ calcd for $\text{C}_{19}\text{H}_{15}\text{O}_2\text{Br}$ 354.0255, found 354.0255.

1-(Naphthalen-2-yl)ethyl 2-Phenylbenzoate 6bf. Compound **1b** (25.0 mg, 145 μmol , 1.0 equiv), **3f** (60.1 mg, 160 μmol , 1.1 equiv), DMAP (886 μg , 7.26 μmol , 0.05 equiv), and Et_3N (30.4 μL , 218 μmol , 1.5 equiv) were dissolved in CH_2Cl_2 (725 μL) and reacted according to

GP E. After purification by column chromatography on silica (isohexane/CH₂Cl₂ 6:4), **6bf** (50.0 mg, 98%) was obtained as an oil: ¹H NMR (400 MHz, CDCl₃) δ 7.85 (dd, *J* = 7.7, 1.3 Hz, 1H, Ar), 7.82–7.72 (m, 3H, Ar), 7.56 (s, 1H, Ar), 7.52 (td, *J* = 7.5, 1.4 Hz, 1H, Ar), 7.48–7.44 (m, 2H, Ar), 7.41 (td, *J* = 7.6, 1.3 Hz, 1H, Ar), 7.37 (dd, *J* = 7.6, 1.3 Hz, 1H, Ar), 7.33–7.29 (m, 4H, Ar), 7.29–7.26 (m, 1H, Ar), 7.18 (dd, *J* = 8.5, 1.8 Hz, 1H, Ar), 6.04 (q, *J* = 6.6 Hz, 1H, CH), 1.40 (d, *J* = 6.6 Hz, 3H, Me) ppm; ¹³C{¹H} NMR (101 MHz, CDCl₃) δ 168.21, 142.59, 141.64, 138.75, 133.24, 133.10, 131.45, 131.29, 130.91, 130.10, 128.70, 128.28, 128.20, 128.17, 127.73, 127.33, 127.30, 126.20, 126.10, 125.20, 124.29, 73.62, 21.99 ppm; IR (ATR) ν (cm⁻¹) 2978, 1706, 1598, 1450, 1275, 1122, 1046, 817, 770; HRMS (EI) *m/z* [M]⁺ calcd for C₂₅H₂₀O₂ 352.1463, found 352.1449.

1-(Naphthalen-2-yl)ethyl 2-(4-Methylphenyl)benzoate 6bg. Compound **1b** (25.0 mg, 145 μmol, 1.0 equiv), **3g** (64.9 mg, 160 μmol, 1.1 equiv), DMAP (886 μg, 7.26 μmol, 0.05 equiv), and Et₃N (30.4 μL, 218 μmol, 1.5 equiv) were dissolved in CH₂Cl₂ (725 μL) and reacted according to GP E. After purification by column chromatography on silica (isohexane/CH₂Cl₂ 6:4), **6bg** (52.0 mg, 98%) was obtained as an oil: ¹H NMR (400 MHz, CDCl₃) δ 7.86–7.71 (m, 4H, Ar), 7.57 (s, 1H, Ar), 7.54–7.42 (m, 3H, Ar), 7.42–7.33 (m, 2H, Ar), 7.19 (dd, *J* = 9.3, 7.6 Hz, 3H, Ar), 7.05 (d, *J* = 7.9 Hz, 2H, Ar), 6.06 (q, *J* = 6.5 Hz, 1H, CH), 2.22 (s, 3H, Me), 1.46 (d, *J* = 6.6 Hz, 3H, Me) ppm; ¹³C{¹H} NMR (101 MHz, CDCl₃) δ 168.40, 142.52, 138.73, 138.54, 137.02, 133.23, 133.08, 131.51, 131.24, 130.89, 129.98, 128.90, 128.50, 128.20, 128.18, 127.73, 127.06, 126.19, 126.08, 125.24, 124.32, 73.55, 22.12, 21.18 ppm; IR (ATR) ν (cm⁻¹) 2978, 1706, 1444, 1273, 1122, 1045, 850, 757; HRMS (EI) *m/z* [M]⁺ calcd for C₂₆H₂₂O₂ 366.1620, found 366.1632.

1-(Naphthalen-2-yl)ethyl 2-(Naphthalene-1-yl)benzoate 6bh. Compound **1b** (20.0 mg, 116 μmol, 1.0 equiv), **3h** (61.1 mg, 127.7 μmol, 1.1 equiv), DMAP (709 μg, 5.81 μmol, 0.05 equiv), and Et₃N (24.3 μL, 174 μmol, 1.5 equiv) were dissolved in CH₂Cl₂ (580 μL) and reacted according to GP E. After purification by column chromatography on silica (isohexane/CH₂Cl₂ 6:4), **6bh** (40.0 mg, 86%) was obtained as an oil (1:1 diastomeric mixture): ¹H NMR (400 MHz, CDCl₃) δ 8.06 (ddd, *J* = 18.7, 7.8, 1.3 Hz, 1H, Ar), 7.87–7.77 (m, 2H, Ar), 7.76–7.70 (m, 1H, Ar), 7.60 (tdd, *J* = 9.1, 6.8, 2.4 Hz, 2H, Ar), 7.57–7.46 (m, 4H, Ar), 7.46–7.36 (m, 5H, Ar), 7.36–7.30 (m, 1H, Ar), 7.27 (s, 0.5H, Ar), 7.16 (s, 0.5H, Ar), 6.81 (dd, *J* = 8.5, 1.7 Hz, 0.5H, Ar), 6.61 (dd, *J* = 8.5, 1.7 Hz, 0.5H, Ar), 5.84–5.71 (m, 1H, CH), 0.94 (d, *J* = 6.6 Hz, 1.5H, Me), 0.69 (d, *J* = 6.6 Hz, 1.5H, Me) ppm; ¹³C{¹H} NMR (101 MHz, CDCl₃) δ 167.37, 167.31, 141.15, 141.09, 140.37, 140.06, 138.53, 138.46, 133.50, 133.43, 133.12, 133.08, 133.00, 132.95, 132.56, 132.49, 132.21, 132.05, 132.01, 131.94, 131.88, 131.44, 130.64, 130.55, 128.31, 128.27, 128.12, 128.09, 128.06, 128.05, 127.78, 127.72, 127.67, 127.66, 127.61, 126.30, 126.28, 126.20, 126.19, 126.13, 126.08, 126.00, 125.99, 125.96, 125.84, 125.84, 125.81, 125.39, 125.23, 125.00, 124.97, 124.19, 124.01, 73.29, 73.25, 21.66, 21.00 ppm; IR (ATR) ν (cm⁻¹) 3055, 1703, 1598, 1506, 1445, 1393, 1278, 1242, 1177, 1120, 1052, 856, 800, 760, 746; HRMS (EI) *m/z* [M]⁺ calcd for C₂₉H₂₂O₂ 402.1620, found 402.1612.

1-(Naphthalen-2-yl)ethyl 2-(Naphthalene-2-yl)benzoate 6bi. Compound **1b** (20.0 mg, 116 μmol, 1.0 equiv), **3i** (61.1 mg, 128 μmol, 1.1 equiv), DMAP (709 μg, 5.81 μmol, 0.05 equiv), and Et₃N (32.4 μL, 232 μmol, 2.0 equiv) were dissolved in CH₂Cl₂ (580 μL) and reacted according to GP E. After purification by column chromatography on silica (isohexane/CH₂Cl₂ 6:4), **6bi** (25.0 mg, 53%) was obtained as an oil: ¹H NMR (400 MHz, CDCl₃) δ 7.92 (dd, *J* = 8.1, 1.4 Hz, 1H, Ar), 7.77–7.65 (m, 5H, Ar), 7.60–7.51 (m, 2H, Ar), 7.49–7.35 (m, 9H, Ar), 6.96 (dd, *J* = 8.5, 1.8 Hz, 1H, Ar), 6.02 (q, *J* = 6.6 Hz, 1H, CH), 1.34 (d, *J* = 6.6 Hz, 3H, Me) ppm; ¹³C{¹H} NMR (101 MHz, CDCl₃) δ 168.25, 142.56, 139.14, 138.40, 133.32, 133.08, 132.99, 132.55, 131.55, 131.40, 131.21, 130.26, 128.10, 128.06, 127.74, 127.70, 127.64, 127.40, 127.28, 127.18, 126.29, 126.08, 126.03, 125.98, 125.16, 124.08, 73.74, 22.03 ppm (one signal is overlapping); IR (ATR) ν (cm⁻¹) 3053, 1704, 1596, 1487, 1445, 1276, 1243, 1122, 1045, 895, 855, 816, 757; HRMS (EI) *m/z* [M]⁺ calcd for C₂₉H₂₂O₂ 402.1620, found 402.1620.

1-(Naphthalen-2-yl)ethyl 2-(6-Methoxynaphthalene-2-yl)benzoate 6bj. Compound **1b** (20.0 mg, 116 μmol, 1.0 equiv), **3j** (70.0 mg, 130 μmol, 1.1 equiv), DMAP (709 μg, 5.81 μmol, 0.05 equiv), and Et₃N (32.4 μL, 232 μmol, 2.0 equiv) were dissolved in CH₂Cl₂ (580 μL) and reacted according to GP E. After purification by column chromatography on silica (isohexane/CH₂Cl₂ 6:4), **6bj** (30.0 mg, 59%) was obtained as an oil: ¹H NMR (400 MHz, CDCl₃) δ 7.92 (dd, *J* = 7.7, 1.0 Hz, 1H, Ar), 7.74–7.69 (m, 1H, Ar), 7.68 (d, *J* = 1.4 Hz, 1H, Ar), 7.62–7.53 (m, 4H, Ar), 7.51–7.36 (m, 7H, Ar), 7.09 (dd, *J* = 8.9, 2.5 Hz, 1H, Ar), 7.00 (dd, *J* = 8.5, 1.7 Hz, 1H, Ar), 6.95 (d, *J* = 2.5 Hz, 1H, Ar), 6.04 (q, *J* = 6.5 Hz, 1H, CH), 3.89 (s, 3H, Me), 1.38 (d, *J* = 6.6 Hz, 3H, Me) ppm; ¹³C{¹H} NMR (101 MHz, CDCl₃) δ 168.49, 157.71, 142.53, 138.40, 136.79, 133.67, 133.03, 132.95, 131.63, 131.31, 131.12, 130.15, 129.50, 128.77, 128.09, 128.02, 127.64, 127.61, 127.17, 126.97, 126.51, 125.99, 125.90, 125.07, 124.07, 119.08, 105.59, 73.68, 55.33, 22.15 ppm; IR (ATR) ν (cm⁻¹) = 2977, 1704, 1597, 1388, 1250, 1202, 1120, 1031, 894, 852, 815, 747, 727; HRMS (EI) *m/z* [M]⁺ calcd for C₃₀H₂₄O₃ 432.1725, found 432.1725.

1-(Naphthalen-2-yl)ethyl 2,6-Dimethoxybenzoate 6bk. Compound **1b** (20.0 mg, 116 μmol, 1.0 equiv), **3k** (44.2 mg, 128 μmol, 1.1 equiv), DMAP (709 μg, 5.81 μmol, 0.05 equiv), and Et₃N (32.4 μL, 232 μmol, 2.0 equiv) were dissolved in CH₂Cl₂ (580 μL) and reacted according to GP E. After purification by column chromatography on silica (isohexane/CH₂Cl₂ 6:4), **6bk** (30.0 mg, 78%) was obtained as a white solid: mp 89–91 °C; ¹H NMR (400 MHz, CDCl₃) δ 7.93 (s, 1H, Ar), 7.84 (tdd, *J* = 5.0, 3.6, 1.5 Hz, 3H, Ar), 7.58 (dd, *J* = 8.5, 1.7 Hz, 1H, Ar), 7.51–7.43 (m, 2H, Ar), 7.28 (t, *J* = 8.4 Hz, 1H, Ar), 6.56 (d, *J* = 8.4 Hz, 2H, Ar), 6.35 (q, *J* = 6.6 Hz, 1H, CH), 3.79 (s, 6H, Me₂), 1.74 (d, *J* = 6.6 Hz, 3H, Me) ppm; ¹³C{¹H} NMR (101 MHz, CDCl₃) δ 166.02, 157.58, 139.28, 133.36, 133.08, 131.11, 128.16, 128.06, 127.76, 126.16, 125.98, 125.13, 124.66, 113.53, 104.12, 73.21, 56.06, 22.31 ppm; IR (ATR) ν (cm⁻¹) 2936, 1726, 1594, 1474, 1251, 1069, 908, 819, 783, 726; HRMS (EI) *m/z* [M]⁺ calcd for C₂₁H₂₀O₄ 336.1362, found 336.1351.

1-(Naphthalen-2-yl)ethyl 2-Methoxy-6-phenylbenzoate 6bl. Compound **1b** (20.0 mg, 116 μmol, 1.0 equiv), **3l** (56.0 mg, 128 μmol, 1.1 equiv), DMAP (709 μg, 5.81 μmol, 0.05 equiv), and Et₃N (32.4 μL, 232 μmol, 2.0 equiv) were dissolved in CH₂Cl₂ (580 μL) and reacted according to GP E. After purification by column chromatography on silica (isohexane/CH₂Cl₂ 6:4), **6bl** (25.0 mg, 56%) was obtained as a white solid: mp 105–108 °C; ¹H NMR (400 MHz, CDCl₃) δ 7.83–7.75 (m, 2H, Ar), 7.73 (d, *J* = 8.5 Hz, 1H, Ar), 7.65 (s, 1H, Ar), 7.50–7.44 (m, 2H, Ar), 7.43–7.33 (m, 3.5H, Ar), 7.24–7.17 (m, 3.5H, Ar), 6.96 (ddd, *J* = 14.4, 8.1, 0.9 Hz, 2H, Ar), 6.11 (q, *J* = 6.6 Hz, 1H, CH), 3.85 (s, 3H, Me), 1.42 (d, *J* = 6.6 Hz, 3H, Me) ppm; ¹³C{¹H} NMR (101 MHz, CDCl₃) δ 167.32, 156.66, 141.37, 139.99, 138.53, 133.23, 133.03, 130.51, 128.56, 128.34, 128.21, 128.14, 127.69, 127.64, 126.11, 126.03, 125.22, 124.47, 123.52, 110.01, 73.18, 56.13, 21.51 ppm (one signal is overlapping); IR (ATR) ν (cm⁻¹) 2938, 1720, 1569, 1465, 1251, 1107, 1251, 1107, 1040, 730, 698; HRMS (EI) *m/z* [M]⁺ calcd for C₂₆H₂₂O₃ 382.1569, found 382.1556.

1-(Naphthalen-2-yl)ethyl 2,6-Dimethylbenzoate 6bm. Compound **1b** (20.0 mg, 116 μmol, 1.0 equiv), **3m** (36.1 mg, 128 μmol, 1.1 equiv), DMAP (709 μg, 5.81 μmol, 0.05 equiv), and Et₃N (32.4 μL, 232 μmol, 2.0 equiv) were dissolved in CH₂Cl₂ (580 μL) and reacted according to GP E. After purification by column chromatography on silica (isohexane/CH₂Cl₂ 6:4), **6bm** (20.0 mg, 57%) was obtained as a white solid: mp 50–54 °C; ¹H NMR (400 MHz, CDCl₃) δ 7.91 (s, 1H, Ar), 7.88–7.80 (m, 3H, Ar), 7.57 (dd, *J* = 8.5, 1.8 Hz, 1H, Ar), 7.54–7.46 (m, 2H, Ar), 7.22–7.17 (m, 1H, Ar), 7.03 (d, *J* = 7.8 Hz, 2H, Ar), 6.37 (q, *J* = 6.6 Hz, 1H, CH), 2.27 (s, 6H, Me₂), 1.77 (d, *J* = 6.6 Hz, 3H, Me) ppm; ¹³C{¹H} NMR (101 MHz, CDCl₃) δ 169.42, 138.70, 134.94, 134.17, 133.32, 133.23, 129.37, 128.52, 128.21, 127.82, 127.67, 126.39, 126.28, 125.55, 124.45, 73.34, 22.35, 19.75 ppm; IR (ATR) ν (cm⁻¹) 2926, 1720, 1596, 1465, 1245, 1113, 1052, 855, 817, 746; HRMS (EI) *m/z* [M]⁺ calcd for C₂₁H₂₀O₂ 304.1463, found 304.1456.

1-(Naphthalen-2-yl)ethyl 2-Methyl-6-phenylbenzoate 6bn. Compound **1b** (15.0 mg, 87.1 μmol, 1.0 equiv), **3n** (38.9 mg, 95.8 μmol, 1.1 equiv), DMAP (532 μg, 4.35 μmol, 0.05 equiv), and Et₃N (18.2 μL, 131 μmol, 1.5 equiv) were dissolved in CH₂Cl₂ (435 μL) and reacted

according to GP E. After purification by column chromatography on silica (isohexane/CH₂Cl₂ 6:4), **6bn** (10.0 mg, 31%) was obtained as an oil: ¹H NMR (400 MHz, CDCl₃) δ 7.84–7.75 (m, 2H, Ar), 7.74 (d, J = 8.6 Hz, 1H, Ar), 7.63 (d, J = 1.8 Hz, 1H, Ar), 7.50–7.44 (m, 2H, Ar), 7.38–7.31 (m, 3H, Ar), 7.25–7.15 (m, 6H, Ar), 6.04 (q, J = 6.6 Hz, 1H, CH), 2.34 (s, 3H, Me), 1.35 (d, J = 6.6 Hz, 3H, Me) ppm; ¹³C{¹H} NMR (101 MHz, CDCl₃) δ 169.13, 140.89, 140.26, 138.45, 135.55, 133.51, 133.24, 133.11, 129.43, 129.23, 128.59, 128.32, 128.21, 127.72, 127.43, 127.41, 126.20, 126.14, 125.32, 124.34, 73.30, 21.53, 19.83 ppm (one signal is overlapping); IR (ATR) ν (cm⁻¹) 2826, 1719, 1590, 1451, 1258, 1121, 1057, 756, 700; HRMS (EI) *m/z* [M]⁺ calcd for C₂₆H₂₂O₃ 366.1620, found 366.1614.

1-(Naphthalen-2-yl)ethyl 2-Methyl-6-nitrobenzoate 6bo. Compound **1b** (20.0 mg, 116 μmol, 1.0 equiv), **3o** (44.0 mg, 128 μmol, 1.1 equiv), DMAP (709 μg, 5.81 μmol, 0.05 equiv), and Et₃N (32.4 μL, 232 μmol, 2.0 equiv) were dissolved in CH₂Cl₂ (580 μL) and reacted according to GP E. After purification by column chromatography on silica (isohexane/CH₂Cl₂ 6:4), **6bo** (29.0 mg, 75%) was obtained as an oil: ¹H NMR (400 MHz, CDCl₃) δ 8.00 (d, J = 8.1 Hz, 1H, Ar), 7.90 (s, 1H, Ar), 7.89–7.82 (m, 3H, Ar), 7.55 (dd, J = 8.5, 1.8 Hz, 1H, Ar), 7.52–7.47 (m, 3H, Ar), 7.44 (t, J = 7.9 Hz, 1H, Ar), 6.41 (q, J = 6.6 Hz, 1H, CH), 2.29 (d, J = 0.7 Hz, 3H, Me), 1.80 (d, J = 6.6 Hz, 3H, Me) ppm; ¹³C{¹H} NMR (101 MHz, CDCl₃) δ 165.90, 146.10, 137.95, 137.71, 136.13, 133.32, 133.28, 129.76, 129.72, 128.59, 128.25, 127.81, 126.42, 126.38, 125.74, 124.48, 121.91, 74.74, 21.42, 19.14 ppm; IR (ATR) ν (cm⁻¹) 2931, 1729, 1529, 1451, 1342, 1247, 1113, 1051, 893, 856, 802, 740; HRMS (EI) *m/z* [M]⁺ calcd for C₂₀H₁₇O₄N 335.1158, found 335.1136.

1-(Naphthalen-2-yl)ethyl 2-Fluoro-6-(trifluoromethyl)benzoate 6bp. Compound **1b** (15.0 mg, 87.1 μmol, 1.0 equiv), **3p** (38.2 mg, 95.8 μmol, 1.1 equiv), DMAP (532 μg, 4.35 μmol, 0.05 equiv), and Et₃N (18.2 μL, 131 μmol, 1.5 equiv) were dissolved in CH₂Cl₂ (435 μL) and reacted according to GP E. After purification by column chromatography on silica (isohexane/CH₂Cl₂ 6:4), **6bp** (15.0 mg, 41%) was obtained as an oil: ¹H NMR (400 MHz, CDCl₃) δ 7.90–7.81 (m, 4H, Ar), 7.57–7.46 (m, 5H, Ar), 7.36–7.29 (m, 1H, Ar), 6.36 (q, J = 6.6 Hz, 1H, CH), 1.77 (d, J = 6.6 Hz, 3H, Me) ppm; ¹³C{¹H} NMR (101 MHz, CDCl₃) δ 162.65, 160.70, 158.20, 137.72, 133.16, 133.14, 131.52, 131.44, 128.40, 128.14, 127.67, 126.25, 126.21, 125.39, 124.15, 121.95 (qd, J = 4.9, 3.3 Hz), 119.83 (q, J = 1.0 Hz), 119.61 (q, J = 1.0 Hz), 75.17, 21.62 ppm; ¹⁹F NMR (377 MHz, CDCl₃) δ -59.57, -113.11 ppm; IR (ATR) ν (cm⁻¹) 2918, 1738, 1464, 1320, 1270, 1171, 1127, 1050, 914, 802, 746; HRMS (EI) *m/z* [M]⁺ calcd for C₂₀H₁₄O₂F₄ 362.0930, found 362.0929.

1-(Naphthalen-2-yl)ethyl 1-Naphthoate 6bq. Compound **1b** (50.0 mg, 290 μmol, 1.0 equiv), **3q** (113 mg, 348 μmol, 1.2 equiv), DMAP (1.77 mg, 14.5 μmol, 0.05 equiv), and Et₃N (60.0 μL, 435 μmol, 1.5 equiv) were dissolved in CH₂Cl₂ (1.5 mL) and reacted according to GP E. After purification by column chromatography on silica (isohexane/CH₂Cl₂ 6:4), **6bq** (90.0 mg, 95%) was obtained as an oil: ¹H NMR (400 MHz, CDCl₃) δ 8.91 (d, J = 8.6 Hz, 1H, Ar), 8.27 (d, J = 8.2 Hz, 1H, Ar), 8.03 (d, J = 8.2 Hz, 1H, Ar), 7.95 (s, 1H, Ar), 7.91–7.83 (m, 4H, Ar), 7.66–7.56 (m, 2H, Ar), 7.56–7.46 (m, 4H, Ar), 6.42 (q, J = 6.6 Hz, 1H, CH), 1.83 (d, J = 6.6 Hz, 3H, Me) ppm; ¹³C{¹H} NMR (101 MHz, CDCl₃) δ 166.93, 139.28, 133.99, 133.47, 133.41, 133.23, 131.56, 130.30, 128.66, 128.63, 128.23, 127.86, 127.83, 127.61, 126.39, 126.34, 126.23, 125.98, 125.29, 124.65, 124.30, 73.36, 22.59 ppm; IR (ATR) ν (cm⁻¹) 2978, 1707, 1593, 1508, 1449, 1274, 1237, 1194, 1126, 1056, 1000, 854, 814, 745; HRMS (EI) *m/z* [M]⁺ calcd for C₂₃H₁₈O₂ 326.1307, found 326.1297.

1-(Naphthalen-2-yl)ethyl 2-Methoxy-1-naphthoate 6br. Compound **1b** (20.0 mg, 116 μmol, 1.0 equiv), **3r** (53.8 mg, 139 μmol, 1.2 equiv), DMAP (709 μg, 5.81 μmol, 0.05 equiv), and Et₃N (32.4 μL, 232 μmol, 2.0 equiv) were dissolved in CH₂Cl₂ (580 μL) and reacted according to GP E. After purification by column chromatography on silica (isohexane/CH₂Cl₂ 6:4), **6br** (34.0 mg, 83%) was obtained as an oil: ¹H NMR (400 MHz, CDCl₃) δ 7.97 (s, 1H, Ar), 7.92–7.83 (m, 4H, Ar), 7.79 (d, J = 7.5 Hz, 1H, Ar), 7.67 (d, J = 8.8 Hz, 1H, Ar), 7.61 (dd, J = 8.5, 1.8 Hz, 1H, Ar), 7.53–7.46 (m, 2H, Ar), 7.41 (ddd, J = 8.4, 6.8, 1.4 Hz, 1H, Ar), 7.35 (ddd, J = 8.0, 6.9, 1.2 Hz, 1H, Ar), 7.29 (d, J = 9.1

Hz, 1H, Ar), 6.49 (q, J = 6.6 Hz, 1H, CH), 3.94 (s, 3H, Me), 1.81 (d, J = 6.6 Hz, 3H, Me) ppm; ¹³C{¹H} NMR (101 MHz, CDCl₃) δ 167.57, 154.58, 139.12, 133.39, 133.20, 131.68, 131.15, 128.71, 128.36, 128.22, 128.19, 127.82, 127.70, 126.32, 126.17, 125.37, 124.57, 124.24, 123.87, 118.00, 113.43, 73.61, 56.90, 22.54 ppm; IR (ATR) ν (cm⁻¹) 2976, 1720, 1295, 1510, 2461, 1344, 1281, 1226, 1127, 1058, 1017, 809, 700; HRMS (EI) *m/z* [M]⁺ calcd for C₂₄H₂₀O₃ 356.1412, found 356.1407.

1-(Naphthalen-2-yl)ethyl 2-Ethoxy-1-naphthoate 6bs. Compound **1b** (20.0 mg, 116 μmol, 1.0 equiv), **3s** (57.8 mg, 139 μmol, 1.2 equiv), DMAP (709 μg, 5.81 μmol, 0.05 equiv), and Et₃N (32.4 μL, 232 μmol, 2.0 equiv) were dissolved in CH₂Cl₂ (580 μL) and reacted according to GP E. After purification by column chromatography on silica (isohexane/CH₂Cl₂ 6:4), **6bs** (20.0 mg, 47%) was obtained as an oil: ¹H NMR (600 MHz, CDCl₃) δ 7.96 (s, 1H, Ar), 7.89–7.83 (m, 4H, Ar), 7.78 (d, J = 8.1 Hz, 1H, Ar), 7.68 (d, J = 8.5 Hz, 1H, Ar), 7.62 (dd, J = 8.5, 1.8 Hz, 1H, Ar), 7.51–7.47 (m, 2H, Ar), 7.41 (ddd, J = 8.3, 6.8, 1.3 Hz, 1H, Ar), 7.35 (ddd, J = 8.0, 6.8, 1.1 Hz, 1H, Ar), 7.26 (d, J = 9.0 Hz, 1H, Ar), 6.51 (q, J = 6.6 Hz, 1H, CH), 4.19 (q, J = 7.0 Hz, 2H, CH₂), 1.82 (d, J = 6.7 Hz, 3H, Me), 1.33 (t, J = 7.0 Hz, 3H, Me) ppm; ¹³C{¹H} NMR (151 MHz, CDCl₃) δ 167.68, 153.90, 139.08, 133.37, 133.19, 131.51, 131.18, 128.69, 128.39, 128.21, 128.15, 127.80, 127.63, 126.30, 126.15, 125.36, 124.60, 124.20, 123.87, 118.42, 114.55, 73.49, 65.44, 22.43, 15.07 ppm; IR (ATR) ν (cm⁻¹) 2979, 1719, 1595, 1510, 1466, 1434, 1341, 1280, 1214, 1137, 1058, 1023, 858, 907, 744; HRMS (EI) *m/z* [M]⁺ calcd for C₂₅H₂₂O₃ 370.1569, found 370.1564.

1-(Naphthalen-2-yl)ethyl 2-Butoxy-1-naphthoate 6bt. Compound **1b** (20.0 mg, 116 μmol, 1.0 equiv), **3t** (60.1 mg, 128 μmol, 1.1 equiv), DMAP (709 μg, 5.81 μmol, 0.05 equiv), and Et₃N (32.4 μL, 232 μmol, 2.0 equiv) were dissolved in CH₂Cl₂ (580 μL) and reacted according to GP E. After purification by column chromatography on silica (isohexane/CH₂Cl₂ 6:4), **6bt** (45.0 mg, 97%) was obtained as a white solid: mp 67–70 °C; ¹H NMR (400 MHz, CDCl₃) δ 7.95 (s, 1H, Ar), 7.86 (td, J = 7.8, 6.7, 3.0 Hz, 4H, Ar), 7.78 (d, J = 7.9 Hz, 1H, Ar), 7.65 (d, J = 8.3 Hz, 1H, Ar), 7.61 (dd, J = 8.5, 1.6 Hz, 1H, Ar), 7.52–7.45 (m, 2H, Ar), 7.40 (ddd, J = 8.4, 6.9, 1.3 Hz, 1H, Ar), 7.36–7.31 (m, 1H, Ar), 7.26 (d, J = 9.1 Hz, 1H, Ar), 6.50 (q, J = 6.6 Hz, 1H, CH), 4.10 (t, J = 6.5 Hz, 2H, CH₂), 1.81 (d, J = 6.6 Hz, 3H, Me), 1.71–1.60 (m, 2H, CH₂), 1.41–1.29 (m, 2H, CH₂), 0.81 (t, J = 7.4 Hz, 3H, Me) ppm; ¹³C{¹H} NMR (101 MHz, CDCl₃) δ 167.54, 153.88, 138.94, 133.24, 133.08, 131.32, 131.05, 128.48, 128.26, 128.09, 128.02, 127.66, 127.48, 126.15, 126.02, 125.30, 124.47, 123.99, 123.67, 118.12, 114.29, 73.41, 69.34, 31.40, 22.34, 19.05, 13.71 ppm; IR (ATR) ν (cm⁻¹) 2957, 1713, 1595, 1513, 1461, 1342, 1282, 1233, 1127, 1009, 807; HRMS (EI) *m/z* [M]⁺ calcd for C₂₇H₂₆O₃ 398.1882, found 398.1879.

1-(Naphthalen-2-yl)ethyl 2-(hexanoyloxy)-1-naphthoate 6bu. Compound **1b** (10.0 mg, 58.1 μmol, 1.0 equiv), **3u** (33.6 mg, 63.87 μmol, 1.1 equiv), DMAP (355 μg, 2.90 μmol, 0.05 equiv), and Et₃N (16.2 μL, 116 μmol, 2.0 equiv) were dissolved in CH₂Cl₂ (300 μL) and reacted according to GP E. After purification by column chromatography on silica (isohexane/CH₂Cl₂ 6:4), **6bu** (10.0 mg, 40%) was obtained as an oil: ¹H NMR (600 MHz, CDCl₃) δ 7.95 (s, 1H, Ar), 7.85 (td, J = 9.2, 4.7 Hz, 4H, Ar), 7.77 (d, J = 8.1 Hz, 1H, Ar), 7.66 (d, J = 8.4 Hz, 1H, Ar), 7.61 (dd, J = 8.5, 1.7 Hz, 1H, Ar), 7.51–7.46 (m, 2H, Ar), 7.40 (ddd, J = 8.3, 6.9, 1.2 Hz, 1H, Ar), 7.36–7.31 (m, 1H, Ar), 7.26 (d, J = 9.1 Hz, 1H, Ar), 6.50 (q, J = 6.6 Hz, 1H, CH), 4.09 (t, J = 6.6 Hz, 2H, CH₂), 1.84–1.78 (m, 3H, Me), 1.70–1.61 (m, 2H, CH₂), 1.33 (dt, J = 15.0, 7.4 Hz, 2H, CH₂), 1.24–1.13 (m, 4H, 2xCH₂), 0.84 (t, J = 7.0 Hz, 3H, Me) ppm; ¹³C{¹H} NMR (151 MHz, CDCl₃) δ 167.66, 154.06, 139.11, 133.40, 133.23, 131.45, 131.21, 128.66, 128.40, 128.23, 128.16, 127.81, 127.61, 126.29, 126.16, 125.41, 124.61, 124.14, 123.84, 118.33, 114.52, 73.53, 69.89, 31.62, 29.48, 25.66, 22.66, 22.52, 14.16 ppm; IR (ATR) ν (cm⁻¹) 2929, 1721, 1595, 1511, 1463, 1343, 1281, 1200, 1136, 1059, 810, 745; HRMS (EI) *m/z* [M]⁺ calcd for C₂₉H₃₀O₃ 426.2195, found 426.2187.

1-(Naphthalen-2-yl)ethyl 2-isopropoxy-1-naphthoate 6bv. Compound **1b** (15.0 mg, 87.1 μmol, 1.0 equiv), **3v** (41.1 mg, 95.8 μmol, 1.1 equiv), DMAP (532 μg, 4.35 μmol, 0.05 equiv), and Et₃N (18.2 μL, 131 μmol, 1.5 equiv) were dissolved in CH₂Cl₂ (435 μL) and reacted according to GP E. After purification by column chromatography on silica (isohexane/CH₂Cl₂ 6:4), **6bv** (25.0 mg, 75%) was obtained as a

oil: $^1\text{H NMR}$ (400 MHz, CDCl_3) δ 7.97–7.95 (m, 1H, Ar), 7.86 (ddd, $J = 7.1, 4.7, 3.1$ Hz, 4H, Ar), 7.78 (d, $J = 7.5$ Hz, 1H, Ar), 7.66 (d, $J = 9.2$ Hz, 1H, Ar), 7.62 (dd, $J = 8.5, 1.8$ Hz, 1H, Ar), 7.52–7.46 (m, 2H, Ar), 7.41 (ddd, $J = 8.4, 6.9, 1.4$ Hz, 1H, Ar), 7.35 (ddd, $J = 8.0, 6.9, 1.3$ Hz, 1H, Ar), 7.27 (d, $J = 9.1$ Hz, 1H, Ar), 6.51 (q, $J = 6.6$ Hz, 1H, CH), 4.77–4.60 (m, 1H, CH), 1.83 (d, $J = 6.6$ Hz, 3H, Me), 1.27 (dd, $J = 6.1, 1.8$ Hz, 6H, Me_2) ppm; $^{13}\text{C}\{^1\text{H}\}$ NMR (101 MHz, CDCl_3) δ 167.62, 152.78, 138.98, 133.24, 133.07, 131.13, 131.12, 128.61, 128.26, 128.08, 127.98, 127.67, 127.42, 126.16, 126.01, 125.24, 124.51, 124.15, 123.73, 119.67, 115.97, 73.29, 72.10, 22.37, 22.26 ppm; IR (ATR) ν (cm^{-1}) 2976, 1720, 1594, 1509, 1434, 1382, 1279, 1200, 1177, 1135, 1106, 1041, 995, 808, 645; HRMS (EI) m/z [M] $^+$ calcd for $\text{C}_{26}\text{H}_{24}\text{O}_3$ 384.1725, found 384.1719.

1-(Naphthalen-2-yl)ethyl 2-methyl-1-naphthoate 6bw. Compound **1b** (20.0 mg, 116 μmol , 1.0 equiv), **3w** (45.3 mg, 128 μmol , 1.1 equiv), DMAP (709 μg , 5.81 μmol , 0.05 equiv), and Et_3N (32.4 μL , 232 μmol , 2.0 equiv) were dissolved in CH_2Cl_2 (580 μL) and reacted according to GP E. After purification by column chromatography on silica (isohexane/ CH_2Cl_2 6:4), **6bw** (20.0 mg, 51%) was obtained as an oil: $^1\text{H NMR}$ (400 MHz, CDCl_3) δ 7.96 (s, 1H, Ar), 7.91–7.83 (m, 3H, Ar), 7.83–7.79 (m, 2H, Ar), 7.76–7.70 (m, 1H, Ar), 7.60 (dd, $J = 8.5, 1.8$ Hz, 1H, Ar), 7.54–7.48 (m, 2H, Ar), 7.46–7.39 (m, 2H, Ar), 7.32 (d, $J = 8.4$ Hz, 1H, Ar), 6.53 (q, $J = 6.6$ Hz, 1H, CH), 2.46 (s, 3H, Me), 1.84 (d, $J = 6.6$ Hz, 3H, Me) ppm; $^{13}\text{C}\{^1\text{H}\}$ NMR (101 MHz, CDCl_3) δ 169.20, 138.77, 133.36, 133.27, 133.25, 131.76, 130.41, 130.15, 129.68, 128.59, 128.50, 128.23, 128.15, 127.84, 127.11, 126.43, 126.31, 125.58, 125.57, 124.55, 124.43, 73.75, 22.58, 20.16 ppm; IR (ATR) ν (cm^{-1}) 2925, 1716, 1508, 1450, 1379, 1276, 1240, 1214, 1137, 1043, 858, 812, 700; HRMS (EI) m/z [M] $^+$ calcd for $\text{C}_{24}\text{H}_{20}\text{O}_2$ 340.1463, found 340.1461.

1-(Naphthalen-2-yl)ethyl 3-phenylbenzoate 6bx. Compound **1b** (20.0 mg, 116 μmol , 1.0 equiv), **3x** (48.3 mg, 127 μmol , 1.1 equiv), DMAP (709 μg , 5.81 μmol , 0.05 equiv), and Et_3N (32.4 μL , 232 μmol , 1.5 equiv) were dissolved in CH_2Cl_2 (580 μL) and reacted according to GP E. After purification by column chromatography on silica (isohexane/ CH_2Cl_2 6:4), **6bx** (35.0 mg, 85%) was obtained as an oil: $^1\text{H NMR}$ (600 MHz, CDCl_3) δ 8.33 (s, 1H, Ar), 8.09 (d, $J = 7.7$, 1H, Ar), 7.91 (s, 1H, Ar), 7.88–7.82 (m, 3H, Ar), 7.79 (d, $J = 7.8$, 1H, Ar), 7.62 (d, $J = 7.4$, 2H, Ar), 7.61–7.57 (m, 1H, Ar), 7.53 (t, $J = 7.8$ Hz, 1H, Ar), 7.51–7.45 (m, 4H, Ar), 7.38 (t, $J = 7.3$ Hz, 1H, Ar), 6.33 (q, $J = 6.6$ Hz, 1H, CH), 1.78 (d, $J = 6.6$ Hz, 3H, Me) ppm; $^{13}\text{C}\{^1\text{H}\}$ NMR (151 MHz, CDCl_3) δ 165.97, 141.66, 140.34, 139.20, 133.35, 133.20, 131.76, 131.21, 129.04, 128.99, 128.61, 128.60, 128.50, 128.22, 127.88, 127.82, 127.35, 126.39, 126.23, 125.20, 124.24, 73.35, 22.47 ppm; IR (ATR) ν (cm^{-1}) 2978, 1711, 1600, 1453, 1295, 1233, 1175, 1113, 1047, 896, 854, 816, 740, 694; HRMS (EI) m/z [M] $^+$ calcd for $\text{C}_{25}\text{H}_{20}\text{O}_2$ 352.1463, found 352.1457.

1-(Naphthalen-2-yl)ethyl thiophen-2-yl-carboxylate 6by. Compound **1b** (25.0 mg, 145 μmol , 1.0 equiv), **3y** (38.1 mg, 160 μmol , 1.1 equiv), DMAP (886 μg , 7.26 μmol , 0.05 equiv), and Et_3N (30.4 μL , 218 μmol , 1.5 equiv) were dissolved in CH_2Cl_2 (725 μL) and reacted according to GP E. After purification by column chromatography on silica (isohexane/ CH_2Cl_2 6:4), **6by** (40.0 mg, 98%) was obtained as a white solid: mp 64–66 $^\circ\text{C}$; $^1\text{H NMR}$ (400 MHz, CDCl_3) δ 7.91–7.81 (m, 5H, Ar), 7.60–7.54 (m, 2H, Ar), 7.52–7.45 (m, 2H, Ar), 7.11 (dd, $J = 5.0, 3.7$ Hz, 1H, Ar), 6.27 (q, $J = 6.6$ Hz, 1H, CH), 1.75 (d, $J = 6.6$ Hz, 3H, Me) ppm; $^{13}\text{C}\{^1\text{H}\}$ NMR (151 MHz, CDCl_3) δ 161.67, 139.00, 134.29, 133.61, 133.32, 133.20, 132.52, 128.57, 128.22, 127.88, 127.81, 126.38, 126.23, 125.18, 124.17, 73.44, 22.49 ppm; IR (ATR) ν (cm^{-1}) 2977, 1691, 1519, 1417, 1281, 1099, 830, 710; HRMS (EI) m/z [M] $^+$ calcd for $\text{C}_{17}\text{H}_{14}\text{O}_2\text{S}$ 282.0715, found 282.0707.

1-(Naphthalen-2-yl)ethyl 2-naphthoate 6bz. Compound **1b** (50.0 mg, 290 μmol , 1.0 equiv), **3z** (113 mg, 348 μmol , 1.2 equiv), DMAP (1.77 mg, 14.5 μmol , 0.05 equiv), and Et_3N (60.0 μL , 435 μmol , 1.5 equiv) were dissolved in CH_2Cl_2 (1.5 mL) and reacted according to GP E. After purification by column chromatography on silica (isohexane/ CH_2Cl_2 6:4), **6bz** (90.0 mg, 95%) was obtained as a white solid: mp 60–63 $^\circ\text{C}$; $^1\text{H NMR}$ (400 MHz, CDCl_3) δ 8.67 (s, 1H, Ar), 8.13 (dd, $J = 8.6, 1.7$ Hz, 1H, Ar), 7.98 (d, $J = 8.0$ Hz, 1H, Ar), 7.96–7.93 (m, 1H, Ar), 7.92–7.82 (m, 5H, Ar), 7.66–7.62 (m, 1H, Ar), 7.62–7.52 (m,

2H, Ar), 7.52–7.45 (m, 2H, Ar), 6.38 (q, $J = 6.6$ Hz, 1H, CH), 1.83 (d, $J = 6.6$ Hz, 3H, Me) ppm; $^{13}\text{C}\{^1\text{H}\}$ NMR (151 MHz, CDCl_3) δ 166.17, 139.27, 135.69, 133.37, 133.21, 132.64, 131.25, 129.51, 128.61, 128.37, 128.28, 128.22, 127.91, 127.90, 127.82, 126.77, 126.39, 126.23, 125.47, 125.21, 124.28, 73.36, 22.51 ppm; IR (ATR) ν (cm^{-1}) 2983, 1705, 1630, 1506, 1438, 1353, 1276, 1225, 1197, 1128, 1095, 1051, 993, 955, 905, 864, 822, 779, 762; HRMS (EI) m/z [M] $^+$ calcd for $\text{C}_{23}\text{H}_{18}\text{O}_2$ 326.1307, found 326.1300.

2-(Naphthalen-2-yl)ethyl benzoate 7ba. Compound **2b** (60.0 mg, 348 μmol , 1.0 equiv), **3a** (118 mg, 522 μmol , 1.5 equiv), DMAP (2.13 mg, 17.4 μmol , 0.05 equiv), and Et_3N (100 μL , 696 μmol , 1.5 equiv) were dissolved in CH_2Cl_2 (2 mL) and reacted according to GP E. After purification by column chromatography on silica (isohexane/ CH_2Cl_2 6:4), **7ba** (80 mg, 83%) was obtained as a white solid: mp 70–73 $^\circ\text{C}$; $^1\text{H NMR}$ (400 MHz, CDCl_3) δ 8.07–8.00 (m, 2H, Ar), 7.86–7.76 (m, 3H, Ar), 7.75 (s, 1H, Ar), 7.60–7.51 (m, 1H, Ar), 7.51–7.40 (m, 5H, Ar), 4.64 (t, $J = 7.0$ Hz, 2H, CH_2), 3.26 (t, $J = 7.0$ Hz, 2H, CH_2) ppm; $^{13}\text{C}\{^1\text{H}\}$ NMR (101 MHz, CDCl_3) δ 166.69, 135.55, 133.73, 133.05, 132.46, 130.43, 129.72, 128.49, 128.29, 127.79, 127.65, 127.52, 127.51, 126.22, 125.66, 65.52, 35.55 ppm; IR (ATR) ν (cm^{-1}) 3058, 1711, 1579, 1447, 1315, 1267, 1106, 1023, 963, 818, 686; HRMS (EI) m/z [M] $^+$ calcd for $\text{C}_{19}\text{H}_{16}\text{O}_2$ 276.1150, found 276.1158.

2-(Naphthalen-2-yl)ethyl 2-Methoxybenzoate 7bb. Compound **2b** (20.0 mg, 116 μmol , 1.0 equiv), **3b** (39.9 mg, 139 μmol , 1.2 equiv), DMAP (709 μg , 5.81 μmol , 0.05 equiv), and Et_3N (32.4 μL , 232 μmol , 2.0 equiv) were dissolved in CH_2Cl_2 (580 μL) and reacted according to GP E. After purification by column chromatography on silica (isohexane/ CH_2Cl_2 6:4), **7bb** (30.0 mg, quant.) was obtained as an oil: $^1\text{H NMR}$ (400 MHz, CDCl_3) δ 7.85–7.76 (m, 3H, Ar), 7.77–7.71 (m, 2H, Ar), 7.49–7.41 (m, 4H, Ar), 6.99–6.91 (m, 2H, Ar), 4.61 (t, $J = 7.0$ Hz, 2H, CH_2), 3.85 (s, 3H, Me), 3.24 (t, $J = 7.0$ Hz, 2H, CH_2) ppm; $^{13}\text{C}\{^1\text{H}\}$ NMR (151 MHz, CDCl_3) δ 166.28, 159.38, 135.73, 133.72, 133.62, 132.44, 131.77, 128.20, 127.78, 127.65, 127.59, 127.55, 126.16, 125.59, 120.28, 120.24, 112.15, 65.37, 56.05, 35.48 ppm; IR (ATR) ν (cm^{-1}) 2295.6, 1721, 1599, 1490, 1435, 1298, 1241, 1128, 1078, 814, 730; HRMS (EI) m/z [M] $^+$ calcd for $\text{C}_{20}\text{H}_{18}\text{O}_3$ 306.1256, found 306.1252.

2-(Naphthalen-2-yl)ethyl 2-Methylbenzoate 7bc. Compound **2b** (20.0 mg, 116 μmol , 1.0 equiv), **3c** (32.5 mg, 128 μmol , 1.1 equiv), DMAP (709 μg , 5.81 μmol , 0.05 equiv), and Et_3N (32.4 μL , 232 μmol , 2.0 equiv) were dissolved in CH_2Cl_2 (580 μL) and reacted according to GP E. After purification by column chromatography on silica (isohexane/ CH_2Cl_2 6:4), **7bc** (20.0 mg, 59%) was obtained as an oil: $^1\text{H NMR}$ (600 MHz, CDCl_3) δ 7.87 (dd, $J = 8.3, 1.5$ Hz, 1H, Ar), 7.85–7.78 (m, 3H, Ar), 7.74 (s, 1H, Ar), 7.46 (tdd, $J = 16.3, 7.6, 1.7$ Hz, 3H, Ar), 7.38 (td, $J = 7.5, 1.2$ Hz, 1H, Ar), 7.22 (t, $J = 7.1$ Hz, 2H, Ar), 4.63 (t, $J = 7.0$ Hz, 2H, CH_2), 3.25 (t, $J = 7.0$ Hz, 2H, CH_2), 2.55 (s, 3H, Me) ppm; $^{13}\text{C}\{^1\text{H}\}$ NMR (151 MHz, CDCl_3) δ 167.70, 140.31, 135.57, 133.72, 132.45, 132.05, 131.78, 130.69, 129.81, 128.29, 127.78, 127.64, 127.53, 127.46, 126.21, 125.81, 125.65, 65.29, 35.52, 21.83 ppm; IR (ATR) ν (cm^{-1}) 2926, 1715, 1456, 1259, 1141, 1259, 1141, 179, 814, 750; HRMS (EI) m/z [M] $^+$ calcd for $\text{C}_{20}\text{H}_{18}\text{O}_2$ 290.1307, found 290.1297.

2-(Naphthalen-2-yl)ethyl 2-Chlorobenzoate 7bd. Compound **2b** (20.0 mg, 116 μmol , 1.0 equiv), **3d** (37.7 mg, 128 μmol , 1.1 equiv), DMAP (709 μg , 5.81 μmol , 0.05 equiv), and Et_3N (24.3 μL , 174 μmol , 1.5 equiv) were dissolved in CH_2Cl_2 (580 μL) and reacted according to GP E. After purification by column chromatography on silica (isohexane/ CH_2Cl_2 6:4), **7bd** (20.0 mg, 56%) was obtained as an oil: $^1\text{H NMR}$ (600 MHz, CDCl_3) δ 7.84–7.79 (m, 3H, Ar), 7.76–7.73 (m, 2H, Ar), 7.50–7.37 (m, 5H, Ar), 7.29–7.26 (m, 1H, Ar), 4.65 (t, $J = 7.0$ Hz, 2H, CH_2), 3.26 (t, $J = 7.0$ Hz, 2H, CH_2) ppm; $^{13}\text{C}\{^1\text{H}\}$ NMR (151 MHz, CDCl_3) δ 165.64, 135.13, 133.71, 133.54, 132.49, 132.30, 131.37, 131.04, 130.13, 128.17, 127.64, 127.50, 127.45, 127.30, 126.53, 126.09, 125.54, 65.90, 35.20 ppm; IR (ATR) ν (cm^{-1}) 2956, 1726, 1592, 1435, 1289, 1245, 1115, 1047, 813, 719; HRMS (EI) m/z [M] $^+$ calcd for $\text{C}_{19}\text{H}_{15}\text{O}_2\text{Cl}$ 310.0761, found 310.0767.

2-(Naphthalen-2-yl)ethyl 2-Bromobenzoate 7be. Compound **2b** (20.0 mg, 116 μmol , 1.0 equiv), **3e** (49.0 mg, 128 μmol , 1.1 equiv),

DMAP (709 μg , 5.81 μmol , 0.05 equiv), and Et_3N (24.3 μL , 174 μmol , 1.5 equiv) were dissolved in CH_2Cl_2 (580 μL) and reacted according to GP E. After purification by column chromatography on silica (isohexane/ CH_2Cl_2 6:4), **7be** (20.0 mg, 48%) was obtained as an oil: ^1H NMR (600 MHz, CDCl_3) δ 7.84–7.78 (m, 3H, Ar), 7.74 (s, 1H, Ar), 7.72–7.69 (m, 1H, Ar), 7.66–7.63 (m, 1H, Ar), 7.50–7.44 (m, 2H, Ar), 7.43 (dd, $J = 8.4, 1.8$ Hz, 1H, Ar), 7.34–7.29 (m, 2H, Ar), 4.66 (t, $J = 7.1$ Hz, 2H, CH_2), 3.27 (t, $J = 7.0$ Hz, 2H, CH_2) ppm; $^{13}\text{C}\{^1\text{H}\}$ NMR (151 MHz, CDCl_3) δ 166.26, 135.23, 134.46, 133.69, 132.65, 132.45, 132.34, 131.43, 128.33, 127.79, 127.64, 127.61, 127.45, 127.26, 126.24, 125.69, 121.81, 66.10, 35.32 ppm; IR (ATR) ν (cm^{-1}) 2923, 1726, 1589, 1431, 1287, 1245, 1106, 1027, 962, 813, 710; HRMS (EI) m/z [M] $^+$ calcd for $\text{C}_{19}\text{H}_{15}\text{O}_2\text{Br}$ 354.0255, found 354.0253.

2-(Naphthalen-2-yl)ethyl 2-Phenylbenzoate 7bf. Compound **2b** (25.0 mg, 145 μmol , 1.0 equiv), **3f** (60.1 mg, 160 μmol , 1.1 equiv), DMAP (886 μg , 7.26 μmol , 0.05 equiv), and Et_3N (30.4 μL , 218 μmol , 1.5 equiv) were dissolved in CH_2Cl_2 (725 μL) and reacted according to GP E. After purification by column chromatography on silica (isohexane/ CH_2Cl_2 6:4), **7bf** (40.0 mg, 78%) was obtained as an oil: ^1H NMR (400 MHz, CDCl_3) δ 7.82–7.73 (m, 4H, Ar), 7.54–7.50 (m, 2H, Ar), 7.48–7.41 (m, 2H, Ar), 7.41–7.35 (m, 3H, Ar), 7.35–7.32 (m, 2H, Ar), 7.32–7.29 (m, 2H, Ar), 7.22 (dd, $J = 8.4, 1.8$ Hz, 1H, Ar), 4.35 (t, $J = 7.1$ Hz, 2H, CH_2), 2.82 (t, $J = 7.1$ Hz, 2H, CH_2) ppm; $^{13}\text{C}\{^1\text{H}\}$ NMR (101 MHz, CDCl_3) δ 168.85, 142.64, 141.61, 135.33, 133.63, 132.37, 131.36, 131.17, 130.81, 129.97, 128.55, 128.18, 128.15, 127.75, 127.62, 127.41, 127.40, 127.36, 127.30, 126.15, 125.60, 65.51, 34.94 ppm; IR (ATR) ν (cm^{-1}) 3055, 1714, 1598, 1450, 1276, 1123, 1086, 1046, 814, 698; HRMS (EI) m/z [M] $^+$ calcd for $\text{C}_{25}\text{H}_{20}\text{O}_2$ 352.1463, found 352.1473.

2-(Naphthalen-2-yl)ethyl 2-(4-Methylphenyl)benzoate 7bg. Compound **2b** (25.0 mg, 145 μmol , 1.0 equiv), **3g** (64.9 mg, 160 μmol , 1.1 equiv), DMAP (886 μg , 7.26 μmol , 0.05 equiv), and Et_3N (30.4 μL , 218 μmol , 1.5 equiv) were dissolved in CH_2Cl_2 (725 μL) and reacted according to GP E. After purification by column chromatography on silica (isohexane/ CH_2Cl_2 6:4), **2bg** (45.0 mg, 85%) was obtained as an oil: ^1H NMR (400 MHz, CDCl_3) δ 7.81 (dd, $J = 6.6, 2.6$ Hz, 1H, Ar), 7.79–7.73 (m, 3H, Ar), 7.55 (s, 1H, Ar), 7.54–7.41 (m, 3H, Ar), 7.40–7.34 (m, 2H, Ar), 7.25–7.23 (m, 1H, Ar), 7.22–7.13 (m, 4H, Ar), 4.38 (t, $J = 7.0$ Hz, 2H, CH_2), 2.88 (t, $J = 7.0$ Hz, 2H, CH_2), 2.37 (s, 3H, Me) ppm; $^{13}\text{C}\{^1\text{H}\}$ NMR (101 MHz, CDCl_3) δ 168.92, 142.62, 138.59, 137.05, 135.41, 133.63, 132.37, 131.30, 131.16, 130.83, 129.87, 128.91, 128.41, 128.14, 127.75, 127.62, 127.41, 127.40, 127.06, 126.15, 125.60, 65.48, 35.03, 21.33 ppm; IR (ATR) ν (cm^{-1}) 2919, 1714, 1599, 1444, 1239, 1123, 1085, 816, 746; HRMS (EI) m/z [M] $^+$ calcd for $\text{C}_{26}\text{H}_{22}\text{O}_2$ 366.1620, found 366.1620.

2-(Naphthalen-2-yl)ethyl 2-(Naphthalene-1-yl)benzoate 7bh. Compound **1b** (20.0 mg, 116 μmol , 1.0 equiv), **3h** (61.1 mg, 127.7 μmol , 1.1 equiv), DMAP (709 μg , 5.81 μmol , 0.05 equiv), and Et_3N (24.3 μL , 174 μmol , 1.5 equiv) were dissolved in CH_2Cl_2 (580 μL) and reacted according to GP E. After purification by column chromatography on silica (isohexane/ CH_2Cl_2 6:4), **6bh** (45.0 mg, 97%) was obtained as an oil: ^1H NMR (400 MHz, CDCl_3) δ 8.00 (dd, $J = 7.8, 1.3$ Hz, 1H, Ar), 7.90 (d, $J = 8.1$ Hz, 1H, Ar), 7.86 (d, $J = 8.3$ Hz, 1H, Ar), 7.79–7.74 (m, 1H, Ar), 7.72–7.68 (m, 1H, Ar), 7.67 (d, $J = 8.5$ Hz, 1H, Ar), 7.61 (td, $J = 7.5, 1.4$ Hz, 1H, Ar), 7.55–7.45 (m, 4H, Ar), 7.45–7.35 (m, 4H, Ar), 7.35–7.31 (m, 2H, Ar), 7.00 (dd, $J = 8.4, 1.7$ Hz, 1H, Ar), 4.03 (dddd, $J = 32.2, 10.8, 7.8, 6.7$ Hz, 2H, CH_2), 2.33 (qt, $J = 14.2, 7.2$ Hz, 2H, CH_2) ppm; $^{13}\text{C}\{^1\text{H}\}$ NMR (101 MHz, CDCl_3) δ 167.90, 141.28, 139.98, 135.21, 133.53, 133.41, 132.30, 132.27, 131.94, 131.92, 131.73, 130.34, 128.34, 128.00, 127.74, 127.70, 127.67, 127.57, 127.27, 127.15, 126.24, 126.16, 126.07, 125.84, 125.77, 125.53, 125.32, 65.23, 34.39 ppm; IR (ATR) ν (cm^{-1}) 3053, 1709, 1598, 1445, 1393, 1280, 1243, 118, 1078, 962, 800, 760, 746; HRMS (EI) m/z [M] $^+$ calcd for $\text{C}_{29}\text{H}_{22}\text{O}_2$ 402.1620, found 402.1608.

2-(Naphthalen-2-yl)ethyl 2-(Naphthalene-2-yl)benzoate 7bi. Compound **2b** (20.0 mg, 116 μmol , 1.0 equiv), **3i** (61.1 mg, 128 μmol , 1.1 equiv), DMAP (709 μg , 5.81 μmol , 0.05 equiv), and Et_3N (24.3 μL , 174 μmol , 1.5 equiv) were dissolved in CH_2Cl_2 (580 μL) and reacted according to GP E. After purification by column chromatography on silica (isohexane/ CH_2Cl_2 6:4), **7bi** (25.0 mg, 53%) was

obtained as an oil: ^1H NMR (400 MHz, CDCl_3) δ 7.88–7.82 (m, 3H, Ar), 7.80–7.75 (m, 3H, Ar), 7.73–7.67 (m, 1H, Ar), 7.64 (d, $J = 8.4$ Hz, 1H, Ar), 7.56 (td, $J = 7.5, 1.4$ Hz, 1H, Ar), 7.52–7.45 (m, 3H, Ar), 7.45–7.40 (m, 4H, Ar), 7.37 (s, 1H, Ar), 7.06 (dd, $J = 8.4, 1.7$ Hz, 1H, Ar), 4.32 (t, $J = 7.1$ Hz, 2H, CH_2), 2.70 (t, $J = 7.1$ Hz, 2H, CH_2) ppm; $^{13}\text{C}\{^1\text{H}\}$ NMR (151 MHz, CDCl_3) δ 168.82, 142.61, 139.17, 135.20, 135.12, 133.56, 133.40, 132.62, 132.31, 131.47, 131.26, 131.13, 130.12, 128.18, 128.06, 127.86, 127.73, 127.59, 127.56, 127.42, 127.27, 127.23, 127.06, 126.41, 126.14, 126.09, 125.54, 65.51, 34.86 ppm; IR (ATR) ν (cm^{-1}) 2922, 1716, 1597, 1445, 1363, 1280, 1242, 1122, 1082, 1045, 962, 856, 816, 758, 707; HRMS (EI) m/z [M] $^+$ calcd for $\text{C}_{29}\text{H}_{22}\text{O}_2$ 402.1620, found 402.1617.

2-(Naphthalen-2-yl)ethyl 2-(6-Methoxynaphthalene-2-yl)benzoate 7bj. Compound **2b** (20.0 mg, 116 μmol , 1.0 equiv), **3j** (70.0 mg, 130 μmol , 1.1 equiv), DMAP (709 μg , 5.81 μmol , 0.05 equiv), and Et_3N (32.4 μL , 232 μmol , 2.0 equiv) were dissolved in CH_2Cl_2 (580 μL) and reacted according to GP E. After purification by column chromatography on silica (isohexane/ CH_2Cl_2 6:4), **7bj** (20.0 mg, 40%) was obtained as an oil: ^1H NMR (400 MHz, CDCl_3) δ 7.82 (dd, $J = 7.7, 1.2$ Hz, 1H, Ar), 7.78–7.67 (m, 5H, Ar), 7.64 (d, $J = 8.4$ Hz, 1H, Ar), 7.55 (td, $J = 7.5, 1.4$ Hz, 1H, Ar), 7.47 (dd, $J = 7.7, 1.0$ Hz, 1H, Ar), 7.45–7.36 (m, 5H, Ar), 7.17 (dd, $J = 8.9, 2.5$ Hz, 1H, Ar), 7.13 (d, $J = 2.5$ Hz, 1H, Ar), 7.07 (dd, $J = 8.4, 1.7$ Hz, 1H, Ar), 4.32 (t, $J = 7.1$ Hz, 2H, CH_2), 3.94 (s, 3H, Me), 2.71 (t, $J = 7.0$ Hz, 2H, CH_2) ppm; $^{13}\text{C}\{^1\text{H}\}$ NMR (101 MHz, CDCl_3) δ 169.07, 157.93, 142.59, 136.87, 135.26, 133.79, 133.55, 132.29, 131.42, 131.31, 131.08, 130.06, 129.68, 128.89, 128.03, 127.72, 127.67, 127.59, 127.27, 127.26, 127.22, 126.92, 126.47, 126.08, 125.53, 119.26, 105.81, 65.53, 55.48, 34.88 ppm; IR (ATR) ν (cm^{-1}) 2955, 1712, 1633, 1597, 1492, 1387, 1247, 1122, 1083, 1030, 895, 851, 811, 746; HRMS (EI) m/z [M] $^+$ calcd for $\text{C}_{30}\text{H}_{24}\text{O}_3$ 432.1725, found 432.1721.

2-(Naphthalen-2-yl)ethyl 2,6-Dimethoxybenzoate 7bk. Compound **2b** (20.0 mg, 116 μmol , 1.0 equiv), **3k** (44.2 mg, 128 μmol , 1.1 equiv), DMAP (709 μg , 5.81 μmol , 0.05 equiv), and Et_3N (32.4 μL , 232 μmol , 2.0 equiv) were dissolved in CH_2Cl_2 (580 μL) and reacted according to GP E. After purification by column chromatography on silica (isohexane/ CH_2Cl_2 6:4), **7bk** (30.0 mg, 78%) was obtained as a white solid: mp 85–87 $^\circ\text{C}$; ^1H NMR (600 MHz, CDCl_3) δ 7.83–7.77 (m, 3H, Ar), 7.73 (s, 1H, Ar), 7.47–7.40 (m, 3H, Ar), 7.27 (t, $J = 8.4$ Hz, 1H, Ar), 6.53 (d, $J = 8.4$ Hz, 2H, Ar), 4.65 (t, $J = 7.1$ Hz, 2H, CH_2), 3.73 (s, 6H, Me_2), 3.24 (t, $J = 7.1$ Hz, 2H, CH_2) ppm; $^{13}\text{C}\{^1\text{H}\}$ NMR (151 MHz, CDCl_3) δ 166.70, 157.51, 135.67, 133.71, 132.42, 131.15, 128.08, 127.74, 127.67, 127.64, 127.55, 126.07, 125.53, 113.34, 104.06, 65.70, 56.07, 35.34 ppm; IR (ATR) ν (cm^{-1}) 2967, 1723, 1596, 1475, 1295, 1255, 1079, 755; HRMS (EI) m/z [M] $^+$ calcd for $\text{C}_{21}\text{H}_{20}\text{O}_4$ 336.1362, Found 336.1354.

2-(Naphthalen-2-yl)ethyl 2-Methoxy-6-phenylbenzoate 7bl. Compound **2b** (20.0 mg, 116 μmol , 1.0 equiv), **3l** (56.0 mg, 128 μmol , 1.1 equiv), DMAP (709 μg , 5.81 μmol , 0.05 equiv), and Et_3N (32.4 μL , 232 μmol , 2.0 equiv) were dissolved in CH_2Cl_2 (580 μL) and reacted according to GP E. After purification by column chromatography on silica (isohexane/ CH_2Cl_2 6:4), **7bl** (30.0 mg, 68%) was obtained as an oil: ^1H NMR (400 MHz, CDCl_3) δ 7.82–7.70 (m, 3H, Ar), 7.52 (s, 1H, Ar), 7.48–7.38 (m, 3H, Ar), 7.38–7.33 (m, 2H, Ar), 7.30–7.27 (m, 3H, Ar), 7.20 (dd, $J = 8.4, 1.7$ Hz, 1H, Ar), 6.98 (dd, $J = 7.7, 0.9$ Hz, 1H, Ar), 6.93 (dd, $J = 8.4, 0.8$ Hz, 1H, Ar), 4.35 (t, $J = 7.2$ Hz, 2H, CH_2), 3.83 (s, 3H, Me), 2.81 (t, $J = 7.2$ Hz, 2H, CH_2) ppm; $^{13}\text{C}\{^1\text{H}\}$ NMR (101 MHz, CDCl_3) δ 168.12, 156.63, 141.45, 140.23, 135.39, 133.60, 132.33, 130.62, 128.45, 128.40, 128.08, 127.72, 127.71, 127.63, 127.44, 127.37, 126.08, 125.55, 123.24, 122.08, 109.97, 65.68, 56.13, 34.88 ppm; IR (ATR) ν (cm^{-1}) 2957, 1725, 1584, 1465, 1431, 1250, 1103, 1065, 1017, 814, 756, 699; HRMS (EI) m/z [M] $^+$ calcd for $\text{C}_{26}\text{H}_{22}\text{O}_3$ 382.1569, found 382.1561.

2-(Naphthalen-2-yl)ethyl 2,6-Dimethylbenzoate 7bm. Compound **2b** (20.0 mg, 116 μmol , 1.0 equiv), **3m** (36.1 mg, 128 μmol , 1.1 equiv), DMAP (709 μg , 5.81 μmol , 0.05 equiv), and Et_3N (32.4 μL , 232 μmol , 2.0 equiv) were dissolved in CH_2Cl_2 (580 μL) and reacted according to GP E. After purification by column chromatography on silica (isohexane/ CH_2Cl_2 6:4), **7bm** (20.0 mg, 57%) was obtained as a white solid: mp 60–62 $^\circ\text{C}$; ^1H NMR (400 MHz, CDCl_3) δ 7.84–7.76

(m, 3H, Ar), 7.72 (d, $J = 1.6$ Hz, 1H, Ar), 7.50–7.43 (m, 2H, Ar), 7.41 (dd, $J = 8.4, 1.8$ Hz, 1H, Ar), 7.17 (t, $J = 7.6$ Hz, 1H, Ar), 7.00 (d, $J = 7.6$ Hz, 2H, Ar), 4.66 (t, $J = 7.1$ Hz, 2H, CH₂), 3.24 (t, $J = 7.0$ Hz, 2H, CH₂), 2.21 (s, 6H, Me₂) ppm; ¹³C{¹H} NMR (101 MHz, CDCl₃) δ 170.15, 135.21, 135.04, 133.99, 133.68, 132.46, 129.40, 128.33, 127.78, 127.66, 127.63, 127.55, 127.35, 126.24, 125.68, 65.36, 35.36, 19.75 ppm; IR (ATR) ν (cm⁻¹) 2923, 1719, 1597, 1465, 1267, 1081, 1065, 964, 821, 774, 747; HRMS (EI) m/z [M]⁺ calcd for C₂₁H₂₀O₂ 304.1463, found 304.1453.

2-(Naphthalen-2-yl)ethyl 2-Methyl-6-phenylbenzoate 7bn. Compound **2b** (15.0 mg, 87.1 μ mol, 1.0 equiv), **3n** (38.9 mg, 95.8 μ mol, 1.1 equiv), DMAP (532 μ g, 4.35 μ mol, 0.05 equiv), and Et₃N (18.2 μ L, 131 μ mol, 1.5 equiv) were dissolved in CH₂Cl₂ (435 μ L) and reacted according to GP E. After purification by column chromatography on silica (isohexane/CH₂Cl₂ 6:4), **7bn** (25.0 mg, 78%) was obtained as a white solid: mp 85–88 °C; ¹H NMR (400 MHz, CDCl₃) δ 7.83–7.79 (m, 1H, Ar), 7.75 (dd, $J = 8.6, 4.8$ Hz, 2H, Ar), 7.53 (s, 1H, Ar), 7.50–7.41 (m, 2H, Ar), 7.40–7.28 (m, 6H, Ar), 7.24–7.19 (m, 3H, Ar), 4.31 (t, $J = 7.2$ Hz, 2H, CH₂), 2.78 (t, $J = 7.2$ Hz, 2H, CH₂), 2.35 (s, 3H, Me) ppm; ¹³C{¹H} NMR (101 MHz, CDCl₃) δ 169.91, 141.14, 140.38, 135.66, 135.22, 133.61, 133.31, 132.37, 129.51, 129.27, 128.47, 128.37, 128.17, 127.73, 127.60, 127.47, 127.36, 127.35, 127.33, 126.14, 125.60, 65.47, 34.86, 19.81 ppm; IR (ATR) ν (cm⁻¹) 2191, 1716, 1591, 1464, 1260, 1128, 1077, 964, 824, 763, 700; HRMS (EI) m/z [M]⁺ calcd for C₂₆H₂₂O₂ 366.1620, found 366.1618.

2-(Naphthalen-2-yl)ethyl 2-Methyl-6-nitrobenzoate 7bo. Compound **2b** (20.0 mg, 116 μ mol, 1.0 equiv), **3o** (44.0 mg, 128 μ mol, 1.1 equiv), DMAP (709 μ g, 5.81 μ mol, 0.05 equiv), and Et₃N (32.4 μ L, 232 μ mol, 2.0 equiv) were dissolved in CH₂Cl₂ (580 μ L) and reacted according to GP E. After purification by column chromatography on silica (isohexane/CH₂Cl₂ 6:4), **7bo** (25.0 mg, 65%) was obtained as an oil: ¹H NMR (400 MHz, CDCl₃) δ 7.97 (d, $J = 8.7$ Hz, 1H, Ar), 7.84–7.77 (m, 3H, Ar), 7.71 (s, 1H, Ar), 7.50–7.38 (m, 5H, Ar), 4.73 (t, $J = 7.1$ Hz, 2H, CH₂), 3.30–3.22 (m, 2H, CH₂), 2.27 (s, 3H, Me) ppm; ¹³C{¹H} NMR (101 MHz, CDCl₃) δ 166.55, 146.25, 137.66, 136.08, 134.94, 133.65, 132.42, 129.79, 129.56, 128.31, 127.74, 127.64, 127.50, 127.27, 126.21, 125.67, 121.88, 66.45, 34.90, 19.08 ppm; IR (ATR) ν (cm⁻¹) 2850, 1730, 1530, 1334, 1268, 1115, 1077, 990, 815, 725; HRMS (EI) m/z [M]⁺ calcd for C₂₀H₁₇O₄N 335.1158, found 335.1144.

2-(Naphthalen-2-yl)ethyl 2-Fluoro-6-(trifluoromethyl)benzoate 7bp. Compound **2b** (15.0 mg, 87.1 μ mol, 1.0 equiv), **3p** (38.2 mg, 95.8 μ mol, 1.1 equiv), DMAP (532 μ g, 4.35 μ mol, 0.05 equiv), and Et₃N (18.2 μ L, 131 μ mol, 1.5 equiv) were dissolved in CH₂Cl₂ (435 μ L) and reacted according to GP E. After purification by column chromatography on silica (isohexane/CH₂Cl₂ 6:4), **7bp** (15.0 mg, 41%) was obtained as an oil: ¹H NMR (400 MHz, CDCl₃) δ 7.86–7.76 (m, 3H, Ar), 7.72 (s, 1H, Ar), 7.57–7.42 (m, 4H, Ar), 7.40 (dd, $J = 8.4, 1.7$ Hz, 1H, Ar), 7.33 (td, $J = 8.1, 7.5, 1.9$ Hz, 1H, Ar), 4.69 (t, $J = 7.3$ Hz, 2H, CH₂), 3.25 (t, $J = 7.3$ Hz, 2H, CH₂) ppm; ¹³C{¹H} NMR (101 MHz, CDCl₃) δ 163.48, 160.75, 158.25, 134.76, 133.69, 132.47, 131.75, 131.67, 128.34, 127.77, 127.68, 127.52, 127.31, 126.22, 125.70, 122.12 (qd, $J = 4.7, 3.5$ Hz), 119.96 (q, $J = 1.0$ Hz), 119.74 (q, $J = 1.4$ Hz), 66.93, 35.02 ppm; ¹⁹F NMR (377 MHz, CDCl₃) δ -59.73, -113.04 ppm; IR (ATR) ν (cm⁻¹) 2960, 1738, 1586, 1464, 1317, 1271, 1172, 1120, 1061, 960, 913, 803, 745; HRMS (EI) m/z [M]⁺ calcd for C₂₀H₁₄O₂F₄ 362.0930, found 362.0915.

2-(Naphthalen-2-yl)ethyl 1-Naphthoate 7bq. Compound **2b** (50.0 mg, 290 μ mol, 1.0 equiv), **3q** (113 mg, 348 μ mol, 1.2 equiv), DMAP (1.77 mg, 14.5 μ mol, 0.05 equiv), and Et₃N (60.0 μ L, 435 μ mol, 1.5 equiv) were dissolved in CH₂Cl₂ (1.5 mL) and reacted according to GP E. After purification by column chromatography on silica (isohexane/CH₂Cl₂ 6:4), **7bq** (80.0 mg, 84%) was obtained as a white solid: mp 47–50 °C; ¹H NMR (400 MHz, CDCl₃) δ 8.76 (d, $J = 8.4$ Hz, 1H, Ar), 8.12 (dd, $J = 7.3, 1.3$ Hz, 1H, Ar), 8.00 (d, $J = 8.2$ Hz, 1H, Ar), 7.90–7.77 (m, 5H, Ar), 7.54–7.43 (m, 6H, Ar), 4.74 (t, $J = 6.9$ Hz, 2H, CH₂), 3.32 (t, $J = 6.9$ Hz, 2H, CH₂) ppm; ¹³C{¹H} NMR (101 MHz, CDCl₃) δ 167.75, 135.60, 133.93, 133.75, 133.43, 132.48, 131.40, 130.31, 128.61, 128.37, 127.81, 127.80, 127.68, 127.65, 127.50, 127.43, 126.30, 126.24, 125.94, 125.69, 124.63, 65.70, 35.55 ppm; IR (ATR) ν (cm⁻¹)

2957, 1711, 1505, 1344, 1288, 1244, 1195, 1134, 1072, 1011, 796, 747; HRMS (EI) m/z [M]⁺ calcd for C₂₃H₁₈O₂ 326.1307, found 326.1290.

2-(Naphthalen-2-yl)ethyl 2-Methoxy-1-naphthoate 7br. Compound **2b** (20.0 mg, 116 μ mol, 1.0 equiv), **3r** (53.8 mg, 139 μ mol, 1.2 equiv), DMAP (709 μ g, 5.81 μ mol, 0.05 equiv), and Et₃N (32.4 μ L, 232 μ mol, 2.0 equiv) were dissolved in CH₂Cl₂ (580 μ L) and reacted according to GP E. After purification by column chromatography on silica (isohexane/CH₂Cl₂ 6:4), **7br** (20.0 mg, 48%) was obtained as a white solid: mp 99–102 °C; ¹H NMR (400 MHz, CDCl₃) δ 7.90–7.86 (m, 1H, Ar), 7.85–7.80 (m, 2H, Ar), 7.78–7.73 (m, 3H, Ar), 7.49–7.44 (m, 4H, Ar), 7.30 (ddd, $J = 8.1, 6.8, 1.2$ Hz, 1H, Ar), 7.25 (d, $J = 9.1$ Hz, 1H, Ar), 7.18 (ddd, $J = 8.3, 6.8, 1.4$ Hz, 1H, Ar), 4.80 (t, $J = 6.9$ Hz, 2H, CH₂), 3.87 (s, 3H, Me), 3.30 (t, $J = 6.9$ Hz, 2H, CH₂) ppm; ¹³C{¹H} NMR (101 MHz, CDCl₃) δ 168.15, 154.55, 135.48, 133.73, 132.49, 131.74, 131.03, 128.60, 128.29, 128.09, 127.77, 127.74, 127.72, 127.63, 127.54, 126.16, 125.65, 124.19, 123.90, 117.69, 113.19, 65.83, 56.82, 35.47 ppm; IR (ATR) ν (cm⁻¹) 2917, 1724, 1593, 1508, 1468, 1255, 1213, 1133, 1074, 1024, 790, 737; HRMS (EI) m/z [M]⁺ calcd for C₂₄H₂₀O₃ 356.1412, found 356.1405.

2-(Naphthalen-2-yl)ethyl 2-Ethoxy-1-naphthoate 7bs. Compound **2b** (20.0 mg, 116 μ mol, 1.0 equiv), **3s** (57.8 mg, 139 μ mol, 1.2 equiv), DMAP (709 μ g, 5.81 μ mol, 0.05 equiv), and Et₃N (32.4 μ L, 232 μ mol, 2.0 equiv) were dissolved in CH₂Cl₂ (580 μ L) and reacted according to GP E. After purification by column chromatography on silica (isohexane/CH₂Cl₂ 6:4), **7bs** (40.0 mg, 93%) was obtained as a white solid: mp 70–73 °C; ¹H NMR (600 MHz, CDCl₃) δ 7.87–7.80 (m, 3H, Ar), 7.78–7.74 (m, 3H, Ar), 7.50 (d, $J = 8.5$ Hz, 1H, Ar), 7.48–7.44 (m, 3H, Ar), 7.33–7.29 (m, 1H, Ar), 7.24 (d, $J = 9.1$ Hz, 1H, Ar), 7.22 (ddd, $J = 8.3, 6.8, 1.3$ Hz, 1H, Ar), 4.79 (t, $J = 7.1$ Hz, 2H, CH₂), 4.17 (q, $J = 7.0$ Hz, 2H, CH₂), 3.31 (t, $J = 7.1$ Hz, 2H, CH₂), 1.34 (t, $J = 7.0$ Hz, 3H, Me) ppm; ¹³C{¹H} NMR (151 MHz, CDCl₃) δ 168.22, 153.93, 135.43, 133.72, 132.48, 131.56, 131.05, 128.64, 128.31, 128.07, 127.76, 127.72, 127.67, 127.54, 127.53, 126.16, 125.65, 124.19, 123.91, 118.35, 114.59, 65.76, 65.53, 35.52, 15.06 ppm; IR (ATR) ν (cm⁻¹) 2917, 1714, 1597, 1508, 1453, 1300, 1234, 1111, 975, 811, 720, 695; HRMS (EI) m/z [M]⁺ calcd for C₂₅H₂₂O₃ 370.1569, found 370.1563.

2-(Naphthalen-2-yl)ethyl 2-Butoxy-1-naphthoate 7bt. Compound **2b** (20.0 mg, 116 μ mol, 1.0 equiv), **3t** (60.1 mg, 128 μ mol, 1.1 equiv), DMAP (709 μ g, 5.81 μ mol, 0.05 equiv), and Et₃N (32.4 μ L, 232 μ mol, 2.0 equiv) were dissolved in CH₂Cl₂ (580 μ L) and reacted according to GP E. After purification by column chromatography on silica (isohexane/CH₂Cl₂ 6:4), **7bt** (41.0 mg, 89%) was obtained as a white solid: mp 49–52 °C; ¹H NMR (600 MHz, CDCl₃) δ 7.87–7.79 (m, 3H, Ar), 7.78–7.73 (m, 3H, Ar), 7.50–7.43 (m, 4H, Ar), 7.30 (ddd, $J = 8.1, 6.8, 1.2$ Hz, 1H, Ar), 7.25 (d, $J = 9.1$ Hz, 1H, Ar), 7.22 (ddd, $J = 8.3, 6.8, 1.3$ Hz, 1H, Ar), 4.77 (t, $J = 7.1$ Hz, 2H, CH₂), 4.10 (t, $J = 6.5$ Hz, 2H, CH₂), 3.30 (t, $J = 7.1$ Hz, 2H, CH₂), 1.71 (ddt, $J = 8.9, 7.7, 6.4$ Hz, 2H, CH₂), 1.50–1.40 (m, 2H, CH₂), 0.94 (t, $J = 7.4$ Hz, 3H, Me) ppm; ¹³C{¹H} NMR (151 MHz, CDCl₃) δ 168.23, 154.12, 135.42, 133.75, 132.51, 131.54, 131.09, 128.62, 128.32, 128.08, 127.77, 127.73, 127.67, 127.55, 127.53, 126.17, 125.66, 124.15, 123.89, 118.22, 114.52, 69.60, 65.76, 35.54, 31.55, 19.24, 13.96; IR (ATR) ν (cm⁻¹) 2956, 1721, 1625, 1594, 11510, 1463, 1434, 1341, 1281, 1226, 1134, 1071, 1024, 807; HRMS (EI) m/z [M]⁺ calcd for C₂₇H₂₆O₃ 398.1882, found 398.1878.

2-(Naphthalen-2-yl)ethyl 2-(Hexanoyloxy)-1-naphthoate 7bu. Compound **2b** (10.0 mg, 58.1 μ mol, 1.0 equiv), **3u** (33.6 mg, 63.87 μ mol, 1.1 equiv), DMAP (355 μ g, 2.90 μ mol, 0.05 equiv), and Et₃N (16.2 μ L, 116 μ mol, 2.0 equiv) were dissolved in CH₂Cl₂ (300 μ L) and reacted according to GP E. After purification by column chromatography on silica (isohexane/CH₂Cl₂ 6:4), **7bu** (10.0 mg, 40%) was obtained as an oil: ¹H NMR (400 MHz, CDCl₃) δ 7.87–7.79 (m, 3H, Ar), 7.78–7.73 (m, 3H, Ar), 7.51–7.43 (m, 4H, Ar), 7.30 (ddd, $J = 8.1, 6.8, 1.1$ Hz, 1H, Ar), 7.25 (d, $J = 9.1$ Hz, 1H, Ar), 7.22 (ddd, $J = 8.2, 6.8, 1.3$ Hz, 1H, Ar), 4.77 (t, $J = 7.2$ Hz, 2H, CH₂), 4.10 (t, $J = 6.6$ Hz, 2H, CH₂), 3.30 (t, $J = 7.1$ Hz, 2H, CH₂), 1.76–1.68 (m, 2H, CH₂), 1.47–1.38 (m, 2H, CH₂), 1.35–1.28 (m, 4H, 2xCH₂), 0.89 (t, $J = 6.8$ Hz, 3H, Me) ppm; ¹³C{¹H} NMR (101 MHz, CDCl₃) δ 168.23, 154.07, 135.37, 133.69, 132.45, 131.54, 131.03, 128.54, 128.30, 128.06, 127.75, 127.71, 127.66, 127.53, 127.51, 126.16, 125.65, 124.12, 123.84, 118.07, 114.53,

69.82, 65.75, 35.51, 31.66, 29.43, 25.69, 22.77, 14.20 ppm; IR (ATR) ν (cm⁻¹) 2924, 1722, 1593, 1511, 1462, 1281, 1226, 1135, 1074, 898, 809, 740; HRMS (EI) m/z [M]⁺ calcd for C₂₉H₃₀O₃ 426.2195, found 426.2186.

2-(Naphthalen-2-yl)ethyl 2-Isopropoxy-1-naphthoate 7bv. Compound **2b** (15.0 mg, 87.1 μ mol, 1.0 equiv), **3v** (41.1 mg, 95.8 μ mol, 1.1 equiv), DMAP (532 μ g, 4.35 μ mol, 0.05 equiv), and Et₃N (18.2 μ L, 131 μ mol, 1.5 equiv) were dissolved in CH₂Cl₂ (435 μ L) and reacted according to GP E. After purification by column chromatography on silica (isohexane/CH₂Cl₂ 6:4), **7bv** (20.0 mg, 59%) was obtained as a white solid: mp 101–104 °C; ¹H NMR (400 MHz, CDCl₃) δ 7.88–7.82 (m, 3H, Ar), 7.81–7.75 (m, 3H, Ar), 7.53–7.45 (m, 4H, Ar), 7.33 (ddd, *J* = 8.1, 6.9, 1.2 Hz, 1H, Ar), 7.29–7.23 (m, 2H, Ar), 4.80 (t, *J* = 7.1 Hz, 2H, CH₂), 4.68 (hept, *J* = 6.1 Hz, 1H, CH), 3.32 (t, *J* = 7.1 Hz, 2H, CH₂), 1.33 (d, *J* = 6.1 Hz, 6H, Me₂) ppm; ¹³C{¹H} NMR (101 MHz, CDCl₃) δ 168.31, 153.04, 135.43, 133.73, 132.49, 131.32, 131.12, 128.75, 128.33, 128.03, 127.76, 127.73, 127.66, 127.52, 127.47, 126.16, 125.65, 124.31, 123.94, 119.84, 116.35, 72.61, 65.72, 35.56, 22.46 ppm; IR (ATR) ν (cm⁻¹) 2978, 1730, 1592, 1504, 1465, 1331, 1279, 1249, 1208, 1132, 1105, 1039, 999, 808, 748; HRMS (EI) m/z [M]⁺ calcd for C₂₆H₂₄O₃ 384.1725, found 384.1722.

2-(Naphthalen-2-yl)ethyl 2-Methyl-1-naphthoate 7bw. Compound **2b** (20.0 mg, 116 μ mol, 1.0 equiv), **3w** (45.3 mg, 128 μ mol, 1.1 equiv), DMAP (709 μ g, 5.81 μ mol, 0.05 equiv), and Et₃N (32.4 μ L, 232 μ mol, 2.0 equiv) were dissolved in CH₂Cl₂ (580 μ L) and reacted according to GP E. After purification by column chromatography on silica (isohexane/CH₂Cl₂ 6:4), **7bw** (20.0 mg, 51%) was obtained as a white solid: mp 80–84 °C; ¹H NMR (600 MHz, CDCl₃) δ 7.85–7.79 (m, 2H, Ar), 7.79–7.73 (m, 4H, Ar), 7.55 (d, *J* = 8.5 Hz, 1H, Ar), 7.49–7.45 (m, 2H, Ar), 7.44 (d, *J* = 8.3 Hz, 1H, Ar), 7.38 (t, *J* = 7.5 Hz, 1H, Ar), 7.28 (d, *J* = 8.4 Hz, 1H, Ar), 7.21 (t, *J* = 7.6 Hz, 1H, Ar), 4.81 (t, *J* = 6.9 Hz, 2H, CH₂), 3.30 (t, *J* = 6.9 Hz, 2H, CH₂), 2.39 (s, 3H, Me) ppm; ¹³C{¹H} NMR (151 MHz, CDCl₃) δ 169.83, 135.27, 133.73, 133.51, 132.53, 131.72, 130.22, 130.12, 129.75, 128.46, 128.41, 128.06, 127.79, 127.73, 127.72, 127.41, 127.05, 126.24, 125.73, 125.54, 124.63, 65.74, 35.48, 20.18 ppm; IR (ATR) ν (cm⁻¹) 2090, 1720, 1598, 1510, 1468, 11426, 1386, 1282, 1243, 1212, 1136, 1064, 997, 801, 742; HRMS (EI) m/z [M]⁺ calcd for C₂₄H₂₀O₂ 340.1463, found 340.1463.

2-(Naphthalen-2-yl)ethyl 3-Phenylbenzoate 7bx. Compound **2b** (20.0 mg, 116 μ mol, 1.0 equiv), **3x** (48.3 mg, 127 μ mol, 1.1 equiv), DMAP (709 μ g, 5.81 μ mol, 0.05 equiv), and Et₃N (32.4 μ L, 232 μ mol, 1.5 equiv) were dissolved in CH₂Cl₂ (580 μ L) and reacted according to GP E. After purification by column chromatography on silica (isohexane/CH₂Cl₂ 6:4), **7bx** (40 mg, 98%) was obtained as a white solid: mp 59–61 °C; ¹H NMR (400 MHz, CDCl₃) δ 8.24 (t, *J* = 2.0 Hz, 1H, Ar), 8.00 (dt, *J* = 7.7, 1.4 Hz, 1H, Ar), 7.85–7.75 (m, 5H, Ar), 7.61–7.56 (m, 2H, Ar), 7.52–7.42 (m, 6H, Ar), 7.41–7.36 (m, 1H, Ar), 4.66 (t, *J* = 6.9 Hz, 2H, CH₂), 3.27 (t, *J* = 6.9 Hz, 2H, CH₂) ppm; ¹³C{¹H} NMR (101 MHz, CDCl₃) δ 166.62, 141.58, 140.25, 135.57, 133.74, 132.48, 131.66, 130.98, 129.04, 128.99, 128.49, 128.43, 128.33, 127.87, 127.81, 127.67, 127.61, 127.54, 127.28, 126.24, 125.68, 65.61, 35.59 ppm; IR (ATR) ν (cm⁻¹) 3054, 1706, 1598, 1454, 1302, 1235, 1174, 1114, 978, 818, 720, 695; HRMS (EI) m/z [M]⁺ calcd for C₂₅H₂₀O₂ 352.1463, found 352.1458.

2-(Naphthalen-2-yl)ethyl Thiophen-2-yl-carboxylate 7by. Compound **2b** (25.0 mg, 145 μ mol, 1.0 equiv), **3y** (38.1 mg, 160 μ mol, 1.1 equiv), DMAP (886 μ g, 7.26 μ mol, 0.05 equiv), and Et₃N (30.4 μ L, 218 μ mol, 1.5 equiv) were dissolved in CH₂Cl₂ (725 μ L) and reacted according to GP E. After purification by column chromatography on silica (isohexane/CH₂Cl₂ 6:4), **7by** (40.0 mg, 98%) was obtained as an oil: ¹H NMR (600 MHz, CDCl₃) δ 7.84–7.76 (m, 4H, Ar), 7.74 (s, 1H, Ar), 7.55 (dd, *J* = 5.0, 1.3 Hz, 1H, Ar), 7.49–7.39 (m, 3H, Ar), 7.09 (dd, *J* = 5.0, 3.7 Hz, 1H, Ar), 4.59 (t, *J* = 7.0 Hz, 2H, CH₂), 3.23 (t, *J* = 7.0 Hz, 2H, CH₂) ppm; ¹³C{¹H} NMR (151 MHz, CDCl₃) δ 162.28, 135.38, 133.90, 133.69, 133.59, 132.52, 132.43, 128.26, 127.87, 127.78, 127.66, 127.61, 127.55, 126.20, 125.66, 65.67, 35.51 ppm; IR (ATR) ν (cm⁻¹) 2918, 1703, 1524, 1417, 1223, 1091, 856, 814, 745; HRMS (EI) m/z [M]⁺ calcd for C₁₇H₁₄O₂S 282.0715, found 282.0716.

Naphthalen-2-yl)ethyl 2-Naphthoate 7bz. Compound **2b** (50.0 mg, 290 μ mol, 1.0 equiv), **3z** (113 mg, 348 μ mol, 1.2 equiv), DMAP

(1.77 mg, 14.5 μ mol, 0.05 equiv), and Et₃N (60.0 μ L, 435 μ mol, 1.5 equiv) were dissolved in CH₂Cl₂ (1.5 mL) and reacted according to GP E. After purification by column chromatography on silica (isohexane/CH₂Cl₂ 6:4), **7bz** (95 mg, 99%) was obtained as a white solid: mp 124–126 °C; ¹H NMR (400 MHz, CDCl₃) δ 8.58 (s, 1H, Ar), 8.04 (dd, *J* = 8.6, 1.7 Hz, 1H, Ar), 7.93 (d, *J* = 8.0 Hz, 1H, Ar), 7.90–7.76 (m, 6H, Ar), 7.63–7.51 (m, 2H, Ar), 7.51–7.43 (m, 3H, Ar), 4.70 (t, *J* = 7.0 Hz, 2H, CH₂), 3.31 (t, *J* = 7.0 Hz, 2H, CH₂) ppm; ¹³C{¹H} NMR (151 MHz, CDCl₃) δ 166.85, 135.69, 135.57, 133.76, 132.64, 132.48, 131.24, 129.51, 128.37, 128.33, 128.29, 127.90, 127.82, 127.68, 127.67, 127.60, 127.56, 126.77, 126.25, 125.69, 125.37, 65.66, 35.63 ppm; IR (ATR) ν (cm⁻¹) 3053, 1707.1442, 1289, 1194, 1129, 1093, 951, 829, 781, 729; HRMS (EI) m/z [M]⁺ calcd for C₂₃H₁₈O₂ 326.1307, found 326.1291.

1-(Pyren-2-yl)ethyl Benzoate 6ca. Compound **1c** (20.0 mg, 81.2 μ mol, 1.0 equiv), **3a** (20.0 mg, 89.3 μ mol, 1.1 equiv), DMAP (496 μ g, 4.06 μ mol, 0.05 equiv), and Et₃N (22.6 μ L, 162 μ mol, 2.0 equiv) were dissolved in CH₂Cl₂ (400 μ L) and reacted according to GP E. After purification by column chromatography on silica (isohexane/CH₂Cl₂ 6:4), **6ca** (10.0 mg, 35%) was obtained as an oil: ¹H NMR (400 MHz, CDCl₃) δ 8.27 (s, 2H, Ar), 8.22–8.14 (m, 4H, Ar), 8.09 (s, 4H, Ar), 8.03–7.97 (m, 1H, Ar), 7.58 (t, *J* = 8.0 Hz, 1H, Ar), 7.47 (t, *J* = 7.6 Hz, 2H, Ar), 6.59 (q, *J* = 6.6 Hz, 1H, CH), 1.91 (d, *J* = 6.6 Hz, 3H, Me) ppm; ¹³C{¹H} NMR (101 MHz, CDCl₃) δ 166.08, 139.66, 133.12, 131.49, 131.23, 130.70, 129.87, 128.53, 127.91, 127.51, 126.07, 125.26, 124.64, 124.49, 122.66, 73.59, 23.21 ppm; IR (ATR) ν (cm⁻¹) 2852, 1713, 1450, 1269, 1064, 1024, 841, 710; HRMS (EI) m/z [M]⁺ calcd for C₂₅H₁₈O₂ 350.1307, found 350.1293.

1-(Pyren-2-yl)ethyl 2-Phenylbenzoate 6cf. Compound **1c** (20.0 mg, 81.2 μ mol, 1.0 equiv), **3f** (33.8 mg, 89.3 μ mol, 1.1 equiv), DMAP (496 μ g, 4.06 μ mol, 0.05 equiv), and Et₃N (22.6 μ L, 162 μ mol, 2.0 equiv) were dissolved in CH₂Cl₂ (400 μ L) and reacted according to GP E. After purification by column chromatography on silica (isohexane/CH₂Cl₂ 6:4), **6cf** (25.0 mg, 72%) was obtained as an oil: ¹H NMR (400 MHz, CDCl₃) δ 8.18 (d, *J* = 7.6 Hz, 2H, Ar), 8.07 (d, *J* = 9.0 Hz, 2H, Ar), 8.03–7.98 (m, 3H, Ar), 7.92–7.87 (m, 3H, Ar), 7.53 (td, *J* = 7.5, 1.4 Hz, 1H, Ar), 7.42 (td, *J* = 7.6, 1.2 Hz, 1H, Ar), 7.38 (dd, *J* = 7.7, 1.3 Hz, 1H, Ar), 7.36–7.31 (m, 2H, Ar), 7.26 (d, *J* = 14.9 Hz, 2H, Ar), 7.21–7.15 (m, 1H, Ar), 6.32 (q, *J* = 6.6 Hz, 1H, CH), 1.55 (d, *J* = 6.6 Hz, 3H, Me) ppm; ¹³C{¹H} NMR (101 MHz, CDCl₃) δ 168.36, 142.59, 141.62, 139.01, 131.42, 131.34, 131.26, 131.21, 130.93, 130.19, 128.70, 128.19, 127.71, 127.52, 127.32, 126.03, 125.17, 124.60, 124.38, 122.81, 74.06, 22.74 ppm (one signal is overlapping); IR (ATR) ν (cm⁻¹) 2918, 1705, 1597, 1449, 1276, 1239, 1124, 1062, 841, 744, 712; HRMS (EI) m/z [M]⁺ calcd for C₃₁H₂₂O₂ 426.1620, found 426.1614.

1-(Pyren-2-yl)ethyl 2-(Naphthalene-1-yl)benzoate 6ch. Compound **1c** (20.0 mg, 81.2 μ mol, 1.0 equiv), **3h** (42.7 mg, 89.3 μ mol, 1.1 equiv), DMAP (496 μ g, 4.06 μ mol, 0.05 equiv), and Et₃N (22.6 μ L, 162 μ mol, 2.0 equiv) were dissolved in CH₂Cl₂ (400 μ L) and reacted according to GP E. After purification by column chromatography on silica (isohexane/CH₂Cl₂ 6:4), **6ch** (25.0 mg, 65%) was obtained as an oil (diastereomeric mixture of 1:1). ¹H NMR (400 MHz, CDCl₃) δ 8.17 (d, *J* = 4.7 Hz, 1H, Ar), 8.15 (d, *J* = 4.8 Hz, 1H, Ar), 8.11 (dd, *J* = 7.6, 1.7 Hz, 0.5H, Ar), 8.09–8.02 (m, 2.5H, Ar), 8.01–7.96 (m, 1H, Ar), 7.94 (d, *J* = 9.0 Hz, 1H, Ar), 7.83 (d, *J* = 9.0 Hz, 1H, Ar), 7.80–7.75 (m, 1H, Ar), 7.71 (d, *J* = 7.4 Hz, 0.5H, Ar), 7.66 (d, *J* = 8.1 Hz, 0.5H, Ar), 7.64–7.49 (m, 4.5H, Ar), 7.48–7.44 (m, 0.5H, Ar), 7.44–7.37 (m, 4H, Ar), 7.34 (m, 1H, Ar), 6.05 (dq, *J* = 7.9, 6.6 Hz, 1H, CH), 1.10 (d, *J* = 6.6 Hz, 1.5H, Me), 0.85 (d, *J* = 6.6 Hz, 1.5H, Me) ppm; ¹³C{¹H} NMR (101 MHz, CDCl₃) δ 167.54, 167.47, 141.17, 141.10, 140.37, 140.05, 138.73, 138.59, 133.42, 133.39, 132.56, 132.42, 132.19, 132.07, 132.03, 131.95, 131.94, 131.52, 131.19, 131.17, 131.11, 131.09, 130.67, 130.61, 128.28, 128.25, 127.81, 127.75, 127.71, 127.66, 127.59, 127.53, 127.49, 126.31, 126.25, 126.20, 126.17, 126.14, 126.00, 125.97, 125.85, 125.84, 125.78, 125.42, 125.17, 125.12, 125.08, 124.58, 124.54, 124.29, 124.25, 122.75, 122.69, 73.72, 73.63, 22.25, 21.60 ppm (one signal is overlapping); IR (ATR) ν (cm⁻¹) 3039, 1703, 1598, 1445, 1279, 1123, 1061, 1016, 841, 755, 700; HRMS (EI) m/z [M]⁺ calcd for C₃₅H₂₄O₂ 476.1776, found 476.1763.

1-(Pyren-2-yl)ethyl 2-Methyl-1-naphthoate 6cw. Compound **1c** (15.0 mg, 60.9 μ mol, 1.0 equiv), **3w** (25.8 mg, 67.0 μ mol, 1.1 equiv), DMAP (372 μ g, 3.04 μ mol, 0.05 equiv), and Et_3N (12.7 μ L, 91.4 μ mol, 1.5 equiv) were dissolved in CH_2Cl_2 (300 μ L) and reacted according to GP E. After purification by column chromatography on silica (isohexane/ CH_2Cl_2 6:4), **6cw** (10.0 mg, 59%) was obtained as a white solid: mp 114–116 $^\circ\text{C}$; ^1H NMR (400 MHz, CDCl_3) δ 8.30 (s, 2H, Ar), 8.20 (d, $J = 7.6$ Hz, 2H, Ar), 8.13–8.05 (m, 4H, Ar), 8.05–8.00 (m, 1H, Ar), 7.81 (d, $J = 8.2$ Hz, 2H, Ar), 7.72 (d, $J = 8.4$ Hz, 1H, Ar), 7.45–7.34 (m, 2H, Ar), 7.32 (d, $J = 8.5$ Hz, 1H, Ar), 6.79 (q, $J = 6.6$ Hz, 1H, CH), 2.45 (s, 3H, Me), 1.97 (d, $J = 6.7$ Hz, 3H, Me) ppm; $^{13}\text{C}\{^1\text{H}\}$ NMR (101 MHz, CDCl_3) δ 169.30, 139.20, 133.29, 131.78, 131.51, 131.27, 130.42, 130.18, 129.71, 128.52, 128.16, 127.99, 127.50, 127.14, 126.16, 125.60, 125.32, 124.63, 124.58, 122.98, 74.16, 23.34, 20.17 ppm (one signal is overlapping); IR (ATR) ν (cm^{-1}) 2923, 1716, 1597, 1453, 1372, 1221, 1135, 1065, 879, 821, 742; HRMS (EI) m/z $[\text{M}]^+$ calcd for $\text{C}_{30}\text{H}_{22}\text{O}_2$ 414.1620, found 414.1616.

2-(Pyren-2-yl)ethyl Benzoate 7ca. Compound **2c** (20.0 mg, 81.2 μ mol, 1.0 equiv), **3a** (20.0 mg, 89.3 μ mol, 1.1 equiv), DMAP (496 μ g, 4.06 μ mol, 0.05 equiv), and Et_3N (22.6 μ L, 162 μ mol, 2.0 equiv) were dissolved in CH_2Cl_2 (400 μ L) and reacted according to GP E. After purification by column chromatography on silica (isohexane/ CH_2Cl_2 6:4), **7ca** (10.0 mg, 35%) was obtained as a brown solid: mp 108–111 $^\circ\text{C}$; ^1H NMR (400 MHz, CDCl_3) δ 8.18 (d, $J = 7.6$ Hz, 2H, Ar), 8.13–7.97 (m, 9H, Ar), 7.55 (t, $J = 7.4$ Hz, 1H, Ar), 7.43 (t, $J = 7.7$ Hz, 2H, Ar), 4.76 (t, $J = 7.0$ Hz, 2H, CH_2), 3.53 (t, $J = 7.0$ Hz, 2H, CH_2) ppm; $^{13}\text{C}\{^1\text{H}\}$ NMR (151 MHz, CDCl_3) δ 166.73, 135.77, 133.08, 131.53, 131.09, 130.41, 129.73, 128.51, 127.81, 127.24, 125.87, 125.61, 125.18, 124.70, 123.71, 65.88, 35.95 ppm; IR (ATR) ν (cm^{-1}) 2921, 1717, 1599, 1451, 1254, 1108, 869, 685 (cm^{-1}); HRMS (EI) m/z $[\text{M}]^+$ calcd for $\text{C}_{25}\text{H}_{18}\text{O}_2$ 350.1307, found 350.1298.

2-(Pyren-2-yl)ethyl 2-Phenylbenzoate 7cf. Compound **2c** (20.0 mg, 81.2 μ mol, 1.0 equiv), **3f** (33.8 mg, 89.3 μ mol, 1.1 equiv), DMAP (496 μ g, 4.06 μ mol, 0.05 equiv), and Et_3N (22.6 μ L, 162 μ mol, 2.0 equiv) were dissolved in CH_2Cl_2 (400 μ L) and reacted according to GP E. After purification by column chromatography on silica (isohexane/ CH_2Cl_2 6:4), **7cf** (14.0 mg, 41%) was obtained as a white solid: mp 137–140 $^\circ\text{C}$; ^1H NMR (400 MHz, CDCl_3) δ 8.17 (d, $J = 7.6$ Hz, 2H, Ar), 8.07 (d, $J = 9.0$ Hz, 2H, Ar), 8.02–7.97 (m, 3H, Ar), 7.90 (s, 2H, Ar), 7.79 (d, $J = 7.9$ Hz, 1H, Ar), 7.52 (td, $J = 7.6$, 1.2 Hz, 1H, Ar), 7.38 (t, $J = 7.7$ Hz, 2H, Ar), 7.34–7.30 (m, 4H, Ar), Ar, 7.29–7.26 (m, 1H, Ar), 4.49 (t, $J = 7.1$ Hz, 2H, CH_2), 3.10 (t, $J = 7.1$ Hz, 2H, CH_2) ppm; $^{13}\text{C}\{^1\text{H}\}$ NMR (101 MHz, CDCl_3) δ 168.93, 142.62, 141.58, 135.60, 131.40, 131.37, 131.16, 131.07, 130.81, 130.00, 128.52, 128.15, 127.71, 127.33, 127.30, 127.23, 125.83, 125.51, 125.13, 124.68, 123.64, 65.93, 35.34 ppm; IR (ATR) ν (cm^{-1}) 2954, 1720, 1476, 1263, 1091, 959, 841, 751, 714; HRMS (EI) m/z $[\text{M}]^+$ calcd for $\text{C}_{31}\text{H}_{22}\text{O}_2$ 426.1620, found 426.1615.

2-(Pyren-2-yl)ethyl 2-(Naphthalene-1-yl)benzoate 7ch. Compound **2c** (20.0 mg, 81.2 μ mol, 1.0 equiv), **3h** (42.7 mg, 89.3 μ mol, 1.1 equiv), DMAP (496 μ g, 4.06 μ mol, 0.05 equiv), and Et_3N (22.6 μ L, 162 μ mol, 2.0 equiv) were dissolved in CH_2Cl_2 (400 μ L) and reacted according to GP E. After purification by column chromatography on silica (isohexane/ CH_2Cl_2 6:4), **7ch** (15.0 mg, 38%) was obtained as a white solid: mp 103–105 $^\circ\text{C}$; ^1H NMR (400 MHz, CDCl_3) δ 8.16 (d, $J = 7.6$ Hz, 2H, Ar), 8.07–7.91 (m, 6H, Ar), 7.90–7.80 (m, 2H, Ar), 7.69 (s, 2H, Ar), 7.61 (td, $J = 7.5$, 1.5 Hz, 1H, Ar), 7.56–7.41 (m, 5H, Ar), 7.41–7.32 (m, 2H, Ar), 4.25–4.07 (m, 2H, CH_2), 2.60 (qt, $J = 14.1$, 7.2 Hz, 2H, CH_2) ppm; $^{13}\text{C}\{^1\text{H}\}$ NMR (101 MHz, CDCl_3) δ 167.98, 141.29, 139.98, 135.47, 133.39, 132.29, 131.95, 131.93, 131.76, 131.30, 131.05, 130.36, 128.32, 127.76, 127.67, 127.64, 127.21, 126.24, 126.16, 125.83, 125.80, 125.75, 125.32, 125.30, 125.10, 124.67, 123.55, 65.60, 34.79 ppm; IR (ATR) ν (cm^{-1}) 2922, 1704, 1599, 1463, 1380, 1286, 1129, 959, 838, 796, 755, 709; HRMS (EI) m/z $[\text{M}]^+$ calcd for $\text{C}_{35}\text{H}_{24}\text{O}_2$ 476.1776, found 476.1769.

2-(Pyren-2-yl)ethyl 2,6-Dimethylbenzoate 7cm. Compound **2c** (15.0 mg, 60.9 μ mol, 1.0 equiv), **3m** (20.6 mg, 73.1 μ mol, 1.2 equiv), DMAP (372 μ g, 3.04 μ mol, 0.05 equiv), and Et_3N (12.7 μ L, 91.4 μ mol, 1.5 equiv) were dissolved in CH_2Cl_2 (300 μ L) and reacted according to GP E. After purification by column chromatography on silica

(isohexane/ CH_2Cl_2 6:4), **7cm** (10.0 mg, 43%) was obtained as a white solid: mp 144–148 $^\circ\text{C}$; ^1H NMR (400 MHz, CDCl_3) δ 8.18 (d, $J = 7.6$ Hz, 2H, Ar), 8.10–7.96 (m, 7H, Ar), 7.19–7.12 (m, 1H, Ar), 6.98 (d, $J = 7.9$ Hz, 2H, Ar), 4.80 (t, $J = 7.1$ Hz, 2H, CH_2), 3.53 (t, $J = 7.1$ Hz, 2H, CH_2), 2.19 (d, $J = 0.7$ Hz, 6H, Me₂) ppm; $^{13}\text{C}\{^1\text{H}\}$ NMR (101 MHz, CDCl_3) δ 170.21, 135.51, 135.04, 133.99, 131.54, 131.11, 129.41, 127.83, 127.66, 127.23, 125.89, 125.54, 125.19, 124.68, 123.73, 65.82, 35.75, 19.75 ppm; IR (ATR) ν (cm^{-1}) 2923, 1714, 1595, 1465, 1274, 1120, 970, 877, 772, 700; HRMS (EI) m/z $[\text{M}]^+$ calcd for $\text{C}_{27}\text{H}_{22}\text{O}_2$ 378.1620, found 378.1620.

2-(Pyren-2-yl)ethyl 2-Methyl-6-phenylbenzoate 7cn. Compound **2c** (15.0 mg, 60.9 μ mol, 1.0 equiv), **3n** (27.2 mg, 67.0 μ mol, 1.1 equiv), DMAP (372 μ g, 3.04 μ mol, 0.05 equiv), and Et_3N (12.7 μ L, 91.4 μ mol, 1.5 equiv) were dissolved in CH_2Cl_2 (300 μ L) and reacted according to GP E. After purification by column chromatography on silica (isohexane/ CH_2Cl_2 6:4), **7cn** (10.0 mg, 38%) was obtained as an oil: ^1H NMR (400 MHz, CDCl_3) δ 8.17 (d, $J = 7.6$ Hz, 2H, Ar), 8.06 (d, $J = 9.0$ Hz, 2H, Ar), 8.01–7.96 (m, 3H, Ar), 7.89 (s, 2H, Ar), 7.38–7.30 (m, 3H, Ar), 7.26–7.17 (m, 5H, Ar), 4.44 (t, $J = 7.2$ Hz, 2H, CH_2), 3.06 (t, $J = 7.2$ Hz, 2H, CH_2), 2.34 (s, 3H, Me) ppm; $^{13}\text{C}\{^1\text{H}\}$ NMR (101 MHz, CDCl_3) δ 169.84, 140.97, 140.26, 135.55, 135.38, 133.17, 131.28, 130.94, 129.39, 129.14, 128.29, 128.20, 127.58, 127.29, 127.23, 127.10, 125.71, 125.33, 125.01, 124.54, 123.51, 65.80, 35.14, 19.69 ppm; IR (ATR) ν (cm^{-1}) 2919, 1715, 1461, 1258, 1121, 1091, 841, 756, 700; HRMS (EI) m/z $[\text{M}]^+$ calcd for $\text{C}_{32}\text{H}_{24}\text{O}_2$ 440.1776, found 440.1772.

2-(Pyren-2-yl)ethyl 2-Methyl-6-nitrobenzoate 7co. Compound **2c** (20.0 mg, 81.2 μ mol, 1.0 equiv), **3o** (30.8 mg, 89.3 μ mol, 1.1 equiv), DMAP (496 μ g, 4.06 μ mol, 0.05 equiv), and Et_3N (22.6 μ L, 162 μ mol, 2.0 equiv) were dissolved in CH_2Cl_2 (400 μ L) and reacted according to GP E. After purification by column chromatography on silica (isohexane/ CH_2Cl_2 6:4), **7co** (17.0 mg, 52%) was obtained as a yellow solid: mp 154–156 $^\circ\text{C}$; ^1H NMR (400 MHz, CDCl_3) δ 8.17 (d, $J = 7.6$ Hz, 2H, Ar), 8.09–7.95 (m, 8H, Ar), 7.47–7.38 (m, 2H, Ar), 4.86 (t, $J = 7.1$ Hz, 2H, CH_2), 3.53 (t, $J = 7.1$ Hz, 2H, CH_2), 2.22 (s, 3H, Me) ppm; $^{13}\text{C}\{^1\text{H}\}$ NMR (101 MHz, CDCl_3) δ 166.60, 137.70, 136.07, 135.27, 131.54, 131.10, 129.81, 129.60, 127.80, 127.24, 125.88, 125.48, 125.17, 124.67, 123.72, 121.91, 66.89, 35.33, 19.09 ppm (one signal is overlapping); IR (ATR) ν (cm^{-1}) 2926, 1730, 1529, 1342, 1267, 1112, 1077, 950, 874, 840, 818, 801, 739, 699; HRMS (EI) m/z $[\text{M}]^+$ calcd for $\text{C}_{26}\text{H}_{19}\text{O}_4\text{N}$ 409.1314, found 409.1305.

2-(Pyren-2-yl)ethyl 2-Methoxy-1-naphthoate 7cr. Compound **2c** (20.0 mg, 81.2 μ mol, 1.0 equiv), **3r** (34.5 mg, 89.3 μ mol, 1.1 equiv), DMAP (496 μ g, 4.06 μ mol, 0.05 equiv), and Et_3N (22.6 μ L, 162 μ mol, 2.0 equiv) were dissolved in CH_2Cl_2 (400 μ L) and reacted according to GP E. After purification by column chromatography on silica (isohexane/ CH_2Cl_2 6:4), **7cr** (20.0 mg, 56%) was obtained as a brown solid: mp 190–193 $^\circ\text{C}$; ^1H NMR (600 MHz, CDCl_3) δ 8.19 (d, $J = 7.6$ Hz, 2H, Ar), 8.13 (s, 2H, Ar), 8.07 (d, $J = 8.9$ Hz, 2H, Ar), 8.03–7.98 (m, 3H, Ar), 7.87 (d, $J = 9.1$ Hz, 1H, Ar), 7.74 (d, $J = 8.2$ Hz, 1H, Ar), 7.45 (d, $J = 8.5$ Hz, 1H, Ar), 7.24 (d, $J = 9.2$ Hz, 2H, Ar), 7.12–7.06 (m, 1H, Ar), 4.94 (t, $J = 6.9$ Hz, 2H, CH_2), 3.81 (s, 3H, Me), 3.58 (t, $J = 6.9$ Hz, 2H, CH_2) ppm; $^{13}\text{C}\{^1\text{H}\}$ NMR (151 MHz, CDCl_3) δ 168.21, 154.58, 135.83, 131.76, 131.52, 131.13, 131.03, 128.60, 128.08, 127.73, 127.65, 127.36, 125.86, 125.76, 125.15, 124.72, 124.17, 123.84, 123.73, 113.18, 66.30, 56.81, 35.85 ppm (one signal is overlapping); IR (ATR) ν (cm^{-1}) 2926, 1715, 1594, 1512, 1433, 1339, 1231, 1141, 1073, 1029, 884, 811, 744, 700; HRMS (EI) m/z $[\text{M}]^+$ calcd for $\text{C}_{30}\text{H}_{22}\text{O}_3$ 430.1569, found 430.1564.

2-(Pyren-2-yl)ethyl 2-Ethoxy-1-naphthoate 7cs. Compound **2c** (20.0 mg, 81.2 μ mol, 1.0 equiv), **3s** (27.0 mg, 89.3 μ mol, 1.1 equiv), DMAP (496 μ g, 4.06 μ mol, 0.05 equiv), and Et_3N (22.6 μ L, 162 μ mol, 2.0 equiv) were dissolved in CH_2Cl_2 (400 μ L) and reacted according to GP E. After purification by column chromatography on silica (isohexane/ CH_2Cl_2 6:4), **7cs** (10.0 mg, 28%) was obtained as a yellow solid: mp 131–134 $^\circ\text{C}$; ^1H NMR (400 MHz, CDCl_3) δ 8.19 (d, $J = 7.6$ Hz, 2H, Ar), 8.13 (s, 2H, Ar), 8.10–7.97 (m, 5H, Ar), 7.85 (d, $J = 8.8$ Hz, 1H, Ar), 7.74 (dd, $J = 8.3$, 1.2 Hz, 1H, Ar), 7.48 (d, $J = 8.5$ Hz, 1H, Ar), 7.29–7.22 (m, 2H, Ar), 7.13 (ddd, $J = 8.3$, 6.8, 1.3 Hz, 1H, Ar), 4.92 (t, $J = 7.1$ Hz, 2H, CH_2), 4.14 (q, $J = 7.0$ Hz, 2H, CH_2), 3.58 (t, $J =$

7.0 Hz, 2H, CH₂), 1.29 (t, *J* = 7.0 Hz, 3H, Me) ppm; ¹³C{¹H} NMR (101 MHz, CDCl₃) δ 168.43, 154.11, 135.91, 131.74, 131.68, 131.27, 131.20, 128.80, 128.21, 127.88, 127.72, 127.48, 126.01, 125.88, 125.30, 124.85, 124.34, 124.02, 123.89, 118.51, 114.76, 66.38, 65.70, 36.06, 15.18 ppm; IR (ATR) ν (cm⁻¹) 2894, 1724, 1592, 1504, 1464, 1434, 1286, 1220, 1137, 1109, 1060, 963, 861, 806, 749, 705; HRMS (EI) *m/z* [M]⁺ calcd for C₃₁H₂₄O₃ 444.1725, found 444.1710.

2-(Pyren-2-yl)ethyl 2-Butoxy-1-naphthoate 7ct. Compound **2c** (10.0 mg, 40.6 μmol, 1.0 equiv), **3t** (21.0 mg, 44.7 μmol, 1.1 equiv), DMAP (248 μg, 2.03 μmol, 0.05 equiv), and Et₃N (11.3 μL, 81.2 μmol, 2.0 equiv) were dissolved in CH₂Cl₂ (200 μL) and reacted according to GP E. After purification by column chromatography on silica (isohexane/CH₂Cl₂ 6:4), **7ct** (18.0 mg, 95%) was obtained as a yellow solid: mp 76–78 °C; ¹H NMR (400 MHz, CDCl₃) δ 8.18 (d, *J* = 7.6 Hz, 2H, Ar), 8.12 (s, 2H, Ar), 8.07 (d, *J* = 8.9 Hz, 2H, Ar), 8.04–7.97 (m, 3H, Ar), 7.85 (d, *J* = 9.0 Hz, 1H, Ar), 7.74 (d, *J* = 8.2 Hz, 1H, Ar), 7.49 (d, *J* = 8.5 Hz, 1H, Ar), 7.30–7.22 (m, 2H, Ar), 7.15 (ddd, *J* = 8.3, 6.8, 1.3 Hz, 1H, Ar), 4.91 (t, *J* = 7.1 Hz, 2H, CH₂), 4.07 (t, *J* = 6.5 Hz, 2H, CH₂), 3.58 (t, *J* = 7.1 Hz, 2H, CH₂), 1.68–1.58 (m, 2H, CH₂), 1.44–1.33 (m, 2H, CH₂), 0.87 (t, *J* = 7.4 Hz, 3H, Me) ppm; ¹³C{¹H} NMR (101 MHz, CDCl₃) δ 168.27, 154.15, 135.76, 131.55, 131.14, 131.09, 128.62, 128.07, 127.74, 127.57, 127.34, 125.86, 125.73, 125.15, 124.73, 124.14, 123.85, 123.76, 118.22, 114.52, 69.60, 66.22, 35.94, 31.50, 19.19, 13.89 ppm (one signal is overlapping); IR (ATR) ν (cm⁻¹) 2927, 1721, 1594, 1510, 1462, 1341, 1281, 1210, 1133, 1070, 807, 745, 700; HRMS (EI) *m/z* [M]⁺ calcd for C₃₃H₂₈O₃ 472.2038, found 472.2037.

2-(Pyren-2-yl)ethyl 2-(Hexanoyloxy)-1-naphthoate 7cu. Compound **2c** (10.0 mg, 40.6 μmol, 1.0 equiv), **3u** (23.5 mg, 44.7 μmol, 1.1 equiv), DMAP (248 μg, 2.03 μmol, 0.05 equiv), and Et₃N (11.3 μL, 81.2 μmol, 2.0 equiv) were dissolved in CH₂Cl₂ (200 μL) and reacted according to GP E. After purification by column chromatography on silica (isohexane/CH₂Cl₂ 6:4), **7cu** (10.0 mg, 50%) was obtained as a white solid: mp 97–100 °C; ¹H NMR (600 MHz, CDCl₃) δ 8.18 (d, *J* = 7.6 Hz, 2H, Ar), 8.12 (s, 2H, Ar), 8.07 (d, *J* = 8.9 Hz, 2H, Ar), 8.03–7.98 (m, 3H, Ar), 7.85 (d, *J* = 9.0 Hz, 1H, Ar), 7.74 (d, *J* = 8.2 Hz, 1H, Ar), 7.50 (d, *J* = 8.5 Hz, 1H, Ar), 7.27 (t, *J* = 7.8 Hz, 1H, Ar), 7.24 (d, *J* = 9.1 Hz, 1H, Ar), 7.15 (t, *J* = 7.7 Hz, 1H, Ar), 4.91 (t, *J* = 7.1 Hz, 2H, CH₂), 4.05 (t, *J* = 6.6 Hz, 2H, CH₂), 3.58 (t, *J* = 7.1 Hz, 2H, CH₂), 1.66–1.59 (m, 2H, CH₂), 1.32 (p, *J* = 7.5 Hz, 2H, CH₂), 1.27–1.15 (m, 4H, CH₂), 0.84 (t, *J* = 7.1 Hz, 3H, Me) ppm; ¹³C{¹H} NMR (151 MHz, CDCl₃) δ 168.27, 154.16, 135.77, 131.55, 131.55, 131.14, 131.09, 128.61, 128.07, 127.73, 127.57, 127.34, 125.86, 125.73, 125.15, 124.73, 124.13, 123.85, 123.76, 118.20, 114.53, 69.92, 66.21, 35.93, 31.61, 29.42, 25.64, 22.72, 14.15 ppm; IR (ATR) ν (cm⁻¹) 2922, 1712, 1593, 1511, 1466, 1435, 1338, 1279, 1226, 1136, 1063, 1033, 881, 841, 814, 737, 700; HRMS (EI) *m/z* [M]⁺ calcd for C₃₅H₃₂O₃ 500.2351, found 500.2339.

2-(Pyren-2-yl)ethyl 2-Isopropoxy-1-naphthoate 7cv. Compound **2c** (10.0 mg, 40.6 μmol, 1.0 equiv), **3v** (23.5 mg, 44.7 μmol, 1.1 equiv), DMAP (248 μg, 2.03 μmol, 0.05 equiv), and Et₃N (11.3 μL, 81.2 μmol, 2.0 equiv) were dissolved in CH₂Cl₂ (200 μL) and reacted according to GP E. After purification by column chromatography on silica (isohexane/CH₂Cl₂ 6:4), **7cv** (10.0 mg, 50%) was obtained as a brown solid: mp 95–97 °C; ¹H NMR (400 MHz, CDCl₃) δ 8.19 (d, *J* = 7.6 Hz, 2H, Ar), 8.13 (s, 2H, Ar), 8.10–7.97 (m, 5H, Ar), 7.84 (d, *J* = 9.0 Hz, 1H, Ar), 7.74 (d, *J* = 8.2 Hz, 1H, Ar), 7.47 (d, *J* = 8.4 Hz, 1H, Ar), 7.32–7.21 (m, 2H, Ar), 7.15 (t, *J* = 8.3 Hz, 1H, Ar), 4.91 (t, *J* = 7.1 Hz, 2H, CH₂), 4.65 (hept, *J* = 5.8 Hz, 1H, CH), 3.58 (t, *J* = 7.1 Hz, 2H, CH₂), 1.27 (d, *J* = 6.1 Hz, 6H, Me₂) ppm; ¹³C{¹H} NMR (101 MHz, CDCl₃) δ 168.36, 153.09, 135.74, 131.56, 131.34, 131.13, 128.77, 128.04, 127.73, 127.49, 127.34, 125.85, 125.71, 125.15, 124.71, 124.31, 123.91, 123.76, 119.88, 116.39, 72.66, 66.18, 35.97, 22.45 ppm (one signal is overlapping); IR (ATR) ν (cm⁻¹) 2916, 1731, 1592, 1504, 1465, 1371, 1280, 1221, 1105, 1024, 842, 750, 700; HRMS (EI) *m/z* [M]⁺ calcd for C₃₂H₂₆O₃ 458.1882, found 458.1875.

2-(Pyren-2-yl)ethyl 2-Methyl-1-naphthoate 7cw. Compound **2d** (15.0 mg, 60.9 μmol, 1.0 equiv), **3w** (25.8 mg, 67.0 μmol, 1.1 equiv), DMAP (372 μg, 3.04 μmol, 0.05 equiv), and Et₃N (12.7 μL, 91.4 μmol, 1.5 equiv) were dissolved in CH₂Cl₂ (300 μL) and reacted according to GP E. After purification by column chromatography on silica

(isohexane/CH₂Cl₂ 6:4), **7dw** (10.0 mg, 59%) was obtained as a white solid: mp 160–163 °C; ¹H NMR (400 MHz, CDCl₃) δ 8.20 (d, *J* = 7.6 Hz, 2H, Ar), 8.13–8.07 (m, 4H, Ar), 8.05–7.98 (m, 3H, Ar), 7.77 (d, *J* = 8.3 Hz, 2H, Ar), 7.56 (d, *J* = 8.5 Hz, 1H, Ar), 7.35 (d, *J* = 16.0 Hz, 1H, Ar), 7.27 (d, *J* = 6.6 Hz, 1H, Ar), 7.15 (ddd, *J* = 8.3, 6.9, 1.2 Hz, 1H, Ar), 4.96 (t, *J* = 6.9 Hz, 2H, CH₂), 3.59 (t, *J* = 6.9 Hz, 2H, CH₂), 2.37 (s, 3H, Me) ppm; ¹³C{¹H} NMR (101 MHz, CDCl₃) δ 169.88, 135.57, 133.52, 131.69, 131.55, 131.11, 130.17, 130.08, 129.75, 128.43, 128.04, 127.79, 127.28, 127.05, 125.89, 125.63, 125.51, 125.18, 124.67, 124.56, 123.75, 66.21, 35.82, 20.16 ppm; IR (ATR) ν (cm⁻¹) 3034, 1709, 1599, 1386, 1284, 1214, 1138, 1048, 946, 877, 841, 747, 710; HRMS (EI) *m/z* [M]⁺ calcd for C₃₀H₂₂O₂ 414.1620, found 414.1619.

1-(Pyren-1-yl)ethyl Benzoate 6da. Compound **1d** (20.0 mg, 81.2 μmol, 1.0 equiv), **3a** (20.0 mg, 89.3 μmol, 1.1 equiv), DMAP (496 μg, 4.06 μmol, 0.05 equiv), and Et₃N (22.6 μL, 162 μmol, 2.0 equiv) were dissolved in CH₂Cl₂ (400 μL) and reacted according to GP E. After purification by column chromatography on silica (isohexane/CH₂Cl₂ 6:4), **6da** (25.0 mg, 89%) was obtained as a white solid: mp 105–108 °C; ¹H NMR (400 MHz, CDCl₃) δ 8.48 (d, *J* = 9.3 Hz, 1H, Ar), 8.28–8.13 (m, 7H, Ar), 8.07 (d, *J* = 1.3 Hz, 2H, Ar), 8.02 (t, *J* = 7.6 Hz, 1H, Ar), 7.57 (t, *J* = 8.1 Hz, 1H, Ar), 7.46 (t, *J* = 7.6 Hz, 2H, Ar), 7.20 (q, *J* = 6.6 Hz, 1H, CH), 1.97 (d, *J* = 6.6 Hz, 3H, Me) ppm; ¹³C{¹H} NMR (101 MHz, CDCl₃) δ 166.10, 135.29, 133.15, 131.45, 131.14, 130.77, 129.86, 128.54, 128.17, 127.74, 127.65, 127.51, 126.15, 125.53, 125.35, 125.20, 125.05, 124.99, 123.56, 122.64, 70.66, 22.75 ppm (one signal is overlapping); IR (ATR) ν (cm⁻¹) 2920, 1709, 1597, 1449, 1270, 1109, 1068, 1023, 840, 760, 704, 681; HRMS (EI) *m/z* [M]⁺ calcd for C₂₅H₁₈O₂ 350.1307, found 350.1296.

1-(Pyren-1-yl)ethyl 2-Phenylbenzoate 6df. Compound **1d** (20.0 mg, 81.2 μmol, 1.0 equiv), **3f** (33.8 mg, 89.3 μmol, 1.1 equiv), DMAP (496 μg, 4.06 μmol, 0.05 equiv), and Et₃N (22.6 μL, 162 μmol, 2.0 equiv) were dissolved in CH₂Cl₂ (400 μL) and reacted according to GP E. After purification by column chromatography on silica (isohexane/CH₂Cl₂ 6:4), **6df** (34.0 mg, 98%) was obtained as a yellow solid: mp 58–62 °C; ¹H NMR (400 MHz, CDCl₃) δ 8.25 (d, *J* = 9.3 Hz, 1H, Ar), 8.19 (d, *J* = 7.6 Hz, 2H, Ar), 8.12–7.98 (m, 5H, Ar), 7.89 (dd, *J* = 7.7, 1.1 Hz, 1H, Ar), 7.70 (d, *J* = 8.0 Hz, 1H, Ar), 7.53 (td, *J* = 7.5, 1.3 Hz, 1H, Ar), 7.45–7.34 (m, 4H, Ar), 7.31–7.26 (m, 2H, Ar), 7.24–7.18 (m, 1H, Ar), 6.98 (q, *J* = 6.6 Hz, 1H, CH), 1.60 (d, *J* = 6.6 Hz, 3H, Me) ppm; ¹³C{¹H} NMR (101 MHz, CDCl₃) δ 168.33, 142.64, 141.60, 134.84, 131.40, 131.37, 131.36, 130.93, 130.73, 130.20, 128.70, 128.17, 127.95, 127.53, 127.47, 127.33, 127.31, 126.07, 125.44, 125.26, 125.07, 124.94, 124.89, 123.78, 122.67, 70.82, 22.28 ppm (two signals are overlapping); IR (ATR) ν (cm⁻¹) 2920, 1705, 1596, 1449, 1276, 1239, 1122, 1068, 1041, 842, 744, 700, 681; HRMS (EI) *m/z* [M]⁺ calcd for C₃₁H₂₂O₂ 426.1620, found 426.1614.

1-(Pyren-1-yl)ethyl 2-(Naphthalene-1-yl)benzoate 6dh. Compound **1d** (20.0 mg, 81.2 μmol, 1.0 equiv), **3h** (42.7 mg, 89.3 μmol, 1.1 equiv), DMAP (496 μg, 4.06 μmol, 0.05 equiv), and Et₃N (22.6 μL, 162 μmol, 2.0 equiv) were dissolved in CH₂Cl₂ (400 μL) and reacted according to GP E. After purification by column chromatography on silica (isohexane/CH₂Cl₂ 6:4), **6dh** (15.0 mg, 38%) was obtained as a yellow solid (diastomeric mixture of 1:1): mp 139–140 °C; ¹H NMR (400 MHz, CDCl₃) δ 8.15 (m, 2.5H, Ar), 8.09–7.92 (m, 6H, Ar), 7.80 (d, *J* = 8.0 Hz, 1H, Ar), 7.77–7.69 (m, 1.5H, Ar), 7.65–7.57 (m, 2H, Ar), 7.56–7.48 (m, 1H, Ar), 7.48–7.34 (m, 5H, Ar), 7.24 (d, *J* = 8.0 Hz, 0.5H, Ar), 7.03 (d, *J* = 8.0 Hz, 0.5H, Ar), 6.74 (dq, *J* = 13.1, 6.6 Hz, 1H, CH), 1.18 (d, *J* = 6.6 Hz, 1.5H, Me), 0.93 (d, *J* = 6.6 Hz, 1.5H, Me) ppm; ¹³C{¹H} NMR (101 MHz, CDCl₃) δ 167.53, 167.46, 141.19, 141.13, 140.26, 139.94, 134.63, 134.56, 133.43, 133.42, 132.52, 132.42, 132.20, 132.06, 132.02, 131.96, 131.91, 131.50, 131.36, 131.35, 130.80, 130.75, 130.74, 130.70, 130.69, 130.64, 128.28, 128.24, 127.80, 127.79, 127.78, 127.74, 127.65, 127.62, 127.44, 127.42, 127.41, 127.24, 127.23, 126.31, 126.25, 126.16, 126.16, 126.16, 125.98, 125.96, 125.84, 125.82, 125.72, 125.34, 125.31, 125.19, 125.17, 125.16, 125.14, 124.92, 124.91, 124.90, 124.90, 124.74, 124.71, 123.69, 123.48, 122.50, 122.41, 77.48, 70.24, 70.08, 21.85, 21.27 ppm; IR (ATR) ν (cm⁻¹) 3041, 1703, 1593, 1444, 1393, 1280, 1242, 1116, 1068, 1040, 905, 842, 800, 777, 759, 700; HRMS (EI) *m/z* [M]⁺ calcd for C₃₅H₂₄O₂ 476.1776, found 476.1769.

1-(Pyren-1-yl)ethyl 2,6-Dimethylbenzoate 6dm. Compound **1d** (15.0 mg, 60.9 μmol , 1.0 equiv), **3m** (20.6 mg, 73.1 μmol , 1.2 equiv), DMAP (372 μg , 3.04 μmol , 0.05 equiv), and Et_3N (12.7 μL , 91.4 μmol , 1.5 equiv) were dissolved in CH_2Cl_2 (300 μL) and reacted according to GP E. After purification by column chromatography on silica (isohexane/ CH_2Cl_2 6:4), **6dm** (10.0 mg, 43%) was obtained as a white solid: mp 104–105 °C; $^1\text{H NMR}$ (400 MHz, CDCl_3) δ 8.48 (d, J = 9.3 Hz, 1H, Ar), 8.25–8.16 (m, 5H, Ar), 8.12–8.00 (m, 3H, Ar), 7.30 (q, J = 6.6 Hz, 1H, CH), 7.19 (t, J = 7.6 Hz, 1H, Ar), 7.02 (d, J = 7.6 Hz, 2H, Ar), 2.27 (s, 6H, Me₂), 1.96 (d, J = 6.6 Hz, 3H, Me) ppm; $^{13}\text{C}\{^1\text{H}\}$ NMR (101 MHz, CDCl_3) δ 169.55, 135.01, 134.67, 134.18, 131.46, 131.22, 130.80, 129.40, 128.18, 127.81, 127.72, 127.69, 127.51, 126.17, 125.58, 125.40, 125.12, 125.04, 125.00, 123.91, 122.67, 70.31, 22.56, 19.83 ppm; IR (ATR) ν (cm^{-1}) 2923, 1714, 1595, 1463, 1264, 1244, 1110, 1067, 830, 773, 716; HRMS (EI) m/z [M]⁺ calcd for $\text{C}_{27}\text{H}_{22}\text{O}_2$ 378.1620, found 378.1623.

1-(Pyren-1-yl)ethyl 2-Methyl-6-phenylbenzoate 6dn. Compound **1d** (15.0 mg, 60.9 μmol , 1.0 equiv), **3n** (27.2 mg, 67.0 μmol , 1.1 equiv), DMAP (372 μg , 3.04 μmol , 0.05 equiv), and Et_3N (12.7 μL , 91.4 μmol , 1.5 equiv) were dissolved in CH_2Cl_2 (300 μL) and reacted according to GP E. After purification by column chromatography on silica (isohexane/ CH_2Cl_2 6:4), **6dn** (10.0 mg, 38%) was obtained as an oil: $^1\text{H NMR}$ (400 MHz, CDCl_3) δ 8.29 (d, J = 9.3 Hz, 1H, Ar), 8.19 (d, J = 7.7 Hz, 2H, Ar), 8.13–7.99 (m, 5H, Ar), 7.86 (d, J = 8.0 Hz, 1H, Ar), 7.39–7.32 (m, 3H, Ar), 7.24–7.18 (m, 2H, Ar), 7.19–7.12 (m, 2H, Ar), 7.11–7.04 (m, 1H, Ar), 6.95 (q, J = 6.6 Hz, 1H, CH), 2.34 (s, 3H, Me), 1.50 (d, J = 6.6 Hz, 3H, Me) ppm; $^{13}\text{C}\{^1\text{H}\}$ NMR (101 MHz, CDCl_3) δ 169.20, 140.91, 140.41, 135.69, 134.71, 133.50, 131.43, 131.00, 130.78, 129.46, 129.26, 128.61, 128.24, 127.93, 127.58, 127.50, 127.43, 127.34, 126.09, 125.45, 125.28, 125.08, 124.97, 124.97, 123.82, 122.78, 70.63, 22.06, 19.92 ppm (one signal is overlapping); IR (ATR) ν (cm^{-1}) 2926, 1715, 1588, 1461, 1235, 1119, 1089, 1063, 1040, 842, 756, 719, 700; HRMS (EI) m/z [M]⁺ calcd for $\text{C}_{32}\text{H}_{24}\text{O}_2$ 440.1776, found 440.1772.

1-(Pyren-1-yl)ethyl 2-Methyl-6-nitrobenzoate 6do. Compound **1d** (20.0 mg, 81.2 μmol , 1.0 equiv), **3o** (30.8 mg, 89.3 μmol , 1.1 equiv), DMAP (496 μg , 4.06 μmol , 0.05 equiv), and Et_3N (22.6 μL , 162 μmol , 2.0 equiv) were dissolved in CH_2Cl_2 (400 μL) and reacted according to GP E. After purification by column chromatography on silica (isohexane/ CH_2Cl_2 6:4), **6do** (17.0 mg, 52%) was obtained as a brown solid: mp 127–129 °C; $^1\text{H NMR}$ (600 MHz, CDCl_3) δ 8.50 (d, J = 9.3 Hz, 1H, Ar), 8.24–8.14 (m, 5H, Ar), 8.08 (q, J = 8.9 Hz, 2H, Ar), 8.05–8.01 (m, 2H, Ar), 7.50–7.42 (m, 2H, Ar), 7.33 (q, J = 6.6 Hz, 1H, CH), 2.25 (s, 3H, Me), 1.99 (d, J = 6.6 Hz, 3H, Me) ppm; $^{13}\text{C}\{^1\text{H}\}$ NMR (151 MHz, CDCl_3) δ 165.98, 137.88, 136.15, 134.06, 131.48, 131.40, 130.82, 129.80, 129.76, 128.29, 127.96, 127.85, 127.51, 126.22, 125.64, 125.48, 125.13, 125.08, 125.01, 123.99, 122.65, 121.97, 71.85, 21.87, 19.28 ppm (one signal is overlapping); IR (ATR) ν (cm^{-1}) 2984, 1727, 1537, 1442, 1340, 1271, 1110, 1065, 1040, 850, 805, 741, 714; HRMS (EI) m/z [M]⁺ calcd for $\text{C}_{26}\text{H}_{19}\text{O}_4\text{N}$ 409.1314, found 409.1311.

1-(Pyren-1-yl)ethyl 2-Methoxy-1-naphthoate 6dr. Compound **1d** (20.0 mg, 81.2 μmol , 1.0 equiv), **3r** (34.5 mg, 89.3 μmol , 1.1 equiv), DMAP (496 μg , 4.06 μmol , 0.05 equiv), and Et_3N (22.6 μL , 162 μmol , 2.0 equiv) were dissolved in CH_2Cl_2 (400 μL) and reacted according to GP E. After purification by column chromatography on silica (isohexane/ CH_2Cl_2 6:4), **6dr** (20.0 mg, 58%) was obtained as a yellow solid: mp 163–165 °C; $^1\text{H NMR}$ (400 MHz, CDCl_3) δ 8.55 (d, J = 9.3 Hz, 1H, Ar), 8.30–8.18 (m, 5H, Ar), 8.11–8.00 (m, 3H, Ar), 7.89 (d, J = 9.1 Hz, 1H, Ar), 7.78 (d, J = 8.7 Hz, 1H, Ar), 7.74 (d, J = 8.0 Hz, 1H, Ar), 7.44–7.31 (m, 3H, Ar and CH), 7.28 (d, J = 9.1 Hz, 1H, Ar), 3.92–3.87 (m, 3H, Me), 2.03 (d, J = 6.6 Hz, 3H, Me) ppm; $^{13}\text{C}\{^1\text{H}\}$ NMR (101 MHz, CDCl_3) δ 167.69, 154.66, 135.02, 131.70, 131.47, 131.19, 131.16, 130.83, 128.68, 128.18, 128.02, 127.90, 127.69, 127.63, 127.54, 126.12, 125.49, 125.34, 125.07, 125.01, 124.22, 124.01, 123.92, 122.96, 117.94, 113.37, 70.91, 56.81, 22.61 ppm (one signal is overlapping); IR (ATR) ν (cm^{-1}) 2840, 1714, 1595, 1510, 1434, 1343, 1280, 1225, 1136, 1069, 1017, 907, 830, 808, 719; HRMS (EI) m/z [M]⁺ calcd for $\text{C}_{30}\text{H}_{22}\text{O}_3$ 430.1569, found 430.1557.

1-(Pyren-1-yl)ethyl 2-Ethoxy-1-naphthoate 6ds. Compound **1d** (20.0 mg, 81.2 μmol , 1.0 equiv), **3s** (37.0 mg, 89.3 μmol , 1.1 equiv), DMAP (496 μg , 4.06 μmol , 0.05 equiv), and Et_3N (22.6 μL , 162 μmol , 2.0 equiv) were dissolved in CH_2Cl_2 (400 μL) and reacted according to GP E. After purification by column chromatography on silica (isohexane/ CH_2Cl_2 6:4), **6ds** (14.0 mg, 39%) was obtained as a brown solid: mp 136–137 °C; $^1\text{H NMR}$ (400 MHz, CDCl_3) δ 8.54 (d, J = 9.3 Hz, 1H, Ar), 8.28 (d, J = 8.1 Hz, 1H, Ar), 8.24–8.17 (m, 4H, Ar), 8.07 (d, J = 2.3 Hz, 2H, Ar), 8.03 (t, J = 7.6 Hz, 1H, Ar), 7.88 (d, J = 9.1 Hz, 1H, Ar), 7.78 (d, J = 8.1 Hz, 1H, Ar), 7.72 (d, J = 8.4 Hz, 1H, Ar), 7.44–7.36 (m, 2H, Ar and CH), 7.33 (ddd, J = 8.0, 6.8, 1.3 Hz, 1H, Ar), 7.28 (s, 1H, Ar), 4.19 (qd, J = 7.0, 1.5 Hz, 2H, CH_2), 2.01 (d, J = 6.6 Hz, 3H, Me), 1.29 (t, J = 7.0 Hz, 3H, Me); $^{13}\text{C}\{^1\text{H}\}$ NMR (101 MHz, CDCl_3) δ 167.76, 154.02, 135.13, 131.56, 131.48, 131.22, 131.15, 130.85, 128.68, 128.15, 128.09, 127.83, 127.63, 127.60, 127.55, 126.12, 125.49, 125.34, 125.11, 125.05, 125.03, 124.19, 123.95, 123.90, 122.87, 118.36, 114.50, 70.75, 65.41, 22.72, 15.05 ppm; IR (ATR) ν (cm^{-1}) 2924, 1716, 1594, 1511, 1434, 1340, 1279, 1213, 1136, 1064, 1024, 850, 807, 745, 719, 981; HRMS (EI) m/z [M]⁺ calcd for $\text{C}_{31}\text{H}_{24}\text{O}_3$ 444.1725, found 444.1726.

1-(Pyren-1-yl)ethyl 2-Butoxy-1-naphthoate 6dt. Compound **1d** (10.0 mg, 40.6 μmol , 1.0 equiv), **3t** (21.0 mg, 44.7 μmol , 1.1 equiv), DMAP (248 μg , 2.03 μmol , 0.05 equiv), and Et_3N (11.3 μL , 81.2 μmol , 2.0 equiv) were dissolved in CH_2Cl_2 (200 μL) and reacted according to GP E. After purification by column chromatography on silica (isohexane/ CH_2Cl_2 6:4), **6dt** (10.0 mg, 53%) was obtained as a white solid: mp 120–123 °C; $^1\text{H NMR}$ (400 MHz, CDCl_3) δ 8.55 (d, J = 9.3 Hz, 1H, Ar), 8.29–8.17 (m, 5H, Ar), 8.11–8.00 (m, 3H, Ar), 7.87 (d, J = 9.0 Hz, 1H, Ar), 7.80–7.75 (m, 1H, Ar), 7.71 (ddt, J = 8.4, 1.3, 0.8 Hz, 1H, Ar), 7.44–7.30 (m, 3H, Ar and CH), 7.26 (d, J = 9.1 Hz, 1H, Ar), 4.08 (td, J = 6.6, 3.8 Hz, 2H, CH_2), 2.02 (d, J = 6.6 Hz, 3H, Me), 1.64–1.55 (m, 2H, CH_2), 1.34–1.23 (m, 2H, CH_2), 0.73 (t, J = 7.4 Hz, 3H, Me) ppm; $^{13}\text{C}\{^1\text{H}\}$ NMR (101 MHz, CDCl_3) δ 167.76, 154.15, 135.12, 131.51, 131.49, 131.24, 131.16, 130.85, 128.61, 128.15, 128.08, 127.85, 127.61, 127.54, 126.12, 125.48, 125.33, 125.12, 125.06, 125.05, 124.12, 124.00, 123.90, 122.90, 118.19, 114.39, 70.76, 69.46, 31.48, 22.73, 19.13, 13.77 ppm (one signal is overlapping); IR (ATR) ν (cm^{-1}) 2955, 1700, 1594, 1512, 1434, 1379, 1341, 1279, 1248, 1225, 1153, 1068, 1026, 1003, 840, 803, 740, 722, 682; HRMS (EI) m/z [M]⁺ calcd for $\text{C}_{33}\text{H}_{28}\text{O}_3$ 472.2038, found 472.2032.

1-(Pyren-1-yl)ethyl 2-(Hexanoyloxy)-1-naphthoate 6du. Compound **1d** (10.0 mg, 40.6 μmol , 1.0 equiv), **3u** (23.5 mg, 44.7 μmol , 1.1 equiv), DMAP (248 μg , 2.03 μmol , 0.05 equiv), and Et_3N (11.3 μL , 81.2 μmol , 2.0 equiv) were dissolved in CH_2Cl_2 (200 μL) and reacted according to GP E. After purification by column chromatography on silica (isohexane/ CH_2Cl_2 6:4), **6du** (10.0 mg, 50%) was obtained as a white solid: mp 92–95 °C; $^1\text{H NMR}$ (400 MHz, CDCl_3) δ 8.55 (d, J = 9.3 Hz, 1H, Ar), 8.29–8.16 (m, 5H, Ar), 8.11–8.00 (m, 3H, Ar), 7.87 (d, J = 9.0 Hz, 1H, Ar), 7.77 (d, J = 7.5 Hz, 1H, Ar), 7.72 (d, J = 8.4 Hz, 1H, Ar), 7.44–7.36 (m, 2H, Ar and CH), 7.33 (ddd, J = 8.0, 6.9, 1.3 Hz, 1H, Ar), 7.27–7.24 (m, 1H, Ar), 4.06 (td, J = 6.7, 2.7 Hz, 2H, CH_2), 2.01 (d, J = 6.6 Hz, 3H, Me), 1.60–1.50 (m, 2H, CH_2), 1.25–1.17 (m, 2H, CH_2), 1.16–0.99 (m, 4H, 2 \times CH_2), 0.75 (t, J = 7.0 Hz, 3H, Me) ppm; $^{13}\text{C}\{^1\text{H}\}$ NMR (101 MHz, CDCl_3) δ 167.75, 154.19, 135.13, 131.52, 131.51, 131.26, 131.18, 130.87, 128.65, 128.16, 128.08, 127.88, 127.62, 127.62, 127.55, 126.12, 125.49, 125.34, 125.12, 125.08, 125.08, 124.14, 124.04, 123.93, 122.93, 118.27, 114.49, 70.75, 69.87, 31.56, 29.42, 25.61, 22.75, 22.60, 14.07 ppm; IR (ATR) ν (cm^{-1}) 2950, 1701, 1595, 1512, 1463, 1433, 1340, 1278, 1249, 1215, 1152, 1123, 1044, 1004, 830, 805, 739, 720; HRMS (EI) m/z [M]⁺ calcd for $\text{C}_{35}\text{H}_{32}\text{O}_3$ 500.2351, found 500.2351.

1-(Pyren-1-yl)ethyl 2-Isopropoxy-1-naphthoate 6dv. Compound **1d** (15.0 mg, 60.9 μmol , 1.0 equiv), **3v** (29.6 mg, 67.0 μmol , 1.1 equiv), DMAP (372 μg , 3.04 μmol , 0.05 equiv), and Et_3N (12.7 μL , 91.4 μmol , 1.5 equiv) were dissolved in CH_2Cl_2 (300 μL) and reacted according to GP E. After purification by column chromatography on silica (isohexane/ CH_2Cl_2 6:4), **6dv** (10.0 mg, 55%) was obtained as a white solid: mp 147–150 °C; $^1\text{H NMR}$ (400 MHz, CDCl_3) δ 8.54 (d, J = 9.3 Hz, 1H, Ar), 8.29–8.16 (m, 5H, Ar), 8.11–7.99 (m, 3H, Ar), 7.86 (d, J = 9.1 Hz, 1H, Ar), 7.77 (dd, J = 7.4, 1.2 Hz, 1H, Ar), 7.71–7.65 (m,

1H, Ar), 7.44–7.30 (m, 3H, Ar and CH), 7.28 (d, $J = 9.2$ Hz, 1H, Ar), 4.70 (hept, $J = 6.0$ Hz, 1H, CH), 2.01 (d, $J = 6.6$ Hz, 3H, Me), 1.26 (t, $J = 6.3$ Hz, 6H, Me₂) ppm; ¹³C{¹H} NMR (101 MHz, CDCl₃) δ 167.84, 153.03, 135.22, 131.49, 131.32, 131.31, 131.12, 130.86, 128.73, 128.11, 127.76, 127.58, 127.56, 127.55, 126.12, 125.49, 125.34, 125.13, 125.05, 125.04, 124.27, 123.95, 122.87, 119.71, 116.02, 72.18, 70.68, 22.87, 22.41 ppm (two signals are overlapping); IR (ATR) ν (cm⁻¹) 2924, 1715, 1593, 1509, 1466, 1434, 1372, 1279, 1225, 1107, 1038, 995, 906, 850, 807, 720; HRMS (EI) m/z [M]⁺ calcd for C₃₂H₂₆O₃ 458.1882, found 458.1881.

1-(Pyren-1-yl)ethyl 2-Methyl-1-naphthoate 6dw. Compound **1d** (15.0 mg, 60.9 μ mol, 1.0 equiv), **3w** (25.8 mg, 67.0 μ mol, 1.1 equiv), DMAP (372 μ g, 3.04 μ mol, 0.05 equiv), and Et₃N (12.7 μ L, 91.4 μ mol, 1.5 equiv) were dissolved in CH₂Cl₂ (300 μ L) and reacted according to GP E. After purification by column chromatography on silica (isohexane/CH₂Cl₂ 6:4), **6dw** (10.0 mg, 59%) was obtained as a yellow solid: mp 101–104 °C; ¹H NMR (400 MHz, CDCl₃) δ 8.55 (d, $J = 9.3$ Hz, 1H, Ar), 8.25–8.16 (m, 5H, Ar), 8.12–8.01 (m, 3H, Ar), 7.81 (d, $J = 8.0$ Hz, 2H, Ar), 7.76 (dd, $J = 8.1, 1.4$ Hz, 1H, Ar), 7.49–7.36 (m, 3H, Ar and CH), 7.31 (d, $J = 8.5$ Hz, 1H, Ar), 2.46 (s, 3H, Me), 2.03 (d, $J = 6.6$ Hz, 3H, Me) ppm; ¹³C{¹H} NMR (101 MHz, CDCl₃) δ 169.19, 134.64, 133.24, 131.64, 131.35, 131.13, 130.70, 130.27, 130.05, 129.59, 128.40, 128.11, 128.02, 127.66, 127.62, 127.40, 126.98, 126.07, 125.48, 125.44, 125.30, 125.04, 124.94, 124.90, 124.50, 123.83, 122.55, 70.68, 22.72, 20.11 ppm; IR (ATR) ν (cm⁻¹) 2919, 1716, 1597, 1508, 1376, 1277, 1239, 1216, 1136, 1067, 1039, 907, 840, 812, 719; HRMS (EI) m/z [M]⁺ calcd for C₃₀H₂₂O₂ 414.1620, found 414.1614.

2-(Pyren-1-yl)ethyl Benzoate 7da. Compound **2d** (20.0 mg, 81.2 μ mol, 1.0 equiv), **3a** (20.0 mg, 89.3 μ mol, 1.1 equiv), DMAP (496 μ g, 4.06 μ mol, 0.05 equiv), and Et₃N (22.6 μ L, 162 μ mol, 2.0 equiv) were dissolved in CH₂Cl₂ (400 μ L) and reacted according to GP E. After purification by column chromatography on silica (isohexane/CH₂Cl₂ 6:4), **7da** (20.0 mg, 70%) was obtained as a white solid: mp 82–85 °C; ¹H NMR (400 MHz, CDCl₃) δ 8.42 (d, $J = 9.2$ Hz, 1H, Ar), 8.22–8.13 (m, 4H, Ar), 8.07–7.99 (m, 5H, Ar), 7.97 (d, $J = 7.8$ Hz, 1H, Ar), 7.58–7.52 (m, 1H, Ar), 7.45–7.39 (m, 2H, Ar), 4.77 (t, $J = 7.3$ Hz, 2H, CH₂), 3.83 (t, $J = 7.3$ Hz, 2H, CH₂) ppm; ¹³C{¹H} NMR (101 MHz, CDCl₃) δ 166.81, 133.08, 131.77, 131.51, 130.99, 130.56, 130.35, 129.77, 129.44, 128.48, 127.99, 127.91, 127.58, 127.19, 126.07, 125.25, 125.21, 125.10, 125.02, 123.32, 65.62, 32.97 ppm (one signal is overlapping); IR (ATR) ν (cm⁻¹) 2953, 1716, 1449, 1268, 1176, 1109, 1025, 960, 840, 700, 678; HRMS (EI) m/z [M]⁺ calcd for C₂₅H₁₈O₂ 350.1307, found 350.1298.

2-(Pyren-1-yl)ethyl 2-Phenylbenzoate 7df. Compound **2d** (20.0 mg, 81.2 μ mol, 1.0 equiv), **3f** (33.8 mg, 89.3 μ mol, 1.1 equiv), DMAP (496 μ g, 4.06 μ mol, 0.05 equiv), and Et₃N (22.6 μ L, 162 μ mol, 2.0 equiv) were dissolved in CH₂Cl₂ (400 μ L) and reacted according to GP E. After purification by column chromatography on silica (isohexane/CH₂Cl₂ 6:4), **7df** (33.0 mg, 95%) was obtained as an oil: ¹H NMR (400 MHz, CDCl₃) δ 8.21–8.15 (m, 3H, Ar), 8.13–8.06 (m, 2H, Ar), 8.05–7.98 (m, 3H, Ar), 7.80 (dd, $J = 8.0, 1.4$ Hz, 1H, Ar), 7.74 (d, $J = 7.8$ Hz, 1H, Ar), 7.56–7.50 (m, 1H, Ar), 7.42–7.29 (m, 7H, Ar), 4.47 (t, $J = 7.6$ Hz, 2H, CH₂), 3.39 (t, $J = 7.6$ Hz, 2H, CH₂) ppm; ¹³C{¹H} NMR (101 MHz, CDCl₃) δ 169.01, 142.59, 141.64, 131.48, 131.48, 131.37, 131.23, 130.95, 130.76, 130.47, 129.97, 129.25, 128.56, 128.18, 127.85, 127.78, 127.56, 127.36, 127.32, 127.13, 126.05, 125.21, 125.13, 125.06, 124.99, 124.93, 123.22, 65.47, 32.34; IR (ATR) ν (cm⁻¹) 2955, 1713, 1597, 1450, 1276, 1240, 1123, 1085, 1047, 964, 840, 748, 700; HRMS (EI) m/z [M]⁺ calcd for C₃₁H₂₂O₂ 426.1620, found 426.1618.

2-(Pyren-1-yl)ethyl 2-(Naphthalene-1-yl)benzoate 7dh. Compound **2d** (20.0 mg, 81.2 μ mol, 1.0 equiv), **3h** (42.7 mg, 89.3 μ mol, 1.1 equiv), DMAP (496 μ g, 4.06 μ mol, 0.05 equiv), and Et₃N (22.6 μ L, 162 μ mol, 2.0 equiv) were dissolved in CH₂Cl₂ (400 μ L) and reacted according to GP E. After purification by column chromatography on silica (isohexane/CH₂Cl₂ 6:4), **7dh** (15.0 mg, 40%) was obtained as a white solid: mp 115–118 °C; ¹H NMR (400 MHz, CDCl₃) δ 8.20–8.14 (m, 2H, Ar), 8.08–7.96 (m, 6H, Ar), 7.91 (d, $J = 8.6$ Hz, 1H, Ar), 7.88 (d, $J = 8.3$ Hz, 1H, Ar), 7.85 (d, $J = 9.3$ Hz, 1H, Ar), 7.63 (td, $J = 7.5, 1.4$ Hz, 1H, Ar), 7.58 (d, $J = 8.8$ Hz, 1H, Ar), 7.55–7.41 (m, 6H, Ar), 7.38 (dd, $J = 7.0, 1.3$ Hz, 1H, Ar), 4.13 (qdd, $J = 10.8, 8.9, 6.7$ Hz,

2H, CH₂), 2.81 (qdd, $J = 13.9, 8.9, 6.4$ Hz, 2H, CH₂) ppm; ¹³C{¹H} NMR (101 MHz, CDCl₃) δ 168.01, 141.25, 140.11, 133.44, 132.39, 131.98, 131.91, 131.81, 131.45, 131.26, 130.90, 130.36, 130.35, 129.08, 128.36, 127.79, 127.69, 127.64, 127.54, 127.52, 127.06, 126.30, 126.21, 126.01, 125.89, 125.84, 125.37, 125.16, 125.01, 125.01, 124.93, 124.82, 123.09, 64.96, 31.69 ppm; IR (ATR) ν (cm⁻¹) 2921, 1699, 1598, 1505, 1443, 1392, 1283, 1131, 1041, 972, 830, 799, 761, 711; HRMS (EI) m/z [M]⁺ calcd for C₃₃H₂₄O₂ 476.1776, found 476.1770.

2-(Pyren-1-yl)ethyl 2,6-Dimethylbenzoate 7dm. Compound **2d** (15.0 mg, 60.9 μ mol, 1.0 equiv), **3m** (20.6 mg, 73.1 μ mol, 1.2 equiv), DMAP (372 μ g, 3.04 μ mol, 0.05 equiv), and Et₃N (12.7 μ L, 91.4 μ mol, 1.5 equiv) were dissolved in CH₂Cl₂ (300 μ L) and reacted according to GP E. After purification by column chromatography on silica (isohexane/CH₂Cl₂ 6:4), **7dm** (10.0 mg, 43%) was obtained as a white solid: mp 120–123 °C; ¹H NMR (400 MHz, CDCl₃) δ 8.39 (d, $J = 9.3$ Hz, 1H, Ar), 8.22–8.12 (m, 4H, Ar), 8.06 (s, 2H, Ar), 8.02 (t, $J = 7.6$ Hz, 1H, Ar), 7.96 (d, $J = 7.8$ Hz, 1H, Ar), 7.19 (t, $J = 7.6$ Hz, 1H, Ar), 7.02 (d, $J = 7.4$ Hz, 2H, Ar), 4.77 (dd, $J = 8.0, 7.2$ Hz, 2H, CH₂), 3.83 (t, $J = 7.6$ Hz, 2H, CH₂), 2.26 (s, 6H, Me₂) ppm; ¹³C{¹H} NMR (101 MHz, CDCl₃) δ 170.19, 135.10, 133.94, 131.51, 131.29, 130.99, 130.62, 129.47, 129.37, 128.03, 127.99, 127.71, 127.59, 127.23, 126.11, 125.30, 125.23, 125.17, 125.02, 123.15, 115.13, 65.45, 32.96, 19.86 ppm; IR (ATR) ν (cm⁻¹) 2891, 1721, 1585, 1462, 1416, 1264, 1114, 1077, 963, 840, 768, 707; HRMS (EI) m/z [M]⁺ calcd for C₂₇H₂₂O₂ 378.1620, found 378.1620.

2-(Pyren-1-yl)ethyl 2-Methyl-6-phenylbenzoate 7dn. Compound **2d** (15.0 mg, 60.9 μ mol, 1.0 equiv), **3n** (27.2 mg, 67.0 μ mol, 1.1 equiv), DMAP (372 μ g, 3.04 μ mol, 0.05 equiv), and Et₃N (12.7 μ L, 91.4 μ mol, 1.5 equiv) were dissolved in CH₂Cl₂ (300 μ L) and reacted according to GP E. After purification by column chromatography on silica (isohexane/CH₂Cl₂ 6:4), **7dn** (10.0 mg, 38%) was obtained as an oil: ¹H NMR (400 MHz, CDCl₃) δ 8.21–8.16 (m, 2H, Ar), 8.16–8.09 (m, 2H, Ar), 8.08–7.98 (m, 4H, Ar), 7.72 (d, $J = 7.7$ Hz, 1H, Ar), 7.40–7.35 (m, 3H, Ar), 7.34–7.29 (m, 2H, Ar), 7.28–7.20 (m, 3H, Ar), 4.41 (t, $J = 7.2$ Hz, 2H, CH₂), 3.31 (t, $J = 7.8$ Hz, 2H, CH₂), 2.41 (s, 3H, Me) ppm; ¹³C{¹H} NMR (101 MHz, CDCl₃) δ 169.93, 141.23, 140.50, 135.76, 133.24, 131.48, 131.30, 130.95, 130.49, 129.59, 129.33, 129.21, 128.50, 128.38, 127.83, 127.80, 127.56, 127.46, 127.38, 127.14, 126.06, 125.22, 125.14, 125.08, 124.99, 124.93, 123.18, 65.41, 32.30, 19.89 ppm; IR (ATR) ν (cm⁻¹) 2924, 1721, 1588, 1461, 1236, 1090, 842, 758, 700; HRMS (EI) m/z [M]⁺ calcd for C₃₂H₂₄O₂ 440.1776, found 440.1775.

2-(Pyren-1-yl)ethyl 2-Methyl-6-nitrobenzoate 7do. Compound **2d** (20.0 mg, 81.2 μ mol, 1.0 equiv), **3o** (30.8 mg, 89.3 μ mol, 1.1 equiv), DMAP (496 μ g, 4.06 μ mol, 0.05 equiv), and Et₃N (22.6 μ L, 162 μ mol, 2.0 equiv) were dissolved in CH₂Cl₂ (400 μ L) and reacted according to GP E. After purification by column chromatography on silica (isohexane/CH₂Cl₂ 6:4), **7do** (20.0 mg, 60%) was obtained as a yellow solid: mp 101–104 °C; ¹H NMR (400 MHz, CDCl₃) δ 8.37 (d, $J = 9.3$ Hz, 1H, Ar), 8.22–8.17 (m, 2H, Ar), 8.17–8.12 (m, 2H, Ar), 8.05 (s, 2H, Ar), 8.04–7.97 (m, 2H, Ar), 7.95 (d, $J = 7.8$ Hz, 1H, Ar), 7.52–7.42 (m, 2H, Ar), 4.82 (dd, $J = 8.1, 7.2$ Hz, 2H, CH₂), 3.84 (t, $J = 7.6$ Hz, 2H, CH₂), 2.28 (d, $J = 0.5$ Hz, 3H, Me) ppm; ¹³C{¹H} NMR (101 MHz, CDCl₃) δ 166.61, 137.76, 136.13, 131.50, 131.09, 130.98, 130.63, 129.88, 129.57, 129.41, 128.02, 127.93, 127.58, 127.24, 126.10, 125.28, 125.21, 125.16, 125.04, 125.00, 123.15, 121.97, 66.54, 32.45, 19.20 ppm. (one signal is overlapping); IR (ATR) ν (cm⁻¹) 2949, 1728, 1530, 1337, 1268, 1115, 1079, 987, 830, 802, 740, 721; HRMS (EI) m/z [M]⁺ calcd for C₂₆H₁₉O₄N 409.1314, found 409.1315.

2-(Pyren-1-yl)ethyl 2-Methoxy-1-naphthoate 7dr. Compound **2d** (20.0 mg, 81.2 μ mol, 1.0 equiv), **3r** (34.5 mg, 89.3 μ mol, 1.1 equiv), DMAP (496 μ g, 4.06 μ mol, 0.05 equiv), and Et₃N (22.6 μ L, 162 μ mol, 2.0 equiv) were dissolved in CH₂Cl₂ (400 μ L) and reacted according to GP E. After purification by column chromatography on silica (isohexane/CH₂Cl₂ 6:4), **7dr** (20.0 mg, 57%) was obtained as a white solid: mp 130–133 °C; ¹H NMR (400 MHz, CDCl₃) δ 8.43 (d, $J = 9.3$ Hz, 1H, Ar), 8.19 (ddd, $J = 7.8, 4.6, 1.2$ Hz, 2H, Ar), 8.15–8.10 (m, 2H, Ar), 8.06 (s, 2H, Ar), 8.04–7.98 (m, 2H, Ar), 7.89 (d, $J = 9.0$ Hz, 1H, Ar), 7.77 (ddd, $J = 7.3, 2.0, 1.0$ Hz, 1H, Ar), 7.61–7.55 (m, 1H, Ar), 7.34–7.25 (m, 3H, Ar), 4.92 (t, $J = 7.5$ Hz, 2H, CH₂), 3.94–3.84

(m, 5H, CH₂ and Me) ppm; ¹³C{¹H} NMR (101 MHz, CDCl₃) δ 168.20, 154.60, 131.80, 131.59, 131.48, 131.05, 130.99, 130.55, 129.45, 128.59, 128.13, 128.08, 127.87, 127.64, 127.56, 127.17, 126.03, 125.19, 125.09, 125.02, 125.01, 124.18, 123.85, 123.34, 117.57, 113.14, 65.92, 56.79, 32.99 ppm (one signal is overlapping); IR (ATR) ν (cm⁻¹) 2953, 1724, 1625, 1596, 1512, 1466, 1435, 1282, 1257, 1231, 1134, 1074, 1014, 943, 841, 800, 745, 708; HRMS (EI) *m/z* [M]⁺ calcd for C₃₀H₂₂O₃ 430.1569, found 430.1563.

2-(Pyren-1-yl)ethyl 2-Ethoxy-1-naphthoate 7ds. Compound **2d** (20.0 mg, 81.2 μmol, 1.0 equiv), **3s** (37.0 mg, 89.3 μmol, 1.1 equiv), DMAP (496 μg, 4.06 μmol, 0.05 equiv), and Et₃N (22.6 μL, 162 μmol, 2.0 equiv) were dissolved in CH₂Cl₂ (400 μL) and reacted according to GP E. After purification by column chromatography on silica (isohexane/CH₂Cl₂ 6:4), **7ds** (33.0 mg, 92%) was obtained as a yellow solid: mp 101–104 °C; ¹H NMR (400 MHz, CDCl₃) δ 8.45 (d, *J* = 9.3 Hz, 1H, Ar), 8.19 (dd, *J* = 8.1, 2.5 Hz, 2H, Ar), 8.15–8.11 (m, 2H, Ar), 8.06 (s, 2H, Ar), 8.04–7.97 (m, 2H, Ar), 7.88 (d, *J* = 9.0 Hz, 1H, Ar), 7.80–7.75 (m, 1H, Ar), 7.63–7.57 (m, 1H, Ar), 7.35–7.28 (m, 2H, Ar), 7.27 (d, *J* = 9.1 Hz, 1H, Ar), 4.89 (t, *J* = 8.1, 7.1 Hz, 2H, CH₂), 4.19 (q, *J* = 7.0 Hz, 2H, CH₂), 3.90 (t, *J* = 7.6 Hz, 2H, CH₂), 1.37 (t, *J* = 7.0 Hz, 3H, Me) ppm; ¹³C{¹H} NMR (101 MHz, CDCl₃) δ 168.31, 154.05, 131.66, 131.56, 131.51, 131.09, 131.03, 130.60, 129.48, 128.68, 128.13, 128.10, 127.94, 127.59, 127.59, 127.20, 126.07, 125.24, 125.23, 125.13, 125.06, 125.05, 124.22, 123.90, 123.35, 118.25, 114.56, 65.84, 65.55, 33.11, 15.13 ppm; IR (ATR) ν (cm⁻¹) 2894, 1724, 1529, 1505, 1464, 1433, 1285, 1251, 1137, 1107, 1060, 1021, 962, 837, 807, 747, 705; HRMS (EI) *m/z* [M]⁺ calcd for C₃₁H₂₄O₃ 444.1725, found 444.1721.

2-(Pyren-1-yl)ethyl 2-Butoxy-1-naphthoate 7dt. Compound **2d** (10.0 mg, 40.6 μmol, 1.0 equiv), **3t** (21.0 mg, 44.7 μmol, 1.1 equiv), DMAP (248 μg, 2.03 μmol, 0.05 equiv), and Et₃N (11.3 μL, 81.2 μmol, 2.0 equiv) were dissolved in CH₂Cl₂ (200 μL) and reacted according to GP E. After purification by column chromatography on silica (isohexane/CH₂Cl₂ 6:4), **7dt** (10 mg, 53%) was obtained as a white solid: mp 72–74 °C; ¹H NMR (400 MHz, CDCl₃) δ 8.44 (d, *J* = 9.3 Hz, 1H, Ar), 8.19 (dd, *J* = 8.1, 2.1 Hz, 2H, Ar), 8.16–8.11 (m, 2H, Ar), 8.06 (s, 2H, Ar), 8.04–7.97 (m, 2H, Ar), 7.88 (d, *J* = 9.0 Hz, 1H, Ar), 7.81–7.74 (m, 1H, Ar), 7.60 (dt, *J* = 6.7, 3.3 Hz, 1H, Ar), 7.32 (dt, *J* = 6.4, 3.4 Hz, 2H, Ar), 7.27 (d, *J* = 8.9 Hz, 1H, Ar), 4.88 (t, 2H, CH₂), 4.12 (t, *J* = 6.5 Hz, 2H, CH₂), 3.89 (t, *J* = 7.7 Hz, 2H, CH₂), 1.79–1.67 (m, 2H, CH₂), 1.52–1.41 (m, 2H, CH₂), 0.91 (t, *J* = 7.4 Hz, 3H, Me) ppm; ¹³C{¹H} NMR (101 MHz, CDCl₃) δ 168.31, 154.21, 131.64, 131.54, 131.52, 131.11, 131.03, 130.61, 129.47, 128.62, 128.13, 128.10, 127.95, 127.59, 127.21, 126.07, 125.24, 125.23, 125.12, 125.06, 125.05, 124.17, 123.87, 123.33, 118.07, 114.45, 77.48, 69.56, 65.82, 33.11, 31.59, 19.27, 13.96 ppm; IR (ATR) ν (cm⁻¹) 2925, 1719, 1624, 1594, 1510, 1461, 1281, 1213, 1134, 1070, 1027, 830, 809, 746, 711; HRMS (EI) *m/z* [M]⁺ calcd for C₃₃H₂₈O₃ 472.2038, found 472.2033.

2-(Pyren-1-yl)ethyl 2-(Hexanoyloxy)-1-naphthoate 7du. Compound **2d** (10.0 mg, 40.6 μmol, 1.0 equiv), **3u** (23.5 mg, 44.7 μmol, 1.1 equiv), DMAP (248 μg, 2.03 μmol, 0.05 equiv), and Et₃N (11.3 μL, 81.2 μmol, 2.0 equiv) were dissolved in CH₂Cl₂ (200 μL) and reacted according to GP E. After purification by column chromatography on silica (isohexane/CH₂Cl₂ 6:4), **7du** (10.0 mg, 50%) was obtained as an oil: ¹H NMR (400 MHz, CDCl₃) δ 8.44 (d, *J* = 9.3 Hz, 1H, Ar), 8.19 (dd, *J* = 7.6, 1.7 Hz, 2H, Ar), 8.16–8.11 (m, 2H, Ar), 8.06 (s, 2H, Ar), 8.05–7.97 (m, 2H, Ar), 7.88 (d, *J* = 9.1 Hz, 1H, Ar), 7.77 (dq, *J* = 6.9, 3.6 Hz, 1H, Ar), 7.64–7.57 (m, 1H, Ar), 7.32 (dt, *J* = 6.4, 3.4 Hz, 2H, Ar), 7.29–7.24 (m, 1H, Ar), 4.89 (t, *J* = 7.6 Hz, 2H, CH₂), 4.10 (t, *J* = 6.6 Hz, 2H, CH₂), 3.90 (t, *J* = 7.6 Hz, 2H, CH₂), 1.77–1.65 (m, 2H, CH₂), 1.42 (p, *J* = 7.3 Hz, 2H, CH₂), 1.32–1.20 (m, 4H, 2 × CH₂), 0.84 (t, *J* = 7.0 Hz, 3H, Me) ppm; ¹³C{¹H} NMR (101 MHz, CDCl₃) δ 168.31, 154.22, 131.64, 131.56, 131.52, 131.11, 131.03, 130.60, 129.47, 128.61, 128.13, 128.09, 127.93, 127.59, 127.20, 126.07, 125.24, 125.23, 125.12, 125.05, 124.16, 123.87, 123.34, 118.05, 114.46, 69.88, 65.81, 33.12, 31.65, 29.50, 25.73, 22.75, 14.16 ppm (two signals are overlapping); IR (ATR) ν (cm⁻¹) 2920, 1722, 1625, 1594, 1463, 1282, 1230, 1134, 1067, 1019, 843, 808, 746, 710; HRMS (EI) *m/z* [M]⁺ calcd for C₃₅H₃₂O₃ 500.2351, found 500.2340.

2-(Pyren-1-yl)ethyl 2-Isopropoxy-1-naphthoate 7dv. Compound **2d** (15.0 mg, 60.9 μmol, 1.0 equiv), **3v** (29.6 mg, 67.0 μmol, 1.1 equiv), DMAP (372 μg, 3.04 μmol, 0.05 equiv), and Et₃N (12.7 μL, 91.4 μmol, 1.5 equiv) were dissolved in CH₂Cl₂ (300 μL) and reacted according to GP E. After purification by column chromatography on silica (isohexane/CH₂Cl₂ 6:4), **7dv** (10.0 mg, 55%) was obtained as an oil: ¹H NMR (400 MHz, CDCl₃) δ 8.45 (d, *J* = 9.3 Hz, 1H, Ar), 8.19 (d, *J* = 7.4 Hz, 2H, Ar), 8.17–8.11 (m, 2H, Ar), 8.06 (s, 2H, Ar), 8.05–7.97 (m, 2H, Ar), 7.86 (d, *J* = 9.1 Hz, 1H, Ar), 7.80–7.75 (m, 1H, Ar), 7.66–7.57 (m, 1H, Ar), 7.37–7.30 (m, 2H, Ar), 7.28 (d, *J* = 9.2 Hz, 1H, Ar), 4.88 (t, *J* = 7.7 Hz, 2H, CH₂), 4.69 (hept, *J* = 6.1 Hz, 1H, CH), 3.90 (t, *J* = 7.7 Hz, 2H, CH₂), 1.34 (d, *J* = 6.1 Hz, 6H, Me₂) ppm; ¹³C{¹H} NMR (101 MHz, CDCl₃) δ 168.40, 153.14, 131.52, 131.40, 131.17, 131.03, 130.61, 129.46, 128.79, 128.09, 127.97, 127.59, 127.51, 127.19, 126.06, 125.25, 125.23, 125.13, 125.07, 125.06, 124.34, 123.93, 123.32, 119.80, 116.36, 72.66, 65.74, 33.16, 22.53 (two signals are overlapping); IR (ATR) ν (cm⁻¹) 2925, 1720, 1624, 1593, 1465, 1271, 1280, 1225, 1132, 1106, 1044, 998, 905, 830, 807, 724; HRMS (EI) *m/z* [M]⁺ calcd for C₃₂H₂₆O₃ 458.1882, found 458.1881.

2-(Pyren-1-yl)ethyl 2-Methyl-1-naphthoate 7dw. Compound **2d** (15.0 mg, 60.9 μmol, 1.0 equiv), **3w** (25.8 mg, 67.0 μmol, 1.1 equiv), DMAP (372 μg, 3.04 μmol, 0.05 equiv), and Et₃N (12.7 μL, 91.4 μmol, 1.5 equiv) were dissolved in CH₂Cl₂ (300 μL) and reacted according to GP E. After purification by column chromatography on silica (isohexane/CH₂Cl₂ 6:4), **7dw** (10.0 mg, 59%) was obtained as a white solid: mp 129–132 °C; ¹H NMR (400 MHz, CDCl₃) δ 8.41 (d, *J* = 9.3 Hz, 1H, Ar), 8.24–8.16 (m, 2H, Ar), 8.14 (s, 1H, Ar), 8.12 (d, *J* = 2.4 Hz, 1H, Ar), 8.07 (s, 2H, Ar), 8.02 (t, *J* = 7.6 Hz, 1H, Ar), 7.98 (d, *J* = 7.8 Hz, 1H, Ar), 7.79 (d, *J* = 8.3 Hz, 2H, Ar), 7.64 (d, *J* = 8.5 Hz, 1H, Ar), 7.39 (ddd, *J* = 8.1, 6.9, 1.1 Hz, 1H, Ar), 7.33–7.27 (m, 2H, Ar), 4.92 (t, *J* = 7.4 Hz, 2H, CH₂), 3.90 (t, *J* = 7.4 Hz, 2H, CH₂), 2.42 (s, 3H, Me) ppm; ¹³C{¹H} NMR (101 MHz, CDCl₃) δ 169.87, 133.58, 131.73, 131.51, 131.36, 131.00, 130.65, 130.13, 130.12, 129.82, 129.42, 128.48, 128.11, 128.10, 128.01, 127.59, 127.26, 127.07, 126.10, 125.55, 125.29, 125.25, 125.17, 125.07, 125.04, 124.60, 123.20, 65.86, 33.01, 20.28 ppm; IR (ATR) ν (cm⁻¹) 2919, 1715, 1597, 1510, 1385, 1282, 1245, 1202, 1216, 1148, 1118, 1010, 958, 835, 814, 746, 725, 707; HRMS (EI) *m/z* [M]⁺ calcd for C₃₀H₂₂O₂ 414.1620, found 414.1616.

1-(Naphthalen-1-yl)ethyl Benzoate 6ea. Compound **1e** (60.0 mg, 348 μmol, 1.0 equiv), **3a** (94.6 mg, 418 μmol, 1.5 equiv), DMAP (2.13 mg, 17.4 μmol, 0.05 equiv), and Et₃N (100 μL, 696 μmol, 1.5 equiv) were dissolved in CH₂Cl₂ (2 mL) and reacted according to GP E. After purification by column chromatography on silica (isohexane/CH₂Cl₂ 6:4), **6ea** (95.0 mg, 99%) was obtained as a white solid: mp 70–72 °C; ¹H NMR (400 MHz, CDCl₃) δ 8.20 (d, *J* = 8.6 Hz, 1H, Ar), 8.14–8.10 (m, 2H, Ar), 7.91–7.87 (m, 1H, Ar), 7.82 (d, *J* = 8.2 Hz, 1H, Ar), 7.71 (d, *J* = 7.1 Hz, 1H, Ar), 7.60–7.54 (m, 2H, Ar), 7.53–7.50 (m, 1H, Ar), 7.50–7.43 (m, 3H, Ar), 6.90 (q, *J* = 6.6 Hz, 1H, CH), 1.85 (d, *J* = 6.6 Hz, 3H, Me) ppm; ¹³C{¹H} NMR (101 MHz, CDCl₃) δ 165.99, 137.70, 134.01, 133.11, 130.63, 130.43, 129.84, 129.07, 128.63, 128.52, 126.50, 125.83, 125.54, 123.38, 70.42, 22.08 (one signal is overlapping) ppm; HRMS (EI) *m/z* [M]⁺ calcd for C₁₉H₁₆O₂ 276.1150, found 276.1162. The ¹H spectrum is in full agreement with this reported in literature.⁴³

1-(Naphthalen-1-yl)ethyl 2-Phenylbenzoate 6ef. Compound **1e** (20.0 mg, 116 μmol, 1.0 equiv), **3f** (48.3 mg, 127 μmol, 1.1 equiv), DMAP (709 μg, 5.81 μmol, 0.05 equiv), and Et₃N (32.4 μL, 232 μmol, 1.5 equiv) were dissolved in CH₂Cl₂ (580 μL) and reacted according to GP E. After purification by column chromatography on silica (isohexane/CH₂Cl₂ 6:4), **6ef** (40 mg, 97%) was obtained as an oil: ¹H NMR (400 MHz, CDCl₃) δ 7.99–7.93 (m, 1H, Ar), 7.88–7.81 (m, 2H, Ar), 7.75 (d, *J* = 8.2 Hz, 1H, Ar), 7.55–7.44 (m, 3H, Ar), 7.43–7.27 (m, 8H, Ar), 7.21 (d, *J* = 7.1 Hz, 1H, Ar), 6.68 (q, *J* = 6.6 Hz, 1H, CH), 1.50 (d, *J* = 6.5 Hz, 3H, Me) ppm; ¹³C{¹H} NMR (101 MHz, CDCl₃) δ 168.19, 142.61, 141.57, 137.17, 133.86, 131.43, 131.31, 130.92, 130.21, 130.15, 128.93, 128.71, 128.35, 128.16, 127.35, 127.30, 126.30, 125.67, 125.47, 123.54, 123.36, 70.63, 21.62 ppm; IR (ATR) ν (cm⁻¹) 3056, 1707, 1597, 1511, 1464, 1277, 1237, 1125, 1041, 857, 799, 774, 697; HRMS (EI) *m/z* [M]⁺ calcd for C₂₅H₂₀O₂ 352.1463, found 352.1452.

1-(Naphthalen-1-yl)ethyl 2,6-Dimethylbenzoate 6em. Compound **1e** (20.0 mg, 116 μmol , 1.0 equiv), **3m** (36.1 mg, 128 μmol , 1.1 equiv), DMAP (709 μg , 5.81 μmol , 0.05 equiv), and Et_3N (32.4 μL , 232 μmol , 2.0 equiv) were dissolved in CH_2Cl_2 (580 μL) and reacted according to GP E. After purification by column chromatography on silica (isohexane/ CH_2Cl_2 6:4), **6em** (20.0 mg, 57%) was obtained as a white solid: mp 47–49 $^\circ\text{C}$; ^1H NMR (400 MHz, CDCl_3) δ 8.20 (d, J = 7.9 Hz, 1H, Ar), 7.90 (d, J = 8.0 Hz, 1H, Ar), 7.83 (d, J = 8.2 Hz, 1H, Ar), 7.68 (d, J = 7.1 Hz, 1H, Ar), 7.60–7.44 (m, 3H, Ar), 7.21–7.15 (m, 1H, Ar), 7.05–6.96 (m, 3H, Ar and CH), 2.28 (d, J = 0.6 Hz, 6H, Me_2), 1.86 (d, J = 6.5 Hz, 3H, Me) ppm; $^{13}\text{C}\{^1\text{H}\}$ NMR (101 MHz, CDCl_3) δ 169.47, 137.07, 134.98, 134.17, 133.95, 130.41, 129.38, 129.07, 128.73, 127.69, 126.49, 125.88, 125.48, 123.70, 123.33, 70.02, 21.88, 19.81; IR (ATR) ν (cm^{-1}) 2920, 1716, 1595, 1463, 1248, 1111, 1063, 804; HRMS (EI) m/z [M] $^+$ calcd for $\text{C}_{21}\text{H}_{20}\text{O}_2$ 304.1463, found 304.1457.

1-(Naphthalen-1-yl)ethyl 2-Methyl-6-phenylbenzoate 6en. Compound **1e** (15.0 mg, 87.1 μmol , 1.0 equiv), **3n** (38.9 mg, 95.8 μmol , 1.1 equiv), DMAP (532 μg , 4.35 μmol , 0.05 equiv), and Et_3N (18.2 μL , 131 μmol , 1.5 equiv) were dissolved in CH_2Cl_2 (435 μL) and reacted according to GP E. After purification by column chromatography on silica (isohexane/ CH_2Cl_2 6:4), **6en** (25.0 mg, 78%) was obtained as an oil: ^1H NMR (400 MHz, CDCl_3) δ 8.03–7.95 (m, 1H, Ar), 7.87–7.81 (m, 1H, Ar), 7.75 (d, J = 7.8 Hz, 1H, Ar), 7.53–7.44 (m, 2H, Ar), 7.39–7.29 (m, 5H, Ar), 7.29–7.19 (m, 5H, Ar), 6.65 (q, J = 6.6 Hz, 1H, CH), 2.35 (s, 3H, Me), 1.36 (d, J = 6.6 Hz, 3H, Me) ppm; $^{13}\text{C}\{^1\text{H}\}$ NMR (101 MHz, CDCl_3) δ 169.11, 140.94, 140.38, 137.04, 135.65, 133.88, 133.50, 130.22, 129.43, 129.26, 128.93, 128.68, 128.38, 128.30, 127.44, 127.42, 126.28, 125.69, 125.47, 123.52, 123.42, 70.45, 21.36, 19.91 ppm; IR (ATR) ν (cm^{-1}) 2919, 1718, 1461, 1261, 1125, 1063, 775, 698; HRMS (EI) m/z [M] $^+$ calcd for $\text{C}_{26}\text{H}_{22}\text{O}_2$ 366.1620, found 366.1606.

1-(Naphthalen-1-yl)ethyl 2-Methyl-6-nitrobenzoate 6eo. Compound **2e** (20.0 mg, 116 μmol , 1.0 equiv), **3o** (44.0 mg, 128 μmol , 1.2 equiv), DMAP (709 μg , 5.81 μmol , 0.05 equiv), and Et_3N (32.4 μL , 232 μmol , 2.0 equiv) were dissolved in CH_2Cl_2 (580 μL) and reacted according to GP E. After purification by column chromatography on silica (isohexane/ CH_2Cl_2 6:4), **6eo** (20.0 mg, 52%) was obtained as an oil: ^1H NMR (400 MHz, CDCl_3) δ 8.21 (d, J = 8.2 Hz, 1H, Ar), 8.00 (d, J = 7.9 Hz, 1H, Ar), 7.89 (d, J = 8.0 Hz, 1H, Ar), 7.83 (d, J = 8.2 Hz, 1H, Ar), 7.63 (d, J = 7.0 Hz, 1H, Ar), 7.58 (ddd, J = 8.5, 6.8, 1.5 Hz, 1H, Ar), 7.54–7.41 (m, 4H, Ar), 7.03 (q, J = 6.6 Hz, 1H, CH), 2.29 (s, 3H, Me), 1.89 (d, J = 6.6 Hz, 3H, Me) ppm; $^{13}\text{C}\{^1\text{H}\}$ NMR (101 MHz, CDCl_3) δ 165.88, 146.24, 137.82, 136.48, 136.14, 133.96, 130.40, 129.78, 129.68, 129.06, 128.93, 126.55, 125.92, 125.45, 123.86, 123.32, 121.93, 71.58, 21.14, 19.27 ppm; IR (ATR) ν (cm^{-1}) 2959, 1732, 1520, 1462, 1343, 1264, 1112, 1068, 954, 798, 776, 738; HRMS (EI) m/z [M] $^+$ calcd for $\text{C}_{20}\text{H}_{17}\text{O}_4\text{N}$ 335.1158, found 335.1154.

1-(Naphthalen-1-yl)ethyl 2-Methoxy-1-naphthoate 6er. Compound **1e** (20.0 mg, 116 μmol , 1.0 equiv), **3r** (53.8 mg, 139 μmol , 1.2 equiv), DMAP (709 μg , 5.81 μmol , 0.05 equiv), and Et_3N (32.4 μL , 232 μmol , 2.0 equiv) were dissolved in CH_2Cl_2 (580 μL) and reacted according to GP E. After purification by column chromatography on silica (isohexane/ CH_2Cl_2 6:4), **6er** (35.0 mg, 84%) was obtained as an oil: ^1H NMR (400 MHz, CDCl_3) δ 8.27 (d, J = 8.3 Hz, 1H, Ar), 7.93–7.87 (m, 2H, Ar), 7.83 (d, J = 8.2 Hz, 1H, Ar), 7.78 (d, J = 8.4 Hz, 1H, Ar), 7.75–7.71 (m, 2H, Ar), 7.59 (ddd, J = 8.5, 6.8, 1.5 Hz, 1H, Ar), 7.52 (ddd, J = 8.0, 6.9, 1.2 Hz, 1H, Ar), 7.50–7.45 (m, 1H, Ar), 7.42 (ddd, J = 8.4, 6.8, 1.4 Hz, 1H, Ar), 7.35 (ddd, J = 8.0, 6.9, 1.2 Hz, 1H, Ar), 7.27 (d, J = 9.5 Hz, 1H, Ar), 7.10 (q, J = 6.5 Hz, 1H, CH), 3.93–3.82 (s, 3H, Me), 1.92 (d, J = 6.6 Hz, 3H, Me) ppm; $^{13}\text{C}\{^1\text{H}\}$ NMR (101 MHz, CDCl_3) δ 167.62, 154.61, 137.24, 133.98, 131.66, 131.13, 130.58, 128.98, 128.68, 128.67, 128.18, 127.67, 126.37, 125.79, 125.48, 124.21, 123.90, 123.79, 123.64, 117.96, 113.36, 70.58, 56.77, 21.81 ppm; IR (ATR) ν (cm^{-1}) 2934, 1716, 1595, 1511, 1433, 1342, 1281, 1254, 1225, 1136, 1068, 1017, 918, 859, 797, 745; HRMS (EI) m/z [M] $^+$ calcd for $\text{C}_{24}\text{H}_{20}\text{O}_3$ 356.1412, found 356.1402.

1-(Naphthalen-1-yl)ethyl 2-Ethoxy-1-naphthoate 6es. Compound **1e** (20.0 mg, 116 μmol , 1.0 equiv), **3s** (57.8 mg, 139 μmol , 1.2 equiv), DMAP (709 μg , 5.81 μmol , 0.05 equiv), and Et_3N (32.4 μL , 232 μmol , 2.0 equiv) were dissolved in CH_2Cl_2 (580 μL) and reacted

according to GP E. After purification by column chromatography on silica (isohexane/ CH_2Cl_2 6:4), **6es** (40.0 mg, 93%) was obtained as an oil: ^1H NMR (400 MHz, CDCl_3) δ 8.27 (d, J = 8.3 Hz, 1H, Ar), 7.90 (d, J = 8.6 Hz, 1H, Ar), 7.87 (d, J = 9.1 Hz, 1H, Ar), 7.82 (d, J = 8.2 Hz, 1H, Ar), 7.78 (d, J = 8.1 Hz, 1H, Ar), 7.74 (dd, J = 7.6, 3.9 Hz, 2H, Ar), 7.59 (ddd, J = 8.5, 6.8, 1.5 Hz, 1H, Ar), 7.52 (ddd, J = 8.0, 6.9, 1.2 Hz, 1H, Ar), 7.48 (d, J = 8.0 Hz, 1H, Ar), 7.44–7.38 (m, 1H, Ar), 7.37–7.31 (m, 1H, Ar), 7.26 (d, J = 9.1 Hz, 1H, Ar), 7.12 (q, J = 6.6 Hz, 1H, CH), 4.17 (qd, J = 7.0, 1.8 Hz, 2H, CH_2), 1.92 (d, J = 6.6 Hz, 3H, Me), 1.31 (t, J = 7.0 Hz, 3H, Me) ppm; $^{13}\text{C}\{^1\text{H}\}$ NMR (101 MHz, CDCl_3) δ 167.67, 153.97, 137.32, 133.96, 131.52, 131.20, 130.55, 129.00, 128.66, 128.59, 128.15, 127.60, 126.43, 125.79, 125.49, 124.17, 123.93, 123.68, 123.54, 118.34, 114.45, 70.40, 65.36, 21.92, 15.01 ppm; IR (ATR) ν (cm^{-1}) 2979, 1715, 1595, 1511, 1434, 1340, 1225, 1136, 1063, 859, 797, 746; HRMS (EI) m/z [M] $^+$ calcd for $\text{C}_{25}\text{H}_{22}\text{O}_3$ 370.1569, found 370.1568.

1-(Naphthalen-1-yl)ethyl 2-methyl-1-naphthoate 6ew. Compound **1e** (20.0 mg, 116 μmol , 1.0 equiv), **3w** (45.3 mg, 128 μmol , 1.1 equiv), DMAP (709 μg , 5.81 μmol , 0.05 equiv), and Et_3N (32.4 μL , 232 μmol , 2.0 equiv) were dissolved in CH_2Cl_2 (580 μL) and reacted according to GP E. After purification by column chromatography on silica (isohexane/ CH_2Cl_2 6:4), **6ew** (20.0 mg, 51%) was obtained as an oil: ^1H NMR (400 MHz, CDCl_3) δ 8.27 (d, J = 8.5 Hz, 1H, Ar), 7.95–7.88 (m, 1H, Ar), 7.87–7.75 (m, 4H, Ar), 7.69 (d, J = 7.1 Hz, 1H, Ar), 7.60 (ddd, J = 8.5, 6.8, 1.5 Hz, 1H, Ar), 7.54 (ddd, J = 8.0, 6.9, 1.2 Hz, 1H, Ar), 7.50–7.45 (m, 1H, Ar), 7.45–7.39 (m, 2H, Ar), 7.32 (d, J = 8.4 Hz, 1H, Ar), 7.16 (q, J = 6.6 Hz, 1H, CH), 2.47 (s, 3H, Me), 1.94 (d, J = 6.5 Hz, 3H, Me) ppm; $^{13}\text{C}\{^1\text{H}\}$ NMR (101 MHz, CDCl_3) δ 169.23, 137.16, 133.99, 133.33, 131.77, 130.41, 130.38, 130.17, 129.70, 129.11, 128.76, 128.52, 128.15, 127.08, 126.54, 125.91, 125.57, 125.52, 124.63, 123.76, 123.34, 70.52, 22.17, 20.21 ppm; IR (ATR) ν (cm^{-1}) 2958, 1710, 1593, 1511, 1470, 1390, 1285, 1247, 1215, 1150, 1046, 957, 813, 770, 751; HRMS (EI) m/z [M] $^+$ calcd for $\text{C}_{24}\text{H}_{20}\text{O}_2$ 340.1463, found 340.1459.

2-(Naphthalen-1-yl)ethyl Benzoate 7ea. Compound **2e** (60.0 mg, 348 μmol , 1.0 equiv), **3a** (94.6 mg, 418 μmol , 1.5 equiv), DMAP (2.13 mg, 17.4 μmol , 0.05 equiv), and Et_3N (100 μL , 696 μmol , 1.5 equiv) were dissolved in CH_2Cl_2 (2 mL) and reacted according to GP E. After purification by column chromatography on silica (isohexane/ CH_2Cl_2 6:4), **7ea** (94.0 mg, 98%) was obtained as an oil: ^1H NMR (400 MHz, CDCl_3) δ 8.23–8.16 (m, 1H, Ar), 8.06–7.99 (m, 2H, Ar), 7.92–7.86 (m, 1H, Ar), 7.81–7.76 (m, 1H, Ar), 7.61–7.53 (m, 2H, Ar), 7.54–7.48 (m, 1H, Ar), 7.47–7.41 (m, 4H, Ar), 4.68 (t, J = 7.3 Hz, 2H, CH_2), 3.57 (t, J = 7.3 Hz, 2H, CH_2) ppm; $^{13}\text{C}\{^1\text{H}\}$ NMR (101 MHz, CDCl_3) δ 166.76, 134.03, 133.91, 133.07, 132.23, 130.39, 129.75, 128.97, 128.47, 127.63, 127.22, 126.36, 125.82, 125.66, 123.80, 65.12, 32.48 ppm; HRMS (EI) m/z [M] $^+$ calcd for $\text{C}_{19}\text{H}_{16}\text{O}_2$ 276.1150, found 276.1136. The $^1\text{H}/^{13}\text{C}\{^1\text{H}\}$ NMR spectra are in full agreement with them reported in literature.⁴²

2-(Naphthalen-1-yl)ethyl 2-Phenylbenzoate 7ef. Compound **2e** (20.0 mg, 116 μmol , 1.0 equiv), **3f** (48.3 mg, 127 μmol , 1.1 equiv), DMAP (709 μg , 5.81 μmol , 0.05 equiv), and Et_3N (32.4 μL , 232 μmol , 1.5 equiv) were dissolved in CH_2Cl_2 (580 μL) and reacted according to GP E. After purification by column chromatography on silica (isohexane/ CH_2Cl_2 6:4), **7ef** (31 mg, 76%) was obtained as an oil: ^1H NMR (400 MHz, CDCl_3) δ 7.93 (d, J = 8.2 Hz, 1H, Ar), 7.87–7.82 (m, 1H, Ar), 7.79 (d, J = 6.9 Hz, 1H, Ar), 7.73 (d, J = 8.2 Hz, 1H, Ar), 7.57–7.45 (m, 3H, Ar), 7.43–7.32 (m, 8H, Ar), 7.20 (d, J = 6.9 Hz, 1H, Ar), 4.37 (t, J = 7.6 Hz, 2H, CH_2), 3.11 (t, J = 7.6 Hz, 2H, CH_2) ppm; $^{13}\text{C}\{^1\text{H}\}$ NMR (101 MHz, CDCl_3) δ 168.96, 142.59, 141.69, 133.94, 133.61, 132.07, 131.36, 131.29, 130.76, 129.94, 128.91, 128.59, 128.22, 127.51, 127.39, 127.33, 127.02, 126.26, 125.75, 125.60, 123.69, 64.96, 31.82 ppm; IR (ATR) ν (cm^{-1}) 3058, 1714, 1597, 1436, 1276, 1123, 1047, 774, 698; HRMS (EI) m/z [M] $^+$ calcd for $\text{C}_{25}\text{H}_{20}\text{O}_2$ 352.1463, found 352.1465.

2-(Naphthalen-1-yl)ethyl 2,6-Dimethylbenzoate 7em. Compound **2e** (20.0 mg, 116 μmol , 1.0 equiv), **3m** (36.1 mg, 128 μmol , 1.1 equiv), DMAP (709 μg , 5.81 μmol , 0.05 equiv), and Et_3N (32.4 μL , 232 μmol , 2.0 equiv) were dissolved in CH_2Cl_2 (580 μL) and reacted according to GP E. After purification by column chromatography on silica (isohexane/ CH_2Cl_2 6:4), **7em** (20.0 mg, 57%) was obtained as a

white solid; mp 81–82 °C; $^1\text{H NMR}$ (400 MHz, CDCl_3) δ 8.16 (d, J = 8.5 Hz, 1H, Ar), 7.88 (dd, J = 8.1, 1.3 Hz, 1H, Ar), 7.82–7.75 (m, 1H, Ar), 7.57 (ddd, J = 8.4, 6.8, 1.5 Hz, 1H, Ar), 7.51 (ddd, J = 8.0, 6.8, 1.3 Hz, 1H, Ar), 7.43 (q, J = 3.5 Hz, 2H, Ar), 7.22–7.17 (m, 1H, Ar), 7.03 (d, J = 7.5 Hz, 2H, Ar), 4.69 (dd, J = 7.8, 7.2 Hz, 2H, CH_2), 3.57 (t, J = 7.5 Hz, 2H, CH_2), 2.28 (s, 6H, Me_2) ppm; $^{13}\text{C}\{^1\text{H}\}$ NMR (101 MHz, CDCl_3) δ 169.47, 137.07, 134.98, 134.17, 133.95, 130.41, 129.38, 129.07, 128.73, 127.69, 126.49, 125.88, 125.48, 123.70, 123.33, 70.02, 21.88, 19.81 ppm; IR (ATR) ν (cm^{-1}) 2920, 1720, 1596, 1443, 1271, 1117, 1065, 1003, 801.741; HRMS (EI) m/z [M] $^+$ calcd for $\text{C}_{21}\text{H}_{20}\text{O}_2$ 304.1463, found 304.1460.

2-(Naphthalen-1-yl)ethyl 2-Methyl-6-phenylbenzoate 7en. Compound **2e** (15.0 mg, 87.1 μmol , 1.0 equiv), **3n** (38.9 mg, 95.8 μmol , 1.1 equiv), DMAP (532 μg , 4.35 μmol , 0.05 equiv), and Et_3N (18.2 μL , 131 μmol , 1.5 equiv) were dissolved in CH_2Cl_2 (435 μL) and reacted according to GP E. After purification by column chromatography on silica (isohexane/ CH_2Cl_2 6:4), **7en** (25.0 mg, 78%) was obtained as an oil: $^1\text{H NMR}$ (400 MHz, CDCl_3) δ 7.90 (d, J = 8.2 Hz, 1H, Ar), 7.87–7.82 (m, 1H, Ar), 7.73 (d, J = 8.2 Hz, 1H, Ar), 7.50 (dddd, J = 15.9, 8.1, 6.8, 1.5 Hz, 2H, Ar), 7.40–7.28 (m, 7H, Ar), 7.23 (d, J = 7.6 Hz, 2H, Ar), 7.18 (d, J = 6.9 Hz, 1H, Ar), 4.32 (dd, J = 8.2, 7.3 Hz, 2H, CH_2), 3.04 (t, J = 7.7 Hz, 2H, CH_2), 2.40 (s, 3H, Me) ppm; $^{13}\text{C}\{^1\text{H}\}$ NMR (101 MHz, CDCl_3) δ 169.87, 141.24, 140.46, 135.70, 133.93, 133.44, 133.30, 132.02, 129.55, 129.31, 128.90, 128.54, 128.42, 127.51, 127.50, 127.36, 126.99, 126.26, 125.75, 125.60, 123.66, 64.89, 31.78, 19.87 ppm; IR (ATR) ν (cm^{-1}) 2956, 1720, 1591, 1461, 1261, 1122, 1061, 907, 775, 699; HRMS (EI) m/z [M] $^+$ calcd for $\text{C}_{26}\text{H}_{22}\text{O}_2$ 366.1620, found 366.1612.

2-(Naphthalen-1-yl)ethyl 2-Methyl-6-nitrobenzoate 7eo. Compound **2e** (20.0 mg, 116 μmol , 1.0 equiv), **3o** (44.0 mg, 128 μmol , 1.2 equiv), DMAP (709 μg , 5.81 μmol , 0.05 equiv), and Et_3N (32.4 μL , 232 μmol , 2.0 equiv) were dissolved in CH_2Cl_2 (580 μL) and reacted according to GP E. After purification by column chromatography on silica (isohexane/ CH_2Cl_2 6:4), **7eo** (30.0 mg, 78%) was obtained as an oil: $^1\text{H NMR}$ (400 MHz, CDCl_3) δ 8.14 (d, J = 7.8 Hz, 1H, Ar), 8.00 (d, J = 8.1 Hz, 1H, Ar), 7.89–7.86 (m, 1H, Ar), 7.80–7.75 (m, 1H, Ar), 7.58–7.48 (m, 3H, Ar), 7.47 (d, J = 8.0 Hz, 1H, Ar), 7.42 (dd, J = 5.3, 3.9 Hz, 2H, Ar), 4.74 (dd, J = 7.9, 7.2 Hz, 2H, CH_2), 3.57 (t, J = 7.6 Hz, 2H, CH_2), 2.32 (s, 3H, Me) ppm; $^{13}\text{C}\{^1\text{H}\}$ NMR (101 MHz, CDCl_3) δ 166.56, 146.30, 137.71, 136.11, 134.00, 133.27, 132.11, 129.84, 129.57, 128.95, 127.70, 127.15, 126.43, 125.83, 125.63, 123.62, 121.92, 66.07, 31.91, 19.18 ppm; IR (ATR) ν (cm^{-1}) 2959, 1732, 1500, 1462, 1343, 1264, 1112, 1068, 954, 776; HRMS (EI) m/z [M] $^+$ calcd for $\text{C}_{20}\text{H}_{17}\text{O}_4\text{N}$ 335.1158, found 335.1158.

2-(Naphthalen-1-yl)ethyl 2-Methoxy-1-naphthoate 7er. Compound **2e** (20.0 mg, 116 μmol , 1.0 equiv), **3r** (53.8 mg, 139 μmol , 1.2 equiv), DMAP (709 μg , 5.81 μmol , 0.05 equiv), and Et_3N (32.4 μL , 232 μmol , 2.0 equiv) were dissolved in CH_2Cl_2 (580 μL) and reacted according to GP E. After purification by column chromatography on silica (isohexane/ CH_2Cl_2 6:4), **7er** (40.0 mg, 97%) was obtained as a white solid; mp 74–75 °C; $^1\text{H NMR}$ (400 MHz, CDCl_3) δ 8.21 (d, J = 8.4 Hz, 1H, Ar), 7.90 (t, J = 8.1 Hz, 2H, Ar), 7.79 (d, J = 8.1 Hz, 2H, Ar), 7.66 (d, J = 8.3 Hz, 1H, Ar), 7.59–7.40 (m, 5H, Ar), 7.36 (ddd, J = 8.1, 6.8, 1.2 Hz, 1H, Ar), 7.29 (d, J = 9.1 Hz, 1H, Ar), 4.82 (t, J = 7.5 Hz, 2H, CH_2), 3.93 (s, 3H, Me), 3.63 (t, J = 7.5 Hz, 2H, CH_2) ppm; $^{13}\text{C}\{^1\text{H}\}$ NMR (101 MHz, CDCl_3) δ 168.20, 154.64, 134.03, 133.72, 132.23, 131.82, 131.10, 128.94, 128.65, 128.19, 127.75, 127.61, 127.30, 126.39, 125.82, 125.67, 124.24, 123.93, 123.82, 117.65, 113.23, 65.47, 56.87, 32.49 ppm; IR (ATR) ν (cm^{-1}) 2953, 1726, 1593, 1511, 1468, 1282, 1256, 1227, 1139, 1073, 1018, 965, 779, 745; HRMS (EI) m/z [M] $^+$ calcd for $\text{C}_{24}\text{H}_{20}\text{O}_3$ 356.1412, found 356.1409.

2-(Naphthalen-1-yl)ethyl 2-Ethoxy-1-naphthoate 7es. Compound **2e** (20.0 mg, 116 μmol , 1.0 equiv), **3s** (57.8 mg, 139 μmol , 1.2 equiv), DMAP (709 μg , 5.81 μmol , 0.05 equiv), and Et_3N (32.4 μL , 232 μmol , 2.0 equiv) were dissolved in CH_2Cl_2 (580 μL) and reacted according to GP E. After purification by column chromatography on silica (isohexane/ CH_2Cl_2 6:4), **7es** (43.0 mg, quant.) was obtained as an oil: $^1\text{H NMR}$ (400 MHz, CDCl_3) δ 8.22 (d, J = 8.3 Hz, 1H, Ar), 7.89 (d, J = 8.9 Hz, 2H, Ar), 7.79 (d, J = 8.1 Hz, 2H, Ar), 7.69 (d, J = 8.4 Hz, 1H, Ar), 7.59–7.34 (m, 6H, Ar), 7.27 (d, J = 10.5 Hz, 1H, Ar), 4.80 (t, J

= 7.6 Hz, 2H, CH_2), 4.21 (q, J = 7.0 Hz, 2H, CH_2), 3.64 (t, J = 7.6 Hz, 2H, CH_2), 1.40 (t, J = 7.0 Hz, 3H, Me) ppm; $^{13}\text{C}\{^1\text{H}\}$ NMR (101 MHz, CDCl_3) δ 168.30, 154.04, 134.04, 133.69, 132.23, 131.65, 131.11, 128.94, 128.69, 128.17, 127.67, 127.63, 127.27, 126.41, 125.83, 125.68, 124.25, 123.96, 123.81, 118.27, 114.57, 65.54, 65.38, 32.58, 15.16 ppm; IR (ATR) ν (cm^{-1}) 2895, 1719, 1594, 1510, 1465, 1280, 1212, 1134, 1063, 1023, 776; HRMS (EI) m/z [M] $^+$ calcd for $\text{C}_{25}\text{H}_{22}\text{O}_3$ 370.1569, found 370.1563.

2-(Naphthalen-1-yl)ethyl 2-Methyl-1-naphthoate 7ew. Compound **2e** (20.0 mg, 116 μmol , 1.0 equiv), **3w** (45.3 mg, 128 μmol , 1.1 equiv), DMAP (709 μg , 5.81 μmol , 0.05 equiv), and Et_3N (32.4 μL , 232 μmol , 2.0 equiv) were dissolved in CH_2Cl_2 (580 μL) and reacted according to GP E. After purification by column chromatography on silica (isohexane/ CH_2Cl_2 6:4), **7ew** (20.0 mg, 51%) was obtained as a white solid; mp 65–67 °C; $^1\text{H NMR}$ (400 MHz, CDCl_3) δ 8.19 (d, J = 8.4 Hz, 1H, Ar), 7.92–7.88 (m, 1H, Ar), 7.83–7.78 (m, 3H, Ar), 7.77–7.71 (m, 1H, Ar), 7.54 (dddd, J = 19.4, 8.1, 6.8, 1.4 Hz, 2H, Ar), 7.48–7.40 (m, 4H, Ar), 7.32 (d, J = 8.4 Hz, 1H, Ar), 4.83 (t, J = 7.4 Hz, 2H, CH_2), 3.64 (t, J = 7.4 Hz, 2H, CH_2), 2.45 (s, 3H, Me) ppm; $^{13}\text{C}\{^1\text{H}\}$ NMR (101 MHz, CDCl_3) δ 169.84, 134.06, 133.58, 133.51, 132.14, 131.76, 130.16, 129.81, 129.00, 128.50, 128.15, 127.73, 127.36, 127.14, 126.45, 125.86, 125.67, 125.58, 124.66, 123.69, 65.38, 32.49, 20.27 ppm (one signal is overlapping); IR (ATR) ν (cm^{-1}) 2958, 1710, 1539, 1511, 1390, 1285, 1247, 1215, 1150, 1046, 957, 813, 780, 751; HRMS (EI) m/z [M] $^+$ calcd for $\text{C}_{24}\text{H}_{20}\text{O}_2$ 340.1463, found 340.1459.

1-(Anthracen-2-yl)ethyl 2-Phenylbenzoate 6ff. Compound **1f** (15.0 mg, 67.5 μmol , 1.0 equiv), **3f** (28.1 mg, 74.2 μmol , 1.1 equiv), DMAP (412 μg , 3.37 μmol , 0.05 equiv), and Et_3N (18.8 μL , 134 μmol , 2.0 equiv) were dissolved in CH_2Cl_2 (340 μL) and reacted according to GP E. After purification by column chromatography on silica (isohexane/ CH_2Cl_2 6:4), **6ff** (15.0 mg, 55%) was obtained as a brown solid; mp 115–118 °C; $^1\text{H NMR}$ (400 MHz, CDCl_3) δ 8.36 (d, J = 11.8 Hz, 2H, Ar), 8.04–7.97 (m, 2H, Ar), 7.89 (t, J = 8.2 Hz, 2H, Ar), 7.73 (s, 1H, Ar), 7.53 (td, J = 7.5, 1.4 Hz, 1H, Ar), 7.49–7.45 (m, 2H, Ar), 7.45–7.40 (m, 1H, Ar), 7.38 (dd, J = 7.6, 1.0 Hz, 1H, Ar), 7.36–7.28 (m, 4H, Ar), 7.26–7.21 (m, 1H, Ar), 7.14 (dd, J = 8.8, 1.6 Hz, 1H, Ar), 6.08 (q, J = 6.6 Hz, 1H, CH), 1.44 (d, J = 6.6 Hz, 3H, Me) ppm; $^{13}\text{C}\{^1\text{H}\}$ NMR (151 MHz, CDCl_3) δ 168.25, 142.59, 141.62, 138.00, 131.98, 131.91, 131.47, 131.35, 131.31, 131.30, 130.91, 130.09, 128.69, 128.30, 128.28, 128.21, 127.34, 127.31, 126.61, 126.11, 125.56, 125.54, 125.19, 124.02, 73.67, 21.70 ppm (one signal is overlapping); IR (ATR) ν (cm^{-1}) 2919, 1715, 1597, 1530, 1448, 1278, 1243, 1126, 1091, 1044, 989, 894, 750, 701 HRMS (EI) m/z [M] $^+$ calcd for $\text{C}_{29}\text{H}_{22}\text{O}_2$ 402.1620, found 402.1615.

2-(Anthracen-2-yl)ethyl 2-Phenylbenzoate 7ff. Compound **2f** (15.0 mg, 67.5 μmol , 1.0 equiv), **3f** (28.1 mg, 74.2 μmol , 1.1 equiv), DMAP (412 μg , 3.37 μmol , 0.05 equiv), and Et_3N (18.8 μL , 134 μmol , 2.0 equiv) were dissolved in CH_2Cl_2 (340 μL) and reacted according to GP E. After purification by column chromatography on silica (isohexane/ CH_2Cl_2 6:4), **7ff** (15.0 mg, 55%) was obtained as a yellow solid; mp 102–104 °C; $^1\text{H NMR}$ (400 MHz, CDCl_3) δ 8.35 (d, J = 24.5 Hz, 2H, Ar), 8.02–7.95 (m, 2H, Ar), 7.91 (d, J = 8.7 Hz, 1H, Ar), 7.79 (d, J = 8.0 Hz, 1H, Ar), 7.67 (s, 1H, Ar), 7.52 (td, J = 7.6, 1.4 Hz, 1H, Ar), 7.49–7.42 (m, 2H, Ar), 7.42–7.29 (m, 7H, Ar), 7.20 (dd, J = 8.7, 1.6 Hz, 1H, Ar), 4.39 (t, J = 7.1 Hz, 2H, CH_2), 2.85 (t, J = 7.1 Hz, 2H, CH_2) ppm; $^{13}\text{C}\{^1\text{H}\}$ NMR (151 MHz, CDCl_3) δ 168.88, 142.64, 141.61, 134.76, 131.99, 131.84, 131.62, 131.37, 131.16, 130.81, 130.78, 129.98, 128.54, 128.48, 128.31, 128.22, 128.18, 127.37, 127.31, 127.28, 127.13, 126.13, 125.76, 125.51, 125.32, 65.27, 35.10 ppm; IR (ATR) ν (cm^{-1}) 2954, 1715, 1597, 1530, 1452, 1275, 1124, 1045, 972, 959, 893, 780, 760, 705; HRMS (EI) m/z [M] $^+$ calcd for $\text{C}_{29}\text{H}_{22}\text{O}_2$ 402.1620, found 402.1616.

Computational Details. All geometry optimizations and vibrational frequency calculations have been performed using the B3LYP-D3 hybrid functional^{16e,g,h} in combination with the 6-31+G(d) basis set.⁴⁴ Solvent effects for chloroform have been taken into account with the SMD continuum solvation model.^{16d} This combination has recently been found to perform well for the description of charge-separated intermediates.^{15,18} Thermochemical corrections to 298.15 K have been calculated for all stationary points from unscaled vibrational frequencies

obtained at this same level. Solvation energies have been obtained as the difference between the energies computed at B3LYP-D3/6-31+G(d) in solution and in the gas phase. For the elucidation of the mechanism, the thermochemical corrections of optimized structures have been combined with single-point energies calculated at the DLPNO-CCSD(T)/def2-TZVPP//B3LYP-D3/6-31+G(d) level.^{16b,c,f,45} Solvation energies have been added to the energy computed at the DLPNO-CCSD(T)/def2-TZVPP//SMD(CHCl₃)/B3LYP-D3/6-31+G(d) level to yield free energies G_{298} at 298.15 K. Free energies in solution have been corrected to a reference state of 1 mol/L at 298.15 K through the addition of $RT\ln(24.46) = +7.925$ kJ/mol to the free energies. All calculations have been performed with Gaussian 09⁴⁶ and ORCA, version 4.0.⁴⁷ Conformation search was performed with Maestro.⁴⁸ The charges have been analyzed using the NBO formalism⁴⁹ on the B3LYP-D3/6-31+G(d) results.

■ ASSOCIATED CONTENT

SI Supporting Information

The Supporting Information is available free of charge at <https://pubs.acs.org/doi/10.1021/acs.joc.0c02848>.

NMR spectroscopic data and crystallographic data (PDF)

Details regarding kinetic study (PDF)

Details regarding computational details about reaction path, thermochemical data, and Cartesian coordinates (PDF)

Crystallographic information file and data (PDF)

Accession Codes

CCDC 1970478–1970499 contain the supplementary crystallographic data for this paper. These data can be obtained free of charge via www.ccdc.cam.ac.uk/data_request/cif, or by emailing data_request@ccdc.cam.ac.uk, or by contacting The Cambridge Crystallographic Data Centre, 12 Union Road, Cambridge CB2 1EZ, UK; fax: +44 1223 336033.

■ AUTHOR INFORMATION

Corresponding Author

Hendrik Zipse – Department of Chemistry, Ludwig-Maximilians-Universität, 81377 München, Germany;
orcid.org/0000-0002-0534-3585; Email: zipse@cup.lmu.de

Authors

Stefanie Mayr – Department of Chemistry, Ludwig-Maximilians-Universität, 81377 München, Germany;
orcid.org/0000-0002-8766-9852

Marta Marin-Luna – Department of Chemistry, Ludwig-Maximilians-Universität, 81377 München, Germany;
orcid.org/0000-0003-3531-6622

Complete contact information is available at: <https://pubs.acs.org/doi/10.1021/acs.joc.0c02848>

Notes

The authors declare no competing financial interest.

■ ACKNOWLEDGMENTS

This work was financially supported by the Deutsche Forschungsgemeinschaft (DFG) through the Priority Program “Control of London Dispersion Interactions in Molecular Chemistry” (SPP 1807), grant ZI 436/17-1. M.M.-L. thanks Xunta de Galicia for her postdoctoral contract (ED481B 2016/166-0).

■ REFERENCES

- (1) (a) Robles, O.; Romo, D. Chemo- and site-selective derivatizations of natural products enabling biological studies. *Nat. Prod. Rep.* **2014**, *31*, 318–334. (b) Nicolaou, K. C.; Chen, J. S. *Classics in Total Synthesis III*; Wiley-VCH: Weinheim, 2011.
- (2) (a) Zong, G.; Barber, E.; Aljewari, H.; Zhou, J.; Hu, Z.; Du, Y.; Shi, W. Q. Total Synthesis and Biological Evaluation of Ipomoeassin F and Its Unnatural 11R-Epimer. *J. Org. Chem.* **2015**, *80*, 9279–9291. (b) Baran, P. S.; Maimone, T. J.; Richter, J. M. Total synthesis of marine natural products without using protecting groups. *Nature* **2007**, *446*, 404–408. (c) Koshimizu, M.; Nagatomo, M.; Inoue, M. Unified Total Synthesis of 3-epi-Ryanodol, Cinnzeylanol, Cinnacassiol A and B, and Structural Revision of Natural Ryanodol and Cinnacassiol. *Angew. Chem., Int. Ed.* **2016**, *55*, 2493–2497.
- (3) Polyakova, S. M.; Nizovtsev, A. V.; Kunetskiy, R. A.; Bovin, N. V. New protecting groups in the synthesis of oligosaccharides. *Russ. Chem. Bull.* **2015**, *64*, 973–989.
- (4) (a) Wuts, P. G. M. *Greene's Protective Groups in Organic Synthesis*; John Wiley & Sons: Hoboken, NJ, 2014. (b) Araki, S.; Kambe, S.; Kameda, K.; Hirashita, T. A New Synthesis of Lavandulol via Indium/Palladium-Mediated Umpolung of Vinyloxirane. *Synthesis* **2003**, *2003*, 0751–0754. (c) Baldessari, A.; Mangone, C. P.; Gros, E. G. Lipase-Catalyzed Acylation and Deacylation Reactions of Pyridoxine, a Member of Vitamin-B6 Group. *Helv. Chim. Acta* **1998**, *81*, 2407–2413. (d) Lewis, C. A.; Miller, S. J. Site-Selective Derivatization and Remodeling of Erythromycin A by Using Simple Peptide-Based Chiral Catalysts. *Angew. Chem., Int. Ed.* **2006**, *45*, 5616–5619.
- (5) (a) Haines, A. H. Relative Reactivities of Hydroxyl Groups in Carbohydrates. *Adv. Carbohydr. Chem. Biochem.* **1976**, *33*, 11–109. (b) Nahmany, M.; Melman, A. Chemoselectivity in reactions of esterification. *Org. Biomol. Chem.* **2004**, *2*, 1563–1572. (c) Afagh, N. A.; Yudin, A. K. Chemoselectivity and the Curious Reactivity Preferences of Functional Groups. *Angew. Chem., Int. Ed.* **2010**, *49*, 262–310. (d) Peng, P.; Linseis, M.; Winter, R. F.; Schmidt, R. R. Regioselective Acylation of Diols and Triols: The Cyanide Effect. *J. Am. Chem. Soc.* **2016**, *138*, 6002–6009.
- (6) Ishihara, K.; Kurihara, H.; Yamamoto, H. An extremely simple, convenient, and selective method for acetylating primary alcohols in the presence of secondary alcohols. *J. Org. Chem.* **1993**, *58*, 3791–3793.
- (7) Toda, Y.; Sakamoto, T.; Komiyama, Y.; Kikuchi, A.; Suga, H. A Phosphonium Ylide as an Ionic Nucleophilic Catalyst for Primary Hydroxyl Group Selective Acylation of Diols. *ACS Catal.* **2017**, *7*, 6150–6154.
- (8) (a) Ishihara, K.; Nakayama, M.; Ohara, S.; Yamamoto, H. Direct ester condensation from a 1:1 mixture of carboxylic acids and alcohols catalyzed by hafnium(IV) or zirconium(IV) salts. *Tetrahedron* **2002**, *58*, 8179–8188. (b) Inanaga, J.; Hirata, K.; Saeki, H.; Katsuki, T.; Yamaguchi, M. A Rapid Esterification by Means of Mixed Anhydride and Its Application to Large-ring Lactonization. *Bull. Chem. Soc. Jpn.* **1979**, *52*, 1989–1993. (c) Kawanami, Y.; Dainobu, Y.; Inanaga, J.; Katsuki, T.; Yamaguchi, M. Synthesis of Thiol Esters by Carboxylic Trichlorobenzoic Anhydrides. *Bull. Chem. Soc. Jpn.* **1981**, *54*, 943–944. (d) Shiina, I.; Kubota, M.; Oshiumi, H.; Hashizume, M. An Effective Use of Benzoic Anhydride and Its Derivatives for the Synthesis of Carboxylic Esters and Lactones: A Powerful and Convenient Mixed Anhydride Method Promoted by Basic Catalysts. *J. Org. Chem.* **2004**, *69*, 1822–1830.
- (9) (a) Kawabata, T.; Muramatsu, W.; Nishio, T.; Shibata, T.; Schedel, H. A Catalytic One-Step Process for the Chemo- and Regioselective Acylation of Monosaccharides. *J. Am. Chem. Soc.* **2007**, *129*, 12890–12895. (b) Ueda, Y.; Furuta, T.; Kawabata, T. Final-Stage Site-Selective Acylation for the Total Syntheses of Multifidosides A–C. *Angew. Chem.* **2015**, *127*, 12134–12138. (c) Merad, J.; Borkar, P.; Caijo, F.; Pons, J.-M.; Parrain, J.-L.; Chuzel, O.; Bressy, C. Double Catalytic Kinetic Resolution (DoCKR) of Acyclic anti-1,3-Diols: The Additive Horeau Amplification. *Angew. Chem., Int. Ed.* **2017**, *56*, 16052–16056. (d) Merad, J.; Borkar, P.; Bouyon Yenda, T.; Roux, C.; Pons, J.-M.; Parrain, J.-L.; Chuzel, O.; Bressy, C. Highly Enantioselective Acylation of Acyclic Meso 1,3-Diols through Synergistic Isothiourea-Catalyzed

Desymmetrization/Chiroablative Kinetic Resolution. *Org. Lett.* **2015**, *17* (9), 2118–2121. (e) Roux, C.; Candy, M.; Pons, J.-M.; Chuzel, O.; Bressy, C. Stereocontrol of All-Carbon Quaternary Centers through Enantioselective Desymmetrization of Meso Primary Diols by Organocatalyzed Acyl Transfer. *Angew. Chem., Int. Ed.* **2014**, *53*, 766–770.

(10) Kattinig, E.; Albert, M. Counterion-Directed Regioselective Acetylation of Octyl β -D-Glucopyranoside. *Org. Lett.* **2004**, *6*, 945–948.

(11) Helberg, J.; Marin-Luna, M.; Zipse, H. Chemoselectivity in Esterification Reactions – Size Matters after All. *Synthesis* **2017**, *49*, 3460–3470.

(12) (a) Wei, Y.; Held, I.; Zipse, H. Stacking interactions as the principal design element in acyl-transfer catalysts. *Org. Biomol. Chem.* **2006**, *4*, 4223–4230. (b) Xu, S.; Held, I.; Kempf, B.; Mayr, H.; Steglich, W.; Zipse, H. The DMAP-Catalyzed Acetylation of Alcohols—A Mechanistic Study (DMAP = 4-(Dimethylamino)pyridine). *Chem. - Eur. J.* **2005**, *11*, 4751–4757. (c) Held, I.; Villinger, A.; Zipse, H. The Stability of Acylpyridinium Cations and Their Relation to the Catalytic Activity of Pyridine Bases. *Synthesis* **2005**, *2005*, 1425–1430. (d) Larionov, E.; Mahesh, M.; Spivey, A. C.; Wei, Y.; Zipse, H. Theoretical Prediction of Selectivity in Kinetic Resolution of Secondary Alcohols Catalyzed by Chiral DMAP Derivatives. *J. Am. Chem. Soc.* **2012**, *134*, 9390–9399.

(13) Tandon, R.; Nigst, T. A.; Zipse, H. Inductive Effects through Alkyl Groups – How Long is Long Enough? *Eur. J. Org. Chem.* **2013**, *2013*, 5423–5430.

(14) Alcohols carrying 1-naphthyl (**1e/2e**) or 2-anthracenyl substituents (**1f/2f**) were also tested for a smaller set of anhydrides as compared to phenyl alcohols **1a/2a** (see [Supporting Information](#)). However, due to severe practical problems (low solubility, ^1H NMR signal overlap), these substrates were not investigated further.

(15) Marin-Luna, M.; Pölloth, B.; Zott, F.; Zipse, H. Size-dependent rate acceleration in the silylation of secondary alcohols: the bigger the faster. *Chem. Sci.* **2018**, *9*, 6509–6515.

(16) (a) Park, S. Y.; Lee, J.-W.; Song, C. E. Parts-per-million level loading organocatalyzed enantioselective silylation of alcohols. *Nat. Commun.* **2015**, *6*, 7512. (b) Riplinger, C.; Sandhoefer, B.; Hansen, A.; Neese, F. Natural triple excitations in local coupled cluster calculations with pair natural orbitals. *J. Chem. Phys.* **2013**, *139*, 134101. (c) Riplinger, C.; Neese, F. An efficient and near linear scaling pair natural orbital based local coupled cluster method. *J. Chem. Phys.* **2013**, *138*, 034106. (d) Marenich, A. V.; Cramer, C. J.; Truhlar, D. G. Universal Solvation Model Based on Solute Electron Density and on a Continuum Model of the Solvent Defined by the Bulk Dielectric Constant and Atomic Surface Tensions. *J. Phys. Chem. B* **2009**, *113*, 6378–6396. (e) Grimme, S. Semiempirical hybrid density functional with perturbative second-order correlation. *J. Chem. Phys.* **2006**, *124*, 034108. (f) Weigend, F.; Ahlrichs, R. Balanced basis sets of split valence, triple zeta valence and quadruple zeta valence quality for H to Rn: Design and assessment of accuracy. *Phys. Chem. Chem. Phys.* **2005**, *7*, 3297–3305. (g) Becke, A. D. Density-functional thermochemistry. III. The role of exact exchange. *J. Chem. Phys.* **1993**, *98*, 5648–5652. (h) Lee, C.; Yang, W.; Parr, R. G. Development of the Colle-Salvetti correlation-energy formula into a functional of the electron density. *Phys. Rev. B: Condens. Matter Mater. Phys.* **1988**, *37*, 785–789.

(17) Marin-Luna, M.; Patschinski, P.; Zipse, H. Substituent Effects in the Silylation of Secondary Alcohols: A Mechanistic Study. *Chem. - Eur. J.* **2018**, *24*, 15052–15058.

(18) Legault, C. *CYLview*, version 1.0b; Université de Sherbrooke, 2009 (<http://www.cylview.org/>). 3D pictures were generated with the *CYLview* program.

(19) (a) Johnson, E. R.; Keinan, S.; Mori-Sánchez, P.; Contreras-García, J.; Cohen, A. J.; Yang, W. Revealing Noncovalent Interactions. *J. Am. Chem. Soc.* **2010**, *132*, 6498–6506. (b) Contreras-García, J.; Johnson, E. R.; Keinan, S.; Chaudret, R.; Piquemal, J.-P.; Beratan, D. N.; Yang, W. NCIPLOT: A Program for Plotting Noncovalent Interaction Regions. *J. Chem. Theory Comput.* **2011**, *7*, 625–632.

(20) Chen, Y.-Z.; Ni, C.-W.; Teng, F.-L.; Ding, Y.-S.; Lee, T.-H.; Ho, J.-H. Construction of polyaromatics via photocyclization of 2-(fur-3-

yl)ethenylarenes, using a 3-furyl group as an isopropenyl equivalent synthon. *Tetrahedron* **2014**, *70*, 1748–1762.

(21) Nishimura, T.; Xu, S.-Y.; Jiang, Y.-B.; Fossey, J. S.; Sakurai, K.; Bull, S. D.; James, T. D. A simple visual sensor with the potential for determining the concentration of fluoride in water at environmentally significant levels. *Chem. Commun.* **2013**, *49*, 478–480.

(22) Casas-Solvas, J. M.; Mooibroek, T. J.; Sandramurthy, S.; Howgego, J. D.; Davis, A. P. A Practical, Large-Scale Synthesis of Pyrene-2-Carboxylic Acid. *Synlett* **2014**, *25*, 2591–2594.

(23) Laali, K. K.; Arrica, M. A.; Okazaki, T.; Bunge, S. D. Synthesis and Stable-Ion Studies of Regioisomeric Acetylnitropyrenes and Nitropyrenyl Carbinols and GIAO-DFT Study of Nitro Substituent Effects on α -Pyrenyl Carbocations. *Eur. J. Org. Chem.* **2008**, *2008*, 6093–6105.

(24) Harvey, R. G.; Konieczny, M.; Pataki, J. Synthesis of the isomeric mono- and bisoxiranylpyrenes. *J. Org. Chem.* **1983**, *48*, 2930–2932.

(25) Deck, L. M.; Daub, G. H. Synthesis of 10-(chloromethyl)benzo[a]pyrene. *J. Org. Chem.* **1983**, *48*, 3577–3580.

(26) Adib, M.; Pashazadeh, R.; Rajai-Daryasari, S.; Mirzaei, P.; Jamal Addin Gohari, S. Metal-free cross-dehydrogenative coupling of aryl aldehydes to give symmetrical carboxylic anhydrides promoted by the TBHP/ $n\text{Bu}_4\text{PBr}$ system. *Tetrahedron Lett.* **2016**, *57*, 3071–3074.

(27) Phakhodee, W.; Duangkamol, C.; Wangngae, S.; Pattarawarapan, M. Acid anhydrides and the unexpected N,N-diethylamides derived from the reaction of carboxylic acids with $\text{Ph}_3\text{P}/\text{I}_2/\text{Et}_3\text{N}$. *Tetrahedron Lett.* **2016**, *57*, 325–328.

(28) Kita, Y.; Akai, S.; Ajimura, N.; Yoshigi, M.; Tsugoshi, T.; Yasuda, H.; Tamura, Y. Facile and efficient syntheses of carboxylic anhydrides and amides using (trimethylsilyl)ethoxyacetylene. *J. Org. Chem.* **1986**, *51*, 4150–4158.

(29) Kazemi, F.; Sharghi, H.; Nasser, M. A. A Cheap, Simple and Efficient Method for the Preparation of Symmetrical Carboxylic Acid Anhydrides. *Synthesis* **2004**, *2004*, 205–207.

(30) Chen, J.; Shao, Y.; Ma, L.; Ma, M.; Wan, X. In situ generation of nitrilium from nitrile ylide and the subsequent Mumm rearrangement: copper-catalyzed synthesis of unsymmetrical diacylglycine esters. *Org. Biomol. Chem.* **2016**, *14*, 10723–10732.

(31) Shiina, I.; Tono, T. Expedient synthesis of carboxylic esters and high yielding macrolactones using trifluoromethyl-substituted benzoic anhydrides with 4-(dimethylamino)pyridine: an evaluation of the reactivities of aromatic acid anhydrides as dehydration reagents compared with 2-methyl-6-nitrobenzoic anhydride. *Heterocycles* **2017**, *94*, 255–275.

(32) Wang, C.; Rakshit, S.; Glorius, F. Palladium-Catalyzed Intermolecular Decarboxylative Coupling of 2-Phenylbenzoic Acids with Alkynes via C-H and C-C Bond Activation. *J. Am. Chem. Soc.* **2010**, *132*, 14006–14008.

(33) Fukuyama, T.; Maetani, S.; Miyagawa, K.; Ryu, I. Synthesis of Fluorenones through Rhodium-Catalyzed Intramolecular Acylation of Biarylcarboxylic Acids. *Org. Lett.* **2014**, *16*, 3216–3219.

(34) Biafora, A.; Krause, T.; Hackenberger, D.; Belitz, F.; Gooßen, L. J. *ortho*-C-H Arylation of Benzoic Acids with Aryl Bromides and Chlorides Catalyzed by Ruthenium. *Angew. Chem., Int. Ed.* **2016**, *55*, 14752–14755.

(35) Phillion, D. P.; Pratt, J. K. A New Method for Hydrolyzing 2-Aryl-4,4-Dimethyl-2-Oxazolines to Aryl Carboxylic Acids. *Synth. Commun.* **1992**, *22*, 13–22.

(36) Attygalle, A. B.; Bialecki, J. B.; Nishshanka, U.; Weisbecker, C. S.; Ruzicka, J. Loss of benzene to generate an enolate anion by a site-specific double-hydrogen transfer during CID fragmentation of *o*-alkyl ethers of *ortho*-hydroxybenzoic acids. *J. Mass Spectrom.* **2008**, *43*, 1224–1234.

(37) (a) Guo, W.; Li, J.; Fan, N.; Wu, W.; Zhou, P.; Xia, C. A Simple and Effective Method for Chemoselective Esterification of Phenolic Acids. *Synth. Commun.* **2005**, *35*, 145–152. (b) Ballantine, M.; Menard, M. L.; Tam, W. Isomerization of 7-Oxabenzonorbomadienes into Naphthols Catalyzed by $[\text{RuCl}_2(\text{CO})_3]_2$. *J. Org. Chem.* **2009**, *74*, 7570–7573.

(38) (a) Liu, Z.; Ma, Q.; Liu, Y.; Wang, Q. 4-(N,N-Dimethylamino)-pyridine Hydrochloride as a Recyclable Catalyst for Acylation of Inert

Alcohols: Substrate Scope and Reaction Mechanism. *Org. Lett.* **2014**, *16*, 236–239. (b) Subaramanian, M.; Ramar, P. M.; Rana, J.; Gupta, V. K.; Balaraman, E. Catalytic conversion of ketones to esters via C(O)–C bond cleavage under transition-metal free conditions. *Chem. Commun.* **2020**, *56*, 8143–8146.

(39) Feng, J.; Liang, S.; Chen, S.-Y.; Zhang, J.; Fu, S.-S.; Yu, X.-Q. A Metal-Free Oxidative Esterification of the Benzyl C-H Bond. *Adv. Synth. Catal.* **2012**, *354*, 1287–1292.

(40) Weng, S.-S.; Ke, C.-S.; Chen, F.-K.; Lyu, Y.-F.; Lin, G.-Y. Transesterification catalyzed by iron(III) β -diketonate species. *Tetrahedron* **2011**, *67*, 1640–1648.

(41) Zhang, C.; Feng, P.; Jiao, N. Cu-Catalyzed Esterification Reaction via Aerobic Oxygenation and C–C Bond Cleavage: An Approach to α -Ketoesters. *J. Am. Chem. Soc.* **2013**, *135*, 15257–15262.

(42) Blümel, M.; Noy, J.-M.; Enders, D.; Stenzel, M. H.; Nguyen, T. V. Development and Applications of Transesterification Reactions Catalyzed by N-Heterocyclic Olefins. *Org. Lett.* **2016**, *18*, 2208–2211.

(43) Slungård, S. V.; Krakeli, T.-A.; Thvedt, T. H. K.; Fuglseth, E.; Sundby, E.; Hoff, B. H. Investigation into the enantioselection mechanism of ruthenium–arene–diamine transfer hydrogenation catalysts using fluorinated substrates. *Tetrahedron* **2011**, *67*, 5642–5650.

(44) Spitznagel, G. W.; Clark, T.; Chandrasekhar, J.; Schleyer, P. V. R. Stabilization of methyl anions by first-row substituents. The superiority of diffuse function-augmented basis sets for anion calculations. *J. Comput. Chem.* **1982**, *3*, 363–371.

(45) Curtiss, L. A.; Redfern, P. C.; Raghavachari, K.; Rassolov, V.; Pople, J. A. Gaussian-3 theory using reduced Møller-Plesset order. *J. Chem. Phys.* **1999**, *110*, 4703–4709.

(46) Frisch, M. J.; Trucks, G. W.; Schlegel, H. B.; Scuseria, G. E.; Robb, M. A.; Cheeseman, J. R.; Scalmani, G.; Barone, V.; Mennucci, B.; Petersson, G. A.; Nakatsuji, H.; Caricato, M.; Li, X.; Hratchian, H. P.; Izmaylov, A. F.; Bloino, J.; Zheng, G.; Sonnenberg, J. L.; Hada, M.; Ehara, M.; Toyota, K.; Fukuda, R.; Hasegawa, J.; Ishida, M.; Nakajima, T.; Honda, Y.; Kitao, O.; Nakai, H.; Vreven, T.; Montgomery, J. A., Jr.; Peralta, J. E.; Ogliaro, F.; Bearpark, M.; Heyd, J. J.; Brothers, E.; Kudin, K. N.; Staroverov, V. N.; Kobayashi, R.; Normand, J.; Raghavachari, K.; Rendell, A.; Burant, J. C.; Iyengar, S. S.; Tomasi, J.; Cossi, M.; Rega, N.; Millam, J. M.; Klene, M.; Knox, J. E.; Cross, J. B.; Bakken, V.; Adamo, C.; Jaramillo, J.; Gomperts, R.; Stratmann, R. E.; Yazyev, O.; Austin, A. J.; Cammi, R.; Pomelli, C.; Ochterski, J. W.; Martin, R. L.; Morokuma, K.; Zakrzewski, V. G.; Voth, G. A.; Salvador, P.; Dannenberg, J. J.; Dapprich, S.; Daniels, A. D.; Farkas, Ö.; Foresman, J. B.; Ortiz, J. V.; Cioslowski, J.; Fox, D. J. *Gaussian 09*; version D.01; Gaussian, Inc.: Wallingford, CT, 2010.

(47) Neese, F. The ORCA program system. *Wiley Interdiscip. Rev.: Comput. Mol. Sci.* **2012**, *2* (1), 73–78.

(48) *Schrödinger Release 2019–2: Jaguar*; Schrödinger, LLC: New York, NY, 2019.

(49) Reed, A. E.; Curtiss, L. A.; Weinhold, F. Intermolecular interactions from a natural bond orbital, donor-acceptor viewpoint. *Chem. Rev.* **1988**, *88*, 899–926.

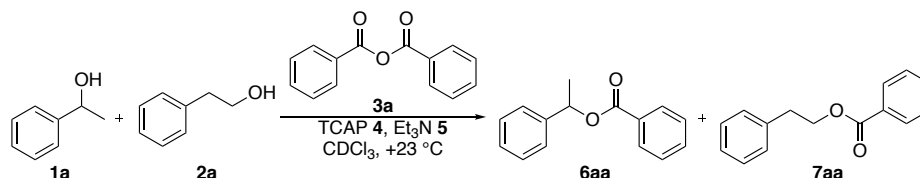
3.1 Experimental Part

3.1.1 Turnover-limited Competition Experiments of Aryl-Substituted Ethanol

3.1.1.1 Experimental Design

Technical details: NMR tubes were dried in the oven for at least 12 h. CDCl_3 and Et_3N were freshly distilled under N_2 over CaH_2 before use. Hamilton syringes were cleaned with acetone, dried under vacuum, and flushed with nitrogen prior to use. A GC vial holder (Shimadzu 221-44998-91) was connected to the coolant circuit of a cryostat maintaining $+23\text{ }^\circ\text{C}$ constantly and placed on a magnetic stirrer. The speed of stirring was fixed at 750 rpm for all the experiments described here.

Preparation of stock solutions: A guideline for the preparation of stock solutions for turnover-limited competition experiments is described in the following:



Temperature control: $+23\text{ }^\circ\text{C}$

Three CDCl_3 stock solutions are prepared under nitrogen (Table 3.1). Stock solution A contains the secondary alcohol **1a** and primary alcohol **2a** each at a concentration of 0.05 M. Stock solution B contains benzoic anhydride **3a** (0.1 M), while stock solution C consists of a 0.15 M Et_3N and catalyst TCAP at a concentration of 0.005 M.

Table 3.1. Preparation of initial CDCl_3 stock solutions.

Stock solution	Compound	Concentration (mol L ⁻¹)	Volume (mL)	n (mol)	M.W. (g mol ⁻¹)	Mass (mg)
Stock A	1a	0.05	2	$100 \cdot 10^{-6}$	122.16	12.2
	2a	0.05	2	$100 \cdot 10^{-6}$	122.16	12.2
Stock B	3a	0.1	2	$200 \cdot 10^{-6}$	226.23	45.2
Stock C	TCAP	0.005	5	$25 \cdot 10^{-6}$	174.24	4.4
	Et₃N	0.15	5	$750 \cdot 10^{-3}$	101.19	75.9

Following these initial preparations, stock solution B was diluted in four discrete steps as shown in Table 3.2. The concentrations of the new solutions have been fixed at 20, 35, 50, and 70% of the initial stock solution B.

Table 3.2. Dilution of stock solution B.

Stock solution	Concentration (mol L ⁻¹)	Vol. B ^[b] (mL)	Volume (mL)
Stock B1 (20%)^[a]	0.020	0.20	1
Stock B2 (35%)^[a]	0.035	0.35	1
Stock B3 (50%)^[a]	0.050	0.50	1
Stock B4 (70%)^[a]	0.070	0.70	1

^[a]Concentration relative to stock solution B; ^[b]Initial volume of stock solution B.

Methodology: Under nitrogen 0.4 mL of stock solution A, 0.4 mL of stock solution C, and 0.4 mL of stock solution B1 are transferred to a GC vial by use of a Hamilton syringe. The GC vial is then capped under nitrogen and placed in the GC vial holder with stirring.

Composition of each prepared GC vial for one turnover-limited competition experiment (method A):

In order to run turnover-limited competition experiments to defined turnover points, reaction solutions with identical concentrations for catalyst, substrate alcohols, and auxiliary base, but different initial anhydride concentrations were prepared in four different GC vials:

GC vial 1: 0.4 mL Stock A; 0.4 mL Stock C; 0.4 mL Stock B1

GC vial 2: 0.4 mL Stock A; 0.4 mL Stock C; 0.4 mL Stock B2

Size-Driven Inversion of Selectivity in Esterfication

GC vial 3: 0.4 mL Stock A; 0.4 mL Stock C; 0.4 mL Stock B3

GC vial 4: 0.4 mL Stock A; 0.4 mL Stock C; 0.4 mL Stock B4

In terms of the actual starting concentrations (mol/L) for all components this yields:

GC vial 1: **1a** and **2a:** 0.017, **3a:** 0.007, **Et₃N:** 0.050, **TCAP:** 0.002

GC vial 2: **1a** and **2a:** 0.017, **3a:** 0.012, **Et₃N:** 0.050, **TCAP:** 0.002

GC vial 3: **1a** and **2a:** 0.017, **3a:** 0.017, **Et₃N:** 0.050, **TCAP:** 0.002

GC vial 4: **1a** and **2a:** 0.017, **3a:** 0.023, **Et₃N:** 0.050, **TCAP:** 0.002

Composition of each prepared GC vial for one turnover-limited competition experiment (method B):

For anhydride **3m**, **3n**, **3v**, and **3w** a higher TCAP concentration is used (Table 3.3).

Table 3.3. Preparation of initial CDCl₃ stock solutions for anhydrides **3m**, **3n**, **3v**, and **3w**.

Stock	Compound	Molarity (mol L ⁻¹)	Volume (mL)	n (mol)	M.W. (g mol ⁻¹)	Mass (mg)
Stock A	1a	0.05	2	100·10 ⁻⁶	122.16	12.2
	2a	0.05	2	100·10 ⁻⁶	122.16	12.2
Stock B	3m	0.1	2	200·10 ⁻⁶	282.13	56.4
Stock C	TCAP	0.02	5	100·10 ⁻⁶	174.24	17.4
	Et₃N	0.15	5	750·10 ⁻³	101.19	75.9

In terms of the actual starting concentrations (mol/L) for all components this yields:

GC-vial 1: **1a** and **2a:** 0.017, **3a:** 0.007, **Et₃N:** 0.050, **TCAP:** 0.007

GC-vial 2: **1a** and **2a:** 0.017, **3a:** 0.012, **Et₃N:** 0.050, **TCAP:** 0.007

GC-vial 3: **1a** and **2a:** 0.017, **3a:** 0.017, **Et₃N:** 0.050, **TCAP:** 0.007

GC-vial 4: **1a** and **2a:** 0.017, **3a:** 0.023, **Et₃N:** 0.050, **TCAP:** 0.007

Preparation of NMR samples: The turnover-limited competition experiment is considered finished when the reaction with the highest anhydride concentration (GC vial 4) is completed. The reaction is monitored by ¹H NMR. NMR tubes are dried under vacuum using a Schlenk-based glassware and flushed with nitrogen three times to eliminate moisture. The GC vials are placed in a Schlenk flask and flushed with nitrogen three times as well. Then, 0.6 mL of the solution contained in the GC vial is transferred to the NMR tube under nitrogen. The NMR tube is then capped and the relative concentrations of all reactants/products determined by ¹H NMR spectroscopy.

3.1.1.2 ¹H NMR Analysis

The ¹H NMR spectra of the turnover-limited competition experiments were edited by *MestReNova* 10.0. The spectra were corrected by using automatic phase correction and Bernstein polynomial fit with polynomial order 3 and referenced by the solvent signal of CDCl₃ (δ = 7.26 ppm). For the secondary alcohol **1** and ester **6** the hydrogen signal of the methyl group was integrated as a measure of the evolution of the reaction. If there was an overlap with other signals, the corresponding CH signal was used instead. For the primary alcohol **2** and ester **7** the hydrogen signal of one of the two CH₂ groups was integrated as a measure of turnover.

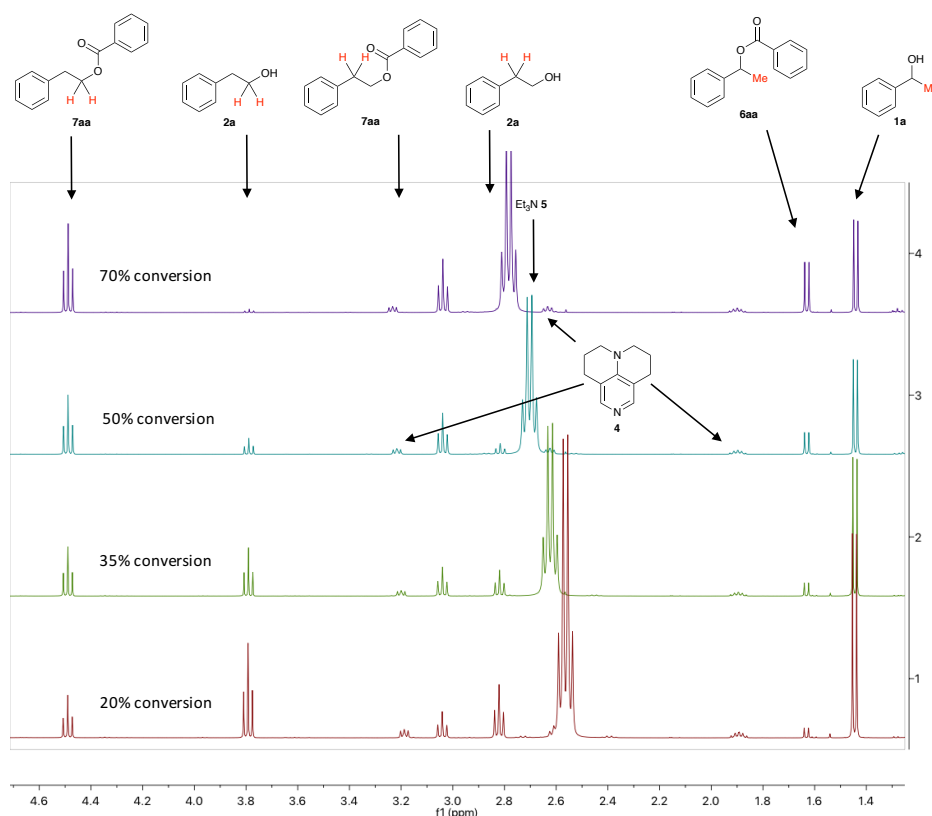
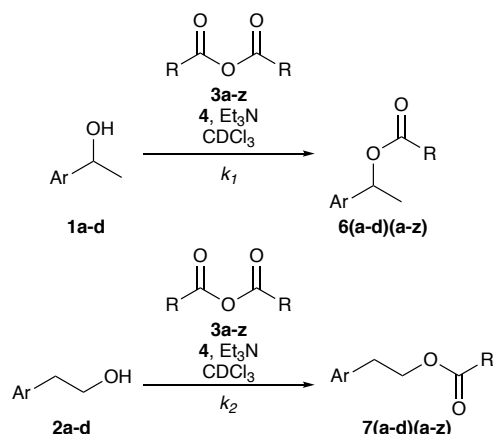


Figure 3.1. Example of the stacked ^1H NMR spectra for the turnover-limited competition experiment between **1a** and **2a** with **3a**.



Scheme 3.1. General equation for the turnover-limited competition experiment.

We determined that after full conversion of the reaction the composition of the products is varied through equilibrium processes. Because of this, we can calculate the relative natural logarithm of rate constants from the product ratios as defined in Eq. 3.1.

$$\ln(k_{\text{rel}}) = \ln\left(\frac{k_2}{k_1}\right) = \ln\left(\frac{k(2a-d+3a-z)}{k(1a-d+3a-z)}\right) \quad \text{Eq. 3.1}$$

The relative rate constant is directly related to the chemoselectivity and the degree of conversion (Eq. 3.2).^[1]

$$k_{\text{rel}} = \frac{\ln[1-\text{conv}(1+C)]}{\ln[1-\text{conv}(1-C)]} \quad \text{Eq. 3.2}$$

The conversion is defined by Eq. 3.3, whereby the integrals of the ^1H NMR correspond to the concentrations.

$$\text{Conversion}(\%) = \left(\frac{[6(a-d)(a-z)] + [7(a-d)(a-z)]}{[1a-d] + [2a-d] + [6(a-d)(a-z)] + [7(a-d)(a-z)]} \right) \cdot 100 \quad \text{Eq. 3.3}$$

The chemoselectivity is defined by Eq. 3.4:

$$\text{Chemoselectivity}_{\text{exp}}(C_{\text{exp}}) = \frac{[7(a-d)(a-z)] - [6(a-d)(a-z)]}{[7(a-d)(a-z)] + [6(a-d)(a-z)]} \quad \text{Eq. 3.4}$$

Size-Driven Inversion of Selectivity in Esterfication

A correction factor f was introduced, which defines the exact ratio of both reactants present in the reaction medium (this should be close to the ideal 1:1), to avoid the human error in the preparation of the samples (Eq. 3.5):

$$f = \frac{[1a-d]+[6(a-d)(a-z)]}{[2a-d]+[7(a-d)(a-z)]} \quad \text{Eq. 3.5}$$

This correction factor f was now allowed in the equation for chemoselectivity and Eq. 3.6 was defined.

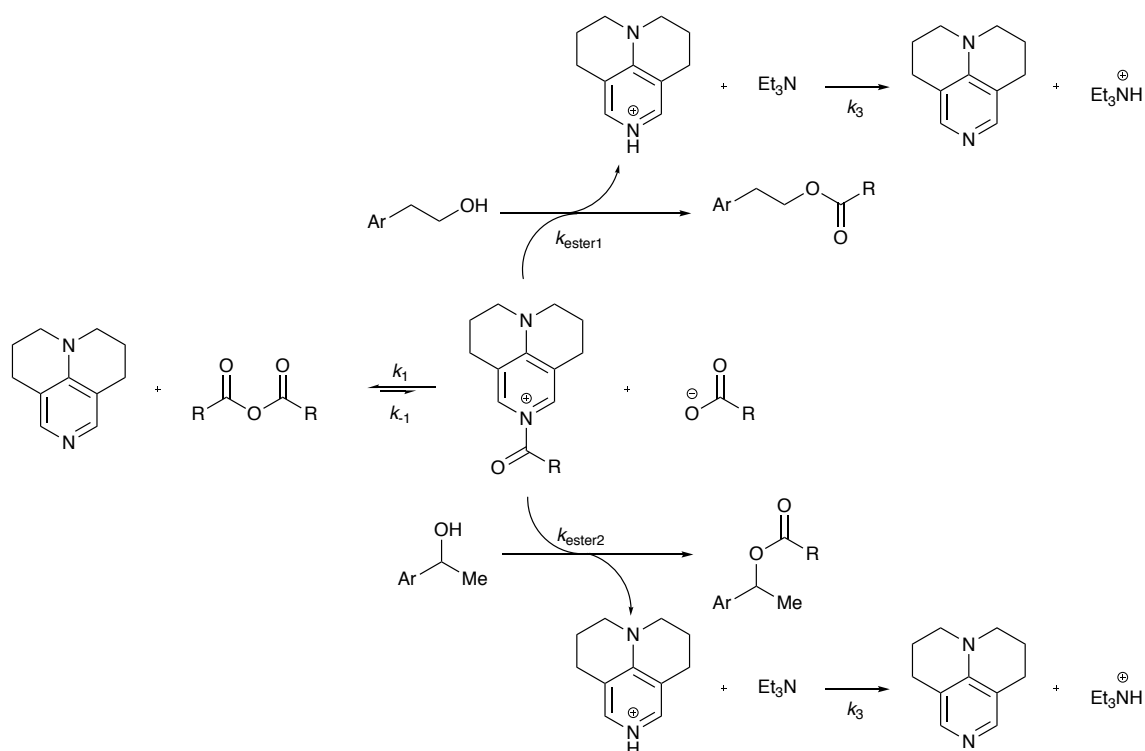
$$\text{Chemoselectivity } (C) = \frac{[7(a-d)(a-z)] \cdot f - [6(a-d)(a-z)]}{[7(a-d)(a-z)] \cdot f + [6(a-d)(a-z)]} \quad \text{Eq. 3.6}$$

3.1.1.3 Simulation of Turnover-limited Competition Experiments

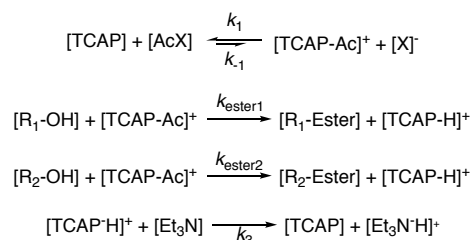
With the help of the CoPaSi^[2] and Pro Fit7 programs the k_{rel} values for the turnover-limited competition experiments have been simulated. Scheme 3.2 shows the reactions used in Copasi, in which the k values have been modified in order to achieve the k_{rel} values. The values k_1 , k_{-1} and k_3 have been used as constants:

$k_1 = 0.1 \text{ L} \cdot \text{mol}^{-1} \cdot \text{s}^{-1}$; $k_{-1} = 0.001 \text{ L} \cdot \text{mol}^{-1} \cdot \text{s}^{-1}$; $k_3 = 0.1 \text{ L} \cdot \text{mol}^{-1} \cdot \text{s}^{-1}$, while k_{ester1} and k_{ester2} have been allowed to vary.

a)



b)

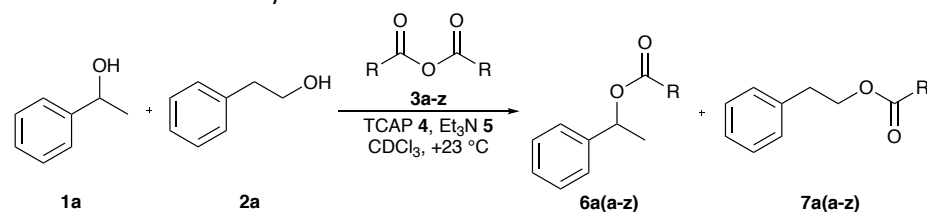


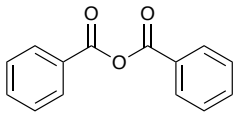
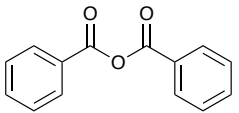
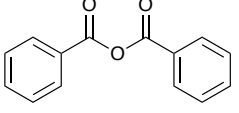
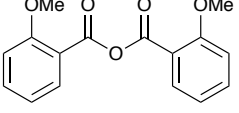
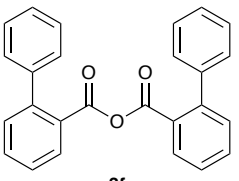
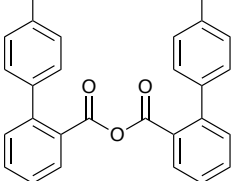
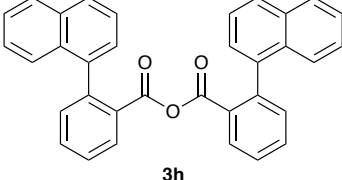
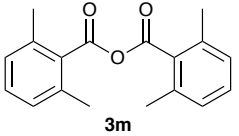
Scheme 3.2. Model reaction used in CoPaSi for the simulation of the rate constants.

The rate constants of the different turnover-limited competition experiments were simulated by CoPaSi by using the starting concentrations of the experiments. The simulated concentrations over the time were used to calculate the conversion by Eq. 3.3 and chemoselectivity by Eq. 3.6. In Figures 3.3 to 3.20 the conversion was plotted against the chemoselectivity, which allows us the illustrative comparison of experimental and simulated results.

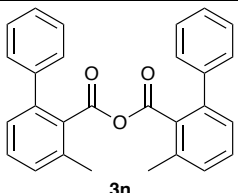
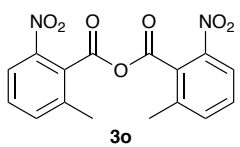
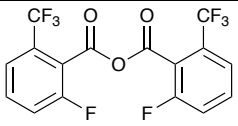
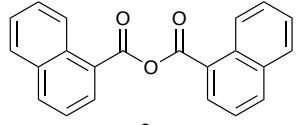
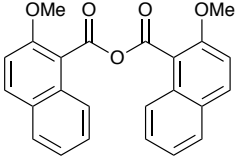
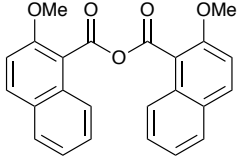
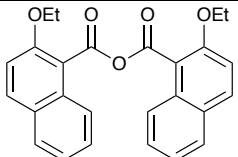
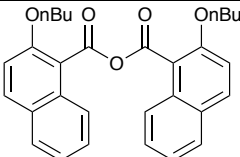
3.1.1.4 Results of Turnover-limited Competition Experiments

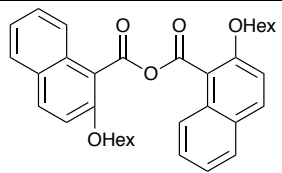
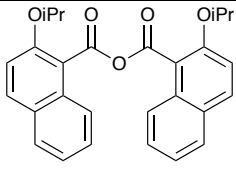
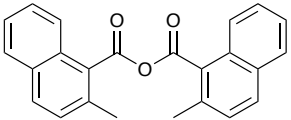
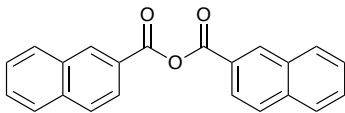
Table 3.4. Conversion, corrected chemoselectivity, relative rate and natural logarithm of relative rate with standard derivations calculated from corresponding ^1H NMR measurements for turnover-limited competition experiments between **1a** and **2a** with the benzoic anhydride derivatives **3a-z**.



 3a [a]				 3a [a]			
<i>Conv.</i>	<i>Chem.</i>	k_{rel}	$\ln(k_{\text{rel}})$	<i>Conv.</i>	<i>Chem.</i>	k_{rel}	$\ln(k_{\text{rel}})$
17.327	0.747	8.030	2.083	18.800	0.739	7.883	2.065
32.458	0.682	7.237	1.979	30.782	0.692	7.390	2.000
44.865	0.630	7.235	1.979	49.786	0.600	7.184	1.972
65.024	0.466	7.197	1.974	67.421	0.434	7.109	1.961
		7.425 ± 0.404	2.004 ± 0.053			7.392 ± 0.349	2.000 ± 0.046
 3a [a]				 3b [a]			
<i>Conv.</i>	<i>Chem.</i>	k_{rel}	$\ln(k_{\text{rel}})$	<i>Conv.</i>	<i>Chem.</i>	k_{rel}	$\ln(k_{\text{rel}})$
18.064	0.738	7.787	2.052	21.398	0.770	9.447	2.246
34.050	0.678	7.291	1.987	32.000	0.704	7.936	2.071
48.181	0.613	7.260	1.982	43.279	0.638	7.253	1.981
68.460	0.422	7.217	1.976	64.039	0.528	10.629	2.364
		7.389 ± 0.267	2.000 ± 0.036			8.816 ± 1.517	2.166 ± 0.172
 3f [a]				 3g [a]			
<i>Conv.</i>	<i>Chem.</i>	k_{rel}	$\ln(k_{\text{rel}})$	<i>Conv.</i>	<i>Chem.</i>	k_{rel}	$\ln(k_{\text{rel}})$
20.941	0.561	4.099	1.411	17.566	0.649	5.369	1.681
35.654	0.514	4.082	1.407	31.215	0.608	5.342	1.676
49.668	0.474	4.343	1.469	45.859	0.542	5.217	1.652
70.432	0.334	4.433	1.489	64.013	0.423	5.234	1.655
		4.239 ± 0.176	1.444 ± 0.041			5.291 ± 0.076	1.666 ± 0.014
 3h [a]				 3m [a]			
<i>Conv.</i>	<i>Chem.</i>	k_{rel}	$\ln(k_{\text{rel}})$	<i>Conv.</i>	<i>Chem.</i>	k_{rel}	$\ln(k_{\text{rel}})$
28.594	0.546	4.202	1.436	14.772	0.235	1.658	0.505
31.968	0.522	4.014	1.390	27.764	0.216	1.678	0.518

Size-Driven Inversion of Selectivity in Esterfication

43.895	0.490	4.190	1.433	41.483	0.189	1.680	0.519
64.131	0.392	4.515	1.507	50.951	0.179	1.693	0.527
		4.230 ± 0.208	1.441 ± 0.049			1.677 ± 0.015	0.517 ± 0.009
 3n [b]				 3o [a]			
<i>Conv.</i>	<i>Chem.</i>	k_{rel}	$\ln(k_{rel})$	<i>Conv.</i>	<i>Chem.</i>	k_{rel}	$\ln(k_{rel})$
15.100	0.409	2.556	0.938	17.862	0.251	1.759	0.565
25.211	0.391	2.592	0.952	29.042	0.234	1.763	0.567
37.344	0.361	2.606	0.958	45.374	0.204	1.762	0.566
51.015	0.309	2.533	0.929	59.984	0.171	1.765	0.568
		2.572 ± 0.033	0.944 ± 0.013			1.762 ± 0.002	0.566 ± 0.001
 3p [a]				 3q [a]			
<i>Conv.</i>	<i>Chem.</i>	k_{rel}	$\ln(k_{rel})$	<i>Conv.</i>	<i>Chem.</i>	k_{rel}	$\ln(k_{rel})$
17.788	0.494	3.271	1.185	19.518	0.727	7.506	2.016
30.707	0.465	3.331	1.203	33.004	0.668	6.878	1.928
45.640	0.414	3.333	1.204	48.070	0.591	6.601	1.887
63.113	0.330	3.323	1.201	67.513	0.427	6.752	1.910
		3.315 ± 0.029	1.198 ± 0.009			6.934 ± 0.397	1.935 ± 0.056
 3r [a]				 3r [a]			
<i>Conv.</i>	<i>Chem.</i>	k_{rel}	$\ln(k_{rel})$	<i>Conv.</i>	<i>Chem.</i>	k_{rel}	$\ln(k_{rel})$
16.011	0.278	1.866	0.624	15.990	0.241	1.709	0.536
29.034	0.227	1.734	0.550	29.613	0.215	1.685	0.522
42.598	0.196	1.697	0.529	44.272	0.191	1.688	0.524
60.549	0.148	1.636	0.492	59.847	0.152	1.649	0.500
		1.733 ± 0.097	0.549 ± 0.055			1.683 ± 0.025	0.520 ± 0.015
 3s [a]				 3t [a]			
<i>Conv.</i>	<i>Chem.</i>	k_{rel}	$\ln(k_{rel})$	<i>Conv.</i>	<i>Chem.</i>	k_{rel}	$\ln(k_{rel})$
17.294	0.192	1.534	0.428	18.603	0.156	1.417	0.349
28.528	0.189	1.576	0.455	30.733	0.139	1.403	0.338
42.451	0.161	1.542	0.433	44.669	0.106	1.336	0.290
60.189	0.174	1.782	0.578	56.151	0.091	1.328	0.283
		1.609 ± 0.117	0.473 ± 0.071			1.371 ± 0.046	0.315 ± 0.033

 3u [a]				 3v [b]			
<i>Conv.</i>	<i>Chem.</i>	k_{rel}	$\ln(k_{rel})$	<i>Conv.</i>	<i>Chem.</i>	k_{rel}	$\ln(k_{rel})$
11.958	0.168	1.436	0.362	18.228	0.287	1.920	0.652
22.578	0.146	1.396	0.334	32.025	0.190	1.597	0.468
31.121	0.120	1.339	0.292	45.787	0.185	1.673	0.514
40.183	0.118	1.363	0.310	60.648	0.150	1.648	0.499
		1.384 ± 0.042	0.324 ± 0.031			1.709 ± 0.144	0.534 ± 0.081
 3w [b]				 3z [a]			
<i>Conv.</i>	<i>Chem.</i>	k_{rel}	$\ln(k_{rel})$	<i>Conv.</i>	<i>Chem.</i>	k_{rel}	$\ln(k_{rel})$
16.326	0.150	1.393	0.332	18.236	0.771	9.148	2.213
26.380	0.149	1.422	0.352	35.773	0.699	8.218	2.106
39.869	0.138	1.437	0.362	48.018	0.641	8.200	2.104
64.087	0.097	1.405	0.340	70.144	0.420	10.706	2.371
		1.414 ± 0.019	0.346 ± 0.013			9.068 ± 1.178	2.199 ± 0.126

[a] Turnover-limited competition experiments were carrying out by method A. [b] Turnover-limited competition experiments were carrying out by method B.

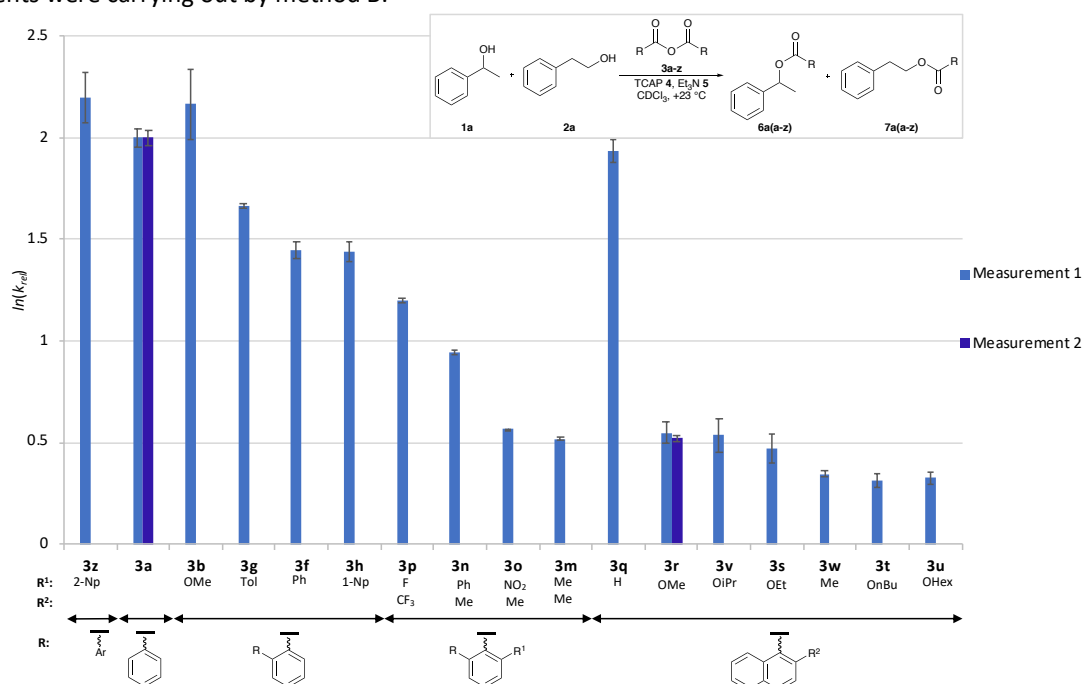


Figure 3.2. $\ln(k_{rel})$ of turnover-limited competition experiment between **1a** and **2a** with the benzoic anhydride derivatives **3a-z**.

Size-Driven Inversion of Selectivity in Esterfication

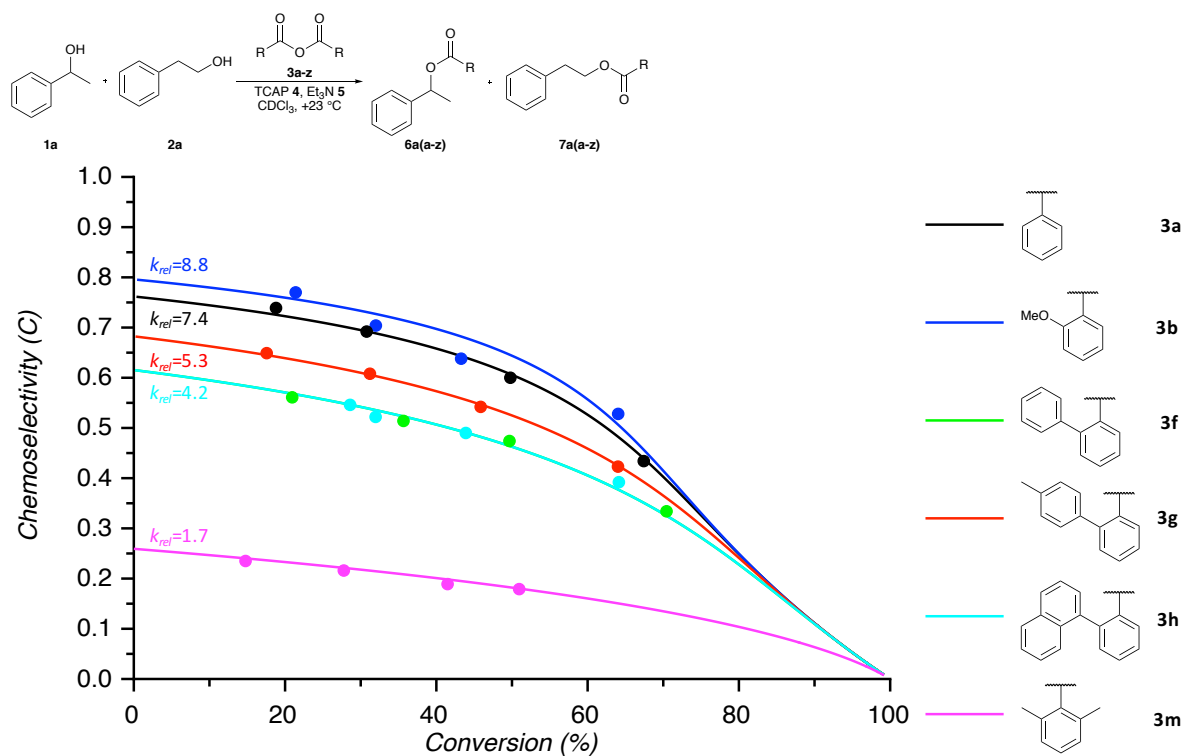


Figure 3.3. Plot of conversion vs. corrected chemoselectivity for turnover-limited competition experiment 1a vs. 2a with the benzoic anhydride derivatives 3a-m.

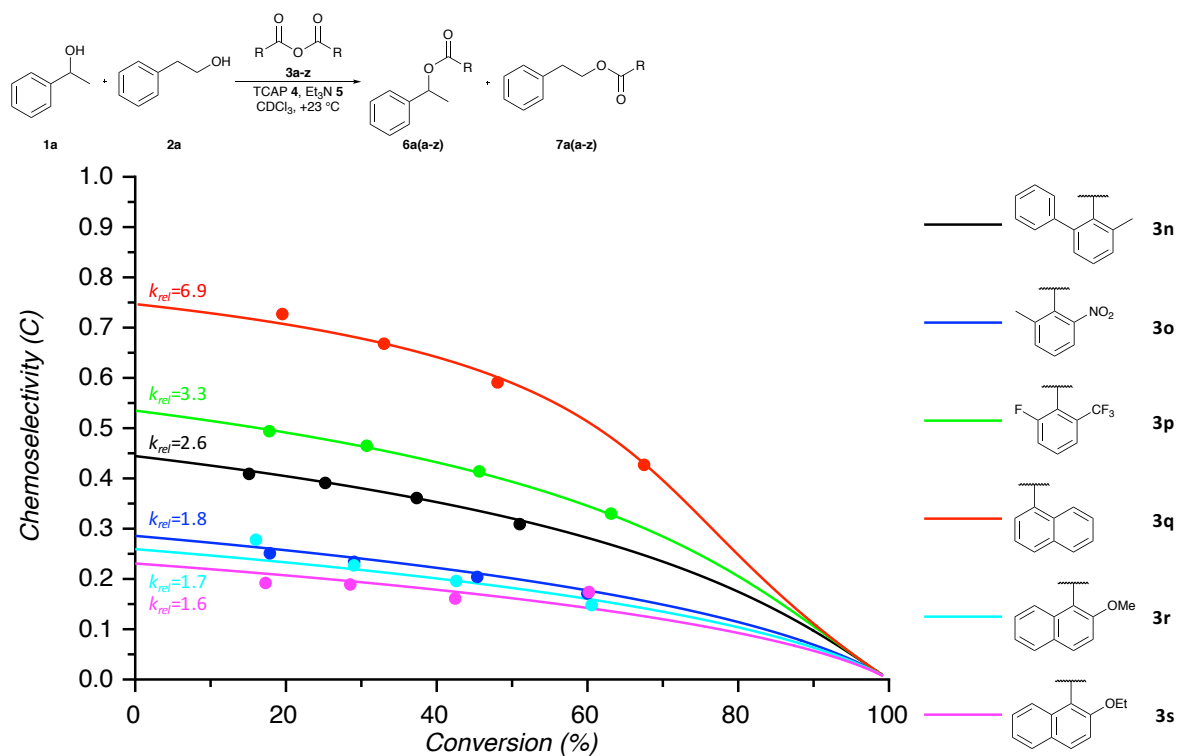


Figure 3.4. Plot of conversion vs. corrected chemoselectivity for turnover-limited competition experiment 1a vs. 2a with the benzoic anhydride derivatives 3n-s.

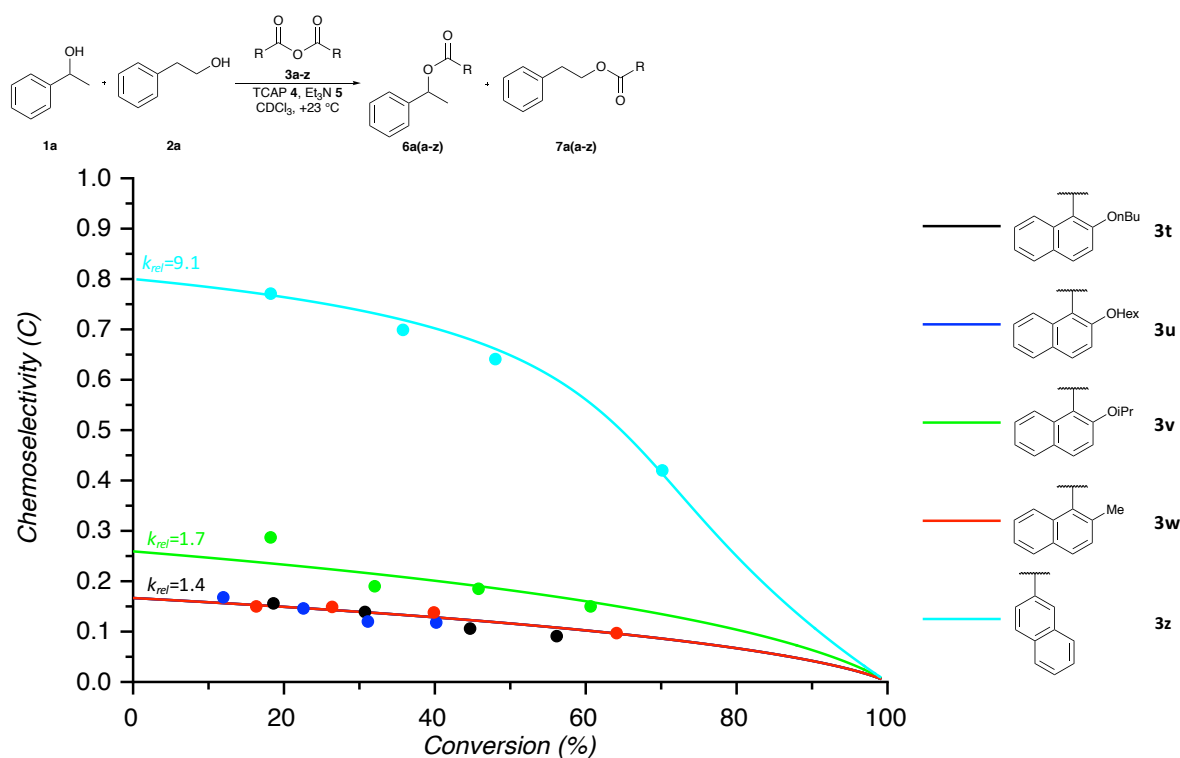
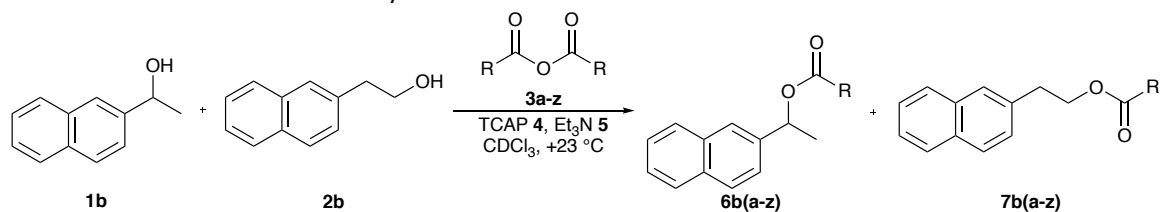
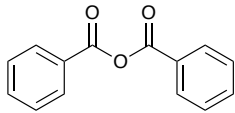
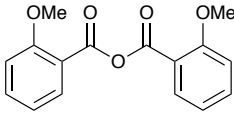
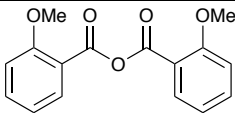
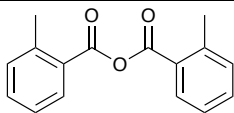


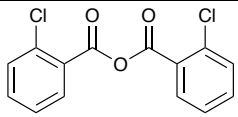
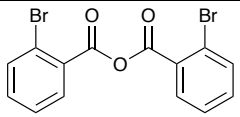
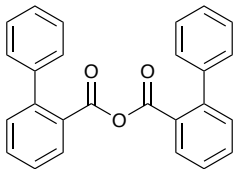
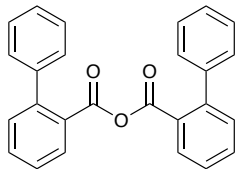
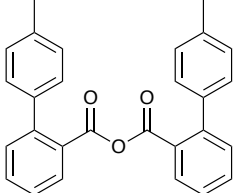
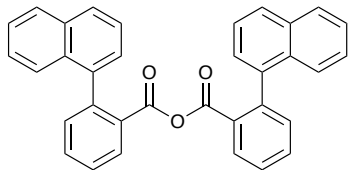
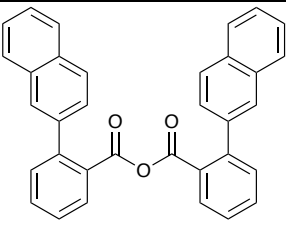
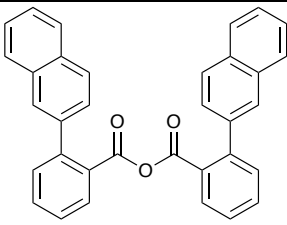
Figure 3.5. Plot of conversion vs. corrected chemoselectivity for turnover-limited competition experiment **1a** vs. **2a** with the benzoic anhydride derivatives **3t-z**.

Table 3.5. Conversion, corrected chemoselectivity, relative rate, and natural logarithm of relative rate with standard derivations calculated from corresponding ^1H NMR measurements for turnover-limited competition experiments between **1b** and **2b** with the benzoic anhydride derivatives **3a-z**.



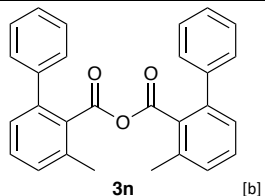
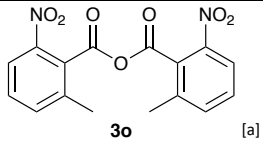
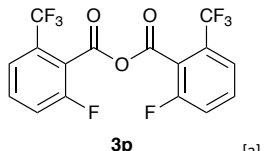
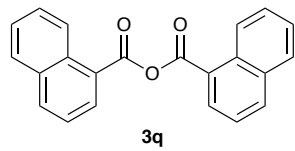
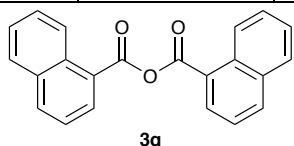
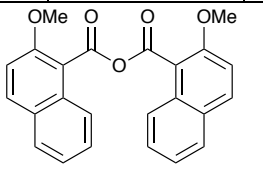
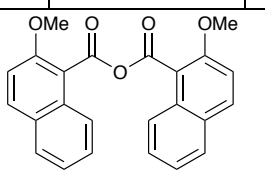
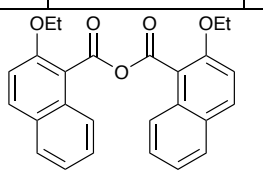
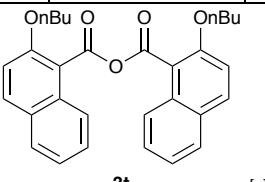
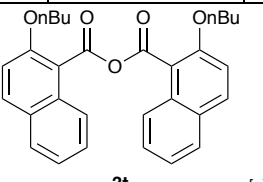
 3a [a]				 3b [a]			
Conv.	Chem.	k_{rel}	$\ln(k_{rel})$	Conv.	Chem.	k_{rel}	$\ln(k_{rel})$
19.239	0.533	3.717	1.313	20.723	0.568	4.187	1.432
34.266	0.485	3.664	1.298	32.491	0.505	3.830	1.343
48.215	0.430	3.639	1.292	45.970	0.441	3.659	1.297
62.151	0.356	3.623	1.287	65.137	0.350	3.841	1.346
		3.661 ± 0.041	1.298 ± 0.011			3.879 ± 0.221	1.354 ± 0.056
 3b [a]				 3c [a]			
Conv.	Chem.	k_{rel}	$\ln(k_{rel})$	Conv.	Chem.	k_{rel}	$\ln(k_{rel})$
21.169	0.558	4.070	1.404	18.492	0.369	2.352	0.855
32.628	0.500	3.778	1.329	31.427	0.315	2.197	0.787
46.360	0.447	3.753	1.323	44.290	0.283	2.198	0.787
66.561	0.344	3.916	1.365	65.192	0.230	2.320	0.841
		3.879 ± 0.146	1.355 ± 0.037			2.267 ± 0.081	0.818 ± 0.036

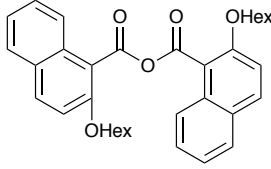
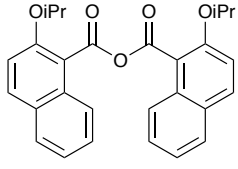
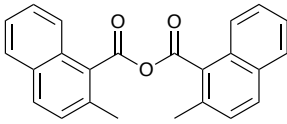
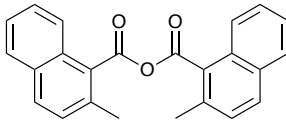
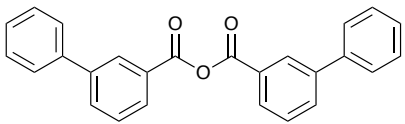
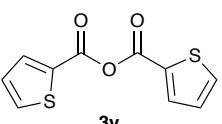
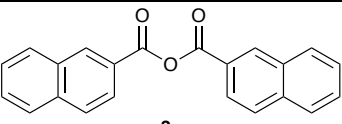
Size-Driven Inversion of Selectivity in Esterfication

 3d [a]				 3e [a]			
Conv.	Chem.	k_{rel}	$\ln(k_{rel})$	Conv.	Chem.	k_{rel}	$\ln(k_{rel})$
18.949	0.487	3.233	1.173	13.654	0.516	3.393	1.222
29.913	0.460	3.259	1.181	23.631	0.473	3.217	1.168
47.512	0.398	3.243	1.176	35.691	0.439	3.228	1.172
58.269	0.350	3.243	1.177	46.499	0.404	3.257	1.181
		3.244 ± 0.011	1.177 ± 0.003			3.274 ± 0.081	1.186 ± 0.025
 3f [a]				 3f [a]			
Conv.	Chem.	k_{rel}	$\ln(k_{rel})$	Conv.	Chem.	k_{rel}	$\ln(k_{rel})$
18.843	0.328	2.127	0.755	23.536	0.316	2.110	0.747
34.398	0.290	2.094	0.739	33.180	0.308	2.183	0.780
47.819	0.264	2.135	0.758	46.687	0.278	2.211	0.793
66.389	0.211	2.197	0.787	66.382	0.216	2.240	0.807
		2.138 ± 0.043	0.760 ± 0.020			2.186 ± 0.056	0.782 ± 0.026
 3g [a]				 3h [a]			
Conv.	Chem.	k_{rel}	$\ln(k_{rel})$	Conv.	Chem.	k_{rel}	$\ln(k_{rel})$
19.399	0.354	2.273	0.821	19.368	0.253	1.777	0.575
34.474	0.320	2.275	0.822	28.270	0.260	1.875	0.629
49.636	0.281	2.289	0.828	41.916	0.270	2.083	0.734
69.299	0.213	2.331	0.846	62.767	0.226	2.206	0.791
		2.292 ± 0.027	0.829 ± 0.012			1.985 ± 0.195	0.682 ± 0.098
 3i [a]				 3i [a]			
Conv.	Chem.	k_{rel}	$\ln(k_{rel})$	Conv.	Chem.	k_{rel}	$\ln(k_{rel})$
17.483	0.409	2.593	0.953	23.250	0.384	2.511	0.921
30.816	0.376	2.584	0.949	31.630	0.375	2.592	0.952
42.731	0.345	2.602	0.956	46.187	0.334	2.605	0.958
58.687	0.298	2.701	0.994	58.494	0.298	2.691	0.990
		2.620 ± 0.054	0.963 ± 0.021			2.600 ± 0.074	0.955 ± 0.028

<p style="text-align: center;">3j [a]</p>				<p style="text-align: center;">3j [a]</p>			
<i>Conv.</i>	<i>Chem.</i>	k_{rel}	$\ln(k_{rel})$	<i>Conv.</i>	<i>Chem.</i>	k_{rel}	$\ln(k_{rel})$
22.952	0.412	2.703	0.994	26.185	0.361	2.410	0.879
38.811	0.382	2.799	1.029	31.560	0.393	2.723	1.002
44.061	0.362	2.779	1.022	42.462	0.364	2.748	1.011
61.048	0.302	2.856	1.049	62.318	0.302	2.919	1.071
		2.784 ± 0.063	1.024 ± 0.023			2.700 ± 0.212	0.991 ± 0.080
<p style="text-align: center;">3k [a]</p>				<p style="text-align: center;">3k [a]</p>			
<i>Conv.</i>	<i>Chem.</i>	k_{rel}	$\ln(k_{rel})$	<i>Conv.</i>	<i>Chem.</i>	k_{rel}	$\ln(k_{rel})$
16.231	0.516	3.457	1.240	16.069	0.550	3.821	1.340
29.872	0.508	3.762	1.325	30.568	0.516	3.887	1.358
42.676	0.466	3.798	1.334	42.732	0.470	3.856	1.350
56.251	0.402	3.790	1.332	55.942	0.406	3.821	1.341
		3.702 ± 0.164	1.308 ± 0.045			3.846 ± 0.032	1.347 ± 0.008
<p style="text-align: center;">3l a</p>				<p style="text-align: center;">3m [b]</p>			
<i>Conv.</i>	<i>Chem.</i>	k_{rel}	$\ln(k_{rel})$	<i>Conv.</i>	<i>Chem.</i>	k_{rel}	$\ln(k_{rel})$
18.625	0.541	3.780	1.330	18.603	-0.196	0.643	-0.441
31.082	0.511	3.842	1.346	30.400	-0.174	0.656	-0.422
46.478	0.451	3.806	1.337	44.337	-0.160	0.644	-0.439
61.580	0.375	3.867	1.352	61.599	-0.127	0.652	-0.428
		3.824 ± 0.038	1.341 ± 0.010			0.649 ± 0.006	-0.432 ± 0.009
<p style="text-align: center;">3m [b]</p>				<p style="text-align: center;">3n [b]</p>			
<i>Conv.</i>	<i>Chem.</i>	k_{rel}	$\ln(k_{rel})$	<i>Conv.</i>	<i>Chem.</i>	k_{rel}	$\ln(k_{rel})$
17.076	-0.202	0.637	-0.451	16.893	-0.041	0.913	-0.091
30.772	-0.182	0.642	-0.443	28.427	-0.015	0.965	-0.036
43.008	-0.160	0.648	-0.434	38.912	-0.021	0.948	-0.053
60.680	-0.123	0.663	-0.411	60.625	-0.012	0.960	-0.041
		0.648 ± 0.011	-0.435 ± 0.017			0.946 ± 0.023	-0.055 ± 0.025

Size-Driven Inversion of Selectivity in Esterfication

 <p style="text-align: center;">3n [b]</p>				 <p style="text-align: center;">3o [a]</p>			
<i>Conv.</i>	<i>Chem.</i>	k_{rel}	$\ln(k_{rel})$	<i>Conv.</i>	<i>Chem.</i>	k_{rel}	$\ln(k_{rel})$
16.011	-0.034	0.928	-0.075	17.773	-0.172	0.682	-0.383
28.114	-0.014	0.968	-0.033	32.992	-0.145	0.698	-0.359
42.178	-0.009	0.977	-0.024	47.610	-0.133	0.687	-0.376
58.384	-0.014	0.957	-0.044	68.379	-0.093	0.702	-0.353
		0.957 ± 0.021	-0.044 ± 0.022			0.692 ± 0.010	-0.368 ± 0.014
 <p style="text-align: center;">3p [a]</p>				 <p style="text-align: center;">3q [a]</p>			
<i>Conv.</i>	<i>Chem.</i>	k_{rel}	$\ln(k_{rel})$	<i>Conv.</i>	<i>Chem.</i>	k_{rel}	$\ln(k_{rel})$
18.641	0.183	1.507	0.410	19.275	0.481	3.187	1.159
35.592	0.161	1.504	0.408	29.512	0.447	3.122	1.138
49.588	0.140	1.501	0.406	43.631	0.400	3.105	1.133
69.022	0.105	1.498	0.404	64.929	0.302	3.092	1.129
		1.502 ± 0.004	0.407 ± 0.003			3.127 ± 0.042	1.140 ± 0.013
 <p style="text-align: center;">3q [a]</p>				 <p style="text-align: center;">3r [a]</p>			
<i>Conv.</i>	<i>Chem.</i>	k_{rel}	$\ln(k_{rel})$	<i>Conv.</i>	<i>Chem.</i>	k_{rel}	$\ln(k_{rel})$
19.488	0.478	3.170	1.154	22.681	-0.130	0.741	-0.299
31.878	0.442	3.141	1.145	29.273	-0.113	0.763	-0.271
44.590	0.397	3.117	1.137	42.486	-0.105	0.755	-0.281
65.116	0.314	3.277	1.187	56.599	-0.095	0.741	-0.299
		3.176 ± 0.071	1.156 ± 0.022			0.750 ± 0.011	-0.287 ± 0.014
 <p style="text-align: center;">3r [a]</p>				 <p style="text-align: center;">3s [a]</p>			
<i>Conv.</i>	<i>Chem.</i>	k_{rel}	$\ln(k_{rel})$	<i>Conv.</i>	<i>Chem.</i>	k_{rel}	$\ln(k_{rel})$
16.922	-0.144	0.728	-0.318	23.857	-0.205	0.620	-0.478
28.651	-0.105	0.779	-0.250	29.637	-0.189	0.633	-0.457
42.269	-0.105	0.755	-0.280	41.733	-0.169	0.636	-0.452
56.040	-0.097	0.740	-0.301	58.905	-0.134	0.647	-0.436
		0.750 ± 0.022	-0.287 ± 0.029			0.634 ± 0.011	-0.456 ± 0.017
 <p style="text-align: center;">3t [a]</p>				 <p style="text-align: center;">3t [a]</p>			

Conv.	Chem.	k_{rel}	$\ln(k_{rel})$	Conv.	Chem.	k_{rel}	$\ln(k_{rel})$
17.563	-0.267	0.548	-0.602	16.163	-0.284	0.528	-0.638
31.600	-0.241	0.550	-0.597	28.314	-0.256	0.539	-0.618
45.793	-0.219	0.542	-0.612	41.220	-0.230	0.540	-0.616
62.014	-0.182	0.535	-0.625	54.527	-0.201	0.538	-0.620
		0.544 ± 0.007	-0.609 ± 0.012			0.536 ± 0.005	-0.623 ± 0.010
 <p>3u [a]</p>				 <p>3v [b]</p>			
Conv.	Chem.	k_{rel}	$\ln(k_{rel})$	Conv.	Chem.	k_{rel}	$\ln(k_{rel})$
19.083	-0.299	0.505	-0.684	19.475	-0.206	0.628	-0.466
30.529	-0.274	0.509	-0.675	34.864	-0.165	0.661	-0.414
41.613	-0.240	0.524	-0.646	48.620	-0.141	0.668	-0.404
59.167	-0.195	0.527	-0.640	68.114	-0.114	0.651	-0.429
		0.516 ± 0.011	-0.661 ± 0.022			0.652 ± 0.018	-0.428 ± 0.027
 <p>3w [b]</p>				 <p>3w [b]</p>			
Conv.	Chem.	k_{rel}	$\ln(k_{rel})$	Conv.	Chem.	k_{rel}	$\ln(k_{rel})$
17.016	-0.250	0.571	-0.561	16.766	-0.218	0.615	-0.487
25.050	-0.241	0.566	-0.569	25.953	-0.221	0.593	-0.522
35.847	-0.209	0.587	-0.533	34.853	-0.181	0.634	-0.456
50.242	-0.183	0.587	-0.534	51.164	-0.172	0.601	-0.509
		0.578 ± 0.011	-0.549 ± 0.019			0.611 ± 0.018	-0.493 ± 0.029
 <p>3x [a]</p>				 <p>3y [a]</p>			
Conv.	Chem.	k_{rel}	$\ln(k_{rel})$	Conv.	Chem.	k_{rel}	$\ln(k_{rel})$
18.473	0.528	3.636	1.291	16.035	0.669	5.720	1.744
26.315	0.512	3.688	1.305	26.757	0.640	5.711	1.742
39.035	0.460	3.570	1.272	36.368	0.603	5.612	1.725
50.393	0.422	3.662	1.298	49.745	0.548	5.770	1.753
		3.639 ± 0.051	1.292 ± 0.014			5.703 ± 0.066	1.741 ± 0.012
 <p>3z [a]</p>							
Conv.	Chem.	k_{rel}	$\ln(k_{rel})$				
20.198	0.590	4.482	1.500				
34.311	0.533	4.269	1.451				
50.038	0.465	4.243	1.445				
68.626	0.345	4.287	1.456				
		4.320 ± 0.109	1.463 ± 0.025				

[a] Turnover-limited competition experiments were carrying out by method A. [b] Turnover-limited competition experiments were carrying out by method B.

Size-Driven Inversion of Selectivity in Esterfication

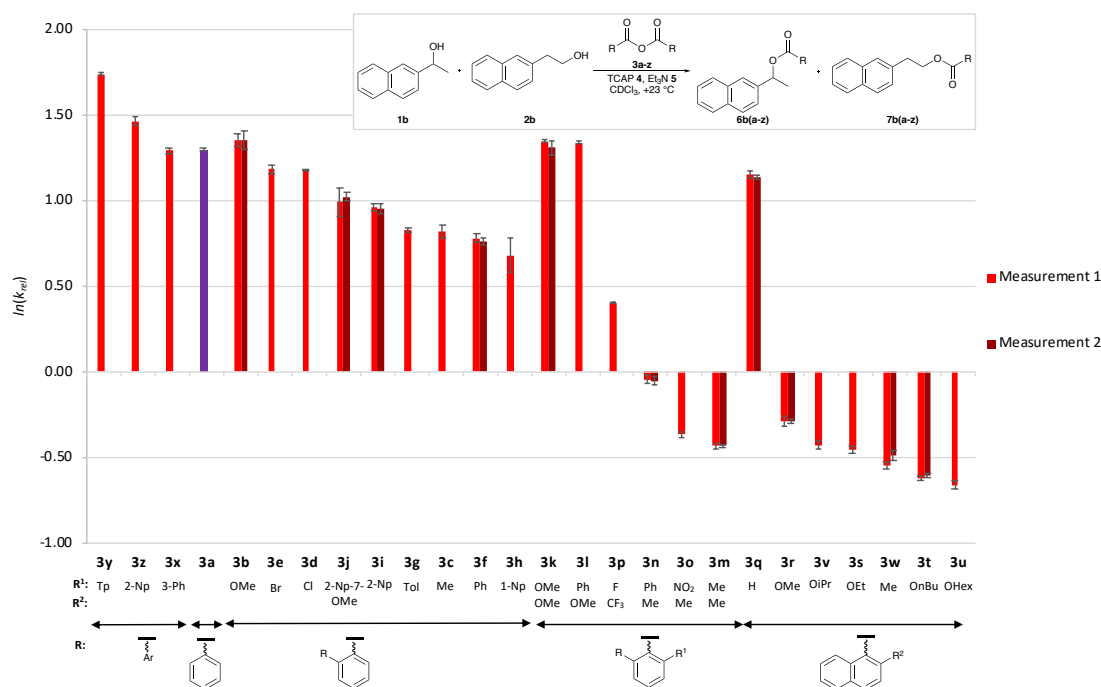


Figure 3.6. $\ln(k_{rel})$ of turnover-limited competition experiment between **1b** and **2b** with the benzoic anhydride derivatives **3a-z**.

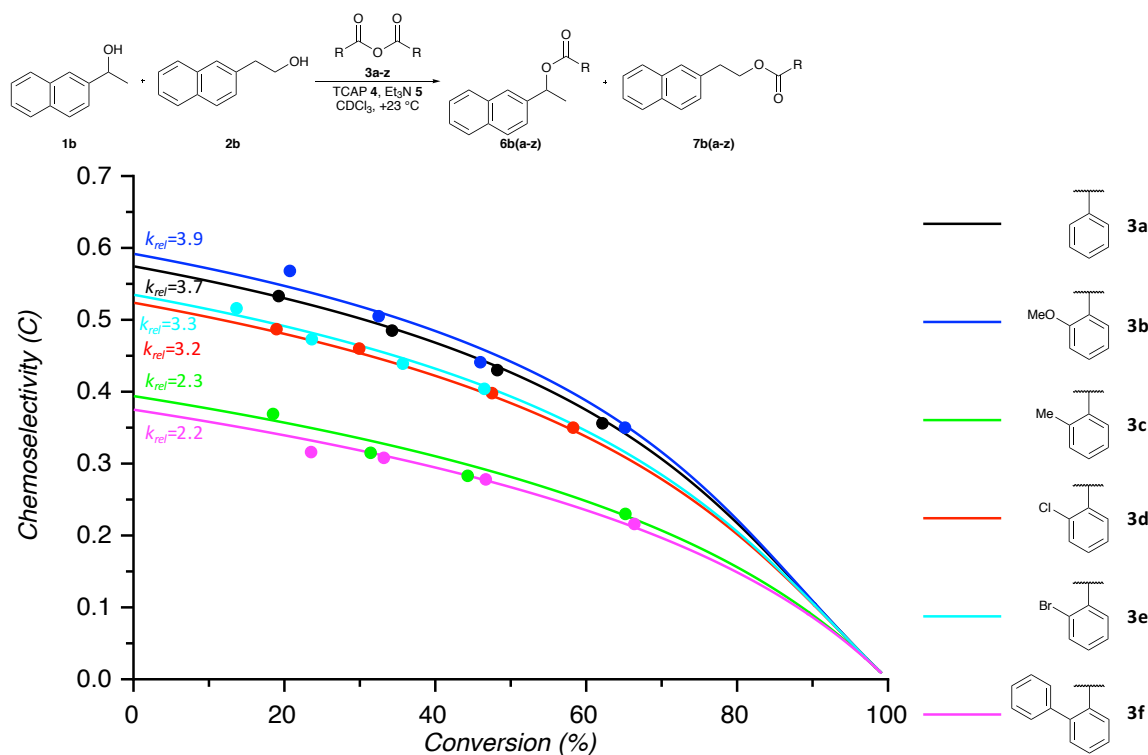


Figure 3.7. Plot of conversion vs. corrected chemoselectivity for turnover-limited competition experiment **1b** vs. **2b** with the benzoic anhydride derivatives **3a-f**.

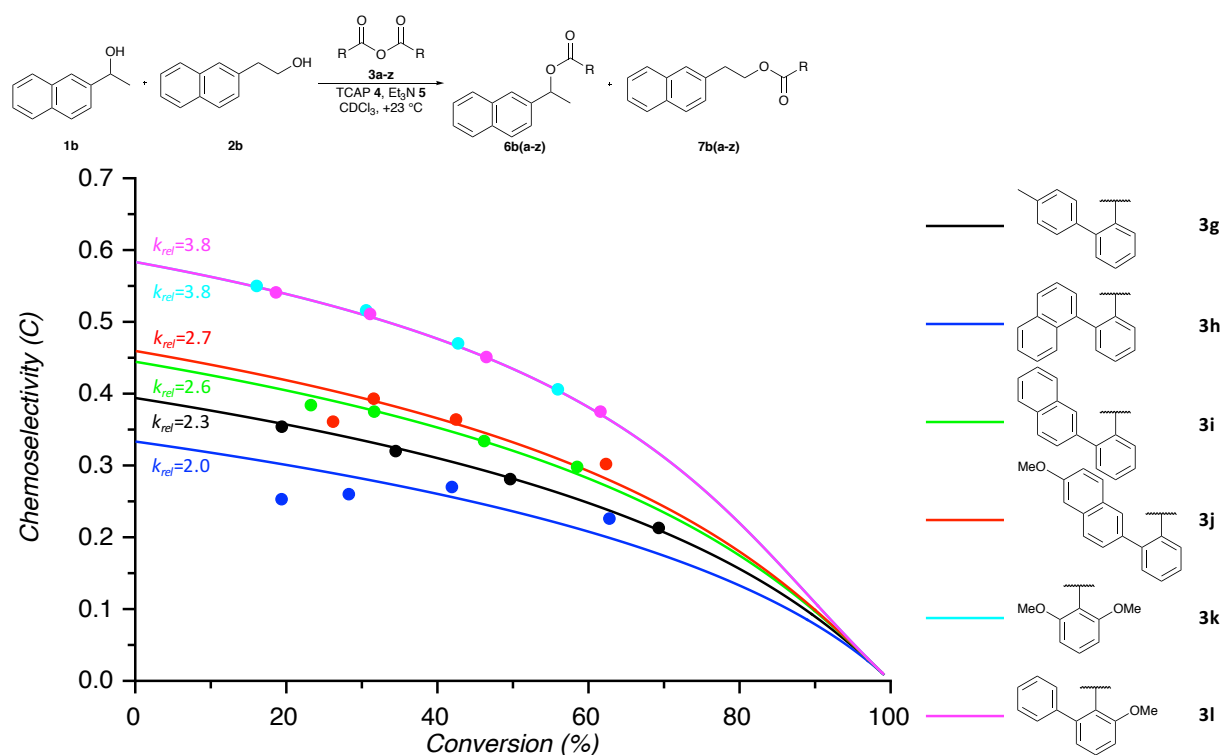


Figure 3.8. Plot of conversion vs. corrected chemoselectivity for turnover-limited competition experiment **1b** vs. **2b** with the benzoic anhydride derivatives **3g-l**.

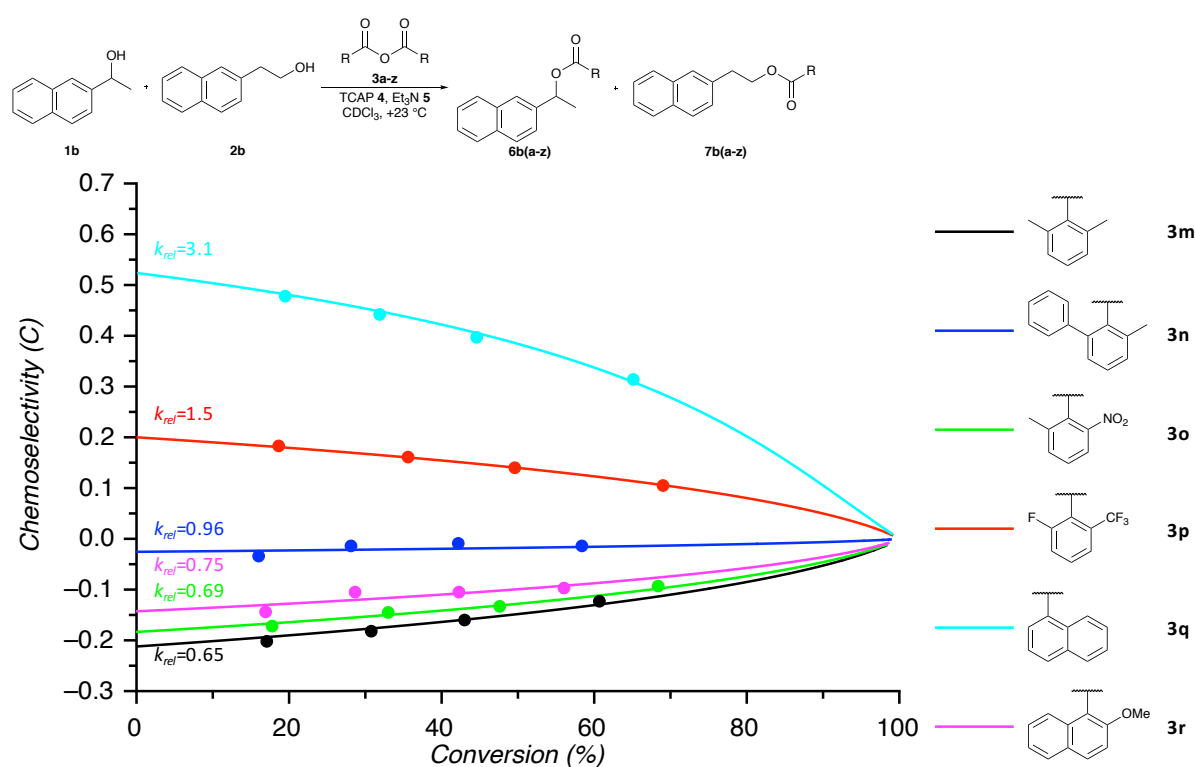


Figure 3.9. Plot of conversion vs. corrected chemoselectivity for turnover-limited competition experiment **1b** vs. **2b** with the benzoic anhydride derivatives **3m-r**.

Size-Driven Inversion of Selectivity in Esterification

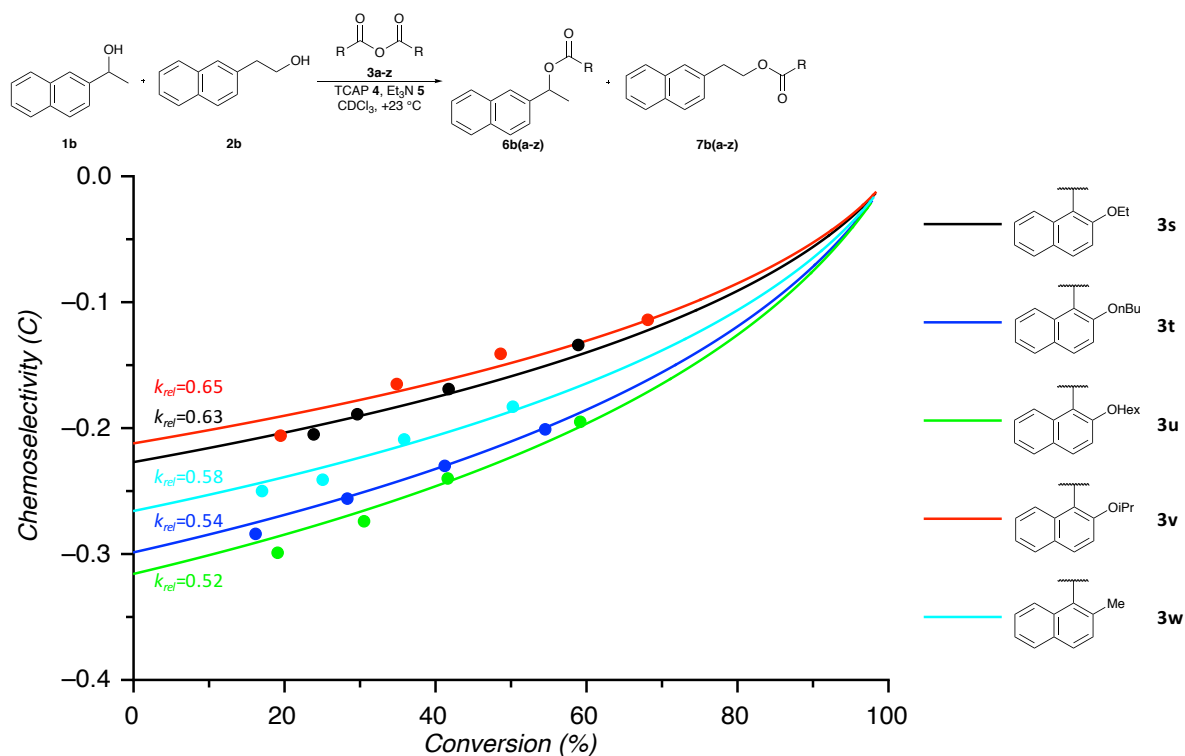


Figure 3.10. Plot of conversion vs. corrected chemoselectivity for turnover-limited competition experiment **1b** vs. **2b** with the benzoic anhydride derivatives **3s-w**.

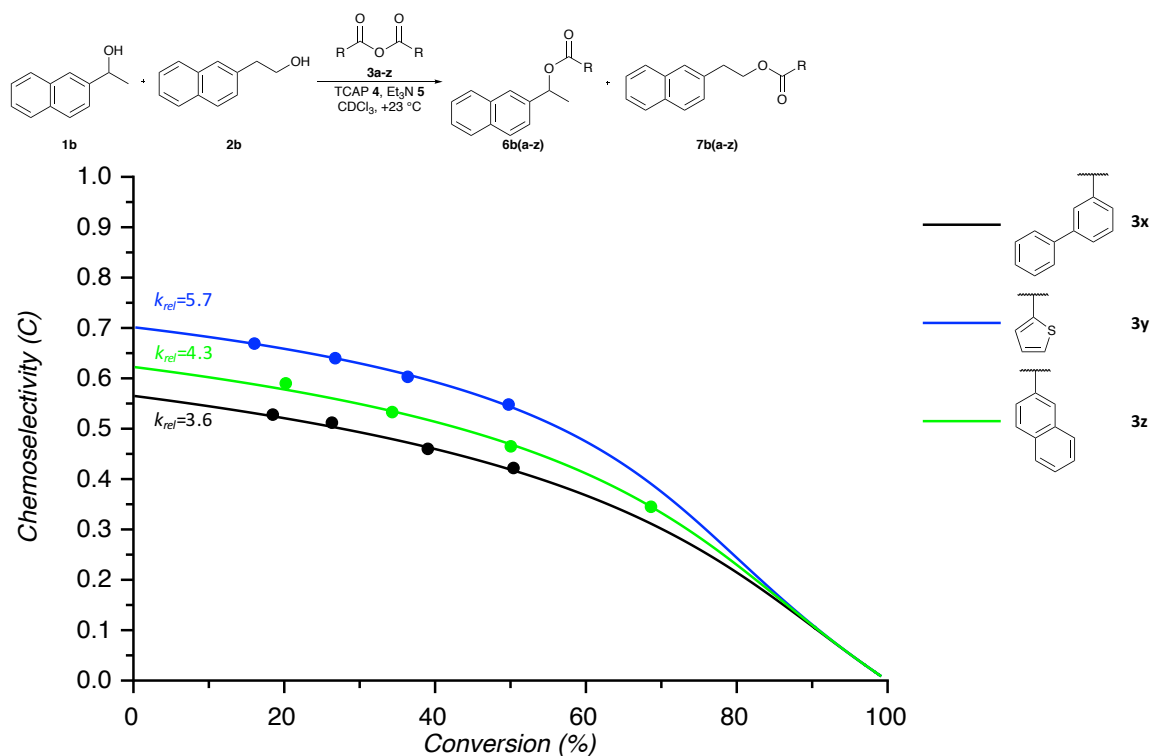
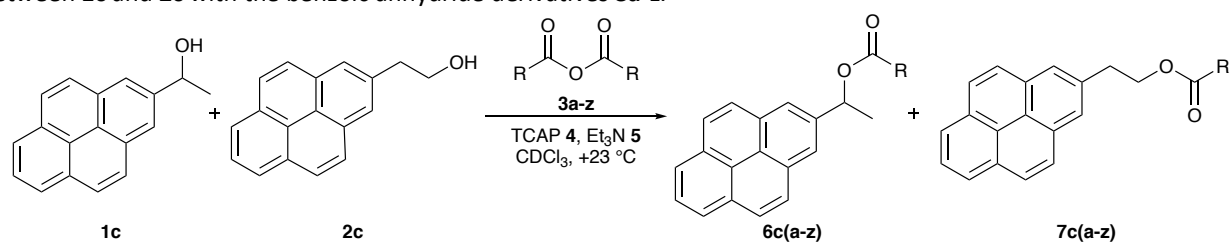
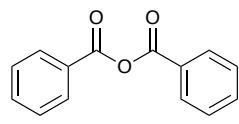
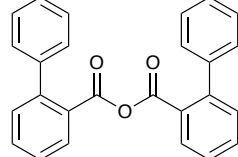
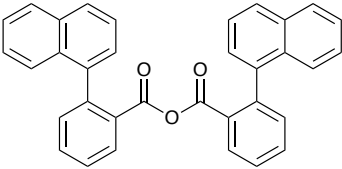
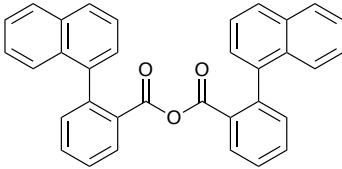
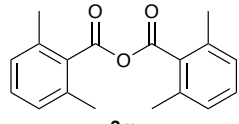
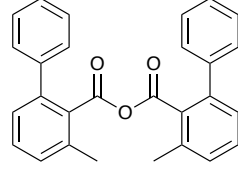
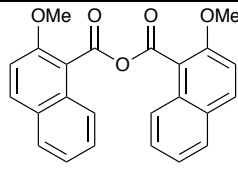


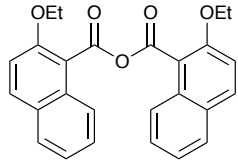
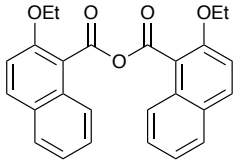
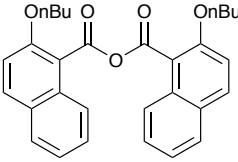
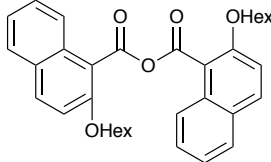
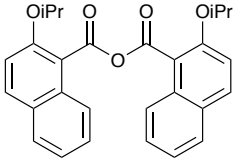
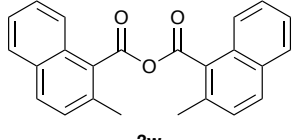
Figure 3.11. Plot of conversion vs. corrected chemoselectivity for turnover-limited competition experiment **1b** vs. **2b** with the benzoic anhydride derivatives **3x-z**.

Table 3.6. Conversion, corrected chemoselectivity, relative rate and natural logarithm of relative rate with standard derivations calculated from corresponding ^1H NMR measurements for turnover-limited competition experiments between **1c** and **2c** with the benzoic anhydride derivatives **3a-z**.



 3a [a]				 3f [a]			
<i>Conv.</i>	<i>Chem.</i>	k_{rel}	$\ln(k_{\text{rel}})$	<i>Conv.</i>	<i>Chem.</i>	k_{rel}	$\ln(k_{\text{rel}})$
17.714	0.483	3.174	1.155	21.350	0.203	1.590	0.464
31.491	0.419	2.931	1.075	34.215	0.197	1.639	0.494
45.678	0.386	3.049	1.115	48.643	0.174	1.646	0.498
61.985	0.312	3.019	1.105	62.690	0.152	1.688	0.524
		3.043 ± 0.100	1.113 ± 0.033			1.641 ± 0.040	0.495 ± 0.024
 3h [a]				 3h [a]			
<i>Conv.</i>	<i>Chem.</i>	k_{rel}	$\ln(k_{\text{rel}})$	<i>Conv.</i>	<i>Chem.</i>	k_{rel}	$\ln(k_{\text{rel}})$
20.753	0.298	1.995	0.691	27.961	0.294	2.041	0.714
33.008	0.267	1.957	0.671	36.446	0.258	1.948	0.667
49.300	0.224	1.920	0.652	51.136	0.222	1.936	0.660
72.569	0.157	1.937	0.661	71.888	0.162	1.955	0.670
		1.952 ± 0.032	0.669 ± 0.016			1.970 ± 0.048	0.678 ± 0.024
 3m [b]				 3n [b]			
<i>Conv.</i>	<i>Chem.</i>	k_{rel}	$\ln(k_{\text{rel}})$	<i>Conv.</i>	<i>Chem.</i>	k_{rel}	$\ln(k_{\text{rel}})$
20.998	-0.305	0.493	-0.708	17.933	-0.208	0.627	-0.467
39.156	-0.277	0.480	-0.733	29.165	-0.188	0.636	-0.453
50.350	-0.243	0.488	-0.718	44.854	-0.168	0.629	-0.463
62.223	-0.200	0.501	-0.691	59.468	-0.140	0.632	-0.459
		0.491 ± 0.009	-0.712 ± 0.018			0.631 ± 0.004	-0.460 ± 0.006
 3o [a]				 3r [a]			
<i>Conv.</i>	<i>Chem.</i>	k_{rel}	$\ln(k_{\text{rel}})$	<i>Conv.</i>	<i>Chem.</i>	k_{rel}	$\ln(k_{\text{rel}})$
18.877	-0.282	0.526	-0.642	17.336	-0.110	0.785	-0.242

Size-Driven Inversion of Selectivity in Esterfication

30.094	-0.265	0.521	-0.651	28.334	-0.106	0.777	-0.252
49.260	-0.233	0.508	-0.678	41.481	-0.101	0.764	-0.269
65.218	-0.178	0.524	-0.646	57.474	-0.092	0.747	-0.292
		0.520 ± 0.008	-0.654 ± 0.016			0.768 ± 0.017	-0.264 ± 0.022
 3s [a]				 3s [a]			
<i>Conv.</i>	<i>Chem.</i>	k_{rel}	$\ln(k_{rel})$	<i>Conv.</i>	<i>Chem.</i>	k_{rel}	$\ln(k_{rel})$
16.889	-0.204	0.635	-0.453	15.789	-0.242	0.584	-0.537
28.245	-0.217	0.593	-0.522	27.534	-0.226	0.582	-0.542
41.994	-0.223	0.548	-0.602	37.978	-0.197	0.601	-0.510
56.535	-0.146	0.631	-0.461	54.467	-0.202	0.536	-0.624
		0.602 ± 0.041	-0.509 ± 0.069			0.576 ± 0.028	-0.553 ± 0.049
 3t [a]				 3u [a]			
<i>Conv.</i>	<i>Chem.</i>	k_{rel}	$\ln(k_{rel})$	<i>Conv.</i>	<i>Chem.</i>	k_{rel}	$\ln(k_{rel})$
15.078	-0.290	0.524	-0.647	15.933	-0.286	0.527	-0.640
30.097	-0.283	0.498	-0.698	28.877	-0.283	0.502	-0.690
40.906	-0.266	0.490	-0.714	39.925	-0.270	0.487	-0.719
56.014	-0.219	0.502	-0.690	64.994	-0.176	0.531	-0.634
		0.503 ± 0.018	-0.687 ± 0.035			0.512 ± 0.021	-0.671 ± 0.041
 3v [b]				 3w [b]			
<i>Conv.</i>	<i>Chem.</i>	k_{rel}	$\ln(k_{rel})$	<i>Conv.</i>	<i>Chem.</i>	k_{rel}	$\ln(k_{rel})$
17.945	-0.215	0.617	-0.483	18.698	-0.355	0.440	-0.820
30.058	-0.193	0.625	-0.470	31.586	-0.333	0.433	-0.836
48.717	-0.167	0.619	-0.479	47.193	-0.291	0.434	-0.834
69.207	-0.131	0.603	-0.506	66.237	-0.222	0.436	-0.829
		0.616 ± 0.009	-0.485 ± 0.015			0.436 ± 0.003	-0.830 ± 0.007

^[a]Turnover-limited competition experiments were carrying out by method A. ^[b]Turnover-limited competition experiments were carrying out by method B.

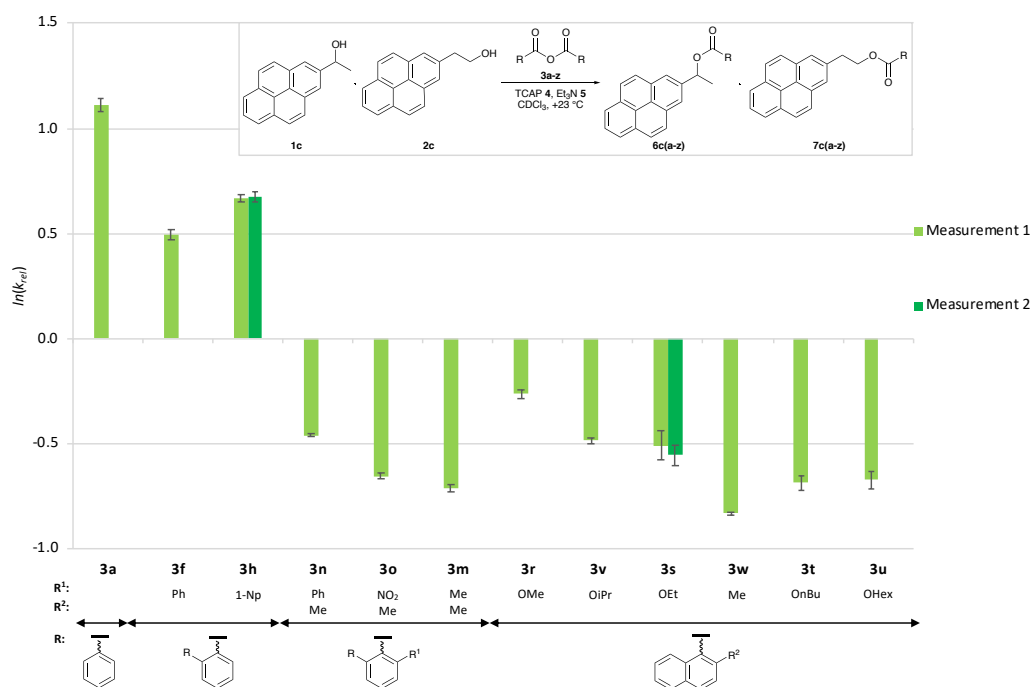


Figure 3.12. $\ln(k_{rel})$ of turnover-limited competition experiment between **1c** and **2c** with the benzoic anhydride derivatives **3a-z**.

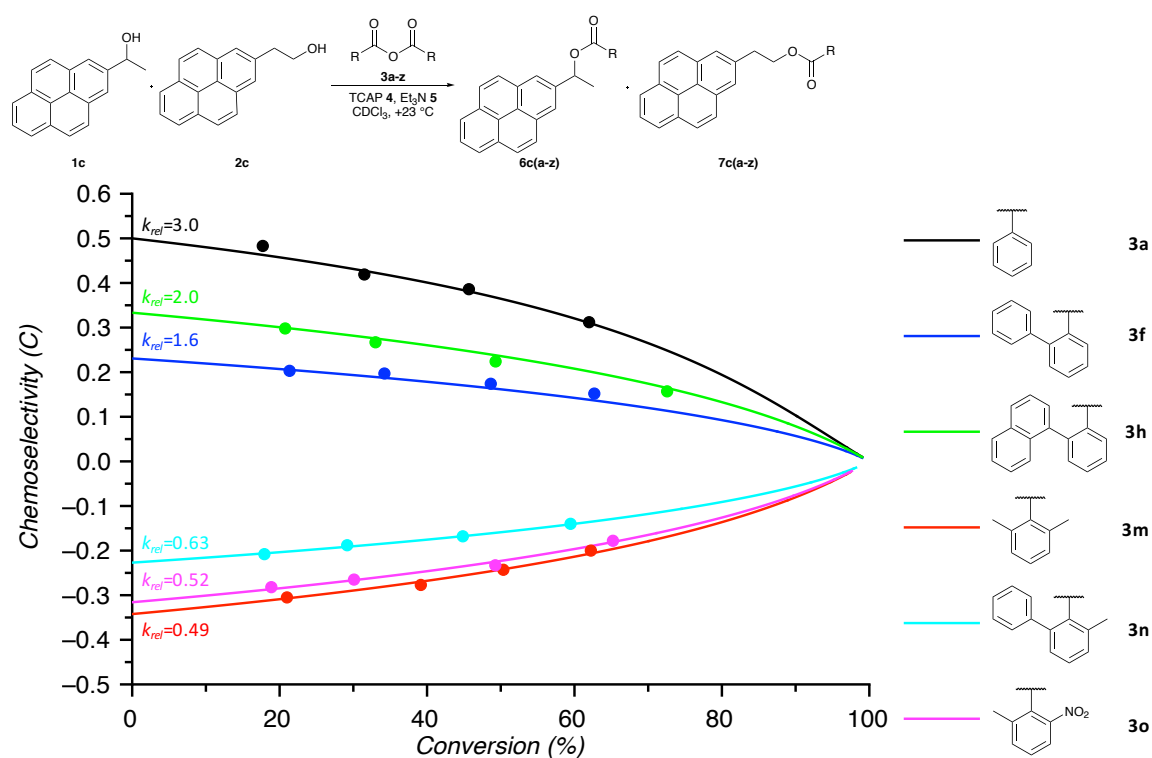


Figure 3.13. Plot of conversion vs. corrected chemoselectivity for turnover-limited competition experiment **1c** vs. **2c** with the benzoic anhydride derivatives **3a-o**.

Size-Driven Inversion of Selectivity in Esterification

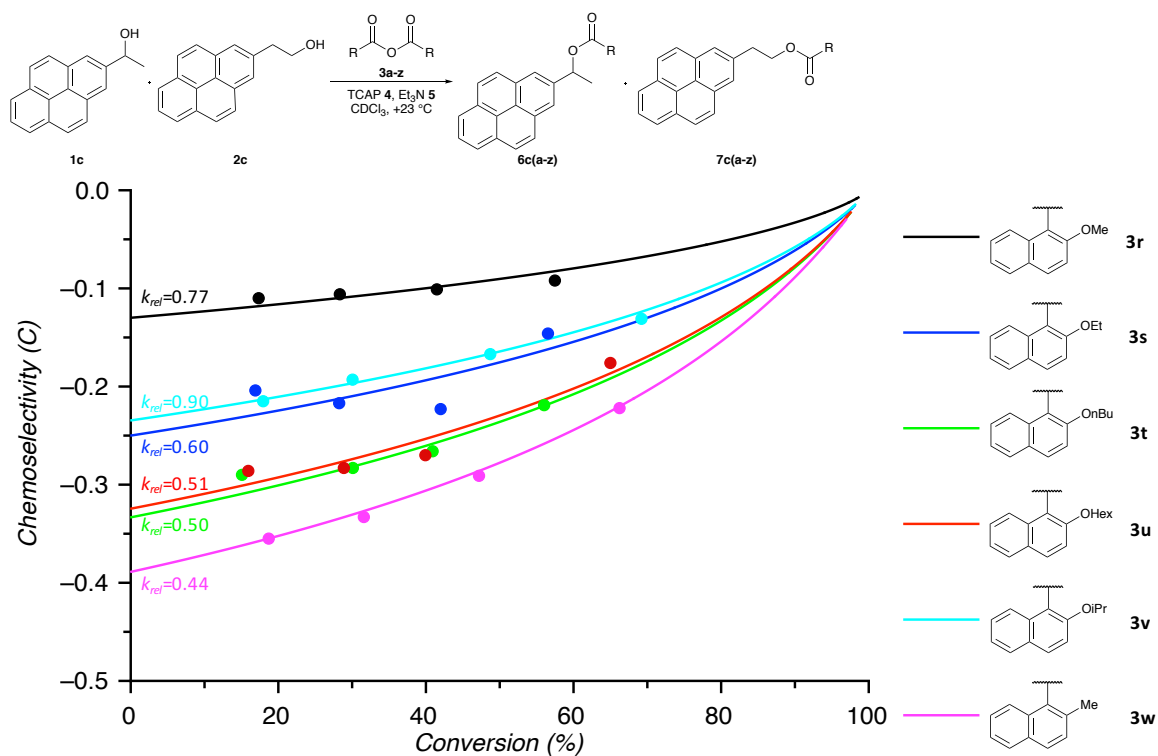
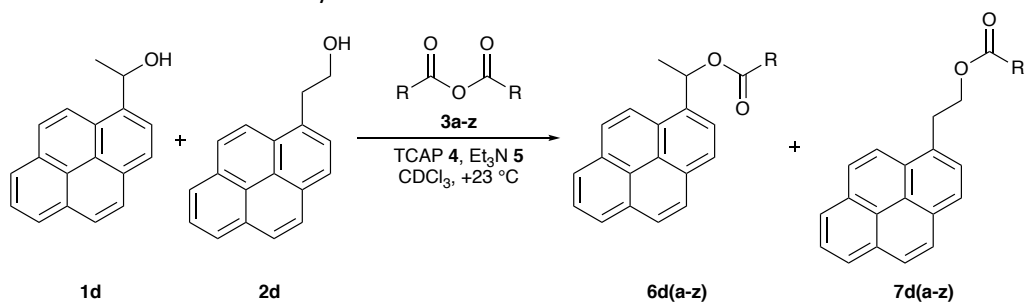
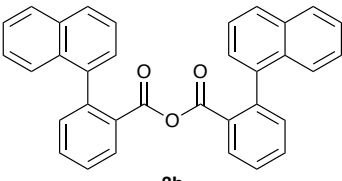
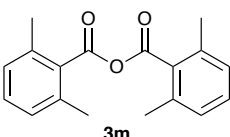
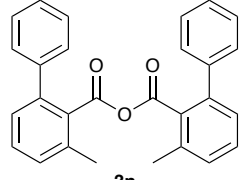
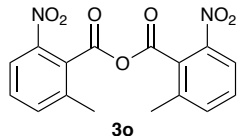
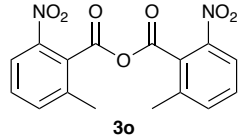
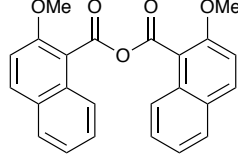
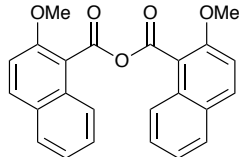
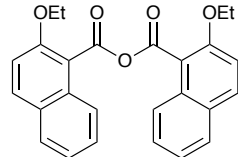


Figure 3.14. Plot of conversion vs. corrected chemoselectivity for turnover-limited competition experiment **1c** vs. **2c** with the benzoic anhydride derivatives **3r-w**.

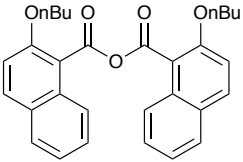
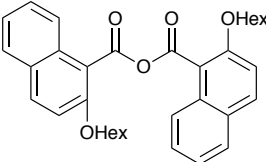
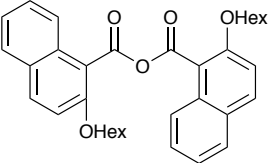
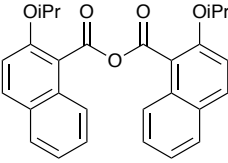
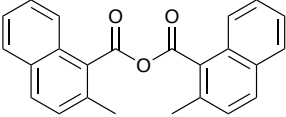
Table 3.7. Conversion, corrected chemoselectivity, relative rate and natural logarithm of relative rate with standard derivations calculated from corresponding ^1H NMR measurements for turnover-limited competition experiments between **1d** and **2d** with the benzoic anhydride derivatives **3a-z**.



3a [a]				3f [a]			
Conv.	Chem.	k_{rel}	$\ln(k_{rel})$	Conv.	Chem.	k_{rel}	$\ln(k_{rel})$
19.064	0.468	3.069	1.121	19.818	0.416	2.679	0.986
34.010	0.399	2.826	1.039	31.226	0.417	2.908	1.067
46.989	0.365	2.897	1.064	47.469	0.363	2.895	1.063
67.907	0.264	2.821	1.037	65.222	0.286	2.909	1.068
		2.903 ± 0.116	1.065 ± 0.039			2.848 ± 0.112	1.046 ± 0.040
3f [a]				3h [a]			
Conv.	Chem.	k_{rel}	$\ln(k_{rel})$	Conv.	Chem.	k_{rel}	$\ln(k_{rel})$

7.242	0.343	2.100	0.742	24.366	0.549	4.065	1.402
32.996	0.388	2.716	0.999	34.690	0.428	3.097	1.130
56.133	0.332	2.930	1.075	49.087	0.363	2.949	1.081
78.670	0.211	3.140	1.144	70.556	0.253	2.882	1.059
		2.721 ± 0.449	0.990 ± 0.176			3.248 ± 0.552	1.168 ± 0.159
 <p>3h [a]</p>				 <p>3m [b]</p>			
<i>Conv.</i>	<i>Chem.</i>	k_{rel}	$\ln(k_{rel})$	<i>Conv.</i>	<i>Chem.</i>	k_{rel}	$\ln(k_{rel})$
28.496	0.470	3.318	1.199	20.908	-0.324	0.471	-0.754
34.266	0.418	2.993	1.096	34.746	-0.275	0.496	-0.701
47.848	0.362	2.891	1.062	48.333	-0.232	0.512	-0.670
69.707	0.258	2.878	1.057	64.942	-0.195	0.495	-0.704
		3.020 ± 0.205	1.104 ± 0.066			0.493 ± 0.017	-0.707 ± 0.043
 <p>3n [b]</p>				 <p>3o [a]</p>			
<i>Conv.</i>	<i>Chem.</i>	k_{rel}	$\ln(k_{rel})$	<i>Conv.</i>	<i>Chem.</i>	k_{rel}	$\ln(k_{rel})$
16.904	-0.025	0.947	-0.055	21.167	-0.231	0.589	-0.530
25.895	0.009	1.021	0.021	38.493	-0.185	0.617	-0.482
42.796	-0.001	0.997	-0.003	50.943	-0.159	0.627	-0.467
58.368	-0.028	0.914	-0.090	73.652	-0.108	0.631	-0.461
		0.970 ± 0.048	-0.032 ± 0.050			0.616 ± 0.019	-0.485 ± 0.031
 <p>3o [a]</p>				 <p>3r [a]</p>			
<i>Conv.</i>	<i>Chem.</i>	k_{rel}	$\ln(k_{rel})$	<i>Conv.</i>	<i>Chem.</i>	k_{rel}	$\ln(k_{rel})$
19.744	-0.213	0.617	-0.483	18.527	-0.185	0.660	-0.416
33.775	-0.181	0.637	-0.451	30.336	-0.159	0.680	-0.386
50.721	-0.153	0.639	-0.447	46.938	-0.135	0.685	-0.378
66.828	-0.117	0.650	-0.431	/	/	/	/
		0.636 ± 0.014	-0.453 ± 0.021			0.675 ± 0.013	-0.393 ± 0.020
 <p>3r [a]</p>				 <p>3s [a]</p>			
<i>Conv.</i>	<i>Chem.</i>	k_{rel}	$\ln(k_{rel})$	<i>Conv.</i>	<i>Chem.</i>	k_{rel}	$\ln(k_{rel})$
25.608	-0.155	0.695	-0.364	17.449	-0.373	0.423	-0.860
32.899	-0.151	0.688	-0.374	24.990	-0.306	0.482	-0.729
48.263	-0.128	0.695	-0.365	45.871	-0.256	0.486	-0.721
61.162	-0.108	0.696	-0.363	65.663	-0.193	0.493	-0.707
		0.693 ± 0.003	-0.366 ± 0.005			0.471 ± 0.032	-0.754 ± 0.071

Size-Driven Inversion of Selectivity in Esterfication

 <p>3t [a]</p>				 <p>3u [a]</p>			
Conv.	Chem.	k_{rel}	$\ln(k_{rel})$	Conv.	Chem.	k_{rel}	$\ln(k_{rel})$
16.534	-0.402	0.395	-0.929	18.834	-0.385	0.408	-0.897
28.117	-0.352	0.420	-0.868	30.891	-0.347	0.418	-0.872
45.059	-0.307	0.421	-0.866	42.056	-0.318	0.418	-0.871
54.431	-0.280	0.417	-0.874	56.572	-0.262	0.432	-0.838
		0.413 ± 0.012	-0.884 ± 0.030			0.419 ± 0.010	-0.870 ± 0.015
 <p>3u [a]</p>				 <p>3v [b]</p>			
Conv.	Chem.	k_{rel}	$\ln(k_{rel})$	Conv.	Chem.	k_{rel}	$\ln(k_{rel})$
25.902	-0.359	0.419	-0.871	19.218	-0.306	0.495	-0.702
32.081	-0.344	0.419	-0.869	31.273	-0.279	0.500	-0.694
45.851	-0.305	0.421	-0.865	43.831	-0.241	0.515	-0.663
62.440	-0.255	0.409	-0.895	67.123	-0.175	0.519	-0.657
		0.417 ± 0.006	-0.875 ± 0.013			0.507 ± 0.011	-0.679 ± 0.022
 <p>3w [b]</p>							
Conv.	Chem.	k_{rel}	$\ln(k_{rel})$				
18.189	-0.380	0.414	-0.881				
28.084	-0.342	0.432	-0.840				
42.387	-0.296	0.445	-0.810				
58.476	-0.239	0.456	-0.785				
		0.437 ± 0.018	-0.829 ± 0.036				

^[a]Turnover-limited competition experiments were carrying out by method A. ^[b]Turnover-limited competition experiments were carrying out by method B.

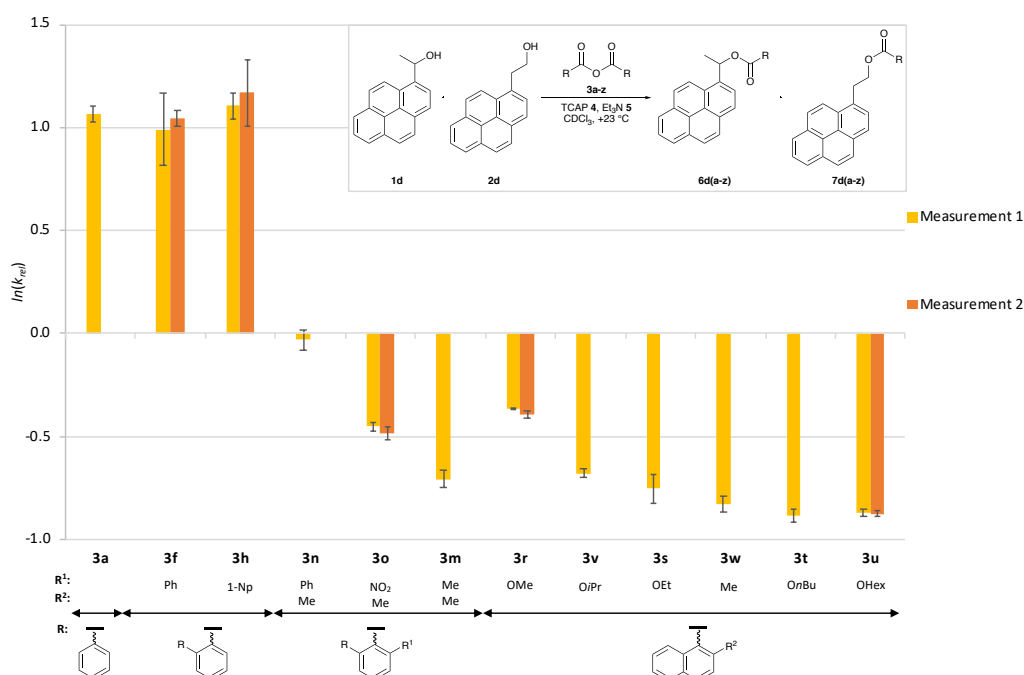


Figure 3.15. $\ln(k_{rel})$ of turnover-limited competition experiment between **1d** and **2d** with the benzoic anhydride derivatives **3a-z**.

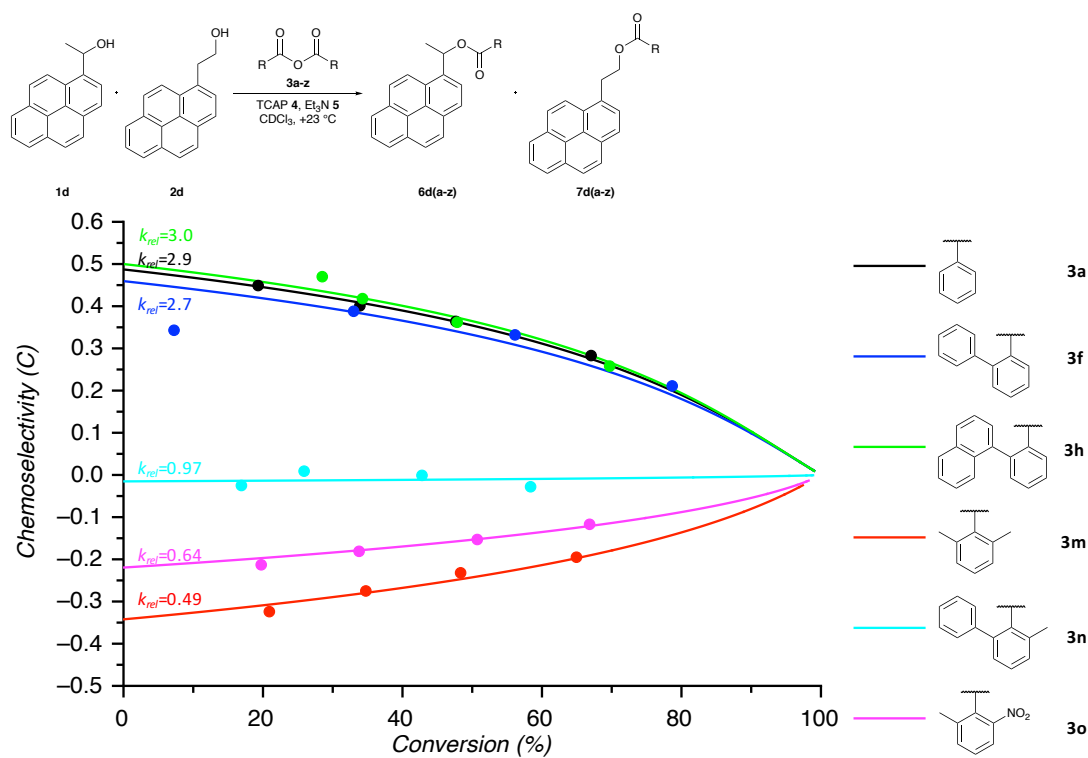


Figure 3.16. Plot of conversion vs. corrected chemoselectivity for turnover-limited competition experiment **1d** vs. **2d** with the benzoic anhydride derivatives **3a-o**.

Size-Driven Inversion of Selectivity in Esterification

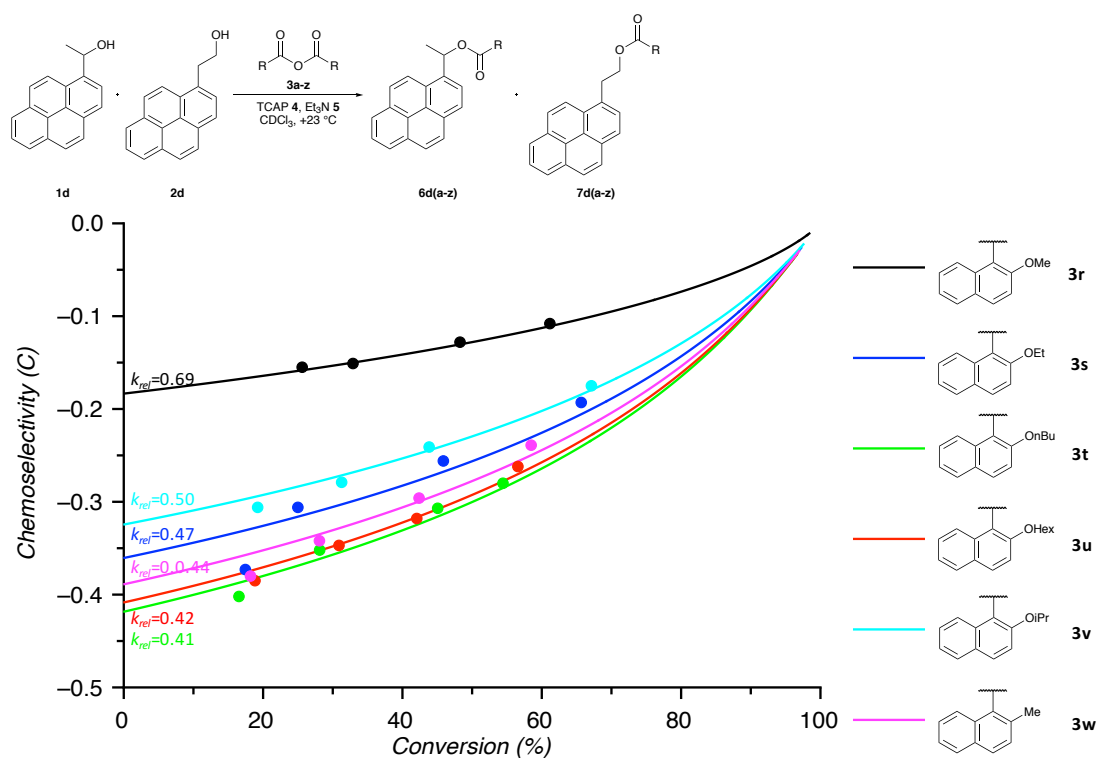
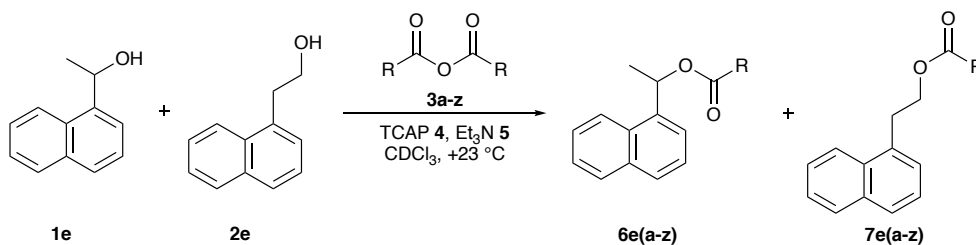
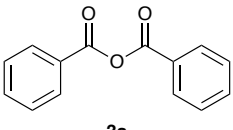
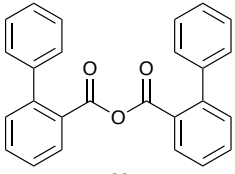
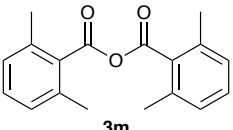
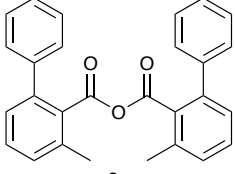
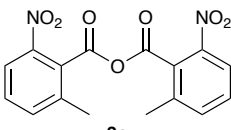
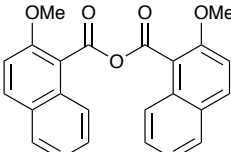
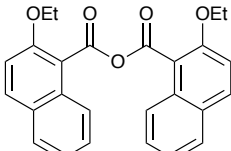
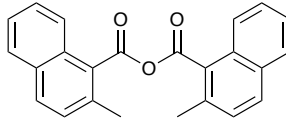


Figure 3.17. Plot of conversion vs. corrected chemoselectivity for turnover-limited competition experiment **1d** vs. **2d** with the benzoic anhydride derivatives **3r-w**.

Table 3.8. Conversion, corrected chemoselectivity, relative rate and natural logarithm of relative rate with standard derivations calculated from corresponding ^1H NMR measurements for turnover-limited competition experiments between **1e** and **2e** with the benzoic anhydride derivatives **3a-z**.



 3a [a]				 3f [a]			
<i>Conv.</i>	<i>Chem.</i>	k_{rel}	$\ln(k_{rel})$	<i>Conv.</i>	<i>Chem.</i>	k_{rel}	$\ln(k_{rel})$
19.042	0.688	6.329	1.845	20.815	0.545	3.894	1.360
34.538	0.636	6.194	1.824	33.349	0.494	3.736	1.318
44.548	0.601	6.377	1.853	44.413	0.474	3.994	1.385
61.044	0.486	6.298	1.840	65.286	0.365	4.139	1.420
		6.299 ± 0.077	1.840 ± 0.012			3.941 ± 0.170	1.371 ± 0.043
 3m [b]				 3n [b]			
<i>Conv.</i>	<i>Chem.</i>	k_{rel}	$\ln(k_{rel})$	<i>Conv.</i>	<i>Chem.</i>	k_{rel}	$\ln(k_{rel})$
24.829	0.117	1.311	0.271	20.074	0.368	2.364	0.860

32.182	0.104	1.291	0.256	33.108	0.372	2.597	0.954
43.399	0.081	1.245	0.219	43.460	0.348	2.645	0.973
58.687	0.073	1.267	0.237	61.522	0.285	2.701	0.994
		1.279 ± 0.029	0.246 ± 0.022			2.577 ± 0.148	0.945 ± 0.059
 3o [a]				 3r [a]			
<i>Conv.</i>	<i>Chem.</i>	k_{rel}	$\ln(k_{rel})$	<i>Conv.</i>	<i>Chem.</i>	k_{rel}	$\ln(k_{rel})$
17.994	0.277	1.872	0.627	15.328	0.258	1.774	0.573
31.244	0.253	1.868	0.625	27.452	0.188	1.567	0.449
44.754	0.136	1.453	0.374	39.457	0.187	1.631	0.489
58.697	0.146	1.606	0.474	54.583	0.080	1.277	0.245
		1.700 ± 0.206	0.525 ± 0.124			1.562 ± 0.209	0.439 ± 0.139
 3s [a]				 3w [b]			
<i>Conv.</i>	<i>Chem.</i>	k_{rel}	$\ln(k_{rel})$	<i>Conv.</i>	<i>Chem.</i>	k_{rel}	$\ln(k_{rel})$
17.458	0.186	1.515	0.415	17.812	-0.053	0.890	-0.116
29.492	0.120	1.335	0.289	26.456	0.003	1.008	0.008
41.841	0.135	1.433	0.359	39.266	0.022	1.059	0.057
57.750	0.089	1.328	0.283	54.764	0.019	1.061	0.059
		1.402 ± 0.089	0.337 ± 0.063			1.004 ± 0.080	0.002 ± 0.082

[a] Turnover-limited competition experiments were carrying out by method A. [b] Turnover-limited competition experiments were carrying out by method B.

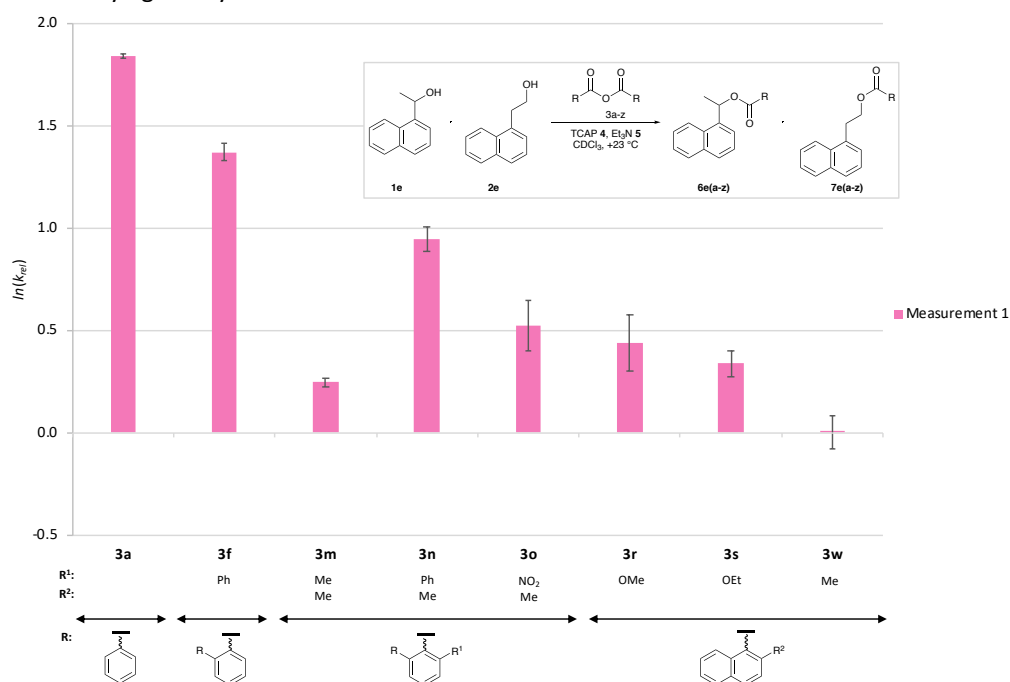


Figure 3.18. $\ln(k_{rel})$ of turnover-limited competition experiment between **1e** and **2e** with the benzoic anhydride derivatives **3a-z**.

Size-Driven Inversion of Selectivity in Esterification

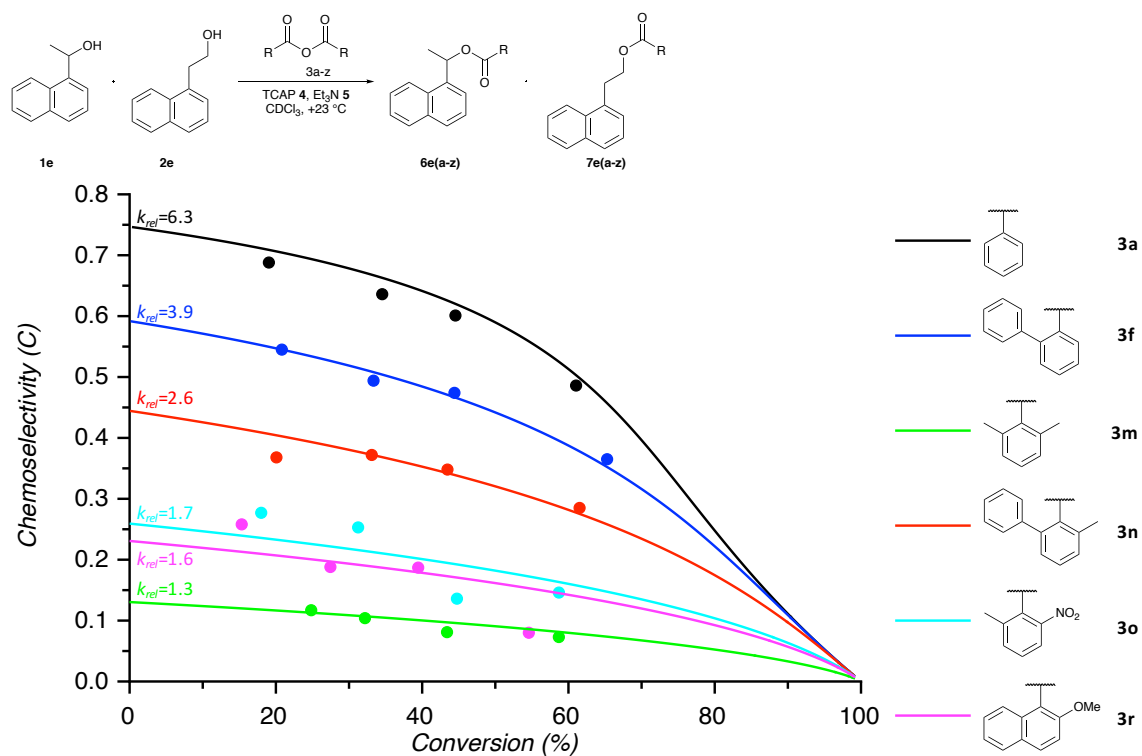


Figure 3.19. Plot of conversion vs. corrected chemoselectivity for turnover-limited competition experiment **1e** vs. **2e** with the benzoic anhydride derivatives **3a-r**.

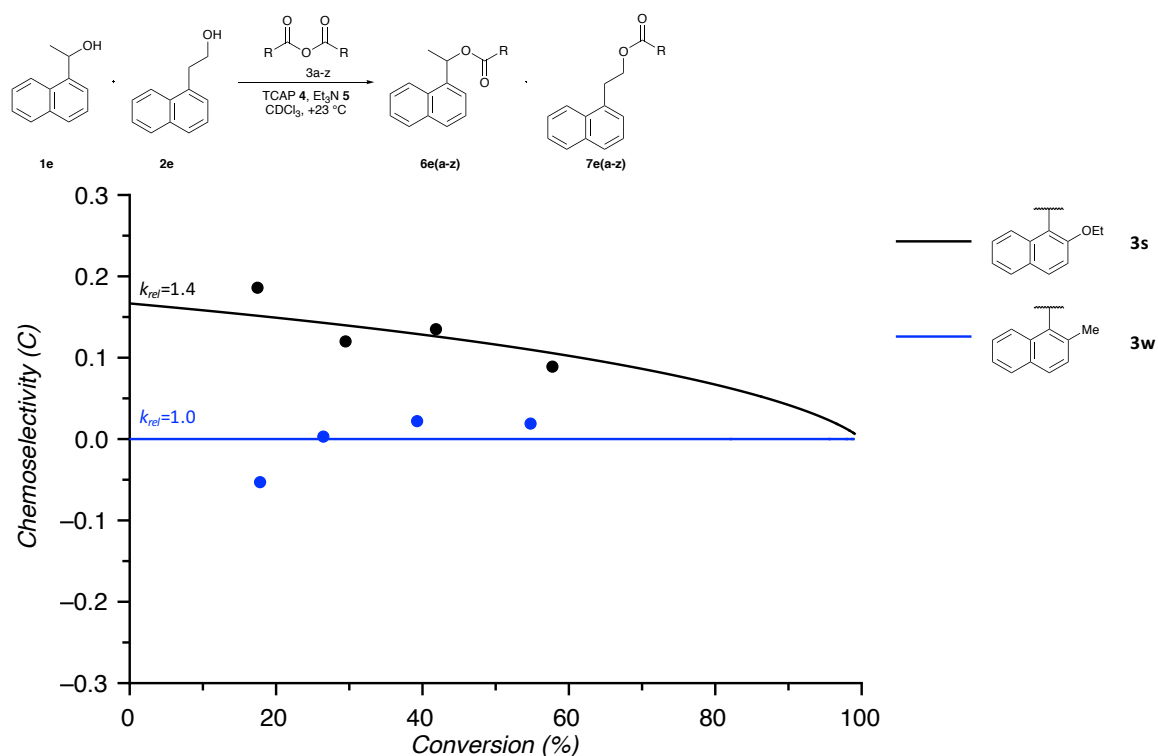
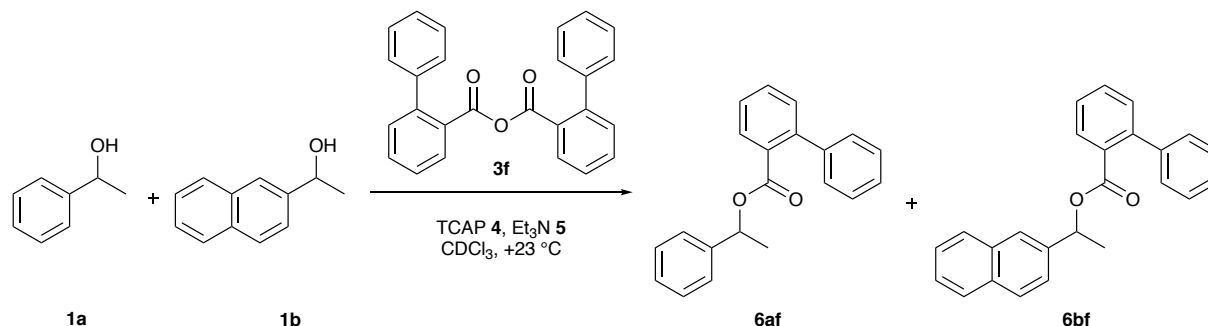


Figure 3.20. Plot of conversion vs. corrected chemoselectivity for turnover-limited competition experiment **1e** vs. **2e** with the benzoic anhydride derivatives **3s,w**.

3.1.2 Investigation of Size Effects of the Alcohol Starting Materials

To explore the influence of the aromatic surface of the alcohol substrates in the selectivity, two secondary alcohols **1** bearing different-size aromatic surfaces were tested with acid anhydrides **3f** and **3s**. These were repeated for the primary alcohols **2** bearing different-size aromatic surfaces.

The preparation of the turnover-limited competition experiments is shown for the following example:



For these three CDCl₃ stock solutions are prepared under nitrogen (Table 3.9). Stock A contains the secondary alcohols **1a** and **1b** and having a concentration of 0.05 M each. Stock B gathers anhydride **3f** (0.1 M) while Stock C consists of a 0.15 M Et₃N and catalyst TCAP in a concentration of 0.005 M (method C).

Table 3.9. Preparation of initial CDCl₃ stock solutions.

Stock	Compound	Molarity (mol L ⁻¹)	Volume (mL)	n (mol)	M.W. (g mol ⁻¹)	Mass (mg)
Stock A	1a	0.05	2	100·10 ⁻⁶	122.16	12.2
	1b	0.05	2	100·10 ⁻⁶	172.08	17.2
Stock B	3f	0.1	2	200·10 ⁻⁶	378.13	75.6
Stock C	TCAP	0.005	5	25·10 ⁻⁶	174.24	4.4
	Et ₃ N	0.15	5	750·10 ⁻³	101.19	75.9

Because the anthracene alcohols **1f/2f** are not soluble with this concentration, stock solutions with lower concentration are prepared. Stock A contains the secondary alcohols **1a** and **1b** and having a concentration of 0.02 M each. Stock B gathers anhydride **3f** (0.04 M) while Stock C consists of a 0.06 M Et₃N and catalyst TCAP in a concentration of 0.002 M (method D).

The following procedure is equivalent to the procedure explained in chapter 3.1.1.

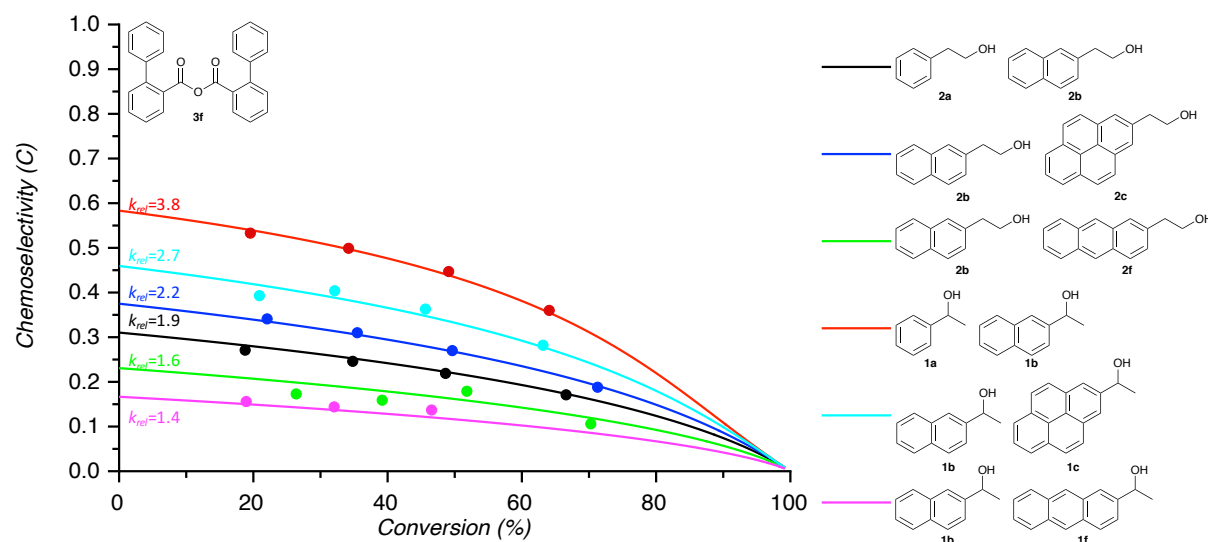


Figure 3.21. Plot of conversion vs. corrected chemoselectivity for turnover-limited competition experiment between primary alcohols **2** and between secondary alcohols **1** with **3f**.

Table 3.10. Conversion, corrected chemoselectivity, relative rate and natural logarithm of relative rate with standard derivations calculated from corresponding ¹H NMR measurements for turnover-limited competition experiments between primary alcohols **2** and between secondary alcohols **1** with **3f**.

Primary Alcohol 2				Secondary Alcohol 1			
2a vs. 2b ^[a]				1a vs. 1b ^[a]			
Conv.	Chem.	k _{rel}	ln(k _{rel})	Conv.	Chem.	k _{rel}	ln(k _{rel})
18.777	0.271	1.850	0.615	19.550	0.533	3.727	1.316
34.802	0.246	1.870	0.626	34.182	0.499	3.822	1.341

Size-Driven Inversion of Selectivity in Esterfication

48.628	0.219	1.881	0.632	49.097	0.447	3.911	1.364
66.587	0.171	1.886	0.635	64.076	0.360	3.878	1.355
		1.872 ± 0.016	0.627 ± 0.008			3.835 ± 0.081	1.344 ± 0.021
2a vs. 2b^[a]				1a vs. 1b^[a]			
<i>Conv.</i>	<i>Chem.</i>	k_{rel}	$\ln(k_{rel})$	<i>Conv.</i>	<i>Chem.</i>	k_{rel}	$\ln(k_{rel})$
17.667	0.287	1.918	0.651	19.317	0.560	4.033	1.395
33.648	0.258	1.917	0.651	32.417	0.509	3.871	1.354
49.330	0.222	1.909	0.647	48.055	0.439	3.745	1.320
65.984	0.175	1.901	0.642	63.610	0.375	4.106	1.413
		1.911 ± 0.008	0.648 ± 0.004			3.939 ± 0.163	1.370 ± 0.041
2b vs. 2c^[a]				1b vs. 1c^[a]			
<i>Conv.</i>	<i>Chem.</i>	k_{rel}	$\ln(k_{rel})$	<i>Conv.</i>	<i>Chem.</i>	k_{rel}	$\ln(k_{rel})$
22.051	0.341	2.230	0.802	20.901	0.393	2.538	0.931
35.480	0.310	2.223	0.799	32.116	0.404	2.821	1.037
49.631	0.270	2.211	0.793	45.634	0.363	2.831	1.041
71.284	0.188	2.169	0.774	63.152	0.282	2.744	1.009
		2.208 ± 0.027	0.792 ± 0.012			2.733 ± 0.136	1.005 ± 0.051
2b vs. 2f^[b]				1b vs. 1f^[b]			
<i>Conv.</i>	<i>Chem.</i>	k_{rel}	$\ln(k_{rel})$	<i>Conv.</i>	<i>Chem.</i>	k_{rel}	$\ln(k_{rel})$
26.382	0.173	1.504	0.408	18.936	0.156	1.419	0.350
39.193	0.159	1.516	0.416	32.038	0.144	1.423	0.353
51.806	0.179	1.701	0.531	46.550	0.137	1.465	0.382
70.269	0.106	1.515	0.415				
		1.559 ± 0.107	0.443 ± 0.067			1.436 ± 0.030	0.362 ± 0.021

^[a]Turnover-limited competition experiments were carrying out by method C. ^[b]Turnover-limited competition experiments were carrying out by method D.

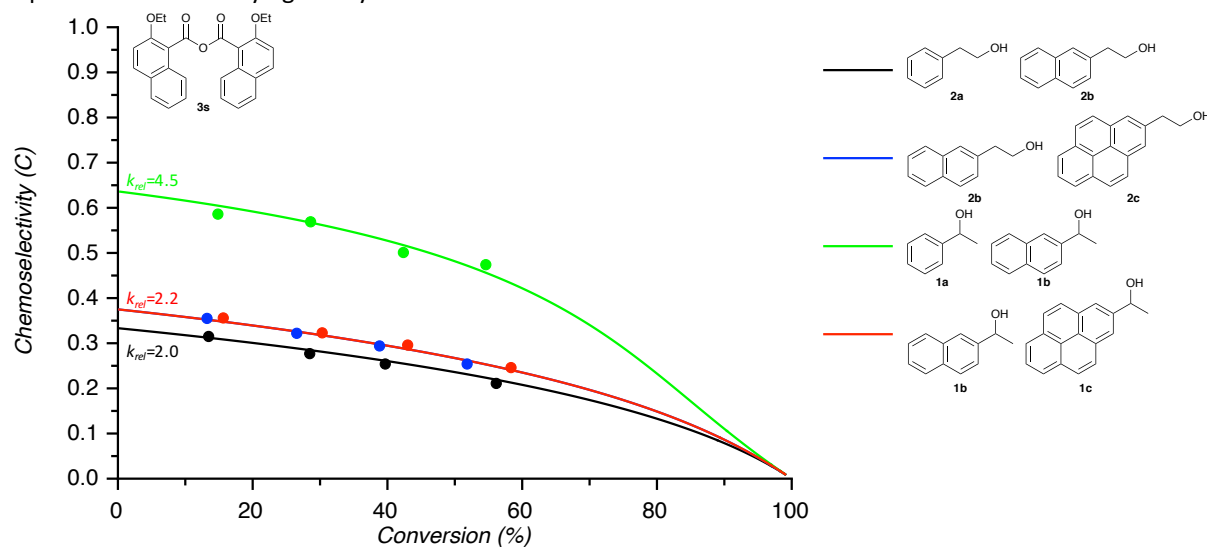


Figure 3.22. Plot of conversion vs. corrected chemoselectivity for turnover-limited competition experiment between primary alcohols **2** and between secondary alcohols **1** with **3s**.

Table 3.11. Conversion, corrected chemoselectivity, relative rate and natural logarithm of relative rate with standard derivations calculated from corresponding ¹H NMR measurements for turnover-limited competition experiments between primary alcohols **2** and between secondary alcohols **1** with **3s**.

Primary Alcohol 2				Secondary Alcohol 1			
2a vs. 2b ^[a]				1a vs. 1b ^[a]			
<i>Conv.</i>	<i>Chem.</i>	k_{rel}	$\ln(k_{rel})$	<i>Conv.</i>	<i>Chem.</i>	k_{rel}	$\ln(k_{rel})$
13.462	0.315	2.012	0.699	14.839	0.586	4.233	1.443
28.467	0.277	1.963	0.674	28.598	0.569	4.530	1.511
39.676	0.254	1.960	0.673	42.367	0.501	4.258	1.449

56.147	0.211	1.945	0.665	54.601	0.474	4.826	1.574
		1.970 ± 0.029	0.678 ± 0.015			4.462 ± 0.278	1.494 ± 0.062
2b vs. 2c^[a]				1b vs. 1c^[a]			
<i>Conv.</i>	<i>Chem.</i>	<i>k_{rel}</i>	<i>ln(k_{rel})</i>	<i>Conv.</i>	<i>Chem.</i>	<i>k_{rel}</i>	<i>ln(k_{rel})</i>
13.224	0.355	2.217	0.796	15.636	0.356	2.244	0.808
26.538	0.322	2.179	0.779	30.318	0.323	2.232	0.803
38.829	0.294	2.181	0.780	43.002	0.296	2.260	0.816
51.825	0.254	2.147	0.764	58.341	0.246	2.240	0.807
		2.181 ± 0.019	0.780 ± 0.009			2.244 ± 0.014	0.808 ± 0.006

^[a]Turnover-limited competition experiments were carrying out by method C.

3.1.3 Effects of Reaction Conditions

3.1.3.1 Investigation of Temperature Effects

Giese *et al.*^[3] documented that a decrease in the reaction temperature often implies an increase in selectivity. We thus tested the effects of reaction temperature on selectivities for the anhydrides **3f** and **3t**, and the alcohol system **1b/2b**. By varying the temperature from +40 °C to -10 °C we observed only moderate changes in the rate constants for anhydride **3f**. By using the well-known Eyring equation Eq. 3.14 an activation entropy difference of -7.4 J K⁻¹·mol was found for anhydride **3f** and a slightly larger value of -10.3 J K⁻¹·mol for anhydride **3t**. Because of the rather similar rate constants at different temperatures, these small differences hardly merit any further discussion.

$$k_1 = \frac{k_B T}{h} \cdot e^{-\frac{\Delta G_1^\ddagger}{RT}} \quad \text{Eq. 3.7}$$

$$\frac{k_2}{k_1} = \frac{e^{-\frac{\Delta G_2^\ddagger}{RT}}}{e^{-\frac{\Delta G_1^\ddagger}{RT}}} \quad \text{Eq. 3.8}$$

$$\frac{k_2}{k_1} = e^{-\frac{\Delta G_2^\ddagger}{RT} + \frac{\Delta G_1^\ddagger}{RT}} \quad \text{Eq. 3.9}$$

$$\ln \frac{k_2}{k_1} = -\frac{\Delta G_2^\ddagger}{RT} + \frac{\Delta G_1^\ddagger}{RT} \quad \text{Eq. 3.10}$$

$$\ln \frac{k_2}{k_1} = -\frac{\Delta H_2^\ddagger - T\Delta S_2^\ddagger}{RT} + \frac{\Delta H_1^\ddagger - T\Delta S_1^\ddagger}{RT} \quad \text{Eq. 3.11}$$

$$\ln \frac{k_2}{k_1} = -\frac{\Delta H_2^\ddagger}{RT} + \frac{\Delta S_2^\ddagger}{R} + \frac{\Delta H_1^\ddagger}{RT} - \frac{\Delta S_1^\ddagger}{R} \quad \text{Eq. 3.12}$$

$$\ln \frac{k_2}{k_1} = \frac{\Delta H_1^\ddagger - \Delta H_2^\ddagger}{RT} - \frac{\Delta S_1^\ddagger - \Delta S_2^\ddagger}{R} \quad \text{Eq. 3.13}$$

With:

$$\begin{aligned} \Delta\Delta H^\ddagger &= \Delta H_1^\ddagger - \Delta H_2^\ddagger \\ \Delta\Delta S^\ddagger &= \Delta S_1^\ddagger - \Delta S_2^\ddagger \\ R &= 8.31451 \text{ J K}^{-1} \cdot \text{mol} \end{aligned}$$

$$\ln(k_{\text{rel}}) = \ln \frac{k_2(2a-d)}{k_1(1a-d)} = \frac{\Delta\Delta H^\ddagger}{R \cdot T} - \frac{\Delta\Delta S^\ddagger}{R} \quad \text{Eq. 3.14}$$

Anhydride 3f

$$\ln \frac{k_2}{k_1} = \frac{-32.544}{T} + 0.887 \quad \text{Eq. 3.15}$$

$$\Delta\Delta H^\ddagger = \Delta H_1^\ddagger - \Delta H_2^\ddagger = -270.587 \text{ J mol}^{-1} \quad \text{Eq. 3.16}$$

$$\Delta\Delta S^\ddagger = \Delta S_1^\ddagger - \Delta S_2^\ddagger = -7.37 \text{ J K}^{-1} \cdot \text{mol} \quad \text{Eq. 3.17}$$

Size-Driven Inversion of Selectivity in Esterfication

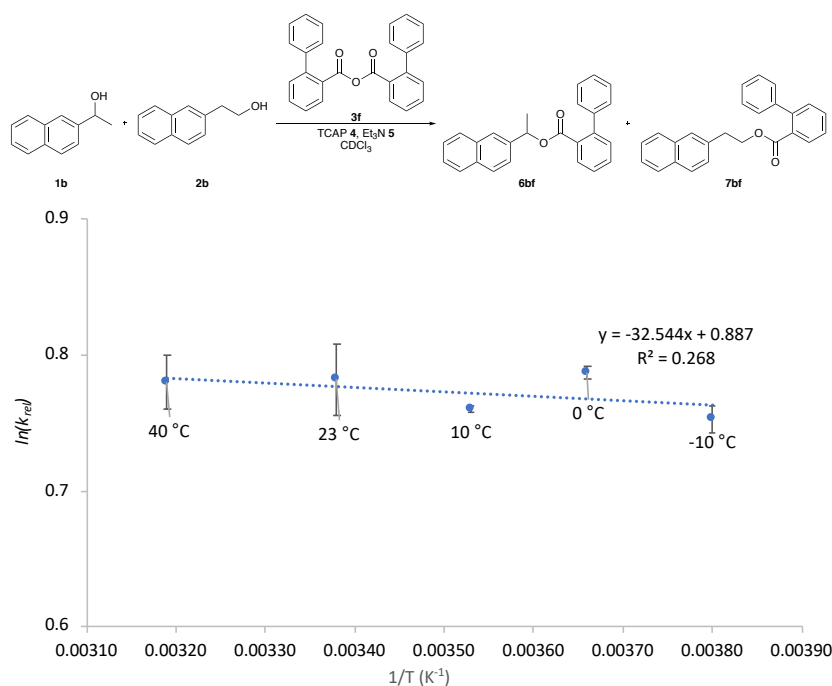
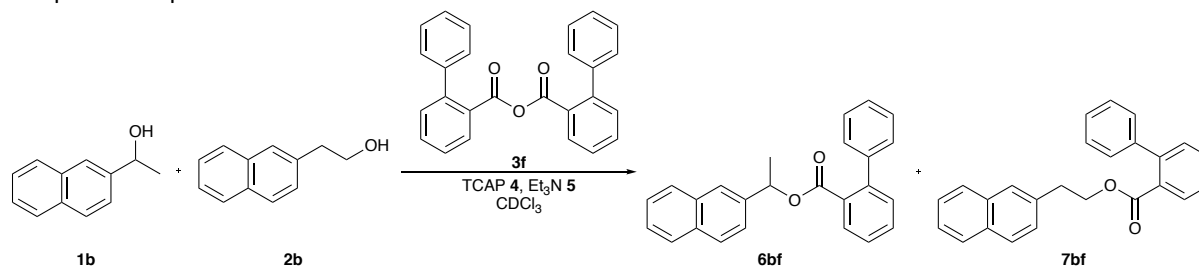


Figure 3.23. Eyring plot of $\ln(k_{rel})$ at different temperatures.

Table 3.12. Conversion, corrected chemoselectivity, relative rate and natural logarithm of relative rate with standard derivations calculated from corresponding ¹H NMR measurements for temperature depending turnover-limited competition experiments.



-10 °C (263.15 K)				0 °C (273.15 K)			
Conv.	Chem.	k_{rel}	$\ln(k_{rel})$	Conv.	Chem.	k_{rel}	$\ln(k_{rel})$
28.549	0.307	2.118	0.751	21.380	0.333	2.180	0.780
35.849	0.288	2.101	0.742	35.652	0.306	2.205	0.791
49.554	0.261	2.153	0.767	51.628	0.263	2.204	0.790
68.366	0.194	2.119	0.751	67.267	0.208	2.198	0.788
		2.123 ± 0.022	0.753 ± 0.010			2.197 ± 0.011	0.787 ± 0.005
10 °C (283.15 K)				23 °C (296.15 K)			
Conv.	Chem.	k_{rel}	$\ln(k_{rel})$	Conv.	Chem.	k_{rel}	$\ln(k_{rel})$
21.311	0.325	2.137	0.760	23.536	0.316	2.11	0.747
33.809	0.299	2.136	0.759	33.18	0.308	2.183	0.78
49.121	0.261	2.145	0.763	46.687	0.278	2.211	0.793
66.701	0.203	2.137	0.759	66.382	0.216	2.24	0.807
		2.139 ± 0.004	0.760 ± 0.002			2.186 ± 0.056	0.782 ± 0.026
40 °C (313.15 K)							
Conv.	Chem.	k_{rel}	$\ln(k_{rel})$				
19.077	0.329	2.137	0.759				
33.251	0.303	2.154	0.767				
49.391	0.273	2.225	0.800				
66.915	0.211	2.212	0.794				
		2.182 ± 0.043	0.780 ± 0.020				

Anhydride **3t**

$$\ln \frac{k_2}{k_1} = \frac{-545.281}{T} + 1.235 \quad \text{Eq. 3.18}$$

$$\Delta\Delta H^\ddagger = \Delta H_1^\ddagger - \Delta H_2^\ddagger = -4533.744 \text{ J mol}^{-1} = -4.534 \text{ kJ mol}^{-1} \quad \text{Eq. 3.19}$$

$$\Delta\Delta S^\ddagger = \Delta S_1^\ddagger - \Delta S_2^\ddagger = -10.268 \text{ J K}^{-1} \cdot \text{mol} \quad \text{Eq. 3.20}$$

These results show that primary alcohol **2b** has a higher activation enthalpy than secondary alcohol **1b**. The activation entropy for alcohol **1b** is less negative as the activation entropy for alcohol **2b**. This means that the transition state for reaction of secondary alcohol **1b** is more highly organized as compared to primary alcohol **2b**.

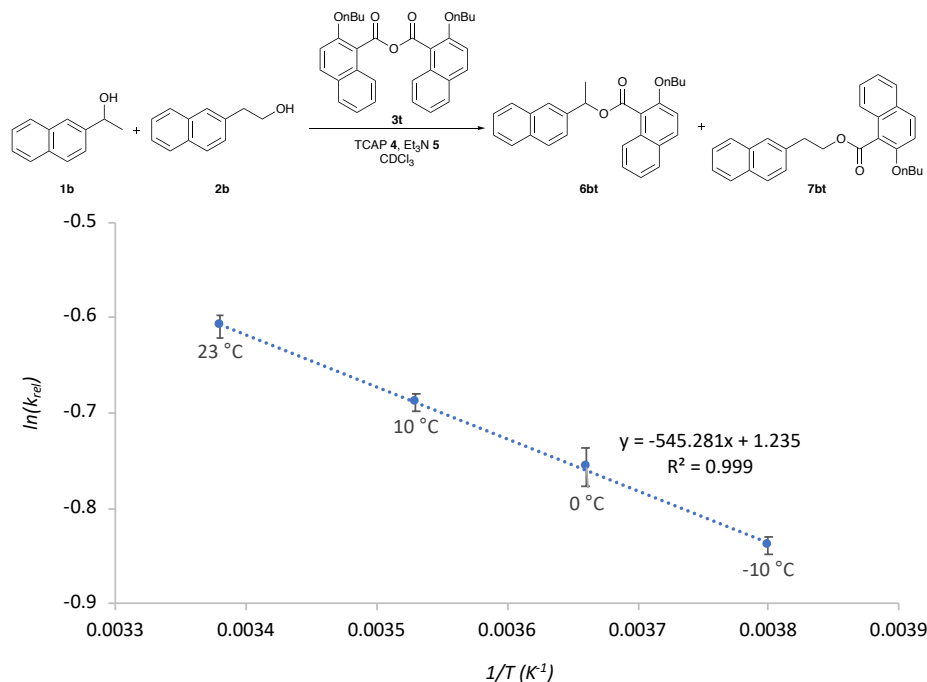


Figure 3.24. Eyring plot of $\ln(k_{rel})$ at different temperatures.

Table 3.13. Conversion, corrected chemoselectivity, relative rate and natural logarithm of relative rate with standard derivations calculated from corresponding ¹H NMR measurements for temperature depending turnover-limited competition experiments.

-10 °C (263.15 K)				-10 °C (263.15 K)			
Conv.	Chem.	k _{rel}	ln(k _{rel})	Conv.	Chem.	k _{rel}	ln(k _{rel})
19.611	-0.363	0.429	-0.847	17.231	-0.354	0.445	-0.811
29.796	-0.336	0.435	-0.833	30.063	-0.330	0.441	-0.820
39.880	-0.309	0.437	-0.828	40.531	-0.310	0.434	-0.835
56.167	-0.265	0.429	-0.846	55.966	-0.258	0.440	-0.820
		0.432 ± 0.004	-0.839 ± 0.009			0.440 ± 0.004	-0.821 ± 0.010
0 °C (273.15 K)				0 °C (273.15 K)			
Conv.	Chem.	k _{rel}	ln(k _{rel})	Conv.	Chem.	k _{rel}	ln(k _{rel})
13.716	-0.346	0.460	-0.776	11.669	-0.318	0.497	-0.700
28.087	-0.304	0.477	-0.740	21.103	-0.324	0.469	-0.757
34.965	-0.300	0.463	-0.771	31.796	-0.297	0.475	-0.744
47.670	-0.257	0.478	-0.739	45.346	-0.270	0.469	-0.758

Size-Driven Inversion of Selectivity in Esterfication

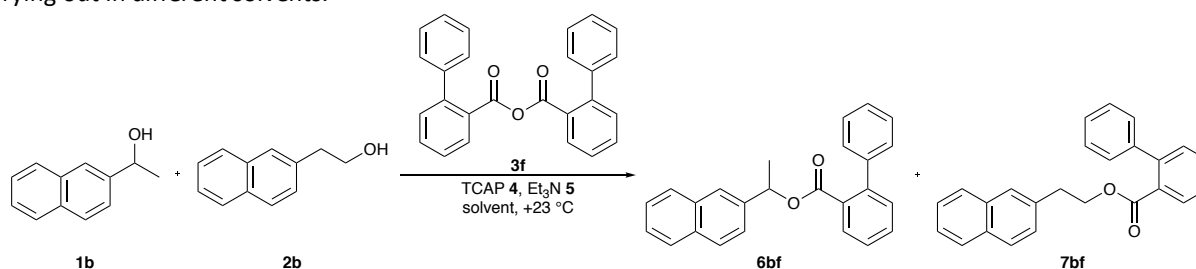
		0.469 ± 0.009	-0.757 ± 0.020			0.477 ± 0.013	-0.740 ± 0.027
10 °C (283.15 K)				10 °C (283.15 K)			
<i>Conv.</i>	<i>Chem.</i>	k_{rel}	$\ln(k_{rel})$	<i>Conv.</i>	<i>Chem.</i>	k_{rel}	$\ln(k_{rel})$
13.443	-0.308	0.505	-0.684	13.636	-0.316	0.495	-0.704
22.639	-0.299	0.497	-0.700	24.994	-0.296	0.494	-0.705
33.320	-0.275	0.500	-0.693	34.766	-0.270	0.503	-0.687
47.716	-0.237	0.507	-0.680	52.725	-0.227	0.504	-0.686
		0.502 ± 0.005	-0.689 ± 0.009			0.499 ± 0.005	-0.695 ± 0.010
23 °C (296.15 K)				23 °C (296.15 K)			
<i>Conv.</i>	<i>Chem.</i>	k_{rel}	$\ln(k_{rel})$	<i>Conv.</i>	<i>Chem.</i>	k_{rel}	$\ln(k_{rel})$
17.563	-0.267	0.548	-0.602	16.163	-0.284	0.528	-0.638
31.600	-0.241	0.550	-0.597	28.314	-0.256	0.539	-0.618
45.793	-0.219	0.542	-0.612	41.220	-0.230	0.540	-0.616
62.014	-0.182	0.535	-0.625	54.527	-0.201	0.538	-0.620
		0.544 ± 0.007	-0.609 ± 0.012			0.536 ± 0.005	-0.623 ± 0.010

3.1.3.2 Investigation of Solvent Effects

As shown in earlier studies,^[4] the solvent can in principle change the relative rate constants determined here. Turnover-limited competition experiments with the alcohol system **1b/2b** were thus carried out with anhydride **3f** in CH₂Cl₂, MeCN, THF, and trifluorotoluene. Instead of the common four different conversion points, only the 50% conversion point of the turnover-limited competition experiments was used for this type of solvent testing in triplicate form. For the solvent CDCl₃ the computed rate constant from the results in chapter 3.1.1 was used [$k_{rel}=2.4$, $\ln(k_{rel}) = 0.76$, $\alpha = 2.2$, $\beta = 0.8$]. No significant differences in the rate constants were found for these solvents. When plotting the $\ln(k_{rel})$ values against Hunter's parameter for solvent hydrogen bond donor and acceptor ability (α and β , Eq. 3.21), no systematic solvent dependence can be identified.

$$\ln(k_{rel}) = 0.60 + 0.07 \cdot \alpha + 0.05 \beta \quad \text{Eq. 3.21}$$

Table 3.14. Conversion, corrected chemoselectivity, relative rate, and natural logarithm of relative rate with standard derivations calculated from corresponding ¹H NMR measurements for turnover-limited competition experiments carrying out in different solvents.



TFT $\alpha = 1.3; \beta = 1.7$				MeCN $\alpha = 1.7; \beta = 5.1$			
<i>Conv.</i>	<i>Chem.</i>	k_{rel}	$\ln(k_{rel})$	<i>Conv.</i>	<i>Chem.</i>	k_{rel}	$\ln(k_{rel})$
48.266	0.259	2.117	0.750	45.912	0.342	2.665	0.980
49.435	0.259	2.132	0.757	46.518	0.324	2.534	0.930
49.729	0.247	2.061	0.723	46.850	0.329	2.584	0.949
		2.103 ± 0.037	0.743 ± 0.018			2.594 ± 0.066	0.953 ± 0.025
THF $\alpha = 0.8; \beta = 5.9$				CH ₂ Cl ₂ $\alpha = 1.9; \beta = 2.0$			
<i>Conv.</i>	<i>Chem.</i>	k_{rel}	$\ln(k_{rel})$	<i>Conv.</i>	<i>Chem.</i>	k_{rel}	$\ln(k_{rel})$
48.721	0.356	2.868	1.053	51.120	0.309	2.539	0.932
48.942	0.334	2.686	0.988	51.345	0.299	2.463	0.901
49.896	0.325	2.636	0.969	52.132	0.305	2.538	0.931
		2.730 ± 0.122	1.004 ± 0.044			2.513 ± 0.044	0.921 ± 0.018

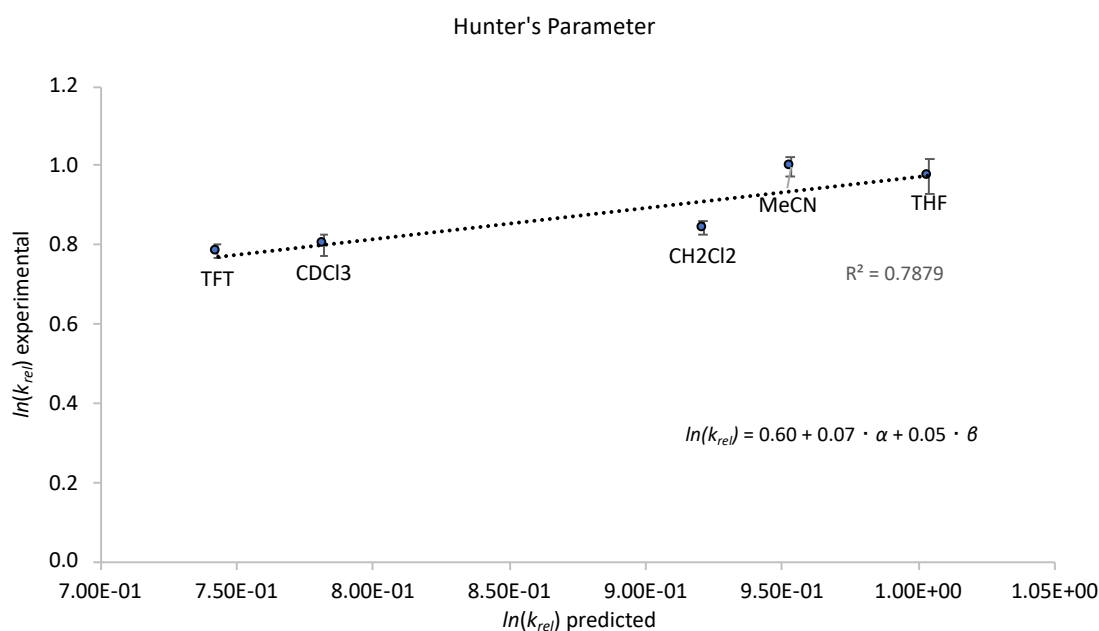


Figure 3.25. Plot of predicted $\ln(k_{rel})$ values against experimental $\ln(k_{rel})$ values. The predicted $\ln(k_{rel})$ values are using the Hunter's parameter and Eq. 3.21.

3.1.3.3 Investigation of Catalyst Concentration

To quantify the role of the catalyst concentration on the selectivity values, two types of turnover-limited competition experiments were carried out. First, the alcohol system **1a/2a** was tested with anhydride **3a** and TCAP (**4**) concentrations of 2, 5, 10, and 20 mol%. No differences in the relative rate constants were found in these experiments. Additionally, the alcohol system **1b/2b** with anhydride **3f** was explored with TCAP concentrations of 1, 2, 5, 10, and 20 mol%, and again no significant changes of the relative rate constant were observed. In the case of alcohol system **1a/2a**, the uncatalyzed background reaction with anhydride **3a** was also studied. Et_3N (**5**) was still used as the auxiliary base in excess. After a reaction time of approx. 4 weeks, the turnover of anhydride **3a** was not yet fully complete by ^1H NMR spectroscopy. However, for the background reaction, a selectivity value of around $\ln(k_{rel}) = 3.28$ was obtained, which indicated a significant increase in selectivity in comparison to the catalyzed reaction of **1a/2a** with **3a** [$\ln(k_{rel}) = 2.00$]. No background reaction was found for the reaction of the alcohol system **1b/2b** with anhydride **3o** (one of the selectivity-inverting anhydrides). Even after 4 weeks, no significant formation of product esters **1bo/2bo** could be observed.

Table 3.15. Conversion, corrected chemoselectivity, relative rate, and natural logarithm of relative rate with standard deviations calculated from corresponding ^1H NMR measurements for catalyst concentration-dependent turnover-limited competition experiments.

uncatalysed				2 mol%			
Conv.	Chem.	k_{rel}	$\ln(k_{rel})$	Conv.	Chem.	k_{rel}	$\ln(k_{rel})$
9.777	0.918	25.794	3.250	19.286	0.732	7.675	2.038
18.354	0.922	30.120	3.405	33.515	0.683	7.378	1.998
27.557	0.897	25.593	3.242	50.440	0.595	7.153	1.967
38.102	0.872	24.991	3.219	67.167	0.439	7.201	1.974
		26.624 ± 2.040	3.279 ± 0.074			7.352 ± 0.236	1.995 ± 0.032

Size-Driven Inversion of Selectivity in Esterification

5 mol%				10 mol%			
Conv.	Chem.	k_{rel}	$\ln(k_{rel})$	Conv.	Chem.	k_{rel}	$\ln(k_{rel})$
17.327	0.747	8.030	2.083	18.163	0.742	7.939	2.072
32.458	0.682	7.237	1.979	33.282	0.676	7.146	1.967
44.865	0.630	7.235	1.979	50.866	0.593	7.151	1.967
65.024	0.466	7.197	1.974	70.882	0.390	7.415	2.004
		7.425 ± 0.404	2.004 ± 0.053			7.413 ± 0.373	2.002 ± 0.049
20 mol%							
Conv.	Chem.	k_{rel}	$\ln(k_{rel})$				
18.645	0.735	7.700	2.041				
31.963	0.679	7.105	1.961				
49.558	0.595	6.983	1.944				
70.055	0.399	7.140	1.966				
		7.232 ± 0.319	1.978 ± 0.043				

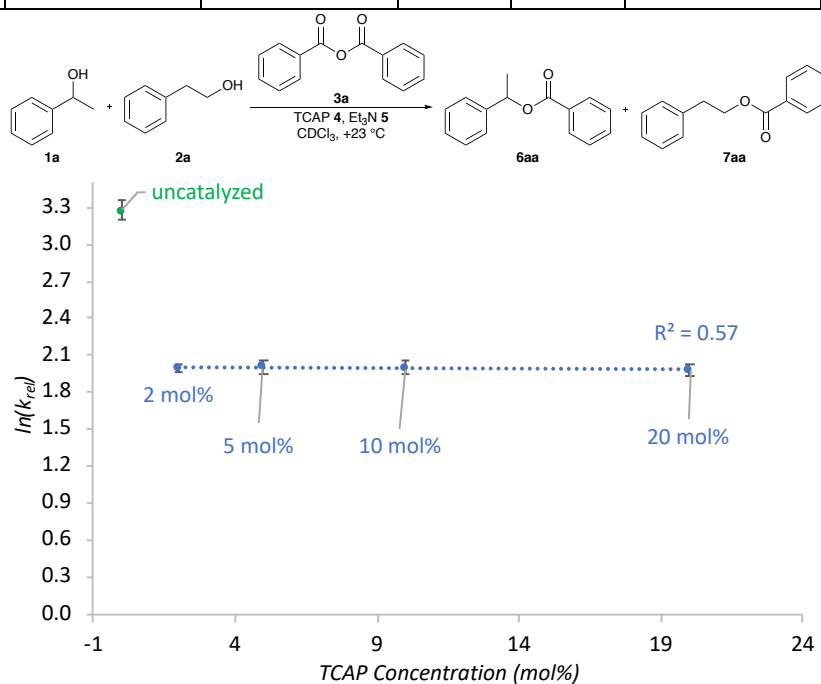


Figure 3.26. Plot of TCAP concentration vs. $\ln(k_{rel})$ for the turnover-limited competition experiment of alcohol **1a** and **2a** with **3a**.

Table 3.16. Conversion, corrected chemoselectivity, relative rate, and natural logarithm of relative rate with standard derivations calculated from corresponding ^1H NMR measurements for catalyst concentration depending turnover-limited competition experiments.

Reaction scheme: 1b + 2b $\xrightarrow[\text{CDCl}_3, +23^\circ\text{C}]{\text{TCAP 4, Et}_3\text{N 5}}$ 6bf + 7bf (catalyzed by 3f)

1 mol%				1 mol%			
Conv.	Chem.	k_{rel}	$\ln(k_{rel})$	Conv.	Chem.	k_{rel}	$\ln(k_{rel})$
27.324	0.315	2.146	0.764	20.870	0.327	2.143	0.762
34.258	0.302	2.162	0.771	32.600	0.310	2.184	0.781
49.193	0.269	2.194	0.786	47.006	0.281	2.232	0.803
69.128	0.202	2.211	0.794	66.423	0.210	2.191	0.785
		2.178 ± 0.030	0.779 ± 0.014			2.188 ± 0.036	0.783 ± 0.020

2 mol%				2 mol%			
Conv.	Chem.	k_{rel}	$\ln(k_{rel})$	Conv.	Chem.	k_{rel}	$\ln(k_{rel})$
20.995	0.328	2.151	0.766	27.483	0.320	2.179	0.779
32.915	0.307	2.174	0.776	34.042	0.303	2.162	0.771
46.458	0.272	2.167	0.773	49.806	0.266	2.191	0.784
65.069	0.216	2.198	0.787	68.877	0.203	2.216	0.796
		2.172 ± 0.019	0.776 ± 0.009			2.187 ± 0.023	0.782 ± 0.010
5 mol%				5 mol%			
Conv.	Chem.	k_{rel}	$\ln(k_{rel})$	Conv.	Chem.	k_{rel}	$\ln(k_{rel})$
23.536	0.316	2.110	0.747	18.843	0.328	2.127	0.755
33.180	0.308	2.183	0.780	34.398	0.290	2.094	0.739
46.687	0.278	2.211	0.793	47.819	0.264	2.135	0.758
66.382	0.216	2.240	0.807	66.389	0.211	2.197	0.787
		2.186 ± 0.056	0.782 ± 0.026			2.138 ± 0.043	0.760 ± 0.020
10 mol%				10 mol%			
Conv.	Chem.	k_{rel}	$\ln(k_{rel})$	Conv.	Chem.	k_{rel}	$\ln(k_{rel})$
21.143	0.331	2.167	0.773	28.456	0.308	2.123	0.753
34.967	0.297	2.141	0.761	33.425	0.301	2.144	0.763
50.527	0.263	2.181	0.780	49.678	0.262	2.159	0.770
69.336	0.200	2.208	0.792	66.691	0.208	2.183	0.781
		2.174 ± 0.028	0.777 ± 0.013			2.152 ± 0.025	0.767 ± 0.012
20 mol%				20 mol%			
Conv.	Chem.	k_{rel}	$\ln(k_{rel})$	Conv.	Chem.	k_{rel}	$\ln(k_{rel})$
28.479	0.316	2.170	0.775	21.600	0.321	2.120	0.751
34.753	0.296	2.131	0.757	33.006	0.302	2.143	0.762
47.043	0.272	2.173	0.776	43.784	0.268	2.099	0.741
68.129	0.206	2.216	0.796	65.116	0.211	2.151	0.766
		2.173 ± 0.035	0.776 ± 0.016			2.128 ± 0.024	0.755 ± 0.011

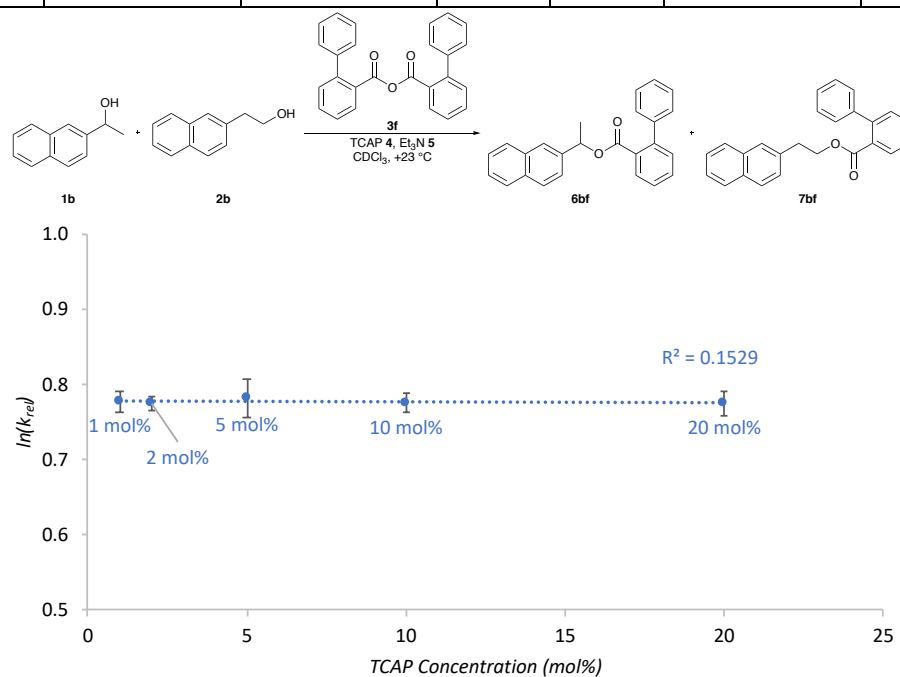
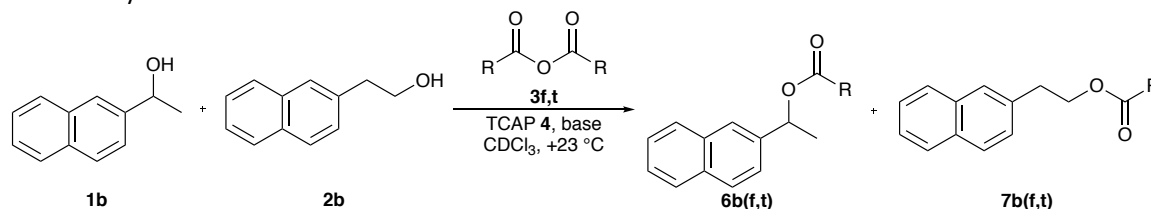


Figure 3.27. Plot of TCAP concentration vs. $\ln(k_{rel})$ for turnover-limited competition experiment of alcohol **1b** and **2b** with **3f**.

3.1.3.4 Investigation of Auxiliary Base Effects

The auxiliary base can, in principle, also influence the rate constant and thus the selectivity.^[5] The alcohol system **1b/2b** with anhydrides **3f** and **3t** was tested with Et₃N and the larger Hünig base. For both anhydrides, no differences in selectivity were found.

Table 3.17. Conversion, corrected chemoselectivity, relative rate and natural logarithm of relative rate with standard derivations calculated from corresponding ¹H NMR measurements for turnover-limited competition experiments using different auxiliary bases.

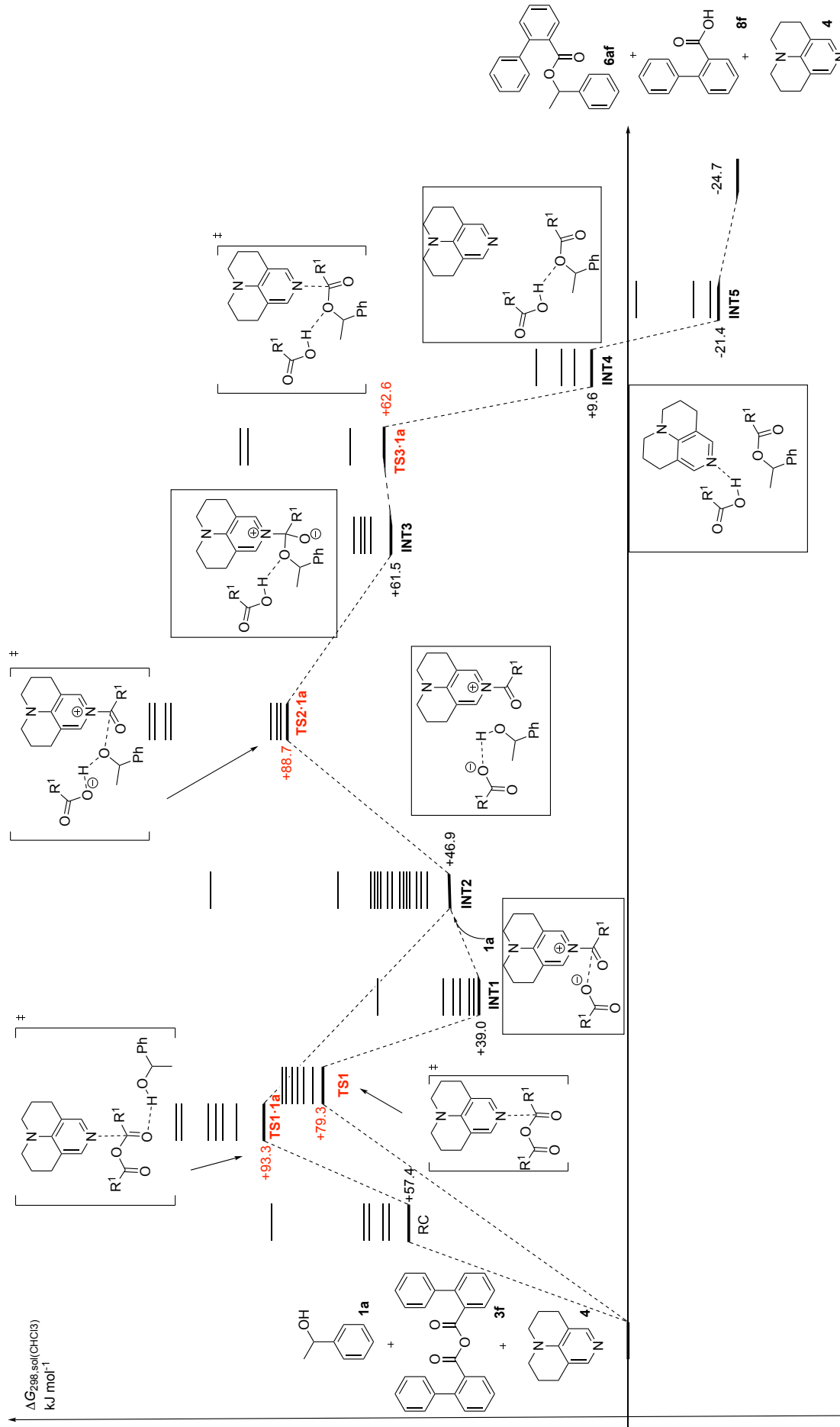


<p>3f</p>				<p>3f</p>			
Et₃N				Hünig base			
<i>Conv.</i>	<i>Chem.</i>	<i>k_{rel}</i>	<i>ln(k_{rel})</i>	<i>Conv.</i>	<i>Chem.</i>	<i>k_{rel}</i>	<i>ln(k_{rel})</i>
23.536	0.316	2.110	0.747	20.706	0.312	2.064	0.725
33.180	0.308	2.183	0.780	34.832	0.292	2.111	0.747
46.687	0.278	2.211	0.793	50.053	0.260	2.156	0.768
66.382	0.216	2.240	0.807	70.545	0.188	2.139	0.760
		2.186 ± 0.056	0.782 ± 0.026			2.117 ± 0.040	0.750 ± 0.019
<p>3t</p>				<p>3t</p>			
Et₃N				Hünig base			
<i>Conv.</i>	<i>Chem.</i>	<i>k_{rel}</i>	<i>ln(k_{rel})</i>	<i>Conv.</i>	<i>Chem.</i>	<i>k_{rel}</i>	<i>ln(k_{rel})</i>
17.563	-0.267	0.548	-0.602	15.860	-0.275	0.540	-0.616
31.600	-0.241	0.550	-0.597	27.068	-0.249	0.551	-0.596
45.793	-0.219	0.542	-0.612	38.198	-0.248	0.523	-0.648
62.014	-0.182	0.535	-0.625	52.567	-0.204	0.541	-0.615
		0.544 ± 0.007	-0.609 ± 0.012			0.539 ± 0.012	-0.619 ± 0.022

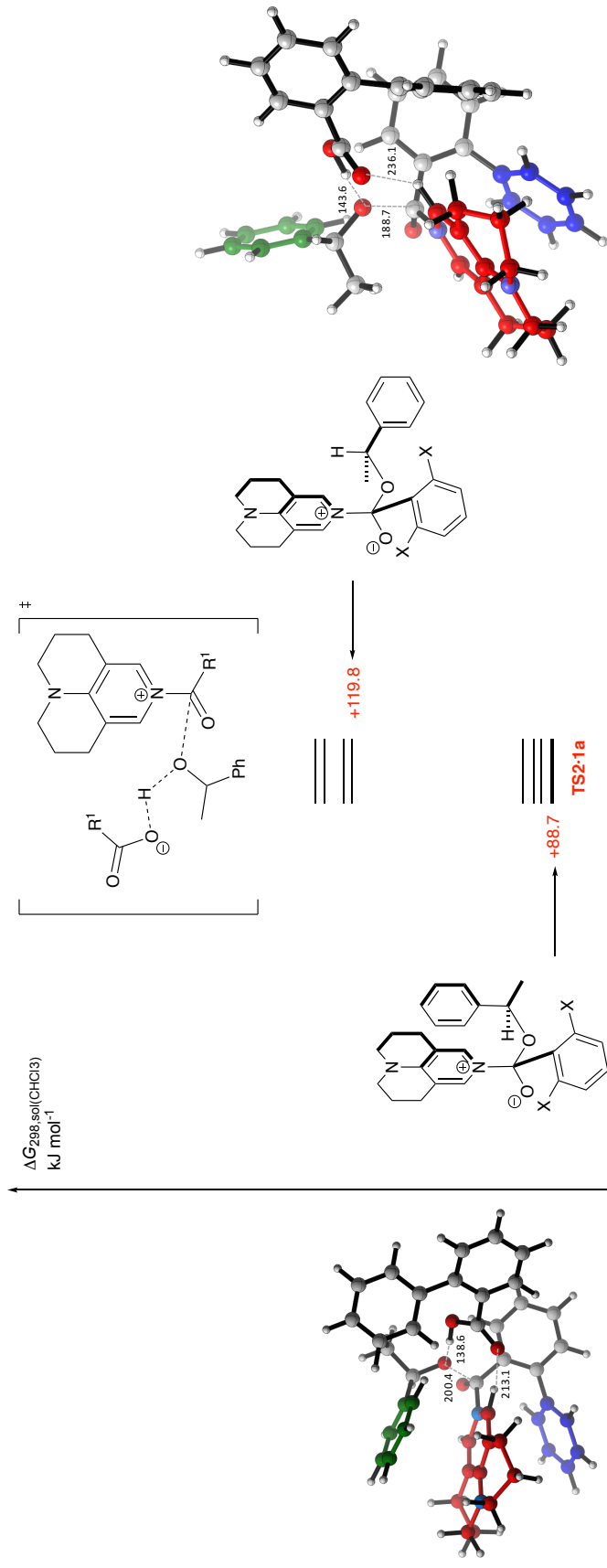
3.2 Computational Data

All geometry optimizations and vibrational frequency calculations have been performed using the B3LYP-D3 hybrid functional^[6] in combination with the 6-31+G(d) basis set.^[7] Solvent effects for chloroform have been taken into account with the SMD continuum solvation model.^[8] This combination has recently been found to perform well for the description of charge-separated intermediates.^[4,9] Thermochemical corrections to 298.15 K have been calculated for all minima from unscaled vibrational frequencies obtained at this same level. Solvation energies have been obtained as the difference between the energies computed at B3LYP-D3/6-31+G(d) in solution and in gas phase. For the elucidation of the mechanism, the thermochemical corrections of optimized structures have been combined with single point energies calculated at the DLPNO-CCSD(T)/def2-TZVPP//B3LYP-D3/6-31+G(d) level.^[10] Solvation energies have been added to the energy computed at DLPNO-CCSD(T)/def2-TZVPP//SMD(CHCl₃)/B3LYP-D3/6-31+G(d) level to yield free energies G_{298} at 298.15 K. Free energies in solution of the reaction pathway analysis have been corrected to a reference state of 1 mol l⁻¹ at 298.15 K through addition of $RT\ln(24.46) = +7.925$ kJ mol⁻¹ to the free energies. All calculations have been performed with Gaussian 09^[11] and ORCA version 4.0.^[12] Conformational search was performed with Maestro.^[13] The charges have been analyzed using the NBO formalism^[14] on the B3LYP-D3/6-31+G(d) results.

3.2.1 Reaction Path Calculations



Scheme 3.3. Computed stationary points in the Lewis base-catalyzed reaction of secondary alcohol **1a** with benzoic anhydride derivative **3f** at the SMD(CHCl₃)/DLPNO-CCSD(T)/def2-TZVPP//SMD(CHCl₃)/B3LYP-D3/6-31+G(d) level of theory.



Scheme 3.4. Computed stationary points of **TS2-1a** in the Lewis base-catalyzed reaction of secondary alcohol **1a** with benzoic anhydride derivative **3f** at SMD(CHCl₃)/DLPNO-CCSD(T)/def2-TZVPP//SMD(CHCl₃)/B3LYP-D3/6-31+G(d) theoretical level.

Table 3.18. Total energies and free energies for all systems shown in Scheme 3.3 (in Hartree). Molar free energies in solution at 298.15 K ($G_{298, \text{sol}}$) have been calculated at the SMD(CHCl₃)/DLPNO-CCSD(T)/def2-TZVPP// SMD(CHCl₃)/B3LYP-D3/6-31+G(d) level and corrected for a solution standard state of 1 M through addition of +7.925 kJ mol⁻¹ (0.00301848 Hartree). The SMD(CHCl₃)/B3LYP-D3/6-31+G(d) level of theory has been used to optimize the geometries and calculate solute thermal corrections and solvation energies. Note that the filenames are used in our calculations and do not follow any guide.

Filename	Freqs	E_{tot} SMD/B3LYP-D3/6-31+G(d)	G_{298} SMD/B3LYP-D3/6-31+G(d)	E_{tot} B3LYP-D3/6-31+G(d)	E_{tot} SMD/DLPNO-CCSD(T)/def2-TZVPP	$G_{298, \text{sol}}$ SMD/DLPNO-CCSD(T)/def2-TZVPP
1a						
roh1_1	0	-386.1353498	-386.0074480	-386.1148119	-385.4196861	-385.3093038
roh1_2	0	-386.1335902	-386.0061890	-386.1123578	-385.4178436	-385.3086563
4						
tcap_02	0	-537.1790980	-536.9785760	-537.1599167	-536.1519628	-535.9676036

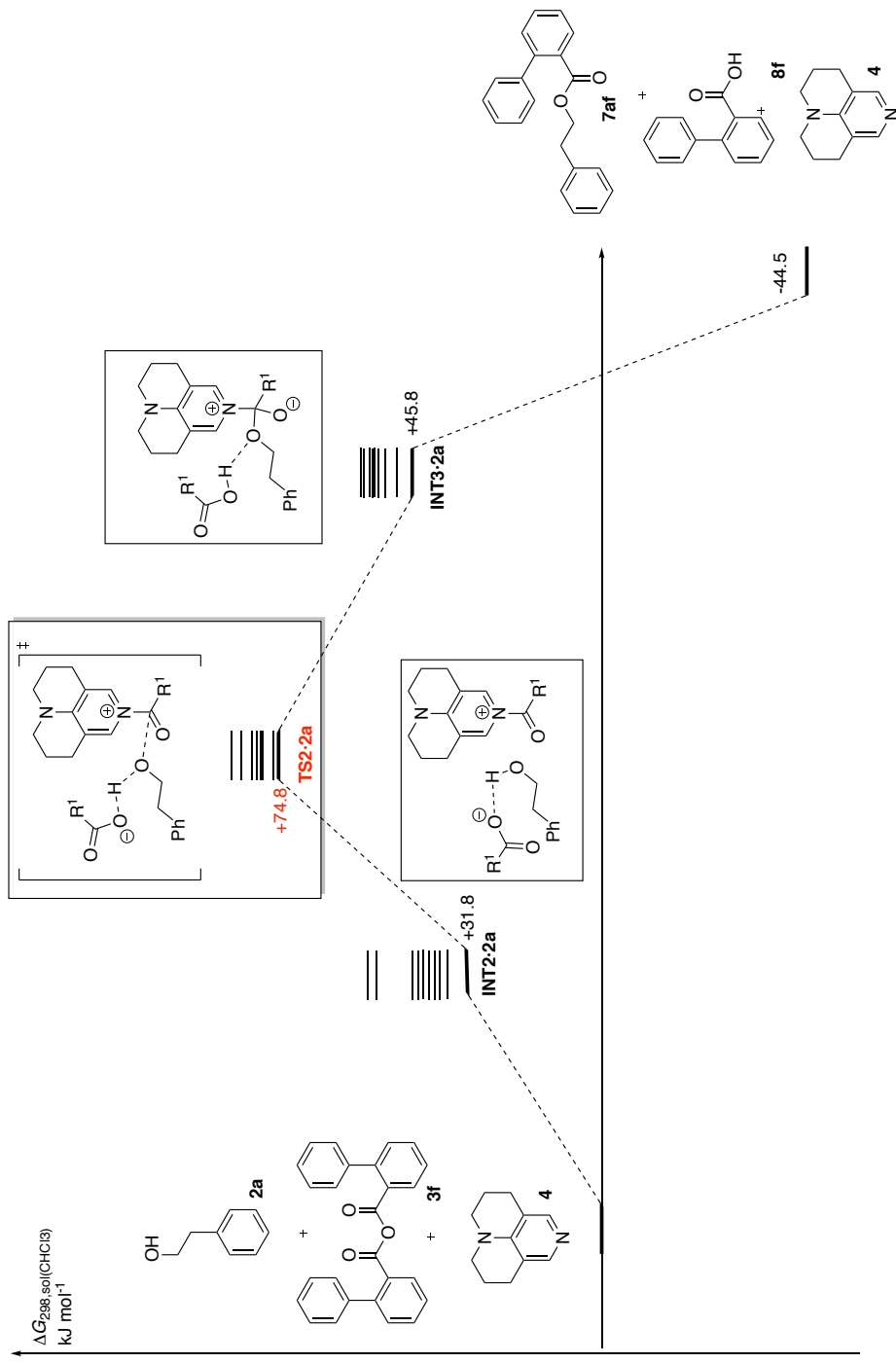
tcap_01	0	-537.1786137	-536.9781170	-537.1591861	-536.1505343	-535.9664467
3f						
anh_op_37	0	-1227.4350491	-1227.1223200	-1227.4008583	-1225.1506553	-1224.8690985
anh_op_4	0	-1227.4309646	-1227.1177170	-1227.3982001	-1225.1491985	-1224.8656969
8f						
acid_op_2	0	-651.9379573	-651.7808020	-651.9176414	-650.7482377	-650.6083799
acid_op_1	0	-651.9379573	-651.7808020	-651.9176414	-650.7482374	-650.6083795
6af						
ester_op_2	0	-961.6484609	-961.3651860	-961.6213434	-959.8386028	-959.5794270
ester_op_4	0	-961.6489639	-961.3638630	-961.6220887	-959.8395539	-959.5783097
TS1						
ts01_op_03_rt	1(-161.9)	-1764.6060573	-1764.0679390	-1764.5579542	-1761.2995340	-1760.8065003
ts01_op_05	1(-159.9)	-1764.6065202	-1764.0681560	-1764.5583383	-1761.2991476	-1760.8059468
INT1						
int0_op_01	0	-1764.6258440	-1764.0889450	-1764.5651617	-1761.3011006	-1760.8218654
int1_op_04	0	-1764.6258361	-1764.0885950	-1764.5652427	-1761.3012603	-1760.8215942
RC						
rcomp_op_08	0	-2150.7772349	-2150.0912360	-2150.7264374	-2146.7623597	-2146.1241398
rcomp_op_06_opt	0	-2150.7762570	-2150.0877690	-2150.7266034	-2146.7643756	-2146.1225227
TS1.1a						
ts1b_op_12_red_opt	1(-152.8)	-2150.7637299	-2150.0756890	-2150.7106985	-2146.7485072	-2146.1104792
ts1b_op_09_red_opt	1(-135.1)	-2150.7602281	-2150.0732070	-2150.7055489	-2146.7432215	-2146.1078611
INT2						
int2_op_10	0	-2150.7889434	-2150.0999900	-2150.7299648	-2146.7611170	-2146.1281238
int2_op_01	0	-2150.7882251	-2150.0972850	-2150.7213503	-2146.7533228	-2146.1262390
TS2.1a						
ts_op_09	1(-144.4)	-2150.7697081	-2150.0824380	-2150.7128124	-2146.7456323	-2146.1122395
ts_op_04	1(-210.4)	-2150.7724321	-2150.0832620	-2150.7192017	-2146.7509196	-2146.1119615
ts_op_14	1(-208.4)	-2150.7599349	-2150.0707990	-2150.7039118	-2146.7365214	-2146.1003901
INT3						
int3_op_01	0	-2150.7786996	-2150.0869040	-2150.7269232	-2146.7656279	-2146.1225902
int3_op_02	0	-2150.7788773	-2150.0857410	-2150.7269064	-2146.7648065	-2146.1206227
TS3.1a						

ts3_op_26	1(-115.7)	-2150.774997	-2150.0878460	-2150.7221686	-2146.7594929	-2146.1221518
ts3_op_21	1(-120.4)	-2150.7745811	-2150.0849690	-2150.7230528	-2146.7599466	-2146.1188444
INT4						
int3_op_04	0	-2150.7951295	-2150.1091990	-2150.7447488	-2146.7809012	-2146.1423329
int3_op_06	0	-2150.7948694	-2150.1078170	-2150.7434487	-2146.7797138	-2146.1410636
INT5						
int3_op_14	0	-2150.8064769	-2150.1220540	-2150.7509289	-2146.7860493	-2146.1541560
int3_op_19	0	-2150.8071959	-2150.1227540	-2150.7571210	-2146.7912914	-2146.1539059

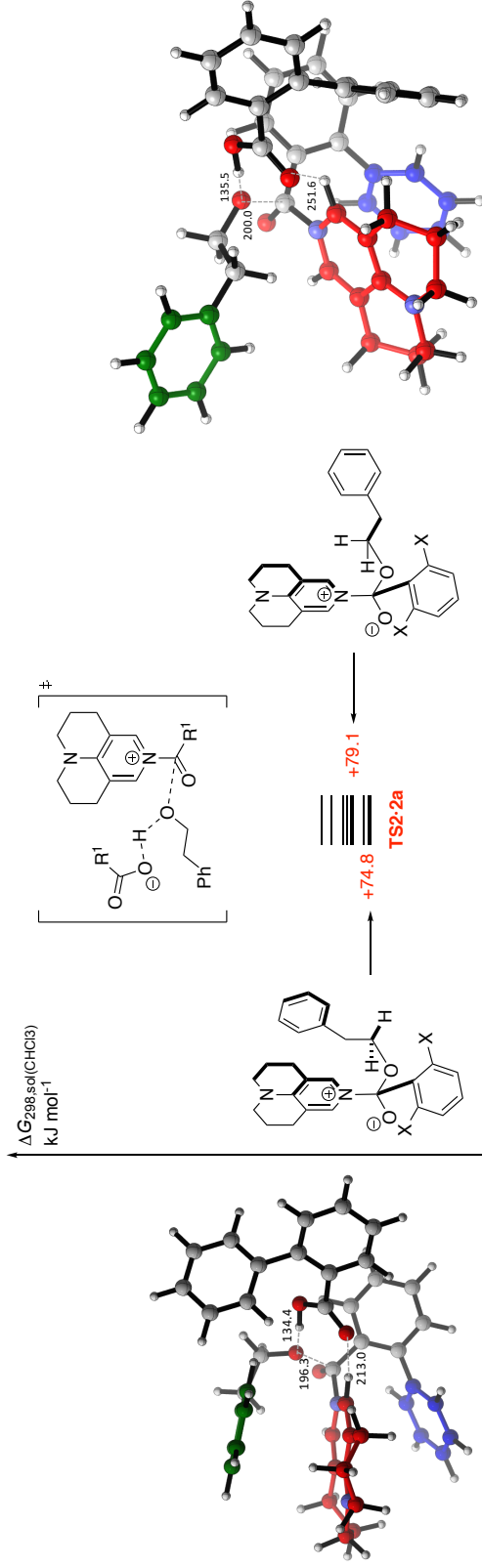
Table 3.19. Total energies and enthalpy energies for all systems shown in Scheme 3.3 (in Hartree). Molar enthalpy energies in solution at 298.15 K ($H_{298,\text{sol}}$) have been calculated at the SMD(CHCl₃)/DLPNO-CCSD(T)/def2-TZVPP// SMD(CHCl₃)/B3LYP-D3/6-31+G(d) level and corrected for a solution standard state of 1 M through addition of +7.925 kJ mol⁻¹ (0.00301848 Hartree). The SMD(CHCl₃)/B3LYP-D3/6-31+G(d) level of theory has been used to optimize the geometries and calculate solute enthalpy corrections and solvation energies. Note that the filenames are used in our calculations and do not follow any guide.

Filename	Freqs	E_{tot} SMD/B3LYP-D3/6-31+G(d)	H_{298} SMD/B3LYP-D3/6-31+G(d)	E_{tot} B3LYP-D3/6-31+G(d)	E_{tot} SMD/DLPNO- CCSD(T)/def2-TZVPP	$H_{298,\text{sol}}$ SMD/DLPNO-CCSD(T)/def2- TZVPP
1a						
roh1_1	0	-386.1353498	-385.9648590	-386.1148119	-385.4196861	-385.2667148
roh1_2	0	-386.1335902	-385.9632620	-386.1123578	-385.4178436	-385.2657293
4						
tcap_02	0	-537.1790980	-536.9321520	-537.1599167	-536.1519628	-535.9211796
tcap_01	0	-537.1786137	-536.9317010	-537.1591861	-536.1505343	-535.9200307
3f						
anh_op_37	0	-1227.4350491	-1227.0440650	-1227.4008583	-1225.1506553	-1224.7908435
anh_op_4	0	-1227.4309646	-1227.0399530	-1227.3982001	-1225.1491985	-1224.7879329
8f						
acid_op_2	0	-651.9379573	-651.7291790	-651.9176414	-650.7482377	-650.5567569
acid_op_1	0	-651.9379573	-651.7291790	-651.9176414	-650.7482374	-650.5567565
6af						
ester_op_2	0	-961.6484609	-961.2947420	-961.6213434	-959.8386028	-959.5089830
ester_op_4	0	-961.6489639	-961.2950840	-961.6220887	-959.8395539	-959.5095307
TS1						
ts01_op_03_rt	1(-161.9)	-1764.6060573	-1763.9671460	-1764.5579542	-1761.2995340	-1760.7057073

ts01_op_05	1(-159.9)	-1764.6065202	-1763.9674430	-1764.5583383	-1761.2991476	-1760.7052338
INT1						
int0_op_01	0	-1764.6258440	-1763.9842970	-1764.5651617	-1761.3011006	-1760.7172174
int1_op_04	0	-1764.6258361	-1763.9843850	-1764.5652427	-1761.3012603	-1760.7173842
RC						
rcomp_op_08	0	-2150.7772349	-2149.9628140	-2150.7264374	-2146.7623597	-2145.9957178
rcomp_op_06_opt	0	-2150.7762570	-2149.9622820	-2150.7266034	-2146.7643756	-2145.9970357
TS1·1a						
ts1b_op_12_red_opt	1(-152.8)	-2150.7637299	-2149.9514390	-2150.7106985	-2146.7485072	-2145.9862292
ts1b_op_09_red_opt	1(-135.1)	-2150.7602281	-2149.9480860	-2150.7055489	-2146.7432215	-2145.9827401
INT2						
int2_op_10	0	-2150.7889434	-2149.9739860	-2150.7299648	-2146.7611170	-2146.0021198
int2_op_01	0	-2150.7882251	-2149.9730490	-2150.7213503	-2146.7533228	-2146.0020030
TS2·1a						
ts_op_09	1(-144.4)	-2150.7697081	-2149.9592230	-2150.7128124	-2146.7456323	-2145.9890245
ts_op_04	1(-210.4)	-2150.7724321	-2149.9625150	-2150.7192017	-2146.7509196	-2145.9912145
ts_op_14	1(-208.4)	-2150.7599349	-2149.9486800	-2150.7039118	-2146.7365214	-2145.9782711
INT3						
int3_op_01	0	-2150.7786996	-2149.9646870	-2150.7269232	-2146.7656279	-2146.0003732
int3_op_02	0	-2150.7788773	-2149.9648640	-2150.7269064	-2146.7648065	-2145.9997457
TS3·1a						
ts3_op_26	1(-115.7)	-2150.7749997	-2149.9623690	-2150.7221686	-2146.7594929	-2145.9966748
ts3_op_21	1(-120.4)	-2150.7745811	-2149.9617670	-2150.7230528	-2146.7599466	-2145.9956424
INT4						
int3_op_04	0	-2150.7951295	-2149.9809060	-2150.7447488	-2146.7809012	-2146.0140399
int3_op_06	0	-2150.7948694	-2149.9805380	-2150.7434487	-2146.7797138	-2146.0137846
INT5						
int3_op_14	0	-2150.8064769	-2149.9932200	-2150.7509289	-2146.7860493	-2146.0253220
int3_op_19	0	-2150.8071959	-2149.9939540	-2150.7571210	-2146.7912914	-2146.0251059



Scheme 3.5. Computed stationary points in the Lewis base-catalyzed reaction of primary alcohol **2a** with the benzoic anhydride derivative **3f** at the SMD(CHCl₃)/DLPNO-CCSD(T)/def2-TZVPP//SMD(CHCl₃)/B3LYP-D3/6-31+G(d) level of theory.

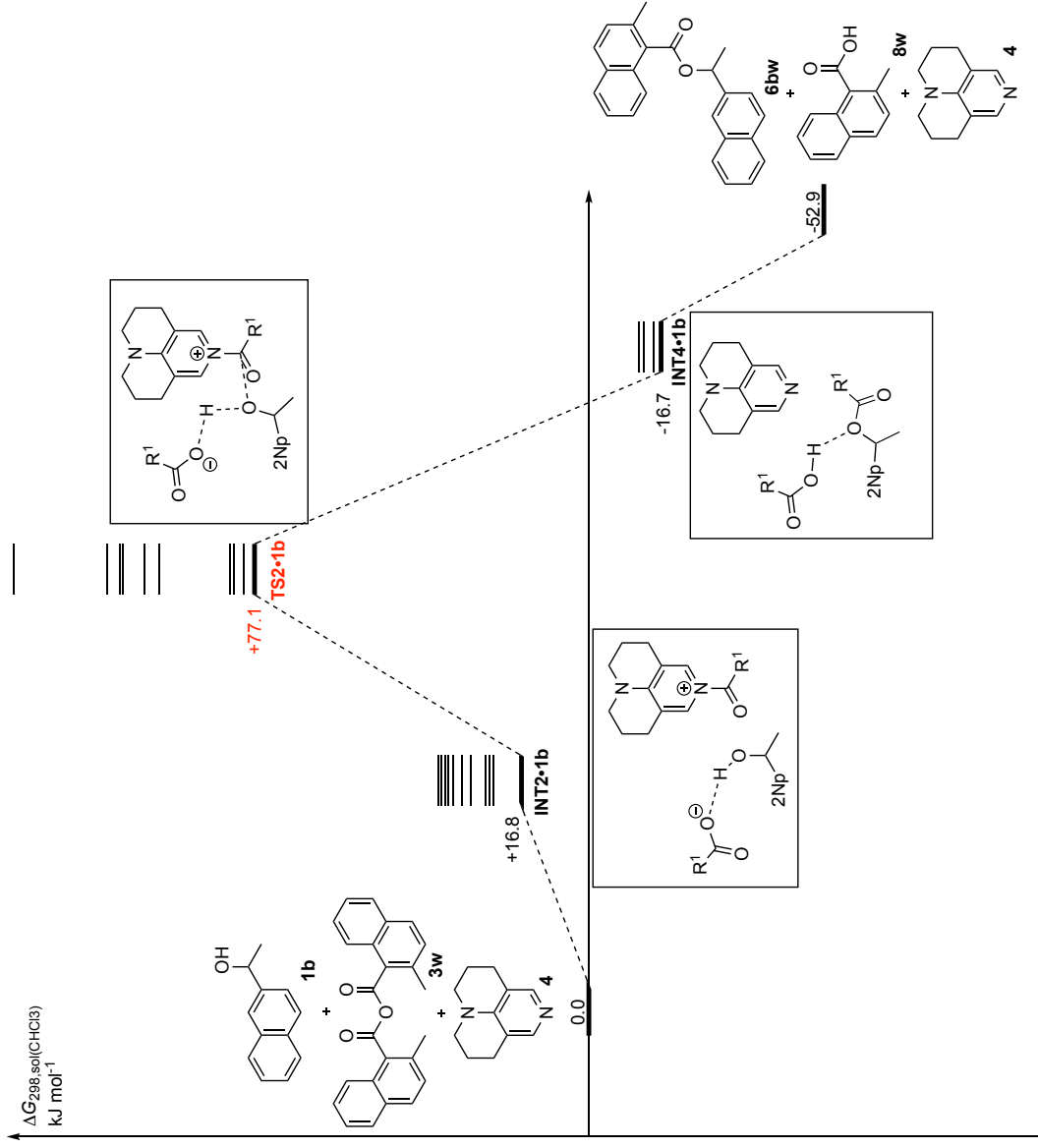


Scheme 3.6. Computed stationary points of **TS2-2a** in the Lewis base-catalyzed reaction of primary alcohol **2a** with anhydride **3f** at the SMD(CHCl₃)/DLPNO-CCSD(T)/def2-TZVPP//SMD(CHCl₃)/B3LYP-D3/6-31+G(d) level of theory.

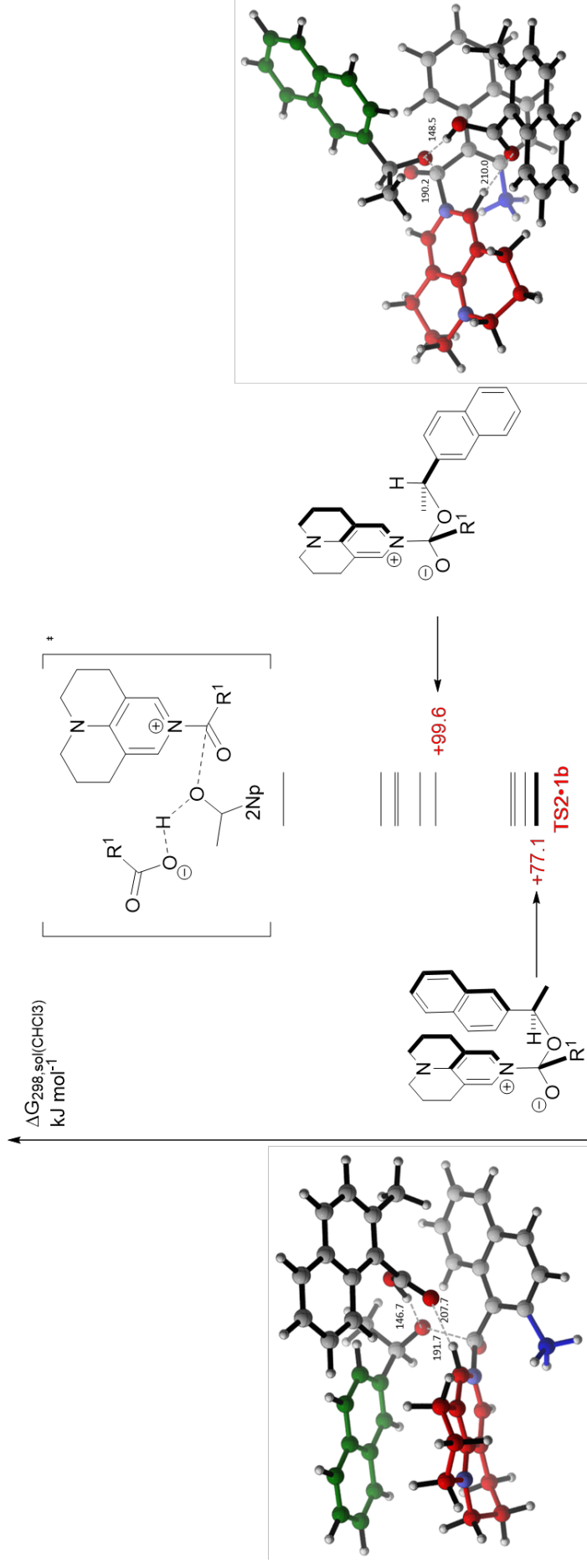
Table 3.20. Total energies and free energies for relevant systems shown in Scheme 3.5 (in Hartree). Molar free energies in solution at 298.15 K ($G_{298, \text{sol}}$) have been calculated at the SMD(CHCl₃)/DLPNO-CCSD(T)/def2-TZVPP// SMD(CHCl₃)/B3LYP-D3/6-31+G(d) level of theory and corrected for a solution standard state of 1 M through addition of +7.925 kJ mol⁻¹ (0.00301848 Hartree). The SMD(CHCl₃)/B3LYP-D3/6-31+G(d) level of theory has been used to optimize the geometries and calculate solute thermal corrections and solvation energies. Note that the filenames are used in our calculations and do not follow any guide.

Filename	Freqs	E_{tot} SMD/B3LYP-D3/6-31+G(d)	G_{298} SMD/B3LYP-D3/6-31+G(d)	E_{tot} B3LYP-D3/6-31+G(d)	E_{tot} SMD/DLPNO-CCSD(T)/def2-TZVPP	$G_{298, \text{sol}}$ SMD/DLPNO-CCSD(T)/def2-TZVPP
2a						
roh_primary_1	0	-386.1332627	-386.0046850	-386.1189416	-385.4167044	-385.2994292
roh_primary_5	0	-386.1316294	-386.0039470	-386.1164728	-385.4146374	-385.2990931
7af						
ester_prim_16	0	-961.6468798	-961.3639740	-961.6186760	-959.8348017	-959.5770812
ester_prim_6	0	-961.6468050	-961.3623120	-961.6188670	-959.8361660	-959.5765925
INT2-2a						
int2_prim_03	0	-2150.7840316	-2150.0965830	-2150.7247089	-2146.7551562	-2146.1240119
int2_prim_01	0	-2150.7825448	-2150.0960150	-2150.7161915	-2146.7454174	-2146.1222224
TS2-2a						
ts_prim_op_11	1(-290.0)	-2150.7639967	-2150.0794170	-2150.7065606	-2146.7377929	-2146.1076309

ts_prim_op_05_red_opt	1(-356.6)	-2150.7643065	-2150.0784220	-2150.7076253	-2146.7397420	-2146.1075202
ts_prim_op_13	1(-271.5)	-2150.7648423	-2150.0791840	-2150.7071316	-2146.7369579	-2146.1059919
INT3-2a						
int3_prim_05	0	-2150.7707793	-2150.0856660	-2150.7144086	-2146.7504392	-2146.1186781
int3_prim_04	0	-2150.7707919	-2150.0846970	-2150.7144519	-2146.7506245	-2146.1178512
Table 3.21. Total energies and enthalpy energies for relevant systems shown in Scheme 3.5 (in Hartree). Molar enthalpy energies in solution at 298.15 K ($H_{298, \text{sol}}$) have been calculated at the SMD(CHCl ₃)/DLPNO-CCSD(T)/def2-TZVPP// SMD(CHCl ₃)/B3LYP-D3/6-31+G(d) level and corrected for a solution standard state of 1 M through addition of +7.925 kJ mol ⁻¹ (0.00301848 Hartree). The SMD(CHCl ₃)/B3LYP-D3/6-31+G(d) level of theory has been used to optimize the geometries and calculate solute enthalpy corrections and solvation factor. Note that the filenames are used in our calculations and do not follow any guide.						
Filename	Freqs	E_{tot} SMD/B3LYP-D3/6-31+G(d)	H_{298} SMD/B3LYP-D3/6-31+G(d)	E_{tot} B3LYP-D3/6-31+G(d)	E_{tot} SMD/DLPNO-CCSD(T)/def2-TZVPP	$H_{298, \text{sol}}$ SMD/DLPNO-CCSD(T)/def2-TZVPP
2a						
roh_primary_1	0	-386.1332627	-385.9620400	-386.1189416	-385.4167044	-385.2567842
roh_primary_5	0	-386.1316294	-385.9602950	-386.1164728	-385.4146374	-385.2554411
7af						
ester_prim_16	0	-961.6468798	-961.2923810	-961.6186760	-959.8348017	-959.5054882
ester_prim_6	0	-961.6468050	-961.2923460	-961.6188670	-959.8361660	-959.5066265
INT2-2a						
int2_prim_03	0	-2150.7840316	-2149.9690990	-2150.7247089	-2146.7551562	-2145.9965279
int2_prim_01	0	-2150.7825448	-2149.9671360	-2150.7161915	-2146.7454174	-2145.9933434
TS2-2a						
ts_prim_op_11	1(-290.0)	-2150.7639967	-2149.9540200	-2150.7065606	-2146.7377929	-2145.9822339
ts_prim_op_05_red_opt	1(-356.6)	-2150.7643065	-2149.9544430	-2150.7076253	-2146.7397420	-2145.9835412
ts_prim_op_13	1(-271.5)	-2150.7648423	-2149.9544960	-2150.7071316	-2146.7369579	-2145.9813039
INT3-2a						
int3_prim_05	0	-2150.7707793	-2149.9563180	-2150.7144086	-2146.7504392	-2145.9893301
int3_prim_04	0	-2150.7707919	-2149.9562580	-2150.7144519	-2146.7506245	-2145.9894122



Scheme 3.7. Computed stationary points in the Lewis base-catalyzed reaction of secondary alcohol **1b** with the 1-naphthyl anhydride derivative **3w** at the SMD(CHCl₃)/DLPNO-CCSD(T)/def2-TZVPP//SMD(CHCl₃)/B3LYP-D3/6-31+G(d) level of theory.



Scheme 3.8. Computed stationary points of **TS2-1b** in the Lewis base-catalyzed reaction of secondary alcohol **1b** with anhydride **3w** at the SMD(CHCl₃)/DLPNO-CCSD(T)/def2-TZVPP//SMD(CHCl₃)/B3LYP-D3/6-31+G(d) level of theory.

Table 3.22. Total energies and free energies for relevant systems shown in Scheme 3.7 (in Hartree). Molar free energies in solution at 298.15 K ($G_{298,so}$) have been calculated at the SMD(CHCl₃)/DLPNO-CCSD(T)/def2-TZVPP// SMD(CHCl₃)/B3LYP-D3/6-31+G(d) level of theory and corrected for a solution standard state of 1 M through addition of +7.925 kJ mol^{-1} (0.00301848 Hartree). The SMD(CHCl₃)/B3LYP-D3/6-31+G(d) level of theory has been used to optimize the geometries and calculate solute thermal corrections and solvation energies. Note that the filenames are used in our calculations and do not follow any guide. The calculations using int=finegrid are marked **green**, this one using int=ultrafinegrid are marked **purple**.

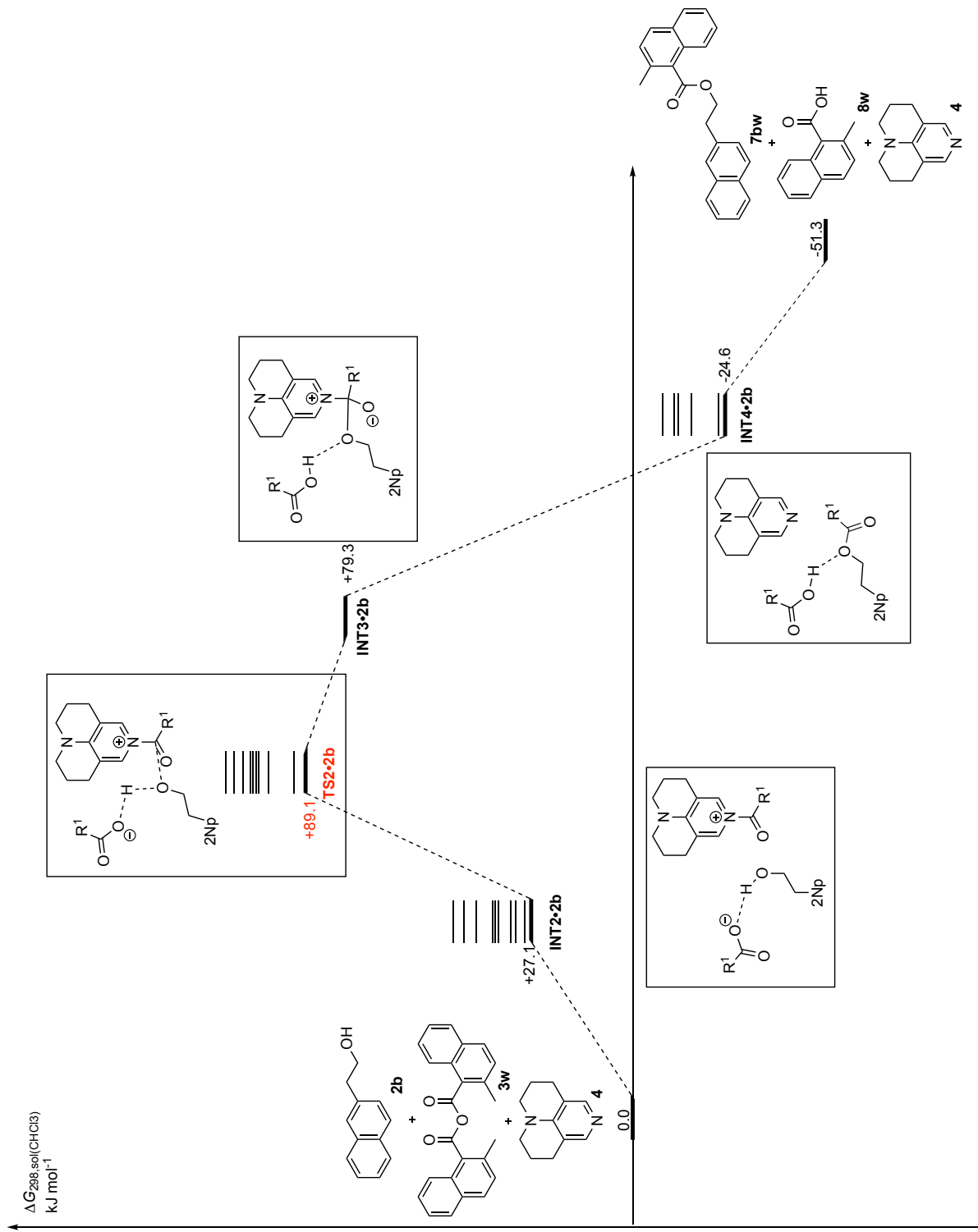
Filename	Freqs	E_{tot} SMD/B3LYP-D3/ 6-31+G(d)	ΔG_{298} SMD/B3LYP-D3/ 6-31+G(d)	E_{tot} SMD/B3LYP-D3/ 6-31+G(d)	E_{tot} B3LYP-D3/ 6-31+G(d)	E_{tot} SMD/DLPNO-CCSD(T)/ def2-TZVPP	$G_{298,so}$ SMD/DLPNO-CCSD(T)/ def2-TZVPP
1b							
1b_2	0	-539.7944796	0.1714430	-539.7944796	-539.7763073	-538.7728240	-538.6165348
1b_1	0	-539.7940810	0.1714070	-539.7940810	-539.7758285	-538.7725477	-538.6163748
4							
tcap_02	0	-537.1790980	0.2005220	-537.1790980	-537.1599167	-536.1519628	-535.9211796
tcap_01	0	-537.1786137	0.2004967	-537.1786137	-537.1591861	-536.1505343	-535.9200307

3w														
naph2me_1_17	0	-1151.2254841	0.3033640	-1151.2254841	-1151.1972173	-1149.0983812	-1148.8202655							
naph2me_1_16	0	-1151.2264728	0.3043320	-1151.2264728	-1151.1979161	-1149.0980048	-1148.8192111							
8w														
8w_2	0	-613.8354473	0.1517970	-613.8354473	-613.8165917	-612.7211184	-612.5851585							
8w_1	0	-613.8356696	0.1522630	-613.8356696	-613.8168063	-612.7214362	-612.5850180							
6bw														
1bw_1	0	-1077.2043288	0.3200170	-1077.2043288	-1077.1737614	-1075.1636403	-1074.8711722							
1bw_15	0	-1077.2044305	0.3217300	-1077.2044305	-1077.1738179	-1075.1633997	-1074.8692638							
INT2-1b														
sek_003	0	-2228.2425548	0.7191980	-2228.2427960	-2228.1785974	-2224.0560083	-2223.3979904							
int2_s_02	0	-2228.2434628	0.7206950	-2228.2437308	-2228.1812571	-2224.0571788	-2223.3959390							
TS2-1b														
ts2_s_01	1 (-130)	-2228.2211644	0.7218680	-2228.2214314	-2228.1662817	-2224.0447741	-2223.3750373							
sek_002	1 (-142)	-2228.2205667	0.7223650	-2228.2208191	-2228.1654747	-2224.0440763	-2223.3740372							
sek_001	1 (-152)	-2228.2118061	0.7193540	-2228.2119592	-2228.1507721	-2224.0276381	-2223.3664527							
INT4-1b														
int3_s_03	0	-2228.2528707	0.7202050	-2228.2530978	-2228.2000567	-2224.0809578	-2223.4107754							
int3_s_01	0	-2228.2517820	0.7190540	-2228.2522176	-2228.1975094	-2224.0768405	-2223.4094762							

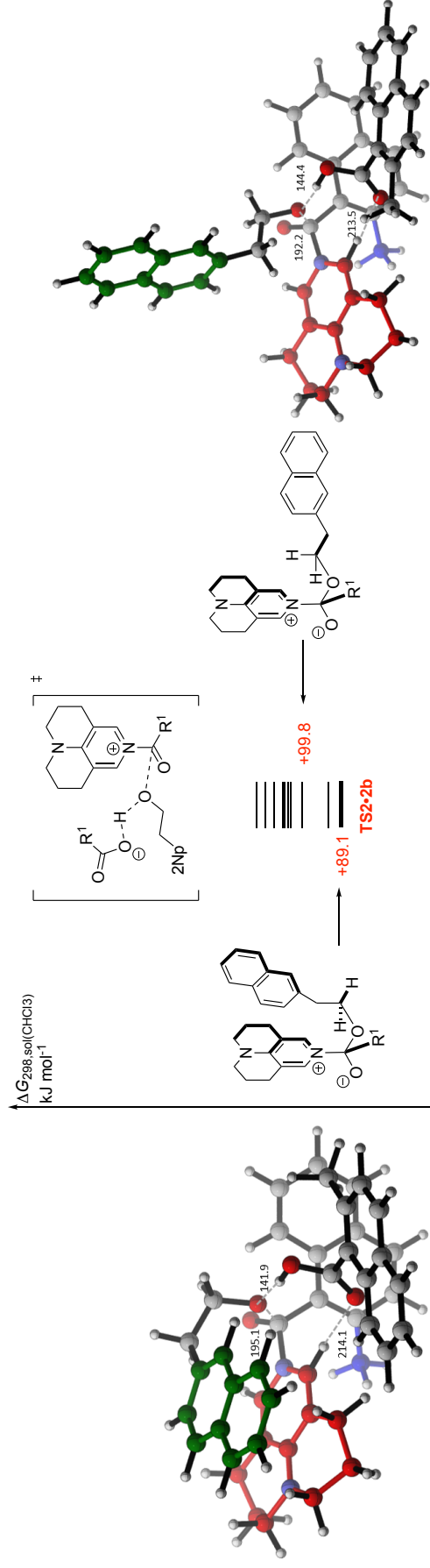
Table 3.23. Total energies and enthalpy energies for relevant systems shown in Scheme 3.7 (in Hartree). Molar enthalpy energies in solution at 298.15 K ($H_{298, sol}$) have been calculated at the SMD(CHCl₃)/DLPNO-CCSD(T)/def2-TZVPP//SMD(CHCl₃)/B3LYP-D3/6-31+G(d) level and corrected for a solution standard state of 1 M through addition of +7.925 kJ mol⁻¹ (0.00301848 Hartree). The SMD(CHCl₃)/B3LYP-D3/6-31+G(d) level of theory has been used to optimize the geometries and calculate solute enthalpy corrections and solvation factor. Note that the filenames are used in our calculations and do not follow any guide. The calculations using int=ultrafinegrid are marked green, this one using int=ultrafinegrid are marked purple.

Filename	Freqs	E_{tot}	ΔH_{298}	E_{tot}	E_{tot}	E_{tot}	$H_{298, sol}$
		SMD/B3LYP-D3/6-31+G(d)	SMD/B3LYP-D3/6-31+G(d)	SMD/B3LYP-D3/6-31+G(d)	B3LYP-D3/6-31+G(d)	SMD/DLPNO-CCSD(T)/def2-TZVPP	SMD/DLPNO-CCSD(T)/def2-TZVPP
1b							
1b_2	0	-539.7944796	0.2200570	-539.7944796	-539.7763073	-538.7728240	-538.5679208
1b_1	0	-539.7940810	0.2200640	-539.7940810	-539.7758285	-538.7725477	-538.5677178
4							
tcap_02	0	-537.1790980	0.2469460	-537.1790980	-537.1599167	-536.1519628	-535.9211796
tcap_01	0	-537.1786137	0.2469127	-537.1786137	-537.1591861	-536.1505343	-535.9200307
3w							

naph2me_1_17	0	-1151.2254841	0.3774420	-1151.2254841	-1151.1972173	-1149.0983812	-1148.7461875
naph2me_1_16	0	-1151.2264728	0.3777680	-1151.2264728	-1151.1979161	-1149.0980048	-1148.7457751
8w							
8w_2	0	-613.8354473	0.2019990	-613.8354473	-613.8165917	-612.7211184	-612.5349565
8w_1	0	-613.8356696	0.2021170	-613.8356696	-613.8168063	-612.7214362	-612.5351640
6bw							
1bw_1	0	-1077.2043288	0.3966150	-1077.2043288	-1077.1737614	-1075.1636403	-1074.7945742
1bw_15	0	-1077.2044305	0.3964890	-1077.2044305	-1077.1738179	-1075.1633997	-1074.7945048
INT2·1b							
sek_003	0	-2228.2425548	0.8503620	-2228.2427960	-2228.1785974	-2224.0560083	-2223.2668264
int2_s_02	0	-2228.2434628	0.8507890	-2228.2437308	-2228.1812571	-2224.0571788	-2223.2658450
TS2·1b							
ts2_s_01	1 (-130)	-2228.2211644	0.8476010	-2228.2214314	-2228.1662817	-2224.0447741	-2223.2493043
sek_002	1 (-142)	-2228.2205667	0.8476230	-2228.2208191	-2228.1654747	-2224.0440763	-2223.2487792
sek_001	1 (-152)	-2228.2118061	0.8475650	-2228.2119592	-2228.1507721	-2224.0276381	-2223.2382417
INT4·1b							
int3_s_03	0	-2228.2528707	0.8508550	-2228.2530978	-2228.2000567	-2224.0809578	-2223.2801254
int3_s_01	0	-2228.2517820	0.8510730	-2228.2522176	-2228.1975094	-2224.0768405	-2223.2774572



Scheme 3.9. Computed stationary points in the Lewis base-catalyzed reaction of primary alcohol **2b** with the 1-naphthyl anhydride derivative **3w** at the SMD(CHCl₃)/DLPNO-CCSD(T)/def2-TZVPP//SMD(CHCl₃)/B3LYP-D3/6-31+G(d) level of theory.



Scheme 3.10. Computed stationary points of **TS2-2b** in the Lewis base-catalyzed reaction of primary alcohol **2b** with anhydride **3w** at the SMD(CHCl₃)/DLPNO-CCSD(T)/def2-TZVPP//SMD(CHCl₃)/B3LYP-D3/6-31+G(d) level of theory.

Table 3.24. Total energies and free energies for relevant systems shown in Scheme 3.9 (in Hartree). Molar free energies in solution at 298.15 K ($G_{298, \text{sol}}$) have been calculated at the SMD(CHCl₃)/DLPNO-CCSD(T)/def2-TZVPP// SMD(CHCl₃)/B3LYP-D3/6-31+G(d) level of theory and corrected for a solution standard state of 1 M through addition of +7.925 kJ mol⁻¹ (0.00301848 Hartree). The SMD(CHCl₃)/B3LYP-D3/6-31+G(d) level of theory has been used to optimize the geometries and calculate solute thermal corrections and solvation energies. Note that the filenames are used in our calculations and do not follow any guideline. The calculations using int=finegrid are marked **green**, this one using int=ultrafinegrid are marked **purple**.

Filename	Freqs	E_{tot} SMD/B3LYP-D3/ 6-31+G(d)	ΔG_{298} SMD/B3LYP-D3/ 6-31+G(d)	E_{tot} SMD/B3LYP-D3/ 6-31+G(d)	E_{tot} B3LYP-D3/ 6-31+G(d)	E_{tot} SMD/DLPNO-CCSD(T)/ def2-TZVPP	$G_{298, \text{sol}}$ SMD/DLPNO-CCSD(T)/ def2-TZVPP
2b							
1a_1	0	-539.7923860	0.1720000	-539.7923860	-539.7736596	-538.7699164	-538.6136243
1a_2	0	-539.7917743	0.1722660	-539.7917743	-539.7729833	-538.7691161	-538.6126226
7bw							
2bw_58	0	-1077.2053169	0.3237990	-1077.2053169	-1077.1757431	-1075.1661288	-1074.8688851
2bw_24	0	-1077.2052866	0.3239800	-1077.2052866	-1077.1755855	-1075.1659498	-1074.8686524
INT2-2b							
prim_0045	0	-2228.2408855	0.7215270	-2228.2408855	-2228.1770770	-2224.0519121	-2223.3911752
int2_p_02	0	-2228.2401959	0.7221100	-2228.2406431	-2228.1769086	-2224.0518188	-2223.3904248
TS2-2b							

prim_004d3	1 (-147)	-2228.2166427	0.7234850	-2228.2166727	-2228.1609297	-2224.0383283	-2223.3675679
prim_0082	1 (-151)	-2228.2169715	0.7245450	-2228.2169795	-2228.1610925	-2224.0384535	-2223.3667770
ts2_p_17_freq	1 (-137)	-2228.2095704	0.7191920	-2228.2100171	-2228.1461258	-2224.0218168	-2223.3634977
INT3-2b							
prim_0064	0	-2228.2481516	0.7198060	-2228.2136636	-2228.1507424	-2224.0311952	-2223.3712919
INT4-2b							
int3_p_04	0	-2228.2499722	0.7208180	-2228.2502573	-2228.1989834	-2224.0834154	-2223.4108529
int3_p_03	0	-2228.2504043	0.7191340	-2228.2508264	-2228.1974803	-2224.0793039	-2223.4104975

Table 3.25. Total energies and enthalpy energies for relevant systems shown in Scheme 3.9 (in Hartree). Molar enthalpy energies in solution at 298.15 K ($H_{298, \text{sol}}$) have been calculated at the SMD(CHCl₃)/DLPNO-CCSD(T)/def2-TZVPP//SMD(CHCl₃)/B3LYP-D3/6-31+G(d) level and corrected for a solution standard state of 1 M through addition of +7.925 kJ mol⁻¹ (0.00301848 Hartree). The SMD(CHCl₃)/B3LYP-D3/6-31+G(d) level of theory has been used to optimize the geometries and calculate solute enthalpy corrections and solvation factor. Note that the filenames are used in our calculations and do not follow any guide. The calculations using int=finegrid are marked green, this one using int=ultrafinegrid are marked purple.

Filename	Freqs	E_{tot} SMD/B3LYP-D3/ 6-31+G(d)	ΔH_{298} SMD/B3LYP-D3/ 6-31+G(d)	E_{tot} SMD/B3LYP-D3/ 6-31+G(d)	E_{tot} B3LYP-D3/ 6-31+G(d)	E_{tot} SMD/DLPNO-CCSD(T)/ def2-TZVPP	$H_{298, \text{sol}}$ SMD/DLPNO-CCSD(T)/ def2-TZVPP
1b							
1a_1	0	-539.7923860	0.2207560	-539.7923860	-539.7736596	-538.7699164	-538.5648683
1a_2	0	-539.7917743	0.2208580	-539.7917743	-539.7729833	-538.7691161	-538.5640306
7bw							
2bw_58	0	-1077.2053169	0.3973830	-1077.2053169	-1077.1757431	-1075.1661288	-1074.7953011
2bw_24	0	-1077.2052866	0.3972100	-1077.2052866	-1077.1755855	-1075.1659498	-1074.7954224
INT2-2b							
prim_0045	0	-2228.2408855	0.8516150	-2228.2408855	-2228.1770770	-2224.0519121	-2223.2610872
int2_p_02	0	-2228.2401959	0.8512700	-2228.2406431	-2228.1769086	-2224.0518188	-2223.2612648
TS2-2b							
prim_004d3	1 (-147)	-2228.2166427	0.8475470	-2228.2166727	-2228.1609297	-2224.0383283	-2223.2435059
prim_0082	1 (-151)	-2228.2169715	0.8478580	-2228.2169795	-2228.1610925	-2224.0384535	-2223.2434640
ts2_p_17_freq	1 (-137)	-2228.2095704	0.8476920	-2228.2100171	-2228.1461258	-2224.0218168	-2223.2349977
INT3-2b							
prim_0064	0	-2228.2481516	0.8518480	-2228.2136636	-2228.1507424	-2224.0311952	-2223.2392499
INT4-2b							
int3_p_04	0	-2228.2499722	0.8515710	-2228.2502573	-2228.1989834	-2224.0834154	-2223.2800999
int3_p_03	0	-2228.2504043	0.8513590	-2228.2508264	-2228.1974803	-2224.0793039	-2223.2782725

3.2.2 NCI Analysis

Comparing the transition states **TS2** (**TS2-1a**, **TS2-2a**, **TS2-1b** and **TS2-2b**) of the corresponding best conformer with each other, we see that all four **TS2** are characterized by a triple “sandwich” conformation between the catalyst-derived pyridinium ring system (red) and the aromatic groups of the alcohol moiety (green) and the *ortho*-substituent of the anhydride (blue). In all four structures, the carboxylate counter ion acts as a clamp setting up a hydrogen bond through the hydrogen atom of the hydroxyl group and a C-H...O interaction with one *ortho*-hydrogen atom of the pyridinium ring system (Figure 3.28). In **TS2-1a** the overlapping between the phenyl moiety of **1a** and the catalyst TCAP is better stacked than in **TS2-2a** also visible by the distances between N1-C (325.4 vs. 376.8 pm) and N-C (414.6 vs. 486.3 pm). Also, the overlapping between the naphthyl group of **1b** with the pyridinium ring system in **TS2-1b** is better stacked as in **TS2-2b** visible by the distances N1-C (326.4 vs. 362.3 pm), C-C (381.4 vs. 390.1 pm) and N-C (439.8 vs 539.3 pm). Further we find out, that the distance N-C between the most catalytic active nitrogen and the carbon of the *ortho*-substituent of the anhydride is getting smaller comparing **TS2-1a** with **TS2-1b** (296.1 vs. 288.5 pm). To analyze these non-covalent π - π stacking further a non-covalent interactions (NCI) plot were done with the four **TS2** shown in Figure 3.28 (always with the corresponding best conformer). Yang *et al.* described non-covalent bonds “as regions with low density and low reduced gradient”^[15] and developed a computational algorithm for the visualization of these non-covalent interactions.^[16] In all four **TS2** areas of non-covalent interactions between the aromatic part of the alcohols and the pyridinium ring system of the catalyst are presented. It is also visible that the areas of NCI for secondary alcohols **1a/1b** are bigger than for the corresponding primary alcohols **2a/2b**. This observation agrees with the previous described distances between alcohols and TCAP motifs. Further it is visible that the NCI between the catalytic active N atom of TCAP and the *ortho*-substituent of the anhydride is similar, so that the previous described distance N-C play an important role for the selectivity.

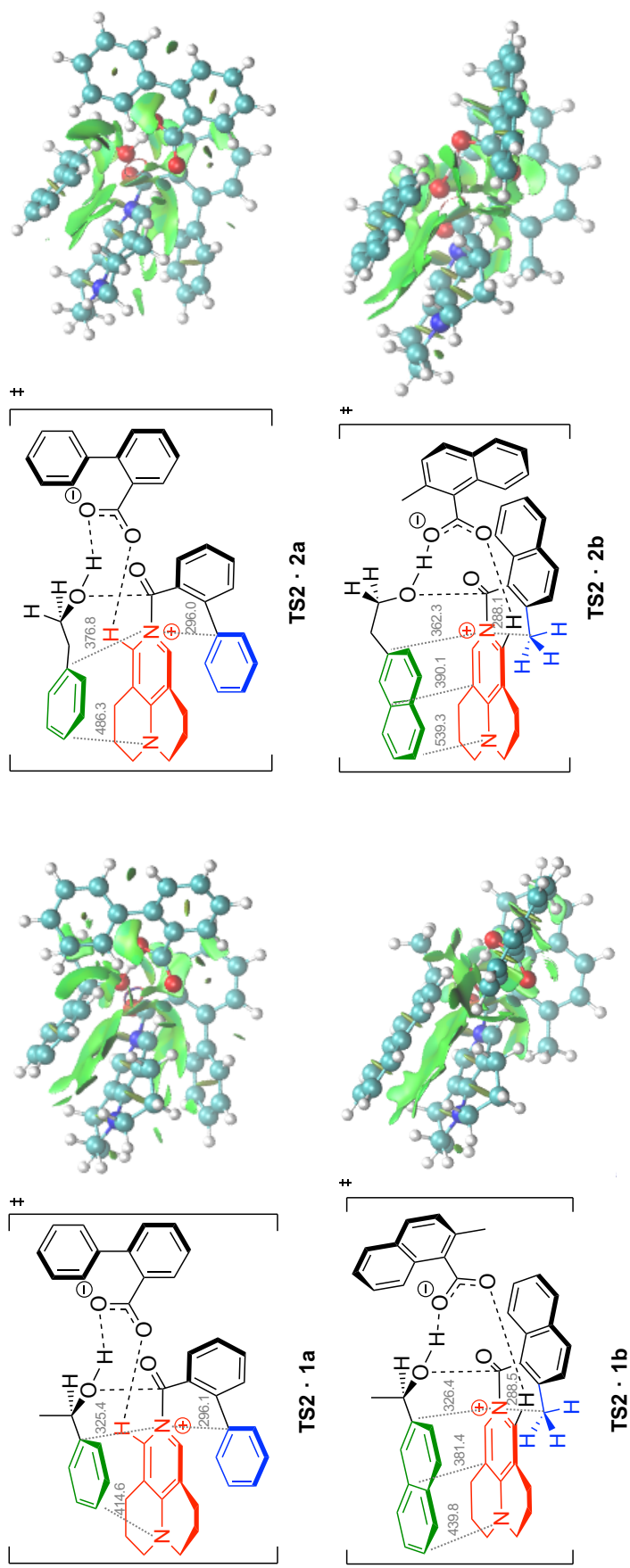


Figure 3.28. TS2 structures and their corresponding NCI plots generated from wavefunction at B3LYP-D3/6-31+G(d) level of theory with NCIplot^[16] and visualized with VMD.^[17]

3.2.3 Computational Study about Acid Anhydride Structures

Table 3.26. Total energies, enthalpies, and free energies for anhydrides **3a-z** (in Hartree). The SMD(CHCl₃)/B3LYP-D3/6-31+G(d) level of theory has been used to optimize the geometries and calculate solute thermal corrections and solvation energies. For the acid anhydrides **3t-v** the conformational search was based on the best 15 conformers of anhydride **3s**. (Note that the filenames are used in our calculations and do not follow any guide.)

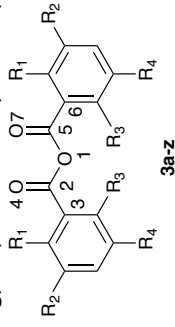
Filename	Freqs	E_{tot}		H_{298}		G_{298}	
		SMD/B3LYP-D3/6-31+G(d) (Hartree)	ΔE_{tot} (kJ mol ⁻¹)	SMD/B3LYP-D3/6-31+G(d) (Hartree)	ΔH_{298} (kJ mol ⁻¹)	SMD/B3LYP-D3/6-31+G(d) (Hartree)	ΔG_{298} (kJ mol ⁻¹)
3a							
anh_031	0	-765.2784970	0.00	-765.0580560	0.07	-765.1154140	0.00
anh_030	0	-765.2784909	0.02	-765.0580840	0.00	-765.1149120	1.32
3b							
ph_2ome_1_5	0	-994.3349746	0.00	-994.0441836	0.00	-994.1108036	3.51

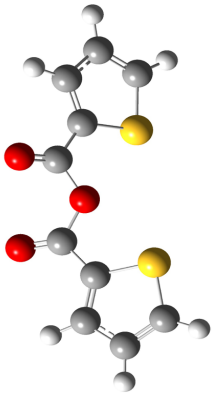
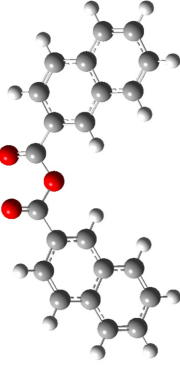
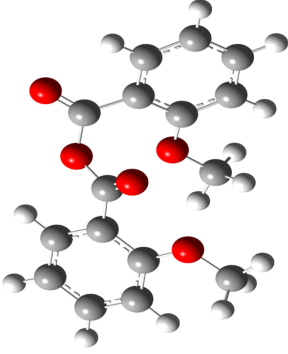
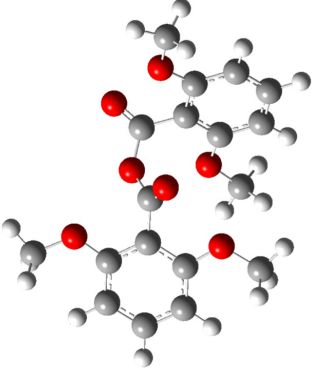
ph_2ome_1_3.com	0	-994.3345061	1.23	-994.0439831	0.53	-994.1121391	0.00
3c							
tol_1_2	0	-843.9173878	0.00	-843.6385218	0.12	-843.7018978	2.09
tol_1_8.com	0	-843.9173166	0.19	-843.6385690	0.00	-843.7026930	0.00
3d							
phcl_2	0	-1684.4578194	0.00	-1684.2548964	0.00	-1684.3197794	0.00
phcl_15	0	-1684.4574567	0.95	-1684.2544387	1.20	-1684.3179287	4.86
3e							
ph_obr_1_13	0	-5907.5356398	0.00	-5907.3318708	0.00	-5907.3970368	0.00
ph_obr_1_2	0	-5907.5337608	4.93	-5907.3299558	5.03	-5907.3968158	0.58
3f							
anh_055	0	-1227.4350563	0.00	-1227.0439910	0.19	-1227.1223790	0.00
anh_op_37	0	-1227.4350491	0.02	-1227.0440650	0.00	-1227.1223200	0.15
3g							
ph_2tol_b_2	0	-1306.0801534	0.00	-1305.6305954	0.00	-1305.7158964	0.00
ph_2tol_b_4	0	-1306.0761545	10.50	-1305.6264895	10.78	-1305.7126605	8.50
3h							
ph_o1naph_1_4	0	-1534.7529959	0.00	-1534.2627289	0.00	-1534.3522029	1.34
ph_o1naph_1_2	0	-1534.7526357	0.95	-1534.2626607	0.18	-1534.3527127	0.00
3i							
ph_2naph_22	0	-1534.7567348	0.00	-1534.2666618	0.00	-1534.3568218	0.78
ph_2naph_10	0	-1534.7561913	1.43	-1534.2659963	1.75	-1534.3554703	4.33
3j							
ph_2naph7ome_19	0	-1763.8228595	0.00	-1763.2621925	0.00	-1763.3625125	0.00
ph_2naph7ome_2 (crystal)	0	-1763.8222769	1.53	-1763.2613489	2.21	-1763.3611389	3.61
3k							
phome2_8	0	-1223.3887796	0.00	-1223.0277706	0.00	-1223.1075986	0.00
phome2_3	0	-1223.3876776	2.89	-1223.0269526	2.15	-1223.1066386	2.52
3l							
phomeph_2	0	-1456.4903640	0.00	-1456.0289550	0.00	-1456.1186460	0.00
phomeph_31	0	-1456.4890217	3.52	-1456.0276497	3.43	-1456.1175917	2.77
3m							
phme2_1_3	0	-922.5528319	0.00	-922.2152349	0.00	-922.2858109	2.23

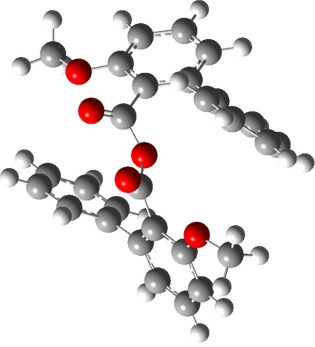
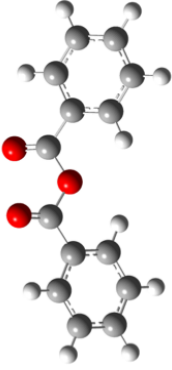
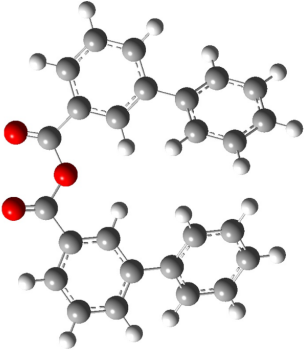
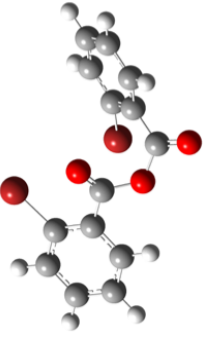
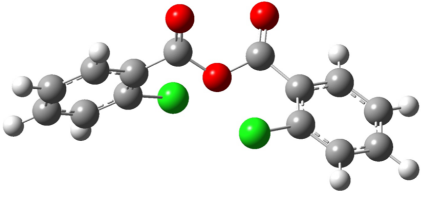
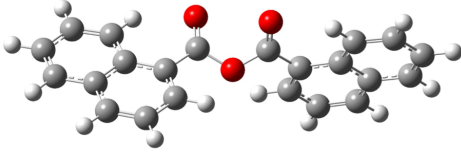
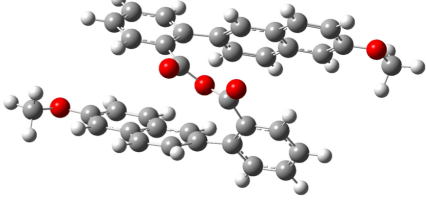
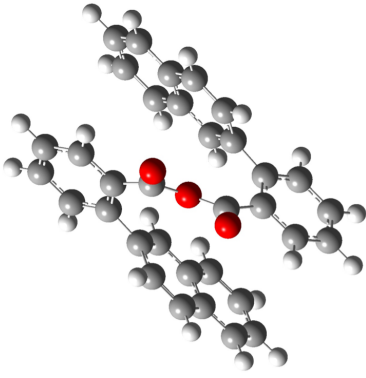
phme2_1_4	0	-922.5526589	0.45	-922.2150079	0.60	-922.2834249	8.50
3n							
ph_me_ph_3_1_2 (crystal)	0	-1306.0750672	0.00	-1305.65207	0.00	-1305.6250762	0.00
ph_me_ph_3_1_7	0	-1306.0715374	9.27	-1305.6489	8.32	-1305.6217724	8.67
3o							
ph_me_no2_1_15.com	0	-1252.9322048	0.00	-1252.6439308	0.04	-1252.7189948	0.74
ph_me_no2_1_11	0	-1252.9321667	0.10	-1252.6439477	0.00	-1252.7191547	0.32
3p							
phfcf3_3	0	-1637.8569065	0.00	-1637.6365235	0.00	-1637.7148185	0.00
phfcf3_1 (crytsal)	0	-1637.8558454	2.79	-1637.6354604	2.79	-1637.7135234	3.40
3q							
naphyl_5	0	-1072.5864642	0.00	-1072.2672142	0.00	-1072.3378572	1.06
naphyl_11	0	-1072.5864175	0.12	-1072.2671995	0.04	-1072.3369765	3.37
3r							
naphyl_methoxy_1	0	-1301.6484172	0.00	-1301.2584632	0.00	-1301.3352042	0.00
naphyl_methoxy_2	0	-1301.6424747	15.60	-1301.2529947	14.36	-1301.3320947	8.16
3s							
naphyl_ethoxy_1	0	-1380.2983871	0.00	-1379.8491851	0.00	-1379.9330211	0.00
naphyl_ethoxy_13	0	-1380.2963418	5.37	-1379.8474998	4.42	-1379.9320478	2.56
3t							
naphyl_nbu_1.com	0	-1537.5729375	0.00	-1537.0042865	0.00	-1537.1022005	0.00
naphyl_nbu_13.com	0	-1537.5712770	4.36	-1537.0022250	5.41	-1537.0999630	5.87
3u							
naphyl_nhex_1.com	0	-1694.8472117	0.00	-1694.1589167	0.00	-1694.2702627	0.00
naphyl_nhex_13.com	0	-1694.8457025	3.96	-1694.1572755	4.31	-1694.2688135	3.80
3v							
naphyl_ipr_1.com	0	-1458.9431647	0.00	-1458.4355107	0.00	-1458.5237787	0.95
naphyl_ipr_5.com	0	-1458.9419562	3.17	-1458.4345542	2.51	-1458.5237202	1.10
3w							
naph2me_1_16	0	-1151.2264728	0.00	-1150.848705	0.00	-1150.9221408	2.63
naph2me_1_15	0	-1151.2262683	0.54	-1150.8481143	1.55	-1150.9206343	6.58
3x							
ph3ph_17	0	-1227.4418346	0.00	-1227.0500336	0.00	-1227.1288686	3.82

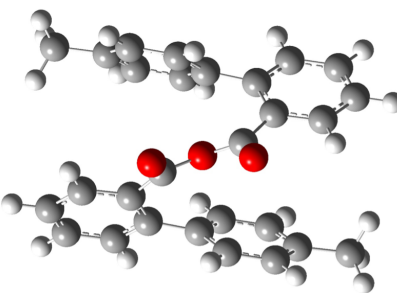
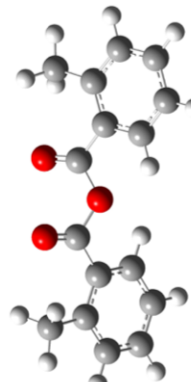
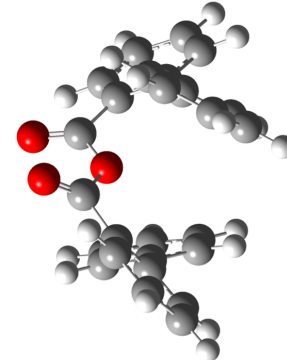
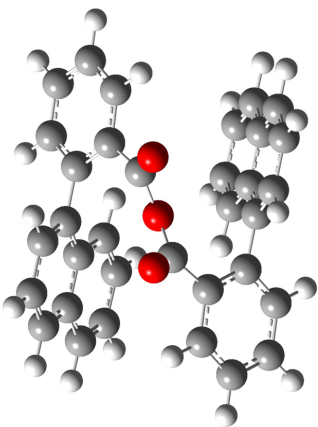
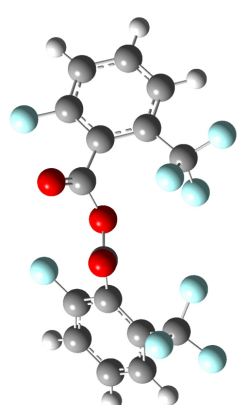
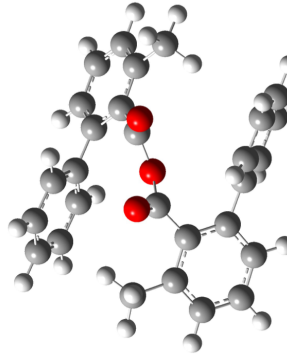
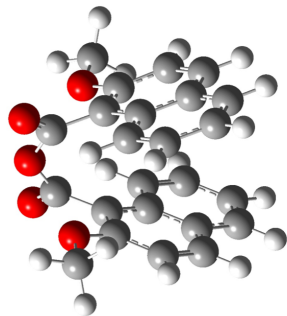
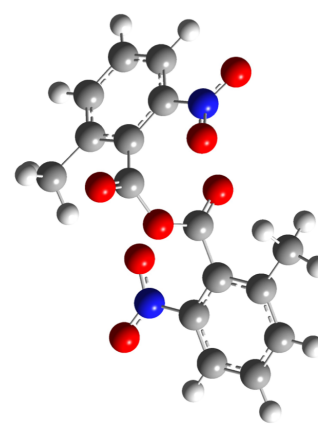
ph3ph_7	0	-1227.4416447	0.50	-1227.0498287	0.54	-1227.1287647	4.09
3y							
thiophen_1_1	0	-1406.7774948	0.00	-1406.6255270	0.00	-1406.6823130	2.53
thiophen_1_2	0	-1406.7773525	0.37	-1406.6253780	0.39	-1406.6832770	0.00
3z							
naph2_1_1.com	0	-1072.5969917	0.00	-1072.2776997	0.00	-1072.3470497	0.00
naph2_1_2.com	0	-1072.5966699	0.84	-1072.2773309	0.97	-1072.3455369	3.97

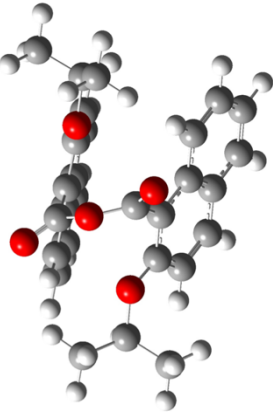
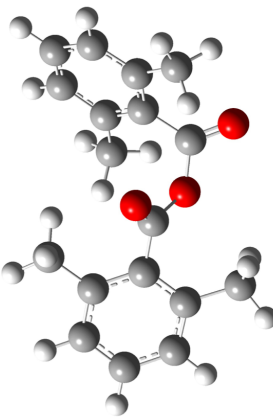
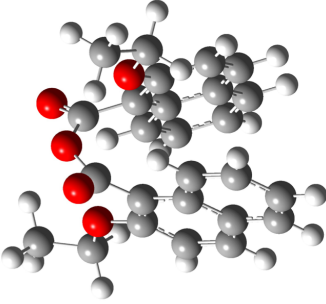
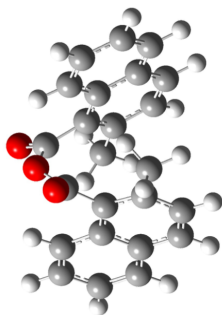
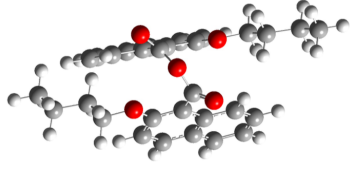
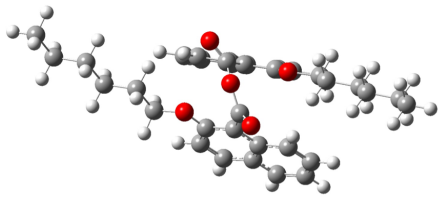
Table 3.27. Structures of optimized acid anhydrides **3a-z** and dihedral angle (θ_A (C5-O1-C2-O4) and θ_B (C2-O1-C5-O7)).



	3y	3z	3b	3k	
$\ln(k_{rel})$	1.74	1.46	1.36	1.35	
θ_A	30.4	32.8	21.5	23.8	
θ_B	30.5	32.8	140.0	149.5	
					
	3l	3a	3x	3e	
$\ln(k_{rel})$	1.34	1.30	1.29	1.19	
θ_A	22.2	31.7	14.0	21.0	

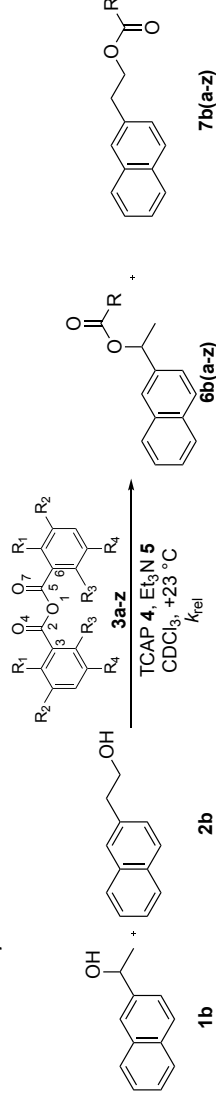
θ_B	22.2	31.7	24.9	143.0
				
	3d	3q	3j	3i
$\ln(k_{rel})$	1.18	1.16	0.99	0.96
θ_A	33.3	38.3	27.4	24.0
θ_B	33.3	38.3	22.0	24.2
				
	3g	3c	3f	3h
$\ln(k_{rel})$	0.83	0.82	0.78	0.68

θ_A	24.1	34.4	25.7	29.3
θ_B	24.1	34.3	25.7	29.3
				
	3p	3n	3r	3o
$\ln(k_{rel})$	0.41	-0.04	-0.29	-0.37
θ_A	28.5	25.0	157.2	13.0
θ_B	25.2	25.0	157.0	167.0
				
	3v	3m	3s	3w
$\ln(k_{rel})$	-0.43	-0.44	-0.46	-0.55

θ_A	155.6	12.1	157.4	149.7
θ_B	156.0	129.2	157.0	150.0
				
	3t	3u		
$\ln(k_{rel})$	-0.62	-0.66		
θ_A	156.9	157.0		
θ_B	157.0	157.0		
				

3.2.3.1 Descriptor Search

In order to identify possible correlations between the relative rate constants and properties of the anhydrides **3a-z**, selected descriptors including electronic or geometrical parameters were explored. NBO charges q_1 (mean value of C2 and C5), q_2 (mean value of C3 and C6) and q_3 (O1), frequencies ν (cm^{-1}) of the C=O stretching vibration, the dihedral angles (deg) θ_A (C5-O1-C2-O4), θ_B (C2-O1-C5-O7) and θ_C (mean value of θ_A and θ_B) and the O1-C2 distance r (Å) were taken from the best optimized conformers of the anhydrides **3a-z** (see Table 3.28). The Taft-type Charton values ν as a steric parameter are taken from literature and used in a non-common way explained in Figure 3.29.^[18] All anhydrides are based on some basic structure like Ph, 2-Np or Tp. These three motifs have the same settings (marked with green cycles) and are defined by the Charton value $\nu = 0$.^[18c] For 1-Np **3q** the motif is based on the Ph settings with an additional Me motif, so that we defined for the 1-Np basic structure the Charton value $\nu = 0.57 + 0.52 = 1.09$.^[18a,18c] In a second step we are adding the Charton values of the *ortho*-substituents found in literature^[18] to the basic structure motif and end up in the here used Charton values. For the rate constants the turnover-limited competition experiment **1b** vs. **2b** with acid anhydrides **3a-z** were used (Scheme 3.11 and Table 3.5). In the Figures 3.30 – 3.38 the different descriptors were plotted against the natural logarithm of rate constants. In the case of the dihedral angles θ_A or θ_B where only on part of the conformer is twisted (**3b**, **e**, **k** and **o**), the smaller angles were put to θ_A and the angles with higher values were put to θ_B . Because of these third group of anhydrides we generated θ_C , the mean value of θ_A and θ_B . For the NBO charges always the NBO charge of the best conformer was taken. These is possible, because q between the single conformers is not changing so much. To proof this statement, q_1 for the conformers of **3s** till a ΔE difference from 10 kJ mol^{-1} were checked (Table 3.29). The mean value of these five conformers is $q_1 = 0.8429 \pm 0.0012$.



Scheme 3.11. Turnover-limited competition experiment between secondary alcohol **1b** and primary alcohol **2b** with anhydride derivatives **3a-z** catalyzed by TCAP **4**.

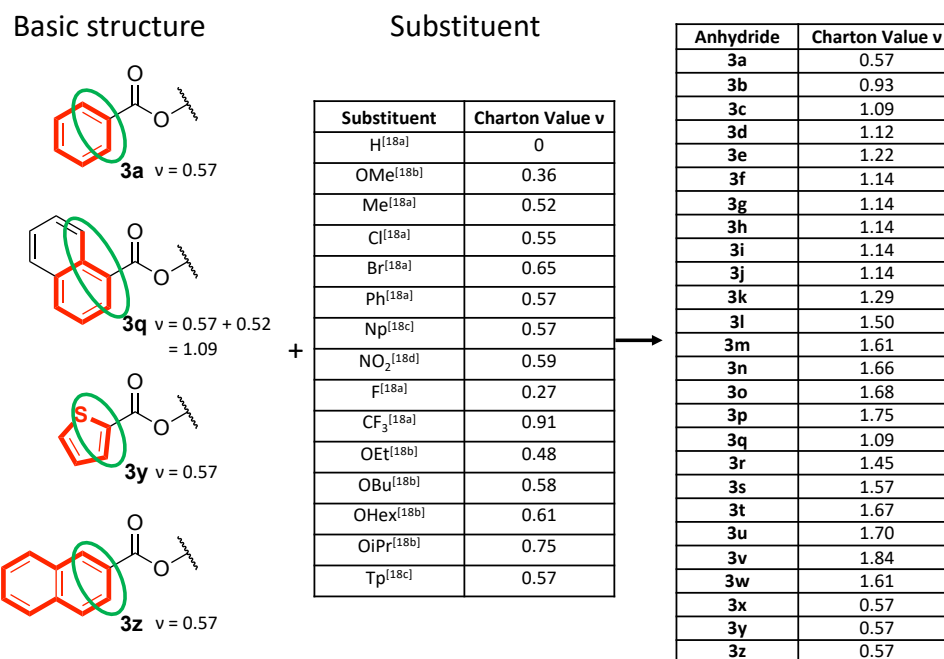
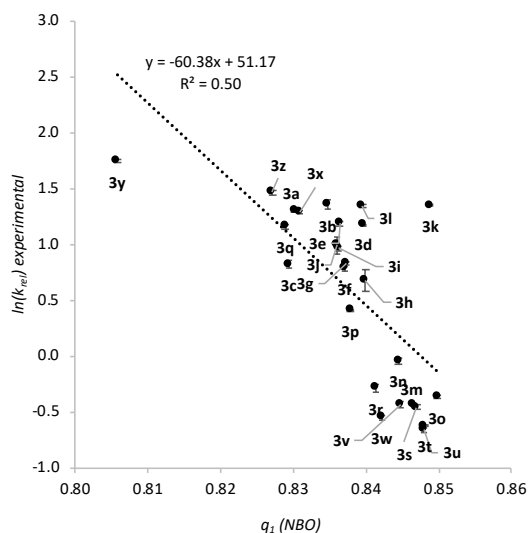
Table 3.28. Relative natural logarithm of rate constants $\ln(k_{rel})$ and standard derivation of $\ln(k_{rel})$ for the turnover-limited competition experiment between **1b** and **2b** using anhydride reagents **3a-z**. NBO charges q_1 (mean value of C2 and C5), q_2 (mean value of C3 and C6) and q_3 (O1), Taft-type Charton parameters ν , frequencies ν (cm^{-1}) of the C=O stretching vibration, the dihedral angles (deg) θ_A (C5-O1-C2-O4), θ_B (C2-O1-C5-O7) and θ_C (mean value of A and B) and the O1-C2 distance r (Å).

Anhydride	$\ln k_{rel}$	st. dev.	q_1	q_2	q_3	Charton ν	θ_A (deg)	θ_B (deg)	θ_C (deg)	r (Å)
3a	1.30	0.01	0.83	-0.19	-0.59	0.56	31.72	31.70	31.71	1.39
3b	1.36	0.04	0.83	-0.22	-0.58	0.92	21.53	140.00	80.77	1.39
3c	0.82	0.04	0.83	-0.20	-0.60	1.08	34.40	34.30	34.35	1.39
3d	1.18	0.00	0.84	-0.19	-0.57	1.11	33.26	33.26	33.26	1.38
3e	1.19	0.03	0.84	-0.19	-0.57	1.21	20.99	143.00	82.00	1.39
3f	0.78	0.03	0.84	-0.17	-0.58	1.12	25.70	25.70	25.70	1.38

3g	0.83	0.01	0.84	-0.17	-0.58	1.12	1813.91	24.13	24.13	24.13	1.38
3h	0.68	0.10	0.84	-0.16	-0.58	1.13	1818.81	29.33	29.33	29.33	1.38
3i	0.96	0.02	0.84	-0.17	-0.58	1.13	1811.85	23.98	24.23	24.11	1.38
3j	0.99	0.08	0.84	-0.17	-0.58	1.13	1809.77	27.40	21.99	24.70	1.38
3k	1.35	0.01	0.85	-0.26	-0.56	1.28	1805.95	23.80	149.48	86.64	1.39
3l	1.34	0.01	0.84	-0.19	-0.59	1.48	1836.86	22.24	22.24	22.24	1.39
3m	-0.44	0.02	0.85	-0.18	-0.59	1.60	1810.41	12.10	129.18	70.64	1.41
3n	-0.04	0.02	0.84	-0.16	-0.59	1.64	1828.59	25.00	25.00	25.00	1.39
3o	-0.37	0.01	0.85	-0.13	-0.56	1.67	1830.49	12.97	167.00	89.99	1.39
3p	0.41	0.00	0.84	-0.19	-0.58	1.74	1861.46	28.53	25.20	26.87	1.39
3q	1.16	0.02	0.83	-0.16	-0.60	1.08	1802.59	38.33	38.30	38.32	1.40
3r	-0.29	0.03	0.84	-0.22	-0.57	1.44	1798.86	157.24	157.00	157.12	1.38
3s	-0.46	0.02	0.85	-0.23	-0.55	1.56	1797.69	157.42	157.00	157.21	1.38
3t	-0.62	0.01	0.85	-0.23	-0.56	1.66	1797.89	156.90	157.00	156.95	1.38
3u	-0.66	0.02	0.85	-0.23	-0.56	1.69	1797.65	157.03	157.00	157.02	1.38
3v	-0.43	0.03	0.84	-0.22	-0.55	1.83	1800.91	155.55	156.00	155.78	1.39
3w	-0.55	0.02	0.84	-0.18	-0.59	1.60	1811.38	149.66	150.00	149.83	1.40
3x	1.29	0.01	0.83	-0.18	-0.59	0.56	1823.84	14.03	24.88	19.45	1.39
3y	1.74	0.01	0.81	-0.38	-0.60	0.57	1806.83	30.37	30.50	30.44	1.39
3z	1.46	0.03	0.83	-0.18	-0.60	0.57	1808.92	32.78	32.80	32.79	1.39

Table 3.29. q_1 for the conformers from **3s** until a $\Delta E_{\text{tot}} = 10 \text{ kJ mol}^{-1}$.

Filename	E_{tot} (Hartree)	ΔE_{tot} (kJ mol^{-1})	q_1
naphyl_ethoxy_1	-1380.2983871	0.00	0.8435
naphyl_ethoxy_13	-1380.2963418	5.37	0.8435
naphyl_ethoxy_4	-1380.2950793	8.68	0.8409
naphyl_ethoxy_5	-1380.2948947	9.17	0.8434
naphyl_ethoxy_78	-1380.2945458	10.09	0.8435
			mean: 0.8429±0.0012

**Figure 3.29.** Calculation of the Taft-type Charton parameters v .**Figure 3.30.** Plot of q_1 (NBO) vs. $\ln(k_{\text{rel}})$ for turnover-limited competition experiment **1b** vs. **2b** with the **3a-z**.

Size-Driven Inversion of Selectivity in Esterfication

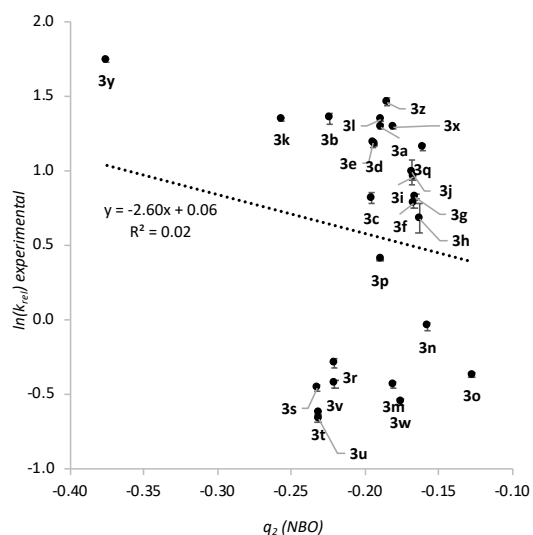


Figure 3.31. Plot of $q_2(NBO)$ vs. $\ln(k_{rel})$ for turnover-limited competition experiment **1b** vs. **2b** with the **3a-z**.

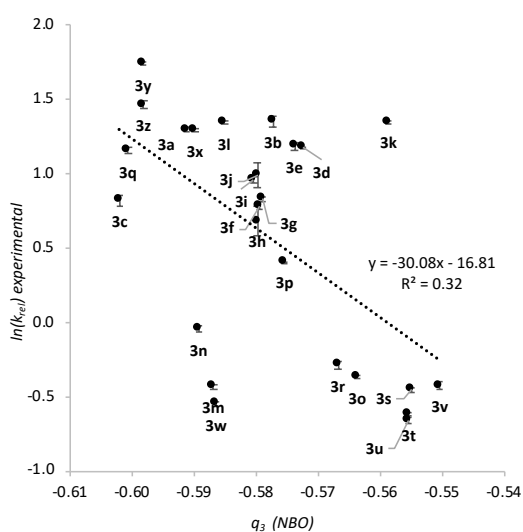


Figure 3.32. Plot of $q_3(NBO)$ vs. $\ln(k_{rel})$ for turnover-limited competition experiment **1b** vs. **2b** with the **3a-z**.

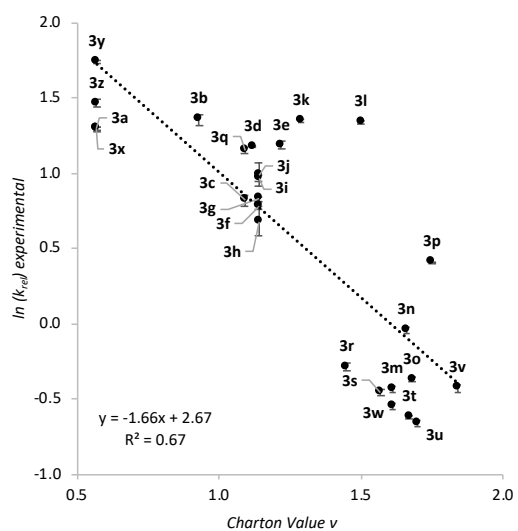


Figure 3.33. Plot of Charton values v of R_{1-4} vs. $\ln(k_{rel})$ for turnover-limited competition experiment **1b** vs. **2b** with the **3a-z**.

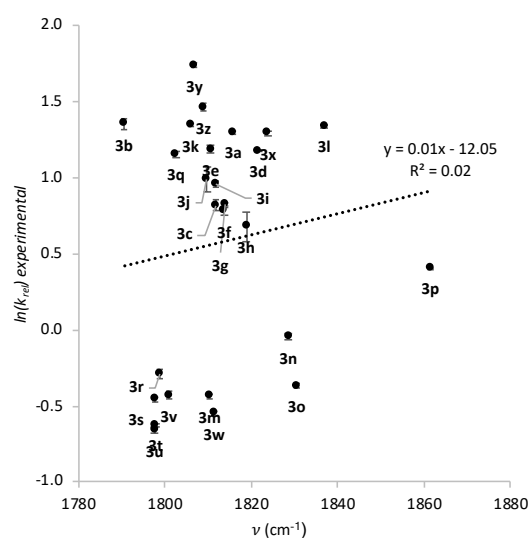


Figure 3.34. Plot of ν (cm^{-1}) vs. $\ln(k_{rel})$ for turnover-limited competition experiment **1b** vs. **2b** with the **3a-z**.

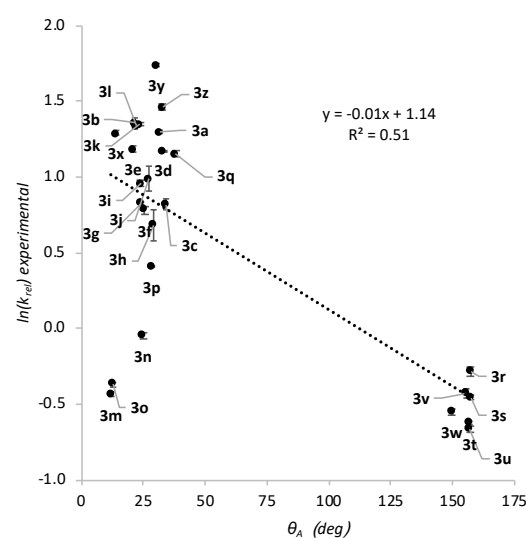


Figure 3.35. Plot θ_A (deg) vs. $\ln(k_{rel})$ for turnover-limited competition experiment **1b** vs. **2b** with the **3a-z**.

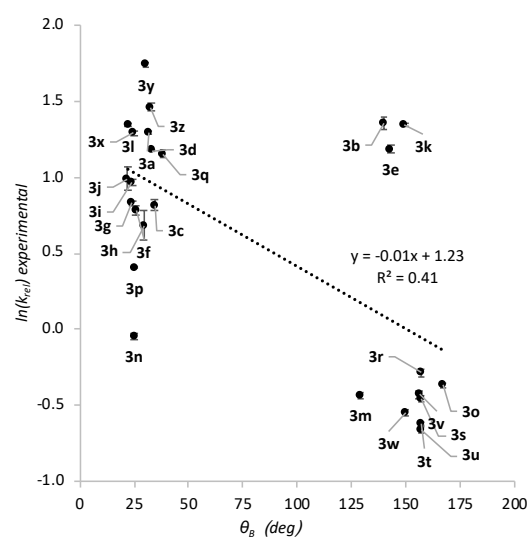


Figure 3.36. Plot of θ_B (deg) vs. $\ln(k_{rel})$ for turnover-limited competition experiment **1b** vs. **2b** with the **3a-z**.

Size-Driven Inversion of Selectivity in Esterification

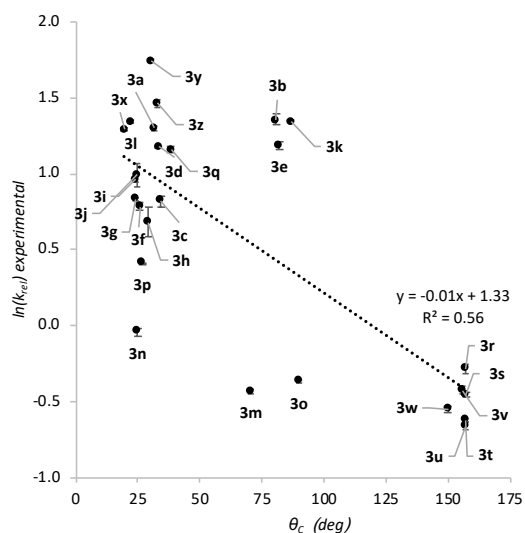


Figure 3.37. Plot of the θ_C (deg) vs. $\ln(k_{rel})$ for turnover-limited competition experiment **1b** vs. **2b** with the **3a-z**.

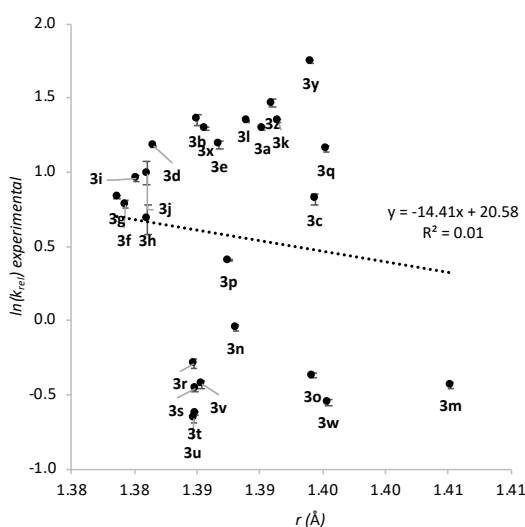


Figure 3.38. Plot of r (Å) vs. $\ln(k_{rel})$ for turnover-limited competition experiment **1b** vs. **2b** with the **3a-z**.

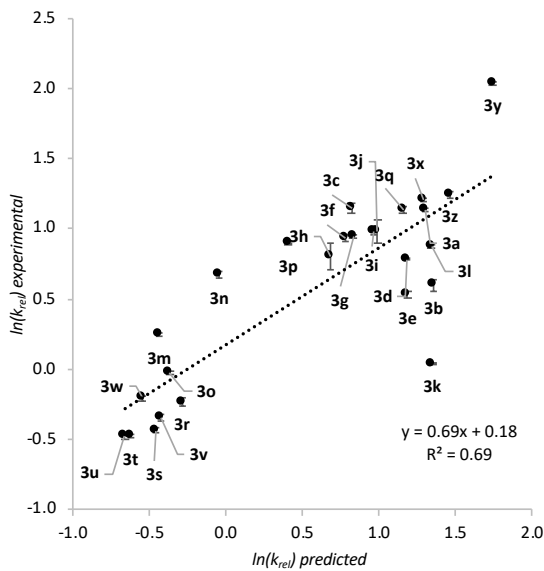
Only when plotting the relative rate constants against q_1 ($R^2 = 0.50$), against the Charton value ν ($R^2 = 0.67$) or against $\theta_{A/B}$ ($R^2 = 0.51$ and 0.41), could correlations of any relevance be identified (Figure 3.30, 3.33, 3.35 and 3.36). In the case of Figure 3.35 and 3.36 we can see that the data points divide up into two well-separated clusters. The first one is characterized by $\theta \approx 25^\circ$ (where both anhydride C-O double bonds point in the same direction) and by "normal" anhydride reactivity. The second cluster is characterized by $\theta \approx 150^\circ$ (where the anhydride C-O double bonds point in opposite directions) and by "invers" anhydride reactivity with a preference for the secondary alcohol **1b**. There are five anhydrides (**3b**, **e**, **k**, **m** and **o**) between these two groups which have two different dihedral angles with around 150° and 25° . **3b** and **3e** are monosubstituted anhydrides, which are not inverting the selectivity. **3m** and **3o** are disubstituted anhydrides which are able to invert the selectivity. The exception is **3k**, which is a disubstituted anhydride with a twist in the conformation but displays a reactivity like **3a**. Using θ_C (the mean value of θ_A and θ_B) for a plot against the relative rate constants a new correlation with $R^2 = 0.56$ (Figure 3.37) is obtained. Based on the work of Sigman *et al.*^[19] a multivariate analysis was performed. For these first a Pearson correlation matrix of the different descriptors were performed with the program StatPlus (Table 3.30).^[20] The correlations which aren't allowed are marked red. The descriptors having a low-quality linear correlation and are used in a multivariate analysis are marked green in Table 3.30. Because of the good performance of q_1 ($R^2=0.5$) with the θ_C ($R^2=0.56$) against the $\ln(k_{rel})$ and the low-quality linear correlation between q_1 and θ_C ($R=0.54$, Table 3.30), these two descriptors were used for a multivariate analysis. Based on Eq. 3.21 $\ln(k_{rel})_{pred.}$ could be calculated which shows a linear correlation with $R^2=0.69$ and which depends on steric and electronical parameters (Figure

3.39). Between q_3 and ν the linear correlation is of low-quality with $R=0.58$, too. Based on Eq. 3.22 a $R^2=0.54$ were obtained (Figure 3.40). The Charton value ν against $\ln(k_{rel})$ was performing the best with $R^2=0.67$. Because ν shows a low-quality linear correlation with q_3 ($R=0.63$) and θ_{A-c} ($R=0.50, 0.55$ and 0.58) further two-parameter analyses were performed, described in Eq. 3.23-3.36 (Figures 3.41-3.44). The two steric parameters θ_A and ν result in a $R^2=0.8$ (Eq. 3.24). Finally, we are making a three-parameter multivariate analysis including q_3 , θ_A and ν . Based on Eq. 3.27 $\ln(k_{rel})_{pred.}$ could be calculated and it was found a linear correlation with $R^2=0.80$, which now depends on steric, geometrical and electrical parameters (Figure 3.45).

Table 3.30. Correlation matrix of the natural logarithm of rate constants $\ln(k_{rel})$ for turnover-limited competition experiment between **1b** and **2b** using anhydride reagents **3a-z**, NBO charges q_1 , q_2 and q_3 , ν (cm^{-1}) of the C=O stretching vibration, the dihedral angles (deg) θ_A (C5-O1-C2-O4), θ_B (C2-O1-C5-O7) and θ_C (mean value of A and B), the O1-C2 distance r (\AA) from the best conformers of the acid anhydrides **3a-z** and Taft-type Charton parameters ν expressed by the respective Pearson correlations. The forbidden linear correlations are marked red (p-value > 5%). The descriptors used in a multivariate analysis are marked green.

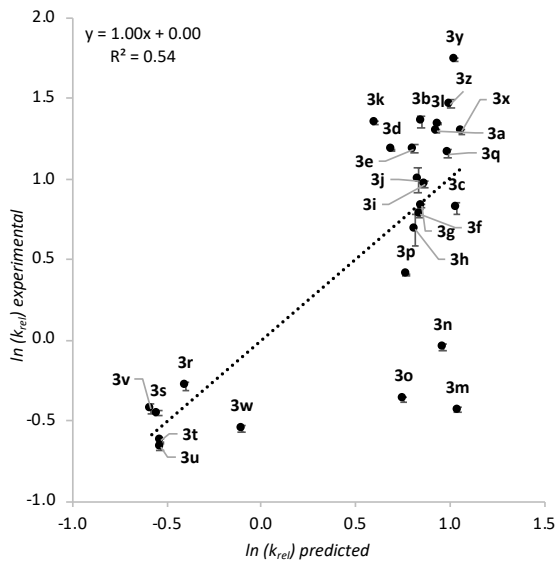
		$\ln k_{rel}$	q_1	q_2	q_3	ν (cm^{-1})	θ_A (deg)	θ_B (deg)	θ_C (deg)	r (\AA)	Charton ν
$\ln k_{rel}$	R	1.00									
	p-value										
q_1	R	-0.71	1.00								
	p-value	0.00									
q_2	R	-0.15	0.41	1.00							
	p-value	0.46	0.04								
q_3	R	-0.57	0.73	-0.13	1.00						
	p-value	0.00	0.00	0.53							
ν (cm^{-1})	R	0.13	0.01	0.38	-0.23	1.00					
	p-value	0.53	0.98	0.06	0.26						
θ_A (deg)	R	-0.72	0.38	-0.27	0.58	-0.48	1.00				
	p-value	0.00	0.05	0.18	0.00	0.01					
θ_B (deg)	R	-0.64	0.59	-0.21	0.70	-0.49	0.63	1.00			
	p-value	0.00	0.00	0.31	0.00	0.01	0.00				
θ_C (deg)	R	-0.75	0.54	-0.26	0.72	-0.54	0.89	0.91	1.00		
	p-value	0.00	0.00	0.19	0.00	0.00	0.00	0.00			
r (\AA)	R	-0.11	-0.10	-0.11	-0.38	0.04	-0.11	0.22	0.07	1.00	
	p-value	0.58	0.62	0.58	0.06	0.85	0.59	0.28	0.73		
Charton ν	R	-0.82	0.79	0.18	0.63	0.13	0.50	0.55	0.58	0.06	1.00
	p-value	0.00	0.00	0.38	0.00	0.52	0.01	0.00	0.00	0.75	

Size-Driven Inversion of Selectivity in Esterfication



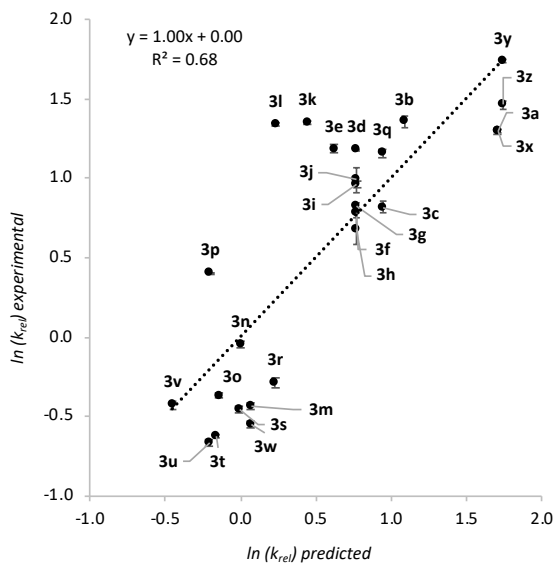
$$\ln(k_{rel})_{exp} = 31.58 - 36.38 \cdot q_1 - 0.008 \cdot \theta_C \quad \text{Eq. 3.21}$$

Figure 3.39. Plot of *pred.* $\ln(k_{rel})$ values against *exp.* $\ln(k_{rel})$ values. The *predicted* $\ln(k_{rel})$ values are based on Eq. 3.21.



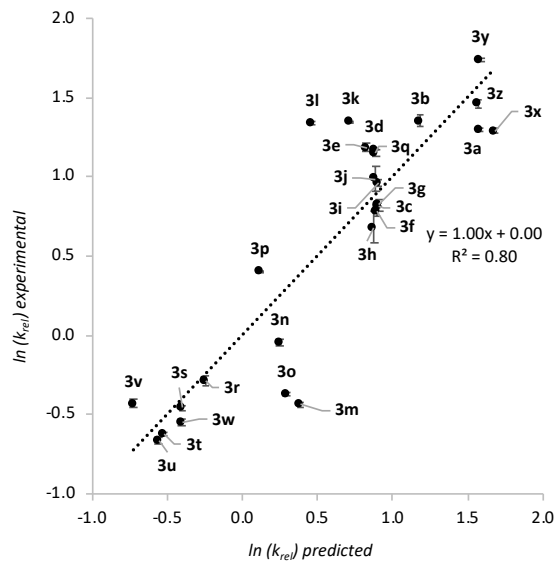
$$\ln(k_{rel})_{exp} = -5.88 - 11.97 \cdot q_3 - 0.008 \cdot \theta_A \quad \text{Eq. 3.22}$$

Figure 3.40. Plot of *pred.* $\ln(k_{rel})$ values against *exp.* $\ln(k_{rel})$ values. The *predicted* $\ln(k_{rel})$ values are based on Eq. 3.22.



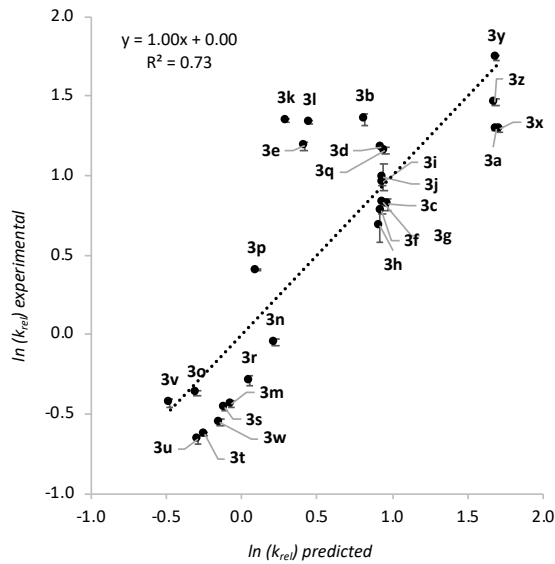
$$\ln(k_{rel})_{exp} = 0.01 + 4.37 \cdot q_3 - 1.56 \cdot v \quad \text{Eq. 3.23}$$

Figure 3.41. Plot of *pred.* $\ln(k_{rel})$ values against *exp.* $\ln(k_{rel})$ values. The *predicted* $\ln(k_{rel})$ values are based on Eq. 3.23.



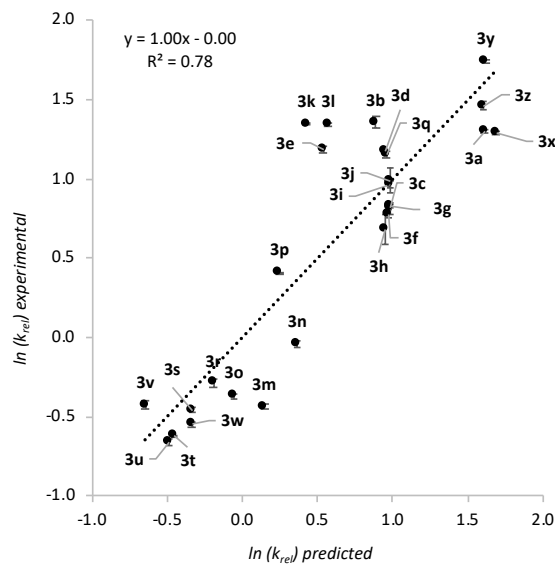
$$\ln(k_{rel})_{exp} = 2.47 - 0.006 \cdot \theta_A - 1.25 \cdot v \quad \text{Eq. 3.24}$$

Figure 3.42. Plot of *pred.* $\ln(k_{rel})$ values against *exp.* $\ln(k_{rel})$ values. The *predicted* $\ln(k_{rel})$ values are based on Eq. 3.24.



$$\ln(k_{rel})_{exp} = 2.57 - 0.003 \cdot \theta_B - 1.36 \cdot v \quad \text{Eq. 3.25}$$

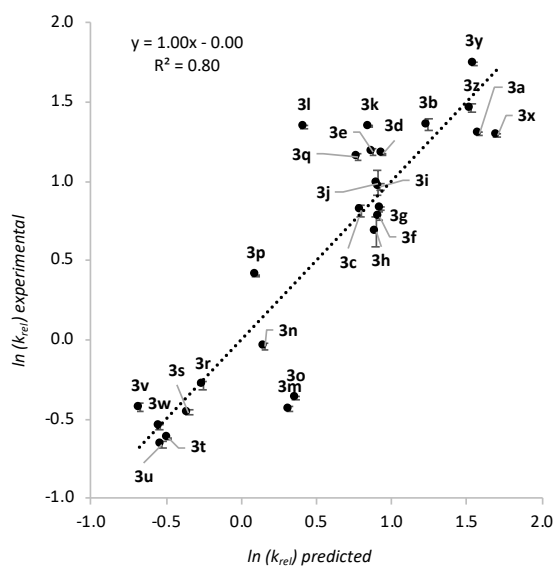
Figure 3.43. Plot of *pred.* $\ln(k_{rel})$ values against *exp.* $\ln(k_{rel})$ values. The *predicted* $\ln(k_{rel})$ values are based on Eq. 3.25.



$$\ln(k_{rel})_{exp} = 2.48 - 0.006 \cdot \theta_C - 1.18 \cdot v \quad \text{Eq. 3.26}$$

Figure 3.44. Plot of *pred.* $\ln(k_{rel})$ values against *exp.* $\ln(k_{rel})$ values. The *predicted* $\ln(k_{rel})$ values are based on Eq. 3.26.

Size-Driven Inversion of Selectivity in Esterfication



$$\ln(k_{rel})_{exp} = 6.17 + 6.11 \cdot q_3 - 0.006 \cdot \theta_A - 1.36 \cdot v \text{ Eq. 3.27}$$

Figure 3.45. Plot of *pred.* $\ln(k_{rel})$ values against *exp.* $\ln(k_{rel})$ values. The *predicted* $\ln(k_{rel})$ values are based on Eq. 3.27.

3.3 References

- [1] H. B. Kagan, J. C. Fiaud, *Top. Stereochem.* **1988**, *18*, 249-330.
- [2] S. Hoops, S. Sahle, R. Gauges, C. Lee, J. Pahle, N. Simus, M. Singhal, L. Xu, P. Mendes, U. Kummer, *Bioinformatics* **2006**, *22*, 3067-3074.
- [3] B. Giese, *Angew. Chem. Int. Ed.* **1977**, *16*, 125-136.
- [4] M. Marin-Luna, B. Pölloth, F. Zott, H. Zipse, *Chem. Sci.* **2018**, *9*, 6509-6515.
- [5] K. Ishihara, H. Kurihara, H. Yamamoto, *J. Org. Chem.* **1993**, *58*, 3791-3793.
- [6] a) A. D. Becke, *J. Chem. Phys.* **1993**, *98*, 5648-5652; b) C. Lee, W. Yang, R. G. Parr, *Phys. Rev. B* **1988**, *37*, 785-789; c) S. Grimme, *J. Chem. Phys.* **2006**, *124*, 034108.
- [7] G. W. Spitznagel, T. Clark, J. Chandrasekhar, P. V. R. Schleyer, *J. Comput. Chem.* **1982**, *3*, 363-371.
- [8] A. V. Marenich, C. J. Cramer, D. G. Truhlar, *J. Phys. Chem. B* **2009**, *113*, 6378-6396.
- [9] M. Marin-Luna, P. Patschinski, H. Zipse, *Chem. Eur. J.* **2018**, *24*, 15052-15058.
- [10] a) C. Riplinger, F. Neese, *J. Chem. Phys.* **2013**, *138*, 034106; b) C. Riplinger, B. Sandhoefer, A. Hansen, F. Neese, *J. Chem. Phys.* **2013**, *139*, 134101; c) F. Weigend, R. Ahlrichs, *Phys. Chem. Chem. Phys.* **2005**, *7*, 3297-3305; d) L. A. Curtiss, P. C. Redfern, K. Raghavachari, V. Rassolov, J. A. Pople, *J. Chem. Phys.* **1999**, *110*, 4703-4709.
- [11] Gaussian 09, R. D.01, M. J. Frisch, G. W. Trucks, H. B. Schlegel, G. E. Scuseria, M. A. Robb, J. R. Cheeseman, G. Scalmani, V. Barone, B. Mennucci, G. A. Petersson, H. Nakatsuji, M. Caricato, X. Li, H. P. Hratchian, A. F. Izmaylov, J. Bloino, G. Zheng, J. L. Sonnenberg, M. Hada, M. Ehara, K. Toyota, R. Fukuda, J. Hasegawa, M. Ishida, T. Nakajima, Y. Honda, O. Kitao, H. Nakai, T. Vreven, J. A. Montgomery Jr., J. E. Peralta, F. Ogliaro, M. Bearpark, J. J. Heyd, E. Brothers, K. N. Kudin, V. N. Staroverov, R. Kobayashi, J. Normand, K. Raghavachari, A. Rendell, J. C. Burant, S. S. Iyengar, J. Tomasi, M. Cossi, N. Rega, J. M. Millam, M. Klene, J. E. Knox, J. B. Cross, V. Bakken, C. Adamo, J. Jaramillo, R. Gomperts, R. E. Stratmann, O. Yazyev, A. J. Austin, R. Cammi, C. Pomelli, J. W. Ochterski, R. L. Martin, K. Morokuma, V. G. Zakrzewski, G. A. Voth, P. Salvador, J. J. Dannenberg, S. Dapprich, A. D. Daniels, Ö. Farkas, J. B. Foresman, J. V. Ortiz, J. Cioslowski, D. J. Fox, Gaussian, Inc., W. CT, **2010**.
- [12] F. Neese, *Wiley Interdiscip. Rev. Comput. Mol. Sci.* **2012**, *2*, 73-78.
- [13] Schrödinger Release 2019-2: Jaguar, Schrödinger, LLC, New York, NY, **2019**.
- [14] A. E. Reed, L. A. Curtiss, F. Weinhold, *Chem. Rev.* **1988**, *88*, 899-926.
- [15] E. R. Johnson, S. Keinan, P. Mori-Sánchez, J. Contreras-García, A. J. Cohen, W. Yang, *J. Am. Chem. Soc.* **2010**, *132*, 6498-6506.
- [16] J. Contreras-García, E. R. Johnson, S. Keinan, R. Chaudret, J.-P. Piquemal, D. N. Beratan, W. Yang, *J. Chem. Theory. Comput.* **2011**, *7*, 625-632.
- [17] W. Humphrey, A. Dalke, K. Schulten, *J. Mol. Graphics* **1996**, *14*, 33-38.
- [18] a) M. Charton, *J. Am. Chem. Soc.* **1975**, *97*, 1552-1556; b) M. Charton, *J. Org. Chem.* **1978**, *43*, 3995-4001; c) M. Charton, H. Ziffer, *J. Org. Chem.* **1987**, *52*, 2400-2403; d) M. Charton, *J. Org. Chem.* **1977**, *42*, 2528-2529.
- [19] a) C. B. Santiago, J.-Y. Guo, M. S. Sigman, *Chem. Sci.* **2018**, *9*, 2398-2412; b) J.-Y. Guo, Y. Minko, C. B. Santiago, M. S. Sigman, *ACS Catal.* **2017**, *7*, 4144-4151; c) K. C. Harper, M. S. Sigman, *Science* **2011**, *333*, 1875-1878.
- [20] StatPlus:mac LE, AnalystSoft.

Chapter 4. Size-Induced Inversion of Selectivity in the Acylation of 1,2-Diols

Stefanie Mayr and Hendrik Zipse*

Chem. Eur. J. **2021**, *27*, 18084-18092. – Published by © 2021 Wiley-VCH Verlag GmbH & Co. KGaA

DOI: 10.1002/chem.202101905

Author contributions: The project was conceived by S.M. and H.Z. The experimental study was performed by S.M. The computational studies were performed by S.M. and H.Z. The manuscript was jointly written by S.M. and H.Z. The supporting information was prepared by S.M.

Copyright: Reprinted with permission from *Chemistry – A European Journal* **2021**, *27*, 18084-18092 - Copyright © 2021 Wiley-VCH Verlag GmbH & Co. KGaA, Weinheim

Additional Information: The herein printed Supporting Information (SI) is an altered version of the published SI. NMR spectra, integral tables for kinetic experiments, crystal structures, original CoPaSi program simulations, tables of energies, enthalpies and free energies for all conformers, and Cartesian coordinates and number of imaginary frequencies of the best conformers can be found in the original version of the SI file free of charge (<https://doi.org/10.1002/chem.202101905>).

Size-Induced Inversion of Selectivity in the Acylation of 1,2-Diols

Stefanie Mayr^[a] and Hendrik Zipse*^[a]

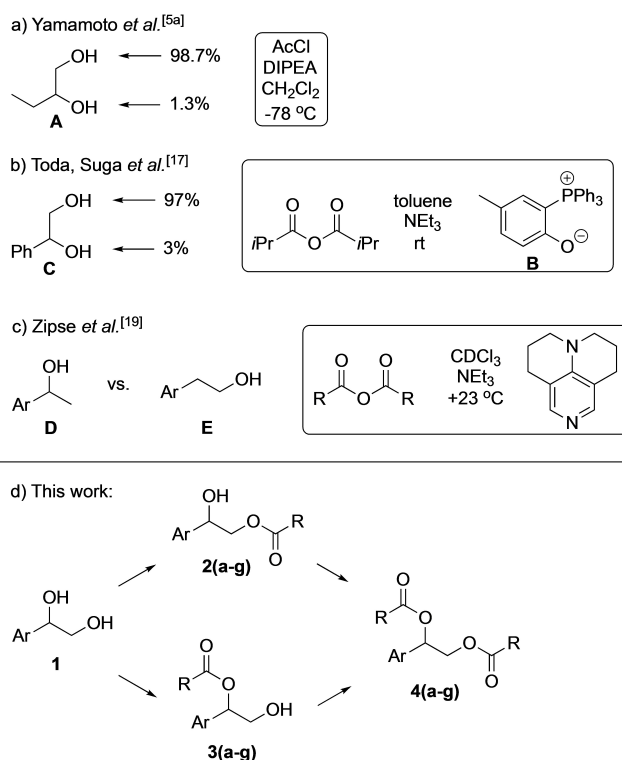
Abstract: Relative rates for the Lewis base-catalyzed acylation of aryl-substituted 1,2-diols with anhydrides differing in size have been determined by turnover-limited competition experiments and absolute kinetics measurements. Depending on the structure of the anhydride reagent, the secondary hydroxyl group of the 1,2-diol reacts faster than the primary

one. This preference towards the secondary hydroxyl group is boosted in the second acylation step from the monoesters to the diester through size and additional steric effects. In absolute terms the first acylation step is found to be up to 35 times faster than the second one for the primary alcohols due to neighboring group effects.

Introduction

In many organic syntheses the protection of functional groups play a strategically important role.^[1] In molecular targets of pharmaceutical or biological importance hydroxyl groups count among the most relevant functional groups,^[2] and their selective protection and deprotection thus dominates synthetic strategies.^[3] Despite all efforts that have already been invested in the development of chemo- and regioselective protection strategies,^[4] it is still today difficult to selectively address a single hydroxyl group in a polyol-system.^[5] The most common reagents for hydroxyl group protection are carboxylic acid derivatives such as acid chlorides, acid cyanides, or acid anhydrides,^[6] and several selective protection strategies of polyols^[7] with these reagents can thus be found in the literature. One strategy focuses on the in situ formation of transient cyclic intermediates such as (dialkyltin) acetals,^[5b,c,8] borinates,^[9] boronates,^[10] or cyclic *ortho*-esters.^[11] Subsequent ring opening reactions of these transient intermediates usually lead to preferred formation of the primary reaction products in 1,*n*-diols (except for the Lewis acid-mediated opening of *ortho*-esters).^[11] It should be added that this selectivity is also observed in reactions involving the transient formation of trialkyltin alkoxides.^[8b,c] A second strategy employs transient complexation of polyol substrates through anionic hydrogen bond acceptors (carboxylates,^[12] cyanide^[6a,e]) as a tool for directing acylation reactions. In selected cases, Lewis base

catalysts have been combined with carboxylate side chains in order to exploit this effect.^[5f,13] A third (and fully complementary) strategy employs Lewis base catalysts with or without the additional aid of auxiliary bases. When using highly reactive acylation reagents such as acid chlorides, already the combination with sterically hindered auxiliary bases such as *N,N*-diisopropyl-*N*-ethyl amine (DIPEA, Huenig base) may be sufficient for the effective acylation of 1,2-diols. For butane-1,2-diol **A** as an example Yamamoto *et al.*^[5a] reported an exceedingly high selectivity for transformation of the primary hydroxyl group under these conditions (Scheme 1a). A strong preference



Scheme 1. Intra- and intermolecular competition in acylation reactions of primary and secondary hydroxyl groups.

[a] S. Mayr, Dr. H. Zipse

Department of Chemistry
LMU München

Butenandstr. 5–13, 81366 München (Germany)

E-mail: zipse@cup.uni-muenchen.de

Supporting information for this article is available on the WWW under <https://doi.org/10.1002/chem.202101905>

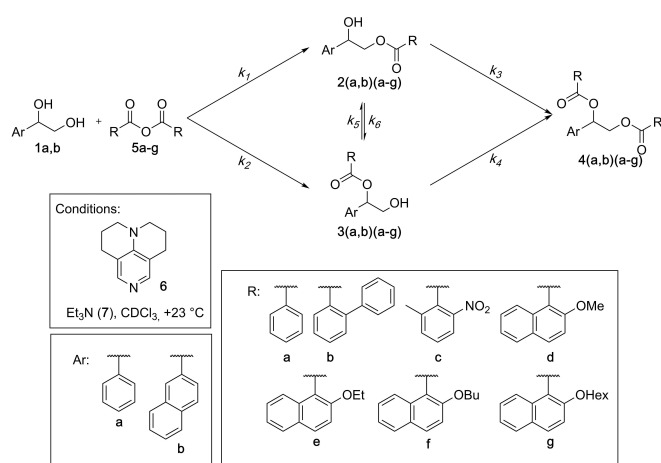
© 2021 The Authors. Chemistry - A European Journal published by Wiley-VCH GmbH. This is an open access article under the terms of the Creative Commons Attribution Non-Commercial NoDerivs License, which permits use and distribution in any medium, provided the original work is properly cited, the use is non-commercial and no modifications or adaptations are made.

for the reaction of primary hydroxyl groups has also been reported by Dong et al. in reactions of polyol substrates with anhydrides mediated by DIPEA,^[14] DBU,^[15] or DBN.^[16]

That the high preference for the acylation of primary hydroxyl groups is not a privilege of nitrogen bases has recently been illustrated by Toda, Suga et al.^[17] with phosphonium ylide **B** as a zwitterionic nucleophilic catalyst for the regioselective acylation of 1,*n*-diols such as **C** (Scheme 1b). For higher polyols (such as carbohydrates) it is also known that acylation selectivity depends on the hydroxyl group hydrogen bonding network.^[7b,18] Very recently we have explored the use of anhydride size-effects for favoring the acylation of secondary alcohol **D** in the presence of primary alcohol **E** (Scheme 1c).^[19] For substrates carrying sizeable aromatic side chains Ar, it was found that secondary alcohols **D** can react up to two times faster than primary alcohols **E** with anhydrides derived from 2-substituted 1-naphthoic acids. In this study we therefore address whether the same selectivity switch can be found for 1,2-diols of general structure **1** decorated by aromatic side chains Ar of variable size. As shown in Scheme 1(d) this reaction potentially involves two mono-acylated and one doubly acylated diol derivative. Rather than providing product distributions at a single conversion point,^[5d,16,17] we have used three different quantitative approaches to determine the rate constants intrinsic to this type of reaction scheme. The resulting rate data can then be used to simulate the experimentally measured turnover curves and thus predict selectivities at any given turnover point.^[20]

Results and Discussion

As illustrated in Scheme 2, the acylation of 1,2-diols **1a,b** with acid anhydride reagents **5a-g** is characterized by effective rate constants k_1-k_6 , that can be combined into three relative rate constants reflective of primary/secondary selectivities. Relative rate constant $k_{rel,a}$ is defined as the ratio of the effective rate



Scheme 2. General mechanistic scheme for the acylation of 1,2-diols **1a,b** with acid anhydrides **5a-g** catalyzed by TCAP (**6**) in the presence of Et₃N (**7**) at +23 °C.

constants for the acylation of the primary and secondary hydroxyl groups of diols **1a,b**. The ratio of effective reaction rates for acylation of secondary monoester **3(a,b)(a-g)** and primary monoester **2(a,b)(a-g)** is given by the relative rate constant $k_{rel,b}$ and thus characterizes the second acylation process. The third relative rate constant $k_{rel,c}$ describes the ratio between the migration rates of secondary monoester **3(a,b)(a-g)** and primary monoester **2(a,b)(a-g)** and thus the transesterification dynamics between monoesters **2** and **3**. 1,2-Ethandiol diols carrying aryl substituents such as phenyl (**a**) and 2-naphthyl (**b**) were employed as diol substrates.^[21]

As reagents we selected the seven anhydrides **5a-g** shown in Scheme 2, two with a preference for primary alcohols (**5a-b**) and five with a preference for secondary alcohols (**5c-g**) based on our earlier studies.^[19] All acylation reactions were catalyzed by TCAP (**6**) in the presence of Et₃N (**7**) at a temperature of +23 °C in CDCl₃. The conversion of all hydroxyl groups involved in the acylation of diols **1** to doubly acylated diols **4** can be expressed by equation I (Figure 1), and the mole fraction of a given species as given by equation II (using diol substrate **1a,b** as an example).^[22] Three different approaches have been employed for measuring the relative reaction rates for the first acylation of 1,2-diol **1b**, and two of these also lend themselves for the second acylation of the monoesters **2b(a-g)** and **3b(a-g)** to the diester **4**. The results obtained with these three different approaches will in the following be discussed for the acylation of **1b** with anhydride **c** catalyzed by TCAP (Figure 2). In the first approach we adapted our procedures developed for intermolecular turnover-limited competition experiments^[19,23] to the 1,2-diol substrate **1b** where anhydride **5c** was added as the limiting reagent such that a maximum of 2%–95% of all hydroxyl groups in **1b** can react in the presence of 0.1 equiv. TCAP (**6**) and 1.5 equiv. Et₃N (**7**) (for details see Supporting Information). Effective rate constants k_1-k_4 were then determined so that the best possible agreement was achieved between experimentally measured and theoretically predicted concentrations of all compounds shown in Scheme 2 using the overall conversion of hydroxyl groups as the reaction variable (Figure 2a). In addition, the product distribution obtained at the 30% conversion point was selected in order to compare the relative ratios of **2b(a-g)** versus **3b(a-g)**.

In kinetic resolution experiments and other 1 : 1 competition experiments it is common practice to select a single conversion point for the determination of relative reaction rates, often at conversions of around 50%.^[5d,16,17,24] However, in order to limit the influence of the second acylation step on the ratio of the mono-acylation, the 30% conversion point seems more appropriate. From these measurements we derived the relative rate

$$\text{Conversion} = \frac{[2(a,b)(a-g)] + [3(a,b)(a-g)] + 2 \cdot [4(a,b)(a-g)]}{2 \cdot [1a,b] + 2 \cdot [2(a,b)(a-g)] + 2 \cdot [3(a,b)(a-g)] + 2 \cdot [4(a,b)(a-g)]} \quad (\text{I})$$

$$\text{Mole fraction}_{(1a,b)} = \frac{[1a,b]}{[1a,b] + [2(a,b)(a-g)] + [3(a,b)(a-g)] + [4(a,b)(a-g)]} \quad (\text{II})$$

Figure 1. Conversion (I) of all OH-groups present in compounds **1-4** and mole fraction (II) of **1a,b** for the acylation of **1a,b** with **5a-g** catalyzed by TCAP (**6**) in the presence of Et₃N (**7**).

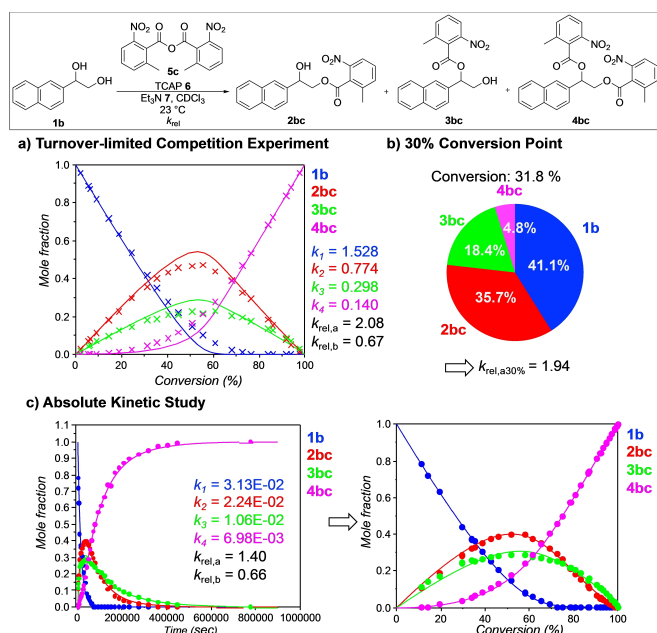


Figure 2. Relative rate constant $k_{rel,a}$ between the primary and secondary hydroxyl groups of diol **1b** and relative rate constant $k_{rel,b}$ between primary alcohol **3bc** and secondary alcohol **2bc** with anhydride reagent **5c** catalyzed by TCAP (**6**) quantified by three types of measurements: a) turnover-limited competition experiments, b) turnover-limited competition measurements at the 30% conversion point, and c) absolute kinetics measurements. The lines represent turnover curves predicted by numerical kinetics simulations while the crosses or dots represent experimentally measured values in the turnover-limited competition experiments or absolute kinetics measurements. The effective rate constants k_1 – k_4 are given in $L mol^{-1} s^{-1}$.

constant $k_{rel,a,30\%}$ defined as the ratio between the concentrations of monoesters **2b(a–g)** and **3b(a–g)** (Figure 2b, for more details see Supporting Information). In a third approach, adapted again from our earlier studies,^[25] we follow the reaction of diol **1b** with an excess of anhydride **5** (1.5 equiv.) in the presence of 0.1 equiv. TCAP (**6**) and 2.0 equiv. Et_3N (**7**) via absolute kinetics measurements (for details see Supporting Information).^[26] Effective rate constants k_1 – k_4 were again determined such that the best possible agreement was achieved between experimentally measured and theoretically predicted concentrations of all compounds shown in Scheme 2 with numerical kinetics simulations (Figure 2c).

In the following, we first focus on the results obtained in the absolute kinetics studies. Results for the reaction of diol **1b** with anhydrides **5a–g** are shown in Figure 3. Anhydrides **5a,c** based on the benzoate parent structure favor acylation of the primary hydroxyl group in diol **1b**. For benzoic anhydride **5a** as the reference system we find a selectivity of $k_{rel,a} = 3.38$. Introduction of substituents in the 1- and 6-positions as in anhydride **5c** reduces the selectivity to $k_{rel,a} = 1.47$.

Selectivities then invert (that is, switch to preferred acylation of the secondary hydroxyl group in diol **1b**) with anhydrides derived from 2-substituted naphthoic acids. The selectivities show only a minor dependence on the length of the 2-substituent with selectivity factors of $k_{rel,a} = 0.96$ (**5d**), 0.96 (**5e**), 0.89 (**5f**), and 0.95 (**5g**). In absolute terms, however, the

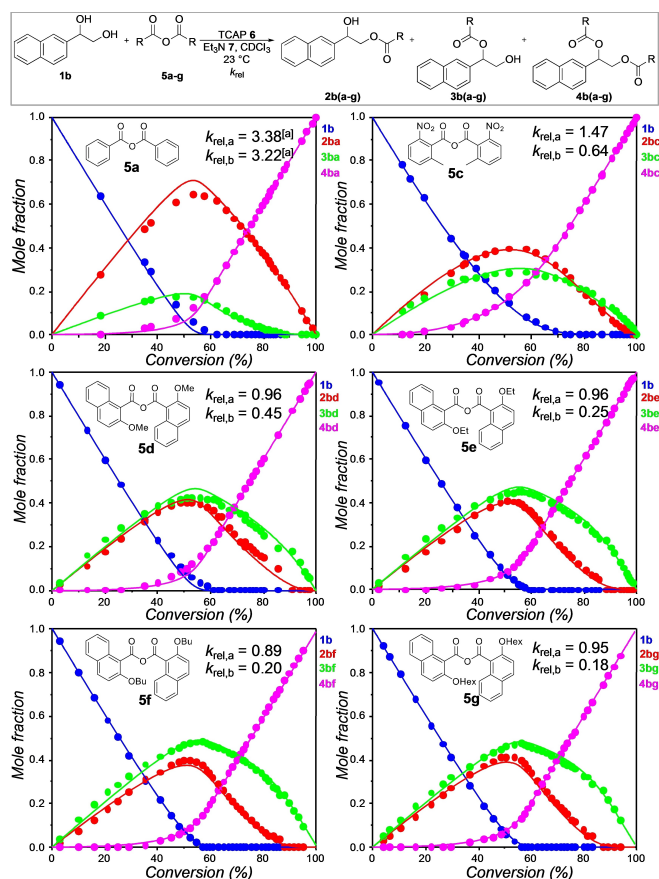


Figure 3. Relative rate constant $k_{rel,a}$ between primary and secondary hydroxyl groups of diol **1b** and relative rate constant $k_{rel,b}$ between primary alcohol **3b(a–g)** and secondary alcohol **2b(a–g)** with anhydride reagents **5a–g** catalyzed by TCAP (**6**). The lines represent simulated curves from numerical kinetics simulations and the dots represent experimentally measured values in the absolute kinetics study.^[a] The acylation of **1b** was catalyzed by 1 mol % TCAP (**6**).

observed preference for acylation of the secondary hydroxyl group is very moderate.

The second acylation step shown in Scheme 2 shows, in part, quite different primary/secondary selectivities as compared to the first one. It is only for benzoic anhydride (**5a**) that both steps show a comparable preference for acylation of the primary hydroxyl group ($k_{rel,a} = 3.38$ versus $k_{rel,b} = 3.22$, Figure 3). Already for anhydride **5c** we observe a preference for reaction of the secondary hydroxyl group with $k_{rel,b} = 0.64$, which is quite similar to earlier findings in intermolecular turnover-limited competition experiments.^[19] Even higher preferences for reaction of the secondary hydroxyl group are found for the 2-substituted naphthoic anhydrides with $k_{rel,b} = 0.45$ (**5d**), $k_{rel,b} = 0.25$ (**5e**), $k_{rel,b} = 0.20$ (**5f**), and $k_{rel,b} = 0.18$ (**5g**). This final value implies that acylation of **2bg** is 5.6 times faster than acylation of **3bg**. This inversion of selectivity is quite contrary to what is commonly found for significantly smaller substrates^[27] and can best be understood as a consequence of size effects between the π -systems present in substrate **1b**, reagents **5**, and catalyst **6** in the respective transition states for acyl group transfer.^[19]

How the selectivity values presented in Figure 3 vary as a function of the method of determination is illustrated in Figure 4. The methodological influence on $k_{rel,a}$ is generally found to be quite moderate, except for anhydride **5c**, where a larger difference can be noted between the turnover-limited competition experiments and the absolute kinetics measurements. Additional experiments were therefore undertaken for this latter system in order to determine, whether interconversion between mono-esters **3bc** and **2bc** are responsible for this observation (for details see Supporting Information). It was indeed found that this process becomes notable at the extended reaction times reached in some of the turnover-limited competition experiments, but less so in the absolute kinetics experiments (which are more reliable at this point). For all other anhydrides studied here, the interconversion between monoesters **2b** and **3b** appears to be too slow to contribute. The values of $k_{rel,b}$ show a somewhat larger dependence on methodological choice as shown in Figure 5. It is now only for the most reactive anhydride **5c** that we find consistent results for turnover-limited competition experiments and absolute kinetics studies, which require reaction times on the order of

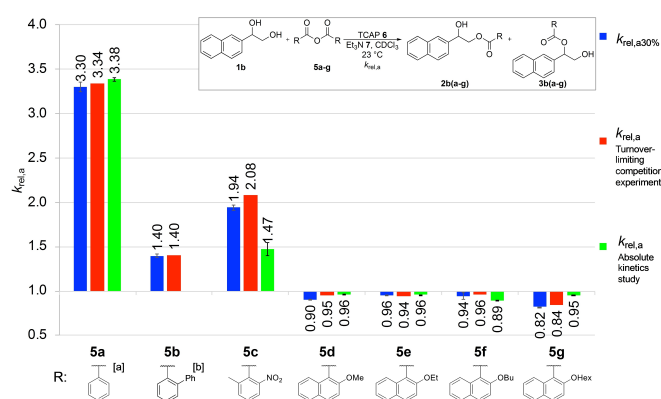


Figure 4. Relative rate constant $k_{rel,a}$ between the primary and secondary hydroxyl groups of diol **1b** in its reaction with anhydrides **5a-g** catalyzed by TCAP (**6**).^[a] The acylation of **1b** was catalyzed by 1 mol % TCAP (**6**).^[b] No absolute kinetics study was performed.^[26]

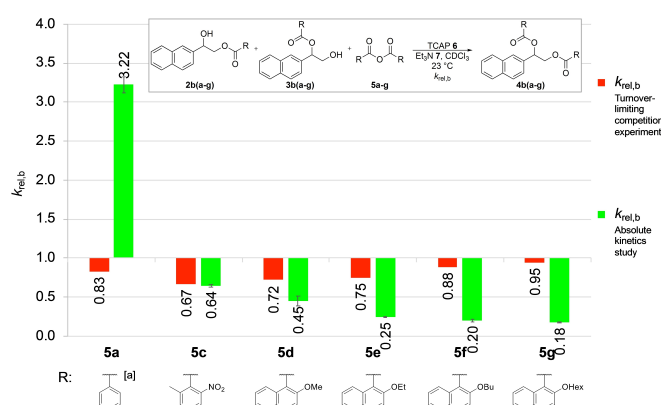


Figure 5. Relative rate constants $k_{rel,b}$ between primary alcohols **3b(a-g)** and secondary alcohols **2b(a-g)** with anhydrides **5a-g** catalyzed by TCAP (**6**).^[a] The acylation of **1b** was catalyzed by 1 mol % TCAP (**6**).^[a]

eight days to run to completion. For all other substituted systems reaction times are much longer, which may, in part, be responsible for the fact that selectivities are found to be much closer to $k_{rel,b} = 1.0$ as compared to the $k_{rel,b}$ values from absolute kinetics experiments.

The hypothesis of stronger attractive interactions between the π -systems present in substrate **1b**, reagents **5**, and catalyst **6** in the acylation transition state for the secondary hydroxyl group in **1b** can be tested by repeating the absolute kinetics experiments with anhydrides **5c,e** for the smaller diol **1a**.^[28] The effective reaction rates k_1 – k_4 for the acylation of 1,2-diols **1a,b** are shown in Figure 6. In reactions of 2,6-disubstituted anhydride **5c** (Figure 6a) we see an increase in the preference for acylation of the primary hydroxyl group in diol **1a** ($k_{rel,a} = 5.32$) as compared to **1b** ($k_{rel,a} = 1.47$). The origin of this selectivity change through increasing the side chain size from Ph to 2-Np can be found in a rather moderate increase in k_1 (red line in Figure 6a) from $k_1 = 29.7 \times 10^{-3} \text{ L mol}^{-1} \text{ s}^{-1}$ (**1a**) to $k_1 = 36.6 \times 10^{-3} \text{ L mol}^{-1} \text{ s}^{-1}$ (**1b**), and a much larger increase in k_2 from $k_2 = 5.6 \times 10^{-3} \text{ L mol}^{-1} \text{ s}^{-1}$ (**1a**) to $k_2 = 24.7 \times 10^{-3} \text{ L mol}^{-1} \text{ s}^{-1}$ (**1b**). In the second acylation, both Ph and 2-Np side chains prefer the acylation of secondary alcohols, whereby the preference for **2bc** is larger in **1b** ($k_{rel,a} = 0.64$) as compared to **1a** ($k_{rel,a} = 0.90$). Again with increasing side chain of the monoesters **2(a,b)c/3(a,b)c** the effective rate constants k_3 and k_4 (purple and orange lines, Figure 6a) increase from $k_3 = 3.6 \times 10^{-3} \text{ L mol}^{-1} \text{ s}^{-1}$ (**2ac**) to $k_3 = 14.6 \times 10^{-3} \text{ L mol}^{-1} \text{ s}^{-1}$ (**2bc**) and $k_4 = 3.3 \times 10^{-3} \text{ L mol}^{-1} \text{ s}^{-1}$ (**3ac**) to $k_4 = 9.3 \times 10^{-3} \text{ L mol}^{-1} \text{ s}^{-1}$ (**3bc**). The simple conclusion from all these rate measurements is that ALL rate constants increase when increasing the substrate side chain from Ph to 2-Np, but that the gains are larger for the secondary hydroxyl group (dashed lines) as compared to the primary one (solid line).

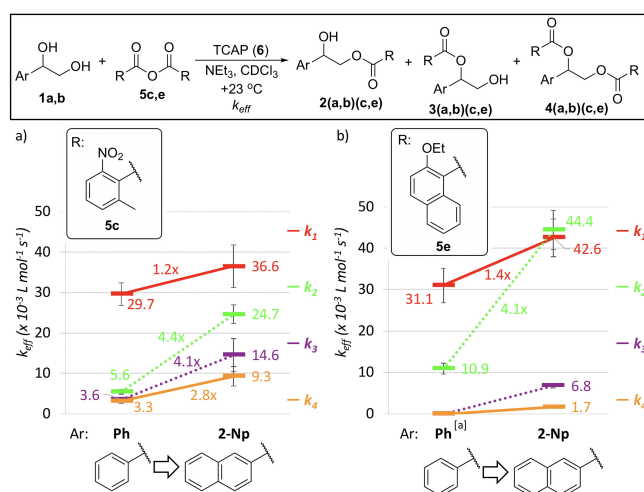


Figure 6. Averaged effective rate constants k_1 – k_4 for diols **1a** and **1b** in their reaction with anhydrides a) **5c** and b) **5e** catalyzed by TCAP (**6**) as obtained from absolute kinetics experiments. Solid lines correspond to transformations of the primary hydroxyl groups (k_1, k_2), and dashed lines correspond to transformations of the secondary hydroxyl groups (k_3, k_4).^[a] The effective rate constants k_3 and k_4 could not be determined reliably for **1a** due to technical problems.

This is also found to be the case for the sterically more demanding anhydride **5e**, which shows an intrinsically larger preference for the conversion of secondary hydroxyl groups (dotted lines, Figure 6b). Unfortunately, the second acylation step for substrate **1a** is so slow that conversions beyond 60% (and thus the rate constants k_3 and k_4) could not be measured reliably. Despite this latter complication, the trends shown in Figure 6 for two anhydrides are largely similar to earlier results obtained in intermolecular competition experiments with the same anhydrides^[19] and are thus in full support of the hypothesis of size effects between the substituents present in substrates **1**, reagents **5**, and catalyst **6** in the acylation transition states.

The influence of the reaction temperature on the first acylation of diols **1a** and **1b** with anhydride **5c** was studied in the range from -20°C to $+40^\circ\text{C}$ using the 30% conversion point method (Figure 7). For diol **1a** the relative rate constant $k_{\text{rel},a30\%}$ varies from $k_{\text{rel},a30\%} = 2.2$ (-20°C) to $k_{\text{rel},a30\%} = 7.0$ ($+40^\circ\text{C}$). Analyzing these results with aid of the Eyring equation shows a difference in activation enthalpy and entropy of $-12.1 \text{ kJ mol}^{-1}$ and $-54.1 \text{ J K}^{-1} \text{ mol}^{-1}$. Larger temperature effects were subsequently found for diol **1b** with differences in activation enthalpy and entropy of $-22.9 \text{ kJ mol}^{-1}$ and $-81.3 \text{ J K}^{-1} \text{ mol}^{-1}$ (see Supporting Information). From the difference of around $\sim 30 \text{ J K}^{-1} \text{ mol}^{-1}$ in the activation entropy values obtained for **1a** and **1b** it appears that reaction of the naphthyl-substituted system involves a more highly ordered transition state. That the activation enthalpy difference for reaction of the primary and secondary hydroxyl groups is larger for **1b** ($\Delta H^\ddagger = -22.9 \text{ kJ mol}^{-1}$) than for **1a** ($\Delta H^\ddagger = -12.1 \text{ kJ mol}^{-1}$) is also in line with the presence of attractive size-dependent interactions between the diol substrates, anhydride **5c**, and catalyst **6** in the acylation transition states.

The reaction of diol **1b** with anhydride **5c** was subsequently also studied in different solvents. A general trend of decreasing selectivity values $k_{\text{rel},a}$ with increasing solvent polarity could be identified, but the range of solvents was, unfortunately, too

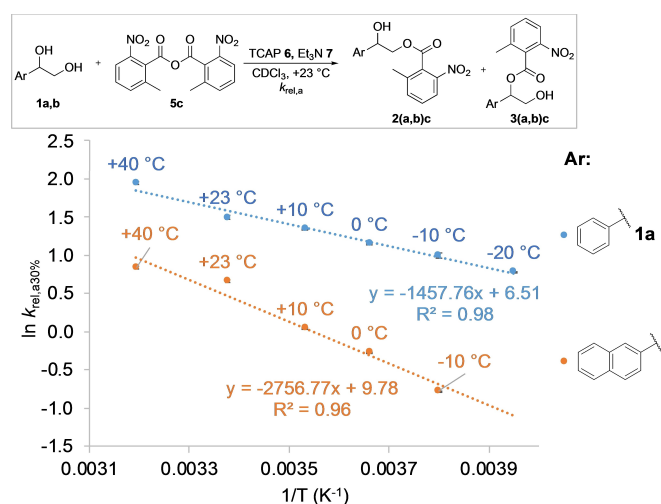


Figure 7. Eyring plot of $\ln k_{\text{rel},a30\%}$ for the reaction of diols **1a** and **1b** with anhydride **5c** mediated by TCAP (**6**).

limited due to solubility issues to allow for a systematic analysis (see Supporting Information).^[29] Similar reaction times for full conversion were also obtained when using different concentrations of the Et_3N auxiliary base (from 0.02 to 0.08 M) in the acylation of **1b** with anhydride **5c**. However, based on changes in polarity caused through the different concentration of Et_3N , the relative selectivities change from $k_{\text{rel},a} = 1.52$ (0.02 M) to $k_{\text{rel},a} = 1.12$ (0.08 M) and from $k_{\text{rel},b} = 0.62$ (0.02 M) to $k_{\text{rel},b} = 0.69$ (0.08 M). The background reactivity was studied for the acylation **1b** with anhydride **5c** and an excess of auxiliary base Et_3N , whereby only traces of **2bc** are detected.

The large selectivity differences between the first and the second acylation steps shown in Figure 3 can potentially arise from repulsive steric effects introduced through the first-formed ester unit or from activating neighboring group effects of one hydroxyl group on the other. In order to differentiate these effects, the 1- and 2-substituted propanol substrates **8b** and **9b** shown in Figure 8 were reacted with the same anhydrides **5** under the same reaction conditions as before. Formally, these two substrates replace one of the hydroxyl groups present in diol **1b** by an unreactive methyl substituent unable to form intramolecular hydrogen bonds. In these experiments the relative rate constant $k_{\text{rel,prop}}$ is defined as the ratio between the acylation rate of primary alcohols **9b** over the secondary alcohols **8b**. A 1:1 mixture of alcohols **8b** and **9b** were therefore reacted with anhydrides **5** as the limiting reagents up to a final conversion of 20%–70%. The esterification reactions were catalyzed by TCAP (**6**) in the presence of Et_3N (**7**) at a reaction temperature of $+23^\circ\text{C}$ in CDCl_3 (for details see Supporting Information). The experimentally measured turnover data were subsequently converted to relative rate constants $k_{\text{rel,prop}}$ using the same approach as in earlier studies.^[19,30]

For the 2-naphthyl substituted alcohol pair **8b/9b** we note a general decrease in the selectivity values (towards a reduced preference for primary alcohol **9b**) in the same range as could be seen before for the first acylation of diol substrate **1b** in

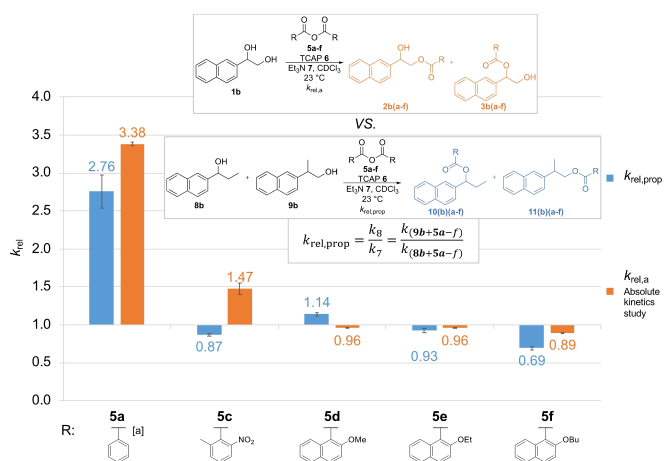


Figure 8. Relative rate constant $k_{\text{rel,prop}}$ between primary alcohols **9b** versus secondary alcohols **8b** in their reaction with anhydride reagents **5a–f** and $k_{\text{rel},a}$ of the acylation of **1b** with **5a–f** catalyzed by TCAP (**6**).^[a] The acylation of **1b** was catalyzed by 1 mol% TCAP (**6**).

Figure 4. This can already be seen in the selectivity for benzoic anhydride **5a** with $k_{\text{rel,prop}} = 2.76$, and becomes more prominent already in the 2,6-disubstituted benzoic anhydride **5c** with $k_{\text{rel,prop}} = 0.87$ and in the 2-substituted naphthyl anhydrides such as **5f** with $k_{\text{rel,prop}} = 0.69$. Thus, the propanol system shows the same trends found earlier in acylation reactions of ethanol systems.^[19] Comparing these results with the first acylation of diol substrate **1b** ($k_{\text{rel,a}}$), we see a small impact through activating neighboring group effects of one hydroxyl group on the other. This is illustrated through the slightly reduced preference for the secondary OH group, for example **5c** with $k_{\text{rel,prop}} = 0.87$ versus $k_{\text{rel,a}} = 1.47$ or **5f** with $k_{\text{rel,prop}} = 0.69$ versus $k_{\text{rel,a}} = 0.89$. An alternative strategy for quantifying the neighboring group effects in acylation reactions of diol **1b** exists in comparing the effective rate constants for the same hydroxyl group in the first and the second acylation steps shown in Scheme 2. A relative rate constant k_{prim} can, for example, be defined as the ratio of effective rate constants k_1 (for acylation of the primary hydroxyl group in **1b**) and k_4 (for acylation of the primary hydroxyl group in monoesters **3b(a–g)**). Similarly, k_{sec} can be defined as the ratio of effective rate constants k_2 and k_3 for reaction of the secondary hydroxyl groups in diol **1b** and in monoesters **2b(a–g)**). The results obtained for selected anhydrides are shown in Figure 9. For the unhindered anhydride **5a** we see that k_{prim} and k_{sec} assume values larger than 10, which simply indicates that both hydroxyl groups in diol **1b** are more reactive than the same hydroxyl groups in the intermediate monoesters **2ba** or **3ba**. For the 2,6-disubstituted (and electronically most activated) benzoic anhydride **5c** both values are reduced to $k_{\text{prim}} = 4.0$ and $k_{\text{sec}} = 1.8$. In particular this latter value indicates that the transition state for acylation of the secondary hydroxyl group in **1b** can hardly benefit from its primary hydroxyl group neighbor in this case. For the series of 2-substituted 1-naphthoic anhydrides **5d–g**, we find increasingly larger values of $k_{\text{prim}} = 20.1$ (**5d**), 25.0 (**5e**), 29.9 (**5f**), and 35.5 (**5g**) for increasingly long side chains.^[19,25] In contrast, the values for k_{sec} are much smaller and show an inverse trend with side chain size with $k_{\text{sec}} = 9.2$ (**5d**), 6.5 (**5e**), 6.8 (**5f**), and 6.8 (**5g**). These results again highlight that for all anhydrides studied here (except for **5c**) the first acylation is significantly faster than

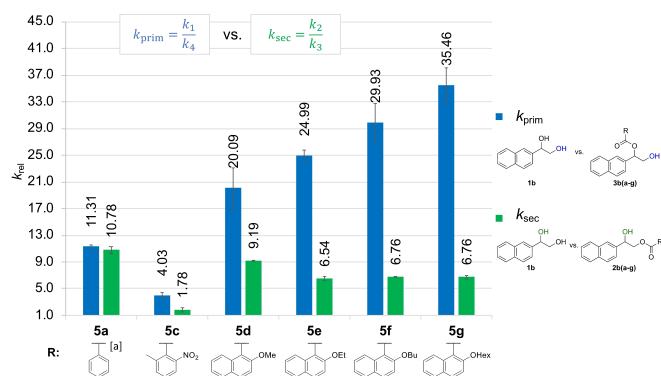
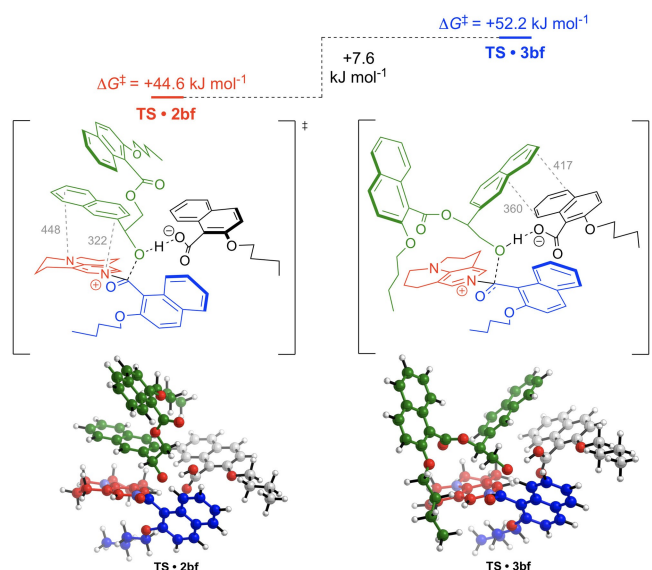


Figure 9. Relative rate constant $k_{\text{rel,prim}}$ versus $k_{\text{rel,sec}}$ of the acylation of **1b** with **5a–g** catalyzed by TCAP (**6**). [a] The acylation of **1b** was catalyzed by 1 mol % TCAP (**6**).

the second, the effects being particularly large for the primary hydroxyl group in diol **1b**.

The acylation of diol **1b** with anhydrides **5c–g** is much slower in absolute terms as compared to that with benzoic anhydride **5a** (see Supporting Information for more details). Whether this is a thermochemical or kinetic issue was tested by quantum mechanical calculation of the Gibbs free energy of reaction ΔG_{298} for the formation of esters **2b(c,f)**, **3b(c,f)**, and **4b(c,f)** at the SMD(CHCl₃)/DLPNO-CCSD(T)/def2-TZVPP//SMD(CHCl₃)/B3LYP-D3/6-31+G(d) level of theory.^[31] As expected from a previous study^[19] the first acylation of **1b** to either **2b(c,f)** or **3b(c,f)** is similarly exothermic with reaction free energies of $\Delta G_{298} = -61.5$ kJ mol⁻¹ (**2bc**) versus -58.9 kJ mol⁻¹ (**3bc**) and $\Delta G_{298} = -44.6$ kJ mol⁻¹ (**2bf**) versus -40.1 kJ mol⁻¹ (**3bf**). The overall diacylation of **1b** to **4(c,f)** is almost exactly twice as exergonic with $\Delta G_{298} = -122.2$ kJ mol⁻¹ (**4bc**) and $\Delta G_{298} = -76.9$ kJ mol⁻¹ (**4bf**), which indicates that the acylation of **1b** is under kinetic control. With respect to Marcus theory^[33] this implies that the intrinsic barrier for the reaction of **2b(c,f)**/**3b(c,f)** with anhydride **5c,f** mediated by **6** is much higher than the intrinsic barrier for the reaction of diol **1b** under the same conditions. The results in Figures 3 and 6 for 1,2-diol substrates **1a/1b** can be rationalized with the same “triple” sandwich acylation transition state between catalyst **6** (red), the substrate aryl substituent (green), and the *ortho*-substituent of the acid anhydrides **5c–g** (blue) as shown in our previous study (Scheme 3).^[19] This structure provides a natural basis for the experimentally observed rate differences between diol **1a** (phenyl side chain) and **1b** (2-naphthyl side chain) under the condition that side chain/catalyst interactions are attractive in nature through a combination of electrostatic and London dispersion interactions. The strong decrease in effective reaction rates from benzoic anhydride **5a** to the bulky anhydrides such as **5f** (by a factor of ca. 1000 for primary hydroxyl groups and



Scheme 3. Computed transition state structures for the second acylation of monoesters **2bf** and **3bf** with anhydride **5f**. Distances are given in pm.^[32]

< 370 for secondary hydroxyl groups excluding **5c**, see Supporting Information) point to strong differential steric hinderances in the acylation. These repulsive size effects are enhanced in the second acylation step and appear to be more substantial for transformations of primary as compared to secondary hydroxyl groups. Based on the transition states calculated earlier for the respective mono-alcohol systems^[19] and the X-ray solid state structure of **2bf**, the TCAP-mediated acylation of monoesters **2bf** and **3bf** to diester **4bf** was explored at the SMD(CHCl₃)/B3LYP-D3/6-31+G(d) level of theory (Scheme 3a).^[31a,d,e,g,h,34] The Gibbs free energy of activation for the acylation of secondary alcohol **2bf** is located +44.6 kJ mol⁻¹ above the separated reactants **2bf**, **5f** and **6** and thus 7.6 kJ mol⁻¹ lower than the transition state for the acylation of primary alcohol **3bf** ($\Delta G_{298}^\ddagger = +52.2$ kJ mol⁻¹). The transition state for the secondary alcohol displays the “triple” sandwich motif found earlier in reactions of the respective mono-alcohols, where the butyloxy side chain of anhydride **5f** is located below and the naphthyl substituent of alcohol substrate **2bf** is located on top of the TCAP-derived pyridinium ring system. This latter structural characteristic is missing in the transition state for the primary alcohol **3bf**, whose naphthyl substituent is oriented towards that of the carboxylate counter ion. That non-covalent interactions (NCIs) exist between several of the three butyloxy side chains, the four naphthyl substituents, and the TCAP pyridinium ring system is readily seen in the NCI plots for these transition states (see Supporting Information for full details). Identification of a single interaction responsible for the barrier difference seen in Scheme 3 is, however, not possible.^[35]

Conclusion

We demonstrate here three possible ways to measure and quantify the acylation of different hydroxyl groups in a diol system. Best results for the first and second acylation steps of 1-substituted ethylene-1,2-diols **1** were obtained using direct kinetics measurements. These were complemented by turnover-limited competition experiments and single conversion point measurements for defining relative rate constants for the first acylation in cases, where internal acyl migration between monoesters **2** and **3** is minimal. Reactions of diol **1b** carrying a large 2-naphthyl side chain with sterically hindered anhydrides display a selectivity inversion favoring acylation of the secondary hydroxyl group in **1b**. Variation of the size of the diol π -system leads to systematic changes in reaction rates as well as selectivities best rationalized by assuming attractive interactions between the substrate side chains and the catalyst-derived pyridinium core. Differential size effects strongly decrease the absolute reaction rates from benzoic anhydride **5a** to bulky anhydrides **5c–5g** and the acylation of the monoesters relative to those of the diols. Surprisingly, the effective acylation rates of primary alcohols respond more strongly to steric hinderance than those of secondary alcohols. The full exploitation of these effects may require catalysts optimally tailored for these structurally demanding reagents.

Experimental Section

Competition experiments

Three different CDCl₃ stock solutions consisting of 0.02 M 1,2-diol **1a,b** (A), 0.04 M acid anhydride **5a–g** (B), and a combination of 0.06 M Et₃N and 0.004 M TCAP (C) are prepared under nitrogen. Afterwards stock solution B is diluted such that new solutions with 23 different concentrations are obtained. The concentration of these solutions has been fixed at 2, 5, 7, 10, 15, 20, 25, 30, 35, 40, 45, 50, 55, 60, 65, 70, 75, 80, 85, 90 and 95% of the initial stock solution B, whereby the solutions of the 30% concentration point are prepared three times. Subsequently 0.4 mL of stock solution A, 0.4 mL of stock solution C and 0.4 mL of diluted stock solution B1 are transferred under nitrogen to a GC vial equipped with a magnetic stir bar by use of a Hamilton syringe. The GC vial is then capped under nitrogen and placed in the GC vial holder with stirring for 3–4 weeks. The reaction is subsequently analyzed by ¹H NMR recorded by Bruker Avance III 800 machine.

Kinetic studies

Three different CDCl₃ stock solutions consisting of 0.02 M 1,2-diol **1a,b** (A), 0.06 M acid anhydride **5a–g** (B), and a combination of 0.08 M Et₃N and 0.004 M TCAP (C) are prepared under nitrogen. The reaction is analyzed by ¹H NMR recorded on a Bruker Avance III 400 machine. NMR tubes are dried under vacuum using a special home-made apparatus and flushed with nitrogen. 0.2 mL of stock solution A, 0.2 mL of stock solution C and 0.2 mL of stock solution B are transferred under nitrogen to an NMR tube by use of a Hamilton syringe. After closing the NMR tube, the reaction mixture is shaken and introduced into the NMR machine.

Computational details

All geometry optimizations and vibrational frequency calculations have been performed using the B3LYP-D3 hybrid functional^[31e,g,36] in combination with the 6-31+G(d) basis set.^[37] Solvent effects for chloroform have been taken into account with the SMD continuum solvation model.^[31d] This combination has recently been found to perform well for Lewis base-catalyzed reactions.^[23b,c] Thermochemical corrections to 298.15 K have been calculated for all stationary points from unscaled vibrational frequencies obtained at this same level. Solvation energies have been obtained as the difference between the energies computed at B3LYP-D3/6-31+G(d) in solution and in gas phase. For the calculations of Gibbs free energies, the thermochemical corrections of optimized structures have been combined with single point energies calculated at the DLPNO-CCSD(T)/def2-TZVPP//B3LYP-D3/6-31+G(d) level.^[31b,c,f,38] Solvation energies have been added to the energy computed at DLPNO-CCSD(T)/def2-TZVPP//SMD(CHCl₃)/B3LYP-D3/6-31+G(d) level to yield free energies G_{298} at 298.15 K. Free energies in solution have been corrected to a reference state of 1 molL⁻¹ at 298.15 K through addition of $RT\ln(24.46) = +7.925$ kJ mol⁻¹ to the free energies. All calculations have been performed with Gaussian 09^[39] and ORCA version 4.0.^[40] Conformation search was performed with Maestro.^[41]

Deposition Number(s) 2085895 (for **4bc**), 2085896 (for **2ac**), 2085897 (for **2ba**), 2085898 (for **4ac**), 2085899 (for **3bc**), 2085900 (for **2bc**), 2085901 (for **2ad**), 2085902 (for **2be**) contain(s) the supplementary crystallographic data for this paper. These data are provided free of charge by the joint Cambridge Crystallographic Data Centre and Fachinformationszentrum Karlsruhe Access Structures service.

Acknowledgements

This work was financially supported by the Deutsche Forschungsgemeinschaft (DFG) through the Priority Program "Control of London Dispersion Interactions in Molecular Chemistry" (SPP 1807), grant ZI 436/17-1. Open Access funding enabled and organized by Projekt DEAL.

Conflict of Interest

The authors declare no conflict of interest.

Keywords: acylation · anhydrides · noncovalent interaction · organocatalysis · regioselectivity

- [1] a) O. Robles, D. Romo, *Nat. Prod. Rep.* **2014**, *31*, 318–334; b) K. C. Nicolaou, J. S. Chen, in *Classics in Total Synthesis III*, Wiley-VCH, Weinheim, **2011**.
- [2] a) P. S. Baran, T. J. Maimone, J. M. Richter, *Nature* **2007**, *446*, 404–408; b) G. Zong, E. Barber, H. Aljewari, J. Zhou, Z. Hu, Y. Du, W. Q. Shi, *J. Org. Chem.* **2015**, *80*, 9279–9291; c) M. Koshimizu, M. Nagatomo, M. Inoue, *Angew. Chem. Int. Ed.* **2016**, *55*, 2493–2497; *Angew. Chem.* **2016**, *128*, 2539–2543.
- [3] S. M. Polyakova, A. V. Nizovtsev, R. A. Kunetskiy, N. V. Bovin, *Russ. Chem. Bull.* **2015**, *64*, 973–989.
- [4] a) C. A. Lewis, S. J. Miller, *Angew. Chem. Int. Ed.* **2006**, *45*, 5616–5619; *Angew. Chem.* **2006**, *118*, 5744–5747; b) S. Araki, S. Kambe, K. Kameda, T. Hirashita, *Synthesis* **2003**, *2003*, 0751–0754; c) P. G. M. Wuts, in *Greene's Protective Groups in Organic Synthesis*, John Wiley & Sons, Hoboken, New Jersey, **2014**; d) A. Baldessari, C. P. Mangone, E. G. Gros, *Helv. Chim. Acta* **1998**, *81*, 2407–2413.
- [5] a) K. Ishihara, H. Kurihara, H. Yamamoto, *J. Org. Chem.* **1993**, *58*, 3791–3793; b) T. Maki, F. Iwasaki, Y. Matsumura, *Tetrahedron Lett.* **1998**, *39*, 5601–5604; c) F. Iwasaki, T. Maki, W. Nakashima, O. Onomura, Y. Matsumura, *Org. Lett.* **1999**, *1*, 969–972; d) J. E. Taylor, J. M. J. Williams, S. D. Bull, *Tetrahedron Lett.* **2012**, *53*, 4074–4076; e) S. Yoganathan, S. J. Miller, *J. Med. Chem.* **2015**, *58*, 2367–2377; f) Y. Ueda, T. Furuta, T. Kawabata, *Angew. Chem. Int. Ed.* **2015**, *54*, 11966–11970; *Angew. Chem.* **2015**, *127*, 12134–12138.
- [6] a) P. Peng, M. Linseis, R. F. Winter, R. R. Schmidt, *J. Am. Chem. Soc.* **2016**, *138*, 6002–6009; b) M. Nahmany, A. Melman, *Org. Biomol. Chem.* **2004**, *2*, 1563–1572; c) N. A. Afagh, A. K. Yudin, *Angew. Chem. Int. Ed.* **2010**, *49*, 262–310; *Angew. Chem.* **2010**, *122*, 270–320; d) A. H. Haines, *Adv. Carbohydr. Chem. Biochem.* **1976**, *33*, 11–109; e) E. Kattnig, M. Albert, *Org. Lett.* **2004**, *6*, 945–948; f) E. Guibe-Jampel, G. Le Corre, M. Wakselman, *Tetrahedron Lett.* **1979**, *20*, 1157–1160.
- [7] a) V. Dimakos, M. S. Taylor, *Chem. Rev.* **2018**, *118*, 11457–11517; b) J. Lawandi, S. Rocheleau, N. Moitessier, *Tetrahedron* **2016**, *72*, 6283–6319.
- [8] a) H. Dong, Y. Zhou, X. Pan, F. Cui, W. Liu, J. Liu, O. Ramström, *J. Org. Chem.* **2012**, *77*, 1457–1467; b) T. Ogawa, M. Matsui, *Carbohydr. Res.* **1977**, *56*, c1–c6; c) T. Ogawa, M. Matsui, *Tetrahedron* **1981**, *37*, 2363–2369; d) H. Dong, Z. Pei, S. Byström, O. Ramström, *J. Org. Chem.* **2007**, *72*, 1499–1502; e) F. Iwasaki, T. Maki, O. Onomura, W. Nakashima, Y. Matsumura, *J. Org. Chem.* **2000**, *65*, 996–1002.
- [9] a) D. Lee, C. L. Williamson, L. Chan, M. S. Taylor, *J. Am. Chem. Soc.* **2012**, *134*, 8260–8267; b) M. S. Taylor, *Acc. Chem. Res.* **2015**, *48*, 295–305.
- [10] S. Kusano, S. Miyamoto, A. Matsuoka, Y. Yamada, R. Ishikawa, O. Hayashida, *Eur. J. Org. Chem.* **2020**, *2020*, 1598–1602.
- [11] M. Ikejiri, K. Miyashita, T. Tsunemi, T. Imanishi, *Tetrahedron Lett.* **2004**, *45*, 1243–1246.
- [12] a) X. Zhang, B. Ren, J. Ge, Z. Pei, H. Dong, *Tetrahedron* **2016**, *72*, 1005–1010; b) Y. Zhou, M. Rahm, B. Wu, X. Zhang, B. Ren, H. Dong, *J. Org. Chem.* **2013**, *78*, 11618–11622; c) B. Ren, M. Rahm, X. Zhang, Y. Zhou, H. Dong, *J. Org. Chem.* **2014**, *79*, 8134–8142.
- [13] a) T. Kawabata, W. Muramatsu, T. Nishio, T. Shibata, H. Schedel, *J. Am. Chem. Soc.* **2007**, *129*, 12890–12895; b) T. Kurahashi, T. Mizutani, J.-i. Yoshida, *Tetrahedron* **2002**, *58*, 8669–8677.
- [14] B. Ren, L. Gan, L. Zhang, N. Yan, H. Dong, *Org. Biomol. Chem.* **2018**, *16*, 5591–5597.
- [15] Y. Lu, C. Hou, J. Ren, X. Xin, H. Xu, Y. Pei, H. Dong, Z. Pei, *Molecules* **2016**, *21*, 641–649.
- [16] B. Ren, M. Zhang, S. Xu, L. Gan, L. Zhang, L. Tang, *Eur. J. Org. Chem.* **2019**, *2019*, 4757–4762.
- [17] Y. Toda, T. Sakamoto, Y. Komiyama, A. Kikuchi, H. Suga, *ACS Catal.* **2017**, *7*, 6150–6154.
- [18] T. Kurahashi, T. Mizutani, J.-i. Yoshida, *J. Chem. Soc. Perkin Trans. 1* **1999**, 465–474.
- [19] S. Mayr, M. Marin-Luna, H. Zipse, *J. Org. Chem.* **2021**, *86*, 3456–3489.
- [20] S. Hoops, S. Sahle, R. Gauges, C. Lee, J. Pahle, N. Simus, M. Singhal, L. Xu, P. Mendes, U. Kummer, *Bioinformatics* **2006**, *22*, 3067–3074.
- [21] 1-(1-Naphthyl)-1,2-ethanediol **1c** was investigated as an additional substrate in its reaction with anhydrides **5c,e**. Because the relative rate constants are close to the results obtained with phenyl-1,2-ethanediol **1a** and due to practical problems (¹H NMR signal overlapping), this substrate was not investigated further. 1-Pyrenyl-1,2-ethanediol **1d** was initially considered as an additional substrate in this study, but eventually dismissed due to solubility problems.
- [22] The mole fractions of **2(a,b)**(a–g), **3(a,b)**(a–g), and **4a,b)**(a–g) were calculated in the same way. See Supporting Information for more information..
- [23] a) J. Helberg, M. Marin-Luna, H. Zipse, *Synthesis* **2017**, *49*, 3460–3470; b) M. Marin-Luna, B. Pölloth, F. Zott, H. Zipse, *Chem. Sci.* **2018**, *9*, 6509–6515; c) M. Marin-Luna, P. Patschinski, H. Zipse, *Chem. Eur. J.* **2018**, *24*, 15052–15058.
- [24] B. Pölloth, M. P. Sibi, H. Zipse, *Angew. Chem. Int. Ed.* **2021**, *60*, 774–778; *Angew. Chem.* **2021**, *133*, 786–791.
- [25] R. Tandon, T. A. Nigst, H. Zipse, *Eur. J. Org. Chem.* **2013**, *2013*, 5423–5430.
- [26] In the case of anhydride **5a** 0.01 equiv. TCAP was used as diol **1b** reacts otherwise too fast to allow accurate determination of the rates for acylation to the monoesters **2bb** and **3bb**.
- [27] C. B. Fischer, S. Xu, H. Zipse, *Chem. Eur. J.* **2006**, *12*, 5779–5784.
- [28] The $k_{rel,a}$ of **1a** and **1b** with all anhydrides **5a–g** are studied via turnover-limited competition experiments and are shown in the Supporting Information.
- [29] C. Reichardt, in *Solvents and Solvent Effects in Organic Chemistry*, Wiley-VCH, Weinheim, **2003**.
- [30] H. B. Kagan, J. C. Fiaud, *Top. Stereochem.* **1988**, *18*, 249–330.
- [31] a) S. Y. Park, J.-W. Lee, C. E. Song, *Nat. Commun.* **2015**, *6*, 7512; b) C. Riplinger, F. Neese, *J. Chem. Phys.* **2013**, *138*, 034106; c) C. Riplinger, B. Sandhoefer, A. Hansen, F. Neese, *J. Chem. Phys.* **2013**, *139*, 134101; d) A. V. Marenich, C. J. Cramer, D. G. Truhlar, *J. Phys. Chem. B* **2009**, *113*, 6378–6396; e) S. Grimme, *J. Chem. Phys.* **2006**, *124*, 034108; f) F. Weigend, R. Ahlrichs, *Phys. Chem. Chem. Phys.* **2005**, *7*, 3297–3305; g) A. D. Becke, *J. Chem. Phys.* **1993**, *98*, 5648–5652.
- [32] CYLVIEW: CYLview, 1.0b; Legault, C. Y., Université de Sherbrooke, **2009** (<http://www.cylview.org/>); 3D-Pictures were generated with the CYL-view program.
- [33] a) F. A. Carey, R. J. Sundberg, in *Advanced Organic Chemistry Part A: Structure and Mechanisms*, Springer Science+Business Media, New York, **2007**; b) J. P. Guthrie, *Can. J. Chem.* **1996**, *74*, 1283–1296; c) M. Breugst, H. Zipse, J. P. Guthrie, H. Mayr, *Angew. Chem. Int. Ed.* **2010**, *49*, 5165–5169; *Angew. Chem.* **2010**, *122*, 5291–5295; d) H. Zipse, in *Reactivity and Mechanism in Organic Chemistry*, Shaker Verlag, Düren, **2019**.
- [34] The free energy profile of the second acylation from **2bf** and **3bf** to **4bf** is shown in detail in the Supporting Information.
- [35] a) E. R. Johnson, S. Keinan, P. Mori-Sánchez, J. Contreras-García, A. J. Cohen, W. Yang, *J. Am. Chem. Soc.* **2010**, *132*, 6498–6506; b) J. Contreras-García, E. R. Johnson, S. Keinan, R. Chaudret, J.-P. Piquemal, D. N. Beratan, W. Yang, *J. Chem. Theory Comput.* **2011**, *7*, 625–632.
- [36] C. Lee, W. Yang, R. G. Parr, *Phys. Rev. B* **1988**, *37*, 785–789.
- [37] G. W. Spitznagel, T. Clark, J. Chandrasekhar, P. V. R. Schleyer, *J. Comput. Chem.* **1982**, *3*, 363–371.
- [38] L. A. Curtiss, P. C. Redfern, K. Raghavachari, V. Rassolov, J. A. Pople, *J. Chem. Phys.* **1999**, *110*, 4703–4709.
- [39] Gaussian 09, R. D.01, M. J. Frisch, G. W. Trucks, H. B. Schlegel, G. E. Scuseria, M. A. Robb, J. R. Cheeseman, G. Scalmani, V. Barone, B. Mennucci, G. A. Petersson, H. Nakatsuji, M. Caricato, X. Li, H. P. Hratchian, A. F. Izmaylov, J. Bloino, G. Zheng, J. L. Sonnenberg, M. Hada, M. Ehara, K. Toyota, R. Fukuda, Y. Hasegawa, M. Ishida, T. Nakajima, Y. Honda, O. Kitao, H. Nakai, T. Vreven, J. A. Montgomery Jr., J. E. Peralta, F.

Ogliaro, M. Bearpark, J. J. Heyd, E. Brothers, K. N. Kudin, V. N. Staroverov, R. Kobayashi, J. Normand, K. Raghavachari, A. Rendell, J. C. Burant, S. S. Iyengar, J. Tomasi, M. Cossi, N. Rega, J. M. Millam, M. Klene, J. E. Knox, J. B. Cross, V. Bakken, C. Adamo, J. Jaramillo, R. Gomperts, R. E. Stratmann, O. Yazyev, A. J. Austin, R. Cammi, C. Pomelli, J. W. Ochterski, R. L. Martin, K. Morokuma, V. G. Zakrzewski, G. A. Voth, P. Salvador, J. J. Dannenberg, S. Dapprich, A. D. Daniels, Ö. Farkas, J. B. Foresman, J. V. Ortiz, J. Cioslowski, D. J. Fox, Gaussian, Inc., W. CT, **2010**.

[40] F. Neese, *Wiley Interdiscip. Rev.: Comput. Mol. Sci.* **2012**, *2*, 73–78.

[41] Schrödinger Release 2019–2: Jaguar, Schrödinger, LLC, New York, NY, **2019**.

Manuscript received: May 31, 2021
Accepted manuscript online: October 25, 2021
Version of record online: November 29, 2021

4.1 Experimental Part

General Methods

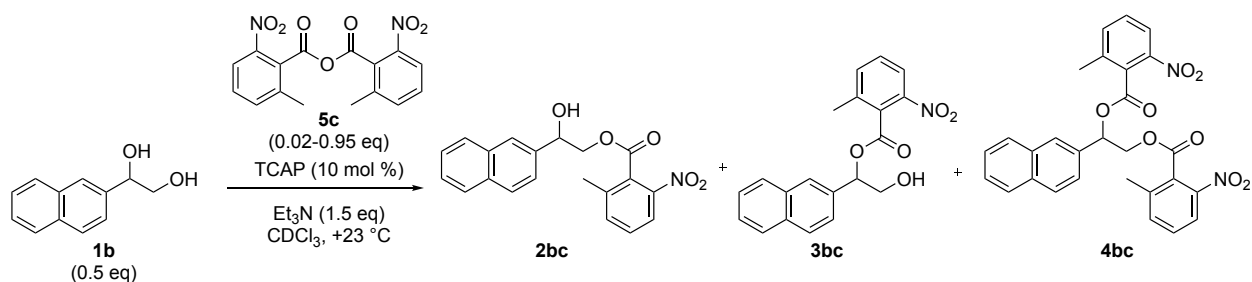
All reactions sensitive to air and moisture were performed under a nitrogen atmosphere and the glassware as well as magnetic stir bars were dried overnight in a dry oven at 110 °C. As heat source for temperature-controlled reactions an oil bath was used. CDCl₃, Et₃N and CH₂Cl₂ were freshly distilled over calcium hydride (CaH₂) under a nitrogen atmosphere. CDCl₃ was also dried and stored over molecular sieve. Acetone-*d*₆, MeCN-*d*₃, THF-*d*₈ and CD₂Cl₂ were dried and stored over molecular sieve. All reagents were purchased from the companies TCI, Sigma Aldrich, ABCR, or Acros and used without further purification, if not mentioned otherwise. The aryl alcohols **1a**, **8a**, and **9a**, the acid anhydrides **5a,c** and TCAP (**6**) have been obtained from commercial sources. The synthesis of acid anhydride reagents **5b,d-h** has been described by Zipse *et al.*^[1] and in chapter 3 of this work. All air- or water-sensitive reagents were stored under nitrogen. If not further specified, solvents were obtained from the companies Acros Organics, Sigma Aldrich or Merck and purified by distillation in a rotary evaporator. Silica gel for column chromatography was purchased from Acros Organics (mesh 35-70). Thin-layer chromatography was performed by using TLC plates purchased from Merck (silica gel 60 F254, thickness 0.2 mm). All ¹H NMR spectra were recorded by Varian INOVA 400, 600 and Bruker 400, 800 machines in CDCl₃ or DMSO-*d*₆ at 400 MHz, 600 or 800 MHz at 23 °C. All ¹³C NMR spectra were recorded respectively at 101 MHz and 151 MHz. The chemical shifts are reported in ppm (δ), relative to the resonance of CDCl₃ at δ = 7.26 ppm and DMSO-*d*₆ at δ = 2.50 ppm for ¹H and for ¹³C relative to the resonance of CDCl₃ δ = 77.16 ppm. In the case of solvent turnover-limited competition experiments the chemical shifts are reported in ppm (δ) relative to the resonance of acetone-*d*₆ at δ = 2.05 ppm, MeCN-*d*₃ at δ = 1.94 ppm, THF-*d*₈ at δ = 3.58 ppm and CD₂Cl₂ at δ = 5.32 ppm for ¹H. Spectra were imported and processed in the MestreNova 10.0.2 program. HRMS spectra were obtained by using a Thermo Finnigan LTQ FT machine of the MAT 95 type with a direct exposure probe (DEP) and electron impact ionization (EI, 70 eV). For ESI measurements a Thermo Finnigan LTQ FT Ultra Fourier Transform Ion Cyclotron Resonance machine was used. IR spectra were measured on a Perkin-Elmer FT-IR BX spectrometer mounting an ATR technology module. Melting points were measured at a Stuart SMP10 and are stated uncorrected. Crystallographic measurements were done using an Oxford Diffraction XCalibur with Saphir CCD-detector and a molybdenum-K α -source (λ = 0.71073) with a concentric circle kappa-device. Structures were resolved using SHELXS or SIR97 and refined with SHELXS. All obtained crystals from the compounds **2ac**, **4ac**, **2ad**, **2ba**, **2bc**, **3bc**, **4bc** and **2be** were grown in a CDCl₃ solution in NMR tube. The determination of the relative rate constants in turnover-limited competition experiments is based on previous work of the Zipse group.^[1] The used techniques and instructions are the same as in the previous work of Zipse *et al.*^[1] NMR tubes were dried in the oven for at least 12 h. CDCl₃ and Et₃N were freshly distilled under N₂ over CaH₂ before use. In case of the turnover curves the CDCl₃ was dried over molecular sieve and stored under N₂. Hamilton syringes were cleaned with acetone, dried under vacuum, and flushed with nitrogen prior to use. A GC vial holder (Shimadzu 221-44998-91) was connected to the coolant circuit of a cryostat maintaining +23 °C constantly and placed on a magnetic stirrer. The speed of stirring was fixed at 750 rpm for all the experiments described here.

4.1.1 Turnover-limited Competition Experiments of Aryl Substituted 1,2-Ethanedioles

In this part of the work, we chose the model of turnover-limited competition experiments shown in previous work of the Zipse group^[1] modified for aryl-substituted 1,2-ethanedioles. The guideline is based on this previous work.

4.1.1.1 Experimental Design

In the following, a general guideline for the design of a turnover-limited competition experiment is described based on the experiment shown in Scheme 4.1. Three different CDCl₃ stock solutions consisting of 0.02 M diol **1b** (A), 0.04 M acid anhydride **5c** (B), and a combination of 0.06 M Et₃N and 0.004 M TCAP (C) are prepared under nitrogen.



Scheme 4.1. Example for a turnover-limited competition experiment of 2-naphthylethane-1,2-diol **1b** with acid anhydride **5c** at $+23^\circ\text{C}$.

Table 4.1. Preparation of initial CDCl_3 stock solutions.

Stock solution	Compound	Concentration (mol L ⁻¹)	Volume (mL)	n (mol)	M.W. (g mol ⁻¹)	Mass (mg)
Stock A	1b	0.02	10	$200 \cdot 10^{-6}$	188	37.6
Stock B	5c	0.04	10	$400 \cdot 10^{-6}$	344	137.6
Stock C	Et₃N	0.06	10	$600 \cdot 10^{-6}$	101	60.7
	TCAP	0.004	10	$80 \cdot 10^{-6}$	174	13.9

Afterwards, stock solution B is diluted to the 23 differently concentrated solutions of B shown in Table 4.2. The concentration of these solutions has been fixed at 2, 5, 7, 10, 15, 20, 25, 30, 35, 40, 45, 50, 55, 60, 65, 70, 75, 80, 85, 90 and 95% of the initial stock solution B, whereby the solutions of the 30% concentration point are prepared three times.

Table 4.2. Preparation of stock solutions B with different concentration of B.

	Stock solution ^a	Concentration (mol L ⁻¹)	Vol. B ^b (mL)	Volume (mL)
1	Stock B1 (2%)	0.0008	0.02	1
2	Stock B2 (5%)	0.0020	0.05	1
3	Stock B3 (7%)	0.0028	0.07	1
4	Stock B4 (10%)	0.0040	0.10	1
5	Stock B5 (15%)	0.0060	0.15	1
6	Stock B6 (20%)	0.0080	0.20	1
7	Stock B7 (25%)	0.0100	0.25	1
8	Stock B8 (30%)	0.0120	0.30	1
9	Stock B9 (30%)	0.0120	0.30	1
10	Stock B10 (30%)	0.0120	0.30	1
11	Stock B11 (35%)	0.0140	0.35	1
12	Stock B12 (40%)	0.0160	0.40	1
13	Stock B13 (45%)	0.0180	0.45	1
14	Stock B14 (50%)	0.0200	0.50	1
15	Stock B15 (55%)	0.0220	0.55	1
16	Stock B16 (60%)	0.0240	0.60	1
17	Stock B17 (65%)	0.0260	0.65	1
18	Stock B18 (70%)	0.0280	0.70	1
19	Stock B19 (75%)	0.0300	0.75	1
20	Stock B20 (80%)	0.0320	0.80	1
21	Stock B21 (85%)	0.0340	0.85	1
22	Stock B22 (90%)	0.0360	0.90	1
23	Stock B23 (95%)	0.0380	0.95	1

^aRelative to Stock B; ^bSolution volume got from initial Stock B

For some turnover-limited competition experiments only 10 diluted stock solutions of B are prepared with the fixed concentrations of 10, 20, 30, 40, 50, 60, 70 and 80%. Here the solutions of the 30% concentration point are prepared three times, too.

Size-Induced Inversion of Selectivity in the Acylation of 1,2-Diols

Subsequently, 0.4 mL of Stock A, 0.4 mL of Stock C and 0.4 mL of diluted Stock B1 are transferred under nitrogen to a GC-vial equipped with a magnetic stir bar by use of a Hamilton syringe. Then, the GC-vial is capped under nitrogen and placed in the GC-vial holder with stirring for 3-4 weeks.

Composition of each prepared GC vial for one turnover-limited competition experiment:

GC vial 1: 0.4 mL Stock A; 0.4 mL Stock C; 0.4 mL Stock B1

GC vial 2: 0.4 mL Stock A; 0.4 mL Stock C; 0.4 mL Stock B2

GC vial 3: 0.4 mL Stock A; 0.4 mL Stock C; 0.4 mL Stock B3

GC vial 4: 0.4 mL Stock A; 0.4 mL Stock C; 0.4 mL Stock B4

GC vial 5: 0.4 mL Stock A; 0.4 mL Stock C; 0.4 mL Stock B5

GC vial ...

In terms of the actual starting concentrations (mol/L) for all components:

GC vial 1: **1b:** 0.006667, **5c:** 0.000267, **Et₃N:** 0.020000, **TCAP:** 0.001333

GC vial 2: **1b:** 0.006667, **5c:** 0.000667, **Et₃N:** 0.020000, **TCAP:** 0.001333

GC vial 3: **1b:** 0.006667, **5c:** 0.000933, **Et₃N:** 0.020000, **TCAP:** 0.001333

GC vial 4: **1b:** 0.006667, **5c:** 0.001344, **Et₃N:** 0.020000, **TCAP:** 0.001333

GC vial 5: **1b:** 0.006667, **5c:** 0.002000, **Et₃N:** 0.020000, **TCAP:** 0.001333

GC vial ...

The reaction is analysed by ¹H NMR, recorded by Bruker Avance III 800 machine. NMR tubes are dried under vacuum using Schlenk based glassware and flushed with nitrogen. Then, 0.6 mL of the solution contained in the GC-vial is transferred to the NMR-tube under nitrogen.

The ¹H NMR spectra of the turnover-limited competition experiments are edited by MestReNova 10.0. The spectra are corrected by using automatic phase correction and Whittaker Smoother (I) fit with autodetected parameters referenced by the solvent signal of CDCl₃ ($\delta = 7.26$ ppm). If Whittaker Smoother fit does not result in a good baseline the Polynomial Fit (II) with polynomial order 3 is used.

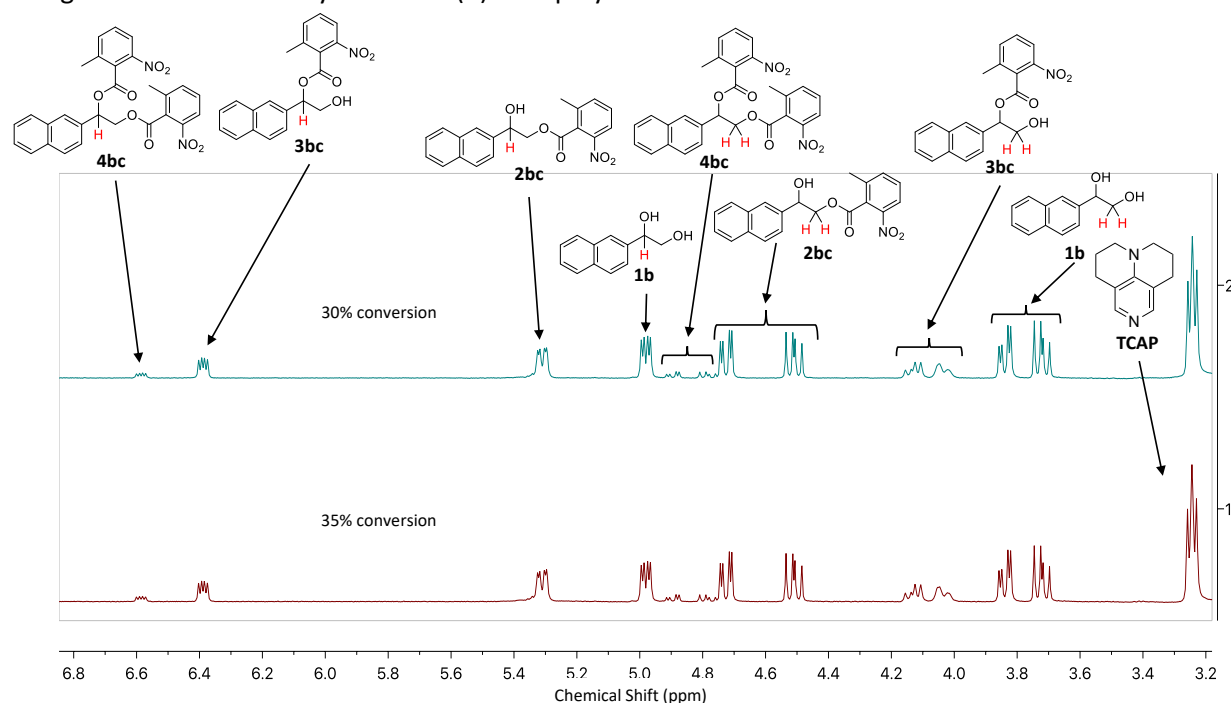
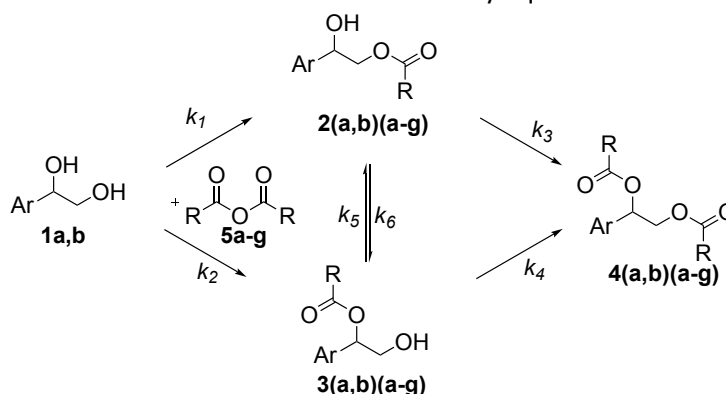


Figure 4.1. Example of the stacked ¹H NMR spectra for the turnover-limited competition experiment for **1b** with **5c**.

For the 1,2-diol **1**, primary ester **2**, secondary ester **3** or diester **4**, the hydrogen signal of the CH group is integrated as guide for the evolution of the reaction. If there is an overlapping with other signals, one of the corresponding hydrogen signals of the CH₂-group is used. If the hydrogen signals of the CH₂-group are not separated, the signal of the CH₂-group itself is used.

The acylation of 1,2-diol **1** is based on the complex two step process of a first and a second acylation and also migration step consisting of six different rate constants, which are influencing each other (Scheme 4.2). Because of this, the reaction has to be separated into three parts. The first part is the first acylation of the two OH groups of **1** to primary ester **2** and secondary ester **3**, defined by the rate constants k_1 and k_2 . The relative rate constant of the first acylation is defined by Eq. 4.1. The second part of this complex process is the acylation of the remaining OH-groups in the monoesters **2** and **3** to the diester **4**, defined by the rate constants k_3 and k_4 . The relative rate constant of the second acylation is defined by Eq. 4.2. The migration between the monoesters **2** and **3** is the third part of this reaction, defined by the rate constants k_5 and k_6 . The relative rate constant of the transesterification is defined by Eq. 4.3.



Scheme 4.2. General model of acylation reaction from 1,2-diol **1**.

$$k_{\text{rel,a}} = \frac{k_1}{k_2}, \quad \text{Eq. 4.1,}$$

$$k_{\text{rel,b}} = \frac{k_4}{k_3} \quad \text{Eq. 4.2}$$

$$k_{\text{rel,c}} = \frac{k_5}{k_6} \quad \text{Eq. 4.3}$$

The conversion of all OH-groups in the system is defined by Eq. 4.4, whereby the integrals of the ^1H NMR spectra were corresponding to the concentration.

$$\text{Conversion (\%)} = \left(\frac{[2(a,b)(a-g)] + [3(a,b)(a-g)] + 2 \cdot [4(a,b)(a-g)]}{2 \cdot [1a,b] + 2 \cdot [2(a,b)(a-g)] + 2 \cdot [3(a,b)(a-g)] + 2 \cdot [4(a,b)(a-g)]} \right) \cdot 100 \quad \text{Eq. 4.4}$$

The proportion of all components to each other are also called mole fractions are defined by Eq. 4.5-4.8:

$$\text{Mole fraction}_{1a,b} (\%) = \left(\frac{[1a,b]}{[1a,b] + [2(a,b)(a-g)] + [3(a,b)(a-g)] + [4(a,b)(a-g)]} \right) \cdot 100 \quad \text{Eq. 4.5}$$

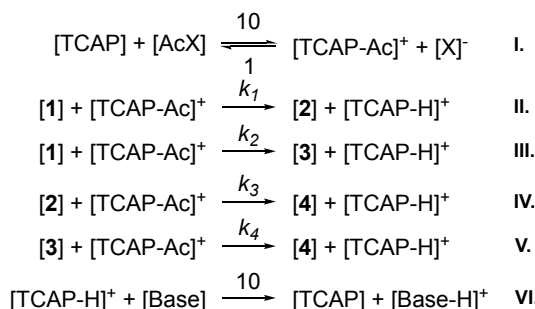
$$\text{Mole fraction}_{2(a,b)(a-g)} (\%) = \left(\frac{[2(a,b)(a-g)]}{[1a,b] + [2(a,b)(a-g)] + [3(a,b)(a-g)] + [4(a,b)(a-g)]} \right) \cdot 100 \quad \text{Eq. 4.6}$$

$$\text{Mole fraction}_{3(a,b)(a-g)} (\%) = \left(\frac{[3(a,b)(a-g)]}{[1a,b] + [2(a,b)(a-g)] + [3(a,b)(a-g)] + [4(a,b)(a-g)]} \right) \cdot 100 \quad \text{Eq. 4.7}$$

$$\text{Mole fraction}_{4(a,b)(a-g)} (\%) = \left(\frac{[4(a,b)(a-g)]}{[1a,b] + [2(a,b)(a-g)] + [3(a,b)(a-g)] + [4(a,b)(a-g)]} \right) \cdot 100 \quad \text{Eq. 4.8}$$

4.1.1.2 Simulation of Turnover-Limited Competition Experiments

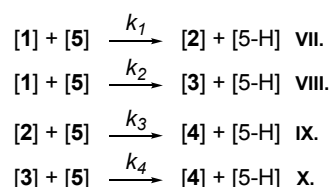
With the help of the CoPaSi^[2] and Origin programs the $k_1 - k_4$ values for the turnover-limited competition experiments have been fitted and simulated. Scheme 4.3 shows the reactions **I-VI**. for the simulations used in CoPaSi.



Scheme 4.3. Model reaction used in CoPaSi for the simulation of the rate constants.

The effective rate constants $k_1 - k_4$ are fitted by CoPaSi using the simplified reactions **VII-X**. shown in Scheme 4.4.

Size-Induced Inversion of Selectivity in the Acylation of 1,2-Diols



Scheme 4.4. Model reaction used in CoPaSi for the fitting of the rate constants.

There are three options (**A**, **B** or **C**) to fit the rate constants $k_1 - k_4$ values (Figure 4.4). In all three options the conversion is applied as “effective time” scale, so that the CoPaSi program is able to fit any effective rate constant. The mole fraction of the single components is recalculated to absolute concentrations originated of the starting concentration of 1,2-diol **1a,b** (0.0067 M) shown on Eq. 4.9-4.12.

$$\text{Concentration}_{1a,b} (\text{mol/L}) = \left(\frac{[1a,b]}{[1a,b] + [2(a,b)(a-g)] + [3(a,b)(a-g)] + [4(a,b)(a-g)]} \right) \cdot 0.0067 \quad \text{Eq. 4.9}$$

$$\text{Concentration}_{2(a,b)(a-g)} (\text{mol/L}) = \left(\frac{[2(a,b)(a-g)]}{[1a,b] + [2(a,b)(a-g)] + [3(a,b)(a-g)] + [4(a,b)(a-g)]} \right) \cdot 0.0067 \quad \text{Eq. 4.10}$$

$$\text{Concentration}_{3(a,b)(a-g)} (\text{mol/L}) = \left(\frac{[3(a,b)(a-g)]}{[1a,b] + [2(a,b)(a-g)] + [3(a,b)(a-g)] + [4(a,b)(a-g)]} \right) \cdot 0.0067 \quad \text{Eq. 4.11}$$

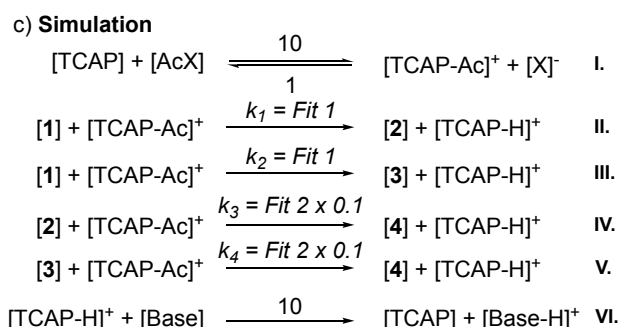
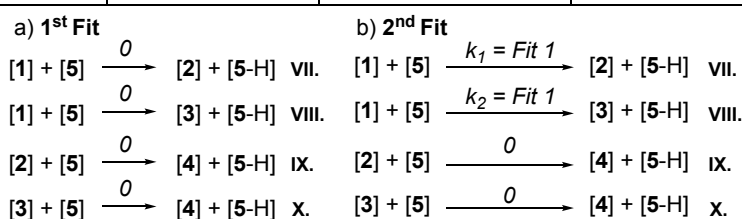
$$\text{Concentration}_{4(a,b)(a-g)} (\text{mol/L}) = \left(\frac{[4(a,b)(a-g)]}{[1a,b] + [2(a,b)(a-g)] + [3(a,b)(a-g)] + [4(a,b)(a-g)]} \right) \cdot 0.0067 \quad \text{Eq. 4.12}$$

For all fits, the initial values of the effective rate constants are set as $k_1 - k_4 = 0$, as method the Differential Evolution is chosen and the fits are run once. The fitted rate constants $k_1 - k_4$ of the different turnover-limited competition experiments are used for simulating the reaction by CoPaSi with the model reaction shown in Scheme 4.3. For the fitting and for the simulation, the starting concentration of **1b** (0.0067 M) up to full conversion of **5c** (0.0133 M) is used. For the simulation the initial concentration Et_3N (0.0200 M) and TCAP (0.0013 M) is also specified. The simulated concentrations over the time were used to calculate the conversion by Eq. 4.4 and mole fractions by Eq. 4.5-4.8. Afterwards the conversion was plotted over the mole fractions to be able to validate the experimental and numerical simulated mole fractions.

In the following methods **A-C** are explained by using the same turnover-limited competition example shown in Scheme 4.1 and are based on the technique shown in Table 4.3 and Scheme 4.5.

Table 4.3. Instructions of Fitting and Simulation in CoPaSi for turnover-limited competition experiments.

CoPaSi	Included Reaction	k_x constant	Fitted k_x	Fitted Reaction	Fitted Compound
Fit 1	VII.-X.	$k_3, k_4 = 0$	k_1, k_2 , Start Value = 0	VII, VIII	1, 2 and 3
Fit 2	VII.-X.	$k_1, k_2 = \text{Fit 1}$	k_3, k_4 , Start Value = 0	IX, X	2, 3 and 4
Simulation	I.-VI.	$k_1, k_2 = \text{Fit 1}$ $k_3, k_4 = \text{Fit 2} \times 0.1$	/	/	/



Scheme 4.5. Instructions of Fitting and Simulations of turnover-limited competition experiments of 1,2-diols in CoPaSi for a) 1st Fit, b) 2nd Fit and c) Simulation.

Method A:

In this case only 8 conversion points are available (10, 20, 30, 40, 50, 60, 70 and 80%). First, the first acylation with the rate constants k_1 (VII.) and k_2 (VIII.) are fitted by the 1st Fit (Scheme4.5a), by taking **1**, **2** and **3** as dependent concentrations (CoPaSi Parameter estimation: dependent). The concentration of **4** is excluded in the 1st fit, because in the first acylation no diester is formed (CoPaSi Parameter estimation: ignored). In this 1st Fit, only the values up to the highest concentration of **2** or **3** are included, in this model up to conversion point of 50% (Figure 4.2).

1st Fit: Reactions:
VII.-X., $k_1 - k_4 = 0$

1st Fit: Parameter estimation:
1, **2**, and **3** dependent
4 ignored

Figure 4.2 shows the CoPaSi software interface for the 1st fit. The left pane displays the species list (P1, P2, P3, R1-OH, TCAP-Ac, TCAP-H) and reactions (P1-P3, P2-p3, Global Quantities [0]). The center pane shows the reaction R1-OH + TCAP-Ac -> P1 + TCAP-H with a mass action rate law. The parameter table is as follows:

Role	Name	Mapping	Value	Unit
Parameter	k1	--local--	0	l/(mol*s)
Substrate	substrate	R1-OH		mol/l
		TCAP-Ac		mol/l

The right pane shows the 'Experimental Data' dialog box with 'Experiment' selected. The table below shows the data points:

Column Name	Type	Model Object	Weight
1 time	Time		
2 e	dependent	[R1-OH]	(0.1...)
3 p1	dependent	[P1]	(0.2...)
4 p2	dependent	[P2]	(1)
5 p3	ignored	[P3]	

Figure 4.2. Instructions of fitting for 1st fit in CoPaSi for turnover-limited competition experiments.

In the 2nd fit, the rate constants k_3 (IX.) and k_4 (X.) from the second acylation are fitted (Scheme 4.5b), by taking **2**, **3** and **4** as dependent concentrations (CoPaSi Parameter estimation: dependent), whereby this time **1** is excluded in the 2nd fit (CoPaSi Parameter estimation: ignored). For k_1 and k_2 the values from the 1st fit are kept constant and all conversion points are used (Figure 4.3). Finally, the resulting values for k_3 and k_4 are multiplied with 0.1. k_3 and k_4 should be slower than k_1 and k_2 , which is clearly visible in the absolute kinetic measurements. In these fitting process no real time dependency is included. We estimate that k_3 and k_4 should be slower by a factor of 10 in the simulations, because in our reference system with benzoic anhydride the first acylation is 10 times faster than the second acylation (see Chapter 4.1.2).

2nd Fit: Reactions:
VII., VIII., $k_1, k_2 = \text{Fit 1}$
IX., X., $k_3, k_4 = 0$

2nd Fit: Parameter estimation:
2, **3** and **4** dependent
1 ignored

Figure 4.3 shows the CoPaSi software interface for the 2nd fit. The left pane displays the species list (P1, P2, P3, R1-OH, TCAP-Ac, TCAP-H) and reactions (P1-P3, P2-p3, Global Quantities [0]). The center pane shows the reaction R1-OH + TCAP-Ac -> P1 + TCAP-H with a mass action rate law. The parameter table is as follows:

Role	Name	Mapping	Value	Unit
Parameter	k1	--local--	1.562584599	l/(mol*s)
Substrate	substrate	R1-OH		mol/l
		TCAP-Ac		mol/l

The right pane shows the 'Experimental Data' dialog box with 'Experiment' selected. The table below shows the data points:

Column Name	Type	Model Object	Weight
1 time	Time		
2 e	ignored	[R1-OH]	
3 p1	dependent	[P1]	(0.2814675523)
4 p2	dependent	[P2]	(1)
5 p3	dependent	[P3]	(0.32500448...)

Figure 4.3. Instructions of Fitting for fit 2 in CoPaSi for turnover-limited competition experiments.

Finally, the fitted effective rate constants $k_1 - k_4$ are putted in the reaction model defined for the simulation (II. – V., Scheme 4.5c) and the reaction was simulated for the full catalytic reaction cycle. After the conversion and mole fractions are calculated for the numerical simulation by using Eq. 4.4-4.8, the *conversion (%)* could plotted against the *mole fractions* for the experimental and numerical simulated values. In Figure 4.4a the final plot of *conversion (%)* vs. *mole fractions* of Method A is shown.

Method B:

In this case, all 21 conversion points are available (2, 5, 7, 10, 15, 20, 25, 30, 35, 40, 45, 50, 55, 60, 65, 70, 75, 80, 85, 90 and 95%). The guideline is the same as in Method A only with more data points. In Figure 4.4b the final plot of *conversion (%)* vs. *mole fractions* of Method B, is shown after simulation of the corresponding concentration by CoPaSi.

Method C:

In this case, all 21 conversion points are available (2, 5, 7, 10, 15, 20, 25, 30, 35, 40, 45, 50, 55, 60, 65, 70, 75, 80, 85, 90 and 95%). In the 1st Fit only the concentrations are used until no diester **4** is formed, in this model up to conversion point of 15%. The approach guideline is the same as in Method A. In Figure 4.4c the final plot of *conversion (%)* vs. *mole fraction* of Method C is shown after the simulation of the corresponding concentration by CoPaSi.

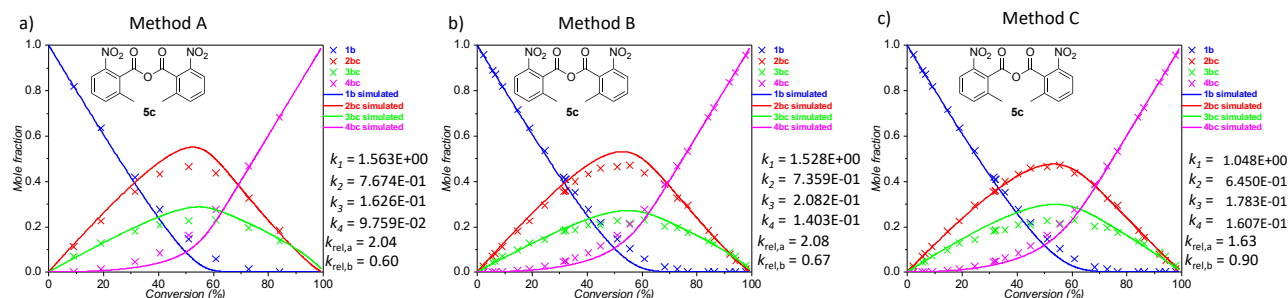


Figure 4.4. Plot of *conversion (%)* vs. *mole fraction* for 2-naphthylethane-1,2-diol **1b** with **5c** generated by turnover-limited competition experiment. The simulations were fitted by a) Method A, b) Method B and c) Method C. The rate constants $k_1 - k_4$ are given in L mol⁻¹s⁻¹.

Comparing the three options, all three plots seem to model well the acylation reaction of **1b** with **5c**. However, in each method the simulated mole fractions do not hit each point of mole fractions determined by the turnover-limited competition experiment. Comparing the relative rate constants $k_{rel,a}$ and $k_{rel,b}$ of the three fitting options (Table 4.4), there exist only small differences.

Table 4.4. Comparison of effective and relative rate constants of the three fitting Methods A, B, C.

Rate constants	Method A	Method B	Method C
k_1 (L mol ⁻¹ s ⁻¹)	1.563E+00	1.528E+00	1.048E+00
k_2 (L mol ⁻¹ s ⁻¹)	7.674E-01	7.359E-01	6.450E-01
k_3 (L mol ⁻¹ s ⁻¹)	1.626E-01	2.082E-01	1.783E-01
k_4 (L mol ⁻¹ s ⁻¹)	9.759E-02	1.403E-01	1.607E-01
$k_{rel,a}$	2.04	2.08	1.63
$k_{rel,b}$	0.60	0.67	0.90

In Figures 4.5 to 4.18 of *total conversion (%)* was plotted against the *mole fraction*, which allows us the illustrative comparison of experimental and simulated results using methods **A**, **B** or **C**. In the manuscript the relative rate constants obtained by Methods A or B are discussed. Method A and B are better comparable to each other, because of the same strategy in the 1st. fit. Furthermore, varying the simulated and experimental obtained mole fractions for the Ph substituted 1,2-diol **1a**, in method C strong derivations are visible (Figure 4.12-4.16).

Table 4.6. Fitted values of k_1 - k_4 by CoPaSi program in ($\text{L mol}^{-1}\text{s}^{-1}$), RMSD (root-mean-square deviation) values of the fitted compounds **1a**, **2a(a-g)**, **3a(a-g)** and **4a(a-g)** and the corresponding relative rate constants $k_{\text{rel,a}}$, $k_{\text{rel,b}}$, k_{prim} and k_{sec} for the acylation of **1a** with **5a-g** catalyzed by TCAP via turnover-limited competition experiments.

		Method A/B										Method C									
Fit		$k_1 - k_4$ ($\text{L mol}^{-1}\text{s}^{-1}$)	RMSD 1a	RMSD 2a(a-g)	RMSD 3a(a-g)	RMSD 4a(a-g)	k_{rel}	$k_1 - k_4$ ($\text{L mol}^{-1}\text{s}^{-1}$)	RMSD 1a	RMSD 2a(a-g)	RMSD 3a(a-g)	RMSD 4a(a-g)	k_{rel}	$k_1 - k_4$ ($\text{L mol}^{-1}\text{s}^{-1}$)	RMSD 1a	RMSD 2a(a-g)	RMSD 3a(a-g)	RMSD 4a(a-g)	k_{rel}		
5a	1	k_1	6.15E-04	3.57E-04	7.87E-05		$k_{\text{rel,a}}$	1.375E+00	5.88E-05	4.63E-05	1.27E-05		$k_{\text{rel,a}}$	1.375E+00	5.88E-05	4.63E-05	1.27E-05		$k_{\text{rel,a}}$		
		k_2					3.68	4.124E-01						4.124E-01						3.33	
	2	k_3		9.11E-04	2.46E-04	8.95E-04	$k_{\text{rel,b}}$	1.178E-01		1.33E-03	2.83E-04	9.12E-04	$k_{\text{rel,b}}$	1.178E-01		1.33E-03	2.83E-04	9.12E-04		$k_{\text{rel,b}}$	
		k_4					1.09	1.040E-01						1.09							0.88
5b		k_1	7.03E-04	4.28E-04	1.71E-04		$k_{\text{rel,a}}$	1.334E+00	1.32E-04	9.15E-05	4.07E-05		$k_{\text{rel,a}}$	1.334E+00	1.32E-04	9.15E-05	4.07E-05		$k_{\text{rel,a}}$		
		k_2					2.16	6.201E-01						6.201E-01						2.15	
		k_3		9.07E-04	4.86E-04	1.14E-03	$k_{\text{rel,b}}$	1.115E-01		1.19E-03	5.47E-04	1.16E-03	$k_{\text{rel,b}}$	1.115E-01		1.19E-03	5.47E-04	1.16E-03		$k_{\text{rel,b}}$	
		k_4					1.50	1.354E-01						1.50							1.21
5c		k_1	8.07E-03	5.90E-03	9.01E-03		$k_{\text{rel,a}}$	1.331E+00	2.28E-05	2.09E-05	7.04E-06		$k_{\text{rel,a}}$	1.331E+00	2.28E-05	2.09E-05	7.04E-06		$k_{\text{rel,a}}$		
		k_2					4.69	3.702E-01						3.702E-01						3.60	
		k_3		1.02E-03	1.69E-04	1.06E-03	$k_{\text{rel,b}}$	1.507E-01		1.31E-03	1.80E-04	1.14E-03	$k_{\text{rel,b}}$	1.507E-01		1.31E-03	1.80E-04	1.14E-03		$k_{\text{rel,b}}$	
		k_4					0.81	1.526E-01						0.81							1.01
5d		k_1	6.38E-04	4.43E-04	6.34E-05		$k_{\text{rel,a}}$	1.105E+00	2.52E-05	2.66E-05	2.24E-06		$k_{\text{rel,a}}$	1.105E+00	2.52E-05	2.66E-05	2.24E-06		$k_{\text{rel,a}}$		
		k_2					2.74	5.910E-01						5.910E-01						1.87	
		k_3		8.16E-04	1.70E-04	5.77E-04	$k_{\text{rel,b}}$	7.752E-02		1.45E-03	2.24E-04	5.74E-04	$k_{\text{rel,b}}$	7.752E-02		1.45E-03	2.24E-04	5.74E-04		$k_{\text{rel,b}}$	
		k_4					0.69	8.982E-02						8.982E-02						1.16	
5e		k_1	7.04E-04	5.07E-04	7.81E-05		$k_{\text{rel,a}}$	1.189E+00	3.63E-05	3.77E-05	3.97E-06		$k_{\text{rel,a}}$	1.189E+00	3.63E-05	3.77E-05	3.97E-06		$k_{\text{rel,a}}$		
		k_2					2.99	5.439E-01						5.439E-01						2.19	
		k_3		7.60E-04	1.22E-04	4.12E-04	$k_{\text{rel,b}}$	6.882E-02		1.45E-03	1.84E-04	4.03E-04	$k_{\text{rel,b}}$	6.882E-02		1.45E-03	1.84E-04	4.03E-04		$k_{\text{rel,b}}$	
		k_4					0.54	5.476E-02						5.476E-02						0.80	
5f		k_1	7.46E-04	5.59E-04	1.06E-04		$k_{\text{rel,a}}$			1.06E-04			$k_{\text{rel,a}}$								
		k_2					2.63						2.63								
		k_3		6.68E-04	1.21E-04	1.23E-04	$k_{\text{rel,b}}$			1.21E-04			$k_{\text{rel,b}}$								
		k_4					0.52						0.52								
5g		k_1	1.03E-03	7.61E-04	1.86E-04		$k_{\text{rel,a}}$			1.86E-04			$k_{\text{rel,a}}$								
		k_2					2.46						2.46								
		k_3		8.00E-04	1.90E-04	7.12E-05	$k_{\text{rel,b}}$			1.90E-04			$k_{\text{rel,b}}$								
		k_4					0.25						0.25								

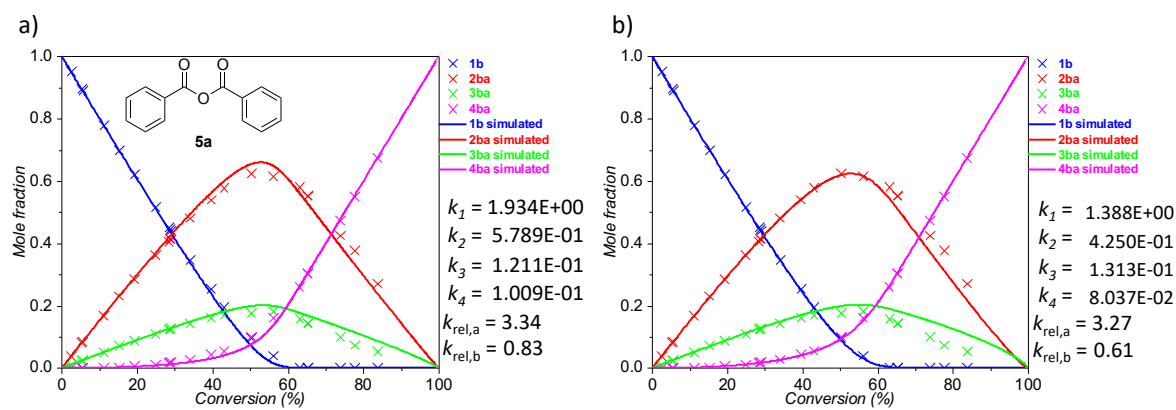


Figure 4.5. Plot of conversion (%) vs. mole fraction for **1b** with **5a** generated by turnover-limited competition experiment. a) Fitted by Method B. b) Fitted by Method C. The rate constants $k_1 - k_4$ are given in $\text{L mol}^{-1}\text{s}^{-1}$.

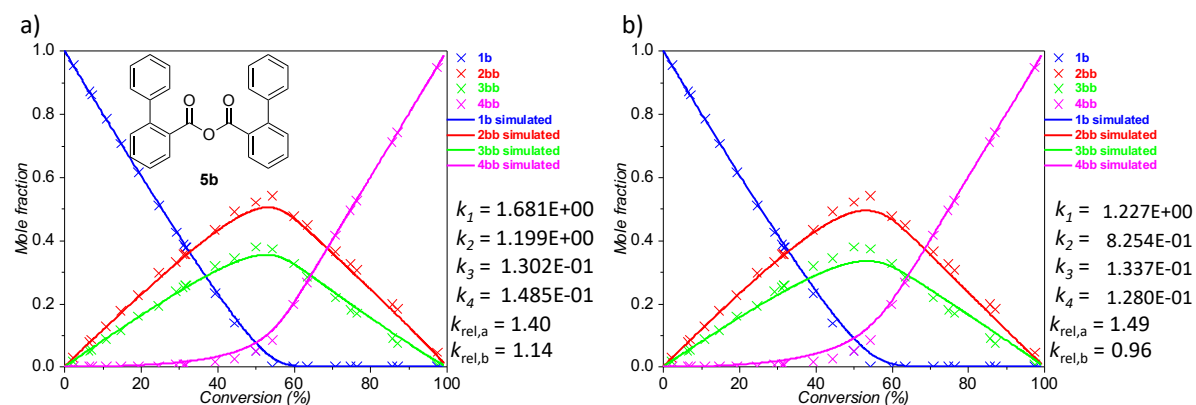


Figure 4.6. Plot of conversion (%) vs. mole fraction for **1b** with **5b** generated by turnover-limited competition experiment. a) Fitted by Method B. b) Fitted by Method C. The rate constants $k_1 - k_4$ are given in $\text{L mol}^{-1}\text{s}^{-1}$.

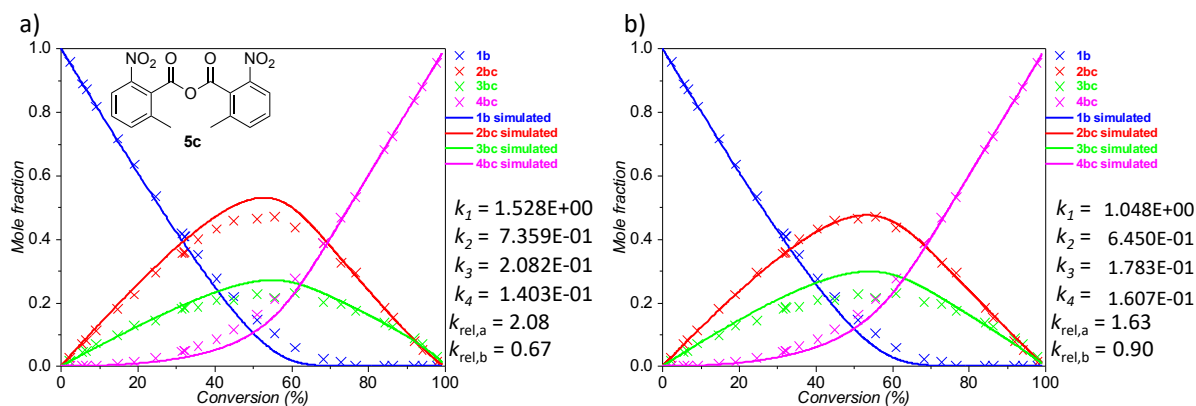


Figure 4.7. Plot of conversion (%) vs. mole fraction for **1b** with **5c** generated by turnover-limited competition experiment. a) Fitted by Method B. b) Fitted by Method C. The rate constants $k_1 - k_4$ are given in $\text{L mol}^{-1}\text{s}^{-1}$.

Size-Induced Inversion of Selectivity in the Acylation of 1,2-Diols

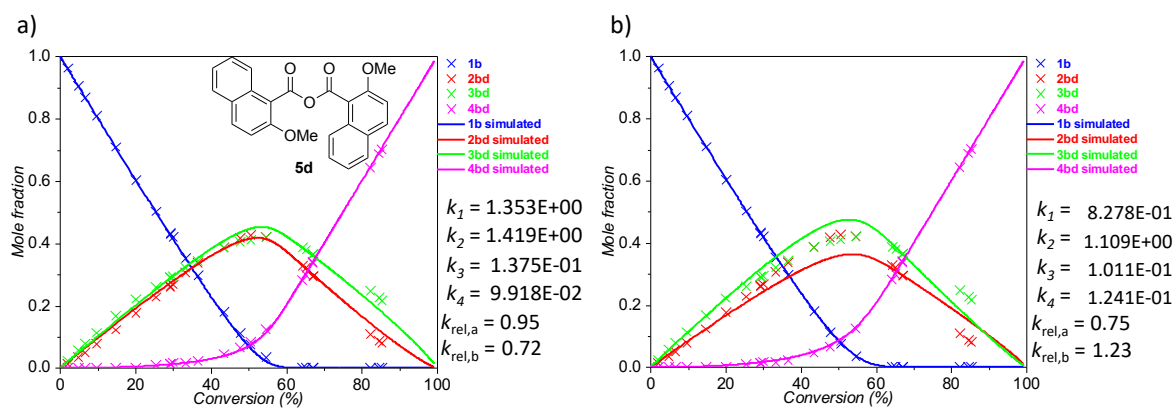


Figure 4.8. Plot of conversion (%) vs. mole fraction for **1b** with **5d** generated by turnover-limited competition experiment. a) Fitted by Method B. b) Fitted by Method C. The rate constants $k_1 - k_4$ are given in $\text{L mol}^{-1}\text{s}^{-1}$.

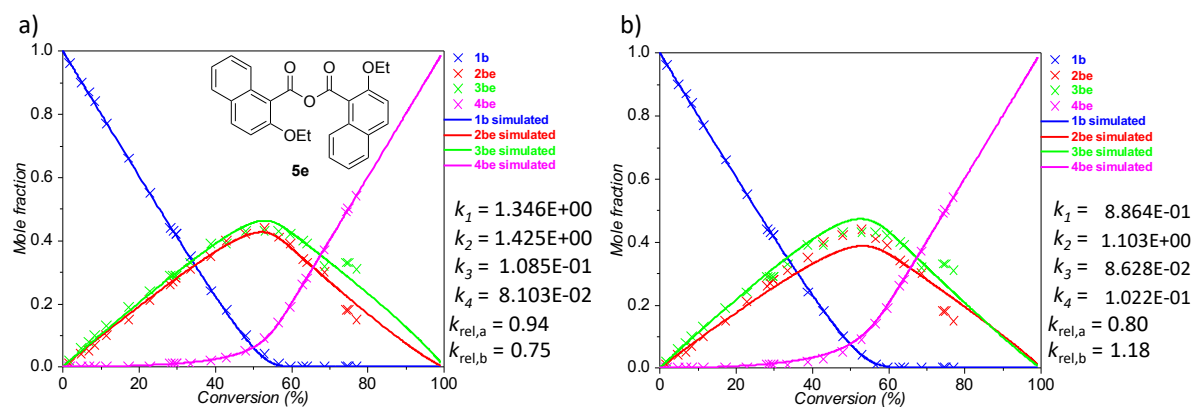


Figure 4.9. Plot of conversion (%) vs. mole fraction for **1b** with **5e** generated by turnover-limited competition experiment. a) Fitted by Method B. b) Fitted by Method C. The rate constants $k_1 - k_4$ are given in $\text{L mol}^{-1}\text{s}^{-1}$.

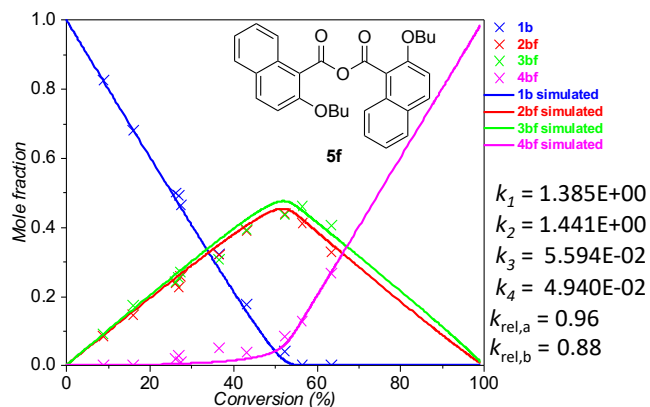


Figure 4.10. Plot of conversion (%) vs. mole fraction for **1b** with **5f** generated by turnover-limited competition experiment. Fitted by Method A. The rate constants $k_1 - k_4$ are given in $\text{L mol}^{-1}\text{s}^{-1}$.

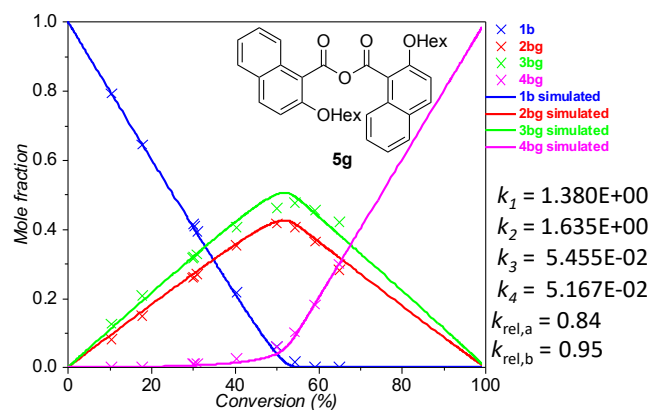


Figure 4.11. Plot of conversion (%) vs. mole fraction for **1b** with **5g** generated by turnover-limited competition experiment. Fitted by Method A. The rate constants $k_1 - k_4$ are given in $L \text{ mol}^{-1} \text{ s}^{-1}$.

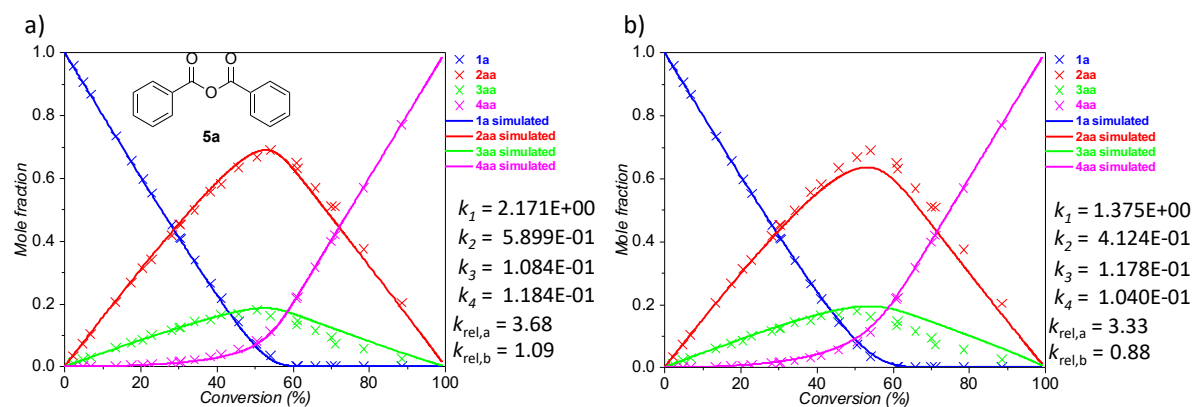


Figure 4.12. Plot of conversion (%) vs. mole fraction for **1a** with **5a** generated by turnover-limited competition experiment. a) Fitted by Method B. b) Fitted by Method C. The rate constants $k_1 - k_4$ are given in $L \text{ mol}^{-1} \text{ s}^{-1}$.

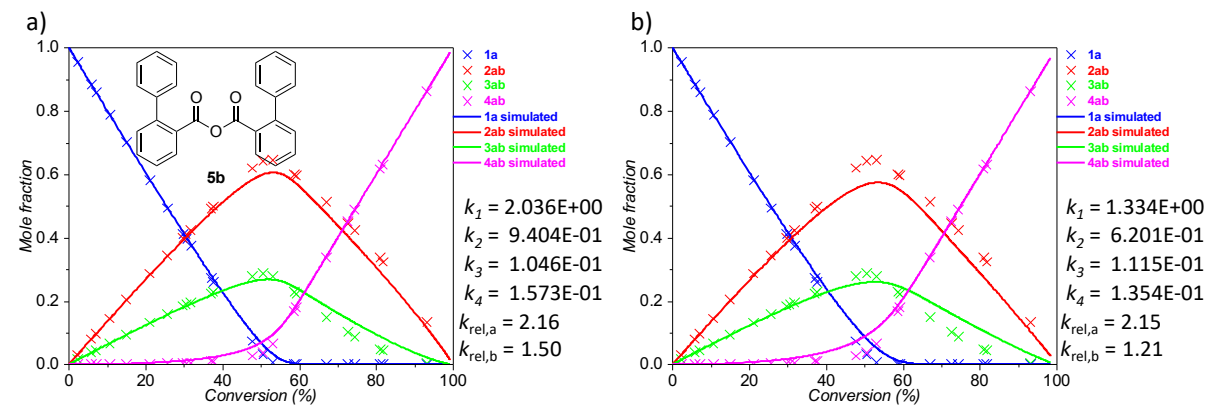


Figure 4.13. Plot of conversion (%) vs. mole fraction for **1a** with **5b** generated by turnover-limited competition experiment. a) Fitted by Method B. b) Fitted by Method C. The rate constants $k_1 - k_4$ are given in $L \text{ mol}^{-1} \text{ s}^{-1}$.

Size-Induced Inversion of Selectivity in the Acylation of 1,2-Diols

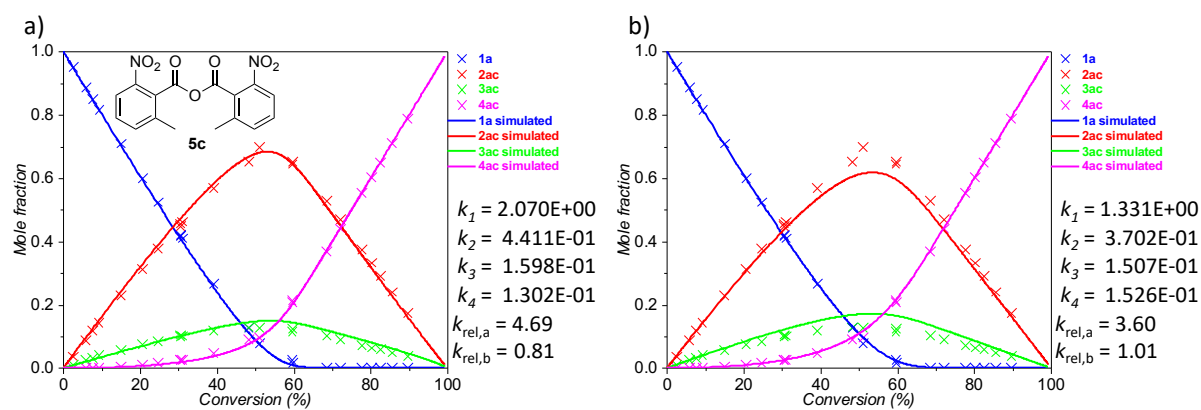


Figure 4.14. Plot of conversion (%) vs. mole fraction for **1a** with **5c** generated by turnover-limited competition experiment. a) Fitted by Method B. b) Fitted by Method C. The rate constants $k_1 - k_4$ are given in $L \text{ mol}^{-1} \text{ s}^{-1}$.

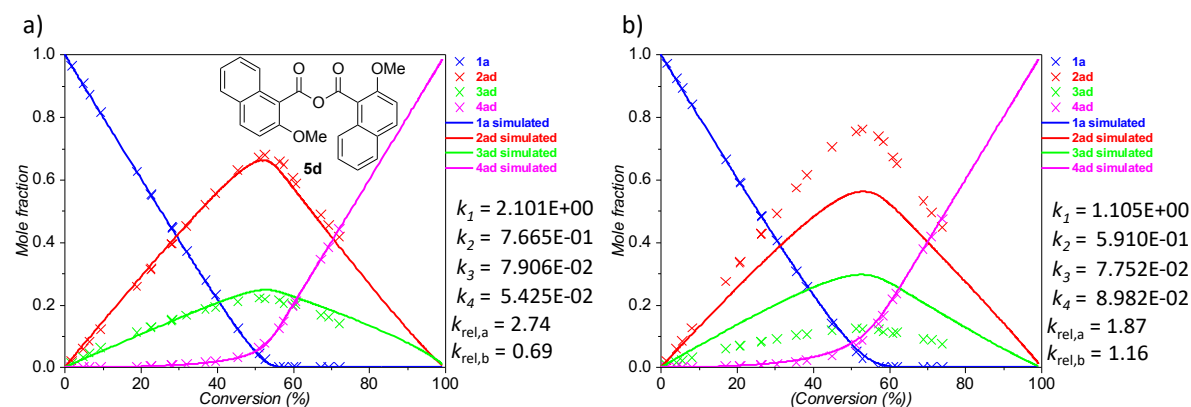


Figure 4.15. Plot of conversion (%) vs. mole fraction for **1a** with **5d** generated by turnover-limited competition experiment. a) Fitted by Method B. b) Fitted by Method C. The rate constants $k_1 - k_4$ are given in $L \text{ mol}^{-1} \text{ s}^{-1}$.

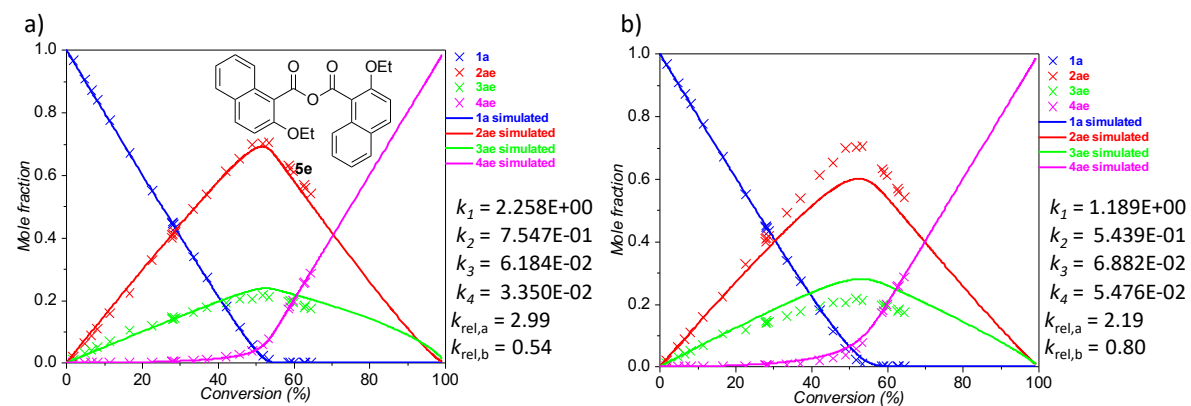


Figure 4.16. Plot of conversion (%) vs. mole fraction for **1a** with **5e** generated by turnover-limited competition experiment. a) Fitted by Method B. b) Fitted by Method C. The rate constants $k_1 - k_4$ are given in $L \text{ mol}^{-1} \text{ s}^{-1}$.

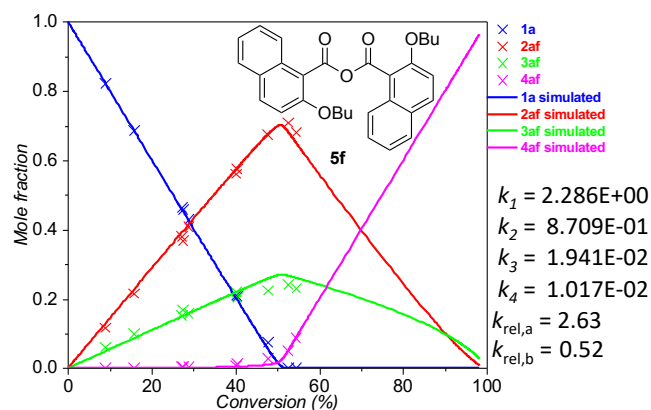


Figure 4.17. Plot of conversion (%) vs. mole fraction for **1a** with **5f** generated by turnover-limited competition experiment. Fitted by Method A. The rate constants $k_1 - k_4$ are given in $\text{L mol}^{-1}\text{s}^{-1}$.

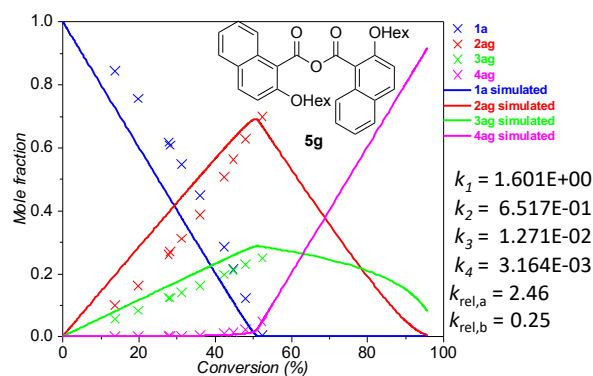


Figure 4.18. Plot of conversion (%) vs. mole fraction for **1a** with **5g** generated by turnover-limited competition experiment. Fitted by Method A. The rate constants $k_1 - k_4$ are given in $\text{L mol}^{-1}\text{s}^{-1}$.

Table 4.7. Conversion (%) and mole fractions of **1b:2b(a-g):3b(ag):4b(a-g)** for turnover-limited competition experiments of **1b** with **5a-g**.

Conv (%)	Mole fraction (%)				Conv (%)	Mole fraction (%)			
Conv _{exp}	1b ^a	2ba ^a	3ba ^a	4ba ^a	Conv _{exp}	1b ^a	2bb ^a	3bb ^a	4bb ^a
2.40	95.20	3.75	1.05	0.00	2.25	95.49	2.83	1.67	0.00
5.18	89.65	8.03	2.33	0.00	6.42	87.16	7.76	5.08	0.00
5.56	88.88	8.53	2.59	0.00	7.00	86.01	8.60	5.40	0.00
11.16	77.92	16.72	5.12	0.24	10.78	78.44	12.72	8.85	0.00
15.09	69.82	23.08	7.11	0.00	14.68	70.65	17.72	11.63	0.00
19.29	62.15	28.37	8.75	0.73	19.29	61.42	22.57	16.01	0.00
24.76	51.66	36.32	10.84	1.18	24.49	51.01	29.65	19.34	0.00
28.28	45.25	40.51	12.42	1.82	29.02	42.56	33.05	23.78	0.61
28.64	44.46	41.53	12.29	1.73	31.00	38.71	35.59	24.99	0.71
28.90	44.12	41.29	12.68	1.91	31.51	37.71	35.69	25.87	0.73
33.99	34.78	48.09	14.38	2.75	31.57	37.69	35.70	25.77	0.83
39.41	25.52	53.94	16.19	4.35	39.17	23.21	43.29	31.95	1.55
42.95	19.65	57.74	17.07	5.54	44.40	13.88	49.10	34.34	2.68
50.20	9.72	62.48	17.68	10.12	49.95	5.05	52.08	37.93	4.95
56.11	3.95	61.48	18.41	16.16	54.29	0.00	54.14	37.29	8.58
62.98	0.00	58.09	15.95	25.97	59.85	0.00	47.63	32.68	19.69
65.12	0.00	55.44	14.31	30.25	63.36	0.00	44.76	28.51	26.73
65.18	0.00	55.16	14.48	30.36	70.83	0.00	36.49	21.86	41.66
73.70	0.00	42.56	10.04	47.40	74.68	0.00	32.67	17.96	49.36
77.50	0.00	37.63	7.37	55.00	76.25	0.00	30.57	16.92	52.51
83.72	0.00	27.11	5.45	67.44	85.59	0.00	19.82	9.00	71.19
					87.07	0.00	18.27	7.58	74.14

Size-Induced Inversion of Selectivity in the Acylation of 1,2-Diols

					97.33	0.00	4.59	0.75	94.66
Conv_{exp}	1b^a	2bc^a	3bc^a	4bc^a	Conv_{exp}	1b^a	2bd^a	3bd^a	4bd^a
2.13	95.74	2.69	1.57	0.00	1.88	96.24	1.34	2.41	0.00
5.59	88.82	6.86	4.33	0.00	4.72	90.57	3.61	5.82	0.00
6.47	87.06	8.18	4.76	0.00	6.56	86.87	5.12	8.01	0.00
9.13	81.74	11.21	7.05	0.00	9.58	80.85	7.74	11.41	0.00
14.61	71.57	17.98	9.65	0.80	14.54	70.93	12.34	16.73	0.00
18.94	63.49	22.49	12.64	1.37	19.90	60.21	17.66	22.13	0.00
24.48	53.58	29.54	14.34	2.54	25.33	50.27	22.77	26.04	0.92
31.35	41.86	35.46	18.10	4.57	29.01	43.34	26.23	29.07	1.36
32.01	40.84	35.59	18.70	4.87	29.21	43.08	26.16	29.26	1.50
32.08	40.73	35.98	18.39	4.90	29.87	42.05	26.81	29.36	1.79
35.60	35.11	39.92	18.66	6.31	33.18	35.33	30.74	32.24	1.70
40.40	27.61	43.15	20.85	8.40	36.37	29.65	33.65	34.30	2.39
44.84	21.87	45.72	20.85	11.55	43.25	18.09	38.65	38.68	4.58
50.84	14.67	46.43	22.54	16.35	47.71	11.18	41.66	40.55	6.61
55.44	10.21	47.11	21.59	21.10	50.48	7.54	42.79	41.16	8.50
60.89	5.85	43.66	22.87	27.63	54.56	3.40	42.08	41.99	12.52
68.22	2.31	38.80	20.14	38.75	64.14	0.00	32.93	38.78	28.29
72.78	1.24	32.42	19.53	46.81	65.02	0.00	32.08	37.89	30.03
76.60	0.00	29.42	17.38	53.20	66.92	0.00	29.58	36.58	33.84
84.08	0.00	18.24	13.60	68.16	66.97	0.00	29.35	36.70	33.94
86.12	0.00	15.14	12.61	72.25	82.20	0.00	10.78	24.83	64.39
91.77	0.00	7.77	8.69	83.54	84.38	0.00	8.70	22.55	68.75
93.95	0.00	5.01	7.08	87.90	85.13	0.00	8.04	21.70	70.26
97.77	0.00	1.41	3.04	95.55					
Conv_{exp}	1b^a	2be^a	3be^a	4be^a	Conv_{exp}	1b^b	2bf^b	3bf^b	4bf^b
1.75	96.50	1.27	2.23	0.00	8.70	82.60	8.40	9.01	0.00
4.78	90.44	3.69	5.87	0.00	15.99	68.03	14.65	17.32	0.00
6.70	86.59	5.34	8.07	0.00	26.82	49.14	22.72	25.37	2.78
8.20	83.60	6.62	9.78	0.00	25.99	49.97	23.85	24.24	1.95
11.30	77.41	9.68	12.92	0.00	27.42	46.29	25.67	26.92	1.12
17.10	65.80	15.24	18.96	0.00	36.53	32.10	32.03	30.72	5.15
22.75	54.82	20.97	23.88	0.32	43.07	17.70	39.09	39.37	3.84
28.15	44.25	25.91	29.30	0.54	52.14	4.19	43.81	43.51	8.48
28.81	43.24	27.25	28.65	0.87	56.39	0.00	41.12	46.10	12.78
29.54	41.88	28.03	29.14	0.95	63.36	0.00	32.84	40.44	26.72
29.63	41.70	28.00	29.34	0.96					
33.43	34.53	31.45	32.63	1.39					
38.84	24.40	34.58	38.93	2.09					
42.76	17.95	39.73	38.84	3.47					
47.85	9.76	42.14	42.64	5.46					
52.86	3.54	43.80	43.42	9.25					
56.49	1.08	41.46	43.40	14.07					
59.54	0.00	39.03	41.90	19.08					
62.94	0.00	33.63	40.48	25.88					
63.81	0.00	33.31	39.08	27.61					
68.60	0.00	30.35	32.46	37.19					
74.39	0.00	18.12	33.10	48.78					
74.80	0.00	17.66	32.74	49.60					
76.97	0.00	14.66	31.40	53.94					

Conv _{exp}	1b ^a	2bg ^a	3bg ^a	4bg ^a					
10.37	79.26	8.15	12.59	0.00					
17.78	64.45	14.82	20.73	0.00					
29.84	41.43	25.88	31.58	1.11					
30.15	40.78	26.21	31.94	1.07					
30.98	39.25	26.89	32.66	1.20					
40.38	21.70	35.38	40.46	2.46					
49.95	6.16	41.65	46.13	6.06					
54.22	1.69	40.58	47.61	10.12					
59.06	0.00	36.37	45.51	18.12					
64.95	0.00	28.11	41.98	29.91					

^aBaseline of ¹H NMR for integration was corrected by Whittaker Smoother (I) fit; ^bBaseline of ¹H NMR for integration was corrected by Polynomial Fit (II).

Table 4.8. Conversion (%) and mole fractions of **1a:2a(a-g):3a(ag):4a(a-g)** for turnover-limited competition experiments of **1a** with **5a-g**.

Conv (%)	Mole fraction (%)				Conv (%)	Mole fraction(%)			
Conv _{exp}	1a ^a	2aa ^a	3aa ^a	4aa ^a	Conv _{exp}	1a ^a	2ab ^a	3ab ^a	4ab ^a
2.16	95.69	3.34	0.97	0.00	2.28	95.44	3.03	1.53	0.00
4.75	90.50	7.27	2.23	0.00	5.83	88.35	7.94	3.71	0.00
6.68	86.65	10.28	3.08	0.00	7.03	85.94	9.64	4.42	0.00
13.30	73.40	20.49	6.11	0.00	10.57	78.85	14.45	6.70	0.00
17.48	65.40	26.76	7.48	0.36	14.91	70.17	20.40	9.42	0.00
20.42	59.76	31.26	8.39	0.59	20.95	58.10	28.66	13.24	0.00
22.78	55.20	34.01	10.05	0.75	25.51	49.34	34.47	15.83	0.36
28.07	45.17	41.88	11.64	1.31	30.50	39.50	41.06	18.93	0.50
30.21	41.02	45.29	12.26	1.43	31.59	37.41	42.43	19.57	0.59
30.43	40.73	45.22	12.47	1.59	29.65	41.18	39.86	18.48	0.48
34.09	33.90	49.80	14.22	2.08	36.98	27.23	49.22	22.36	1.19
38.27	26.52	55.54	14.87	3.07	37.52	25.99	49.97	23.01	1.03
40.99	21.78	58.01	16.45	3.76	47.68	7.38	61.99	27.90	2.73
45.66	14.23	63.40	16.83	5.54	50.36	3.15	64.28	28.70	3.87
50.50	7.16	66.75	17.93	8.17	52.96	0.74	64.66	27.94	6.67
53.92	3.47	69.03	16.18	11.32	58.45	0.00	60.07	23.04	16.90
60.91	0.00	64.95	13.23	21.82	59.02	0.00	59.56	22.41	18.03
61.07	0.00	63.13	14.72	22.15	66.84	0.00	51.44	14.89	33.67
65.77	0.00	56.97	11.50	31.53	72.57	0.00	44.47	10.39	45.14
69.89	0.00	50.93	9.30	39.77	74.39	0.00	42.40	8.81	48.78
70.95	0.00	50.87	7.24	41.89	81.58	0.00	32.39	4.45	63.16
78.47	0.00	37.36	5.69	56.94	80.83	0.00	33.64	4.69	61.67
88.53	0.00	20.30	2.64	77.06	93.10	0.00	13.29	0.52	86.19
Conv _{exp}	1a ^a	2ac ^a	3ac ^a	4ac ^a	Conv _{exp}	1a ^a	2ad ^a	3ad ^a	4ad ^a
2.40	95.21	3.66	1.13	0.00	1.75	96.49	2.11	1.40	0.00
5.72	88.56	8.86	2.57	0.00	4.64	90.72	5.91	3.38	0.00
7.54	84.91	11.96	3.13	0.00	6.41	87.17	8.26	4.56	0.00
9.17	81.66	14.30	4.04	0.00	9.25	81.50	12.24	6.26	0.00
14.81	70.96	22.83	5.64	0.57	18.84	62.61	25.87	11.23	0.29
20.55	59.96	31.34	7.64	1.06	22.50	55.38	31.32	12.92	0.38
24.58	52.38	37.64	8.45	1.53	22.66	55.12	31.59	12.86	0.43
30.32	42.05	44.82	10.44	2.69	27.97	44.79	39.46	15.02	0.73
30.41	41.74	45.64	10.06	2.56	27.99	44.77	39.43	15.05	0.75
30.83	40.97	46.27	10.14	2.62	28.07	44.57	39.47	15.26	0.70

Size-Induced Inversion of Selectivity in the Acylation of 1,2-Diols

39.08	26.63	56.80	11.77	4.80	31.92	37.20	45.14	16.63	1.04
48.11	12.78	65.28	12.94	9.00	36.86	27.86	52.06	18.50	1.58
50.89	7.81	69.88	12.72	9.59	39.41	23.20	55.62	19.17	2.01
59.46	2.51	64.45	11.61	21.43	45.38	12.53	63.11	21.06	3.30
59.50	1.70	65.14	12.47	20.69	51.00	4.40	67.03	22.18	6.39
68.47	0.00	52.78	10.28	36.94	52.52	2.61	67.87	21.86	7.66
72.03	0.00	46.93	9.01	44.06	56.29	0.00	65.85	21.57	12.58
77.61	0.00	37.48	7.31	55.21	57.40	0.00	64.79	20.41	14.79
80.14	0.00	33.27	6.45	60.28	59.82	0.00	60.55	19.81	19.64
82.47	0.00	29.12	5.94	64.94	60.58	0.00	58.78	20.07	21.16
85.52	0.00	24.05	4.91	71.04	67.26	0.00	48.80	16.69	34.51
89.43	0.00	17.37	3.77	78.86	69.23	0.00	45.50	16.04	38.47
					72.09	0.00	41.76	14.07	44.17
Conv_{exp}	1a^a	2ae^a	3ae^a	4ae^a	Conv_{exp}	1a^b	2af^b	3af^b	4af^b
1.62	96.75	2.03	1.22	0.00	8.91	82.18	11.66	6.16	0.00
4.67	90.66	6.20	3.15	0.00	15.70	68.61	21.54	9.86	0.00
6.48	87.04	8.81	4.15	0.00	27.04	46.33	38.10	15.15	0.42
8.04	83.93	10.89	5.18	0.00	27.29	45.77	36.94	16.94	0.36
11.26	77.48	15.74	6.78	0.00	28.72	43.01	40.77	15.76	0.46
16.55	67.09	22.25	10.46	0.19	39.94	20.98	56.11	22.05	0.86
22.58	55.12	32.74	11.85	0.29	40.32	20.71	57.53	20.42	1.34
27.74	45.01	40.00	14.51	0.49	47.70	7.40	67.32	22.49	2.79
27.94	44.63	40.75	14.10	0.51	52.50	0.00	70.92	24.09	4.99
28.09	44.29	41.26	13.98	0.48	54.37	0.00	68.12	23.14	8.74
28.64	43.27	41.85	14.32	0.55					
33.46	33.85	49.13	16.26	0.76					
36.92	27.31	53.79	17.76	1.14					
41.98	17.91	61.10	19.12	1.87					
45.70	11.36	65.33	20.55	2.76					
49.02	5.83	69.73	20.57	3.87					
51.71	2.39	70.13	21.68	5.80					
53.35	0.99	70.34	21.00	7.68					
58.61	0.00	63.23	19.54	17.23					
58.94	0.00	62.24	19.88	17.88					
59.92	0.00	61.05	19.12	19.83					
62.68	0.00	56.83	17.80	25.37					
62.89	0.00	55.90	18.33	25.77					
64.33	0.00	54.04	17.29	28.67					
Conv_{exp}	1a^a	2ag^a	3ag^a	4ag^a					
8.12	83.75	10.46	5.78	0.00					
12.43	75.15	16.43	8.42	0.00					
17.88	64.41	22.80	12.63	0.16					
19.84	60.49	27.00	12.35	0.16					
20.57	58.97	27.84	13.10	0.10					
28.07	44.33	39.04	16.16	0.47					
36.03	28.91	50.43	19.69	0.98					
38.93	23.45	53.59	21.65	1.31					
45.24	11.97	60.31	25.27	2.45					
52.62	0.00	67.47	27.28	5.25					

^aBaseline of ¹H NMR for integration was corrected by Whittaker Smoother (I) fit; ^bBaseline of ¹H NMR for integration was corrected by Polynomial Fit (II).

4.1.1.3 Determination of Selectivity by Measurement of the 30% Conversion Point

In the literature it is common to concentrate on only one conversion point, mostly the 50% conversion point.^[3] For this reason, the turnover-limited competition experiments at the 30% conversion point is prepared three times and shown in Figures 4.20 and 4.21. Since the formation of the diester **4** is still negligible here, it is possible to calculate the relative rate constant $k_{rel,a30\%}$ through the ratio between the concentrations of monoester **2(a,b)(a-g)** over **3(a,b)(a-g)** (Eq. 4.13).

$$k_{rel,a30\%} = \frac{\text{Mole fraction}_{2(a,b)(a-g)}}{\text{Mole fraction}_{3(a,b)(a-g)}} = \frac{[2(a,b)(a-g)]}{[3(a,b)(a-g)]} \quad \text{Eq. 4.13}$$

Based on the work of Giese^[4] the relative rate constant s of the turnover-limited competition acylation of 1,2-diol **1** with anhydride **5** to product **2** and **3** (Figure 4.19) is described as the ratio of the effective rate constant k_1 of the formation of **2** over the effective rate constant k_2 of the formation of **3** (Eq. 4.14).^[4]

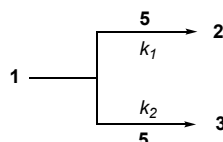


Figure 4.19. Turnover-limited competition acylation of 1,2-diol **1** with anhydride **5** to product **2** and **3**.

Because **1** reacts to the two different products **2** and **3** in an irreversible (pseudo-)first order reaction, the reaction could be described via the first-order rate law which results in Eq. 4.15 and 4.16. by activating the equation towards the effective rate constants k_1 , k_2 , Eq. 4.17 and 4.18 are generated. Inserting the parameters of Eq. 4.17 and 4.18 in Eq. 14, it is shown that the relative rate constant is proportional to the product compositions (Eq. 19).

$$s = \frac{k_1}{k_2} \quad \text{Eq. 4.14}$$

$$\frac{d[2]}{dt} = +k_1[1][5] \quad \text{Eq. 4.15}$$

$$\frac{d[3]}{dt} = +k_2[1][5] \quad \text{Eq. 4.16}$$

$$k_1 = \frac{d[2]}{[1][5]dt} \quad \text{Eq. 4.17}$$

$$k_2 = \frac{d[3]}{[1][5]dt} \quad \text{Eq. 4.18}$$

$$s = \frac{k_1}{k_2} = \frac{\frac{d[2]}{[1][5]dt}}{\frac{d[3]}{[1][5]dt}} = \frac{d[2]}{d[3]} \approx \frac{\Delta[2]}{\Delta[3]} \quad \text{Eq. 4.19}$$

Finally, it is possible to compare the rate constants generated by looking at one point ($k_{rel,a30\%}$) or by fitting the rate constants by simulating the reaction ($k_{rel,a}$). Even for the acylation of **1b** as for **1a**, the two ways of generating relative rate constants show similar $k_{rel,a}$ for the first acylation. A further discussion will be made in chapter 4.1.3.

Size-Induced Inversion of Selectivity in the Acylation of 1,2-Diols

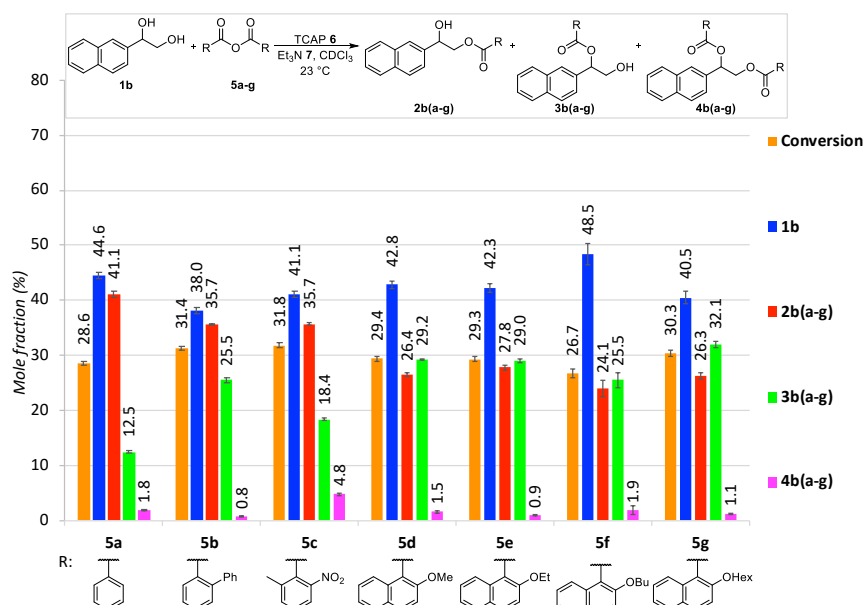


Figure 4.20. Mole fraction (%) of 1b:2b(a-g):3b(a-g):4b(a-g) and total conversion (%) for turnover-limited competition experiments of 1b with 5a-g at the 30% conversion point.

Table 4.9. Comparison of $k_{rel,a}$ by different validation methods for turnover-limited competition experiments of 1b with 5a-g.

Anhydride	$k_{rel,a30\%}$	$k_{rel,a}$
5a	3.30 ± 0.057	3.34
5b	1.40 ± 0.020	1.40
5c	1.94 ± 0.026	2.08
5d	0.90 ± 0.008	0.95
5e	0.96 ± 0.005	0.94
5f	0.94 ± 0.037	0.96
5g	0.82 ± 0.002	0.84

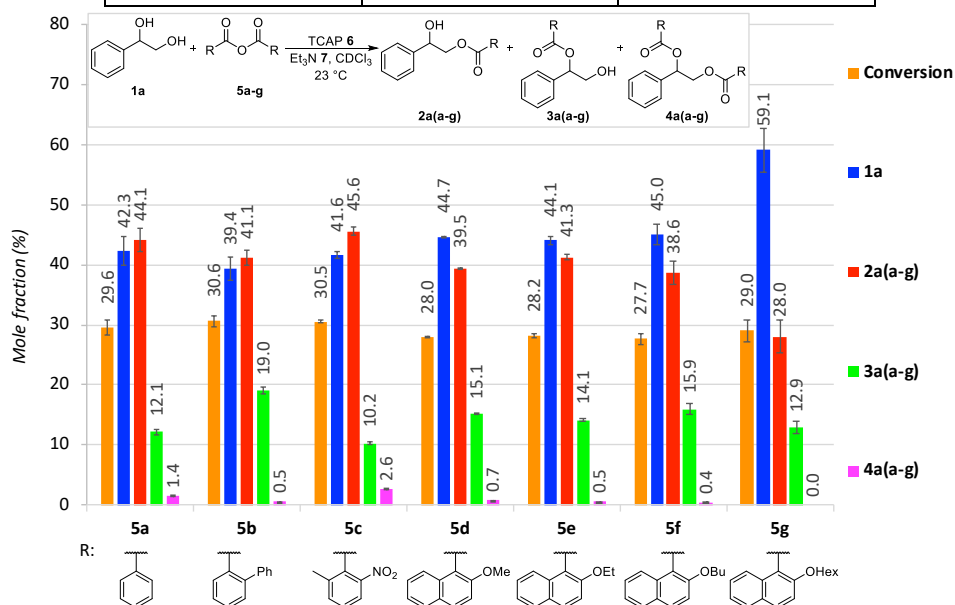


Figure 4.21. Mole fraction (%) of 1a:2a(a-g):3a(a-g):4a(a-g) and total conversion (%) for turnover-experiments of 1a with 5a-g at the 30% conversion point.

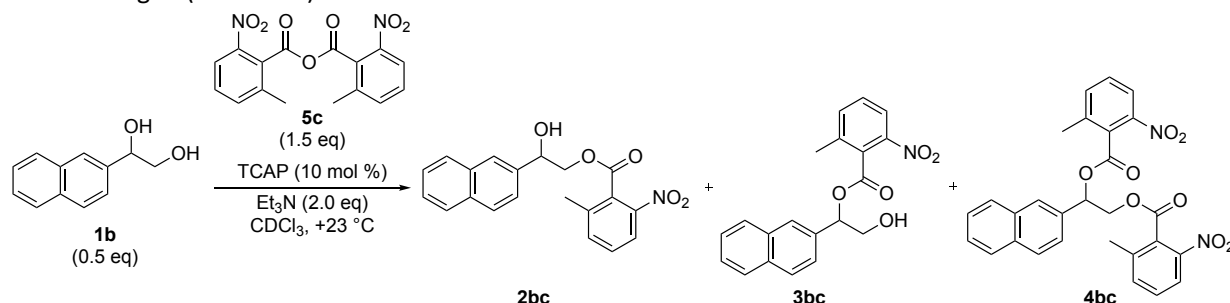
Table 4.10. Comparison of $k_{rel,a}$ by different validation methods for turnover-limited competition experiments of **1a** with **5a-g**.

Anhydride	$k_{rel,a30\%}$	$k_{rel,a}$
5a	3.64 ± 0.040	3.68
5b	2.17 ± 0.005	2.16
5c	4.46 ± 0.120	4.69
5d	2.61 ± 0.018	2.74
5e	2.92 ± 0.025	2.99
5f	2.43 ± 0.177	2.63
5g	2.13 ± 0.266	2.46

4.1.2 Absolute Kinetic Studies of Aryl Substituted 1,2-Ethanediols

4.1.2.1 Experimental Design

In the following, a general guideline for the performance of an absolute kinetic experiment is described, based on the experiment shown in Scheme 4.6. Three different $CDCl_3$ stock solutions, consisting of 0.02 M 1,2-diol **1b** (A), 0.06 M acid anhydride **5c** (B) and a combination of 0.08 M Et_3N and 0.004 M TCAP (C) are prepared under nitrogen (method A).

**Scheme 4.6.** Model example for an absolute kinetic experiment of **1b** with **5c**.**Table 4.11.** Preparation of initial $CDCl_3$ stock solutions (Method A).

Stock solution	Compound	Concentration (mol L ⁻¹)	Volume (mL)	n (mol)	M.W. (g mol ⁻¹)	Mass (mg)
Stock A	1b	0.02	1	$20 \cdot 10^{-6}$	188	3.8
Stock B	5c	0.06	1	$60 \cdot 10^{-6}$	344	20.6
Stock C	Et_3N	0.08	2	$160 \cdot 10^{-6}$	101	16.2
	TCAP	0.004	2	$8 \cdot 10^{-6}$	174	1.4

For acid anhydride derivative like **5a** a lower concentration of catalyst TCAP is used (Method B, Table 4.12):

Table 4.12. Preparation of initial $CDCl_3$ stock solutions (Method B).

Stock solution	Compound	Concentration (mol L ⁻¹)	Volume (mL)	n (mol)	M.W. (g mol ⁻¹)	Mass (mg)
Stock A	1b	0.02	1	$20 \cdot 10^{-6}$	188	3.8
Stock B	5a	0.06	1	$60 \cdot 10^{-6}$	344	20.6
Stock C	Et_3N	0.08	20	$1.6 \cdot 10^{-3}$	101	16.2
	TCAP	0.0004	20	$8 \cdot 10^{-6}$	174	1.4

The reaction is analysed by 1H NMR recorded by Bruker Avance III 400 machines. NMR tubes are dried under vacuum using a Schlenk based glassware and flushed with nitrogen. 0.2 mL of Stock A, 0.2 mL of Stock C and 0.2 mL of Stock B are transferred under nitrogen to the NMR tube by using a Hamilton syringe. After closing the NMR tubes, the reaction mixture is shaken and put in the NMR machine. Because of the low concentration of the reaction mixtures for each 1H NMR spectrum, 32 scans are recorded.

In terms of the actual starting concentrations (mol/L) for all components:

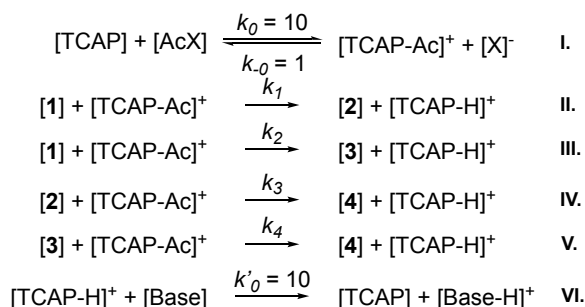
NMR Tube: 1b: 0.00667, **5c:** 0.02000, **Et_3N :** 0.02667, **TCAP:** 0.00133

NMR Tube: 1b: 0.00667, **5a:** 0.02000, **Et_3N :** 0.02667, **TCAP:** 0.00013

The following procedure is equivalent to the procedure explained in Chapter 4.1.1.1.

4.1.2.2 Simulation of the Absolute Kinetics Experiments

With the help of the CoPaSi^[2] and Origin programs, the $k_1 - k_4$ values for the turnover-limited competition experiments have been fitted and simulated. Scheme 4.7 shows the reactions for the fitting and simulations used in CoPaSi.



Scheme 4.7. Model reaction used in CoPaSi for the fitting and subsequently simulation of the rate constants.

Before the fitting process was started the values of k_0 , k_{-0} (I.) and k'_0 (VI.) has to set. Although in the literature it is reported that the equilibrium in the catalyst loading step (I.) should be on the left side with acid anhydride reagents,^[5] we state this equilibrium to be on the right side by defining $k_0 = 10$ and $k_{-0} = 1$. This fixation is reasonable because the loaded catalyst cation intermediat “[TCAP-Ac]⁺” is visible in the ¹H NMR for most of our acid anhydride derivatives. The effective rate for catalyst recovery was also fixed with $k'_0 = 10$. k_0 , k_{-0} (I.) and k'_0 (VI.) was not changed during the fitting process to guarantee a reproducibility and comparability of the acylation reaction. For the fitting the actual starting concentrations of **1b** (0.0067 M), **5c** (0.020 M), Et₃N (0.0267 M) and TCAP (0.0013 M) are specified (Method A). In the absolute kinetic model for Method B the concentration of TCAP was adjusted (0.00013 M).

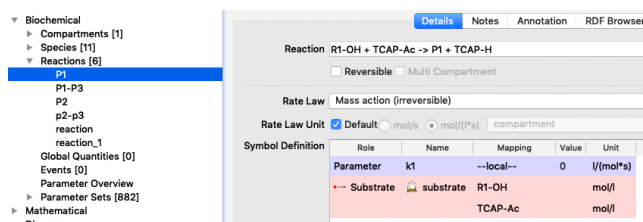
The fitting-process has to be separated into four steps, based on the “two-step” process of first- and second acylation and that the rate constants affecting each other. In Table 4.13, each single fit and the associated modifications are shown and discussed in the following:

Table 4.13. Procedure for fitting of $k_1 - k_4$ in CoPaSi in an absolut kinetic study.

Fit	k_x always constant	k_x modified	Fitted k_x	Fitted Reaction	Fitted compound
1	k_0, k_{-0}, k'_0	k_3 and $k_4 = 0$	k_1 and k_2 start value =0	II. and III.	1, 2 and 3
2	k_0, k_{-0}, k'_0	k_1 and $k_2 = \text{Fit 1}$	k_3 and k_4 start value =0	IV. and V.	2, 3 and 4
3	k_0, k_{-0}, k'_0	k_3 and $k_4 = \text{Fit 2}$	k_1 and k_2 start value =0	II. and III.	1, 2 and 3
4	k_0, k_{-0}, k'_0	k_1 and $k_2 = \text{Fit 3}$	k_3 and k_4 start value =0	IV. and V.	2, 3 and 4

In the 1st fit all effective rate constants $k_1 - k_4$ are initially set as 0, as the method the “Differential Evolution” is chosen and the fit runs only once (Scheme 4.8a). k_1 (II.) and k_2 (III.) are fitted, by taking **1**, **2** and **3** as dependent concentrations and only the values up to the highest concentrations of **2** or **3** were performed (CoPaSi Parameter estimation: dependent). The concentration of **4** is excluded in the 1st fit, because in the first acylation no diester is formed (CoPaSi Parameter estimation: ignored). As start value k_1 and $k_2 = 0$ was set and the 1. fit was allowed to run (Figure 4.22 and 24a).

1st Fit: Reactions:
II.-V., $k_1 - k_4 = 0$



1st Fit: Parameter estimation:
1, 2, and 3 dependent
4 ignored

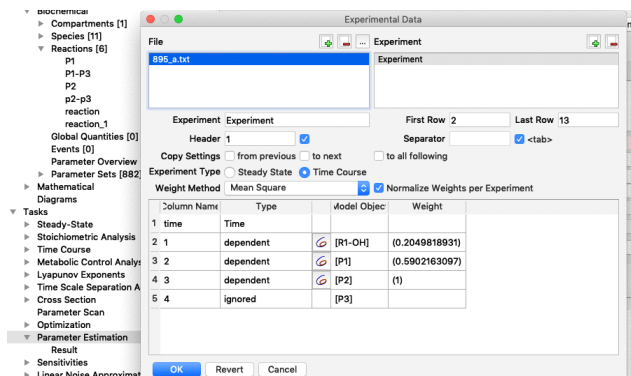
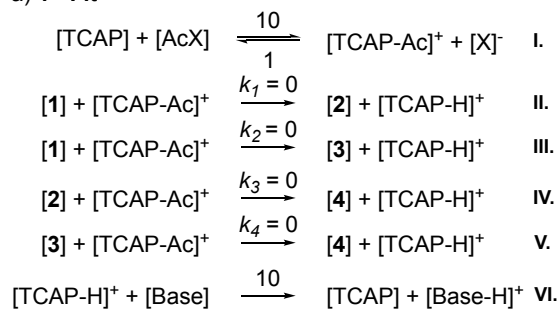


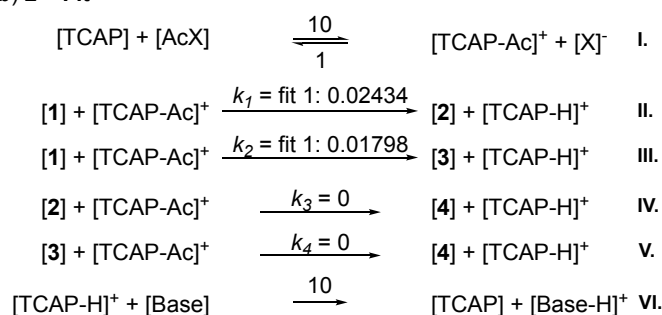
Figure 4.22. Instructions of fitting for the 1st fit in CoPaSi for the absolute kinetic experiments.

In the 2nd fit, effective rate constants k_3 and k_4 are still set as 0, effective rate constants k_1 and k_2 are defined through Fit 1, as method the “Differential Evolution” is chosen and the fit runs only once (Scheme 4.8b).

a) 1st Fit



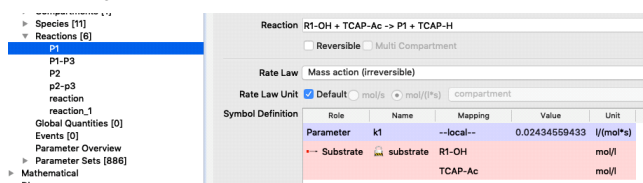
b) 2nd Fit



Scheme 4.8. Model reaction used in CoPaSi for the a) 1st Fit and b) 2nd Fit.

k_3 and k_4 are fitted, by taking 2, 3 and 4 as dependent concentrations and all measured concentration points are used this time (CoPaSi Parameter estimation: dependent). The concentration of 1 is excluded, because in the second acylation the diol is not existence (CoPaSi Parameter estimation: ignored). As starting value k_3 and $k_4 = 0$ was set and the 2nd fit was allowed to run (Figure 4.23 and 24b).

2nd Fit: Reactions:
II., III., $k_1, k_2 = \text{Fit 1}$
III., IV., $k_3, k_4 = 0$



2nd Fit: Parameter estimation:
2, 3 and 4 dependent
1 ignored

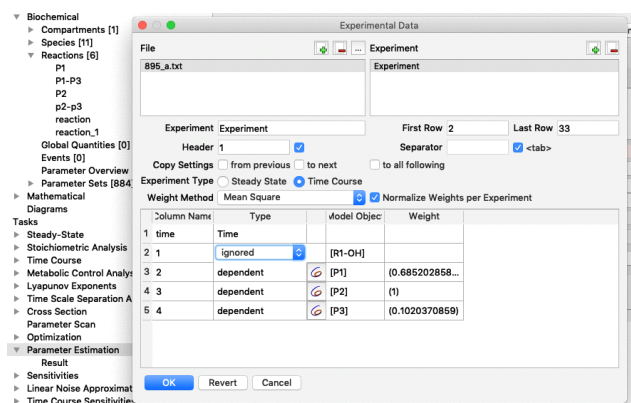


Figure 4.23. Instructions of fitting for the 2nd fit in CoPaSi for the absolute kinetic experiments.

Size-Induced Inversion of Selectivity in the Acylation of 1,2-Diols

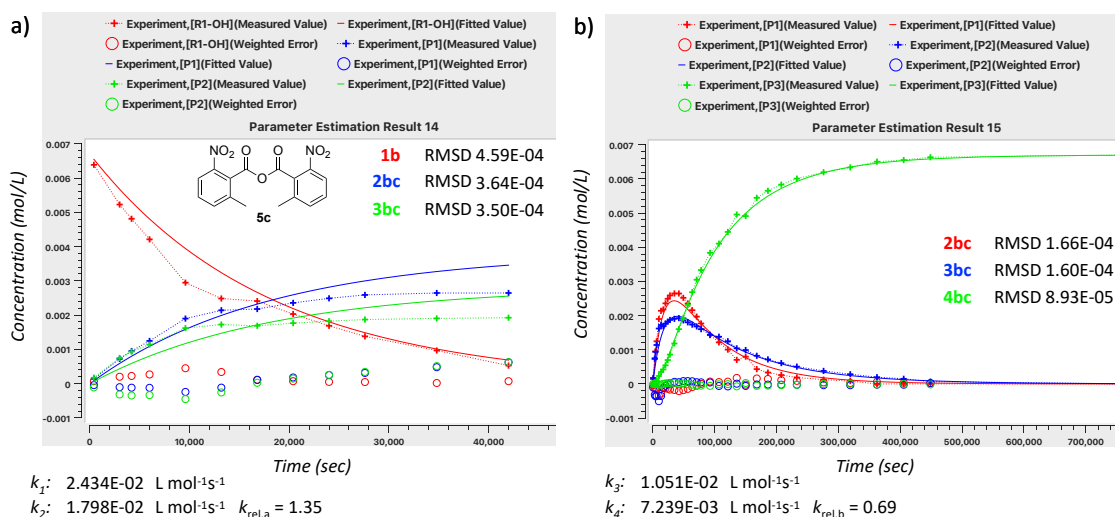


Figure 4.24. Plot of time (sec) vs. concentration (mol/L) for **1b** with **5c** for measurement 1 fitted by CoPaSi. a) Fitting of rate constants k_1 and k_2 up to the highest concentration of **2bc** (1st Fit). b) Fitting of rate constants k_3 and k_4 (2nd Fit).

In the additional fits, we are doing a so called “refitting”, because k_3 and k_4 influence the fitted values of k_1 and k_2 .

In the 3rd fit, effective rate constants k_1 and k_2 are defined through fit 1, the effective rate constants k_3 and k_4 are defined through fit 2 “Differential Evolution” is chosen and the fit runs only for one time (Scheme 4.9a). k_1 and k_2 are fitted, by taking **1**, **2** and **3** as dependent concentrations and only the values up to the highest concentration of **2** or **3** were considered (CoPaSi Parameter estimation: dependent). The concentration of **4** is excluded again in the 3rd fit (CoPaSi Parameter estimation: ignored). As starting value k_1 and $k_2 = 0$ was set and the 3rd fit was allowed to run (Figure 4.25 and 27a).

3rd Fit: Reactions:

- II., III., $k_1, k_2 = \text{Fit 1}$
- III., IV., $k_3, k_4 = \text{Fit 2}$

3rd Fit: Parameter estimation:

- 1, 2**, and **3** dependent
- 4** ignored
- Start values: $k_1, k_2 = 0$

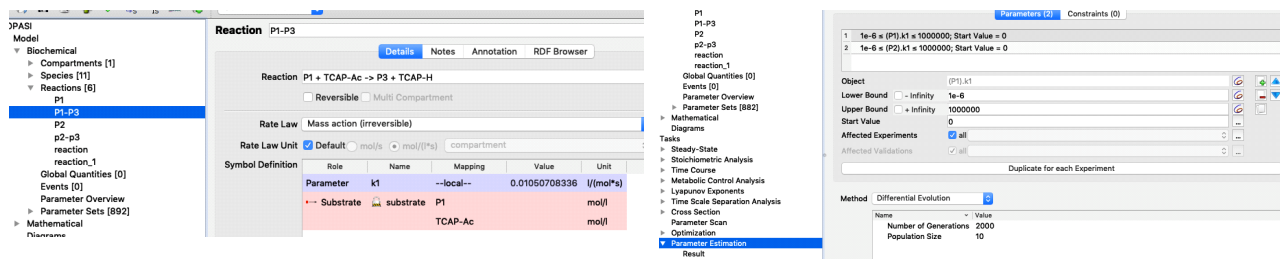
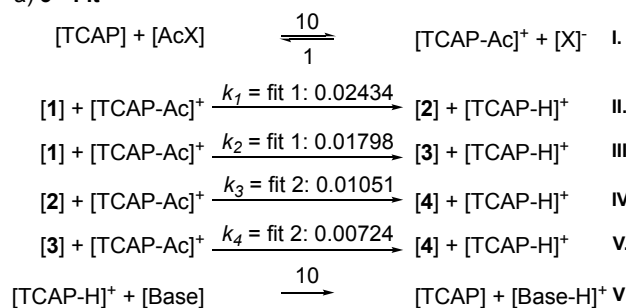
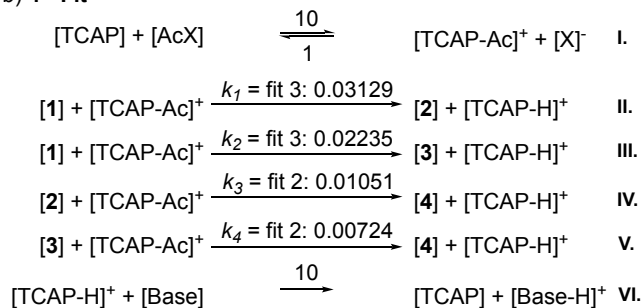


Figure 4.25. Instructions of fitting for the 3rd fit in CoPaSi for the absolute kinetic experiments.

a) 3rd Fit



b) 4th Fit



Scheme 4.9. Model reaction used in CoPaSi for the a) 3rd Fit with effective rate constants k_1/k_2 defined by the 1st fit and k_3/k_4 defined by the 2nd fit and b) 4th Fit with effective rate constants k_1/k_2 defined by the 3rd fit and k_3/k_4 defined by the 2nd.

In the 4th fit, effective rate constants k_1/k_2 are defined through fit 3, effective rate constants k_3/k_4 are defined through fit 2, as method the “Differential Evolution” is chosen and the fit runs only for one time (Scheme 4.9b). k_3 and k_4 are fitted, by taking **2**, **3** and **4** as dependent concentrations and all measured concentration

points are used this time (CoPaSi Parameter estimation: dependent). The concentration of **1** is again excluded in the 4th fit (CoPaSi Parameter estimation: ignored). As starting value $k_3/k_4 = 0$ was set and the 4th fit was allowed to run (Figure 4.26 and 27b).

4th Fit: Reactions:
II., III., k_3 , k_2 = Fit 3
III., IV., k_3 , k_4 = Fit 2

4th Fit: Parameter estimation:
2,3 and 4 dependent
1 ignored
 Start values: $k_3, k_4 = 0$

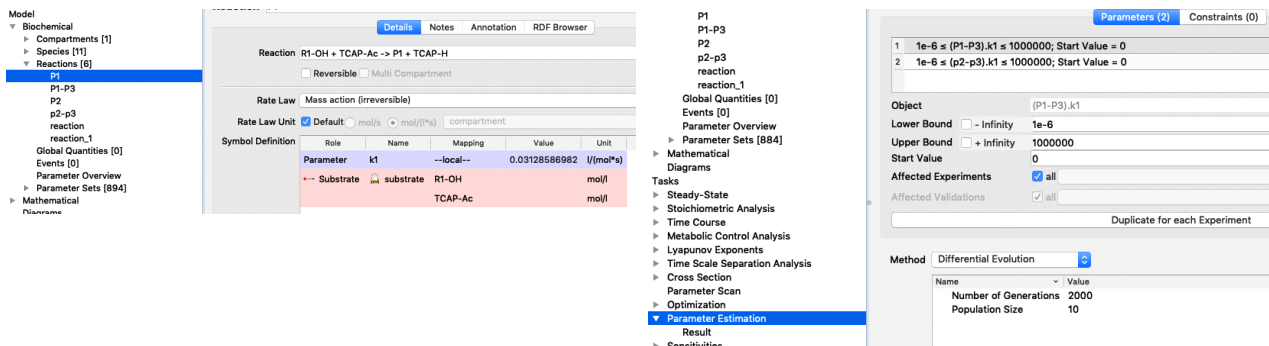


Figure 4.26. Instructions of fitting for the 4th fit in CoPaSi for the absolute kinetic experiments.

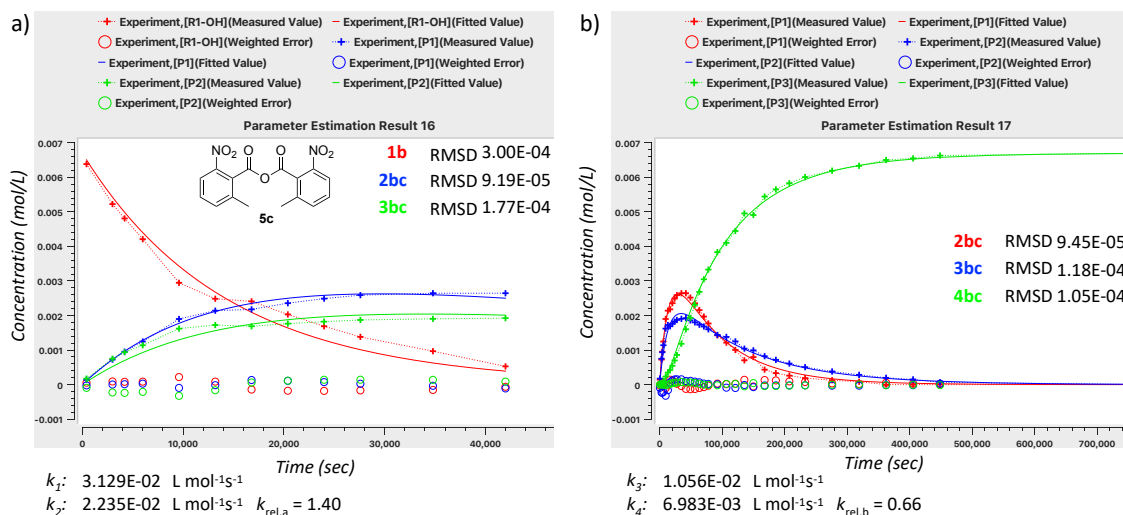


Figure 4.27. Plot of time (sec) vs. concentration (mol/L) for **1b** with **5c** for measurement 1 fitted by CoPaSi. a) Fitting of rate constants k_1 and k_2 up to the highest concentration of **2bc** (3rd Fit). b) Fitting of rate constants k_3 and k_4 (4th fit).

The now final fitted effective rate constants $k_1 - k_4$ are used for simulating the reaction by CoPaSi. The simulated concentrations over the time were used to calculate the conversion by Eq. 4.4 and mole fractions by Eq. 4.5-4.8. The time (sec) or the conversion (%) was plotted against the mole fractions, obtained by experiments and numerical simulations to verify the simulated effective rate constants (Figure 4.28)

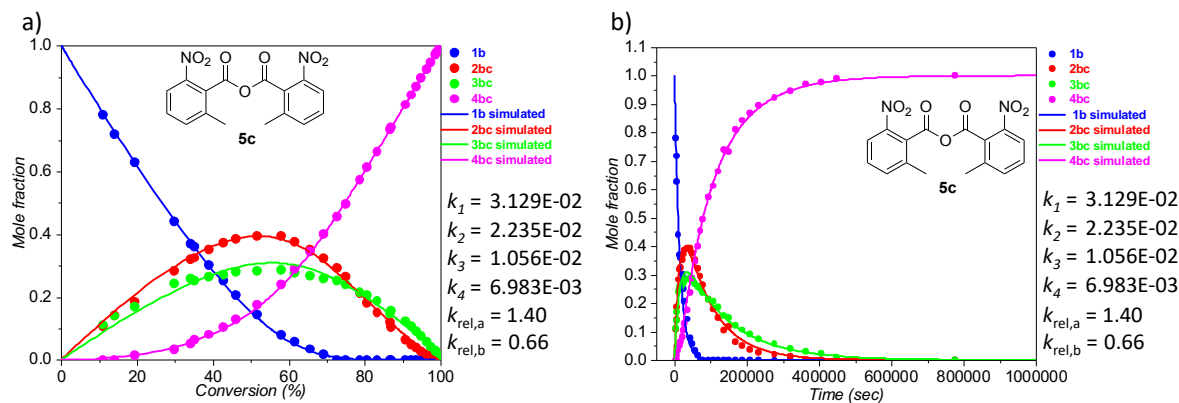
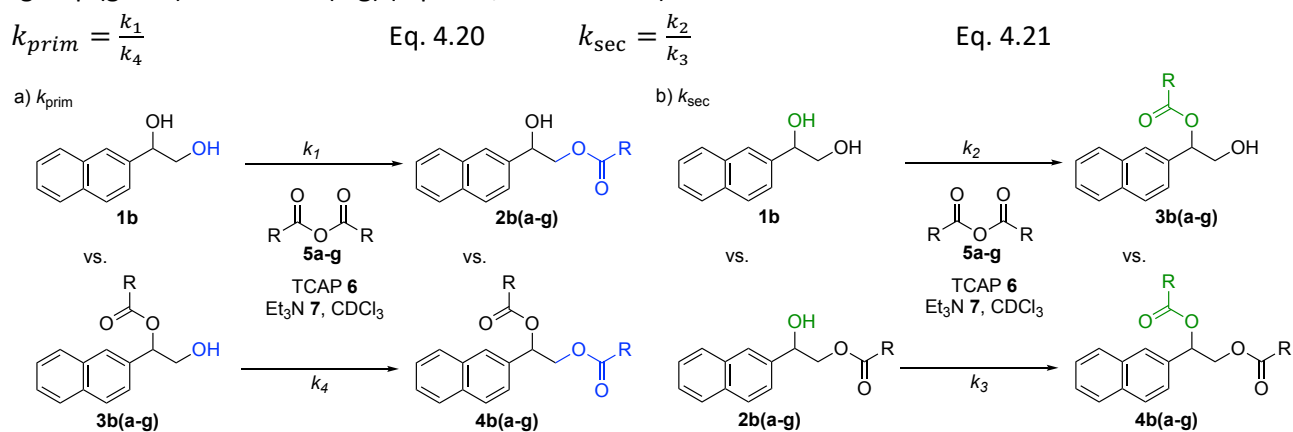


Figure 4.28. a) Plot of time (sec) vs. mole fraction and b) plot of conversion (%) vs. mole fraction for **1b** with **5c**. The rate constants $k_1 - k_4$ are given in L mol⁻¹s⁻¹.

Size-Induced Inversion of Selectivity in the Acylation of 1,2-Diols

In Figures 4.30 to 4.52 the *total conversion (%)* or the *time (sec)* was plotted against the *mole fraction*, which allows us the illustrative comparison of experimental and simulated results. Figures 4.29, 4.43 and 4.48 show the plot of *time (sec)* over the *total conversion (%)* of all OH groups in the system. For acid anhydride **5b** we were not measuring the absolute kinetic, because **5b** already performs as fast as **5a** in the separated ethanol system from our previous studied system^[1] and the first acylation of the 1,2 diol **1b** is very fast already with **5a**, even with 1 mol% of catalyst. This make it difficult to allow accurate determination of the effective rate. For the 2-substituted 1-naphthoic anhydrides **5d-g**, mainly for over 90 % conversion, the relative mole fractions do not plot well anymore with the simulated mole fractions. We believe that some hydrolysis processes started, which is influencing the effective rate constants of our second acylations. Because these competing side reactions start influence the system after more or less than one week and to leave the fitting process as simple as possible, we decided to neglect this hydrolysis process in our simulations. In Table 4.14 the fitted rate constants $k_1 - k_4$ are shown as well as the corresponding relative rate constants $k_{rel,a}$ and $k_{rel,b}$. Because of the measured effective rate constants $k_1 - k_4$ we can also make a statement of how much the hydrogen bonding of a second OH-group in the system in comparison to a protected further OH-group is influencing the acylation of the primary OH-group (blue) in **1b** vs. **3b(a-g)** (Eq. 4.20) and of the secondary OH-group (green) in **1b** vs. **2b(a-g)** (Eq. 4.21, Scheme 4.10).



Scheme 4.10. General equation for k_{prim} and k_{sec} for the acylation of **1b** with **5a-g**.

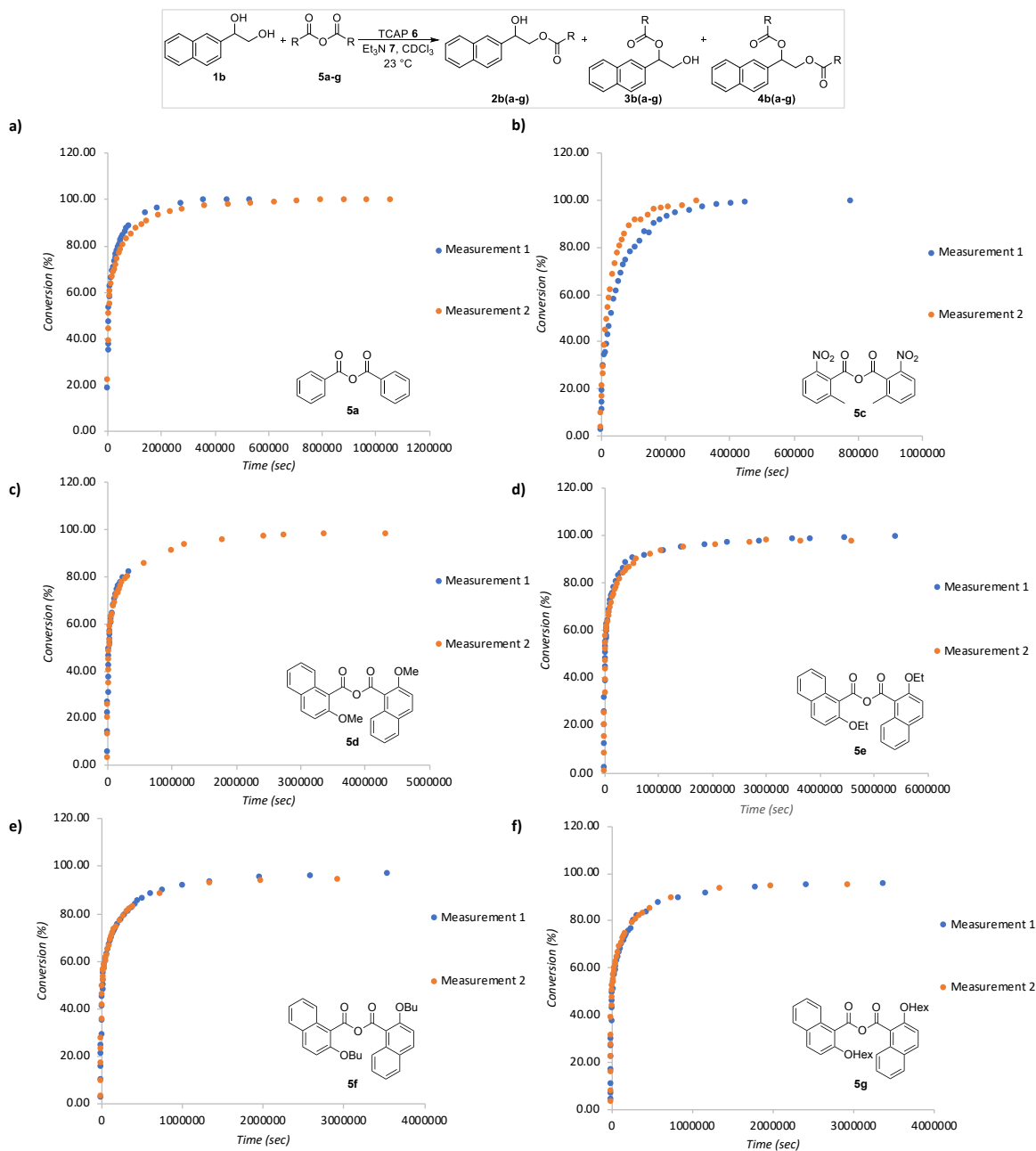


Figure 4.29. Plot of time (sec) vs. conversion (%) of all OH-groups for **1b** with a) **5a**, b) **5c**, c) **5d**, d) **5e**, e) **5f** and f) **5g**.

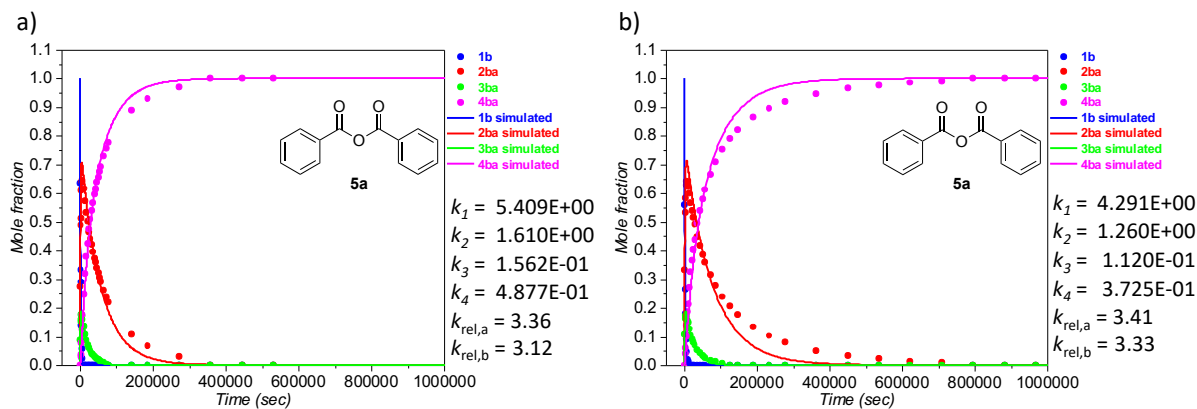


Figure 4.30. Plot of time (sec) vs. mole fraction for **1b** with **5a** for a) measurement 1 and b) measurement 2 (Method B). The effective rate constants $k_1 - k_4$ are given in $\text{L mol}^{-1} \text{s}^{-1}$.

Size-Induced Inversion of Selectivity in the Acylation of 1,2-Diols

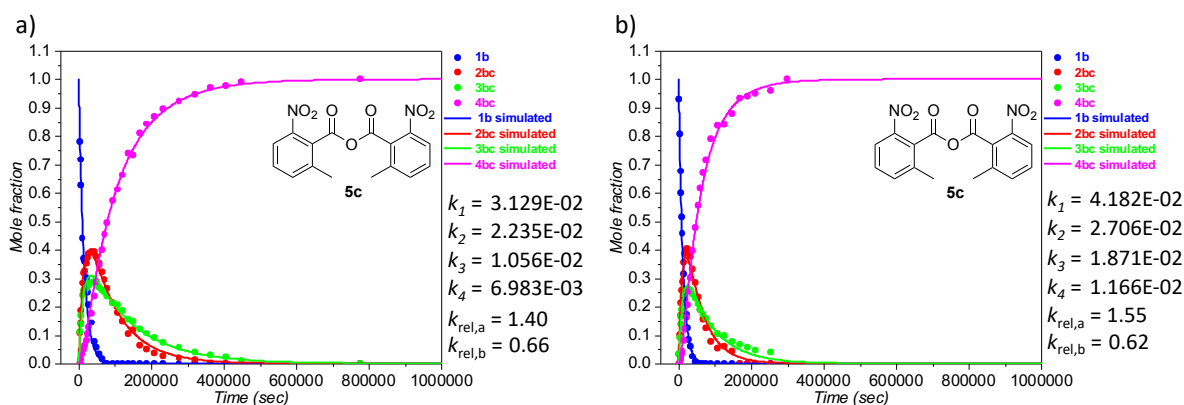


Figure 4.31. Plot of time (sec) vs. mole fraction for **1b** with **5c** for a) measurement 1 and b) measurement 2 (Method A). The effective rate constants $k_1 - k_4$ are given in L mol⁻¹ s⁻¹.

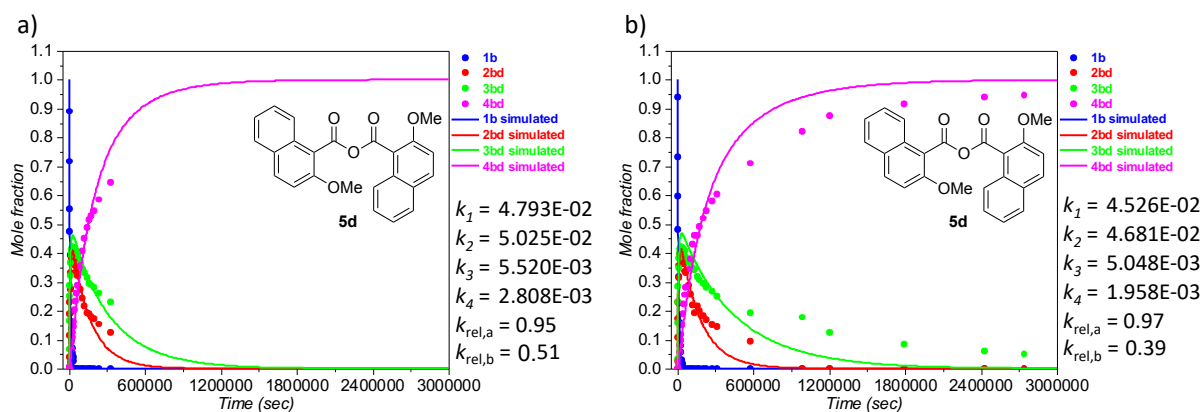


Figure 4.32. Plot of time (sec) vs. mole fraction for **1b** with **5d** for a) measurement 1 and b) measurement 2 (Method A). The effective rate constants $k_1 - k_4$ are given in L mol⁻¹ s⁻¹.

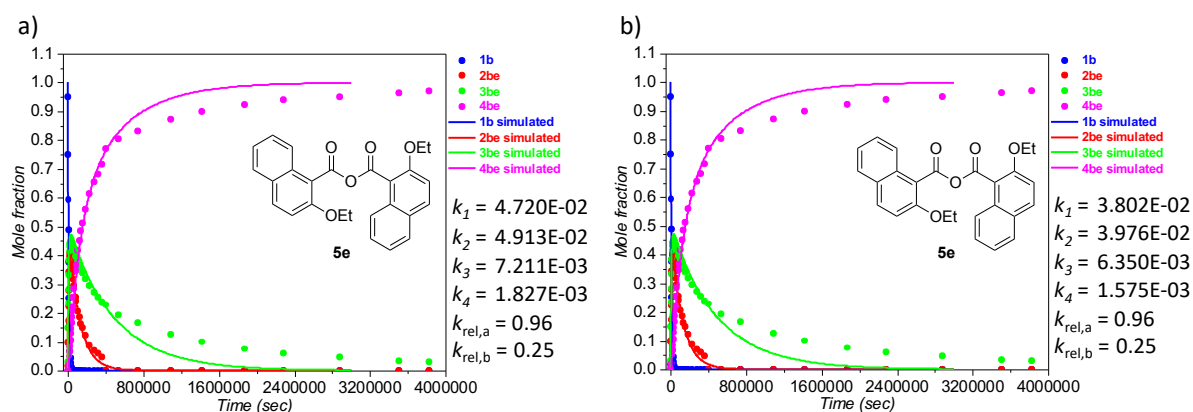


Figure 4.33. Plot of time (sec) vs. mole fraction for **1b** with **5e** for a) measurement 1 and b) measurement 2 (Method A). The effective rate constants $k_1 - k_4$ are given in L mol⁻¹ s⁻¹.

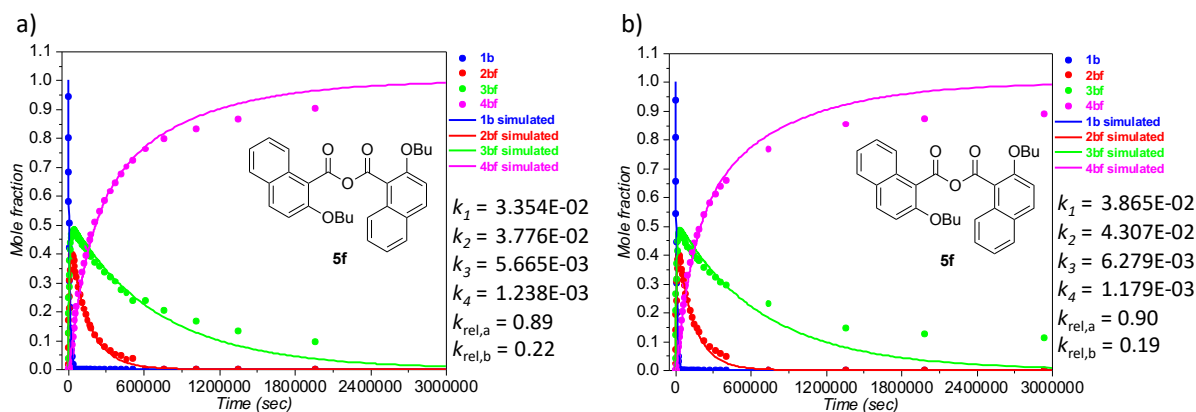


Figure 4.34. Plot of time (sec) vs. mole fraction for **1b** with **5f** for a) measurement 1 and b) measurement 2 (Method A). The effective rate constants $k_1 - k_4$ are given in $L mol^{-1} s^{-1}$.

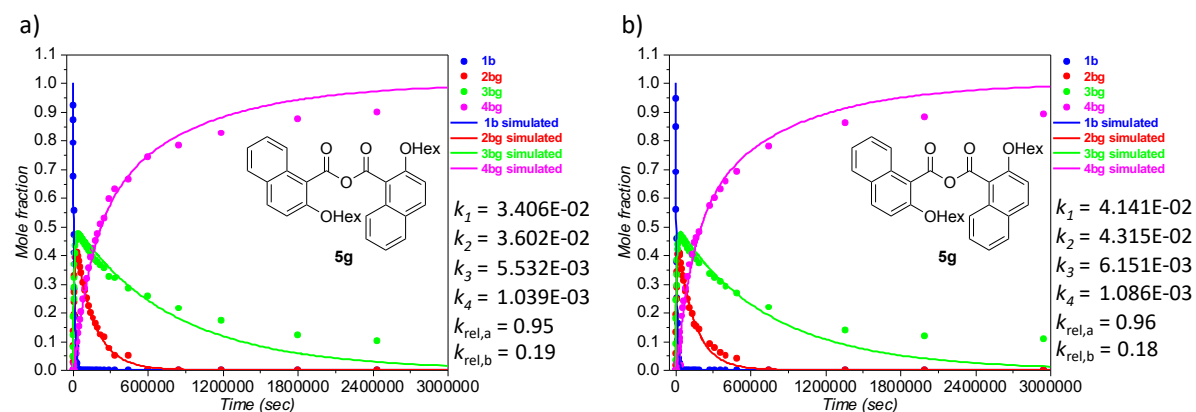


Figure 4.35. Plot of time (sec) vs. mole fraction for **1b** with **5g** for a) measurement 1 and b) measurement 2 (Method A). The effective rate constants $k_1 - k_4$ are given in $L mol^{-1} s^{-1}$.

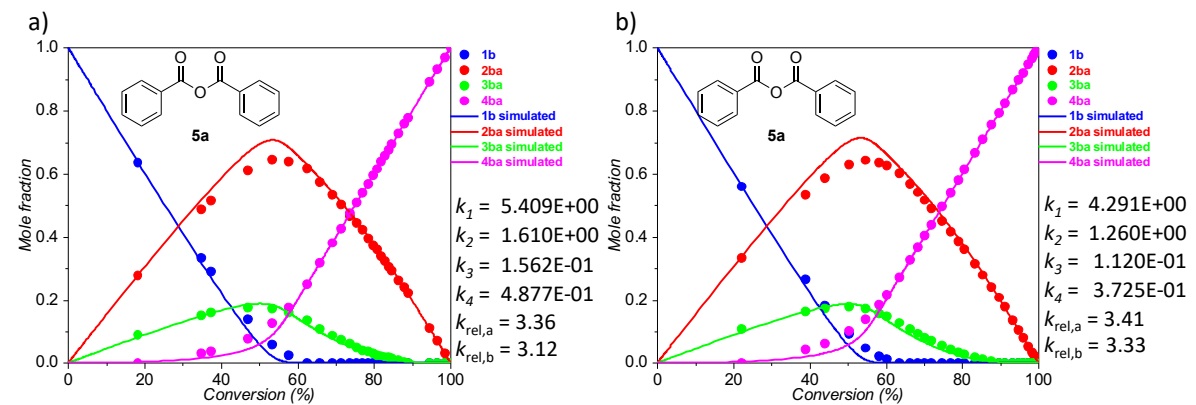


Figure 4.36. Plot of conversion (%) vs. mole fraction for **1b** with **5a** for a) measurement 1 and b) measurement 2 (Method B). The effective rate constants $k_1 - k_4$ are given in $L mol^{-1} s^{-1}$.

Size-Induced Inversion of Selectivity in the Acylation of 1,2-Diols

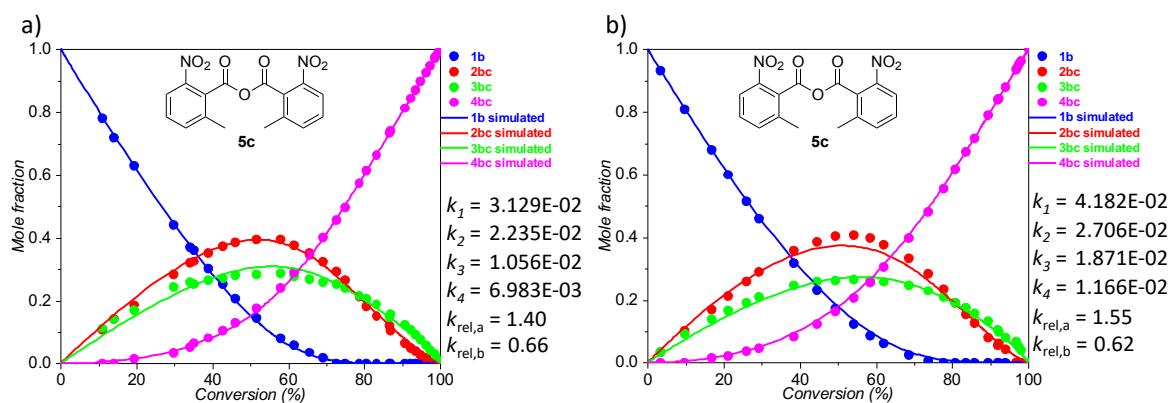


Figure 4.37. Plot of conversion (%) vs. mole fraction for **1b** with **5c** for a) measurement 1 and b) measurement 2 (Method A). The effective rate constants $k_1 - k_4$ are given in $\text{L mol}^{-1} \text{s}^{-1}$.

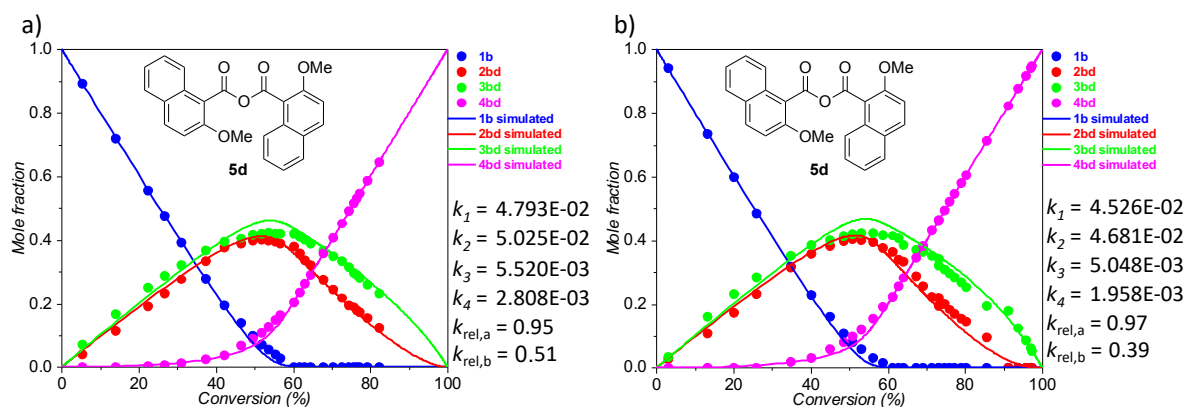


Figure 4.38. Plot of conversion (%) vs. mole fraction for **1b** with **5d** for a) measurement 1 and b) measurement 2 (Method A). The effective rate constants $k_1 - k_4$ are given in $\text{L mol}^{-1} \text{s}^{-1}$.

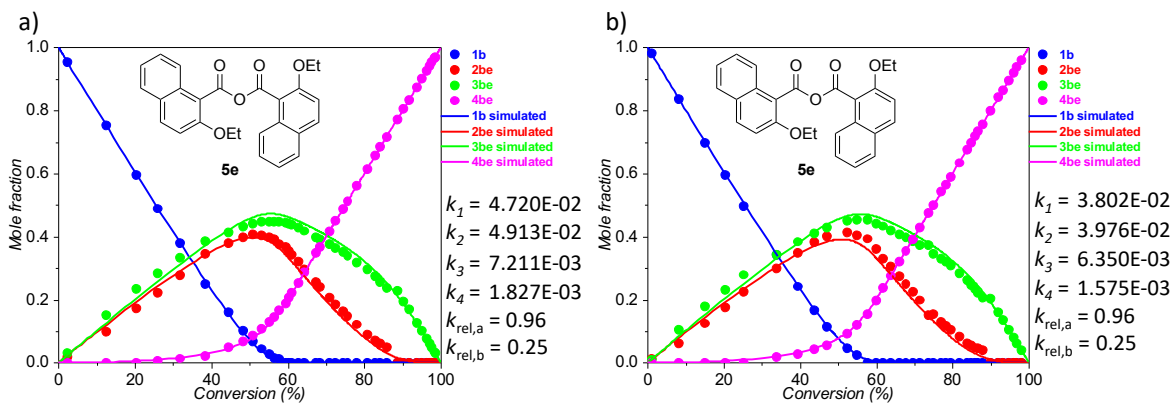


Figure 4.39. Plot of conversion (%) vs. mole fraction for **1b** with **5e** for a) measurement 1 and b) measurement 2 (Method A). The effective rate constants $k_1 - k_4$ are given in $\text{L mol}^{-1} \text{s}^{-1}$.

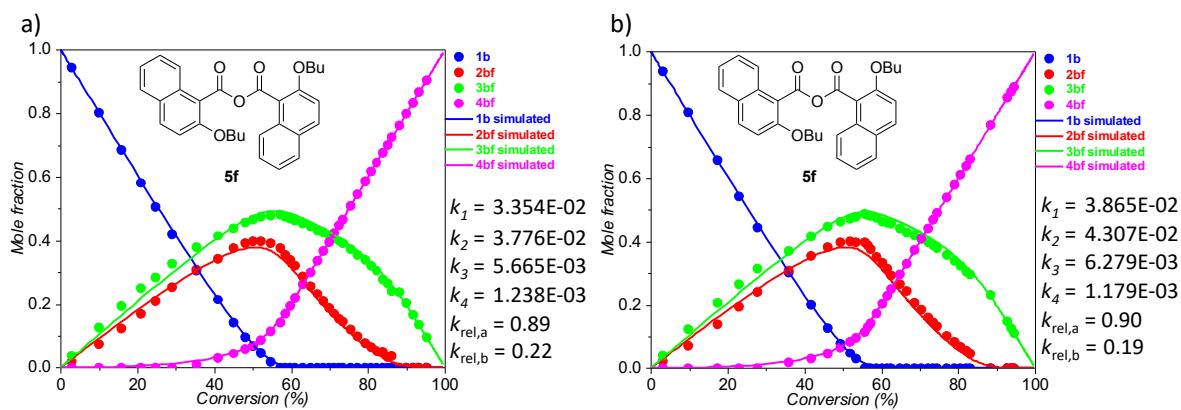


Figure 4.40. Plot of *conversion (%)* vs. *mole fraction* for **1b** with **5f** for a) measurement 1 and b) measurement 2 (Method A). The effective rate constants $k_1 - k_4$ are given in $\text{L mol}^{-1} \text{s}^{-1}$.

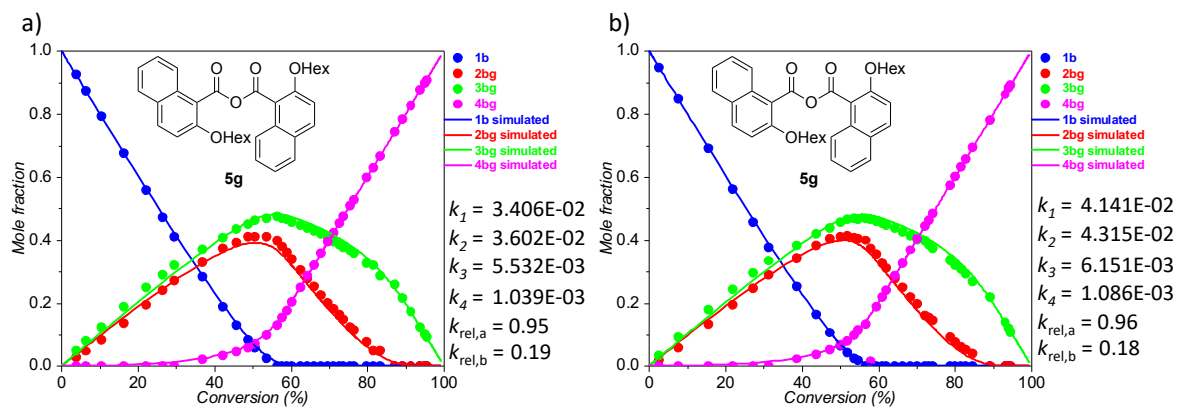


Figure 4.41. Plot of *conversion (%)* vs. *mole fraction* for **1b** with **5g** for a) measurement 1 and b) measurement 2 (Method A). The effective rate constants $k_1 - k_4$ are given in $\text{L mol}^{-1} \text{s}^{-1}$.

Size-Induced Inversion of Selectivity in the Acylation of 1,2-Diols

Despite a high catalyst loading of 10 mol% the acylation of diol **1b** with anhydrides **5c-g** is comparatively to **5a** slow in absolute terms, which suggest to highly differential sterical hinderances. About which relative rate $k_{rel,5a}$ the effective rates of **5a** are faster than the bulky anhydrides **5c-g** are determined by the ratio between the effective rate constants of **5a** $k_{eff,5a}$ and the effective rate constants of **5c-g** $k_{eff,5c-g}$ (Eq. 4.22). The effective rate constant of **5a** was multiplied with 10. The absolute kinetics with **5a** were performed with 1 mol% TCAP, whereby the absolute kinetics with **5c-g** were performed with 10 mol% TCAP

$$k_{rel,5a} = \frac{k_{eff,5a} \cdot 10}{k_{eff,5c-g}} \quad \text{Eq. 4.22}$$

In Figure 4.42 the decrease in speed is shown for the effective rate constants $k_1 - k_4$ of the different bulky anhydrides **5c-g**. Whereby the acylation of the primary alcohols (k_1, k_4) is slowed down about a factor of $k_{rel,5a} > 10000$, except k_4 of **5c** ($k_{rel,5a} = 509$), the effective rate constants of secondary alcohols are less impacted by a factor of only $k_{rel,5a} = 104 - 369$, except k_2 of **5c** ($k_{rel,5a} = 593$). That the effective rates of **5c** occupied a special role is shown in chapter 4.1.5 and are based on the NO₂ – group in the system. Interestingly, the $k_{rel,5a}$ for the second acylation of monoesters **3b(d-g)** are increasing with the side chain of the 1-naphthoic anhydrides **5d-g** from $k_{rel,5a} = 1820$ up to $k_{rel,5a} = 4062$, whereby for $k_1 - k_3$ no strong trendicity is visible. It is suspected, that the acylation of primary alcohols is more depending from repulsive size effects, than the acylation of secondary alcohols. Thus, sterical hindereance is increasing in the second acylation of monoesters **3b(d-g)**.

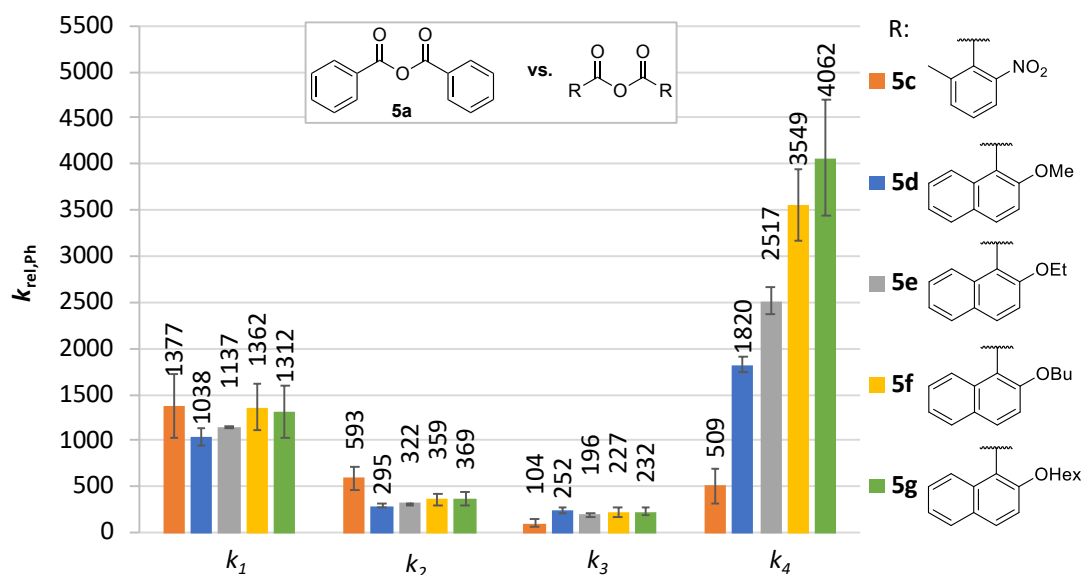


Figure 4.42. Relative rate constant $k_{rel,5a}$ from effective rates $k_1 - k_4$ of anhydrides **5c-g**.

Table 4.15. Relative rate constant $k_{rel,5a}$ from effective rates $k_1 - k_4$ of anhydrides **5c-g**.

Anhydride	k_{eff}	$k_{rel,5a}$ I.	$k_{rel,5a}$ II.	Mean $k_{rel,5a}$
5c	k_1	1728.52	1026.17	1377.34 ± 351.18
	k_2	720.15	465.66	592.90 ± 127.25
	k_3	147.82	59.86	103.84 ± 43.98
	k_4	698.38	319.39	508.88 ± 189.50
5d	k_1	1128.63	948.10	1038.37 ± 90.27
	k_2	320.32	269.21	294.76 ± 25.56
	k_3	282.93	221.81	252.37 ± 30.56
	k_4	1736.97	1902.46	1819.72 ± 82.75
5e	k_1	1146.11	1128.64	1137.37 ± 8.73
	k_2	327.64	316.98	322.31 ± 5.33
	k_3	216.55	176.31	196.43 ± 20.12
	k_4	2669.16	2364.73	2516.95 ± 152.21
5f	k_1	1612.94	1110.36	1361.65 ± 251.29
	k_2	426.34	292.60	359.47 ± 66.87

	k_3	275.65	178.31	226.98 ± 48.67
	k_4	3939.52	3158.71	3549.11 ± 390.41
5g	k_1	1588.07	1036.37	1312.22 ± 275.85
	k_2	446.93	292.07	369.50 ± 77.43
	k_3	282.31	182.01	232.16 ± 50.15
	k_4	4693.62	3429.73	4061.6 ± 8631.95

Table 4.16. Time (sec), conversion total (%) and ratio of **1b:2b(a-g):3b(ag):4b(a-g)** for absolute kinetic measurement of 2-naphthylethane-1,2-diol **1b** with acid anhydride derivatives **5a-g**. Baseline of ^1H NMR for integration was corrected by Whittaker Smoother (I) fit.

Time (sec)	Conv (%)	Ratio (%)				Time (sec)	Conv (%)	Ratio (%)			
Time ^a	Conv _{exp}	1b ^a	2ba ^a	3ba ^a	4ba ^a	time ^a	Conv _{exp}	1b ^a	2ba ^a	3ba ^a	4ba ^a
600	18.20	63.59	27.59	8.82	0.00	900	22.02	55.96	33.23	10.81	0.00
1500	34.87	33.22	48.73	15.09	2.96	2100	38.83	26.46	53.20	16.21	4.13
1680	37.32	29.01	51.40	15.93	3.66	3000	44.03	18.08	58.44	17.34	6.14
2880	46.92	13.83	60.96	17.54	7.67	4500	50.42	9.28	62.78	17.82	10.12
4680	53.38	5.87	64.35	17.15	12.63	6300	54.60	4.72	64.28	17.09	13.91
6480	57.61	2.44	63.93	15.96	17.66	8700	58.17	2.21	63.48	15.77	18.55
10080	62.47	0.00	61.59	13.47	24.93	10200	60.11	1.25	62.48	14.81	21.47
13680	65.91	0.00	57.36	10.83	31.81	13800	63.61	0.00	60.03	12.74	27.22
17280	69.02	0.00	53.22	8.74	38.04	17400	66.29	0.00	56.78	10.63	32.59
20880	71.28	0.00	50.19	7.25	42.56	21000	68.29	0.00	54.09	9.34	36.57
24480	73.71	0.00	46.55	6.02	47.43	24600	70.15	0.00	51.64	8.07	40.30
28080	75.39	0.00	44.25	4.97	50.77	28200	71.91	0.00	49.09	7.09	43.82
31680	76.93	0.00	42.11	4.03	53.86	35400	74.78	0.00	44.89	5.54	49.56
35280	78.41	0.00	39.56	3.63	56.81	42600	77.00	0.00	41.68	4.32	54.00
38880	79.80	0.00	37.42	2.98	59.61	49800	78.97	0.00	38.65	3.42	57.93
42480	80.75	0.00	35.96	2.55	61.49	57000	80.63	0.00	35.94	2.81	61.26
46080	81.88	0.00	33.98	2.25	63.77	71400	83.32	0.00	31.50	1.86	66.64
49680	82.82	0.00	32.41	1.94	65.65	85800	85.43	0.00	27.85	1.28	70.87
53280	83.80	0.00	30.57	1.83	67.60	103800	87.71	0.00	23.94	0.64	75.42
56880	84.68	0.00	29.18	1.45	69.37	125400	89.61	0.00	20.79	0.00	79.21
64080	86.45	0.00	26.15	0.95	72.90	147000	91.13	0.00	17.74	0.00	82.26
71280	87.87	0.00	23.90	0.35	75.74	190200	93.30	0.00	13.40	0.00	86.60
78480	88.91	0.00	22.18	0.00	77.82	233400	94.84	0.00	10.33	0.00	89.67
142080	94.51	0.00	10.98	0.00	89.02	276600	95.96	0.00	8.09	0.00	91.91
185280	96.54	0.00	6.92	0.00	93.08	363000	97.39	0.00	5.22	0.00	94.78
271680	98.46	0.00	3.07	0.00	96.93	449400	98.30	0.00	3.41	0.00	96.59
358080	100	0.00	0.00	0.00	100.00	535800	98.82	0.00	2.35	0.00	97.65
444480	100	0.00	0.00	0.00	100.00	622200	99.30	0.00	1.41	0.00	98.59
530880	100	0.00	0.00	0.00	100.00	708600	99.56	0.00	0.88	0.00	99.12
						795000	100.00	0.00	0.00	0.00	100.00
						881400	100.00	0.00	0.00	0.00	100.00
						967800	100.00	0.00	0.00	0.00	100.00
						1054200	100.00	0.00	0.00	0.00	100.00
Time ^b	Conv _{exp}	1b ^b	2bc ^b	3bc ^b	4bc ^b	time ^b	Conv _{exp}	1b ^b	2bc ^b	3bc ^b	4bc ^b
420	2.35	95.29	2.11	2.60	0.00	600	3.44	93.12	3.43	3.45	0.00
3000	11.00	78.00	10.81	11.19	0.00	2400	9.68	80.64	10.14	9.22	0.00
4200	14.10	71.80	14.22	13.98	0.00	4200	16.83	67.71	16.95	13.97	1.37
6000	19.34	62.85	18.61	17.00	1.54	6000	21.09	59.96	21.34	16.55	2.15
9600	29.74	43.99	28.35	24.19	3.46	7800	25.98	51.57	25.80	19.11	3.52
13200	34.06	37.09	31.95	25.75	5.21	9600	29.34	45.80	28.86	20.87	4.48
16800	35.17	35.97	32.51	25.20	6.31	13200	38.29	31.66	35.61	24.49	8.24
20400	38.91	30.32	35.19	26.36	8.14	16800	44.53	23.14	38.66	25.99	12.21
24000	42.61	25.21	37.16	27.21	10.42	20400	49.42	17.34	40.25	26.22	16.19
27600	46.10	20.61	38.65	27.93	12.81	24000	54.09	12.43	40.58	26.38	20.61

Size-Induced Inversion of Selectivity in the Acylation of 1,2-Diols

34800	51.60	14.44	39.49	28.42	17.64	27600	58.53	8.51	39.69	26.23	25.58
42000	58.02	7.88	39.49	28.72	23.91	31200	62.06	6.25	37.68	25.71	30.37
49200	61.51	5.81	37.60	27.75	28.84	38400	68.57	2.55	33.20	24.56	39.70
56400	65.50	3.49	35.13	26.90	34.48	45600	73.61	0.71	28.44	22.92	47.93
63600	69.12	1.84	32.20	25.89	40.07	52800	77.80	0.00	23.40	21.01	55.59
70800	72.75	0.00	29.39	25.10	45.51	60000	80.87	0.00	19.11	19.14	61.74
78000	74.85	0.00	26.41	23.89	49.70	67200	83.55	0.00	15.48	17.43	67.10
92400	78.62	0.00	21.29	21.46	57.24	74400	85.74	0.00	12.69	15.83	71.48
106800	80.63	0.00	18.13	20.61	61.25	88800	89.47	0.00	7.94	13.13	78.94
121200	83.18	0.00	14.97	18.66	66.37	106800	91.96	0.00	5.51	10.56	83.93
135600	86.98	0.00	10.49	15.54	73.97	124800	92.12	0.00	6.04	9.72	84.24
150000	86.64	0.00	11.92	14.80	73.29	146400	93.95	0.00	4.27	7.83	87.90
168000	90.63	0.00	6.46	12.28	81.26	168000	96.68	0.00	0.00	6.65	93.35
186000	92.17	0.00	4.95	10.70	84.34	189600	97.05	0.00	0.00	5.89	94.11
207600	93.51	0.00	3.87	9.10	87.03	211200	97.59	0.00	0.00	4.83	95.17
232800	94.82	0.00	2.81	7.54	89.65	254400	98.04	0.00	0.00	3.92	96.08
276000	96.22	0.00	1.89	5.67	92.44	297600	100.00	0.00	0.00	0.00	100.00
319200	97.27	0.00	1.23	4.23	94.54						
362400	98.53	0.00	0.00	2.94	97.06						
405600	98.88	0.00	0.00	2.24	97.76						
448800	99.49	0.00	0.00	1.02	98.98						
776400	100.00		0.00	0.00	100.00						
time^b	Conv_{exp}	1b^b	2bd^b	3bd^b	4bd^b	time^b	Conv_{exp}	1b^b	2bd^b	3bd^b	4bd^b
600	5.46	89.09	3.99	6.92	0.00	600	3.00	93.99	2.75	3.25	0.00
1800	14.10	71.80	11.46	16.75	0.00	1800	13.32	73.37	10.79	15.85	0.00
4200	22.44	55.49	19.08	25.07	0.36	3600	20.17	59.65	17.27	23.08	0.00
5400	26.59	47.47	23.16	28.72	0.64	6000	25.83	48.34	23.21	28.45	0.00
7200	30.92	39.23	27.56	32.14	1.07	9600	34.93	31.84	31.43	35.03	1.70
10800	37.34	27.73	33.20	36.67	2.41	13200	40.09	22.80	35.81	38.40	2.99
14400	42.09	19.36	37.63	39.47	3.54	16800	45.04	15.83	38.29	39.95	5.92
18000	46.53	13.79	38.85	40.50	6.85	20400	48.59	10.87	39.80	41.30	8.04
21600	49.59	9.84	39.66	41.48	9.02	24600	50.94	7.99	40.21	41.94	9.87
25200	51.84	7.10	40.16	41.95	10.79	28200	53.06	5.72	40.18	42.27	11.84
28800	53.56	5.41	39.84	42.21	12.54	35400	56.15	3.07	39.45	42.11	15.38
32400	55.36	3.94	39.49	41.91	14.66	42600	58.71	1.61	37.63	41.72	19.04
36000	56.73	2.82	38.90	42.00	16.29	49800	61.14	0.00	36.28	41.44	22.28
43200	60.18	0.00	37.76	41.88	20.36	57000	62.81	0.00	33.76	40.62	25.62
50400	61.68	0.00	35.80	40.83	23.37	66000	64.09	0.00	33.26	38.56	28.18
57600	63.13	0.00	33.59	40.15	26.26	85800	67.22	0.00	28.70	36.85	34.44
65700	64.48	0.00	32.10	38.93	28.97	100200	69.04	0.00	25.67	36.25	38.08
84600	67.87	0.00	27.48	36.78	35.74	118200	71.50	0.00	22.01	34.99	43.00
102600	70.39	0.00	24.42	34.80	40.78	136200	73.14	0.00	19.47	34.25	46.28
120600	72.58	0.00	21.70	33.15	45.16	154200	73.10	0.00	21.77	32.03	46.20
138600	74.50	0.00	19.49	31.51	49.01	175800	74.64	0.00	20.01	30.71	49.29
156600	75.74	0.00	18.93	29.59	51.48	201000	76.05	0.00	18.32	29.58	52.10
174600	76.51	0.00	17.95	29.02	53.03	226200	77.34	0.00	17.05	28.28	54.67
192600	77.26	0.00	17.33	28.14	54.52	271200	78.97	0.00	15.23	26.83	57.94
238200	79.27	0.00	15.45	26.01	58.54	312600	80.16	0.00	14.50	25.17	60.33
324600	82.24	0.00	12.43	23.09	64.48	575400	85.56	0.00	9.46	19.42	71.12
Further integration not possible because of some other integrals						989400	91.09	0.00	0.00	17.83	82.17
						1201800	93.78	0.00	0.00	12.44	87.56
						1791000	95.75	0.00	0.00	8.49	91.51
						2424600	96.98	0.00	0.00	6.05	93.95
						2739600	97.38	0.00	0.00	5.25	94.75
						3373200	98.21	0.00	0.00	3.58	96.42
						4323600	97.95	0.00	0.00	4.11	95.89

time^b	Conv_{exp}	1b^b	2be^b	3be^b	4be^b	time^b	Conv_{exp}	1b^b	2be^b	3be^b	4be^b
300	2.41	95.19	1.65	3.17	0.00	300	1.03	97.94	1.05	1.00	0.00
2100	12.44	75.12	9.83	15.05	0.00	1800	8.28	83.45	6.25	10.30	0.00
3900	20.28	59.44	17.28	23.28	0.00	3600	15.14	69.72	12.46	17.83	0.00
5700	25.90	48.84	22.28	28.25	0.64	5400	20.27	59.46	17.46	23.08	0.00
8400	31.80	37.74	27.79	33.13	1.33	7200	25.23	49.54	22.61	27.85	0.00
11100	38.49	25.08	34.40	38.45	2.07	10800	33.75	34.15	29.96	34.24	1.65
14700	44.49	15.95	37.77	41.35	4.93	14400	39.29	24.17	34.74	38.36	2.74
18300	48.28	10.20	39.86	43.17	6.77	18000	43.78	16.63	38.06	41.12	4.19
21900	50.86	6.75	40.64	44.15	8.46	21600	47.11	11.42	40.00	42.95	5.63
25500	53.14	4.40	40.33	44.59	10.68	25200	52.23	4.68	41.27	44.91	9.14
29100	55.06	2.65	39.77	44.81	12.77	28800	54.81	2.38	40.33	45.28	12.00
32700	56.45	1.60	39.09	44.82	14.49	32400	57.68	0.00	39.28	45.35	15.37
36300	57.75	1.09	37.69	44.63	16.59	43200	59.89	0.00	36.10	44.11	19.78
39900	59.39	0.00	36.75	44.47	18.78	54000	61.81	0.00	33.09	43.30	23.61
43500	60.26	0.00	35.52	43.96	20.52	64800	63.78	0.00	30.54	41.90	27.56
47100	61.05	0.00	34.14	43.76	22.10	79200	65.94	0.00	27.54	40.57	31.89
54300	62.68	0.00	31.89	42.76	25.35	93600	67.70	0.00	24.96	39.63	35.41
61500	64.32	0.00	29.60	41.76	28.65	108000	69.57	0.00	22.51	38.35	39.13
79500	67.33	0.00	25.51	39.83	34.66	126000	71.44	0.00	19.85	37.27	42.88
86700	68.37	0.00	24.04	39.22	36.74	144000	73.80	0.00	15.14	37.27	47.59
104700	70.83	0.00	20.75	37.58	41.67	165600	75.01	0.00	15.41	34.57	50.02
119100	72.52	0.00	18.56	36.41	45.03	194400	77.10	0.00	12.76	33.04	54.20
137100	74.34	0.00	16.34	34.99	48.67	216000	78.16	0.00	11.68	31.99	56.33
155100	75.58	0.00	14.84	33.99	51.17	237600	79.43	0.00	10.48	30.67	58.85
185700	77.99	0.00	12.14	31.87	55.98	280800	81.68	0.00	8.17	28.48	63.36
228900	80.73	0.00	8.92	29.62	61.47	342000	83.80	0.00	6.18	26.22	67.60
272100	82.82	0.00	7.07	27.29	65.64	385200	84.87	0.00	5.56	24.71	69.74
315300	84.16	0.00	6.21	25.47	68.33	428400	85.93	0.00	4.74	23.39	71.87
358500	85.79	0.00	4.75	23.67	71.58	471600	86.72	0.00	4.57	22.00	73.44
401700	88.55	0.00	0.00	22.91	77.09	542400	87.82	0.00	3.86	20.49	75.65
536700	90.27	0.00	0.00	19.46	80.54	585600	89.86	0.00	0.00	20.29	79.71
743700	91.61	0.00	0.00	16.78	83.22	847800	92.03	0.00	0.00	15.94	84.06
1089300	93.64	0.00	0.00	12.72	87.28	1062900	93.21	0.00	0.00	13.58	86.42
1420500	94.99	0.00	0.00	10.02	89.98	1474200	94.73	0.00	0.00	10.54	89.46
1873200	96.18	0.00	0.00	7.64	92.36	2064600	96.00	0.00	0.00	8.00	92.00
2285400	97.01	0.00	0.00	5.99	94.01	2698200	96.88	0.00	0.00	6.25	93.75
2875800	97.59	0.00	0.00	4.83	95.17	3013200	98.00	0.00	0.00	4.01	95.99
3509400	98.25	0.00	0.00	3.49	96.51	3646800	97.52	0.00	0.00	4.95	95.05
3824400	98.48	0.00	0.00	3.04	96.96	4597200	97.60	0.00	0.00	4.80	95.20
4458000	98.79	0.00	0.00	2.42	97.58						
5408400	99.39	0.00	0.00	1.23	98.77						
time^b	Conv_{exp}	1b^b	2bf^b	3bf^b	4bf^b	time^b	Conv_{exp}	1b^b	2bf^b	3bf^b	4bf^b
600	2.75	94.49	1.70	3.80	0.00	600	3.13	93.73	2.20	4.07	0.00
2400	9.96	80.08	7.40	12.53	0.00	2400	9.68	80.64	7.16	12.20	0.00
4200	15.82	68.35	12.39	19.26	0.00	4200	17.21	65.58	13.84	20.58	0.00
6000	20.95	58.11	16.97	24.92	0.00	6000	22.89	54.23	19.27	26.50	0.00
7800	24.74	50.51	21.06	28.43	0.00	7800	27.80	44.40	24.09	31.51	0.00
9600	28.97	42.05	25.24	32.71	0.00	11400	35.76	30.28	30.87	37.06	1.79
13200	35.25	30.43	30.81	37.83	0.93	15000	41.59	19.95	35.41	41.51	3.13
16800	40.80	21.37	34.23	41.43	2.98	18600	46.08	12.47	38.29	44.62	4.63
20400	45.10	14.22	37.67	43.70	4.41	22200	49.31	7.79	39.69	46.10	6.41
24000	48.14	9.50	39.11	45.63	5.77	25800	51.78	4.74	39.96	47.01	8.29
27600	50.04	6.80	39.66	46.65	6.89	29400	53.26	3.10	39.63	47.66	9.61
31200	51.99	4.49	39.68	47.37	8.46	33000	55.72	0.00	39.87	48.69	11.44
38400	54.72	1.84	39.00	47.88	11.28	36600	56.45	0.00	38.80	48.29	12.91

Size-Induced Inversion of Selectivity in the Acylation of 1,2-Diols

45600	57.11	0.00	37.64	48.13	14.23	40200	57.10	0.00	37.63	48.17	14.20
52800	58.45	0.00	35.54	47.57	16.90	47400	58.65	0.00	35.12	47.58	17.31
60000	59.67	0.00	33.75	46.91	19.34	54600	60.15	0.00	33.38	46.32	20.30
67200	60.87	0.00	31.94	46.32	21.75	61800	61.40	0.00	31.32	45.88	22.81
81600	63.09	0.00	28.57	45.25	26.18	69000	62.52	0.00	29.38	45.57	25.04
96000	64.98	0.00	25.69	44.36	29.96	83400	64.73	0.00	26.47	44.08	29.46
110400	66.84	0.00	23.23	43.10	33.67	97800	66.46	0.00	24.25	42.84	32.92
124800	68.36	0.00	20.88	42.39	36.73	115800	68.66	0.00	20.67	42.00	37.33
139200	69.75	0.00	18.89	41.61	39.50	133800	70.44	0.00	18.49	40.62	40.89
153600	71.16	0.00	17.07	40.61	42.32	151800	72.09	0.00	15.95	39.88	44.17
169800	72.34	0.00	15.43	39.90	44.67	169800	73.36	0.00	14.58	38.71	46.71
182400	73.34	0.00	14.31	39.02	46.67	187800	74.49	0.00	13.08	37.93	48.99
211200	75.43	0.00	12.00	37.13	50.87	231000	77.00	0.00	10.23	35.78	53.99
247200	77.30	0.00	9.86	35.54	54.60	274200	78.96	0.00	8.20	33.89	57.92
290400	79.26	0.00	7.75	33.74	58.51	317400	80.58	0.00	6.64	32.21	61.15
333600	80.81	0.00	6.46	31.93	61.61	360600	81.94	0.00	5.63	30.48	63.89
376800	82.17	0.00	5.27	30.39	64.35	403800	82.97	0.00	4.63	29.42	65.95
420000	83.81	0.00	4.76	27.61	67.63	742200	88.39	0.00	0.00	23.22	76.78
463200	85.05	0.00	3.42	26.48	70.10	1354200	92.67	0.00	0.00	14.65	85.35
510000	86.16	0.00	3.78	23.90	72.32	1987800	93.69	0.00	0.00	12.62	87.38
612600	88.10	0.00	0.00	23.81	76.19	2938200	94.44	0.00	0.00	11.11	88.89
764400	89.86	0.00	0.00	20.29	79.71						
1014000	91.64	0.00	0.00	16.71	83.29						
1352400	93.32	0.00	0.00	13.37	86.63						
1964400	95.21	0.00	0.00	9.57	90.43						
2598000	95.91	0.00	0.00	8.17	91.83						
3548400	96.72	0.00	0.00	6.57	93.43						
time^b	Conv_{exp}	1b^b	2bg^b	3bg^b	4bg^b	time^b	Conv_{exp}	1b^b	2bg^b	3bg^b	4bg^b
1200	3.76	92.49	2.65	4.86	0.00	600	2.60	94.79	1.83	3.38	0.00
1800	6.35	87.29	4.74	7.97	0.00	1800	7.57	84.87	5.84	9.30	0.00
3000	10.37	79.26	8.40	12.34	0.00	3600	15.47	69.07	13.09	17.84	0.00
4800	16.18	67.64	13.63	18.74	0.00	5400	21.99	56.02	19.51	24.47	0.00
6600	22.15	55.69	19.48	24.83	0.00	7200	27.15	45.69	24.65	29.66	0.00
8400	26.42	47.15	23.90	28.95	0.00	9000	31.16	37.68	28.89	33.43	0.00
10200	29.55	40.90	27.01	32.09	0.00	12600	38.55	25.16	34.32	38.26	2.26
13800	36.92	28.22	32.86	36.85	2.07	16200	43.63	16.34	38.12	41.94	3.60
17400	42.27	18.75	37.17	40.81	3.28	19800	47.27	10.58	40.45	43.85	5.12
21000	45.74	12.96	39.22	43.37	4.45	23400	50.14	6.47	41.09	45.67	6.76
24600	48.83	8.20	40.98	44.96	5.85	27000	51.93	4.18	41.25	46.53	8.04
28200	50.59	5.82	41.08	46.10	7.00	30600	53.61	2.55	40.82	46.87	9.77
35400	53.67	2.42	40.91	46.90	9.77	34200	54.75	1.78	40.29	46.64	11.28
42600	56.39	0.00	39.80	47.41	12.79	37800	56.59	0.00	39.89	46.93	13.18
49800	57.61	0.00	38.00	46.78	15.22	45000	58.02	0.00	37.30	46.66	16.05
57000	58.83	0.00	35.92	46.42	17.66	52200	59.41	0.00	35.34	45.83	18.82
64200	60.20	0.00	33.96	45.63	20.41	59400	60.93	0.00	32.79	45.34	21.87
78600	62.42	0.00	30.48	44.68	24.85	66600	62.04	0.00	31.18	44.73	24.09
93000	64.27	0.00	27.68	43.78	28.54	81000	64.28	0.00	27.59	43.85	28.56
107400	66.01	0.00	25.14	42.84	32.02	95400	66.30	0.00	24.89	42.50	32.60
125400	67.86	0.00	22.46	41.82	35.72	113400	68.42	0.00	21.83	41.33	36.84
143400	69.66	0.00	20.04	40.64	39.32	131400	70.15	0.00	19.70	40.00	40.30
161400	71.16	0.00	18.17	39.50	42.33	149400	72.16	0.00	15.86	39.81	44.33
179400	72.64	0.00	16.34	38.39	45.27	167400	73.05	0.00	15.38	38.52	46.10
197400	73.80	0.00	14.79	37.62	47.59	185400	74.17	0.00	14.31	37.35	48.34
222600	75.40	0.00	12.39	36.81	50.80	271800	78.64	0.00	9.16	33.56	57.27
247800	76.41	0.00	11.45	35.73	52.83	315000	80.07	0.00	7.70	32.17	60.14
291000	79.85	0.00	7.64	32.66	59.70	358200	81.54	0.00	6.13	30.79	63.08

334200	81.48	0.00	4.95	32.08	62.97	401400	82.87	0.00	5.12	29.13	65.75
445200	83.26	0.00	4.96	28.53	66.51	487800	84.63	0.00	3.93	26.81	69.27
597300	87.14	0.00	0.00	25.73	74.27	747000	89.06	0.00	0.00	21.89	78.11
846900	89.23	0.00	0.00	21.55	78.45	1359000	93.09	0.00	0.00	13.82	86.18
1185300	91.32	0.00	0.00	17.36	82.64	1992600	94.05	0.00	0.00	11.91	88.09
1797300	93.84	0.00	0.00	12.33	87.67	2943000	94.56	0.00	0.00	10.87	89.13
2430900	94.90	0.00	0.00	10.20	89.80						
3381300	95.39	0.00	0.00	9.23	90.77						

^aAbsolute kinetic experiments were carrying out by method B. ^b Ablolute kinetic experiments were carrying out by method A.

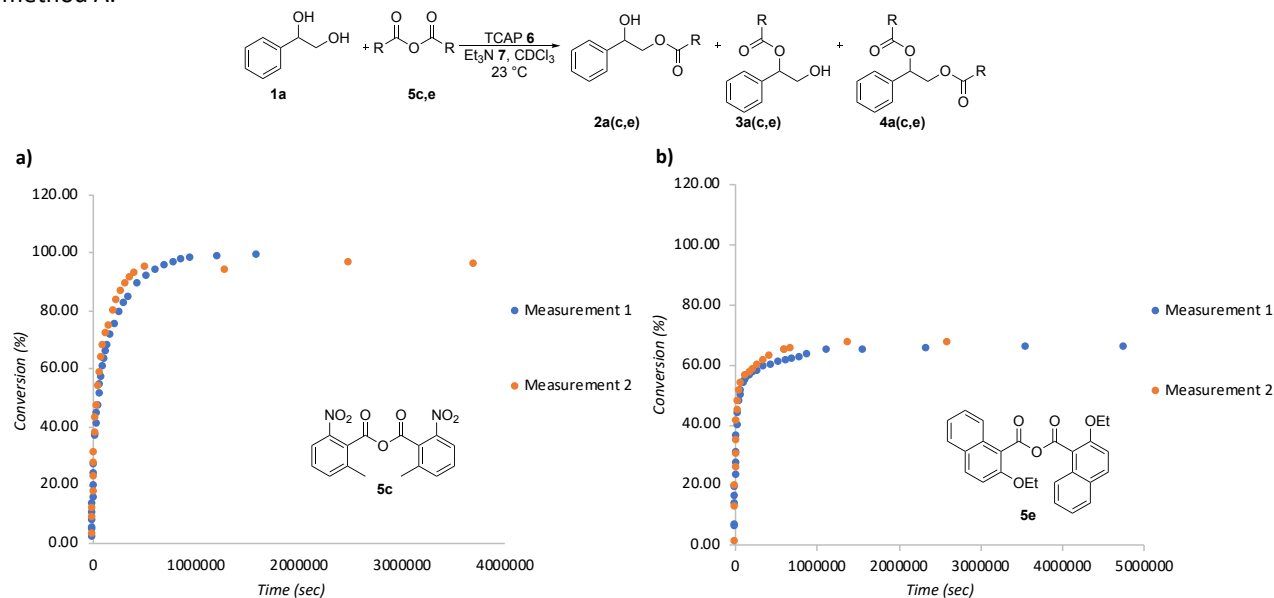


Figure 4.43. Plot of time (sec) vs. conversion (%) of all OH-groups for 1a with a) 5c and b) 5e.

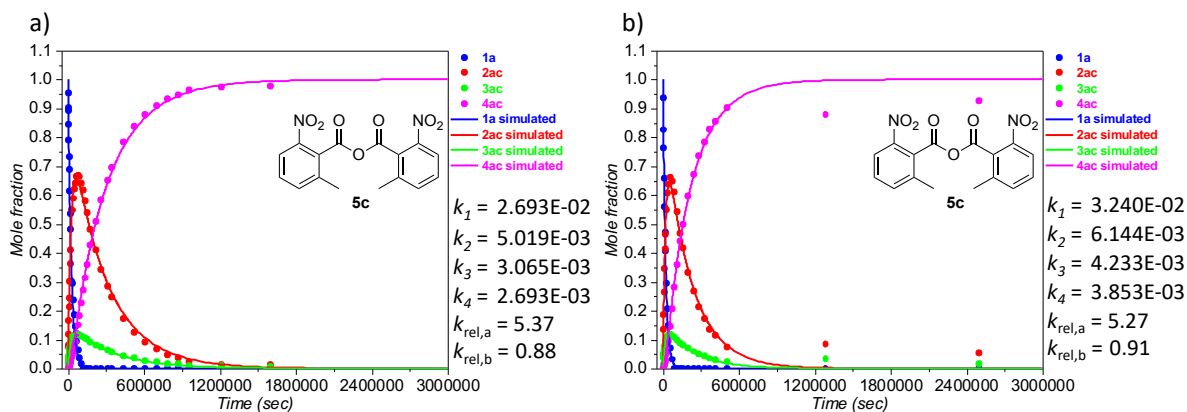


Figure 4.44. Plot of conversion (%) vs. mole fraction for 1a with 5c for a) measurement 1 and b) measurement 2 (Method B). The effective rate constants $k_1 - k_4$ are given in $\text{L mol}^{-1} \text{s}^{-1}$.

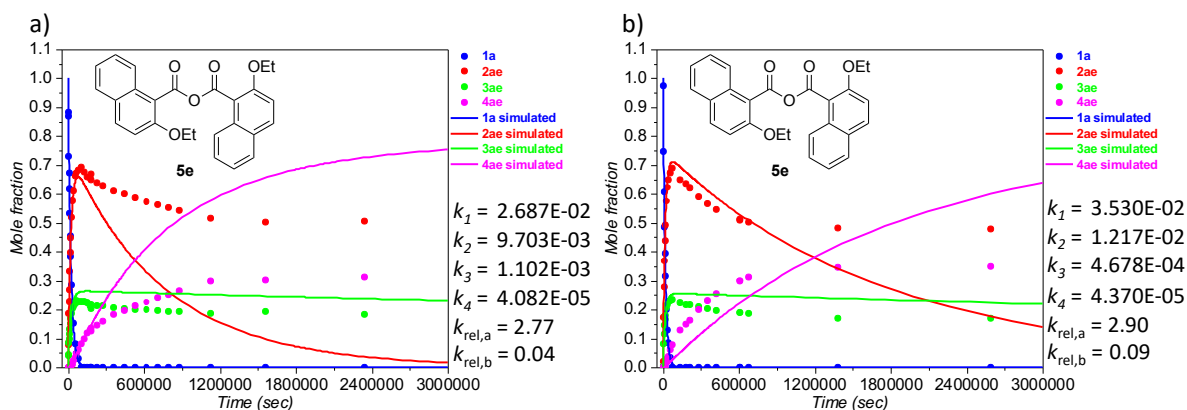


Figure 4.45. Plot of conversion (%) vs. mole fraction for 1a with 5e for a) measurement 1 and b) measurement 2 (Method B). The effective rate constants $k_1 - k_4$ are given in $\text{L mol}^{-1} \text{s}^{-1}$.

Size-Induced Inversion of Selectivity in the Acylation of 1,2-Diols

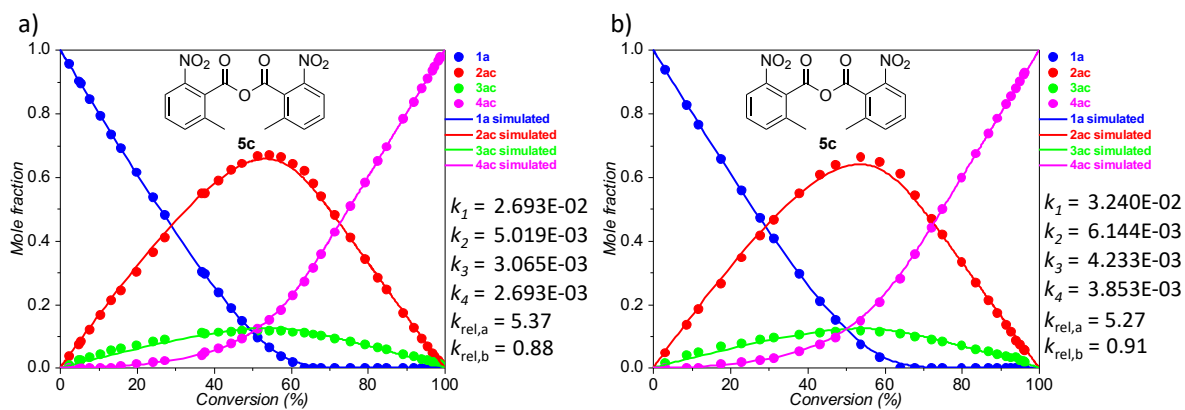


Figure 4.46. Plot of time (sec) vs. mole fraction for **1a** with **5c** for a) measurement 1 and b) measurement 2 (Method B). The effective rate constants $k_1 - k_4$ are given in L mol⁻¹ s⁻¹.

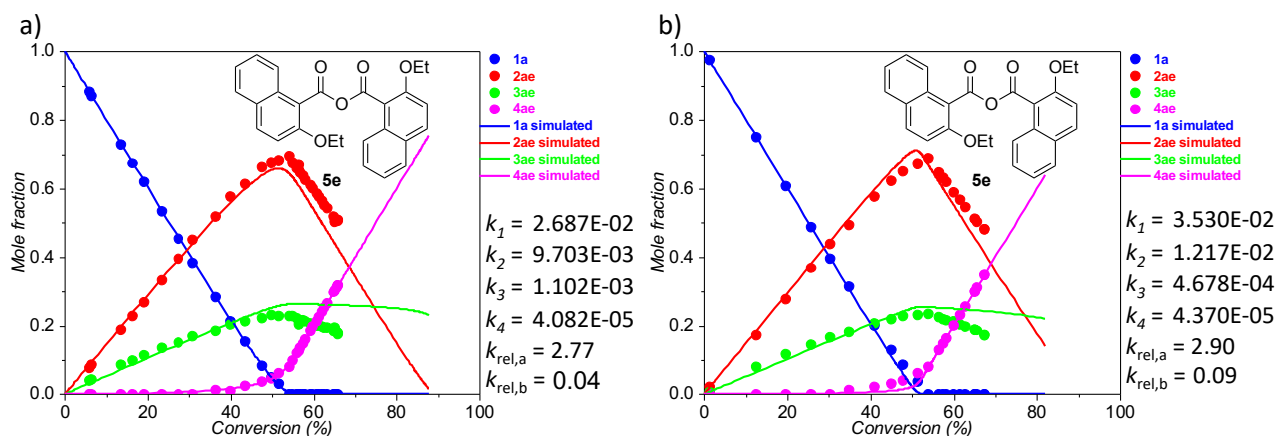


Figure 4.47. Plot of time (sec) vs. mole fraction **1a** with **5e** for a) measurement 1 and b) measurement 2 (Method B). The effective rate constants $k_1 - k_4$ are given in L mol⁻¹ s⁻¹.

Table 4.17. Fitted values of $k_1 - k_4$ by CoPaSi program in ($\text{L mol}^{-1} \text{s}^{-1}$), RMSD (root-mean-square deviation) values of the fitted compounds **1a**, **2a(c,e)**, **3a(c,e)** and **4a(c,e)** and the corresponding relative rate constants $k_{\text{rel},a}$, $k_{\text{rel},b}$, $k_{\text{rel},c}$, $k_{\text{rel},d}$, $k_{\text{rel},e}$, $k_{\text{rel},f}$, $k_{\text{rel},g}$ and $k_{\text{rel},h}$ for the acylation of **1a** with **5c,e** catalyzed by TCAP via absolute kinetic experiments.

Fit	$k_1 - k_4$ ($\text{L mol}^{-1} \text{s}^{-1}$)	RMSD	RMSD	RMSD	RMSD	RMSD	RMSD	RMSD	$k_1 - k_4$	RMSD	k_{rel}	RMSD	RMSD	RMSD	RMSD	k_{rel}	Mean $k_1 - k_4$	Mean k_{rel}	
		1a	2a(c,e)	3a(c,e)	4a(c,e)	1a	2a(c,e)	3a(c,e)	4a(c,e)	(L mol s^{-1})	1a	2a(c,e)	3a(c,e)	4a(c,e)	($\times 10^{-3} \text{L}^{-1} \text{mol s}^{-1}$)				
5c	k_1	2.392E-02	2.13E-04	3.81E-04	1.02E-04	1.63E-04	3.12E-04	9.45E-05	2.943E-02	1.63E-04									
	k_2	4.240E-03							5.300E-03										
	k_3	3.122E-03		1.23E-04	6.43E-05		1.84E-04	8.03E-05	4.308E-03										
	k_4	2.498E-03			7.77E-05				3.593E-03										
5e	k_1	2.693E-02	2.05E-04	1.38E-04	6.75E-05	1.27E-04	1.11E-04	6.24E-05	3.240E-02	1.27E-04						29.66 ± 2.737	Mean $k_{\text{rel},a}$	Mean k_{prim}	
	k_2	5.019E-03							6.144E-03							5.27	8.41	5.32 ± 0.046	9.20 ± 0.794
	k_3	3.065E-03		1.25E-04	4.93E-05	1.25E-04	1.81E-04	7.19E-05	4.233E-03								3.65 ± 0.584	Mean $k_{\text{rel},b}$	Mean k_{sec}
	k_4	2.693E-03							3.853E-03							0.91	1.45	0.90 ± 0.016	1.54 ± 0.093
5e	k_1	2.723E-02	7.63E-05	1.72E-04	1.03E-04	7.00E-05	1.57E-04	8.58E-05	3.493E-02	7.00E-05									
	k_2	9.228E-03							1.213E-02										
	k_3	4.718E-05		6.45E-04	4.92E-04	3.57E-04	5.05E-04	2.48E-04	4.621E-04										
	k_4	1.058E-03							5.115E-05										
3	k_1	2.687E-02	7.66E-05	1.12E-04	7.63E-05	6.80E-05	1.13E-04	8.17E-05	3.530E-02	6.80E-05						31.08 ± 4.216	Mean $k_{\text{rel},a}$	Mean k_{prim}	
	k_2	9.703E-03							1.217E-02						2.90	/	10.94 ± 1.234	2.84 ± 0.066	/
4^a	k_3	1.102E-03		6.10E-04	4.89E-04	3.32E-04	5.11E-04	2.49E-04	4.678E-04							/	Mean $k_{\text{rel},b}$	Mean k_{sec}	
	k_4	4.082E-05							4.370E-05						0.09	/	0.07 ± 0.028	/	/

^a k_3 and k_4 were manual interchanged.

Size-Induced Inversion of Selectivity in the Acylation of 1,2-Diols

Table 4.18. Time (sec), conversion total (%) and ratio of **1a:2a(c,e):3a(c,e):4a(c,e)** for absolute kinetic measurement of phenylethane-1,2-diol **1a** with acid anhydride derivatives **5c,e**. All absolute kinetic experiments were carrying out by method A. Baseline of ¹H NMR for integration was corrected by Whittaker Smoother (I) fit.

Time (sec)	Conv (%)	Ratio (%)				Time (sec)	Conv (%)	Ratio (%)			
Time	Conv _{exp}	1a	2ac	3ac	4ac	time	Conv _{exp}	1a	2ac	3ac	4ac
900	2.26	95.49	3.50	1.02	0.00	900	3.09	93.83	4.72	1.45	0.00
1800	4.90	90.19	7.49	2.32	0.00	3000	8.68	82.64	13.54	3.82	0.00
1980	5.34	89.33	8.29	2.38	0.00	4800	11.75	76.51	18.52	4.97	0.00
3180	7.70	84.59	12.02	3.39	0.00	8400	17.66	65.75	26.58	6.59	1.08
4980	10.42	79.17	16.49	4.34	0.00	12000	22.94	55.86	34.65	7.73	1.75
6780	13.37	73.26	21.31	5.43	0.00	15600	27.62	47.23	41.46	8.84	2.47
8580	15.88	68.91	24.35	6.07	0.66	19200	31.19	40.70	46.62	9.61	3.07
12180	19.92	61.49	30.10	7.07	1.34	26400	37.82	29.46	54.91	10.53	5.10
15780	24.16	53.58	36.37	8.16	1.89	33600	43.25	20.81	60.82	11.06	7.31
19380	27.09	48.07	40.91	8.77	2.25	40800	47.35	14.95	63.94	11.47	9.64
26580	36.77	30.29	54.92	10.96	3.83	55200	53.74	7.24	66.27	11.77	14.72
33780	37.57	29.67	54.82	10.70	4.81	69600	58.67	3.23	64.84	11.36	20.56
40980	41.21	23.75	58.88	11.21	6.17	87600	64.04	0.00	61.09	10.84	28.07
48180	44.51	18.64	62.20	11.50	7.66	109200	67.92	0.00	54.31	9.86	35.83
55380	47.30	14.71	64.27	11.71	9.31	134400	72.04	0.00	46.98	8.95	44.07
67980	51.43	9.46	66.48	11.75	12.31	156000	74.94	0.00	41.84	8.27	49.88
76980	54.37	6.35	66.81	11.74	15.10	197400	79.88	0.00	33.21	7.04	59.75
87780	57.33	3.64	66.36	11.70	18.30	240600	83.68	0.00	26.70	5.95	67.35
102180	60.53	1.83	64.06	11.21	22.90	283800	86.83	0.00	21.30	5.04	73.66
116580	63.54	0.00	61.88	11.04	27.08	327000	89.24	0.00	17.23	4.29	78.47
134580	65.70	0.00	58.00	10.60	31.40	370200	91.43	0.00	13.56	3.58	82.86
152580	67.93	0.00	54.01	10.13	35.86	413400	92.71	0.00	11.38	3.19	85.43
174180	71.35	0.00	48.16	9.15	42.69	507000	95.07	0.00	7.41	2.45	90.14
217380	75.40	0.00	40.97	8.22	50.80	1284600	94.00	0.00	8.51	3.49	88.00
260580	79.16	0.00	34.26	7.43	58.32	2494200	96.37	0.00	5.46	1.80	92.74
310980	82.55	0.00	28.43	6.46	65.11	3703800	96.08	0.00	5.88	1.97	92.16
346980	84.76	0.00	24.75	5.74	69.52						
436980	89.13	0.00	17.35	4.39	78.26						
523380	91.85	0.00	12.64	3.67	83.69						
609780	93.97	0.00	9.21	2.85	87.93						
696180	95.48	0.00	6.65	2.40	90.95						
782580	96.72	0.00	4.72	1.84	93.44						
868980	97.37	0.00	3.59	1.68	94.73						
955380	98.21	0.00	2.44	1.14	96.42						
1207380	98.72	0.00	1.47	1.09	97.43						
1596180	98.83	0.00	1.48	0.86	97.67						
Time	Conv _{exp}	1a	2ae	3ae	4ae	time	Conv _{exp}	1a	2ae	3ae	4ae
2400	5.86	88.29	7.70	4.02	0.00	900	1.32	97.37	2.13	0.50	0.00
2700	6.47	87.06	8.63	4.32	0.00	4500	12.61	74.78	17.22	8.00	0.00
6000	13.57	72.85	18.68	8.47	0.00	8100	19.69	60.63	27.69	11.68	0.00
7800	16.33	67.35	22.77	9.88	0.00	11700	25.70	48.59	36.83	14.57	0.00
9600	19.09	61.83	26.78	11.39	0.00	15300	30.30	39.40	43.89	16.71	0.00
13200	23.31	53.39	33.24	13.37	0.00	18900	34.85	31.44	49.30	18.11	1.15
16800	27.33	45.33	39.57	15.09	0.00	26100	41.04	19.92	57.53	20.56	1.99
20400	30.84	38.32	44.87	16.81	0.00	33300	44.96	13.00	62.28	21.80	2.92
27600	36.34	28.47	51.84	18.53	1.15	40500	47.66	8.53	64.91	22.71	3.85
34800	39.90	21.15	57.70	20.20	0.95	54900	51.28	3.56	67.24	23.07	6.12
42000	43.56	15.27	61.24	21.10	2.39	69300	53.97	0.00	68.80	23.26	7.94
56400	47.62	8.30	66.15	22.02	3.53	137700	56.46	0.00	64.72	22.35	12.93
67200	49.88	4.92	67.39	23.01	4.68	180900	57.41	0.00	63.32	21.87	14.81
81600	51.49	3.04	68.25	22.68	6.03	213300	58.15	0.00	62.09	21.62	16.29

103200	54.02	0.00	69.28	22.68	8.03	281700	59.98	0.00	58.94	21.10	19.96
124800	54.93	0.00	67.47	22.66	9.87	350100	61.48	0.00	56.73	20.31	22.97
146400	55.95	0.00	65.81	22.30	11.89	418500	62.76	0.00	54.69	19.79	25.51
175200	56.53	0.00	65.45	21.49	13.07	607500	64.97	0.00	51.22	18.84	29.94
178800	56.33	0.00	66.94	20.40	12.66	609300	65.02	0.00	51.02	18.93	30.04
182400	56.77	0.00	64.85	21.60	13.55	677700	65.61	0.00	50.18	18.59	31.23
229200	57.37	0.00	63.82	21.43	14.74	1382400	67.38	0.00	48.15	17.09	34.76
272400	58.02	0.00	62.65	21.31	16.04	2592000	67.44	0.00	48.00	17.11	34.89
358800	59.17	0.00	61.11	20.56	18.33						
445200	59.79	0.00	60.06	20.35	19.58						
531600	60.66	0.00	58.67	20.00	21.33						
618000	61.29	0.00	57.50	19.92	22.58						
704400	62.03	0.00	56.32	19.63	24.05						
790800	62.62	0.00	55.26	19.49	25.25						
877200	63.30	0.00	54.18	19.23	26.59						
1129200	64.86	0.00	51.72	18.56	29.72						
1561200	65.12	0.00	50.36	19.40	30.24						
2338800	65.59	0.00	50.53	18.30	31.17						
3548400	65.84	0.00	50.59	17.73	31.68						
4758000	65.85	0.00	50.88	17.42	31.70						

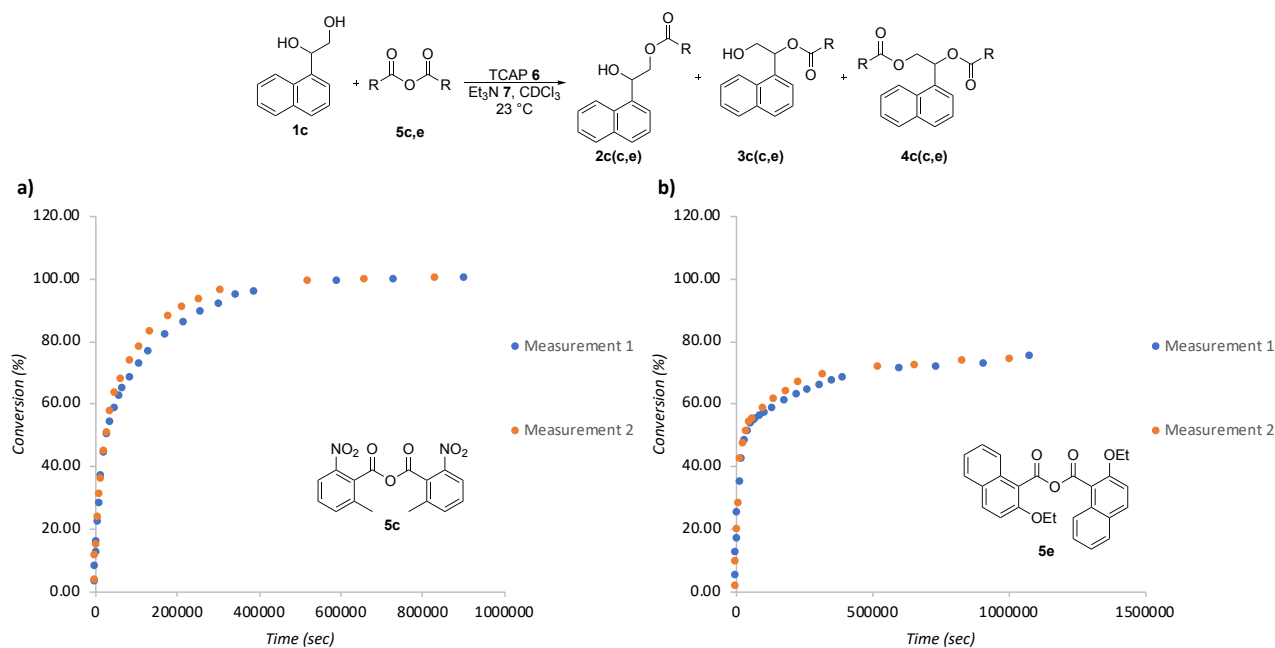


Figure 4.48. Plot of time (sec) vs. conversion (%) of all OH-groups for **1c** with a) **5c** and b) **5e**.

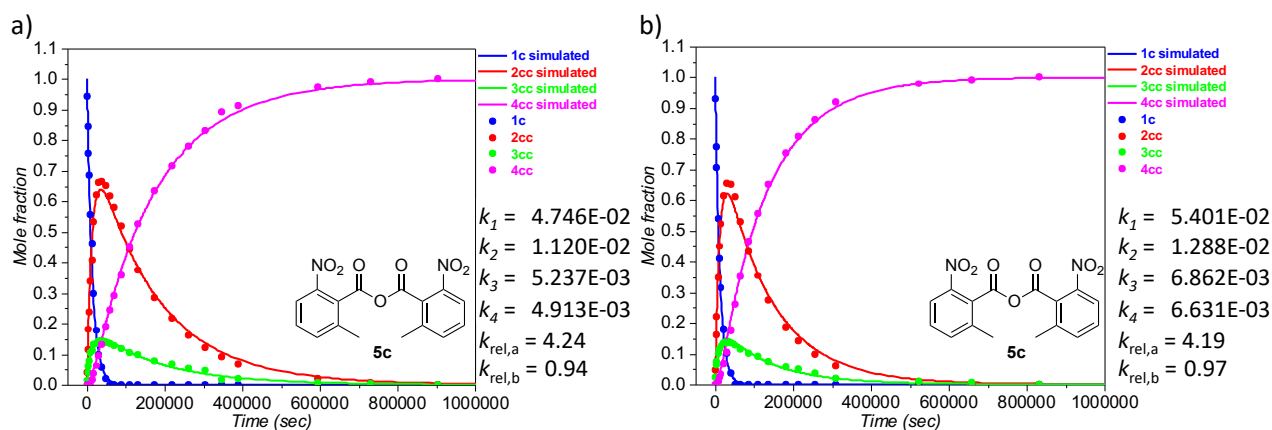


Figure 4.49. Plot of time (sec) vs. mole fraction for **1c** with **5c** for a) measurement 1 and b) measurement 2 (Method A). The effective rate constants $k_1 - k_4$ are given in $\text{L mol}^{-1} \text{s}^{-1}$.

Size-Induced Inversion of Selectivity in the Acylation of 1,2-Diols

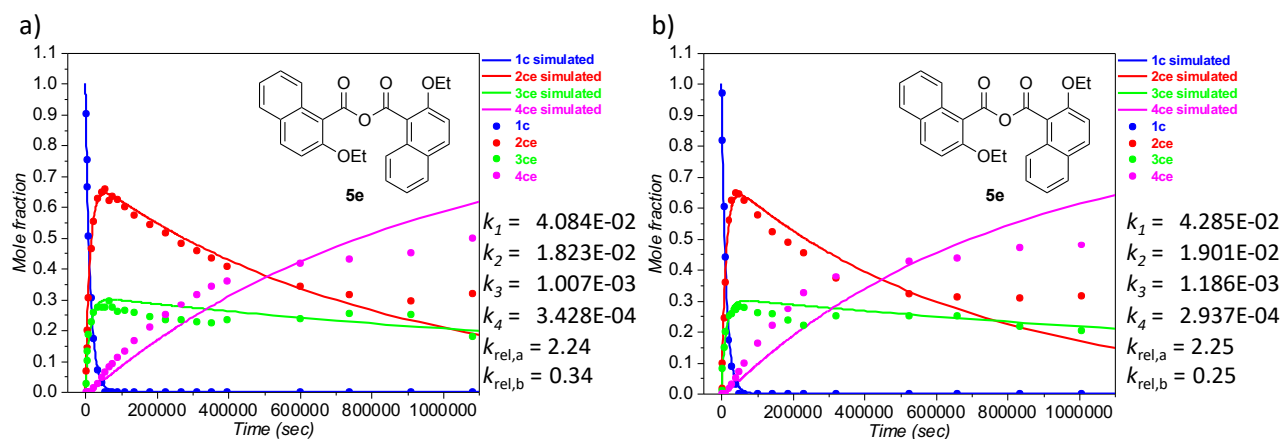


Figure 4.50. Plot of time (sec) vs. mole fraction for **1c** with **5e** for a) measurement 1 and b) measurement 2 (Method A). The effective rate constants $k_1 - k_4$ are given in $\text{L mol}^{-1} \text{s}^{-1}$.

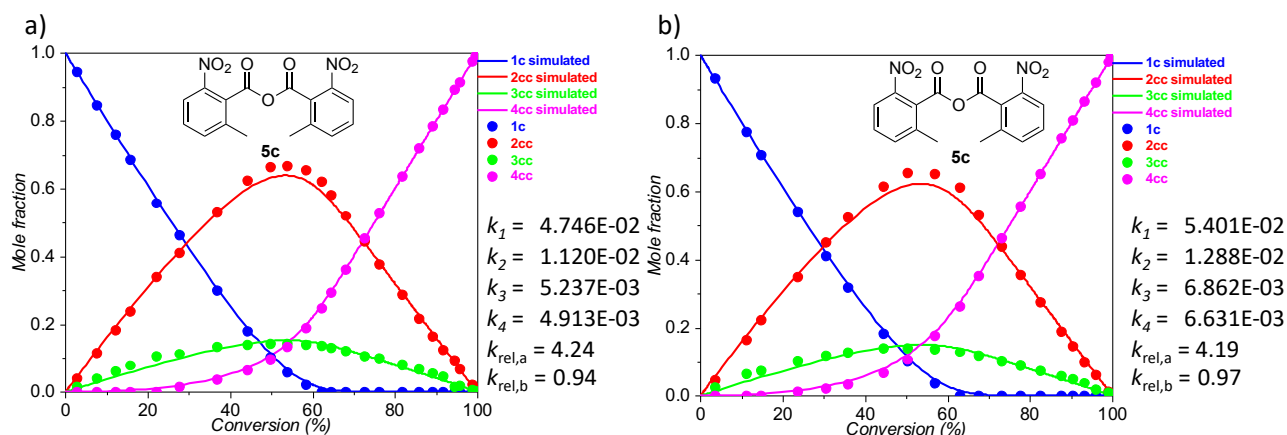


Figure 4.51. Plot of conversion (%) vs. mole fraction for **1c** with **5c** for a) measurement 1 and b) measurement 2 (Method A). The effective rate constants $k_1 - k_4$ are given in $\text{L mol}^{-1} \text{s}^{-1}$.

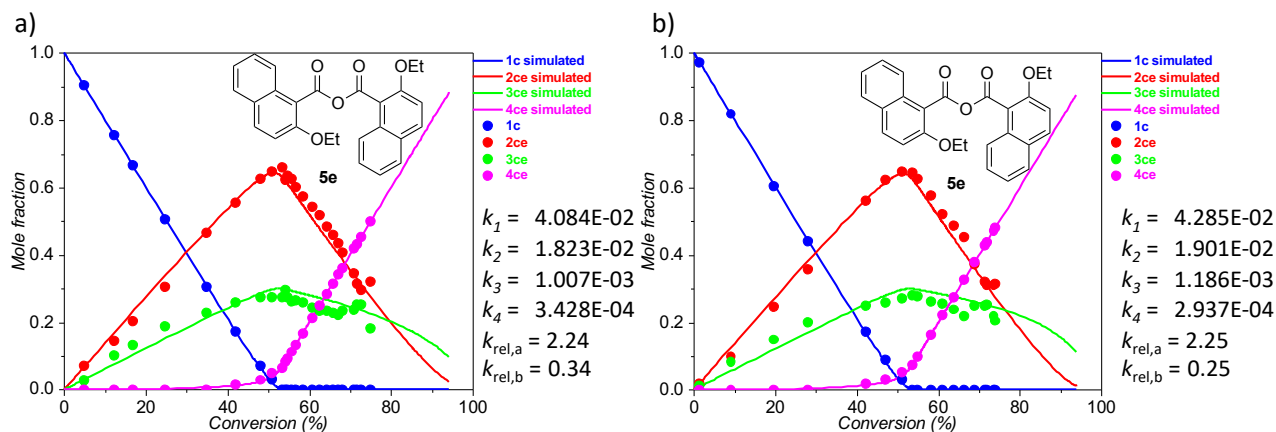


Figure 4.52. Plot of conversion (%) vs. mole fraction for **1c** with **5e** for a) measurement 1 and b) measurement 2 (Method A). The effective rate constants $k_1 - k_4$ are given in $\text{L mol}^{-1} \text{s}^{-1}$.

Table 4.19. Fitted values of $k_1 - k_4$ by CoPaSi program in ($\text{L mol}^{-1}\text{s}^{-1}$), RMSD (root-mean-square deviation) values of the fitted compounds **1c**, **2c(c,e)**, **3c(c,e)** and **4c(c,e)** and the corresponding relative rate constants $k_{\text{rel,a}}$, $k_{\text{rel,b}}$, k_{prim} and k_{sec} for the acylation of **1c** with **5c,e** catalyzed by TCAP (10 mol%) via absolute kinetic experiments.

Fit	$k_1 - k_4$ ($\text{L mol}^{-1}\text{s}^{-1}$)	RMSD	RMSD	RMSD	$k_1 - k_4$ (L mol s^{-1})	RMSD	k_{rel}	$k_1 - k_4$ (L mol s^{-1})	RMSD	RMSD	RMSD	RMSD	RMSD	k_{rel}	Mean $k_1 - k_4$ ($\times 10^{-3} \text{ L}^{-1} \text{ mol s}^{-1}$)	Mean k_{rel}	
		1c	2c(a-g)	3c(a-g)	4c(a-g)	1c	2c(a-g)	3c(a-g)	4c(a-g)	1c	2c(a-g)	3c(a-g)	4c(a-g)	1c	2c(a-g)	3c(a-g)	4c(a-g)
5c	k_1	1.85E-04	2.69E-04	1.18E-04	4.912E-02	1.37E-04		4.912E-02	1.37E-04	1.31E-04							
	k_2				1.113E-02			1.113E-02									
	k_3		1.34E-04	7.32E-05	6.997E-03			6.997E-03	1.33E-04	7.69E-05							
	k_4				6.205E-03			6.205E-03									
	k_1	1.88E-04	1.87E-04	7.90E-05	5.401E-02	1.56E-04	$k_{\text{rel,a}}$	5.401E-02	1.56E-04	9.23E-05				$k_{\text{rel,a}}$	50.74 ± 3.277	Mean k_{prim}	
	k_2				1.288E-02		4.24	1.288E-02						4.19	12.04 ± 0.838	4.22 ± 0.021	Mean $k_{\text{rel,a}}$
	k_3		1.44E-04	6.04E-05	6.862E-03		$k_{\text{rel,b}}$	6.862E-03	1.33E-04	6.55E-05				$k_{\text{rel,b}}$	6.05 ± 0.813	Mean $k_{\text{rel,b}}$	
	k_4				6.631E-03		0.94	6.631E-03						0.97	5.77 ± 0.859	0.95 ± 0.014	Mean k_{sec}
5e	k_1	8.71E-05	1.45E-04	1.53E-04	4.192E-02	2.03E-04		4.192E-02	2.03E-04	1.35E-04							
	k_2				1.877E-02			1.877E-02									
	k_3		2.27E-04	2.04E-04	1.179E-03			1.179E-03	3.59E-04	1.89E-04							
	k_4				3.049E-04			3.049E-04									
	k_1	9.32E-05	1.43E-04	1.40E-04	4.285E-02	2.04E-04	$k_{\text{rel,a}}$	4.285E-02	2.04E-04	1.27E-04				$k_{\text{rel,b}}$	41.85 ± 1.003	Mean $k_{\text{rel,a}}$	
	k_2				1.901E-02		2.24	1.901E-02						2.25	18.62 ± 0.387	2.25 ± 0.007	Mean $k_{\text{rel,b}}$
	k_3		2.33E-04	2.01E-04	1.186E-03		k_{sec}	1.186E-03	3.64E-04	1.84E-04				k_{sec}	1.10 ± 0.090	Mean $k_{\text{rel,b}}$	
	k_4				2.937E-04		0.34	2.937E-04						0.25	0.32 ± 0.025	0.29 ± 0.046	Mean k_{sec}

Size-Induced Inversion of Selectivity in the Acylation of 1,2-Diols

Table 4.20. Time (sec), conversion total (%) and ratio of **1c:2c(c,e):3c(c,e):4c(c,e)** for absolute kinetic measurement of 1-naphthylethane-1,2-diol **1c** with acid anhydride derivatives **5c,e**. All absolute kinetic experiments were carried out by method A. Baseline of ¹H NMR for integration was corrected by Whittaker Smoother (I) fit.

Time (sec)	Conv (%)	Ratio (%)				Time (sec)	Conv (%)	Ratio (%)			
Time	Conv _{exp}	1c	2cc	3cc	4cc	time	Conv _{exp}	1c	2cc	3cc	4cc
600	2.75	94.49	3.97	1.54	0.00	540	3.50	93.01	4.65	2.34	0.00
1800	7.72	84.56	11.50	3.93	0.00	2700	11.33	77.33	16.37	6.30	0.00
3300	12.13	75.75	18.18	6.08	0.00	3900	14.76	70.49	22.16	7.35	0.00
5100	15.79	68.43	23.75	7.82	0.00	7500	23.58	53.94	34.82	10.14	1.10
8700	22.18	55.63	34.01	10.36	0.00	11100	30.56	41.12	44.98	11.66	2.24
12300	27.65	46.31	40.87	11.20	1.62	14700	35.90	31.62	52.30	12.66	3.43
15900	36.84	30.00	53.14	13.17	3.68	21900	44.37	18.09	61.35	13.74	6.83
23100	44.24	17.83	62.19	13.68	6.30	29100	50.20	10.20	65.49	13.72	10.60
30300	49.80	9.99	66.16	14.26	9.59	39900	56.99	3.67	65.18	13.50	17.65
37500	53.80	5.72	66.67	14.28	13.33	50700	63.04	0.00	61.18	12.74	26.08
48300	58.36	2.14	65.23	13.77	18.86	65100	67.63	0.00	53.08	11.66	35.25
59100	62.24	0.00	61.88	13.64	24.48	86700	73.17	0.00	43.61	10.05	46.34
69900	64.60	0.00	58.01	12.80	29.20	108300	77.76	0.00	35.46	9.02	55.52
87900	68.03	0.00	51.94	12.00	36.06	137100	82.55	0.00	27.45	7.46	65.09
109500	72.60	0.00	44.33	10.47	45.20	180300	87.72	0.00	18.80	5.76	75.45
131100	76.29	0.00	37.50	9.93	52.57	212700	90.37	0.00	14.31	4.94	80.74
174300	81.77	0.00	28.63	7.83	63.54	255900	93.15	0.00	9.90	3.80	86.29
217500	85.88	0.00	21.58	6.67	71.75	309900	96.01	0.00	6.08	1.90	92.02
260700	89.10	0.00	16.20	5.60	78.21	522300	98.96	0.00	1.14	0.94	97.92
303900	91.59	0.00	12.21	4.61	83.18	659100	99.58	0.00	0.26	0.57	99.17
347100	94.60	0.00	9.16	1.63	89.21	831900	100.00	0.00	0.00	0.00	100.00
390300	95.67	0.00	6.77	1.90	91.33						
593700	98.67	0.00	2.11	0.54	97.35						
730500	99.48	0.00	0.62	0.41	98.97						
903300	100.00	0.00	0.00	0.00	100.00						
Time	Conv _{exp}	1c	2ce	3ce	4ce	time	Conv _{exp}	1b	2ce	3ce	4ce
1800	4.8	90.4	6.9	2.7	0.0	1200	1.4	97.2	1.7	1.1	0.0
3600	12.3	75.4	14.4	10.2	0.0	3000	9.1	81.9	9.9	8.2	0.0
5400	16.8	66.5	20.2	13.4	0.0	6600	19.7	60.6	24.5	14.9	0.0
9000	24.7	50.7	30.6	18.7	0.0	10200	28.0	44.0	35.9	20.1	0.0
16200	34.7	30.5	46.6	22.9	0.0	21000	42.2	17.3	56.1	25.0	1.7
23400	42.0	17.3	55.5	25.8	1.4	28200	47.1	8.8	62.3	26.0	3.0
34200	47.9	7.0	62.7	27.4	2.9	39000	51.0	3.2	64.8	27.0	5.1
45000	50.9	3.0	64.8	27.4	4.8	49800	53.6	0.0	64.6	28.2	7.3
55800	53.3	0.0	65.9	27.5	6.5	64200	54.9	0.0	62.5	27.8	9.7
66600	54.1	0.0	62.1	29.6	8.3	100200	58.1	0.0	57.7	26.0	16.3
74400	54.6	0.0	63.5	27.4	9.2	143400	61.1	0.0	52.2	25.7	22.1
90600	55.6	0.0	62.6	26.2	11.2	186600	63.7	0.0	48.8	23.9	27.3
108600	56.7	0.0	60.2	26.5	13.3	229800	66.4	0.0	45.3	22.0	32.7
137400	58.3	0.0	57.4	25.9	16.7	319800	68.9	0.0	37.2	25.0	37.8
180600	60.6	0.0	54.4	24.4	21.2	523200	71.4	0.0	32.2	25.0	42.9
223800	62.5	0.0	51.7	23.4	25.0	660000	71.9	0.0	31.1	25.2	43.7
267000	64.2	0.0	48.3	23.4	28.3	832800	73.6	0.0	31.0	21.9	47.1
310200	65.8	0.0	45.9	22.6	31.5	1005600	74.0	0.0	31.5	20.5	48.0
353400	67.1	0.0	43.5	22.3	34.2						
396600	68.0	0.0	40.7	23.3	36.1						
600000	70.9	0.0	34.4	23.7	41.9						
736800	71.6	0.0	31.5	25.3	43.2						
909600	72.6	0.0	29.5	25.2	45.2						
1082400	75.0	0.0	32.0	18.1	49.9						

4.1.3 Turnover-limited Competition vs. Absolute Kinetic Experiments

In Table 4.21 the three different methods used to quantify the relative rate constants are compared. For all cases, the $k_{rel,a}$ values are close to each other. If differences are detected, the changes in $k_{rel,a}$ may be due to transesterification reaction, which we will discuss further in Chapter 4.1.5. Comparing the two methods of quantifying $k_{rel,b}$, the results for the relative rate constants don't follow the same trend. Because $k_{rel,b}$ is dependent from time, which constant we could not integrate well in the fitting of the turnover-limited competition experiments, the $k_{rel,b}$ values plotted from the absolute kinetic experiments seen more reliable. Only for **5c** $k_{rel,b}$ is comparable, because here the difference between $k_1 - k_4$ is very small, so that the time difference is small.

Table 4.21. Comparison of $k_{rel,a}$ and $k_{rel,b}$ by the different validation methods for acylation of **1b** with **5a-g** and **1a** with **5c,e**.

Anhydride	$k_{rel,a}$ 30% Conversion	$k_{rel,a}$ Turnover-limited competition experiment	$k_{rel,a}$ Absolute Kinetic study	$k_{rel,b}$ Turnover-limited competition experiment	$k_{rel,b}$ Absolute Kinetic study
Naphthyl-1,2-ethanediol 1b					
5a	3.30 ± 0.057	3.34	3.38 ± 0.023	0.83	3.22 ± 0.102
5b	1.40 ± 0.020	1.40	/	1.14	/
5c	1.94 ± 0.026	2.08	1.47 ± 0.073	0.67	0.64 ± 0.019
5d	0.90 ± 0.008	0.95	0.96 ± 0.007	0.72	0.45 ± 0.060
5e	0.96 ± 0.005	0.94	0.96 ± 0.002	0.75	0.25 ± 0.003
5f	0.94 ± 0.037	0.96	0.89 ± 0.005	0.88	0.20 ± 0.015
5g	0.82 ± 0.002	0.84	0.95 ± 0.007	0.95	0.18 ± 0.006
Phenyl-1,2-ethanediol 1a					
5c	4.46 ± 0.120	4.69	5.32 ± 0.046	0.81	0.90 ± 0.016
5e	2.92 ± 0.025	2.99	2.84 ± 0.066		

4.1.4 Influence of Alcohol Size

Size effects on the selectivities through varying the side chain of the diols from Ph (**1a**) to 2-Np (**1b**) are shown in Figure 4.53. The respective $k_{rel,a}$ values of anhydrides **5a-5g** are obtained from turnover-limited competition. For benzoic anhydride (**5a**) there exists no significant difference between the selectivities for both diol substrates with $k_{rel,a} = 3.68$ (**1a**) vs. $k_{rel,a} = 3.34$ (**1b**). For *ortho*-substituted benzoic anhydrides **5b** and **5c** we see an increasingly larger preference for acylation of the primary hydroxyl group in diol **1a** as compared to **1b**. For the anhydrides derived from 2-substituted naphthoic acids this effect becomes even more pronounced, the largest selectivity change being that for anhydride **5e** with $k_{rel,a} = 2.99$ (**1a**) vs. $k_{rel,a} = 0.94$ (**1b**). These trends are, together with the influence of the variable chain length in anhydrides **5d - 5g**, largely similar to earlier results obtained in intermolecular turnover-limited competition experiments with the same anhydrides.^[1]

Size-Induced Inversion of Selectivity in the Acylation of 1,2-Diols

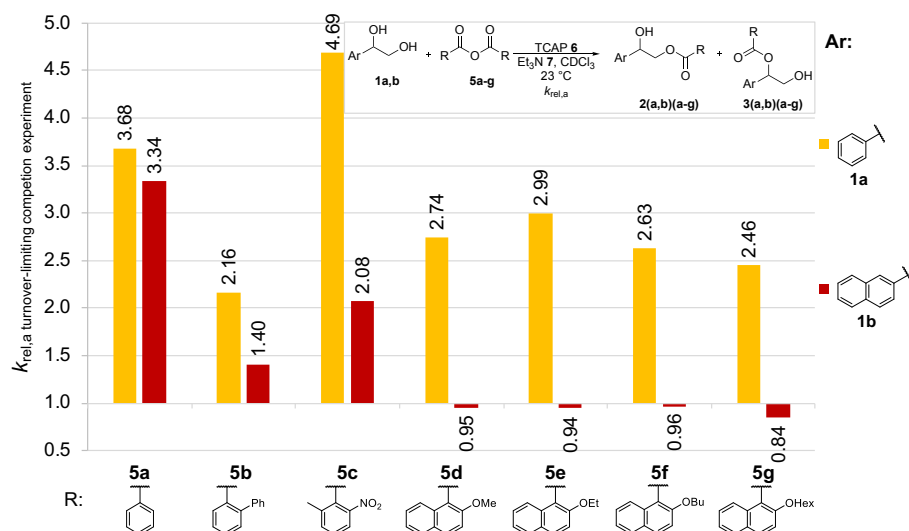


Figure 4.53. Relative rate constants $k_{rel,a}$ for diols **1a** and **1b** in their reaction with anhydrides **5a-g** catalyzed by TCAP (**6**) as obtained from turnover-limited competition experiments.

Size effects on the selectivities through varying the side chain of the diols from Ph (**1a**) over 1-Np (**1c**) to 2-Np (**1b**) are shown in Figure 4.54. The respective $k_{rel,a}$ values of anhydrides **5c,e** are obtained from absolute kinetic studies. For both anhydrides **5c,e** the selectivities of the diol **1c** [$k_{rel,a} = 4.22$ (**5c**) and $k_{rel,a} = 2.25$ (**5e**)] are close to the selectivities of the diol **1a** [$k_{rel,a} = 5.32$ (**5c**) and $k_{rel,a} = 2.84$ (**5e**)]. A larger change in selectivity is obtained with the diol **1b** [$k_{rel,a} = 1.47$ (**5c**) and $k_{rel,a} = 0.96$ (**5e**)].

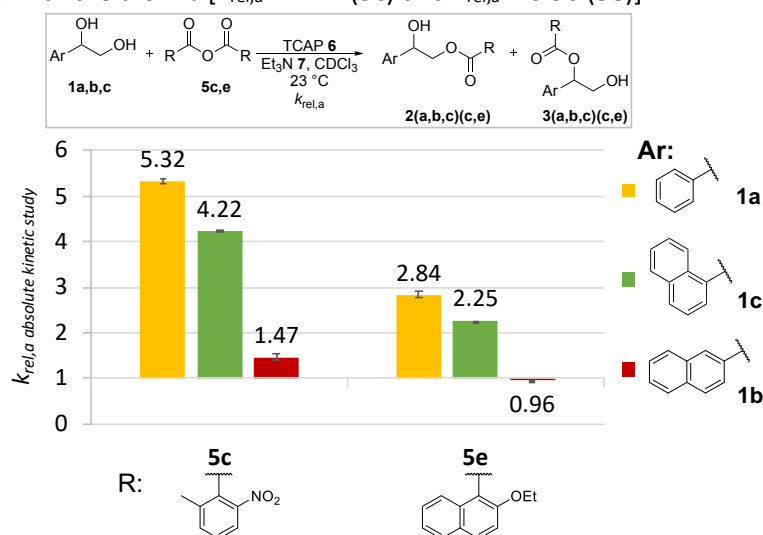
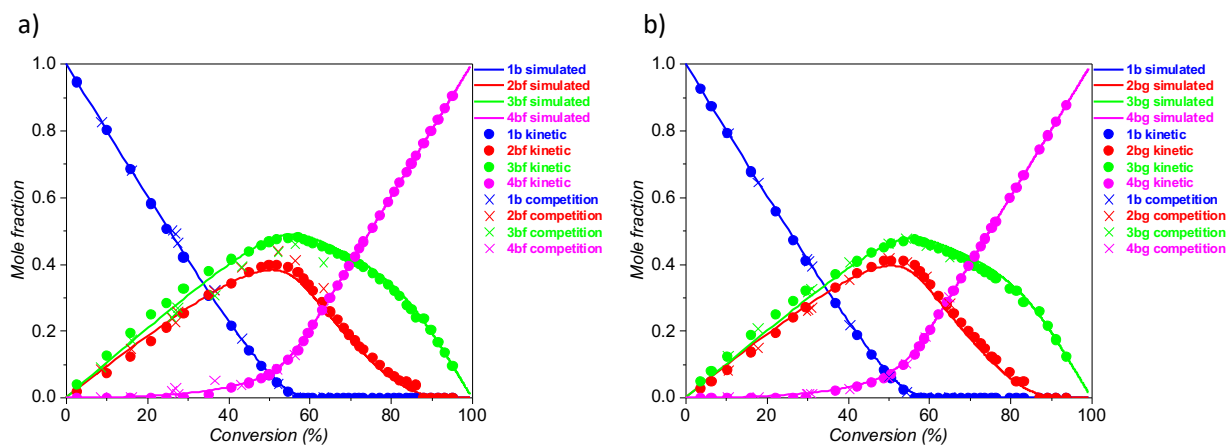
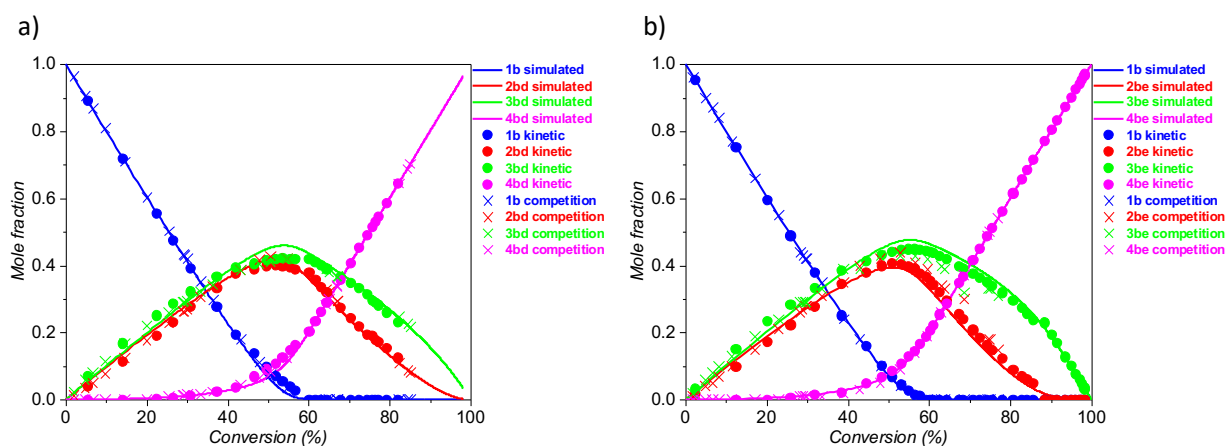
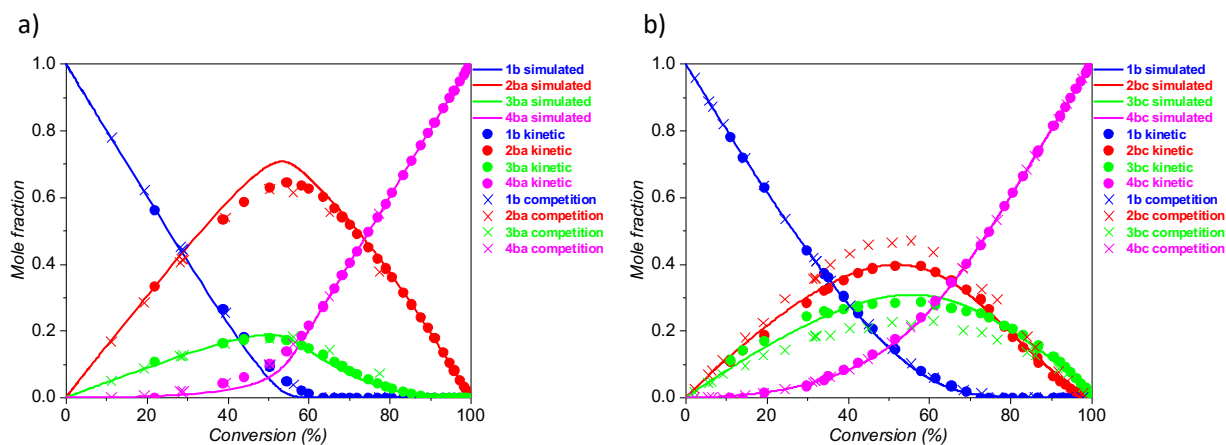
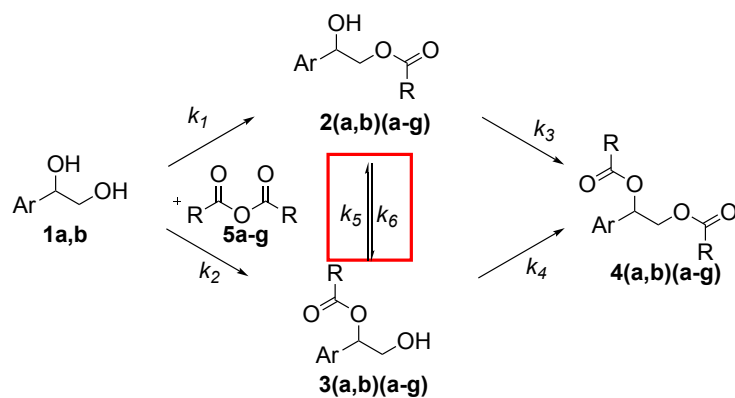


Figure 4.54. Relative rate constants $k_{rel,a}$ for diols **1a,b,c** in their reaction with anhydrides **5c,e** catalyzed by TCAP (**6**) as obtained from absolute kinetic study.

4.1.5 Transesterification

Because of the long reaction times of 3-4 weeks or longer, the monoesters **2** and **3** can potentially undergo transesterification (Scheme 4.11). This process is expected to be very slow, so that in the absolute kinetic experiments this migration process should be negligible. This is different for the turnover-limited competition experiments, because here only a defined amount of anhydride **5a-g** is available for the acylation reaction. If the reagent **5** is gone, the system is more likely to transesterify. In Figures 4.55 until 4.57, the total conversion is plotted against the mole fractions for **1b:2b(a-g):3b(a-g):4b(a-g)** obtained in turnover-limited competition experiments. In the same plots the corresponding data obtained in absolute kinetics are included, too. Only with reagent **5c**, significant differences are clearly visible (Figure 4.55b).



Size-Induced Inversion of Selectivity in the Acylation of 1,2-Diols

An attempt has been made for **5c** to quantify k_5 and k_6 by using the simulation option of CoPaSi program. Scheme 4.12 shows the reactions for the simulations process used in CoPaSi. The effective rate constants k_1 - k_4 are defined by previous fitting shown in Chapter 4.1.2.2. Different values for k_5 and k_6 are tested, some are shown in Table 4.22 (**A-D**). Test **A** seems to describe the noted transesterification the best.

Via the Van-'t Hoff equation (Eq. 4.23) the difference in free energy $\Delta G_{k_{rel,c}}$ of the transesterification could be calculate by inserting $k_{rel,c}$ in Eq. 4.23 (Eq. 4.24, Table 4.22). In Chapter 4.2 the free energy of reaction ΔG_{298} for the formation of monoesters **2bc** and **3bc** are listed at SMD-(CHCl3)/DLPNOCCSD(T)/def2-TZVPP//SMD-(CHCl3)/B3LYP-D3/6-31+G(d) level of theory.^[6] The first acylation of **1b** to either **2bc** or **3bc** is similarly exothermic with reaction free energies of $\Delta G_{298} = -61.5 \text{ kJ mol}^{-1}$ (**2bc**) and $-58.9 \text{ kJ mol}^{-1}$ (**3bc**) (for more details see Chapter 4.2). We are assuming that the transesterification from **2bc** to **3bc** has a Gibbs free energy barrier of $x \text{ kJ mol}^{-1}$ (Eq. 4.28), whereby the transesterification from **3bc** to **2bc** has a free energy barrier of $(x - 2.55) \text{ kJ mol}^{-1}$ (Eq. 4.29) justified by the same single transition state and **2bc** is around 2.55 kJ mol^{-1} more stable than **3bc**. Again via the Van-'t Hoff equation (Eq. 4.27) and $\Delta G_{k_{rel,c}} = -2.55 \text{ kJ mol}^{-1}$ the relative rate constant of the transesterification could be determined as $k_{rel,c} = 2.82$. Comparing the $\Delta G_{k_{rel,c}} = -2.55 \text{ kJ mol}^{-1}$ with the modulated free energy of test **A** with $\Delta G_{k_{rel,c}} = -5.67 \text{ kJ mol}^{-1}$, the modulated free energy is around 3 kJ mol^{-1} lower. Based on this findings, further values for k_5 and k_6 originating from the effective rate constants by test **A** are tested which illustrating a relative rate constant of $k_{rel,c} = 2.82$ (Test **E,F**, Table 4.22). It looks as if the effective rate constant by Test **F** is reflecting the effective rates of the transesterification (Figure 4.59).

$$\Delta G = -R T \ln k \quad \text{Eq. 4.23}$$

$$\Delta G_{k_{rel,c}}^{\ddagger} = -R T \ln k_{rel,c} = -R T \ln \frac{k_5}{k_6} \quad \text{Eq. 4.24}$$

$$\frac{k_5}{k_6} = \frac{e^{-\frac{\Delta G_{k_5}^{\ddagger}}{RT}}}{e^{-\frac{\Delta G_{k_6}^{\ddagger}}{RT}}} = e^{-\frac{\Delta G_{k_5}^{\ddagger}}{RT} + \frac{\Delta G_{k_6}^{\ddagger}}{RT}} \quad \text{Eq. 4.25}$$

$$\ln \frac{k_5}{k_6} = -\frac{\Delta G_{k_5}^{\ddagger}}{RT} + \frac{\Delta G_{k_6}^{\ddagger}}{RT} \quad \text{Eq. 4.26}$$

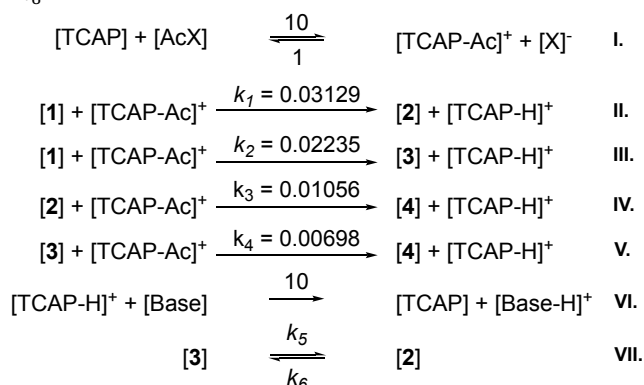
$$\Delta G_{k_5}^{\ddagger} - \Delta G_{k_6}^{\ddagger} = -R T \ln \frac{k_5}{k_6} \quad \text{Eq. 4.27}$$

With

$$\Delta G_{k_6}^{\ddagger} = x \text{ kJ mol}^{-1} \quad \text{Eq. 4.28}$$

$$\Delta G_{k_5}^{\ddagger} = x \text{ kJ mol}^{-1} - 2.55 \text{ kJ mol}^{-1} \quad \text{Eq. 4.29}$$

$$-2.55 \text{ kJ mol}^{-1} = -R T \ln \frac{k_5}{k_6} \quad \text{Eq. 4.30}$$



Scheme 4.12. Model reaction used in CoPaSi simulation of the rate constants.

Table 4.22. Defined rate constants for k_5 and k_6 used in the simulations.

Test	k_5 (L mol ⁻¹ s ⁻¹)	k_6 (L mol ⁻¹ s ⁻¹)	$k_{rel,c}$	$\Delta G_{k_{rel,c}}$ (kJ mol ⁻¹)
A	1.0x10 ⁻⁵	1.0x10 ⁻⁶	10.0	-5.67
B	1.0x10 ⁻⁶	1.0x10 ⁻⁵	0.1	5.67

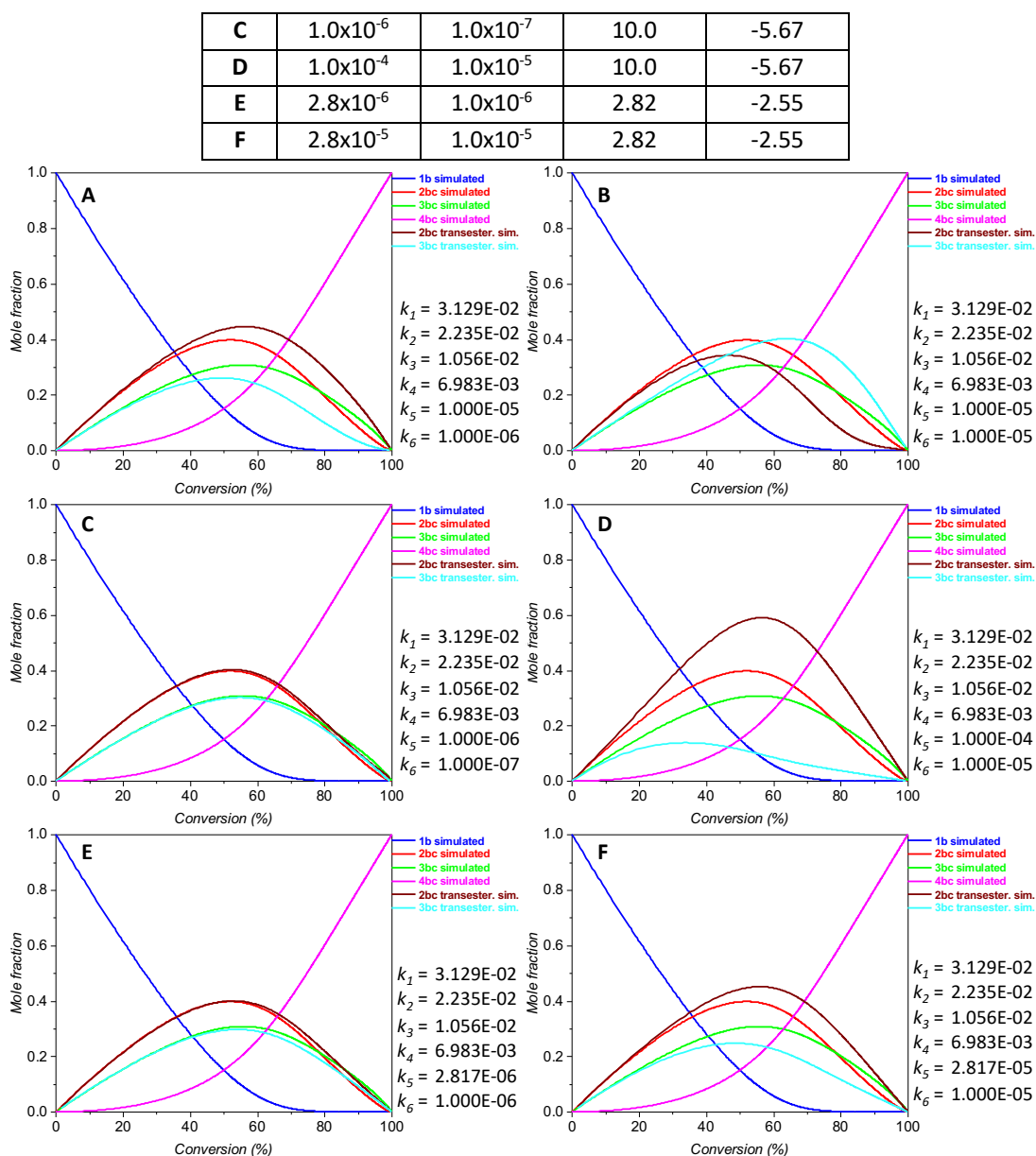


Figure 4.58. Plot of *conversion (%)* vs. *mole fraction* for the reaction of **1b** with **5c** excluding (red and green line) and including transesterification reaction (brown and cyan line). The rate constants $k_1 - k_6$ are given in $\text{L mol}^{-1} \text{s}^{-1}$.

Size-Induced Inversion of Selectivity in the Acylation of 1,2-Diols

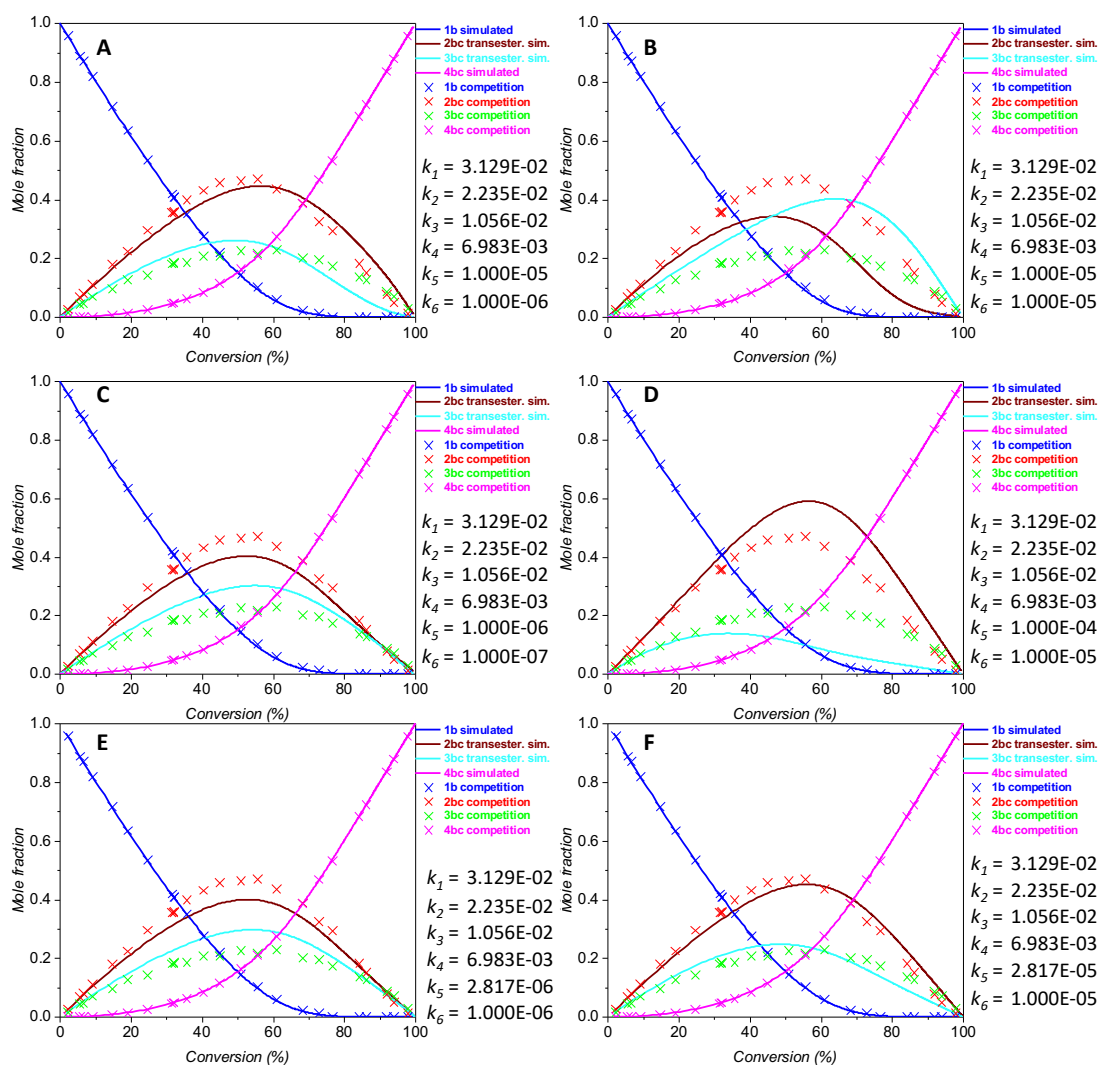
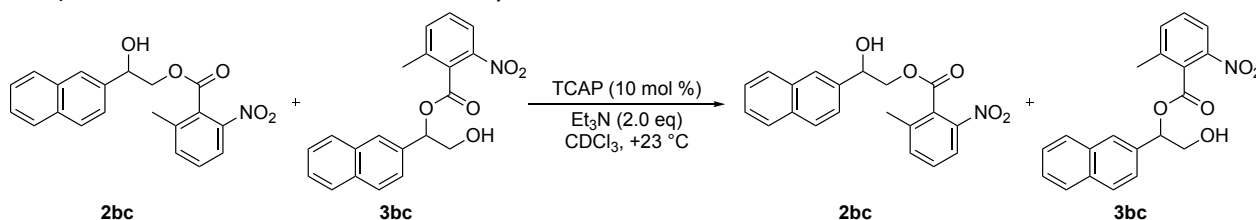


Figure 4.59. Plot of conversion (%) vs. mole fraction for the reaction of **1b** with **5c** including transesterification reaction. The rate constants $k_1 - k_6$ are given in $\text{L mol}^{-1} \text{s}^{-1}$.

In a separate experiment, transesterification was quantified. In the following a general guideline for the performance of a transesterification absolute kinetic experiment is described, based on the experiment shown in Scheme 4.13. Two different CDCl_3 stock solutions containing a 0.04 M mixture of monoesters **2bc** and **3bc** (A) and a combination of 0.08 M Et_3N and 0.004 M TCAP (C) are prepared under nitrogen (Table 4.23). The monoester **2bc** and **3bc** initially exist in a 13:10 ratio:



Scheme 4.13. Model reaction for transesterification of monoesters **2bc** and **3bc**.

Table 4.23. Preparation of initial CDCl_3 stock solutions.

Stock solution	Compound	Concentration (mol L^{-1})	Volume (mL)	n (mol)	M.W. (g mol^{-1})	Mass (mg)
Stock A	2bc:3bc (13:10)	0.04	1	$4 \cdot 10^{-5}$	351	14.0
Stock C	Et_3N	0.08	2	$160 \cdot 10^{-6}$	101	16.2
	TCAP	0.004	2	$8 \cdot 10^{-6}$	174	1.4

The reaction is analysed by ^1H NMR recorded by Bruker Avance III 400 machines. NMR tubes are dried under vacuum using a Schlenk based glassware and flushed with nitrogen. 0.4 mL of stock A and 0.2 mL of stock C

are transferred under nitrogen to the NMR tube by use of a Hamilton syringe. After closing the NMR tubes, the reaction mixture is shaken and put into the NMR machine. Because of the low concentrations in the reaction mixture, for each ^1H NMR spectrum 32 scans are recorded. In Figure 4.60 the migration from **3bc** into **2bc** over time is clearly visible. In the beginning the migration starts slowly and increases over time.

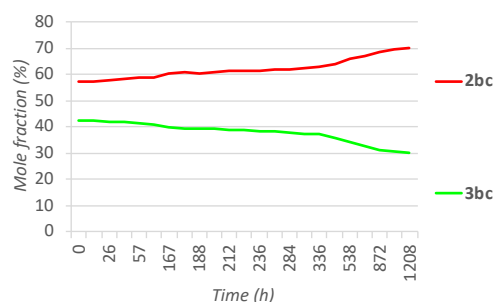


Figure 4.60. Plot of mole fraction (%) vs. time (h) for the migration of **3bc** into **2bc**.

Table 4.24. Integral limits (ppm), relative and absolute integral values for transesterification of monoesters **2bc** and **3bc** and the corresponding mole fractions of **2bc** and **3bc**.

Time (h)	integral limits (ppm)		integral	absolute	integral limits (ppm)		integral	absolute	mole fraction (%)	
	2bc				3bc				2bc	3bc
0	5.36	5.27	1.36	83135.60	6.43	6.34	1.00	61335.20	57.5	42.5
9	5.34	5.28	1.35	92803.80	6.42	6.34	1.00	68634.60	57.5	42.5
26	5.28	5.21	1.37	99180.70	6.36	6.28	1.00	72369.20	57.8	42.2
33	5.37	5.23	1.39	83121.30	6.44	6.32	1.00	59920.20	58.1	41.9
57	5.36	5.24	1.42	88968.20	6.44	6.33	1.00	62847.10	58.6	41.4
81	5.36	5.26	1.44	81640.80	6.43	6.36	1.00	56693.80	59.0	41.0
167	5.35	5.26	1.52	80915.00	6.44	6.33	1.00	53229.50	60.3	39.7
177	5.35	5.23	1.55	100934.00	6.43	6.34	1.00	65196.40	60.8	39.2
188	5.35	5.27	1.54	82782.40	6.44	6.34	1.00	53801.60	60.6	39.4
200	5.36	5.28	1.55	83934.30	6.44	6.34	1.00	54150.50	60.8	39.2
212	5.37	5.26	1.58	84684.10	6.43	6.35	1.00	53667.90	61.2	38.8
224	5.36	5.27	1.58	81304.10	6.43	6.34	1.00	51386.00	61.3	38.7
236	5.36	5.25	1.60	83972.70	6.45	6.34	1.00	52325.10	61.6	38.4
260	5.36	5.26	1.62	96704.50	6.45	6.34	1.00	59598.90	61.9	38.1
284	5.34	5.28	1.64	83201.80	6.41	6.36	1.00	50802.60	62.1	37.9
308	5.34	5.28	1.66	97627.70	6.41	6.36	1.00	58793.30	62.4	37.6
336	5.36	5.27	1.70	90003.80	6.44	6.35	1.00	53093.40	62.9	37.1
438	5.36	5.27	1.78	84974.70	6.48	6.34	1.00	47645.80	64.1	35.9
538	5.36	5.26	1.93	101404.00	6.42	6.36	1.00	52438.80	65.9	34.1
718	5.35	5.27	2.04	99687.80	6.42	6.35	1.00	48832.50	67.1	32.9
872	5.34	5.26	2.18	96060.40	6.42	6.35	1.00	44000.00	68.6	31.4
1064	5.34	5.27	2.26	99560.70	6.44	6.36	1.00	43972.30	69.4	30.6
1208	5.35	5.26	2.34	102418.00	6.41	6.34	1.00	43792.30	70.0	30.0

4.1.6 Investigation of Reaction Conditions

4.1.6.1 Investigation of Temperature Effects

A decrease in temperature often implies an increase in selectivity, what was documented by Giese *et al.*^[7] Thus we tested the effects of reaction temperature on selectivities of the first acylation for the anhydride **5c** with the diol system **1a** and **1b** by measuring a turnover-limited competition experiment at the 30% point. This analytical model was chosen, because the 30% conversion point is a practical experimental method, which give us moderate results in a conceivable time ranch. To mimic the effect of transesterification during the ^1H NMR analysis due to change in temperature, the samples were immediately measured after sample extraction. By varying the temperature from +40 °C to -20 °C we observed moderate changes in the relative rate constants $k_{\text{rel},a30\%}$ for anhydride **5c**, which are stronger for the 2-Np substitutes 1,2-diol **1b**. By using the well-known Eyring equation Eq. 4.31, an activation entropy difference of -54.1 J K⁻¹·mol was found for **1a** with **5c**. For diol **1b** the activation entropy difference increases to -81.3 J K⁻¹.

$$k_1 = \frac{k_B T}{h} \cdot e^{-\frac{\Delta G_1^\ddagger}{RT}} \quad \text{Eq. 4.31}$$

Size-Induced Inversion of Selectivity in the Acylation of 1,2-Diols

$$\frac{k_1}{k_2} = \frac{e^{-\frac{\Delta G_1^\ddagger}{RT}}}{e^{-\frac{\Delta G_2^\ddagger}{RT}}} \quad \text{Eq. 4.32}$$

$$\frac{k_1}{k_2} = e^{-\frac{\Delta G_1^\ddagger + \Delta G_2^\ddagger}{RT}} \quad \text{Eq. 4.33}$$

$$\ln \frac{k_1}{k_2} = -\frac{\Delta G_1^\ddagger}{RT} + \frac{\Delta G_2^\ddagger}{RT} \quad \text{Eq. 4.34}$$

$$\ln \frac{k_1}{k_2} = -\frac{\Delta H_1^\ddagger - T\Delta S_1^\ddagger}{RT} + \frac{\Delta H_2^\ddagger - T\Delta S_2^\ddagger}{RT} \quad \text{Eq. 4.35}$$

$$\ln \frac{k_1}{k_2} = -\frac{\Delta H_1^\ddagger}{T} + \frac{\Delta S_1^\ddagger}{R} + \frac{\Delta H_2^\ddagger}{RT} - \frac{\Delta S_2^\ddagger}{R} \quad \text{Eq. 4.36}$$

$$\ln \frac{k_1}{k_2} = \frac{\Delta H_2^\ddagger - \Delta H_1^\ddagger}{RT} - \frac{\Delta S_2^\ddagger - \Delta S_1^\ddagger}{R} \quad \text{Eq. 4.37}$$

With

$$\Delta\Delta H^\ddagger = \Delta H_2^\ddagger - \Delta H_1^\ddagger$$

$$\Delta\Delta S^\ddagger = \Delta S_2^\ddagger - \Delta S_1^\ddagger$$

$$R = 8.31451 \text{ J K}^{-1} \cdot \text{mol}$$

$$\ln(k_{rel}) = \ln \frac{k_1[2(a,b)c]}{k_2[3(a,b)c]} = \frac{\Delta\Delta H^\ddagger}{R \cdot T} - \frac{\Delta\Delta S^\ddagger}{R} \quad \text{Eq. 4.38}$$

Phenylethane-1,2-diol **1a**

$$\ln \frac{k_1}{k_2} = \frac{-1457.76}{T} + 6.51 \quad \text{Eq. 4.39}$$

$$\Delta\Delta H^\ddagger = \Delta H_2^\ddagger - \Delta H_1^\ddagger = -12.1 \text{ kJ mol}^{-1} \quad \text{Eq. 4.40}$$

$$\Delta\Delta S^\ddagger = \Delta S_2^\ddagger - \Delta S_1^\ddagger = -54.1 \text{ J K}^{-1} \cdot \text{mol} \quad \text{Eq. 4.41}$$

2-Naphthylethane-1,2-diol **1b**

$$\ln \frac{k_1}{k_2} = \frac{-2756.77}{T} + 9.78 \quad \text{Eq. 4.42}$$

$$\Delta\Delta H^\ddagger = \Delta H_2^\ddagger - \Delta H_1^\ddagger = -22.9 \text{ kJ mol}^{-1} \quad \text{Eq. 4.43}$$

$$\Delta\Delta S^\ddagger = \Delta S_2^\ddagger - \Delta S_1^\ddagger = -81.3 \text{ J K}^{-1} \cdot \text{mol} \quad \text{Eq. 4.44}$$

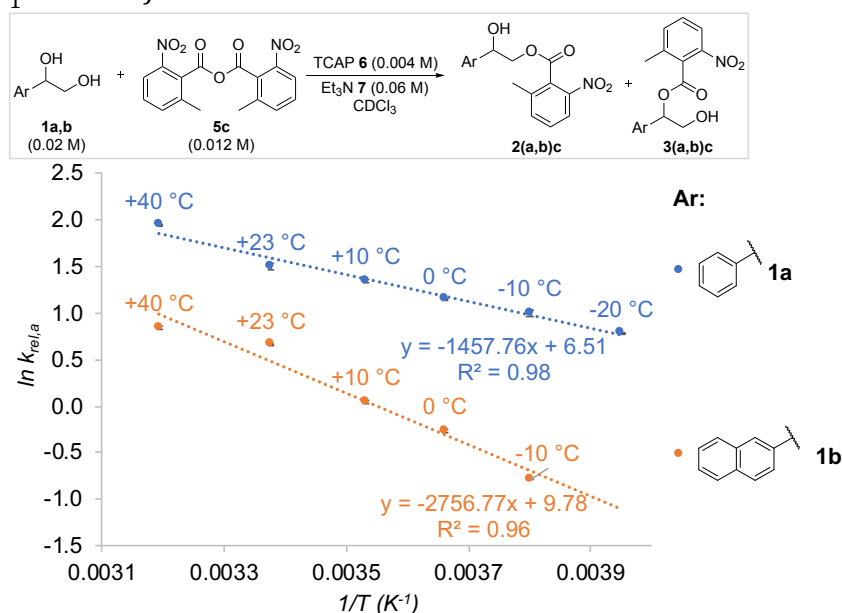


Figure 4.61. Eyring plot of $\ln k_{rel}$ at different temperatures.

Table 4.25. Conversion, mole fractions, relative rate and natural logarithm of relative rate with standard derivations calculated from corresponding ^1H NMR measurements for temperature depending turnover-limited competition experiments at 30% conversion.

Temperature	Conv. (%)	1a (%)	2ac (%)	3ac (%)	4ac (%)	$k_{rel,a30\%}$	$\ln k_{rel,a30\%}$
+40 °C	28.20	45.73	45.63	6.51	2.13	7.007	1.947
313.15 K	29.47	43.42	47.53	6.70	2.35	7.095	1.959

	27.55	46.95	44.60	6.40	2.05	6.964	1.941	
						7.022 ± 0.055	1.949 ± 0.008	
+23 °C	30.48	41.60	45.80	10.03	2.57	4.565	1.518	
296.15 K	30.21	42.11	45.37	9.98	2.53	4.547	1.514	
	29.92	42.81	44.26	10.27	2.66	4.310	1.461	
						4.474 ± 0.116	1.498 ± 0.026	
+10 °C	29.48	43.87	42.31	10.98	2.84	3.853	1.349	
283.15 K	29.78	43.38	42.60	11.07	2.95	3.848	1.348	
	28.23	46.13	40.59	10.70	2.58	3.792	1.333	
						3.831 ± 0.028	1.343 ± 0.007	
0 °C	32.86	38.10	44.08	14.00	3.81	3.148	1.147	
273.15 K	32.18	39.33	43.33	13.66	3.68	3.172	1.154	
	32.64	38.53	43.79	13.86	3.82	3.160	1.151	
						3.160 ± 0.010	1.151 ± 0.003	
-10 °C	32.82	37.36	43.54	16.10	3.00	2.704	0.995	
263.15 K	33.77	35.97	43.92	16.59	3.52	2.647	0.973	
	33.28	36.82	44.09	15.71	3.39	2.807	1.032	
						2.719 ± 0.067	1.000 ± 0.024	
-20 °C	30.71	42.45	36.79	16.90	3.87	2.177	0.778	
253.15 K	30.23	43.19	36.43	16.73	3.65	2.178	0.778	
	29.99	43.66	36.22	16.47	3.64	2.199	0.788	
						2.185 ± 0.010	0.781 ± 0.005	
Temperature	Conv. (%)	1b (%)	2bc (%)	3bc (%)	4bc (%)	$k_{rel,a30\%}$	$\ln k_{rel,a30\%}$	
+40 °C	29.84	44.68	35.73	15.24	4.36	2.345	0.852	
313.15 K	30.42	43.64	36.27	15.61	4.48	2.324	0.843	
	29.96	44.53	35.48	15.54	4.45	2.284	0.826	
						2.318 ± 0.025	0.840 ± 0.011	
+23 °C	31.35	41.88	35.43	18.11	4.58	1.956	0.671	
296.15 K	32.10	40.69	36.00	18.42	4.89	1.954	0.670	
	31.84	41.17	35.48	18.49	4.85	1.918	0.652	
						1.943 ± 0.017	0.664 ± 0.009	
+10 °C	33.95	37.43	29.25	27.99	5.33	1.045	0.044	
283.15 K	32.93	39.17	28.38	27.43	5.03	1.035	0.034	
	32.59	39.78	28.47	26.80	4.95	1.063	0.061	
						1.047 ± 0.011	0.046 ± 0.011	
0 °C	32.56	38.99	24.55	32.35	4.11	0.759	-0.276	
273.15 K	41.09	23.04	31.01	40.73	5.22	0.762	-0.272	
	31.78	40.70	24.04	31.00	4.26	0.775	-0.254	
						0.765 ± 0.007	-0.268 ± 0.009	
-10 °C	30.82	41.29	17.51	38.29	2.92	0.457	-0.783	
263.15 K	33.40	36.33	19.21	41.32	3.14	0.465	-0.766	
	30.83	40.08	18.16	40.02	1.74	0.454	-0.790	
						0.459 ± 0.005	-0.779 ± 0.010	
-20 °C	Precipitation available. Not analysable.							
253.15 K								

4.1.6.2 Investigation of Solvent Effects

As shown in earlier study of the Zipse group with related system,^[8] the solvent can in principle change the relative rate constants of the first acylation step. We thus tested the effects of solvent on selectivities for anhydride **5c** with the diol system **1b** in CD₂Cl₂, MeCN-*d*3, THF-*d*8, CDCl₃ and acetone-*d*6. Only a limited range of solvents could be used in this study due to the low solubility of **1b** and **5c**. Deuterated solvents were used in all cases in order to facilitate analysis of reaction samples running for exactly two weeks because of mimicking the effect of transesterification in the reaction system with **5c**. In all solvents except acetonitrile was this sufficient to reach full conversion of added anhydride **5c** (see Figure 4.62). A change in selectivity of around 1.2 was detected ($k_{rel,a30\%} = 2.5$ to 1.3) on moving from the least polar (THF-*d*8), to the most polar solvent (MeCN-*d*3). A good correlation ($R^2=0.86$) was obtained when plotting $\ln k_{rel,a30\%}$ against the Reichardt solvent parameter $E_T(30)^{[9]}$ as shown in Figure 4.63.

Size-Induced Inversion of Selectivity in the Acylation of 1,2-Diols

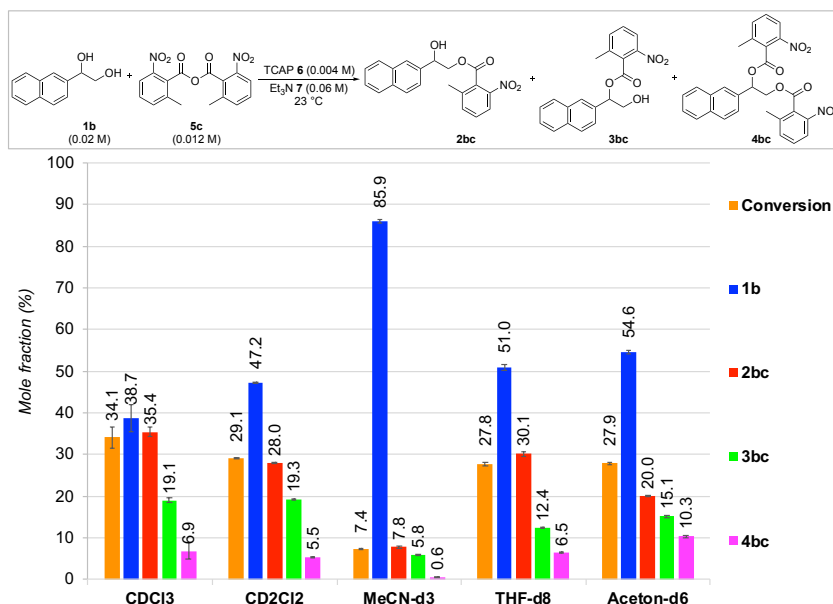


Figure 4.62. Mole fractions (%) of **1b:2bc:3bc:4bc** and total conversion (%) for the acylation of diol **1b** with anhydride **5c** at the 30 % conversion point in different solvents.

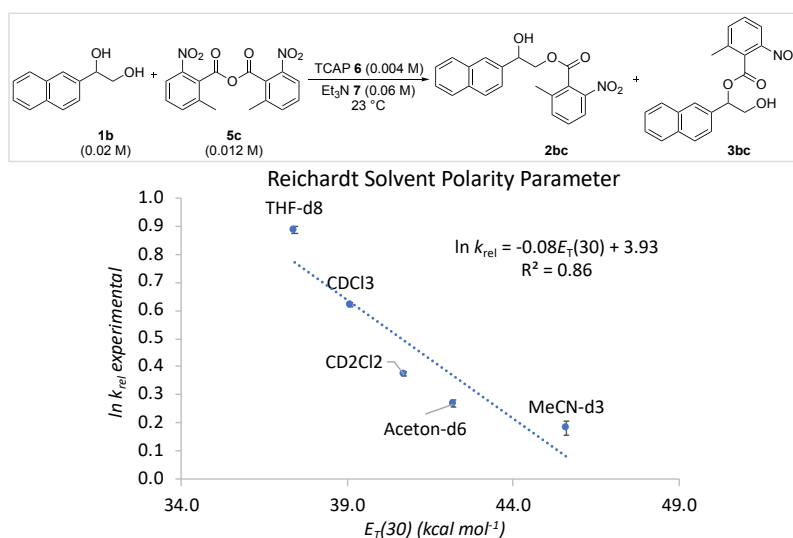


Figure 4.63. Plot of $E_T(30) k_{rel,a30\%}$ vs. $k_{rel,a30\%}$ for the results shown in Table 4.26.

Table 4.26. Conversion, mole fractions, relative rates and natural logarithms of relative rates with standard derivations calculated from the corresponding ¹H NMR measurements for solvent-dependent turnover-limited competition experiments. The Reichardt solvent polarity parameter $E_T(30)$ (kcal mol⁻¹) of the non deuterated solvents have been used.^[9]

Solvent	Conv. (%)	1a (%)	2ac (%)	3ac (%)	4ac (%)	$k_{rel,a30\%}$	ln $k_{rel,a30\%}$
CDCl ₃	35.64	36.31	36.57	19.52	7.60	1.873	0.628
$E_T(30) = 39.1$	35.54	37.36	35.20	18.98	8.45	1.855	0.618
	31.12	42.36	34.38	18.65	4.61	1.843	0.612
						1.857 ± 0.012	0.619 ± 0.007
MeCN-d ₃	9.03	83.14	8.54	7.12	1.20	1.200	0.182
$E_T(30) = 45.6$	10.68	80.46	9.70	8.01	1.83	1.210	0.191
	9.84	81.82	9.05	7.62	1.51	1.187	0.171
						1.199 ± 0.010	0.181 ± 0.008
MeCN-d ₃	7.13	86.41	7.32	5.61	0.66	1.304	0.266
	7.49	85.66	7.90	5.81	0.64	1.361	0.308
	7.46	85.57	8.04	5.90	0.49	1.362	0.309
						1.343 ± 0.027	0.294 ± 0.020
THF-d ₈	27.91	50.60	30.46	12.52	6.42	2.433	0.889
$E_T(30) = 37.4$	27.36	51.76	29.46	12.31	6.47	2.394	0.873
	28.03	50.52	30.45	12.44	6.59	2.448	0.895
						2.425 ± 0.023	0.886 ± 0.009

Solvent	Conv. (%)	1b (%)	2bc (%)	3bc (%)	4bc (%)	$k_{rel,a30\%}$	$\ln k_{rel,a30\%}$
CD_2Cl_2 $E_T(30) = 40.7$	29.09	47.26	27.97	19.32	5.44	1.448	0.370
	29.06	47.33	27.91	19.32	5.44	1.445	0.368
	29.20	47.15	28.10	19.20	5.55	1.464	0.381
						1.452 ± 0.009	0.373 ± 0.006
Aceton- d_6 $E_T(30) = 42.2$	28.30	54.12	20.09	15.05	10.73	1.335	0.289
	27.60	55.03	19.77	14.97	10.23	1.321	0.278
	27.71	54.58	20.00	15.42	10.00	1.297	0.260
						1.309 ± 0.016	0.269 ± 0.012

4.1.6.3 Investigation of Auxiliary Base

4.1.6.3.1 Background Reaction

To quantify the uncatalyzed background reaction for 1,2-diol **1b** two further reaction were carried out with anhydride derivatives **5a** and **5c**. Et_3N was still used as auxiliary base in excess. The uncatalyzed absolute kinetic experiment was running around 3 months. In the case of **5a** small amounts of esters are formed till are full conversion around 50 %, whereby in the case of **5c** only traces of monoester **2bc** were formed.

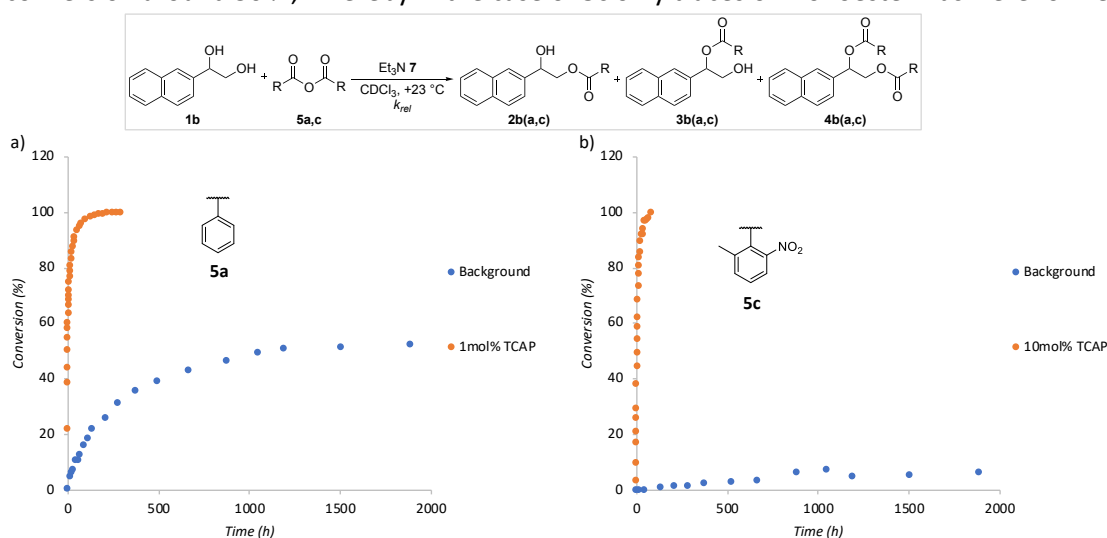


Figure 4.64. Plot of time (sec) vs. conversion (%) of all OH-groups for **1b** with a) **5a** and b) **5c**.

Table 4.27. Time (h), conversion total (%) and ratio of **1b:2b(a,c):3b(a,c):4b(a,c)** for absolute kinetic measurement from the background reaction of 2-naphthyl-ethane-1,2-diol **1b** with acid anhydride derivatives **5a,c**. Baseline of 1H NMR for integration was corrected by Whittaker Smoother (I) fit.

Time (h)	Conv (%)	Ratio (%)				Time (h)	Conv (%)	Ratio (%)			
Time	Conv _{exp}	1b	2ba	3ba	4ba	time	Conv _{exp}	1b	2bc	3bc	4bc
2	0.3	1.0	0.0	0.0	0.0	2	0.0	/	/	/	/
18	5.0	0.9	0.1	0.0	0.0	18	0.0	/	/	/	/
23	6.2	0.9	0.1	0.0	0.0	42	0.0	/	/	/	/
27	7.0	0.9	0.1	0.0	0.0	138	0.8	/	/	/	/
44	10.7	0.8	0.2	0.0	0.0	210	1.3	/	/	/	/
61	10.6	0.7	0.2	0.0	0.0	282	1.4	/	/	/	/
68	12.8	0.7	0.3	0.0	0.0	378	2.1	/	/	/	/
88	16.3	0.6	0.3	0.0	0.0	522	2.7	/	/	/	/
112	18.5	0.6	0.4	0.0	0.0	666	3.3	/	/	/	/
136	21.9	0.5	0.5	0.0	0.0	882	6.5	/	/	/	/
208	26.0	0.4	0.5	0.1	0.0	1050	7.5	/	/	/	/
280	31.3	0.3	0.6	0.1	0.0	1194	4.8	/	/	/	/
376	35.4	0.2	0.6	0.1	0.0	1506	5.2	/	/	/	/
496	39.3	0.2	0.7	0.1	0.0	1890	6.5	/	/	/	/
664	42.8	0.1	0.7	0.1	0.0						
880	46.4	0.1	0.7	0.1	0.1						
1048	49.3	0.0	0.7	0.2	0.1						
1192	50.9	0.0	0.7	0.2	0.1						

1504	51.4	0.0	0.8	0.2	0.1					
1888	52.5	0.0	0.7	0.2	0.1					

4.1.6.3.2 Concentration of Auxiliary Base

We tested the effect of auxiliary base Et_3N concentration on selectivities for the anhydride **5c** with the diol system **1b** by measuring an absolute kinetic study. By varying the Et_3N concentration from 0.020 M to 0.080 M we observed no changes in absolute reaction time for anhydride **5c** (Figure 4.65a). However, the selectivities for $k_{\text{rel},a}$ and k_{sec} are changing caused in polarity effects (Figure 4.65b). The selectivities for the first acylation are changing from $k_{\text{rel},a} = 1.52$ (0.02 M) to $k_{\text{rel},a} = 1.12$ (0.08 M), whereby the selectivities for the acylation of secondary OH-groups are changing from $k_{\text{sec}} = 1.57$ (0.02 M) to $k_{\text{sec}} = 2.52$ (0.08 M).

In terms of the actual starting concentrations (mol/L) for all components:

1.5 eq. Et_3N NMR Tube: **1b** 0.00667, **5c**: 0.02000, **Et_3N** : 0.02000, **TCAP**: 0.00133

2.0 eq. Et_3N NMR Tube: **1b** 0.00667, **5c**: 0.02000, **Et_3N** : 0.02667, **TCAP**: 0.00133 (see Chapter 4.1.2.1)

3.0 eq. Et_3N NMR Tube: **1b** 0.00667, **5c**: 0.02000, **Et_3N** : 0.04000, **TCAP**: 0.00133

6.0 eq. Et_3N NMR Tube: **1b** 0.00667, **5c**: 0.02000, **Et_3N** : 0.08000, **TCAP**: 0.00133

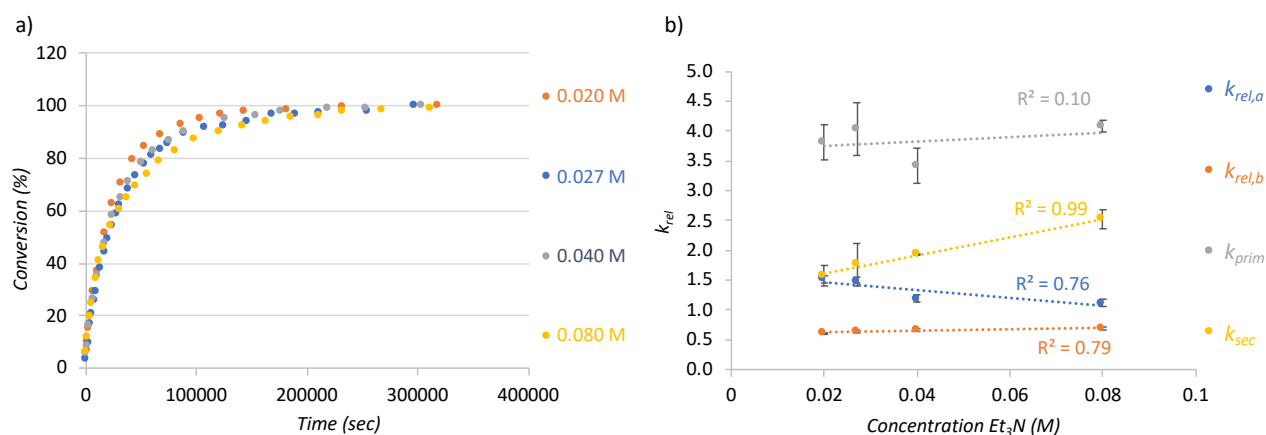


Figure 4.65. a) Plot of *time (sec)* vs. *conversion (%)* of all OH-groups for **1b** with **5c** and different concentrations of the auxiliary base Et_3N . b) Changes in selectivities for the acylation of **1b** with **5c** and different concentrations of the auxiliary base Et_3N .

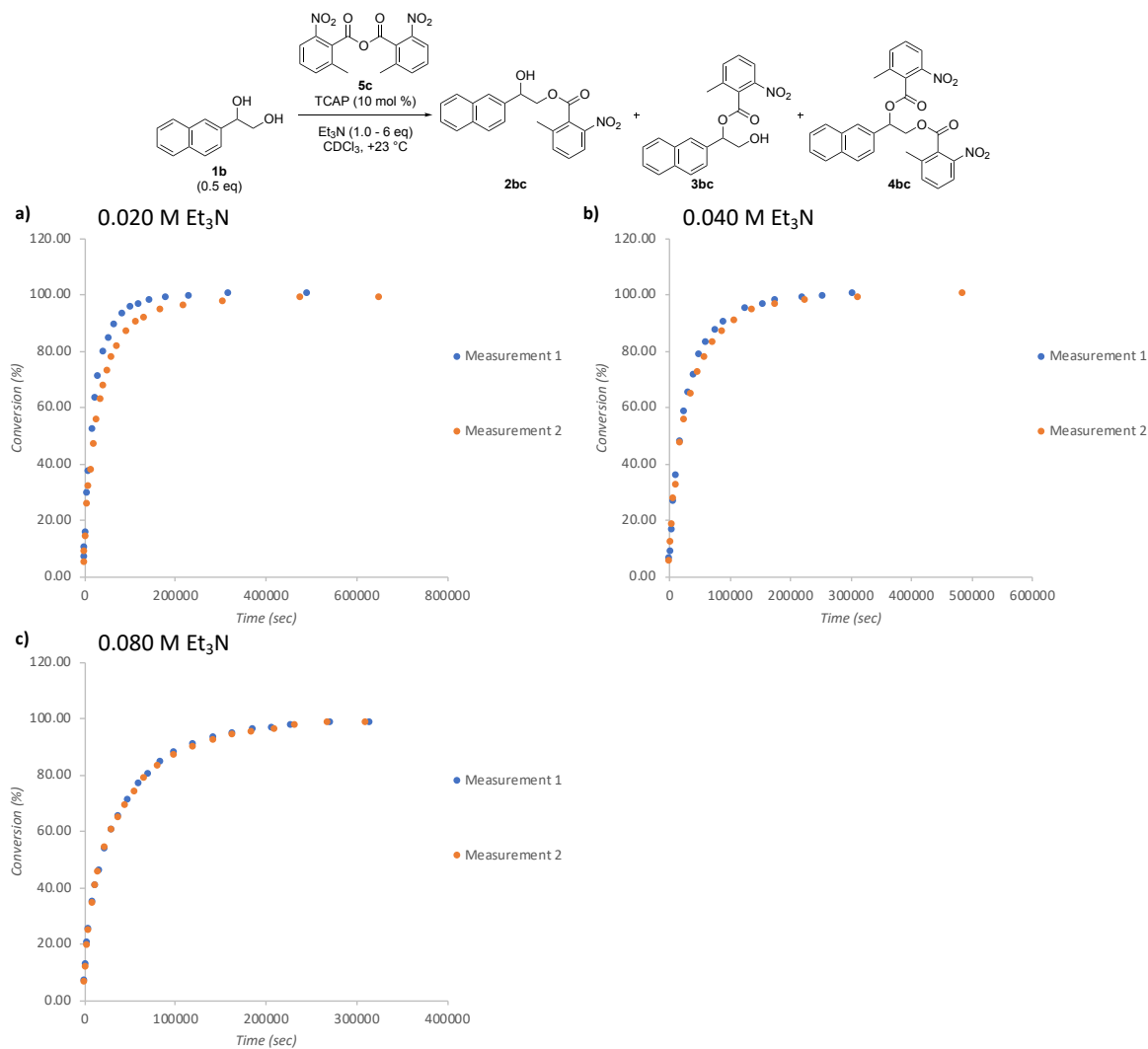


Figure 4.66. Plot of time (sec) vs. conversion (%) of all OH-groups for **1b** with **5c** and a) 0.02 M Et_3N , b) 0.04 M Et_3N and c) 0.08 M Et_3N

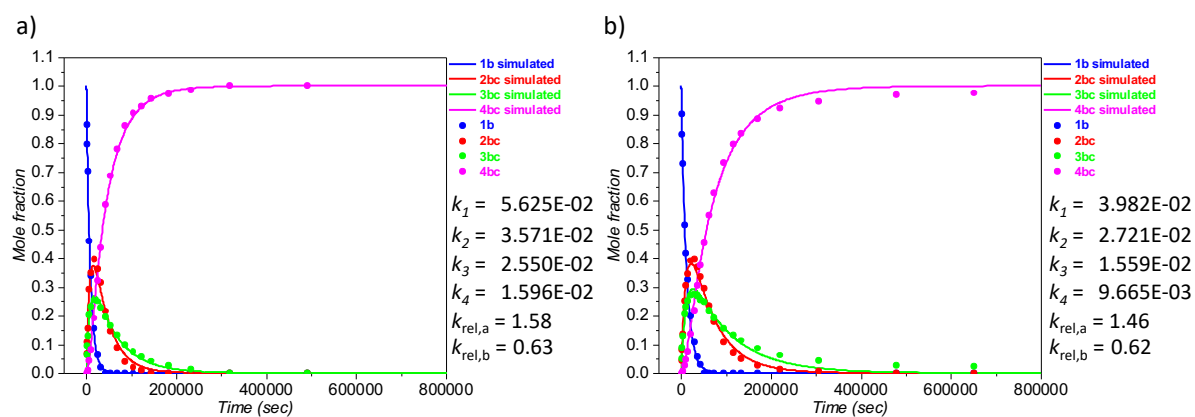


Figure 4.67. Plot of time (sec) vs. mole fraction for **1b** with **5c** and 0.020 M Et_3N for a) measurement 1 and b) measurement 2. The effective rate constants $k_1 - k_4$ are given in $\text{L mol}^{-1} \text{s}^{-1}$.

Size-Induced Inversion of Selectivity in the Acylation of 1,2-Diols

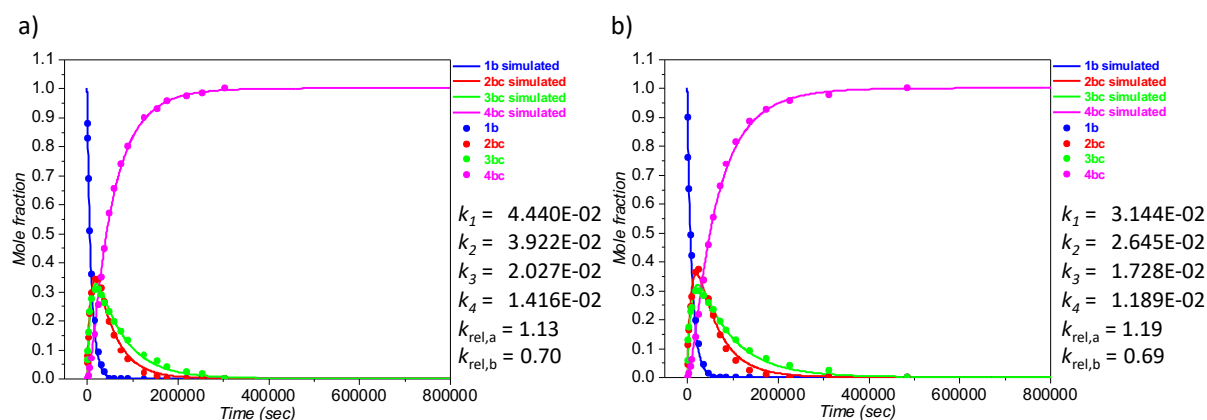


Figure 4.68. Plot of time (sec) vs. mole fraction for **1b** with **5c** and 0.040 M Et₃N for a) measurement 1 and b) measurement 2. The effective rate constants $k_1 - k_4$ are given in L mol⁻¹ s⁻¹.

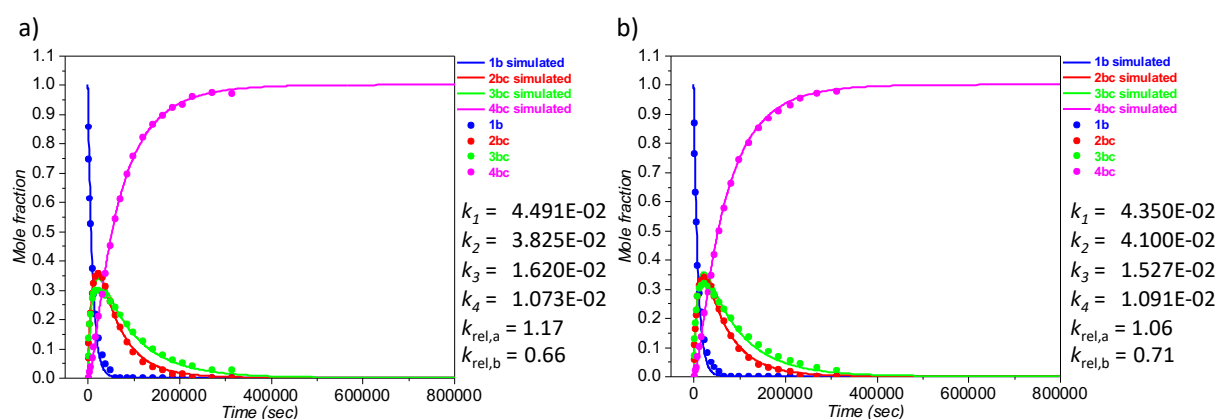


Figure 4.69. Plot of time (sec) vs. mole fraction for **1b** with **5c** and 0.080 M Et₃N for a) measurement 1 and b) measurement 2. The effective rate constants $k_1 - k_4$ are given in L mol⁻¹ s⁻¹.

Figure 4.70. Time (sec), conversion total (%) and ratio of **1b:2bc:3bc:4bc** for absolute kinetic measurement of 2-naphthylethane-1,2-diol **1b** with acid anhydride derivate **5c** and variations of auxiliary base Et₃N concentrations.

Time (h)	Conv (%)	Ratio (%)				Time (h)	Conv (%)	Ratio (%)			
Time	Conv _{exp}	1b	2bc	3bc	4bc	time	Conv _{exp}	1b	2bc	3bc	4bc
0.020 M Et₃N											
1080	6.7	86.6	6.9	6.6	0.0	780	4.8	90.4	4.5	5.1	0.0
1800	10.1	79.9	10.7	9.4	0.0	1740	8.4	83.2	8.0	8.8	0.0
3000	15.3	70.3	15.6	13.0	1.0	3540	13.9	72.8	13.6	12.9	0.6
6600	29.2	46.0	29.1	20.5	4.4	7140	25.6	51.4	25.0	20.9	2.7
10200	37.1	33.9	34.9	23.1	8.1	10740	31.6	41.6	30.4	23.1	4.9
17400	51.8	15.7	39.8	25.4	19.2	14340	37.4	32.7	34.6	25.1	7.6
24600	62.9	6.4	36.3	25.0	32.3	21540	46.8	20.1	39.2	27.0	13.7
31800	70.8	2.2	31.5	22.6	43.7	28740	55.4	10.9	39.8	27.5	21.8
42600	79.3	0.1	21.6	19.6	58.7	35940	62.4	5.7	37.0	26.7	30.6
53400	84.4	0.0	14.6	16.7	68.7	43140	67.3	3.2	33.5	25.6	37.7
67800	89.1	0.0	8.7	13.2	78.1	50340	72.8	0.0	29.7	24.8	45.5
85800	93.1	0.0	4.2	9.7	86.1	61140	77.5	0.0	23.3	21.7	55.0
103800	95.3	0.0	2.0	7.3	90.6	71940	81.3	0.0	17.9	19.4	62.7
121800	96.6	0.0	1.1	5.7	93.1	93540	86.7	0.0	11.0	15.7	73.3
143400	97.9	0.0	0.0	4.2	95.8	115140	89.9	0.0	7.1	13.1	79.7
181800	98.7	0.0	0.0	2.6	97.4	133140	91.7	0.0	5.2	11.4	83.4
232200	99.3	0.0	0.0	1.4	98.6	169140	94.3	0.0	2.7	8.6	88.7
318600	100.0	0.0	0.0	0.0	100.0	219540	96.1	0.0	1.5	6.3	92.2
491400	100.0	0.0	0.0	0.0	100.0	305940	97.4	0.0	0.7	4.5	94.8
						478740	98.6	0.0	0.0	2.8	97.2
						651540	98.8	0.0	0.0	2.4	97.6
0.040 M Et₃N											

600	6.0	88.0	5.4	6.6	0.0	600	5.0	89.9	4.5	5.6	0.0
1200	8.6	82.8	7.8	9.4	0.0	2100	12.0	75.9	11.3	12.8	0.0
3000	16.1	68.8	14.1	16.0	1.1	3600	18.1	65.2	16.2	17.2	1.4
6600	26.5	50.8	22.4	23.0	3.8	7200	27.2	49.2	24.5	22.7	3.6
10200	35.4	36.1	29.6	27.4	7.0	10800	32.0	42.0	27.9	24.1	6.0
17400	47.6	20.0	34.2	30.6	15.2	18000	47.2	19.7	36.4	29.9	14.0
24600	58.2	9.3	34.2	31.0	25.6	25200	55.2	11.4	37.2	29.7	21.7
31800	65.0	4.9	31.4	28.7	35.0	36000	64.5	4.5	33.6	28.3	33.6
39000	71.2	2.5	26.4	26.2	44.9	46800	72.2	1.3	27.1	25.8	45.8
49800	78.6	0.0	19.8	23.1	57.1	57600	77.7	0.0	21.4	23.3	55.4
60600	82.8	0.0	14.9	19.5	65.6	72000	83.1	0.0	14.5	19.4	66.2
75000	87.0	0.0	9.7	16.4	74.0	86400	86.9	0.0	9.8	16.3	73.8
89400	90.0	0.0	6.7	13.3	80.1	108000	90.7	0.0	5.7	13.0	81.3
125400	95.0	0.0	1.9	8.0	90.0	136800	94.2	0.0	2.4	9.1	88.5
154200	96.5	0.0	1.0	6.1	93.0	174600	96.3	0.0	1.0	6.4	92.6
175800	97.9	0.0	0.0	4.2	95.8	225000	97.9	0.0	0.0	4.1	95.9
219000	98.8	0.0	0.0	2.5	97.5	311400	98.9	0.0	0.0	2.2	97.8
253800	99.2	0.0	0.0	1.7	98.3	484200	100.0	0.0	0.0	0.0	100.0
304200	100.0	0.0	0.0	0.0	100.0						
0.080 M Et₃N											
780	7.1	85.7	6.9	7.4	0.0	720	6.5	87.0	5.7	7.3	0.0
1980	12.7	74.6	11.9	13.5	0.0	1620	11.8	76.4	10.9	12.8	0.0
3780	20.4	61.3	18.4	18.3	2.0	3420	19.5	63.1	16.3	18.5	2.1
5580	25.5	52.5	22.0	21.9	3.6	5220	25.0	53.1	21.0	22.7	3.1
9180	34.8	37.2	28.7	27.2	6.8	8820	34.4	38.0	27.6	27.6	6.8
12780	41.0	28.5	32.1	28.8	10.5	12420	40.8	28.6	31.2	30.1	10.2
16380	46.0	21.8	34.5	29.9	13.8	16020	45.7	22.2	32.9	31.2	13.7
23580	53.7	13.6	35.7	29.7	21.0	23220	54.5	12.7	33.8	31.9	21.6
30780	60.4	7.8	34.2	29.4	28.6	30420	60.4	8.0	32.3	30.7	28.9
37980	65.5	4.8	31.2	28.2	35.8	37620	64.9	4.9	31.1	29.3	34.8
48780	71.2	2.7	26.0	26.2	45.1	44820	69.2	3.2	27.4	27.7	41.7
59580	77.2	0.0	21.4	24.1	54.4	55620	74.1	1.8	23.0	25.3	49.9
70380	80.6	0.0	17.3	21.6	61.1	66420	78.9	0.0	19.0	23.1	57.8
84780	84.8	0.0	12.2	18.3	69.5	80820	83.1	0.0	13.9	20.0	66.1
99180	87.9	0.0	8.7	15.6	75.7	98820	87.1	0.0	9.6	16.2	74.2
120780	91.1	0.0	5.4	12.4	82.1	120420	90.1	0.0	6.3	13.5	80.1
142380	93.2	0.0	3.7	9.9	86.5	142020	92.5	0.0	4.1	10.8	85.1
163980	94.8	0.0	2.6	7.9	89.5	163620	94.2	0.0	2.9	8.7	88.4
185580	96.2	0.0	1.4	6.1	92.5	185220	95.5	0.0	2.2	6.9	90.9
207180	96.7	0.0	1.5	5.1	93.4	210420	96.4	0.0	1.7	5.5	92.9
228780	98.0	0.0	0.0	4.1	95.9	232020	97.7	0.0	0.3	4.3	95.4
271980	98.6	0.0	0.0	2.7	97.3	268020	98.5	0.0	0.0	3.0	97.0
315180	98.6	0.0	0.0	2.8	97.2	311220	98.9	0.0	0.0	2.2	97.8

Table 4.28. Fitted values of $k_1 - k_4$ by CoPaSi program in ($L \cdot mol^{-1} \cdot s^{-1}$), RMSD (root-mean-square deviation) values of the fitted compounds **1b**, **2bc**, **3bc** and **4bc** and the corresponding relative rate constants $k_{rel,a}$, $k_{rel,b}$, k_{prim} and k_{sec} for the acylation of **1b** with **5c** catalyzed by TCAP (10 mol%) and variations of auxiliary base Et_3N concentrations via absolute kinetic experiments.

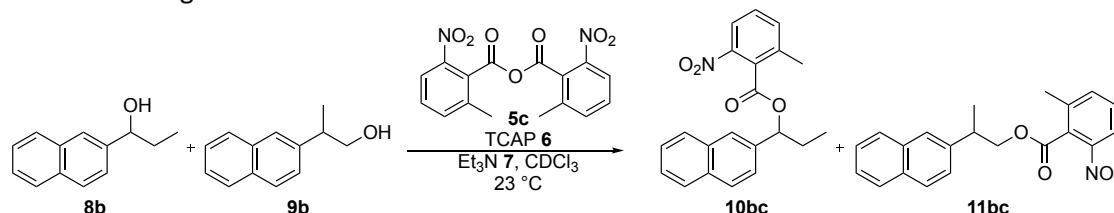
Conc. Et_3N (mol/L)	Fit	$k_1 - k_4$ ($L \cdot mol^{-1} \cdot s^{-1}$)	RMSD 1b	RMSD 2bc	RMSD 3bc	RMSD 4bc	k_{rel}	$k_1 - k_4$ ($L \cdot mol^{-1} \cdot s^{-1}$)	RMSD 1b	RMSD 2bc	RMSD 3bc	RMSD 4bc	k_{rel}	Mean $k_1 - k_4$ ($\times 10^{-3} L^{-1} \cdot mol \cdot s^{-1}$)	Mean k_{rel}	Mean $k_{rel,a}$	Mean $k_{rel,b}$	Mean k_{rel}	
0.020	1	k_1 4.283E-02	3.72E-04	2.41E-04	2.37E-04			3.029E-02	4.07E-04	2.84E-04	2.95E-04								
		k_2 2.824E-02						2.156E-02											
	2	k_3 2.541E-02		1.83E-04	1.14E-04	1.18E-04		1.548E-02		1.82E-04	1.66E-04	1.49E-04							
		k_4 1.657E-02						1.010E-02											
0.040	3	k_1 5.625E-02	1.36E-04	9.29E-05	1.01E-04		$k_{rel,a}$ k_{prim}	3.982E-02	1.88E-04	8.82E-05	1.42E-04		$k_{rel,a}$ k_{prim}	48.04 ± 8.218	Mean $k_{rel,a}$	Mean $k_{rel,b}$	Mean k_{rel}	Mean k_{prim}	
		k_2 3.571E-02					1.58	2.721E-02					1.46	4.12	31.46 ± 4.249	1.52 ± 0.056	1.52 ± 0.056	3.82 ± 0.298	
	4	k_3 2.550E-02		1.04E-04	6.77E-05	1.01E-04	$k_{rel,b}$ k_{sec}	1.559E-02		9.55E-05	1.24E-04	1.28E-04	$k_{rel,b}$ k_{sec}	4.12	20.55 ± 4.958	Mean $k_{rel,b}$	Mean k_{sec}	Mean k_{sec}	
		k_4 1.596E-02					0.63	9.665E-03					0.62	1.75	12.81 ± 3.147	0.62 ± 0.003	0.62 ± 0.003	1.57 ± 0.173	
0.080	1	k_1 3.131E-02	5.31E-04	3.10E-04	3.74E-04			3.144E-02	4.94E-04	2.83E-04	3.57E-04								
		k_2 2.906E-02						2.645E-02											
	2	k_3 2.007E-02		1.86E-04	1.76E-04	1.17E-04		1.728E-02		1.84E-04	1.79E-04	9.49E-05							
		k_4 1.484E-02						1.189E-02											
0.080	3	k_1 4.440E-02	2.55E-04	1.00E-04	1.64E-04		$k_{rel,a}$ k_{prim}	4.199E-02	2.92E-04	1.22E-04	1.96E-04		$k_{rel,a}$ k_{prim}	43.20 ± 1.206	Mean $k_{rel,a}$	Mean $k_{rel,b}$	Mean k_{rel}	Mean k_{prim}	
		k_2 3.922E-02					1.13	3.375E-02					1.24	3.70	36.48 ± 2.736	1.19 ± 0.056	1.19 ± 0.056	3.42 ± 0.284	
	4	k_3 2.027E-02		9.17E-05	1.12E-04	8.58E-05	$k_{rel,b}$ k_{sec}	1.742E-02		1.14E-04	1.32E-04	8.86E-05	$k_{rel,b}$ k_{sec}	1.94	18.84 ± 1.426	Mean $k_{rel,b}$	Mean k_{sec}	Mean k_{sec}	
		k_4 1.416E-02					0.70	1.134E-02					0.65	1.94	12.75 ± 1.412	0.67 ± 0.024	0.67 ± 0.024	1.94 ± 0.001	
0.080	1	k_1 3.524E-02	4.97E-04	3.20E-04	3.80E-04			3.420E-02	5.10E-04	3.10E-04	3.90E-04								
		k_2 3.133E-02						3.352E-02											
	2	k_3 1.594E-02		1.31E-04	1.76E-04	7.10E-05		1.503E-02		1.22E-04	1.88E-04	8.77E-05							
		k_4 1.116E-02						1.130E-02											
0.080	3	k_1 4.491E-02	3.00E-04	1.11E-04	2.08E-04		$k_{rel,a}$ k_{prim}	4.350E-02	3.08E-04	1.10E-04	2.18E-04		$k_{rel,a}$ k_{prim}	44.21 ± 0.706	Mean $k_{rel,a}$	Mean $k_{rel,b}$	Mean k_{rel}	Mean k_{prim}	
		k_2 3.825E-02					1.17	4.100E-02					1.06	3.99	39.63 ± 1.377	1.12 ± 0.057	1.12 ± 0.057	4.09 ± 0.099	
	4	k_3 1.620E-02		8.03E-05	1.46E-04	6.47E-05	$k_{rel,b}$ k_{sec}	1.527E-02		7.57E-05	1.62E-04	6.72E-05	$k_{rel,b}$ k_{sec}	2.68	15.73 ± 0.462	Mean $k_{rel,b}$	Mean k_{sec}	Mean k_{sec}	
		k_4 1.073E-02					0.66	1.091E-02					0.71	2.68	10.82 ± 0.088	0.69 ± 0.026	0.69 ± 0.026	2.52 ± 0.162	

4.1.7 Turnover-limited Competition Experiments with Aryl Substituted Propanols

In this part of the work, we chose the model of turnover-limited competition experiments shown in previous work of the Zipse group^[1] with other kinds of alcohols. The guideline is based on this previous work.

4.1.7.1 Experimental Design

A guideline for the preparation of stock solutions for turnover-limited competition experiments is described in the following:



Scheme 4.14. Model example for a turnover-limited competition experiment of secondary alcohol **8b** vs primary alcohol **9b** with acid anhydride **5c** at a temperature of +23°C.

Three CDCl₃ stock solutions are prepared under nitrogen (Table 4.29). Stock solution A contains the secondary alcohol **8b** and primary alcohol **9b**, each at a concentration of 0.1 M. Stock solution B contains anhydride **5c** (0.2 M), while stock solution C consists of a 0.3 M Et₃N and catalyst TCAP at a concentration of 0.01 M.

Table 4.29. Preparation of initial CDCl₃ stock solutions.

Stock	Compound	Molarity (mol L ⁻¹)	Volume (mL)	n (mol)	M.W. (g mol ⁻¹)	Mass (mg)
Stock A	8b	0.1	2	200·10 ⁻⁶	186	37.2
	9b	0.1	2	200·10 ⁻⁶	186	37.2
Stock B	5c	0.2	2	400·10 ⁻⁶	344	137.6
Stock C	TCAP	0.01	2	20·10 ⁻⁶	174	3.5
	Et ₃ N	0.3	2	600·10 ⁻³	101	60.7

Following these initial preparations, stock solution B is diluted in four discrete steps as shown in Table 4.30. The concentrations of the new solutions have been fixed at 20, 35, 50, and 70% of the initial stock solution B.

Table 4.30. Dilution of stock solution B.

Stock solution	Concentration (mol L ⁻¹)	Vol. B ^b (mL)	Volume (mL)
Stock B1 (20%)^a	0.040	0.20	1
Stock B2 (35%)^a	0.070	0.35	1
Stock B3 (50%)^a	0.100	0.50	1
Stock B4 (70%)^a	0.140	0.70	1

^aConcentration relative to stock solution B; ^bInitial volume of stock solution B.

Under nitrogen 0.4 mL of stock solution A, 0.4 mL of stock solution C, and 0.4 mL of stock solution B1 are transferred to a GC vial by use of a Hamilton syringe. The GC vial is then capped under nitrogen and placed in the GC vial holder with stirring. The turnover-limited competition experiment is considered finished when the reaction with the highest anhydride concentration (GC vial 4, 70% of stock solution B) is completed.

Composition of each prepared GC vial for one turnover-limited competition experiment:

GC vial 1: 0.4 mL Stock A; 0.4 mL Stock C; 0.4 mL Stock B1

GC vial 2: 0.4 mL Stock A; 0.4 mL Stock C; 0.4 mL Stock B2

GC vial 3: 0.4 mL Stock A; 0.4 mL Stock C; 0.4 mL Stock B3

GC vial 4: 0.4 mL Stock A; 0.4 mL Stock C; 0.4 mL Stock B4

In terms of the actual starting concentrations (mol/L) for all components:

GC vial 1: **8b** and **9b**: 0.0333, **5c**: 0.0133, **Et₃N**: 0.1000, **TCAP**: 0.0033

GC vial 2: **8b** and **9b**: 0.0333, **5c**: 0.0233, **Et₃N**: 0.1000, **TCAP**: 0.0033

GC vial 3: **8b** and **9b**: 0.0333, **5c**: 0.0333, **Et₃N**: 0.1000, **TCAP**: 0.0033

GC vial 4: **8b** and **9b**: 0.0333, **5c**: 0.0467, **Et₃N**: 0.1000, **TCAP**: 0.0033

Size-Induced Inversion of Selectivity in the Acylation of 1,2-Diols

The reaction is monitored by ^1H NMR. NMR tubes are dried under vacuum using a Schlenk based glassware. 0.6 mL of the solution contained in the GC vial is transferred to the NMR tube under nitrogen. The NMR tube is then capped and the relative concentrations of all reactants/products determined by ^1H NMR spectroscopy.

4.1.7.2 ^1H NMR Analysis

The ^1H NMR spectra of the turnover-limited competition experiments were edited by MestReNova 10.0. The spectra were corrected by using automatic phase correction and Bernstein polynomial fit with polynomial order 3 and referenced by the solvent signal of CDCl_3 ($\delta = 7.26$ ppm). For the secondary alcohol **8** and ester **10** the hydrogen signal of the CH group was integrated as a guide for the evolution of the reaction. If there was an overlap with other signals, the corresponding CH_2 - or CH_3 group signals were used. For the primary alcohol **9** and ester **11** the hydrogen signal of the CH_2 group was integrated as a guide. If there was an overlap with other signals, the corresponding CH- or CH_3 group signal was used.

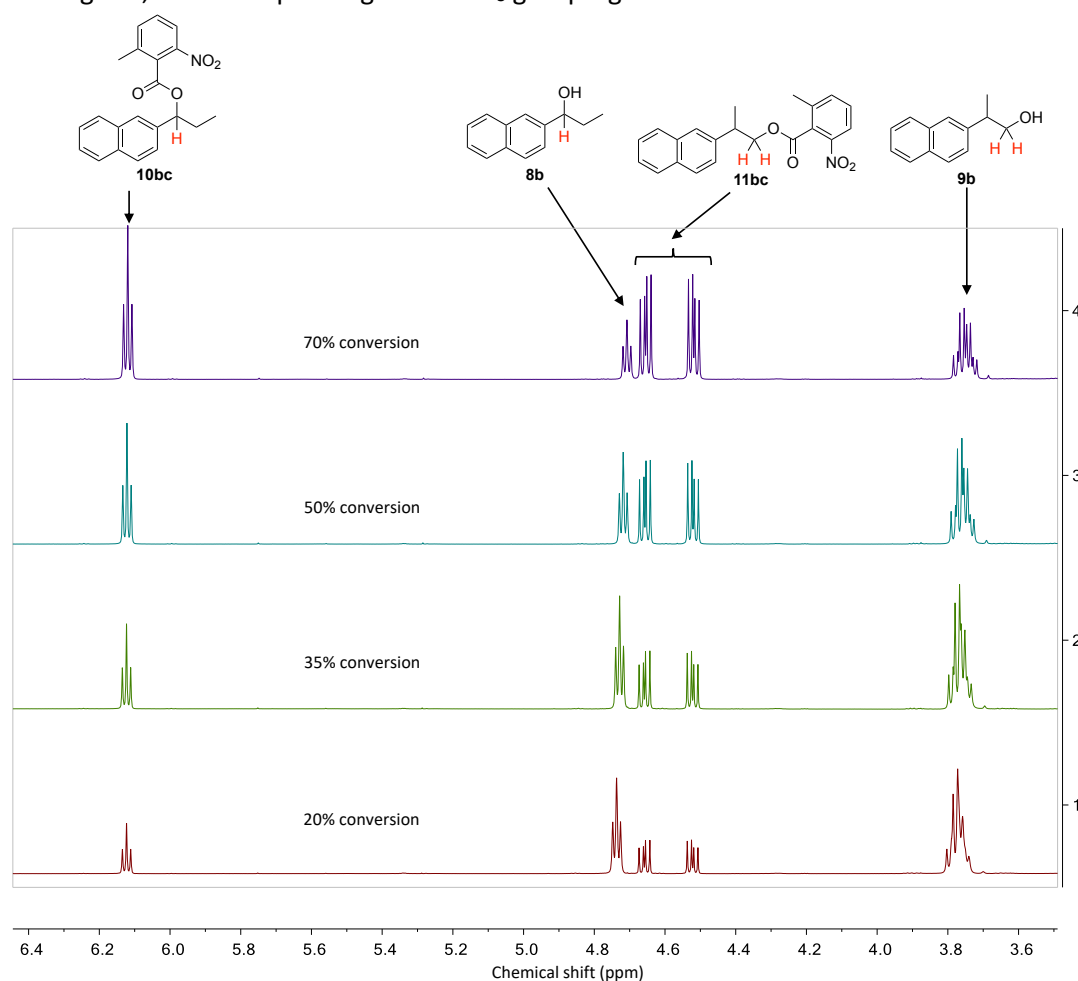
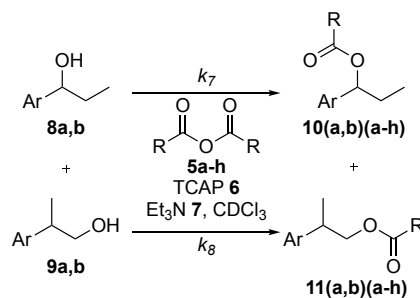


Figure 4.71. Example of the stacked ^1H NMR spectra for the turnover-limited competition experiment between **8b** and **9b** with **5c**.



Scheme 4.15. General equation for the turnover-limited competition experiment.

We determined that after full conversion of the reaction the composition of the products is varied through equilibrium processes. Because of this, we can calculate the relative rate constants from the product ratios, defined in Eq. 4.45.

$$k_{rel,prop} = \frac{k_8}{k_7} = \frac{k_{(9a,b+5a-h)}}{k_{(8a,b+5a-h)}} \quad \text{Eq. 4.45}$$

The relative rate constant is directly related to the chemoselectivity and the degree of conversion (Eq. 4.46).^[10]

$$k_{rel,prop} = \frac{\ln[1-conv(1+C)]}{\ln[1-conv(1-C)]} \quad \text{Eq. 4.46}$$

The conversion is defined by Eq. 4.47, whereby the integrals of the ¹H NMR spectra were those corresponding to the concentrations.

$$Conversion(\%) = \left(\frac{[10(a,b)(a-h)] + [11(a,b)(a-h)]}{[8a,b] + [9a,b] + [10(a,b)(a-h)] + [11(a,b)(a-h)]} \right) \cdot 100 \quad \text{Eq. 4.47}$$

The chemoselectivity is defined by Eq. 4.48:

$$Chemoselectivity_{exp} (C_{exp}) = \frac{[11(a,b)(a-h)] - [10(a,b)(a-h)]}{[11(a,b)(a-h)] + [10(a,b)(a-h)]} \quad \text{Eq. 4.48}$$

A correction factor f was introduced, which defines the exact ratio of both reactants present in the reaction medium (this should be close to the ideal 1:1), to avoid the human-error in the preparation of the samples (Eq. 4.49):

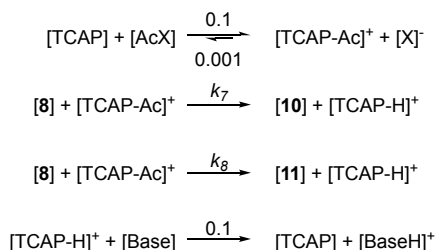
$$f = \frac{[8a,b] + [10(a,b)(a-h)]}{[9a,b] + [11(a,b)(a-h)]} \quad \text{Eq. 4.49}$$

This correction factor f was now inverted in the equation for chemoselectivity and Eq. 4.50 was defined.

$$Chemoselectivity (C) = \frac{[11(a,b)(a-h)] \cdot f - [10(a,b)(a-h)]}{[11(a,b)(a-h)] \cdot f + [10(a,b)(a-h)]} \quad \text{Eq. 4.50}$$

4.1.7.3 Simulation of Turnover-limited Competition Experiments

With the help of the CoPaSi^[2] and Origin programs the $k_{rel,prop}$ values for the turnover-limited competition experiments have been simulated. Scheme 4.16 shows the reactions used in CoPaSi, in which the k values have been modified in order to obtain the $k_{rel,prop}$ values. k_7 and k_8 have been used as variable in the fitting process, while the other rate constants were held constant.



Scheme 4.16. Model reaction used in CoPaSi for simulation of the rate constants.

The rate constants of the different turnover-limited competition experiments were simulated by CoPaSi by using the starting concentrations of the experiments. The simulated concentrations over the time were used to calculate the conversion by Eq. 4.47 and chemoselectivity by Eq. 4.50. In Figures 4.72 and 4.73 the conversion was plotted against the chemoselectivity, which allows us the illustrative comparison of experimental and simulated results.

4.1.7.4 Results of Turnover-limited Competition Experiments

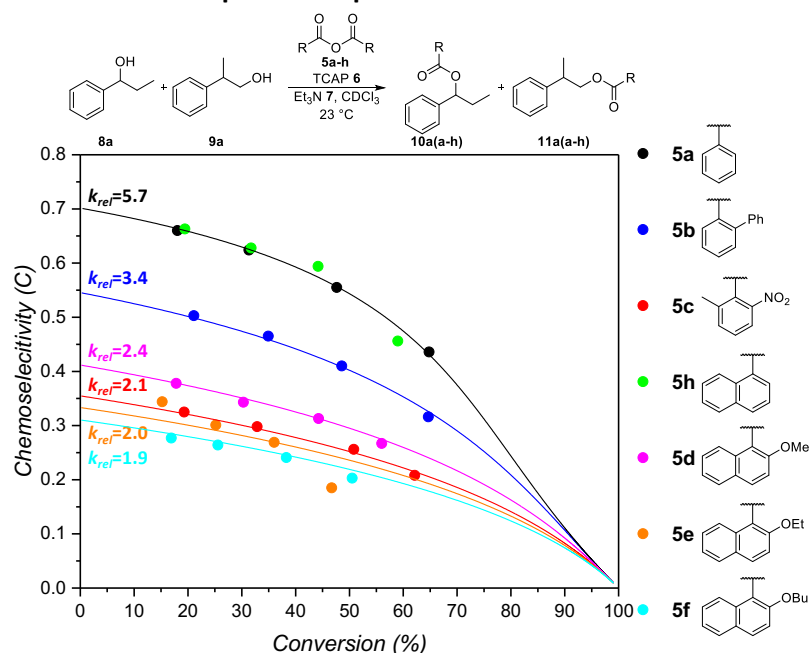
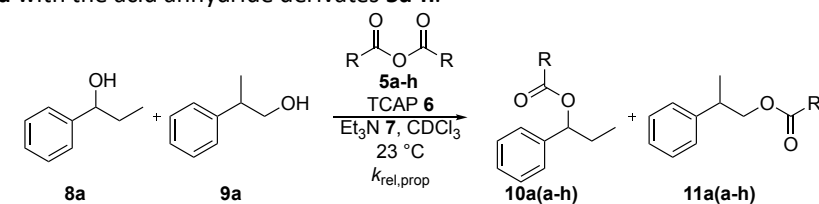
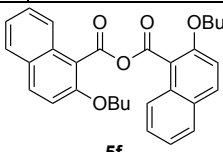
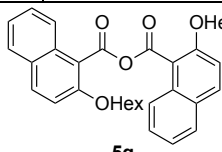


Figure 4.72. Plot of conversion vs. corrected chemoselectivity for turnover-limited competition experiment **8a** vs. **9a** with **5a-h**.

Table 4.31. Conversion, corrected chemoselectivity, relative rate and natural logarithm of relative rate with standard derivations calculated from corresponding ^1H NMR measurements for turnover-limited competition experiments between **8a** and **9a** with the acid anhydride derivatives **5a-h**.



5a				5b			
Conv.	Chem.	$k_{rel,prop}$	$\ln(k_{rel,prop})$	Conv.	Chem.	$k_{rel,prop}$	$\ln(k_{rel,prop})$
18.050	0.660	5.624	1.727	21.109	0.503	3.445	1.237
31.317	0.624	5.680	1.737	34.935	0.465	3.467	1.243
47.653	0.555	5.670	1.735	48.586	0.410	3.417	1.229
64.798	0.436	5.873	1.770	64.664	0.316	3.255	1.180
		5.712 ± 0.095	1.742 ± 0.017			3.396 ± 0.083	1.222 ± 0.025
5c				5h			
Conv.	Chem.	$k_{rel,prop}$	$\ln(k_{rel,prop})$	Conv.	Chem.	$k_{rel,prop}$	$\ln(k_{rel,prop})$
19.307	0.325	2.114	0.749	19.445	0.663	5.754	1.750
32.848	0.298	2.120	0.752	31.749	0.628	5.781	1.754
50.805	0.256	2.138	0.760	44.180	0.594	6.164	1.819
62.141	0.208	2.052	0.719	58.996	0.456	5.053	1.620
		2.106 ± 0.033	0.745 ± 0.016			5.688 ± 0.401	1.736 ± 0.072
5d				5e			

Conv.	Chem.	$k_{rel,prop}$	$\ln(k_{rel,prop})$	Conv.	Chem.	$k_{rel,prop}$	$\ln(k_{rel,prop})$
17.814	0.378	2.397	0.874	15.210	0.344	2.175	0.777
30.309	0.343	2.356	0.857	25.187	0.301	2.052	0.719
44.275	0.313	2.401	0.876	36.032	0.269	2.000	0.693
56.012	0.267	2.337	0.849	46.712	0.185	1.682	0.520
		2.373 ± 0.027	0.864 ± 0.011			1.977 ± 0.182	0.677 ± 0.096
 5f				 5g ^a			
Conv.	Chem.	$k_{rel,prop}$	$\ln(k_{rel,prop})$	Conv.	Chem.	$k_{rel,prop}$	$\ln(k_{rel,prop})$
16.897	0.277	1.866	0.624	/	/	/	/
25.556	0.264	1.871	0.626	/	/	/	/
38.277	0.241	1.875	0.629	/	/	/	/
50.517	0.203	1.814	0.595	/	/	/	/
		1.857 ± 0.025	0.619 ± 0.013	/	/	/	/

^aSignal overlapping, no integration possible

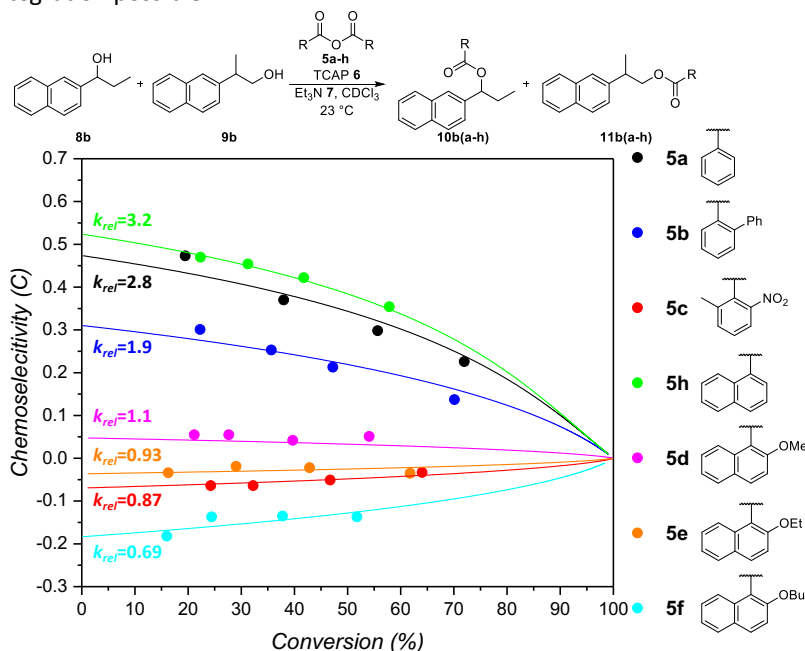
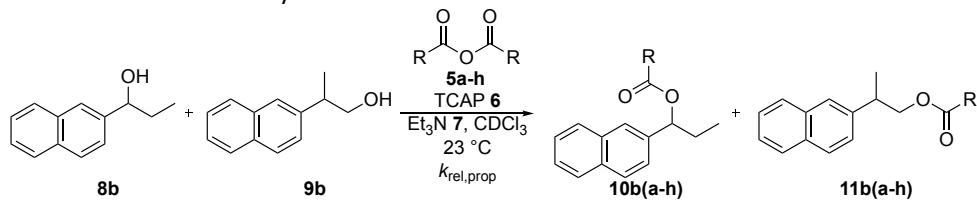


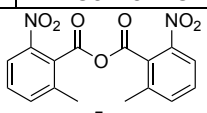
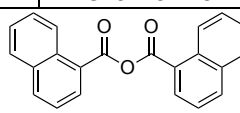
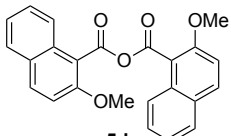
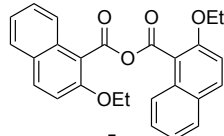
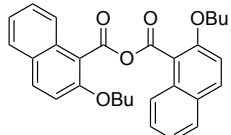
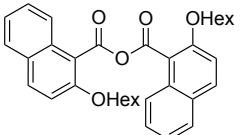
Figure 4.73. Plot of conversion vs. corrected chemoselectivity for turnover-limited competition experiment **8b** vs. **9b** with **5a-h**.

Table 4.32. Conversion, corrected chemoselectivity, relative rate and natural logarithm of relative rate with standard derivations calculated from corresponding ¹H NMR measurements for turnover-limited competition experiments between **8b** and **9b** with the acid anhydride derivatives **5a-h**.



Conv.	Chem.	$k_{rel,prop}$	$\ln(k_{rel,prop})$	Conv.	Chem.	$k_{rel,prop}$	$\ln(k_{rel,prop})$
19.459	0.473	3.124	1.139	22.265	0.301	2.021	0.704
37.980	0.370	2.688	0.989	35.649	0.253	1.909	0.647
55.654	0.298	2.586	0.950	47.241	0.213	1.830	0.604

Size-Induced Inversion of Selectivity in the Acylation of 1,2-Diols

71.955	0.226	2.629	0.967	70.103	0.137	1.720	0.543
		2.756 ± 0.215	1.011 ± 0.075			1.870 ± 0.110	0.624 ± 0.059
 5c				 5h			
<i>Conv.</i>	<i>Chem.</i>	<i>k_{rel,prop}</i>	<i>ln(k_{rel,prop})</i>	<i>Conv.</i>	<i>Chem.</i>	<i>k_{rel,prop}</i>	<i>ln(k_{rel,prop})</i>
24.263	-0.064	0.863	-0.148	22.338	0.470	3.162	1.151
32.238	-0.064	0.856	-0.156	31.264	0.454	3.238	1.175
46.732	-0.051	0.869	-0.141	41.764	0.422	3.260	1.182
64.016	-0.033	0.891	-0.115	57.851	0.354	3.262	1.182
		0.870 ± 0.013	-0.140 ± 0.015			3.230 ± 0.041	1.173 ± 0.013
 5d				 5e			
<i>Conv.</i>	<i>Chem.</i>	<i>k_{rel,prop}</i>	<i>ln(k_{rel,prop})</i>	<i>Conv.</i>	<i>Chem.</i>	<i>k_{rel,prop}</i>	<i>ln(k_{rel,prop})</i>
21.162	0.055	1.134	0.125	16.275	-0.034	0.927	-0.075
27.667	0.055	1.139	0.130	29.016	-0.019	0.956	-0.045
39.693	0.042	1.116	0.110	42.862	-0.022	0.943	-0.059
54.072	0.051	1.169	0.156	61.767	-0.035	0.888	-0.119
		1.139 ± 0.019	0.130 ± 0.017			0.929 ± 0.026	-0.074 ± 0.028
 5f				 5g ^a			
<i>Conv.</i>	<i>Chem.</i>	<i>k_{rel,prop}</i>	<i>ln(k_{rel,prop})</i>	<i>Conv.</i>	<i>Chem.</i>	<i>k_{rel,prop}</i>	<i>ln(k_{rel,prop})</i>
15.987	-0.182	0.669	-0.401				
24.420	-0.137	0.727	-0.319				
37.787	-0.135	0.707	-0.346				
51.768	-0.137	0.667	-0.404				
		0.693 ± 0.025	-0.368 ± 0.037				

^aSignal overlapping, no integration possible

4.1.7.5 Investigation of Temperature Effects

Here we tested the effects of reaction temperature on selectivities for the anhydride **5c** and the alcohol system **8b/9b** based on the work of Giese.^[7] By varying the temperature from +40 °C to -20 °C, we observed only moderate changes in the rate constants for anhydride **5c**. By using the well-known Eyring equation Eq. 4.51 an activation entropy difference of -8.05 J K⁻¹·mol was found. Because of the rather similar rate constants at different temperatures, these small differences hardly merit any further discussion.

$$\frac{k_2}{k_1} = \frac{e^{-\frac{\Delta G_2^\ddagger}{RT}}}{e^{-\frac{\Delta G_1^\ddagger}{RT}}} \quad \text{Eq. 4.51}$$

$$\frac{k_2}{k_1} = e^{-\frac{\Delta G_2^\ddagger}{RT} + \frac{\Delta G_1^\ddagger}{RT}} \quad \text{Eq. 4.52}$$

$$\ln \frac{k_2}{k_1} = -\frac{\Delta G_2^\ddagger}{RT} + \frac{\Delta G_1^\ddagger}{RT} \quad \text{Eq. 4.53}$$

$$\ln \frac{k_2}{k_1} = -\frac{\Delta H_2^\ddagger - T\Delta S_2^\ddagger}{RT} + \frac{\Delta H_1^\ddagger - T\Delta S_1^\ddagger}{RT} \quad \text{Eq. 4.54}$$

$$\ln \frac{k_2}{k_1} = -\frac{\Delta H_2^\ddagger}{RT} + \frac{\Delta S_2^\ddagger}{R} + \frac{\Delta H_1^\ddagger}{RT} - \frac{\Delta S_1^\ddagger}{R} \quad \text{Eq. 4.55}$$

$$\ln \frac{k_2}{k_1} = \frac{\Delta H_1^\ddagger - \Delta H_2^\ddagger}{RT} - \frac{\Delta S_1^\ddagger - \Delta S_2^\ddagger}{R} \quad \text{Eq. 4.56}$$

$$\begin{aligned} \Delta\Delta H^\ddagger &= \Delta H_1^\ddagger - \Delta H_2^\ddagger \\ \Delta\Delta S^\ddagger &= \Delta S_1^\ddagger - \Delta S_2^\ddagger \\ R &= 8.31451 \text{ J K}^{-1} \cdot \text{mol} \end{aligned}$$

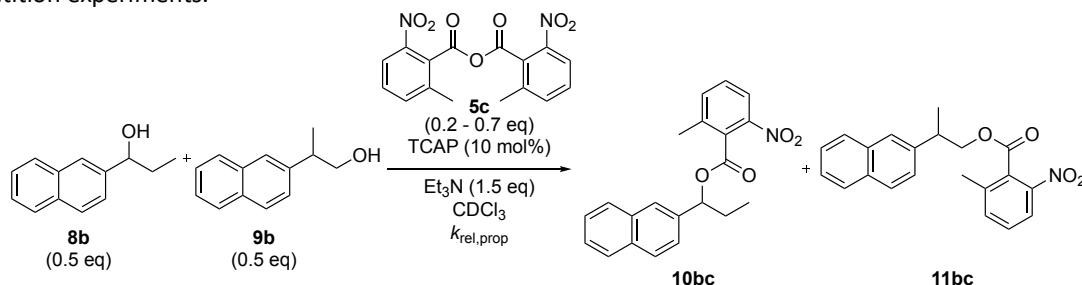
$$\ln(k_{rel}) = \ln \frac{k_2(9b)}{k_1(8b)} = \frac{\Delta\Delta H^\ddagger}{R \cdot T} - \frac{\Delta\Delta S^\ddagger}{R} \quad \text{Eq. 4.57}$$

$$\ln \frac{k_2}{k_1} = \frac{-331.80}{T} + 0.97 \quad \text{Eq. 4.58}$$

$$\Delta\Delta H^\ddagger = \Delta H_1^\ddagger - \Delta H_2^\ddagger = -2.76 \text{ kJ mol}^{-1} \quad \text{Eq. 4.59}$$

$$\Delta\Delta S^\ddagger = \Delta S_1^\ddagger - \Delta S_2^\ddagger = -8.05 \text{ J K}^{-1} \cdot \text{mol} \quad \text{Eq. 4.60}$$

Table 4.33. Conversion, corrected chemoselectivity, relative rate and natural logarithm of relative rate with standard derivations calculated from corresponding ¹H NMR measurements for temperature depending turnover-limited competition experiments.



+40 °C (313.15 K)				+40 °C (313.15 K)			
Conv.	Chem.	<i>k_{rel,prop}</i>	ln(<i>k_{rel,prop}</i>)	Conv.	Chem.	<i>k_{rel,prop}</i>	ln(<i>k_{rel,prop}</i>)
17.979	-0.043	0.910	-0.094	17.993	-0.035	0.926	-0.077
33.235	-0.037	0.912	-0.092	34.023	-0.036	0.915	-0.089
47.232	-0.026	0.930	-0.072	50.738	-0.027	0.924	-0.079
67.708	-0.020	0.929	-0.074	67.354	-0.021	0.927	-0.076
		0.920 ± 0.009	-0.083 ± 0.010			0.923 ± 0.005	-0.080 ± 0.005
+40 °C (313.15 K)				+10 °C (283.15 K)			
Conv.	Chem.	<i>k_{rel,prop}</i>	ln(<i>k_{rel,prop}</i>)	Conv.	Chem.	<i>k_{rel,prop}</i>	ln(<i>k_{rel,prop}</i>)
18.630	-0.039	0.917	-0.087	20.113	-0.103	0.794	-0.231
33.529	-0.031	0.927	-0.076	34.356	-0.090	0.800	-0.223
50.580	-0.025	0.929	-0.073	49.601	-0.075	0.806	-0.215
70.583	-0.019	0.927	-0.076	68.277	-0.057	0.807	-0.214
		0.925 ± 0.005	-0.078 ± 0.005			0.802 ± 0.006	-0.221 ± 0.007
+10 °C (283.15 K)				+10 °C (283.15 K)			
Conv.	Chem.	<i>k_{rel,prop}</i>	ln(<i>k_{rel,prop}</i>)	Conv.	Chem.	<i>k_{rel,prop}</i>	ln(<i>k_{rel,prop}</i>)
20.713	-0.108	0.783	-0.245	20.213	-0.098	0.803	-0.220
34.419	-0.093	0.792	-0.233	35.641	-0.089	0.799	-0.225
49.022	-0.077	0.802	-0.221	50.159	-0.075	0.804	-0.218
66.116	-0.060	0.805	-0.217	73.718	-0.050	0.810	-0.211
		0.796 ± 0.009	-0.229 ± 0.011			0.804 ± 0.004	-0.218 ± 0.005
0 °C (273.15 K)				0 °C (273.15 K)			
Conv.	Chem.	<i>k_{rel,prop}</i>	ln(<i>k_{rel,prop}</i>)	Conv.	Chem.	<i>k_{rel,prop}</i>	ln(<i>k_{rel,prop}</i>)
20.099	-0.129	0.748	-0.290	19.772	-0.127	0.752	-0.285
37.525	-0.104	0.767	-0.266	34.870	-0.112	0.756	-0.280
51.781	-0.090	0.767	-0.266	49.620	-0.093	0.764	-0.269
69.436	-0.070	0.763	-0.271	66.003	-0.072	0.771	-0.260
		0.761 ± 0.009	-0.273 ± 0.011			0.761 ± 0.005	-0.273 ± 0.007
0 °C (273.15 K)				-20 °C (253.15 K)			
Conv.	Chem.	<i>k_{rel,prop}</i>	ln(<i>k_{rel,prop}</i>)	Conv.	Chem.	<i>k_{rel,prop}</i>	ln(<i>k_{rel,prop}</i>)
19.375	-0.118	0.767	-0.265	21.296	-0.144	0.721	-0.327
35.000	-0.111	0.757	-0.279	37.363	-0.128	0.721	-0.327
50.798	-0.092	0.764	-0.269	51.507	-0.107	0.730	-0.315
68.560	-0.070	0.768	-0.263	74.617	-0.073	0.730	-0.315
		0.764 ± 0.005	-0.269 ± 0.006			0.725 ± 0.004	-0.321 ± 0.006
-20 °C (253.15 K)				-20 °C (253.15 K)			
Conv.	Chem.	<i>k_{rel,prop}</i>	ln(<i>k_{rel,prop}</i>)	Conv.	Chem.	<i>k_{rel,prop}</i>	ln(<i>k_{rel,prop}</i>)
21.335	-0.151	0.709	-0.343	21.100	-0.150	0.711	-0.341
35.322	-0.129	0.722	-0.326	37.973	-0.125	0.725	-0.321
51.787	-0.109	0.724	-0.324	53.507	-0.108	0.721	-0.327

69.820	-0.080	0.732	-0.312	73.813	-0.071	0.741	-0.300
		0.722 ± 0.008	-0.326 ± 0.011			0.725 ± 0.011	-0.322 ± 0.015

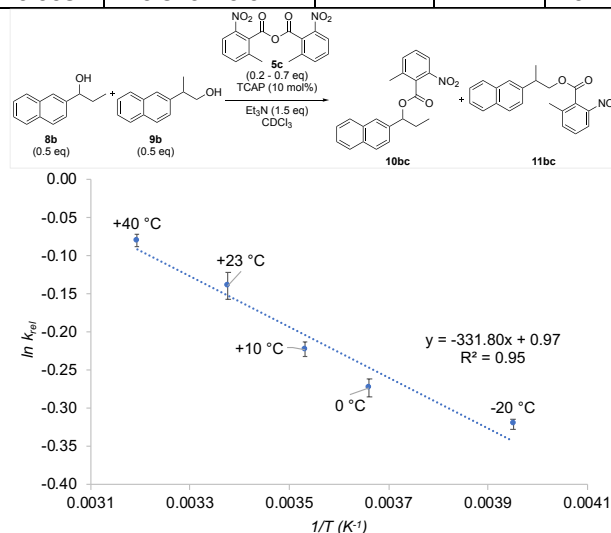
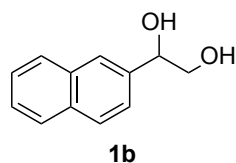


Figure 4.74. Eyring plot of $\ln k_{rel}$ at different temperatures.

4.1.8 Analytical Data

4.1.8.1 Synthesis of Alcohols

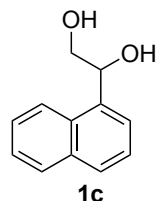
1-(2-Naphthyl)-1,2-ethanediol 1b. (The synthesis of aryl diols **1b-d** is based on the procedure reported by Moreno-Dorado *et al.*^[11])



2-Vinylnaphthalene (616 mg, 3.99 mmol, 1.0 eq.) was dissolved in a 1:1 mixture of *t*BuOH (10 mL) and water (10 mL). AD-mix β (5.96 g, 1.49 g per 1 mmol olefin) was added to the reaction mixture and stirred at room temperature for 2 h. The reaction mixture was quenched by adding Na_2SO_3 (1.00g) and stirring for 10 min. *t*BuOH was removed in vacuum and the aqueous phase was extracted with EtOAc (3 x 20 mL). The combined organic phase was washed with brine, dried over MgSO_4 , filtered and concentrated in vacuum. After purification by column chromatography on silica (isohexane/EtOAc 3:7) 1-(2-naphthyl)-1,2-ethanediol (**1b**, 707 mg, 94 %) was obtained as a white solid.

$^1\text{H NMR}$ (CDCl_3 , 400 MHz) δ = 7.89 – 7.79 (m, 4H, Ar), 7.53 – 7.44 (m, 3H, Ar), 5.02 (dt, J = 7.6, 3.5 Hz, 1H, CH), 3.87 (ddd, J = 11.1, 7.4, 3.6 Hz, 1H, CHH), 3.77 (ddd, J = 11.2, 8.0, 4.7 Hz, 1H, CHH), 2.58 (d, J = 3.4 Hz, 1H, OH), 2.02 (dd, J = 7.4, 4.8 Hz, 1H, OH) ppm; $^{13}\text{C NMR}$ (CDCl_3 , 101 MHz) δ = 137.87, 133.24, 133.15, 128.37, 127.95, 127.71, 126.32, 126.09, 125.03, 123.94, 74.78, 68.05 ppm; **HRMS** (EI): m/z calcd for $\text{C}_{12}\text{H}_{12}\text{O}_2^+$ [M] $^+$: 188.0832; found: 188.0842. The $^1\text{H NMR}$ spectrum is in full agreement with literature reports.^[11]

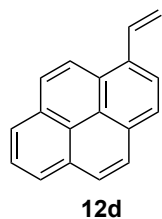
1-(1-Naphthyl)-1,2-ethanediol 1c.



2-Vinylnaphthalene (616 mg, 3.99 mmol, 1.0 eq.) was dissolved in a 1:1 mixture of *t*BuOH (20 mL) and water (20 mL). AD-mix β (5.96 g, 1.49 g per 1 mmol olefin) was added to the reaction mixture and stirred at room temperature for 3 days. The reaction mixture was quenched by adding Na_2SO_3 (1.00g) and stirring for 10 min. *t*BuOH was removed in vacuum and the aqueous phase was extracted with EtOAc (3 x 20 mL). The combined organic phase was washed with brine, dried over MgSO_4 , filtered and concentrated in vacuum. After purification by column chromatography on silica (isohexane/EtOAc 3:7) 1-(1-naphthyl)-1,2-ethanediol (**1c**, 100 mg, 13 %) was obtained as a white solid.

$^1\text{H NMR}$ (CDCl_3 , 400 MHz) δ = 8.04 – 7.98 (m, 1H, Ar), 7.85 – 7.80 (m, 1H, Ar), 7.75 (dt, J = 8.4, 1.0 Hz, 1H, Ar), 7.65 (dt, J = 7.2, 1.0 Hz, 1H, Ar), 7.51 – 7.38 (m, 3H, Ar), 5.59 (dt, J = 7.1, 3.2 Hz, 1H, CH), 3.93 (ddd, J = 11.2, 7.8, 3.2 Hz, 1H, CHH), 3.73 (ddd, J = 11.4, 8.2, 4.1 Hz, 1H, CHH), 2.51 (d, J = 3.4 Hz, 1H, OH), 2.07 (dd, J = 8.0, 4.3 Hz, 1H, OH) ppm; $^{13}\text{C NMR}$ (CDCl_3 , 101 MHz) δ = 136.13, 133.81, 130.50, 129.14, 128.58, 126.46, 125.84, 125.59, 123.62, 122.76, 71.78, 67.60 ppm; **HRMS** (EI): m/z calcd for $\text{C}_{12}\text{H}_{12}\text{O}_2^+$ [M] $^+$: 188.0832; found: 188.0830. The $^1\text{H NMR}$ spectrum is in full agreement with literature reports.^[11]

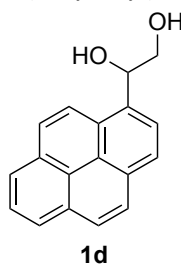
1-Vinylpyrene 12d. (The synthesis of **12d** is based on the procedure reported by Nishimura *et al.*^[12])



In a Schlenk flask methyltriphenylphosphonium bromide (443 mg, 1.24 mmol, 1.4 eq.) was suspended in dry THF (2.4 mL) and cooled down to 0 °C. *n*-BuLi (2.5 M in hexane, 500 μ L, 1.24 mmol, 1.4 eq.) was added dropwise to the solution. The reaction mixture was allowed to warm up to room temperature and was stirred for 10 min. 1-Pyrenecarboxaldehyde (200 μ L, 861 μ mol, 1.0 eq.) dissolved in dry THF (2.4 mL) was added dropwise. The resulting yellow suspension was stirred over night. After filtration of the reaction mixture, water (30 mL) was added and extracted with ether (3 x 40 mL). The combined organic phase was dried over MgSO₄, filtered and concentrated in vacuum. After purification by column chromatography on silica (isohexane/CH₂Cl₂, 10:1) 1-vinylpyrene (**12d**, 78.0 mg, 40 %) was obtained as a yellow solid.

¹H NMR (CDCl₃, 400 MHz) δ = 8.40 (d, *J* = 9.3 Hz, 1H, Ar), 8.24 – 8.09 (m, 5H, Ar), 8.05 (s, 2H, Ar), 8.00 (dd, *J* = 8.0, 7.2 Hz, 1H, Ar), 7.80 (dd, *J* = 17.3, 11.0 Hz, 1H, CH), 6.00 (dd, *J* = 17.3, 1.3 Hz, 1H, CHH), 5.62 (dd, *J* = 11.0, 1.3 Hz, 1H, CHH) ppm. The ¹H NMR spectrum is in full agreement with literature reports.^[12]

1-(1-Pyrenyl)-1,2-ethanediol 1d.

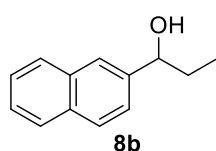


1-Vinylpyrene **12d** (78 mg, 338 μ mol, 1.0 eq.) was dissolved in a 1:1 mixture of *t*BuOH (2 mL) and water (2 mL). AD-mix β (500 mg, 1.49 g per 1 mmol olefin) was added to the reaction mixture and stirred at room temperature for one week. The reaction mixture was quenched by adding Na₂SO₃ (170 mg) and stirring for 10 min. *t*BuOH was removed in vacuum and the aqueous phase was extracted with EtOAc (3 x 20 mL). The combined organic phase was washed with brine, dried over MgSO₄, filtered and concentrated in vacuum.

Purification and further characterisations were not possible because of the very low

solubility of **1d**.

1-(Naphthalen-2-yl)propan-1-ol 8b. (The synthesis of **8b** is based on the procedure reported by Musolino *et al.*^[13])

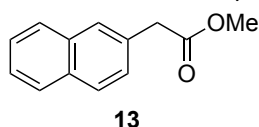


In a Schlenk tube 2-naphthaldehyde (500 mg, 3.20 mmol, 1.0 eq.) was dissolved in THF (3.2 mL). After cooling to 0 °C, EtMgCl (1 M in THF, 4.80 mL, 4.80 mmol, 1.5 eq.) was added dropwise and the reaction mixture was stirred at room temperature for 4 h. The mixture was quenched with sat. NH₄Cl-solution and extracted with EtOAc (3 x 15 mL).

The combined organic phase was washed with brine, dried over MgSO₄, filtered and concentrated in vacuum. After purification by column chromatography on silica (isohexane/EtOAc 8:2), 1-(naphthalen-2-yl)propan-1-ol (**8b**, 463 mg, 78 %) was obtained as colorless oil.

¹H NMR (CDCl₃, 400 MHz) δ = 7.87 – 7.80 (m, 3H, Ar), 7.78 (s, 1H, Ar), 7.54 – 7.43 (m, 3H, Ar), 4.77 (td, *J* = 6.6, 3.1 Hz, 1H, CH), 1.98 (d, *J* = 3.2 Hz, 1H, OH), 1.96 – 1.79 (m, 2H, CH₂), 0.95 (t, *J* = 7.4 Hz, 3H, Me) ppm; ¹³C NMR (CDCl₃, 101 MHz) δ = 142.05, 133.39, 133.11, 128.35, 128.05, 127.80, 126.23, 125.90, 124.86, 124.26, 76.25, 31.89, 10.29 ppm; HRMS (EI): *m/z* calcd for C₁₃H₁₄O⁺ [M]⁺: 186.1039; found: 186.1035. The ¹H NMR spectrum is in full agreement with literature reports.^[13]

Methyl 2-(naphthalene-2-yl)acetate 13. (The synthesis of **13** is based on the procedure reported by Tsukamoto *et al.*^[14])



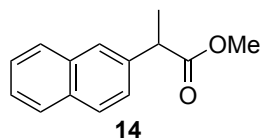
2-(Naphthalen-2-yl)acetic acid (2 g, 10.7 mmol, 1.0 eq.) was dissolved in MeOH (3.50 mL, 85.9 mmol, 8.0 eq.) and 5 drops of conc. H₂SO₄ was added. After heating under reflux for 3 h, the mixture was quenched with sat. NaHCO₃ solution and extracted with CH₂Cl₂ (3 x 20 mL). The combined organic phase was washed with H₂O, dried

over MgSO₄, filtered and concentrated in vacuum. Methyl 2-(naphthalene-2-yl)acetate (**13**, 2.00 g, 93 %) was obtained without any further purification as a colorless oil.

¹H NMR (CDCl₃, 400 MHz) δ = 7.85 – 7.78 (m, 3H, Ar), 7.74 (s, 1H, Ar), 7.51 – 7.44 (m, 2H, Ar), 7.42 (dd, *J* = 8.5, 1.8 Hz, 1H, Ar), 3.80 (s, 2H, CH₂), 3.71 (s, 3H, Me) ppm. The ¹H NMR spectrum is in full agreement with literature reports.^[14]

Size-Induced Inversion of Selectivity in the Acylation of 1,2-Diols

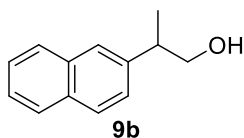
Methyl 2-(naphthalene-2-yl)propanoate 14. (The synthesis of **14** is based on the procedure reported by Cruz *et al.*^[15])



In a Schlenk tube NaH (60% dispersion in mineral oil, 439 mg, 11.0 mmol, 1.1 eq.) was dissolved in DMF (33 mL) and cooled down to 0 °C. **13** (2.00 g, 9.99 mmol, 1.0 eq.) dissolved in DMF (25 mL) was added dropwise to the reaction mixture. After the mixture was stirred at 0 °C for 5 min, MeI (683 μ L, 11.0 mmol, 1.1 eq.) was added carefully. The mixture was warmed up to room temperature, stirred for 1 h and quenched with sat. NH_4Cl solution and extracted with ether (3 x 20 mL). The collected organic phase was washed with water, brine, dried over MgSO_4 , filtered and concentrated in vacuum. After purification by column chromatography on silica (isohexan/EtOAc 8:2), methyl 2-(naphthalene-2-yl)propanoate (**14**, 1.70 g, 79%) was obtained as a colorless oil.

$^1\text{H NMR}$ (CDCl_3 , 400 MHz) δ = 7.82 (d, J = 8.8 Hz, 3H, Ar), 7.75 (s, 1H, Ar), 7.53 – 7.41 (m, 3H, Ar), 3.91 (q, J = 7.2 Hz, 1H, CH), 3.68 (s, 3H, Me), 1.60 (d, J = 7.2 Hz, 3H, Me) ppm. The $^1\text{H NMR}$ spectrum is in full agreement with literature reports.^[14]

2-(Naphthalen-2-yl)propan-1-ol 9b. (Synthesis of **9b** is based on the procedure reported by Cruz *et al.*^[15])



In a Schlenk tube **14** (1.70 g 7.94 mmol, 1.0 eq.) was dissolved in THF (20 ml) and was cooled down to 0 °C. LiAlH_4 (1.20 g, 31.8 mmol, 4.0 eq.) was carefully added and the reaction mixture was stirred at room temperature over night. The reaction mixture was quenched by adding 2 M NaOH solution and water. The water phase was extracted by EtOAc (3 x 10 mL) and CH_2Cl_2 (3 x 30 mL). The combined organic phase was dried over MgSO_4 , filtered and concentrated in vacuum. After purification by column chromatography on silica (isohexan/EtOAc 8:2), 2-(naphthalen-1-yl)propan-1-ol (**9b**, 1.16 g, 79 %) was obtained as a white solid.

$^1\text{H NMR}$ (CDCl_3 , 400 MHz) δ = 7.88 – 7.77 (m, 3H Ar), 7.69 (s, 1H Ar), 7.52 – 7.42 (m, 2H Ar), 7.39 (dd, J = 8.5, 1.7 Hz, 1H Ar), 3.80 (m, 2H, CH_2), 3.14 (p, J = 6.9 Hz, 1H, CH), 1.38 (d, J = 7.0 Hz, 4H, Me and OH) ppm; $^{13}\text{C NMR}$ (CDCl_3 , 101 MHz) δ = 141.19, 133.69, 132.64, 128.51, 127.76 (2x), 126.24, 126.21, 125.91, 125.67, 68.71, 42.72, 17.74 ppm; **HRMS** (EI): m/z calcd for $\text{C}_{13}\text{H}_{14}\text{O}^+$ [M] $^+$: 186.1039; found: 186.1041. Synthesis of **9b** is based on the procedure reported by Cruz *et al.*^[15] The $^1\text{H NMR}$ spectrum is in full agreement with literature reports.^[16]

4.1.8.2 Synthesis of Esters

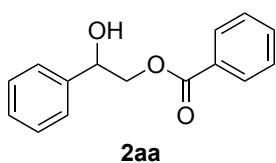
General Procedure A (GP A)

In a round bottom flask the corresponding alcohol (1.0 eq.), anhydride (0.9, 1.0 or 1.2 eq.), DMAP (0.05 eq.) and Et_3N (1.5 or 2.0 eq.) were dissolved in CH_2Cl_2 or CHCl_3 and stirred at room temperature for 24 h. After full conversion, the reaction mixture was extracted with CH_2Cl_2 (3 x 10 mL), dried over MgSO_4 , filtered and concentrated in vacuum. The mixture was purified by column chromatography on silica (isohexan/EtOAc 9:1) and column chromatography on silica (isohexan/ CH_2Cl_2 6:4).

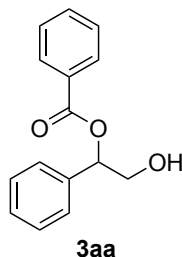
4.1.8.2.1 Phenyl Diol Esters

1a (1.00 g, 7.24 mmol, 1.0 eq.), **5a** (3.44 g, 15.2 mmol, 2.1 eq.), DMAP (44.0 mg, 362 μ mol, 0.05 eq.), and Et_3N (1.01 mL, 7.24 mmol, 1.0 eq.) were dissolved in CH_2Cl_2 (36 mL) and reacted according to GP A. **2aa** (1.74 g, 68%) was obtained as a white solid, **3aa** (199 mg, 11%) was obtained as an oil and **4aa** (28.0 mg, 1.6%) was obtained as a white solid.

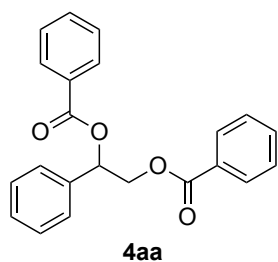
2-Hydroxy-2-phenylethyl benzoate 2aa.



$^1\text{H NMR}$ (CDCl_3 , 400 MHz) δ = 8.09 – 8.03 (m, 2H, Ar), 7.63 – 7.55 (m, 1H, Ar), 7.50 – 7.37 (m, 6H, Ar), 7.37 – 7.30 (m, 1H, Ar), 5.13 (dt, J = 8.2, 3.3 Hz, 1H, CH), 4.54 (dd, J = 11.6, 3.4 Hz, 1H, CHH), 4.44 (dd, J = 11.6, 8.2 Hz, 1H, CHH), 2.56 (d, J = 3.3 Hz, 1H, OH) ppm; $^{13}\text{C NMR}$ (CDCl_3 , 151 MHz) δ = 166.87, 140.01, 133.37, 129.92, 129.85, 128.77, 128.58, 128.41, 126.35, 72.74, 69.94 ppm; **HRMS** (ESI): m/z calcd for $\text{C}_{15}\text{H}_{14}\text{O}_3 + \text{Cl}^-$ [M+Cl] $^-$: 277.0637; found: 277.0638. The $^1\text{H}/^{13}\text{C NMR}$ spectra are in full agreement with literature reports.^[3b,17]

2-Hydroxy-1-phenylethyl benzoate 3aa.

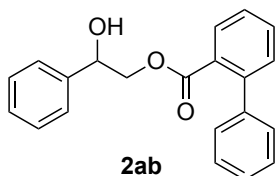
$^1\text{H NMR}$ (CDCl_3 , 400 MHz) δ = 8.15 – 8.09 (m, 2H, Ar), 7.63 – 7.56 (m, 1H, Ar), 7.46 (td, J = 7.8, 1.6 Hz, 4H, Ar), 7.42 – 7.30 (m, 3H, Ar), 6.12 (dd, J = 7.5, 3.9 Hz, 1H, CH), 4.05 (dd, J = 12.2, 7.5 Hz, 1H, CHH), 3.95 (dd, J = 12.1, 4.0 Hz, 1H, CHH), 1.30 – 1.16 (m, 1H, OH) ppm; $^{13}\text{C NMR}$ (CDCl_3 , 101 MHz) δ = 166.28, 137.17, 133.42, 130.04, 129.90, 128.86, 128.65, 128.60, 126.75, 77.57, 66.39 ppm; **HRMS** (ESI): m/z calcd for $\text{C}_{15}\text{H}_{14}\text{O}_3 + \text{Cl}^-$ [$\text{M} + \text{Cl}$]: 277.0637; found: 277.0637. The $^1\text{H}/^{13}\text{C}$ NMR spectra are in full agreement with literature reports.^[17a,18]

1-Phenylethane-1,2-diyl dibenzoate 4aa.

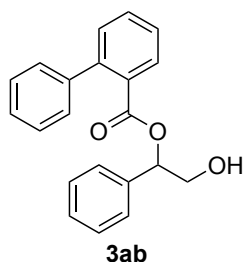
$^1\text{H NMR}$ (CDCl_3 , 400 MHz) δ = 8.12 – 8.08 (m, 2H, Ar), 8.02 – 7.97 (m, 2H, Ar), 7.63 – 7.50 (m, 4H, Ar), 7.50 – 7.33 (m, 7H, Ar), 6.42 (dd, J = 8.2, 3.8 Hz, 1H, CH), 4.75 (dd, J = 11.9, 8.1 Hz, 1H, CHH), 4.67 (dd, J = 11.9, 3.7 Hz, 1H, CHH) ppm; $^{13}\text{C NMR}$ (CDCl_3 , 151 MHz) δ = 166.35, 165.76, 136.75, 133.34, 133.27, 130.07, 129.91, 129.86, 129.83, 128.91, 128.88, 128.59, 128.54, 126.86, 74.15, 66.83 ppm; **HRMS** (ESI): m/z calcd for $\text{C}_{22}\text{H}_{18}\text{O}_4 + \text{Na}^+$ [$\text{M} + \text{Na}$]: 369.1097; found: 369.1101.

The ^1H NMR spectrum is in full agreement with literature reports.^[19]

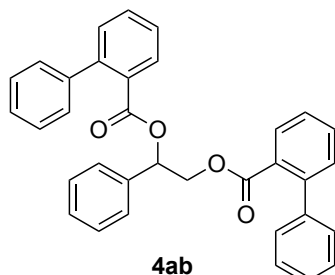
1a (200 mg, 1.45 mmol, 1.0 eq.), **5b** (548 mg, 1.45 mmol, 1.0 eq.), DMAP (8.84 mg, 72.4 μmol , 0.05 eq.), and Et_3N (404 μL , 2.90 mmol, 2.0 eq.) were dissolved in CH_2Cl_2 (7.24 mL) and reacted according to GP A. **2ab** (300 mg, 65%) was obtained as an oil, **3ab** (75.0 mg, 16%) was obtained as a white solid and **4ab** (60.0 mg, 8.3%) was obtained as an oil.

2-Hydroxy-2-phenylethyl [1,1'-biphenyl]-2-carboxylate 2ab.

$^1\text{H NMR}$ (CDCl_3 , 600 MHz) δ = 7.90 (dd, J = 7.8, 1.2 Hz, 1H, Ar), 7.57 (td, J = 7.6, 1.4 Hz, 1H, Ar), 7.50 – 7.42 (m, 4H, Ar), 7.40 – 7.38 (m, 3H, Ar), 7.35 – 7.30 (m, 2H, Ar), 7.29 – 7.25 (m, 3H, Ar), 4.53 (dt, J = 9.2, 2.8 Hz, 1H, CH), 4.29 (dd, J = 11.4, 2.8 Hz, 1H, CHH), 3.98 (dd, J = 11.4, 9.1 Hz, 1H, CHH), 1.60 (d, J = 3.1 Hz, 1H, OH) ppm; $^{13}\text{C NMR}$ (CDCl_3 , 151 MHz) δ = 168.77, 142.48, 142.20, 139.08, 131.72, 130.87, 130.55, 130.48, 128.59, 128.49, 128.48, 128.21, 127.75, 127.56, 126.20, 71.93, 70.49 ppm; **IR** (ATR): ν (cm^{-1}) = 3457, 2948, 1714, 1597, 1451, 1240, 1126, 1087, 1046, 973, 912, 744, 697; **HRMS** (EI): m/z calcd for $\text{C}_{21}\text{H}_{18}\text{O}_3^+$ [M]: 318.1250; found: 318.1216.

2-Hydroxy-1-phenylethyl [1,1'-biphenyl]-2-carboxylate 3ab.

m.p. 60-62 $^\circ\text{C}$; $^1\text{H NMR}$ (CDCl_3 , 600 MHz) δ = 7.86 (dd, J = 7.8, 1.4 Hz, 1H, Ar), 7.55 (td, J = 7.6, 1.5 Hz, 1H, Ar), 7.45 – 7.40 (m, 4H, Ar), 7.41 – 7.36 (m, 4H, Ar), 7.28 – 7.26 (m, 2H, Ar), 7.13 – 7.09 (m, 2H, Ar), 5.79 (dd, J = 7.1, 4.3 Hz, 1H, CH), 3.55 – 3.44 (m, 2H, CH_2), 1.11 (dd, J = 8.0, 6.1 Hz, 1H, OH) ppm (traces of **2ab** are available, **3ab:2ab** 100:9); $^{13}\text{C NMR}$ (CDCl_3 , 151 MHz) δ = 168.32, 142.34, 142.25, 136.84, 131.58, 130.91, 130.81, 130.46, 128.61, 128.55, 128.41, 128.38, 127.67, 127.54, 126.64, 78.29, 66.05 ppm; **IR** (ATR): ν (cm^{-1}) = 3458, 2917, 1689, 1449, 1352, 1277, 1126, 1007, 863, 742, 694; **HRMS** (EI): m/z calcd for $\text{C}_{21}\text{H}_{18}\text{O}_3^+$ [M]: 318.1250; found: 318.1248.

1-Phenylethane-1,2-diyl bis([1,1'-biphenyl]-2-carboxylate) 4ab.

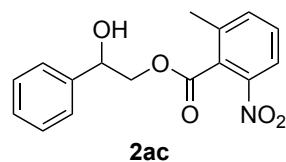
$^1\text{H NMR}$ (CDCl_3 , 600 MHz) δ = 7.84 (dd, J = 7.8, 1.0 Hz, 1H, Ar), 7.78 (dd, J = 7.8, 1.0 Hz, 1H, Ar), 7.54 (tdd, J = 7.6, 4.6, 1.4 Hz, 2H, Ar), 7.41 (tdd, J = 7.6, 3.6, 1.2 Hz, 2H, Ar), 7.38 – 7.32 (m, 5H, Ar), 7.26 (ddt, J = 6.1, 4.4, 1.3 Hz, 6H, Ar), 7.23 (d, J = 3.4 Hz, 4H, Ar), 7.03 (dd, J = 7.7, 1.6 Hz, 2H, Ar), 5.83 (dd, J = 8.0, 4.0 Hz, 1H, CH), 4.14 (dd, J = 11.8, 4.1 Hz, 1H, CHH), 4.07 (dd, J = 11.8, 8.1 Hz, 1H, CHH) ppm; $^{13}\text{C NMR}$ (CDCl_3 , 151 MHz) δ = 167.91, 167.30, 143.05, 142.89, 141.47, 141.35, 136.28, 131.57, 131.53, 131.06, 130.96, 130.53, 130.40, 130.35, 130.11, 128.60, 128.57, 128.54, 128.47, 128.20, 128.09, 127.42, 127.34, 127.29, 127.27, 126.96, 74.01, 66.51

Size-Induced Inversion of Selectivity in the Acylation of 1,2-Diols

ppm; IR (ATR): ν (cm⁻¹) = 3060, 2953, 1722, 1597, 1450, 1236, 1120, 1075, 743, 696; HRMS (EI): m/z calcd for C₃₄H₂₆O₄⁺ [M]⁺: 498.1826; found: 498.1824.

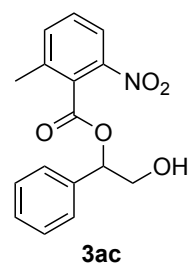
1a (200 mg, 1.45 mmol, 1.0 eq.), **5c** (498 mg, 1.45 mmol, 1.0 eq.), DMAP (8.84 mg, 72.4 μ mol, 0.05 eq.), and Et₃N (404 μ L, 2.90 mmol, 2.0 eq.) were dissolved in CHCl₃ (7.2 mL) and reacted according to GP A. **2ac** (175 mg, 40%) was obtained as a white solid, **3ac** (42.0 mg, 10%) was obtained as an oil and **4ac** (90.0 mg, 13%) was obtained as a white solid.

2-Hydroxy-2-phenylethyl 2-methyl-6-nitrobenzoate **2ac**.



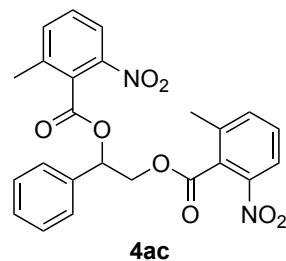
m.p. 118-120 °C; ¹H NMR (CDCl₃, 600 MHz) δ = 8.01 (d, J = 8.2 Hz, 1H, Ar), 7.55 (d, J = 7.7 Hz, 1H, Ar), 7.49 (t, J = 7.9 Hz, 1H, Ar), 7.45 (d, J = 7.5 Hz, 2H, Ar), 7.39 (t, J = 7.6 Hz, 2H, Ar), 7.33 (t, J = 7.3 Hz, 1H, Ar), 5.14 (d, J = 8.8 Hz, 1H, CH), 4.63 (dd, J = 11.5, 3.1 Hz, 1H, CHH), 4.43 (dd, J = 11.4, 8.8 Hz, 1H, CHH), 2.52 (d, J = 3.1 Hz, 1H, OH), 2.40 (s, 3H, Me) ppm (traces of **3ac** are available, **2ac**:**3ac** 100:10); ¹³C NMR (CDCl₃, 151 MHz) δ = 166.57, 139.49, 137.88, 136.29, 130.06, 129.28, 128.80, 128.48, 127.21, 126.35, 121.99, 72.05, 70.97, 19.27 ppm; IR (ATR): ν (cm⁻¹) = 3422, 2959, 1698, 1529, 1450, 1339, 1291, 1262, 1131, 1103, 1076, 1019, 967, 918, 806, 754, 705, 673; HRMS (EI): m/z calcd for C₁₆H₁₃O₄N⁺ [M-H₂O]⁺: 283.0839; found: 284.0850.

2-Hydroxy-1-phenylethyl 2-methyl-6-nitrobenzoate **3ac**.



¹H NMR (CDCl₃, 400 MHz) δ = 8.01 (ddd, J = 8.1, 1.3, 0.7 Hz, 1H, Ar), 7.56 – 7.46 (m, 2H, Ar), 7.44 – 7.33 (m, 5H, Ar), 6.22 (dd, J = 7.3, 3.8 Hz, 1H, CH), 4.08 – 3.90 (m, 2H, CH₂), 2.29 (s, 3H, Me), 2.09 (dd, J = 7.9, 5.5 Hz, 1H, OH) ppm; ¹³C NMR (CDCl₃, 101 MHz) δ = 166.08, 146.05, 137.98, 136.36, 136.23, 130.02, 129.32, 128.92, 128.83, 127.21, 121.98, 78.96, 65.78, 19.20 ppm; IR (ATR): ν (cm⁻¹) = 3444, 2926, 1730, 1539, 1454, 1342, 1249, 1113, 1072, 1015, 921, 803, 739, 697; HRMS (EI): m/z calcd for C₁₆H₁₄O₄N⁺ [M-HO]⁺: 284.0917; found: 284.0918.

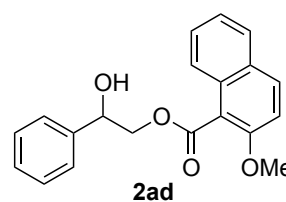
1-Phenylethane-1,2-diyl bis(2-methyl-6-nitrobenzoate) **4ac**.



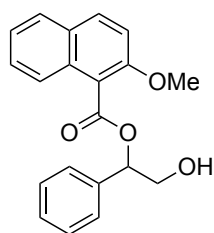
m.p. 121 - 122 °C; ¹H NMR (CDCl₃, 600 MHz) δ = 7.99 (d, J = 8.1 Hz, 1H, Ar), 7.96 (d, J = 8.5 Hz, 1H, Ar), 7.53 (d, J = 7.6 Hz, 1H, Ar), 7.49 – 7.44 (m, 5H, Ar), 7.44 – 7.36 (m, 3H, Ar), 6.41 (dd, J = 7.9, 3.9 Hz, 1H, CH), 4.82 (dd, J = 12.0, 3.9 Hz, 1H, CHH), 4.69 (dd, J = 11.9, 7.9 Hz, 1H, CHH), 2.32 (s, 3H, Me), 2.17 (s, 3H, Me) ppm; ¹³C NMR (CDCl₃, 151 MHz) δ = 166.25, 165.62, 146.27, 146.03, 137.98, 137.80, 136.18, 136.11, 135.30, 130.02, 129.97, 129.27, 129.06, 128.97, 128.91, 127.40, 121.91, 121.90, 75.04, 67.12, 19.13, 18.94 ppm; IR (ATR): ν (cm⁻¹) = 2925, 1856, 1736, 1525, 1452, 1343, 1247, 1109, 1070, 922, 804, 739, 697; HRMS (EI): m/z calcd for C₁₆H₁₃O₄N⁺ [M-O-C₈H₇O₃N]⁺: 283.0839; found: 283.0867.

1a (150 mg, 1.09 mmol, 1.0 eq.), **5d** (420 mg, 1.09 mmol, 1.0 eq.), DMAP (6.63 mg, 54.3 μ mol, 0.05 eq.), and Et₃N (302 μ L, 2.17 mmol, 2.0 eq.) were dissolved in CH₂Cl₂ (5.4 mL) and reacted according to GP A. **2ad** (110 mg, 31%) was obtained as a white solid, **3ad** (35.0 mg, 10%) was obtained as an oil and **4ad** (35.0 mg, 6%) was obtained as an oil.

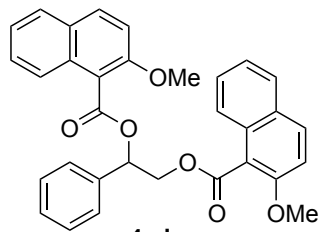
2-Hydroxy-2-phenylethyl 2-methoxy-1-naphthoate **2ad**.



m.p. 93-95 °C; ¹H NMR (CDCl₃, 600 MHz) δ = 7.94 (d, J = 9.1 Hz, 1H, Ar), 7.81 (d, J = 8.9 Hz, 2H, Ar), 7.52 – 7.48 (m, 3H, Ar), 7.40 (q, J = 8.7, 8.1 Hz, 3H, Ar), 7.35 (t, J = 7.3 Hz, 1H, Ar), 7.31 (d, J = 9.1 Hz, 1H, Ar), 5.17 (d, J = 7.7 Hz, 1H, CH), 4.67 (dd, J = 11.2, 3.2 Hz, 1H, CHH), 4.53 (dd, J = 11.2, 9.1 Hz, 1H, CHH), 4.01 (s, 3H, Me), 3.17 (d, J = 2.5 Hz, 1H, OH) ppm; ¹³C NMR (CDCl₃, 151 MHz) δ = 167.75, 154.74, 139.34, 132.31, 131.19, 128.75, 128.74, 128.35, 128.24, 128.06, 126.46, 124.51, 123.99, 116.96, 112.96, 72.20, 70.27, 56.98 ppm; IR (ATR): ν (cm⁻¹) = 3450, 2926, 1688, 1593, 1511, 1451, 1295, 1239, 1139, 1073, 1017, 966, 910, 815, 738, 697; HRMS (EI): m/z calcd for C₂₀H₁₈O₄⁺ [M]⁺: 322.1200; found: 322.1195.

2-Hydroxy-1-phenylethyl 2-methoxy-1-naphthoate 3ad.**3ad**

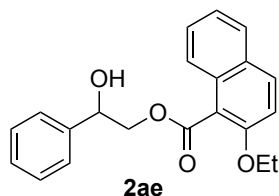
$^1\text{H NMR}$ (CDCl_3 , 400 MHz) δ = 7.94 (d, J = 9.1 Hz, 1H, Ar), 7.81 (dd, J = 8.0, 1.3 Hz, 1H, Ar), 7.75 (dd, J = 8.5, 1.1 Hz, 1H, Ar), 7.49 – 7.43 (m, 3H, Ar), 7.43 – 7.35 (m, 4H, Ar), 7.32 (d, J = 9.2 Hz, 1H, Ar), 6.32 (dd, J = 7.9, 4.4 Hz, 1H, CH), 4.01 (s, 3H, Me), 3.99 – 3.93 (m, 2H, CH_2), 2.80 (dd, J = 8.6, 5.0 Hz, 1H, OH); $^{13}\text{C NMR}$ (CDCl_3 , 101 MHz) δ = 167.32, 154.54, 136.89, 132.21, 131.21, 128.76, 128.74, 128.56, 128.20, 128.05, 126.80, 124.53, 123.95, 117.18, 112.99, 78.13, 66.37, 56.97 ppm; **IR** (ATR): ν (cm^{-1}) = 3444, 2935, 1717, 1595, 1511, 1434, 1342, 1225, 1135, 1072, 1017, 917, 809, 747, 698; **HRMS** (EI): m/z calcd for $\text{C}_{20}\text{H}_{18}\text{O}_4^+$ [M] $^+$: 322.1200; found: 322.1194.

1-Phenylethane-1,2-diyl bis(2-methoxy-1-naphthoate) 4ad.**4ad**

$^1\text{H NMR}$ (CDCl_3 , 800 MHz) δ = 7.92 (d, J = 9.0 Hz, 1H, Ar), 7.86 (d, J = 9.0 Hz, 1H, Ar), 7.79 – 7.77 (m, 1H, Ar), 7.73 (dd, J = 8.2, 1.1 Hz, 1H, Ar), 7.68 – 7.65 (m, 1H, Ar), 7.64 – 7.60 (m, 2H, Ar), 7.59 – 7.56 (m, 1H, Ar), 7.46 – 7.42 (m, 2H, Ar), 7.42 – 7.39 (m, 1H, Ar), 7.32 (ddd, J = 8.1, 6.8, 1.1 Hz, 1H, Ar), 7.27 (d, J = 9.1 Hz, 1H, Ar), 7.24 (dtd, J = 8.0, 6.8, 1.2 Hz, 2H, Ar), 7.22 (d, J = 9.0 Hz, 1H, Ar), 6.96 (ddd, J = 8.3, 6.8, 1.3 Hz, 1H, Ar), 6.65 (dd, J = 8.4, 3.9 Hz, 1H, CH), 5.02 (dd, J = 11.9, 3.9 Hz, 1H, CHH), 4.73 (dd, J = 11.9, 8.4 Hz, 1H, CHH), 3.85 (s, 3H, Me), 3.73 (s,

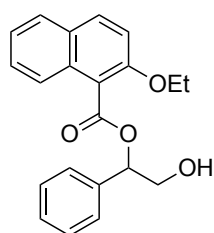
3H, Me) ppm; $^{13}\text{C NMR}$ (CDCl_3 , 201 MHz) δ = 167.86, 167.24, 154.80, 154.66, 136.70, 131.92, 131.78, 131.09, 131.07, 128.74, 128.71, 128.50, 128.50, 128.03, 127.97, 127.79, 127.53, 127.20, 124.21, 124.12, 124.03, 123.92, 117.35, 117.14, 113.22, 113.07, 74.46, 66.97, 56.71, 56.55 ppm; **IR** (ATR): ν (cm^{-1}) = 2935, 2843, 1723, 1595, 1511, 1434, 1342, 1210, 1131, 1072, 1017, 808, 745, 698; **HRMS** (EI): m/z calcd for $\text{C}_{32}\text{H}_{26}\text{O}_6^+$ [M] $^+$: 506.1724; found: 506.1722.

1a (100 mg, 724 μmol , 1.0 eq.), **5e** (360 mg, 869 μmol , 1.2 eq.), DMAP (4.42 mg, 36.2 μmol , 0.05 eq.), and Et_3N (202 μL , 1.45 mmol, 2.0 eq.) were dissolved in CH_2Cl_2 (3.6 mL) and reacted according to GP A. **2ae** (85.0 mg, 35%) was obtained as a white solid, **3ae** (30.0 mg, 12%) was obtained as an oil and **4ae** (20.0 mg, 5%) was obtained as a white solid.

2-Hydroxy-2-phenylethyl 2-ethoxy-1-naphthoate 2ae.**2ae**

m.p. 88-89 $^\circ\text{C}$; $^1\text{H NMR}$ (CDCl_3 , 600 MHz) δ = 7.91 (d, J = 9.1 Hz, 1H, Ar), 7.80 (dd, J = 8.4, 4.5 Hz, 2H, Ar), 7.52 – 7.47 (m, 3H, Ar), 7.43 – 7.37 (m, 3H, Ar), 7.35 (t, J = 7.3 Hz, 1H, Ar), 7.30 (d, J = 9.1 Hz, 1H, Ar), 5.17 (dt, J = 9.3, 2.8 Hz, 1H, CH), 4.66 (dd, J = 11.2, 3.1 Hz, 1H, CHH), 4.51 (dd, J = 11.2, 9.2 Hz, 1H, CHH), 4.28 (q, J = 7.0 Hz, 2H, CH_2), 3.08 (d, J = 2.6 Hz, 1H, OH), 1.47 (t, J = 7.0 Hz, 3H, Me) ppm; $^{13}\text{C NMR}$ (CDCl_3 ,

151 MHz) δ = 167.92, 154.11, 139.32, 132.10, 131.18, 128.76, 128.74, 128.36, 128.21, 127.96, 126.47, 124.49, 123.98, 117.59, 114.27, 72.26, 70.30, 65.76, 15.12 ppm; **IR** (ATR): ν (cm^{-1}) = 3436, 2876, 1692, 1593, 1513, 1464, 1340, 1292, 1236, 1116, 1061, 1024, 966, 811, 740, 699; **HRMS** (EI): m/z calcd for $\text{C}_{21}\text{H}_{20}\text{O}_4^+$ [M] $^+$: 336.1356; found: 336.1355.

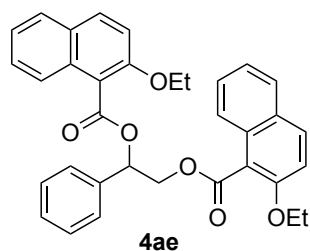
2-Hydroxy-1-phenylethyl 2-methoxy-1-naphthoate 3ae.**3ae**

$^1\text{H NMR}$ (CDCl_3 , 600 MHz) δ = 7.91 (d, J = 9.1 Hz, 1H, Ar), 7.80 (d, J = 8.2 Hz, 1H, Ar), 7.70 (d, J = 8.5 Hz, 1H, Ar), 7.45 (tdd, J = 8.4, 6.9, 1.5 Hz, 3H, Ar), 7.41 – 7.32 (m, 4H, Ar), 7.31 (d, J = 9.1 Hz, 1H, Ar), 6.32 (dd, J = 8.4, 3.9 Hz, 1H, CH), 4.31 (dq, J = 9.3, 6.9 Hz, 1H, CHH), 4.23 (dq, J = 9.4, 7.0 Hz, 1H, CHH), 4.02 – 3.91 (m, 2H, CH_2), 2.62 (dd, J = 9.2, 4.4 Hz, 1H, OH), 1.43 (t, J = 7.0 Hz, 3H, Me) ppm; $^{13}\text{C NMR}$ (CDCl_3 , 151 MHz) δ = 167.52, 153.84, 136.94, 131.95, 131.21, 128.76, 128.75, 128.55, 128.18, 127.96, 126.80, 124.50, 123.91, 117.84, 114.23, 78.06, 66.44, 65.79, 15.05 ppm; **IR** (ATR): ν (cm^{-1}) = 3445, 2927, 1719,

1595, 1511, 1466, 1435, 1340, 1227, 1136, 1023, 807, 748, 698; **HRMS** (EI): m/z calcd for $\text{C}_{21}\text{H}_{20}\text{O}_4^+$ [M] $^+$: 336.1356; found: 336.1356.

Size-Induced Inversion of Selectivity in the Acylation of 1,2-Diols

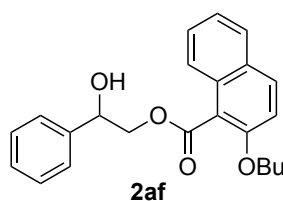
1-Phenylethane-1,2-diyl bis(2-ethoxy-1-naphthoate) **4ae**.



m.p. 116–118 °C; $^1\text{H NMR}$ (CDCl_3 , 400 MHz) δ = 7.90 (d, J = 9.1 Hz, 1H, Ar), 7.83 (d, J = 9.0 Hz, 1H, Ar), 7.78 (d, J = 8.0 Hz, 1H, Ar), 7.70 (d, J = 8.2 Hz, 1H, Ar), 7.66 – 7.59 (m, 3H, Ar), 7.50 (d, J = 8.5 Hz, 1H, Ar), 7.46 – 7.36 (m, 3H, Ar), 7.31 (ddd, J = 8.1, 6.9, 1.1 Hz, 1H, Ar), 7.25 (d, J = 8.5 Hz, 2H, Ar), 7.23 – 7.17 (m, 2H, Ar), 6.84 (ddd, J = 8.3, 6.9, 1.2 Hz, 1H, Ar), 6.62 (dd, J = 8.6, 3.7 Hz, 1H, CH), 5.00 (dd, J = 11.8, 3.7 Hz, 1H, CHH), 4.69 (dd, J = 11.8, 8.6 Hz, 1H, CHH), 4.23 – 3.94 (m, 4H; $2 \times \text{CH}_2$), 1.31 (t, J = 7.0 Hz, 3H, Me), 1.13 (t, J = 7.0 Hz, 3H, Me) ppm; $^{13}\text{C NMR}$ (CDCl_3 , 101 MHz) δ = 168.01, 167.42, 154.21, 153.84, 136.65, 131.75, 131.54, 131.13, 131.06, 128.73, 128.71, 128.53, 128.48, 128.00, 127.88, 127.72, 127.42, 127.22, 124.21, 124.07, 124.05, 123.94, 117.85, 117.71, 114.37, 114.26, 74.47, 66.94, 65.42, 65.29, 14.99, 14.77 ppm; **IR** (ATR): ν (cm^{-1}) = 3290, 2975, 1726, 1594, 1509, 1436, 1340, 1287, 1229, 1135, 1064, 1023, 810, 742, 696; **HRMS** (EI): m/z calcd for $\text{C}_{34}\text{H}_{30}\text{O}_6^+$ [M] $^+$: 534.2037; found: 534.2036.

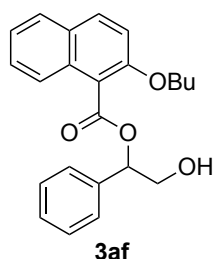
1a (100 mg, 724 μmol , 1.0 eq.), **5f** (306 mg, 651 μmol , 0.9 eq.), DMAP (4.42 mg, 36.2 μmol , 0.05 eq.), and Et_3N (202 μL , 1.45 mmol, 2.0 eq.) were dissolved in CHCl_3 (3.6 mL) and reacted according to GP A. **2af** (96.0 mg, 36%) was obtained as a white solid, **3af** (50.0 mg, 19%) was obtained as an oil and **4af** (20.0 mg, 5%) was obtained as an oil.

2-Hydroxy-2-phenylethyl 2-butoxy-1-naphthoate **2af**.



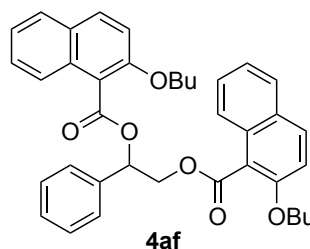
m.p. 61–63 °C; $^1\text{H NMR}$ (CDCl_3 , 400 MHz) δ = 7.91 (d, J = 9.1 Hz, 1H, Ar), 7.82 – 7.75 (m, 2H, Ar), 7.52 – 7.46 (m, 3H, Ar), 7.43 – 7.32 (m, 4H, Ar), 7.30 (d, J = 9.1 Hz, 1H, Ar), 5.15 (dt, J = 9.1, 3.0 Hz, 1H, CH), 4.66 (dd, J = 11.3, 3.1 Hz, 1H, CHH), 4.51 (dd, J = 11.3, 9.1 Hz, 1H, CHH), 4.20 (t, J = 6.6 Hz, 2H, CH_2), 3.01 (d, J = 2.9 Hz, 1H, OH), 1.86 – 1.77 (m, 2H, CH_2), 1.56 – 1.45 (m, 2H, CH_2), 0.99 (t, J = 7.4 Hz, 3H, Me) ppm; $^{13}\text{C NMR}$ (CDCl_3 , 101 MHz) δ = 167.99, 154.25, 139.41, 132.01, 131.17, 128.76, 128.68, 128.36, 128.21, 127.92, 126.45, 124.42, 123.92, 117.52, 114.28, 72.33, 70.33, 69.83, 31.45, 19.25, 13.96 ppm; **IR** (ATR): ν (cm^{-1}) = 3473, 2957, 1721, 1595, 1511, 1463, 1342, 1227, 1136, 1070, 1025, 809, 747, 699; **HRMS** (EI): m/z calcd for $\text{C}_{23}\text{H}_{24}\text{O}_4^+$ [M] $^+$: 364.1669; found: 364.1669.

2-Hydroxy-1-phenylethyl 2-butoxy-1-naphthoate **3af**.



$^1\text{H NMR}$ (CDCl_3 , 400 MHz) δ = 7.91 (d, J = 9.1 Hz, 1H, Ar), 7.80 (d, J = 8.1 Hz, 1H, Ar), 7.71 – 7.66 (m, 1H, Ar), 7.49 – 7.43 (m, 3H, Ar), 7.43 – 7.34 (m, 4H, Ar), 7.30 (d, J = 9.1 Hz, 1H, Ar), 6.31 (dd, J = 8.1, 4.2 Hz, 1H, CH), 4.27 – 4.09 (m, 2H, CH_2), 4.05 – 3.85 (m, 2H, CH_2), 2.53 (dd, J = 8.8, 4.9 Hz, 1H, OH), 1.81 – 1.72 (m, 2H, CH_2), 1.49 – 1.37 (m, 2H, CH_2), 0.94 (t, J = 7.4 Hz, 3H, Me) ppm (traces of **2af** are available, **3af:2af** 100:8); $^{13}\text{C NMR}$ (CDCl_3 , 101 MHz) δ = 167.55, 153.95, 136.96, 131.86, 131.20, 128.75, 128.70, 128.55, 128.17, 127.92, 126.85, 124.43, 123.87, 117.78, 114.24, 78.06, 69.91, 66.44, 31.42, 19.18, 13.93 ppm; **IR** (ATR): ν (cm^{-1}) = 3444, 2958, 1723, 1595, 1511, 1464, 1342, 1227, 1136, 1072, 1023, 809, 748, 698; **HRMS** (EI): m/z calcd for $\text{C}_{23}\text{H}_{24}\text{O}_4^+$ [M] $^+$: 364.1669; found: 364.1670.

1-Phenylethane-1,2-diyl bis(2-butoxy-1-naphthoate) **4af**.

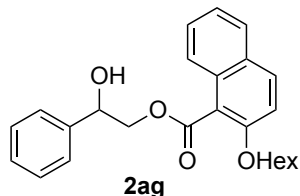


$^1\text{H NMR}$ (CDCl_3 , 400 MHz) δ = 7.90 (d, J = 9.1 Hz, 1H, Ar), 7.82 (d, J = 9.1 Hz, 1H, Ar), 7.78 (dd, J = 8.3, 1.3 Hz, 1H, Ar), 7.69 (d, J = 8.2 Hz, 1H, Ar), 7.65 – 7.58 (m, 3H, Ar), 7.48 (dd, J = 8.6, 1.0 Hz, 1H, Ar), 7.46 – 7.38 (m, 3H, Ar), 7.31 (ddd, J = 8.2, 6.8, 1.2 Hz, 1H, Ar), 7.26 (d, J = 8.9 Hz, 2H, Ar), 7.23 – 7.15 (m, 2H, Ar), 6.76 (ddd, J = 8.3, 6.8, 1.3 Hz, 1H, Ar), 6.61 (dd, J = 8.7, 3.8 Hz, 1H, CH), 4.96 (dd, J = 11.9, 3.8 Hz, 1H, CHH), 4.69 (dd, J = 11.8, 8.7 Hz, 1H, CHH), 4.13 – 3.86 (m, 4H, $2 \times \text{CH}_2$), 1.74 – 1.63 (m, 2H, CH_2), 1.54 – 1.44 (m, 2H, CH_2), 1.40 (qt, J = 8.1, 3.8 Hz, 2H, CH_2), 1.20 (dq, J = 14.8, 7.4 Hz, 2H, CH_2), 0.90 (t, J = 7.4 Hz, 3H, Me), 0.77 (t, J = 7.4 Hz, 3H, Me) ppm; $^{13}\text{C NMR}$ (CDCl_3 , 101 MHz) δ = 168.02, 167.38, 154.37, 153.97, 136.64, 131.71, 131.47, 131.14, 131.06, 128.74, 128.51, 128.42, 128.00, 127.84, 127.72, 127.37, 127.30, 124.18, 124.04, 124.00, 123.94, 117.77,

117.63, 114.34, 114.21, 74.45, 69.49, 69.40, 66.94, 31.43, 31.31, 19.21, 19.04, 13.96, 13.87 ppm (one signal is overlapping); **IR** (ATR): ν (cm^{-1}) = 2957, 2872, 1726, 1594, 1511, 1463, 1434, 1341, 1208, 1131, 1021, 807, 744, 697; **HRMS** (EI): m/z calcd for $\text{C}_{38}\text{H}_{38}\text{O}_6^+$ $[\text{M}]^+$: 590.2663; found: 590.2664.

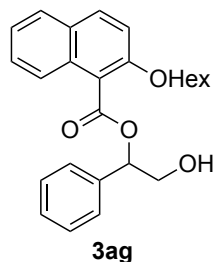
1a (100 mg, 724 μmol , 1.0 eq.), **5g** (344 mg, 651 μmol , 0.9 eq.), DMAP (4.42 mg, 36.2 μmol , 0.05 eq.), and Et_3N (202 μL , 1.45 mmol, 2.0 eq.) were dissolved in CHCl_3 (3.6 mL) and reacted according to GP A. **2ag** (105 mg, 37%) was obtained as a white solid, **3ag** (18.0 mg, 6%) was obtained as a white solid and **4ag** (10.0 mg, 2%) was obtained as an oil.

2-Hydroxy-2-phenylethyl 2-(hexanoyloxy)-1-naphthoate 2ag.



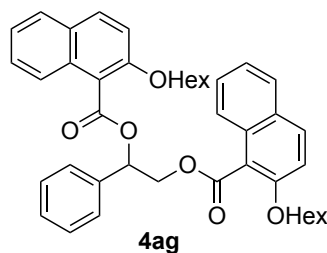
m.p. 53–54 °C; $^1\text{H NMR}$ (CDCl_3 , 400 MHz) δ = 7.91 (d, J = 9.1 Hz, 1H, Ar), 7.79 (ddd, J = 10.4, 8.3, 1.1 Hz, 2H, Ar), 7.51 – 7.46 (m, 3H, Ar), 7.44 – 7.32 (m, 4H, Ar), 7.30 (d, J = 9.1 Hz, 1H, Ar), 5.15 (dt, J = 9.2, 2.9 Hz, 1H, CH), 4.65 (dd, J = 11.3, 3.1 Hz, 1H, CHH), 4.50 (dd, J = 11.3, 9.2 Hz, 1H, CHH), 4.19 (t, J = 6.7 Hz, 2H, CH_2), 3.02 (d, J = 2.8 Hz, 1H, OH), 1.83 (dt, J = 15.0, 6.8 Hz, 2H, CH_2), 1.53 – 1.41 (m, 2H, CH_2), 1.35 (pd, J = 5.6, 3.4 Hz, 4H, $2\times\text{CH}_2$), 0.97 – 0.85 (m, 3H, Me) ppm; $^{13}\text{C NMR}$ (CDCl_3 , 101 MHz) δ = 167.98, 154.24, 139.36, 132.02, 131.15, 128.75, 128.65, 128.35, 128.20, 127.92, 126.44, 124.41, 123.90, 117.45, 114.25, 72.30, 70.33, 70.11, 31.64, 29.38, 25.68, 22.77, 14.18 ppm; **IR** (ATR): ν (cm^{-1}) = 3462, 2950, 1705, 1626, 1596, 1437, 1339, 1287, 1214, 1141, 1066, 1013, 914, 816, 738, 702; **HRMS** (EI): m/z calcd for $\text{C}_{25}\text{H}_{28}\text{O}_4^+$ $[\text{M}]^+$: 392.1982; found: 391.1980.

2-Hydroxy-1-phenylethyl 2-(hexanoyloxy)-1-naphthoate 3ag.



m.p. 75–77 °C; $^1\text{H NMR}$ (CDCl_3 , 600 MHz) δ = 7.91 (d, J = 9.0 Hz, 1H, Ar), 7.81 – 7.78 (m, 1H, Ar), 7.69 (dt, J = 8.5, 1.0 Hz, 1H, Ar), 7.47 – 7.44 (m, 2H, Ar), 7.43 (dd, J = 8.5, 1.4 Hz, 1H, Ar), 7.41 – 7.33 (m, 4H, Ar), 7.30 (d, J = 9.1 Hz, 1H, Ar), 6.31 (dd, J = 8.4, 3.9 Hz, 1H, CH), 4.18 (ddt, J = 41.1, 9.3, 6.8 Hz, 2H, CH_2), 4.01 – 3.88 (m, 2H, CH_2), 2.54 (dd, J = 9.1, 4.5 Hz, 1H, OH), 1.85 – 1.72 (m, 2H, CH_2), 1.45 – 1.35 (m, 2H, CH_2), 1.35 – 1.27 (m, 4H, $2\times\text{CH}_2$), 0.95 – 0.86 (m, 3H, Me) ppm; $^{13}\text{C NMR}$ (CDCl_3 , 151 MHz) δ = 167.55, 153.98, 136.97, 131.88, 131.22, 128.76, 128.71, 128.55, 128.18, 127.93, 126.84, 124.44, 123.88, 117.78, 114.28, 78.07, 70.26, 66.47, 31.64, 29.37, 25.61, 22.72, 14.18 ppm; **IR** (ATR): ν (cm^{-1}) = 3502, 2926, 1709, 1596, 1512, 1467, 1435, 1394, 1343, 1287, 1242, 1143, 1058, 1015, 802, 746, 701; **HRMS** (EI): m/z calcd for $\text{C}_{25}\text{H}_{28}\text{O}_4^+$ $[\text{M}]^+$: 392.1982; found: 391.1983.

1-Phenylethane-1,2-diyl bis(2-(hexanoyloxy)-1-naphthoate) 4ag.



$^1\text{H NMR}$ (CDCl_3 , 600 MHz) δ = 7.89 (d, J = 9.0 Hz, 1H, Ar), 7.82 (d, J = 9.0 Hz, 1H, Ar), 7.78 (d, J = 8.2 Hz, 1H, Ar), 7.69 (d, J = 8.2 Hz, 1H, Ar), 7.61 (ddd, J = 14.1, 8.2, 1.1 Hz, 3H, Ar), 7.48 (d, J = 8.5 Hz, 1H, Ar), 7.45 – 7.36 (m, 3H, Ar), 7.31 (ddd, J = 8.1, 6.8, 1.1 Hz, 1H, Ar), 7.24 (dd, J = 8.8, 7.3 Hz, 2H, Ar), 7.21 – 7.14 (m, 2H, Ar), 6.78 (t, J = 7.7 Hz, 1H, Ar), 6.61 (dd, J = 8.8, 3.7 Hz, 1H, CH), 4.95 (dd, J = 11.8, 3.8 Hz, 1H, CHH), 4.68 (dd, J = 11.8, 8.8 Hz, 1H, CHH), 4.06 (dt, J = 9.1, 6.5 Hz, 1H, CHH), 3.97 (ddt, J = 24.7, 9.1, 6.6 Hz, 2H, CH_2), 3.90 (dt, J = 9.0, 6.8 Hz, 1H, CHH), 1.67 (p, J = 7.0 Hz, 2H, CH_2), 1.49 (dtd, J = 14.2, 6.8, 2.8 Hz, 2H, CH_2), 1.35 (ddt, J = 18.2, 14.7, 7.5 Hz, 2H, CH_2), 1.29 – 1.23 (m, 4H, $2\times\text{CH}_2$), 1.23 – 1.09 (m, 6H, $3\times\text{CH}_2$), 0.85 (dt, J = 9.1, 7.0 Hz, 6H, $2\times\text{Me}$) ppm; $^{13}\text{C NMR}$ (CDCl_3 , 151 MHz) δ = 168.01, 167.37, 154.40, 154.01, 136.68, 131.69, 131.46, 131.16, 131.10, 128.73, 128.72, 128.53, 128.46, 128.00, 127.84, 127.72, 127.37, 127.28, 124.18, 124.07, 124.01, 123.98, 117.87, 117.68, 114.40, 114.32, 74.43, 69.84, 69.82, 66.97, 31.65, 31.58, 29.36, 29.25, 25.64, 25.49, 22.72, 22.65, 14.18 (2x) ppm; **IR** (ATR): ν (cm^{-1}) = 2927, 2856, 1728, 1595, 1511, 1464, 1341, 1282, 1223, 1131, 1065, 1018, 903, 807, 744, 697; **HRMS** (EI): m/z calcd for $\text{C}_{42}\text{H}_{46}\text{O}_6^+$ $[\text{M}]^+$: 646.3289; found: 646.3293.

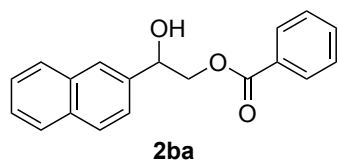
4.1.8.2.2 2-Naphthyl Diol Esters

1b (100 mg, 531 μmol , 1.0 eq.), **5a** (120 mg, 531 μmol , 1.0 eq.), DMAP (3.25 mg, 26.6 μmol , 0.05 eq.), and Et_3N (148 μL , 1.06 mmol, 2.0 eq.) were dissolved in CH_2Cl_2 (27 mL) and reacted according to GP A. **2ba** (77

Size-Induced Inversion of Selectivity in the Acylation of 1,2-Diols

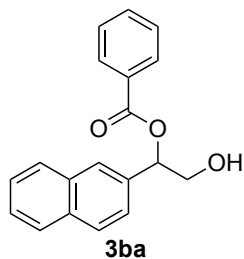
mg, 50%) was obtained as a white solid, **3ba** (20.0 mg, 13%) was obtained as a white solid and **4ba** (20.0 mg, 10%) was obtained as a white solid.

2-Hydroxy-2-(naphthalen-2-yl)ethyl benzoate **2ba**.



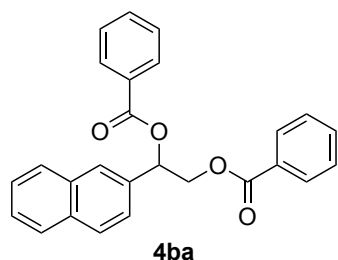
m.p. 95-97 °C; $^1\text{H NMR}$ (CDCl_3 , 600 MHz) δ = 8.07 (dd, J = 8.2, 1.1 Hz, 2H, Ar), 7.95 (s, 1H, Ar), 7.88 (d, J = 8.5 Hz, 1H, Ar), 7.87 – 7.84 (m, 2H, Ar), 7.61 – 7.55 (m, 2H, Ar), 7.53 – 7.48 (m, 2H, Ar), 7.46 (t, J = 7.8 Hz, 2H, Ar), 5.30 (d, J = 6.0 Hz, 1H, CH), 4.64 (dd, J = 11.6, 3.4 Hz, 1H, CHH), 4.52 (dd, J = 11.6, 8.2 Hz, 1H, CHH), 2.69 (s, 1H, OH) ppm; $^{13}\text{C NMR}$ (CDCl_3 , 151 MHz) δ = 166.93, 137.39, 133.41, 133.40, 129.91, 129.89, 128.61, 128.17, 127.88, 126.49, 126.33, 125.42, 124.14, 72.95, 69.97 ppm (two signals are overlapping); **IR** (ATR): ν (cm^{-1}) = 3542, 3056, 1702, 1597, 1449, 1276, 1085, 967, 822, 740, 707; **HRMS** (EI): m/z calcd for $\text{C}_{19}\text{H}_{16}\text{O}_3^+$ [M] $^+$: 292.1094; found: 292.1097. The $^1\text{H}/^{13}\text{C}$ NMR spectra are in full agreement with literature reports.^[17a,20]

2-Hydroxy-1-(naphthalen-2-yl)ethyl benzoate **3ba**.



m.p. 80-82 °C; $^1\text{H NMR}$ (CDCl_3 , 400 MHz) δ = 8.17 – 8.12 (m, 2H, Ar), 7.94 – 7.81 (m, 4H, Ar), 7.62 – 7.54 (m, 2H, Ar), 7.53 – 7.45 (m, 4H, Ar), 6.28 (dd, J = 7.4, 4.1 Hz, 1H, CH), 4.15 (ddd, J = 12.5, 7.4, 5.3 Hz, 1H, CHH), 4.04 (ddd, J = 11.8, 7.0, 4.1 Hz, 1H, CHH), 2.06 (t, J = 6.5 Hz, 1H, OH) ppm (traces of **2ba** are available, **3ba:2ba** 100:10); $^{13}\text{C NMR}$ (CDCl_3 , 101 MHz) δ = 166.28, 134.58, 133.43, 133.42, 133.27, 130.09, 129.93, 128.78, 128.62, 128.20, 127.86, 126.57, 126.51, 126.16, 124.27, 77.73, 66.29 ppm; **IR** (ATR): ν (cm^{-1}) = 3227, 2926, 1713, 1600, 1450, 1266, 1112, 1025, 821, 704; **HRMS** (EI): m/z calcd for $\text{C}_{19}\text{H}_{16}\text{O}_3^+$ [M] $^+$: 292.1094; found: 292.1101.

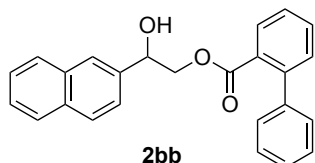
1-(Naphthalen-2-yl)ethane-1,2-diyl dibenzoate **4ba**.



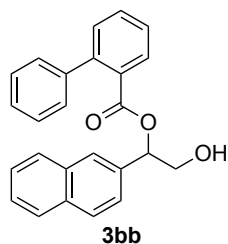
m.p. 103-104 °C; $^1\text{H NMR}$ (CDCl_3 , 800 MHz) δ = 8.13 (dd, J = 8.3, 1.3 Hz, 2H, Ar), 8.01 (dd, J = 8.3, 1.3 Hz, 2H, Ar), 8.00 (s, 1H, Ar), 7.90 (d, J = 8.5 Hz, 1H, Ar), 7.86 (td, J = 9.4, 4.1 Hz, 2H, Ar), 7.65 (dd, J = 8.5, 1.7 Hz, 1H, Ar), 7.61 – 7.57 (m, 1, Ar), 7.56 – 7.52 (m, 1H, Ar), 7.52 – 7.49 (m, 2H, Ar), 7.48 – 7.44 (m, 2H, Ar), 7.41 (td, J = 7.5, 1.7 Hz, 2H, Ar), 6.58 (dd, J = 8.2, 3.7 Hz, 1H, CH), 4.85 (dd, J = 12.0, 8.3 Hz, 1H, CHH), 4.76 (dd, J = 12.0, 3.7 Hz, 1H, CHH) ppm; $^{13}\text{C NMR}$ (CDCl_3 , 201 MHz) δ = 166.43, 165.86, 134.16, 133.57, 133.42, 133.34, 130.10, 129.99, 129.90, 129.88, 128.88, 128.66, 128.60, 128.29, 127.94, 126.66, 126.65, 126.36, 124.37, 74.40, 66.82 ppm (one signal is overlapping); **IR** (ATR): ν (cm^{-1}) = 3058, 1711, 1599, 1449, 1245, 1175, 1096, 832, 710; **HRMS** (EI): m/z calcd for $\text{C}_{26}\text{H}_{20}\text{O}_4^+$ [M] $^+$: 396.1356; found: 396.1349.

1b (100 mg, 531 μmol , 1.0 eq.), **5b** (201 mg, 531 μmol , 1.0 eq.), DMAP (3.25 mg, 26.6 μmol , 0.05 eq.), and Et_3N (148 μL , 1.06 mmol, 2.0 eq.) were dissolved in CHCl_3 (27 mL) and reacted according to GP A. **2bb** (90.0 mg, 46%) was obtained as an oil, **3bb** (20.0 mg, 10%) was obtained as an oil and **4bb** (30.0 mg, 10%) was obtained as an oil.

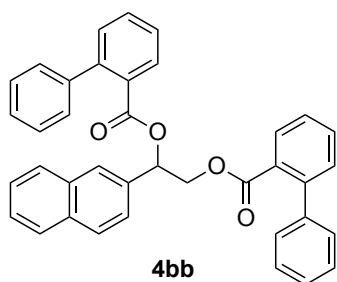
2-Hydroxy-2-(naphthalen-2-yl)ethyl [1,1'-biphenyl]-2-carboxylate **2bb**.



$^1\text{H NMR}$ (CDCl_3 , 400 MHz) δ = 7.91 (dd, J = 7.7, 1.4 Hz, 1H, Ar), 7.84 – 7.78 (m, 3H, Ar), 7.75 (s, 1H, Ar), 7.57 (td, J = 7.5, 1.4 Hz, 1H, Ar), 7.52 – 7.42 (m, 6H, Ar), 7.42 – 7.37 (m, 3H, Ar), 7.36 (dd, J = 8.5, 1.7 Hz, 1H, Ar), 4.71 (dt, J = 8.9, 2.8 Hz, 1H, CH), 4.40 (dd, J = 11.5, 2.8 Hz, 1H, CHH), 4.06 (dd, J = 11.5, 9.0 Hz, 1H, CHH), 1.70 (d, J = 3.2 Hz, 1H, OH) ppm; $^{13}\text{C NMR}$ (CDCl_3 , 101 MHz) δ = 168.81, 142.50, 142.23, 136.50, 133.32, 133.26, 131.75, 130.90, 130.54, 130.52, 128.51, 128.37, 128.12, 127.80, 127.78, 127.58, 126.35, 126.20, 125.23, 124.02, 72.06, 70.45 ppm (one signal is overlapping); **IR** (ATR): ν (cm^{-1}) = 3445, 3056, 1713, 1597, 1450, 1240, 1124, 1075, 1046, 976, 818, 743, 698; **HRMS** (EI): m/z calcd for $\text{C}_{25}\text{H}_{20}\text{O}_4^+$ [M] $^+$: 368.1407; found: 368.1405.

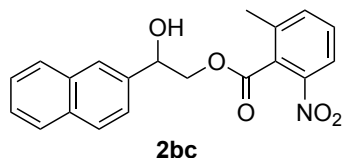
2-Hydroxy-1-(naphthalen-2-yl)ethyl [1,1'-biphenyl]-2-carboxylate **3bb**.

¹H NMR (CDCl₃, 400 MHz) δ = 7.86 (dd, J = 7.8, 1.4 Hz, 1H, Ar), 7.81 – 7.78 (m, 1H, Ar), 7.78 – 7.76 (m, 1H, Ar), 7.75 (s, 1H, Ar), 7.60 (s, 1H, Ar), 7.56 (td, J = 7.5, 1.4 Hz, 1H, Ar), 7.49 – 7.45 (m, 3H, Ar), 7.44 – 7.42 (m, 2H, Ar), 7.41 (s, 2H, Ar), 7.41 – 7.37 (m, 2H, Ar), 7.23 – 7.18 (m, 1H, Ar), 6.00 – 5.90 (m, 1H, CH), 3.64 – 3.54 (m, 2H, CH₂), 1.18 (t, J = 7.0 Hz, 1H, OH) ppm (traces of **2bb** are available, **3bb**:**2bb** 100:14); ¹³C NMR (CDCl₃, 101 MHz) δ = 168.43, 142.39, 142.25, 134.25, 133.32, 133.18, 131.64, 130.96, 130.82, 130.52, 128.59, 128.49, 128.46, 128.17, 127.79, 127.70, 127.58, 126.40, 126.38, 126.06, 124.33, 78.46, 65.99 ppm; IR (ATR): ν (cm⁻¹) = 3425, 2923, 1709, 1597, 1436, 1240, 1122, 1046, 818, 743, 698; HRMS (EI): m/z calcd for C₂₅H₂₀O₃⁺ [M]⁺: 368.1407; found: 368.1414.

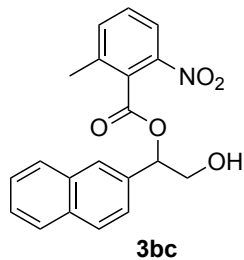
1-(Naphthalen-2-yl)ethane-1,2-diyl bis([1,1'-biphenyl]-2-carboxylate) **4bb**.

¹H NMR (CDCl₃, 400 MHz) δ = 7.90 (dd, J = 7.8, 1.3 Hz, 1H, Ar), 7.86 – 7.77 (m, 3H, Ar), 7.75 (d, J = 8.6 Hz, 1H, Ar), 7.60 – 7.53 (m, 3H, Ar), 7.53 – 7.48 (m, 2H, Ar), 7.47 – 7.40 (m, 2H, Ar), 7.40 – 7.36 (m, 2H, Ar), 7.36 – 7.31 (m, 3H, Ar), 7.30 – 7.24 (m, 4H, Ar), 7.24 – 7.18 (m, 3H, Ar), 7.15 (dd, J = 8.5, 1.7 Hz, 1H, Ar), 6.03 (dd, J = 7.5, 4.5 Hz, 1H, CH), 4.30 – 4.17 (m, 2H, CH₂) ppm; ¹³C NMR (CDCl₃, 101 MHz) δ = 167.96, 167.42, 143.06, 142.92, 141.49, 141.34, 133.66, 133.39, 133.13, 131.59, 131.10, 130.98, 130.52, 130.42, 130.37, 130.17, 128.62, 128.47, 128.43, 128.23, 128.19, 128.11, 127.78, 127.43, 127.37, 127.32, 127.31, 126.49, 126.46, 126.36, 124.51, 74.19, 66.41 ppm (one signal is overlapping); IR (ATR): ν (cm⁻¹) = 3057, 1716, 1597, 1436, 1236, 1120, 1075, 1046, 907, 743, 697; HRMS (EI): m/z calcd for C₃₈H₂₈O₄⁺ [M]⁺: 548.1982; found: 548.1986.

1b (100 mg, 531 μ mol, 1.0 eq.), **5c** (183 mg, 531 μ mol, 1.0 eq.), DMAP (3.25 mg, 26.6 μ mol, 0.05 eq.), and Et₃N (148 μ L, 1.06 mmol, 2.0 eq.) were dissolved in CHCl₃ (27 mL) and reacted according to GP A. **2bc** (49.0 mg, 26%) was obtained as a white solid, **3bc** (31.0 mg, 17%) was obtained as a white solid and **4bc** (40.0 mg, 15%) was obtained as a white solid.

2-Hydroxy-2-(naphthalen-2-yl)ethyl 2-methyl-6-nitrobenzoate **2bc**.

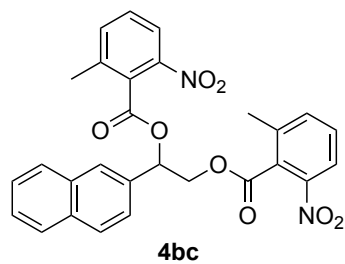
m.p. 115-117 °C; ¹H NMR (CDCl₃, 400 MHz) δ = 8.02 (d, J = 8.1 Hz, 1H, Ar), 7.94 (s, 1H, Ar), 7.92 – 7.82 (m, 3H, Ar), 7.60 – 7.45 (m, 5H, Ar), 5.33 (dt, J = 8.5, 3.2 Hz, 1H, CH), 4.74 (dd, J = 11.5, 3.1 Hz, 1H, CHH), 4.51 (dd, J = 11.5, 8.8 Hz, 1H, CHH), 2.62 (d, J = 3.5 Hz, 1H, OH), 2.40 (s, 3H, Me) ppm; ¹³C NMR (CDCl₃, 101 MHz) δ = 166.61, 146.30, 137.90, 136.87, 136.30, 133.40, 133.40, 130.08, 129.28, 128.63, 128.19, 127.86, 126.49, 126.36, 125.50, 124.07, 122.01, 72.19, 70.93, 19.29 ppm; IR (ATR): ν (cm⁻¹) = 3431, 2924, 1704, 1526, 1340, 1283, 1120, 972, 921, 801, 746, 702; HRMS (EI): m/z calcd for C₂₀H₁₇O₅N⁺ [M]⁺: 351.1101; found: 351.1097.

2-Hydroxy-1-(naphthalen-2-yl)ethyl 2-methyl-6-nitrobenzoate **3bc**.

m.p. 128-130 °C; ¹H NMR (CDCl₃, 400 MHz) δ = 8.01 (d, J = 8.0 Hz, 1H, Ar), 7.93 – 7.81 (m, 4H, Ar), 7.58 – 7.43 (m, 5H, Ar), 6.39 (dd, J = 7.3, 3.9 Hz, 1H, CH), 4.13 (ddd, J = 12.3, 7.3, 5.1 Hz, 1H, CHH), 4.04 (ddd, J = 12.1, 7.6, 3.9 Hz, 1H, CHH), 2.28 (s, 3H, Me), 2.19 – 2.14 (m, 1H, OH) ppm (traces of **2bc** are available, **3bc**:**2bc** 100:4); ¹³C NMR (CDCl₃, 101 MHz) δ = 166.14, 146.08, 138.01, 136.40, 133.65, 133.53, 133.26, 130.06, 129.34, 128.75, 128.27, 127.90, 126.76, 126.66, 126.62, 124.54, 122.01, 79.06, 65.78, 19.25 ppm; IR (ATR): ν (cm⁻¹) = 3520, 2923, 1720, 1528, 1342, 1264, 1116, 1072, 1003, 821, 740; HRMS (EI): m/z calcd for C₂₀H₁₇O₅N⁺ [M]⁺: 351.1101; found: 351.1088.

Size-Induced Inversion of Selectivity in the Acylation of 1,2-Diols

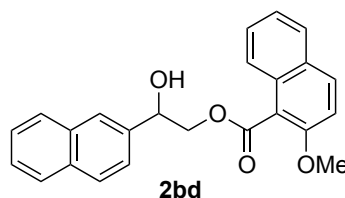
1-(Naphthalen-2-yl)ethane-1,2-diyl bis(2-methyl-6-nitrobenzoate) **4bc**.



m.p. 172-175 °C; $^1\text{H NMR}$ (CDCl_3 , 400 MHz) δ = 8.00 – 7.95 (m, 3H, Ar), 7.90 (d, J = 8.5 Hz, 1H, Ar), 7.86 (dt, J = 6.5, 3.5 Hz, 2H, Ar), 7.56 (dd, J = 8.5, 1.7 Hz, 1H, Ar), 7.54 – 7.49 (m, 3H, Ar), 7.49 – 7.41 (m, 3H, Ar), 6.59 (dd, J = 7.8, 4.0 Hz, 1H, CH), 4.91 (dd, J = 12.0, 4.0 Hz, 1H, CHH), 4.79 (dd, J = 12.0, 7.9 Hz, 1H, CHH), 2.30 (s, 3H, Me), 2.17 (s, 3H, Me) ppm; $^{13}\text{C NMR}$ (CDCl_3 , 101 MHz) δ = 166.27, 165.66, 146.29, 146.06, 137.97, 137.82, 136.17, 136.12, 133.66, 133.24, 132.65, 130.03, 129.99, 129.04, 128.94, 128.86, 128.35, 127.89, 127.14, 126.79, 126.64, 124.45, 121.90 (2x), 75.15, 67.08, 19.11, 18.99 ppm; **IR** (ATR): ν (cm^{-1}) = 2924, 1734, 1537, 1443, 1341, 1247, 1124, 1071, 805, 741; **HRMS** (EI): m/z calcd for $\text{C}_{28}\text{H}_{22}\text{O}_8\text{N}_2^+$ [M] $^+$: 514.1371; found: 514.1377.

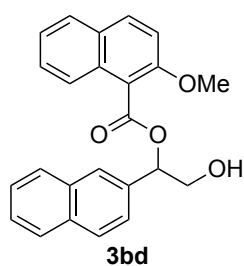
1b (100 mg, 531 μmol , 1.0 eq.), **5d** (205 mg, 531 μmol , 1.0 eq.), DMAP (3.25 mg, 26.6 μmol , 0.05 eq.), and Et_3N (148 μL , 1.06 mmol, 2.0 eq.) were dissolved in CHCl_3 (27 mL) and reacted according to GP A. **2bd** (44.0 mg, 15%) was obtained as a white solid, **3bd** (11.0 mg, 6%) was obtained as an oil and **4bd** (54.0 mg, 18%) was obtained as a white solid.

2-Hydroxy-2-(naphthalen-2-yl)ethyl 2-methoxy-1-naphthoate **2bd**.



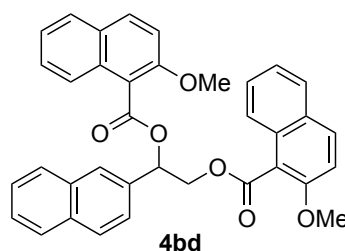
m.p. 149-151 °C; $^1\text{H NMR}$ (CDCl_3 , 400 MHz) δ = 7.98 (s, 1H, Ar), 7.94 (d, J = 9.1 Hz, 1H, Ar), 7.91 – 7.84 (m, 3H, Ar), 7.79 (ddd, J = 13.0, 8.2, 1.5 Hz, 2H, Ar), 7.60 (dd, J = 8.5, 1.7 Hz, 1H, Ar), 7.54 – 7.48 (m, 2H, Ar), 7.40 (dddd, J = 16.4, 8.1, 6.8, 1.4 Hz, 2H, Ar), 7.31 (d, J = 9.1 Hz, 1H, Ar), 5.34 (dt, J = 8.8, 3.0 Hz, 1H, CH), 4.77 (dd, J = 11.3, 3.3 Hz, 1H, CHH), 4.62 (dd, J = 11.3, 8.9 Hz, 1H, CHH), 4.00 (s, 3H, Me), 3.30 (d, J = 2.9 Hz, 1H, OH) ppm; $^{13}\text{C NMR}$ (CDCl_3 , 101 MHz) δ = 167.80, 154.76, 136.80, 133.46, 133.40, 132.32, 131.19, 128.74, 128.56, 128.23, 128.23, 128.04, 127.87, 126.41, 126.28, 125.57, 124.51, 124.23, 123.97, 116.96, 112.96, 72.35, 70.20, 56.98 ppm; **IR** (ATR): ν (cm^{-1}) = 3474, 2947, 1701, 1593, 1508, 1433, 1361, 1231, 1124, 1069, 1014, 814, 749; **HRMS** (EI): m/z calcd for $\text{C}_{24}\text{H}_{20}\text{O}_4^+$ [M] $^+$: 372.1356; found: 372.1363.

2-Hydroxy-1-(naphthalen-2-yl)ethyl 2-methoxy-1-naphthoate **3bd**.



$^1\text{H NMR}$ (CDCl_3 , 400 MHz) δ = 7.96 (dd, J = 5.4, 3.8 Hz, 2H, Ar), 7.90 – 7.80 (m, 4H, Ar), 7.77 – 7.72 (m, 1H, Ar), 7.56 (dd, J = 8.5, 1.8 Hz, 1H, Ar), 7.51 (dt, J = 6.2, 3.4 Hz, 2H, Ar), 7.46 – 7.32 (m, 3H, Ar), 6.48 (dd, J = 8.3, 4.0 Hz, 1H, CH), 4.10 – 3.99 (m, 5H, CH_2 and Me) ppm (traces of **2bd** are available, **3bd:2bd** 100:13); $^{13}\text{C NMR}$ (CDCl_3 , 101 MHz) δ = 167.36, 154.58, 134.32, 133.40, 133.31, 132.24, 131.24, 128.78, 128.59, 128.21, 128.20, 128.09, 127.87, 126.52, 126.46, 126.15, 124.56, 124.46, 123.97, 117.19, 112.99, 78.26, 66.35, 57.00 ppm; **IR** (ATR): ν (cm^{-1}) = 3394, 2924, 1718, 1595, 1510, 1434, 1343, 1281, 1226, 1135, 1017, 810, 745; **HRMS** (EI): m/z calcd for $\text{C}_{21}\text{H}_{20}\text{O}_4^+$ [M] $^+$: 336.1356; found: 372.1354.

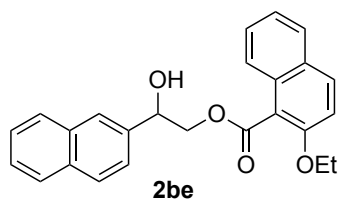
1-(Naphthalen-2-yl)ethane-1,2-diyl bis(2-methoxy-1-naphthoate) **4bd**.



m.p. 80-82°C; $^1\text{H NMR}$ (CDCl_3 , 400 MHz) δ = 8.10 (s, 1H, Ar), 7.95 – 7.82 (m, 5H, Ar), 7.75 (dd, J = 11.4, 8.2 Hz, 2H, Ar), 7.71 (dd, J = 8.5, 1.7 Hz, 1H, Ar), 7.61 – 7.55 (m, 2H, Ar), 7.56 – 7.49 (m, 2H, Ar), 7.32 – 7.21 (m, 4H, Ar), 7.10 (ddd, J = 8.3, 6.8, 1.3 Hz, 1H, Ar), 6.96 (ddd, J = 8.3, 6.8, 1.3 Hz, 1H, Ar), 6.79 (dd, J = 8.1, 3.9 Hz, 1H, CH), 5.09 (dd, J = 11.8, 4.0 Hz, 1H, CHH), 4.81 (dd, J = 11.8, 8.1 Hz, 1H, CHH), 3.82 (s, 3H, Me), 3.75 (s, 3H, Me) ppm; $^{13}\text{C NMR}$ (CDCl_3 , 101 MHz) δ = 167.88, 167.29, 154.81, 154.72, 134.13, 133.54, 133.39, 131.93, 131.84, 131.13, 131.10, 128.58, 128.56, 128.51, 128.33, 128.01, 128.00, 127.90, 127.76, 127.61, 126.71, 126.53, 126.49, 124.74, 124.22, 124.18, 124.01, 123.98, 117.41, 117.16, 113.24, 113.07, 74.62, 66.91, 56.71, 56.62 ppm; **IR** (ATR): ν (cm^{-1}) = 2916, 1732, 1595, 1511, 1231, 1131, 1073, 1018, 809, 746; **HRMS** (EI): m/z calcd for $\text{C}_{36}\text{H}_{28}\text{O}_6^+$ [M] $^+$: 556.1880; found: 556.1881.

1b (100 mg, 531 μmol , 1.0 eq.), **5e** (220 mg, 531 μmol , 1.0 eq.), DMAP (3.25 mg, 26.6 μmol , 0.05 eq.), and Et_3N (148 μL , 1.06 mmol, 2.0 eq.) were dissolved in CHCl_3 (27 mL) and reacted according to GP A. **2be** (40.0 mg, 20%) was obtained as a white solid, **3be** (75.0 mg, 37%) was obtained as a white solid and **4be** (20.0 mg, 6%) was obtained as a white solid.

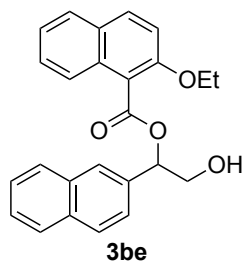
2-Hydroxy-2-(naphthalen-2-yl)ethyl 2-ethoxy-1-naphthoate 2be.



m.p. 127-128 $^{\circ}\text{C}$; $^1\text{H NMR}$ (CDCl_3 , 800 MHz) δ = 7.98 (s, 1H, Ar), 7.92 (d, J = 9.0 Hz, 1H, Ar), 7.89 (d, J = 8.5 Hz, 1H, Ar), 7.88 – 7.84 (m, 2H, Ar), 7.80 (dd, J = 8.1, 1.1 Hz, 1H, Ar), 7.78 – 7.74 (m, 1H, Ar), 7.60 (dd, J = 8.4, 1.7 Hz, 1H, Ar), 7.52 (s, 2H, Ar), 7.42 (ddd, J = 8.4, 6.7, 1.3 Hz, 1H, Ar), 7.37 (ddd, J = 8.0, 6.8, 1.1 Hz, 1H, Ar), 7.30 (d, J = 9.1 Hz, 1H, Ar), 5.34 (d, J = 11.8 Hz, 1H, CH), 4.76 (dd, J = 11.3, 3.2 Hz, 1H, CHH), 4.60 (dd, J = 11.3, 9.1 Hz, 1H, CHH), 4.29 (q, J = 7.0 Hz,

2H, CH_2), 3.21 (d, J = 2.8 Hz, 1H, OH), 1.47 (t, J = 7.0 Hz, 3H, Me) ppm; $^{13}\text{C NMR}$ (CDCl_3 , 201 MHz) δ = 167.96, 154.11, 136.73, 133.45, 133.39, 132.11, 131.16, 128.73, 128.55, 128.21, 128.20, 127.94, 127.86, 126.40, 126.27, 125.56, 124.49, 124.23, 123.95, 117.56, 114.26, 72.40, 70.23, 65.77, 15.13 ppm; IR (ATR): ν (cm^{-1}) = 3458, 2907, 1697, 1592, 1507, 1465, 1342, 1289, 1234, 1138, 1063, 977, 865, 808, 744; HRMS (EI): m/z calcd for $\text{C}_{25}\text{H}_{22}\text{O}_4^+$ [M] $^+$: 386.1513; found: 386.1505.

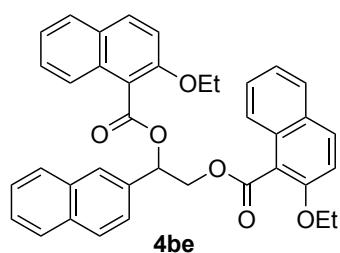
2-Hydroxy-1-(naphthalen-2-yl)ethyl 2-ethoxy-1-naphthoate 3be.



m.p. 91 $^{\circ}\text{C}$; $^1\text{H NMR}$ (CDCl_3 , 400 MHz) δ = 7.96 – 7.91 (m, 2H, Ar), 7.89 – 7.78 (m, 4H, Ar), 7.69 (d, J = 8.3 Hz, 1H, Ar), 7.56 (dd, J = 8.5, 1.5 Hz, 1H, Ar), 7.50 (dt, J = 6.2, 3.4 Hz, 2H, Ar), 7.39 (m, 2H, Ar), 7.32 (d, J = 9.1 Hz, 1H, Ar), 6.48 (dd, J = 8.3, 3.9 Hz, 1H, CH), 4.39 – 4.16 (m, 2H, CH_2), 4.04 (qdd, J = 12.3, 8.6, 4.0 Hz, 2H, CH_2), 2.66 (dd, J = 9.2, 4.4 Hz, 1H, OH), 1.43 (t, J = 7.0 Hz, 3H, Me) ppm (traces of **2be** are available, **3be:2be** 100:5); $^{13}\text{C NMR}$ (CDCl_3 , 101 MHz) δ = 167.54, 153.88, 134.36, 133.43, 133.33, 131.99, 131.24, 128.79, 128.62, 128.21, 128.18, 127.99, 127.88, 126.52, 126.46, 126.13,

124.53, 124.47, 123.94, 117.88, 114.27, 78.17, 66.42, 65.83, 15.07 ppm; IR (ATR): ν (cm^{-1}) = 3455, 2922, 1697, 1539, 1509, 1464, 1233, 1137, 1062, 808, 744; HRMS (EI): m/z calcd for $\text{C}_{25}\text{H}_{22}\text{O}_4^+$ [M] $^+$: 386.1513; found: 386.1510.

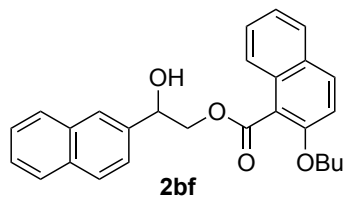
1-(Naphthalen-2-yl)ethane-1,2-diyl bis(2-ethoxy-1-naphthoate) 4be.



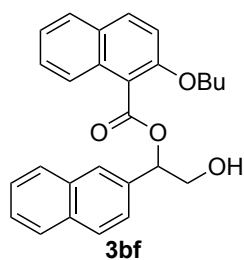
m.p. 226-228 $^{\circ}\text{C}$; $^1\text{H NMR}$ (CDCl_3 , 400 MHz) δ = 8.11 – 8.07 (m, 1H, Ar), 7.94 – 7.82 (m, 5H, Ar), 7.79 – 7.70 (m, 3H, Ar), 7.58 – 7.49 (m, 4H, Ar), 7.31 – 7.18 (m, 4H, Ar), 7.10 (ddd, J = 8.4, 6.8, 1.3 Hz, 1H, Ar), 6.89 (ddd, J = 8.4, 6.9, 1.3 Hz, 1H, Ar), 6.79 (dd, J = 8.2, 3.9 Hz, 1H, CH), 5.10 (dd, J = 11.8, 4.0 Hz, 1H, CHH), 4.81 (dd, J = 11.8, 8.2 Hz, 1H, CHH), 4.18 – 3.94 (m, 4H, $2\times\text{CH}_2$), 1.29 (t, J = 7.0 Hz, 3H, Me), 1.07 (t, J = 7.0 Hz, 3H, Me) ppm; $^{13}\text{C NMR}$ (CDCl_3 , 101 MHz) δ = 168.00, 167.44, 154.19, 153.90, 134.10, 133.53, 133.33, 131.75, 131.61,

131.10, 128.59, 128.51, 128.30, 127.97, 127.92, 127.87, 127.64, 127.47, 126.67, 126.50, 126.46, 124.77, 124.19, 124.11, 123.99, 123.95, 117.86, 117.70, 114.37, 114.35, 74.59, 66.86, 65.43, 65.31, 14.96, 14.75 ppm (two signals are overlapping); IR (ATR): ν (cm^{-1}) = 2929, 1720, 1594, 1509, 1435, 1342, 1278, 1208, 1129, 1024, 859, 804, 750; HRMS (EI): m/z calcd for $\text{C}_{38}\text{H}_{32}\text{O}_6^+$ [M] $^+$: 584.2193; found: 584.2182.

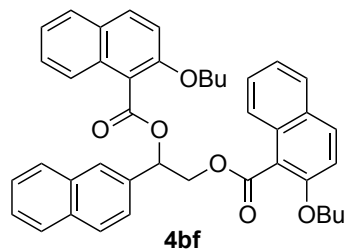
1b (100 mg, 531 μmol , 1.0 eq.), **5f** (250 mg, 531 μmol , 1.0 eq.), DMAP (3.25 mg, 26.6 μmol , 0.05 eq.), and Et_3N (148 μL , 1.06 mmol, 2.0 eq.) were dissolved in CH_2Cl_2 (27 mL) and reacted according to GP A. **2bf** (55.0 mg, 25%) was obtained as a white solid, **3bf** (55.0 mg, 25%) was obtained as an oil and **4bf** (27.0 mg, 8%) was obtained as an oil.

2-Hydroxy-2-(naphthalen-2-yl)ethyl 2-butoxy-1-naphthoate **2bf**.

m.p. 101 °C; $^1\text{H NMR}$ (CDCl_3 , 400 MHz) δ = 7.97 (s, 1H, Ar), 7.93 – 7.84 (m, 4H, Ar), 7.82 – 7.76 (m, 1H, Ar), 7.75 – 7.70 (m, 1H, Ar), 7.60 (dd, J = 8.5, 1.7 Hz, 1H, Ar), 7.53 – 7.47 (m, 2H, Ar), 7.39 (dddd, J = 16.4, 8.1, 6.8, 1.4 Hz, 2H, Ar), 7.30 (d, J = 9.1 Hz, 1H, Ar), 5.33 (dt, J = 9.0, 3.1 Hz, 1H, CH), 4.75 (dd, J = 11.3, 3.2 Hz, 1H, CHH), 4.59 (dd, J = 11.3, 9.0 Hz, 1H, CHH), 4.21 (t, J = 6.7 Hz, 2H, CH_2), 3.13 (d, J = 2.8 Hz, 1H, OH), 1.87 – 1.77 (m, 2H, CH_2), 1.50 (dt, J = 14.8, 7.4 Hz, 2H, CH_2), 0.98 (t, J = 7.4 Hz, 3H, Me) ppm; $^{13}\text{C NMR}$ (CDCl_3 , 101 MHz) δ = 168.05, 154.23, 136.78, 133.43, 133.38, 132.04, 131.13, 128.64, 128.56, 128.21, 128.19, 127.91, 127.86, 126.41, 126.28, 125.55, 124.41, 124.22, 123.87, 117.43, 114.23, 72.46, 70.25, 69.80, 31.43, 19.25, 13.98 ppm; **IR** (ATR): ν (cm^{-1}) = 3466, 2960, 1712, 1593, 1510, 1461, 1347, 1237, 1139, 1048, 964, 858, 807, 744; **HRMS** (EI): m/z calcd for $\text{C}_{27}\text{H}_{26}\text{O}_4^+$ [M] $^+$: 414.1826; found: 414.1818.

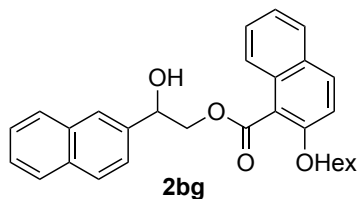
2-Hydroxy-1-(naphthalen-2-yl)ethyl 2-butoxy-1-naphthoate **3bf**.

$^1\text{H NMR}$ (CDCl_3 , 400 MHz) δ = 7.96 (s, 1H, Ar), 7.91 (d, J = 9.1 Hz, 1H, Ar), 7.89 – 7.83 (m, 3H, Ar), 7.81 (d, J = 8.1 Hz, 1H, Ar), 7.71 (d, J = 8.5 Hz, 1H, Ar), 7.57 (dd, J = 8.5, 1.6 Hz, 1H, Ar), 7.51 (dt, J = 6.3, 3.4 Hz, 2H, Ar), 7.42 (ddd, J = 8.4, 6.9, 1.2 Hz, 1H, Ar), 7.37 (td, J = 7.5, 6.9, 1.0 Hz, 1H, Ar), 7.31 (d, J = 9.1 Hz, 1H, Ar), 6.49 (dd, J = 8.5, 3.8 Hz, 1H, CH), 4.23 (dt, J = 9.3, 6.7 Hz, 1H, CHH), 4.15 (dt, J = 9.3, 6.8 Hz, 1H, CHH), 4.08 (ddd, J = 12.5, 8.5, 4.2 Hz, 1H, CHH), 4.02 (ddd, J = 12.4, 9.0, 3.9 Hz, 1H, CHH), 2.64 (dd, J = 9.1, 4.4 Hz, 1H, OH), 1.80 – 1.70 (m, 2H, CH_2), 1.46 – 1.35 (m, 2H, CH_2), 0.89 (t, J = 7.4 Hz, 3H, Me) ppm (traces of **2bf** are available, **3bf**:**2bf** 100: 6); $^{13}\text{C NMR}$ (CDCl_3 , 151 MHz) δ = 167.60, 153.99, 134.37, 133.44, 133.33, 131.90, 131.22, 128.71, 128.61, 128.22, 128.18, 127.96, 127.87, 126.51, 126.46, 126.22, 124.51, 124.45, 123.88, 117.79, 114.27, 78.17, 69.93, 66.39, 31.42, 19.16, 13.86 ppm; **IR** (ATR): ν (cm^{-1}) = 3449, 2957, 1722, 1595, 1510, 1463, 1341, 1226, 1136, 1021, 907, 809, 745; **HRMS** (EI): m/z calcd for $\text{C}_{27}\text{H}_{26}\text{O}_4^+$ [M] $^+$: 414.1826; found: 414.1827.

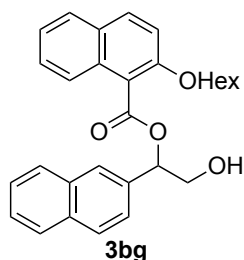
1-(Naphthalen-2-yl)ethane-1,2-diyl bis(2-butoxy-1-naphthoate) **4bf**.

$^1\text{H NMR}$ (CDCl_3 , 400 MHz) δ = 8.09 (s, 1H, Ar), 7.95 – 7.81 (m, 5H, Ar), 7.77 (d, J = 8.2 Hz, 1H, Ar), 7.71 (ddd, J = 8.4, 2.7, 1.4 Hz, 2H, Ar), 7.58 – 7.51 (m, 4H, Ar), 7.31 – 7.18 (m, 4H, Ar), 7.11 (ddd, J = 8.3, 6.8, 1.3 Hz, 1H, Ar), 6.85 – 6.76 (m, 2H, Ar and CH), 5.06 (dd, J = 11.8, 4.1 Hz, 1H, CHH), 4.82 (dd, J = 11.8, 8.4 Hz, 1H, CHH), 4.08 (dt, J = 9.1, 6.5 Hz, 1H, CHH), 4.03 – 3.95 (m, 2H, CH_2), 3.91 (dt, J = 9.1, 6.6 Hz, 1H, CHH), 1.66 (tt, J = 7.8, 6.4 Hz, 2H, CH_2), 1.47 – 1.33 (m, 4H, $2\times\text{CH}_2$), 1.15 – 1.01 (m, 2H, CH_2), 0.90 (t, J = 7.4 Hz, 3H, Me), 0.60 (t, J = 7.4 Hz, 3H, Me) ppm; $^{13}\text{C NMR}$ (CDCl_3 , 101 MHz) δ = 167.99, 167.39, 154.36, 154.05, 134.10, 133.60, 133.37, 131.70, 131.52, 131.12, 131.10, 128.60, 128.51, 128.47, 128.34, 127.96, 127.88, 127.86, 127.65, 127.43, 126.88, 126.52, 126.44, 124.88, 124.16, 124.04, 124.00, 123.96, 117.82, 117.67, 114.36, 114.30, 74.56, 69.52, 69.45, 66.81, 31.42, 31.28, 19.20, 18.96, 13.94, 13.64 ppm; **IR** (ATR): ν (cm^{-1}) = 2926, 1725, 1594, 1510, 1463, 1341, 1281, 1207, 1130, 1069, 1021, 806, 744; **HRMS** (EI): m/z calcd for $\text{C}_{42}\text{H}_{40}\text{O}_6^+$ [M] $^+$: 640.2819; found: 640.2833.

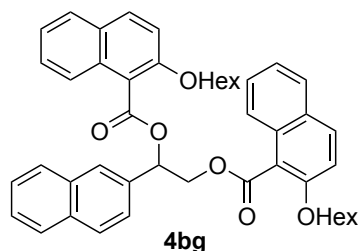
1b (100 mg, 531 μmol , 1.0 eq.), **5g** (238 mg, 452 μmol , 0.9 eq.), DMAP (3.25 mg, 26.6 μmol , 0.05 eq.), and Et_3N (148 μL , 1.06 mmol, 2.0 eq.) were dissolved in CHCl_3 (27 mL) and reacted according to GP A. **2bg** (50.0 mg, 21%) was obtained as a white solid, **3bg** (65.0 mg, 28%) was obtained as an oil and **4bg** (10.0 mg, 3%) was obtained as an oil.

2-Hydroxy-2-(naphthalen-2-yl)ethyl 2-(hexanoyloxy)-1-naphthoate 2bg.

m.p. 108–110 °C; $^1\text{H NMR}$ (CDCl_3 , 400 MHz) δ = 7.97 (s, 1H, Ar), 7.94 – 7.82 (m, 4H, Ar), 7.82 – 7.76 (m, 1H, Ar), 7.75 – 7.71 (m, 1H, Ar), 7.60 (dd, J = 8.5, 1.7 Hz, 1H, Ar), 7.54 – 7.48 (m, 2H, Ar), 7.38 (dddd, J = 16.3, 8.1, 6.8, 1.4 Hz, 2H, Ar), 7.30 (d, J = 9.1 Hz, 1H, Ar), 5.33 (dt, J = 8.9, 3.0 Hz, 1H, CH), 4.76 (dd, J = 11.3, 3.2 Hz, 1H, CHH), 4.60 (dd, J = 11.3, 8.9 Hz, 1H, CHH), 4.19 (t, J = 6.7 Hz, 2H, CH_2), 3.13 (d, J = 2.8 Hz, 1H, OH), 1.88 – 1.76 (m, 2H, CH_2), 1.47 (dt, J = 13.8, 7.1 Hz, 2H, CH_2), 1.41 – 1.31 (m, 4H, $2\times\text{CH}_2$), 0.94 – 0.87 (m, 3H, Me) ppm; $^{13}\text{C NMR}$ (CDCl_3 , 101 MHz) δ = 168.02, 154.26, 136.84, 133.45, 133.40, 132.02, 131.16, 128.67, 128.54, 128.21, 128.19, 127.89, 127.86, 126.40, 126.26, 125.54, 124.41, 124.22, 123.89, 117.50, 114.29, 72.46, 70.25, 70.15, 31.65, 29.41, 25.69, 22.78, 14.19 ppm; **IR** (ATR): ν (cm^{-1}) = 3476, 2923, 1711, 1593, 1461, 1346, 1237, 1138, 1056, 858, 807, 744; **HRMS** (EI): m/z calcd for $\text{C}_{29}\text{H}_{30}\text{O}_4^+$ [M] $^+$: 442.2139; found: 442.2140.

2-Hydroxy-1-(naphthalen-2-yl)ethyl 2-(hexanoyloxy)-1-naphthoate 3bg.

$^1\text{H NMR}$ (CDCl_3 , 600 MHz) δ = 7.96 (d, J = 1.6 Hz, 1H, Ar), 7.92 (d, J = 9.1 Hz, 1H, Ar), 7.89 – 7.83 (m, 3H, Ar), 7.81 – 7.78 (m, 1H, Ar), 7.70 (d, J = 8.4 Hz, 1H, Ar), 7.56 (dd, J = 8.4, 1.7 Hz, 1H, Ar), 7.51 (dt, J = 6.3, 3.4 Hz, 2H, Ar), 7.42 (ddd, J = 8.4, 6.8, 1.4 Hz, 1H, Ar), 7.39 – 7.34 (m, 1H, Ar), 7.31 (d, J = 9.1 Hz, 1H, Ar), 6.48 (dd, J = 8.5, 3.8 Hz, 1H, CH), 4.22 (dt, J = 9.3, 6.9 Hz, 1H, CHH), 4.15 (dt, J = 9.3, 6.9 Hz, 1H, CHH), 4.05 (dddd, J = 34.6, 12.5, 8.7, 4.1 Hz, 2H, CH_2), 2.61 (dd, J = 9.2, 4.4 Hz, 1H, OH), 1.75 (dq, J = 13.2, 8.2, 4.3 Hz, 2H, CH_2), 1.37 (dq, J = 12.1, 7.6 Hz, 2H, CH_2), 1.25 (pd, J = 7.2, 6.2, 3.5 Hz, 4H, $2\times\text{CH}_2$), 0.87 (dd, J = 7.6, 6.2 Hz, 3H, Me) ppm; $^{13}\text{C NMR}$ (CDCl_3 , 151 MHz) δ = 167.59, 153.99, 134.38, 133.42, 133.32, 131.89, 131.22, 128.70, 128.59, 128.20, 128.17, 127.94, 127.85, 126.49, 126.45, 126.20, 124.50, 124.44, 123.88, 117.79, 114.30, 78.15, 70.26, 66.38, 31.57, 29.35, 25.57, 22.66, 14.14 ppm; **IR** (ATR): ν (cm^{-1}) = 3465, 2929, 1723, 1595, 1511, 1464, 1281, 1226, 1135, 1017, 906, 810, 728; **HRMS** (EI): m/z calcd for $\text{C}_{29}\text{H}_{30}\text{O}_4^+$ [M] $^+$: 442.2139; found: 442.2142.

1-(Naphthalen-2-yl)ethane-1,2-diyl bis(2-(hexanoyloxy)-1-naphthoate) 4bg.

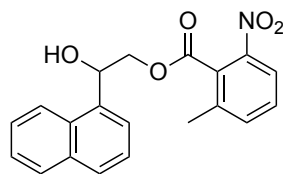
$^1\text{H NMR}$ (CDCl_3 , 600 MHz) δ = 8.08 (d, J = 1.6 Hz, 1H, Ar), 7.92 – 7.87 (m, 3H, Ar), 7.87 – 7.81 (m, 2H, Ar), 7.76 (dd, J = 8.3, 1.1 Hz, 1H, Ar), 7.71 (dd, J = 8.4, 1.5 Hz, 2H, Ar), 7.57 – 7.49 (m, 4H, Ar), 7.28 (ddd, J = 8.4, 6.9, 1.2 Hz, 1H, Ar), 7.24 (d, J = 9.1 Hz, 1H, Ar), 7.22 – 7.17 (m, 2H, Ar), 7.11 (ddd, J = 8.3, 6.8, 1.3 Hz, 1H, Ar), 6.84 – 6.79 (m, 1H, Ar), 6.77 (dd, J = 8.5, 4.0 Hz, 1H, CH), 5.04 (dd, J = 11.9, 4.0 Hz, 1H, CHH), 4.79 (dd, J = 11.8, 8.5 Hz, 1H, CHH), 4.05 (dt, J = 9.1, 6.5 Hz, 1H, CHH), 3.96 (ddt, J = 13.0, 9.1, 6.7 Hz, 2H, CH_2), 3.88 (dt, J = 9.0, 6.8 Hz, 1H, CHH), 1.64 (p, J = 7.1 Hz, 2H, CH_2), 1.40 – 1.36 (m, 2H, CH_2), 1.35 – 1.31 (m, 2H, CH_2), 1.29 – 1.20 (m, 6H, $3\times\text{CH}_2$), 1.05 (h, J = 7.7 Hz, 4H, $2\times\text{CH}_2$), 0.86 (t, J = 7.0 Hz, 3H, Me), 0.75 (t, J = 7.3 Hz, 3H, Me) ppm; $^{13}\text{C NMR}$ (CDCl_3 , 151 MHz) δ = 168.00, 167.40, 154.38, 154.07, 134.10, 133.60, 133.37, 131.70, 131.51, 131.13, 131.11, 128.59, 128.51, 128.48, 128.34, 127.97, 127.88, 127.87, 127.66, 127.43, 126.85, 126.53, 126.45, 124.86, 124.17, 124.04, 124.01, 123.99, 117.88, 117.66, 114.38, 74.53, 69.84 (2x), 66.85, 31.65, 31.43, 29.35, 29.20, 25.63, 25.41, 22.73, 22.53, 14.20, 14.12 (one signal is overlapping) ppm; **IR** (ATR): ν (cm^{-1}) = 2925, 1728, 1594, 1511, 1463, 1341, 1282, 1223, 1130, 1064, 1017, 806, 744; **HRMS** (EI): m/z calcd for $\text{C}_{46}\text{H}_{48}\text{O}_6^+$ [M] $^+$: 696.3445; found: 696.3438.

4.1.8.2.3 1-Naphthyl Diol Esters

1c (50.0 mg, 266 μmol , 1.0 eq.), **5c** (91.5 mg, 266 μmol , 1.00 eq.), DMAP (1.62 mg, 13.8 μmol , 0.05 eq.), and Et_3N (74.1 μL , 531 μmol , 2.0 eq.) were dissolved in CHCl_3 (5 mL) and reacted according to GP A. **2cc** (35.0 mg, 37%) was obtained as a white solid, **3cc** (8.00 mg, 9%) was obtained as an oil and **4cc** (24.0 mg, 18%) was obtained as a white solid.

Size-Induced Inversion of Selectivity in the Acylation of 1,2-Diols

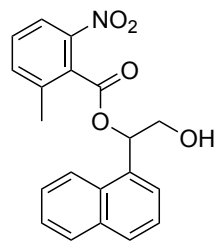
2-Hydroxy-2-(naphthalen-1-yl)ethyl 2-methyl-6-nitrobenzoate **3cc**.



2cc

m.p. 122-125 °C; $^1\text{H NMR}$ (CDCl_3 , 400 MHz) δ = 8.24 (dd, J = 8.6, 1.1 Hz, 1H, Ar), 8.04 (dt, J = 8.1, 1.0 Hz, 1H, Ar), 7.93 – 7.88 (m, 1H, Ar), 7.83 (ddt, J = 11.9, 7.2, 1.1 Hz, 2H, Ar), 7.64 – 7.55 (m, 2H, Ar), 7.55 – 7.47 (m, 3H, Ar), 6.00 (dt, J = 9.2, 3.0 Hz, 1H, CH), 4.92 (dd, J = 11.7, 2.5 Hz, 1H, CHH), 4.40 (dd, J = 11.6, 9.2 Hz, 1H, CHH), 2.71 (d, J = 3.4 Hz, 1H, OH), 2.46 (s, 3H, Me) ppm; $^{13}\text{C NMR}$ (CDCl_3 , 101 MHz) δ = 166.80, 146.31, 137.92, 136.38, 135.05, 133.81, 130.48, 130.13, 129.34, 129.09, 128.91, 126.84, 125.95, 125.61, 123.89, 122.92, 122.07, 70.94, 68.97, 19.36 ppm; **IR** (ATR): ν (cm^{-1}) = 3528, 2915, 1707, 1525, 1436, 1340, 1277, 1166, 1121, 1063, 974, 921, 798, 778, 740; **HRMS** (EI): m/z calcd for $\text{C}_{20}\text{H}_{17}\text{NO}_5^+$ [M] $^+$: 351.1101; found: 351.1105.

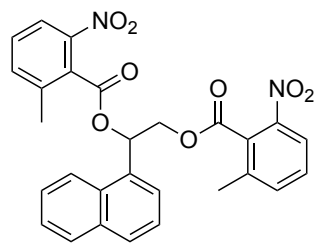
2-Hydroxy-1-(naphthalen-1-yl)ethyl 2-methyl-6-nitrobenzoate **3cc**.



3cc

$^1\text{H NMR}$ (CDCl_3 , 600 MHz) δ = 8.23 (dd, J = 8.5, 1.2 Hz, 1H, Ar), 8.06 – 8.01 (m, 1H, Ar), 7.93 – 7.88 (m, 1H, Ar), 7.86 (dt, J = 8.2, 1.1 Hz, 1H, Ar), 7.63 – 7.58 (m, 2H, Ar), 7.56 – 7.45 (m, 4H), Ar, 7.06 (dd, J = 7.1, 3.5 Hz, 1H, CH), 4.22 – 4.05 (m, 2H, CH_2), 2.29 – 2.23 (m, 4H, Me and OH) ppm (traces of **2dc** are available, **3dc:2dc** 100: 8); $^{13}\text{C NMR}$ (CDCl_3 , 151 MHz) δ = 166.18, 146.18, 138.12, 136.45, 133.96, 132.03, 130.51, 130.10, 129.38, 129.32, 129.18, 126.92, 126.15, 125.30, 124.86, 122.98, 122.05, 76.28, 65.81, 19.32 ppm; **IR** (ATR): ν (cm^{-1}) = 3448, 2926, 1735, 1531, 1343, 1267, 1115, 1072, 802, 779, 738; **HRMS** (EI): m/z calcd for $\text{C}_{20}\text{H}_{17}\text{NO}_5^+$ [M] $^+$: 351.1101; found: 351.1103

1-(Naphthalen-1-yl)ethane-1,2-diyl bis(2-methyl-6-nitrobenzoate) **4cc**.

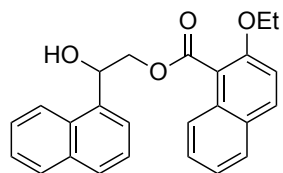


4cc

m.p. 133-135 °C; $^1\text{H NMR}$ (CDCl_3 , 400 MHz) δ = 8.32 (d, J = 8.5 Hz, 1H, Ar), 8.03 – 7.99 (m, 1H, Ar), 7.97 (dd, J = 7.5, 1.9 Hz, 1H, Ar), 7.95 – 7.87 (m, 2H, Ar), 7.68 – 7.60 (m, 2H, Ar), 7.58 – 7.53 (m, 2H, Ar), 7.51 – 7.43 (m, 4H, Ar), 7.24 (dd, J = 8.4, 3.2 Hz, 1H, CH), 4.99 (dd, J = 12.2, 3.3 Hz, 1H, CHH), 4.71 (dd, J = 12.2, 8.5 Hz, 1H, CHH), 2.37 (s, 3H, Me), 2.16 (s, 3H, Me) ppm; $^{13}\text{C NMR}$ (CDCl_3 , 151 MHz) δ = 166.39, 165.66, 146.39, 146.14, 138.12, 137.89, 136.21, 136.14, 133.96, 131.11, 130.47, 130.07, 130.02, 129.77, 129.19, 129.03, 128.88, 127.18, 126.22, 125.28, 125.15, 122.93, 121.92, 72.38, 67.36, 19.22, 19.02 ppm; **IR** (ATR): ν (cm^{-1}) = 217, 1737, 1529, 1462, 1341, 1259, 1108, 1068, 921, 801, 736; **HRMS** (EI): m/z calcd for $\text{C}_{28}\text{H}_{22}\text{N}_2\text{O}_8^+$ [M] $^+$: 514.1371; found: 514.1375.

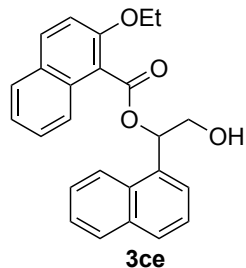
1c (50.0 mg, 266 μmol , 1.0 eq.), **5e** (110 mg, 266 μmol , 1.00 eq.), DMAP (1.62 mg, 13.8 μmol , 0.05 eq.), and Et_3N (74.1 μL , 531 μmol , 2.0 eq.) were dissolved in CHCl_3 (5 mL) and reacted according to GP A. **2ce** (36.0 mg, 31%) was obtained as an oil, **3ce** (20.0 mg, 20%) was obtained as an oil and **4ce** (10.0 mg, 6%) was obtained as a white solid.

2-Hydroxy-2-(naphthalen-1-yl)ethyl 2-ethoxy-1-naphthoate **2ce**.

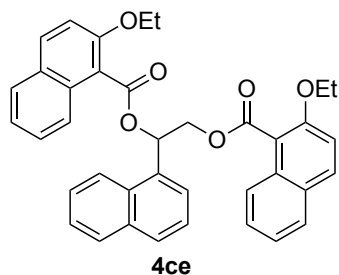


2ce

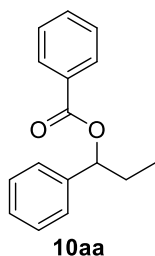
$^1\text{H NMR}$ (CDCl_3 , 400 MHz) δ = 8.29 – 8.24 (m, 1H, Ar), 7.97 – 7.93 (m, 1H, Ar), 7.93 – 7.89 (m, 1H, Ar), 7.89 – 7.81 (m, 4H, Ar), 7.59 (ddd, J = 8.5, 6.8, 1.5 Hz, 1H, Ar), 7.57 – 7.50 (m, 3H, Ar), 7.41 (ddd, J = 8.0, 6.8, 1.2 Hz, 1H, Ar), 7.34 (d, J = 9.1 Hz, 1H, Ar), 6.01 (dt, J = 9.5, 2.6 Hz, 1H, CH), 4.96 (dd, J = 11.4, 2.6 Hz, 1H, CHH), 4.49 (dd, J = 11.4, 9.5 Hz, 1H, CHH), 4.33 (qd, J = 7.0, 3.4 Hz, 2H, CH_2), 3.32 (d, J = 2.5 Hz, 1H, OH), 1.51 (t, J = 7.0 Hz, 3H, Me) ppm; $^{13}\text{C NMR}$ (CDCl_3 , 101 MHz) δ = 168.16, 154.17, 134.78, 133.81, 132.19, 131.18, 130.65, 129.09, 128.76, 128.74, 128.25, 128.02, 126.68, 125.85, 125.72, 124.55, 123.99, 123.90, 122.99, 117.51, 114.20, 70.26, 69.23, 65.81, 15.18 ppm; **IR** (ATR): ν (cm^{-1}) = 3496, 2980, 1715, 1595, 1511, 1435, 1280, 1227, 1135, 1062, 1025, 906, 801, 776, 727; **HRMS** (EI): m/z calcd for $\text{C}_{25}\text{H}_{22}\text{O}_4^+$ [M] $^+$: 386.1513; found: 386.1511.

2-Hydroxy-1-(naphthalen-1-yl)ethyl 2-ethoxy-1-naphthoate 3ce.

$^1\text{H NMR}$ (CDCl_3 , 400 MHz) δ = 8.33 – 8.26 (m, 1H, Ar), 7.97 – 7.89 (m, 2H, Ar), 7.85 (d, J = 8.2 Hz, 1H, Ar), 7.83 – 7.78 (m, 1H, Ar), 7.72 (dd, J = 8.3, 1.2 Hz, 1H, Ar), 7.68 (dt, J = 7.2, 1.0 Hz, 1H, Ar), 7.62 (ddd, J = 8.4, 6.8, 1.5 Hz, 1H, Ar), 7.55 (ddd, J = 8.0, 6.8, 1.2 Hz, 1H), 7.49 – 7.35 (m, 3H, Ar), 7.33 (d, J = 9.2 Hz, 1H, Ar), 7.14 (dd, J = 8.5, 3.5 Hz, 1H, CH), 4.30 (ddq, J = 36.2, 9.4, 7.0 Hz, 2H, CH_2), 4.10 (dddd, J = 27.9, 12.3, 8.9, 3.6 Hz, 2H, CH_2), 2.83 (dd, J = 9.7, 4.0 Hz, 1H, OH), 1.45 (t, J = 7.0 Hz, 3H, Me) ppm; $^{13}\text{C NMR}$ (CDCl_3 , 101 MHz) δ = 167.56, 153.86, 133.86, 132.68, 132.00, 131.22, 130.54, 129.10, 129.01, 128.76, 128.18, 127.98, 126.81, 126.04, 125.43, 124.52, 124.27, 123.95, 123.02, 117.80, 114.18, 75.44, 66.19, 65.80, 15.06 ppm; **IR** (ATR): ν (cm^{-1}) = 8452, 2926, 1722, 1595, 1511, 1434, 1340, 1280, 1213, 1135, 1057, 907, 799, 776, 727; **HRMS** (EI): m/z calcd for $\text{C}_{25}\text{H}_{22}\text{O}_4^+$ [M] $^+$: 386.1513; found: 386.1520.

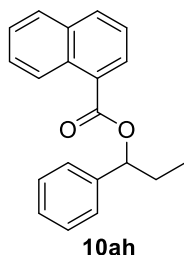
1-(Naphthalen-1-yl)ethane-1,2-diyl bis(2-ethoxy-1-naphthoate) 4ce.

m.p. 168–175 °C; $^1\text{H NMR}$ (CDCl_3 , 400 MHz) δ = 8.56 – 8.49 (m, 1H, Ar), 7.96 – 7.91 (m, 2H, Ar), 7.91 – 7.85 (m, 2H, Ar), 7.86 – 7.80 (m, 2H, Ar), 7.80 – 7.77 (m, 1H, Ar), 7.77 – 7.75 (m, 0.5H, Ar), 7.73 – 7.63 (m, 2H, Ar), 7.57 (ddd, J = 8.0, 6.8, 1.1 Hz, 1H, Ar), 7.55 – 7.50 (m, 2H, Ar), 7.49 – 7.43 (m, 1H, Ar), 7.36 – 7.26 (m, 3.5H, Ar), 7.23 – 7.15 (m, 2H, Ar), 6.75 (ddd, J = 8.4, 6.9, 1.3 Hz, 1H, CH), 5.22 (dd, J = 12.1, 3.0 Hz, 1H, CHH), 4.68 (dd, J = 12.1, 9.1 Hz, 1H, CHH), 4.22 – 3.93 (m, 4H, $2\times\text{CH}_2$), 1.35 (t, J = 7.0 Hz, 3H, Me), 1.05 (t, J = 7.0 Hz, 3H, Me) ppm; $^{13}\text{C NMR}$ (CDCl_3 , 101 MHz) δ = 168.30, 167.40, 154.35, 153.90, 133.93, 132.42, 131.82, 131.57, 131.18, 131.14, 130.72, 129.28, 129.04, 128.57, 128.50, 128.04, 127.87, 127.82, 127.38, 127.03, 126.10, 125.36, 124.79, 124.27, 124.15, 124.08, 123.41, 117.89, 117.74, 114.35, 114.23, 72.05, 67.03, 65.46, 65.23, 15.02, 14.71 (one signal is overlapping) ppm; **IR** (ATR): ν (cm^{-1}) = 2921, 1725, 1595, 1511, 1434, 1281, 1208, 1131, 1061 860, 801, 746; **HRMS** (EI): m/z calcd for $\text{C}_{38}\text{H}_{32}\text{O}_6^+$ [M] $^+$: 584.2193; found: 584.2194.

4.1.8.2.4 Synthesis of Phenylpropanol Esters**1-Phenylpropyl benzoate 10aa.**

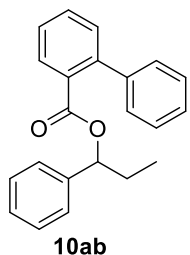
8a (100 mg, 734 μmol , 1.0 eq.), **5a** (250 mg, 1.10 mmol, 1.5 eq.), DMAP (4.49 mg, 36.7 μmol , 0.05 eq.), and Et_3N (205 μL , 1.47 mmol, 2.0 eq.) were dissolved in CH_2Cl_2 (4.0 mL) and reacted according to GP A. **10aa** (141 mg, 80%) was obtained as a clear liquid.

$^1\text{H NMR}$ (CDCl_3 , 400 MHz) δ = 8.12 – 8.06 (m, 2H, Ar), 7.59 – 7.53 (m, 1H, Ar), 7.48 – 7.39 (m, 4H, Ar), 7.39 – 7.32 (m, 2H, Ar), 7.31 – 7.26 (m, 1H, Ar), 5.93 (t, J = 6.8 Hz, 1H, CH), 2.16 – 1.88 (m, 2H, CH_2), 0.97 (t, J = 7.4 Hz, 3H, Me) ppm; $^{13}\text{C NMR}$ (CDCl_3 , 101 MHz) δ = 166.04, 140.77, 133.04, 130.69, 129.78, 128.57, 128.49, 127.98, 126.62, 78.04, 29.72, 10.11; **HRMS** (EI): m/z calcd for $\text{C}_{16}\text{H}_{16}\text{O}_2^+$ [M] $^+$: 240.1145; found: 240.1137. The $^1\text{H}/^{13}\text{C}$ NMR spectrum are in full agreement with literature reports.^[21]

1-Phenylpropyl 1-naphthoate 10ah.

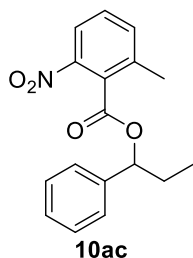
8a (25.0 mg, 184 μmol , 1.0 eq.), **5h** (65.9 mg, 202 μmol , 1.1 eq.), DMAP (1.12 mg, 91.8 μmol , 0.05 eq.), and Et_3N (51.2 μL , 367 μmol , 2.0 eq.) were dissolved in CH_2Cl_2 (1.0 mL) and reacted according to GP A. **10ah** (20.0 mg, 38%) was obtained as an oil.

$^1\text{H NMR}$ (CDCl_3 , 400 MHz) δ = 8.90 (d, J = 8.6 Hz, 1H, Ar), 8.26 (dd, J = 7.3, 1.2 Hz, 1H, Ar), 8.02 (d, J = 8.2 Hz, 1H, Ar), 7.88 (d, J = 8.0 Hz, 1H, Ar), 7.59 (ddd, J = 8.6, 6.8, 1.5 Hz, 1H, Ar), 7.55 – 7.46 (m, 4H, Ar), 7.42 – 7.35 (m, 2H, Ar), 7.35 – 7.28 (m, 1H, Ar), 6.04 (t, J = 6.8 Hz, 1H, CH), 2.23 – 1.94 (m, 2H, CH_2), 1.03 (t, J = 7.4 Hz, 3H, Me) ppm; $^{13}\text{C NMR}$ (CDCl_3 , 101 MHz) δ = 166.95, 140.78, 133.97, 133.42, 131.57, 130.18, 128.63, 128.62, 128.00, 127.82, 127.58, 126.73, 126.32, 125.98, 124.63, 78.23, 29.78, 10.26 ppm; **IR** (ATR): ν (cm^{-1}) = 2927, 1711, 1509, 1454, 1237, 1194, 1132, 1072, 1003, 779, 697; **HRMS** (EI): m/z calcd for $\text{C}_{20}\text{H}_{18}\text{O}_2^+$ [M] $^+$: 290.1301; found: 290.1301.

1-Phenylpropyl 2-phenylbenzoate **10ab**.

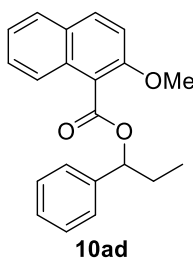
8a (20.0 mg, 147 μmol , 1.0 eq.), **5b** (61.1 mg, 162 μmol , 1.1 eq.), DMAP (897 μg , 7.34 μmol , 0.05 eq.), and Et_3N (40.9 μL , 293 μmol , 2.0 eq.) were dissolved in CH_2Cl_2 (1.0 mL) and reacted according to GP A. **10ab** (45.0 mg, 97%) was obtained as an oil.

$^1\text{H NMR}$ (CDCl_3 , 400 MHz) δ = 7.83 (dd, J = 7.7, 1.4 Hz, 1H, Ar), 7.51 (td, J = 7.5, 1.5 Hz, 1H, Ar), 7.40 (td, J = 7.6, 1.4 Hz, 1H, Ar), 7.35 (dd, J = 7.6, 1.3 Hz, 1H, Ar), 7.34 – 7.22 (m, 8H, Ar), 7.13 – 7.07 (m, 2H, Ar), 5.68 (t, J = 6.8 Hz, 1H, CH), 1.67 (ddq, J = 51.3, 14.0, 7.1 Hz, 2H, CH_2), 0.72 (t, J = 7.4 Hz, 3H, Me) ppm; **$^{13}\text{C NMR}$** (CDCl_3 , 101 MHz) δ = 168.12, 142.54, 141.57, 140.16, 131.46, 131.19, 130.95, 129.99, 128.66, 128.37, 128.16, 127.81, 127.32, 127.25, 126.82, 78.53, 29.11, 9.91 ppm; **IR** (ATR): ν (cm^{-1}) = 2967, 1709, 1597, 1451, 1275, 1123, 1076, 1046, 908, 744, 664; **HRMS** (EI): m/z calcd for $\text{C}_{22}\text{H}_{20}\text{O}_2^+$ [M] $^+$: 316.1458; found: 316.1467.

1-Phenylpropyl 2-methyl-6-nitrobenzoate **10ac**.

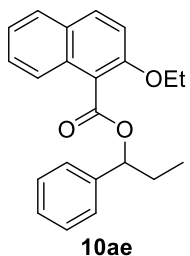
8a (20.0 mg, 147 μmol , 1.0 eq.), **5c** (55.6 mg, 162 μmol , 1.1 eq.), DMAP (897 μg , 7.34 μmol , 0.05 eq.), and Et_3N (40.9 μL , 293 μmol , 2.0 eq.) were dissolved in CH_2Cl_2 (1.0 mL) and reacted according to GP A. **10ac** (40.0 mg, 91%) was obtained as a white solid.

m.p. 35–40 $^\circ\text{C}$; **$^1\text{H NMR}$** (CDCl_3 , 600 MHz) δ = 7.98 (dd, J = 8.0, 1.1 Hz, 1H, Ar), 7.49 (d, J = 7.5 Hz, 1H, Ar), 7.44 (t, J = 7.9 Hz, 1H, Ar), 7.42 – 7.35 (m, 4H), 7.35 – 7.30 (m, 1H, Ar), 5.96 (t, J = 7.0 Hz, 1H, CH), 2.21 (s, 3H, Me), 2.13 (dp, J = 14.6, 7.3 Hz, 1H, CHH), 1.93 (dp, J = 14.6, 7.4 Hz, 1H, CHH), 0.94 (t, J = 7.4 Hz, 3H, Me) ppm; **$^{13}\text{C NMR}$** (CDCl_3 , 151 MHz) δ = 165.94, 146.12, 139.44, 137.78, 136.09, 129.79, 129.69, 128.58, 128.39, 127.28, 121.88, 80.00, 28.74, 19.07, 10.04 ppm; **IR** (ATR): ν (cm^{-1}) = 2923, 1735, 1533, 1453, 1340, 1248, 1113, 1069, 904, 760, 697; **HRMS** (EI): m/z calcd for $\text{C}_8\text{H}_6\text{O}_3\text{N}^+$ [$\text{M}-\text{C}_9\text{H}_{11}\text{O}$] $^+$: 164.0342; found: 164.0348.

1-Phenylpropyl 2-methoxy-1-naphthoate **10ad**.

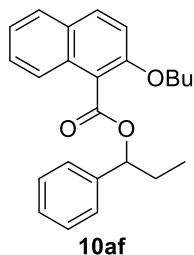
8a (15.0 mg, 110 μmol , 1.0 eq.), **5d** (51.1 mg, 132 μmol , 1.2 eq.), DMAP (673 μg , 5.51 μmol , 0.05 eq.), and Et_3N (30.7 μL , 220 μmol , 2.0 eq.) were dissolved in CH_2Cl_2 (550 μL) and reacted according to GP A. **10ad** (11.0 mg, 34%) was obtained as an oil.

$^1\text{H NMR}$ (CDCl_3 , 400 MHz) δ = 7.89 (d, J = 9.1 Hz, 1H, Ar), 7.78 (d, J = 8.0 Hz, 1H, Ar), 7.58 (d, J = 8.5 Hz, 1H, Ar), 7.51 – 7.44 (m, 2H, Ar), 7.44 – 7.30 (m, 5H, Ar), 7.28 (d, J = 9.1 Hz, 1H, Ar), 6.10 (dd, J = 7.8, 5.9 Hz, 1H, CH), 3.92 (s, 3H, Me), 2.19 – 1.87 (m, 2H, CH_2), 1.04 (t, J = 7.4 Hz, 3H, Me) ppm; **$^{13}\text{C NMR}$** (CDCl_3 , 151 MHz) δ = 167.73, 154.40, 140.72, 131.55, 131.13, 128.68, 128.46, 128.15, 127.96, 127.63, 126.94, 124.20, 123.88, 118.16, 113.36, 78.69, 56.75, 29.75, 10.26 ppm; **IR** (ATR): ν (cm^{-1}) = 2931, 1726, 1596, 1512, 1461, 1230, 1138, 1075, 1019, 919, 811, 749, 700; **HRMS** (EI): m/z calcd for $\text{C}_{21}\text{H}_{20}\text{O}_3^+$ [M] $^+$: 320.1407; found: 320.1403.

1-Phenylpropyl 2-ethoxy-1-naphthoate **10ae**.

8a (15.0 mg, 110 μmol , 1.0 eq.), **5e** (50.2 mg, 121 μmol , 1.1 eq.), DMAP (673 μg , 5.51 μmol , 0.05 eq.), and Et_3N (30.7 μL , 220 μmol , 2.0 eq.) were dissolved in CH_2Cl_2 (550 μL) and reacted according to GP A. **10ae** (17.0 mg, 46%) was obtained as an oil.

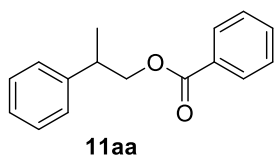
$^1\text{H NMR}$ (CDCl_3 , 400 MHz) δ = 7.86 (d, J = 9.1 Hz, 1H, Ar), 7.78 (d, J = 8.0 Hz, 1H, Ar), 7.58 (d, J = 7.9 Hz, 1H, Ar), 7.51 – 7.45 (m, 2H, Ar), 7.44 – 7.30 (m, 5H, Ar), 7.28 – 7.24 (m, 1H, Ar), 6.11 (dd, J = 8.0, 5.8 Hz, 1H, CH), 4.17 (q, J = 7.0 Hz, 2H, CH_2), 2.20 – 1.88 (m, 2H, CH_2), 1.33 (t, J = 7.0 Hz, 3H, Me), 1.05 (t, J = 7.4 Hz, 3H, Me) ppm; **$^{13}\text{C NMR}$** (CDCl_3 , 101 MHz) δ = 167.88, 153.59, 140.67, 131.33, 131.08, 128.57, 128.44, 128.10, 127.93, 127.53, 126.92, 124.10, 123.80, 118.42, 114.30, 78.61, 65.25, 29.70, 15.00, 10.41 ppm; **IR** (ATR): ν (cm^{-1}) = 2934, 1723, 1595, 1511, 1280, 1228, 1137, 1064, 1024, 807, 746, 698; **HRMS** (EI): m/z calcd for $\text{C}_{22}\text{H}_{22}\text{O}_3^+$ [M] $^+$: 344.1563; found: 344.1563.

1-Phenylpropyl 2-butoxy-1-naphthoate 10af.

8a (15.0 mg, 110 μmol , 1.0 eq.), **5f** (57.0 mg, 121 μmol , 1.1 eq.), DMAP (673 μg , 5.51 μmol , 0.05 eq.), and Et_3N (30.7 μL , 220 μmol , 2.0 eq.) were dissolved in CH_2Cl_2 (550 μL) and reacted according to GP A. **10af** (13.0 mg, 30%) was obtained as an oil.

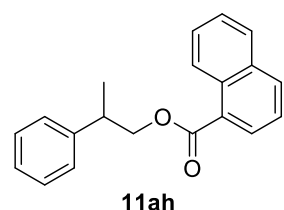
$^1\text{H NMR}$ (CDCl_3 , 400 MHz) δ = 7.86 (dt, J = 9.1, 0.6 Hz, 1H, Ar), 7.77 (ddd, J = 8.5, 1.3, 0.5 Hz, 1H, Ar), 7.60 – 7.53 (m, 1H, Ar), 7.49 – 7.45 (m, 2H, Ar), 7.43 – 7.29 (m, 5H, Ar), 7.26 (d, J = 9.1 Hz, 1H, Ar), 6.11 (dd, J = 7.7, 6.0 Hz, 1H, CH), 4.10 (t, J = 6.5 Hz, 2H, CH_2), 2.18 – 1.90 (m, 2H, CH_2), 1.72 – 1.63 (m, 2H, CH_2), 1.46 – 1.33 (m, 2H, CH_2), 1.04 (t, J = 7.4 Hz, 3H, Me),

0.91 (t, J = 7.4 Hz, 3H, Me) ppm; $^{13}\text{C NMR}$ (CDCl_3 , 101 MHz) δ = 167.82, 153.81, 140.63, 131.30, 131.17, 128.60, 128.46, 128.11, 127.96, 127.51, 127.03, 124.08, 123.83, 118.43, 114.37, 78.64, 69.45, 31.51, 29.69, 19.21, 13.96, 10.34 ppm; IR (ATR): ν (cm^{-1}) = 2933, 1723, 1595, 1511, 1463, 1342, 1280, 1226, 1136, 1070, 1023, 939, 807, 745, 697; HRMS (EI): m/z calcd for $\text{C}_{24}\text{H}_{26}\text{O}_3^+$ [M] $^+$: 362.1876; found: 362.1877.

2-Phenylpropyl benzoate 11aa.

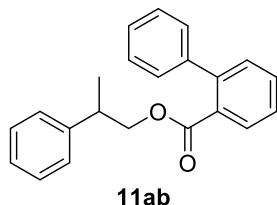
9a (100 mg, 734 μmol , 1.0 eq.), **5a** (250 mg, 1.10 mmol, 1.5 eq.), DMAP (4.49 mg, 36.7 μmol , 0.05 eq.), and Et_3N (205 μL , 1.47 mmol, 2.0 eq.) were dissolved in CH_2Cl_2 (4.0 mL) and reacted according to GP A. **11aa** (170 mg, 96%) was obtained as a clear liquid.

$^1\text{H NMR}$ (CDCl_3 , 400 MHz) δ = 8.02 – 7.95 (m, 2H, Ar), 7.58 – 7.51 (m, 1H, Ar), 7.42 (dd, J = 8.4, 7.1 Hz, 2H, Ar), 7.38 – 7.28 (m, 4H, Ar), 7.26 – 7.21 (m, 1H, Ar), 4.41 (qd, J = 10.8, 7.0 Hz, 2H, CH_2), 3.26 (h, J = 7.0 Hz, 1H, CH), 1.41 (d, J = 7.0 Hz, 3H, Me) ppm; $^{13}\text{C NMR}$ (CDCl_3 , 101 MHz) δ = 166.64, 143.31, 133.03, 130.41, 129.68, 128.67, 128.48, 127.49, 126.87, 70.03, 39.21, 18.19 ppm; HRMS (ESI): m/z calcd for $\text{C}_{16}\text{H}_{17}\text{O}_2^+$ [M+H] $^+$: 241.1223; found: 241.1226. The $^1\text{H}/^{13}\text{C}$ NMR spectrum are in full agreement with literature reports.^[22]

2-Phenylpropyl 1-naphthoate 11ah.

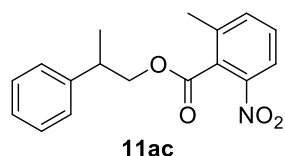
9a (25.0 mg, 184 μmol , 1.0 eq.), **5h** (65.9 mg, 202 μmol , 1.1 eq.), DMAP (1.12 mg, 91.8 μmol , 0.05 eq.), and Et_3N (51.2 μL , 367 μmol , 2.0 eq.) were dissolved in CH_2Cl_2 (1.0 mL) and reacted according to GP A. **11ah** (44.0 mg, 83%) was obtained as an oil.

$^1\text{H NMR}$ (CDCl_3 , 400 MHz) δ = 8.76 – 8.70 (m, 1H, Ar), 8.06 (dd, J = 7.3, 1.3 Hz, 1H, Ar), 8.00 (d, J = 8.2 Hz, 1H, Ar), 7.89 – 7.83 (m, 1H, Ar), 7.57 – 7.49 (m, 2H, Ar), 7.46 (dd, J = 8.2, 7.3 Hz, 1H, Ar), 7.39 – 7.32 (m, 4H, Ar), 7.29 – 7.24 (m, 1H, Ar), 4.59 – 4.46 (m, 2H, CH_2), 3.33 (h, J = 7.1 Hz, 1H, CH), 1.44 (d, J = 7.0 Hz, 3H, Me) ppm; $^{13}\text{C NMR}$ (CDCl_3 , 101 MHz) δ = 167.70, 143.46, 133.94, 133.38, 131.43, 130.25, 128.75, 128.61, 127.80, 127.56, 127.50, 126.92, 126.29, 125.98, 124.63, 70.25, 39.30, 18.42 ppm; IR (ATR): ν (cm^{-1}) = 2965, 1709, 1593, 1510, 1452, 1275, 1240, 1193, 1130, 1011, 760, 698; HRMS (EI): m/z calcd for $\text{C}_{20}\text{H}_{18}\text{O}_2^+$ [M] $^+$: 290.1301; found: 290.1291.

2-Phenylpropyl 2-phenylbenzoate 11ab.

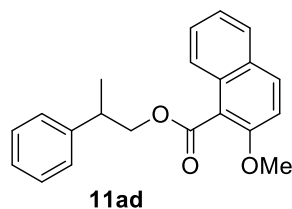
9a (20.0 mg, 147 μmol , 1.0 eq.), **5b** (61.1 mg, 162 μmol , 1.1 eq.), DMAP (897 μg , 7.34 μmol , 0.05 eq.), and Et_3N (40.9 μL , 293 μmol , 2.0 eq.) were dissolved in CH_2Cl_2 (1.0 mL) and reacted according to GP A. **11ab** (44.0 mg, 95%) was obtained as an oil.

$^1\text{H NMR}$ (CDCl_3 , 400 MHz) δ = 7.73 (ddd, J = 7.7, 1.5, 0.6 Hz, 1H, Ar), 7.51 (td, J = 7.5, 1.4 Hz, 1H, Ar), 7.44 – 7.32 (m, 5H, Ar), 7.32 – 7.25 (m, 4H, Ar), 7.23 – 7.17 (m, 1H, Ar), 7.13 – 7.09 (m, 2H, Ar), 4.22 (dd, J = 10.8, 6.4 Hz, 1H, CHH), 4.06 (dd, J = 10.8, 7.8 Hz, 1H, CHH), 2.80 (h, J = 7.0 Hz, 1H, CH), 1.06 (d, J = 7.0 Hz, 3H, Me) ppm; $^{13}\text{C NMR}$ (CDCl_3 , 101 MHz) δ = 168.87, 143.24, 142.57, 141.63, 131.27, 130.84, 129.92, 128.57, 128.55, 128.26, 127.39, 127.39, 127.27, 126.74, 70.22, 38.83, 18.10 ppm (one signal is overlapping); IR (ATR): ν (cm^{-1}) = 2964, 1715, 1598, 1451, 1370, 1277, 1239, 1124, 1085, 1047, 967, 744, 664; HRMS (EI): m/z calcd for $\text{C}_{22}\text{H}_{20}\text{O}_2^+$ [M] $^+$: 316.1458; found: 316.1459.

2-Phenylpropyl 2-methyl-6-nitrobenzoate **11ac**.

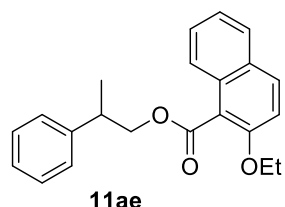
9a (20.0 mg, 147 μmol , 1.0 eq.), **5c** (55.6 mg, 162 μmol , 1.1 eq.), DMAP (897 μg , 7.34 μmol , 0.05 eq.), and Et_3N (40.9 μL , 293 μmol , 2.0 eq.) were dissolved in CH_2Cl_2 (1.0 mL) and reacted according to GP A. **11ac** (40.0 mg, 91%) was obtained as a white solid.

m.p. 35–40 $^\circ\text{C}$; $^1\text{H NMR}$ (CDCl_3 , 600 MHz) δ = 7.96 (d, J = 8.1 Hz, 1H, Ar), 7.48 (d, J = 7.4 Hz, 1H, Ar), 7.43 (t, J = 7.9 Hz, 1H, Ar), 7.31 (t, J = 7.5 Hz, 2H, Ar), 7.28 – 7.25 (m, 2H, Ar), 7.23 (t, J = 7.2 Hz, 1H, Ar), 4.57 (dd, J = 10.8, 7.2 Hz, 1H, CHH), 4.42 (dd, J = 10.8, 7.3 Hz, 1H, CHH), 3.23 (h, J = 7.1 Hz, 1H, CH), 2.23 (s, 3H, Me), 1.35 (d, J = 7.0 Hz, 3H, Me) ppm; $^{13}\text{C NMR}$ (CDCl_3 , 151 MHz) δ = 166.55, 146.28, 143.01, 137.69, 136.04, 129.75, 129.68, 128.69, 127.42, 126.91, 121.86, 71.13, 38.90, 19.04, 18.52 ppm; **IR** (ATR): ν (cm^{-1}) = 2923, 1720, 1533, 1448, 1356, 1270, 1115, 1063, 965, 802, 764, 699; **HRMS** (EI): m/z calcd for $\text{C}_8\text{H}_6\text{O}_3\text{N}^+$ [$\text{M}-\text{C}_9\text{H}_{11}\text{O}$] $^+$: 164.0342; found: 164.0345.

2-Phenylpropyl 2-methoxy-1-naphthoate **11ad**.

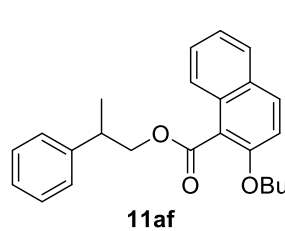
9a (15.0 mg, 110 μmol , 1.0 eq.), **5d** (51.1 mg, 132 μmol , 1.2 eq.), DMAP (673 μg , 5.51 μmol , 0.05 eq.), and Et_3N (30.7 μL , 220 μmol , 2.0 eq.) were dissolved in CH_2Cl_2 (550 μL) and reacted according to GP A. **11ad** (26.0 mg, 74%) was obtained as an oil.

$^1\text{H NMR}$ (CDCl_3 , 400 MHz) δ = 7.88 (d, J = 9.1 Hz, 1H, Ar), 7.79 – 7.75 (m, 1H, Ar), 7.50 (dd, J = 8.5, 1.0 Hz, 1H, Ar), 7.41 – 7.31 (m, 6H, Ar), 7.30 – 7.24 (m, 2H, Ar), 4.68 (dd, J = 10.8, 7.1 Hz, 1H, CHH), 4.51 (dd, J = 10.8, 7.3 Hz, 1H, CHH), 3.91 (s, 3H, Me), 3.31 (h, J = 7.1 Hz, 1H, CH), 1.42 (d, J = 7.0 Hz, 3H, Me) ppm; $^{13}\text{C NMR}$ (CDCl_3 , 101 MHz) δ = 168.12, 154.54, 143.38, 131.68, 131.07, 128.68, 128.60, 128.09, 127.65, 127.60, 126.81, 124.16, 123.96, 117.77, 113.22, 70.39, 56.78, 39.24, 18.54 ppm; **IR** (ATR): ν (cm^{-1}) = 2965, 1721, 1595, 1511, 1453, 1254, 1133, 1073, 1019, 958, 809, 746, 698; **HRMS** (EI): m/z calcd for $\text{C}_{21}\text{H}_{20}\text{O}_3^+$ [M] $^+$: 320.1407; found: 320.1408.

2-Phenylpropyl 2-ethoxy-1-naphthoate **11ae**.

9a (15.0 mg, 110 μmol , 1.0 eq.), **5e** (50.2 mg, 121 μmol , 1.1 eq.), DMAP (673 μg , 5.51 μmol , 0.05 eq.), and Et_3N (30.7 μL , 220 μmol , 2.0 eq.) were dissolved in CH_2Cl_2 (550 μL) and reacted according to GP A. **11ae** (24.0 mg, 65%) was obtained as a white solid.

m.p. 35–40 $^\circ\text{C}$; $^1\text{H NMR}$ (CDCl_3 , 400 MHz) δ = 7.86 (d, J = 9.1 Hz, 1H, Ar), 7.78 – 7.75 (m, 1H, Ar), 7.53 – 7.47 (m, 1H, Ar), 7.41 – 7.30 (m, 6H, Ar), 7.26 (s, 2H, Ar), 4.67 (dd, J = 10.8, 6.7 Hz, 1H, CHH), 4.49 (dd, J = 10.8, 7.6 Hz, 1H, CHH), 4.19 (q, J = 7.0 Hz, 2H, CH_2), 3.30 (h, J = 7.0 Hz, 1H, CH), 1.46 – 1.34 (m, 6H, Me and Me) ppm; $^{13}\text{C NMR}$ (CDCl_3 , 101 MHz) δ = 168.27, 153.79, 143.30, 131.49, 131.03, 128.68, 128.57, 128.06, 127.56, 126.83, 124.14, 123.91, 118.29, 114.43, 70.37, 65.38, 39.25, 18.58, 15.10 ppm (one signal is overlapping); **IR** (ATR): ν (cm^{-1}) = 2977, 1721, 1595, 1511, 1281, 1225, 1133, 1064, 806, 746, 698; **HRMS** (EI): m/z calcd for $\text{C}_{22}\text{H}_{22}\text{O}_3^+$ [M] $^+$: 334.1563; found: 334.1566.

2-Phenylpropyl 2-butoxy-1-naphthoate **11af**.

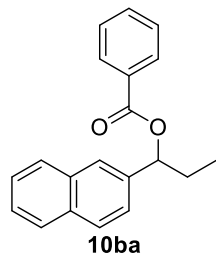
9a (15.0 mg, 110 μmol , 1.0 eq.), **5f** (57.0 mg, 121 μmol , 1.1 eq.), DMAP (673 μg , 5.51 μmol , 0.05 eq.), and Et_3N (30.7 μL , 220 μmol , 2.0 eq.) were dissolved in CH_2Cl_2 (550 μL) and reacted according to GP A. **11af** (15.0 mg, 37%) was obtained as an oil.

$^1\text{H NMR}$ (CDCl_3 , 400 MHz) δ = 7.84 (d, J = 9.0 Hz, 1H, Ar), 7.78 – 7.73 (m, 1H, Ar), 7.47 (d, J = 8.4 Hz, 1H, Ar), 7.37 (ddd, J = 8.4, 6.7, 1.4 Hz, 1H, Ar), 7.34 – 7.29 (m, 5H, Ar), 7.27 – 7.22 (m, 2H, Ar), 4.65 (dd, J = 10.8, 6.7 Hz, 1H, CHH), 4.46 (dd, J = 10.8, 7.7 Hz, 1H, CHH), 4.11 (td, J = 6.5, 1.1 Hz, 2H, CH_2), 3.28 (h, J = 7.0 Hz, 1H, CH), 1.79 – 1.71 (m, 2H, CH_2), 1.53 – 1.44 (m, 2H, CH_2), 1.40 (d, J = 7.0 Hz, 3H, Me), 0.96 (t, J = 7.4 Hz, 3H, Me) ppm; $^{13}\text{C NMR}$ (CDCl_3 , 151 MHz) δ = 168.24, 154.01, 143.32, 131.44, 131.09, 128.70, 128.58, 128.07, 127.58, 127.55, 126.85, 124.11, 123.93, 118.30, 114.47,

70.36, 69.53, 39.30, 31.55, 19.26, 18.58, 13.99 ppm; IR (ATR): ν (cm⁻¹) = 2958, 1723, 1595, 1511, 1463, 1341, 1282, 1212, 1134, 1027, 808, 746, 699; HRMS (EI): m/z calcd for C₂₄H₂₆O₃⁺ [M]⁺: 362.1876; found: 362.1877.

4.1.8.2.5 Synthesis of 2-Naphthylpropanol Esters

1-(Naphthalen-2-yl)propyl benzoate **10ba**.

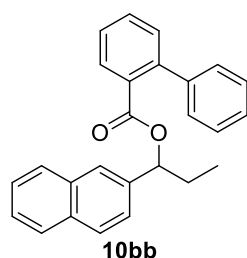


8b (40.0 mg, 215 μ mol, 1.0 eq.), **5a** (58.3 mg, 258 μ mol, 1.1 eq.), DMAP (1.31 mg, 10.7 μ mol, 0.05 eq.), and Et₃N (59.9 μ L, 430 μ mol, 2.0 eq.) were dissolved in CH₂Cl₂ (1.0 μ L) and reacted according to GP A. **10ba** (62.0 mg, 99%) was obtained as an oil.

¹H NMR (CDCl₃, 400 MHz) δ = 8.14 – 8.10 (m, 2H, Ar), 7.89 – 7.80 (m, 4H, Ar), 7.59 – 7.52 (m, 2H, Ar), 7.50 – 7.43 (m, 4H, Ar), 6.09 (t, J = 6.8 Hz, 1H, CH), 2.25 – 1.97 (m, 2H, CH₂), 1.01 (t, J = 7.4 Hz, 3H, Me) ppm; ¹³C NMR (CDCl₃, 101 MHz) δ = 166.07, 138.08, 133.29, 133.21, 133.06, 130.68, 129.80, 128.51, 128.46, 128.19, 127.80, 126.30, 126.14, 125.84,

124.43, 78.23, 29.60, 10.19 ppm; IR (ATR): ν (cm⁻¹) = 2968, 1713, 1601, 1451, 1266, 1107, 1025, 816, 746, 686; HRMS (EI): m/z calcd for C₂₀H₁₈O₂⁺ [M]⁺: 290.1301; found: 290.1304.

1-(Naphthalen-2-yl)propyl 2-phenylbenzoate **10bb**.

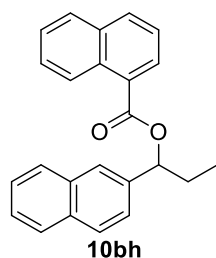


8b (20.0 mg, 107 μ mol, 1.0 eq.), **5b** (44.7 mg, 118 μ mol, 1.1 eq.), DMAP (656 μ g, 5.37 μ mol, 0.05 eq.), and Et₃N (29.9 μ L, 215 μ mol, 2.0 eq.) were dissolved in CH₂Cl₂ (540 μ L) and reacted according to GP A. **10bb** (37.0 mg, 94%) was obtained as an oil.

¹H NMR (CDCl₃, 600 MHz) δ = 7.85 (dd, J = 7.8, 1.3 Hz, 1H, Ar), 7.83 – 7.76 (m, 2H, Ar), 7.74 (d, J = 8.5 Hz, 1H, Ar), 7.59 (s, 1H, Ar), 7.52 (td, J = 7.5, 1.4 Hz, 1H, Ar), 7.49 – 7.44 (m, 2H, Ar), 7.41 (td, J = 7.6, 1.2 Hz, 1H, Ar), 7.36 (dd, J = 7.6, 1.2 Hz, 1H, Ar), 7.31 – 7.23 (m, 5H, Ar), 7.20 (dd, J = 8.5, 1.7 Hz, 1H, Ar), 5.85 (t, J = 6.9 Hz, 1H, CH), 1.89 –

1.78 (m, 1H, CHH), 1.74 – 1.65 (m, 1H, CHH), 0.76 (t, J = 7.4 Hz, 3H, Me) ppm; ¹³C NMR (CDCl₃, 151 MHz) δ = 168.20, 142.55, 141.54, 137.43, 133.19, 133.15, 131.43, 131.23, 130.96, 130.03, 128.64, 128.21, 128.18, 128.15, 127.73, 127.30, 127.27, 126.15, 126.12, 126.07, 124.66, 78.73, 28.96, 9.98 ppm; IR (ATR): ν (cm⁻¹) = 2934, 1708, 1597, 1436, 1275, 121, 1046, 817, 743, 697; HRMS (EI): m/z calcd for C₂₆H₂₂O₂⁺ [M]⁺: 366.1614; found: 366.1616.

1-(Naphthalen-2-yl)propyl 2-phenylbenzoate **10bh**.

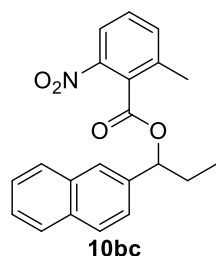


8b (20.0 mg, 107 μ mol, 1.0 eq.), **5h** (38.6 mg, 118 μ mol, 1.1 eq.), DMAP (656 μ g, 5.37 μ mol, 0.05 eq.), and Et₃N (29.9 μ L, 215 μ mol, 2.0 eq.) were dissolved in CH₂Cl₂ (540 μ L) and reacted according to GP A. **10bh** (30.0 mg, 88%) was obtained as an oil.

¹H NMR (CDCl₃, 400 MHz) δ = 8.91 (d, J = 8.6 Hz, 1H, Ar), 8.33 – 8.27 (m, 1H, Ar), 8.03 (d, J = 8.2 Hz, 1H, Ar), 7.94 (s, 1H, Ar), 7.91 – 7.83 (m, 4H, Ar), 7.65 – 7.45 (m, 6H, Ar), 6.21 (t, J = 6.9 Hz, 1H, CH), 2.19 (ddq, J = 45.5, 13.9, 7.1 Hz, 2H, CH₂), 1.06 (t, J = 7.4 Hz, 3H, Me) ppm; ¹³C NMR (CDCl₃, 101 MHz) δ = 166.99, 138.07, 133.95, 133.45, 133.31, 133.21,

131.54, 130.20, 128.63, 128.52, 128.20, 127.84, 127.81, 127.57, 126.32, 126.16, 125.98, 125.96, 124.64, 124.50, 78.40, 29.66, 10.32 ppm (one signal is overlapping); IR (ATR): ν (cm⁻¹) = 2967, 1708, 1593, 1508, 1461, 1274, 1237, 1193, 1131, 1073, 1002, 814, 745; HRMS (EI): m/z calcd for C₂₄H₂₀O₂⁺ [M]⁺: 340.1458; found: 340.1459.

1-(Naphthalen-2-yl)propyl 2-methyl-6-nitrobenzoate **10bc**.



8b (20.0 mg, 107 μ mol, 1.0 eq.), **5c** (40.7 mg, 118 μ mol, 1.1 eq.), DMAP (656 μ g, 5.37 μ mol, 0.05 eq.), and Et₃N (29.9 μ L, 215 μ mol, 2.0 eq.) were dissolved in CH₂Cl₂ (540 μ L) and reacted according to GP A. **10bc** (30.0 mg, 86%) was obtained as white solid.

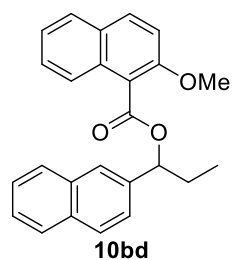
m.p. 80–82 °C; ¹H NMR (CDCl₃, 400 MHz) δ = 8.02 – 7.98 (m, 1H, Ar), 7.89 – 7.81 (m, 4H, Ar), 7.53 – 7.42 (m, 5H, Ar), 6.13 (t, J = 7.0 Hz, 1H, CH), 2.29 – 2.11 (m, 4H, CHH and Me), 2.01 (dt, J = 13.7, 7.4 Hz, 1H, CHH), 0.97 (t, J = 7.4 Hz, 3H, Me) ppm; ¹³C NMR (CDCl₃, 101 MHz) δ = 166.00, 137.80, 136.81, 136.13, 133.38, 133.26, 129.79, 129.73, 128.51, 128.27,

127.85, 126.72, 126.38, 126.33, 124.67, 121.91, 115.13, 80.13, 28.80, 19.13, 10.09 ppm; IR (ATR): ν (cm⁻¹) =

Size-Induced Inversion of Selectivity in the Acylation of 1,2-Diols

2922, 1736, 1523, 1454, 1344, 1243, 1112, 1073, 815, 751, 700; **HRMS** (EI): m/z calcd for $C_{21}H_{19}O_4N^+$ $[M]^+$: 349.1309; found: 349.1302.

1-(Naphthalen-2-yl)propyl 2-methoxy-1-naphthoate **10bd**.

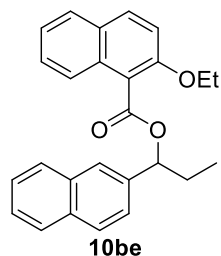


8b (20.0 mg, 107 μ mol, 1.0 eq.), **5d** (45.6 mg, 118 μ mol, 1.1 eq.), DMAP (656 μ g, 5.37 μ mol, 0.05 eq.), and Et_3N (29.9 μ L, 215 μ mol, 2.0 eq.) were dissolved in CH_2Cl_2 (540 μ L) and reacted according to GP A. **10be** (30.0 mg, 75%) was obtained as white solid.

m.p. 65-57 $^{\circ}C$; 1H NMR ($CDCl_3$, 400 MHz) δ = 7.95 (s, 1H, Ar), 7.92 – 7.82 (m, 4H, Ar), 7.78 (dd, J = 7.4, 1.9 Hz, 1H, Ar), 7.59 (td, J = 8.6, 8.2, 1.4 Hz, 2H, Ar), 7.53 – 7.46 (m, 2H, Ar), 7.40 – 7.31 (m, 2H, Ar), 7.29 (d, J = 9.1 Hz, 1H, Ar), 6.26 (dd, J = 7.8, 6.0 Hz, 1H, CH), 3.92 (s, 3H, Me), 2.26 – 1.99 (m, 2H, CH_2), 1.07 (t, J = 7.4 Hz, 3H, Me) ppm; ^{13}C NMR

($CDCl_3$, 101 MHz) δ = 167.77, 154.43, 138.14, 133.36, 133.23, 131.58, 131.15, 128.69, 128.25, 128.22, 128.16, 127.83, 127.68, 126.27, 126.11, 126.02, 124.80, 124.22, 123.89, 118.14, 113.33, 78.79, 56.77, 29.78, 10.30 ppm; **IR** (ATR): ν (cm^{-1}) = 2966, 1721, 1595, 1510, 1433, 1343, 1280, 1254, 1225, 1136, 1072, 1017, 919, 809, 720; **HRMS** (EI): m/z calcd for $C_{25}H_{22}O_3^+$ $[M]^+$: 370.1563; found: 370.1567.

1-(Naphthalen-2-yl)propyl 2-ethoxy-1-naphthoate **10be**.

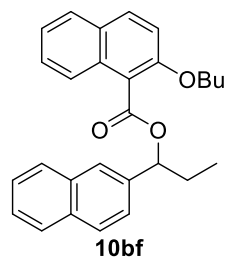


8b (15.0 mg, 80.5 μ mol, 1.0 eq.), **5e** (36.7 mg, 88.6 μ mol, 1.1 eq.), DMAP (492 μ g, 4.03 μ mol, 0.05 eq.), and Et_3N (22.5 μ L, 161 μ mol, 2.0 eq.) were dissolved in CH_2Cl_2 (402 μ L) and reacted according to GP A. **10be** (30.0 mg, 97%) was obtained as a white solid.

m.p. 94-96 $^{\circ}C$; 1H NMR ($CDCl_3$, 400 MHz) δ = 7.96 (s, 1H, Ar), 7.87 (dt, J = 9.3, 2.3 Hz, 4H, Ar), 7.78 (d, J = 7.4 Hz, 1H, Ar), 7.60 (dd, J = 8.4, 1.3 Hz, 2H, Ar), 7.54 – 7.46 (m, 2H, Ar), 7.40 – 7.30 (m, 2H, Ar), 7.27 (d, J = 9.1 Hz, 1H, Ar), 6.30 (dd, J = 7.7, 6.0 Hz, 1H, CH), 4.18 (q, J = 7.0 Hz, 2H, CH_2), 2.26 – 2.00 (m, 2H, CH_2), 1.29 (t, J = 7.0 Hz, 3H, Me), 1.09 (t, J =

7.4 Hz, 3H, Me) ppm; ^{13}C NMR ($CDCl_3$, 101 MHz) δ = 167.87, 153.70, 138.12, 133.36, 133.25, 131.37, 131.18, 128.68, 128.29, 128.20, 128.12, 127.81, 127.57, 126.24, 126.09, 126.07, 124.84, 124.17, 123.89, 118.64, 114.48, 78.72, 65.37, 29.71, 14.99, 10.40 ppm; **IR** (ATR): ν (cm^{-1}) = 2924, 1733, 1595, 1434, 1278, 1213, 1110, 1059, 808, 750; **HRMS** (EI): m/z calcd for $C_{26}H_{24}O_3^+$ $[M]^+$: 384.1720; found: 384.1723.

1-(Naphthalen-2-yl)propyl 2-butoxy-1-naphthoate **10bf**.

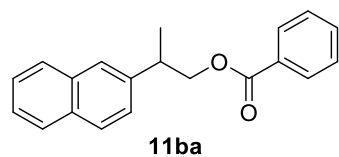


8b (15.0 mg, 80.5 μ mol, 1.0 eq.), **5f** (41.7 mg, 88.6 μ mol, 1.1 eq.), DMAP (492 μ g, 4.03 μ mol, 0.05 eq.), and Et_3N (22.5 μ L, 161 μ mol, 2.0 eq.) were dissolved in CH_2Cl_2 (402 μ L) and reacted according to GP A. **10bf** (10.0 mg, 30%) was obtained as an oil.

1H NMR ($CDCl_3$, 400 MHz) δ = 7.95 (d, J = 1.3 Hz, 1H, Ar), 7.90 – 7.83 (m, 4H, Ar), 7.80 – 7.75 (m, 1H, Ar), 7.58 (ddd, J = 8.7, 2.0, 1.2 Hz, 2H, Ar), 7.53 – 7.46 (m, 2H, Ar), 7.39 – 7.30 (m, 2H, Ar), 7.26 (d, J = 9.1 Hz, 1H, Ar), 6.28 (dd, J = 7.6, 6.2 Hz, 1H, CH), 4.08 (td, J = 6.6, 1.7 Hz, 2H, CH_2), 2.27 – 1.98 (m, 2H, CH_2), 1.62 – 1.55 (m, 2H, CH_2), 1.36 – 1.23 (m,

2H, CH_2), 1.07 (t, J = 7.4 Hz, 3H, Me), 0.78 (t, J = 7.4 Hz, 3H, Me) ppm; ^{13}C NMR ($CDCl_3$, 101 MHz) δ = 167.86, 153.84, 138.02, 133.35, 133.27, 131.33, 131.17, 128.60, 128.30, 128.23, 128.12, 127.81, 127.55, 126.24, 126.22, 126.11, 124.89, 124.10, 123.85, 118.44, 114.39, 78.76, 69.46, 31.47, 29.66, 19.13, 13.81, 10.39 ppm; **IR** (ATR): ν (cm^{-1}) = 2923, 1722, 1595, 1511, 1463, 1226, 1136, 1071, 1022, 909, 808, 744; **HRMS** (EI): m/z calcd for $C_{28}H_{28}O_3^+$ $[M]^+$: 412.2033; found: 412.2033.

2-(Naphthalen-2-yl)propyl benzoate **11ba**.

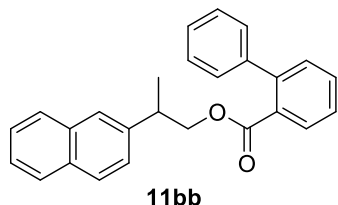


9b (40.0 mg, 215 μ mol, 1.0 eq.), **5a** (58.3 mg, 258 μ mol, 1.1 eq.), DMAP (1.31 mg, 10.7 μ mol, 0.05 eq.), and Et_3N (59.9 μ L, 430 μ mol, 2.0 eq.) were dissolved in CH_2Cl_2 (1.0 μ L) and reacted according to GP A. **11ba** (61.0 mg, 98%) was obtained as an oil.

1H NMR ($CDCl_3$, 400 MHz) δ = 8.01 – 7.97 (m, 2H, Ar), 7.86 – 7.79 (m, 3H, Ar), 7.75 (s, 1H, Ar), 7.57 – 7.51 (m, 1H, Ar), 7.50 – 7.44 (m, 3H, Ar), 7.44 – 7.38 (m, 2H, Ar), 4.52 (qd, J = 10.8, 7.0 Hz, 2H, CH_2), 3.44 (h, J = 7.0 Hz, 1H, CH), 1.50 (d, J = 7.0 Hz, 3H, Me) ppm; ^{13}C NMR ($CDCl_3$, 101 MHz) δ = 166.66, 140.81, 133.70, 133.03, 132.62, 130.40, 129.69, 128.48, 128.29, 127.80, 127.75, 126.18, 126.02, 125.88, 125.66, 69.92, 39.36, 18.32

ppm; **IR** (ATR): ν (cm⁻¹) = 2967, 1714, 1601, 1451, 1267, 1108, 1025, 971, 816, 745, 686; **HRMS** (EI): m/z calcd for C₂₀H₁₈O₂ [M]⁺: 290.1301, found 290.1294.

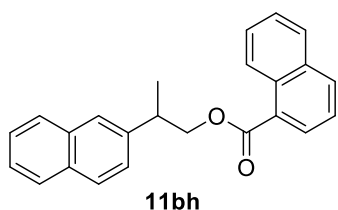
2-(Naphthalen-2-yl)propyl 2-phenylbenzoate 11bb.



9b (20.0 mg, 107 μ mol, 1.0 eq.), **5b** (44.7 mg, 118 μ mol, 1.1 eq.), DMAP (656 μ g, 5.37 μ mol, 0.05 eq.), and Et₃N (29.9 μ L, 215 μ mol, 2.0 eq.) were dissolved in CH₂Cl₂ (540 μ L) and reacted according to GP A. **11bb** (36.0 mg, 91%) was obtained as an oil.

¹H NMR (CDCl₃, 600 MHz) δ = 7.82 – 7.79 (m, 1H, Ar), 7.78 – 7.73 (m, 3H, Ar), 7.55 – 7.53 (m, 1H, Ar), 7.50 (td, J = 7.6, 1.4 Hz, 1H, Ar), 7.48 – 7.41 (m, 2H, Ar), 7.40 – 7.31 (m, 5H, Ar), 7.30 – 7.27 (m, 2H, Ar), 7.27 – 7.24 (m, 1H, Ar), 4.32 (dd, J = 10.9, 6.6 Hz, 1H, CHH), 4.17 (dd, J = 10.9, 7.6 Hz, 1H, CHH), 2.97 (h, J = 7.0 Hz, 1H, CH), 1.16 (d, J = 7.0 Hz, 3H, Me) ppm; **¹³C NMR** (CDCl₃, 151 MHz) δ = 168.90, 142.56, 141.59, 140.70, 133.61, 132.55, 131.30, 131.18, 130.85, 129.95, 128.52, 128.23, 128.17, 127.77, 127.71, 127.37, 127.27, 126.11, 125.93, 125.78, 125.61, 70.13, 38.93, 18.15 ppm; ; **IR** (ATR): ν (cm⁻¹) = 2963, 1714, 1450, 1276, 1125, 951, 967, 817, 743, 698; **HRMS** (EI): m/z calcd for C₂₆H₂₂O₂⁺ [M]⁺: 366.1614; found: 366.1605.

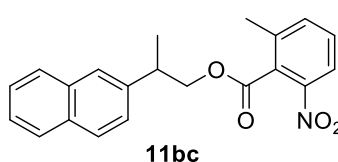
2-(Naphthalen-2-yl)propyl 2-phenylbenzoate 11bh.



9b (20.0 mg, 107 μ mol, 1.0 eq.), **5h** (38.6 mg, 118 μ mol, 1.1 eq.), DMAP (656 μ g, 5.37 μ mol, 0.05 eq.), and Et₃N (29.9 μ L, 215 μ mol, 2.0 eq.) were dissolved in CH₂Cl₂ (540 μ L) and reacted according to GP A. **11bh** (35.0 mg, 96%) was obtained as an oil.

¹H NMR (CDCl₃, 400 MHz) δ = 8.65 (d, J = 8.7 Hz, 1H, Ar), 8.05 (dd, J = 7.3, 1.3 Hz, 1H, Ar), 7.98 (d, J = 8.2 Hz, 1H, Ar), 7.88 – 7.80 (m, 4H, Ar), 7.79 – 7.77 (m, 1H, Ar), 7.52 – 7.44 (m, 4H, Ar), 7.44 – 7.35 (m, 2H, Ar), 4.70 – 4.52 (m, 2H, CH₂), 3.50 (h, J = 7.0 Hz, 1H, CH), 1.53 (d, J = 7.0 Hz, 3H, Me) ppm; **¹³C NMR** (CDCl₃, 101 MHz) δ = 167.78, 140.91, 133.89, 133.74, 133.38, 132.67, 131.35, 130.25, 128.57, 128.41, 127.83, 127.78, 127.74, 127.47, 126.27, 126.21, 126.09, 125.95, 125.92, 125.71, 124.61, 70.18, 39.40, 18.46 ppm; **IR** (ATR): ν (cm⁻¹) = 2964, 1708, 1593, 1509, 1461, 1275, 1239, 1193, 1120, 1012, 951, 815, 745; **HRMS** (EI): m/z calcd for C₂₄H₂₀O₂⁺ [M]⁺: 340.1458; found: 340.1466.

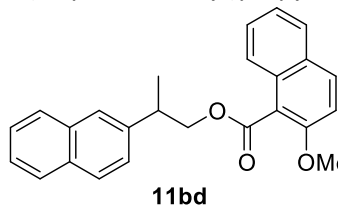
2-(Naphthalen-2-yl)propyl 2-methyl-6-nitrobenzoate 11bc.



9b (20.0 mg, 107 μ mol, 1.0 eq.), **5c** (40.7 mg, 118 μ mol, 1.1 eq.), DMAP (656 μ g, 5.37 μ mol, 0.05 eq.), and Et₃N (29.9 μ L, 215 μ mol, 2.0 eq.) were dissolved in CH₂Cl₂ (540 μ L) and reacted according to GP A. **11bc** (30.0 mg, 86%) was obtained as an oil.

¹H NMR (CDCl₃, 400 MHz) δ = 7.95 (dd, J = 7.9, 1.4 Hz, 1H, Ar), 7.84 – 7.77 (m, 3H, Ar), 7.70 (s, 1H, Ar), 7.49 – 7.38 (m, 5H, Ar), 4.67 (dd, J = 10.9, 7.3 Hz, 1H, CHH), 4.53 (dd, J = 10.8, 7.2 Hz, 1H, CHH), 3.41 (h, J = 7.1 Hz, 1H, CH), 2.19 (s, 3H, Me), 1.44 (d, J = 7.0 Hz, 3H, Me) ppm; **¹³C NMR** (CDCl₃, 101 MHz) δ = 166.60, 140.45, 137.67, 136.05, 133.66, 132.61, 129.76, 129.63, 128.37, 127.80, 127.72, 126.19, 125.97, 125.78, 125.69, 121.88, 70.96, 39.00, 19.03, 18.62 ppm (one signal is overlapping); **IR** (ATR): ν (cm⁻¹) = 2923, 1732, 1529, 1460, 1343, 1266, 1111, 1071, 951, 802, 742; **HRMS** (EI): m/z calcd for C₂₁H₁₉O₄N⁺ [M]⁺: 349.1309; found: 349.1314.

2-(Naphthalen-2-yl)propyl 2-methoxy-1-naphthoate 11bd.



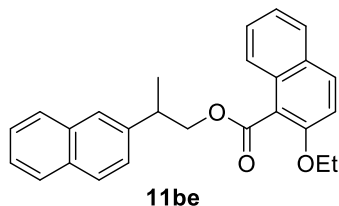
9b (20.0 mg, 107 μ mol, 1.0 eq.), **5d** (45.6 mg, 118 μ mol, 1.1 eq.), DMAP (656 μ g, 5.37 μ mol, 0.05 eq.), and Et₃N (29.9 μ L, 215 μ mol, 2.0 eq.) were dissolved in CH₂Cl₂ (540 μ L) and reacted according to GP A. **11bd** (30.0 mg, 75%) was obtained as a white solid.

m.p. 87-89 °C; **¹H NMR** (CDCl₃, 400 MHz) δ = 7.88 – 7.81 (m, 3H, Ar), 7.81 – 7.76 (m, 1H, Ar), 7.76 – 7.70 (m, 2H, Ar), 7.50 – 7.44 (m, 3H, Ar), 7.34 (d, J = 8.5 Hz, 1H, Ar), 7.29 – 7.21 (m, 2H, Ar), 7.07 (ddd, J = 8.3, 6.9, 1.3 Hz, 1H, Ar), 4.79 (dd, J = 10.9, 7.4 Hz, 1H, CHH), 4.58 (dd, J = 10.9, 7.0 Hz, 1H, CHH), 3.83 (s, 3H, Me), 3.47 (h, J = 7.0 Hz, 1H, CH), 1.49 (d, J = 7.0 Hz, 3H,

Size-Induced Inversion of Selectivity in the Acylation of 1,2-Diols

Me) ppm; ^{13}C NMR (CDCl_3 , 101 MHz) δ = 168.13, 154.51, 140.84, 133.74, 132.67, 131.68, 131.01, 128.56, 128.34, 128.02, 127.88, 127.74, 127.54, 126.19, 126.13, 126.02, 125.66, 124.14, 123.88, 117.71, 113.15, 70.26, 56.74, 39.41, 18.54 ppm; IR (ATR): ν (cm^{-1}) = 2945, 1735, 1596, 1511, 1280, 1210, 1131, 1074, 1033, 816, 730; HRMS (EI): m/z calcd for $\text{C}_{25}\text{H}_{22}\text{O}_3^+$ [M] $^+$: 370.1563; found: 370.1556.

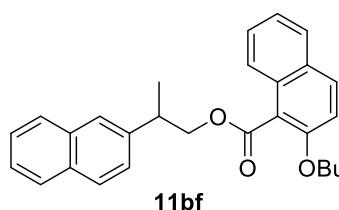
2-(Naphthalen-2-yl)propyl 2-ethoxy-1-naphthoate **11be**.



9b (15.0 mg, 80.5 μmol , 1.0 eq.), **5e** (36.7 mg, 88.6 μmol , 1.1 eq.), DMAP (492 μg , 4.03 μmol , 0.05 eq.), and Et_3N (22.5 μL , 161 μmol , 2.0 eq.) were dissolved in CH_2Cl_2 (402 μL) and reacted according to GP A. **11be** (30.0 mg, 97%) was obtained as a white solid.

m.p. 110-112 $^\circ\text{C}$; ^1H NMR (CDCl_3 , 400 MHz) δ = 7.91 – 7.82 (m, 4H, Ar), 7.80 (s, 1H, Ar), 7.78 (d, J = 8.2 Hz, 1H, Ar), 7.56 – 7.49 (m, 3H, Ar), 7.41 (d, J = 8.5 Hz, 1H, Ar), 7.35 – 7.29 (m, 1H, Ar), 7.27 (d, J = 9.1 Hz, 1H, Ar), 7.14 (ddd, J = 8.4, 6.8, 1.3 Hz, 1H, Ar), 4.84 (dd, J = 10.8, 7.1 Hz, 1H, CHH), 4.63 (dd, J = 10.9, 7.3 Hz, 1H, CHH), 4.20 (qd, J = 7.0, 1.6 Hz, 2H, CH_2), 3.53 (h, J = 7.1 Hz, 1H, CH), 1.56 (d, J = 7.0 Hz, 3H, Me), 1.39 (t, J = 7.0 Hz, 3H, Me) ppm; ^{13}C NMR (CDCl_3 , 101 MHz) δ = 168.34, 153.84, 140.84, 133.76, 132.70, 131.56, 131.06, 128.60, 128.42, 128.07, 127.92, 127.80, 127.53, 126.21, 126.19, 126.08, 125.73, 124.19, 123.91, 118.34, 114.48, 70.30, 65.45, 39.49, 18.67, 15.12 ppm; IR (ATR): ν (cm^{-1}) = 2981, 1725, 1595, 1506, 1460, 1249, 1110, 1066, 807, 748; HRMS (EI): m/z calcd for $\text{C}_{26}\text{H}_{24}\text{O}_3^+$ [M] $^+$: 384.1720; found: 384.1720.

2-(Naphthalen-2-yl)propyl 2-butoxy-1-naphthoate **11bf**.



9b (15.0 mg, 80.5 μmol , 1.0 eq.), **5f** (41.7 mg, 88.6 μmol , 1.1 eq.), DMAP (492 μg , 4.03 μmol , 0.05 eq.), and Et_3N (22.5 μL , 161 μmol , 2.0 eq.) were dissolved in CH_2Cl_2 (402 μL) and reacted according to GP A. **11bf** (16.0 mg, 49%) was obtained as an oil.

^1H NMR (CDCl_3 , 400 MHz) δ = 7.86 – 7.82 (m, 3H, Ar), 7.81 – 7.77 (m, 1H, Ar), 7.76 – 7.71 (m, 2H, Ar), 7.50 – 7.45 (m, 3H, Ar), 7.35 (dq, J = 8.5, 0.9 Hz, 1H, Ar), 7.29 – 7.21 (m, 2H, Ar), 7.10 (ddd, J = 8.4, 6.8, 1.3 Hz, 1H, Ar), 4.79 (dd, J = 10.8, 7.0 Hz, 1H, CHH), 4.57 (dd, J = 10.8, 7.4 Hz, 1H, CHH), 4.09 (td, J = 6.5, 1.6 Hz, 2H, CH_2), 3.47 (h, J = 7.0 Hz, 1H, CH), 1.77 – 1.68 (m, 2H, CH_2), 1.51 (d, J = 7.0 Hz, 3H, Me), 1.49 – 1.40 (m, 2H, CH_2), 0.95 (t, J = 7.4 Hz, 3H, Me) ppm; ^{13}C NMR (CDCl_3 , 101 MHz) δ = 168.11, 153.86, 140.67, 133.61, 132.55, 131.31, 130.91, 128.42, 128.23, 127.87, 127.75, 127.61, 127.32, 126.01, 126.00, 125.89, 125.54, 123.96, 123.72, 118.14, 114.32, 70.09, 69.41, 39.33, 31.39, 19.10, 18.47, 13.85 ppm; IR (ATR): ν (cm^{-1}) = 2957, 1722, 1595, 1510, 1462, 1341, 1224, 1133, 1027, 808, 744; HRMS (EI): m/z calcd for $\text{C}_{28}\text{H}_{28}\text{O}_3^+$ [M] $^+$: 412.2033; found: 412.2032.

4.2 Computational Data

General Information. All geometry optimizations and vibrational frequency calculations have been performed using the B3LYP-D3 hybrid functional^[6e,6g,23] in combination with the 6-31+G(d) basis set.^[24] Solvent effects for chloroform have been taken into account with the SMD continuum solvation model.^[6d] This combination has recently been found to perform well for the description of charge-separated intermediates.^[8,25] Thermochemical corrections to 298.15 K have been calculated for all minima from unscaled vibrational frequencies obtained at this same level. Solvation energies have been obtained as the difference between the energies computed at B3LYP-D3/6-31+G(d) in solution and in gas phase. The thermochemical corrections of optimized structures have been combined with single point energies calculated at the DLPNO-CCSD(T)/def2-TZVPP//B3LYP-D3/6-31+G(d) level.^[6b,6c,6f,26] Solvation energies have been added to the energy computed at DLPNO-CCSD(T)/def2-TZVPP//SMD(CHCl_3)/B3LYP-D3/6-31+G(d) level to yield free energies G_{298} at 298.15 K. Free energies in solution have been corrected to a reference state of 1 mol l^{-1} at 298.15 K through addition of $\text{RTln}(24.46) = +7.925$ kJ mol^{-1} to the free energies. All calculations have been performed with Gaussian 09^[27] and ORCA version 4.0.^[28] Conformational search was performed with Maestro.^[29]

In Table 4.34 the Gibbs free energy of the formation from the monoesters **2bc** and **3bc** and from the diester **4bc** is listed at SMD/B3LYP-D3/6-31+G(d) level of theory and for the corresponding singlepoints at SMD/DLPNO-CCSD(T)/def2-TZVPP level of theory (in each case from the best conformer). The formations of the monoesters **2bc/3bc** are an exothermic process with similar Gibbs free energies of $\Delta G_{298,\text{sol}} = -61.46 \text{ kJ mol}^{-1}$ or $-58.91 \text{ kJ mol}^{-1}$. The formation of the diester **4bc** is an even more exothermic process with $\Delta G_{298,\text{sol}} = -122.23 \text{ kJ mol}^{-1}$. The experimental based rate constants are in contrast to these theoretical based data. Even by the use of catalyst TCAP (10 mol%) the complete formation of the diester **4bc** has a reaction time of at least 3 days. Because of these contrasts, we believe that the reaction is kinetically controlled.

Table 4.34. Free energy for the formation of **2bc**, **3bc** and **4bc** at different level of energy.

Reaction	ΔG_{298} SMD/B3LYP-D3/6-31+G(d)	$\Delta G_{298,\text{sol}}$ SMD/DLPNO-CCSD(T)/def2-TZVPP
1b + 5c → 2bc + 17c	-63.23	-61.46
1b + 5c → 3bc + 17c	-63.83	-58.91
1b + 5c → 4bc + 17c	-123.94	-122.23
2bc + 5c → 4bc + 17c	-60.71	-60.77
3bc + 5c → 4bc + 17c	-60.11	-63.32

By the help of the Marcus equation^[30] the Gibbs free energy of activation ΔG^\ddagger described in Eq. 4.61 via ΔG_0^\ddagger as intrinsic barrier and ΔG^0 as Gibbs free energy of the reaction we are able to understand possible transition states (TS). Thereby ΔG^0 reflects the thermodynamic contribution and ΔG_0^\ddagger the kinetic contribution of the Gibbs free energy of activation ΔG^\ddagger . The term $\frac{(\Delta G^0)^2}{16\Delta G_0^\ddagger}$ is normally so small that it could be neglected.^[31]

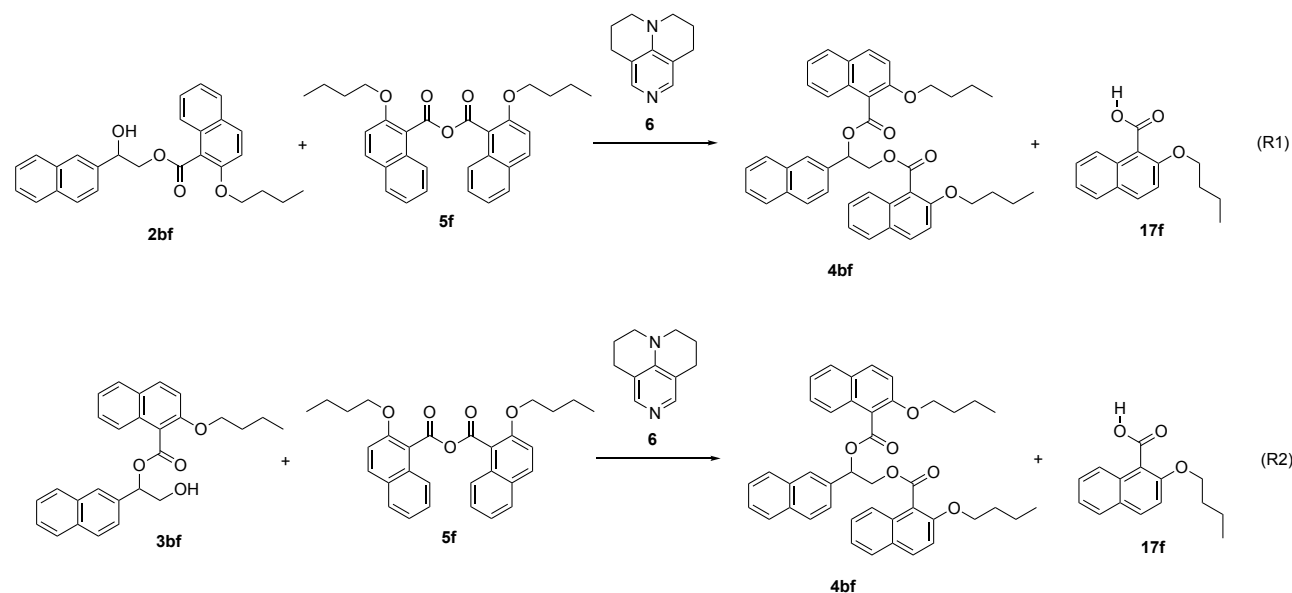
$$\Delta G^\ddagger = \Delta G_0^\ddagger + 0.5\Delta G^0 + \frac{(\Delta G^0)^2}{16\Delta G_0^\ddagger} \quad \text{Eq. 4.61}$$

In addition, Guthrie *et al.*^[30a] defined that the intrinsic barrier ΔG_0^\ddagger can be transferable between similar reactions. In previous work of our group^[1] we calculated the TS for the acylation of secondary and primary alcohol (**A** and **B**). The reaction should be similar to the acylation of the here used polyol **1b**, so that ΔG_0^\ddagger should be nearly the same. However, the acylation of **1b** takes longer, even both acylation steps – formation of mono-esters **2bc/3bc** and diester **4bc** – have the same $\Delta G^0 \approx -60 \text{ kJ mol}^{-1}$. We are assuming that the intrinsic barrier for the second acylation to **4bc** strongly increases, which supported the assumption of a kinetic controlled reaction.^[1]

Furthermore, the reaction of monoesters **2bf** and **3bf** with anhydride **5f** mediated by catalyst **6** was studied at the SMD(CHCl₃)/B3LYP-D3/6-31+G(d) level of theory. This level of theory has recently been used to study the closely related acylation of 1-(2-naphthyl)ethanol with 2-methyl-1-naphthoic anhydride mediated by TCAP (**6**).^[1] The enormous conformational space of the system shown in Scheme 4.17 poses a serious practical limit to possible theoretical studies. We have therefore imposed the following restrictions on the system:

- 1) The conformation of the butyloxy side chains present in all reactants and products is chosen such that it corresponds to the all-*trans* conformation found in anhydride **5f** (where it corresponds to the global minimum).
- 2) The transition state studies for the acylation of **2bf** are based on the best transition state found in our earlier study for 1-(2-naphthyl)ethanol (that is, the alcohol obtained after removing the ester side chain from **2bf**). The transition state studies for the acylation of **3bf** are based on the best transition state found in our earlier study for 2-(2-naphthyl)ethanol (that is, the alcohol obtained after removing the ester side chain from **3bf**).

Size-Induced Inversion of Selectivity in the Acylation of 1,2-Diols



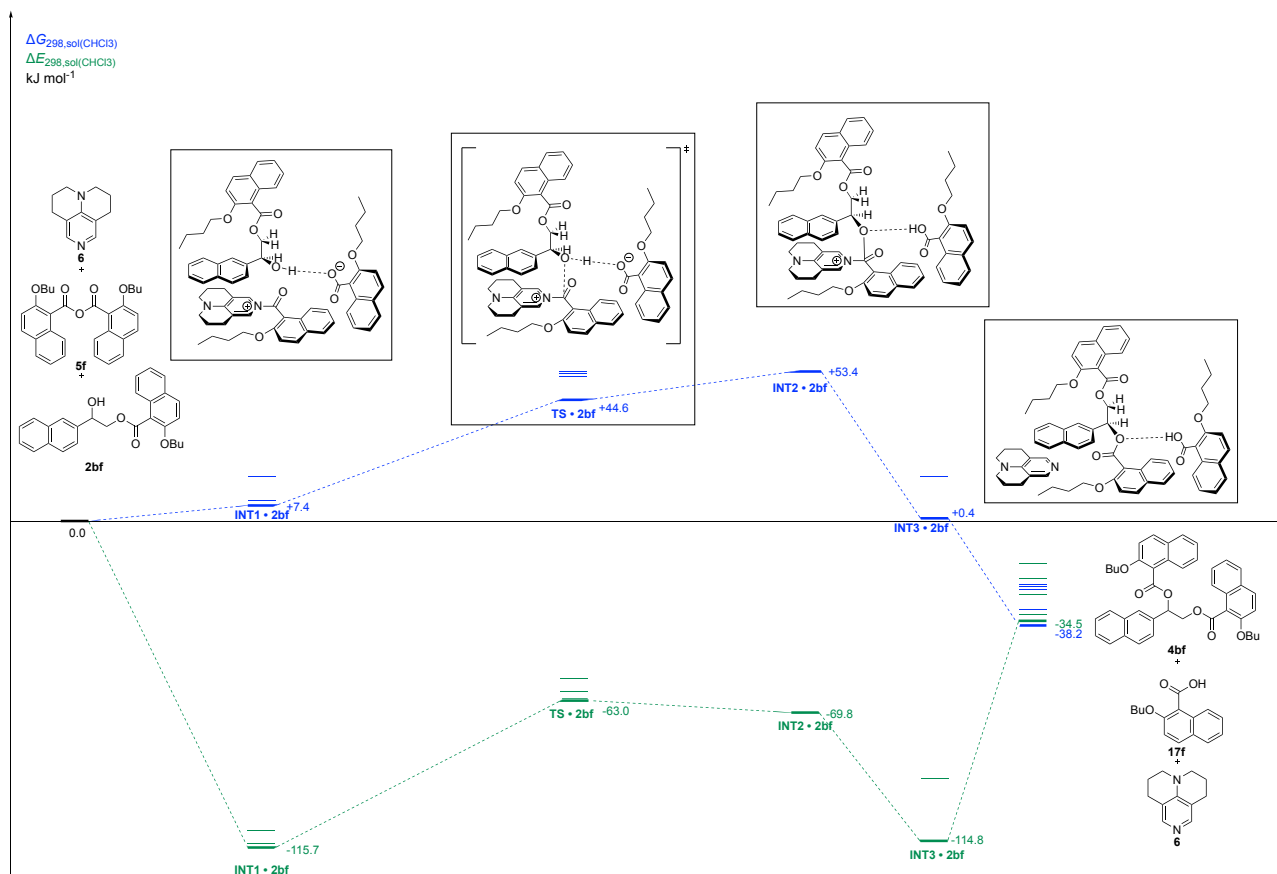
Scheme 4.17. Reaction of monoesters **2bf** and **3bf** with anhydride **5f** mediated by catalyst **6**.

In Table 4.35 the Gibbs free energy of the formation from the monoesters **2bf** and **3bf** and from the diester **4bf** is listed at SMD/B3LYP-D3/6-31+G(d) level of theory and for the corresponding singlepoints at SMD/DLPNO-CCSD(T)/def2-TZVPP level of theory (in each case from the best conformer). Again the formations of the monoesters **2bf/3bf** are an exothermic process with similar Gibbs free energies of $\Delta G_{298,\text{sol}} = -44.56 \text{ kJ mol}^{-1}$ or $-40.01 \text{ kJ mol}^{-1}$. The formation of the diester **4bf** is an even more exothermic process with $\Delta G_{298,\text{sol}} = -76.89 \text{ kJ mol}^{-1}$.

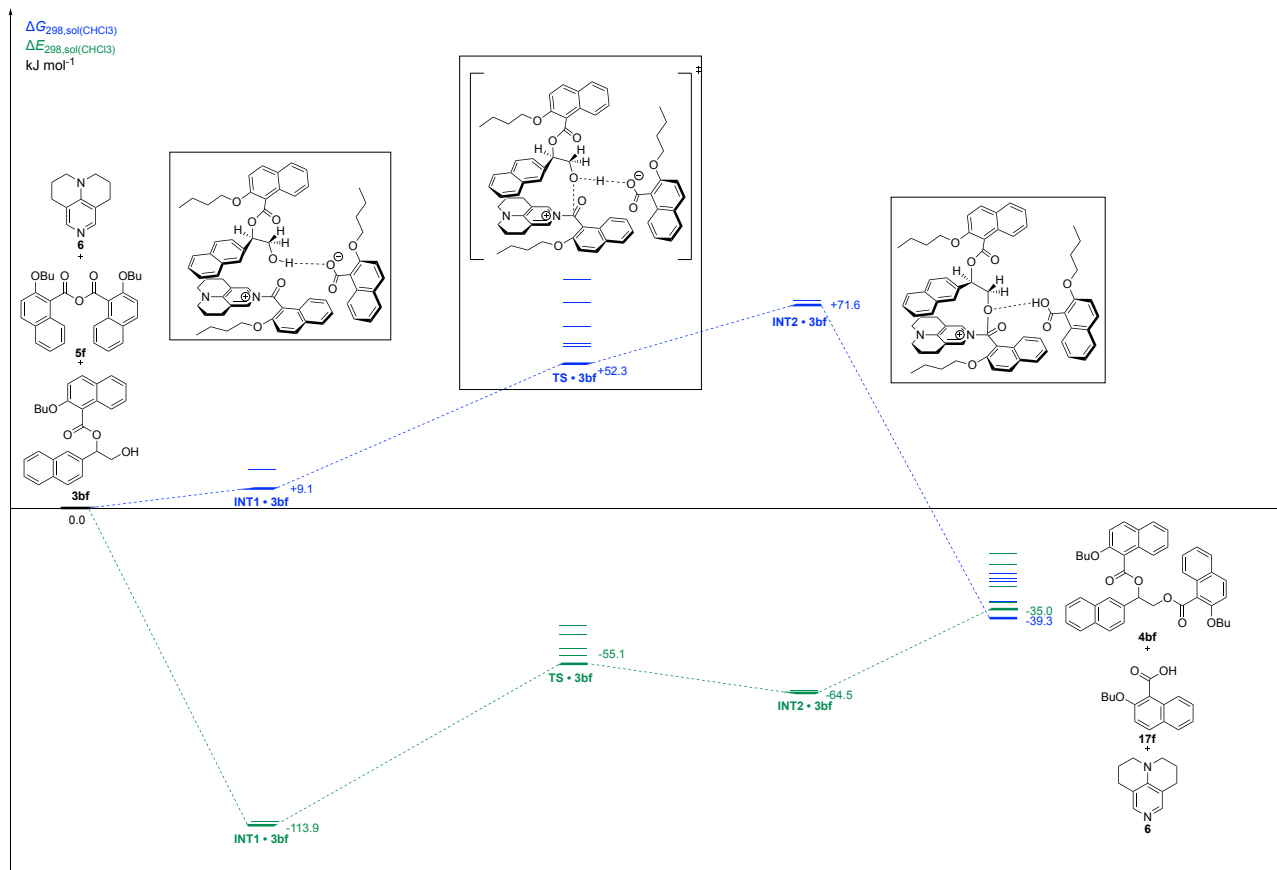
Table 4.35. Free energy for the formation of **2bf**, **3bf** and **4bf** at different level of theory.

Reaction	ΔG_{298}	$\Delta G_{298,\text{sol}}$
	SMD/B3LYP-D3/6-31+G(d)	SMD/DLPNO-CCSD(T)/def2-TZVPP
1b + 5f \rightarrow 2bf + 17f	-47.45	-44.56
1b + 5f \rightarrow 3bf + 17f	-46.36	-40.01
1b + 5f \rightarrow 4bf + 17f	-85.60	-76.89
2bf + 5f \rightarrow 4bf + 17f	-38.15	-32.32
3bf + 5f \rightarrow 4bf + 17f	-39.25	-36.88

The experimental based rate constants are again in contrast to these theoretical based data. Even by the use of catalyst TCAP (10 mol%) the complete formation of the diester **4bf** has a reaction time of at least 14 days. As already mention the rate-determining transition states of the first acylation of **1b** to **2bf/3bf** should be similar to the in the previous study shown “triple” sandwich TS of the primary and secondary ethanol systems (**A** and **B**). The strong decrease in effective reaction rates or the second acylation of **2bf/3bf** to **4bf** with the bulky anhydride **5f** point to strong differential steric hinderances in the acylation. These repulsive size effects are appeared to be more substantial for transformations of primary as compared to secondary hydroxyl groups. To explore this statement in more detail, the second acylation of the monoesters **2bf/3bf** to **4bf** were explored by quantum chemical analysis at the SMD(CHCl₃)/B3LYP-D3/6-31+G(d) level of theory (Scheme 4.18 and 4.19).



Scheme 4.18. Computed stationary points in the Lewis base-catalyzed second acylation step of secondary alcohol **2bf** at the SMD(CHCl₃)/B3LYP-D3/6-31+G(d) level of theory (blue stationary points are based on Gibbs free energy; green stationary points are based on total energy).



Scheme 4.19. Computed stationary points in the Lewis base-catalyzed second acylation step of primary alcohol **3bf** at the SMD(CHCl₃)/B3LYP-D3/6-31+G(d) level of theory (blue stationary points are based on Gibbs free energy; green stationary points are based on total energy).

Size-Induced Inversion of Selectivity in the Acylation of 1,2-Diols

Comparing the transition states **TS-2bf** with **TS-3bf** of the corresponding best conformer with each other it is visible that the **TS-2bf** is characterized by a triple “sandwich” conformation between the catalyst-derived pyridinium ring system (red), the aromatic groups of the alcohol moiety (green) and the *ortho*-substituent of the anhydride (blue) (Figure 4.75). In contrast the **TS-3bf** has an open TS where the the catalyst-derived pyridinium ring system (red) and the *ortho*-substituent of the anhydride (blue) are overlapping, whereby the aromatic motif of the alcohol (green) is overlapping with the aromatic motif of the acid. In both cases the carboxylate counter ion acts as a clamp setting up a hydrogen bond through the hydrogen atom of the hydroxyl group and a C-H...O interaction with one *ortho*-hydrogen atom of the pyridinium ring system. In **TS-2bf** the overlapping between the Np side chain of **2bf** and the catalyst TCAP is better face-to-face stacked than in **TS-3bf** which is visible by the distances between N1-C3 (322 vs. 425 pm) and N2-C4 (448 vs. 915 pm). To analyze these non-covalent interactions (NCI) further NCI plots were done with **TS-2bf** and **TS-3bf** shown in Figure 4.75 (always with the corresponding best conformer). Non-covalent bonds are “regions with low density and low reduced gradient”^[32] from which a computational algorithm was developed for the visualization of these non-covalent interactions.^[33] For **TS-2bf** areas of non-covalent interactions between the butoxy side chain of the anhydride/pyridinium ring, Np-alcohol/pyridinium ring and butoxy-chain monoester/Np-alcohol are presented. In the case of **TS-3bf** areas of non-covalent interactions between the butoxy side chain of the anhydride/pyridinium ring and Np-alcohol/Np-acid. In both transition states NCI with the butoxy side-chain of the counterion are visible.

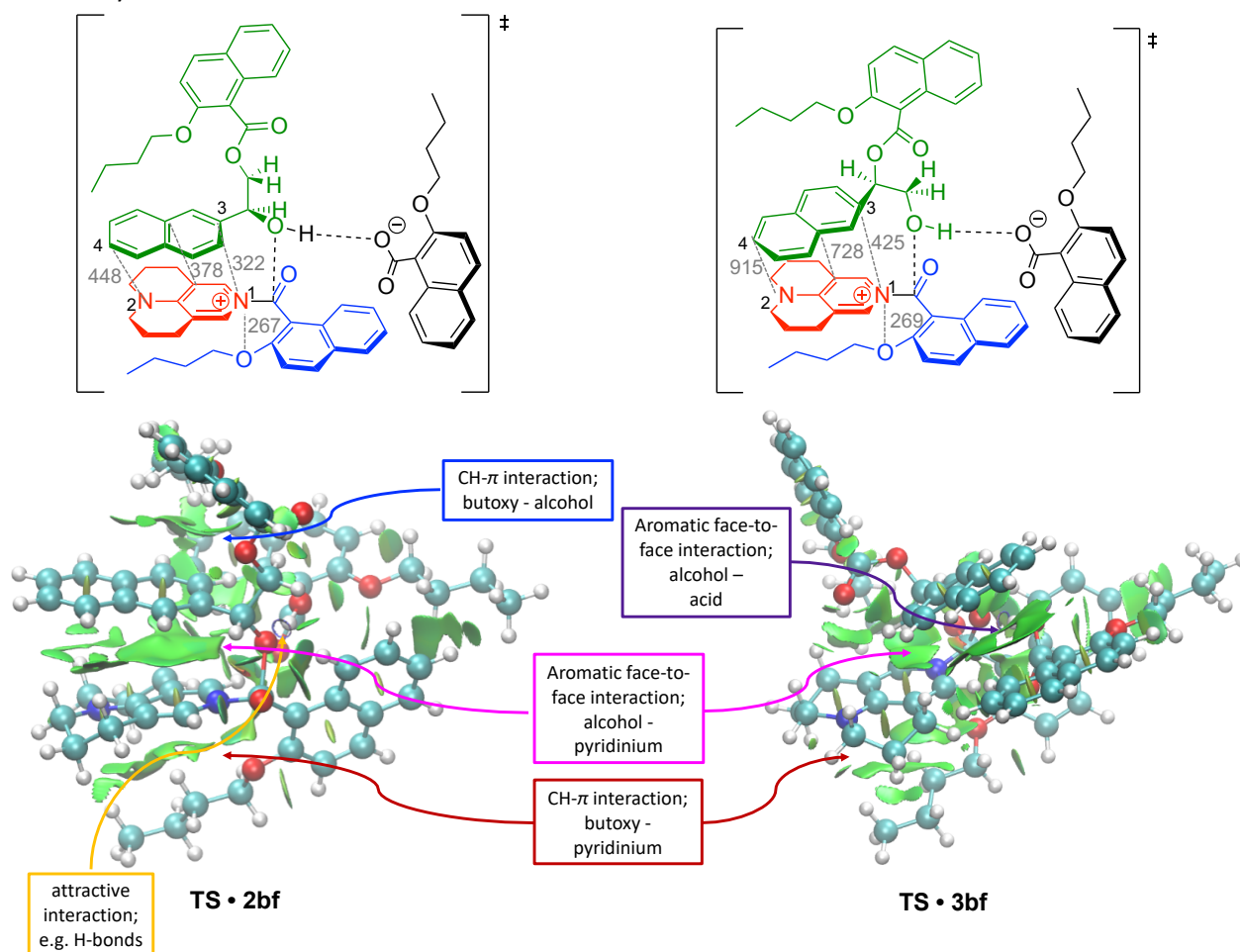


Figure 4.75. Transition state structures and their corresponding NCI plots generated from wavefunction at B3LYP-D3/6-31+G(d) level of theory with NCIplot^[33] and visualized with VMD.^[34]

Table 4.36. Total energies, free energies and enthalpy energies for the systems of polyol **1b**, anhydride **5c**, esters **2bc**, **3bc** and **4bc** and corresponding acid **17c** (in Hartree). Molar free energies in solution at 298.15 K ($G_{298,\text{sol}}$) have been calculated at the SMD(CHCl₃)/DLPNO-CCSD(T)/def2-TZVPP// SMD(CHCl₃)/B3LYP-D3/6-31+G(d) level and corrected for a solution standard state of 1 M through addition of +7.925 kJ mol⁻¹ (0.00301848 Hartree). The SMD(CHCl₃)/B3LYP-D3/6-31+G(d) level of theory has been used to optimize the geometries and calculate solute thermal corrections and solvation energies. Note that the filenames are used in our calculations and do not follow any guide.

Filename	freqs	E_{tot} SMD/B3LYP-D3/ 6-31+G(d)	H_{298} SMD/B3LYP-D3/ 6-31+G(d)	G_{298} SMD/B3LYP-D3/ 6-31+G(d)	E_{tot} B3LYP-D3/ 6-31+G(d)	E_{tot} SMD/DLPNO-CCSD(T)/ def2-TZVPP	$H_{298,\text{sol}}$ SMD/DLPNO-CCSD(T)/ def2-TZVPP	$G_{298,\text{sol}}$ SMD/DLPNO-CCSD(T)/ def2-TZVPP
1b								
1b_3	0	-615.0138161	-614.7876751	-614.8389761	-614.9929054	-613.8994872	-613.6912384	-613.7425394
1b_4	0	-615.0138667	-614.7877457	-614.8390047	-614.9930088	-613.8994865	-613.6912050	-613.7424640
1b_8	0	-615.0119535	-614.7866179	-614.8377175	-614.9908060	-613.8983124	-613.6909381	-613.7422054
2bc								
2bc_125	0	-1203.2769428	-1202.9192278	-1202.9991388	-1203.2454553	-1201.1664661	-1200.8372201	-1200.9171311
2bc_123	0	-1203.2767796	-1202.9191476	-1202.9975086	-1203.2448521	-1201.1674841	-1200.8387611	-1200.9171221
2bc_118	0	-1203.2782255	-1202.9202955	-1202.9976925	-1203.2469062	-1201.1692177	-1200.8395886	-1200.9169856
3bc								
3bc_10	0	-1203.2793036	-1202.921413	-1202.9993676	-1203.2489033	-1201.1687130	-1200.8382039	-1200.9161589
3bc_25	0	-1203.2772922	-1202.91949	-1202.9976922	-1203.2457312	-1201.1671914	-1200.8379319	-1200.9161339
3bc_54	0	-1203.2769190	-1202.919032	-1202.9965780	-1203.2447320	-1201.1667495	-1200.8380310	-1200.9155770
4bc								
4bc_146	0	-1791.5451618	-1791.055552	-1791.1582918	-1791.5036077	-1788.4397940	-1787.9887196	-1788.0914596
4bc_132	0	-1791.5450839	-1791.055527	-1791.1583109	-1791.5034689	-1788.4395394	-1787.9885789	-1788.0913629
4bc_178	0	-1791.5459670	-1791.056319	-1791.1582660	-1791.5048201	-1788.4408242	-1787.9893047	-1788.0912517
5c								
ph_me_no2_1_9	0	-1252.9298177	-1252.6416657	-1252.7186957	-1252.9010773	-1250.8436912	-1250.5812612	-1250.6582912
ph_me_no2_1_1	0	-1252.9319557	-1252.6436087	-1252.7190957	-1252.9043871	-1250.8463401	-1250.5825433	-1250.6580303
ph_me_no2_2_1_22 (crystal)	0	-1252.9317865	-1252.6433925	-1252.7188005	-1252.9040172	-1250.8459559	-1250.5823128	-1250.6577208
17c								
8o_2	0	-664.6896779	-664.5323379	-664.5832259	-664.6721323	-663.5990344	-663.4562215	-663.5071095

Table 4.37. Total energies, free energy and enthalpy energies for the systems of anhydride **5f**, esters **2bf**, **3bf** and **4bf** and corresponding acid **17f**, as well as transition states TS shown in Scheme 4.18 and 4.19 (in Hartree). Molar free energies in solution at 298.15 K ($H_{298, sol}$) have been calculated at the SMD(CHCl₃)/DLPNO-CCSD(T)/def2-TZVPP//SMD(CHCl₃)/B3LYP-D3/6-31+G(d) level and corrected for a solution standard state of 1 M through addition of +7.925 kJ mol⁻¹ (0.00301848 Hartree). The SMD(CHCl₃)/B3LYP-D3/6-31+G(d) level of theory has been used to optimize the geometries and calculate solute thermal corrections and solvation energies. The transition states and intermediates are computed on SMD(CHCl₃)/B3LYP-D3/6-31+G(d) level of theory caused in high costs of calculations. Note that the filenames are used in our calculations and do not follow any guide.

System	Freqs	E_{tot} (SMD)(CHCl ₃)/ B3LYP-D3/ 6-31+G(d)	H_{298} (SMD)(CHCl ₃)/ B3LYP-D3/ 6-31+G(d)	G_{298} (SMD)(CHCl ₃)/ B3LYP-D3/ 6-31+G(d)	E_{tot} (B3LYP-D3/ 6-31+G(d))	E_{tot} (DLPNO-CCSD(T)/ def2-TZVPP)	H_{298} (DLPNO-CCSD(T)/ def2-TZVPP)	G_{298} (DLPNO-CCSD(T)/ def2-TZVPP)
2bf (R)								
diolp_010	0	-1345.5961044	-1345.0950719	-1345.1840209	-1345.5599869	-1343.1295031	-1342.6645881	-1342.7535371
diolp_011	0	-1345.5958840	-1345.0948465	-1345.1822095	-1345.5593479	-1343.1289902	-1342.6644888	-1342.7518518
diolp_022	0	-1345.5956548	-1345.0944853	-1345.1821193	-1345.5596343	-1343.1291630	-1342.6640141	-1342.7516481
3bf (R)								
diolp_023	0	-1345.5957199	-1345.0942924	-1345.1836024	-1345.5594322	-1343.1276313	-1342.6624915	-1342.7518015
diolp_015	0	-1345.5958980	-1345.0944885	-1345.1822185	-1345.5593498	-1343.1279137	-1342.6630524	-1342.7507824
diolp_016	0	-1345.5909201	-1345.0901286	-1345.1800806	-1345.5511287	-1343.1217468	-1342.6607467	-1342.7506987
5f								
naphthyl_nbu_1	0	-1537.5729375	-1537.0012680	-1537.0991820	-1537.5349771	-1534.7734597	-1534.2397506	-1534.3376646
naphthyl_nbu_42	0	-1537.5681967	-1536.9966282	-1537.0983012	-1537.5289415	-1534.7634967	-1534.2311834	-1534.3328564
naphthyl_nbu_50	0	-1537.5696979	-1536.9980794	-1537.0971214	-1537.5328233	-1534.7722305	-1534.2374866	-1534.3365286
6								
TCAP_1	0	-537.1790988	-536.9291043	-536.9755593	-537.1599188	-536.1519420	-535.9211276	-535.9675826
TCAP_2	0	-537.1786144	-536.9286499	-536.9750889	-537.1591846	-536.1505485	-535.9200138	-535.9664528
INT1-2bf								
diols_029f	0	-3420.3902155	-3419.0674971	-3419.2559521	/	/	/	/
diols_002f	0	-3420.3922128	-3419.0691033	-3419.2557173	/	/	/	/
diols_001f	0	-3420.3919661	-3419.0678916	-3419.2521296	/	/	/	/
TS-2bf								
diols_031	1(-110.5)	-3420.3719373	-3419.0525225	-3419.2417655	/	/	/	/
diols_001	1(-206.5)	-3420.3713213	-3419.0507585	-3419.2386885	/	/	/	/
diols_002	3(-113.2; -8.9; -4.1)	-3420.3721360	-3419.0549025	-3419.2383565	/	/	/	/
diols_029	2(-107.4; -5.9)	-3420.3692687	-3419.0504605	-3419.2375685	/	/	/	/
INT2-2bf								
diols_002r	0	-3420.3747069	-3419.0527495	-3419.2384295	/	/	/	/
INT3-2bf								
diols_001r	0	-3420.3918748	-3419.0691593	-3419.2586043	/	/	/	/

diols_029r	0	-3420.3831453	-3419.0608725	-3419.2522375	/	/	/	/
INT1-3bf								
diolp_028f	0	-3420.3913278	-3419.0713568	-3419.2579118	/	/	/	/
diolp_025f	0	-3420.3906113	-3419.07501252	-3419.25300252	/	/	/	/
diolp_027f	0							
TS-3bf								
diolp_026	2(-115.3; -16.3)	-3420.3684593	-3419.0503215	-3419.2384415	/	/	/	/
diolp_028	1(-129.4)	-3420.3689274	-3419.0494145	-3419.2359845	/	/	/	/
diolp_025	2(-136.9; -15.8)	-3420.3672765	-3419.0491585	-3419.2358035	/	/	/	/
diolp_027	2(-125.1; -7.8)	-3420.3657844	-3419.0471765	-3419.2333755	/	/	/	/
diolp_002	3(-152.0; -15.5; -4.7	-3420.3657857	-3419.0480392	-3419.2304802	/	/	/	/
diolp_001	2(-103.6; -11.9)	-3420.3641533	-3419.0446665	-3419.2273245	/	/	/	/
INT2-3bf								
diolp_028r	0	-3420.3725023	-3419.0483445	-3419.2310775	/	/	/	/
diolp_027r	0	-3420.3724556	-3419.0482935	-3419.2310055	/	/	/	/
4bf (R)	0							
diolp_017	0	-2076.1771039	-2075.4040464	-2075.5285114	-2076.1272412	-2072.3586023	-2071.6354076	-2071.7598726
diolp_018	0	-2076.1763437	-2075.4028592	-2075.5260602	-2076.1259044	-2072.3578071	-2071.6347619	-2071.7579629
diolp_020	0	-2076.1716557	-2075.3982572	-2075.5231762	-2076.1221187	-2072.3528777	-2071.6290162	-2071.7539352
17f								
diolp_003	0	-807.0050723	-806.7046318	-806.7692218	-806.9815372	-805.5559557	-805.2790503	-805.3436403
diolp_004	0	-807.0045536	-806.7039281	-806.7674191	-806.9803719	-805.5551815	-805.2787377	-805.3422287

4.3 References

- [1] S. Mayr, M. Marin-Luna, H. Zipse, *J. Org. Chem.* **2021**, *86*, 3456-3489.
- [2] S. Hoops, S. Sahle, R. Gauges, C. Lee, J. Pahle, N. Simus, M. Singhal, L. Xu, P. Mendes, U. Kummer, *Bioinformatics* **2006**, *22*, 3067-3074.
- [3] a) J. E. Taylor, J. M. J. Williams, S. D. Bull, *Tetrahedron Lett.* **2012**, *53*, 4074-4076; b) B. Ren, M. Zhang, S. Xu, L. Gan, L. Zhang, L. Tang, *Eur. J. Org. Chem.* **2019**, *2019*, 4757-4762; c) Y. Toda, T. Sakamoto, Y. Komiyama, A. Kikuchi, H. Suga, *ACS Catal.* **2017**, *7*, 6150-6154.
- [4] B. Giese, *Acc. Chem. Res.* **1984**, *17*, 438-442.
- [5] E. Kattnig, M. Albert, *Org. Lett.* **2004**, *6*, 945-948.
- [6] a) S. Y. Park, J.-W. Lee, C. E. Song, *Nat. Commun.* **2015**, *6*, 7512; b) C. Riplinger, F. Neese, *J. Chem. Phys.* **2013**, *138*, 034106; c) C. Riplinger, B. Sandhoefer, A. Hansen, F. Neese, *J. Chem. Phys.* **2013**, *139*, 134101; d) A. V. Marenich, C. J. Cramer, D. G. Truhlar, *J. Phys. Chem. B* **2009**, *113*, 6378-6396; e) S. Grimme, *J. Chem. Phys.* **2006**, *124*, 034108; f) F. Weigend, R. Ahlrichs, *Phys. Chem. Chem. Phys.* **2005**, *7*, 3297-3305; g) A. D. Becke, *J. Chem. Phys.* **1993**, *98*, 5648-5652.
- [7] B. Giese, *Angew. Chem. Int. Ed.* **1977**, *16*, 125-136.
- [8] M. Marin-Luna, B. Pölloth, F. Zott, H. Zipse, *Chem. Sci.* **2018**, *9*, 6509-6515.
- [9] C. Reichardt, *Solvents and Solvent Effects in Organic Chemistry*, Wiley-VCH, Weinheim, **2003**.
- [10] H. B. Kagan, J. C. Fiaud, *Top. Stereochem.* **1988**, *18*, 249-330.
- [11] F. J. Moreno-Dorado, F. M. Guerra, M. a. J. Ortega, E. Zubía, G. M. Massanet, *Tetrahedron: Asymmetry* **2003**, *14*, 503-510.
- [12] T. Nishimura, S.-Y. Xu, Y.-B. Jiang, J. S. Fossey, K. Sakurai, S. D. Bull, T. D. James, *Chem. Comm.* **2013**, *49*, 478-480.
- [13] S. F. Musolino, O. S. Ojo, N. J. Westwood, J. E. Taylor, A. D. Smith, *Chem. Eur. J.* **2016**, *22*, 18916-18922.
- [14] Y. Tsukamoto, S. Itoh, M. Kobayashi, Y. Obora, *Org. Lett.* **2019**, *21*, 3299-3303.
- [15] F. A. Cruz, V. M. Dong, *J. Am. Chem. Soc.* **2017**, *139*, 1029-1032.
- [16] L. L. W. Cheung, G. Vasapollo, H. Alper, *Adv. Synth. Catal.* **2012**, *354*, 2019-2022.
- [17] a) F. Iwasaki, T. Maki, O. Onomura, W. Nakashima, Y. Matsumura, *J. Org. Chem.* **2000**, *65*, 996-1002; b) M. Gavel, T. Courant, A. Y. P. Joosten, T. Lecourt, *Org. Lett.* **2019**, *21*, 1948-1952.
- [18] A. Khalafi-Nezhad, M. N. Soltani Rad, A. Khoshnood, *Synthesis* **2003**, *2003*, 2552-2558.
- [19] S. Kim, H. Chang, W. J. Kim, *J. Org. Chem.* **1985**, *50*, 1751-1752.
- [20] B. Liu, J. Yan, R. Huang, W. Wang, Z. Jin, G. Zanoni, P. Zheng, S. Yang, Y. R. Chi, *Org. Lett.* **2018**, *20*, 3447-3450.
- [21] A. J. Wommack, J. S. Kingsbury, *J. Org. Chem.* **2013**, *78*, 10573-10587.
- [22] A. M. Foley, D. P. Gavin, I. Joniec, A. R. Maguire, *Tetrahedron: Asymmetry* **2017**, *28*, 1144-1153.
- [23] C. Lee, W. Yang, R. G. Parr, *Phys. Rev. B* **1988**, *37*, 785-789.
- [24] G. W. Spitznagel, T. Clark, J. Chandrasekhar, P. V. R. Schleyer, *J. Comput. Chem.* **1982**, *3*, 363-371.
- [25] M. Marin-Luna, P. Patschinski, H. Zipse, *Chem. Eur. J.* **2018**, *24*, 15052-15058.
- [26] L. A. Curtiss, P. C. Redfern, K. Raghavachari, V. Rassolov, J. A. Pople, *J. Chem. Phys.* **1999**, *110*, 4703-4709.
- [27] Gaussian 09, R. D.01, M. J. Frisch, G. W. Trucks, H. B. Schlegel, G. E. Scuseria, M. A. Robb, J. R. Cheeseman, G. Scalmani, V. Barone, B. Mennucci, G. A. Petersson, H. Nakatsuji, M. Caricato, X. Li, H. P. Hratchian, A. F. Izmaylov, J. Bloino, G. Zheng, J. L. Sonnenberg, M. Hada, M. Ehara, K. Toyota, R. Fukuda, J. Hasegawa, M. Ishida, T. Nakajima, Y. Honda, O. Kitao, H. Nakai, T. Vreven, J. A. Montgomery Jr., J. E. Peralta, F. Ogliaro, M. Bearpark, J. J. Heyd, E. Brothers, K. N. Kudin, V. N. Staroverov, R. Kobayashi, J. Normand, K. Raghavachari, A. Rendell, J. C. Burant, S. S. Iyengar, J. Tomasi, M. Cossi, N. Rega, J. M. Millam, M. Klene, J. E. Knox, J. B. Cross, V. Bakken, C. Adamo, J. Jaramillo, R. Gomperts, R. E. Stratmann, O. Yazyev, A. J. Austin, R. Cammi, C. Pomelli, J. W. Ochterski, R. L. Martin, K. Morokuma, V. G. Zakrzewski, G. A. Voth, P. Salvador, J. J. Dannenberg, S. Dapprich, A. D. Daniels, Ö. Farkas, J. B. Foresman, J. V. Ortiz, J. Cioslowski, D. J. Fox, Gaussian, Inc., W. CT, **2010**.
- [28] F. Neese, *Wiley Interdiscip. Rev. Comput. Mol. Sci.* **2012**, *2*, 73-78.
- [29] Schrödinger Release 2019-2: Jaguar, Schrödinger, LLC, New York, NY, **2019**.
- [30] a) J. P. Guthrie, *Can. J. Chem.* **1996**, *74*, 1283-1296; b) F. A. Carey, R. J. Sundberg, *Advanced Organic Chemistry Part A: Structure and Mechanisms*, 5 ed., Springer Science+Business Media, New York, **2007**; c) M. Breugst, H. Zipse, J. P. Guthrie, H. Mayr, *Angew. Chem. Int. Ed.* **2010**, *49*, 5165-5169.
- [31] H. Zipse, *Reactivity and Mechanism in Organic Chemistry*, Shaker Verlag, Düren, **2019**.
- [32] E. R. Johnson, S. Keinan, P. Mori-Sánchez, J. Contreras-García, A. J. Cohen, W. Yang, *J. Am. Chem. Soc.* **2010**, *132*, 6498-6506.
- [33] J. Contreras-García, E. R. Johnson, S. Keinan, R. Chaudret, J.-P. Piquemal, D. N. Beratan, W. Yang, *J. Chem. Theory. Comput.* **2011**, *7*, 625-632.
- [34] W. Humphrey, A. Dalke, K. Schulten, *J. Mol. Graphics* **1996**, *14*, 33-38.

Chapter 5. Annelated Pyridine Bases for the Selective Acylation of 1,2-Diols

Stefanie Mayr and Hendrik Zipse*

Eur. J. Org. Chem., **2021**, submitted. Manuscript ID: *ejoc.202101521*

Author contributions: The project was conceived by S.M. and H.Z. The experimental and computational study was performed by S.M. The manuscript was jointly written by S.M. and H.Z. The supporting information was prepared by S.M.

Copyright: The manuscript was submitted to *European Journal of Organic Chemistry* on 16th of December 2021 and assigned the manuscript ID *ejoc.202101521* (© 2021 Wiley-VCH Verlag GmbH & Co. KGaA, Weinheim)

Additional Information: The herein printed Supporting Information (SI) is an altered version of the SI file submitted to *Eur. J. Org. Chem.* Original CoPaSi program simulations, tables of energies, enthalpies and free energies for all conformers, Cartesian coordinates and number of imaginary frequencies of the best conformers can be found in the original electronic SI file. Chapter 5.1 and 5.2 contain few additional experimental and computational results from the research report of Ana Mateos Calbet, who worked under the supervision of S.M. All of these results were reanalyzed by S.M. and are explicitly marked.

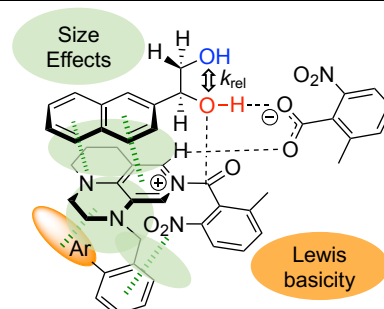
Annelated Pyridine Bases for the Selective Acylation of 1,2-Diols

Stefanie Mayr, Hendrik Zipse*

Dedicated to the memory of Klaus Hafner

[a] S. Mayr, Dr. H. Zipse*
 Department of Chemistry
 LMU München
 Butenandstr. 5-13, 81366 München (Germany)
 E-mail: zipse@cup.uni-muenchen.de

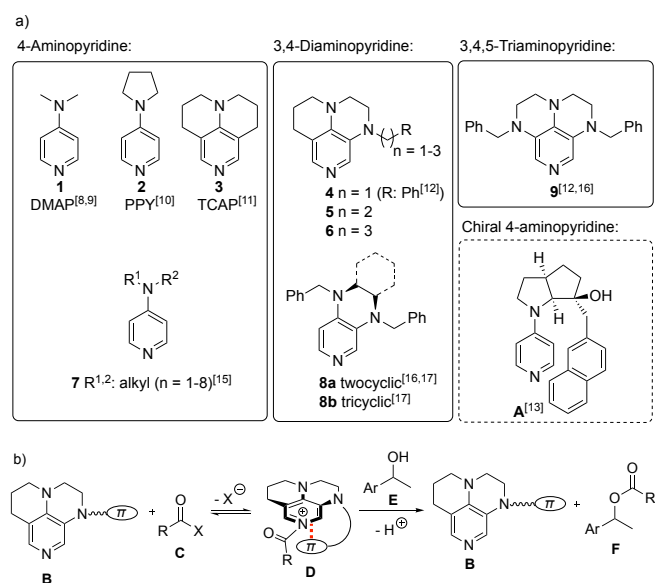
Supporting information for this article is given via a link at the end of the document.



Abstract: A set of 24 annelated derivatives of 4-diaminopyridine (DMAP) has been synthesized and tested with respect to its catalytic potential in the regioselective acylation of 1,2-diol substrates. The Lewis basicities of the catalysts as quantified through quantum chemical calculations vary due to inductive substituent effects and intramolecular stacking interactions between side chain π -systems and the pyridinium core ring system. The primary over secondary hydroxyl group selectivities in catalytic acylations of 1,2-diol substrates depend on the size and the steric demand of the Lewis base and the anhydride reagent.

Introduction

The protection of functional groups plays an important role in organic synthesis.^[1] In most natural products such as sugars or pharmaceutically important molecules, hydroxyl groups are present in large numbers,^[2] and the selective protection and deprotection of these groups is thus highly relevant in organic chemistry.^[3] The highly chemo- and regioselective transformation of hydroxyl groups in polyol systems provides particular challenges, despite the considerable attention this area has seen already in the last decades.^[4] One of the most prominent ways to protect alcohols is the Lewis base-mediated esterification using a variety of acylation reagents such as acid chlorides, cyanides or acid anhydrides.^[5] Aside from phosphanes,^[6] pyridine-based catalysts like 4-dimethylaminopyridine (DMAP, **1**) count among the most often used Lewis base catalysts for these transformations.^[5f,7,8,9] The catalytic activity of **1** can be increased through installation of stronger electron donors at the C4 position as is, for example, the case in 4-(pyrrolidinyl)pyridine (PPY, **2**).^[9a,10] A further improvement in catalytic activity was achieved with tricyclic 4-aminopyridine derivative 9-azajulolidine (TCAP, **3**), where the 4-amino nitrogen atom is conformationally fixed.^[11] A mechanistic study by Steglich *et al.*^[11] indicated that the stability of the respective acylpyridinium ions correlates strongly with experimentally measured acylation rates. Further extensions of this idea led to the more nucleophilic Lewis bases of the 3,4-diaminopyridine type **4** (R = Ph, Me), which perform quite well in the acylation of tertiary alcohols.^[12] For the chiral catalyst **A** employed in kinetic resolution experiments by Fujii *et al.*^[13] it was demonstrated by ¹H NMR analysis (and later confirmed through quantum chemical studies^[14]) that the respective acylpyridinium intermediate is stabilized by cation- π interactions. Combining these concepts one can envision a class of intrinsically electron-rich 3,4-diaminopyridine



Scheme 1. a) Basic motif of pyridinium Lewis based catalysts. b) Stabilization of *N*-acylpyridinium cation intermediate by non-covalent interactions (NCI).

catalysts for the acylation of alcohols carrying a π -system (or dispersion-energy donor, DED) side chain of general structure **B**. Reaction of **B** with acyl donor **C** will generate the acylpyridinium ion **D** as a key intermediate of the catalytic cycle. If designed properly this latter intermediate will be stabilized through stacking interactions between the side chain substituents and the formally cationic pyridinium core ring system as shown in the "closed" conformation **D** in Scheme 1. Subsequent reaction with alcohol **E** then completes the catalytic sequence. Whether or not the closed conformation of acylpyridinium intermediate **D** actually exists will depend on the type of side chain DED donor as well as the length of the linker connecting these two units. The latter aspect is best seen in catalysts **4** - **6**, where the linker length is systematically increased from n = 1 to n = 3. For catalysts of type **7** it is already known that *n*-alkyl substituents can influence catalytic activity also through inductive effects.^[15] This also appears to be a factor in the excellent catalytic performance of 3,4-diaminopyridine catalysts of general structure **8**,^[16,17] where derivative **8b** was found to be similarly active as TCAP (**3**) and **4** in many transformations. 3,4,5-Triaminopyridines such as **9** appear to be even stronger Lewis bases as compared to all other compounds shown in

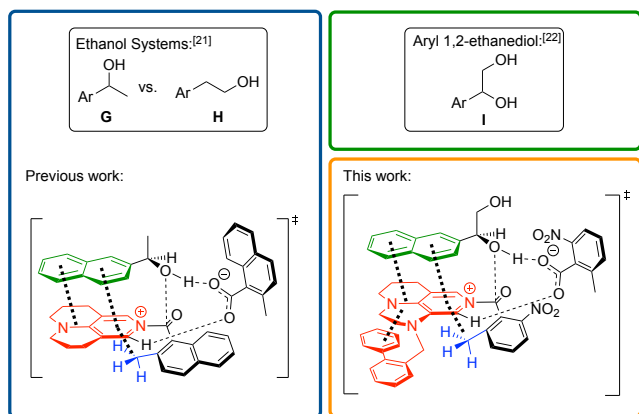


Figure 1. Transition structure for the acylation of 1-(2-naphthyl)ethanol catalysed by TCAP (**3**) (left) and proposed transition structure for the acylation of 1-(2-naphthyl)ethane-1,2-diol catalysed by modified TCAP catalysts **4-6** (right).

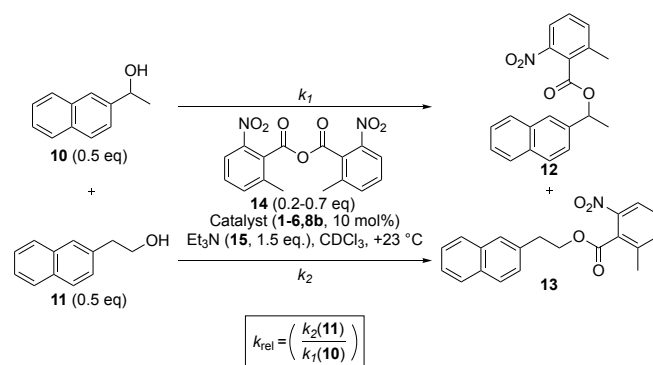
Scheme 1, but this basicity increase does not appear to translate into higher catalytic reactivity.^[12,16] Although the stereoselectivity of Lewis base-mediated acylation reactions has been studied extensively (and successfully),^[5f,7,18] this is much less the case for regioselective acylations in polyol systems. Noteworthy exceptions exist for acylations of carbohydrate substrates, where the use of highly functionalized catalysts based on the PPY substructure^[19] and/or the exploitation of specific hydrogen bonding effects with selected counter ions^[5a,20] lead to selective acylations of secondary over primary OH groups. We have recently analyzed the influence of anhydride size and substitution pattern on the acylation of secondary alcohol **G** over primary alcohol **H** catalysed by the Lewis base TCAP.^[21] Exploiting π - π -interactions between secondary alcohol **G** and the planar TCAP motif as well as size effects of the anhydride reagents, it was indeed possible to steer intermolecular competition reactions towards preferred acylation of the secondary alcohol **G** (Figure 1, left side). The same factors were subsequently also found to impact the *intramolecular* competition between primary and secondary OH groups in 1,2-diols of general structure **I** (Figure 1, right side).^[22] In absolute terms the regioselectivity of the TCAP-mediated process was found to be quite moderate in the first acylation step and then to increase in acylations of the initially formed monoesters. In kinetic resolution experiments it was already demonstrated earlier that size effects can have a strong influence on the enantioselectivity.^[18,23] In the present study we now probe the influence of catalyst structure on the regioselectivity of diols **I**. More specifically we analyze how the DED substituents in catalysts of general structure **4-6** impacts regioselectivity and catalytic efficiency. The Lewis basicities of these catalysts have been quantified by quantum mechanically calculated acetyl cation affinity numbers.

Results and Discussion

Competition Experiments. Catalysts **1-6** and **8b**^[24] were first characterized with respect to their ability to selectively acylate primary or secondary hydroxyl groups in turnover-limited competition experiments. As a benchmark reaction we select the acylation of secondary 1-(naphth-2-yl)ethanol **10** vs. primary 2-(naphth-2-yl)ethanol **11** to the corresponding esters (Scheme 2).^[21,25] The relative rate constant k_{rel} reflecting the selectivities of the formation of the products **12**

and **13** is here defined as the ratio between the effective rate constant k_2 for acylation of primary alcohol **11** and the effective rate constant k_1 for acylation of secondary alcohol **10**. As acylation reagent 2-methyl-6-nitrobenzoic anhydride **14** was selected due to its performance in earlier projects.^[21-22] Turnover-limited competition experiments were performed with a 1:1 mixture of **10** and **11** adding **14** as the limiting acylation reagent to allow conversions of 20-70%, an excess of auxiliary base Et₃N (**15**), and 10 mol% of the corresponding Lewis-base catalyst **1-6,8b** in CDCl₃ at +23 °C. By determining the chemoselectivity at various conversion points, the relative reaction rates can be determined following the analysis method established by Kagan *et al.*^[26] for kinetic resolution experiments (for details see SI). Three different classes of tricyclic pyridine-based catalysts were synthesized (Figure 2). The first class **4a-r** contains a tricyclic 3,4-diaminopyridine core unit connected via a short CH₂-linker ($n = 1$) to a selection of small (**4a-l**, **4n,o** and **4r**) or larger (**4j-m**) aromatic and aliphatic (**4p,q**) side chains. The effects of longer linker units are explored in class II ($n = 2$, **5a-b**) and class III ($n = 3$, **6a-d**), where the attached aromatic side chains can potentially fold back onto the 3,4-diaminopyridine core unit more easily. For the sake of comparison we also include the established catalysts DMAP (**1**), PPY (**2**), and TCAP (**3**) as well as the tricyclic diaminopyridine derivative **8b**.^[12,27]

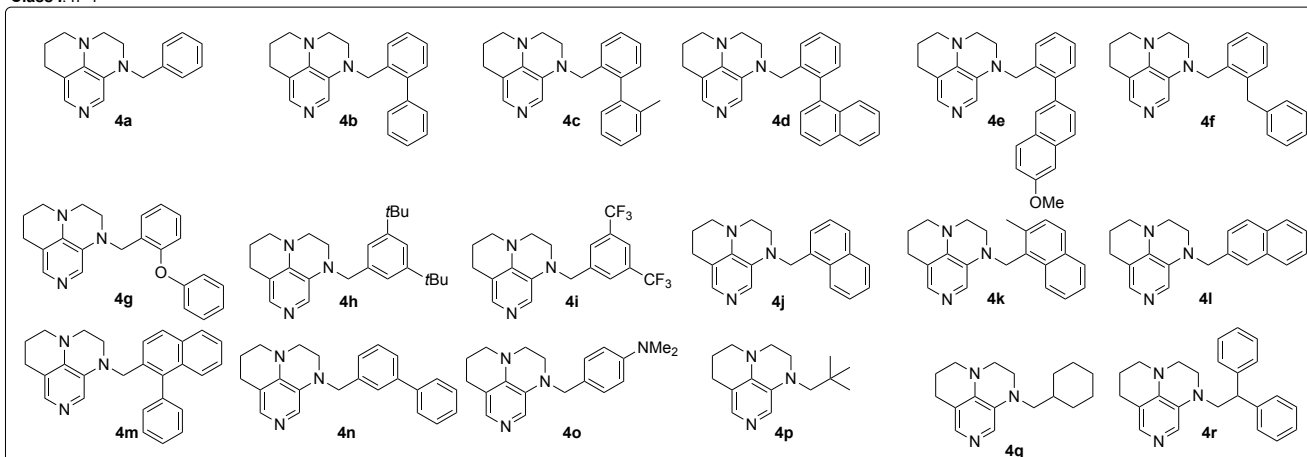
The acylation of **10** and **11** catalysed with the most common 4-aminopyridine based catalyst DMAP (**1**) is a good reference point with $k_{rel} = 1.44$, which indicates that the primary alcohol **11** reacts 1.4 times as fast as the secondary alcohol **10** (red bar in Figure 3). PPY (**2**) shows a drop in selectivity to $k_{rel} = 1.24$ and thus a reduced preference for primary alcohol **11**. The selectivity value inverts to $k_{rel} = 0.68$ when using the tricyclic 4-aminopyridine TCAP (**3**), which implies that secondary alcohol **10** reacts 1.4 times as fast as primary alcohol **11** (green bar in Figure 3). In the 3,4-aminopyridine catalysts **4** we first explored the influence of an attached *ortho*-substituted phenyl group. The catalytic reaction with **4a** ($R = Ph$) shows a selectivity of $k_{rel} = 0.78$. By functionalizing the attached phenyl group in *ortho* position with aryl substituents (such as Ph, Tol, or 1-Np) the selectivity values decrease slightly, the smallest value (and thus the highest preference for secondary alcohol **10**) being found for **4d** with $k_{rel} = 0.63$. Whether the *ortho*-substituent is attached through a CH₂-group (as in **4f**) or an ether oxygen bridge (as in **4g**) appears not to impact the obtained selectivities. The best



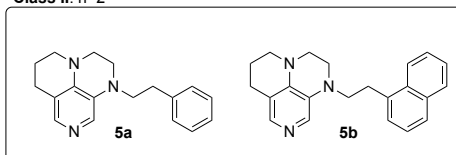
Scheme 2. Turnover-limited competition experiment between alcohols **10** and **11** with anhydride **14** catalysed by Lewis base catalysts **1-6** and **8b**.

Annelated Pyridine Bases

Class I: n=1



Class II: n=2



Class III: n=3

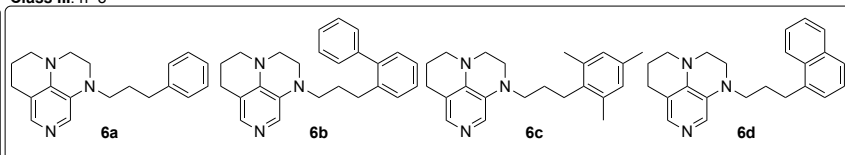


Figure 2. Structures and classifications of catalyst **4-6**.

result in this group with $k_{rel} = 0.57$ is obtained for **4e** carrying a 7-methoxynaphth-2-yl substituent. This selectivity value may reflect the size of the 2-naphthyl substituent as well as the electronic influence of the attached methoxy group. Moving the attached substituents to *meta* (as in **4n**) or *para* position (as in the dimethyl amino-substituted system **4o**) leads to selectivities closely similar to those obtained for **4a**. Slightly better selectivities are obtained for the 3,5-disubstituted systems **4h** with $k_{rel} = 0.69$ (where two *t*Bu units may act as electron donor and DED-groups)^[23b] and **4i** with $k_{rel} = 0.67$ (where CF_3 groups act as electron withdrawing substituents). Expanding the core side chain unit from Ph (as in **4a**) to naphthyl attached at C1 (as in **4j** and **4k**) or C2 (as in **4l**) shows no significant change in selectivity. Addition of a phenyl group at C1 position to this latter system as in **4m** leads to a small, but notable change in selectivity with $k_{rel} = 0.63$. Whether purely aliphatic side chains have systematically different effects as compared to aromatic side

chains of equal carbon count was explored with **4q**, which can be seen as the hydrogenated complement to **4a**. Indeed, the selectivity is notably reduced now to $k_{rel} = 0.90$. Replacing the cyclohexyl by a *t*Bu substituent as in **4p** with does not lead to a major change with $k_{rel} = 0.80$. In conclusion we can see that the 3,4-diaminopyridine variants explored in class I yield selectivity values closely similar to that of TCAP (**3**), where secondary alcohol **10** reacts approx. 1.5 times faster as compared to secondary alcohol **11**. This selectivity can be rationalized assuming the previously reported "triple sandwich" acylation transition states,^[21] where the 2-naphthyl side chain of alcohol **10** can form stronger non-covalent interactions with the catalyst pyridinium core unit as compared to alcohol **11**. If the catalyst surface is big enough (as is the case in the tricyclic pyridinium catalysts of type **3** and **4**), then the acylation of secondary alcohols is slightly preferred.

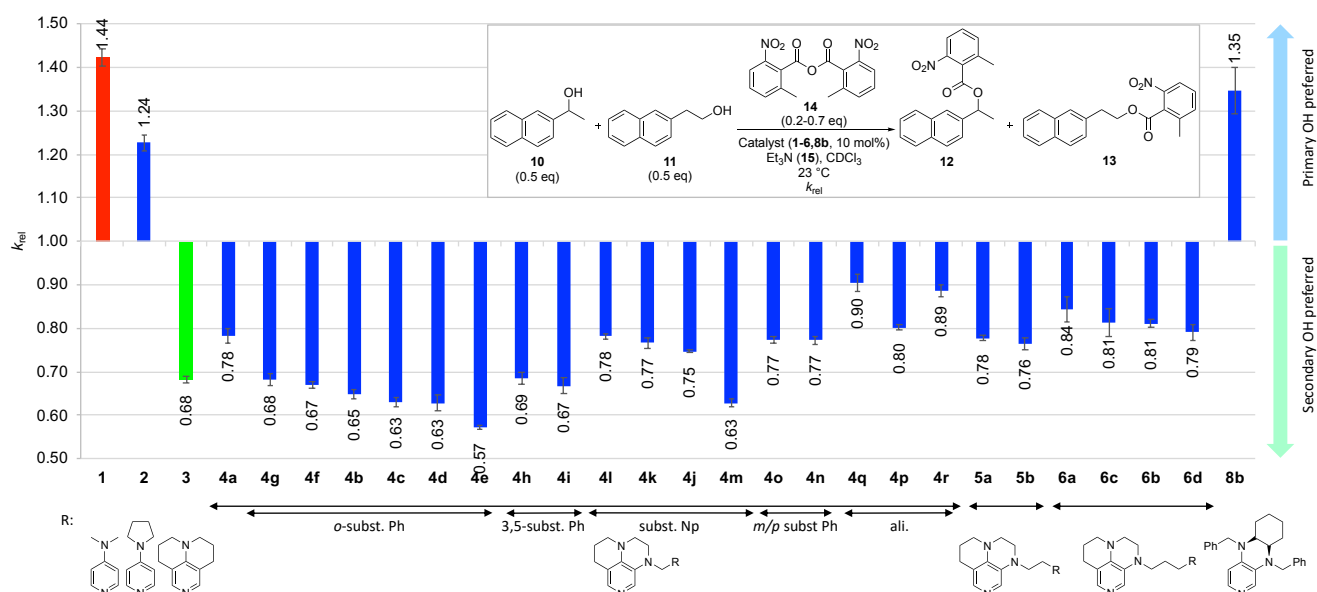
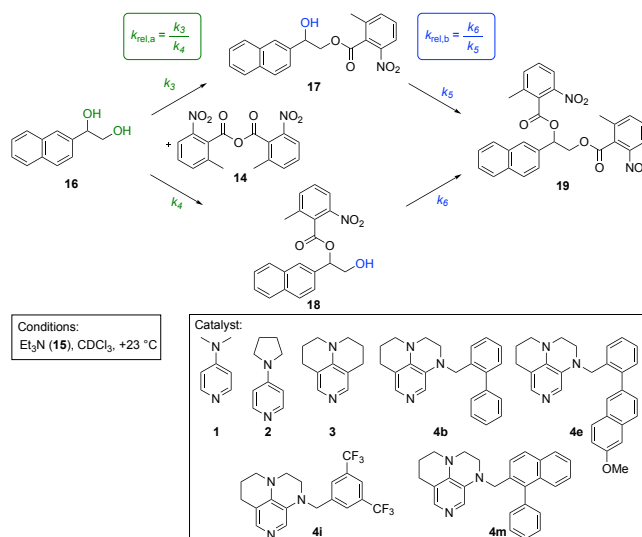


Figure 3. Relative rate constants k_{rel} for secondary alcohol **10** vs primary alcohol **11** with anhydride **14** catalysed by various catalysts **1-6,8b**.

In Class II we find systems where the 3,4-diaminopyridine core unit is connected to the side chain with a slightly longer and thus more flexible C2 linker unit. However, comparing the results for **4a** (R = Ph, n = 1) and **5a** (R = Ph, n = 2) we see that both react with $k_{\text{rel}} = 0.78$. This is similarly true for the two catalysts carrying a naphth-1-yl side chain **4j** (n = 1) and **5b** (n = 2). We note in passing that reduction of linker flexibility as in catalyst **4r** leads to a notable reduction of selectivity. Increasing the linker length to n = 3 (class III) the acylation of secondary alcohol **10** is even less favoured as can be seen for catalyst **6a** (R = Ph, n = 3) with $k_{\text{rel}} = 0.84$. For the larger naphth-1-yl side chain similar selectivities are obtained for all linker lengths with $k_{\text{rel}} = 0.75$ (**4j**, n = 1), $k_{\text{rel}} = 0.76$ (**5b**, n = 2) and $k_{\text{rel}} = 0.79$ (**6d**, n = 3). Further variation of the size of the substituent as in **6b** or **6c** also leads to no notable change in the selectivities, and we thus conclude that the length of the linker unit does NOT impact the catalytic behavior and the selectivity of the reaction. A lack of alignment of the attached aromatic substituents into one plane, which appears to impact acylation of secondary alcohol **10** more than that of primary alcohol **11** is determined for the tricyclic 3,4-diaminopyridine catalyst **8b** with $k_{\text{rel}} = 1.35$.

Absolute Kinetics Studies. Based on their performance in the 1:1 competition studies described above, seven catalysts were selected for further studies in the acylation of 1-(naphth-2-yl)ethane-1,2-diol **16** testing their ability to differentiate vicinal primary and secondary hydroxyl groups. Following earlier work on **16**^[22] the initial formation of monoesters **17** and **18** and the subsequent second acylation to yield diester **19** were followed using absolute kinetics measurements (Scheme 3). Analysis of these results yields selectivity value $k_{\text{rel,a}}$ defined as the ratio between the effective acylation rate of primary hydroxyl group (k_3) and the secondary hydroxyl group of **16** (k_4). The ratio between the effective acylation rate of primary alcohol **18** (k_6) over the secondary alcohol **17** (k_5) is reflected in selectivity value $k_{\text{rel,b}}$ for the second acylation of the monoesters **17/18** to the diester **19**. The migration from **18** to **17** is neglected in this study.^[22] With these definitions both selectivity values $k_{\text{rel,a}}$ and $k_{\text{rel,b}}$ reflect the acylation selectivities for primary over secondary hydroxyl groups. For **16** as a substrate we had found earlier that suitable catalyst/reagent combinations yield to an inversion of selectivity in favour of the secondary hydroxyl group.^[22] As the acylation reagent we employ an excess (1.5 eq.) of 2-methyl-6-nitrobenzoic anhydride **14** in combination with 10 mol% of the corresponding Lewis base catalyst and Et₃N (2.0 eq.) as auxiliary base in CDCl₃ at +23 °C (for details see SI).



Scheme 3. Acylation of 1-(naphth-2-yl)ethane-1,2-diol **16** with 2-methyl-6-nitrobenzoic anhydride **14** mediated by catalysts **1-4** in the presence of Et₃N (**15**) at +23 °C.

The known catalysts DMAP (**1**), PPY (**2**), and TCAP (**3**) were again included as reference systems. The four 3,4-diaminopyridine catalysts tested in the acylation of diol **16** include the *ortho* substituted phenyl-based catalysts **4b,e**, the 3,5-disubstituted phenyl-based catalysts **4i**, and the *ortho*-substituted 2-naphthyl catalyst **4m**. Mole fractions for substrates **16** - **19** have been determined by ¹H NMR spectroscopy at various time intervals, and the effective rate constants $k_3 - k_6$ have then been determined from these data by numerical kinetics simulations (see SI).^[28] From the time dependence of the mole fraction of monoester **17** shown in Figure 4a we see that the effective rate constant k_3 for acylation of the primary hydroxyl group in **16** is largest for DMAP (**1**) and smallest for 3,4-diaminopyridine catalyst **4m**. It is particularly surprising that catalyst **1** is more reactive here than TCAP (**3**), which is in contrast to most other reactivity studies with these two Lewis bases.^[6,12,29] Quantitative analysis in the framework of the mechanistic model shown in Scheme 3 yields the values shown in Table 1 and thus an approx. 10-fold reactivity difference between the fastest and slowest catalysts. A similar reactivity ordering is also found for acylation of the secondary hydroxyl group in **16** as is reflected in the time dependence of the mole fraction of monoester **18** shown in Figure 4b and the numerical values of rate constant k_4 in Table 1, except that **4i** is slightly more active than **1** in this case. A third measure of catalytic activity

Table 1. Effective rate constants k_3 and k_4 and the corresponding relative rate constant $k_{\text{rel,a}}$ for catalysts **1-3**, **4b,e,i** and **m** for the first acylation of polyol **16** determined through absolute kinetics. The relative rate constant k_{rel} for the acylation of alcohols **10** and **11** with **14** catalysed by **1-3**, **4b,e,i** and **m** has been determined through turnover-limited competition experiments.

Entry	Catalyst	k_3 ($\times 10^{-3}$) ^[a,b]	k_4 ($\times 10^{-3}$) ^[a,b]	$k_{\text{rel,a}}$ ^[a]	k_{rel} ^[a]
1	1	69.9±12.39	27.9±2.99	2.49±0.178	1.42±0.016
2	2	38.7±2.30	21.8±1.85	1.78±0.046	1.23±0.017
3	3	36.6±5.26	24.7±2.35	1.47±0.073	0.68±0.006
4	4i	35.7±0.04	32.1±0.04	1.11±0.003	0.67±0.017
5	4b	9.2±0.10	9.6±1.29	0.97±0.026	0.65±0.009
6	4m	5.9±0.84	5.8±0.75	1.03±0.011	0.63±0.008
7	4e	6.7±0.11	6.9±0.08	0.98±0.005	0.57±0.003

^[a]Averaged values (see SI). ^[b]In L mol⁻¹ s⁻¹.

Table 2. Effective rate constants k_5 and k_6 and the corresponding relative rate constant $k_{\text{rel,b}}$ for catalysts **1-3** and **4i** for the second acylation of polyol **16** determined through absolute kinetics. The relative rate constant k_{rel} for the acylation of alcohols **10** and **11** with **14** catalysed by **1-3** and **4i** has been determined through turnover-limited competition experiments.

Entry	Catalyst	k_5 ($\times 10^{-3}$) ^[a,b]	k_6 ($\times 10^{-3}$) ^[a,b]	$k_{\text{rel,b}}$ ^[a]	k_{rel} ^[a]
1	4i	18.2±0.76	10.9±2.21	0.59±0.102	0.67±0.017
2	3	14.6±4.07	9.32±2.34	0.64±0.019	0.68±0.006
3	1	10.3±2.20	11.2±2.00	1.10±0.041	1.42±0.016
4	2	6.9±0.24	8.41±0.80	1.21±0.073	1.23±0.017

^[a]Averaged values (see SI). ^[b]In L mol⁻¹ s⁻¹.

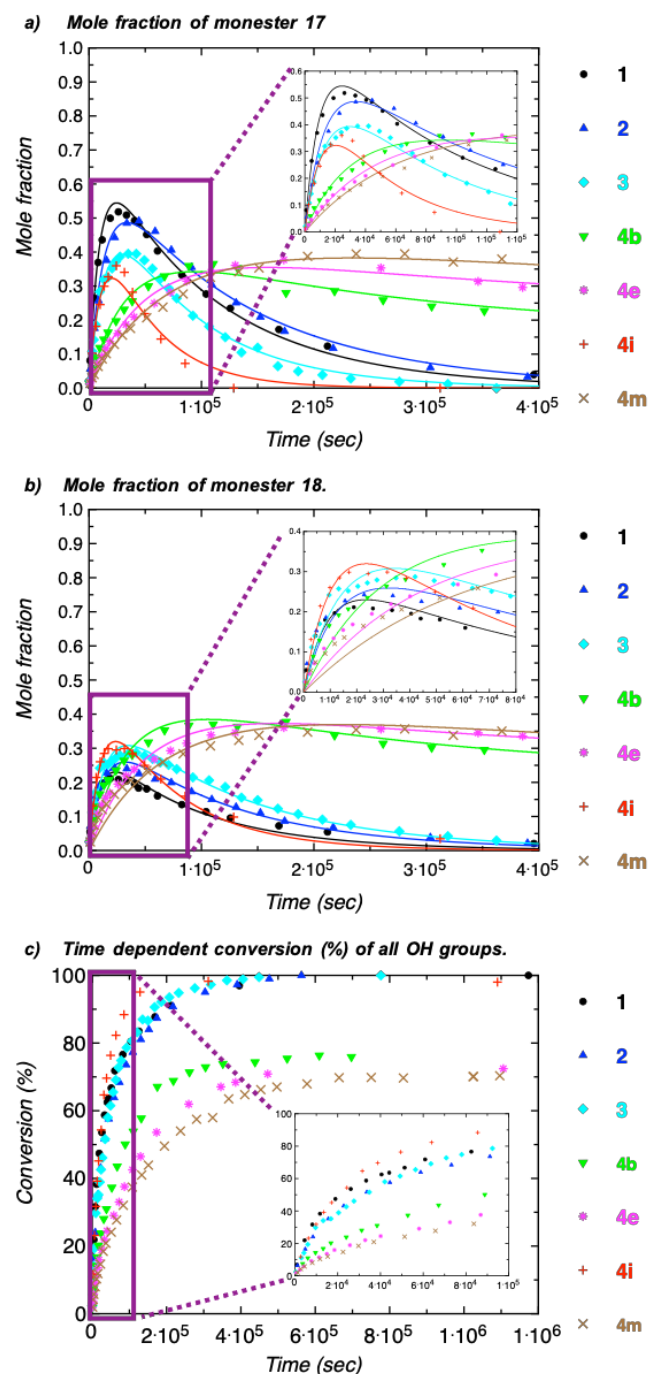
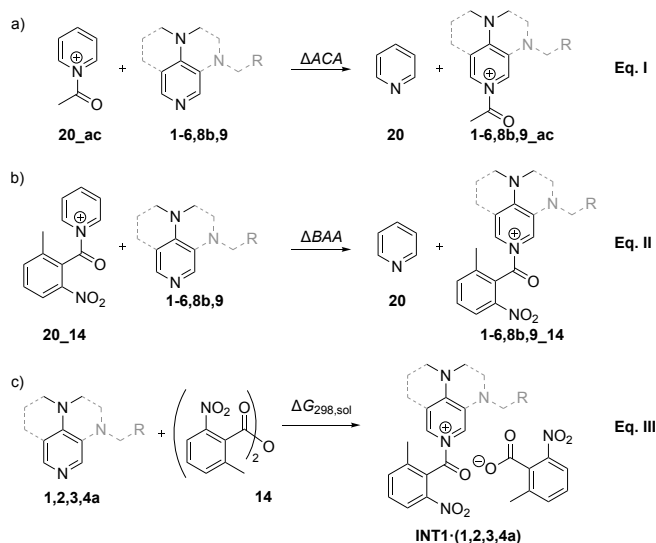


Figure 4. Time development (in sec) of a) the mole fraction of monoester **17**, b) the mole fraction of monoester **18**, and c) of all OH-groups (%) in the acylation of diol **16** with anhydride **14** mediated by catalysts **1-3**, **4b,e,i** and **m**.

can be obtained from analysis of the time dependent conversion of all hydroxyl groups present in **16** - **18** as shown in Figure 4c, where again **4i** appears to be most active. The ratio of k_3 and k_4 and thus the primary/secondary selectivity of the first acylation step ($k_{rel,a}$ values in Table 1) is largest for DMAP (**1**) with $k_{rel,a} = 2.49$ and then approaches unity for the less active catalysts. This parallels the chemoselectivities presented in Figure 3, where **1** showed the largest preference for the acylation of primary alcohol **11** over secondary alcohol **10**. In contrast to these intermolecular competition experiments, TCAP (**3**) is not effective in inverting the primary/secondary selectivity in the acylation of diol **16** with $k_{rel,a} = 1.47$. The 3,4-diaminopyridine catalysts **4b,e,i** and **m**

all show $k_{rel,a}$ values close to 1.0, the individual differences being too small for meaningful structure/ activity analyses. The acylation of monoesters **17** vs. **18** to diester **19** is systematically slower than the initial acylation step, and only for catalysts **1-3** and **4i** could full conversion to **19** be observed. For catalysts **4b,e** and **m** only conversions of up to 60 % could be realized even at extended reaction times (for more details see SI). From the time-dependent decrease of the mole fraction of monoester **17** shown in Figure 4a we see that the effective rate constant k_5 for acylation of the secondary hydroxyl group in **17** is largest for 3,4-diaminopyridine catalyst **4i** and smallest for PPY (**2**). Quantitative analysis in the framework of the mechanistic model shown in Scheme 3 yields the values shown in Table 2 and thus an approx. 2.5-fold reactivity difference between the fastest and slowest catalysts. The acylation of the primary hydroxyl group in **18** as described by the time dependent decrease of the mole fraction of monoester **18** shown in Figure 4b and the numerical values of rate constant k_6 in Table 2 proceeds with similar efficiency with all catalysts. Again DMAP (**1**) has the largest effective rate constant k_6 and PPY (**2**) the smallest. The ratio of k_6 and k_5 and thus the primary/secondary selectivity of the second acylation step ($k_{rel,b}$ values in Table 2) are largest for DMAP (**1**) with $k_{rel,b} = 1.10$ and inverted to the secondary hydroxyl group for tricyclic catalyst systems TCAP (**3**) with $k_{rel,b} = 0.64$ and **4i** with $k_{rel,b} = 0.59$.

Acetyl cation affinity values (ΔACA). In how far intramolecular interactions between catalyst side chains and the *N*-aminopyridinium core unit influences the Lewis basicity of the catalysts was explored by the calculation of acetyl cation affinities (ΔACA) at the SMD(CHCl₃)/B3LYP-D3/6-31+G(d) level of theory.^[30] As shown in Eq. I (Scheme 4a) these are defined as the reaction enthalpies ΔH_{298} for acetyl group transfer from acetylpyridinium cation **20**_{ac}.^[12,14,29a,31] The Lewis basicity of 4-aminopyridine catalysts **1** and **2** is lower than that of 3,4-diaminopyridines and is in the range of $\Delta ACA = -57.9$ to -63.1 kJ mol⁻¹ (Table 3, entries 1 - 2). Around 10 kJ mol⁻¹ higher basicities are found for tricyclic catalysts **4i** ($\Delta ACA = -72.6$ kJ mol⁻¹, entry 4) and **3** ($\Delta ACA = -75.0$ kJ mol⁻¹, entry 5).



Scheme 4. Model of a) acetyl cation affinity number (ΔACA , Eq. I), b) benzoic anhydride affinity number (ΔBAA , Eq. II) and c) Gibbs free reaction energy of the formation of INT1 (Eq. III).

Table 3. Acetyl cation affinity numbers (ΔACA), benzoic anhydride affinity numbers (ΔBAA), and free energy values for the formation of INT1 (in kJ mol^{-1}).

Entry	Catalyst	ΔACA^a	ΔBAA^a	INT1 ^b
1	1	-57.9	-58.4	+20.6
2	2	-63.1	-63.4	+12.5
3	8b	-71.1	-85.8	/
4	4i	-72.6	-91.4	/
5	3	-75.0	-76.9	+8.3
6	4j	-80.3	-83.7	/
7	4a	-81.5	-95.3	-2.7
8	5a	-81.6	-89.5	/
9	5b	-83.8	-88.5	/
10	9	-84.1	-99.9	/
11	6a	-85.2	-93.0	/
12	4b	-85.4	-101.2	/
13	4m	-87.8	-94.6	/
14	6d	-91.0	-93.1	/
15	4e	-93.6	-96.6	/

^a $\Delta H_{298}(\text{SMD}(\text{CHCl}_3)/\text{B3LYP-D3/6-31+G(d)})$, in kJ mol^{-1} . ^b $\Delta G_{298,\text{sol}}(\text{DLPNO-CCSD(T)/def2-TZVPP//SMD}(\text{CHCl}_3)/\text{B3LYP-D3/6-31+G(d)})$, in kJ mol^{-1} .

Most of the catalysts **4**, **5** and **6** have affinity values between $\Delta ACA = -80.3$ - $-93.6 \text{ kJ mol}^{-1}$, whereby **4e** with $\Delta ACA = -93.6 \text{ kJ mol}^{-1}$ is the most Lewis-basic catalyst of this class (entry 15).^[32] The tricyclic catalyst **8b** has a similar basicity as TCAP with $\Delta ACA = -71.1 \text{ kJ mol}^{-1}$, while the triaminopyridine catalyst **9** is of intermediate basicity with $\Delta ACA = -84.1 \text{ kJ mol}^{-1}$. The experimental studies described above employ 2-methyl-6-nitrobenzoic anhydride (**14**) as the electrophilic reagent, and additional benzoic anhydride affinities (ΔBAA) were therefore calculated for this system as defined by Eq. II (Scheme 4b and Table 3). The graphical presentation of ΔACA and ΔBAA values in Figure 5 shows both affinity measures to follow similar trends, but also indicates that the ΔBAA values are slightly larger (more negative) for the tricyclic catalysts. Particularly larger changes in affinity are found for the benzyl-substituted catalysts **4a**, **4b**, and **4i**, as well as **8b** and **9**. With the relative acetyl cation affinity (ΔACA) values in hand, we can analyze the structural differences between the various acylated catalysts and thus test the hypothesis of stabilizing non-covalent interactions presented in Scheme 1. The most stable conformers of the acylpyridinium cations of selected catalysts are shown in Figure 6 together with critical distances between the acylpyridinium core units and the closest side chain atoms. In the (biphen-2-yl)methyl-

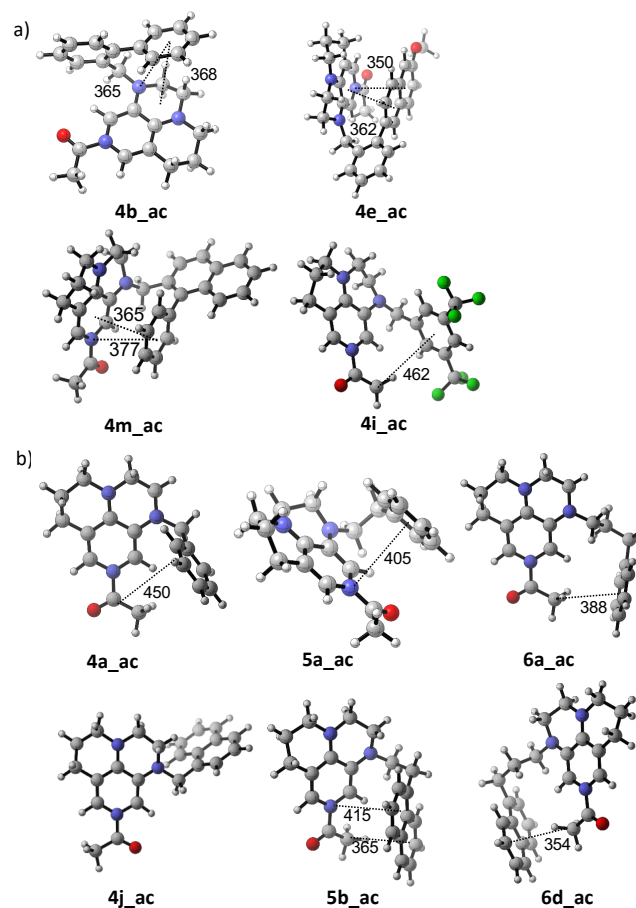
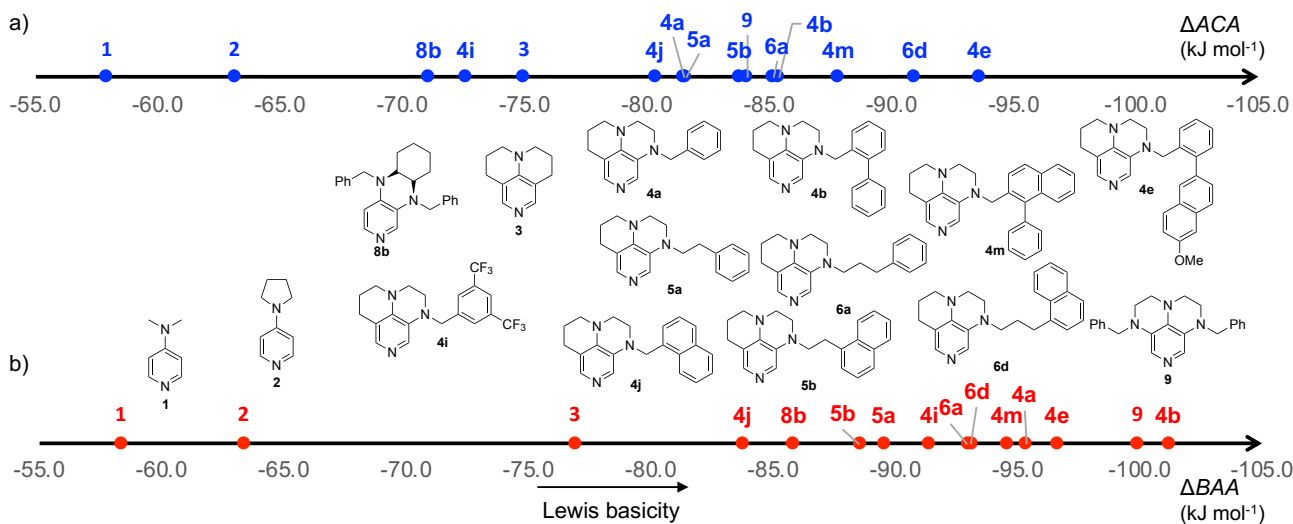


Figure 6. Geometries of acetyl cation adducts optimized at the $\text{SMD}(\text{CHCl}_3)/\text{B3LYP-D3/6-31+G(d)}$ level of theory for a) catalysts **4b**, **4b**, **4m** and **4i**, and b) catalysts **4a,j**, **5a,b** and **6a,d** together with selected distances (in pm) between side chains and the acetylpyridinium core unit.^[33]

substituted 3,4-diaminopyridine intermediates **4b_ac**, **4e_ac**, and **4m_ac** we can indeed recognize the expected sandwich structures between side chain phenyl groups and the acylpyridinium core fragment with ring-to-ring distances of $r = 350$ - 377 pm typical for stacking conformations. The shortest distance of $r = 350 \text{ pm}$ can be found for the most Lewis basic catalyst **4e_ac** where the side chain phenyl group is



Annelated Pyridine Bases

positioned directly over the catalytically active nitrogen atom.^[34] In contrast, no such interactions can be seen in the acylpyridinium intermediate of catalyst **4i** characterized by a comparatively low ΔACA value. Whether alkyl group linkers of different lengths can be employed to steer the attached side chain π -systems into a stacking orientation was tested for catalysts **4a**, **5a**, and **6a** with linker lengths of $n = 1 - 3$. The best alignment between acylpyridinium core and side chain phenyl substituent could be seen in **5a**, but even then, the distances between the two units was significantly larger at $r = 405$ pm as compared to that in **4b_ac**. For the system with the largest linker length **6a_ac** the dominant side chain/acylpyridinium core interaction appears to be a CH- π interaction between the attached π -system and the acetyl C-H bonds.^[35] Effectively the same conclusions were obtained for the acylpyridinium intermediates of 1-naphthyl substituted catalysts **4j**, **5b**, and **6d**, where again the linker length varies from $n = 1 - 3$ (Figure 6b).

In earlier studies it could be shown that cation affinity values of Lewis base catalysts correlate well with their effective rate constants towards electrophiles.^[12,14,29a,31] Whether this is also the case for the first acylation of diol **16** studied here is shown in Figure 7. Plotting the ΔACA values over the natural logarithm of effective rate constant $\ln k_3$ (acylation of primary OH-group in **16**) a linear correlation of good fidelity is obtained (Figure 7, red triangles, $R^2 = 0.89$). It is, however, quite unexpected that catalysts with lower Lewis basicity such as **1** or **2** accelerate the acylation more strongly as compared to more potent Lewis base catalysts such as **3** or **4b,e,m**. This finding (specifically for catalysts **1-3**) is in contrast to the findings of earlier studies on Lewis base-mediated acylation reactions.^[6,12] The same type of correlation, but with a smaller slope, is also found for rate constant $\ln k_4$ (acylation of secondary hydroxyl group in **16**, Figure 7b, green circles, $R^2 = 0.73$). It is the difference in the slopes for the acylation of the primary and the secondary hydroxyl group in diol **16** that leads to a direct link between catalyst Lewis basicity and acylation regioselectivity as quantified by $k_{rel,a}$ in Table 1. In order to identify possible reasons for the comparatively low catalytic activity of the most Lewis basic catalysts studied here, we also calculated the full Gibbs free energy for the reaction of catalysts **1-4** with anhydride **14** to yield the full *N*-acylpyridinium ion pair intermediates **INT1** at the DLPNO-CCSD(T)/def2-TZVPP// SMD(CHCl₃)/B3LYP-D3/6-31+G(d) level of theory (Eq. III, Scheme 4).^[30,36] Based on earlier theoretical studies we assume that the formation of **INT1** is

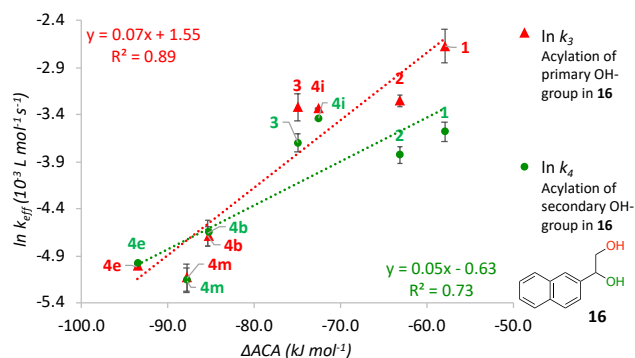


Figure 7. Plot of ΔACA (kJ mol^{-1}) vs. natural logarithm of effective rate constant for the first acylation of primary OH-group (k_3 , red triangle) and of secondary OH-group (k_4 , green circle) catalysed **1-3**, **4b,e,i** and **m**.

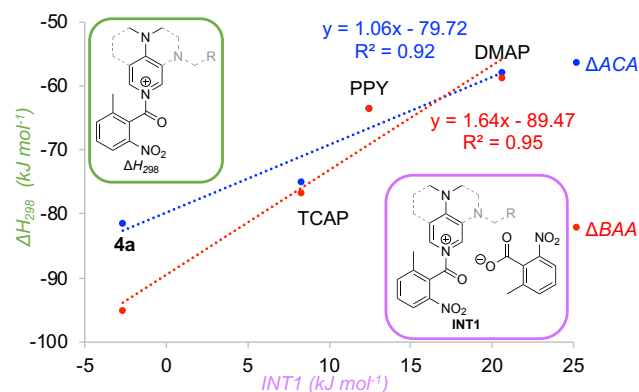


Figure 8. Plot of the stability of **INT1** (ΔG_{298} in kJ mol^{-1}) vs. ΔACA (ΔH_{298} in kJ mol^{-1}) for Lewis base catalysts **1-3** and **4a**

the first step of the catalytic cycle.^[21] If **INT1** is too stable, the energy barrier for the subsequent alcohol acylation step could be negatively affected.^[37] For DMAP a Gibbs free energy of $\Delta G_{298}(\mathbf{1}) = +20.6$ kJ mol^{-1} was obtained (Table 3). For increasingly Lewis basic catalysts these energies become more favorable with values of $\Delta G_{298}(\mathbf{2}) = +12.5$ kJ mol^{-1} , $\Delta G_{298}(\mathbf{3}) = +8.3$ kJ mol^{-1} , and $\Delta G_{298}(\mathbf{4a}) = -2.7$ kJ mol^{-1} . This last value thus implies that the equilibrium between free catalyst **4a** and its acylpyridinium ion pair intermediate **INT1•4a** may tip towards the latter as a function of absolute catalysts/reagent concentrations. As shown in Figure 8, the various measures of Lewis basicity studied here ($\Delta ACA(\mathbf{x})$, $\Delta BAA(\mathbf{x})$ and $\Delta G_{298}(\mathbf{x})$) are well correlated.

Together with the direct ¹H NMR-spectroscopic detection of **INT1** for the catalysts **1**, **3**, and **4a** (see SI for further details) we thus assume that the stabilities of acylpyridinium intermediates formed with anhydride **14** are, at least in part, responsible for the inverse correlation of acylation rate and Lewis basicity. In addition, we note that acylation rates in diol substrate **16** are moderated through intramolecular hydrogen bonding interactions.

Conclusion

A group of 24 tricyclic pyridine-based Lewis base catalysts have been synthesized with the goal of performing selective acylation reactions of secondary hydroxyl groups in aromatic 1,2-ethanediols with 2-methyl-6-nitrobenzoic anhydride. The acylation of secondary instead of primary hydroxyl groups depends on the surface of the Lewis base and its steric demand. The formation of sandwich structures between DED-substituents of Lewis base catalyst and tricyclic pyridinium surface increase the Lewis basicity by stabilization of acylpyridinium cations and supporting the acylation of secondary alcohol in separated ethanol systems as well as in 1,2-diols. Somewhat surprisingly, the positioning of DED-substituents is less effective through flexible CH₂-linker units as compared to *ortho*-substituted aryl units. Some of the highly Lewis basic pyridine-based catalysts studied here form comparatively stable *N*-acylpyridinium cation intermediates detected both by experimental and quantum chemical analysis. This stability may actually impede catalytic turnover in acylation reactions. In contrast, catalyst **4i** containing two CF₃ groups is predicted to be a more active and selective organocatalyst than **1**. The second finding of this study is, that in 1,2-diol systems the acylation is quite fast with less nucleophilic and sterically demanding catalysts. Tests

towards the selectivities obtained with the reagent/catalyst combinations explored here in polyol natural products are currently under way in our laboratories.

Experimental Section

Competition Experiments: Three different CDCl_3 stock solutions were prepared under nitrogen. Stock solution A contained the secondary alcohol **10** and primary alcohol **11** each at a concentration of 0.05 M. Stock solution B contained anhydride **14** (0.1 M), while stock solution C contained 0.15 M Et_3N and catalyst **1-8** at a concentration of 0.01 M. Stock solution B was diluted in four discrete steps. The concentrations of the new solutions were fixed at 20, 35, 50, and 70% of the initial stock solution B. Under nitrogen 0.4 mL of stock solution A, 0.4 mL of stock solution C, and 0.4 mL of stock solution B1-4 were transferred to a GC vial by using a Hamilton syringe. The GC vial was then capped under nitrogen and placed in the GC vial holder with stirring. The competition experiments were considered finished when the reaction with the highest anhydride concentration (GC vial 4) was complete. The reaction was monitored by ^1H NMR spectroscopy.

Kinetic Studies: Three different CDCl_3 stock solutions containing 0.02 M 1,2-diol **16** (A), 0.06 M acid anhydride **14** (B), and a combination of 0.08 M Et_3N and 0.004 M **1-8** (C) are prepared under nitrogen. The reaction is analysed by ^1H NMR as recorded on a Bruker Avance III 400 machine. NMR tubes are first dried under vacuum using a special home-made apparatus and flushed with nitrogen, and 0.2 mL of stock solution A, 0.2 mL of stock solution C and 0.2 mL of stock solution B are then transferred under nitrogen to the NMR tube by use of a Hamilton syringe. After closing the NMR tube, the reaction mixture is shaken and introduced into the NMR machine.

Computational details: All geometry optimizations and vibrational frequency calculations have been performed using the B3LYP-D3 hybrid functional^[30c-e] in combination with the 6-31+G(d) basis set.^[38] Solvent effects for chloroform have been taken into account with the SMD continuum solvation model.^[30b] This combination has recently been found to perform well for Lewis base-catalysed reactions.^[39] Thermochemical corrections to 298.15 K have been calculated for all stationary points from unscaled vibrational frequencies obtained at this same level. Solvation energies have been obtained as the difference between the energies computed at B3LYP-D3/6-31+G(d) in solution and in gas phase. For the elucidation of the mechanism, the thermochemical corrections of optimized structures have been combined with single point energies calculated at the DLPNO-CCSD(T)/def2-TZVPP//B3LYP-D3/6-31+G(d) level.^[36,40] Solvation energies have been added to the energy computed at DLPNO-CCSD(T)/def2-TZVPP//SMD(CHCl_3)/B3LYP-D3/6-31+G(d) level to yield free energies G_{298} at 298.15 K. Free energies in solution have been corrected to a reference state of 1 mol/L at 298.15 K through addition of $\text{RTln}(24.46) = +7.925$ kJ/mol to the free energies. All calculations have been performed with Gaussian 09^[41] and ORCA version 4.0.^[42] Conformation search was performed with Maestro.^[43]

Acknowledgements

This work was financially supported by the Deutsche Forschungsgemeinschaft (DFG) through the Priority Program "Control of London Dispersion Interactions in Molecular Chemistry" (SPP 1807), grant ZI 436/17-1.

Keywords: Acylation • Regioselectivity • Anhydrides • Lewis bases • Noncovalent interactions

- [1] a) O. Robles, D. Romo, *Nat. Prod. Rep.* **2014**, *31*, 318-334; b) K. C. Nicolaou, J. S. Chen, *Classics in Total Synthesis III*, Wiley-VCH, Weinheim, **2011**.
 [2] a) P. S. Baran, T. J. Maimone, J. M. Richter, *Nature* **2007**, *446*, 404-408; b) G. Zong, E. Barber, H. Aljewari, J. Zhou, Z. Hu, Y. Du,

W. Q. Shi, *J. Org. Chem.* **2015**, *80*, 9279-9291; c) M. Koshimizu, M. Nagatomo, M. Inoue, *Angew. Chem., Int. Ed.* **2016**, *55*, 2493-2497.

- [3] S. M. Polyakova, A. V. Nizovtsev, R. A. Kunetskiy, N. V. Bovin, *Russ. Chem. Bull.* **2015**, *64*, 973-989.
 [4] a) C. A. Lewis, S. J. Miller, *Angew. Chem., Int. Ed.* **2006**, *45*, 5616-5619; b) S. Araki, S. Kambe, K. Kameda, T. Hirashita, *Synthesis* **2003**, *2003*, 0751-0754; c) P. G. M. Wuts, *Greene's Protective Groups in Organic Synthesis*, 5 ed., John Wiley & Sons, Hoboken, New Jersey, **2014**; d) A. Baldessari, C. P. Mangone, E. G. Gros, *Helv. Chim. Acta* **1998**, *81*, 2407-2413; e) K. Ishihara, H. Kurihara, H. Yamamoto, *J. Org. Chem.* **1993**, *58*, 3791-3793; f) T. Maki, F. Iwasaki, Y. Matsumura, *Tetrahedron Lett.* **1998**, *39*, 5601-5604; g) F. Iwasaki, T. Maki, W. Nakashima, O. Onomura, Y. Matsumura, *Org. Lett.* **1999**, *1*, 969-972; h) J. E. Taylor, J. M. J. Williams, S. D. Bull, *Tetrahedron Lett.* **2012**, *53*, 4074-4076.
 [5] a) P. Peng, M. Linseis, R. F. Winter, R. R. Schmidt, *J. Am. Chem. Soc.* **2016**, *138*, 6002-6009; b) M. Nahmany, A. Melman, *Org. Biomol. Chem.* **2004**, *2*, 1563-1572; c) N. A. Afagh, A. K. Yudin, *Angew. Chem., Int. Ed.* **2010**, *49*, 262-310; d) A. H. Haines, *Adv. Carbohydr. Chem. Biochem.* **1976**, *33*, 11-109; e) S. E. Denmark, G. L. Beutner, *Angew. Chem., Int. Ed.* **2008**, *47*, 1560-1638; f) A. C. Spivey, S. Arseniyadis, *Angew. Chem., Int. Ed.* **2004**, *43*, 5436-5441.
 [6] C. Lindner, R. Tandon, Y. Liu, B. Maryasin, H. Zipse, *Org. Biomol. Chem.* **2012**, *10*, 3210-3218.
 [7] C. E. Müller, P. R. Schreiner, *Angew. Chem., Int. Ed.* **2011**, *50*, 6012-6042.
 [8] L. M. Litvinenko, A. I. Kirichenko, *Dokl. Akad. Nauk. SSSR Ser. Khim.* **1967**, *176*, 97-100.
 [9] a) G. Höfle, W. Steglich, H. Vorbrüggen, *Angew. Chem., Int. Ed.* **1978**, *17*, 569-583; b) W. Steglich, G. Höfle, *Angew. Chem., Int. Ed.* **1969**, *8*, 981-981.
 [10] a) W. Steglich, G. Höfle, *Tetrahedron Lett.* **1970**, *11*, 4727-4730; b) A. Hassner, L. R. Krepski, V. Alexanian, *Tetrahedron* **1978**, *34*, 2069-2076.
 [11] M. R. Heinrich, H. S. Klisa, H. Mayr, W. Steglich, H. Zipse, *Angew. Chem., Int. Ed.* **2003**, *42*, 4826-4828.
 [12] R. Tandon, T. Unzner, T. A. Nigst, N. De Rycke, P. Mayer, B. Wendt, O. R. P. David, H. Zipse, *Chem. Eur. J.* **2013**, *19*, 6435-6442.
 [13] T. Kawabata, M. Nagato, K. Takasu, K. Fuji, *J. Am. Chem. Soc.* **1997**, *119*, 3169-3170.
 [14] Y. Wei, I. Held, H. Zipse, *Org. Biomol. Chem.* **2006**, *4*, 4223-4230.
 [15] R. Tandon, T. A. Nigst, H. Zipse, *Eur. J. Org. Chem.* **2013**, *2013*, 5423-5430.
 [16] S. Singh, G. Das, O. V. Singh, H. Han, *Org. Lett.* **2007**, *9*, 401-404.
 [17] I. Held, S. Xu, H. Zipse, *Synthesis* **2007**, *2007*, 1185-1196.
 [18] S. Yamada, *Chem. Rev.* **2018**, *118*, 11353-11432.
 [19] T. Kawabata, W. Muramatsu, T. Nishio, T. Shibata, H. Schedel, *J. Am. Chem. Soc.* **2007**, *129*, 12890-12895.
 [20] E. Kattnig, M. Albert, *Org. Lett.* **2004**, *6*, 945-948.
 [21] S. Mayr, M. Marin-Luna, H. Zipse, *J. Org. Chem.* **2021**, *86*, 3456-3489.
 [22] S. Mayr, H. Zipse, *Chem. Eur. J.* **2021**, *27*, 18084-18092.
 [23] a) B. Pölloth, M. P. Sibi, H. Zipse, *Angew. Chem., Int. Ed.* **2021**, *60*, 774-778; b) J. P. Wagner, P. R. Schreiner, *Angew. Chem., Int. Ed.* **2015**, *54*, 12274-12296.
 [24] The strong Lewis base catalyst **9** was not explored in the experimental part of this work. The reported X-ray structure demonstrates that the Ph rings are orientated such that intra- and intermolecular cation- π stacking interactions are not possible.
 [25] J. Helberg, M. Marin-Luna, H. Zipse, *Synthesis* **2017**, *49*, 3460-3470.
 [26] H. B. Kagan, J. C. Fiaud, *Top. Stereochem.* **1988**, *18*, 249-330.
 [27] E. Larionov, F. Achraimer, J. Humin, H. Zipse, *ChemCatChem* **2012**, *4*, 559-566.
 [28] S. Hoops, S. Sahle, R. Gauges, C. Lee, J. Pahle, N. Simus, M. Singhal, L. Xu, P. Mendes, U. Kummer, *Bioinformatics* **2006**, *22*, 3067-3074.
 [29] a) J. Helberg, T. Ampßler, H. Zipse, *J. Org. Chem.* **2020**, *85*, 5390-5402; b) P. Patschinski, C. Zhang, H. Zipse, *J. Org. Chem.* **2014**, *79*, 8348-8357; c) V. Barbier, F. Couty, O. R. P. David, *Eur. J. Org. Chem.* **2015**, *2015*, 3679-3688; d) T. Tsutsumi, A. Saitoh, T. Kasai,

Annelated Pyridine Bases

- M. Chu, S. Karanjit, A. Nakayama, K. Namba, *Tetrahedron Lett.* **2020**, *61*, 152047.
- [30] a) S. Y. Park, J.-W. Lee, C. E. Song, *Nat. Commun.* **2015**, *6*, 7512; b) A. V. Marenich, C. J. Cramer, D. G. Truhlar, *J. Phys. Chem. B* **2009**, *113*, 6378-6396; c) S. Grimme, *J. Chem. Phys.* **2006**, *124*, 034108; d) A. D. Becke, *J. Chem. Phys.* **1993**, *98*, 5648-5652; e) C. Lee, W. Yang, R. G. Parr, *Phys. Rev. B* **1988**, *37*, 785-789.
- [31] a) C. Lindner, R. Tandon, B. Maryasin, E. Larionov, H. Zipse, *Beilstein J. Org. Chem.* **2012**, *8*, 1406-1442; b) I. Held, E. Larionov, C. Bozler, F. Wagner, H. Zipse, *Synthesis* **2009**, *2009*, 2267-2277; c) Y. Wei, T. Singer, H. Mayr, G. N. Sastry, H. Zipse, *J. Comput. Chem.* **2008**, *29*, 291-297; d) Y. Wei, G. N. Sastry, H. Zipse, *J. Am. Chem. Soc.* **2008**, *130*, 3473-3477; e) I. Held, A. Villinger, H. Zipse, *Synthesis* **2005**, *2005*, 1425-1430.
- [32] Here only a selection of calculated cationic affinity numbers is presented. A full analysis of the ΔACA values with all catalysts is shown in the SI.
- [33] CYLVIEW: CYLview,1.0b; Legault, C. Y., Université de Sherbrooke, **2009** (<http://www.cylview.org>); 3D-Pictures were generated with the CYLview program.
- [34] a) C. R. Kennedy, S. Lin, E. N. Jacobsen, *Angew. Chem., Int. Ed.* **2016**, *55*, 12596-12624; b) J. P. Gallivan, D. A. Dougherty, *J. Am. Chem. Soc.* **2000**, *122*, 870-874.
- [35] O. Takahashi, Y. Kohno, M. Nishio, *Chem. Rev.* **2010**, *110*, 6049-6076.
- [36] a) C. Riplinger, B. Sandhoefer, A. Hansen, F. Neese, *J. Chem. Phys.* **2013**, *139*, 134101; b) C. Riplinger, F. Neese, *J. Chem. Phys.* **2013**, *138*, 034106; c) F. Weigend, R. Ahlrichs, *Phys. Chem. Chem. Phys.* **2005**, *7*, 3297-3305.
- [37] F. A. Carey, R. J. Sundberg, *Advanced Organic Chemistry Part A: Structure and Mechanisms*, 5 ed., Springer Science+Business Media, New York, **2007**.
- [38] G. W. Spitznagel, T. Clark, J. Chandrasekhar, P. V. R. Schleyer, *J. Comput. Chem.* **1982**, *3*, 363-371.
- [39] a) M. Marin-Luna, P. Patschinski, H. Zipse, *Chem. Eur. J.* **2018**, *24*, 15052-15058; b) M. Marin-Luna, B. Pölloth, F. Zott, H. Zipse, *Chem. Sci.* **2018**, *9*, 6509-6515.
- [40] L. A. Curtiss, P. C. Redfern, K. Raghavachari, V. Rassolov, J. A. Pople, *J. Chem. Phys.* **1999**, *110*, 4703-4709.
- [41] Gaussion 09, R. D.01, M. J. Frisch, G. W. Trucks, H. B. Schlegel, G. E. Scuseria, M. A. Robb, J. R. Cheeseman, G. Scalmani, V. Barone, B. Mennucci, G. A. Petersson, H. Nakatsuji, M. Caricato, X. Li, H. P. Hratchian, A. F. Izmaylov, J. Bloino, G. Zheng, J. L. Sonnenberg, M. Hada, M. Ehara, K. Toyota, R. Fukuda, J. Hasegawa, M. Ishida, T. Nakajima, Y. Honda, O. Kitao, H. Nakai, T. Vreven, J. A. Montgomery Jr., J. E. Peralta, F. Ogliaro, M. Bearpark, J. J. Heyd, E. Brothers, K. N. Kudin, V. N. Staroverov, R. Kobayashi, J. Normand, K. Raghavachari, A. Rendell, J. C. Burant, S. S. Iyengar, J. Tomasi, M. Cossi, N. Rega, J. M. Millam, M. Klene, J. E. Knox, J. B. Cross, V. Bakken, C. Adamo, J. Jaramillo, R. Gomperts, R. E. Stratmann, O. Yazyev, A. J. Austin, R. Cammi, C. Pomelli, J. W. Ochterski, R. L. Martin, K. Morokuma, V. G. Zakrzewski, G. A. Voth, P. Salvador, J. J. Dannenberg, S. Dapprich, A. D. Daniels, Ö. Farkas, J. B. Foresman, J. V. Ortiz, J. Cioslowski, D. J. Fox, Gaussian, Inc., W. CT, **2010**.
- [42] F. Neese, *Wiley Interdiscip. Rev. Comput. Mol. Sci.* **2012**, *2*, 73-78.
- [43] Schrödinger Release 2019-2: Jaguar, Schrödinger, LLC, New York, NY, **2019**.

5.1 Experimental Part

General Methods

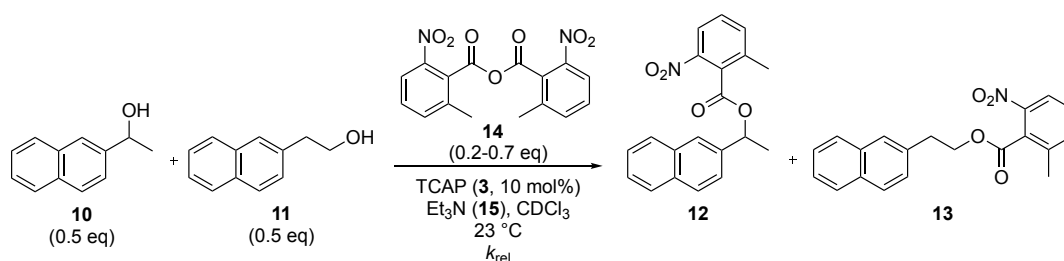
All reactions sensitive to air and moisture were performed under nitrogen atmosphere and the glassware as well as magnetic stir bars were dried overnight in a dry oven at 110 °C. As heat source for temperature controlled reactions an oil bath was used. CDCl_3 , Et_3N and CH_2Cl_2 were freshly distilled over calcium hydride (CaH_2) under nitrogen atmosphere. CDCl_3 was also dried and stored over molecular sieve. All reagents were purchased from the companies TCI, Sigma Aldrich, ABCR or Acros and used without further purification, if not mentioned otherwise. The aromatic alcohol **10**, the acid anhydrides **14**, **29a** and the catalysts DMAP (**1**), PPY (**2**) and TCAP (**3**) have been obtained from commercial sources. The synthesis of acid anhydride precursors **29b,d,e,j,n**, the 1,2-diol **16**, the aromatic alcohol **11**, and the ester products **12**, **13**, **17**, **18** and **19** has been described by Zipse *et al.*^[1] and chapter 4 of this work.^[2] All air- or water-sensitive reagents were stored under nitrogen. If not further specified, solvents were obtained from the companies Acros Organics, Sigma Aldrich or Merck and purified by distillation in a rotary evaporator. Silica gel for column chromatography was purchased from Acros Organics (mesh 35-70). Thin-layer chromatography was performed by using TLC plates purchased from Merck (silica gel 60 F254, thickness 0.2 mm). All ^1H NMR spectra were recorded by Varian Mercury 200, Varian INOVA 400, 600 and Bruker 400, 800 machines in CDCl_3 or $\text{DMSO-}d_6$ at 400 MHz, 600 MHz and 800 MHz at 23 °C. All ^{13}C NMR spectra were recorded respectively at 101 MHz and 151 MHz. The chemical shifts are reported in ppm (δ), relative to the resonance of CDCl_3 at $\delta = 7.26$ ppm and $\text{DMSO-}d_6$ at $\delta = 2.50$ ppm for ^1H and for ^{13}C relative to the resonance of CDCl_3 $\delta = 77.16$ ppm. Spectra were imported and processed in the MestreNova 10.0.2 program. HRMS spectra were obtained by using a Thermo Finnigan LTQ FT machine of the MAT 95 type with a direct exposure probe (DEP) and electron impact ionization (EI, 70 eV). For ESI measurements a Thermo Finnigan LTQ FT Ultra Fourier Transform Ion Cyclotron Resonance machine was used. IR spectra were measured on a Perkin-Elmer FT-IR BX spectrometer mounting an ATR technology module. UV/VIS spectra were measured at the Varian Cary 50 UV/Vis spectrometer. Melting points were measured at a Stuart SMP10 and are stated uncorrected. Crystallographic measurements were done using an Oxford Diffraction XCalibur with Saphir CCD-detector and a molybdenum- K_α -source ($\lambda = 0.71073$) with a concentric circle kappa-device. Structures were resolved using SHELXS or SIR97 and refined with SHELXS. All obtained crystals from the compounds **25c**, **27c** and **4p** were grown in a CDCl_3 solution in NMR tube. The determination of the rate constants of the ethanol system is based on a previous work of the Zipse group^[1] and the determination of the rate constants of the 1,2-ethylenediol system is based on Chapter 4 of this work.^[2] NMR tubes were dried in the oven for at least 12 h. CDCl_3 and Et_3N were freshly distilled under N_2 over CaH_2 before use. In case of the turnover curves the CDCl_3 was dried over molecular sieve and stored under N_2 . Hamilton syringes were cleaned with acetone, dried under vacuum, and flushed with nitrogen prior to use. A GC vial holder (Shimadzu 221-44998-91) was connected to the coolant circuit of a cryostat maintaining +23 °C constantly and placed on a magnetic stirrer. The speed of stirring was fixed at 750 rpm for all the experiments described here. The Lewis base catalysts **4-8** were in each case freshly purified by column chromatography and stored afterwards at 7 °C under N_2 .

5.1.1 Turnover-limited Competition Experiments of 2-Naphthyl Substituted Ethanol

In this part of the work, we chose the model of turnover-limited competition experiments shown in previous work of the Zipse group^[1] with a variation of catalysts. The guideline is based on this previous work.

5.1.1.1 Experimental Design

In the following a general procedure for turnover-limited competition experiments will be described based on the experiment shown in Scheme 5.1. Three different CDCl_3 stock solutions consisting of 0.05 M secondary alcohol **10** and 0.05 M primary alcohol **11** (A), 0.1 M acid anhydride **14** (B) and a combination of 0.15 M Et_3N and 0.01 M TCAP (C) are prepared under nitrogen.



Scheme 5.1. Model example for a competition experiment of secondary alcohol **10** vs. primary alcohol **11** with acid anhydride **14** at a temperature of +23°C.

Table 5.1. Preparation of initial CDCl₃ stock solutions.

Stock solution	Compound	Concentration (mol L ⁻¹)	Volumen (mL)	n (mol)	M.W. (g mol ⁻¹)	Mass (mg)
Stock A	10	0.05	5	250·10 ⁻⁶	172.22	43.1
	11	0.05	5	250·10 ⁻⁶	172.22	43.1
Stock B	14	0.10	2	200·10 ⁻⁶	344	137.6
Stock C	Et₃N	0.15	2	300·10 ⁻⁶	101	60.7
	TCAP	0.01	2	20·10 ⁻⁶	174	3.5

Afterwards stock solution B is diluted into four different concentrated solutions of B shown in Table 5.2. The concentrations of these solutions have been fixed at 20, 35, 50 and 70% of the initial stock solution B.

Table 5.2. Preparation of stock solutions B with different concentrations of B1-B4.

	Stock solution	Concentration (mol L ⁻¹)	Vol. B ^b (mL)	Volumen (mL)
1	Stock B1 (20%) ^a	0.020	0.20	1
2	Stock B2 (35%)	0.035	0.35	1
3	Stock B3 (50%)	0.050	0.50	1
4	Stock B4 (70%)	0.070	0.70	1

^aRelative to Stock B; ^bSolution volume got from initial Stock B

Under nitrogen 0.4 mL of stock solution A, 0.4 mL of stock solution C, and 0.4 mL of stock solution B1 are transferred to a GC vial by use of a Hamilton syringe. The GC vial is then capped under nitrogen and placed in the GC vial holder with stirring. The competition experiment is considered finished when the reaction with the highest anhydride concentration (GC vial 4, 70% of stock solution B) is over.

Composition of each prepared GC vial for one turnover-limited competition experiment:

GC vial 1: 0.4 mL Stock A; 0.4 mL Stock C; 0.4 mL Stock B1

GC vial 2: 0.4 mL Stock A; 0.4 mL Stock C; 0.4 mL Stock B2

GC vial 3: 0.4 mL Stock A; 0.4 mL Stock C; 0.4 mL Stock B3

GC vial 4: 0.4 mL Stock A; 0.4 mL Stock C; 0.4 mL Stock B4

In terms of the actual starting concentrations (mol/L) for all components:

GC vial 1: **10** and **11:** 0.0167, **5c:** 0.0067, **Et₃N:** 0.0500, **TCAP:** 0.0033

GC vial 2: **10** and **11:** 0.0167, **5c:** 0.0117, **Et₃N:** 0.0500, **TCAP:** 0.0033

GC vial 3: **10** and **11:** 0.0167, **5c:** 0.0167, **Et₃N:** 0.0500, **TCAP:** 0.0033

GC vial 4: **10** and **11:** 0.0167, **5c:** 0.0233, **Et₃N:** 0.0500, **TCAP:** 0.0033

The reaction is monitored by ¹H NMR. NMR tubes are dried under vacuum using a Schlenk based glassware. 0.6 mL of the solution contained in the GC vial is transferred to the NMR tube under nitrogen. The NMR tube is then capped and the relative concentrations of all reactants/products determined by ¹H NMR spectroscopy.

5.1.1.2 ^1H NMR Analysis

The ^1H NMR spectra of the competition experiments were edited by MestReNova 10.0. The spectra were corrected by using automatic phase correction and Bernstein polynomial fit with polynomial order 3 for the 600 MHz. The 400 and 800 MHz spectra were corrected by using automatic phase correction and Whittaker Smoother fit. In one of the rather cases of 800 MHz spectra, the Whittaker Smoother fit do not generate a moderate baseline so that the Polynomial fit has to be used. All spectra were referenced by the solvent signal of CDCl_3 ($\delta = 7.26$ ppm). For the secondary alcohol **10** and ester **12** the hydrogen signal of the CH group was integrated as a guide for the evolution of the reaction. If there was an overlap with other signals, the corresponding CH_2 group signals were used. For the primary alcohol **11** and ester **13** the hydrogen signal of one of the CH_2 groups was integrated as a guide.

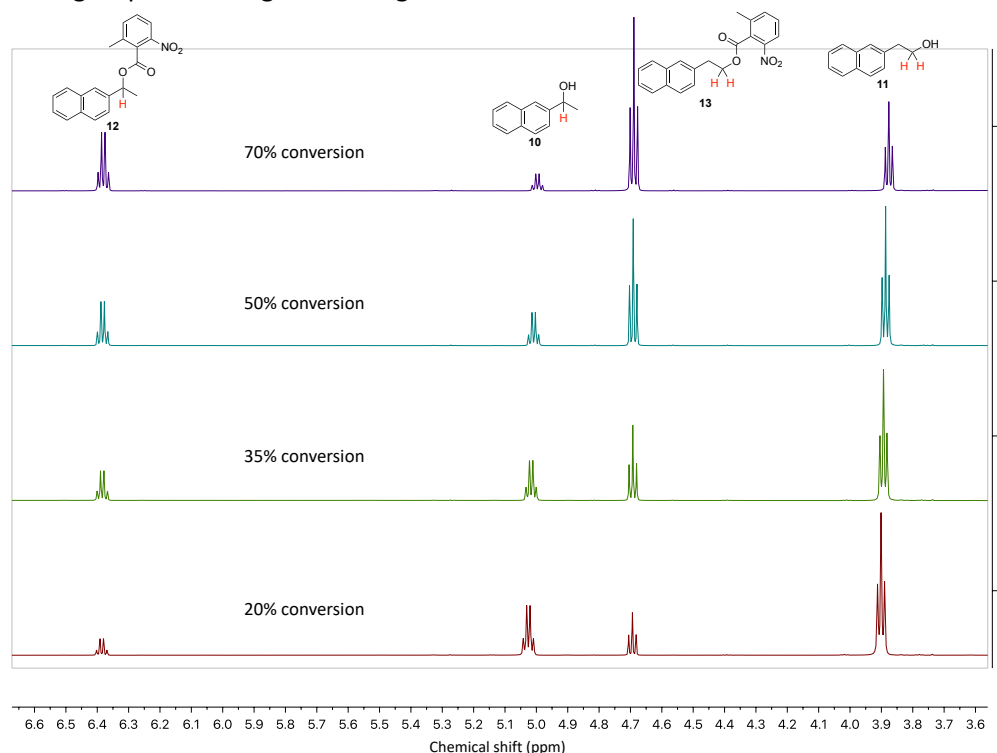
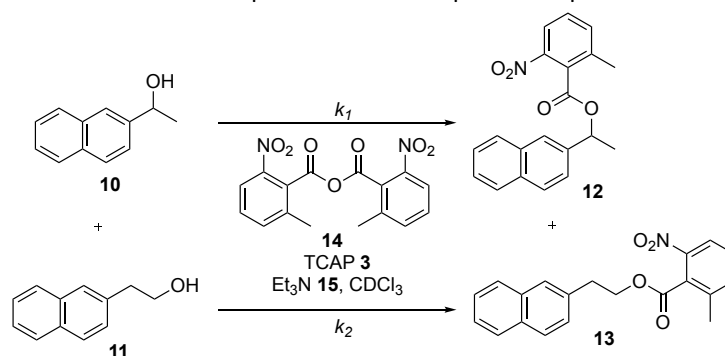


Figure 5.1. Example of the stacked ^1H NMR spectra for the competition experiment between **10** and **11** with **14**.



Scheme 5.2. General equation for the turnover-limited competition experiment.

We determined that after full conversion of the reaction the composition of the products is varied through equilibrium processes. Because of this, we can calculate the relative rate constants from the product ratios defined in Eq. 5.1.

$$k_{\text{rel}} = \frac{k_2}{k_1} = \frac{k_{(11+14)}}{k_{(10+14)}} \quad \text{Eq. 5.1}$$

The relative rate constant k_{rel} is determined through measuring chemoselectivity and conversion according to Eq. 5.2.^[3]

$$k_{\text{rel}} = \frac{\ln[1-\text{conv}(1+C)]}{\ln[1-\text{conv}(1-C)]} \quad \text{Eq. 5.2}$$

Annelated Pyridine Bases

The conversion is defined by Eq. 5.3, where the integrals of the ^1H NMR spectra were assumed to correspond to the concentrations.

$$\text{Conversion}(\%) = \left(\frac{[\mathbf{12}] + [\mathbf{13}]}{[\mathbf{10}] + [\mathbf{11}] + [\mathbf{12}] + [\mathbf{13}]} \right) \cdot 100 \quad \text{Eq. 5.3}$$

The chemoselectivity is defined by Eq. 5.4:

$$\text{Chemoselectivity}_{\text{exp}} (C_{\text{exp}}) = \frac{[\mathbf{13}] - [\mathbf{12}]}{[\mathbf{13}] + [\mathbf{12}]} \quad \text{Eq. 5.4}$$

A correction factor f was introduced, which defines the exact ratio of both reactants present in the reaction medium (this should be close to the ideal 1:1), to avoid the human-error in the preparation of the samples (Eq. 5.5):

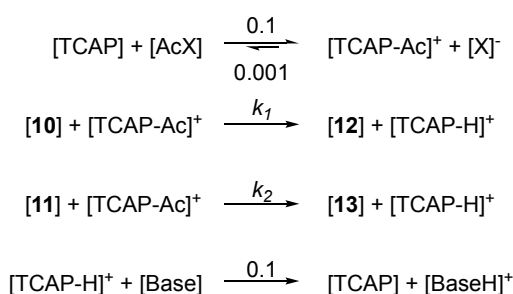
$$f = \frac{[\mathbf{10}] + [\mathbf{12}]}{[\mathbf{11}] + [\mathbf{13}]} \quad \text{Eq. 5.5}$$

This correction factor f was now allowed in the equation for chemoselectivity and Eq. 5.6 was defined.

$$\text{Chemoselectivity} (C) = \frac{[\mathbf{13}] \cdot f - [\mathbf{12}]}{[\mathbf{13}] \cdot f + [\mathbf{12}]} \quad \text{Eq. 5.6}$$

5.1.1.3 Simulation of Turnover-limited Competition Experiments

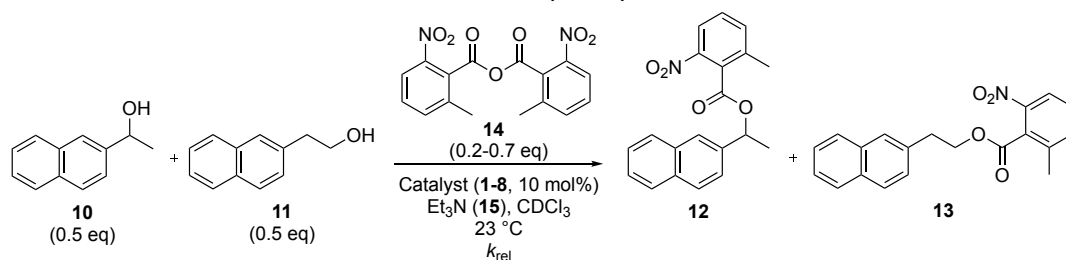
With the help of the CoPaSi^[4] and ProFit programs the k_{rel} values for the turnover-limited competition experiments have been simulated. Scheme 5.3 shows the reactions used in CoPaSi, in which the k values have been modified in order to achieve the k_{rel} values. k_1 and k_2 have been changed, while the other rate constants were held constant.

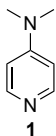
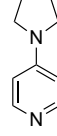
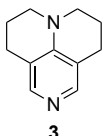
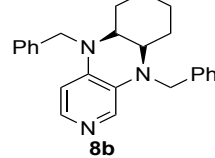
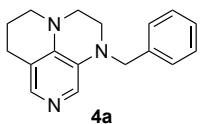
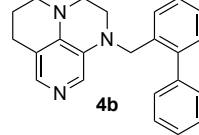
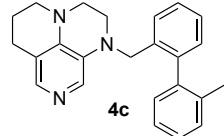
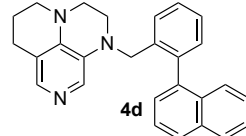


Scheme 5.3. Model reaction used in CoPaSi for simulation of the rate constants.

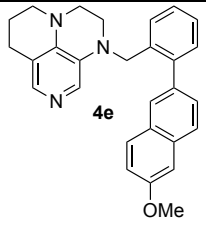
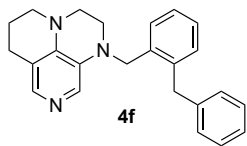
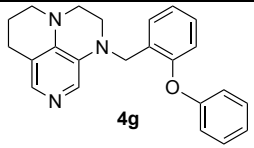
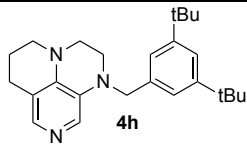
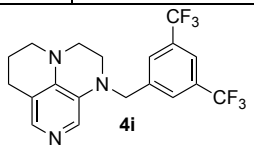
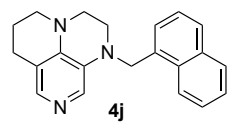
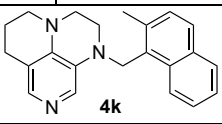
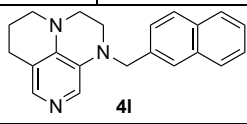
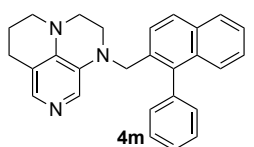
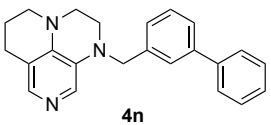
The rate constants of the different turnover-limited competition experiments were simulated by CoPaSi by using the starting concentrations of the experiments. The simulated concentrations over the time were used to calculate the conversion by Eq. 5.3 and chemoselectivity by Eq. 5.6. In Figures 5.2 till 5.9 the conversion was plotted against the chemoselectivity, which allows us the illustrative comparison of experimental and simulated results.

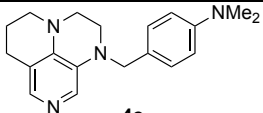
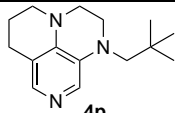
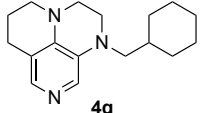
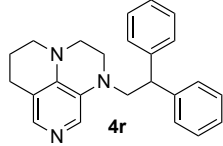
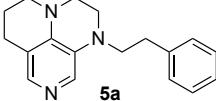
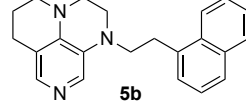
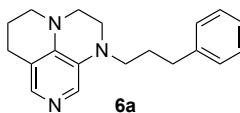
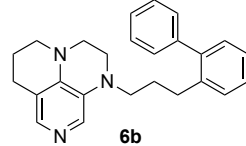
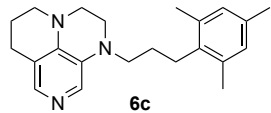
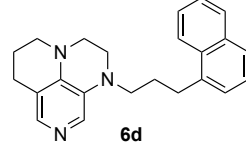
5.1.1.4 Results of Turnover-limited Competition Experiments

Table 5.3. Conversion, corrected chemoselectivity, relative rate and natural logarithm of relative rate with standard deviations calculated from ^1H NMR measurements for turnover-limited competition experiments between **10** and **11**with **14** catalysed by **1-8**.

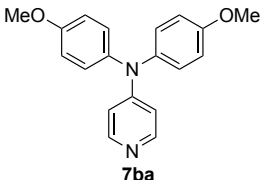
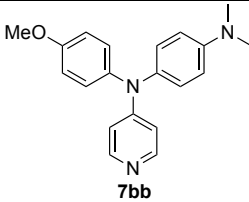
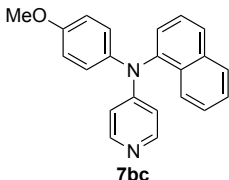
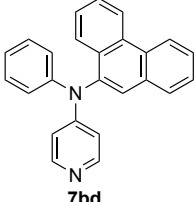
							
Conv.	Chem.	k_{rel}	$\ln(k_{rel})$	Conv.	Chem.	k_{rel}	$\ln(k_{rel})$
19.69	0.15	1.42	0.35	20.11	0.07	1.16	0.151
35.81	0.14	1.44	0.36	35.86	0.09	1.26	0.235
49.95	0.13	1.45	0.37	50.17	0.08	1.27	0.236
68.37	0.10	1.44	0.36	68.37	0.07	1.28	0.25
		1.44 ± 0.015	0.36 ± 0.011			1.24 ± 0.054	0.22 ± 0.045
							
Conv.	Chem.	k_{rel}	$\ln(k_{rel})$	Conv.	Chem.	k_{rel}	$\ln(k_{rel})$
17.59	-0.17	0.69	-0.37	11.65	0.17	1.43	0.35
33.14	-0.16	0.68	-0.39	28.16	0.11	1.31	0.27
47.86	-0.14	0.68	-0.39	38.42	0.11	1.33	0.28
68.74	-0.10	0.68	-0.38	58.59	0.09	1.32	0.28
		0.68 ± 0.006	-0.38 ± 0.008			1.35 ± 0.046	0.30 ± 0.034
							
Conv.	Chem.	k_{rel}	$\ln(k_{rel})$	Conv.	Chem.	k_{rel}	$\ln(k_{rel})$
13.48	-0.11	0.80	-0.23	12.20	-0.19	0.66	-0.41
27.06	-0.12	0.76	-0.27	26.25	-0.18	0.65	-0.43
37.10	-0.10	0.78	-0.25	42.03	-0.17	0.64	-0.44
48.40	-0.08	0.80	-0.23	58.57	-0.14	0.64	-0.45
		0.78 ± 0.014	-0.24 ± 0.018			0.65 ± 0.009	-0.43 ± 0.013
							
Conv.	Chem.	k_{rel}	$\ln(k_{rel})$	Conv.	Chem.	k_{rel}	$\ln(k_{rel})$
20.90	-0.21	0.62	-0.48	10.04	-0.20	0.65	-0.44
27.21	-0.20	0.62	-0.47	22.13	-0.20	0.63	-0.46
42.91	-0.17	0.63	-0.46	42.36	-0.19	0.60	-0.50
56.10	-0.14	0.65	-0.44	55.09	-0.15	0.63	-0.46

Annelated Pyridine Bases

		0.63 ± 0.010	-0.46 ± 0.016			0.63 ± 0.015	-0.47 ± 0.024
 4e				 4f			
<i>Conv.</i>	<i>Chem.</i>	k_{rel}	$\ln(k_{rel})$	<i>Conv.</i>	<i>Chem.</i>	k_{rel}	$\ln(k_{rel})$
25.79	-0.24	0.57	-0.56	15.65	-0.18	0.67	-0.40
31.76	-0.22	0.58	-0.55	28.80	-0.17	0.66	-0.42
43.39	-0.21	0.57	-0.56	43.11	-0.15	0.67	-0.39
		Signaloverlapping	60.20	-0.12	0.67	-0.40	
		0.57 ± 0.003	-0.56 ± 0.005			0.67 ± 0.007	-0.40 ± 0.010
 4g				 4h			
<i>Conv.</i>	<i>Chem.</i>	k_{rel}	$\ln(k_{rel})$	<i>Conv.</i>	<i>Chem.</i>	k_{rel}	$\ln(k_{rel})$
16.52	-0.16	0.70	-0.35	14.32	-0.19	0.67	-0.40
32.00	-0.16	0.67	-0.39	28.36	-0.16	0.69	-0.37
47.94	-0.14	0.67	-0.40	40.00	-0.14	0.69	-0.37
66.29	-0.10	0.68	-0.38	59.08	-0.11	0.70	-0.36
		0.68 ± 0.011	-0.38 ± 0.017			0.69 ± 0.011	-0.38 ± 0.017
 4i				 4j			
<i>Conv.</i>	<i>Chem.</i>	k_{rel}	$\ln(k_{rel})$	<i>Conv.</i>	<i>Chem.</i>	k_{rel}	$\ln(k_{rel})$
17.03	-0.16	0.70	-0.36	11.89	-0.14	0.75	-0.29
30.14	-0.17	0.66	-0.41	24.49	-0.13	0.75	-0.29
47.97	-0.15	0.65	-0.42	36.69	-0.12	0.74	-0.30
64.48	-0.12	0.66	-0.41	55.87	-0.09	0.75	-0.29
		0.67 ± 0.017	-0.40 ± 0.025			0.75 ± 0.003	-0.29 ± 0.004
 4k				 4l			
<i>Conv.</i>	<i>Chem.</i>	k_{rel}	$\ln(k_{rel})$	<i>Conv.</i>	<i>Chem.</i>	k_{rel}	$\ln(k_{rel})$
17.92	-0.12	0.77	-0.26	24.85	-0.11	0.78	-0.25
25.63	-0.11	0.77	-0.26	32.63	-0.10	0.78	-0.25
43.76	-0.11	0.75	-0.29	46.23	-0.09	0.78	-0.25
53.44	-0.09	0.77	-0.26	64.92	-0.07	0.79	-0.24
		0.77 ± 0.010	-0.27 ± 0.014			0.78 ± 0.005	-0.25 ± 0.006
 4m				 4n			
<i>Conv.</i>	<i>Chem.</i>	k_{rel}	$\ln(k_{rel})$	<i>Conv.</i>	<i>Chem.</i>	k_{rel}	$\ln(k_{rel})$
17.39	-0.21	0.62	-0.48	11.98	-0.12	0.77	-0.27
31.42	-0.19	0.62	-0.47	23.04	-0.11	0.78	-0.24
45.91	-0.17	0.63	-0.47	36.61	-0.11	0.77	-0.27
64.17	-0.13	0.64	-0.44	54.12	-0.08	0.78	-0.25

		0.63 ± 0.008	-0.47 ± 0.013			0.77 ± 0.008	-0.26 ± 0.010
 4o				 4p			
<i>Conv.</i>	<i>Chem.</i>	k_{rel}	$\ln(k_{rel})$	<i>Conv.</i>	<i>Chem.</i>	k_{rel}	$\ln(k_{rel})$
18.53	-0.11	0.78	-0.24	19.42	-0.10	0.80	-0.22
33.56	-0.11	0.77	-0.26	32.32	-0.09	0.80	-0.22
45.79	-0.10	0.77	-0.26	45.80	-0.08	0.80	-0.23
		signaloverlapping		67.78	-0.06	0.81	-0.21
		0.77 ± 0.007	-0.26 ± 0.009			0.80 ± 0.005	-0.22 ± 0.006
 4q				 4r			
<i>Conv.</i>	<i>Chem.</i>	k_{rel}	$\ln(k_{rel})$	<i>Conv.</i>	<i>Chem.</i>	k_{rel}	$\ln(k_{rel})$
14.13	-0.03	0.93	-0.07	14.45	-0.06	0.88	-0.13
29.78	-0.04	0.91	-0.10	29.83	-0.04	0.90	-0.10
42.17	-0.04	0.89	-0.12	46.03	-0.05	0.87	-0.14
64.90	-0.03	0.89	-0.12	61.96	-0.04	0.89	-0.12
		0.90 ± 0.017	-0.10 ± 0.019			0.89 ± 0.013	-0.12 ± 0.015
 5a				 5b			
<i>Conv.</i>	<i>Chem.</i>	k_{rel}	$\ln(k_{rel})$	<i>Conv.</i>	<i>Chem.</i>	k_{rel}	$\ln(k_{rel})$
18.78	-0.11	0.78	-0.25	16.54	-0.13	0.75	-0.29
32.88	-0.10	0.79	-0.24	29.49	-0.11	0.77	-0.27
48.72	-0.09	0.77	-0.26	40.72	-0.10	0.78	-0.25
67.51	-0.07	0.78	-0.25	62.16	-0.08	0.77	-0.26
		0.78 ± 0.006	-0.25 ± 0.008			0.76 ± 0.012	-0.27 ± 0.015
 6a				 6b			
<i>Conv.</i>	<i>Chem.</i>	k_{rel}	$\ln(k_{rel})$	<i>Conv.</i>	<i>Chem.</i>	k_{rel}	$\ln(k_{rel})$
13.11	-0.10	0.81	-0.21	14.71	-0.10	0.80	-0.22
25.46	-0.08	0.83	-0.18	28.55	-0.08	0.82	-0.19
38.19	-0.07	0.84	-0.17	44.39	-0.08	0.81	-0.21
52.77	-0.04	0.88	-0.12	62.79	-0.06	0.81	-0.21
		0.84 ± 0.026	-0.17 ± 0.030			0.81 ± 0.008	-0.21 ± 0.010
 6c				 6d			
<i>Conv.</i>	<i>Chem.</i>	k_{rel}	$\ln(k_{rel})$	<i>Conv.</i>	<i>Chem.</i>	k_{rel}	$\ln(k_{rel})$
14.50	-0.12	0.77	-0.26	15.05	-0.11	0.79	-0.24
30.29	-0.09	0.81	-0.21	29.67	-0.09	0.81	-0.21
39.87	-0.08	0.82	-0.20	47.51	-0.09	0.77	-0.26
59.12	-0.05	0.85	-0.16	63.45	-0.07	0.79	-0.23
		0.81 ± 0.028	-0.21 ± 0.034			0.79 ± 0.016	-0.23 ± 0.020

Annelated Pyridine Bases

 7ba a				 7bb a			
Conv.	Chem.	k_{rel}	$\ln(k_{rel})$	Conv.	Chem.	k_{rel}	$\ln(k_{rel})$
18.09	-0.15	0.72	-0.33	17.46	-0.09	0.81	-0.21
30.45	-0.13	0.72	-0.32	29.36	-0.08	0.82	-0.20
45.02	-0.12	0.72	-0.33	43.66	-0.07	0.82	-0.19
56.30	-0.11	0.72	-0.33	61.77	-0.05	0.84	-0.17
		0.72 ± 0.002	-0.33 ± 0.003			0.82 ± 0.010	-0.19 ± 0.012
 7bc a				 7bd a			
Conv.	Chem.	k_{rel}	$\ln(k_{rel})$	Conv.	Chem.	k_{rel}	$\ln(k_{rel})$
17.55	-0.08	0.84	-0.17	24.09	-0.03	0.94	-0.06
32.66	-0.06	0.86	-0.15	28.83	-0.03	0.94	-0.06
48.11	-0.05	0.87	-0.14	43.58	-0.02	0.95	-0.05
66.19	-0.04	0.87	-0.13	56.82	-0.03	0.92	-0.09
		0.86 ± 0.012	-0.15 ± 0.014			0.94 ± 0.012	-0.07 ± 0.013

^a Raw NMR data were experimentally determined by A. Mateos Calbet^[5] under the supervision of S. Mayr. The herein reported data are fully reanalyzed.

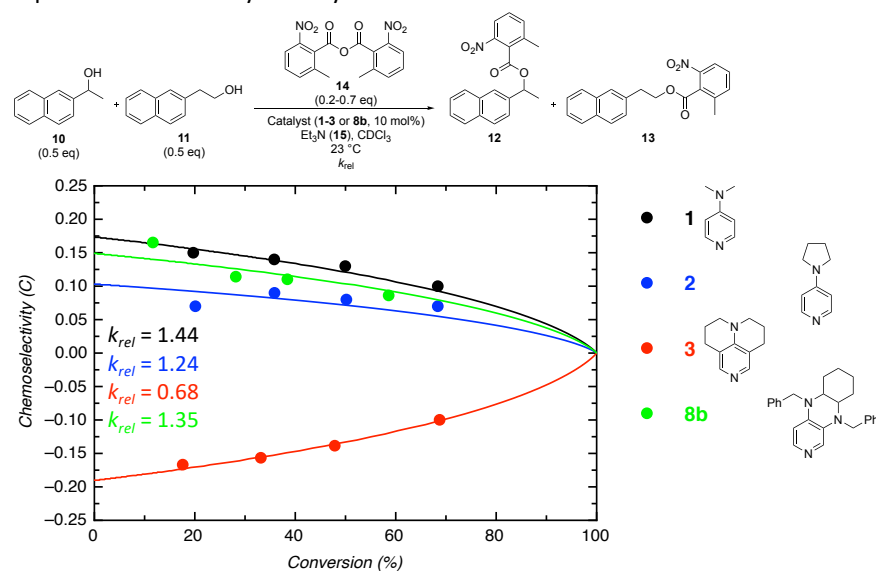


Figure 5.2. Plot of conversion (%) vs. chemoselectivity for turnover-limited competition experiment **10** vs. **11** with **14** catalysed by **1-3**, **8b**.

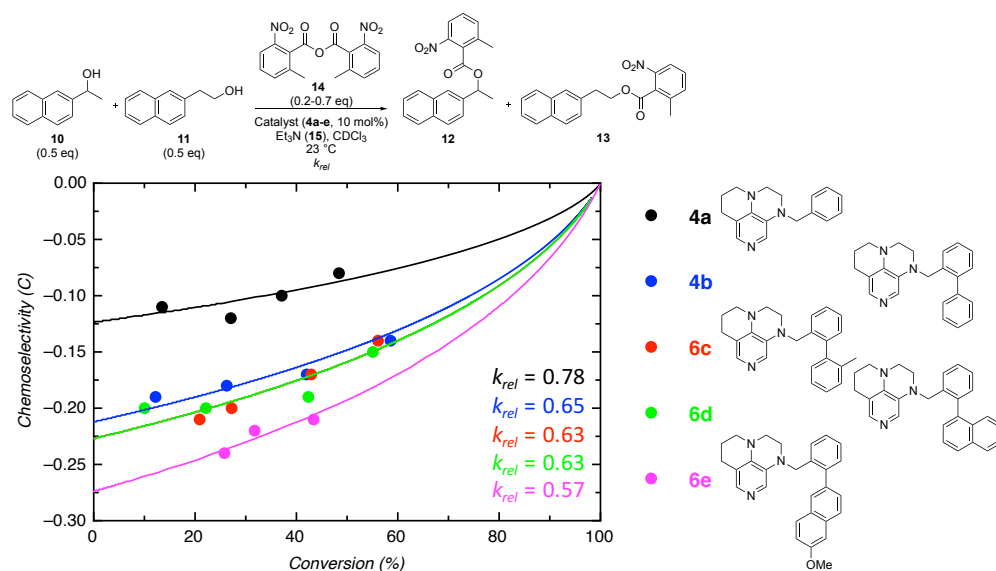


Figure 5.3. Plot of conversion (%) vs. chemoselectivity for turnover-limited competition experiment 10 vs. 11 with 14 catalysed by 4a-e.

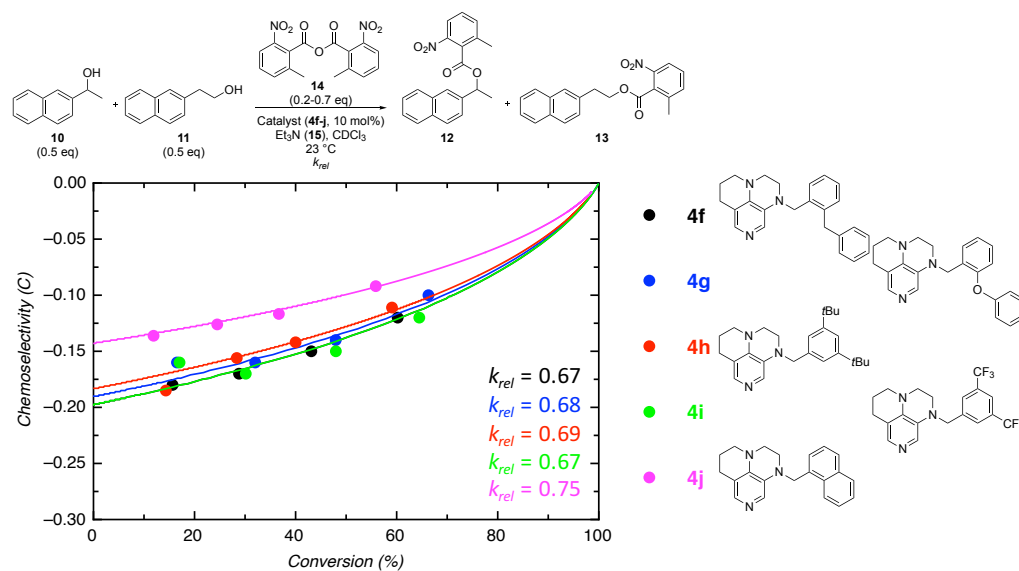


Figure 5.4. Plot of conversion (%) vs. chemoselectivity for turnover-limited competition experiment 10 vs. 11 with 14 catalysed by 4f-j.

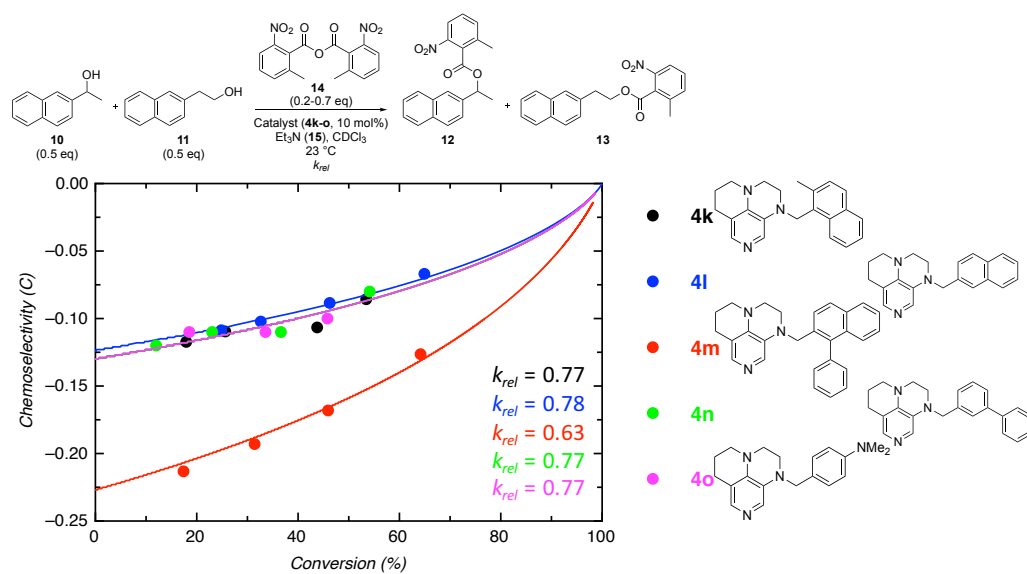


Figure 5.5. Plot of conversion (%) vs. chemoselectivity for turnover-limited competition experiment 10 vs. 11 with 14 catalysed by 4k-o.

Annulated Pyridine Bases

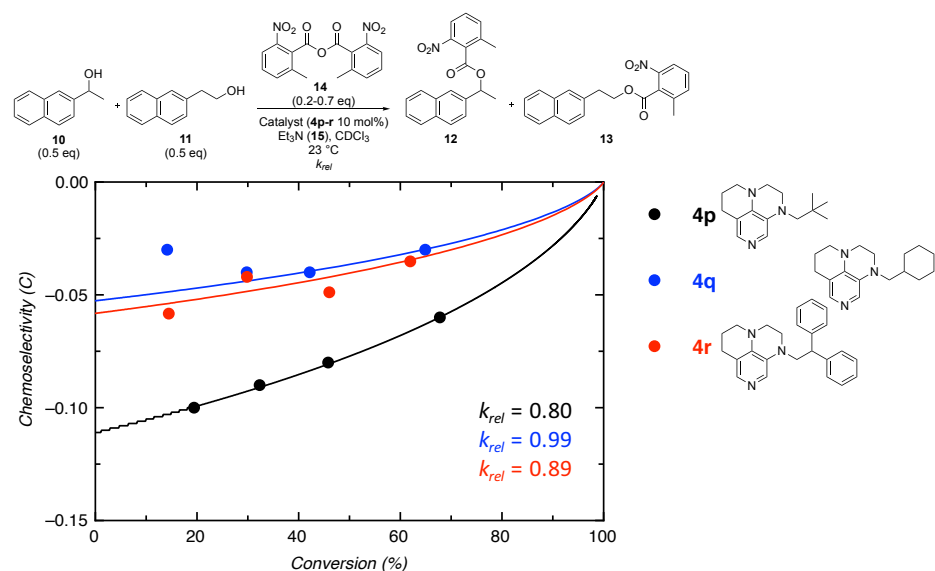


Figure 5.6. Plot of conversion (%) vs. chemoselectivity for turnover-limited competition experiment 10 vs. 11 with 14 catalysed by 4p-r.

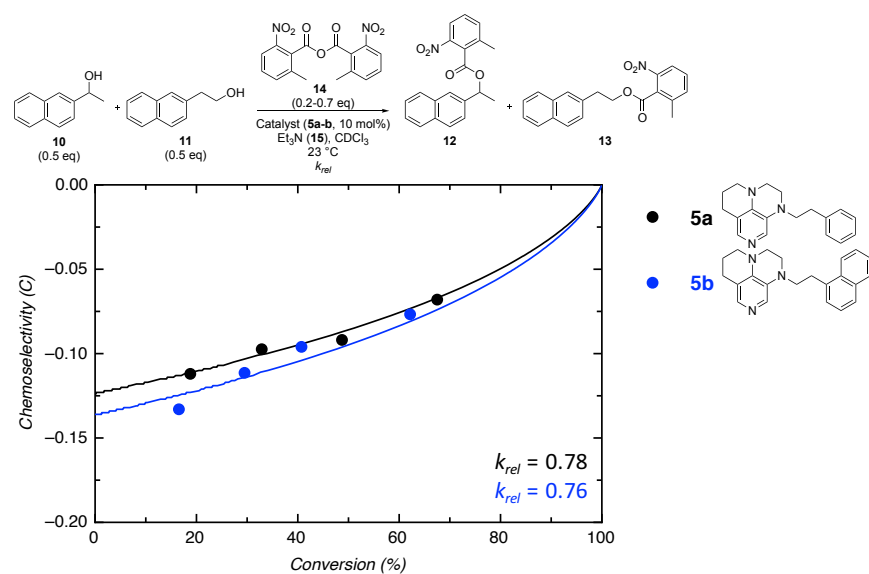


Figure 5.7. Plot conversion (%) vs. chemoselectivity for turnover-limited competition experiment 10 vs. 11 with 14 catalysed by 5a-b.

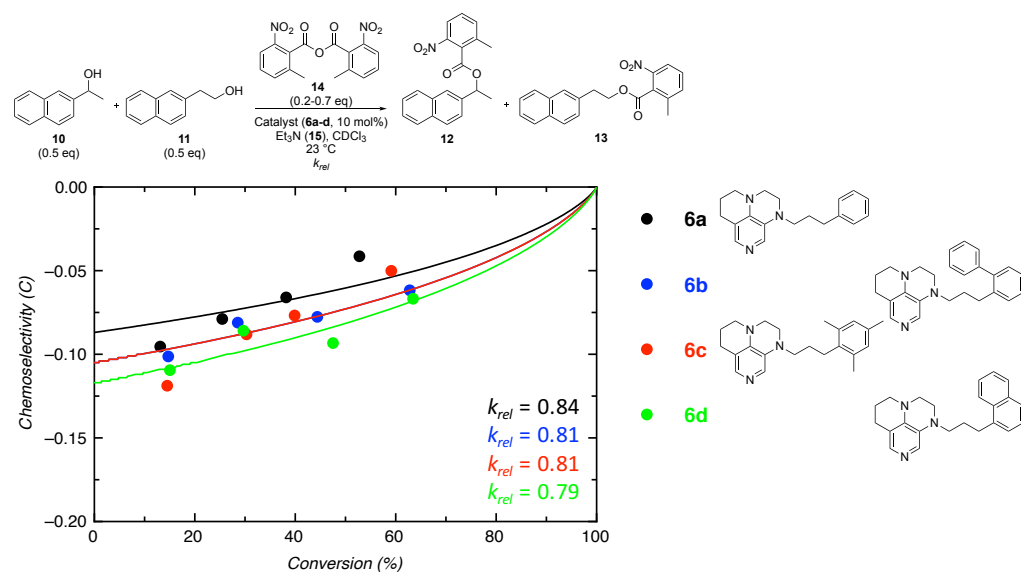


Figure 5.8. Plot of conversion (%) vs. chemoselectivity for turnover-limited competition experiment 10 vs. 11 with 14 catalysed by 6a-d.

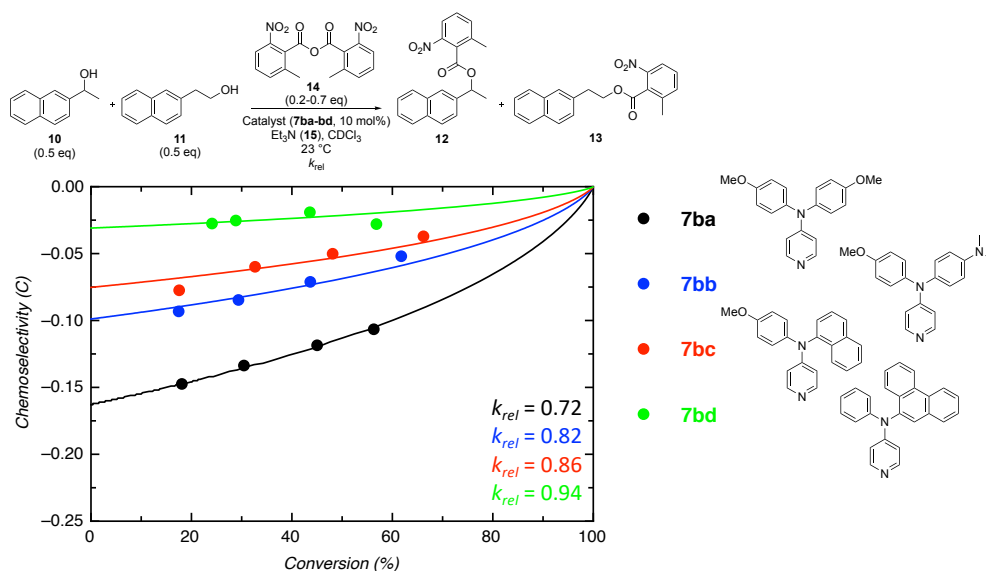


Figure 5.9. Plot of *conversion (%)* vs. *chemoselectivity* for turnover-limited competition experiment **10** vs. **11** with **14** catalysed by **7ba-bd**.

Table 5.4. Integral regions, relative and absolute integral values for turnover-limited competition experiment competition experiments of alcohol **10** vs. **11** using acid anhydride **14** catalyzed by **1-8**.

Conv	1	region	region	integral	absolute	Conv	2	region	region	integral	absolute
20%	10	4.95	5.04	0.52	61719.03	10	1.54	1.60	1.00	192251.60	
	11	3.84	3.92	1.00	118119.72	11	3.90	3.99	0.64	122841.69	
	12	6.28	6.37	0.10	12290.36	12	1.76	1.81	0.23	44387.17	
	13	4.60	4.68	0.29	34628.48	13	4.66	4.75	0.17	33584.13	
35%	10	4.93	5.04	0.57	52118.17	10	1.51	1.61	1.00	164208.82	
	11	3.83	3.90	1.00	91923.15	11	3.90	3.96	0.57	93050.12	
	12	6.29	6.38	0.25	23004.89	12	1.76	1.81	0.48	79453.42	
	13	4.59	4.68	0.69	63437.60	13	4.67	4.74	0.37	60241.00	
50%	10	4.93	5.02	0.63	42414.76	10	1.47	1.52	1.00	109181.85	
	11	3.84	3.89	1.00	67441.45	11	3.83	3.89	0.57	61887.58	
	12	6.27	6.37	0.48	32561.88	12	1.69	1.76	0.85	93281.71	
	13	4.59	4.67	1.29	86822.76	13	4.60	4.68	0.67	73401.16	
70%	10	5.01	5.09	0.73	25743.42	10	1.53	1.58	1.00	72019.94	
	11	3.87	3.97	1.00	35274.53	11	3.90	3.97	0.51	36894.73	
	12	6.36	6.44	1.18	41465.65	12	1.76	1.81	1.76	127018.45	
	13	4.67	4.76	2.97	104613.66	13	4.67	4.75	1.37	98864.10	
Conv	3	region	region	integral	absolute	Conv	8b	region	region	integral	absolute
20%	10	4.99	5.07	1.00	3621.54	10	5.01	5.13	1.00	67574.05	
	11	3.87	3.93	2.25	8152.03	11	3.88	3.97	1.99	134453.97	
	12	6.36	6.42	0.26	939.91	12	6.36	6.44	0.11	7252.42	
	13	4.67	4.73	0.39	1406.47	13	3.20	3.28	0.31	21039.53	
35%	10	4.98	5.05	0.99	2773.01	10	5.01	5.11	1.00	56229.59	
	11	3.86	3.92	2.40	6739.97	11	3.89	3.97	1.90	106572.79	
	12	6.35	6.42	0.62	1731.92	12	6.36	6.44	0.33	18634.62	
	13	4.67	4.73	0.94	2626.20	13	3.21	3.28	0.86	48573.00	
50%	10	4.97	5.03	0.99	2035.56	10	4.99	5.09	1.00	44476.52	
	11	3.86	3.92	2.70	5522.43	11	3.88	3.97	1.76	78435.42	
	12	6.35	6.41	1.20	2454.51	12	6.37	6.43	0.52	23079.12	
	13	4.66	4.72	1.90	3896.49	13	3.18	3.29	1.31	58297.26	
70%	10	4.95	5.04	1.00	1071.04	10	4.99	5.09	1.00	32206.03	
	11	3.85	3.91	3.30	3533.90	11	3.88	3.96	1.63	52415.87	
	12	6.34	6.42	3.13	3352.21	12	1.73	1.82	3.45	110953.01	
	13	4.66	4.72	5.39	5774.03	13	3.20	3.28	2.84	91340.24	
Conv	4a	region	region	integral	absolute	Conv	4b	region	region	integral	absolute

Annelated Pyridine Bases

20%	10	5.03	5.09	1.00	26232.54	20%	10	5.03	5.09	1.00	14617.36
	11	3.92	3.96	1.96	51446.28		11	3.91	3.97	2.21	32358.30
	12	6.38	6.43	0.17	4580.41		12	6.36	6.43	0.17	2497.65
	13	4.69	4.73	0.27	7032.79		13	4.68	4.74	0.24	3563.89
35%	10	5.03	5.08	1.00	21214.49	35%	10	5.03	5.09	1.00	11877.83
	11	3.91	3.95	2.04	43240.75		11	3.90	3.96	2.36	27983.82
	12	6.37	6.43	0.43	9120.10		12	6.37	6.43	0.45	5366.75
	13	4.68	4.74	0.64	13534.77		13	4.68	4.74	0.65	7682.69
50%	10	5.02	5.08	1.00	28259.77	50%	10	5.02	5.08	1.00	8772.93
	11	3.90	3.96	2.01	56906.27		11	3.90	3.97	2.69	23632.72
	12	6.37	6.42	0.68	19248.61		12	6.37	6.43	0.97	8498.23
	13	4.69	4.73	1.00	28399.05		13	4.69	4.74	1.47	12863.08
70%	10	5.01	5.06	1.00	20176.19	70%	10	5.00	5.09	1.00	5751.30
	11	3.90	3.94	2.17	43796.52		11	3.90	3.95	3.19	18336.63
	12	6.37	6.43	1.09	21992.55		12	6.37	6.44	2.03	11648.64
	13	4.69	4.73	1.73	34939.12		13	4.68	4.74	3.28	18888.44
Conv	4c	region	region	integral	absolute	Conv	4d	region	region	integral	absolute
20%	10	4.94	5.04	1.00	57425.14	20%	10	5.01	5.12	1.00	65368.53
	11	3.82	3.91	2.27	130474.97		11	3.89	3.96	2.08	136116.58
	12	6.25	6.39	0.34	19476.18		12	6.34	6.45	0.14	8976.50
	13	4.60	4.69	0.45	25884.80		13	4.66	4.76	0.18	11814.41
35%	10	4.92	5.02	1.01	52595.75	35%	10	4.99	5.13	1.00	53928.10
	11	3.82	3.90	2.38	123944.64		11	3.87	3.97	2.29	123506.80
	12	6.28	6.39	0.49	25514.63		12	6.36	6.45	0.36	19595.05
	13	4.59	4.68	0.66	34636.81		13	4.66	4.77	0.49	26576.04
50%	10	4.94	5.02	1.00	33376.92	50%	10	5.00	5.10	1.00	37558.19
	11	3.82	3.90	2.62	87413.93		11	3.89	3.98	2.71	101903.75
	12	6.27	6.40	1.01	33750.24		12	6.33	6.47	1.02	38164.59
	13	4.60	4.69	1.45	48351.81		13	4.66	4.75	1.43	53783.15
70%	10	5.00	5.09	1.00	23041.15	70%	10	5.00	5.10	1.00	24515.97
	11	3.88	3.95	2.81	64683.57		11	3.87	3.96	2.97	72766.24
	12	6.35	6.45	1.77	40709.98		12	6.34	6.47	1.73	42451.08
	13	4.67	4.73	2.61	60105.99		13	4.64	4.76	2.63	64493.20
Conv	4e	region	region	integral	absolute	Conv	4f	region	region	integral	absolute
20%	10	5.02	5.10	1.00	45530.05	20%	10	5.03	5.09	1.00	3421.32
	11	2.98	3.07	2.71	123223.60		11	3.91	3.96	2.10	7186.07
	12	6.34	6.45	0.48	21820.55		12	6.36	6.44	0.23	772.97
	13	4.66	4.75	0.68	30829.57		13	4.69	4.74	0.31	1057.03
35%	10	5.00	5.10	1.00	42575.36	35%	10	5.02	5.09	1.00	2828.72
	11	2.98	3.06	2.79	118762.01		11	3.91	3.97	2.26	6398.01
	12	6.35	6.45	0.65	27619.70		12	6.37	6.44	0.51	1441.79
	13	4.67	4.75	0.93	39644.25		13	4.69	4.74	0.70	1992.39
50%	10	5.00	5.10	1.00	31775.52	50%	10	5.02	5.08	1.00	2090.23
	11	3.00	3.06	3.13	99391.66		11	3.91	3.96	2.51	5247.67
	12	6.34	6.45	1.13	35825.69		12	6.37	6.43	0.98	2042.75
	13	4.67	4.75	1.68	53237.98		13	4.69	4.74	1.46	3059.02
70%	10					70%	10	5.02	5.07	1.00	1362.02
	11						11	3.90	3.96	2.88	3925.28
	12						12	6.37	6.42	2.07	2822.24
	13						13	4.68	4.74	3.24	4414.83
Conv	4g	region	region	integral	absolute	Conv	4h	region	region	integral	absolute
20%	10	5.01	5.10	1.03	58370.66	20%	10	5.03	5.10	1.00	46494.70
	11	3.90	3.97	2.18	122898.82		11	3.91	3.97	2.12	98614.71
	12	6.35	6.46	0.25	13829.62		12	6.37	6.44	0.20	9500.13
	13	4.67	4.74	0.35	19769.12		13	4.69	4.73	0.28	13020.81
35%	10	5.00	5.10	1.03	45514.43	35%	10	5.02	5.09	1.00	38729.88

	11	3.88	3.97	2.38	104983.10		11	3.90	3.96	2.27	87992.01
	12	6.36	6.44	0.61	26842.96		12	6.37	6.43	0.49	18903.57
	13	4.67	4.74	0.87	38545.55		13	4.68	4.74	0.72	27693.55
50%	10	4.99	5.09	1.05	29053.48	50%	10	5.01	5.08	1.00	31287.53
	11	3.87	3.97	2.71	75032.84		11	3.91	3.95	2.40	75073.20
	12	6.35	6.45	1.26	34987.78		12	6.38	6.44	0.84	26281.69
	13	4.67	4.75	1.90	52614.29		13	4.69	4.74	1.25	39196.42
70%	10	4.99	5.08	1.10	17906.29	70%	10	5.02	5.08	1.00	17926.80
	11	3.89	3.95	3.26	52894.30		11	3.91	3.95	2.73	48946.46
	12	6.35	6.44	3.01	48716.04		12	6.37	6.43	1.91	34154.68
	13	4.67	4.74	4.75	76976.32		13	4.68	4.75	3.02	54107.05
Conv	4i	region	region	integral	absolute	Conv	4j	region	region	integral	absolute
20%	10	5.03	5.09	0.72	6732.04	20%	10	5.02	5.09	1.00	3752.77
	11	3.90	3.97	1.62	15240.88		11	3.91	3.97	2.13	7981.64
	12	6.37	6.44	0.18	1672.85		12	6.37	6.43	0.16	587.27
	13	4.68	4.74	0.27	2548.11		13	4.69	4.73	0.24	915.34
35%	10	5.02	5.09	0.66	5442.91	35%	10	5.03	5.09	1.00	3073.46
	11	3.91	3.96	1.60	13080.08		11	3.90	3.97	2.21	6793.76
	12	6.37	6.43	0.36	2979.67		12	6.37	6.44	0.38	1172.24
	13	4.68	4.74	0.54	4380.51		13	4.68	4.73	0.60	1852.84
50%	10	5.02	5.07	0.62	3698.83	50%	10	5.02	5.09	1.00	2498.56
	11	3.91	3.97	1.70	10137.95		11	3.90	3.95	2.31	5764.65
	12	6.36	6.44	0.77	4574.09		12	6.37	6.44	0.69	1735.42
	13	4.68	4.74	1.18	7016.69		13	4.69	4.73	1.11	2765.52
70%	10	5.00	5.08	0.42	2372.22	70%	10	4.99	5.07	1.00	1655.77
	11	3.90	3.95	1.35	7536.43		11	3.90	3.95	2.55	4221.87
	12	6.36	6.43	1.10	6149.41		12	6.37	6.43	1.57	2592.88
	13	4.68	4.73	1.79	9992.77		13	4.69	4.73	2.63	4350.68
Conv	4k	region	region	integral	absolute	Conv	4l	region	region	integral	absolute
20%	10	5.01	5.12	1.00	57560.11	20%	10	5.02	5.09	1.00	11790.84
	11	3.88	3.98	2.21	127483.79		11	3.91	3.97	2.09	24587.42
	12	6.36	6.45	0.25	14464.79		12	6.36	6.44	0.38	4472.75
	13	4.67	4.74	0.42	24039.39		13	4.68	4.76	0.59	6979.46
35%	10	5.00	5.09	1.00	50665.15	35%	10	5.02	5.09	0.67	10854.00
	11	3.88	3.96	2.24	113471.02		11	3.90	3.96	1.46	23482.35
	12	6.34	6.46	0.40	20189.66		12	6.37	6.44	0.38	6087.64
	13	4.67	4.75	0.66	33637.98		13	4.68	4.74	0.60	9716.46
50%	10	5.00	5.10	1.00	33348.21	50%	10	5.02	5.09	0.61	8428.19
	11	3.88	3.97	2.45	81820.03		11	3.91	3.95	1.38	18971.36
	12	6.35	6.44	0.94	31440.80		12	6.36	6.44	0.62	8512.10
	13	4.68	4.74	1.58	52697.51		13	4.68	4.74	1.00	13784.21
70%	10	5.00	5.10	1.00	27159.41	70%	10	5.00	5.09	0.44	5027.38
	11	3.89	3.97	2.49	67529.07		11	3.90	3.95	1.08	12489.00
	12	6.35	6.45	1.39	37621.44		12	6.37	6.43	0.98	11291.59
	13	4.67	4.75	2.38	64628.34		13	4.68	4.74	1.66	19141.26
Conv	4m	region	region	integral	absolute	Conv	4n	region	region	integral	absolute
20%	10	5.00	5.12	1.03	57159.78	20%	10	5.02	5.09	1.00	2972.41
	11	3.88	3.99	2.25	125293.84		11	3.90	3.96	2.11	6273.83
	12	6.35	6.45	0.28	15287.78		12	6.37	6.44	0.16	463.36
	13	4.66	4.76	0.36	19863.52		13	4.69	4.74	0.25	735.75
35%	10	5.00	5.12	1.05	44587.21	35%	10	5.02	5.08	1.00	2560.74
	11	3.89	3.98	2.49	105916.48		11	3.90	3.96	2.18	5590.09
	12	6.36	6.46	0.63	26715.83		12	6.37	6.43	0.34	877.02
	13	4.67	4.76	0.84	35953.74		13	4.68	4.74	0.57	1452.90
50%	10	5.01	5.10	1.05	33510.74	50%	10	5.01	5.08	1.00	2577.14
	11	3.89	3.97	2.75	87702.50		11	3.90	3.96	2.30	5924.14

Annelated Pyridine Bases

	12	6.36	6.46	1.21	38637.70		12	6.37	6.43	0.68	1753.83
	13	4.67	4.75	1.70	54075.56		13	4.69	4.74	1.12	2890.28
70%	10	4.99	5.10	1.09	17473.64	70%	10	5.01	5.08	1.00	1434.06
	11	3.89	3.95	3.41	54552.55		11	3.90	3.96	2.47	3544.95
	12	6.35	6.44	2.84	45409.69		12	6.37	6.44	1.42	2035.05
	13	4.66	4.77	4.34	69445.70		13	4.68	4.74	2.44	3495.28
Conv	4o	region	region	integral	absolute	Conv	4p	region	region	integral	absolute
20%	10	4.99	5.09	1.00	38329.39	20%	10	5.01	5.10	1.00	57022.97
	11	3.88	3.95	2.03	77798.96		11	3.88	3.99	2.26	128666.46
	12	6.35	6.45	0.26	9900.40		12	6.34	6.44	0.27	15514.49
	13	4.67	4.74	0.40	15328.94		13	4.68	4.76	0.48	27447.40
35%	10	4.99	5.07	1.00	28446.65	35%	10	5.00	5.10	1.00	48721.76
	11	3.85	3.95	2.19	62300.20		11	3.87	3.98	2.34	114222.93
	12	6.35	6.45	0.59	16769.14		12	6.35	6.46	0.55	26672.75
	13	4.67	4.74	0.94	26657.48		13	4.67	4.75	0.98	47718.05
50%	10	4.98	5.06	1.00	21473.53	50%	10	4.99	5.14	1.00	36788.69
	11	3.85	3.97	2.28	49043.63		11	3.89	3.97	2.44	89620.74
	12	6.35	6.45	1.00	21542.83		12	6.35	6.45	0.99	36320.16
	13	4.66	4.74	1.61	34615.40		13	4.66	4.74	1.77	65269.61
70%	10					70%	10	5.00	5.09	1.00	17826.54
	11						11	3.89	3.97	2.70	48076.99
	12						12	6.35	6.46	2.54	45282.99
	13						13	4.65	4.75	4.80	85599.15
Conv	4q	region	region	integral	absolute	Conv	4r	region	region	integral	absolute
20%	10	5.00	5.11	1.00	58560.53	20%	10	5.01	5.12	1.00	59365.70
	11	3.89	3.98	2.13	124604.85		11	3.90	3.97	2.04	120602.24
	12	6.35	6.43	0.17	10033.78		12	6.36	6.44	0.18	10712.20
	13	4.67	4.75	0.34	19722.62		13	4.66	4.77	0.32	18986.17
35%	10	5.01	5.12	1.00	44393.91	35%	10	5.01	5.10	1.02	49400.71
	11	3.89	3.98	2.18	96625.78		11	3.90	3.98	2.10	101567.53
	12	6.33	6.45	0.45	19931.90		12	6.36	6.45	0.46	22274.83
	13	4.67	4.77	0.87	38752.11		13	4.67	4.76	0.84	40623.83
50%	10	5.01	5.10	1.00	33827.47	50%	10	5.01	5.10	1.03	37651.12
	11	3.88	3.97	2.27	76701.26		11	3.90	3.97	2.23	81261.15
	12	6.35	6.45	0.79	26657.83		12	6.35	6.47	0.96	35128.51
	13	4.65	4.77	1.54	51961.60		13	4.67	4.77	1.74	63254.74
70%	10	5.00	5.09	1.00	19991.65	70%	10	4.99	5.11	1.09	26074.15
	11	3.88	3.96	2.40	47986.26		11	3.89	3.96	2.40	57362.81
	12	6.34	6.44	2.05	40961.42		12	6.35	6.45	1.95	46581.01
	13	4.66	4.75	4.04	80748.00		13	4.67	4.75	3.56	85178.17
Conv	5a	region	region	integral	absolute	Conv	5b	region	region	integral	absolute
20%	10	5.01	5.12	1.00	58049.54	20%	10	5.01	5.10	1.00	62294.75
	11	3.89	3.98	2.26	131031.54		11	3.90	3.98	2.16	134769.41
	12	6.34	6.45	0.27	15400.44		12	6.34	6.44	0.23	14394.13
	13	4.66	4.76	0.45	26353.52		13	4.68	4.75	0.36	22601.43
35%	10	4.99	5.10	1.00	46269.88	35%	10	5.01	5.12	1.00	51899.09
	11	3.87	3.96	2.33	107933.47		11	3.90	3.99	2.23	115784.93
	12	6.34	6.45	0.57	26238.27		12	6.34	6.46	0.49	25334.30
	13	4.65	4.75	0.99	45735.82		13	4.67	4.76	0.79	41161.46
50%	10	4.99	5.09	1.00	32798.67	50%	10	4.99	5.13	1.00	37010.64
	11	3.89	3.97	2.54	83300.10		11	3.87	4.00	2.34	86649.00
	12	6.33	6.46	1.14	37511.59		12	6.35	6.44	0.81	29899.89
	13	4.66	4.76	2.03	66432.13		13	4.67	4.76	1.37	50576.94
70%	10	5.00	5.09	1.00	17314.86	70%	10	4.96	5.10	1.00	21663.95
	11	3.89	3.96	2.73	47318.40		11	3.88	3.97	2.60	56327.75
	12	6.34	6.46	2.59	44883.38		12	6.34	6.45	2.03	43883.45

	13	4.66	4.75	4.65	80482.25		13	4.66	4.75	3.51	75937.76
Conv	6a	region	region	integral	absolute	Conv	6b	region	region	integral	absolute
20%	10	5.03	5.08	1.07	25334.69	20%	10	5.01	5.10	1.00	7057.60
	11	3.91	3.96	2.16	50941.39		11	3.91	3.96	2.13	14967.74
	12	6.36	6.43	0.18	4244.63		12	6.37	6.44	0.19	1366.75
	13	4.69	4.73	0.29	6847.91		13	4.67	4.75	0.32	2284.02
35%	10	5.03	5.08	1.11	21759.62	35%	10	5.01	5.09	1.00	5694.54
	11	3.91	3.95	2.21	43460.08		11	3.91	3.96	2.18	12428.66
	12	6.37	6.44	0.42	8217.88		12	6.37	6.42	0.45	2545.84
	13	4.69	4.73	0.67	13280.29		13	4.67	4.74	0.78	4426.17
50%	10	5.02	5.07	1.12	25471.20	50%	10	5.01	5.09	1.00	4300.66
	11	3.91	3.96	2.28	52093.47		11	3.90	3.96	2.31	9954.24
	12	6.37	6.43	0.76	17429.06		12	6.37	6.43	0.92	3950.27
	13	4.69	4.73	1.26	28792.55		13	4.67	4.74	1.61	6911.15
70%	10	5.00	5.08	1.33	11730.11	70%	10	5.00	5.08	1.00	2717.65
	11	3.90	3.94	2.74	24167.99		11	3.89	3.95	2.49	6801.37
	12	6.37	6.43	1.62	14269.96		12	6.36	6.45	2.00	5443.63
	13	4.69	4.73	2.79	24680.85		13	4.67	4.74	3.58	9765.11
Conv	6c	region	region	integral	absolute	Conv	6d	region	region	integral	absolute
20%	10	5.04	5.08	1.00	44878.84	20%	10	5.01	5.11	1.04	57481.67
	11	3.91	3.96	2.08	93699.77		11	3.89	3.97	2.29	125909.60
	12	6.36	6.46	0.19	8693.19		12	6.36	6.45	0.21	11558.63
	13	4.69	4.73	0.30	13731.18		13	4.67	4.76	0.35	19543.07
35%	10	5.03	5.08	1.00	36561.34	35%	10	5.01	5.10	1.05	48241.12
	11	3.92	3.97	2.07	75765.74		11	3.90	3.97	2.37	109066.03
	12	6.36	6.43	0.49	17929.01		12	6.34	6.46	0.50	23008.82
	13	4.69	4.74	0.79	28845.77		13	4.66	4.76	0.88	40713.82
50%	10	5.03	5.08	1.00	31461.10	50%	10	5.01	5.10	1.07	33796.47
	11	3.91	3.95	2.15	67756.10		11	3.88	3.97	2.72	85499.02
	12	6.37	6.43	0.75	23619.75		12	6.34	6.46	1.17	36763.45
	13	4.69	4.74	1.25	39397.72		13	4.67	4.75	2.07	65056.53
70%	10	5.01	5.08	0.98	19171.30	70%	10	4.99	5.08	1.10	20432.48
	11	3.90	3.95	2.15	42109.95		11	3.89	3.97	2.97	55097.59
	12	6.37	6.44	1.59	31275.42		12	6.35	6.45	2.33	43086.77
	13	4.69	4.74	2.74	53778.20		13	4.65	4.77	4.34	80415.96
Conv	7ba^a	region	region	integral	absolute	Conv	7bb^a	region	region	integral	absolute
20%	10	5.03	5.09	1.00	3428.81	20%	10	5.01	5.11	1.07	56609.64
	11	3.91	3.98	2.14	7333.66		11	3.88	4.01	2.28	120034.65
	12	6.38	6.42	0.26	898.31		12	6.36	6.44	0.25	13364.21
	13	4.69	4.73	0.39	1337.54		13	4.68	4.74	0.43	22596.39
35%	10	5.03	5.09	1.00	2891.48	35%	10	5.01	5.11	1.09	48716.17
	11	3.91	3.97	2.25	6507.54		11	3.89	3.99	2.36	105341.46
	12	6.38	6.43	0.53	1524.46		12	6.36	6.44	0.51	22772.70
	13	4.69	4.73	0.81	2331.96		13	4.68	4.75	0.87	38728.61
50%	10	5.03	5.09	1.00	2130.98	50%	10	5.02	5.10	1.09	37282.52
	11	3.91	3.96	2.44	5167.08		11	3.89	3.98	2.47	84534.42
	12	6.37	6.43	1.02	2160.95		12	6.36	6.44	0.96	32785.13
	13	4.69	4.73	1.60	3398.58		13	4.67	4.75	1.68	57719.38
70%	10	5.01	5.07	0.99	1551.90	70%	10	5.01	5.09	1.17	25299.25
	11	3.90	3.95	2.57	4051.82		11	3.90	3.96	2.73	59269.97
	12	6.37	6.43	1.63	2560.97		12	6.36	6.44	2.16	46909.52
	13	4.68	4.75	2.60	4096.50		13	4.67	4.74	3.86	83700.65
Conv	7bc^a	region	region	integral	absolute	Conv	7bd^a	region	region	integral	absolute
20%	10	5.02	5.11	1.07	54997.11	20%	10	5.02	5.10	1.00	3176.40
	11	3.90	3.99	2.22	113979.92		11	3.90	3.98	2.06	6549.20
	12	6.37	6.44	0.25	12830.42		12	6.37	6.44	0.33	1045.32

	13	4.68	4.74	0.43	22029.92		13	4.69	4.74	0.63	2004.42
35%	10	5.02	5.10	1.09	44888.78	35%	10	5.03	5.09	1.00	3052.99
	11	3.90	3.98	2.31	95042.53		11	3.89	3.98	2.06	6307.88
	12	6.37	6.44	0.58	23765.29		12	6.37	6.43	0.42	1281.58
	13	4.68	4.74	1.03	42114.54		13	4.68	4.75	0.81	2466.24
50%	10	5.02	5.09	1.11	34523.26	50%	10	5.02	5.09	1.00	2382.04
	11	3.90	3.97	2.43	75765.24		11	3.89	3.97	2.09	5009.27
	12	6.36	6.44	1.13	35249.87		12	6.37	6.43	0.80	1903.53
	13	4.68	4.74	2.04	63758.32		13	4.68	4.74	1.56	3740.83
70%	10	5.01	5.09	1.17	21768.42	70%	10	5.04	5.09	0.98	1921.42
	11	3.90	3.96	2.69	50169.47		11	3.92	3.98	1.88	3702.54
	12	6.36	6.44	2.56	47643.25		12	6.38	6.43	1.37	2688.80
	13	4.68	4.75	4.73	88141.64		13	4.69	4.75	2.32	4552.84

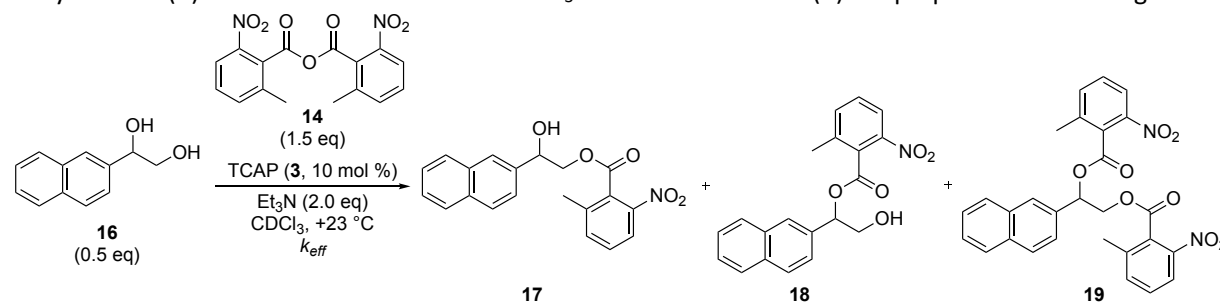
^aRaw NMR data were experimental determined by A. Mateos Calbet^[5] under the supervision of S. Mayr. The herein reported data are fully reanalysed.

5.1.2 Absolute Kinetic Study with 2-Naphthyl-1,2-ethanediol

In this part of the work, we chose the model of absolute kinetic experiments shown in chapter 4 of this thesis with a variation of catalysts. The guideline is based on this previous chapter.^[2]

5.1.2.1 Experimental Design

In the following a general procedure for absolute kinetic studies will be described based on the experiment shown in Scheme 5.4. Three different CDCl₃ stock solution consisting of 0.02 M 1,2-diol **16** (A), 0.06 M acid anhydride **14** (B) and a combination of 0.08 M Et₃N and 0.004 M TCAP (C) are prepared under nitrogen.



Scheme 5.4. Model example for a time dependent kinetic experiment of 2-naphthylethan-1,2-diol **1b** with acid anhydride **5c**.

Table 5.5. Preparation of initial CDCl₃ stock solutions (method A).

Stock solution	Compound	Concentration (mol L ⁻¹)	Volume (mL)	n (mol)	M.W. (g mol ⁻¹)	Mass (mg)
Stock A	16	0.02	1	20·10 ⁻⁶	188	3.8
Stock B	14	0.06	1	60·10 ⁻⁶	344	20.6
Stock C	Et₃N	0.08	2	160·10 ⁻⁶	101	16.2
	TCAP	0.004	2	8·10 ⁻⁶	174	1.4

The reaction is analysed by ¹H NMR recorded by Bruker Avance III 400 machines. NMR tubes are dried under vacuum using a Schlenk based glassware and flushed with nitrogen. 0.2 mL of Stock A, 0.2 mL of Stock C and 0.2 mL of Stock B are transferred under nitrogen to a NMR tube by use of a Hamilton syringe. After closing the NMR tubes, reaction mixture is shaken and put in the NMR machine. Because of the low concentration of the reaction mixtures for each ¹H NMR spectrum 32 scans were recorded.

In terms of the actual starting concentrations (mol/L) for all components:

NMR Tube: **16:** 0.00667, **14:** 0.02000, **Et₃N:** 0.02667, **TCAP:** 0.00133

5.1.2.2 ¹H NMR Analysis

The ¹H NMR spectra of the absolute kinetic studies are edited by MestReNova 10.0. The spectra are corrected by using automatic phase correction and Whittaker Smoother (I) fit with autodected parameters referenced by the solvent signal of CDCl₃ ($\delta = 7.26$ ppm). For the 1,2-diol **16**, primary ester **17**, secondary ester **18** or

diester **19** the hydrogen signal of the CH group is integrated as a guide for the evolution of the reaction. If there is an overlapping with other signals, one of the corresponding hydrogen signals of the CH₂-groups are used.

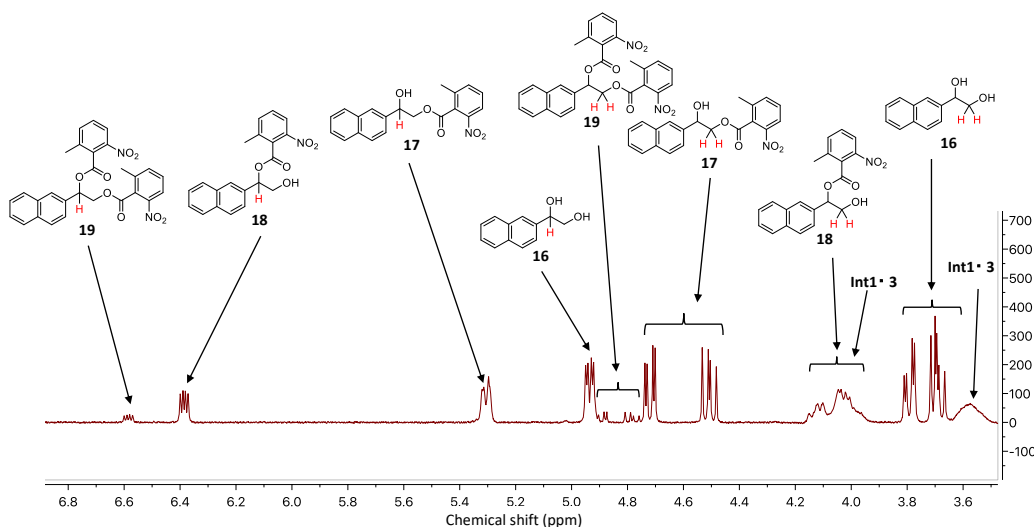
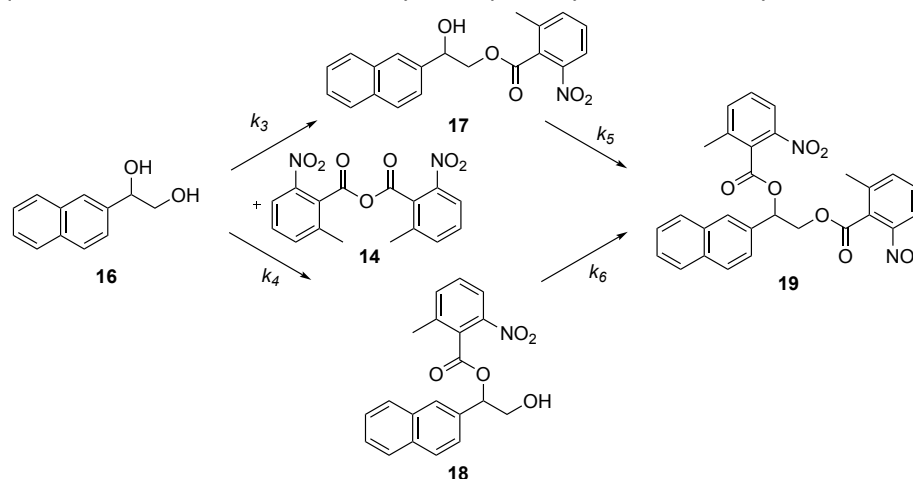


Figure 5.10. Example of the ¹H NMR for the absolute kinetic of **16** with **14**.

The acylation of 1,2-diols **16** is based on complex process with four different effective rate constants, which influence the reaction (Scheme 5.5). The reaction has to be separated in two parts. The first part is the first acylation of **16** to primary ester **17** and secondary ester **18**, defined by the effective rate constants k_3 and k_4 . The relative rate constant $k_{rel,a}$ of the first acylation is defined by Eq. 5.7, which is the ratio of acylation primary over secondary OH-group. The second part of this complex process is the acylation of **17** and **18** to the diester **19**, defined by the effective rate constants k_5 and k_6 . The relative rate constant $k_{rel,b}$ of the second acylation is defined by Eq. 5.8, which is also the ratio of acylation primary over secondary alcohol.



Scheme 5.5. General model for the acylation reaction of 1,2-ethylenediol **16**.

$$k_{rel,a} = \frac{k_3}{k_4}$$

Eq. 5.7

$$k_{rel,b} = \frac{k_6}{k_5}$$

Eq. 5.8

The conversion of all OH-groups in the system is defined by Eq. 5.9, whereby the integrals of the ¹H NMR spectra were assumed to corresponding to the concentrations.

$$\text{Conversion (\%)} = \left(\frac{[17] + [18] + 2 \cdot [16]}{2 \cdot [16] + 2 \cdot [17] + 2 \cdot [18] + 2 \cdot [19]} \right) \cdot 100$$

Eq. 5.9

The proportion of all components to each other are defined as mole fractions by Eq. 5.10-5.13:

$$\text{Mole fraction}_{16} (\%) = \left(\frac{[16]}{[16] + [17] + [18] + [19]} \right) \cdot 100$$

Eq. 5.10

$$\text{Mole fraction}_{17} (\%) = \left(\frac{[17]}{[16] + [17] + [18] + [19]} \right) \cdot 100$$

Eq. 5.11

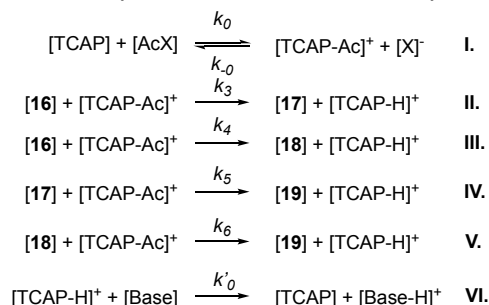
$$\text{Mole fraction}_{18} (\%) = \left(\frac{[18]}{[16] + [17] + [18] + [19]} \right) \cdot 100$$

Eq. 5.12

$$\text{Mole fraction}_{19} (\%) = \left(\frac{[19]}{[16]+[17]+[18]+[19]} \right) \cdot 100 \quad \text{Eq. 5.13}$$

5.1.2.3 Simulation of the Absolute Kinetic Experiments

Based on the model shown in Chapter 4,^[2] again the rate constants of our first and second acylation k_1 - k_4 were fitted and simulated with the help of the CoPaSi^[4] and ProFit programs. In Scheme 5.6 a simplified model used in CoPaSi is shown for the acetylation reaction of 1,2-ethylenediol **16**.



Scheme 5.6. Model reaction used in CoPaSi for the simulation of the rate constants (Method A).

First, the mole fractions of the single components are recalculated to the concentrations, which correspond to the starting concentrations of 1,2-diol in our absolute kinetics studies, as shown on Eq. 5.14-5.17:

$$\text{Concentration}_{16} (\text{mol/L}) = \left(\frac{[16]}{[16]+[17]+[18]+[19]} \right) \cdot 0.0067 \quad \text{Eq. 5.14}$$

$$\text{Concentration}_{17} (\text{mol/L}) = \left(\frac{[17]}{[16]+[17]+[18]+[19]} \right) \cdot 0.0067 \quad \text{Eq. 5.15}$$

$$\text{Concentration}_{18} (\text{mol/L}) = \left(\frac{[18]}{[16]+[17]+[18]+[19]} \right) \cdot 0.0067 \quad \text{Eq. 5.16}$$

$$\text{Concentration}_{19} (\text{mol/L}) = \left(\frac{[19]}{[16]+[17]+[18]+[19]} \right) \cdot 0.0067 \quad \text{Eq. 5.17}$$

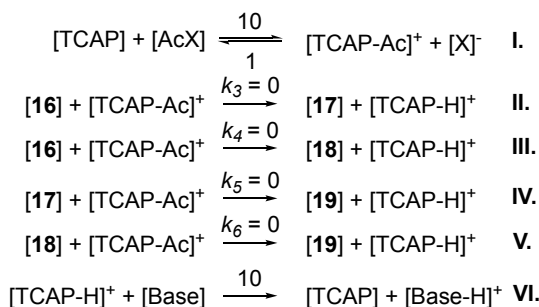
Before we start the fitting process we have to set the values of k_0 , k_{-0} (I.) and k'_0 (VI.). Although in the literature it is reported that the equilibrium in the catalyst loading step (I.) is often found to be on the left side with acid anhydride reagents,^[6] we define this equilibrium to be on the product side by defining $k_0 = 10$ and $k_{-0} = 1$. This choice is reasonable because the loaded catalyst cation intermediate “[TCAP-Ac]⁺” is visible in the ¹H NMR for most of our catalysts systems. The rate for catalyst recovery was also fixed with $k'_0 = 10$. k_0 , k_{-0} (I.) and k'_0 (VI.) were not changed during the fitting process to guarantee a reproducibility and comparability of catalysts activity. For the fitting the actual starting concentrations of **1b** (0.0067 M), **5c** (0.020 M), Et₃N (0.0267 M) and TCAP (0.0013 M) are specified.

Method A: The “fitting”-process has to be separated into four steps based on the “two-step” process of first- and second acylation and the four different effective rate constants k_3 - k_6 affecting each other. In Table 5.6 each single fit and the associated modifications are shown and discussed in the following:

Table 5.6. Instructions of fitting in CoPaSi for Method A.

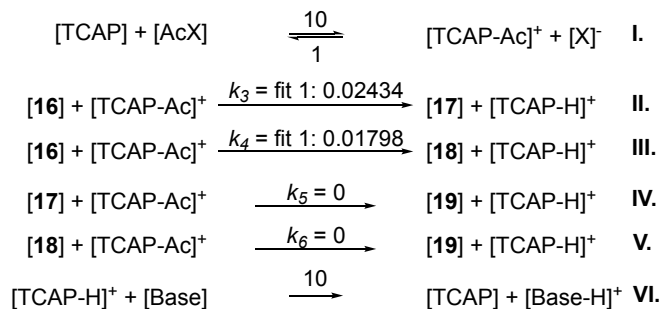
Fit	k_x always constant	k_x modified	Fitted k_x	Fitted Reaction	Fitted compound
1	k_0, k_{-0}, k'_0	k_5 and $k_6 = 0$	k_3 and k_4 Start Value = 0	II. and III.	16, 17 and 18
2	k_0, k_{-0}, k'_0	k_3 and $k_4 = \text{Fit 1}$	k_5 and k_6 Start Value = 0	IV. and V.	17, 18 and 19
3	k_0, k_{-0}, k'_0	k_5 and $k_6 = \text{Fit 2}$	k_3 and k_4 Start Value = 0	II. and III.	16, 17 and 18
4	k_0, k_{-0}, k'_0	k_3 and $k_4 = \text{Fit 3}$	k_5 and k_6 Start Value = 0	IV. and V.	17, 18 and 19

In the 1st fit all effective rate constants k_3 - k_6 are initially set as 0, as the method the “Differential Evolution” is chosen and the fit is running only once (Scheme 5.7). k_3 (II.) and k_4 (III.) are fitted, by taking **16**, **17** and **18** as dependent concentrations and only the values up to the highest concentrations of **17** or **18** were performed (CoPaSi Parameter estimation: dependent). The concentration of **19** is excluded in the 1st fit, because in the first acylation no diester is formed (CoPaSi Parameter estimation: ignored). As start value $k_3/k_4 = 0$ was set and the 1st fit was allowed to run (Figure 5.11a).



Scheme 5.7. Model reaction used in CoPaSi for the 1st fit.

In the 2nd fit rate constants k_5/k_6 still set as 0, rate constants k_3/k_4 are defined through fit 1, as method the “Differential Evolution” is chosen and the fit is running only once (Scheme 5.8).



Scheme 5.8. Model reaction used in CoPaSi for the 2nd fit.

k_5 and k_6 are fitted, by taking **17**, **18** and **19** as dependent concentrations and all measured concentration points are used this time (CoPaSi Parameter estimation: dependent). The concentration of **16** is excluded, because in the second acylation the diol is not existence (CoPaSi Parameter estimation: ignored). As start value $k_5/k_6 = 0$ was set and the 2nd fit was allowed to run (Figure 5.11b).

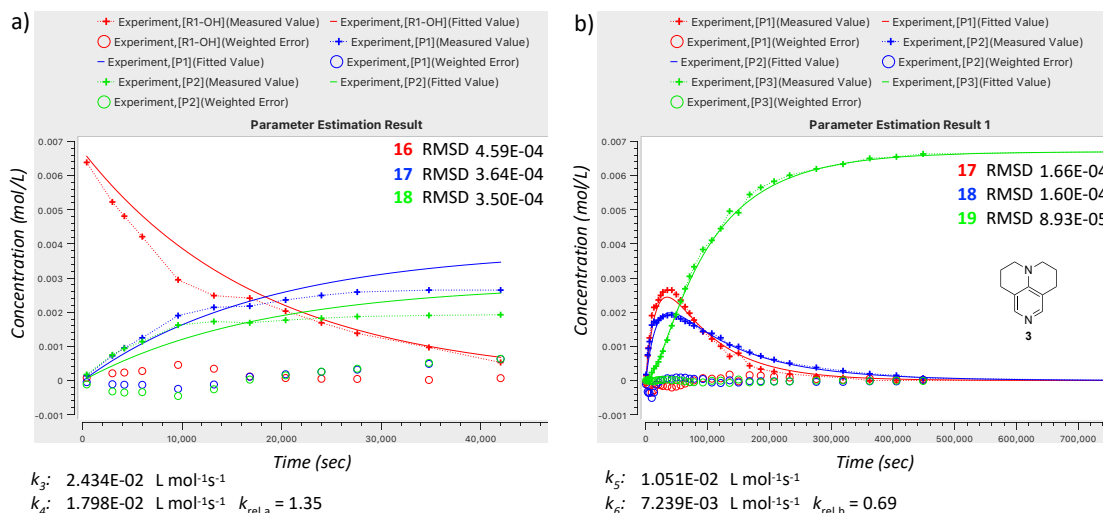
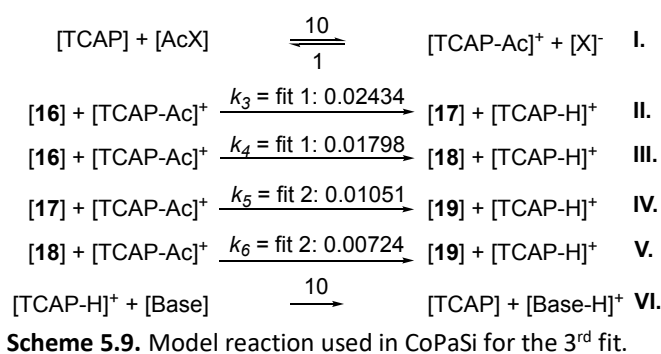


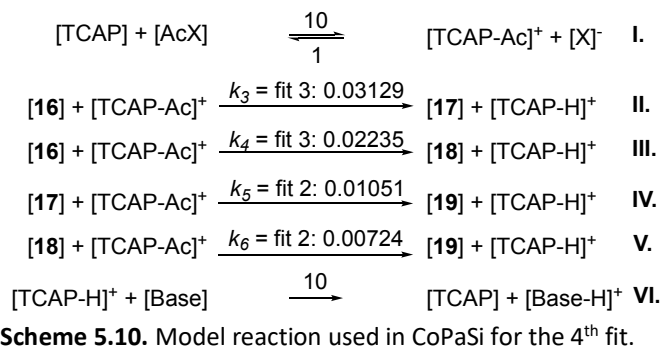
Figure 5.11. Plot of time (sec) vs. concentration (mol/L) for the acylation of **16** with **14** catalyzed by TCAP (**3**) fitted by CoPaSi. a) Fit 1 for k_3 and k_4 up to highest concentration of **17**. b) Fit 2 for k_5 and k_6 .

In the additional fits, a so called “refitting” step was added, because the effective rate constants k_5 and k_6 of the second acylation step already influence k_3 and k_4 significantly in the first acylation step, which was ignored in the 1st fit.

In the 3rd fit rate constants k_3/k_4 are defined through fit 1, the effective rate constants k_5/k_6 are defined through fit 2, as method the “Differential Evolution” is chosen and the fit runs only once (Scheme 5.9). k_3 and k_4 are fitted, by taking **16**, **17** and **18** as dependent concentrations and only the values up to the highest concentration of **17** or **18** was achieved (CoPaSi Parameter estimation: dependent). The concentration of **19** is again excluded in the 3rd fit (CoPaSi Parameter estimation: ignored). As start value $k_3/k_4 = 0$ was set and the 3rd fit was allowed to run (Figure 5.12a).



In the 4th fit, effective rate constants k_3/k_4 are defined through fit 3, effective rate constants k_5/k_6 are defined through fit 2, as method the “Differential Evolution” is chosen and the fit is running only once (Scheme 5.10).



k_5 and k_6 are fitted, by taking **17**, **18** and **19** as dependent concentrations and all measured concentration points are used this time (CoPaSi Parameter estimation: dependent). The concentration of **16** is again excluded in the 4th fit (CoPaSi Parameter estimation: ignored). As start value $k_5/k_6 = 0$ was set and the 4th fit was allowed to run (Figure 5.12b).

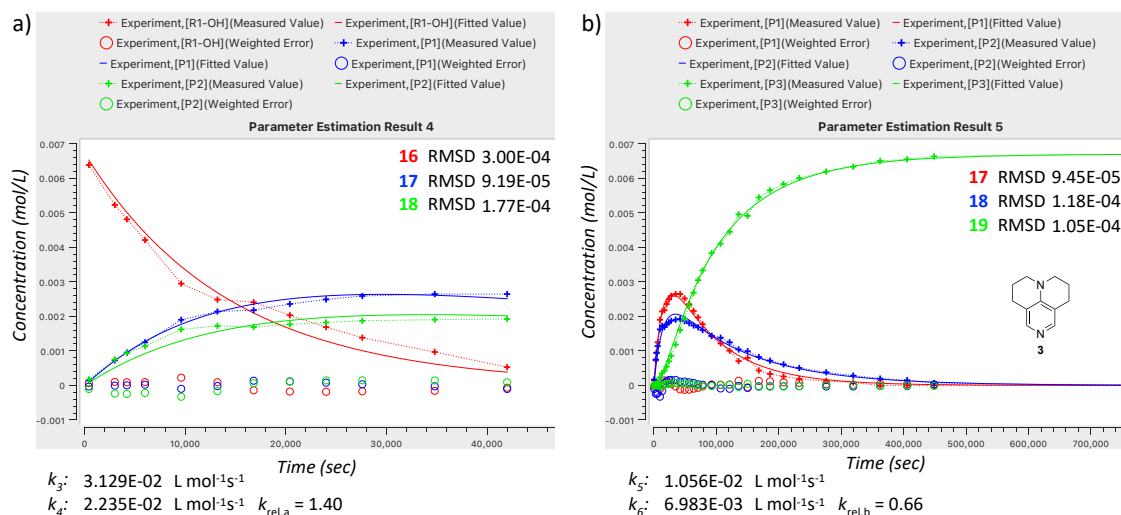


Figure 5.12. Plot of time (sec) vs. concentration (mol/L) for the acylation of **16** with **14** catalyzed by TCAP (**3**) fitted by CoPaSi. a) Fit 3 for k_3 and k_4 up to highest concentration of **17**. b) Fit 4 for k_5 and k_6 .

The now fitted rate constants k_3 - k_6 are finally used for simulating the reaction by CoPaSi. In addition, for the simulated concentrations over the time the mole fractions could be calculated by Eq. 5.14-5.17. The time (sec) was plotted against the mole fractions, obtained by experiments and numerical simulations to verify the simulated effective rate constants (Figure 5.13).

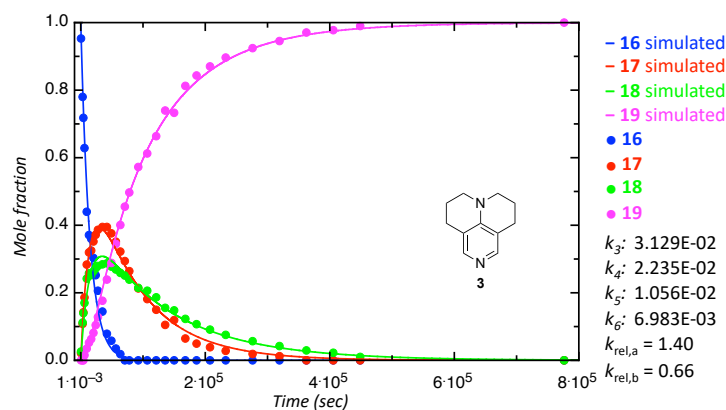
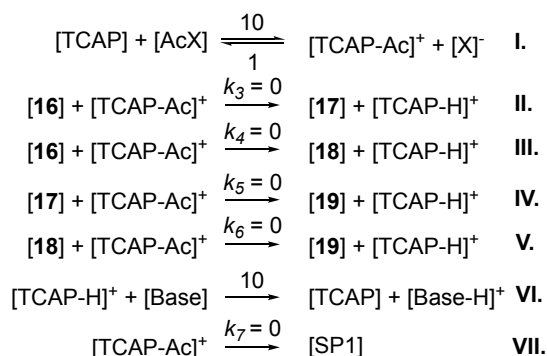


Figure 5.13. Plot of *time (sec)* vs. *mole fraction* for acylation of **16** with **14** catalysed by **3**. Fitted values of $k_3 - k_6$ by Method A and the corresponding relative rate constants $k_{rel,a}$ and $k_{rel,b}$. The rate constants $k_3 - k_6$ are given in $L \text{ mol}^{-1} \text{ s}^{-1}$.

Method B:

In some cases, the reaction stops after 5 days during the second acylation step of **17** and **18** to **19** catalysed with **4** and only a conversion of ~70% is achieved. Because only the catalyst is varied here and the equilibrium of catalysts loading is on the right side, we are thinking that this “problem” is caused by the formation of the *N*-acylpyridinium ion **INT1-4** (equal to [TCAP-Ac]⁺ in the CoPaSi model reaction). It is thinkable that **INT1-4** prioritizes a side reaction, which eliminates the catalysts and/or the anhydride out of the reaction. We decide to include this side reaction in our CoPaSi model by adding reaction **VII** in the model reaction used in CoPaSi (Scheme 5.11).



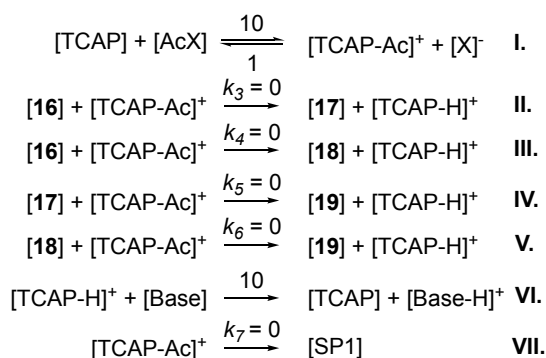
Scheme 5.11. Model reaction used in CoPaSi for the simulation of the rate constants (Method B).

In Table 5.7 each single Fit and the associated modifications are shown and discussed in the following:

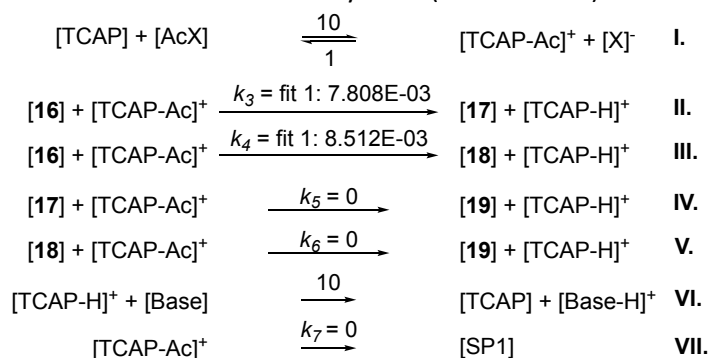
Table 5.7. Instructions of Fitting in CoPaSi for Method B.

Fit	k_x always constant	k_x modified	Fitted k_x	Fitted Reaction	Fitted compound
1	k_0, k_{-0}, k'_0	k_5, k_6 and $k_7 = 0$	k_3 and k_4 , start value = 0	II. and III.	16, 17 and 18
2	k_0, k_{-0}, k'_0	k_3 and $k_4 = \text{Fit 1}$ $k_7 = 0$	k_5, k_6 and $k_7 = 0$, start value = 0	IV., V. and VII.	17, 18 and 19
3	k_0, k_{-0}, k'_0	k_5, k_6 and $k_7 = \text{Fit 2}$	k_3 and k_4 , start value = 0	II. and III.	16, 17 and 18
4	k_0, k_{-0}, k'_0	k_3 and $k_4 = \text{Fit 3}$ $k_7 = \text{Fit 2}$	k_5 and k_6 , start value = 0	IV. and V.	17, 18 and 19

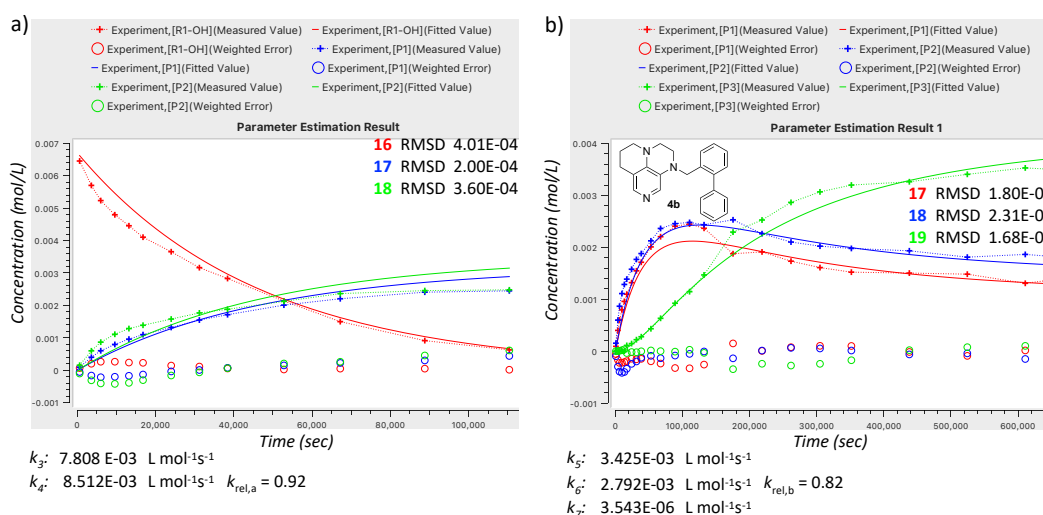
In the 1st fit all effective rate constants $k_3 - k_7$ are initially set as 0, as the method the “Differential Evolution” is chosen and the fit runs only once (Scheme 5.12). k_3 (II.) and k_4 (III.) are fitted, by taking **16, 17** and **18** as dependent concentrations and only the values up to the highest concentrations of **17** or **18** were performed (CoPaSi Parameter estimation: dependent). The concentration of **19** is excluded in the 1st fit, because in the first acylation no diester is formed (CoPaSi Parameter estimation: ignored). As start value $k_3/k_4 = 0$ was set and the 1st fit was allowed to run (Figure 5.14a).


Scheme 5.12. Model reaction used in CoPaSi for the 1st fit.

In the 2nd fit rate constants $k_5 - k_7$ still set as 0, rate constants k_3/k_4 are defined through fit 1, as method the “Differential Evolution” is chosen and the fit runs only once (Scheme 5.13).


Scheme 5.13. Model reaction used in CoPaSi for the 2nd fit.

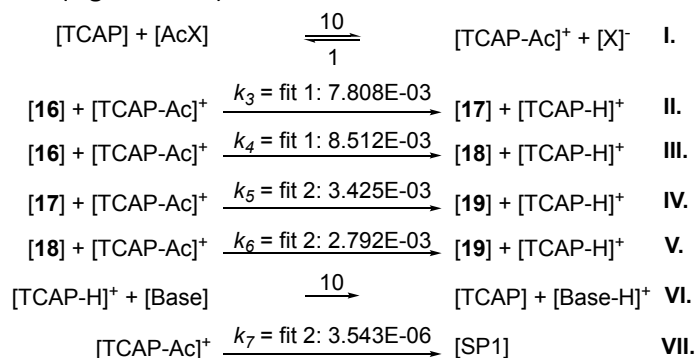
$k_5 - k_7$ are fitted, by taking **17**, **18** and **19** as dependent concentrations and all measured concentration points are used this time (CoPaSi Parameter estimation: dependent). The concentration of **16** is excluded, because in the second acylation the diol is not existence (CoPaSi Parameter estimation: ignored). As start value $k_5 - k_7 = 0$ was set and the 2nd fit was allowed to run (Figure 5.14b). k_7 could be fitted here indirect by the decrease in formation of **19**.


Figure 5.14. Plot of time (sec) vs. concentration (mol/L) for the acylation of **16** with **14** catalyzed by **4b** fitted by CoPaSi. a) Fit 1 for k_1 and k_2 till highest concentration of **17**. b) Fit 2 for k_3 , k_4 and k_6 .

In the additional fits, a so called “refitting” step was added, because the effective rate constants k_5 and k_6 of the second acylation step already influence k_3 and k_4 significantly in the first acylation step, which was ignored in the 1st fit. The effective reate k_7 was not refitted!

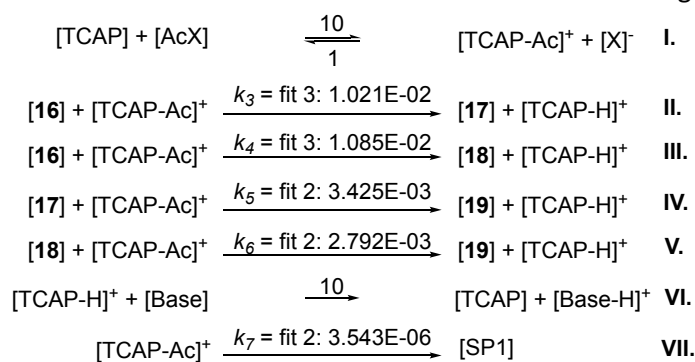
In the 3rd fit rate constants k_3/k_4 are defined through fit 1, the effective rate constants $k_5 - k_7$ are defined through fit 2, as method the “Differential Evolution” is chosen and the fit runs only once (Scheme 5.14). k_3 and k_4 are fitted, by taking **16**, **17** and **18** as dependent concentrations and only the values up to the highest

concentration of **17** or **18** was achieved (CoPaSi Parameter estimation: dependent). The concentration of **19** is again excluded in the 3rd fit (CoPaSi Parameter estimation: ignored). As start value $k_3/k_4 = 0$ was set and the 3rd fit was allowed to run (Figure 5.15a).



Scheme 5.14. Model reaction used in CoPaSi for the 3rd fit.

In the 4th fit, effective rate constants k_3/k_4 are defined through fit 3, effective rate constants k_5-k_7 are defined through fit 2, as method the “Differential Evolution” is chosen and the fit is running only once (Scheme 5.15).



Scheme 5.15. Model reaction used in CoPaSi for the 4th fit.

k_5 and k_6 are fitted, by taking **17**, **18** and **19** as dependent concentrations and all measured concentration points are used this time (CoPaSi Parameter estimation: dependent). The concentration of **16** is again excluded in the 4th fit (CoPaSi Parameter estimation: ignored). As start value $k_5/k_6 = 0$ was set and the 4th fit was allowed to run (Figure 5.15b).

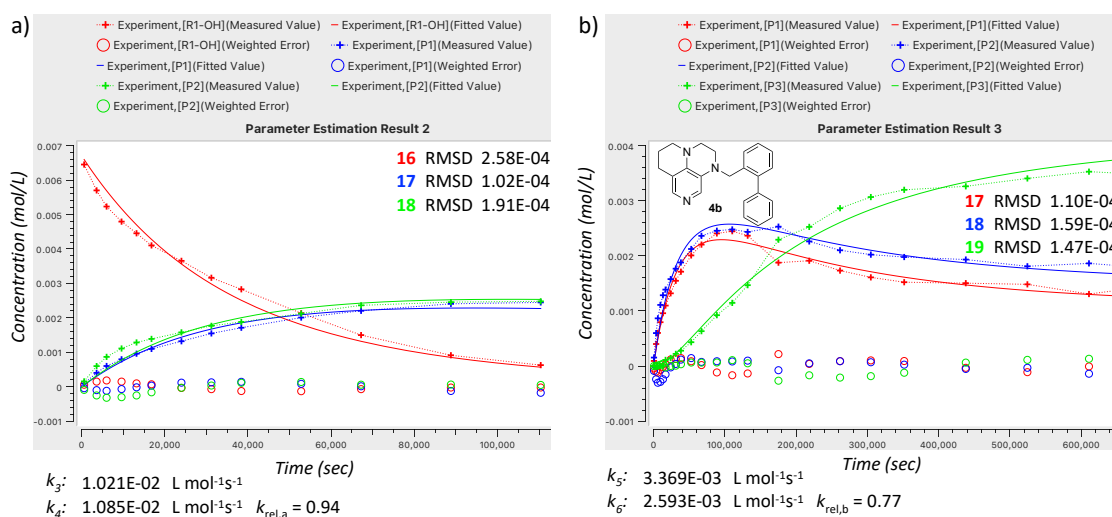


Figure 5.15. Plot of time (sec) vs. concentration (mol/L) for the acylation of **16** with **14** catalyzed by TCAP (**3**) fitted by CoPaSi. a) Fit 3 for k_3 and k_4 up to highest concentration of **17**. b) Fit 4 for k_5 and k_6 .

The now fitted rate constants $k_3 - k_7$ are finally used for simulating the reaction by CoPaSi. In addition, for the simulated concentrations over the time again the mole fractions could be calculated by Eq. 5.14-5.17. The time (sec) was plotted against the mole fractions, obtained by experiments and numerical simulations to verify the simulated effective rate constants (Figure 5.16).

Annulated Pyridine Bases

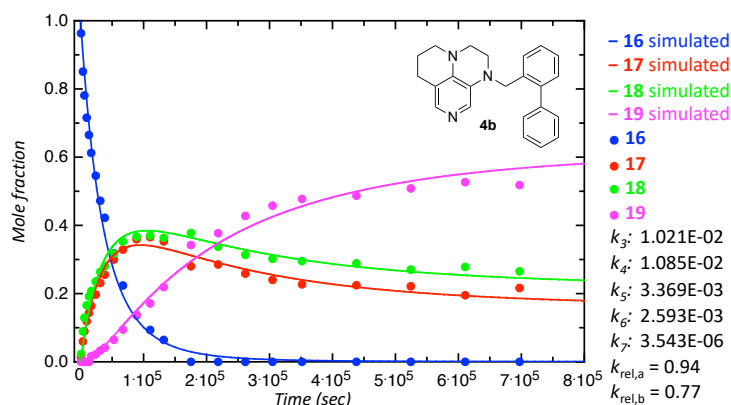


Figure 5.16. Plot of *time (sec)* vs. *mole fraction* for acylation of **16** with **14** catalysed by **4b**. Fitted values of k_{1-4} by Method B and the corresponding relative rate constants $k_{rel,a}$ and $k_{rel,b}$. The rate constants $k_3 - k_7$ are given in $\text{L mol}^{-1} \text{s}^{-1}$. In Figure 5.17 to 5.23 the time (sec) was plotted against the mole fractions, obtained by experiments and numerical simulations for Lewis base catalysts **1-3**, **4b,e,i** and **m**. Figure 5.24 shows the plot of time (sec) over the conversion (%) of all OH groups in the system.

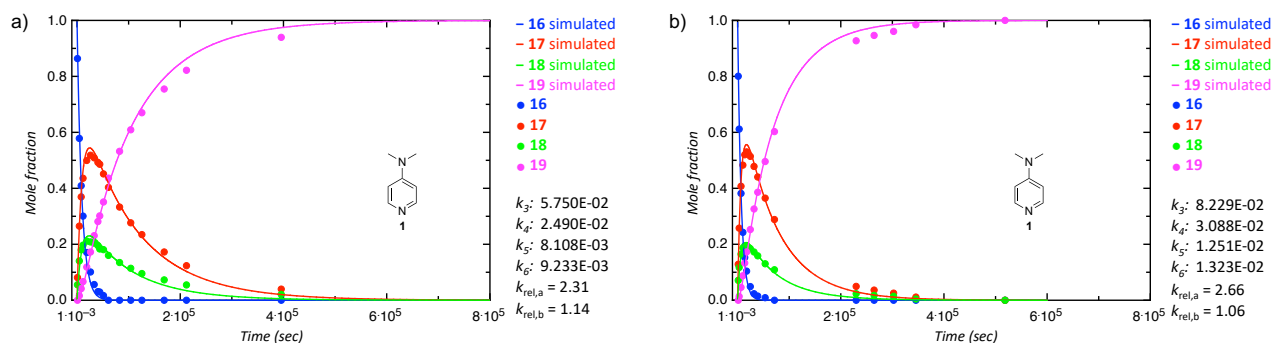


Figure 5.17. Plot of *time (sec)* vs. *mole fraction* for acylation of **16** with **14** catalyzed by **1** for a) measurement 1 and b) measurement 2. The Fitting was done by Method A. The rate constants $k_3 - k_6$ are given in $\text{L mol}^{-1} \text{s}^{-1}$.

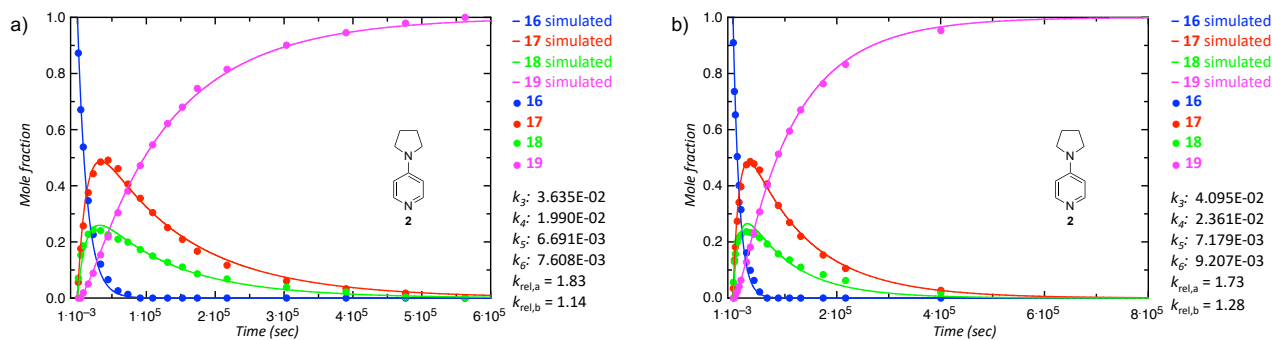


Figure 5.18. Plot of *time (sec)* vs. *mole fraction* for acylation of **16** with **14** catalyzed by **2** for a) measurement 1 and b) measurement 2. The Fitting was done by Method A. The rate constants $k_3 - k_6$ are given in $\text{L mol}^{-1} \text{s}^{-1}$.

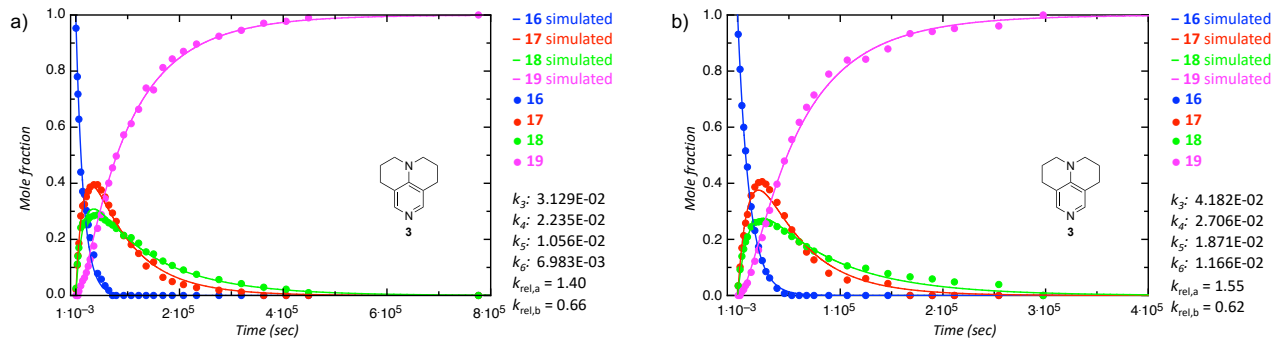


Figure 5.19. Plot of *time (sec)* vs. *mole fraction* for acylation of **16** with **14** catalyzed by **3** for a) measurement 1 and b) measurement 2. The Fitting was done by Method A. The rate constants $k_3 - k_6$ are given in $\text{L mol}^{-1} \text{s}^{-1}$.

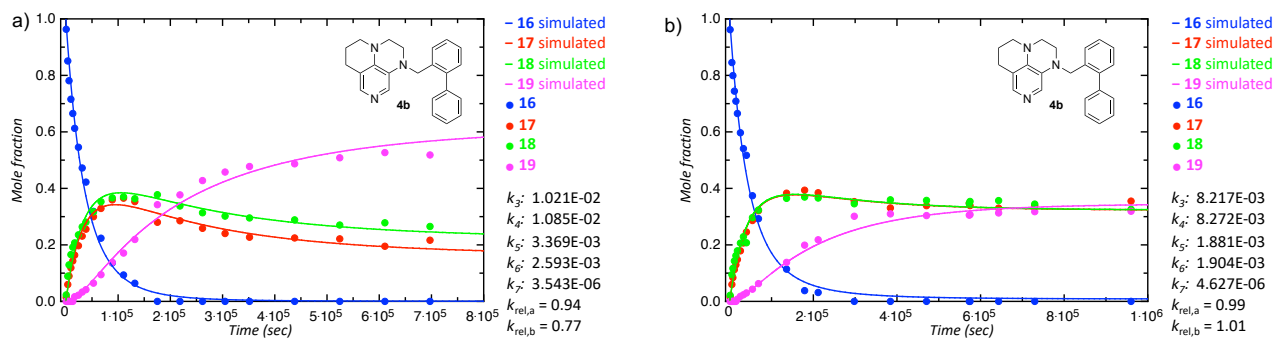


Figure 5.20. Plot of time (sec) vs. mole fraction for acylation of **16** with **14** catalyzed by **4b** for a) measurement 1 and b) measurement 2. The Fitting was done by Method B. The rate constants $k_3 - k_7$ are given in $L mol^{-1} s^{-1}$.

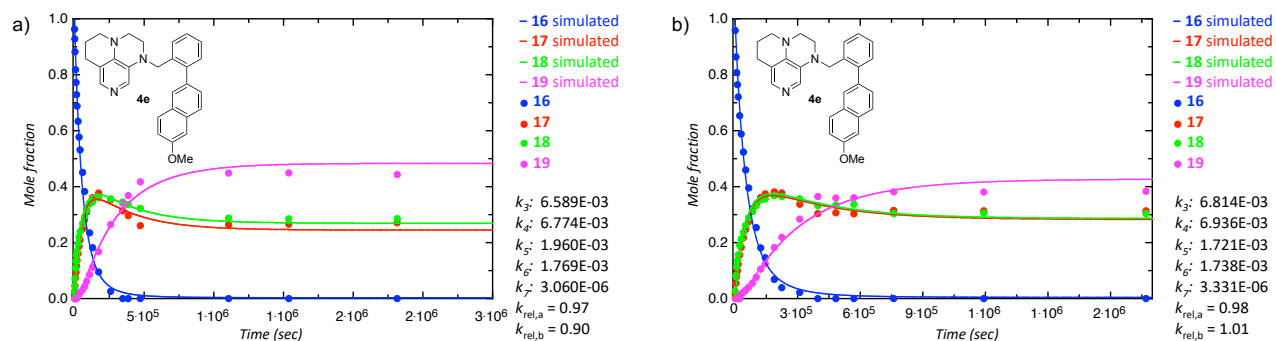


Figure 5.21. Plot of time (sec) vs. mole fraction for acylation of **16** with **14** catalyzed by **4e** for a) measurement 1 and b) measurement 2. The Fitting was done by Method B. The rate constants $k_3 - k_7$ are given in $L mol^{-1} s^{-1}$.

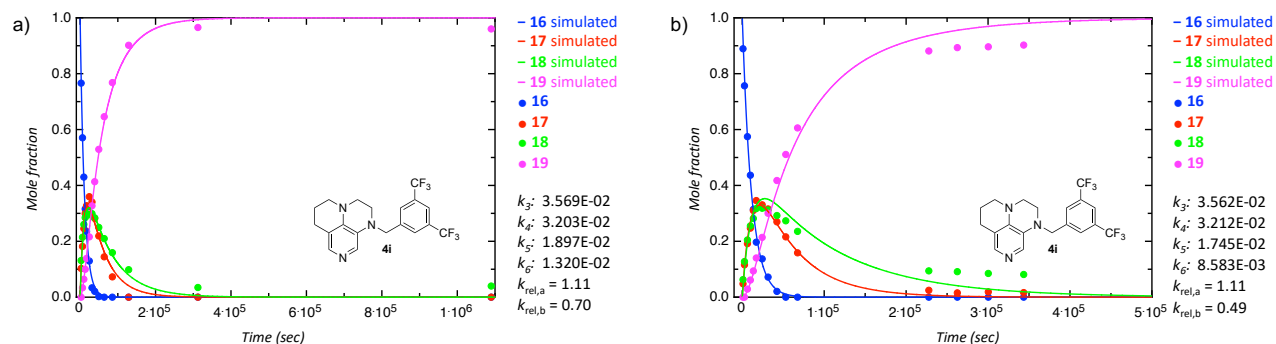


Figure 5.22. Plot of time (sec) vs. mole fraction for acylation of **16** with **14** catalyzed by **4i** for a) measurement 1 and b) measurement 2. The Fitting was done by Method A. The rate constants $k_3 - k_6$ are given in $L mol^{-1} s^{-1}$.

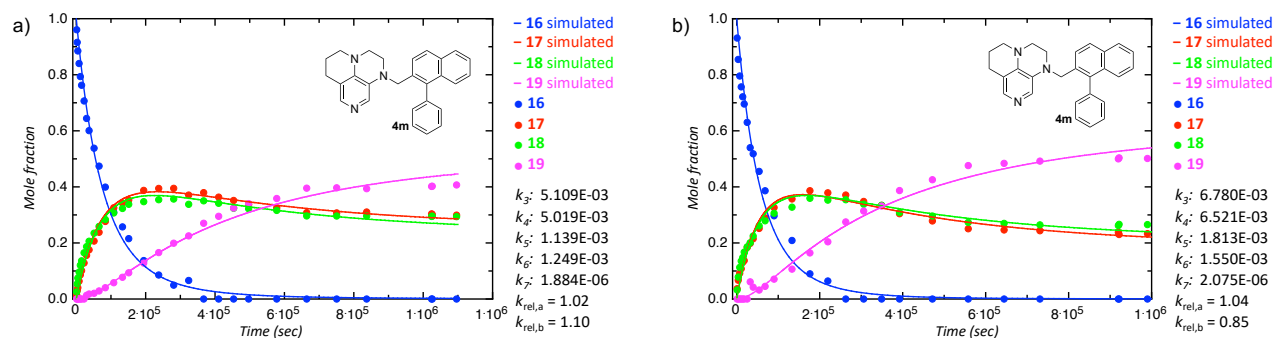


Figure 5.23. Plot of time (sec) vs. mole fraction for acylation of **16** with **14** catalyzed by **4m** for a) measurement 1 and b) measurement 2. The Fitting was done by Method B. The rate constants $k_3 - k_7$ are given in $L mol^{-1} s^{-1}$.

Annulated Pyridine Bases

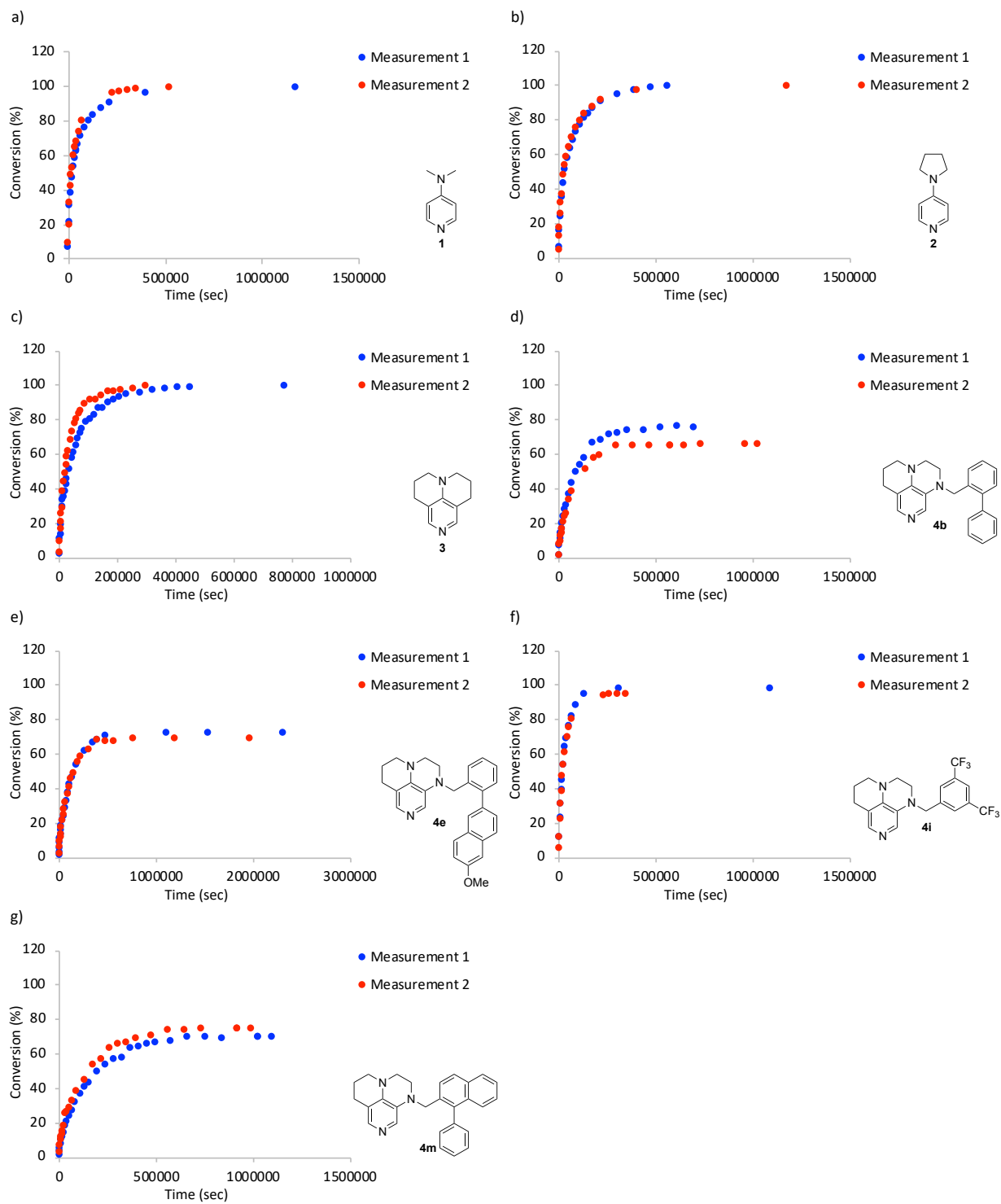


Figure 5.24. Plot of *time (sec)* vs. *conversion (%)* of all OH-groups for acylation of **16** with a) **1**, b) **2**, c) **3**, d) **4b**, e) **4e**, f) **4i** and g) **4m**

Table 5.8. Fitted values of $k_3 - k_7$ by CoPaSi program in ($\text{L mol}^{-1} \text{s}^{-1}$), RMSD (root-mean-square deviation) values of the fitted compounds **16-19** and the corresponding relative rate constants $k_{\text{rel},a}$ and $k_{\text{rel},b}$ for the acylation of **16** with **14** catalysed by **1, 2, 3, 4b,e,i** or **m**.

Cat	Fit	$k_3 - k_7$ ($\text{L mol}^{-1} \text{s}^{-1}$)	RMSD 16	RMSD 17	RMSD 18	RMSD 19	k_{rel}	$k_3 - k_7$ ($\text{L mol}^{-1} \text{s}^{-1}$)	RMSD 16	RMSD 17	RMSD 18	RMSD 19	k_{rel}	Mean $k_3 - k_7$ ($\text{L mol}^{-1} \text{s}^{-1}$)	St. Dev. $k_3 - k_7$	Mean k_{rel}		
1	1	k_3	5.119E-02	3.20E-04	4.41E-04	2.33E-04		k_3	7.263E-02	4.51E-04	1.86E-04							
		k_4	2.094E-02					k_4	2.591E-02									
		k_5	8.447E-03		1.05E-04	1.18E-04	1.37E-04		k_5	1.292E-02	9.55E-05	1.01E-04	1.17E-04					
		k_6	8.600E-03					k_6	1.206E-02									
		k_3	5.750E-02	2.14E-04	1.30E-04	1.38E-04		k_3	8.229E-02	1.58E-04	1.16E-04	1.11E-04		k_3	6.99E-02	1.24E-02	$k_{\text{rel},a}$	
		k_4	2.490E-02				2.31	k_4	3.088E-02					2.66	k_4	2.79E-02	2.99E-03	2.49 ± 0.178
2	1	k_5	8.108E-03		1.07E-04	1.05E-04		k_5	1.251E-02	9.89E-05	7.93E-05	1.04E-04		k_5	1.03E-02	2.20E-03	$k_{\text{rel},b}$	
		k_6	9.233E-03				1.14	k_6	1.323E-02					1.06	k_6	1.12E-02	2.00E-03	1.10 ± 0.041
		k_3	3.070E-02	3.25E-04	4.12E-04	3.61E-04		k_3	3.531E-02	3.47E-04	3.10E-04	3.57E-04						
		k_4	1.559E-02					k_4	1.898E-02									
		k_5	7.031E-03		6.98E-05	1.75E-04	4.01E-05	k_5	7.574E-03	6.28E-05	2.01E-04	4.60E-05						
		k_6	7.157E-03					k_6	8.563E-03									
3	1	k_3	3.635E-02	1.96E-04	1.27E-04	2.06E-04		k_3	4.095E-02	2.51E-04	1.15E-04	2.33E-04		k_3	3.86E-02	2.30E-03	$k_{\text{rel},a}$	
		k_4	1.990E-02				1.83	k_4	2.361E-02					1.73	k_4	2.18E-02	1.85E-03	1.78 ± 0.046
		k_5	6.691E-03		9.78E-05	1.28E-04	6.26E-05	k_5	7.179E-03	9.17E-05	1.67E-04	4.78E-05		k_5	6.94E-03	2.44E-04	$k_{\text{rel},b}$	
		k_6	7.608E-03				1.14	k_6	9.207E-03					1.28	k_6	8.41E-03	7.99E-04	1.21 ± 0.073
		k_3	2.434E-02	4.59E-04	3.64E-04	3.50E-04		k_3	3.294E-02	3.74E-04	2.26E-04	2.11E-04						
		k_4	1.798E-02					k_4	2.210E-02									
4	1	k_5	1.051E-02		1.66E-04	1.60E-04	8.93E-05	k_5	1.858E-02	2.17E-04	1.23E-04	1.68E-04						
		k_6	7.239E-03					k_6	1.208E-02									
		k_3	3.129E-02	3.00E-04	9.19E-05	1.77E-04		$k_{\text{rel},a}$	4.182E-02	9.79E-05	1.31E-04	7.28E-05		$k_{\text{rel},a}$	3.66E-02	5.26E-03	$k_{\text{rel},a}$	
		k_4	2.235E-02				1.40	k_4	2.706E-02					1.55	k_4	2.47E-02	2.35E-03	1.47 ± 0.073
		k_5	1.056E-02		9.45E-05	1.18E-04	1.05E-04	$k_{\text{rel},b}$	1.871E-02	1.36E-04	7.84E-05	1.34E-04		$k_{\text{rel},b}$	1.46E-02	4.07E-03	$k_{\text{rel},b}$	
		k_6	6.983E-03				0.66	k_6	1.166E-02					0.62	k_6	9.32E-03	2.34E-03	0.64 ± 0.019
4b	1	k_3	7.808E-03	4.01E-04	2.00E-04	3.60E-04		k_3	6.480E-03	3.42E-04	2.16E-04	3.48E-04						
		k_4	8.512E-03					k_4	6.480E-03									
		k_5	3.425E-03		1.80E-04	2.31E-04	1.68E-04	k_5	2.019E-03	1.58E-04	2.26E-04	1.39E-04						
		k_6	2.792E-03					k_6	2.006E-03									
		k_7	3.543E-06					k_7	4.627E-06									
		k_3	1.021E-02	2.58E-04	1.02E-04	1.91E-04		k_3	8.217E-03	2.26E-04	8.41E-05	1.85E-04		k_3	9.21E-03	9.96E-04	$k_{\text{rel},a}$	
	k_4	1.085E-02				0.94	k_4	8.272E-03					0.99	k_4	9.56E-03	1.29E-03	0.97 ± 0.026	
	k_5	3.369E-03		1.10E-04	1.59E-04	1.47E-04	k_5	1.881E-03	8.92E-05	1.53E-04	1.21E-04		k_5	2.63E-03	7.44E-04	$k_{\text{rel},b}$		

11700	4.96	4.86	1.0	16448.9	13469.3	4.55	4.45	1.2	19529.0	6.41	6.35	0.5	8823.7	6.62	6.52	0.2	2979.6	38.3	30.1	43.6	19.7	6.7
18900	4.94	4.86	1.0	14431.8	8515.5	4.56	4.46	1.7	24938.4	6.43	6.35	0.7	10554.4	6.64	6.54	0.4	5916.3	47.4	17.1	50.0	21.1	11.9
26100	4.94	4.85	1.0	11784.2	4353.6	4.55	4.46	1.9	22338.2	6.41	6.34	0.8	8983.2	6.61	6.54	0.6	7430.6	53.6	10.1	51.8	20.8	17.2
33300	4.95	4.85	1.0	12866.5	2516.7	4.55	4.46	1.8	22817.1	6.43	6.36	0.7	9157.7	6.62	6.54	0.8	10349.8	58.7	5.6	50.9	20.4	23.1
40500	4.93	4.84	1.0	14112.5	1391.7	4.55	4.44	1.6	22275.4	6.43	6.34	0.6	8834.5	6.62	6.53	0.9	12720.8	62.5	3.1	49.3	19.5	28.1
44100	4.95	4.85	1.0	15524.4	1376.7	4.56	4.45	1.5	22801.5	6.42	6.33	0.6	8600.5	6.62	6.54	0.9	14147.7	63.6	2.9	48.6	18.3	30.2
51300	4.94	4.84	1.0	16338.9	740.1	4.54	4.46	1.2	20053.5	6.41	6.34	0.5	8030.9	6.62	6.55	1.0	15598.8	66.7	1.7	45.1	18.1	35.1
60900						4.57	4.44	1.0	18099.2	6.41	6.34	0.4	7192.3	6.63	6.55	1.1	19587.6	71.8	0.0	40.3	16.0	43.7
82500						4.55	4.46	1.0	14746.0	6.43	6.34	0.4	5969.4	6.65	6.55	1.6	23567.1	76.6	0.0	33.3	13.5	53.2
104100						4.55	4.46	1.0	12457.4	6.42	6.34	0.4	5140.9	6.63	6.53	2.2	27423.8	80.5	0.0	27.7	11.4	60.9
125700						4.57	4.46	1.0	10276.3	6.44	6.35	0.4	4178.3	6.63	6.56	2.9	29353.0	83.5	0.0	23.5	9.5	67.0
168900						4.56	4.46	1.0	7509.5	6.41	6.34	0.4	3165.8	6.63	6.54	4.4	32862.4	87.7	0.0	17.3	7.3	75.5
212100						4.55	4.46	1.0	5307.4	6.42	6.34	0.4	2351.9	6.62	6.53	6.7	35326.8	91.1	0.0	12.4	5.5	82.2
395700						4.55	4.47	1.0	1852.3	6.41	6.35	0.5	967.9	6.63	6.54	23.7	43812.5	97.0	0.0	4.0	2.1	94.0
1173300														6.65	6.55	1.0	38706.7	100.0	0.0	0.0	0.0	100.0
1_b								17				18						Conv	16	17	18	19
1200	4.96	4.89	1.0	33567.1	33567.1	4.76	4.68	0.2	5384.3	6.41	6.34	0.1	2978.4					10.0	80.1	12.8	7.1	0.0
3000	4.96	4.84	1.0	24112.0	23590.8	4.55	4.46	0.4	9939.8	6.40	6.35	0.2	4518.7	6.62	6.56	0.0	521.3	20.1	61.2	25.8	11.7	1.4
6600	4.95	4.85	1.0	17065.6	15231.9	4.56	4.46	1.0	16253.8	6.42	6.35	0.4	6577.3	6.62	6.55	0.1	1833.8	33.2	38.2	40.7	16.5	4.6
10200	4.94	4.86	1.0	13456.7	9889.9	4.56	4.47	1.5	19683.8	6.42	6.34	0.6	7624.4	6.66	6.55	0.3	3566.9	42.2	24.3	48.3	18.7	8.8
13800	4.95	4.85	1.0	11816.8	6322.1	4.55	4.46	1.8	21493.2	6.42	6.34	0.7	8032.8	6.62	6.55	0.5	5494.7	49.0	15.3	52.0	19.4	13.3
17400	4.94	4.85	1.0	11706.5	4400.7	4.54	4.45	1.9	22440.0	6.41	6.35	0.7	8176.9	6.62	6.55	0.6	7305.8	53.4	10.4	53.0	19.3	17.3
24600	4.94	4.85	1.0	12546.2	2030.4	4.54	4.46	1.7	21396.0	6.41	6.34	0.6	7666.7	6.62	6.54	0.8	10515.8	60.2	4.9	51.4	18.4	25.3
31800	4.93	4.86	1.0	14605.1	971.3	4.56	4.46	1.4	19989.0	6.43	6.35	0.5	7209.1	6.62	6.54	0.9	13633.8	65.2	2.3	47.8	17.3	32.6
39000	4.94	4.84	1.0	16821.2	626.4	4.54	4.45	1.1	18482.6	6.43	6.34	0.4	6660.5	6.62	6.54	1.0	16194.8	68.6	1.5	44.0	15.9	38.6
53400	4.93	4.85	1.0	21265.8	382.6	4.54	4.45	0.7	15374.4	6.41	6.34	0.3	5489.0	6.62	6.55	1.0	20883.2	74.3	0.9	36.5	13.0	49.6
71400						4.54	4.46	1.0	12019.1	6.42	6.34	0.4	4539.1	6.63	6.55	2.1	25110.6	80.1	0.0	28.8	10.9	60.3
229800						4.55	4.45	1.0	2101.7	6.41	6.36	0.5	990.5	6.63	6.56	18.7	39373.1	96.4	0.0	5.0	2.3	92.7
264600						4.56	4.47	1.0	1552.4	6.42	6.34	0.5	744.3	6.64	6.55	26.1	40541.3	97.3	0.0	3.6	1.7	94.6
302400						4.57	4.46	1.0	1091.9	6.42	6.35	0.6	601.6	6.62	6.55	37.9	41415.6	98.0	0.0	2.5	1.4	96.1
345600						4.55	4.47	1.0	488.0	6.42	6.35	0.4	184.1	6.62	6.55	87.1	42491.5	99.2	0.0	1.1	0.4	98.4
518400														6.65	6.55	1.0	38706.7	100.0	0.0	0.0	0.0	100.0
2_a								17				18						Conv	16	17	18	19
1200	5.00	4.91	1.0	30544.4	30544.4	4.56	4.47	0.1	1959.0	4.19	3.94	0.2	4987.9					6.4	87.3	5.6	7.1	0.0
4800	4.98	4.91	1.0	24261.3	24261.3	4.57	4.45	0.3	6362.2	4.18	3.97	0.5	11069.5					16.5	67.1	17.6	15.3	0.0
8400	4.99	4.85	1.0	22193.1	21453.4	4.55	4.45	0.5	10259.2	4.17	3.98	0.7	14833.6	6.63	6.54	0.0	739.8	24.0	53.8	25.7	18.6	1.9

15600	4.96	4.84	1.0	14383.6	12566.6	4.56	4.45	1.0	13613.4	4.18	3.96	1.2	16476.1	6.63	6.54	0.1	1817.0	35.2	34.7	37.6	22.7	5.0	
22800	4.96	4.84	1.0	12351.1	8881.4	4.56	4.45	1.4	17384.5	4.18	3.98	1.5	19015.9	6.61	6.55	0.3	3469.7	43.1	22.6	44.3	24.2	8.8	
33600	4.97	4.85	1.0	9902.2	4355.2	4.57	4.46	1.8	17462.3	4.19	3.97	1.8	17291.6	6.62	6.55	0.6	5547.0	51.7	12.1	48.5	24.0	15.4	
44400	4.96	4.84	1.0	10074.1	2330.4	4.55	4.45	1.7	17489.4	4.17	3.96	1.6	16058.6	6.62	6.55	0.8	7743.7	57.6	6.6	49.1	22.6	21.8	
58800	4.94	4.84	1.0	11356.3	891.5	4.54	4.44	1.4	15889.0	4.18	3.97	1.3	14454.4	6.61	6.54	0.9	10464.8	63.9	2.6	46.1	21.0	30.4	
73200	4.96	4.85	1.0	14044.9	473.3	4.55	4.46	1.0	14456.4	4.21	3.96	1.0	14193.3	6.62	6.54	1.0	13571.6	68.4	1.3	40.6	19.9	38.1	
91200						4.56	4.44	1.0	14073.6	4.16	3.97	1.0	13678.9	6.64	6.54	1.3	18682.5	73.6	0.0	35.5	17.3	47.2	
109200						4.55	4.45	1.0	11948.7	4.17	3.97	1.0	11775.4	6.62	6.54	1.8	21426.8	77.3	0.0	30.4	15.0	54.6	
130800						4.57	4.46	1.0	9738.3	4.18	3.97	1.0	9889.7	6.63	6.53	2.5	24115.1	81.1	0.0	25.1	12.8	62.2	
152400						4.56	4.45	1.0	8357.0	4.18	3.98	1.1	8835.9	6.63	6.54	3.3	27182.8	84.0	0.0	20.9	11.1	68.0	
174000						4.56	4.45	1.0	5973.1	4.19	3.98	1.0	6178.9	6.64	6.52	4.5	26716.9	87.3	0.0	16.7	8.6	74.7	
217200						4.55	4.44	1.0	4234.4	4.20	3.96	1.2	4925.3	6.65	6.52	7.0	29490.9	90.8	0.0	11.7	6.8	81.5	
303600						4.57	4.45	1.0	2155.8	4.17	3.98	1.3	2742.4	6.61	6.54	14.9	32108.2	95.1	0.0	6.1	3.9	90.1	
390000						4.54	4.45	1.0	1283.8	4.16	3.98	1.3	1690.7	6.62	6.54	28.6	36744.7	97.3	0.0	3.3	2.2	94.5	
476400							4.56	4.5	1.0	630.37	4.17	4.0	0.4	232.53	6.63	6.63	6.5	56.2	99.0	0.0	1.7	0.3	97.9
562800														6.62	6.54	1.0	38644.1	100.0	0.0	0.0	0.0	100.0	
2_b																			Conv	16	17	18	19
600	5.00	4.90	1.0	46600.9	46600.9	4.58	4.46	0.0	1763.7	4.18	3.96	0.1	5728.3					4.5	91.0	3.4	5.6	0.0	
2700	4.97	4.90	1.0	34395.9	34395.9	4.76	4.67	0.2	6279.9	4.18	3.98	0.4	12119.3					13.2	73.6	13.4	13.0	0.0	
4500	4.99	4.85	1.0	29813.0	29409.2	4.57	4.46	0.3	8180.4	4.17	3.99	0.5	14129.8	6.61	6.54	0.0	403.8	17.8	65.3	18.2	15.7	0.9	
8100	4.97	4.85	1.0	23744.9	22717.4	4.55	4.46	0.5	12333.0	4.18	3.98	0.8	17975.7	6.62	6.54	0.0	1027.5	25.9	50.4	27.4	19.9	2.3	
11700	4.95	4.84	1.0	19573.9	17755.3	4.56	4.46	0.8	15079.2	4.19	3.98	1.0	19170.2	6.61	6.55	0.1	1818.6	32.0	40.1	34.1	21.7	4.1	
15300	4.94	4.85	1.0	19519.3	16241.6	4.56	4.46	1.1	20451.8	4.18	3.97	1.2	23182.6	6.62	6.54	0.2	3277.7	37.4	31.5	39.7	22.5	6.4	
26100	4.95	4.85	1.0	12333.1	6868.7	4.55	4.43	1.6	20262.0	4.18	3.97	1.6	20144.1	6.62	6.55	0.4	5464.4	48.4	16.1	47.5	23.6	12.8	
33300	4.93	4.85	1.0	12652.5	4469.8	4.57	4.46	1.7	21947.0	4.17	3.98	1.7	21056.8	6.62	6.55	0.7	8182.7	54.1	9.9	48.6	23.3	18.1	
40500	4.94	4.85	1.0	13395.6	2855.0	4.55	4.47	1.6	21724.1	4.17	3.98	1.5	20633.3	6.63	6.55	0.8	10540.6	58.5	6.3	47.8	22.7	23.2	
51300	4.93	4.85	1.0	14333.7	954.6	4.55	4.45	1.4	19879.4	4.19	3.97	1.3	18738.7	6.62	6.54	0.9	13379.1	64.3	2.2	45.6	21.5	30.7	
65700						4.56	4.47	1.0	17767.8	4.16	3.98	1.0	16837.6	6.63	6.56	1.0	17519.1	70.0	0.0	40.7	19.3	40.1	
87300						4.54	4.45	1.0	16507.4	4.17	3.96	1.0	15774.8	6.62	6.53	1.6	25662.3	75.6	0.0	33.0	15.8	51.3	
108900						4.57	4.44	1.0	12121.3	4.18	3.97	1.0	12239.1	6.62	6.55	2.2	26773.4	79.7	0.0	26.9	13.6	59.5	
130500						4.57	4.46	1.0	9680.0	4.18	3.98	1.0	9684.1	6.63	6.54	3.1	29510.9	83.5	0.0	22.0	11.0	67.0	
173700						4.56	4.45	1.0	6773.0	4.16	3.98	1.1	7361.9	6.63	6.53	5.0	33709.4	88.2	0.0	15.3	8.3	76.3	
216900						4.55	4.46	1.0	4546.3	4.16	3.98	1.2	5378.9	6.63	6.53	7.9	35908.3	91.6	0.0	10.5	6.2	83.2	
400500						4.57	4.43	1.0	1167.8	4.17	3.97	1.4	1652.1	6.61	6.53	34.9	40706.5	97.7	0.0	2.7	1.9	95.3	
1178100														6.62	6.54	1.0	38644.1	100.0	0.0	0.0	0.0	100.0	
3_a																			Conv	16	17	18	19

420	5.00	4.91	1.0	39007.0	/	4.55	4.46	0.0	865.4	6.43	6.36	0.0	1062.6					2.4	95.3	2.1	2.6	0.0
3000	4.99	4.91	1.0	35182.0	/	4.55	4.46	0.1	4873.9	6.42	6.35	0.1	5047.3					11.0	78.0	10.8	11.2	0.0
4200	4.97	4.92	1.0	28164.9	/	4.55	4.47	0.2	5579.6	6.42	6.33	0.2	5484.4					14.1	71.8	14.2	14.0	0.0
6000	3.74	3.64	1.0	25266.5	/	4.56	4.46	0.3	7483.2	6.43	6.35	0.3	6835.5	6.62	6.54	0.0	617.7	19.3	62.9	18.6	17.0	1.5
9600	3.74	3.64	1.0	15203.5	/	4.56	4.46	0.6	9797.8	6.43	6.33	0.5	8361.6	6.63	6.54	0.1	1197.0	29.7	44.0	28.4	24.2	3.5
13200	3.73	3.64	1.0	13677.4	/	4.56	4.46	0.9	11782.3	6.41	6.34	0.7	9495.0	6.64	6.54	0.1	1919.9	34.1	37.1	32.0	25.8	5.2
16800	3.83	3.75	1.0	15176.5	/	4.55	4.46	0.9	13716.6	6.42	6.35	0.7	10633.5	6.64	6.54	0.2	2663.4	35.2	36.0	32.5	25.2	6.3
20400	3.83	3.73	1.0	12847.7	/	4.55	4.46	1.2	14911.5	6.42	6.34	0.9	11170.7	6.63	6.55	0.3	3447.5	38.9	30.3	35.2	26.4	8.1
24000	3.82	3.73	1.0	10275.9	/	4.57	4.46	1.5	15149.9	6.41	6.35	1.1	11091.0	6.62	6.55	0.4	4249.8	42.6	25.2	37.2	27.2	10.4
27600	3.83	3.74	1.0	8618.0	/	4.57	4.46	1.9	16158.1	6.41	6.33	1.4	11678.0	6.63	6.56	0.6	5354.0	46.1	20.6	38.7	27.9	12.8
34800	3.81	3.74	1.0	5971.5	/	4.55	4.46	2.7	16327.1	6.41	6.34	2.0	11752.0	6.62	6.55	1.2	7295.4	51.6	14.4	39.5	28.4	17.6
42000	3.82	3.73	1.0	3274.6	/	4.56	4.46	5.0	16419.0	6.42	6.34	3.7	11941.8	6.63	6.55	3.0	9941.8	58.0	7.9	39.5	28.7	23.9
49200	3.82	3.74	1.0	2458.1	/	4.56	4.46	6.5	15902.9	6.42	6.34	4.8	11739.6	6.62	6.56	5.0	12199.6	61.5	5.8	37.6	27.8	28.8
56400	3.82	3.74	1.0	1114.7	/	4.56	4.46	10.1	11224.0	6.43	6.35	7.7	8593.2	6.63	6.54	9.9	11016.1	65.5	3.5	35.1	26.9	34.5
63600	3.81	3.73	1.0	761.9	/	4.55	4.46	17.5	13348.3	6.41	6.36	14.1	10730.7	6.62	6.54	21.8	16609.1	69.1	1.8	32.2	25.9	40.1
70800						4.55	4.46	1.0	12187.9	6.41	6.35	0.9	10407.4	6.63	6.54	1.6	18871.0	72.8	0.0	29.4	25.1	45.5
78000						4.56	4.45	1.0	11391.0	6.42	6.34	0.9	10306.2	6.61	6.55	1.9	21437.5	74.9	0.0	26.4	23.9	49.7
92400						4.56	4.45	1.0	9148.5	6.42	6.34	1.0	9220.5	6.61	6.55	2.7	24593.1	78.6	0.0	21.3	21.5	57.2
106800						4.55	4.46	1.0	8332.2	6.42	6.34	1.1	9473.5	6.62	6.55	3.4	28150.2	80.6	0.0	18.1	20.6	61.3
121200						4.55	4.46	1.0	6752.3	6.42	6.34	1.3	8417.0	6.62	6.55	4.4	29935.5	83.2	0.0	15.0	18.7	66.4
135600						4.56	4.45	1.0	4334.4	6.41	6.34	1.5	6418.8	6.64	6.54	7.1	30550.6	87.0	0.0	10.5	15.5	74.0
150000						4.57	4.45	1.0	5561.2	6.41	6.34	1.2	6905.8	6.62	6.55	6.2	34205.0	86.6	0.0	11.9	14.8	73.3
168000						4.55	4.46	1.0	2808.1	6.41	6.34	1.9	5333.6	6.64	6.54	12.6	35305.7	90.6	0.0	6.5	12.3	81.3
186000						4.57	4.46	1.0	2142.1	6.41	6.34	2.2	4628.9	6.62	6.54	17.0	36470.1	92.2	0.0	5.0	10.7	84.3
207600						4.56	4.46	1.0	1616.0	6.40	6.35	2.4	3793.2	6.63	6.55	22.5	36296.5	93.5	0.0	3.9	9.1	87.0
232800						4.56	4.46	1.0	1177.2	6.41	6.34	2.7	3160.9	6.61	6.54	31.9	37575.2	94.8	0.0	2.8	7.5	89.7
276000						4.54	4.46	1.0	819.6	6.41	6.34	3.0	2462.9	6.62	6.55	49.0	40120.0	96.2	0.0	1.9	5.7	92.4
319200						4.56	4.47	1.0	516.3	6.41	6.34	3.4	1774.2	6.62	6.54	76.8	39661.7	97.3	0.0	1.2	4.2	94.5
362400										6.43	6.34	1.0	1209.4	6.62	6.54	33.1	39967.3	98.5	0.0	0.0	2.9	97.1
405600										6.41	6.34	1.0	948.4	6.64	6.54	43.6	41305.8	98.9	0.0	0.0	2.2	97.8
448800										6.40	6.35	1.0	432.5	6.63	6.54	97.5	42151.0	99.5	0.0	0.0	1.0	99.0
776400														6.63	6.55	1.0	40912.4	100.0		0.0	0.0	100.0
3_b								17				18				19		Conv	16	17	18	19
600	4.98	4.90	1.0	38937.5	/	4.57	4.46	0.0	1432.5	6.42	6.34	0.0	1442.4				3.4	93.1	3.4	3.4	3.5	0.0
2400	4.98	4.90	1.0	34228.4	/	4.56	4.47	0.1	4303.9	6.41	6.34	0.1	3913.5				9.7	80.6	10.1	9.2	0.0	0.0
4200	4.97	4.90	1.0	29600.2	/	4.56	4.47	0.3	7409.6	6.42	6.35	0.2	6106.7	6.62	6.54	0.0	600.4	16.8	67.7	17.0	14.0	1.4

6000	3.84	3.74	1.0	25848.7	/	4.57	4.46	0.4	9197.5	6.41	6.36	0.3	7136.5	6.65	6.55	0.0	925.5	21.1	60.0	21.3	16.6	2.2
7800	4.95	4.91	1.0	22139.2	/	4.57	4.46	0.5	11076.0	6.42	6.34	0.4	8206.5	6.62	6.54	0.1	1511.8	26.0	51.6	25.8	19.1	3.5
9600	4.96	4.90	1.0	20012.7	/	4.56	4.47	0.6	12612.5	6.42	6.34	0.5	9119.2	6.63	6.54	0.1	1955.8	29.3	45.8	28.9	20.9	4.5
13200	3.82	3.74	1.0	13237.0	/	4.57	4.46	1.1	14887.3	6.42	6.34	0.8	10236.8	6.64	6.53	0.3	3445.2	38.3	31.7	35.6	24.5	8.2
16800	3.81	3.74	1.0	9658.7	/	4.56	4.46	1.7	16133.9	6.42	6.34	1.1	10848.2	6.63	6.54	0.5	5096.0	44.5	23.1	38.7	26.0	12.2
20400	3.81	3.73	1.0	7434.0	/	4.56	4.45	2.3	17250.5	6.43	6.35	1.5	11239.0	6.65	6.55	0.9	6939.5	49.4	17.3	40.3	26.2	16.2
24000	3.81	3.72	1.0	5349.2	/	4.56	4.46	3.3	17466.8	6.44	6.33	2.1	11353.8	6.64	6.54	1.7	8870.4	54.1	12.4	40.6	26.4	20.6
27600	3.81	3.72	1.0	3760.0	/	4.56	4.47	4.7	17538.8	6.43	6.34	3.1	11589.0	6.63	6.55	3.0	11302.4	58.5	8.5	39.7	26.2	25.6
31200	3.80	3.72	1.0	2761.1	/	4.56	4.47	6.0	16651.5	6.42	6.35	4.1	11359.3	6.63	6.55	4.9	13419.0	62.1	6.3	37.7	25.7	30.4
38400	3.79	3.72	1.0	1097.0	/	4.57	4.45	13.0	14279.4	6.42	6.34	9.6	10563.6	6.62	6.56	15.6	17076.6	68.6	2.6	33.2	24.6	39.7
45600	3.81	3.72	1.0	313.6	/	4.56	4.46	40.1	12571.2	6.44	6.35	32.3	10129.2	6.63	6.55	67.6	21184.5	73.6	0.7	28.4	22.9	47.9
52800						4.57	4.46	1.0	10255.4	6.42	6.34	0.9	9208.9	6.63	6.54	2.4	24368.8	77.8	0.0	23.4	21.0	55.6
60000						4.55	4.46	1.0	8374.3	6.42	6.35	1.0	8386.4	6.63	6.55	3.2	27051.7	80.9	0.0	19.1	19.1	61.7
67200						4.56	4.46	1.0	6620.2	6.42	6.34	1.1	7455.1	6.63	6.54	4.3	28701.6	83.6	0.0	15.5	17.4	67.1
74400						4.56	4.45	1.0	5465.8	6.41	6.34	1.3	6817.0	6.62	6.55	5.6	30781.8	85.7	0.0	12.7	15.8	71.5
88800						4.57	4.45	1.0	3339.8	6.42	6.32	1.7	5524.9	6.65	6.53	10.0	33219.6	89.5	0.0	7.9	13.1	78.9
106800						4.55	4.47	1.0	2464.1	6.42	6.34	1.9	4720.7	6.63	6.54	15.2	37520.3	92.0	0.0	5.5	10.6	83.9
124800						4.56	4.47	1.0	2786.0	6.41	6.34	1.6	4480.8	6.62	6.55	13.9	38840.1	92.1	0.0	6.0	9.7	84.2
146400						4.55	4.47	1.0	1980.8	6.40	6.34	1.8	3631.2	6.61	6.55	20.6	40781.1	94.0	0.0	4.3	7.8	87.9
168000										6.42	6.35	1.0	2965.7	6.62	6.54	14.0	41650.8	96.7	0.0	0.0	6.7	93.4
189600										6.41	6.34	1.0	2421.0	6.63	6.54	16.0	38648.6	97.1	0.0	0.0	5.9	94.1
211200										6.41	6.35	1.0	2200.1	6.62	6.55	19.7	43375.2	97.6	0.0	0.0	4.8	95.2
254400										6.43	6.34	1.0	1765.6	6.63	6.55	24.5	43316.6	98.0	0.0	0.0	3.9	96.1
297600														6.62	6.54	1.0	39376.8	100.0	0.0	0.0	0.0	100.0
4b_a								17				18				19		Conv	16	17	18	19
600	5.00	4.90	1.0	41680.5	/	4.75	4.69	0.0	599.8	6.41	6.35	0.0	992.7					1.8	96.3	1.4	2.3	0.0
3600	4.98	4.90	1.0	43032.6	/	4.76	4.68	0.1	3018.8	6.41	6.35	0.1	4513.9					7.5	85.1	6.0	8.9	0.0
6000	4.98	4.91	1.0	39342.6	/	4.76	4.68	0.1	4517.0	6.40	6.34	0.2	6509.9					11.0	78.1	9.0	12.9	0.0
9600	4.98	4.90	1.0	34963.7	/	4.75	4.69	0.2	5800.5	6.41	6.35	0.2	8090.0					14.2	71.6	11.9	16.6	0.0
13200	4.98	4.91	1.0	22990.3	/	4.75	4.69	0.2	4946.8	6.43	6.34	0.3	6629.9					16.8	66.5	14.3	19.2	0.0
16800	4.97	4.90	1.0	32169.1	/	4.74	4.68	0.3	8605.2	6.42	6.35	0.3	10877.1	6.61	6.55	0.0	870.4	20.2	61.3	16.4	20.7	1.7
24000	4.97	4.90	1.0	25255.8	/	4.74	4.68	0.4	9121.1	6.41	6.33	0.4	10902.7	6.62	6.55	0.0	1012.9	23.8	54.6	19.7	23.6	2.2
31200	4.96	4.91	1.0	24030.2	/	4.75	4.67	0.5	11754.4	6.41	6.34	0.6	13423.9	6.63	6.54	0.1	1679.8	28.0	47.2	23.1	26.4	3.3
38400	4.95	4.90	1.0	22055.6	/	4.74	4.67	0.6	13348.6	6.41	6.34	0.7	14653.8	6.62	6.54	0.1	2168.1	31.0	42.2	25.6	28.1	4.2
52800	3.82	3.72	0.9	14405.1	/	4.74	4.68	0.9	13548.9	6.41	6.35	0.9	14336.8	6.62	6.55	0.2	2917.7	37.3	31.9	30.0	31.7	6.5
67200	3.81	3.74	1.0	9411.9	/	4.74	4.69	1.5	13842.8	6.41	6.34	1.6	14840.5	6.62	6.55	0.4	3975.1	43.5	22.4	32.9	35.3	9.5

88800	3.80	3.75	1.0	7002.3	/	4.73	4.68	2.6	18464.4	6.42	6.35	2.7	18838.3	6.62	6.55	1.0	7082.6	50.1	13.6	35.9	36.7	13.8
110400	3.81	3.74	1.0	4215.5	/	4.74	4.67	3.9	16473.6	6.42	6.34	4.0	16687.0	6.61	6.56	1.8	7712.5	53.9	9.4	36.5	37.0	17.1
132000	3.80	3.74	1.0	2992.2	/	4.74	4.67	5.5	16472.9	6.41	6.34	5.7	16948.7	6.62	6.55	3.4	10219.9	57.8	6.4	35.3	36.3	21.9
175200						4.74	4.69	1.0	11691.9	6.41	6.34	1.4	15763.9	6.62	6.54	1.2	14288.0	67.1	0.0	28.0	37.8	34.2
218400						4.73	4.67	1.0	11429.4	6.42	6.34	1.2	13524.7	6.63	6.54	1.3	15101.9	68.9	0.0	28.5	33.8	37.7
261600						4.74	4.66	1.0	11539.4	6.41	6.33	1.2	13995.9	6.62	6.56	1.7	19079.0	71.4	0.0	25.9	31.4	42.8
304800						4.73	4.66	1.0	10781.9	6.41	6.35	1.3	13544.7	6.62	6.55	1.9	20543.9	72.9	0.0	24.0	30.2	45.8
351600						4.74	4.67	1.0	9538.3	6.41	6.34	1.3	12404.0	6.63	6.54	2.1	20052.2	73.9	0.0	22.7	29.5	47.8
438000						4.73	4.66	1.0	9967.6	6.41	6.34	1.3	12810.3	6.62	6.54	2.2	21618.7	74.4	0.0	22.5	28.9	48.7
524400						4.73	4.67	1.0	10040.3	6.41	6.33	1.2	12258.7	6.62	6.56	2.3	23055.8	75.4	0.0	22.1	27.0	50.8
610800						4.73	4.67	1.0	8207.5	6.42	6.32	1.4	11699.1	6.63	6.55	2.7	22151.0	76.3	0.0	19.5	27.8	52.7
697200						4.74	4.66	1.0	9194.2	6.41	6.34	1.2	11262.4	6.62	6.54	2.4	22009.7	75.9	0.0	21.7	26.5	51.8
4b_b																		Conv	16	17	18	19
900	5.01	4.90	1.0	43364.4	/	4.76	4.67	0.0	746.5	6.42	6.34	0.0	972.0					1.9	96.2	1.7	2.2	0.0
5100	5.00	4.91	1.0	35592.1	/	4.75	4.68	0.1	2519.1	6.43	6.34	0.1	3990.3					7.7	84.5	6.0	9.5	0.0
7500	5.00	4.92	1.0	35639.0	/	4.76	4.67	0.1	3743.4	6.41	6.34	0.2	5209.8					10.0	79.9	8.4	11.7	0.0
11100	4.99	4.92	1.0	35637.5	/	4.78	4.68	0.2	5390.8	6.42	6.35	0.2	6857.0					12.8	74.4	11.3	14.3	0.0
14700	4.99	4.91	1.0	30368.9	/	4.76	4.68	0.2	5548.4	6.41	6.34	0.2	6935.4					14.6	70.9	13.0	16.2	0.0
18300	4.98	4.92	1.0	28675.4	/	4.75	4.67	0.2	6387.1	6.42	6.34	0.3	7717.5	6.62	6.55	0.0	332.1	17.1	66.5	14.8	17.9	0.8
25500	4.99	4.91	1.0	25600.0	/	4.75	4.68	0.3	7672.0	6.42	6.34	0.4	8847.2	6.62	6.53	0.0	763.8	21.0	59.7	17.9	20.6	1.8
32700	4.98	4.91	1.0	24047.1	/	4.75	4.68	0.4	9196.1	6.41	6.34	0.4	10177.3	6.62	6.55	0.0	1041.1	24.1	54.1	20.7	22.9	2.3
39900	4.97	4.91	1.0	21198.9	/	4.75	4.68	0.5	10069.7	6.39	6.35	0.4	8509.2	6.61	6.54	0.1	1223.6	25.6	51.7	24.6	20.8	3.0
54300	3.83	3.75	1.0	16671.3	/	4.74	4.67	0.8	12762.0	6.42	6.34	0.8	13217.7	6.62	6.54	0.1	1924.2	33.5	37.4	28.6	29.7	4.3
68700	3.82	3.75	1.0	12234.3	/	4.74	4.68	1.1	13419.6	6.41	6.34	1.1	13518.5	6.62	6.55	0.2	2628.1	38.5	29.3	32.1	32.3	6.3
135900	3.81	3.75	1.0	4635.1	/	4.74	4.66	3.4	15551.1	6.41	6.34	3.2	14810.0	6.61	6.54	1.2	5604.9	51.2	11.4	38.3	36.5	13.8
179100	3.81	3.74	1.0	1448.3	/	4.74	4.66	10.3	14966.9	6.42	6.34	9.7	14045.2	6.61	6.55	5.2	7567.5	58.1	3.8	39.4	36.9	19.9
211500	3.80	3.75	1.0	1173.4	/	4.73	4.67	12.2	14334.7	6.44	6.34	11.6	13639.3	6.63	6.55	6.9	8126.8	59.3	3.2	38.5	36.6	21.8
297900						4.74	4.67	1.0	14205.3	6.42	6.33	1.0	13895.1	6.62	6.55	0.9	12119.0	65.1	0.0	35.3	34.6	30.1
384300						4.55	4.47	1.0	12252.2	6.42	6.34	1.1	13320.0	6.62	6.55	0.9	11476.0	65.5	0.0	33.1	36.0	31.0
470700						4.56	4.46	1.0	13492.8	6.40	6.33	1.1	14235.3	6.63	6.55	0.9	12097.5	65.2	0.0	33.9	35.7	30.4
573000						4.56	4.46	1.0	14410.6	6.42	6.33	1.0	14354.7	6.63	6.55	0.9	12638.0	65.3	0.0	34.8	34.7	30.5
574800						4.54	4.46	1.0	13787.0	6.40	6.34	1.0	14382.3	6.63	6.56	0.9	12493.5	65.4	0.0	33.9	35.4	30.7
643200						4.53	4.47	1.0	5611.7	6.40	6.33	1.1	6063.2	6.62	6.54	1.0	5319.2	65.7	0.0	33.0	35.7	31.3
729600						4.54	4.46	1.0	6085.8	6.40	6.33	1.0	6201.9	6.63	6.54	0.9	5718.3	65.9	0.0	33.8	34.4	31.8
960000						4.73	4.66	1.0	13484.5	6.41	6.33	0.9	12381.7	4.92	4.85	0.9	12123.5	66.0	0.0	35.5	32.6	31.9
1028400						4.72	4.67	1.0	11640.4	6.41	6.33	1.0	11342.3	4.92	4.85	0.9	10621.3	65.8	0.0	34.6	33.8	31.6

4e_a	16				17				18				19				Conv	16	17	18	19			
	5.00	4.92	1.0	48229.1	48229.1	477	4.68	0.0	592.3	6.42	6.33	0.0	1274.0	6.61	6.52	0.0						361.6	57.7	18.7
480	5.00	4.92	1.0	48229.1	48229.1	477	4.68	0.0	592.3	6.42	6.33	0.0	1274.0	6.61	6.52	0.0	361.6	57.7	18.7	21.9	1.9	96.3	1.2	2.5
2280	5.00	4.92	1.0	44670.6	44670.6	476	4.68	0.0	1248.6	6.43	6.34	0.1	2215.5	6.61	6.52	0.0	538.9	63.3	16.1	19.5	3.6	92.8	2.6	4.6
4080	4.99	4.92	1.0	49119.5	49119.5	478	4.68	0.1	2561.3	6.42	6.34	0.1	4004.3	6.61	6.52	0.0	887.5	68.8	13.7	16.9	5.9	88.2	4.6	7.2
7680	5.00	4.90	1.0	45013.3	45013.3	478	4.68	0.1	4023.6	6.43	6.33	0.1	5988.4	6.61	6.52	0.0	1152.5	72.9	11.6	15.5	9.1	81.8	7.3	10.9
11280	4.99	4.89	1.0	41885.8	41885.8	475	4.66	0.1	5085.1	6.42	6.35	0.2	7271.7	6.61	6.52	0.0	1703.6	77.2	9.4	13.4	11.4	77.2	9.4	13.4
14880	5.00	4.91	1.0	40135.1	40135.1	476	4.68	0.2	6405.4	6.43	6.32	0.2	8527.2	6.61	6.52	0.0	2381.8	82.2	29.3	35.6	13.6	72.9	11.6	15.5
18480	5.00	4.91	1.0	38333.2	38333.2	478	4.67	0.2	7639.6	6.42	6.34	0.3	9396.6	6.61	6.52	0.0	3057.6	88.2	26.4	28.8	15.9	68.8	13.7	16.9
25680	4.98	4.91	1.0	32177.8	32177.8	477	4.67	0.3	8164.2	6.41	6.33	0.3	9917.1	6.61	6.52	0.0	4274.8	92.8	24.9	26.8	18.9	63.3	16.1	19.5
32880	4.99	4.86	1.0	31947.7	31060.2	475	4.67	0.3	10058.6	6.42	6.34	0.4	11803.1	6.61	6.52	0.0	5795.3	95.1	27.1	28.6	22.0	57.7	18.7	21.9
40080	4.99	4.85	1.0	30456.8	29304.3	475	4.68	0.4	11530.8	6.42	6.36	0.4	13169.7	6.61	6.52	0.0	8234.3	100.0	26.6	28.5	24.5	53.1	20.9	23.9
58080	4.98	4.85	1.0	25944.2	24240.6	475	4.68	0.5	13406.2	6.42	6.32	0.6	14416.6	6.61	6.52	0.0	12968.9	105.0	26.6	28.5	29.0	45.1	24.9	26.8
72480	4.97	4.86	1.0	23533.4	21151.6	474	4.67	0.7	15561.8	6.42	6.34	0.7	16187.5	6.61	6.52	0.0	17701.0	109.0	27.1	28.6	33.0	38.3	28.2	29.3
86880	4.96	4.86	1.0	18547.5	15489.9	474	4.68	0.9	15727.9	6.41	6.34	0.9	15734.3	6.61	6.52	0.0	20153.2	112.0	27.1	28.6	37.6	31.0	31.5	31.5
108480	4.96	4.86	1.0	15963.5	11688.7	474	4.68	1.1	16964.3	6.41	6.34	1.1	16854.4	6.61	6.52	0.0	22260.4	115.0	27.1	28.6	42.6	23.5	34.1	33.9
130080	4.96	4.86	1.0	15255.1	9459.8	474	4.68	1.2	18789.4	6.41	6.34	1.2	17996.0	6.61	6.52	0.0	2381.8	118.0	27.1	28.6	46.5	18.2	36.1	34.6
173280	4.96	4.86	1.0	12912.2	4677.9	474	4.66	1.4	18563.7	6.40	6.35	1.4	17748.4	6.61	6.52	0.0	2381.8	120.0	27.1	28.6	53.6	9.5	37.7	36.1
259680	4.94	4.86	1.0	14228.7	1259.8	474	4.66	1.2	17306.1	6.41	6.34	1.2	17445.5	6.61	6.52	0.0	2381.8	122.0	27.1	28.6	62.0	2.6	35.3	35.6
346080						473	4.67	1.0	16661.2	6.42	6.34	1.1	18326.3	6.61	6.52	0.0	2381.8	124.0	27.1	28.6	67.1	0.0	31.4	34.5
385680						474	4.67	1.0	14239.0	6.40	6.34	1.1	16149.0	6.61	6.52	0.0	2381.8	126.0	27.1	28.6	68.4	0.0	29.6	33.6
472080						474	4.66	1.0	12585.4	6.42	6.33	1.2	15568.0	6.61	6.52	0.0	2381.8	128.0	27.1	28.6	70.9	0.0	26.1	32.2
1105680						474	4.65	1.0	12533.7	6.42	6.33	1.1	13666.3	6.61	6.52	0.0	2381.8	130.0	27.1	28.6	72.4	0.0	26.4	28.8
1537680						474	4.67	1.0	13357.4	6.40	6.33	1.1	14312.4	6.61	6.52	0.0	2381.8	132.0	27.1	28.6	72.5	0.0	26.6	28.5
2315280						474	4.66	1.0	13608.4	6.41	6.34	1.1	14345.7	6.61	6.52	0.0	2381.8	134.0	27.1	28.6	72.2	0.0	27.1	28.6
4e_b	16				17				18				19				Conv	16	17	18	19			
5.00	4.90	1.0	36742.3	36742.3	475	4.69	0.0	598.1	6.42	6.35	0.0	1008.9	6.61	6.52 <td>0.0</td> <th>592.1</th> <th>72.2<th>27.1</th><th>28.6</th> <th>2.1</th><th>95.8</th><th>1.6</th><th>2.6</th> </th>	0.0	592.1						72.2 <th>27.1</th> <th>28.6</th> <th>2.1</th> <th>95.8</th> <th>1.6</th> <th>2.6</th>	27.1	28.6
600	5.00	4.90	1.0	36742.3	36742.3	475	4.69	0.0	598.1	6.42	6.35	0.0	1008.9	6.61	6.52	0.0	592.1	72.2	27.1	28.6	2.1	95.8	1.6	2.6
4200	4.99	4.90	1.0	30129.7	30129.7	476	4.68	0.1	1904.7	6.42	6.34	0.1	2853.4	6.61	6.52	0.0	592.1	74.0	27.1	28.6	6.8	86.4	5.5	8.2
7800	5.00	4.91	1.0	31596.3	31596.3	476	4.68	0.1	3108.7	6.43	6.35	0.1	4423.8	6.61	6.52	0.0	592.1	76.0	27.1	28.6	9.6	80.8	7.9	11.3
11400	5.00	4.92	1.0	29142.8	29142.8	476	4.69	0.1	3793.4	6.41	6.34	0.2	5182.2	6.61	6.52	0.0	592.1	78.0	27.1	28.6	11.8	76.5	10.0	13.6
15000	4.99	4.90	1.0	26749.2	26749.2	476	4.68	0.2	4557.0	6.41	6.34	0.2	5809.9	6.61	6.52	0.0	592.1	80.0	27.1	28.6	14.0	72.1	12.3	15.7
22200	4.99	4.92	1.0	24664.1	24664.1	477	4.68	0.2	5884.8	6.42	6.35	0.3	7194.5	6.61	6.52	0.0	592.1	82.0	27.1	28.6	17.3	65.4	15.6	19.1
29400	4.98	4.85	1.0	23061.7	22469.6	475	4.68	0.3	7004.2	6.42	6.35	0.4	8139.3	6.61	6.52	0.0	592.1	84.0	27.1	28.6	21.4	58.8	18.3	21.3
40200	4.99	4.85	1.0	21310.9	20408.6	475	4.66	0.4	8477.0	6.42	6.36	0.4	9194.9	6.61	6.52	0.0	592.1	86.0	27.1	28.6	25.0	52.4	21.8	23.6
51000	4.99	4.85	1.0	17154.6	16084.5	475	4.69	0.5	8659.6	6.41	6.35	0.5	9187.6	6.61	6.52	0.0	592.1	88.0	27.1	28.6	28.6	46.0	24.7	26.3
65400	4.98	4.86	1.0	16555.0	15004.0	474	4.69	0.6	10438.9	6.42	6.35	0.7	10958.5	6.61	6.52	0.0	592.1	90.0	27.1	28.6	32.3	39.5	27.5	28.9
83400	4.98	4.86	1.0	12828.0	10941.5	475	4.67	0.8	10599.6	6.42	6.34	0.8	10593.6	6.61	6.52	0.0	592.1	92.0	27.1	28.6	36.7	32.2	31.2	31.1

101400	4.98	4.85	1.0	12578.3	9671.0	4.74	4.66	1.0	12897.6	6.41	6.35	1.0	12648.2	6.63	6.55	0.2	2907.3	41.1	25.4	33.8	33.2	7.6
123000	4.96	4.86	1.0	9542.2	6037.3	4.74	4.68	1.3	12042.9	6.42	6.35	1.2	11733.1	6.61	6.55	0.4	3504.9	46.2	18.1	36.2	35.2	10.5
144600	4.96	4.85	1.0	10015.8	5413.9	4.74	4.68	1.4	13871.9	6.41	6.34	1.3	13185.2	6.61	6.55	0.5	4601.9	48.9	14.6	37.4	35.6	12.4
187800	4.96	4.86	1.0	9057.4	2471.1	4.74	4.67	1.5	13759.6	6.42	6.35	1.5	13261.9	6.61	6.55	0.7	6586.3	55.7	6.9	38.1	36.8	18.3
223800	4.95	4.86	1.0	8059.2	1215.6	4.74	4.66	1.5	11788.1	6.41	6.33	1.4	11380.2	6.62	6.54	0.9	6843.6	59.0	3.9	37.8	36.4	21.9
310200	4.96	4.85	1.0	9953.2	716.7	4.75	4.69	1.1	10959.3	6.42	6.33	1.2	11584.4	6.63	6.56	0.9	9236.5	63.1	2.2	33.7	35.7	28.4
396600						4.74	4.66	1.0	10865.1	6.41	6.34	1.0	11857.0	6.63	6.55	1.2	13049.9	68.2	0.0	30.4	33.2	36.5
483000						4.74	4.67	1.0	9561.3	6.40	6.34	1.1	10420.3	6.62	6.55	1.2	11207.5	68.0	0.0	30.7	33.4	35.9
569400						4.74	4.67	1.0	10660.4	6.41	6.34	1.1	11859.5	6.63	6.55	1.2	12689.7	68.0	0.0	30.3	33.7	36.0
760200						4.73	4.68	1.0	10234.6	6.40	6.34	1.0	9854.4	4.93	4.85	1.2	12389.4	69.1	0.0	31.5	30.3	38.2
1192200						4.73	4.67	1.0	10491.6	6.41	6.34	1.0	10226.3	4.93	4.85	1.2	12732.4	69.0	0.0	31.4	30.6	38.1
1969800						4.74	4.68	1.0	9669.9	6.42	6.33	1.0	9349.4	4.94	4.84	1.2	11830.3	69.2	0.0	31.4	30.3	38.4
4i_a				16				17				18				19		Conv	16	17	18	19
2700	4.96	4.90	1.0	28717.6	28717.6	4.73	4.67	0.1	3850.5	6.41	6.35	0.2	4915.7					11.7	76.6	10.3	13.1	0.0
6300	4.95	4.85	1.0	20158.5	19040.9	4.74	4.67	0.3	6060.4	6.42	6.33	0.4	7153.5	6.63	6.53	0.1	1117.6	23.2	57.1	18.2	21.4	3.4
9900	4.95	4.85	1.0	15857.8	13797.9	4.73	4.67	0.5	7881.9	6.41	6.32	0.5	8357.9	6.62	6.54	0.1	2059.9	31.7	43.0	24.6	26.0	6.4
13500	4.95	4.84	1.0	14279.1	10848.9	4.74	4.66	0.7	10284.2	6.41	6.33	0.7	9781.0	6.61	6.54	0.2	3430.2	39.2	31.6	29.9	28.5	10.0
17100	4.94	4.85	1.0	12304.8	7741.4	4.73	4.67	0.9	10769.6	6.41	6.33	0.8	9827.0	6.62	6.55	0.4	4563.4	45.2	23.5	32.7	29.9	13.9
24300	4.93	4.84	1.0	12843.9	4816.5	4.74	4.66	1.0	13378.6	6.40	6.34	0.9	10974.7	6.62	6.55	0.6	8027.4	54.3	13.0	36.0	29.5	21.6
31500	4.91	4.85	1.0	12050.4	1119.3	4.73	4.66	0.9	11387.1	6.41	6.34	0.8	9995.1	6.62	6.54	0.9	10931.1	64.7	3.4	34.1	29.9	32.7
38700	4.93	4.84	1.0	14919.8	715.2	4.73	4.66	0.7	9688.6	6.41	6.31	0.7	9753.2	6.62	6.54	1.0	14204.6	69.6	2.1	28.2	28.4	41.3
49500	4.95	4.85	1.0	18997.7	73.2	4.73	4.66	0.4	7832.9	6.39	6.34	0.5	8931.5	6.62	6.53	1.0	18924.5	76.4	0.2	21.9	25.0	52.9
63900						4.73	4.65	1.0	5020.1	6.42	6.34	1.5	7288.8	6.62	6.55	4.5	22460.7	82.3	0.0	14.4	21.0	64.6
85500						4.73	4.66	1.0	2753.4	6.40	6.33	2.2	6035.6	6.64	6.54	10.6	29103.2	88.4	0.0	7.3	15.9	76.8
128700										6.40	6.34	1.0	3575.5	6.62	6.54	9.2	32788.7	95.1	0.0	0.0	9.8	90.2
312300										6.42	6.33	1.0	1266.1	6.64	6.54	27.9	35298.9	98.3	0.0	0.0	3.5	96.5
1089900										6.40	6.34	1.0	1436.3	6.64	6.52	24.1	34613.2	98.0	0.0	0.0	4.0	96.0
4i_b				16				17				18				19		Conv	16	17	18	19
900	4.98	4.91	1.0	32139.0	32139.0	4.75	4.69	0.1	1733.2	6.42	6.35	0.1	2271.2					5.5	88.9	4.8	6.3	0.0
2700	4.98	4.90	1.0	29545.7	29545.7	4.75	4.67	0.2	4525.3	6.41	6.36	0.2	4978.9					12.2	75.7	11.6	12.8	0.0
6300	4.97	4.85	1.0	19860.0	18906.2	4.74	4.68	0.3	6306.4	6.41	6.34	0.3	6735.1	6.64	6.52	0.1	953.9	22.7	57.5	19.2	20.5	2.9
9900	4.97	4.84	1.0	17798.6	15607.1	4.74	4.68	0.5	8832.8	6.40	6.34	0.5	9123.0	6.63	6.56	0.1	2191.5	31.2	43.7	24.7	25.5	6.1
13500	4.96	4.86	1.0	15386.6	11849.0	4.74	4.67	0.8	11698.1	6.41	6.35	0.7	10621.0	6.61	6.55	0.2	3537.6	39.0	31.4	31.0	28.2	9.4
17100	4.93	4.85	1.0	13036.5	7612.5	5.32	5.26	1.0	13371.0	6.41	6.34	0.9	12264.8	6.62	6.55	0.4	5424.0	47.2	19.7	34.6	31.7	14.0
24300	4.95	4.85	1.0	12491.4	4876.8	5.32	5.26	0.9	11765.1	6.40	6.34	0.9	11329.2	6.60	6.54	0.6	7614.6	53.9	13.7	33.1	31.8	21.4
31500	4.95	4.86	1.0	14211.4	2745.3	5.32	5.25	0.9	12058.8	6.40	6.34	0.8	11913.5	6.62	6.55	0.8	11466.1	61.4	7.2	31.6	31.2	30.0

42300	4.95	4.85	1.0	15280.8	720.6	5.32	5.25	0.6	9399.8	6.40	6.34	0.7	10188.2	6.63	6.54	1.0	14560.2	69.9	2.1	27.0	29.2	41.8
53100						5.32	5.25	0.4	8102.3	6.41	6.35	0.5	10259.4	6.62	6.55	1.0	19174.5	75.5	0.0	21.6	27.3	51.1
67500						5.32	5.24	0.3	6581.6	6.41	6.34	0.4	9763.1	6.64	6.53	1.0	25119.2	80.3	0.0	15.9	23.6	60.6
227700						4.73	4.67	1.0	887.2	6.40	6.34	3.8	3388.4	6.62	6.55	35.8	31725.4	94.1	0.0	2.5	9.4	88.1
262500						4.73	4.68	1.0	277.7	6.41	6.35	5.9	1643.3	6.63	6.55	57.9	16077.7	94.7	0.0	1.5	9.1	89.3
300300						4.72	4.66	1.0	381.5	6.40	6.34	4.5	1713.1	6.62	6.53	47.4	18074.7	94.8	0.0	1.9	8.5	89.6
343500						4.73	4.66	1.0	289.6	6.41	6.34	5.0	1433.8	6.63	6.55	55.0	15934.1	95.1	0.0	1.6	8.1	90.2
4m_a				16				17			18					19		Conv	16	17	18	19
1200	5.01	4.93	1.0	39526.6	/	4.57	4.45	0.0	574.6	6.41	6.35	0.0	1046.3					2.0	96.1	1.4	2.5	0.0
2700	5.01	4.93	1.0	37050.5	/	4.55	4.47	0.0	1228.7	6.41	6.36	0.1	2185.7					4.2	91.6	3.0	5.4	0.0
4500	5.00	4.93	1.0	35761.1	/	4.57	4.47	0.1	1632.4	6.42	6.35	0.1	3018.9					5.8	88.5	4.0	7.5	0.0
8100	5.00	4.93	1.0	34441.8	/	4.55	4.46	0.1	2612.0	6.42	6.35	0.1	3941.3					8.0	84.0	6.4	9.6	0.0
11700	5.00	4.92	1.0	32178.5	/	4.55	4.46	0.1	3486.9	6.42	6.35	0.2	4886.4					10.3	79.4	8.6	12.1	0.0
15300	5.00	4.93	1.0	30446.1	/	4.57	4.47	0.1	4042.5	6.42	6.36	0.2	5438.1					11.9	76.3	10.1	13.6	0.0
22500	5.00	4.92	1.0	27380.9	/	4.57	4.47	0.2	4983.6	6.41	6.35	0.2	6390.0					14.7	70.7	12.9	16.5	0.0
29700	5.00	4.92	1.0	26413.2	/	4.56	4.47	0.2	6386.9	6.41	6.35	0.3	7660.0	4.83	4.76	0.0	541.3	18.5	64.4	15.6	18.7	1.3
36900	5.00	4.92	1.0	23992.7	/	4.58	4.46	0.3	7006.4	6.42	6.35	0.3	8232.5	4.83	4.74	0.0	712.4	20.9	60.1	17.5	20.6	1.8
51300	4.99	4.93	1.0	20389.5	/	4.57	4.46	0.4	7834.2	6.41	6.35	0.4	8902.5	4.82	4.76	0.0	772.0	24.1	53.8	20.7	23.5	2.0
65700	4.99	4.92	1.0	20204.7	/	4.58	4.46	0.5	10144.9	6.41	6.35	0.6	11035.2	4.82	4.75	0.1	1226.9	27.7	47.4	23.8	25.9	2.9
83700	4.91	4.86	1.0	15285.2	/	4.48	4.40	0.7	10597.9	6.34	6.29	0.7	10861.5	4.75	4.68	0.1	1542.3	32.1	39.9	27.7	28.4	4.0
108000	4.90	4.85	1.0	11676.8	/	4.68	4.62	1.1	12284.7	6.34	6.29	1.0	11584.7	4.75	4.68	0.2	2192.8	37.4	30.9	32.6	30.7	5.8
133200	4.91	4.85	1.0	9697.3	/	4.50	4.39	1.3	12892.7	6.35	6.29	1.3	12175.6	4.76	4.69	0.3	2922.4	41.0	25.7	34.2	32.3	7.8
151200	4.91	4.85	1.0	8003.0	/	4.49	4.41	1.6	13126.7	6.35	6.29	1.6	12554.0	4.76	4.67	0.4	3473.7	43.9	21.5	35.3	33.8	9.4
194400	4.96	4.92	1.0	5129.9	/	4.74	4.68	2.8	14491.9	6.41	6.35	2.5	12987.3	4.82	4.75	0.9	4791.6	49.6	13.7	38.8	34.7	12.8
237600	4.96	4.92	1.0	3234.9	/	4.74	4.68	4.6	14897.3	6.41	6.35	4.1	13377.8	4.82	4.74	1.9	6254.5	54.0	8.6	39.5	35.4	16.6
280800	4.96	4.92	1.0	1806.8	/	4.74	4.68	8.0	14433.6	6.41	6.34	7.2	13038.1	4.82	4.75	4.0	7278.1	57.5	4.9	39.5	35.7	19.9
324000	4.96	4.91	1.0	2431.8	/	4.74	4.68	5.6	13634.2	6.40	6.34	5.1	12422.4	4.83	4.75	3.4	8280.0	58.0	6.6	37.1	33.8	22.5
367200						4.75	4.67	1.0	12881.0	6.41	6.35	0.9	11889.5	4.83	4.74	0.7	9172.0	63.5	0.0	38.0	35.0	27.0
410400						4.75	4.66	1.0	13374.9	6.40	6.35	0.9	12566.9	4.82	4.75	0.8	10856.5	64.8	0.0	36.4	34.2	29.5
453600						4.75	4.67	1.0	11607.4	6.40	6.34	0.9	10693.4	4.83	4.75	0.9	10717.2	66.2	0.0	35.2	32.4	32.5
496800						4.75	4.66	1.0	11703.7	6.41	6.35	1.0	11170.8	4.82	4.75	1.0	11801.5	67.0	0.0	33.8	32.2	34.0
577800						4.74	4.67	1.0	11332.6	6.41	6.35	1.0	11009.0	6.62	6.55	1.1	12487.1	67.9	0.0	32.5	31.6	35.9
664200						4.74	4.68	1.0	11336.6	6.41	6.35	1.0	10902.5	6.61	6.55	1.3	14545.1	69.8	0.0	30.8	29.6	39.5
750600						4.73	4.67	1.0	9884.8	6.40	6.34	1.0	9528.6	6.61	6.53	1.3	12765.1	69.8	0.0	30.7	29.6	39.7
837000						4.73	4.67	1.0	10541.5	6.41	6.33	1.0	10053.9	6.62	6.55	1.3	13366.5	69.7	0.0	31.0	29.6	39.4
1024200						4.74	4.66	1.0	10304.0	6.41	6.35	1.0	9992.2	6.61	6.55	1.3	13623.3	70.1	0.0	30.4	29.5	40.2

1026000								4.73	4.67	1.0	9666.3	6.41	6.34	1.0	9471.4	6.61	6.55	1.3	12886.4	70.1	0.0	30.2	29.6	40.2																				
1096200								4.74	4.67	1.0	10665.5	6.41	6.33	1.0	10470.8	6.62	6.56	1.4	14501.1	70.4	0.0	29.9	29.4	40.7																				
4m_b	16											17											18											19										
900	5.01	4.93	1.0	40405.5	/			4.76	4.69	0.0	1593.9	6.42	6.35	0.0	1401.2					3.5	93.1	3.7	3.2	0.0																				
3600	5.00	4.92	1.0	34668.6	/			4.75	4.69	0.1	2720.9	6.41	6.35	0.1	3176.1					7.3	85.5	6.7	7.8	0.0																				
7200	4.99	4.92	1.0	33512.9	/			4.76	4.68	0.1	3864.0	6.42	6.35	0.1	4749.6					10.2	79.6	9.2	11.3	0.0																				
10800	4.99	4.92	1.0	27632.3	/			4.75	4.69	0.1	3942.8	6.42	6.35	0.2	4940.7					12.2	75.7	10.8	13.5	0.0																				
14400	4.99	4.91	1.0	30098.6	/			4.75	4.69	0.2	5457.9	6.41	6.35	0.2	6166.0					13.9	72.1	13.1	14.8	0.0																				
18000	5.00	4.91	1.0	26572.7	/			4.75	4.69	0.2	5235.9	6.42	6.35	0.2	6389.8					15.2	69.6	13.7	16.7	0.0																				
25200	4.99	4.92	1.0	25445.1	/			4.74	4.69	0.3	7422.8	6.41	6.36	0.3	7513.9					18.5	63.0	18.4	18.6	0.0																				
32400	4.98	4.92	1.0	23172.2	/			4.75	4.69	0.4	8514.3	6.41	6.35	0.4	8613.2	4.83	4.74	0.1	2629.6	26.1	54.0	19.8	20.1	6.1																				
39600	4.98	4.91	1.0	21148.3	/			4.75	4.68	0.4	8773.3	6.41	6.35	0.4	9173.3	4.83	4.74	0.1	1724.3	26.2	51.8	21.5	22.5	4.2																				
54000	4.92	4.86	1.0	14889.2	/			4.68	4.61	0.6	8237.3	6.35	6.28	0.6	8533.2	4.76	4.68	0.1	1047.2	28.8	45.5	25.2	26.1	3.2																				
68400	4.91	4.85	1.0	14600.4	/			4.68	4.61	0.8	10953.3	6.34	6.29	0.7	10548.0	4.75	4.68	0.1	1705.9	33.0	38.6	29.0	27.9	4.5																				
90000	4.90	4.85	1.0	11237.6	/			4.68	4.61	1.1	12354.9	6.35	6.29	1.0	11582.2	4.76	4.68	0.2	2681.9	38.7	29.7	32.6	30.6	7.1																				
133200	4.89	4.84	1.0	8157.2	/			4.68	4.60	1.7	13943.9	6.34	6.28	1.6	12802.2	4.77	4.68	0.5	4165.0	44.9	20.9	35.7	32.8	10.7																				
176400	4.90	4.85	1.0	3426.3	/			4.68	4.61	4.3	14723.2	6.35	6.27	4.0	13695.2	4.76	4.68	1.8	6266.1	53.7	9.0	38.6	35.9	16.4																				
219600	4.89	4.85	1.0	2147.9	/			4.68	4.60	5.9	12660.5	6.34	6.28	5.5	11789.2	4.75	4.68	3.2	6819.1	57.0	6.4	37.9	35.3	20.4																				
262800								4.74	4.67	1.0	12491.9	6.42	6.34	1.0	11927.7	4.83	4.73	0.7	9259.4	63.8	0.0	37.1	35.4	27.5																				
306000								4.75	4.67	1.0	11422.5	6.40	6.34	1.0	11098.4	4.83	4.73	0.9	10298.7	65.7	0.0	34.8	33.8	31.4																				
349200								4.73	4.66	1.0	10842.4	6.41	6.35	1.0	10862.4	4.81	4.74	1.0	10775.5	66.6	0.0	33.4	33.4	33.2																				
392400								4.73	4.66	1.0	10315.0	6.41	6.34	1.0	10465.9	4.83	4.74	1.3	13114.5	69.4	0.0	30.4	30.9	38.7																				
471600								4.73	4.67	1.0	8537.0	6.40	6.34	1.1	9074.5	4.93	4.85	1.5	13045.4	71.3	0.0	27.9	29.6	42.6																				
558000								4.73	4.66	1.0	7855.3	6.40	6.34	1.1	8567.0	4.93	4.84	1.9	14920.7	73.8	0.0	25.1	27.3	47.6																				
644400								4.74	4.67	1.0	7664.5	6.39	6.34	1.1	8392.9	4.92	4.85	2.0	15057.0	74.2	0.0	24.6	27.0	48.4																				
730800								4.73	4.66	1.0	7559.9	6.40	6.34	1.1	8206.7	4.92	4.85	2.0	15266.8	74.6	0.0	24.4	26.4	49.2																				
919800								4.72	4.67	1.0	7414.2	6.40	6.35	1.1	8166.3	4.92	4.86	2.1	15575.0	75.0	0.0	23.8	26.2	50.0																				
921600								4.73	4.66	1.0	7394.8	6.41	6.35	1.2	8557.7	4.93	4.85	2.2	16179.1	75.2	0.0	23.0	26.6	50.4																				
990000								4.73	4.67	1.0	7228.6	6.40	6.34	1.1	8228.5	4.93	4.86	2.2	15541.2	75.1	0.0	23.3	26.6	50.1																				

5.1.3 INT1 Analytics via ^1H NMR and UV/VIS Spectroscopy

In the ^1H NMR spectrum during the turnover-limited competition experiments of **10** vs. **11** with **14** some proton signals of catalyst **4** disappear and after full conversion of **14** the proton signals of **4** are visible again in the ^1H NMR spectrum. Because of this observation we were measuring ^1H NMR spectra with a 1:1 mixture of catalysts **1**, **3** or **4a** with **14** or the corresponding acid **14OH** (Figure 5.25-5.27). A guideline for the preparation of stock solutions are described in Table 5.10. As internal standard 1,3,5-trimethoxybenzene was used.

Table 5.10. Preparation of initial CDCl_3 stock solutions.

Stock Solution	Compound	Concentration (mol L^{-1})	Volumne (mL)	n (mol)	M.W. (g mol^{-1})	Mass (mg)
Stock A	14	0.05	1	$50 \cdot 10^{-6}$	344	17.2
	14OH	0.05	1	$50 \cdot 10^{-6}$	181	9.1
Stock B	DMAP	0.05	1	$50 \cdot 10^{-6}$	122	6.1
	TCAP	0.05	1	$50 \cdot 10^{-6}$	174	8.7
Stock C	1,3,5-Trimethoxybenzene	0.01	2	$20 \cdot 10^{-6}$	168	3.4
Stock A	14	0.02	1	$20 \cdot 10^{-6}$	344	6.9
	14OH	0.02	1	$20 \cdot 10^{-6}$	181	3.6
Stock B	4a	0.02	1	$20 \cdot 10^{-6}$	265	5.3
Stock C	1,3,5-Trimethoxybenzene	0.01	2	$20 \cdot 10^{-6}$	168	3.4

Thereby we find that for the combination of **1** and **14** (**INT1-1**) more H signals are visible than in the ^1H NMR spectra with only **1** or **14** (Figure 5.25V). Some H signals could be identified as signals corresponding to **1** (orange star) or **14** (green square). In addition, next to the Me group of **14** two further Me groups are visible in the spectrum which contains the counterion and acyl transfer group of **INT1-1** (red circle). When measuring ^1H NMR spectra with mixtures of **3**, **14** and **14OH** (**INT1-3**), then similar ^1H NMR spectra as with **1** are determined (Figure 5.26). However, some broad singulets are discovered in Figure 5.26V in the aliphatic as well as in the aromatic sector. Again, some proton signals could be assigned to proton signals of catalyst **3** (stars) and reagent **14** (squares) as well as the three Me groups, which are the Me group of the anhydride (green square) and Me groups of **INT1-3** (grey circle). Furthermore, in the aromatic field it was possible to match different integrals to the corresponding compounds **INT1-3** (circles), **14** (square) and TCAP (star). It looks as if in the case of catalysts **1** and **3** we are able to see the equilibrium between unloaded and loaded catalysts with anhydride reagent. Using the mass action law, the equilibrium constant K_c could be determined (Eq. 5.18). The equilibrium constant K_c for the formation of INT1 is in the case of DMAP $K_c = 42.7 \text{ L mol}^{-1}$ and of TCAP $K_c = 1462.3 \text{ L mol}^{-1}$, which indicate that in both cases the equilibrium lies on intermediate side (Table 5.11).

$$K_c = \frac{[\text{Int1} \cdot (1,3,4a)]}{[(1,3,4a) \cdot [14]]} \quad \text{Eq. 5.18}$$

Table 5.11. Preparation of initial CDCl_3 stock solutions.

Compound	Integ. Limits (ppm)		Integ.	Absol.	Protons	Concentration (mol L^{-1})	K_c (L mol^{-1})
Standard	3.76	3.78	9.00	262943.62	9	0.0041 ^[a]	
DMAP	2.98	3.01	17.45	509852.26	6	0.0118	
14	2.55	2.58	16.35	477815.38	6	0.0111	
INT1-1	2.45	2.48	4.13	120769.61	3	0.0056	42.7
Standard	6.01	6.03	2.80	80128.66	3	0.0041 ^[a]	
TCAP	7.73	7.78	1.32	37930.51	2	0.0029	
14	7.97	8.02	1.41	40409.38	2	0.0031	
INT1-3	8.36	8.47	2.98	85331.93	1	0.0130	1462.3

^[a]Concentration for weighed-in quantity of $m = 4.1 \text{ mg}$.

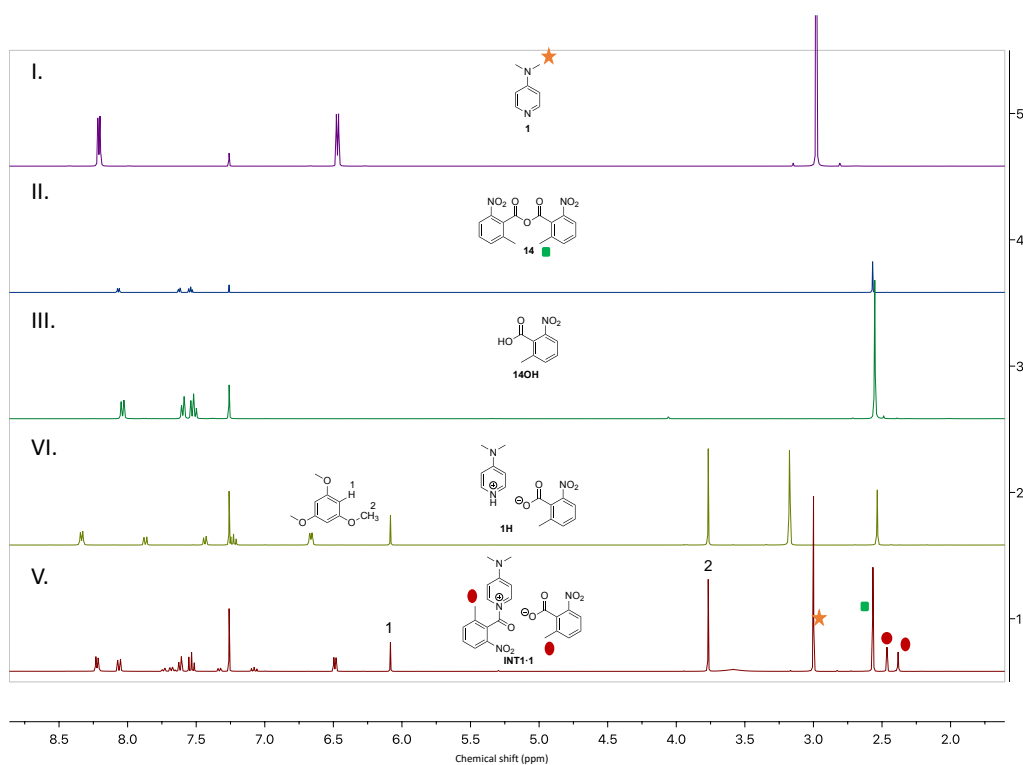


Figure 5.25. ^1H NMR spectra of **1**, **14**, **14OH**, **1H** and **INT1-1**.

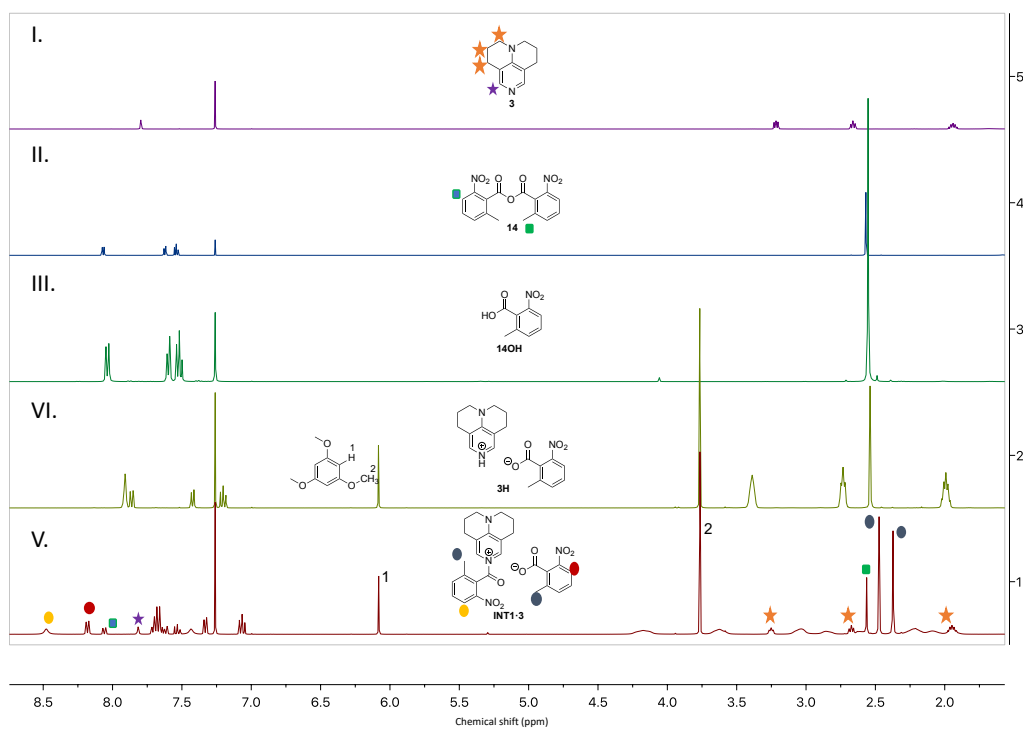


Figure 5.26. ^1H NMR spectra of **3**, **14**, **14OH**, **3H** and **INT1-3**.

In contrast, determining a ^1H NMR spectrum of **INT1-4a** (Figure 5.27V) the spectrum is hard to interpret, because the integrals are getting broad and indistinct, so that an integration and determination of K_c is not possible. Measuring the ^1H NMR spectra at different temperature (Figure 5.28; $-20\text{ }^\circ\text{C}$ till $+40\text{ }^\circ\text{C}$) shows that the equilibrium is shifted from the intermediate side ($-20\text{ }^\circ\text{C}$) to the separated starting material side ($+40\text{ }^\circ\text{C}$).

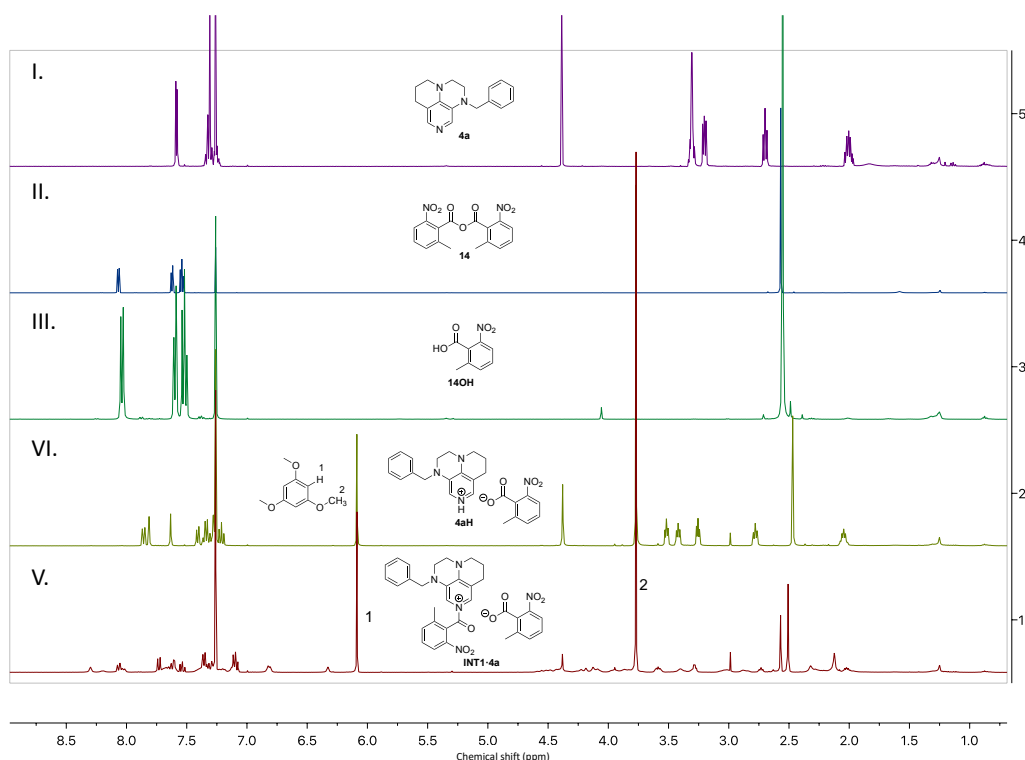


Figure 5.27. ^1H NMR spectra of **4a**, **14**, **14OH**, **4aH** and **INT1-4a**.

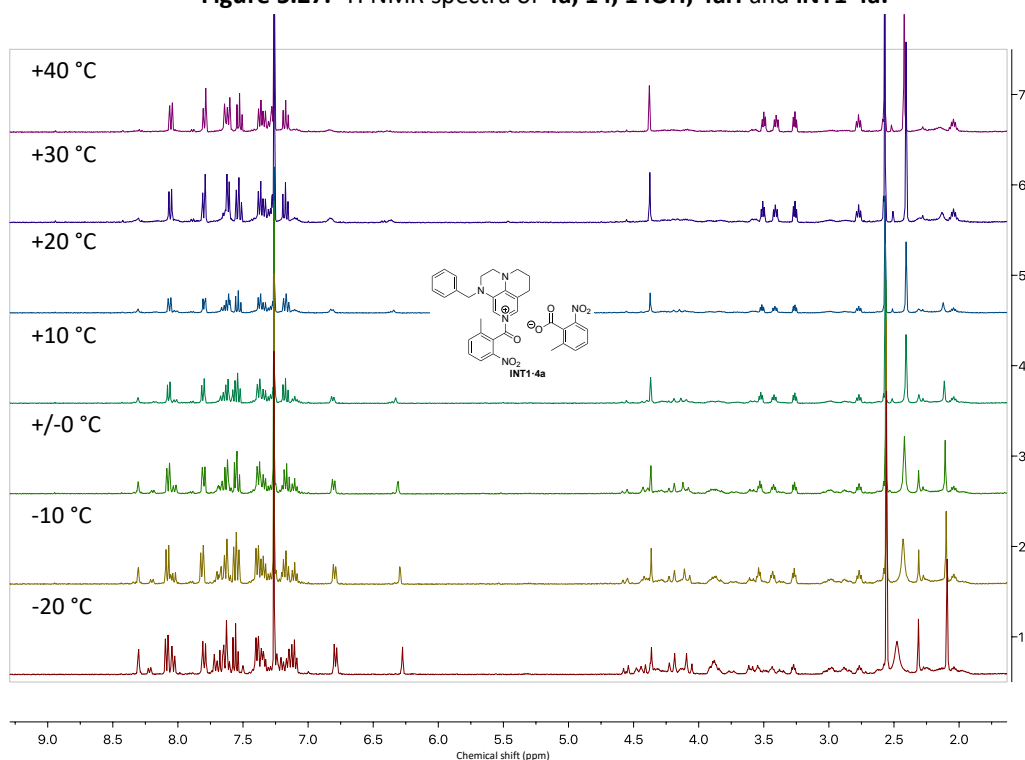


Figure 5.28. ^1H NMR spectra of **INT1-4a** at a temperature range from $-20\text{ }^\circ\text{C}$ till $+40\text{ }^\circ\text{C}$.

The second observation is that a mixture between 3,4-diaminopyridine catalysts **4-6** and **14** change their color from colorless to a yellow solution (Figure 5.29a). After full conversion of reagent **14**, the yellow coloring is reduced (Figure 5.29b). To figure out why this change in color happens UV/VIS - spectra of **4a**, **14** and **INT1-4a** in CHCl_3 were detected (Figure 5.30). The nitro group of **14** shows a significant absorption at $\lambda = 265$ nm, whereby **4a** demonstrates a shoulder at $\lambda = 320$ nm. **INT1-4a** shows a further absorption around $\lambda = 400$ nm which could explain the change of color to yellow. Non-covalent interactions (NCI) between the three parts -the acylated group, the resulted acid and the substituent of **4a**- could result in electronic transitions. Because in 4-aminopyridine catalysts **1-3** or **7b** a substituent closely to the active nitrogen is missing, these electronic transitions do not exist.

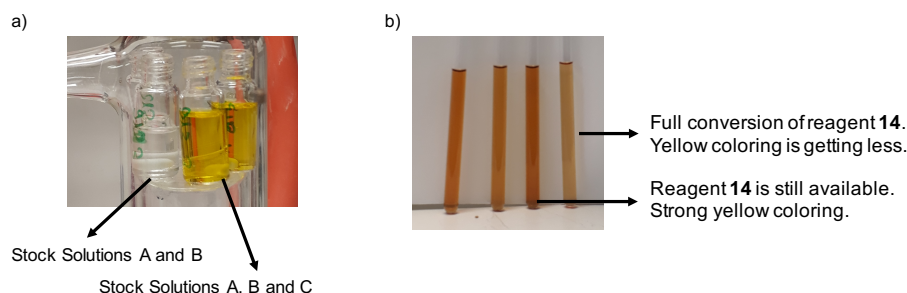


Figure 5.29. Change of the colours in solution by a) Preparing the competition experiments from colorless to yellow by adding catalyst **4,5,6** to a solution of **10,11** and **14** in CDCl_3 b) Fading of yellow coloring after the reaction is finished and no reagent **14** is available in the solution.

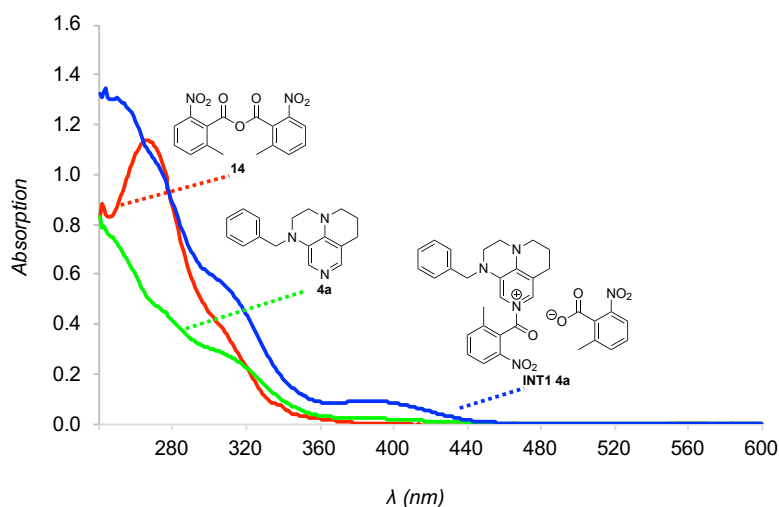


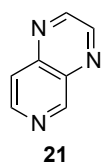
Figure 5.30. UV/Vis spectra of **4a**, **14** and **INT1·4a** in CHCl_3 .

5.1.4 Analytic Data of Synthesised Catalysts

5.1.4.1 Precursor Synthesis for Catalysts 4-6

The synthesis of precursor 1,2,3,5,6,7-Hexahydropyrazino[3,2,1-ij][1,6]naphthyridine **24** is based on procedure reported by Zipse *et al.*:^[7]

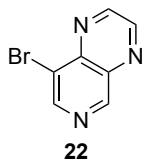
Pyrido[3,4-*b*]pyrazine **21**.



3,4-Diaminopyridine (2.50 g, 22.9 mmol, 1.0 eq.) was put in an 80 mL microwave vessel and dissolved in ethanol (40 mL). After adding glyoxal (40 wt.-% in water, 3.10 mL, 26.8 mmol, 1.2 eq.), the reaction mixture was put into the microwave reactor and stirred for 1 h at 110 °C (70 W). The mixture was concentrated and **21** (3.00 g, quant.) was obtained as a brown solid.

$^1\text{H NMR}$ (400 MHz, CDCl_3) δ = 9.58 (d, J = 0.8 Hz, 1H, Ar), 9.01 (dd, J = 27.5, 1.7 Hz, 2H, Ar), 8.86 (d, J = 5.8 Hz, 1H, Ar), 7.97 (dd, J = 5.8, 0.8 Hz, 1H, Ar) ppm. The $^1\text{H NMR}$ spectrum is in full agreement with literature reports.^[7]

8-Bromopyrido[3,4-*b*]pyrazine **22**.

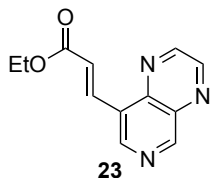


21 (3.00 g, 22.9 mmol, 1.0 eq.) was dissolved in MeCN (130 mL) and stirred in the dark. NBS (4.48 g, 25.2 mmol, 1.1 eq.) was added portionwise and the reaction mixture stirred at room temperature over night. MTBE was added to the reaction mixture as long as no brown solid was falling out, filtered and concentrated in vacuum. After purification by column chromatography on silica (isohexane/EtOAc/ Et_3N 20:15:1) **22** (1.10 g, 23%) was obtained as a yellow solid.

$^1\text{H NMR}$ (400 MHz, CDCl_3) δ = 9.51 (s, 1H, Ar), 9.15 (d, J = 1.7 Hz, 1H, Ar), 9.09 (s, 1H, Ar), 9.03 (d, J = 1.7 Hz, 1H, Ar) ppm. The $^1\text{H NMR}$ spectrum is in full agreement with literature reports.^[7]

Annulated Pyridine Bases

Ethyl-3-(pyrido[3,4-b]pyrazin-8-yl)acrylate **23**.

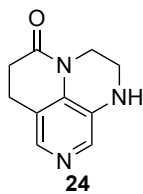


In a pressure tube **22** (3.38 g, 16.1 mmol, 1.0 eq.), ethyl acrylate (3.00 mL, 27.4 mmol, 1.7 eq.), Pd(OAc)₂ (94.0 mg, 418 μmol, 2.6 mol%), P(oTol)₃ (317 mg, 1.05 mmol, 6.5 mol%) and Et₃N (1.53 mL, 16.1 mmol, 1.0 eq.) were suspended in MeCN (20 mL) and stirred for 20 h at 120 °C. The mixture was cooled down to room temperature and concentrated in vacuum. After purification by column chromatography on silica (isohexane/EtOAc 1:0 -

to 3:7) **23** (3.26 g, 88%) was obtained as an oil

¹H NMR (400 MHz, CDCl₃) δ = 9.55 (s, 1H, Ar), 9.13 – 9.00 (m, 3H, Ar), 8.49 (d, *J* = 16.3 Hz, 1H, CH), 7.14 (d, *J* = 16.3 Hz, 1H, CH), 4.33 (q, *J* = 7.2 Hz, 2H, CH₂), 1.38 (t, *J* = 7.1 Hz, 3H, Me) ppm. The ¹H NMR spectrum is in full agreement with literature reports.^[7]

1,2,3,5,6,7-Hexahydropyrazino[3,2,1-ij][1,6]naphthyridine **24**.



23 (1.24 g, 5.41 mmol, 1.0 eq.) was dissolved in EtOH and Pd (10 wt.-% on Carbon, 320 mg) was added. After degassing with nitrogen, the reaction mixture was purged with hydrogen (3x) and stirred for 8 h at room temperature under hydrogen atmosphere. The reaction mixture was filtered over celite, washed well with EtOH and concentrated in vacuum. After purification by column chromatography on neutral Al₂O₃ (Chloroform/MeOH 40:1) **24** (852 mg, 83%) was

obtained as a yellow solid.

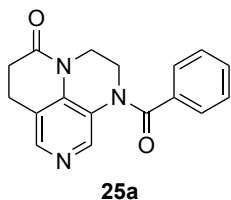
¹H NMR (400 MHz, CDCl₃) δ = 7.88 (s, 1H, Ar), 7.80 (s, 1H, Ar), 4.04 – 3.94 (m, 3H, NH and CH₂), 3.41 – 3.35 (m, 2H, CH₂), 2.94 – 2.87 (m, 2H, CH₂), 2.71 (dd, *J* = 8.6, 6.4 Hz, 2H, CH₂) ppm. The ¹H NMR spectrum is in full agreement with literature reports.^[7]

General Procedure A (GP A, the synthesis of **25**, **26** and **27** are based on procedure reported by Zipse *et al.*^[7]) In an evacuated microwave vessel **24** (1.0 eq.) was dissolved in dry pyridine (2 mL pro mmol **24**). The corresponding acid chloride **28** or acid anhydride **29**, **30** or **31** (2.1 - 3.0 eq.) was added and stirred for 5 min under N₂-atmosphere. The reaction mixture was put into the microwave reactor and stirred for 1-2.5 h at 170 °C (200 W). After cooling to room temperature, the mixture was quenched with methanol and concentrated in vacuum. The mixture was dissolved in CH₂Cl₂ and washed with saturated K₂CO₃-solution (10 mL). The aqueous phase was extracted with CH₂Cl₂ (3 x 10 mL) and the combined organic phase was dried over MgSO₄, filtered and concentrated in vacuum. The pure products **25**, **26** or **27** were obtained by column chromatography on silica (EtOAc/Et₃N/MeOH 95:5:0 to 92:5:3). Because of uncertain ¹H NMR spectra for compounds **25**, **26** and **27** at room temperature only HRMS detection as analytic was been implemented for these kinds of precursor compounds.

General Procedure B (GP B, the synthesis acid anhydride **29** and **31** is based on procedure reported by Zipse *et al.*^[1])

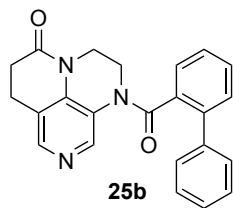
In a round bottom flask the corresponding carboxylic acid (1.0 eq.), TsCl (0.5 eq.), and K₂CO₃ (1.5 eq.) were dissolved in a 1:1 mixture of MeCN and CH₂Cl₂ and stirred at room temperature for 48 h. The mixture was filtered and washed well with CH₂Cl₂. After concentration under vacuum, the anhydride was triturated in *n*-hexane, filtered and washed in *n*-hexane to obtain the pure anhydride derivative **29** or **31**.

1-Benzoyl-2,3,6,7-tetrahydropyrazino[3,2,1-ij][1,6]naphthyridin-5(1H)-one **25a**.



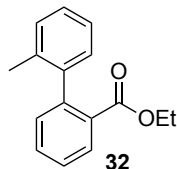
24 (200 mg, 1.06 mmol, 1.0 eq.) and benzoic anhydride (**29a**, 717 mg, 3.17 mmol, 3.0 eq.) was dissolved in dry pyridine (2 mL) and reacted according to GP A. **25a** (301 mg, 97%) was obtained as a yellow solid.

¹H NMR (400 MHz, CDCl₃) δ = 8.12 – 8.00 (m, 2H, Ar), 7.50 – 7.44 (m, 3H, Ar), 7.43 – 7.35 (m, 2H, Ar), 4.06 – 3.96 (m, 4H, 2xCH₂), 3.00 (dd, *J* = 8.6, 6.5 Hz, 2H, CH₂), 2.79 (dd, *J* = 8.7, 6.5 Hz, 2H, CH₂) ppm; HRMS (EI): *m/z* calcd for C₁₇H₁₅O₂N₃⁺ [M]⁺: 293.1159; found: 293.1162. The ¹H NMR spectrum is in full agreement with literature reports.^[7]

1-([1,1'-Biphenyl]-2-carbonyl-2,3,6,7-tetrahydropyrazino[3,2,1-ij][1,6]naphthyridin-5(1H)-one **25b**.

24 (100 mg, 529 μmol , 1.0 eq.) and 2-phenylbenzoic anhydride (**29b**, 600 mg, 1.59 mmol, 3.0 eq.) was dissolved in dry pyridine (1 mL) and reacted according to GP A. **25b** (150 mg, 77%) was obtained as a yellow solid.

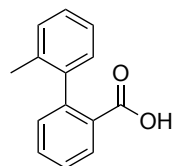
HRMS (EI): m/z calcd for $\text{C}_{23}\text{H}_{19}\text{O}_2\text{N}_3^+$ $[\text{M}]^+$: 369.1472; found: 369.1465.

Ethyl 2-(2-methylphenyl)benzoate **32**.

Ethyl 2-bromobenzoate (1.39 mL, 8.73 mmol, 1.0 eq.), 2-tolylboronic acid (1.78 g, 13.1 mmol, 1.5 eq.), and Na_2CO_3 (1.85 g, 17.5 mmol, 2.0 eq.) were dissolved in a mixture of THF (35 mL) and water (35 mL). After the reaction mixture was degassed with N_2 , $(\text{PPh}_3)_2\text{PdCl}_2$ (306 mg, 437 μmol , 0.05 eq.) was added and the mixture was stirred overnight at 60 $^\circ\text{C}$.

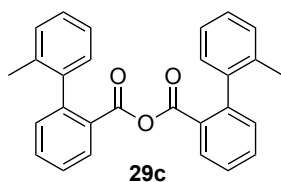
After cooling down to room temperature, water was added to the reaction mixture and extracted with CH_2Cl_2 (3 x 25 mL). The combined organic phase was dried over MgSO_4 , filtered, and concentrated in vacuum. After column chromatography on silica (isohexane/EtOAc 8:2), **32** (2.00 g, 91 %) was obtained as a clear liquid.

$^1\text{H NMR}$ (400 MHz, CDCl_3) δ = 7.96 (dd, J = 7.7, 1.4 Hz, 1H, Ar), 7.53 (td, J = 7.5, 1.5 Hz, 1H, Ar), 7.43 (td, J = 7.6, 1.4 Hz, 1H, Ar), 7.31 – 7.16 (m, 4H, Ar), 7.08 (dd, J = 7.4, 1.4 Hz, 1H, Ar), 4.03 (q, J = 7.1 Hz, 2H, CH_2), 2.08 (s, 3H, Me), 0.95 (t, J = 7.1 Hz, 3H, Me) ppm. The $^1\text{H NMR}$ spectrum is in full agreement with literature reports.^[8]

2-(2-Tolyl)benzoic acid **33a**.

In a round bottom flask **32** (2.00 g, 8.32 mmol, 1.0 eq.) and NaOH (3.33 g, 83.2 mmol, 10.0 eq.) were dissolved in a mixture of water (35 mL) and MeOH (35 mL). The reaction mixture was stirred for 24 h at 100 $^\circ\text{C}$. After adding 2 M HCl until a pH value of 2 was reached, the mixture was extracted with EtOAc (3 x), dried over MgSO_4 , filtered, and concentrated in vacuum to obtained **33a** (1.94 g, *quant.*) as a white solid.

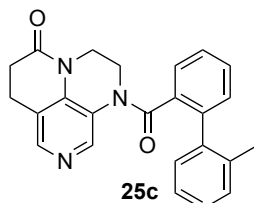
$^1\text{H NMR}$ (400 MHz, $\text{DMSO}-d_6$) δ = 12.53 (s, 1H, OH), 7.84 (dd, J = 7.7, 1.4 Hz, 1H, Ar), 7.58 (td, J = 7.5, 1.4 Hz, 1H, Ar), 7.47 (td, J = 7.7, 1.3 Hz, 1H, Ar), 7.25 – 7.14 (m, 4H, Ar), 7.02 (d, J = 7.3 Hz, 1H, Ar), 2.02 (s, 3H, Me) ppm. The $^1\text{H NMR}$ spectrum is in full agreement with literature reports.^[9]

2-(2-Methylphenyl)benzoic anhydride **29c**.

In a round bottom flask **33a** (1.00 g, 4.71 mmol, 1.0 eq.), TsCl (449 mg, 2.36 mmol, 0.5 eq.), and K_2CO_3 (976 mg, 7.07 mmol, 1.5 eq.) were dissolved in MeCN (25 mL) and CH_2Cl_2 (25 mL) and reacted according to GP B. **29c** (698 mg, 73 %) was obtained as a yellow oil

$^1\text{H NMR}$ (400 MHz, CDCl_3) δ = 7.63 – 7.54 (m, 2H, Ar), 7.38 – 7.33 (m, 1H, Ar), 7.25 – 7.13 (m, 4H, Ar), 7.10 – 7.01 (m, 1H, Ar), 2.04 (s, 3H, Me) ppm.

1-(2'-Methyl-[1,1'-biphenyl]-2-carbonyl-2,3,6,7-tetrahydropyrazino[3,2,1-ij][1,6]naphthyridin-5(1H)-one

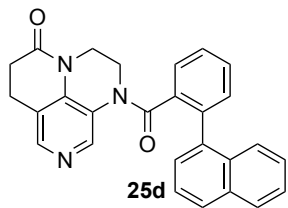
25c.

24 (100 mg, 529 μmol , 1.0 eq.) and **29c** (644 mg, 1.59 mmol, 3.0 eq.) were dissolved in dry pyridine (1 mL) and reacted according to GP A. **25c** (196 mg, 97%) was obtained as a yellow solid

HRMS (EI): m/z calcd for $\text{C}_{24}\text{H}_{21}\text{O}_2\text{N}_3^+$ $[\text{M}]^+$: 383.1628; found: 383.1631.

Annulated Pyridine Bases

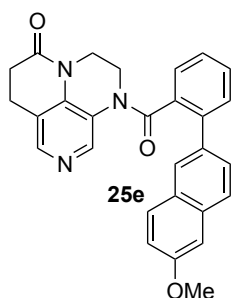
1-(2-(Naphthalen-1-yl)benzoyl)-2,3,6,7-tetrahydropyrazino[3,2,1-ij][1,6]naphthyridin-5(1H)-one **25d**.



24 (100 mg, 529 μmol , 1.0 eq.) and 2-(naphthalen-1-yl)benzoic anhydride (**29d**, 710 mg, 1.49 mmol, 2.8 eq.) were dissolved in dry pyridine (1 mL) and reacted according to GP A. **25d** (192 mg, 87%) was obtained as a yellow solid.

HRMS (EI): m/z calcd for $\text{C}_{27}\text{H}_{21}\text{O}_2\text{N}_3^+$ [M]⁺: 419.1628; found: 419.1614.

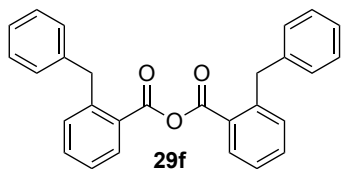
1-(2-(6-methoxynaphthalen-2-yl)benzoyl)-2,3,6,7-tetrahydropyrazino[3,2,1-ij][1,6]naphthyridin-5(1H)-one **25e**.



24 (100 mg, 529 μmol , 1.0 eq.) and 2-(6-methoxynaphthalen-2-yl)benzoic anhydride (**29e**, 600 mg, 1.11 mmol, 2.1 eq.) were dissolved in dry pyridine (1 mL) and reacted according to GP A. **25e** (174 mg, 73%) was obtained as a yellow solid.

HRMS (EI): m/z calcd for $\text{C}_{28}\text{H}_{23}\text{O}_3\text{N}_3^+$ [M]⁺: 449.1734; found: 449.1732.

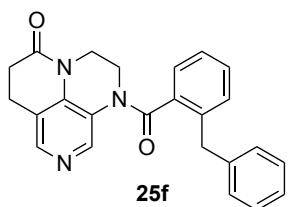
2-Benzylbenzoic anhydride **29f**.



In a round bottom flask α -phenyl-*o*-toluic acid (1.00 g, 4.71 mmol, 1.0 eq.), TsCl (449 mg, 2.36 mmol, 0.5 eq.), and K_2CO_3 (976 mg, 7.07 mmol, 1.5 eq.) were dissolved in MeCN (25 mL) and CH_2Cl_2 (25 mL) and reacted according to GP B. α -Phenyl-*o*-toluic anhydride (**29f**, 836 mg, 87 %) was obtained as brown solid and used in the next step without any further purification or

characterization.

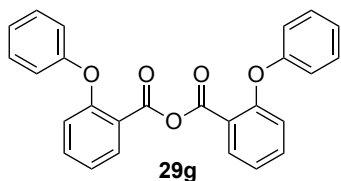
1-(2-Benzylbenzoyl)-2,3,6,7-tetrahydropyrazino[3,2,1-ij][1,6]naphthyridin-5(1H)-one **25f**.



24 (100 mg, 529 μmol , 1.0 eq.) and **29f** (644 mg, 1.59 mmol, 3.0 eq.) were dissolved in dry pyridine (1 mL) and reacted according to GP A. **25f** (194 mg, 82%) was obtained as a yellow solid.

HRMS (EI): m/z calcd for $\text{C}_{24}\text{H}_{21}\text{O}_2\text{N}_3^+$ [M]⁺: 383.1628, found: 383.1633.

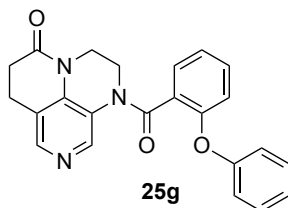
2-Phenoxybenzoic anhydride **29g**.



In a round bottom flask 2-phenoxybenzoic acid (1.00 g, 4.67 mmol, 1.0 eq.), TsCl (445 mg, 2.33 mmol, 0.5 eq.), and K_2CO_3 (967 mg, 7.00 mmol, 1.5 eq.) were dissolved in MeCN (25 mL) and CH_2Cl_2 (25 mL) and reacted according to GP B. **29g** (618 mg, 64 %) was obtained as an oil.

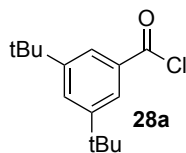
¹H NMR (400 MHz, CDCl_3) δ = 8.01 (dd, J = 7.9, 1.7 Hz, 1H, Ar), 7.51 – 7.43 (m, 1H, Ar), 7.34 – 7.27 (m, 2H, Ar), 7.15 – 7.07 (m, 2H, Ar), 6.93 (dt, J = 9.2, 1.9 Hz, 2H, Ar), 6.91 – 6.88 (m, 1H, Ar) ppm.

1-(2-Phenoxybenzoyl)-2,3,6,7-tetrahydropyrazino[3,2,1-ij][1,6]naphthyridin-5(1H)-one **25g**.

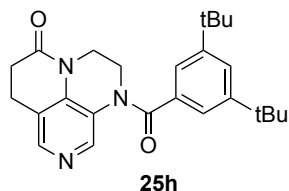


24 (100 mg, 529 μmol , 1.0 eq.) and **29g** (520 mg, 1.27 mmol, 2.4 eq.) were dissolved in dry pyridine (1 mL) and reacted according to GP A. **25g** (180 mg, 88%) was obtained as a yellow solid.

HRMS (EI): m/z calcd for $\text{C}_{23}\text{H}_{19}\text{O}_3\text{N}_3^+$ [M]⁺: 385.1421; found: 385.1421.

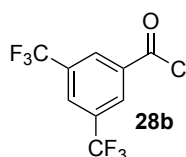
3,5-Di-tert-butylbenzoyl chloride 28a.

3,5-Di-tert-butylbenzoic acid (400 mg, 1.71 mmol, 1.0 eq.) were dissolved in dry CH_2Cl_2 (3 mL) and SOCl_2 (173 μL , 2.39 mmol, 1.4 eq.) and few drops of DMF were added. The mixture was stirred over night at room temperature and concentrated in vacuum. **28a** (430 mg, *quant.*) was obtained as a colourless liquid and used in the next step without any further purification or characterization.

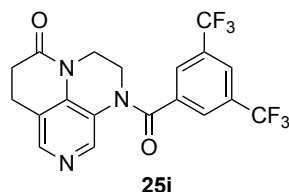
1-(3,5-di-tert-butylbenzoyl)-2,3,6,7-tetrahydropyrazino[3,2,1-ij][1,6]naphthyridin-5(1H)-one 25h.

24 (120 mg, 637 μmol , 1.0 eq.) and **28a** (400 mg, 1.59 mmol, 2.5 eq.) were dissolved in dry pyridine (1 mL) and reacted according to GP A. **25h** (245 mg, 95%) was obtained as a yellow solid.

HRMS (EI): m/z calcd for $\text{C}_{25}\text{H}_{31}\text{O}_2\text{N}_3^+$ $[\text{M}]^+$: 405.2411; found: 405.2419.

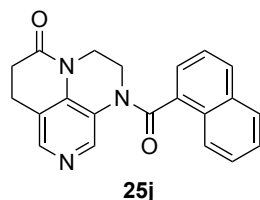
3,5-Bis(trifluoromethyl)benzoic acid chloride 28b.

3,5-Bis(trifluoromethyl)benzoic acid (500 mg, 1.94 mmol, 1.0 eq.) were dissolved in SOCl_2 (5.00 mL) and stirred for 24 h at 80 °C. After purification by kugelrohr distillation **28b** (533 mg, *quant.*) was obtained as brown liquid and used in the next step without any further purification or characterization.

1-(3,5-Bis(trifluoromethyl)benzoyl)-2,3,6,7-tetrahydropyrazino[3,2,1-ij][1,6]naphthyridin-5(1H)-one 25i.

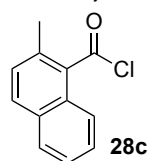
24 (100 mg, 529 μmol , 1.0 eq.) and **28b** (438 mg, 1.59 mmol, 3.0 eq.) were dissolved in dry pyridine (1 mL) and reacted according to GP A. **25i** (150 mg, 68%) was obtained as a yellow solid.

HRMS (EI): m/z calcd for $\text{C}_{19}\text{H}_{13}\text{O}_2\text{N}_3\text{F}_6^+$ $[\text{M}]^+$: 429.0906, found 429.0910.

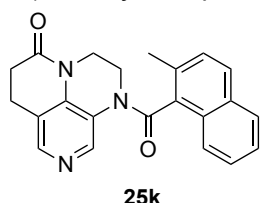
1-(1-Naphthoyl)-2,3,6,7-tetrahydropyrazino[3,2,1-ij][1,6]naphthyridin-5(1H)-one 25j.

24 (100 mg, 529 μmol , 1.0 eq.) and 1-naphthoic anhydride (**25j**, 517 mg, 1.59 mmol, 3.0 eq.) were dissolved in dry pyridine (1 mL) and reacted according to GP A. **25j** (140 mg, 77%) was obtained as a yellow solid.

HRMS (EI): m/z calcd for $\text{C}_{21}\text{H}_{17}\text{O}_2\text{N}_3^+$ $[\text{M}]^+$: 343.1315; found: 343.1317.

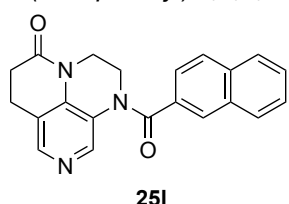
2-Methyl-naphthoic acid chloride 28c.

2-Methyl-naphthoic acid (500 mg, 2.69 mmol, 1.0 eq.) was dissolved in SOCl_2 (5.00 mL, 0.5 M) and stirred for 24 h at 80 °C. After purification by kugelrohr distillation **28c** (548 mg, *quant.*) was obtained and used in the next step without any further purification or characterization.

1-(2-Methyl-1-naphthoyl)-2,3,6,7-tetrahydropyrazino[3,2,1-ij][1,6]naphthyridin-5(1H)-one 25k.

24 (100 mg, 529 μmol , 1.0 eq.) and **28c** (324 mg, 1.59 mmol, 3.0 eq.) were dissolved in dry pyridine (1 mL) and reacted according to GP A. **25k** (100 mg, 53%) was obtained as a yellow solid.

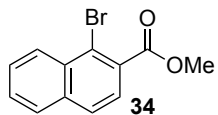
HRMS (EI): m/z calcd for $\text{C}_{22}\text{H}_{19}\text{O}_2\text{N}_3^+$ $[\text{M}]^+$: 357.1472; found: 357.1473.

1-(2-Naphthoyl)-2,3,6,7-tetrahydropyrazino[3,2,1-ij][1,6]naphthyridin-5(1H)-one 25l.

24 (350 mg, 1.85 mmol, 1.0 eq.) and 2-naphthoyl chloride (1.06 g, 5.55 mmol, 3.0 eq.) were dissolved in dry pyridine (4 mL) and reacted according to GP A. **25l** (128 mg, 20%) was obtained as a yellow solid.

HRMS (EI): m/z calcd for $\text{C}_{27}\text{H}_{21}\text{O}_2\text{N}_3^+$ $[\text{M}]^+$: 343.1315; found: 343.1313.

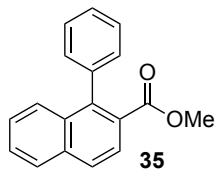
Methyl 1-bromo-2-naphthoate 34.



In a round bottom flask 1-bromo-2-naphthoic acid (1.00 g, 3.98 mmol, 1.0 eq.), MeI (545 μ L, 8.76 mmol, 2.2 eq.), and KHCO_3 (478 μ g, 4.78 mmol, 1.2 eq.) were dissolved in DMF (10 mL) and stirred at room temperature for 24 h. The reaction mixture was quenched with 1 M HCl and extracted with ether (3 x 40 mL). The combined organic phase was washed with brine, dried over MgSO_4 , filtered, and concentrated in vacuum. After purification by column chromatography on silica (isohexane/EtOAc 8:2) **34** (841 mg, 80 %) was obtained as an oil.

$^1\text{H NMR}$ (400 MHz, CDCl_3) δ = 8.46 (d, J = 8.4 Hz, 1H, Ar), 7.88 – 7.81 (m, 2H, Ar), 7.68 (d, J = 8.4 Hz, 1H, Ar), 7.67 – 7.57 (m, 2H, Ar), 4.01 (s, 3H, Me) ppm. The $^1\text{H NMR}$ spectrum is in full agreement with literature reports.^[10]

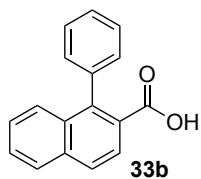
Methyl 1-phenyl-2-naphthoate 35.



In a Schlenk tube **34** (600 mg, 2.26 mmol, 1.0 eq.), phenyl boronic acid (413 mg, 3.39 mmol, 1.5 eq.), Na_2CO_3 (479 mg, 4.53 mmol, 2.0 eq.) and $\text{PdCl}_2(\text{PPh}_3)_2$ (79.0 mg, 113 μ mol, 0.05 eq.) were suspended in a 2:1 mixture of THF (9 mL) and H_2O (4.5 mL) and the reaction mixture were degassed with nitrogen. The mixture was stirred for 24 h at 60 °C. After cooling down to room temperature, H_2O (10 mL) was added and extracted with CH_2Cl_2 (3x20 mL). The combined organic phase was washed with brine, dried over MgSO_4 , filtered, and concentrated in vacuum. After purification by column chromatography on silica (isohexane/EtOAc 8:2) **35** (568 mg, 96 %) was obtained.

$^1\text{H NMR}$ (400 MHz, CDCl_3) δ = 7.95 – 7.89 (m, 3H, Ar), 7.61 – 7.52 (m, 2H, Ar), 7.51 – 7.39 (m, 4H, Ar), 7.33 – 7.28 (m, 2H, Ar), 3.62 (s, 3H, Me) ppm. The $^1\text{H NMR}$ spectrum is in full agreement with literature reports.^[11]

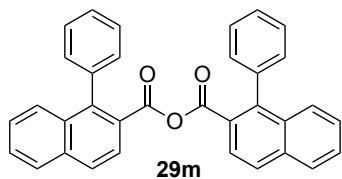
1-Phenyl-2-naphthoic acid 33b.



In a round bottom flask **35** (768 mg, 2.93 mmol, 1.0 eq.) and NaOH (1.17 g, 29.3 mmol, 10.0 eq.) were dissolved in a 1:1 mixture of water (20 mL) and MeOH (20 mL). The reaction mixture was stirred for 24 h at 100 °C. After adding 2 M HCl until a pH value of 2 was reached, the mixture was extracted with EtOAc (3 x), dried over MgSO_4 , filtered, and concentrated in vacuum to obtain **33b** (650 mg, 85%) as a white solid.

$^1\text{H NMR}$ (400 MHz, $\text{DMSO}-d_6$) δ = 12.70 (s, 1H, OH), 8.04 (d, J = 8.4 Hz, 2H, Ar), 7.83 (d, J = 8.6 Hz, 1H, Ar), 7.61 (ddd, J = 8.1, 6.6, 1.3 Hz, 1H, Ar), 7.53 – 7.38 (m, 5H, Ar), 7.32 – 7.24 (m, 2H, Ar) ppm. The $^1\text{H NMR}$ spectrum is in full agreement with literature reports.^[12]

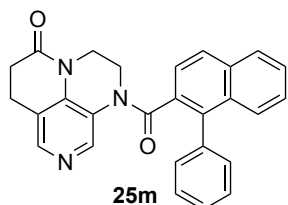
1-Phenyl-2-naphthoic anhydride 29m.



In a round bottom flask **33b** (650 mg, 2.62 mmol, 1.0 eq.), TsCl (250 mg, 1.31 mmol, 0.5 eq.), and K_2CO_3 (543 mg, 3.93 mmol, 1.5 eq.) were dissolved in MeCN (15 mL, 0.2 M) and CH_2Cl_2 (15 mL, 0.2 M) and stirred for 48 h at room temperature. The mixture was filtered and washed well with CH_2Cl_2 . After concentration under vacuum, **29m** (610 mg, 98 %) was obtained as a brown oil.

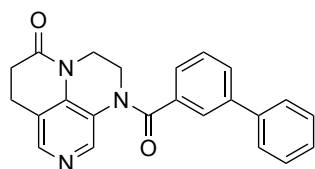
$^1\text{H NMR}$ (400 MHz, CDCl_3) δ = 7.90 (d, J = 8.2 Hz, 1H, Ar), 7.84 (d, J = 8.7 Hz, 1H, Ar), 7.64 (d, J = 8.7 Hz, 1H, Ar), 7.61 – 7.51 (m, 2H, Ar), 7.47 – 7.32 (m, 4H, Ar), 7.31 – 7.23 (m, 2H, Ar) ppm; **HRMS** (EI): m/z calcd for $\text{C}_{34}\text{H}_{22}\text{O}_3^+$ [M] $^+$: 478.1563; found: 478.1552.

1-(1-Phenyl-2-naphthoyl)-2,3,6,7-tetrahydropyrazino[3,2,1-ij][1,6]naphthyridin-5(1H)-one 25m.



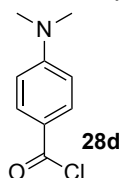
24 (80.0 mg, 423 μ mol, 1.0 eq.) and **29m** (607 mg, 1.27 mmol, 3.0 eq.) were dissolved in dry pyridine (1 mL) and reacted according to GP A. **25m** (110 mg, 62%) was obtained as a yellow solid.

HRMS (EI): m/z calcd for $\text{C}_{27}\text{H}_{21}\text{O}_2\text{N}_3^+$ [M] $^+$: 419.1628; found: 419.1596.

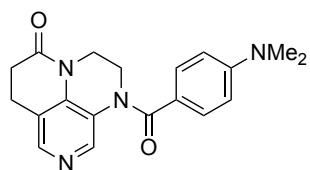
1-([1,1'-Biphenyl]-3-carbonyl)-2,3,6,7-tetrahydropyrazino[3,2,1-ij][1,6]naphthyridin-5(1H)-one **25n**.**25n**

24 (100 mg, 529 μmol , 1.0 eq.) and 3-phenylbenzoic anhydride (**29n**, 600 mg, 1.59 mmol, 3.0 eq.) were dissolved in dry pyridine (1 mL) and reacted according to GP A. **25n** (142 mg, 73%) was obtained as a brown solid.

HRMS (EI): m/z calcd for $\text{C}_{23}\text{H}_{19}\text{O}_2\text{N}_3^+$ $[\text{M}]^+$: 369.1472; found: 369.1475.

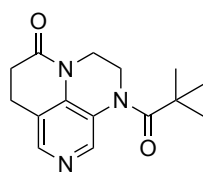
4-Dimethylaminobenzoyl chloride **28d**.**28d**

4-Dimethylaminobenzoic acid (500 mg, 3.03 mmol, 1.0 eq.) was dissolved in dry CH_2Cl_2 (15 mL) and SOCl_2 (1.10 mL, 15.1 mmol, 5.0 eq.) and few drops of DMF were added. The mixture was stirred over night at room temperature and concentrated in vacuum. **28d** (554 mg, *quant.*) was obtained as white solid and used in the next step without any further purification or characterization.

1-(4-(Dimethylamino)benzoyl)-2,3,6,7-tetrahydropyrazino[3,2,1-ij][1,6]naphthyridin-5(1H)-one **25o**.**25o**

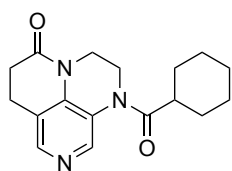
24 (100 mg, 529 μmol , 1.0 eq.) and **28d** (291 mg, 1.59 mmol, 3.0 eq.) were dissolved in dry pyridine (1 mL) and reacted according to GP A. **25o** (111 mg, 63%) was obtained as a yellow solid.

HRMS (EI): m/z calcd for $\text{C}_{19}\text{H}_{20}\text{O}_2\text{N}_4^+$ $[\text{M}]^+$: 336.1581; found: 336.1586.

1-Pivaloyl-2,3,6,7-tetrahydropyrazino[3,2,1-ij][1,6]naphthyridin-5(1H)-one **25p**.**25p**

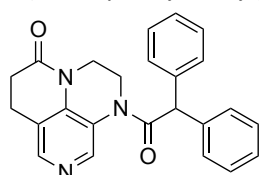
24 (200 mg, 1.06 mmol, 1.0 eq.) and pivaloyl chloride (392 μL , 3.19 mmol, 3.0 eq.) were dissolved in dry pyridine (2 mL) and reacted according to GP A. **25p** (199 mg, 69%) was obtained as a yellow solid.

HRMS (EI): m/z calcd for $\text{C}_{15}\text{H}_{19}\text{O}_2\text{N}_3^+$ $[\text{M}]^+$: 273.1472; found: 273.1476.

1-(Cyclohexanecarbonyl)-2,3,6,7-tetrahydropyrazino[3,2,1-ij][1,6]naphthyridin-5(1H)-one **25q**.**25q**

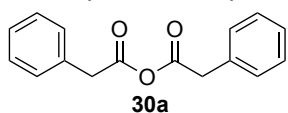
24 (100 mg, 529 μmol , 1.0 eq.) and cyclohexanecarbonyl chloride (212 μL , 1.59 mmol, 3.0 eq.) were dissolved in dry pyridine (1 mL) and reacted according to GP A. **25q** (150 mg, 95%) was obtained as a yellow solid.

HRMS (EI): m/z calcd for $\text{C}_{17}\text{H}_{21}\text{O}_2\text{N}_3^+$ $[\text{M}]^+$: 299.1628; found: 299.1628.

1-(2,2-Diphenylacetyl)-2,3,6,7-tetrahydropyrazino[3,2,1-ij][1,6]naphthyridin-5(1H)-one **25r**.**25r**

24 (100 mg, 529 μmol , 1.0 eq.) and diphenylacetyl chloride (366 mg, 1.59 mmol, 3.0 eq.) were dissolved in dry pyridine (1 mL) and reacted according to GP A. **25r** (144 mg, 71%) was obtained as a brown solid.

HRMS (EI): m/z calcd for $\text{C}_{24}\text{H}_{21}\text{O}_2\text{N}_3^+$ $[\text{M}]^+$: 383.1628; found: 383.1623.

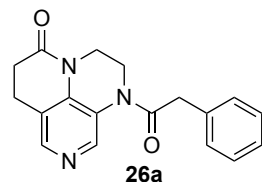
2-Phenylacetic anhydride **30a**.**30a**

Phenyl acetic acid (2.00 g, 14.7 mmol, 1.0 eq.), DCC (1.67 g, 8.08 mmol, 0.6 eq.) were suspended in CH_2Cl_2 (40 mL, 0.4 M) and stirred for 24 h at room temperature. The reaction mixture was filtered and washed carefully with CH_2Cl_2 . After recrystallization in MTBE, **30a** (1.34 g, 72%) was obtained as a white solid.

$^1\text{H NMR}$ (200 MHz, CDCl_3) δ = 7.32 (dd, J = 5.2, 2.0 Hz, 3H, Ar), 7.21 (dt, J = 6.6, 2.4 Hz, 2H, Ar), 3.73 (s, 2H, CH_2) ppm. The $^1\text{H NMR}$ spectrum is in full agreement with literature reports.^[13]

Annelated Pyridine Bases

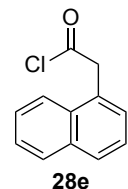
1-(2-phenylacetyl)-2,3,6,7-tetrahydropyrazino[3,2,1-ij][1,6]naphthyridin-5(1H)-one **26a**.



24 (200 mg, 1.06 μmol , 1.0 eq.) and **30a** (806 mg, 3.17 mmol, 3.0 eq.) were dissolved in dry pyridine (2 mL) and reacted according to GP A. **26a** (277 mg, 85%) was obtained as a yellow solid.

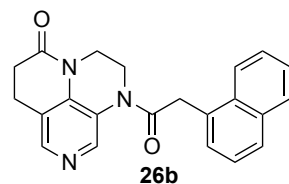
HRMS (EI): m/z calcd for $\text{C}_{18}\text{H}_{17}\text{O}_2\text{N}_3^+$ $[\text{M}]^+$: 307.1315; found: 307.1313.

1-Naphthylacetic acid chloride **28e**.



1-Naphthylacetic acid (2.00 g, 10.7 mmol, 1.0 eq.) was dissolved in dry CH_2Cl_2 (20 mL) and SOCl_2 (4.68 mL, 64.4 mmol, 6.0 eq.) and few drops of DMF were added. The mixture was stirred over night at room temperature and concentrated in vacuum. **28e** (2.18 g, *quant.*) was obtained and used in the next step without any further purification or characterization.

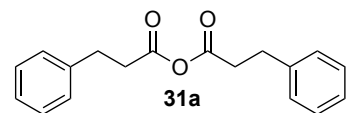
1-(2-(Naphthalen-1-yl)acetyl)-2,3,6,7-tetrahydropyrazino[3,2,1-ij][1,6]naphthyridin-5(1H)-one **26b**.



24 (100 mg, 529 μmol , 1.0 eq.) and **28e** (324 mg, 1.59 mmol, 3.0 eq.) were dissolved in dry pyridine (1 mL) and reacted according to GP A. **26b** (141 mg, 74%) was obtained as a yellow solid.

HRMS (EI): m/z calcd for $\text{C}_{22}\text{H}_{19}\text{O}_2\text{N}_3^+$ $[\text{M}]^+$: 357.1472; found: 357.1473.

3-Phenylpropanoic anhydride **31a**.

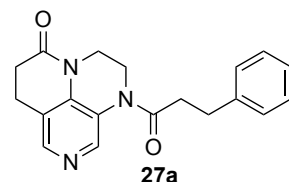


3-Phenylpropionic acid (2.00 g, 13.3 mmol, 1.0 eq.), DCC (1.37 g, 6.66 mmol, 0.6 eq.) were suspended in CH_2Cl_2 (30 mL, 0.4 M) and stirred for 24 h at room temperature. The reaction mixture was filtrated and washed carefully with

CH_2Cl_2 . **31a** (1.34 g, 72%) was obtained as an oil

$^1\text{H NMR}$ (200 MHz, CDCl_3) δ = 7.38 – 7.15 (m, 5H, Ar), 2.97 (t, J = 7.9 Hz, 2H, CH_2), 2.84 – 2.64 (m, 2H, CH_2) ppm. The $^1\text{H NMR}$ spectrum is in full agreement with literature reports.^[14]

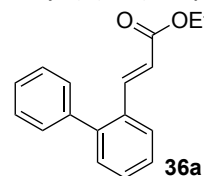
1-(3-Phenylpropanoyl)-2,3,6,7-tetrahydropyrazino[3,2,1-ij][1,6]naphthyridin-5(1H)-one **27a**.



24 (200 mg, 1.06 mmol, 1.0 eq.) and **31a** (806 mg, 3.17 mmol, 3.0 eq.) were dissolved in dry pyridine (2 mL) and reacted according to GP A. **27a** (277 mg, 85%) was obtained as a yellow solid.

HRMS (ESI): m/z calcd for $\text{C}_{19}\text{H}_{19}\text{O}_2\text{N}_3+\text{H}^+$ $[\text{M}+\text{H}]^+$: 322.1550; found: 322.1547.

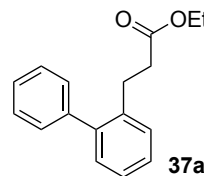
Ethyl (E)-3-(2-biphenyl)-2-propenoate **36a**.



In a pressure tube 2-bromobiphenyl (740 μL , 4.29 mmol, 1.0 eq.), ethyl acrylate (465 μL , 4.29 mmol, 1.0 eq.), $\text{Pd}(\text{OAc})_2$ (24.9 mg, 111 μmol , 2.6 mol%), $\text{P}(\text{oTol})_3$ (84.5 mg, 278 μmol , 6.5 mol%) and Et_3N (422 μL , 3.00 mmol, 0.7 eq.) were suspended in MeCN (5.5 mL) and stirred for 20 h at 120 $^\circ\text{C}$. After cooling to room temperature, the reaction mixture was concentrated in vacuum. After purification by column chromatography on silica (isohexane/EtOAc 1:1) and kugelrohr distillation, **36a** (900 mg, 83%) was obtained as an oil.

$^1\text{H NMR}$ (400 MHz, CDCl_3) δ = 7.78 – 7.68 (m, 2H, Ar and CH), 7.48 – 7.42 (m, 3H, Ar), 7.42 – 7.36 (m, 3H, Ar), 7.35 – 7.29 (m, 2H, Ar), 6.40 (d, J = 15.9 Hz, 1H, CH), 4.21 (q, J = 7.1 Hz, 2H, CH_2), 1.29 (t, J = 7.1 Hz, 3H, Me) ppm. The $^1\text{H NMR}$ spectrum is in full agreement with literature reports.^[15]

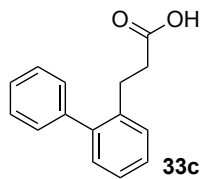
Ethyl 3-([1,1'-biphenyl]-2-yl)propanoate **37a**.



36a (900 mg, 3.60 mmol, 1.0 eq.) was dissolved in EtOH (20 mL) and Pd (10 wt.-% on Carbon, 100 mg) were added. After degassing with nitrogen, the reaction mixture was purged with hydrogen (3x) and stirred for 8 h at room temperature under hydrogen atmosphere. The reaction mixture was filtered over celite, washed well with EtOH and concentrated in vacuum. After purification by column chromatography on silica (isohexane/EtOAc 9:1), **37a** (855 mg, 93%) was obtained.

$^1\text{H NMR}$ (400 MHz, CDCl_3) δ = 7.45 – 7.38 (m, 2H, Ar), 7.38 – 7.34 (m, 1H, Ar), 7.33 – 7.27 (m, 4H, Ar), 7.27 – 7.24 (m, 1H, Ar), 7.23 – 7.19 (m, 1H, Ar), 4.05 (q, J = 7.1 Hz, 2H, CH_2), 3.00 – 2.89 (m, 2H, CH_2), 2.49 – 2.30 (m, 2H, CH_2), 1.18 (t, J = 7.1 Hz, 3H, Me) ppm.

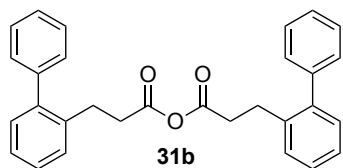
3-([1,1'-Biphenyl]-2-yl)propanoic acid **33c.**



In a round bottom flask **37a** (850 mg, 3.34 mmol, 1.0 eq.) and NaOH (2.01 g, 50.1 mmol, 15.0 eq.) were dissolved in a 1:1 mixture of water (17 mL) and MeOH (17 mL). The reaction mixture was stirred for 24 h at 100 °C. After adding 2 M HCl until a pH value of 2 was reached, the mixture was extracted with EtOAc (3 x), dried over MgSO_4 , filtered, and concentrated in vacuum to obtain **33c** (700 mg, 93%) as a white solid.

$^1\text{H NMR}$ (400 MHz, $\text{DMSO}-d_6$) δ = 7.44 (t, J = 7.3 Hz, 2H, Ar), 7.40 – 7.23 (m, 6H, Ar), 7.15 (dd, J = 7.3, 1.6 Hz, 1H, Ar), 2.83 – 2.70 (m, 2H, CH_2), 2.39 – 2.29 (m, 2H, CH_2) ppm. The $^1\text{H NMR}$ spectrum is in full agreement with literature reports.^[16]

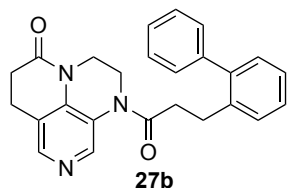
3-([1,2'-Biphenyl]-2-yl)propanoic anhydride **31b**



In a round bottom flask **33c** (670 mg, 2.96 mmol, 1.0 eq.), TsCl (282 mg, 1.48 mmol, 0.5 eq.), and K_2CO_3 (614 mg, 4.44 mmol, 1.5 eq.) were dissolved in MeCN (15 mL) and CH_2Cl_2 (15 mL) and stirred for 48 h at room temperature. The mixture was filtered and washed well with CH_2Cl_2 . After concentration under vacuum, **31b** (450 mg, 70 %) was obtained as an oil.

$^1\text{H NMR}$ (400 MHz, CDCl_3) δ = 7.44 – 7.38 (m, 2H, Ar), 7.38 – 7.34 (m, 1H, Ar), 7.31 – 7.27 (m, 4H, Ar), 7.26 – 7.18 (m, 2H, Ar), 2.92 (dd, J = 8.6, 7.2 Hz, 2H, CH_2), 2.44 (dd, J = 8.6, 7.1 Hz, 2H, CH_2) ppm.

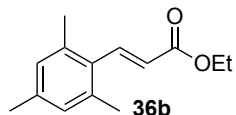
1-(3-([1,1'-biphenyl]-2-yl)propanoyl)-2,3,6,7-tetrahydropyrazino[3,2,1-ij][1,6]naphthyridin-5(1H)-one **27b.**



24 (80.0 mg, 423 μmol , 1.0 eq.) and **31b** (450 mg, 1.04 mmol, 2.5 eq.) were dissolved in dry pyridine (1 mL) and reacted according to GP A. **27b** (128 mg, 76%) was obtained as a yellow solid.

HRMS (EI): m/z calcd for $\text{C}_{25}\text{H}_{23}\text{O}_2\text{N}_3^+$ $[M]^+$: 397.1785; found: 397.1774.

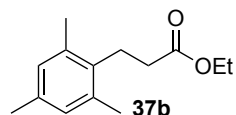
Ethyl (E)-3-mesitylacrylate **36b.**



In a pressure tube 2-bromomesitylene (2.00 g, 10.1 mmol, 1.0 eq.), ethyl acrylate (1.85 mL, 17.1 mmol, 1.7 eq.), $\text{Pd}(\text{OAc})_2$ (58.7 mg, 261 μmol , 2.6 mol%), $\text{P}(\text{oTol})_3$ (199 mg, 653 μmol , 6.5 mol%) and Et_3N (1.00 mL, 7.03 mmol, 0.7 eq.) were suspended in MeCN (12 mL) and stirred for 20 h at 120 °C. After cooling to room temperature, the reaction mixture was concentrated in vacuum. After purification by column chromatography on silica (isohexane/EtOAc 9:1) **36b** (1.36 g, 62%) was obtained as a solid.

$^1\text{H NMR}$ (200 MHz, CDCl_3) δ = 7.84 (d, J = 16.4 Hz, 1H, CH), 6.89 (s, 2H, Ar), 6.05 (d, J = 16.3 Hz, 1H, CH), 4.27 (q, J = 7.1 Hz, 2H, CH_2), 2.33 (s, 6H, 2xMe), 2.28 (s, 3H, Me), 1.35 (t, J = 7.1 Hz, 3H, Me) ppm. The $^1\text{H NMR}$ spectrum is in full agreement with literature reports.^[17]

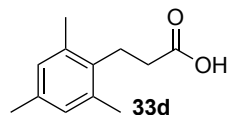
Ethyl 3-mesitylpropanoate **37b.**



36b (1.40 g, 6.41 mmol, 1.0 eq.) was dissolved in EtOH (26 mL) and Pd (10 wt.-% on carbon, 170 mg) were added. After degassing with nitrogen, the reaction mixture was purged with hydrogen (3x) and stirred for 8 h at room temperature under hydrogen atmosphere. The reaction mixture was filtered over celite, washed well with EtOH and concentrated in vacuum. After purification by column chromatography on silica (isohexane/EtOAc 9:1) **37b** (1.35 g, 96%) was obtained as a colorless liquid.

$^1\text{H NMR}$ (200 MHz, CDCl_3) δ = 6.85 (s, 2H, Ar), 4.17 (q, J = 7.1 Hz, 2H, CH_2), 3.01 – 2.84 (m, 2H, CH_2), 2.48 – 2.36 (m, 2H, CH_2), 2.31 (s, 6H, 2xMe), 2.25 (s, 3H, Me), 1.29 (t, J = 7.1 Hz, 3H, Me) ppm.

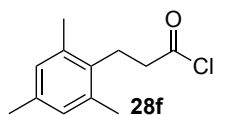
3-Mesitylpropanoic acid 33d.



In a round bottom flask **37b** (1.35 g, 6.13 mmol, 1.0 eq.) and KOH (584 mg, 10.4 mmol, 1-7 eq.) were dissolved in a 3:1 mixture of MeOH (60 mL) and water (20 mL). The reaction mixture was stirred for 24 h at 100 °C. After adding 2 M HCl until a pH value of 2 was reached, the mixture was extracted with EtOAc (3 x), dried over MgSO₄, filtered, and concentrated in vacuum to obtain **32c** (777 mg, 67%) as a white solid.

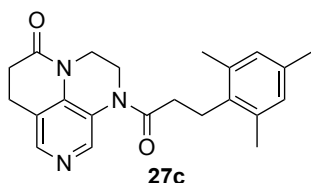
¹H NMR (200 MHz, CDCl₃) δ = 6.81 (s, 2H, Ar), 3.01 – 2.71 (m, 2H, CH₂), 2.45 (m, CH₂), 2.23 (s, 9H, 3xMe) ppm. The ¹H NMR spectrum is in full agreement with literature reports.^[18]

3-Mesitylpropanoic acid chloride 28f.



33d (530 mg, 2.76 mmol, 1.0 eq.) was dissolved in dry CH₂Cl₂ (5 mL) and SOCl₂ (280 μL, 3.87 mmol, 1.4 eq.) and few drops of DMF were added. The mixture was stirred for 3 days at room temperature and concentrated in vacuum. **28f** (470 mg, 81%) was obtained and used in the next step without any further purification or characterization.

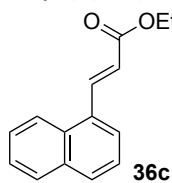
1-(3-Mesitylpropanoyl)-2,3,6,7-tetrahydropyrazino[3,2,1-ij][1,6]naphthyridin-5(1H)-one 27c.



24 (175 mg, 924 μmol, 1.0 eq.) and **28f** (467 mg, 2.22 mmol, 2.4 eq.) were dissolved in dry pyridine (2 mL) and reacted according to GP A. **27c** (276 mg, 82%) was obtained as a yellow solid.

HRMS (ESI): *m/z* calcd for C₂₂H₂₅O₂N₃+H⁺ [M+H]⁺: 364.2020; found: 364.2018.

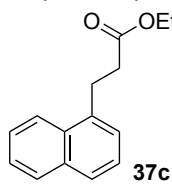
Ethyl (E)-3-(naphthalen-1-yl)acrylate 36c.



In a pressure tube 1-bromonaphthalene (1.35 mL, 9.66 mmol, 1.0 eq.), ethyl acrylate (1.78 mL, 16.4 mmol, 1.7 eq.), Pd(OAc)₂ (56.0 mg, 251 μmol, 2.6 mol%), P(oTol)₃ (191 mg, 628 μmol, 6.5 mol%) and Et₃N (950 μL, 6.76 mmol, 0.7 eq.) were suspended in MeCN (12 mL) and stirred for 20 h at 120 °C. After cooling to room temperature, the reaction mixture was concentrated in vacuum. After purification by column chromatography on silica (isohexane/EtOAc 8:2) and kugelrohr distillation **36c** (1.49 g, 68%) was obtained as an oil.

¹H NMR (400 MHz, CDCl₃) δ = 8.53 (d, *J* = 15.8 Hz, 1H, CH), 8.21 (dd, *J* = 8.6, 1.2 Hz, 1H, Ar), 7.98 – 7.82 (m, 2H, Ar), 7.76 (dt, *J* = 7.2, 0.9 Hz, 1H, Ar), 7.62 – 7.46 (m, 3H, Ar), 6.53 (d, *J* = 15.8 Hz, 1H, CH), 4.32 (q, *J* = 7.1 Hz, 2H, CH₂), 1.38 (t, *J* = 7.2 Hz, 3H, Me) ppm. The ¹H NMR spectrum is in full agreement with literature reports.^[19]

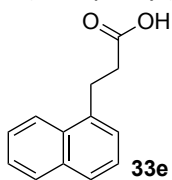
Ethyl-3-(naphthalen-1-yl)propanoate 37c.



36c (1.49 g, 1.64 mmol, 1.0 eq.) was dissolved in EtOH (30 mL) and Pd (10 wt.-% on carbon, 175 mg) was added. After degassing with nitrogen, the reaction mixture was purged with hydrogen (3x) and stirred for 8 h at room temperature under hydrogen atmosphere. The reaction mixture was filtered over celite, washed well with EtOH and concentrated in vacuum. After purification by column chromatography on silica (isohexane/EtOAc 9:1) **37c** (1.39 g, 91%) was obtained.

¹H NMR (400 MHz, CDCl₃) δ = 8.04 (d, *J* = 8.4 Hz, 1H, Ar), 7.87 (d, *J* = 7.8 Hz, 1H, Ar), 7.74 (d, *J* = 8.0 Hz, 1H, Ar), 7.57 – 7.45 (m, 2H, Ar), 7.43 – 7.33 (m, 2H, Ar), 4.16 (q, *J* = 7.1 Hz, 2H, CH₂), 3.47 – 3.39 (m, 2H, CH₂), 2.84 – 2.69 (m, 2H, CH₂), 1.25 (t, *J* = 7.1 Hz, 3H, Me) ppm. The ¹H NMR spectrum is in full agreement with literature reports.^[20]

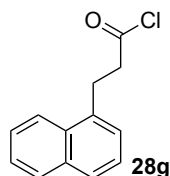
3-(1-Naphthyl)propanoic acid 33e.



In a round bottom flask **37c** (1.40 g, 6.13 mmol, 1.0 eq.) and NaOH (3.68 g, 92.0 mmol, 10.0 eq.) were dissolved in a mixture of water (30 mL) and MeOH (30 mL). The reaction mixture was stirred for 3 days at room temperature. After adding 2 M HCl until a pH value of 2 was reached, the mixture was extracted with EtOAc (3 x), dried over MgSO₄, filtered, and concentrated in vacuum to obtain **33e** (1.21 g, 99%) as a white solid.

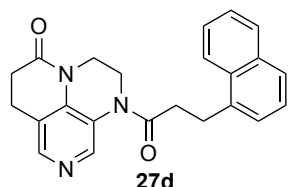
$^1\text{H NMR}$ (400 MHz, DMSO- d_6) δ = 8.09 – 8.03 (m, 1H, Ar), 7.92 (d, J = 7.8 Hz, 1H, Ar), 7.82 – 7.76 (m, 1H, Ar), 7.59 – 7.48 (m, 2H, Ar), 7.45 – 7.35 (m, 2H, Ar), 3.32 – 3.25 (m, 2H, CH_2), 2.63 (t, J = 7.7 Hz, 2H, CH_2) ppm. The $^1\text{H NMR}$ spectrum is in full agreement with literature reports.^[21]

3-(1-Naphthyl)propanoic acid chloride 28g.



33e (500 mg, 2.50 mmol, 1.0 eq.) was dissolved in dry CH_2Cl_2 (3 mL) and SOCl_2 (905 μL , 12.5 mmol, 5.0 eq.) and few drops of DMF were added. The mixture was stirred for 3 days at room temperature and concentrated in vacuum. **28g** (545 mg, *quant.*) was obtained and used in the next step without any further purification or characterization.

1-(3-(Naphthalen-1-yl)propanoyl)-2,3,6,7-tetrahydropyrazino[3,2,1-ij][1,6]naphthyridin-5(1H)-one 27d.



24 (100 mg, 529 μmol , 1.0 eq.) and **28g** (346 mg, 1.59 mmol, 3.0 eq.) were dissolved in dry pyridine (1 mL) and reacted according to GP A. **27d** (142 mg, 73%) was obtained as a yellow solid.

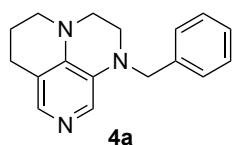
HRMS (EI): m/z calcd for $\text{C}_{23}\text{H}_{21}\text{O}_2\text{N}_3^+$ $[\text{M}]^+$: 371.1628; found: 371.1634.

5.1.4.2 Synthesis of Catalysts 4-6

General Procedure C (GP C, Synthesis of catalyst 4-6 is based on the procedure reported by Zipse *et al.*^[7])

In a Schlenk tube dry THF (1.5 mL) was added and cooled to 0 °C. LiAlH_4 (4.2 eq.) and AlCl_3 (2.6 eq.) were added carefully and the reaction mixture was stirred for 20 min at room temperature. **25**, **26** or **27** (1.0 eq.) diluted in THF (1.5-5 mL, if not soluble in dry THF, dry CH_2Cl_2 was added) was added dropwise at 0 °C. The reaction mixture was stirred for 24 - 48 h under reflux (in less hindered systems the mixture was stirred at room temperature). After cooling to room temperature, the mixture was quenched with water and saturated K_2CO_3 -solution. The mixture was filtered over celite and the filtrate was washed with CH_2Cl_2 and EtOAc. After extraction with $\text{CH}_2\text{Cl}_2/\text{EtOAc}$ (1:1, 3x20 mL), the combined organic phase was washed with saturated K_2CO_3 -solution (50 mL), dried over MgSO_4 , filtered and concentrated in vacuum. The pure product was obtained by column chromatography on silica (EtOAc/ Et_3N /MeOH 95:5:0 to 92:5:3).

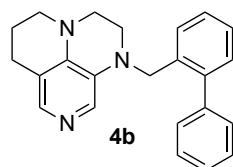
1-Benzyl-1,2,3,5,6,7-hexahydropyrazino[3,2,1-ij][1,6]naphthyridine 4a.



25a (300 mg, 1.02 mmol, 1.0 eq.), LiAlH_4 (163 mg, 4.30 mmol, 4.2 eq.) and AlCl_3 (354 mg, 2.66 mmol, 2.6 eq.) were dissolved in dry THF and reacted according to GP C. **4a** (172 mg, 64%) was obtained as a yellow oil.

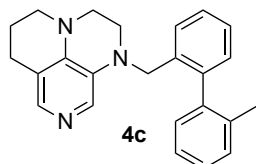
$^1\text{H NMR}$ (400 MHz, CDCl_3) δ = 7.59 (d, J = 4.3 Hz, 2H, Ar), 7.37 – 7.28 (m, 4H, Ar), 7.27 – 7.21 (m, 1H, Ar), 4.39 (s, 2H, CH_2), 3.34 – 3.27 (m, 4H, $2\times\text{CH}_2$), 3.25 – 3.15 (m, 2H, CH_2), 2.70 (t, J = 6.4 Hz, 2H, CH_2), 2.06 – 1.97 (m, 2H, CH_2) ppm; $^{13}\text{C NMR}$ (151 MHz, CDCl_3) δ = 139.90, 138.55, 137.79, 130.34, 129.72, 128.82, 127.56, 127.37, 114.97, 55.26, 49.45, 47.99, 46.24, 24.04, 21.22 ppm; **HRMS** (EI): m/z calcd for $\text{C}_{17}\text{H}_{19}\text{N}_3^+$ $[\text{M}]^+$: 265.1573; found: 265.1568. The $^1\text{H NMR}$ spectrum is in full agreement with literature reports.^[7]

1-([1,1'-Biphenyl]-2-ylmethyl)-1,2,3,5,6,7-hexahydropyrazino[3,2,1-ij][1,6]naphthyridine 4b.



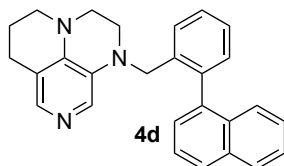
25b (100 mg, 271 μmol , 1.0 eq.), LiAlH_4 (43.1 mg, 1.14 mmol, 4.2 eq.) and AlCl_3 (93.8 mg, 704 μmol , 2.6 eq.) were dissolved in dry THF and reacted according to GP C. **4b** (80.0 mg, 87%) was obtained as a yellow oil.

$^1\text{H NMR}$ (400 MHz, CDCl_3) δ = 7.53 (s, 1H, Ar), 7.44 – 7.38 (m, 3H, Ar), 7.37 – 7.29 (m, 6H, Ar), 7.26 (d, J = 9.1 Hz, 1H, Ar), 4.29 (s, 2H, CH_2), 3.24 (s, 4H, $2\times\text{CH}_2$), 3.20 – 3.15 (m, 2H, CH_2), 2.67 (t, J = 6.4 Hz, 2H, CH_2), 2.02 – 1.94 (m, 2H, CH_2) ppm; $^{13}\text{C NMR}$ (101 MHz, CDCl_3) δ = 141.75, 141.01, 140.11, 138.14, 134.97, 130.39, 130.23, 130.20, 129.19, 128.42, 127.81, 127.53, 127.31, 127.08, 114.92, 53.70, 49.41, 47.77, 46.76, 24.00, 21.28 ppm; **IR** (ATR): ν (cm^{-1}) = 2840, 1578, 1514, 1470, 1349, 1253, 1154, 912, 853, 745, 701; **HRMS** (EI): m/z calcd for $\text{C}_{23}\text{H}_{23}\text{N}_3^+$ $[\text{M}]^+$: 341.1886; found: 341.1889.

1-((2'-Methyl-[1,1'-biphenyl]-2-yl)methyl)-1,2,3,5,6,7-hexahydropyrazino[3,2,1-ij][1,6]naphthyridine **4c**.

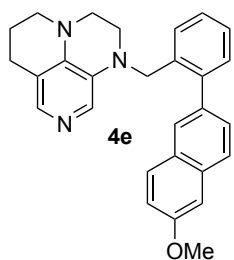
25c (100 mg, 261 μmol , 1.0 eq.), LiAlH_4 (41.6 mg, 1.10 mmol, 4.2 eq.) and AlCl_3 (90.4 mg, 678 μmol , 2.6 eq.) were dissolved in dry THF and reacted according to GP C. **4c** (43.0 mg, 46%) was obtained as a colourless oil.

$^1\text{H NMR}$ (400 MHz, CDCl_3) δ = 7.53 (s, 1H, Ar), 7.42 – 7.37 (m, 1H, Ar), 7.33 (s, 1H, Ar), 7.31 – 7.26 (m, 4H, Ar), 7.25 – 7.20 (m, 1H, Ar), 7.18 – 7.11 (m, 2H, Ar), 4.06 (s, 2H, CH_2), 3.27 – 3.14 (m, 6H, $3\times\text{CH}_2$), 2.67 (t, J = 6.4 Hz, 2H, CH_2), 2.10 (s, 3H, Me), 2.02 – 1.94 (m, 2H, CH_2) ppm; $^{13}\text{C NMR}$ (101 MHz, CDCl_3) δ = 140.98, 140.46, 140.33, 137.98, 135.92, 135.36, 130.64, 130.25, 130.21, 129.94, 129.24, 127.68, 127.64, 127.19, 126.94, 125.85, 114.98, 53.90, 49.39, 47.62, 47.08, 23.98, 21.32, 20.18 ppm; IR (ATR): ν (cm^{-1}) = 2840, 1576, 1514, 1435, 1349, 1196, 1155, 853, 755; HRMS (EI): m/z calcd for $\text{C}_{24}\text{H}_{25}\text{N}_3^+$ [M] $^+$: 355.2043; found: 355.2046.

1-(2-(Naphthalen-1-yl)benzyl)-1,2,3,5,6,7-hexahydropyrazino[3,2,1-ij][1,6]naphthyridine **4d**.

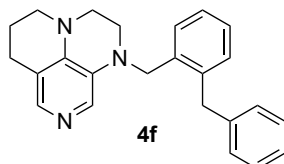
25d (100 mg, 238 μmol , 1.0 eq.), LiAlH_4 (38.0 mg, 1.00 mmol, 4.2 eq.) and AlCl_3 (82.6 mg, 619 μmol , 2.6 eq.) were dissolved in dry THF and reacted according to GP C. **4d** (30.0 mg, 32%) was obtained as a white solid.

m.p. 60-62 $^\circ\text{C}$, $^1\text{H NMR}$ (600 MHz, CDCl_3) δ = 7.90 (d, J = 8.2 Hz, 1H, Ar), 7.87 (d, J = 8.3 Hz, 1H, Ar), 7.53 (dd, J = 8.2, 7.0 Hz, 1H, Ar), 7.50 – 7.45 (m, 4H, Ar), 7.43 – 7.34 (m, 4H, Ar), 7.31 – 7.27 (m, 2H, Ar), 4.03 (s, 2H, CH_2), 3.18 – 3.01 (m, 6H, $3\times\text{CH}_2$), 2.63 (t, J = 6.4 Hz, 2H, CH_2), 1.94 (qd, J = 6.5, 4.6 Hz, 2H, CH_2) ppm; $^{13}\text{C NMR}$ (151 MHz, CDCl_3) δ = 140.23, 139.57, 138.79, 137.83, 136.44, 133.66, 132.18, 130.97, 130.54, 130.05, 128.43, 128.12, 127.86, 127.10, 126.96, 126.53, 126.42, 126.06, 125.88, 125.56, 114.88, 53.87, 49.33, 47.53, 47.08, 23.96, 21.30 ppm; IR (ATR): ν (cm^{-1}) = 2838, 1580, 1512, 1433, 1349, 1253, 1196, 1155, 853, 778; HRMS (EI): m/z calcd for $\text{C}_{27}\text{H}_{25}\text{N}_3^+$ [M] $^+$: 391.2043; found: 391.2043.

1-(2-(6-methoxynaphthalen-2-yl)benzyl)-1,2,3,5,6,7-hexahydropyrazino[3,2,1-ij][1,6]naphthyridine **4e**.

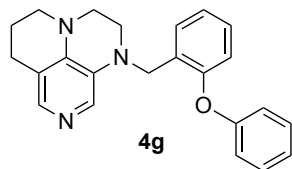
25e (100 mg, 222 μmol , 1.0 eq.), LiAlH_4 (35.5 mg, 934 μmol , 4.2 eq.) and AlCl_3 (77.1 mg, 578 μmol , 2.6 eq.) were dissolved in dry THF and reacted according to GP C. **4e** (73.0 mg, 78%) was obtained as a white solid.

m.p. 60-62 $^\circ\text{C}$, $^1\text{H NMR}$ (400 MHz, CDCl_3) δ = 7.76 (dd, J = 11.3, 9.1 Hz, 2H, Ar), 7.71 (d, J = 1.7 Hz, 1H, Ar), 7.52 (s, 1H, Ar), 7.47 – 7.41 (m, 2H, Ar), 7.39 (s, 1H, Ar), 7.33 (q, J = 2.7 Hz, 3H, Ar), 7.21 – 7.16 (m, 2H, Ar), 4.35 (s, 2H, CH_2), 3.95 (s, 3H, Me), 3.23 (q, J = 1.7 Hz, 4H, $2\times\text{CH}_2$), 3.19 – 3.12 (m, 2H, CH_2), 2.66 (t, J = 6.4 Hz, 2H, CH_2), 1.98 (q, J = 6.0 Hz, 2H, CH_2) ppm; $^{13}\text{C NMR}$ (101 MHz, CDCl_3) δ = 157.94, 141.63, 140.35, 137.96, 136.26, 135.29, 133.66, 130.63, 130.55, 130.14, 129.65, 128.84, 128.03, 127.78, 127.71, 127.41, 127.06, 126.77, 119.36, 114.93, 105.71, 55.52, 53.87, 49.37, 47.71, 46.94, 23.98, 21.29 ppm; IR (ATR): ν (cm^{-1}) = 2838, 1726, 1631, 1580, 1514, 1433, 1388, 1349, 1252, 1202, 1160, 1030, 915, 853, 746; HRMS (EI): m/z calcd for $\text{C}_{28}\text{H}_{27}\text{ON}_3^+$ [M] $^+$: 421.2149; found: 421.2157.

1-(2-Benzylbenzyl)-1,2,3,5,6,7-hexahydropyrazino[3,2,1-ij][1,6]naphthyridine **4f**.

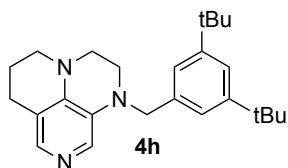
25f (100 mg, 261 μmol , 1.0 eq.), LiAlH_4 (41.6 mg, 1.10 mmol, 4.2 eq.) and AlCl_3 (90.4 mg, 678 μmol , 2.6 eq.) were dissolved in dry THF and reacted according to GP C. **4f** (40.0 mg, 43%) was obtained as a yellow oil.

$^1\text{H NMR}$ (400 MHz, CDCl_3) δ = 7.57 (s, 1H, Ar), 7.39 (s, 1H, Ar), 7.30 – 7.16 (m, 7H, Ar), 7.12 – 7.07 (m, 2H, Ar), 4.25 (s, 2H, CH_2), 4.05 (s, 2H, CH_2), 3.20 – 3.11 (m, 6H, $3\times\text{CH}_2$), 2.69 (t, J = 6.4 Hz, 2H, CH_2), 2.03 – 1.96 (m, 2H, CH_2) ppm; $^{13}\text{C NMR}$ (101 MHz, CDCl_3) δ = 140.37, 140.14, 138.78, 138.19, 135.42, 131.06, 130.19, 130.02, 128.73, 128.60, 128.52, 127.48, 126.85, 126.26, 114.82, 52.95, 49.33, 47.79, 45.77, 38.85, 24.01, 21.23 ppm; IR (ATR): ν (cm^{-1}) = 2842, 1570, 1514, 1451, 1346, 1253, 1196, 1154, 1029, 853, 733, 697; HRMS (EI): m/z calcd for $\text{C}_{24}\text{H}_{25}\text{N}_3^+$ [M] $^+$: 355.2043; found: 355.2043.

1-(2-Phenoxybenzyl)-1,2,3,5,6,7-hexahydropyrazino[3,2,1-ij][1,6]naphthyridine 4g.

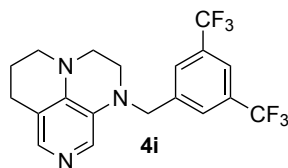
25g (100 mg, 259 μmol , 1.0 eq.), LiAlH_4 (41.3 mg, 1.09 mmol, 4.2 eq.) and AlCl_3 (90.0 mg, 675 μmol , 2.6 eq.) were dissolved in dry THF and reacted according to GP C. **4g** (35.0 mg, 38%) was obtained as an oil.

$^1\text{H NMR}$ (CDCl_3 , 400 MHz) δ = 7.56 (s, 1H, Ar), 7.49 (s, 1H, Ar), 7.38 – 7.29 (m, 3H, Ar), 7.22 (t, J = 8.5 Hz, 1H, Ar), 7.11 – 7.04 (m, 2H, Ar), 7.01 – 6.90 (m, 3H, Ar), 4.43 (s, 2H, CH_2), 3.43 – 3.37 (m, 2H, CH_2), 3.31 – 3.24 (m, 2H, CH_2), 3.21 – 3.14 (m, 2H, CH_2), 2.69 (t, J = 6.4 Hz, 2H, CH_2), 2.06 – 1.95 (m, 2H, CH_2) ppm; **$^{13}\text{C NMR}$** (CDCl_3 , 101 MHz) δ = 157.53, 154.47, 140.39, 137.95, 130.56, 130.18, 129.94, 129.14, 128.91, 128.43, 124.10, 123.04, 119.57, 117.93, 115.06, 50.56, 49.43, 47.71, 47.22, 24.01, 21.34 ppm; **IR** (ATR): ν (cm^{-1}) = 2841, 1579, 1515, 1482, 1350, 1228, 1161, 1093, 870, 746, 691; **HRMS** (EI): m/z calcd for $\text{C}_{23}\text{H}_{23}\text{O}_1\text{N}_3^+$ $[M]^+$: 357.1836; found: 357.1836.

1-(3,5-Di-tert-butylbenzyl)-1,2,3,5,6,7-hexahydropyrazino[3,2,1-ij][1,6]naphthyridine 4h.

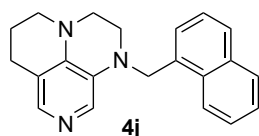
25h (100 mg, 247 μmol , 1.0 eq.), LiAlH_4 (37.4 mg, 986 μmol , 4.2 eq.) and AlCl_3 (85.5 mg, 641 μmol , 2.6 eq.) were dissolved in dry THF and reacted according to GP C. **4h** (70.0 mg, 75%) was obtained as a yellow oil.

$^1\text{H NMR}$ (400 MHz, CDCl_3) δ = 7.67 (s, 1H, Ar), 7.59 (s, 1H, Ar), 7.32 (t, J = 1.9 Hz, 1H, Ar), 7.15 – 7.12 (m, 2H, Ar), 4.35 (s, 2H, CH_2), 3.32 – 3.26 (m, 2H, CH_2), 3.26 – 3.17 (m, 4H, $2 \times \text{CH}_2$), 2.71 (t, J = 6.4 Hz, 2H, CH_2), 2.06 – 1.96 (m, 2H, CH_2), 1.31 (s, 18H, $2 \times \text{tBu}$) ppm; **$^{13}\text{C NMR}$** (101 MHz, CDCl_3) δ = 151.13, 140.59, 138.21, 136.98, 130.65, 130.63, 121.87, 121.22, 114.82, 55.56, 49.33, 48.06, 45.70, 34.92, 31.62, 24.04, 21.30 ppm; **IR** (ATR): ν (cm^{-1}) = 2951, 1580, 1513, 1468, 1348, 1247, 1195, 1156, 873, 746, 712; **HRMS** (EI): m/z calcd for $\text{C}_{25}\text{H}_{35}\text{N}_3^+$ $[M]^+$: 377.2825; found: 377.2826.

1-(3,5-Bis(trifluoromethyl)benzyl)-1,2,3,5,6,7-hexahydropyrazino[3,2,1-ij][1,6]naphthyridine 4i.

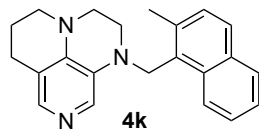
25i (100 mg, 233 μmol , 1.0 eq.), LiAlH_4 (37.1 mg, 978 μmol , 4.2 eq.) and AlCl_3 (80.8 mg, 606 μmol , 2.6 eq.) were dissolved in dry THF and reacted according to GP C. **4i** (46.0 mg, 49%) was obtained as a white solid.

m.p. 63–65 $^\circ\text{C}$; **$^1\text{H NMR}$** (400 MHz, CDCl_3) δ = 7.80 – 7.75 (m, 3H, Ar), 7.62 (s, 1H, Ar), 7.44 (s, 1H, Ar), 4.46 (s, 2H, CH_2), 3.42 – 3.31 (m, 4H, $2 \times \text{CH}_2$), 3.28 – 3.21 (m, 2H, CH_2), 2.71 (t, J = 6.4 Hz, 2H, CH_2), 2.08 – 1.97 (m, 2H, CH_2) ppm; **$^{13}\text{C NMR}$** (151 MHz, CDCl_3) δ = 141.57, 141.36, 138.55, 132.20 (q), 130.85, 129.53, 127.38 – 127.26 (m), 125.63 – 120.52 (q), 121.68 – 121.44 (m), 115.31, 55.45, 49.35, 47.85, 47.36, 24.00, 21.20 ppm; **$^{19}\text{F NMR}$** (CDCl_3 , 377 MHz) δ = -62.78 ppm; **IR** (ATR): ν (cm^{-1}) = 2921, 1579, 1516, 1355, 1275, 1157, 1125, 895, 864, 742, 704. 682; **HRMS** (EI): m/z calcd for $\text{C}_{19}\text{H}_{17}\text{N}_3\text{F}_6^+$ $[M]^+$: 401.1321; found: 401.1323.

1-(Naphthalen-1-ylmethyl)-1,2,3,5,6,7-hexahydropyrazino[3,2,1-ij][1,6]naphthyridine 4j.

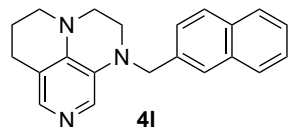
25j (100 mg, 291 μmol , 1.0 eq.), LiAlH_4 (46.4 mg, 1.22 mmol, 4.2 eq.) and AlCl_3 (101 mg, 757 μmol , 2.6 eq.) were dissolved in dry THF and reacted according to GP C. **4j** (35.0 mg, 38%) was obtained as a yellow solid.

m.p. 72–75 $^\circ\text{C}$; **$^1\text{H NMR}$** (400 MHz, CDCl_3) δ = 8.03 (dt, J = 6.4, 3.5 Hz, 1H, Ar), 7.93 – 7.83 (m, 1H, Ar), 7.83 – 7.77 (m, 1H, Ar), 7.64 (d, J = 12.7 Hz, 2H, Ar), 7.51 (tt, J = 6.1, 3.1 Hz, 2H, Ar), 7.46 – 7.38 (m, 2H, Ar), 4.78 (s, 2H, CH_2), 3.30 – 3.16 (m, 6H, $3 \times \text{CH}_2$), 2.72 (q, J = 6.3 Hz, 2H, CH_2), 2.07 – 1.98 (m, 2H, CH_2) ppm; **$^{13}\text{C NMR}$** (101 MHz, CDCl_3) δ = 139.65, 138.85, 133.97, 132.09, 131.72, 130.40, 128.89, 128.86, 128.35, 126.41, 126.31, 126.02, 125.50, 123.51, 114.79, 53.17, 49.40, 48.14, 44.94, 24.04, 21.08 ppm; **IR** (ATR): ν (cm^{-1}) = 2839, 1628, 1566, 1513, 1433, 1346, 1246, 1196, 1155, 791, 744; **HRMS** (EI): m/z calcd for $\text{C}_{21}\text{H}_{21}\text{N}_3^+$ $[M]^+$: 315.1730; found: 315.1733.

1-((2-Methylnaphthalen-1-yl)methyl)-1,2,3,5,6,7-hexahydropyrazino[3,2,1-ij][1,6]naphthyridine **4k**.

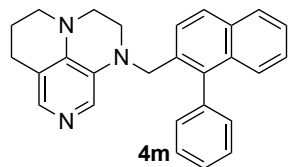
25k (100 mg, 280 μmol , 1.0 eq.), LiAlH_4 (44.6 mg, 1.18 mmol, 4.2 eq.) and AlCl_3 (97.0 mg, 727 μmol , 2.6 eq.) were dissolved in dry THF and reacted according to GP C. **4k** (30.0 mg, 33%) was obtained as a white solid.

m.p. 62–64 $^\circ\text{C}$; $^1\text{H NMR}$ (600 MHz, CDCl_3) δ = 8.04 (d, J = 8.3 Hz, 1H, Ar), 7.97 (s, 1H, Ar), 7.82 (d, J = 7.9 Hz, 1H, Ar), 7.75 (d, J = 8.4 Hz, 1H, Ar), 7.69 (s, 1H, Ar), 7.44 (dt, J = 15.3, 7.3 Hz, 2H, Ar), 7.35 (d, J = 8.4 Hz, 1H, Ar), 4.69 (s, 2H, CH_2), 3.18 – 3.12 (m, 2H, CH_2), 3.06 (ddd, J = 6.1, 3.4, 1.2 Hz, 2H, CH_2), 2.87 – 2.82 (m, 2H, CH_2), 2.72 (t, J = 6.4 Hz, 2H, CH_2), 2.55 (d, J = 1.1 Hz, 3H, Me), 2.01 – 1.93 (m, 2H, CH_2) ppm; $^{13}\text{C NMR}$ (151 MHz, CDCl_3) δ = 141.25, 138.55, 136.29, 133.40, 132.53, 130.75, 129.64, 129.21, 129.18, 128.47, 128.35, 126.63, 125.16, 124.20, 114.42, 49.20, 48.62, 46.73, 41.58, 24.12, 21.17, 20.63 ppm; **IR** (ATR): ν (cm^{-1}) = 2838, 1582, 1515, 1467, 1338, 1243, 1157, 859, 812, 772, 744; **HRMS** (EI): m/z calcd for $\text{C}_{22}\text{H}_{23}\text{N}_3^+$ $[\text{M}]^+$: 329.1886; found: 329.1887.

1-(Naphthalen-2-ylmethyl)-1,2,3,5,6,7-hexahydropyrazino[3,2,1-ij][1,6]naphthyridine **4l**.

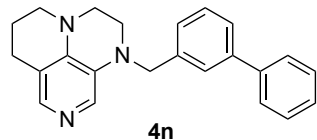
25l (100 mg, 291 μmol , 1.0 eq.), LiAlH_4 (46.4 mg, 1.22 mmol, 4.2 eq.) and AlCl_3 (101 mg, 757 μmol , 2.6 eq.) were dissolved in dry THF and reacted according to GP C. **4l** (60.0 mg, 65%) was obtained as a yellow oil.

$^1\text{H NMR}$ (400 MHz, CDCl_3) δ = 7.84 – 7.77 (m, 3H, Ar), 7.75 (d, J = 1.6 Hz, 1H, Ar), 7.67 (s, 1H, Ar), 7.59 (d, J = 0.9 Hz, 1H, Ar), 7.49 – 7.41 (m, 3H, Ar), 4.53 (s, 2H, CH_2), 3.37 – 3.28 (m, 4H, $2\times\text{CH}_2$), 3.27 – 3.18 (m, 2H, CH_2), 2.71 (t, J = 6.4 Hz, 2H, CH_2), 2.05 – 1.97 (m, 2H, CH_2) ppm; $^{13}\text{C NMR}$ (101 MHz, CDCl_3) δ = 140.15, 138.57, 135.34, 133.58, 132.95, 130.42, 129.98, 128.64, 127.85, 127.82, 126.35, 126.31, 125.89, 125.75, 115.00, 55.50, 49.44, 48.02, 46.13, 24.06, 21.24 ppm; **IR** (ATR): ν (cm^{-1}) = 2847, 1626, 1567, 1513, 1434, 1346, 1256, 1153, 854, 814, 743; **HRMS** (EI): m/z calcd for $\text{C}_{21}\text{H}_{17}\text{N}_3^+$ $[\text{M}]^+$: 315.1730; found: 315.1730.

1-((1-Phenylnaphthalen-2-yl)methyl)-1,2,3,5,6,7-hexahydropyrazino[3,2,1-ij][1,6]naphthyridine **4m**.

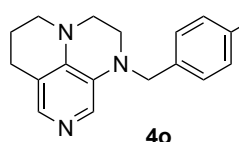
25m (90.0 mg, 214 μmol , 1.0 eq.), LiAlH_4 (34.2 mg, 901 μmol , 4.2 eq.) and AlCl_3 (74.4 mg, 557 μmol , 2.6 eq.) were dissolved in dry THF and reacted according to GP C. **4m** (41.1 mg, 49%) was obtained as a white solid.

m.p. 59–61 $^\circ\text{C}$; $^1\text{H NMR}$ (600 MHz, CDCl_3) δ = 7.85 (d, J = 8.1 Hz, 1H, Ar), 7.83 (d, J = 8.6 Hz, 1H, Ar), 7.57 (d, J = 8.6 Hz, 1H, Ar), 7.55 – 7.49 (m, 3H, Ar), 7.47 – 7.43 (m, 3H, Ar), 7.41 (dd, J = 8.6, 1.1 Hz, 1H, Ar), 7.35 (ddd, J = 8.4, 6.6, 1.3 Hz, 1H, Ar), 7.33 – 7.30 (m, 2H, Ar), 4.23 (s, 2H, CH_2), 3.26 (dd, J = 6.0, 3.5 Hz, 2H, CH_2), 3.23 – 3.16 (m, 4H, $2\times\text{CH}_2$), 2.68 (t, J = 6.4 Hz, 2H, CH_2), 1.99 (dt, J = 11.3, 6.1 Hz, 2H, CH_2) ppm; $^{13}\text{C NMR}$ (151 MHz, CDCl_3) δ = 140.45, 138.60, 138.45, 138.20, 133.13, 133.02, 132.84, 130.54, 130.38, 130.18, 128.76, 128.09, 127.91, 127.60, 126.46, 126.15, 125.66, 125.31, 114.90, 53.71, 49.40, 47.86, 46.40, 24.02, 21.30 ppm; **IR** (ATR): ν (cm^{-1}) = 2922, 1573, 1514, 1432, 1351, 1269, 1195, 1152, 1069, 980, 853, 817, 754, 706; **HRMS** (EI): m/z calcd for $\text{C}_{27}\text{H}_{25}\text{N}_3^+$ $[\text{M}]^+$: 391.2043; found: 391.2045.

1-([1,1'-Biphenyl]-3-ylmethyl)-1,2,3,5,6,7-hexahydropyrazino[3,2,1-ij][1,6]naphthyridine **4n**.

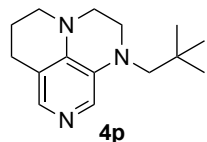
25n (100 mg, 271 μmol , 1.0 eq.), LiAlH_4 (43.1 mg, 1.14 mmol, 4.2 eq.) and AlCl_3 (93.8 mg, 704 μmol , 2.6 eq.) were dissolved in dry THF and reacted according to GP C. **4n** (65.0 mg, 70%) was obtained as a yellow oil.

$^1\text{H NMR}$ (600 MHz, CDCl_3) δ = 7.61 – 7.55 (m, 4H, Ar), 7.52 – 7.47 (m, 2H, Ar), 7.46 – 7.37 (m, 3H, Ar), 7.37 – 7.32 (m, 1H, Ar), 7.28 (d, J = 7.6 Hz, 1H, Ar), 4.43 (s, 2H, CH_2), 3.41 – 3.31 (m, 4H, $2\times\text{CH}_2$), 3.27 – 3.21 (m, 2H, CH_2), 2.71 (t, J = 6.4 Hz, 2H, CH_2), 2.01 (p, J = 6.2 Hz, 2H, CH_2) ppm; $^{13}\text{C NMR}$ (151 MHz, CDCl_3) δ = 141.91, 141.13, 139.06, 138.15, 130.35, 129.30, 128.89, 128.71, 127.51, 127.36, 127.33, 126.48, 126.38, 126.33, 114.89, 55.38, 49.48, 48.07, 46.07, 24.02, 21.06 ppm; **IR** (ATR): ν (cm^{-1}) = 2840, 1566, 1453, 1337, 1254, 1195, 1155, 854, 753, 698; **HRMS** (EI): m/z calcd for $\text{C}_{23}\text{H}_{23}\text{N}_3^+$ $[\text{M}]^+$: 341.1886; found: 341.1886.

1-((*N,N*-Dimethyl-4-aniline)methyl)-1,2,3,5,6,7-hexahydropyrazino[3,2,1-*ij*][1,6]naphthyridine **4o**.**4o**

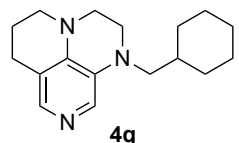
25o (100 mg, 297 μmol , 1.0 eq.), LiAlH_4 (47.4 mg, 1.25 mmol, 4.2 eq.) and AlCl_3 (103 mg, 772 μmol , 2.6 eq.) were dissolved in dry THF and reacted according to GP C. **4o** (36 mg, 39%) was obtained as a yellow oil.

$^1\text{H NMR}$ (400 MHz, CDCl_3) δ = 7.68 (s, 1H, Ar), 7.57 (s, 1H, Ar), 7.17 (d, J = 8.6 Hz, 2H, Ar), 6.70 (d, J = 8.7 Hz, 2H, Ar), 4.27 (s, 2H, CH_2), 3.31 – 3.23 (m, 2H, CH_2), 3.24 – 3.17 (m, 4H, CH_2), 2.93 (s, 6H, Me_2), 2.69 (t, J = 6.4 Hz, 2H), 2.02 – 1.94 (m, 2H, CH_2) ppm; $^{13}\text{C NMR}$ (101 MHz, CDCl_3) δ = 150.06, 140.46, 138.18, 130.64, 128.85, 125.41, 114.83, 112.89, 54.45, 49.36, 48.02, 45.47, 40.84, 24.06, 21.31 ppm; **IR** (ATR): ν (cm^{-1}) = 2841, 1613, 1581, 1519, 1442, 1345, 1163, 946, 803; **HRMS** (EI): m/z calcd for $\text{C}_{19}\text{H}_{24}\text{N}_4^+$ $[\text{M}]^+$: 308.1995; found: 308.1994.

1-Neopentyl-1,2,3,5,6,7-hexahydropyrazino[3,2,1-*ij*][1,6]naphthyridine **4p**.**4p**

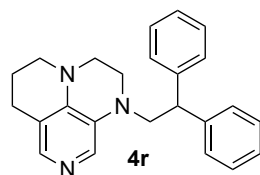
25p (250 mg, 914 μmol , 1.0 eq.), LiAlH_4 (145 mg, 3.84 mmol, 4.2 eq.) and AlCl_3 (317 mg, 2.28 mmol, 2.6 eq.) were dissolved in dry THF and reacted according to GP C. **4p** (183 mg, 82%) was obtained as a white solid.

m.p. 100-102 $^\circ\text{C}$; $^1\text{H NMR}$ (599 MHz, CDCl_3) δ = 7.66 (s, 1H, Ar), 7.51 (s, 1H, Ar), 3.38 – 3.32 (m, 2H, CH_2), 3.29 – 3.21 (m, 2H, CH_2), 3.21 – 3.13 (m, 2, CH_2), 2.96 (s, 2H, CH_2), 2.67 (t, J = 6.4 Hz, 2H, CH_2), 2.00 – 1.94 (m, 2H, CH_2), 0.97 (s, 9H, *t*Bu) ppm; $^{13}\text{C NMR}$ (151 MHz, CDCl_3) δ = 139.76, 137.80, 131.81, 131.01, 114.90, 63.84, 49.97, 49.47, 47.46, 34.76, 28.40, 24.08, 21.34 ppm; **IR** (ATR): ν (cm^{-1}) = 2948, 1576, 1513, 1462, 1345, 1249, 1229, 1154, 1036, 856, 772, 746; **HRMS** (ESI): m/z calcd for $\text{C}_{15}\text{H}_{23}\text{N}_3 + \text{H}^+$ $[\text{M} + \text{H}]^+$: 246.1965; found: 246.1964.

1-(Cyclohexylmethyl)-1,2,3,5,6,7-hexahydropyrazino[3,2,1-*ij*][1,6]naphthyridine **4q**.**4q**

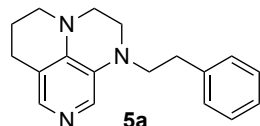
25q (100 mg, 334 μmol , 1.0 eq.), LiAlH_4 (53.3 mg, 1.40 mmol, 4.2 eq.) and AlCl_3 (116 mg, 868 μmol , 2.6 eq.) were dissolved in dry THF and reacted according to GP C. **4q** (33.0 mg, 37%) was obtained as a yellow oil.

$^1\text{H NMR}$ (400 MHz, CDCl_3) δ = 7.52 (d, J = 4.5 Hz, 2H, Ar), 3.34 (dd, J = 5.8, 3.7 Hz, 2H, CH_2), 3.25 (dd, J = 5.8, 3.7 Hz, 2H, CH_2), 3.20 – 3.14 (m, 2H, CH_2), 2.97 (d, J = 6.6 Hz, 2H, CH_2), 2.68 (t, J = 6.4 Hz, 2H, CH_2), 2.04 – 1.95 (m, 2H, CH_2), 1.69 (d, J = 8.6 Hz, 5H, $2 \times \text{CH}_2$ and CH), 1.31 – 1.13 (m, 4H, $2 \times \text{CH}_2$), 0.93 (q, J = 12.9, 12.2 Hz, 2H, CH_2) ppm; $^{13}\text{C NMR}$ (101 MHz, CDCl_3) δ = 139.59, 137.68, 130.71, 129.74, 115.03, 58.70, 49.49, 48.21, 47.63, 36.28, 31.50 (2x), 26.72, 26.13 (2x), 24.05, 21.40 ppm; **IR** (ATR): ν (cm^{-1}) = 2919, 1571, 1512, 1446, 1355, 1253, 1198, 1160, 1144, 1038, 853, 773, 745; **HRMS** (EI): m/z calcd for $\text{C}_{17}\text{H}_{25}\text{N}_3^+$ $[\text{M}]^+$: 271.2043; found: 271.2044.

1-(2,2-Diphenylethyl)-1,2,3,5,6,7-hexahydropyrazino[3,2,1-*ij*][1,6]naphthyridine **4r**.**4r**

25r (100 mg, 261 μmol , 1.0 eq.), LiAlH_4 (41.6 mg, 1.10 mmol, 4.2 eq.) and AlCl_3 (90.4 mg, 678 μmol , 2.6 eq.) were dissolved in dry THF and reacted according to GP C. **4r** (50.0 mg, 54%) was obtained as a yellow solid.

m.p. 95-97 $^\circ\text{C}$; $^1\text{H NMR}$ (600 MHz, CDCl_3) δ = 7.61 (s, 1H, Ar), 7.57 (s, 1H, Ar), 7.29 (d, J = 5.5 Hz, 8H, Ar), 7.23 – 7.19 (m, 2H, Ar), 4.44 (t, J = 7.5 Hz, 1H, CH), 3.85 (d, J = 7.5 Hz, 2H, CH_2), 3.11 – 3.06 (m, 2H, CH_2), 2.98 (dd, J = 5.9, 3.5 Hz, 2H, CH_2), 2.93 (dd, J = 5.8, 3.5 Hz, 2H, CH_2), 2.68 (t, J = 6.4 Hz, 2H, CH_2), 1.96 (dt, J = 11.2, 6.3 Hz, 2H, CH_2) ppm; $^{13}\text{C NMR}$ (151 MHz, CDCl_3) δ = 142.90, 140.07, 137.87, 129.58, 129.37, 128.66, 128.35, 126.73, 115.12, 57.34, 49.37, 48.37, 47.81, 47.33, 24.02, 21.30 ppm; **IR** (ATR): ν (cm^{-1}) = 2929, 1567, 1511, 1433, 1349, 1254, 1152, 1081, 847, 758, 744, 699; **HRMS** (EI): m/z calcd for $\text{C}_{24}\text{H}_{25}\text{N}_3^+$ $[\text{M}]^+$: 355.2043; found: 355.2036.

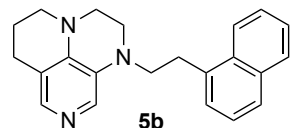
1-Phenylethyl-1,2,3,5,6,7-hexahydropyrazino[3,2,1-*ij*][1,6]naphthyridine **5a**.**5a**

26a (277 mg, 901 μmol , 1.0 eq.), LiAlH_4 (143 mg, 3.79 mmol, 4.2 eq.) and AlCl_3 (312 mg, 2.34 mmol, 2.6 eq.) were dissolved in dry THF and reacted according to GP C. **5a** (203mg, 81%) was obtained as a yellow solid.

m. p. 144-146 $^\circ\text{C}$; $^1\text{H NMR}$ (600 MHz, CDCl_3) δ = 7.67 (s, 1H, Ar), 7.58 (s, 1H, Ar), 7.33 – 7.29 (m, 2H, Ar), 7.25 – 7.20 (m, 3H, Ar), 3.50 – 3.45 (m, 2H, CH_2), 3.29 – 3.26 (m, 2H, CH_2), 3.24 (dt, J = 6.0,

2.1 Hz, 2H, CH_2), 3.18 – 3.14 (m, 2H, CH_2), 2.92 – 2.88 (m, 2H, CH_2), 2.69 (t, $J = 6.4$ Hz, 2H, CH_2), 2.02 – 1.97 (m, 2H, CH_2) ppm; ^{13}C NMR (151 MHz, $CDCl_3$) $\delta = 140.26, 139.75, 138.02, 129.89, 129.36, 128.94, 128.69, 126.39, 115.19, 53.28, 49.43, 47.62, 46.75, 31.95, 24.04, 21.35$; IR (ATR): ν (cm^{-1}) = 2943, 2782, 1681, 1572, 1512, 1355, 1225, 1155, 1067, 997, 914, 849, 774, 743, 698; HRMS (ESI): m/z calcd for $C_{18}H_{21}N_3+H^+$ [M+H] $^+$: 280.1808; found: 280.1807.

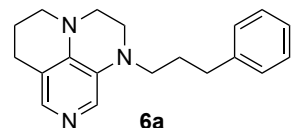
1-(2-Naphtalen-1-yl)ethyl)-1,2,3,5,6,7-hexahydropyrazino[3,2,1-ij][1,6]naphthyridine **5b**.



26b (100 mg, 280 μ mol, 1.0 eq.), $LiAlH_4$ (44.6 mg, 1.18 mmol, 4.2 eq.) and $AlCl_3$ (97.0 mg, 727 μ mol, 2.6 eq.) were dissolved in dry THF and reacted according to GP C. **5b** (40.0 mg, 43%) was obtained as a yellow solid.

m. p. 100-102 $^{\circ}C$; 1H NMR (400 MHz, $CDCl_3$) $\delta = 8.08$ (dd, $J = 8.3, 1.2$ Hz, 1H, Ar), 7.87 (dd, $J = 8.0, 1.6$ Hz, 1H, Ar), 7.78 (s, 1H, Ar), 7.75 (dd, $J = 7.6, 1.8$ Hz, 1H, Ar), 7.60 (d, $J = 0.9$ Hz, 1H, Ar), 7.52 (dddd, $J = 19.4, 8.1, 6.8, 1.4$ Hz, 2H, Ar), 7.44 – 7.36 (m, 2H, Ar), 3.61 (dd, $J = 8.8, 6.4$ Hz, 2H, CH_2), 3.39 (dd, $J = 9.0, 6.2$ Hz, 2H, CH_2), 3.30 (dd, $J = 5.9, 3.6$ Hz, 2H, CH_2), 3.25 – 3.14 (m, 4H, $2 \times CH_2$), 2.71 (t, $J = 6.4$ Hz, 2H, CH_2), 2.05 – 1.94 (m, 2H, CH_2) ppm; ^{13}C NMR (101 MHz, $CDCl_3$) $\delta = 140.23, 138.06, 135.95, 134.03, 132.04, 129.81, 129.44, 129.04, 127.20, 127.09, 126.26, 125.80, 125.76, 123.66, 115.29, 52.48, 49.45, 47.53, 46.85, 29.07, 24.05, 21.35$ ppm; IR (ATR): ν (cm^{-1}) = 2834, 1572, 1515, 1350, 1153, 915, 846, 772; HRMS (EI): m/z calcd $C_{22}H_{23}N_3^+$ [M] $^+$: 329.1886; found: 329.1887.

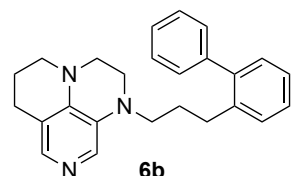
1-(3-Phenylpropyl)-1,2,3,5,6,7-hexahydropyrazino[3,2,1-ij][1,6]naphthyridine **6a**.



27a (300 mg, 933 μ mol, 1.0 eq.), $LiAlH_4$ (148 mg, 3.92 mmol, 4.2 eq.) and $AlCl_3$ (323 mg, 2.43 mmol, 2.6 eq.) were dissolved in dry THF and reacted according to GP C. **6a** (214.0 mg, 75%) was obtained as a yellow oil.

1H NMR (400 MHz, $CDCl_3$) $\delta = 7.54$ (s, 1H, Ar), 7.51 (s, 1H, Ar), 7.31 – 7.26 (m, 2H, Ar), 7.22 – 7.16 (m, 3H, Ar), 3.30 – 3.26 (m, 4H, $2 \times CH_2$), 3.25 – 3.20 (m, 2H, CH_2), 3.19 – 3.13 (m, 2H, CH_2), 2.67 (t, $J = 7.4$ Hz, 4H, $2 \times CH_2$), 2.01 – 1.90 (m, 4H, $2 \times CH_2$) ppm; ^{13}C NMR (101 MHz, $CDCl_3$) $\delta = 141.71, 140.20, 138.06, 130.13, 129.83, 128.55, 128.46, 126.07, 114.99, 50.76, 49.39, 47.80, 46.37, 33.49, 27.22, 24.03, 21.33$ ppm; IR (ATR): ν (cm^{-1}) = 2924, 2840, 1568, 1512, 1466, 1433, 1347, 1253, 1204, 1151, 1036, 853, 745, 698; HRMS (EI): m/z calcd for $C_{19}H_{23}N_3^+$ [M] $^+$: 293.1886; found: 293.1883.

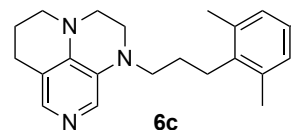
1-(3-([1,1'-Biphenyl]-2-yl)propyl)-1,2,3,5,6,7-hexahydropyrazino[3,2,1-ij][1,6]naphthyridine **6b**.



27b (100 mg, 252 μ mol, 1.0 eq.), $LiAlH_4$ (40.1 mg, 1.06 mmol, 4.2 eq.) and $AlCl_3$ (87.2 mg, 654 μ mol, 2.6 eq.) were dissolved in dry THF and reacted according to GP C. **6b** (58.0 mg, 62%) was obtained as a colorless oil.

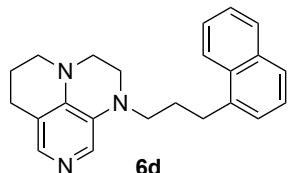
1H NMR (600 MHz, $CDCl_3$) $\delta = 7.53$ (s, 1H, Ar), 7.39 (t, $J = 3.9$ Hz, 3H, Ar), 7.34 (t, $J = 7.3$ Hz, 1H, Ar), 7.31 – 7.27 (m, 4H, Ar), 7.24 (q, $J = 4.1$ Hz, 1H, Ar), 7.20 (d, $J = 7.4$ Hz, 1H, Ar), 3.14 (p, $J = 5.4, 5.0$ Hz, 4H, $2 \times CH_2$), 3.09 – 3.01 (m, 4H, $2 \times CH_2$), 2.64 (dt, $J = 20.5, 7.1$ Hz, 4H, $2 \times CH_2$), 2.00 – 1.93 (m, 2H, CH_2), 1.80 – 1.73 (m, 2H, CH_2) ppm; ^{13}C NMR (151 MHz, $CDCl_3$) $\delta = 141.99, 141.92, 140.03, 139.24, 138.03, 130.24, 129.82, 129.81, 129.34, 129.28, 128.24, 127.64, 126.96, 126.04, 114.85, 50.55, 49.37, 47.75, 45.86, 30.71, 27.26, 24.04, 21.32$ ppm; IR (ATR): ν (cm^{-1}) = 2839, 1572, 1513, 1468, 1348, 1153, 1008, 854, 748, 792; HRMS (EI): m/z calcd for $C_{25}H_{27}N_3^+$ [M] $^+$: 369.2199; found: 369.2207.

1-(3-Mesitylpropyl)-1,2,3,5,6,7-hexahydropyrazino[3,2,1-ij][1,6]naphthyridine **6c**.



27c (100 mg, 275 μ mol, 1.0 eq.), $LiAlH_4$ (43.9 mg, 1.16 mmol, 4.2 eq.) and $AlCl_3$ (95.4 mg, 715 μ mol, 2.6 eq.) were dissolved in dry THF and reacted according to GP C. **6c** (60.0 mg, 65%) was obtained as a yellow oil.

1H NMR (400 MHz, $CDCl_3$) $\delta = 7.58$ (s, 1H, Ar), 7.55 (s, 1H, Ar), 6.82 (s, 2H, Ar), 3.30 (s, 6H, $3 \times CH_2$), 3.20 – 3.15 (m, 2H, CH_2), 2.67 (t, $J = 6.4$ Hz, 2H, CH_2), 2.65 – 2.60 (m, 2H, CH_2), 2.28 (s, 6H, $2 \times Me$), 2.23 (s, 3H, Me), 2.02 – 1.93 (m, 2H, CH_2), 1.83 – 1.74 (m, 2H, CH_2) ppm; ^{13}C NMR (101 MHz, $CDCl_3$) $\delta = 140.01, 138.23, 135.91, 135.54, 135.20, 129.94, 129.83, 129.08, 115.01, 51.42, 49.41, 47.83, 46.23, 26.98, 25.46, 24.04, 21.31, 20.93, 19.94$ ppm; IR (ATR): ν (cm^{-1}) = 2923, 1659, 1571, 1513, 1468, 1347, 1253, 1153, 1038, 840, 745; HRMS (EI): m/z calcd for $C_{22}H_{29}N_3^+$ [M] $^+$: 335.2356; found: 335.2352.

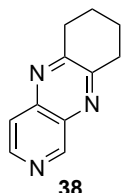
1-(3-(Naphthalen-1-yl)propyl)-1,2,3,5,6,7-hexahydropyrazino[3,2,1-ij][1,6]naphthyridine **6d**.**6d**

27d (100 mg, 269 μmol , 1.0 eq.), LiAlH_4 (42.9 mg, 1.13 mmol, 4.2 eq.) and AlCl_3 (93.3 mg, 700 μmol , 2.6 eq.) were dissolved in dry THF and reacted according to GP C. **6d** (37.0 mg, 40%) was obtained as a yellow oil.

$^1\text{H NMR}$ (400 MHz, CDCl_3) δ = 8.05 – 7.99 (m, 1H, Ar), 7.85 (dd, J = 8.2, 1.2 Hz, 1H, Ar), 7.72 (d, J = 8.1 Hz, 1H, Ar), 7.57 (d, J = 11.4 Hz, 2H, Ar), 7.54 – 7.44 (m, 2H, Ar), 7.42 – 7.37 (m, 1H, Ar), 7.33 (dd, J = 7.0, 1.3 Hz, 1H, Ar), 3.37 – 3.30 (m, 2H, CH_2), 3.31 – 3.26 (m, 4H, $2 \times \text{CH}_2$), 3.20 – 3.10 (m, 4H, $2 \times \text{CH}_2$), 2.67 (t, J = 6.4 Hz, 2H, CH_2), 2.15 – 2.05 (m, 2H, CH_2), 2.01 – 1.95 (m, 2H, CH_2) ppm; $^{13}\text{C NMR}$ (101 MHz, CDCl_3) δ = 140.08, 138.22, 137.82, 134.02, 131.88, 129.94, 129.88, 128.96, 126.91, 126.04 (2x), 125.66, 125.64, 123.74, 114.99, 51.12, 49.39, 47.82, 46.28, 30.57, 26.71, 24.04, 21.29 ppm; IR (ATR): ν (cm^{-1}) = 2926, 1659, 1580, 1512, 1467, 1348, 1254, 1151, 1037, 854, 776, 745; HRMS (ESI): m/z calcd for $\text{C}_{23}\text{H}_{25}\text{N}_3\text{-H}^+$ [$\text{M}+\text{H}$] $^+$: 344.2121; found: 344.2118.

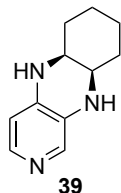
5.1.4.3 Synthesis of Catalysts **7b** and **8b**

The synthesis of **8b** is based on procedure reported by Zipse *et al.*^[22]

6,7,8,9-Tetrahydropyrido[3,4-*b*]chinoxalin **38**.**38**

3,4-Diaminopyridine (2.00 g, 18.3 mmol, 1.0 eq.) was put in a 80 mL microwave vessel and dissolved in ethanol (30 mL). After adding of cyclohexane-1,2-dione (2.50 g, 22.0 mmol, 1.2 eq.), the reaction mixture was put into the microwave reactor, stirred for 1 h at 110 $^\circ\text{C}$ (70 W) and concentrated in vacuum. After purification by column chromatographie on silica (EtOAc), **38** (2.85 g, 84%) was obtained as a white solid.

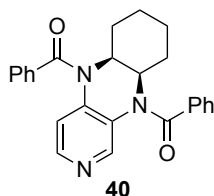
$^1\text{H NMR}$ (400 MHz, CDCl_3) δ = 9.40 (s, 1H, Ar), 8.72 (d, J = 5.8 Hz, 1H, Ar), 7.79 (d, J = 5.8 Hz, 1H, Ar), 3.25 – 3.17 (m, 4H, $2 \times \text{CH}_2$), 2.06 (dq, J = 7.5, 3.8 Hz, 4H, $2 \times \text{CH}_2$) ppm. The $^1\text{H NMR}$ spectrum is in full agreement with literature reports.^[22a]

(rac)-5,5a,6,7,8,9a,10-Octahydropyrido[3,4-*b*]chinoxalin **39**.**39**

38 (2.77 g, 15.4 mmol, 1.0 eq.) was dissolved in dry THF (50 mL) and the reaction mixture was cooled down to 0 $^\circ\text{C}$. LiAlH_4 (1.46 g, 38.5 mmol, 2.5 eq.) was added carefully and the mixture was stirred for 32 h at room temperature. The reaction mixture was quenched with water and saturated K_2CO_3 -solution, filtered over celite and the filtrate was washed with CH_2Cl_2 . After extraction with CH_2Cl_2 (3x20 mL), the combined organic phase was washed with saturated K_2CO_3 -

solution (50 mL), dried over MgSO_4 , filtered and concentrated in vacuum. By column chromatography on silica (EtOAc/ Et_3N /MeOH 10:1:1) **39** (1.74 g, 60 %) was obtained as a white solid.

$^1\text{H NMR}$ (400 MHz, CDCl_3) δ = 7.73 – 7.68 (m, 2H, Ar), 6.30 (d, J = 5.2 Hz, 1H, Ar), 3.99 (s, 1H, NH), 3.59 – 3.49 (m, 1H, CH), 3.49 – 3.42 (m, 2H, NH and CH), 1.81 – 1.63 (m, 6H, $3 \times \text{CH}_2$), 1.38 (dp, J = 15.2, 5.0, 4.5 Hz, 2H, CH_2) ppm. The $^1\text{H NMR}$ spectrum is in full agreement with literature reports.^[22a]

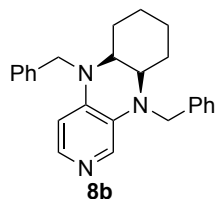
5a,6,7,8,9,9a-hexahydropyrido[3,4-*b*]quinoxaline-5,10-diyl)bis(phenylmethanone) **40**.**40**

In an evacuated microwave vessel **39** (200 mg, 1.06 mmol, 1.0 eq.) was dissolved in dry pyridine (2 mL pro mmol **39**) and benzoyl chloride (891 mg, 6.34 mmol, 6.0 eq.) was added. The mixture was stirred for 5 min under N_2 -atmosphere, put into the microwave reactor and stirred for 2.5 h at 170 $^\circ\text{C}$ (200 W). After cooling to room temperature, the mixture was quenched with methanol and concentrated in vacuum. The mixture was

dissolved in CH_2Cl_2 and washed with saturated K_2CO_3 -solution (10 mL). The aqueous phase was extracted with CH_2Cl_2 (3 x 10 mL). The combined organic phase was dried over MgSO_4 , filtered and concentrated in vacuum. After purification by column chromatography on silica (EtOAc/ Et_3N /MeOH 95:5:0 to 92:5:3), **40** (200 mg, 48 %) was obtained as a solid.

HRMS (EI): m/z calcd for $\text{C}_{25}\text{H}_{23}\text{O}_2\text{N}_3^+$ [M] $^+$: 397.1785; found: 397.1789.

(*rac*)-5,10-Dibenzyl-5,5a,6,7,8,9,9a,10-octahydro-pyrido[3,4-*b*]quinoxaline **8b**.

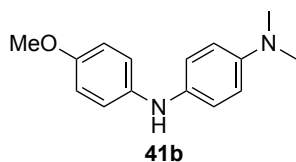


40 (100 mg, 252 μ mol, 1.0 eq.), LiAlH₄ (40.1 mg, 1.06 mmol, 4.2 eq.) and AlCl₃ (87.2 mg, 654 μ mol, 2.6 eq.) were dissolved in dry THF and reacted according to GP C. **8b** (40.0 mg, 43%) was obtained as a colorless oil.

¹H NMR (400 MHz, CDCl₃) δ = 7.72 (d, *J* = 5.4 Hz, 1H, Ar), 7.70 (s, 1H, Ar), 7.37 – 7.30 (m, 6H, Ar), 7.29 – 7.21 (m, 4H, Ar), 6.35 (d, *J* = 5.5 Hz, 1H, Ar), 4.69 (d, *J* = 7.8 Hz, 1H, CHH), 4.65 (d, *J* = 7.3 Hz, 1H, CHH), 4.43 (d, *J* = 17.1 Hz, 1H, CHH), 4.32 (d, *J* = 16.6 Hz, 1H, CHH), 3.62 – 3.53 (m, 1H, CHH), 3.51 – 3.42 (m, 1H, CHH), 1.97 – 1.82 (m, 2H, CH₂), 1.66 – 1.49 (m, 3H, CHH and CH₂), 1.38 – 1.22 (m, 3H, CHH and CH₂) ppm; ¹³C NMR (101 MHz, CDCl₃) δ = 141.57, 141.03, 138.64, 137.81, 133.35, 131.43, 128.85, 128.79, 127.25, 127.08, 127.03, 126.77, 105.66, 57.06, 55.58, 52.17, 51.16, 27.80, 27.05, 22.55, 22.33 ppm; HRMS (ESI): *m/z* calcd for C₂₅H₂₇N₃+H⁺ [M+H]⁺: 370.2278; found: 370.2283. The ¹H NMR spectrum is in full agreement with literature reports.^[22b]

Synthesis and analytical data for the synthesis of **7b(a-d)** were experimental determined by A. Mateos Calbet^[5] under the supervision of S. Mayr. The herein reported analytical data are fully reanalysed.

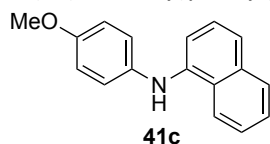
N,N-Dimethyl-*N'*-(4-methoxyphenyl)-1,4-phenyldiamine **41b**.



In a pressure tube 4-bromo-*N,N*-dimethylanilin (500 mg, 2.50 mmol, 1.0 eq.), 4-methoxyanilin (400 mg, 3.25 mmol, 1.3 eq.), Pd₂(dba)₃ (114 mg, 125 μ mol, 0.05 eq.), dppf (208 mg, 375 μ mol, 0.15 eq.) and KOtBu (421 mg, 3.75 mmol, 1.5 eq.) were suspended in dry 1,4-dioxan (10 mL). After the reaction mixture was degassed with N₂, the mixture was stirred for 20 h at 100 °C. After concentration in vacuum, the pure product was obtained by column chromatography on silica (isohexane/EtOAc/Et₃N 75:20:5). **41b** (403 mg, 67%) was obtained as a solid.

¹H NMR (400 MHz, CDCl₃) δ = 7.02 – 6.94 (m, 2H, Ar), 6.93 – 6.87 (m, 2H, Ar), 6.85 – 6.78 (m, 2H, Ar), 6.77 – 6.72 (m, 2H, Ar), 5.23 (s, 1H, NH), 3.78 (s, 3H, Me), 2.96 – 2.86 (m, 6H, Me₂) ppm. The ¹H NMR spectrum is in full agreement with literature reports.^[23]

N-(4-(Methoxy)phenyl)naphthalene-1-amine **41c**.



In a pressure tube 1-bromo-4-methoxybenzene (335 μ L, 2.67 mmol, 1.0 eq.), 1-naphthylamin (498 mg, 3.48 mmol, 1.3 eq.), (dppf)PdCl₂ (97.7 mg, 134 μ mol, 0.05 eq.), dppf (222.0 mg, 401 μ mol, 0.15 eq.) and KOtBu (450 mg, 4.01 mmol, 1.5 eq.) were suspended in dry 1,4-dioxane (10 mL). After the reaction mixture was degassed

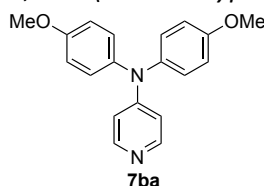
with N₂, the mixture was stirred for 20 h at 90 °C. After concentration in vacuum, the pure product was obtained by column chromatography on silica (isohexane/EtOAc/Et₃N 65:30:5). **41c** (490 mg, 74%) was obtained as a yellow solid.

¹H NMR (400 MHz, CDCl₃) δ = 8.05 – 7.97 (m, 1H, Ar), 7.92 – 7.80 (m, 1H, Ar), 7.47 (ddd, *J* = 14.1, 7.5, 4.8 Hz, 3H, Ar), 7.33 (t, *J* = 7.8 Hz, 1H, Ar), 7.11 (d, *J* = 7.5 Hz, 1H, Ar), 7.07 (d, *J* = 8.8 Hz, 2H, Ar), 6.99 – 6.85 (m, 2H, Ar), 5.89 (bs, 1H, NH), 3.82 (s, 3H, Me) ppm. The ¹H NMR spectrum is in full agreement with literature reports.^[24]

General Procedure D

In a pressure tube the corresponding amin (1.3 eq.), 4-bromopyridine hydrochloride (1.0 eq.), Pd₂(dba)₃ (0.02 eq.), dppf (0.02 eq.) and NaOtBu (1.5 eq.) were suspended in dry toluene. After the reaction mixture was degassed with N₂, the mixture was stirred for 20 h at 140 °C. After concentration in vacuum, the pure product was obtained by column chromatography on silica (isohexane/EtOAc/Et₃N 55:40:5).

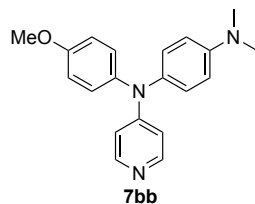
N,N-Di-(4-methoxyphenyl)-4-pyridinamine **7ba**.



4,4-Dimethoxydiphenylamine (283 mg, 1.68 mmol, 1.3 eq.), 4-bromopyridine hydrochloride (250 mg, 1.29 mmol, 1.0 eq.), Pd₂(dba)₃ (24.0 mg, 25.7 μ mol, 0.02 eq.), dppf (14.0 mg, 25.7 μ mol, 0.02 eq.) and NaOtBu (185 mg, 1.93 mmol, 1.5 eq.) were suspended in dry toluene (20 mL) and reacted according to GP D. **7ba** (122 mg, 31%) was obtained as a solid.

m. p. 112–115 °C; $^1\text{H NMR}$ (400 MHz, CDCl_3) δ = 8.16 (dd, J = 5.0, 1.5 Hz, 1H, Ar), 7.17 – 7.10 (m, 2H, Ar), 6.92 – 6.87 (m, 2H, Ar), 6.58 (dd, J = 5.0, 1.5 Hz, 1H, Ar), 3.81 (s, 3H, Me) ppm; $^{13}\text{C NMR}$ (101 MHz, CDCl_3) δ = 157.66, 154.38, 150.08, 138.11, 128.40, 115.21, 110.99, 55.63 ppm; **IR** (ATR): ν (cm^{-1}) = 2948, 1587, 1503, 1340, 1288, 1244, 1178, 1104, 1030, 985, 824, 725; **HRMS** (EI): m/z calcd for $\text{C}_{19}\text{H}_{18}\text{O}_2\text{N}_2^+$ [M] $^+$: 306.1363; found: 306.1357. The $^1\text{H}/^{13}\text{C}$ NMR spectrum are in full agreement with literature reports.^[25]

N-(4-Methoxyphenyl)-*N,N*-dimethyl-*N*-(pyridine-4-yl)benzene-1,4-diamine **7bb**.

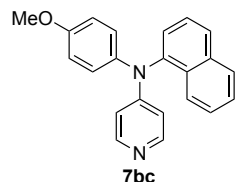


41b (324 mg, 1.34 mmol, 1.3 eq.), 4-bromopyridine hydrochloride (200 mg, 1.03 mmol, 1.0 eq.), $\text{Pd}_2(\text{dba})_3$ (18.8 mg, 20.6 μmol , 0.02 eq.), dppf (11.4 mg, 20.6 μmol , 0.02 eq.) and NaOtBu (148 mg, 1.54 mmol, 1.5 eq.) were suspended in dry 1,4-dioxane (15 mL). After the reaction mixture was degassed with N_2 , the mixture was stirred for 20 h at 110 °C. After concentration in vacuum, the pure product was

obtained by column chromatography on silica (isohexane/EtOAc/ Et_3N 55:40:5). **7bb** (35.0 mg, 11%) was obtained as an oil.

$^1\text{H NMR}$ (400 MHz, CDCl_3) δ = 8.16 – 8.10 (m, 2H, Ar), 7.18 – 7.12 (m, 2H, Ar), 7.11 – 7.05 (m, 2H, Ar), 6.91 – 6.86 (m, 2H, Ar), 6.74 – 6.68 (m, 2H, Ar), 6.60 – 6.56 (m, 2H, Ar), 3.80 (s, 3H, Me), 2.96 (s, 6H, 2xMe) ppm; $^{13}\text{C NMR}$ (151 MHz, CDCl_3) δ = 157.45, 154.65, 149.75, 148.89, 138.24, 134.10, 128.26, 128.22, 115.09, 113.48, 110.62, 55.61, 40.77 ppm; **IR** (ATR): ν (cm^{-1}) = 2893, 1588, 1495, 1336, 1238, 1166, 1030, 987, 813, 730; **HRMS** (EI): m/z calcd for $\text{C}_{20}\text{H}_{21}\text{ON}_3^+$ [M] $^+$: 319.1679; found: 319.1678.

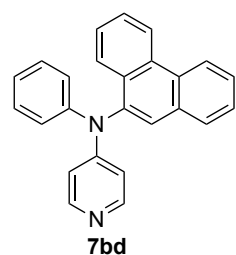
N,N-(4-Methoxyphenyl)-(naphthalene-1-yl)-4-pyridinamine **7bc**.



41c (250 mg, 1.00 mmol, 1.3 eq.), 4-bromopyridine hydrochloride (150 mg, 771 μmol , 1.0 eq.), $\text{Pd}_2(\text{dba})_3$ (14.1 mg, 15.4 μmol , 0.02 eq.), dppf (8.55 mg, 15.4 μmol , 0.02 eq.) and NaOtBu (111 mg, 1.16 mmol, 1.5 eq.) were suspended in dry toluene (11 mL) and reacted according to GP D. **7bc** (51.0 mg, 20%) was obtained as an oil.

$^1\text{H NMR}$ (599 MHz, CDCl_3) δ = 8.16 (d, J = 6.3 Hz, 2H, Ar), 7.91 (t, J = 9.1 Hz, 2H, Ar), 7.84 (d, J = 8.2 Hz, 1H, Ar), 7.53 – 7.49 (m, 2H, Ar), 7.45 (t, J = 8.1 Hz, 1H, Ar), 7.39 (d, J = 7.3 Hz, 1H, Ar), 7.26 (d, J = 8.9 Hz, 2H, Ar), 6.87 (d, J = 9.0 Hz, 2H, Ar), 6.49 (d, J = 6.4 Hz, 2H, Ar), 3.79 (s, 3H, Me) ppm; $^{13}\text{C NMR}$ (151 MHz, CDCl_3) δ = 157.54, 154.59, 150.13, 141.25, 138.17, 135.32, 130.81, 128.80, 127.89, 127.45, 127.32, 127.10, 126.62, 126.52, 123.79, 115.11, 110.81, 55.63 ppm; **IR** (ATR): ν (cm^{-1}) = 2928, 1589, 1492, 1391, 1330, 1291, 1240, 1108, 1030, 770, 680; **HRMS** (EI): m/z calcd for $\text{C}_{22}\text{H}_{18}\text{ON}_2^+$ [M] $^+$: 326.1414; found: 326.1413.

N,N-(4-Methoxyphenyl)-(phenanthren-9-yl)-4-pyridinamine **7bd**.



N-Phenyl-9-phenanthrenamine (360 mg, 1.34 mmol, 1.3 eq.), 4-bromopyridine hydrochloride (200 mg, 1.03 mmol, 1.0 eq.), $\text{Pd}_2(\text{dba})_3$ (18.8 mg, 20.6 μmol , 0.02 eq.), dppf (11.4 mg, 20.6 μmol , 0.02 eq.) and NaOtBu (148 mg, 1.54 mmol, 1.5 eq.) were suspended in dry 1,4-dioxane (15 mL) and reacted according to GP D. **7bd** (160 mg, 45%) was obtained as a solid.

m. p. 80–83 °C; $^1\text{H NMR}$ (400 MHz, CDCl_3) δ = 8.76 (d, J = 8.4 Hz, 1H, Ar), 8.71 (d, J = 8.1 Hz, 1H, Ar), 8.20 (dd, J = 5.1, 1.4 Hz, 2H, Ar), 7.98 – 7.92 (m, 1H, Ar), 7.80 (d, J = 8.4 Hz, 1H, Ar), 7.73 – 7.64 (m, 3H, Ar), 7.59 (t, J = 7.9 Hz, 1H, Ar), 7.52 (t, J = 8.0 Hz, 1H, Ar), 7.36 – 7.26 (m, 4H, Ar), 7.14 (ddd, J = 8.4, 6.1, 2.3 Hz, 1H, Ar), 6.68 (d, J = 6.5 Hz, 2H, Ar) ppm; $^{13}\text{C NMR}$ (101 MHz, CDCl_3) δ = 154.05, 150.41, 145.38, 139.83, 132.33, 132.21, 130.06, 129.82, 128.74, 128.53, 127.51, 127.44, 127.44, 127.25, 125.28, 125.07, 124.63, 123.50, 122.85, 112.04 ppm (one signal is overlapping); **IR** (ATR): ν (cm^{-1}) = 3027, 1583, 1493, 1384, 1337, 1219, 988, 812, 748, 726, 897, 653; **HRMS** (EI): m/z calcd for $\text{C}_{25}\text{H}_{18}\text{N}_2^+$ [M] $^+$: 346.1465; found: 346.1461.

5.1.4.4 $^1\text{H}/^{13}\text{C}$ NMR Spectra

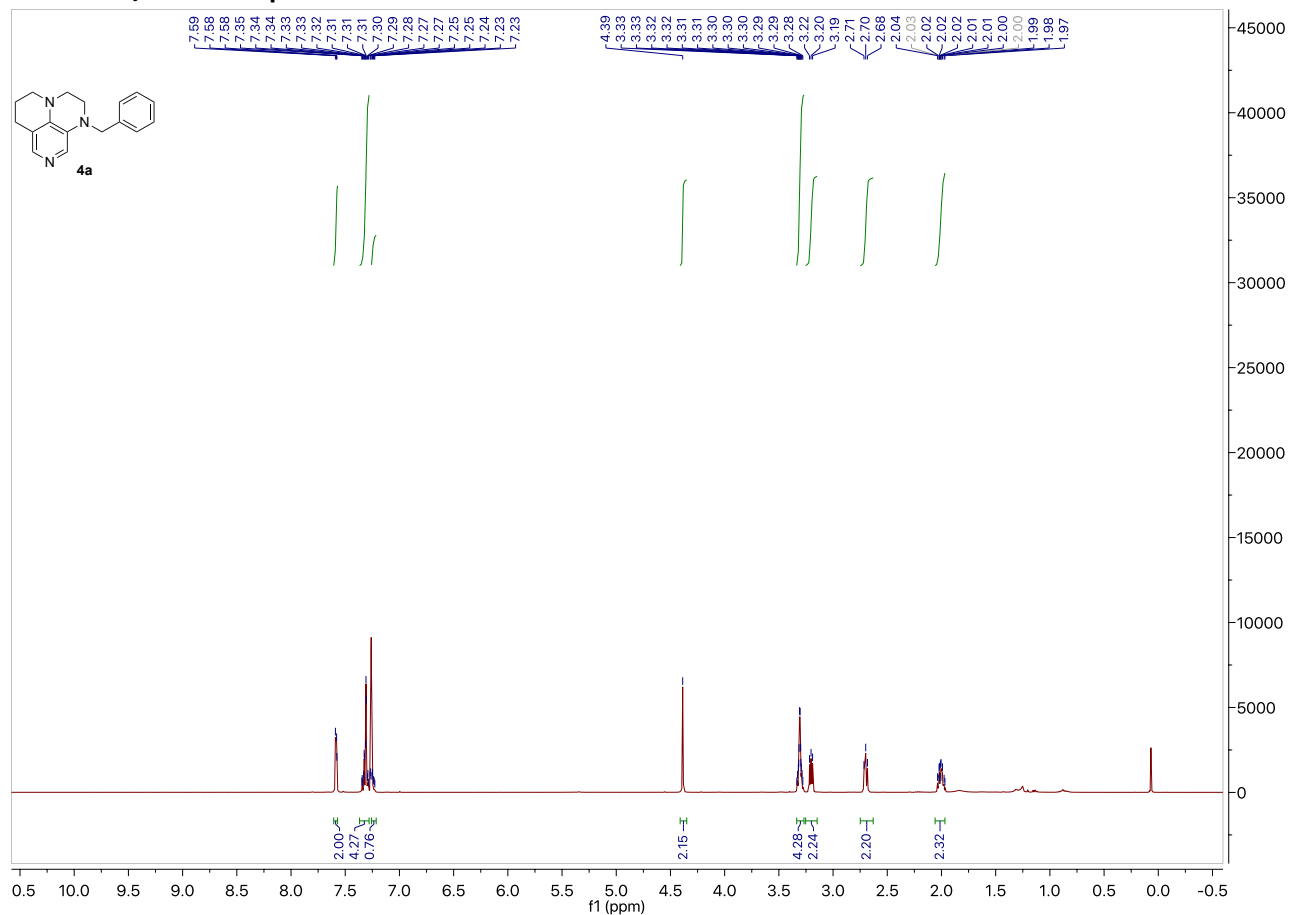


Figure 5.31. ^1H NMR spectrum of **4a** (400 MHz, CDCl_3).

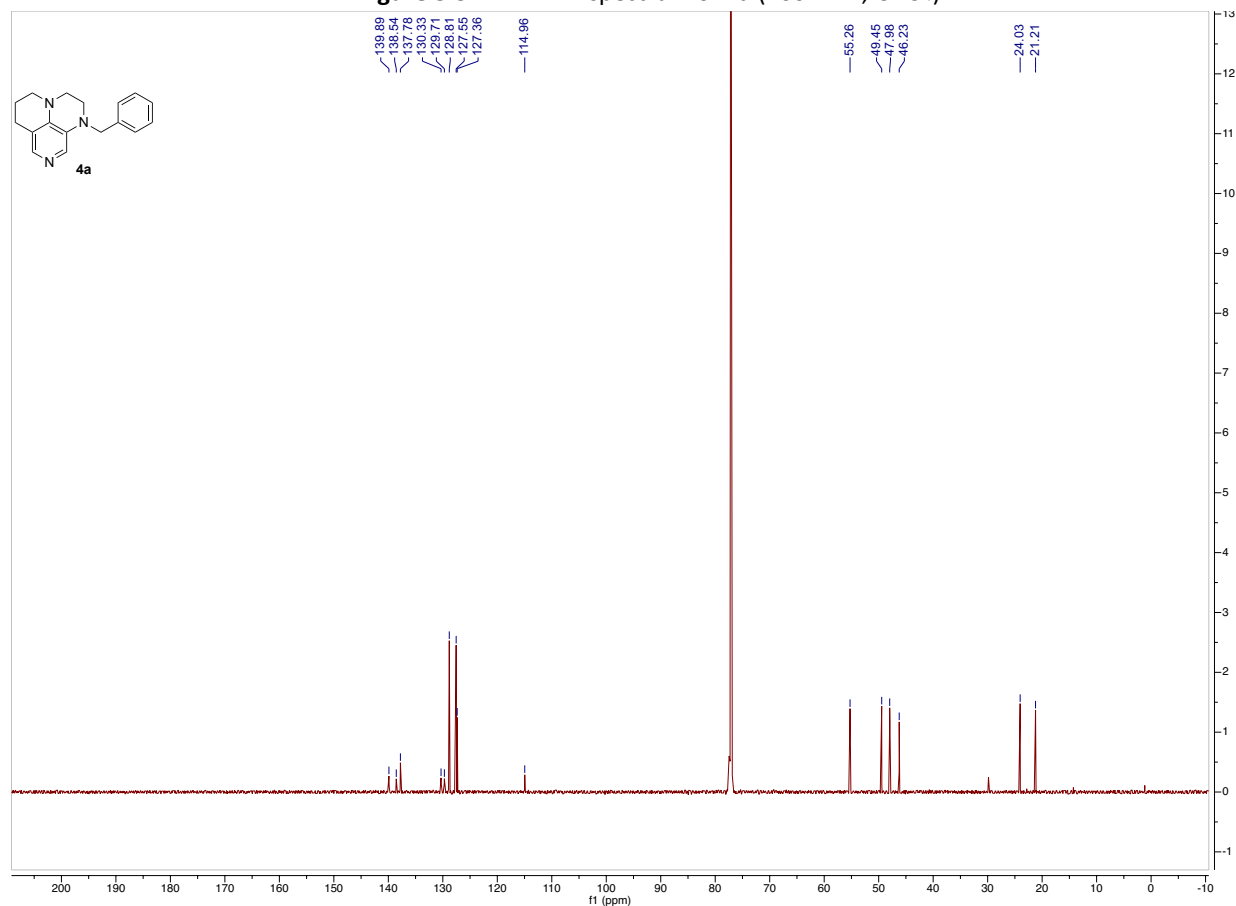


Figure 5.32. ^{13}C NMR spectrum of **4a** (101 MHz, CDCl_3).

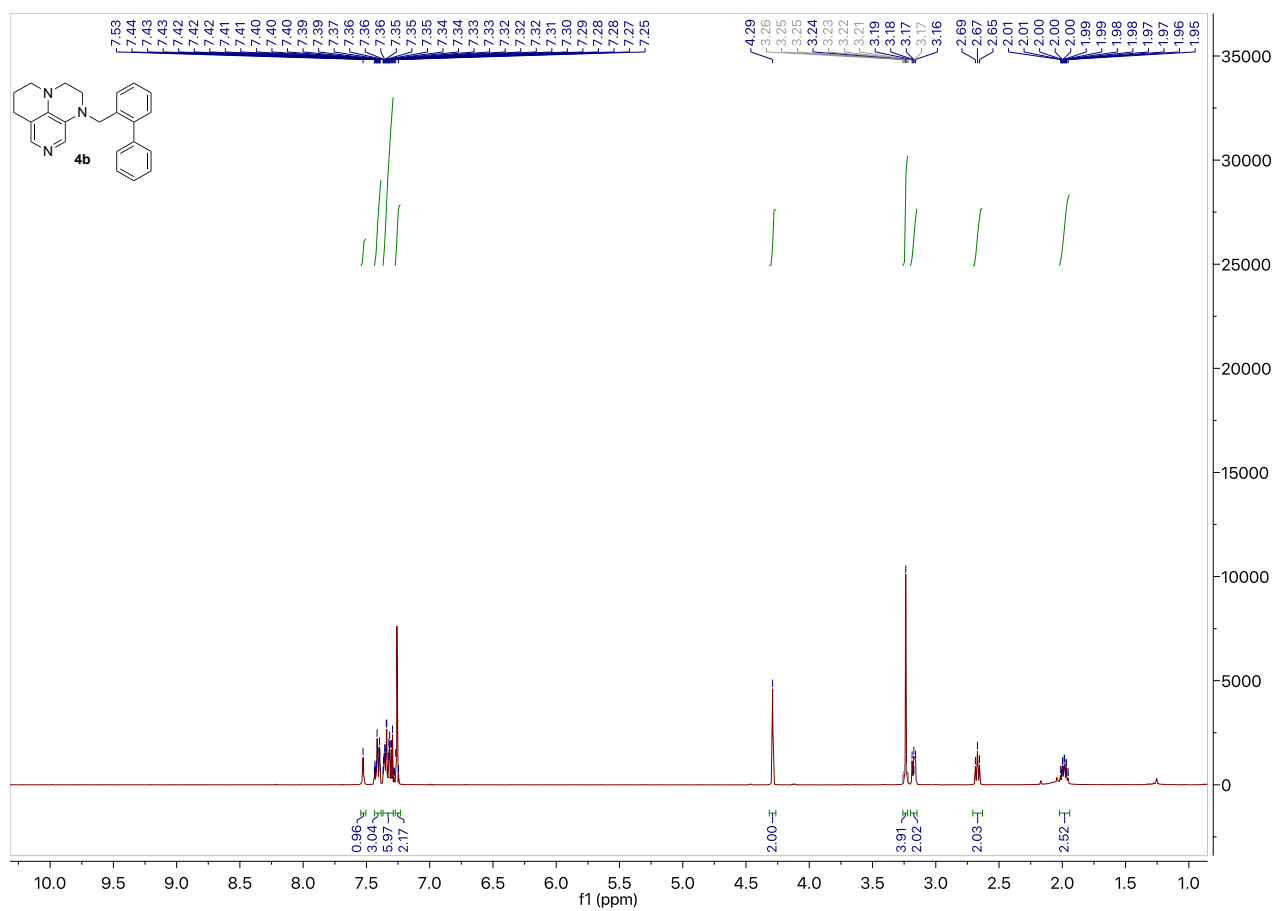


Figure 5.33. ^1H NMR spectrum of **4b** (400 MHz, CDCl_3).

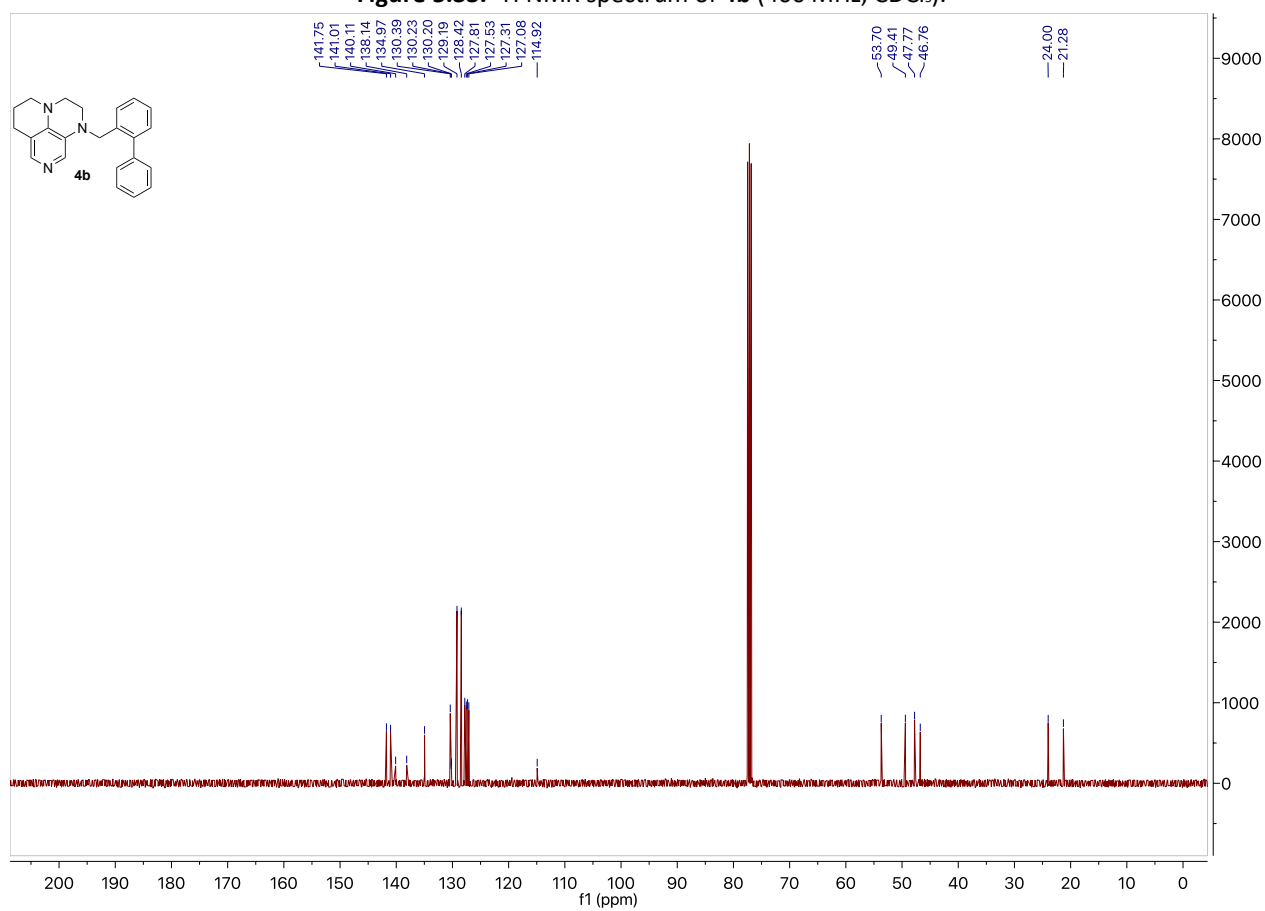


Figure 5.34. ^{13}C NMR spectrum of **4b** (101 MHz, CDCl_3).

Annulated Pyridine Bases

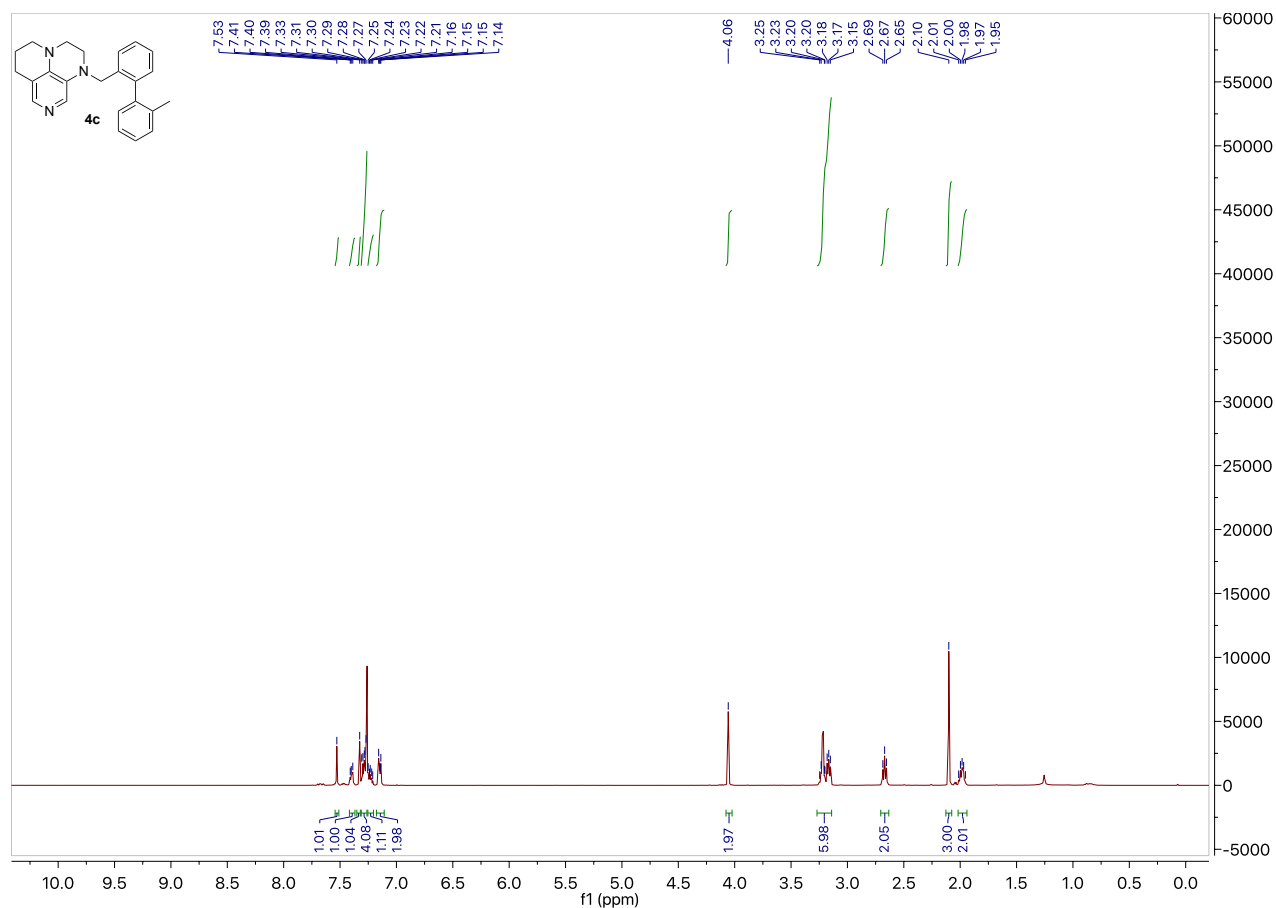


Figure 5.35. ¹H NMR spectrum of 4c (400 MHz, CDCl₃).

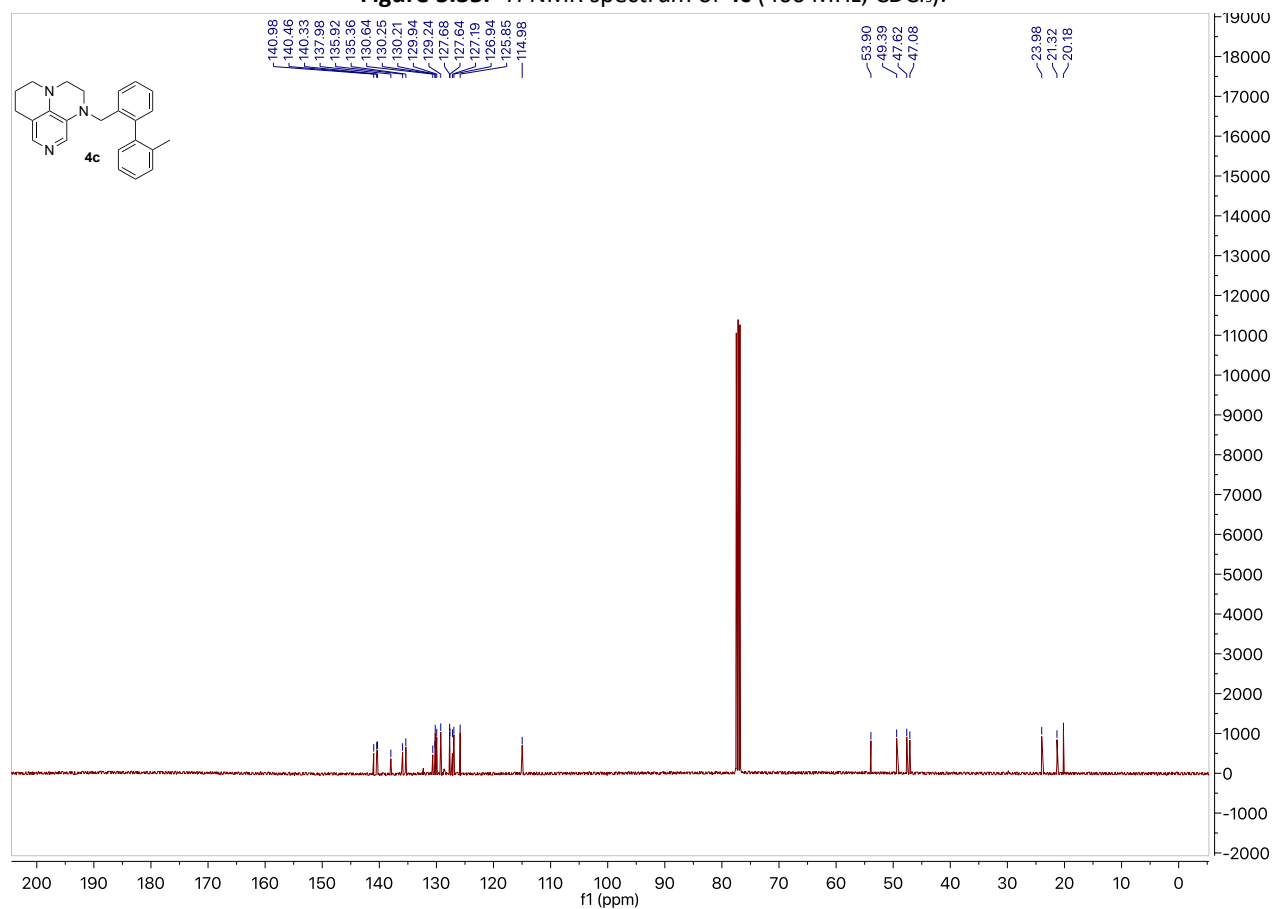


Figure 5.36. ¹³C NMR spectrum of 4c (101 MHz, CDCl₃).

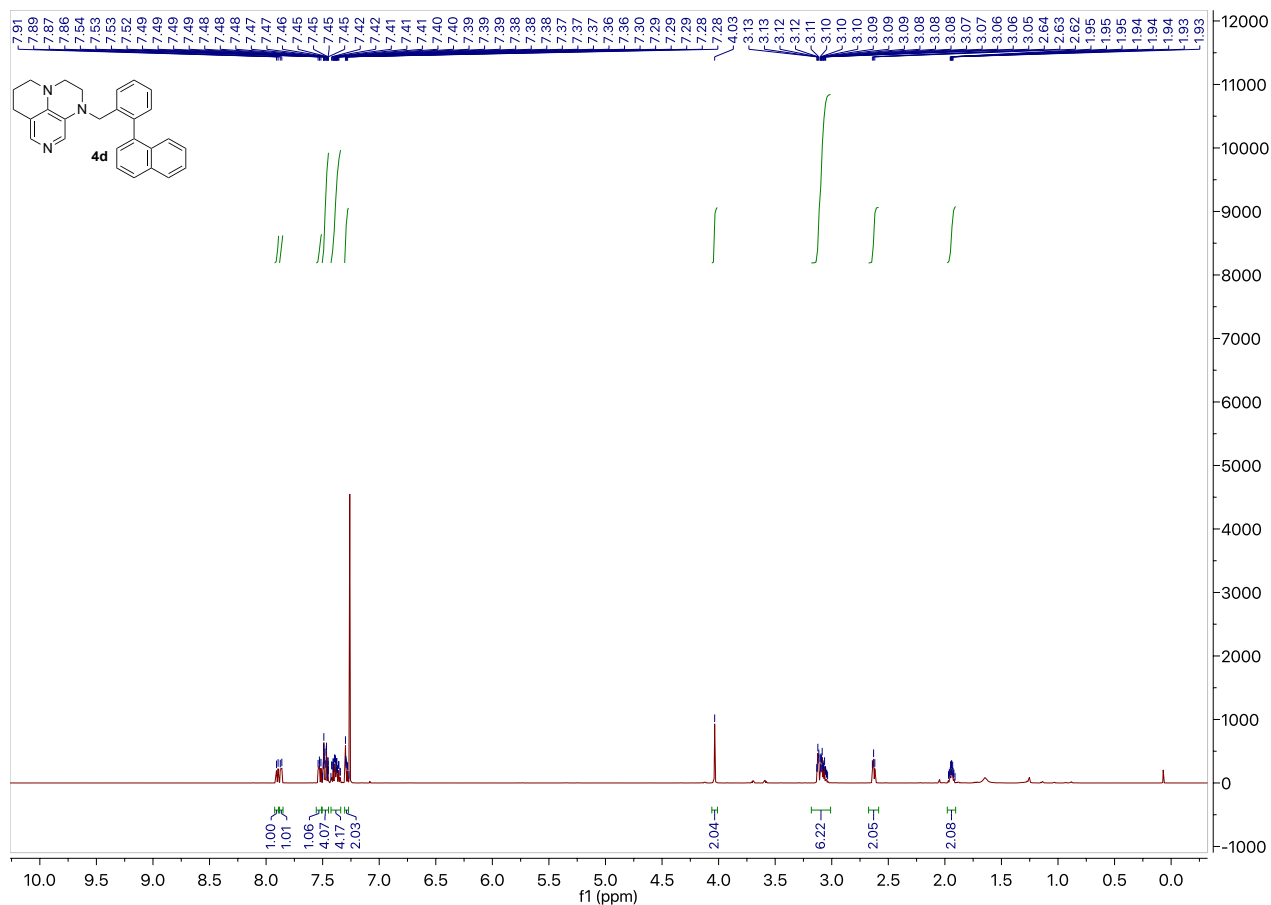


Figure 5.37. ^1H NMR spectrum of **4d** (400 MHz, CDCl_3).

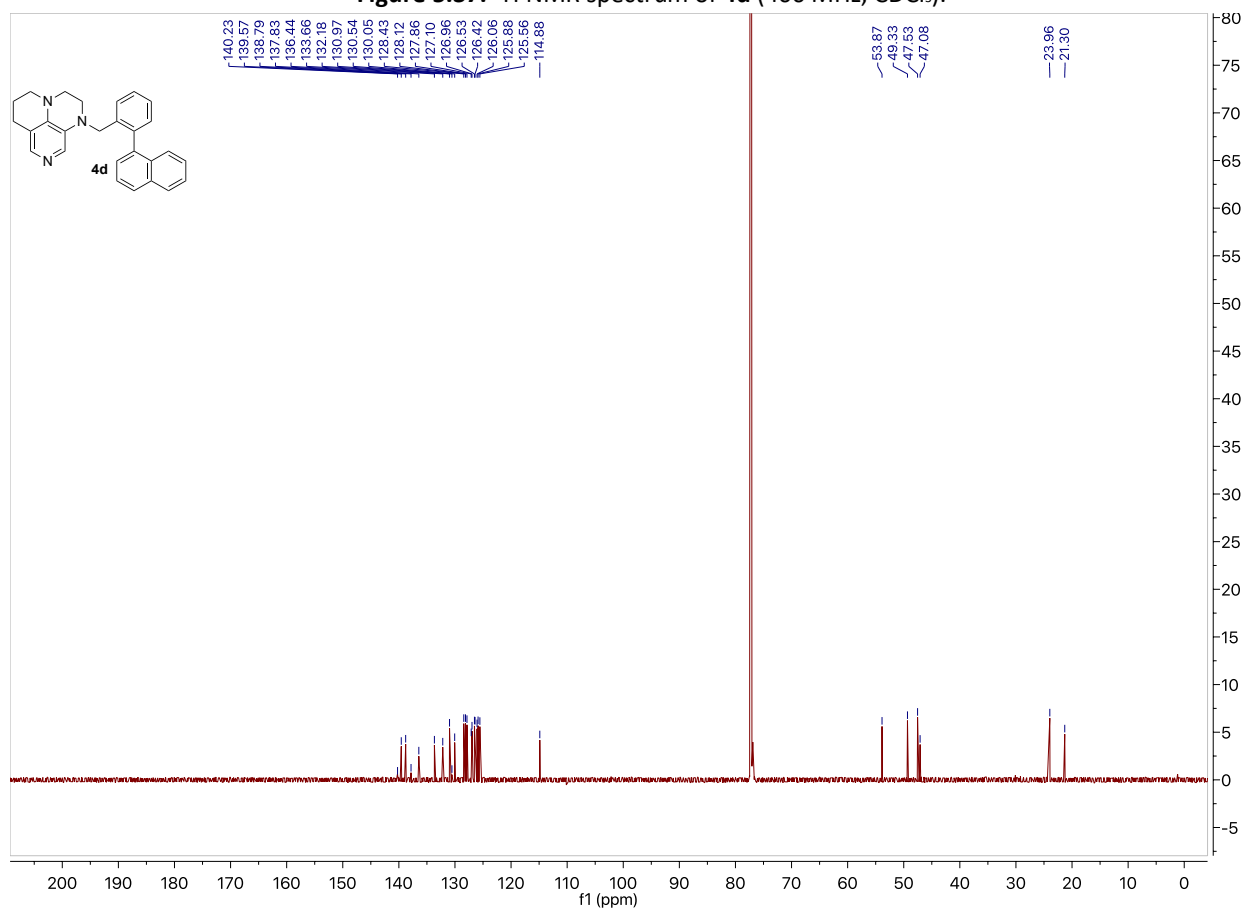


Figure 5.38. ^{13}C NMR spectrum of **4d** (101 MHz, CDCl_3).

Annulated Pyridine Bases

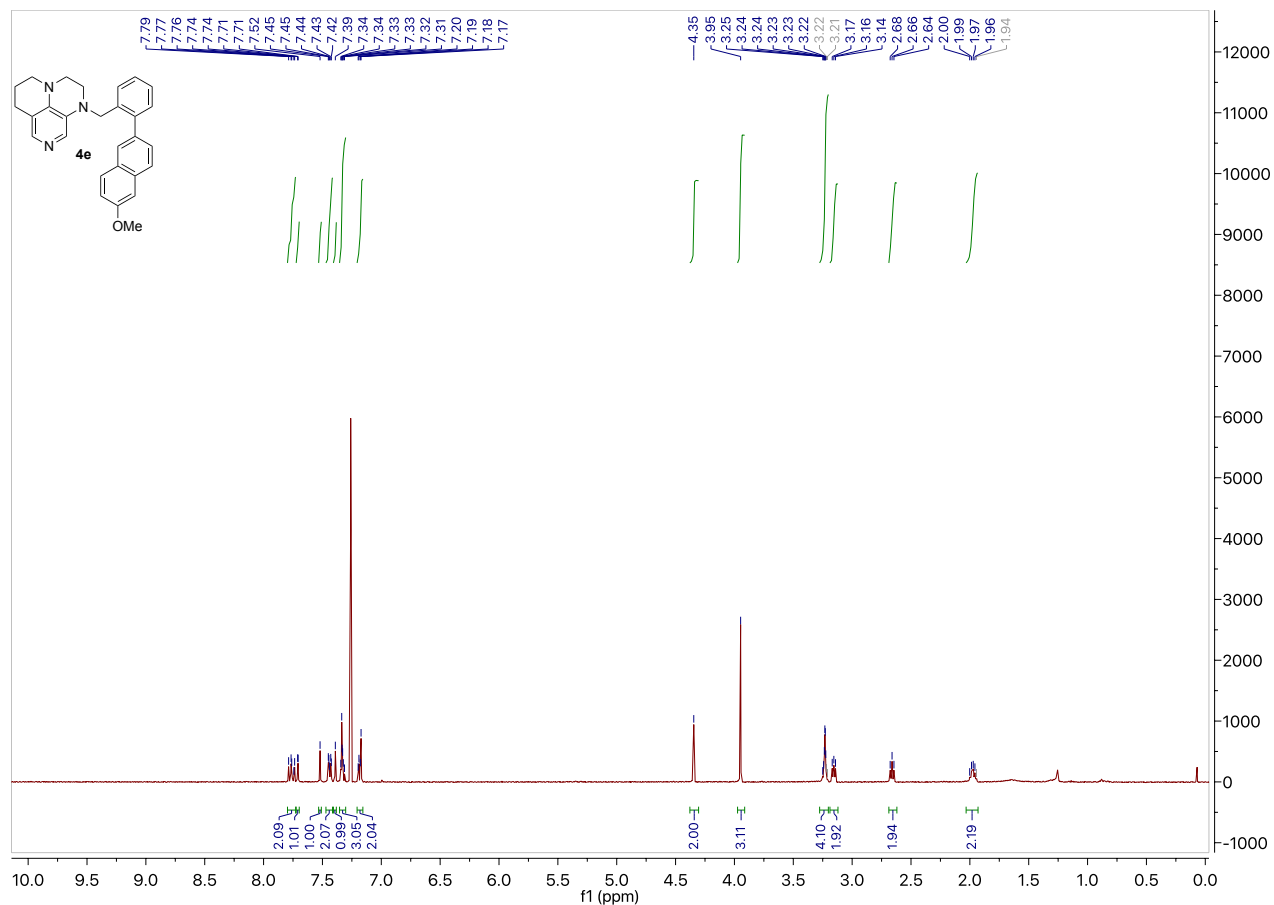


Figure 5.39. ¹H NMR spectrum of 4e (400 MHz, CDCl₃).

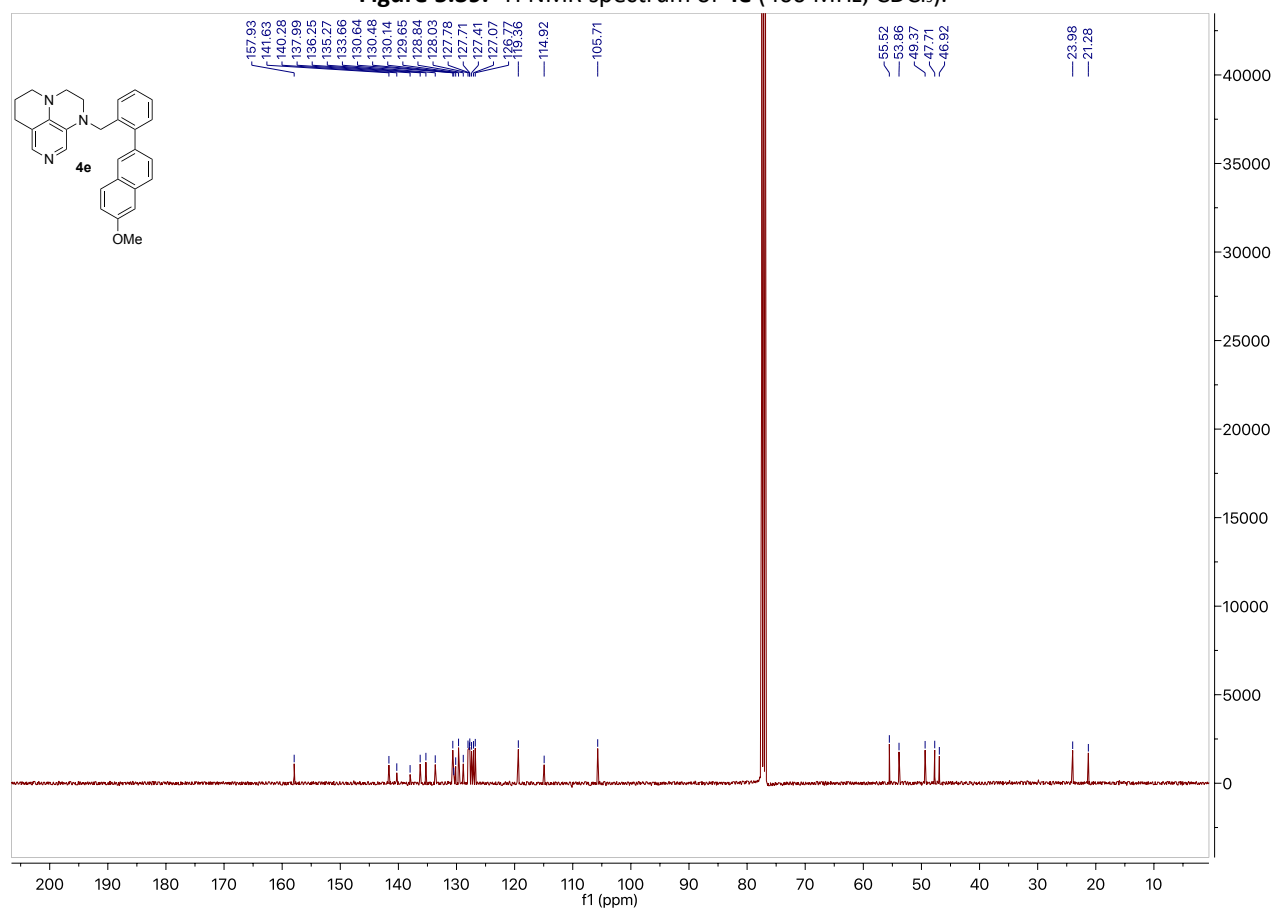


Figure 5.40. ¹³C NMR spectrum of 4e (101 MHz, CDCl₃).

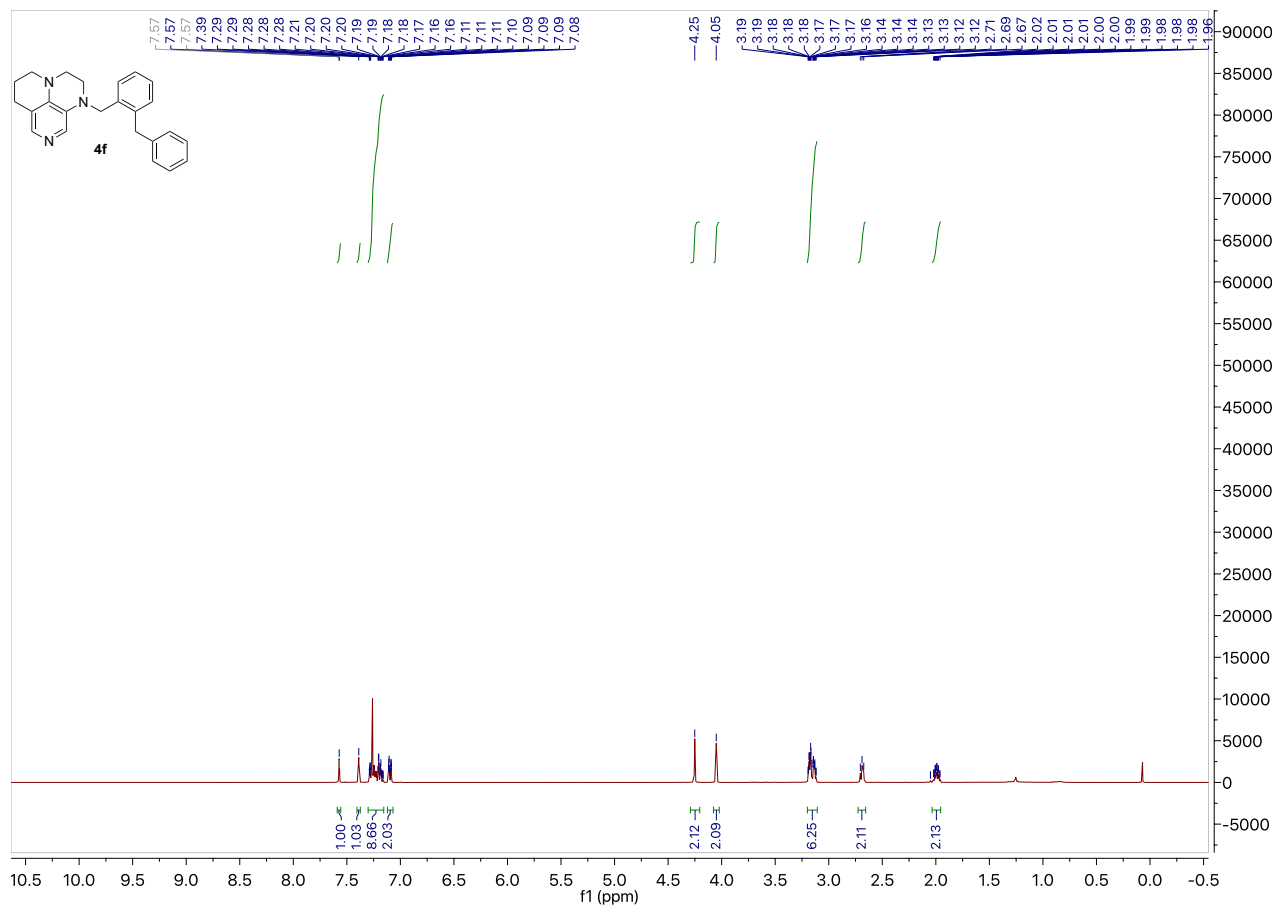


Figure 5.41. ^1H NMR spectrum of **4f** (400 MHz, CDCl_3).

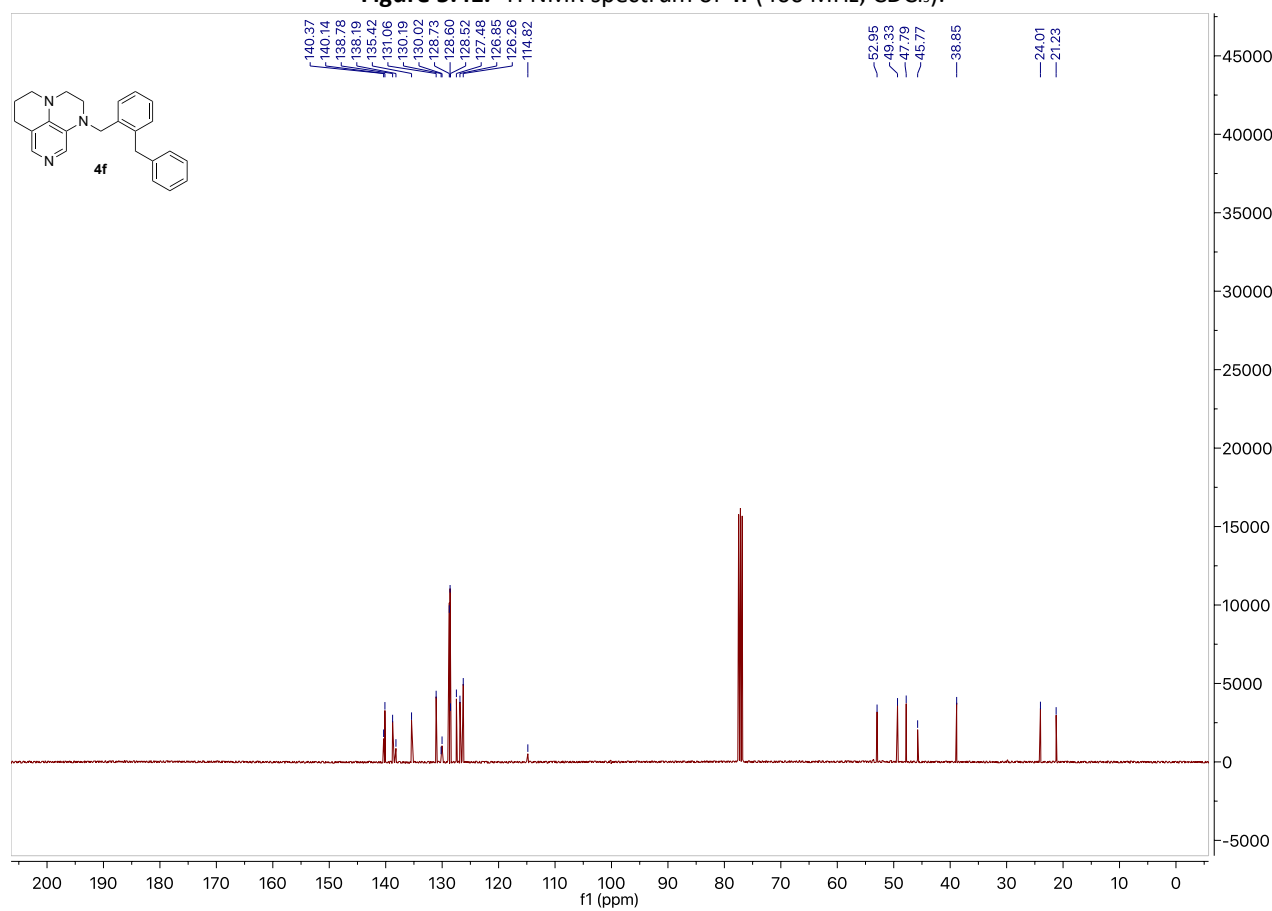


Figure 5.42. ^{13}C NMR spectrum of **4f** (101 MHz, CDCl_3).

Annulated Pyridine Bases

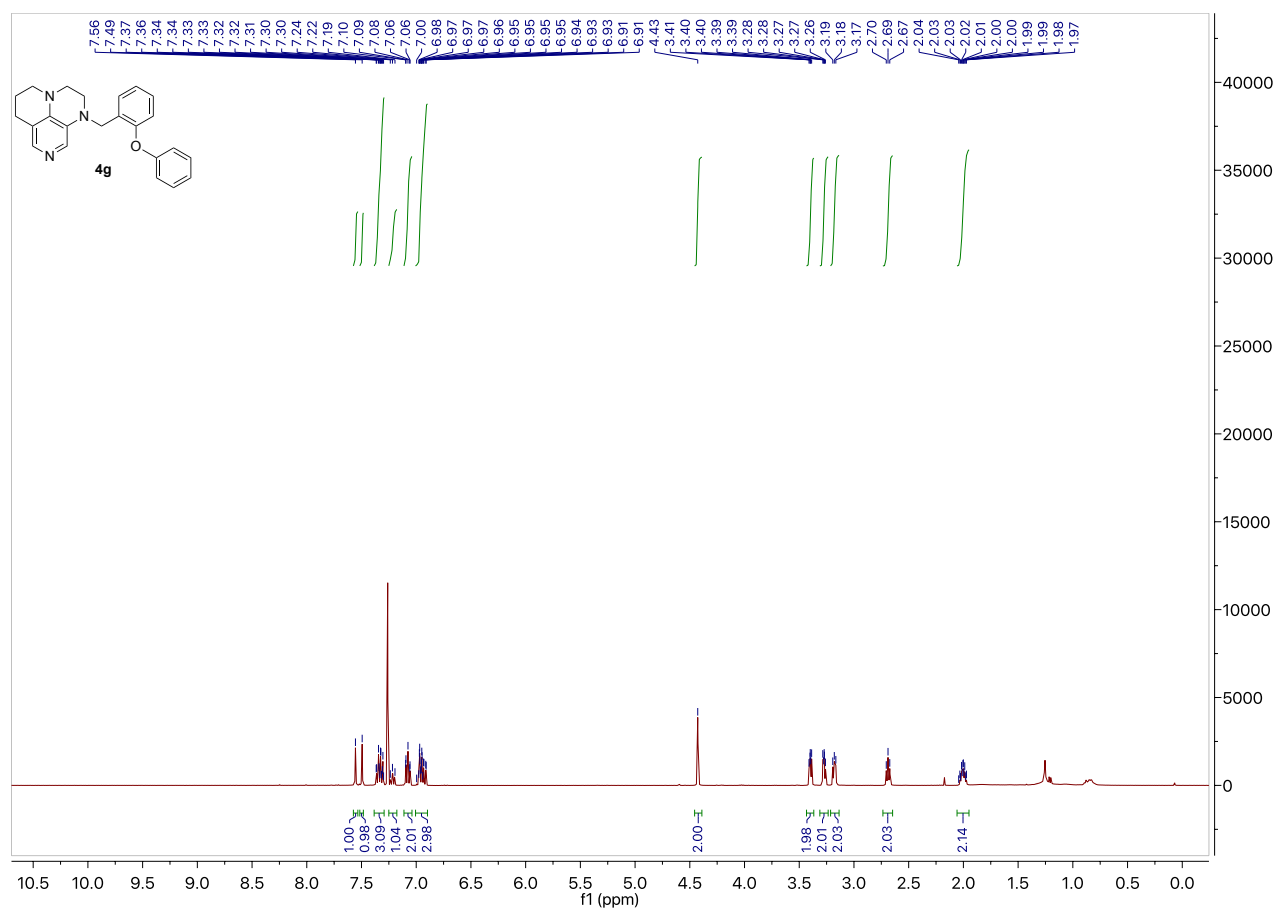


Figure 5.43. ^1H NMR spectrum of **4g** (400 MHz, CDCl_3).

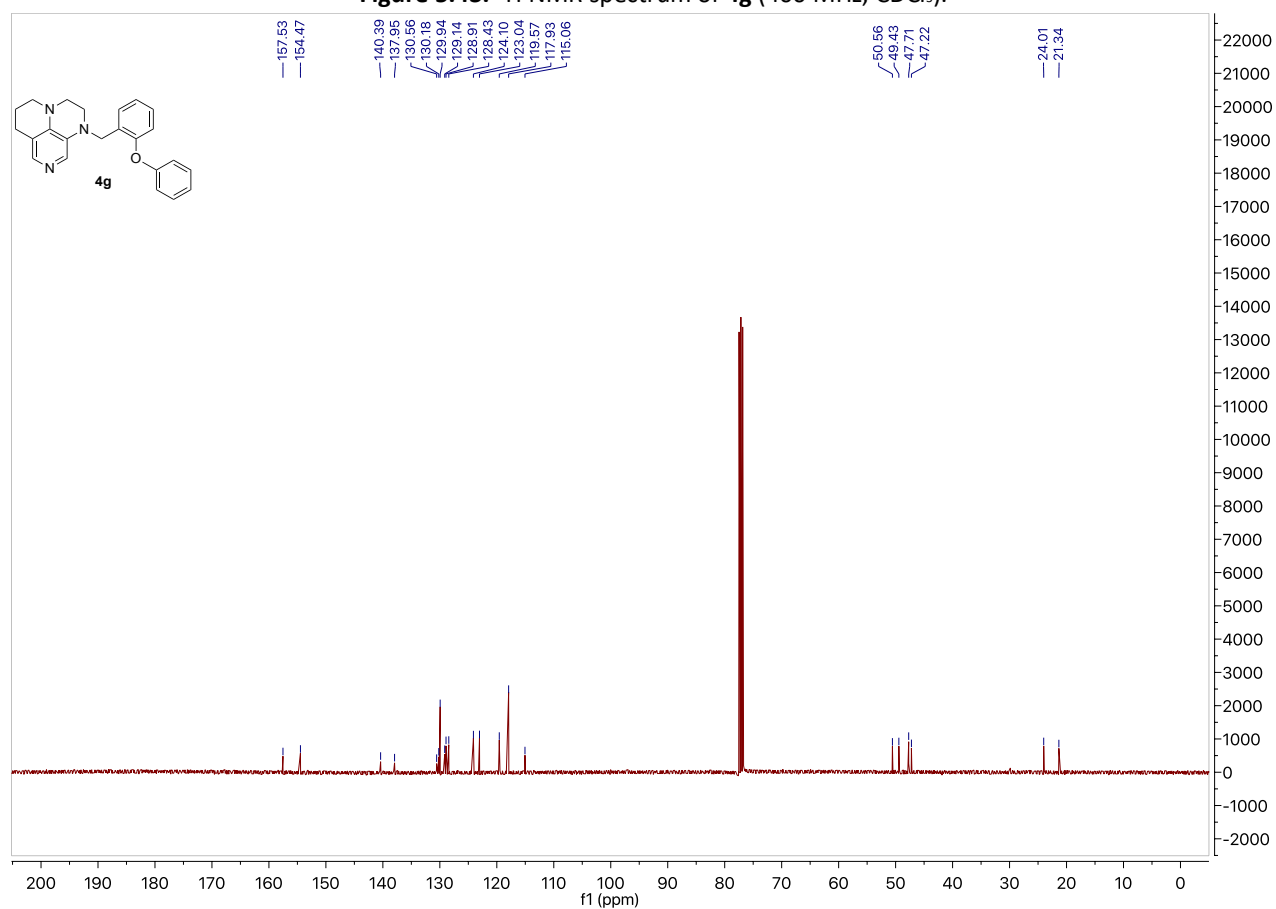
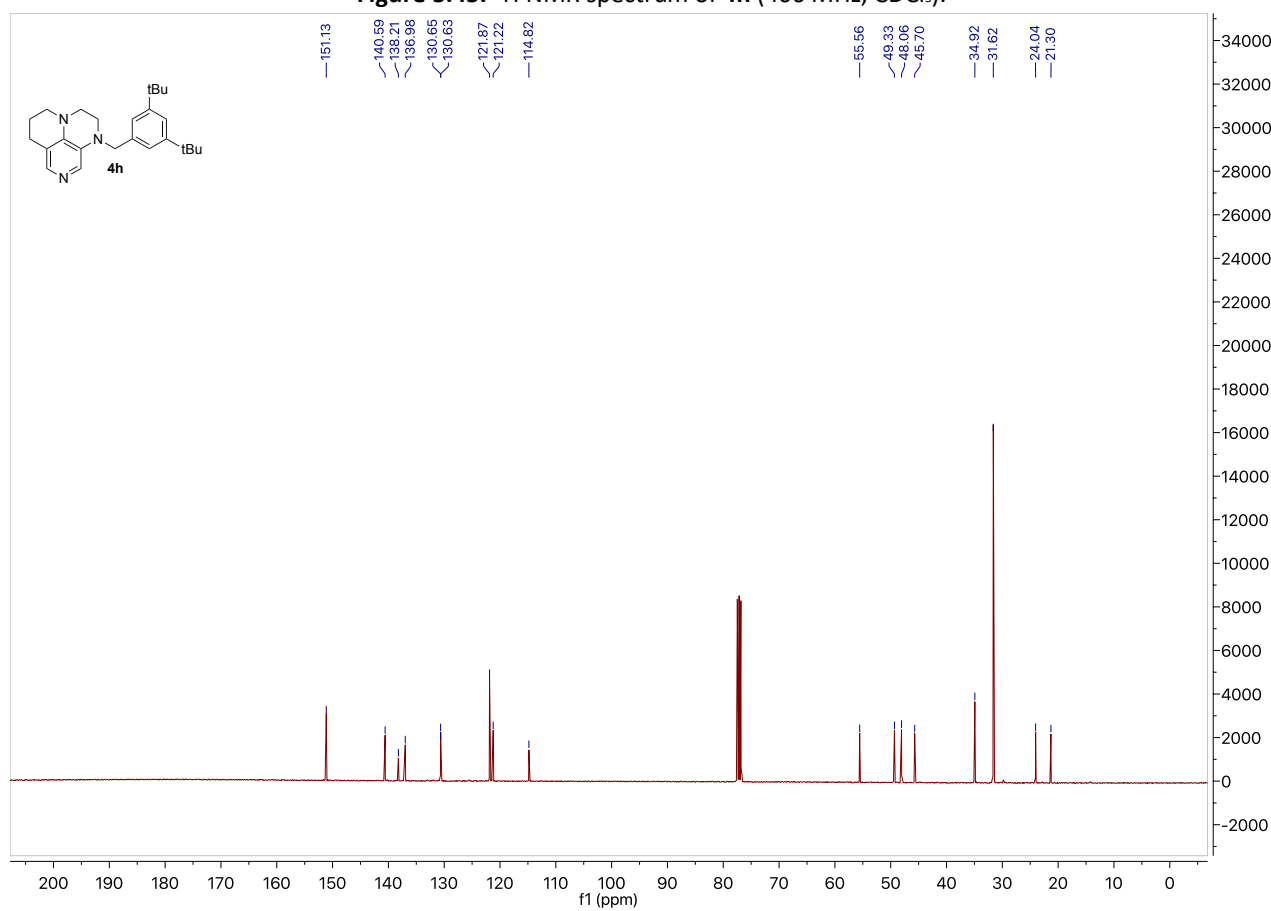
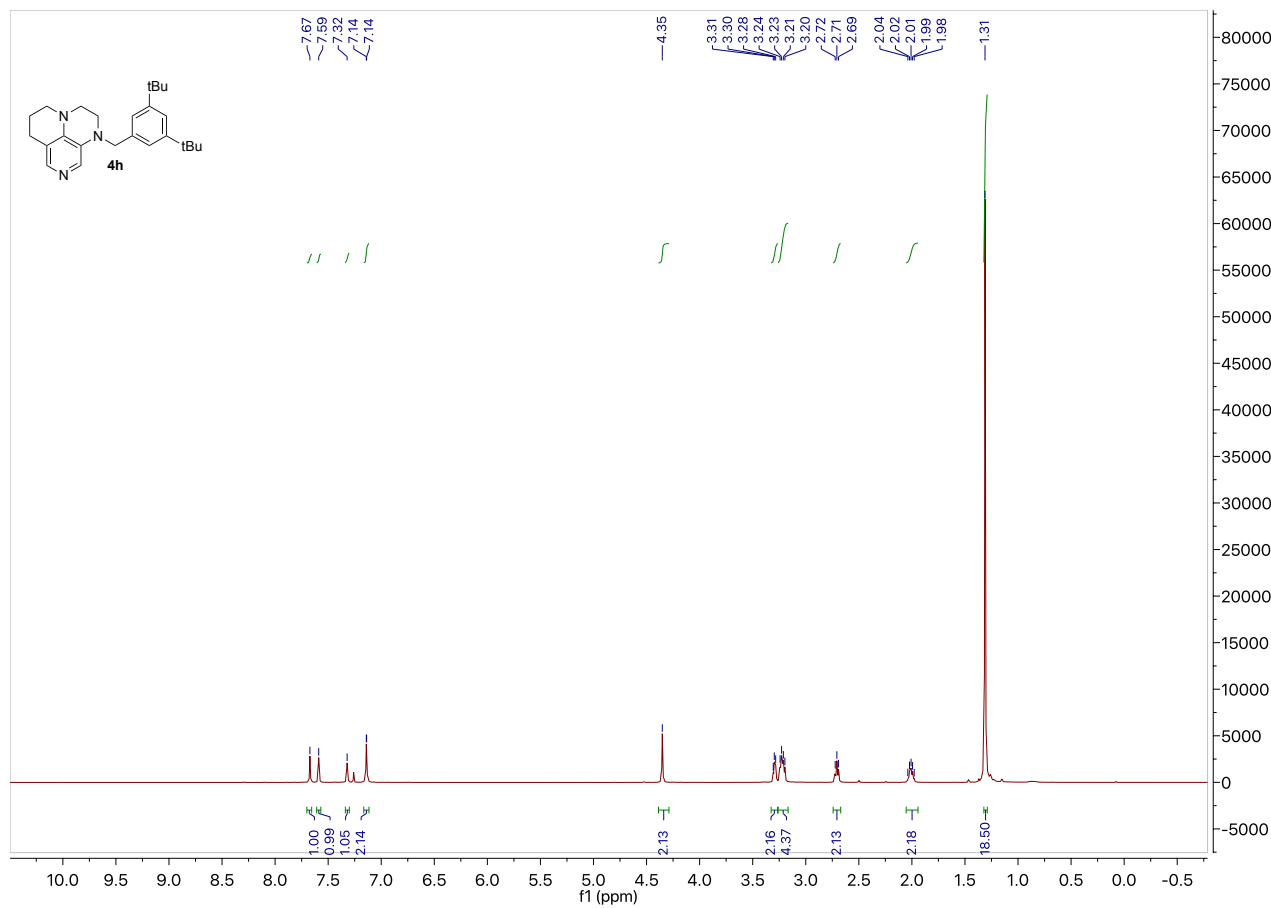


Figure 5.44. ^{13}C NMR spectrum of **4g** (101 MHz, CDCl_3).



Annulated Pyridine Bases

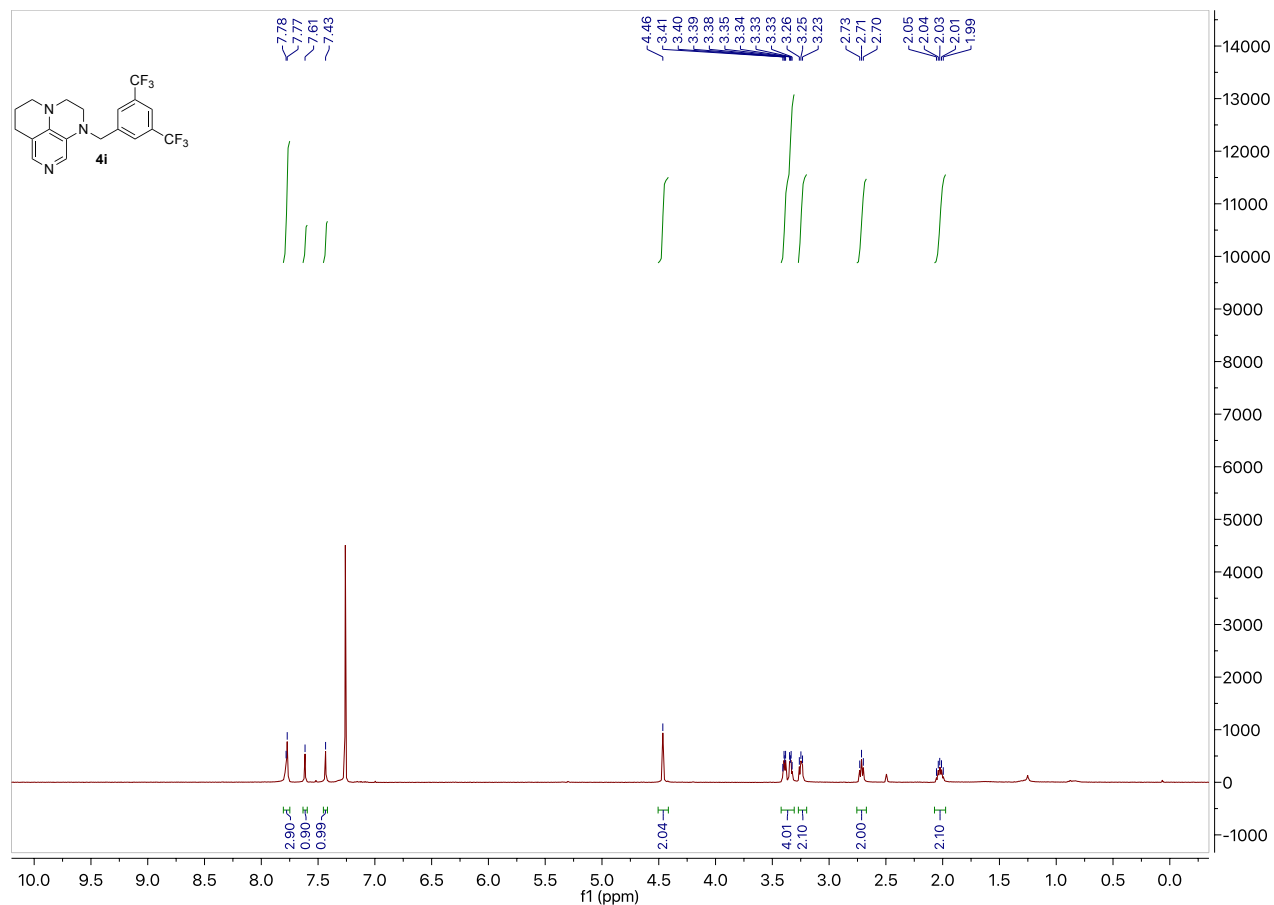


Figure 5.47. ^1H NMR spectrum of **4i** (400 MHz, CDCl_3).

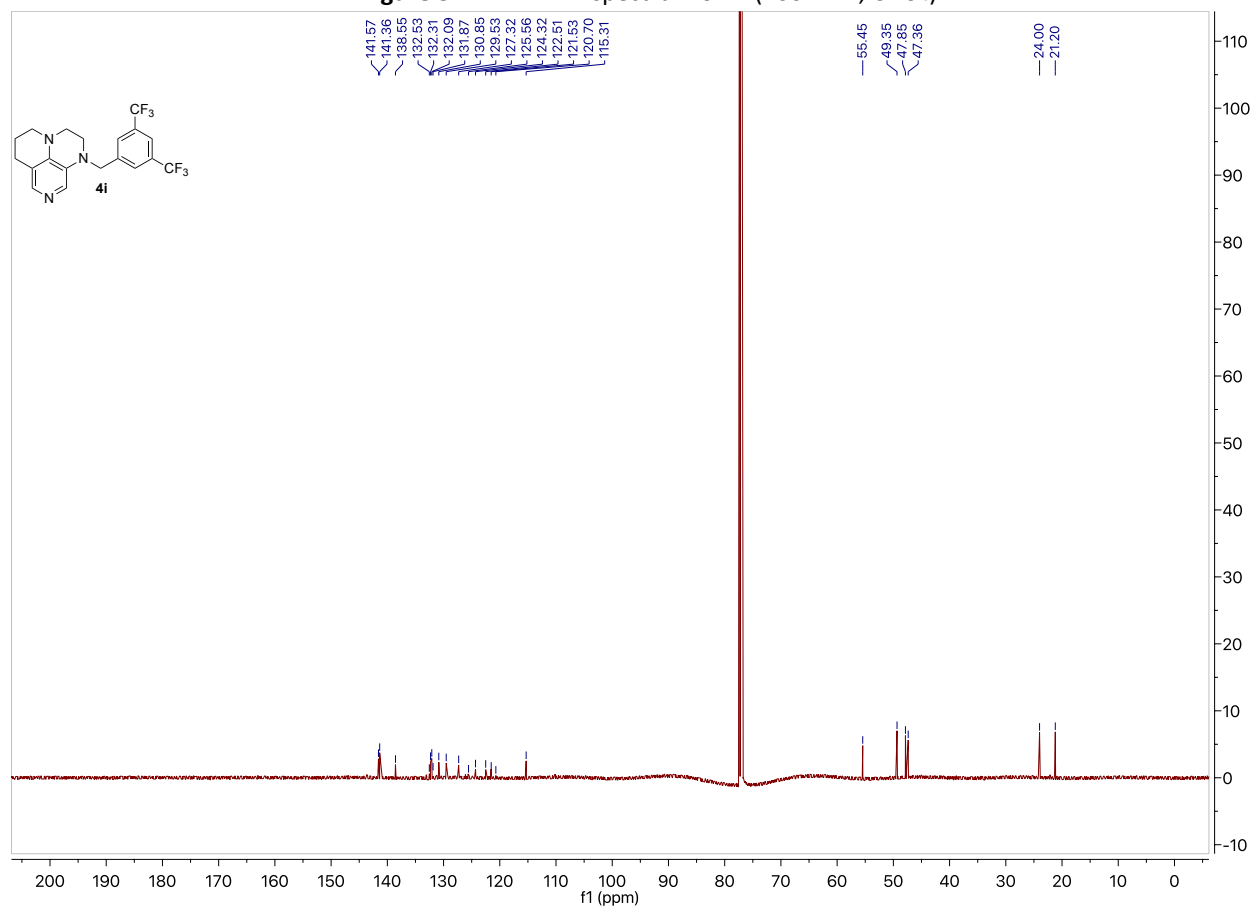
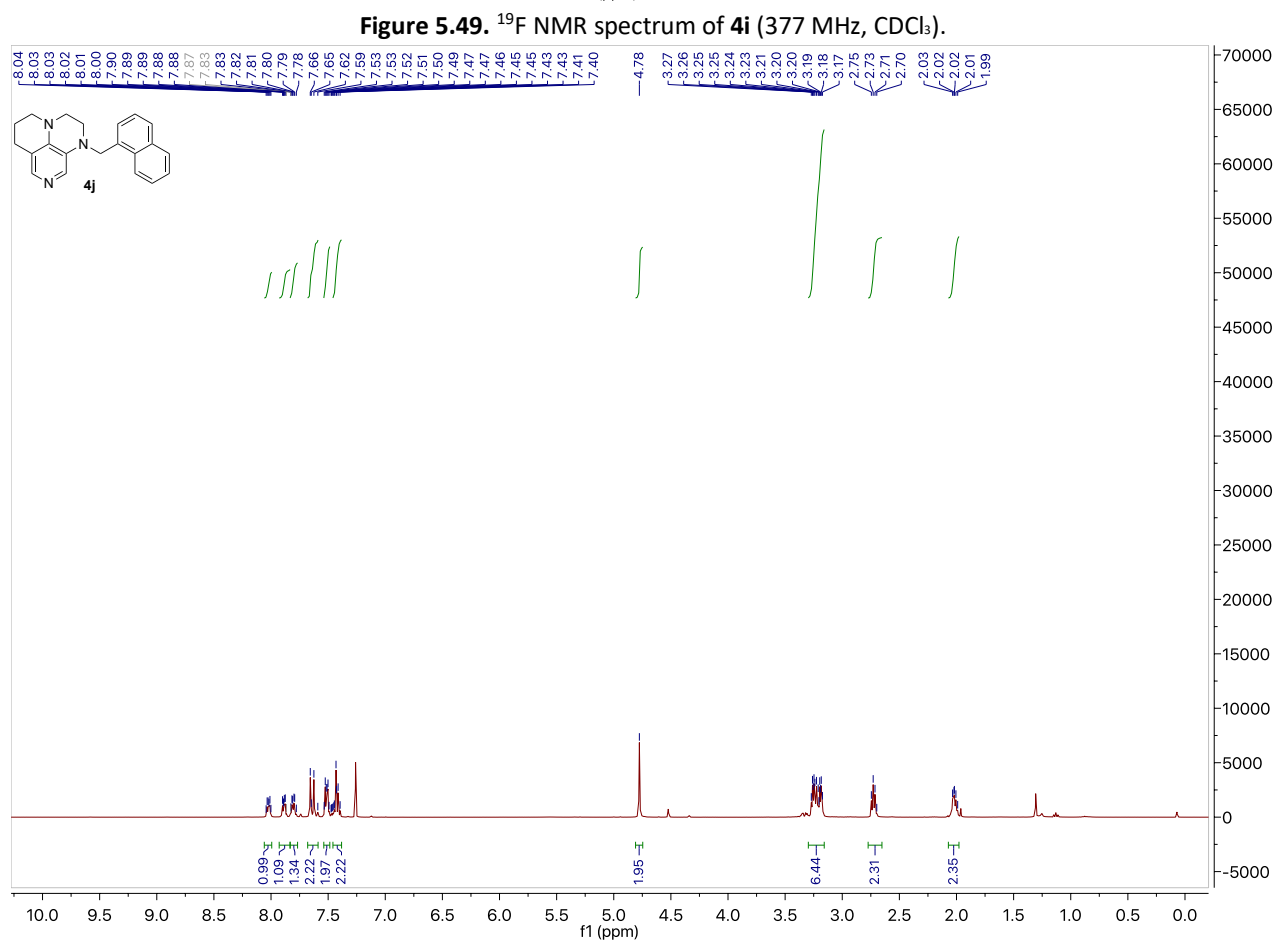
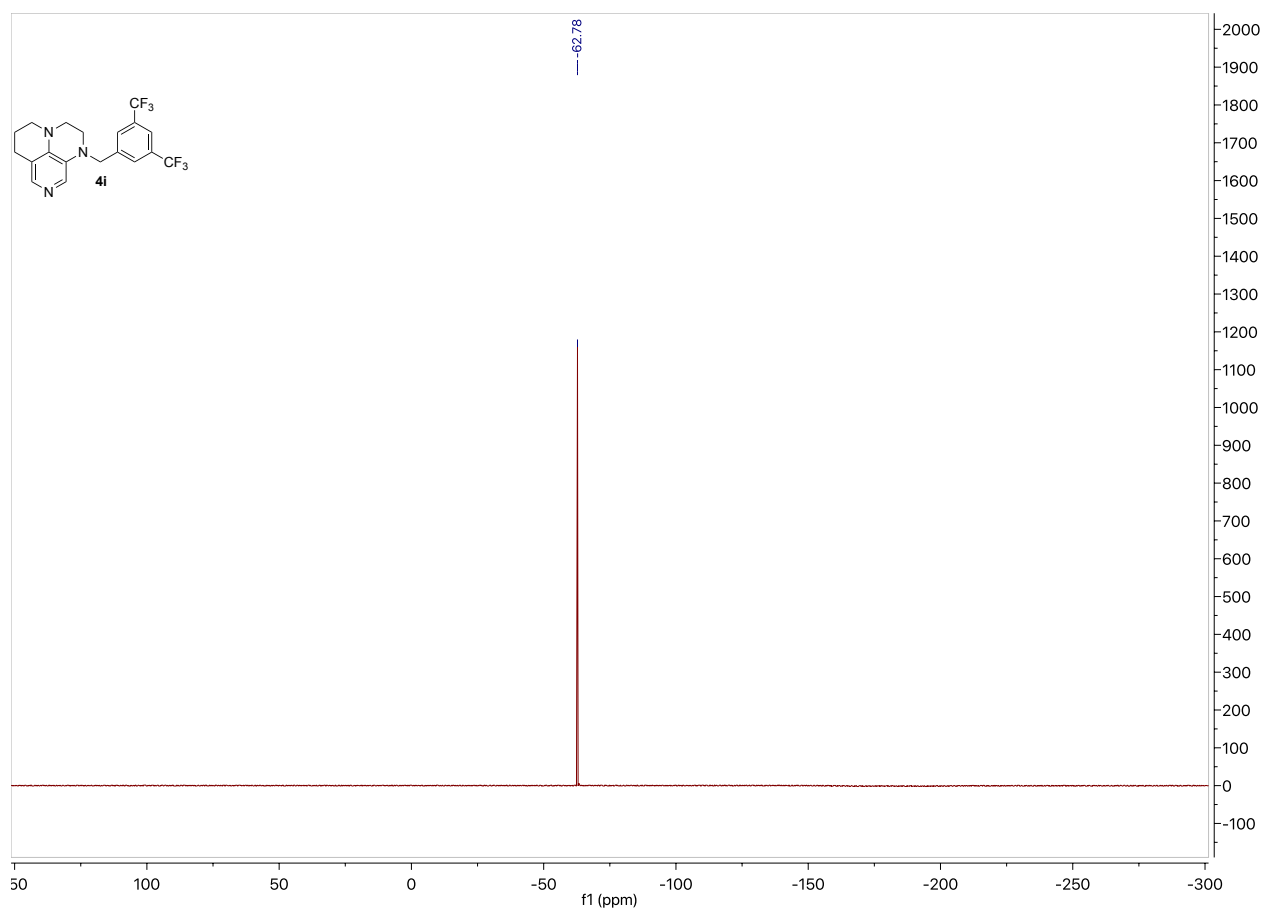


Figure 5.48. ^{13}C NMR spectrum of **4i** (101 MHz, CDCl_3).



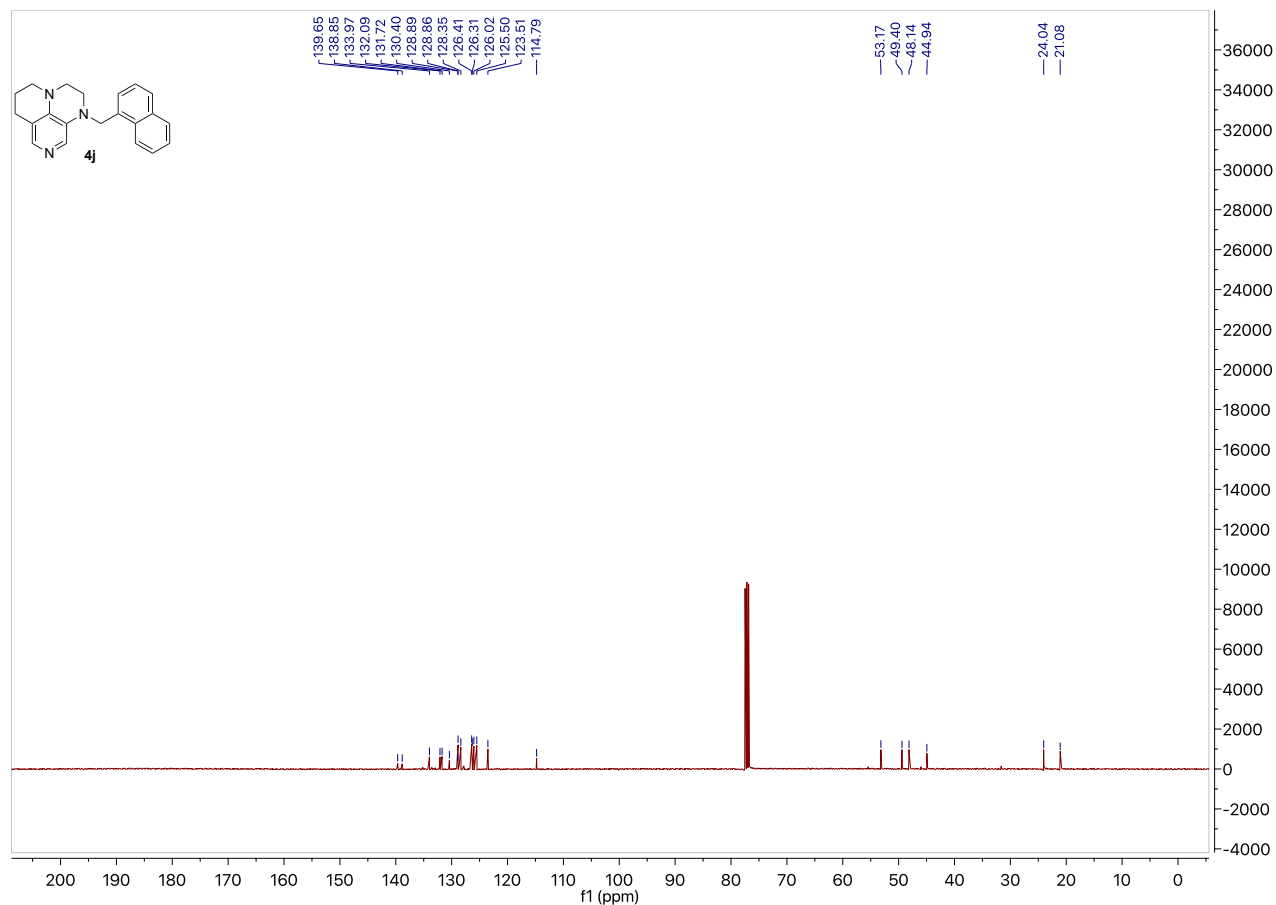


Figure 5.51. ^{13}C NMR spectrum of **4j** (101 MHz, CDCl_3).

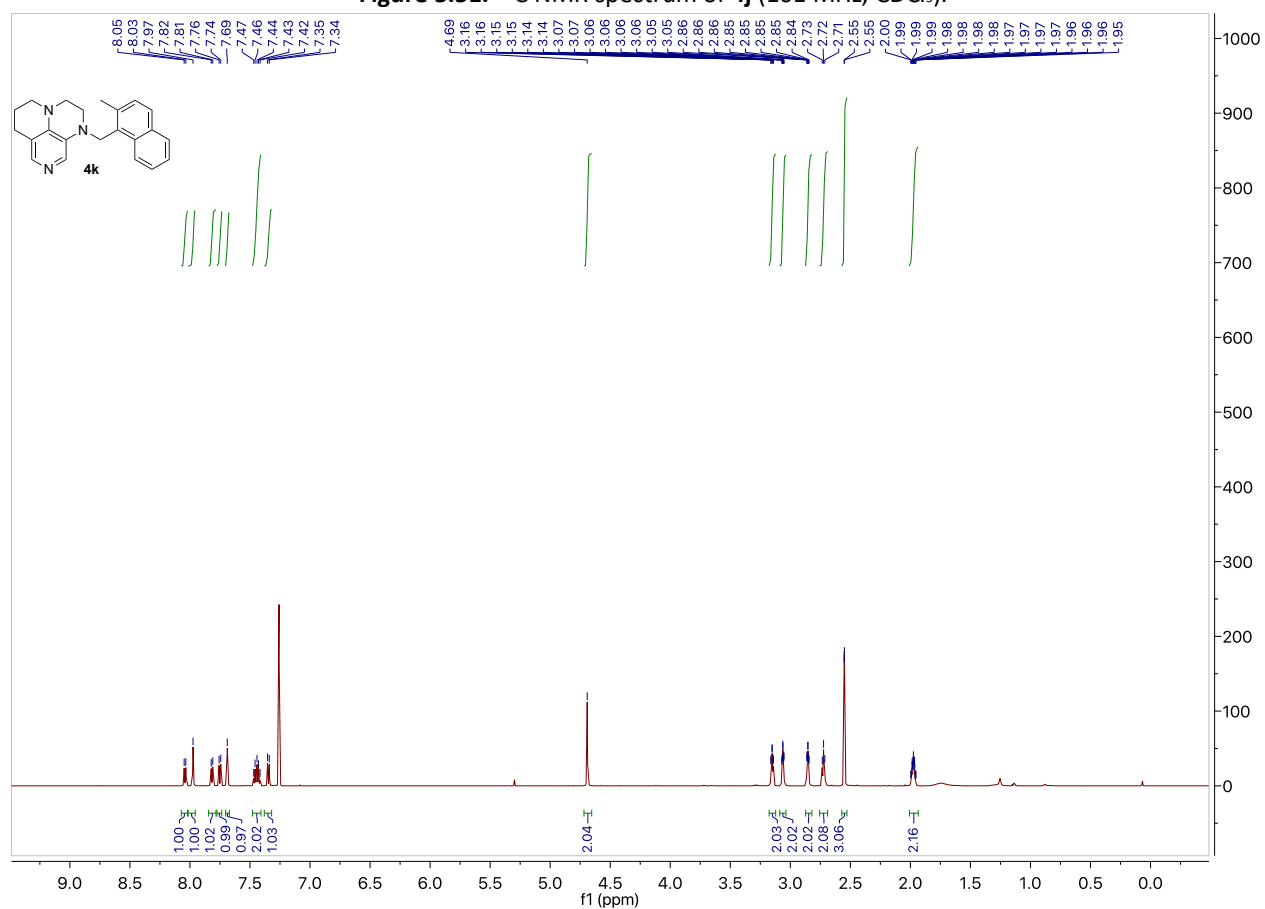
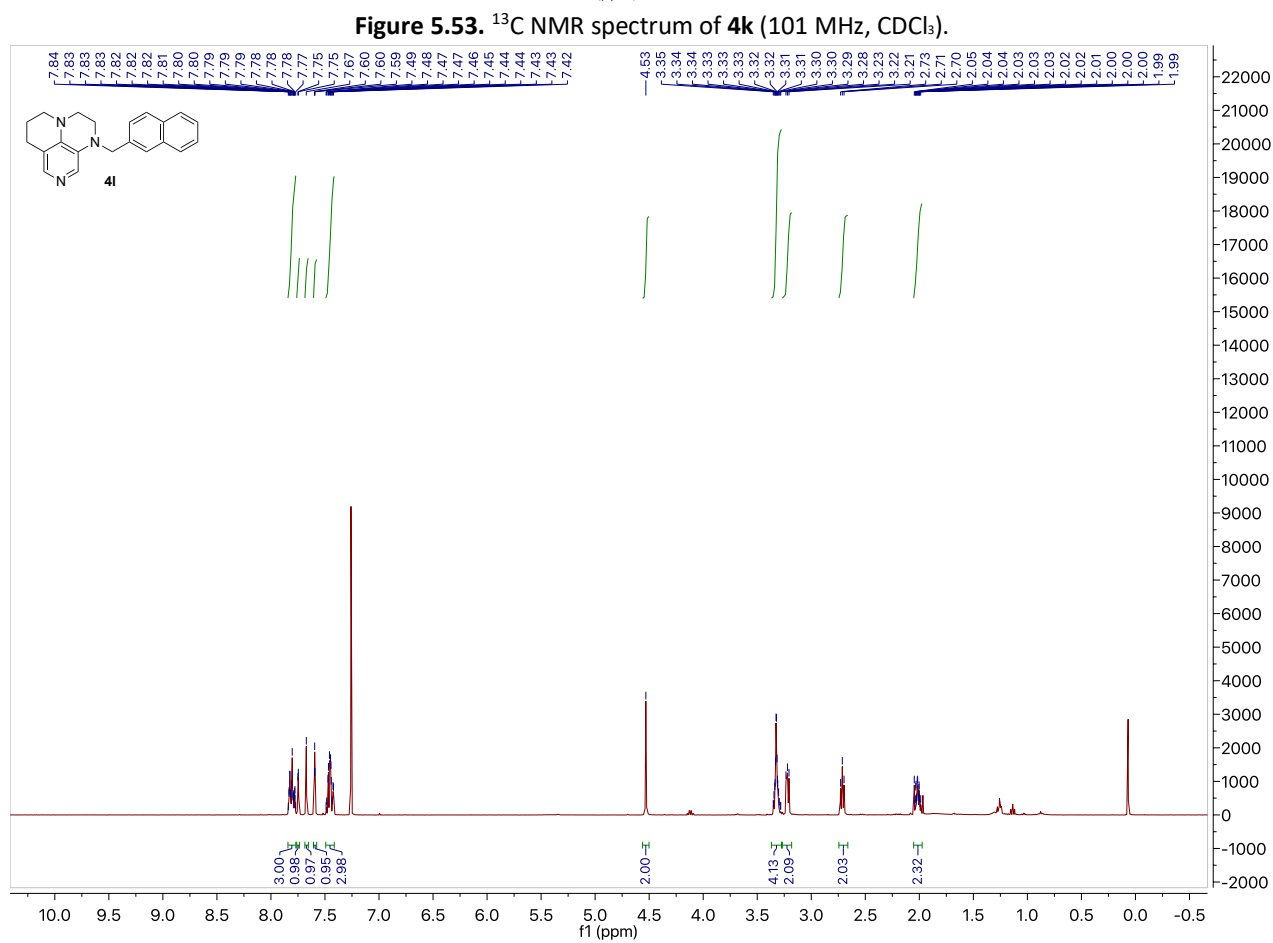
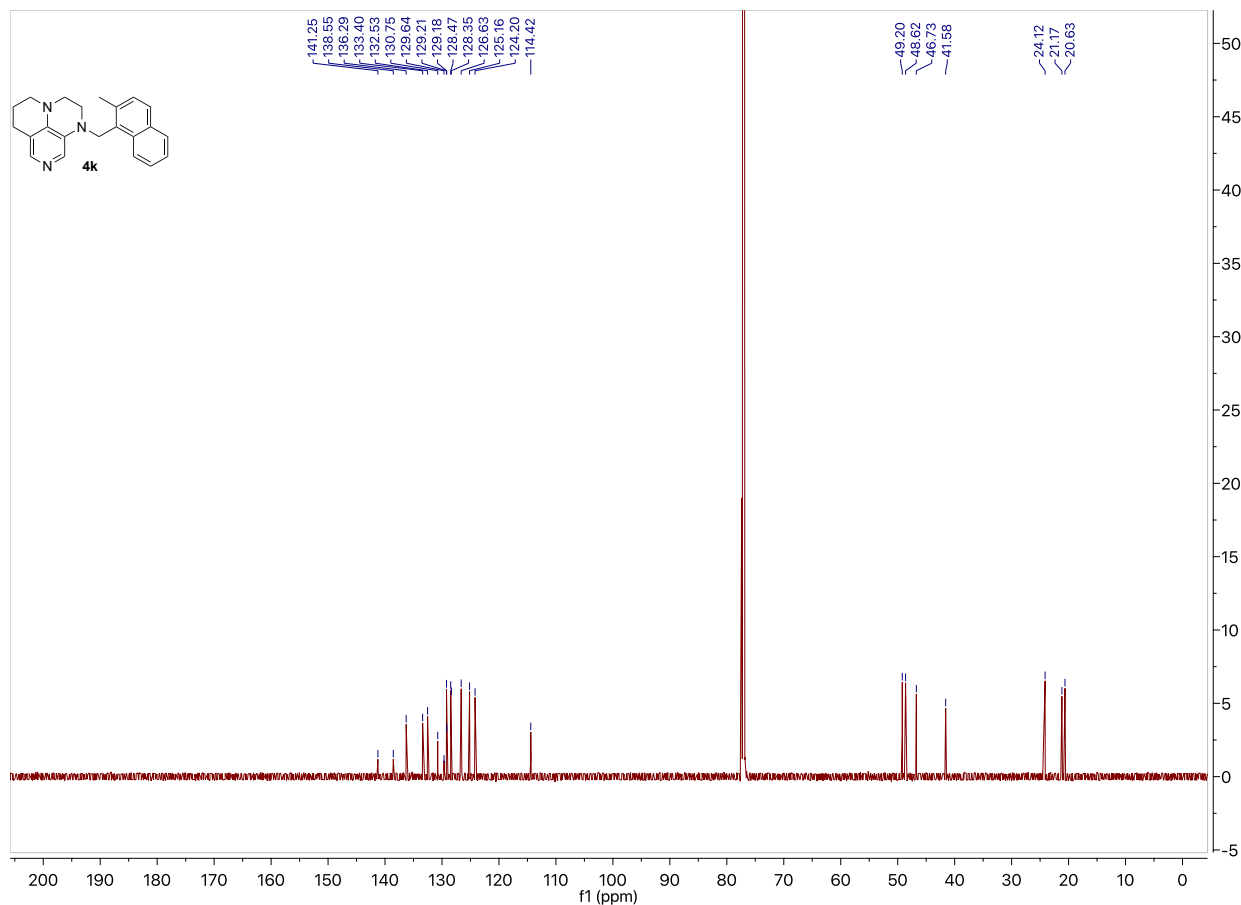


Figure 5.52. ^1H NMR spectrum of **4k** (400 MHz, CDCl_3).



Annulated Pyridine Bases

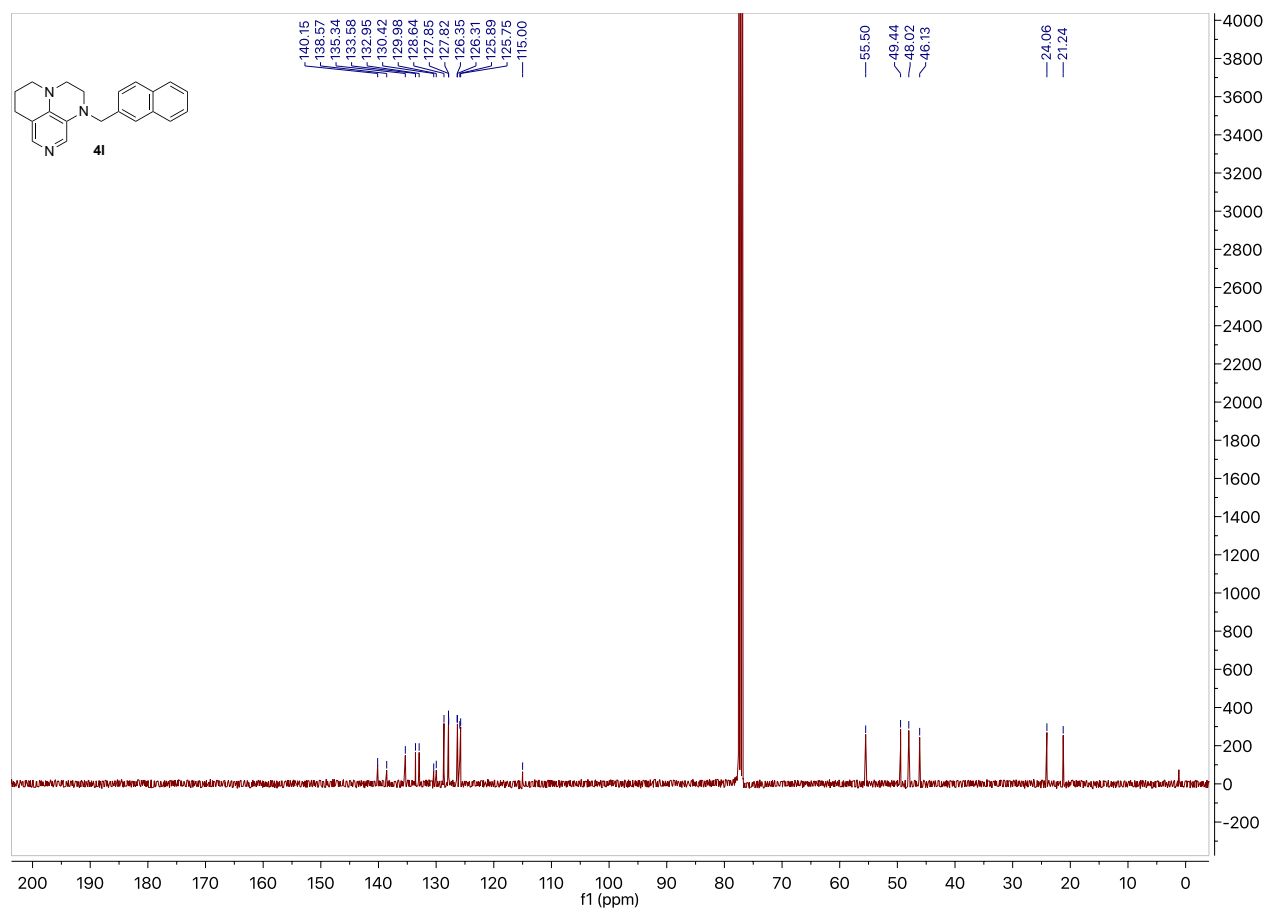


Figure 5.55. ¹³C NMR spectrum of **4l** (101 MHz, CDCl₃).

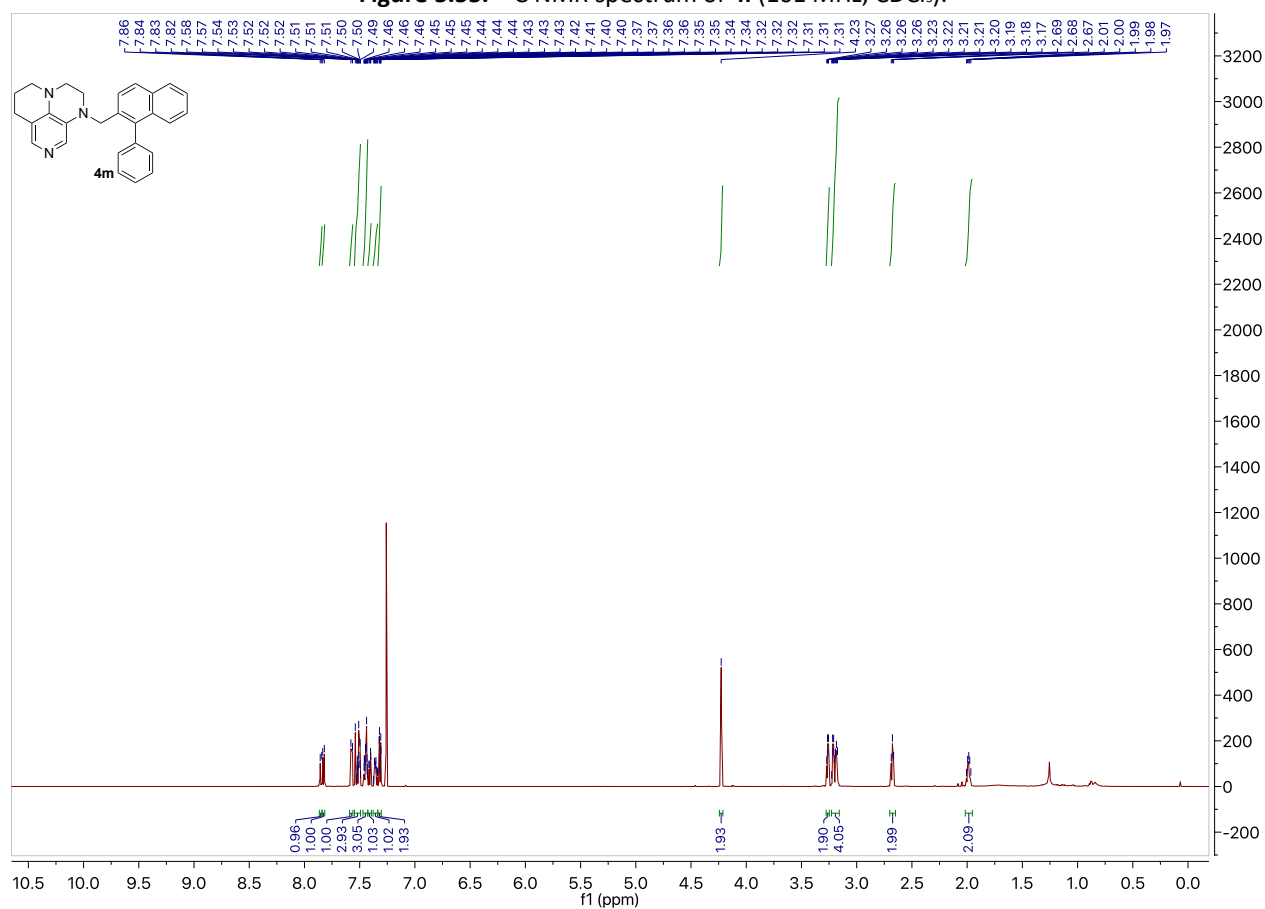
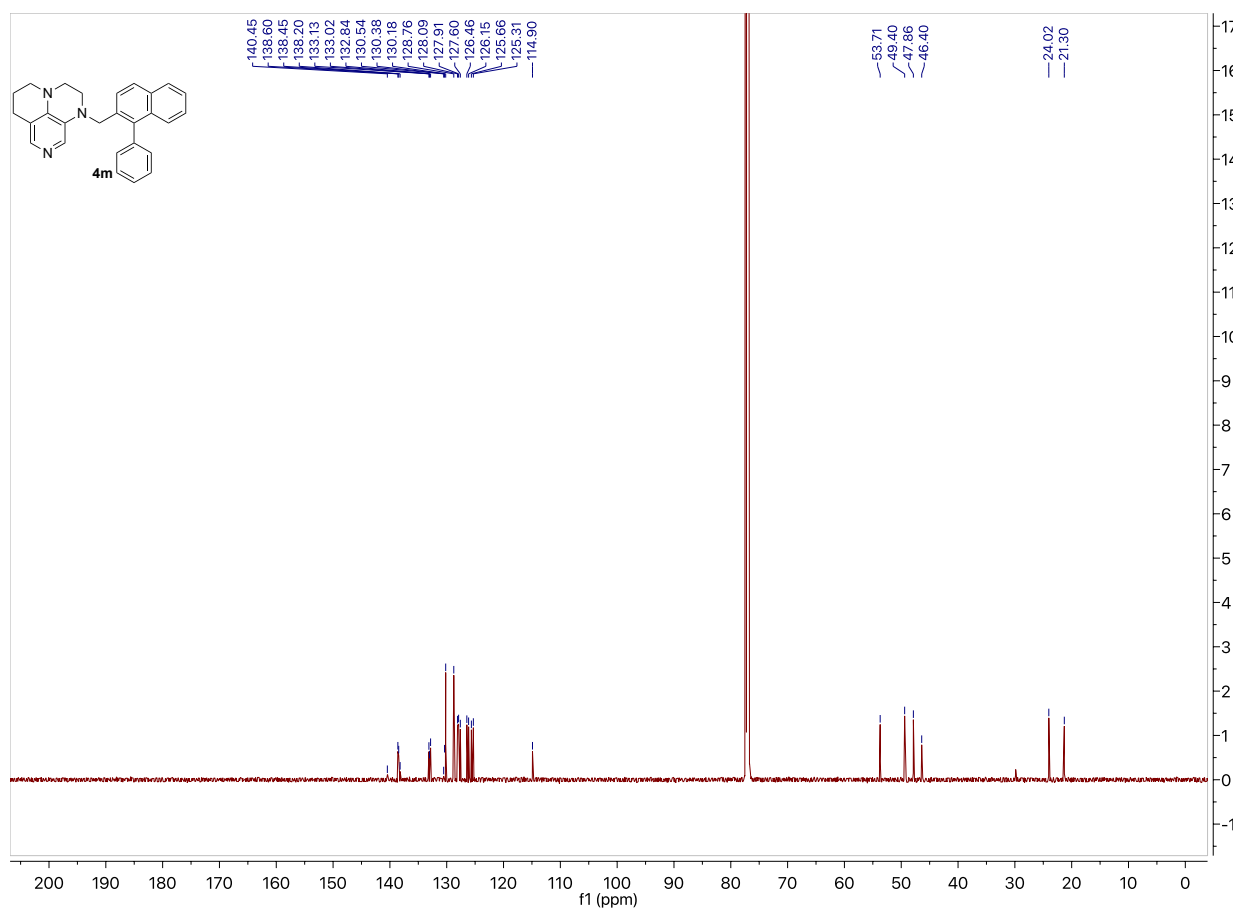
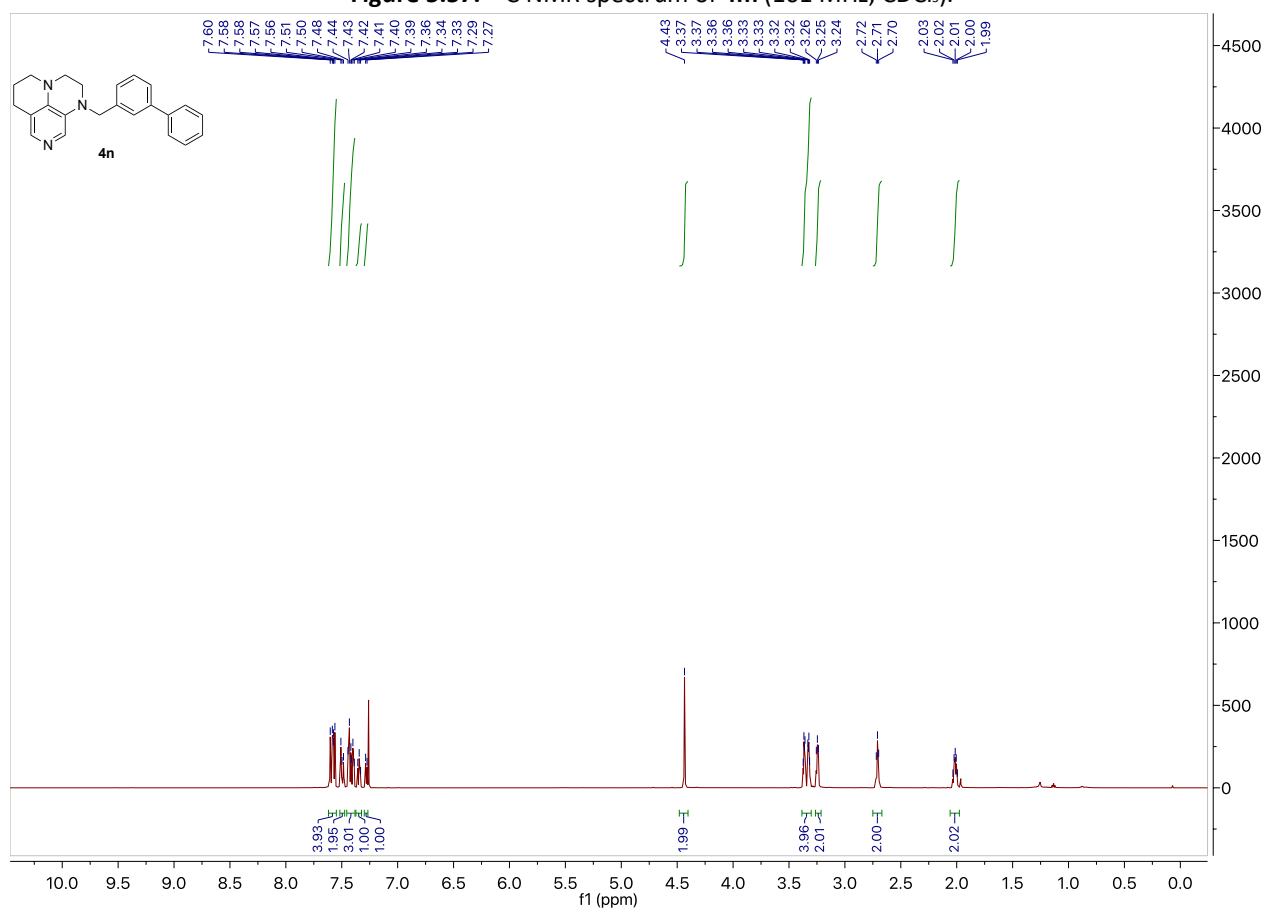
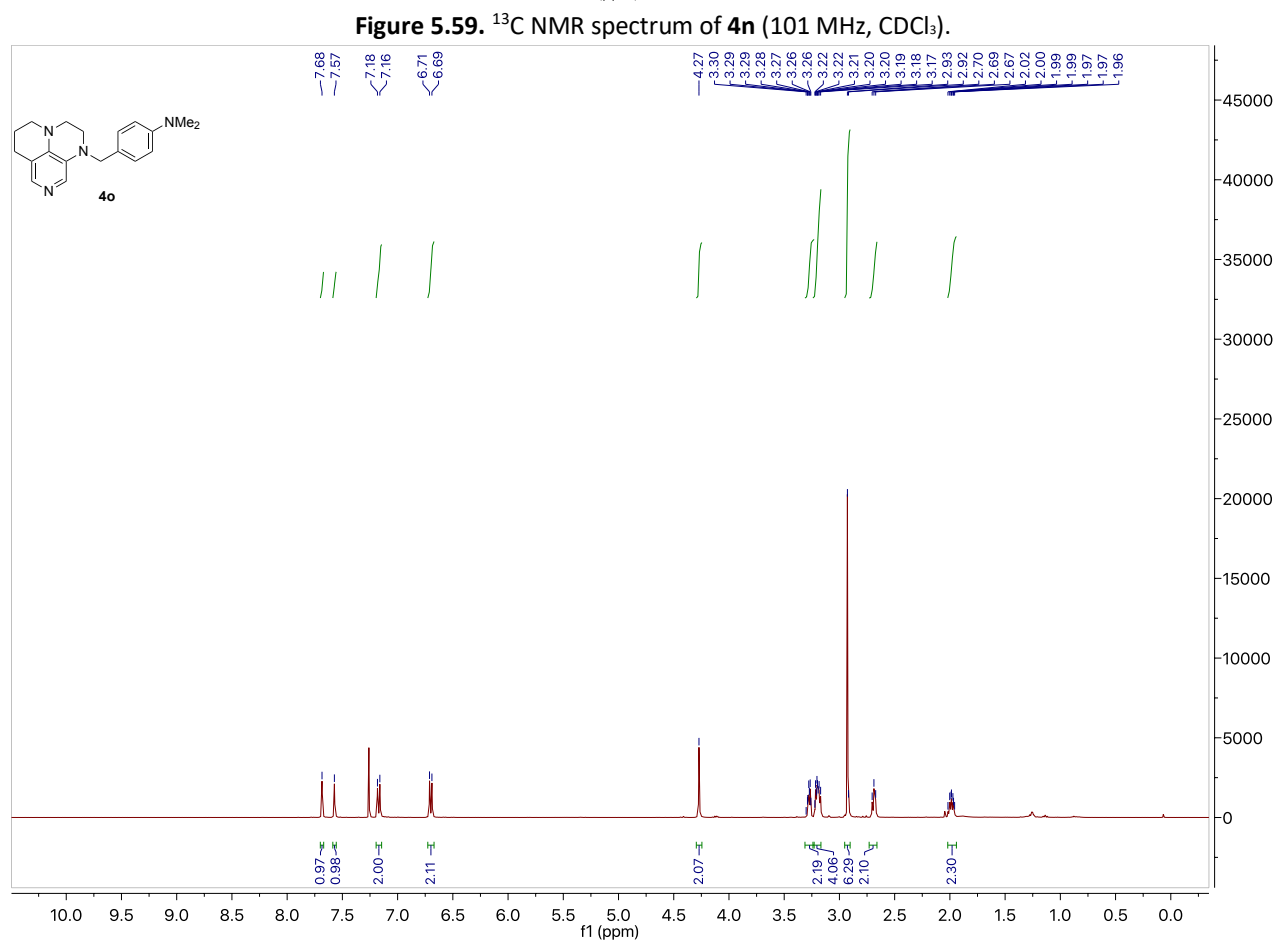
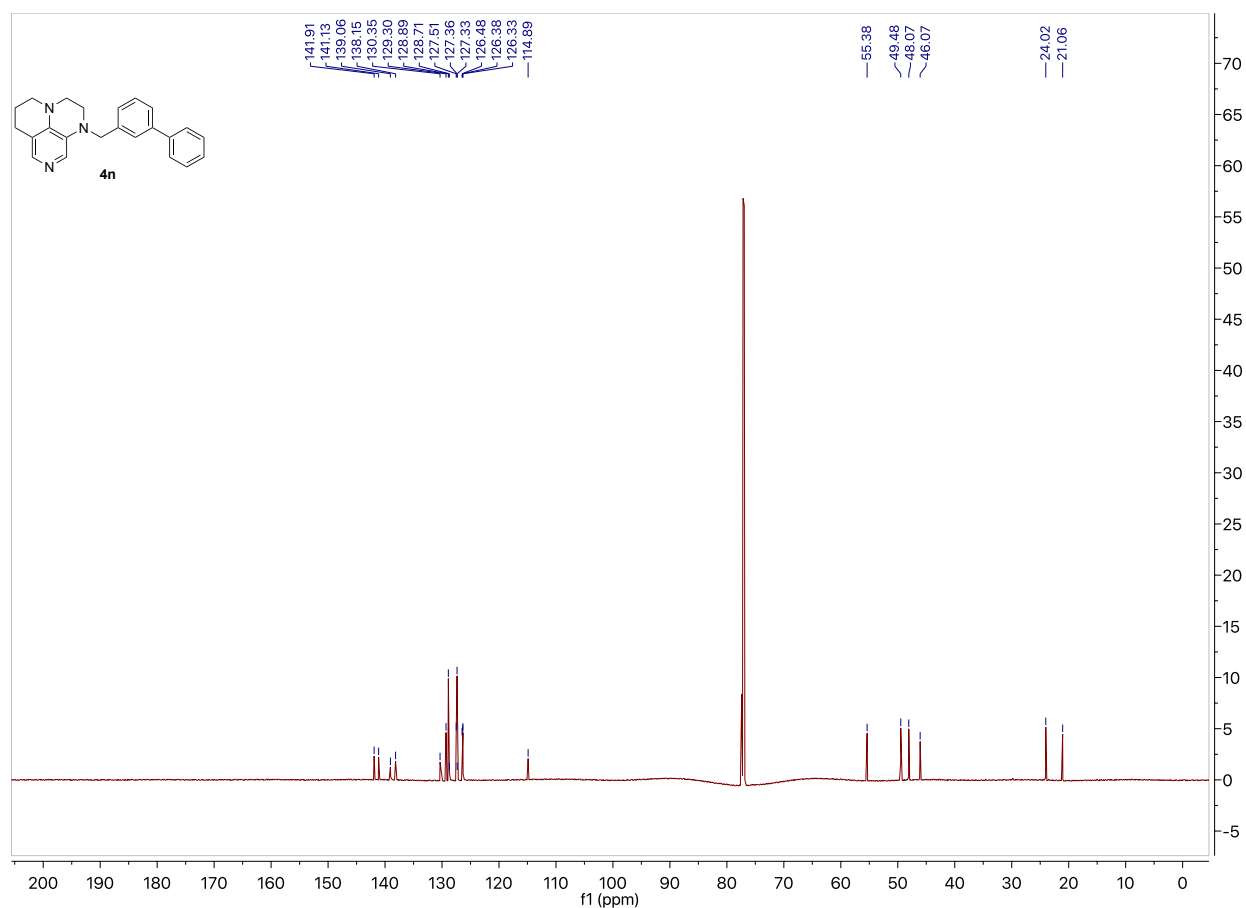
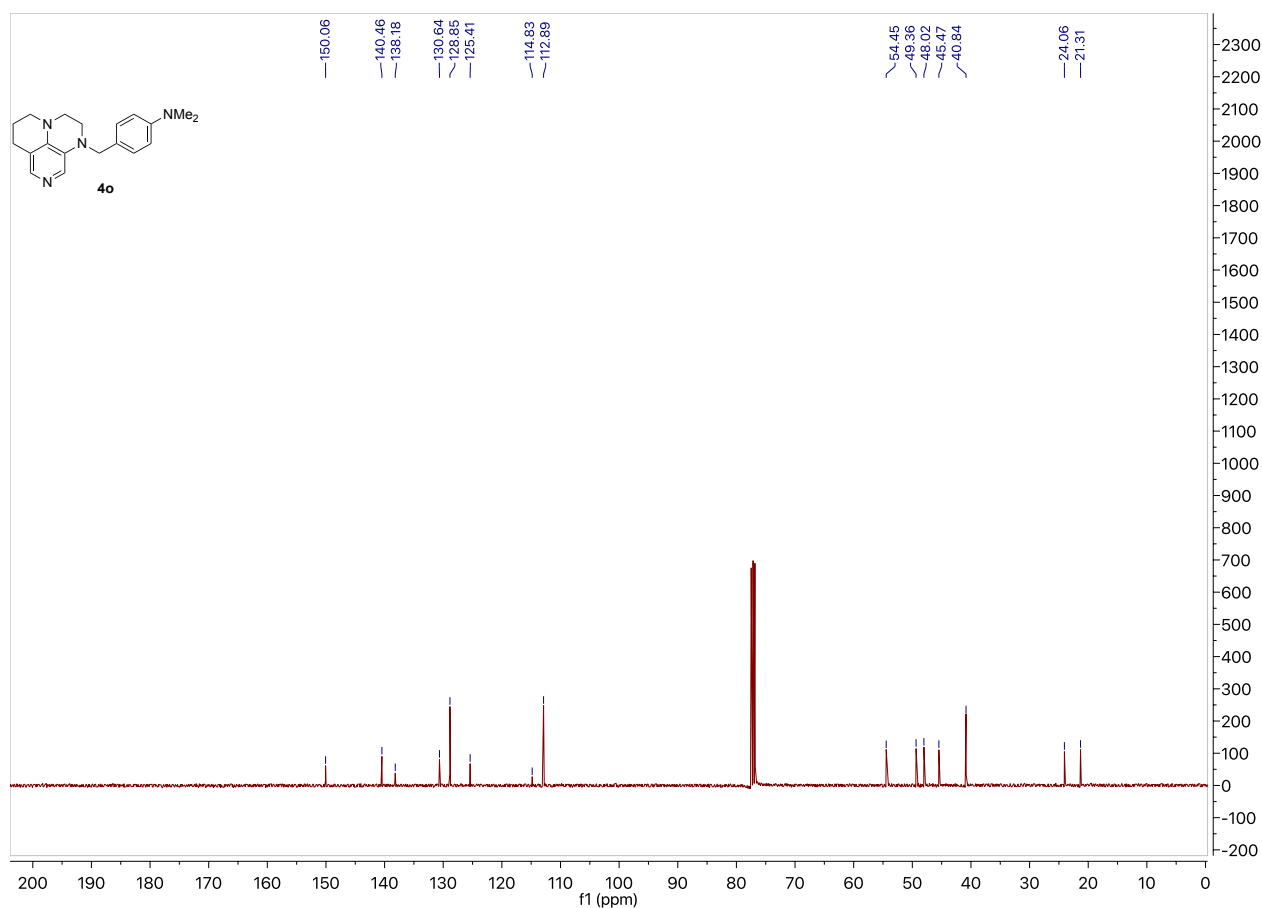
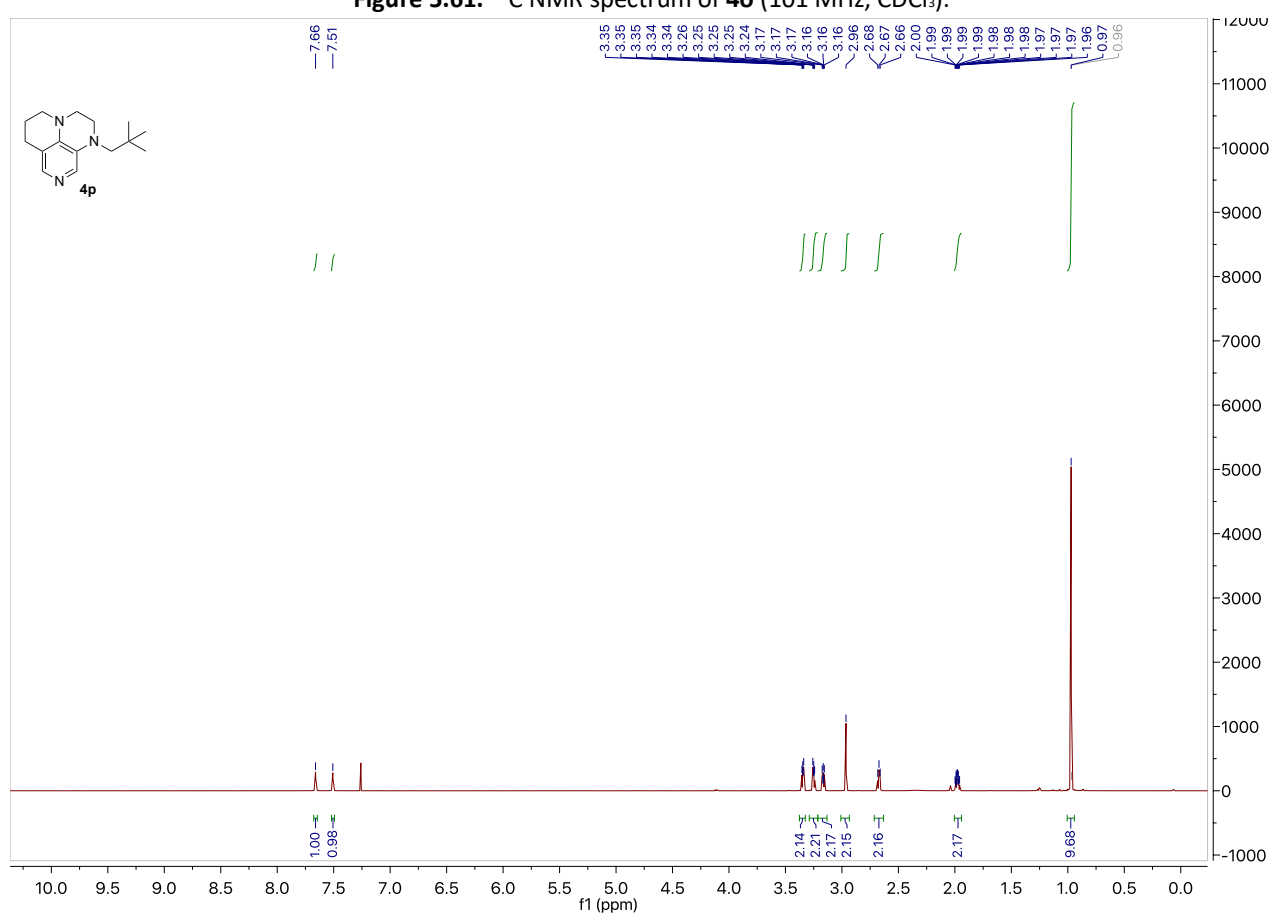
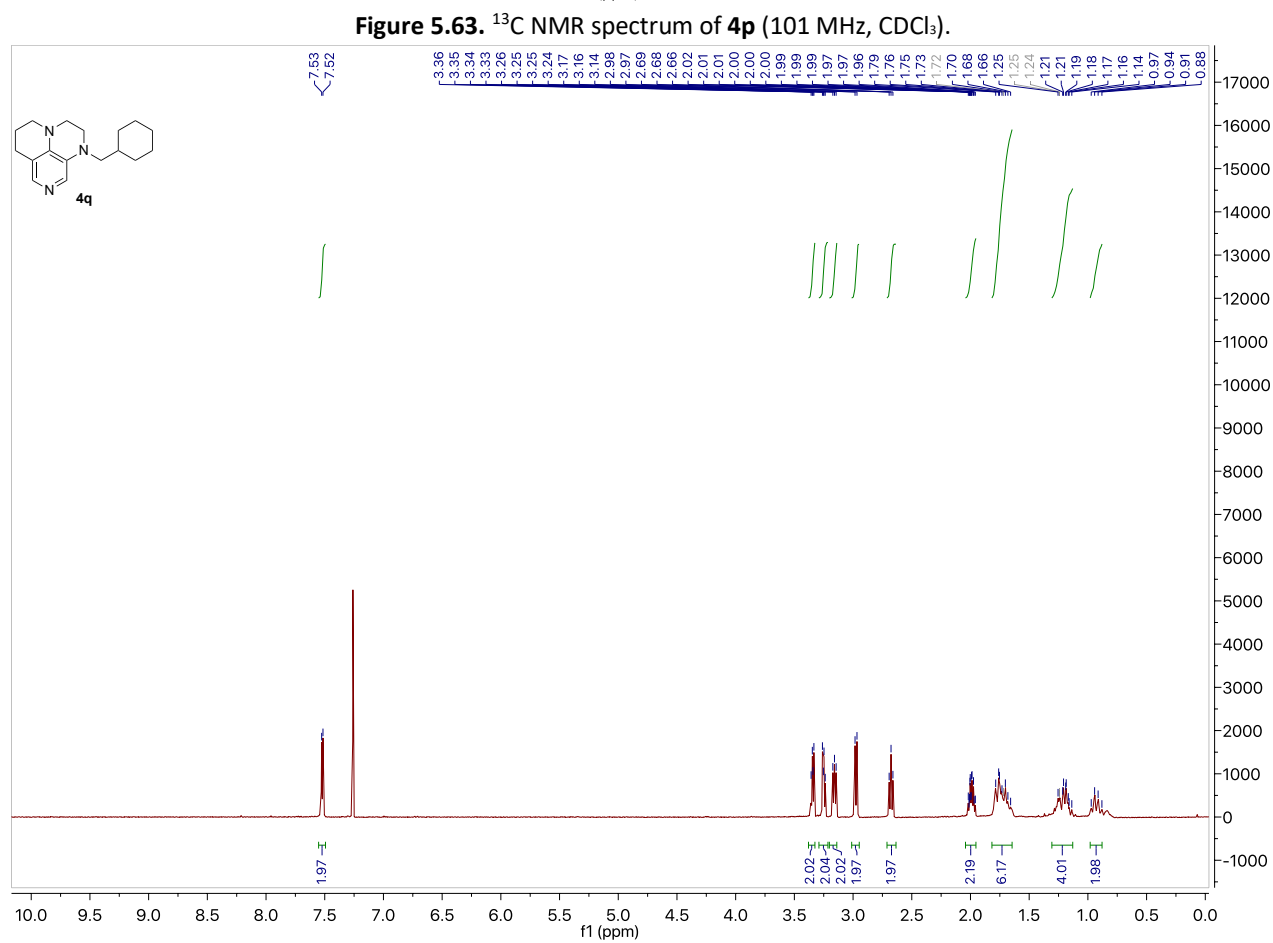
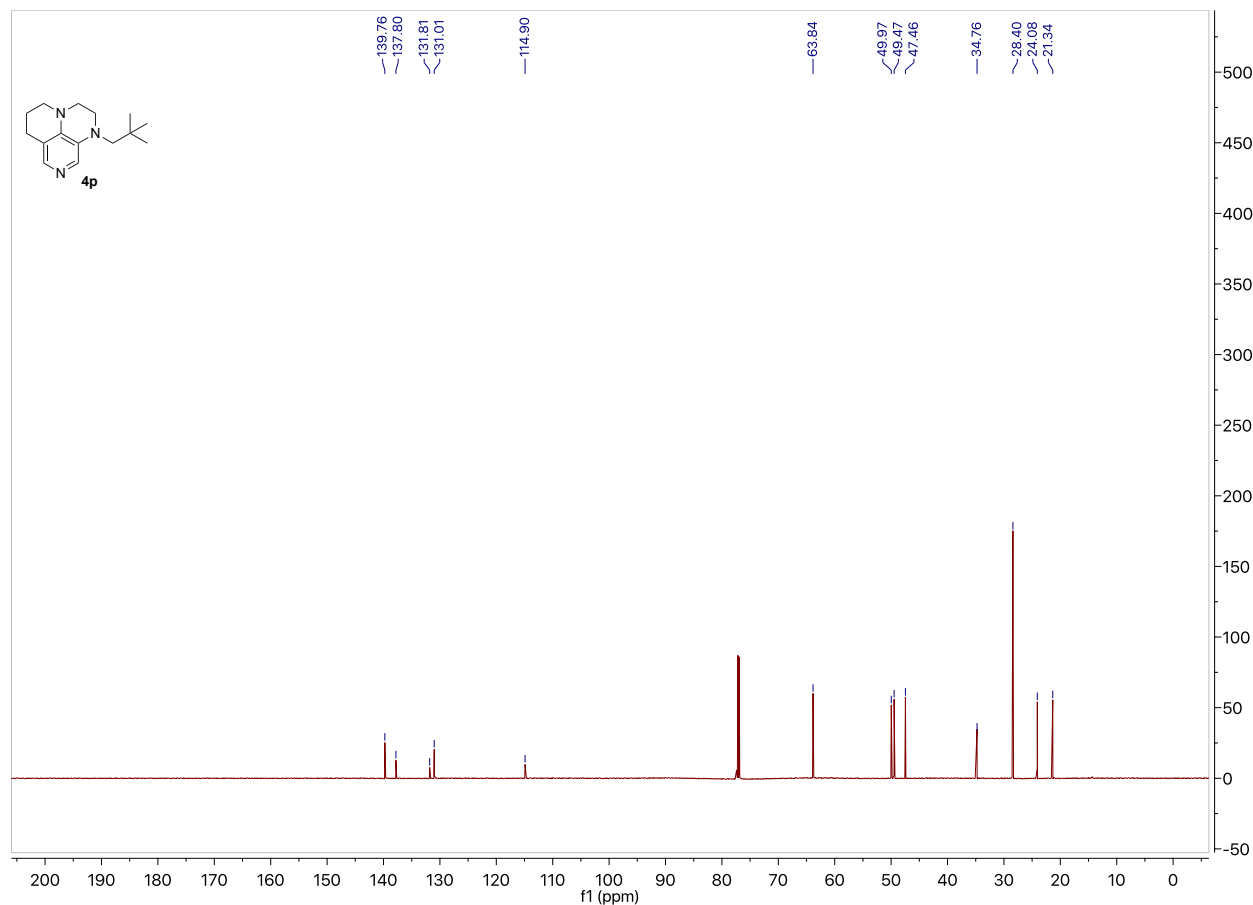


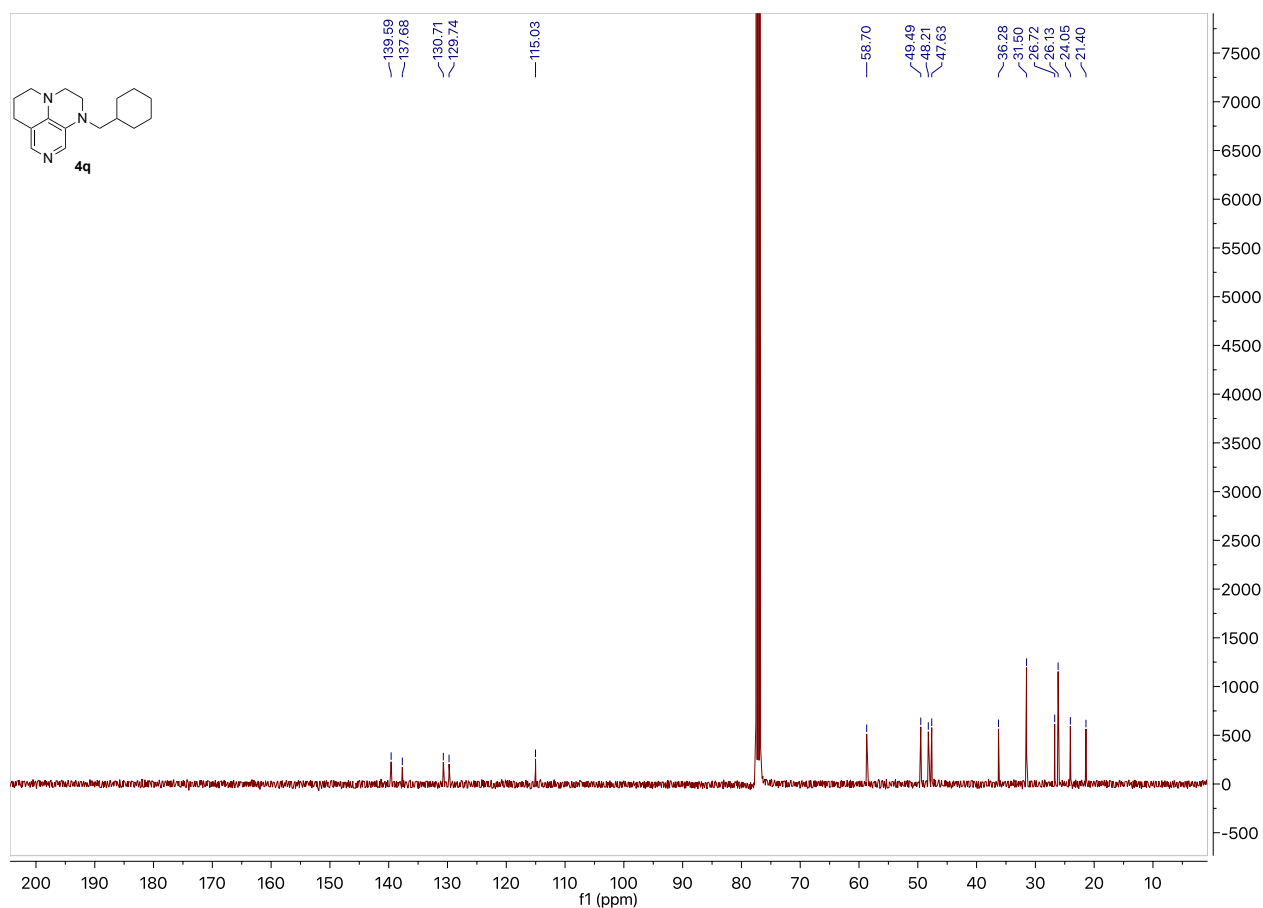
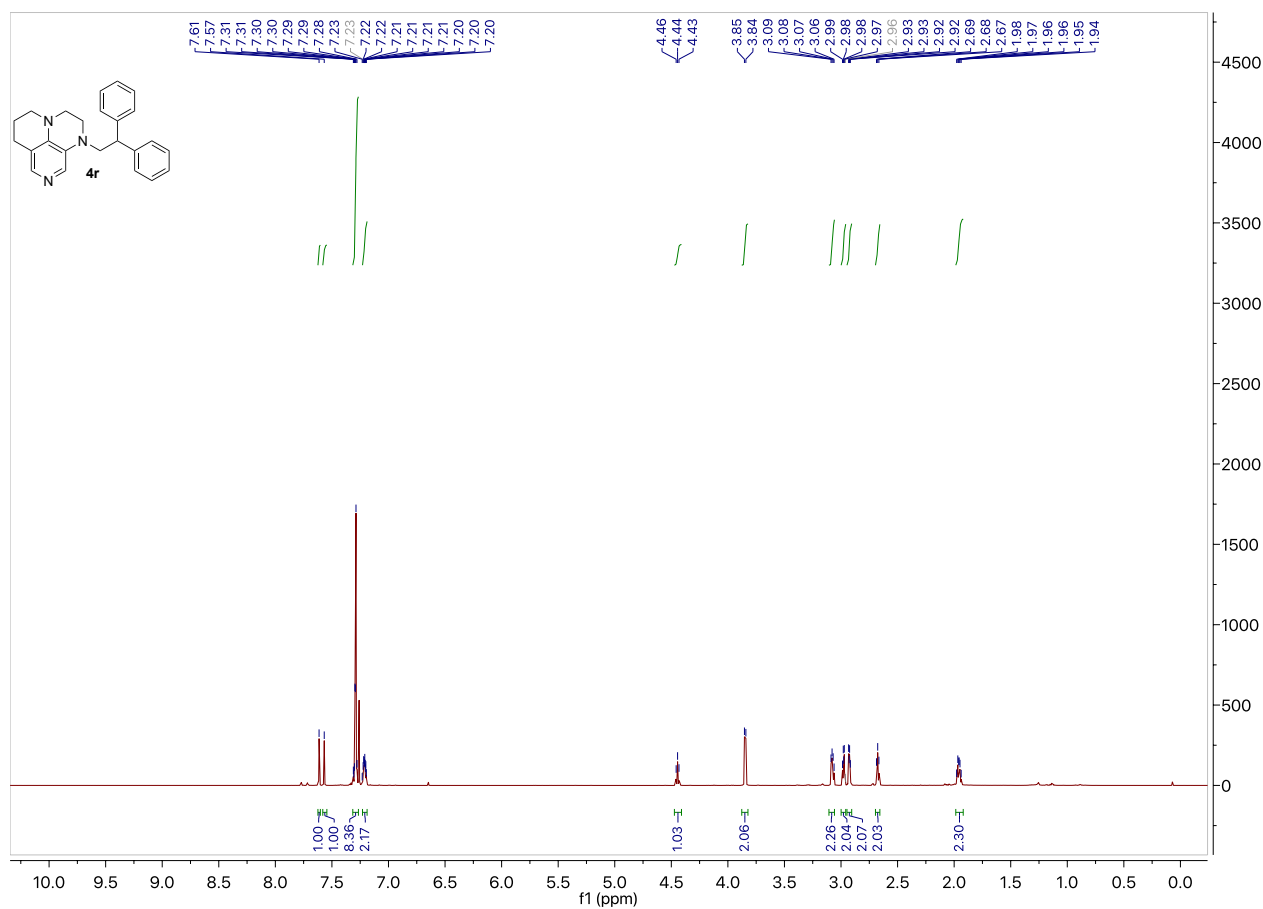
Figure 5.56. ¹H NMR spectrum of **4m** (400 MHz, CDCl₃).

Figure 5.57. ¹³C NMR spectrum of **4m** (101 MHz, CDCl₃).Figure 5.58. ¹H NMR spectrum of **4n** (400 MHz, CDCl₃).



Figure 5.61. ¹³C NMR spectrum of **4o** (101 MHz, CDCl₃).Figure 5.62. ¹H NMR spectrum of **4p** (400 MHz, CDCl₃).



Figure 5.65. ¹³C NMR spectrum of **4q** (101 MHz, CDCl₃).Figure 5.66. ¹H NMR spectrum of **4r** (400 MHz, CDCl₃).

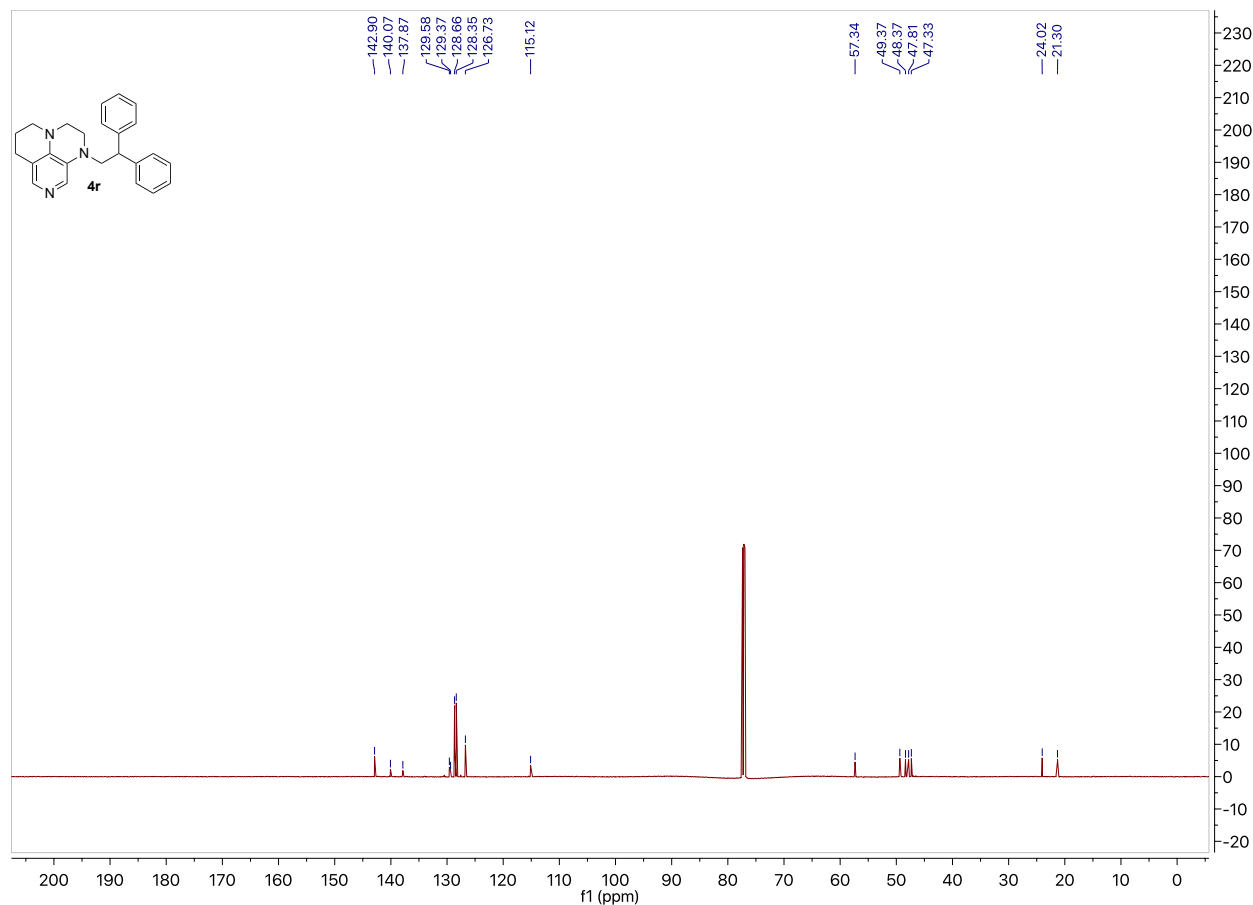


Figure 5.67. ¹³C NMR spectrum of **4r** (101 MHz, CDCl₃).

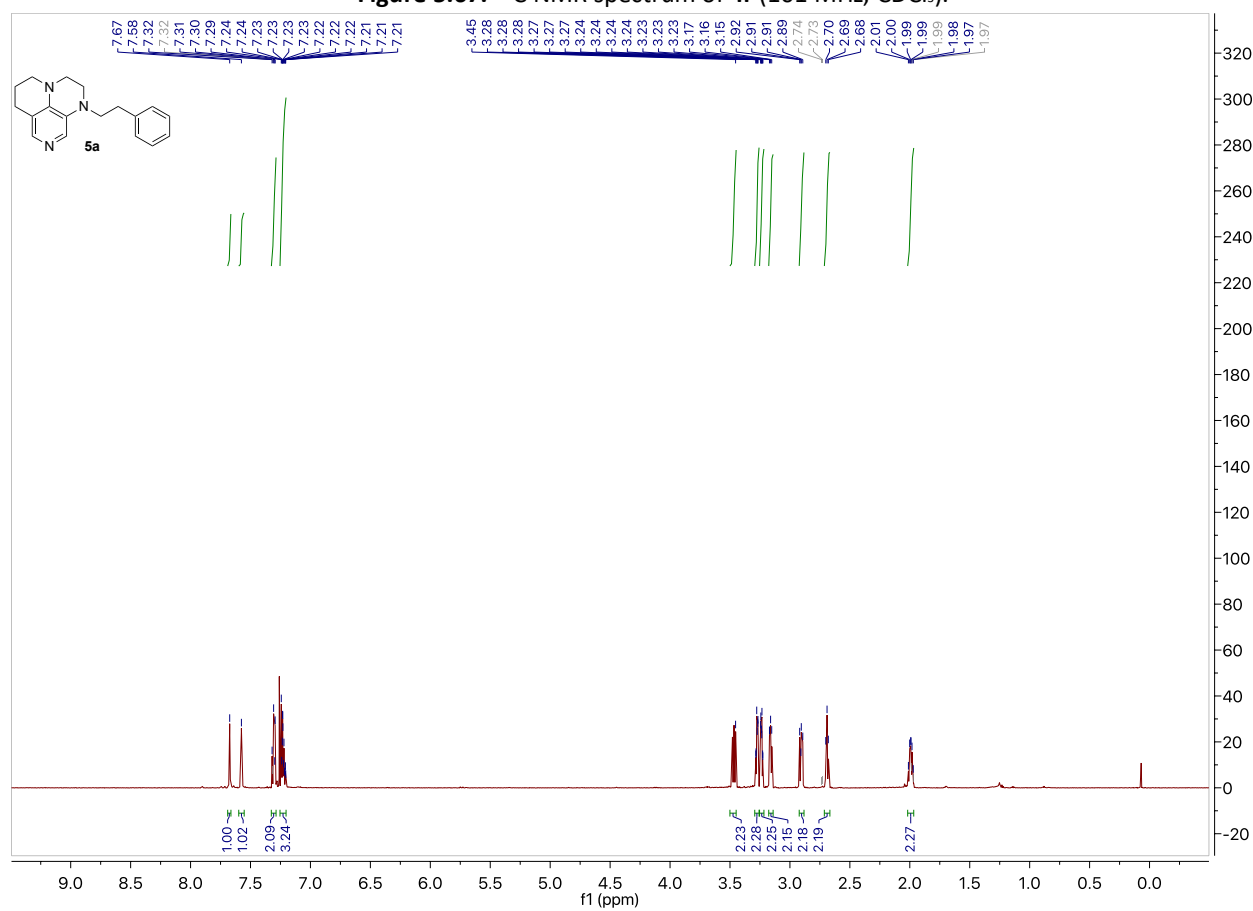
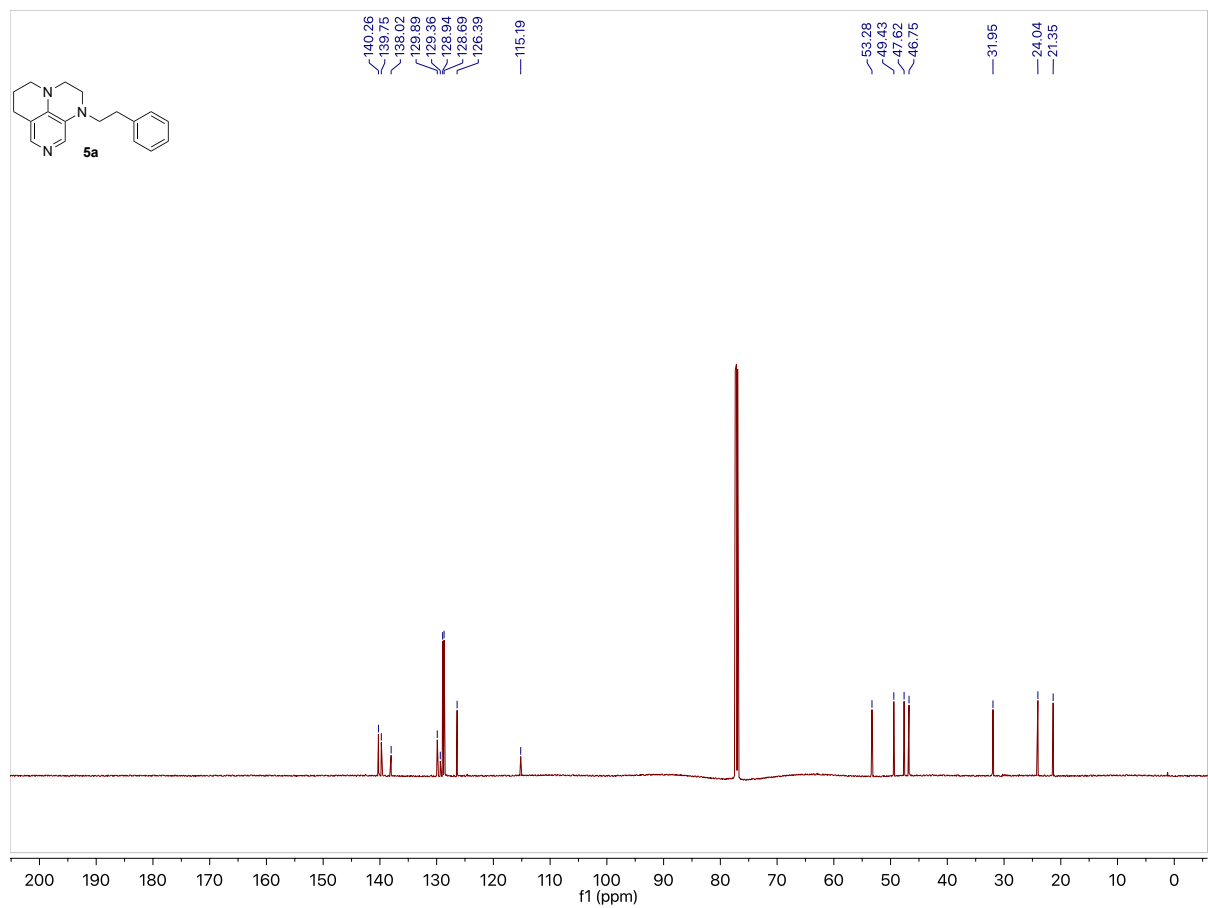
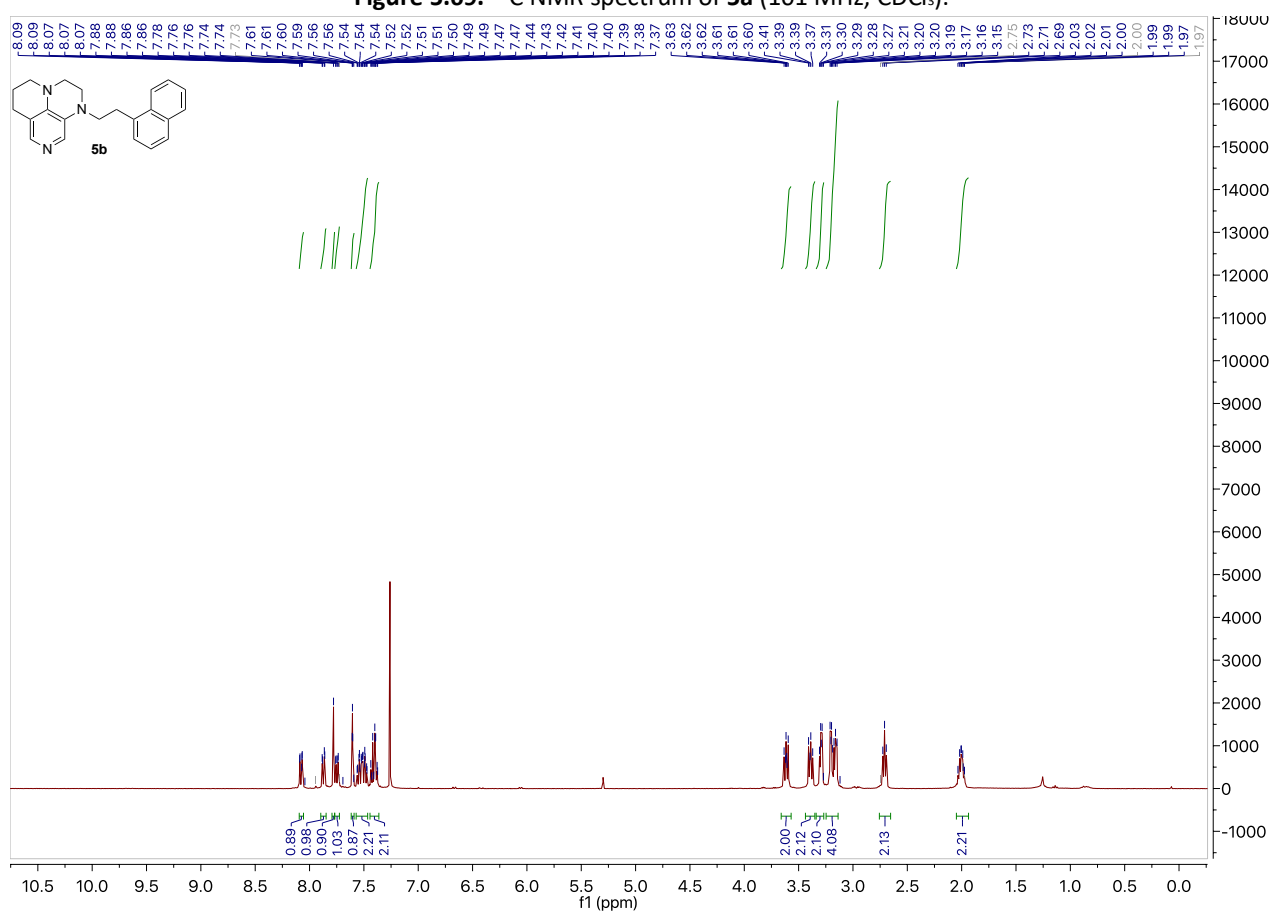


Figure 5.68. ¹H NMR spectrum of **5a** (400 MHz, CDCl₃).

Figure 5.69. ¹³C NMR spectrum of **5a** (101 MHz, CDCl₃).Figure 5.70. ¹H NMR spectrum of **5b** (400 MHz, CDCl₃).

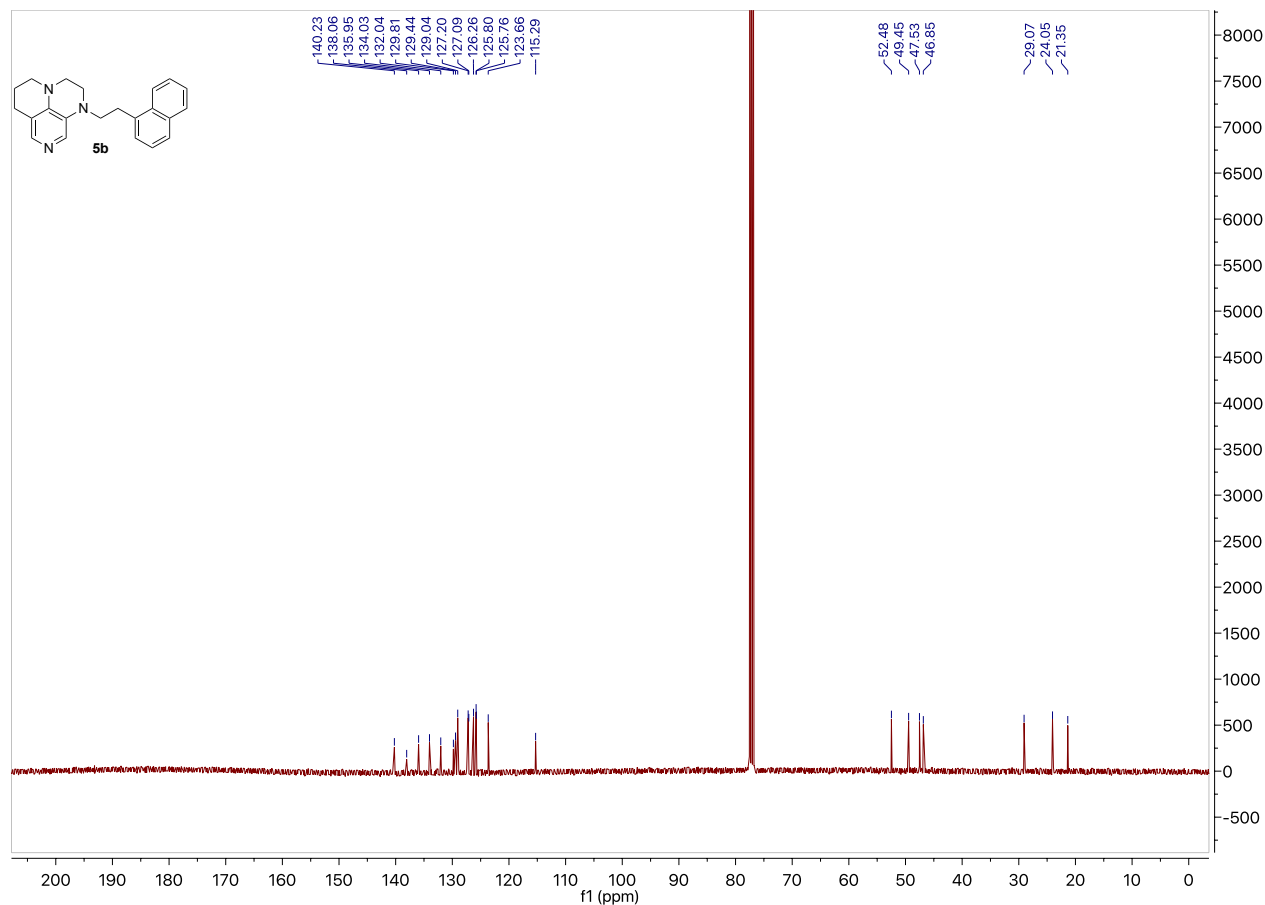


Figure 5.71. ¹³C NMR spectrum of **5b** (101 MHz, CDCl₃).

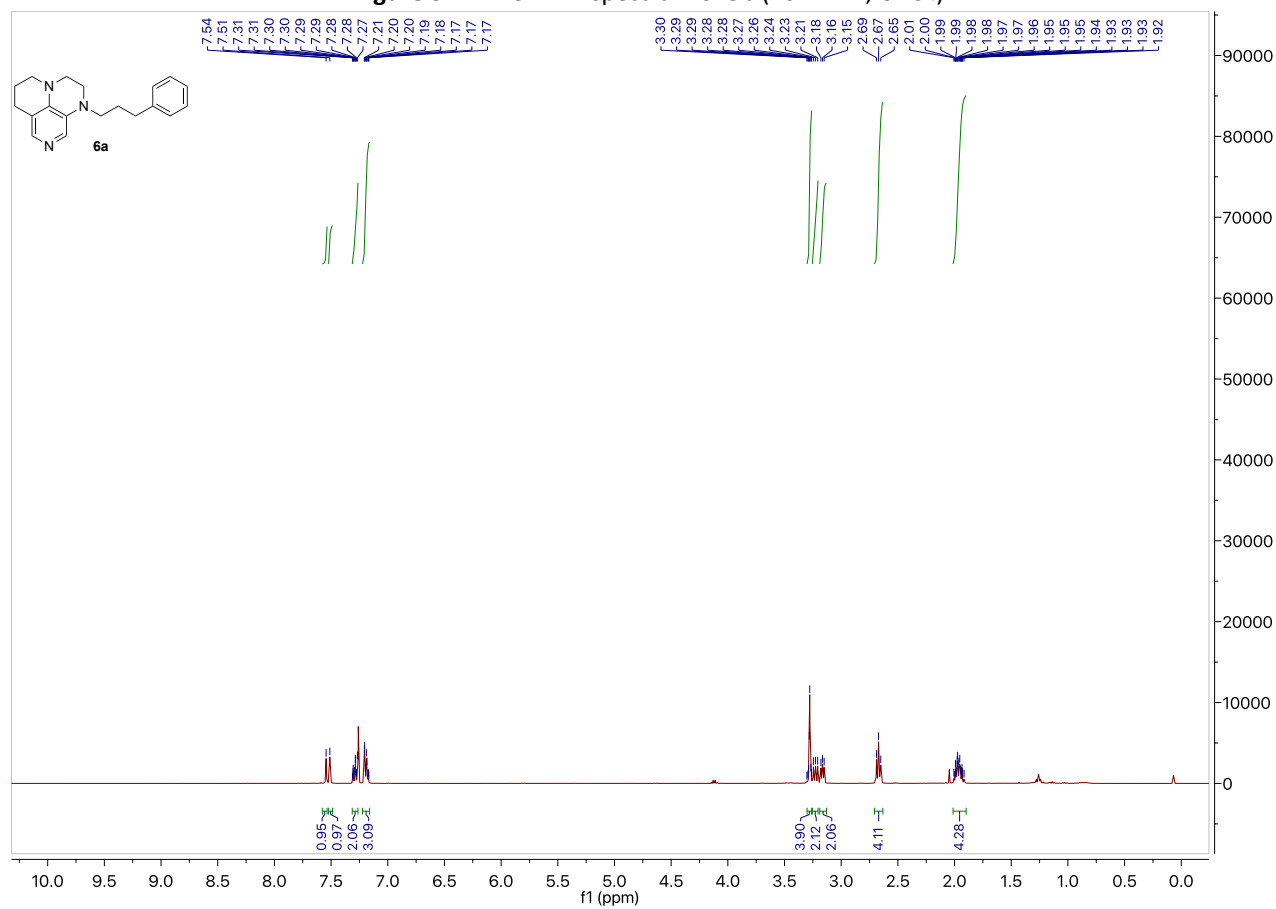
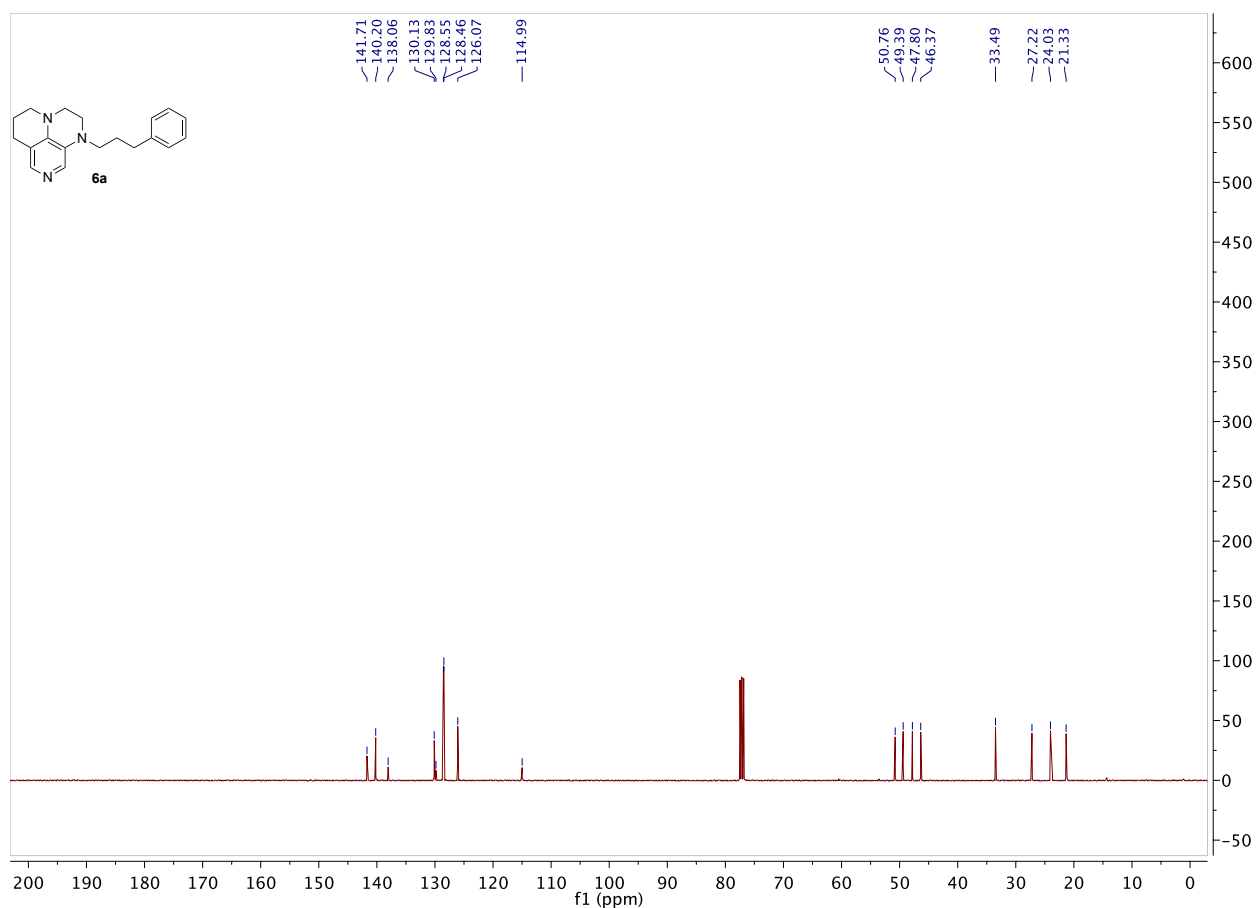
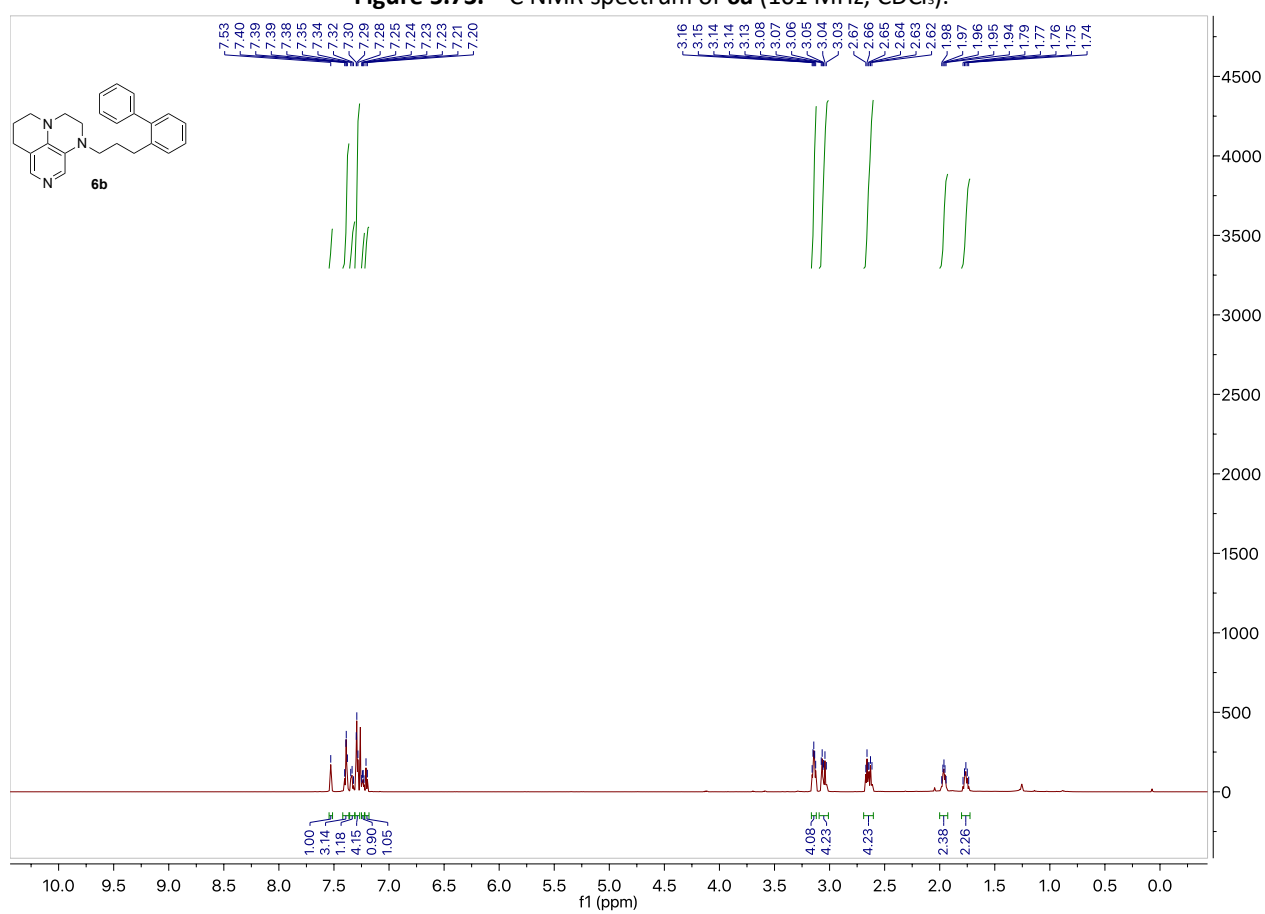


Figure 5.72. ¹H NMR spectrum of **6a** (400 MHz, CDCl₃).

Figure 5.73. ^{13}C NMR spectrum of **6a** (101 MHz, CDCl_3).Figure 5.74. ^1H NMR spectrum of **6b** (400 MHz, CDCl_3).

Annulated Pyridine Bases

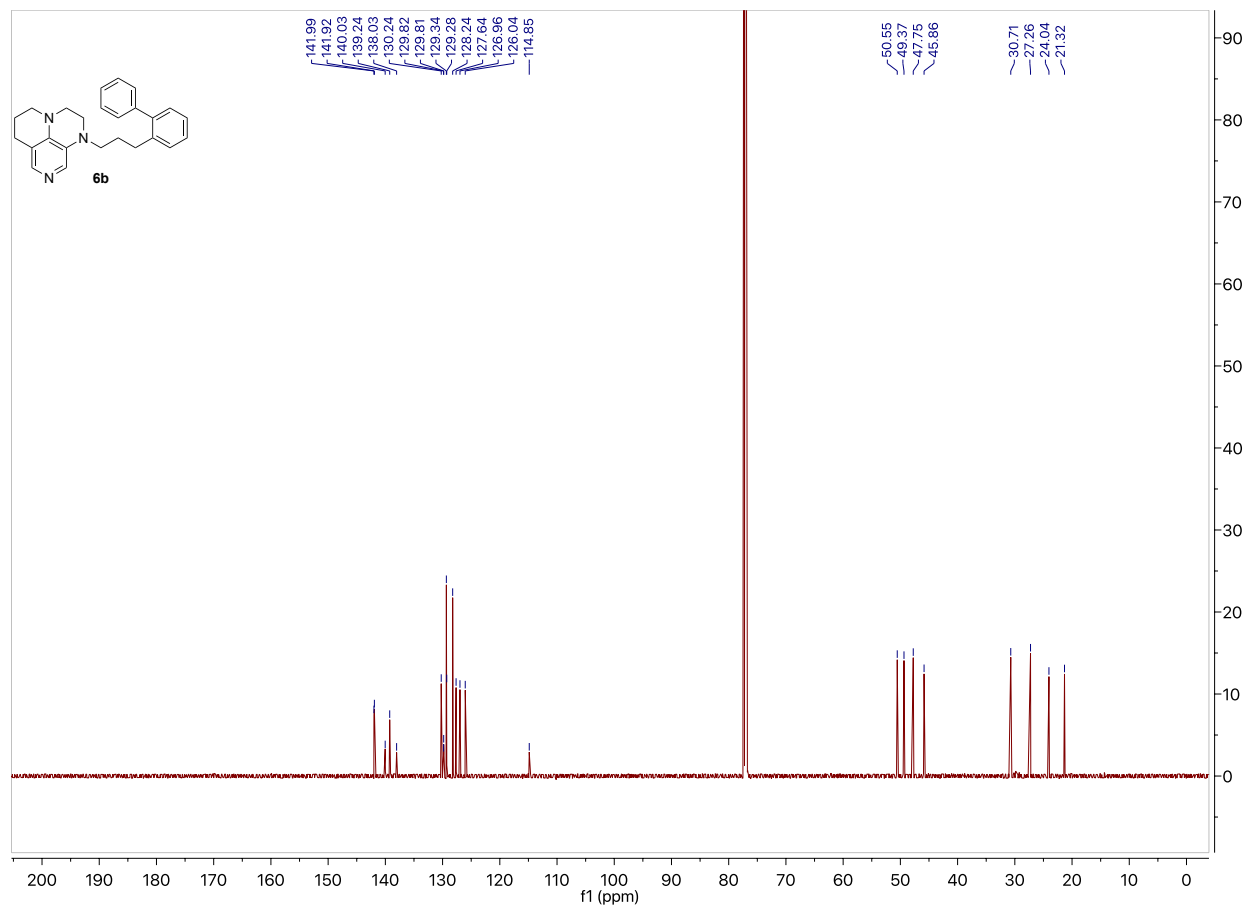


Figure 5.75. ¹³C NMR spectrum of **6b** (101 MHz, CDCl₃).

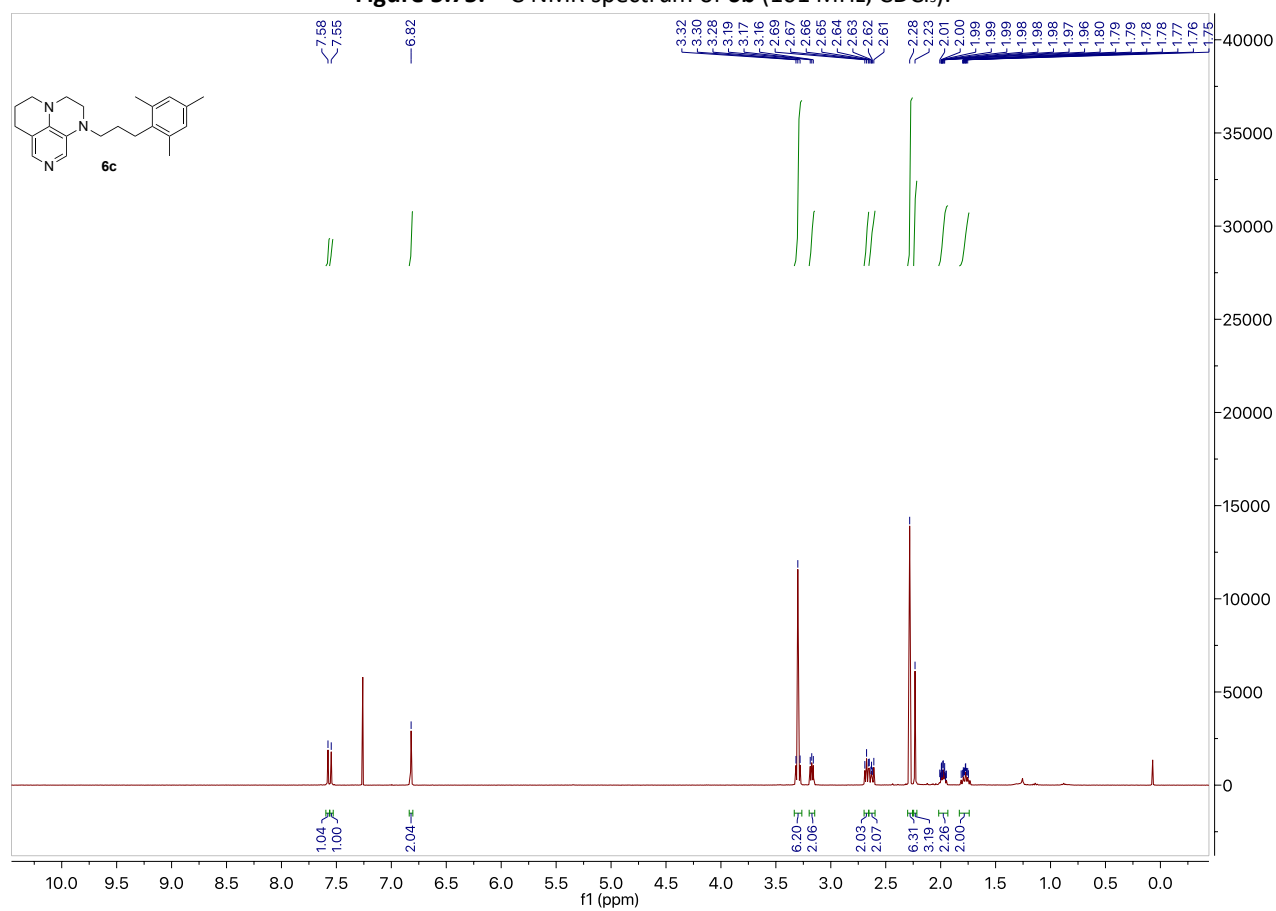
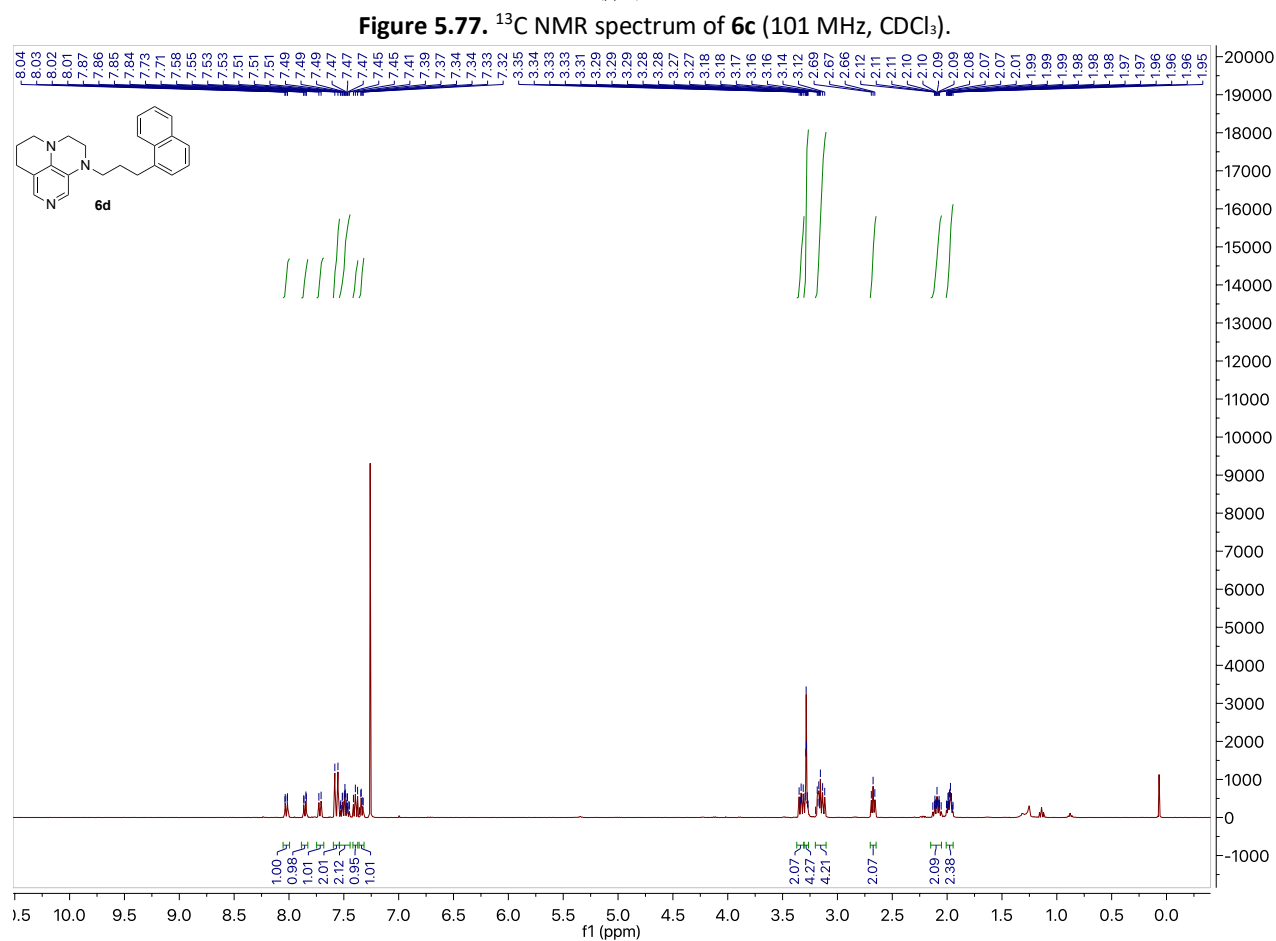
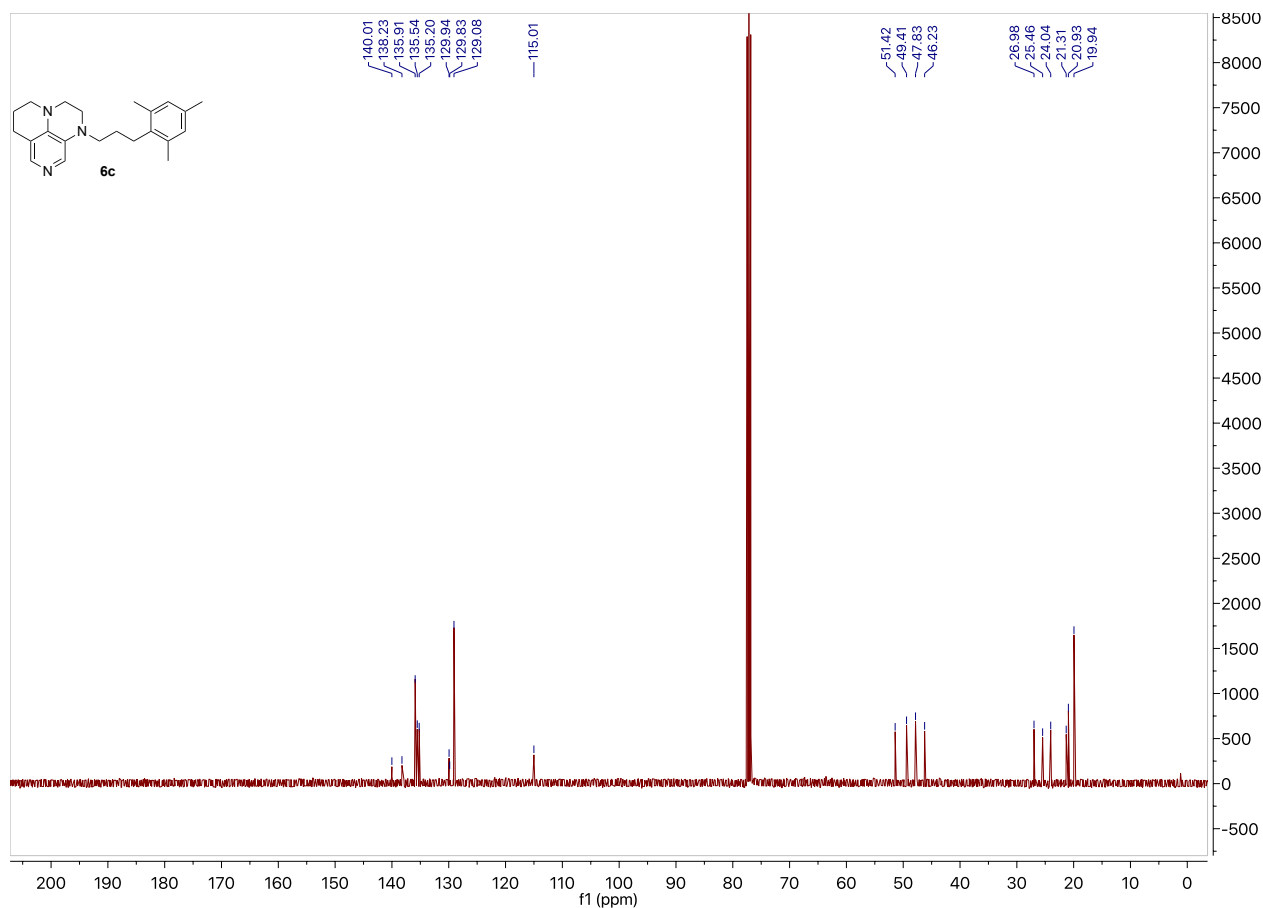


Figure 5.76. ¹H NMR spectrum of **6c** (400 MHz, CDCl₃).



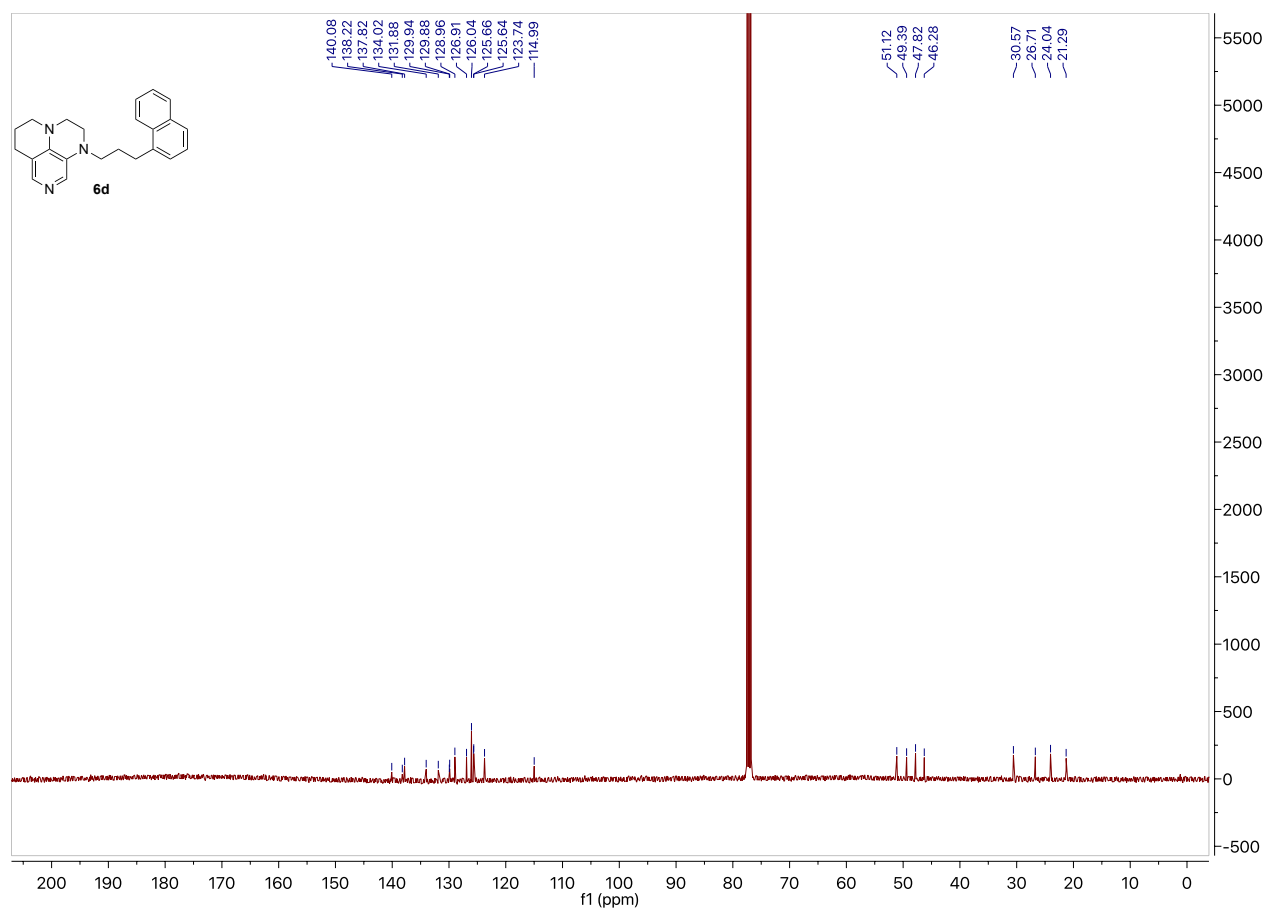


Figure 5.79. ¹³C NMR spectrum of **6d** (101 MHz, CDCl₃).

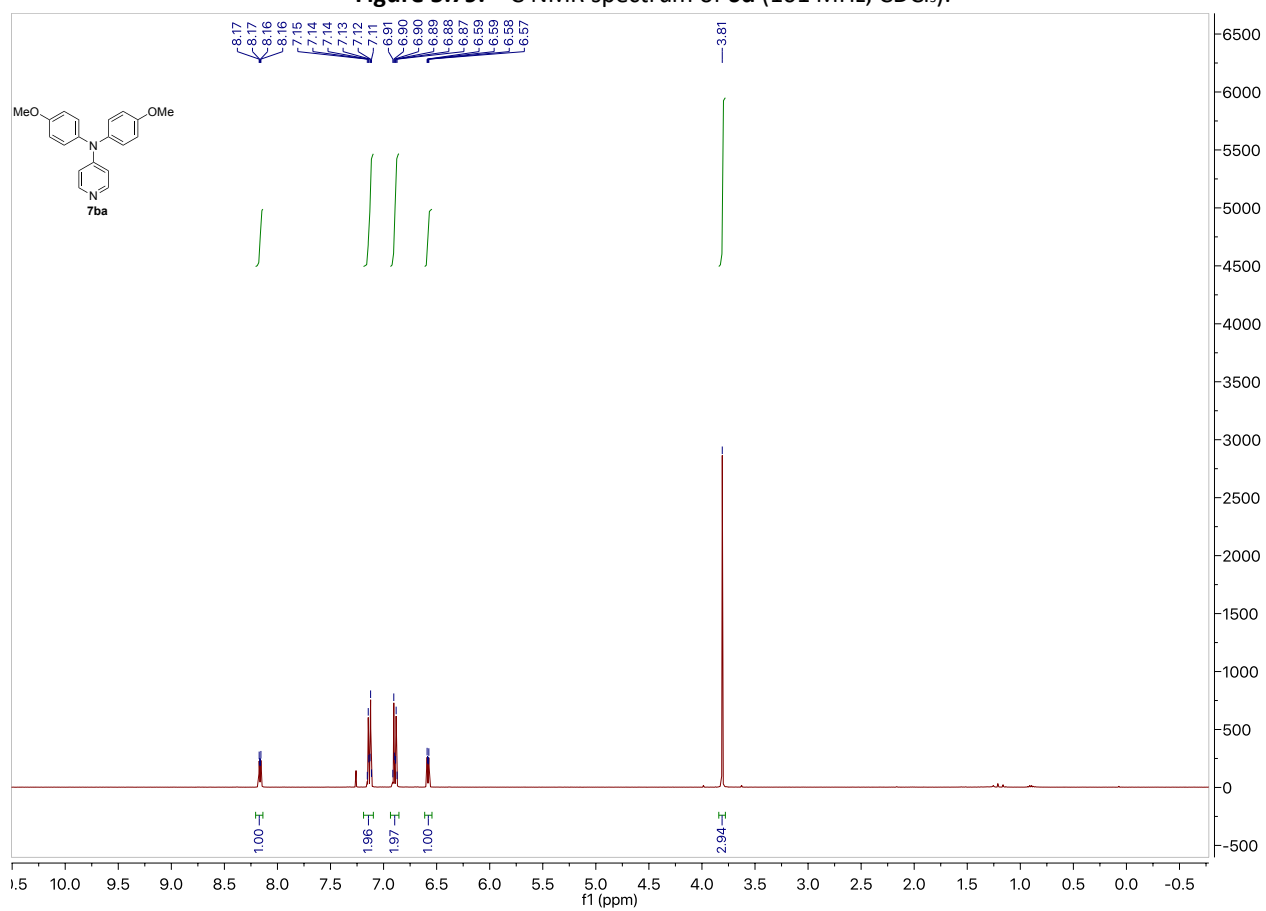
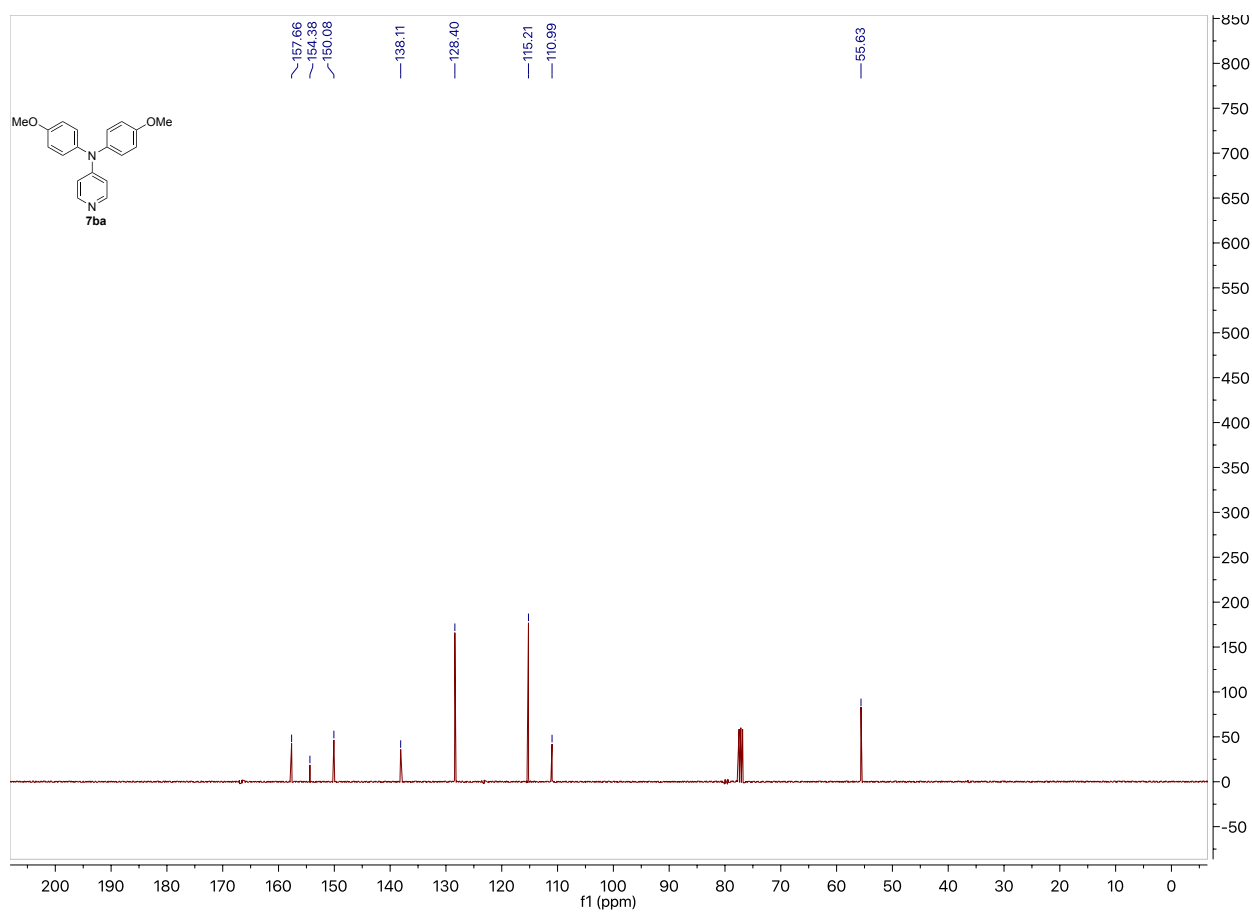
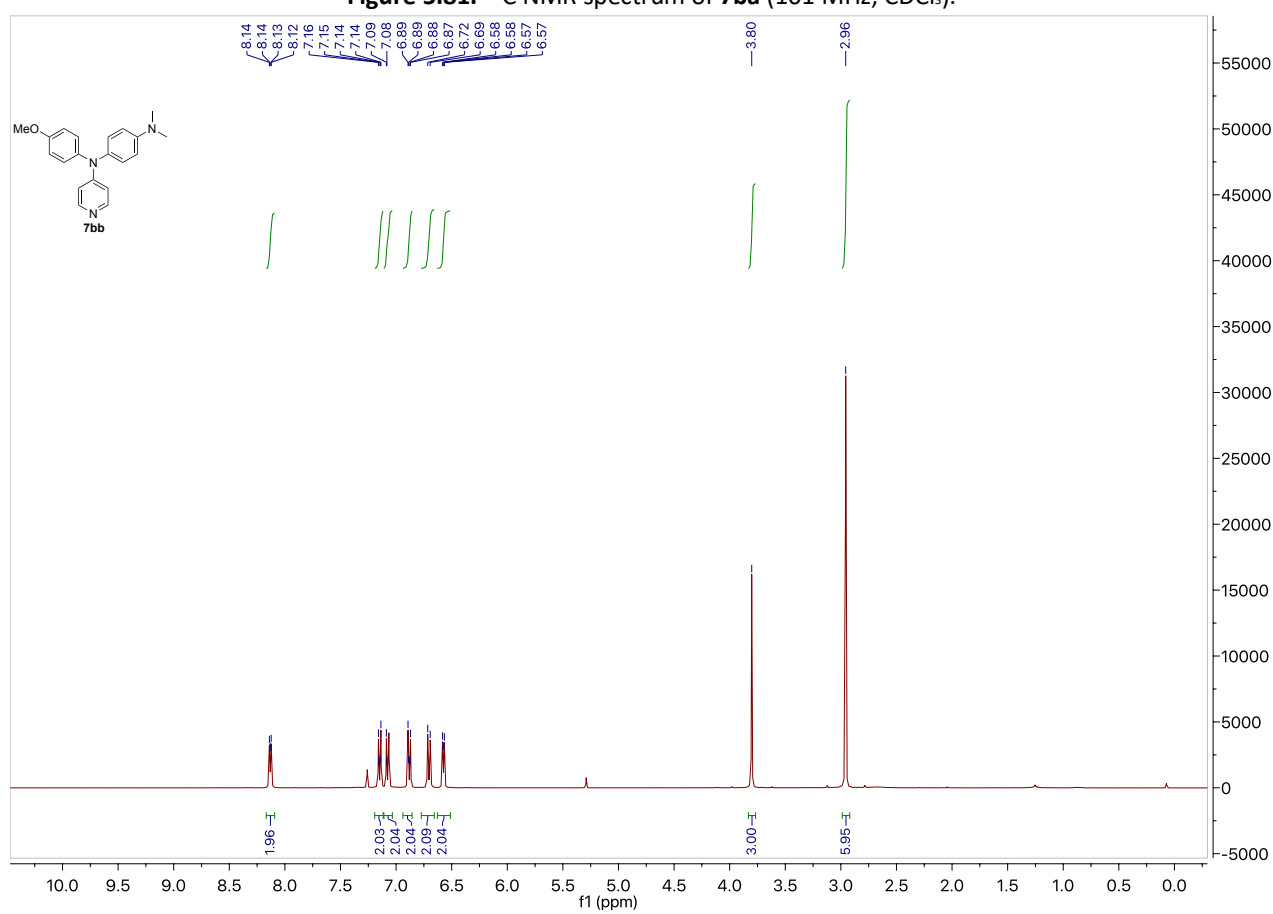
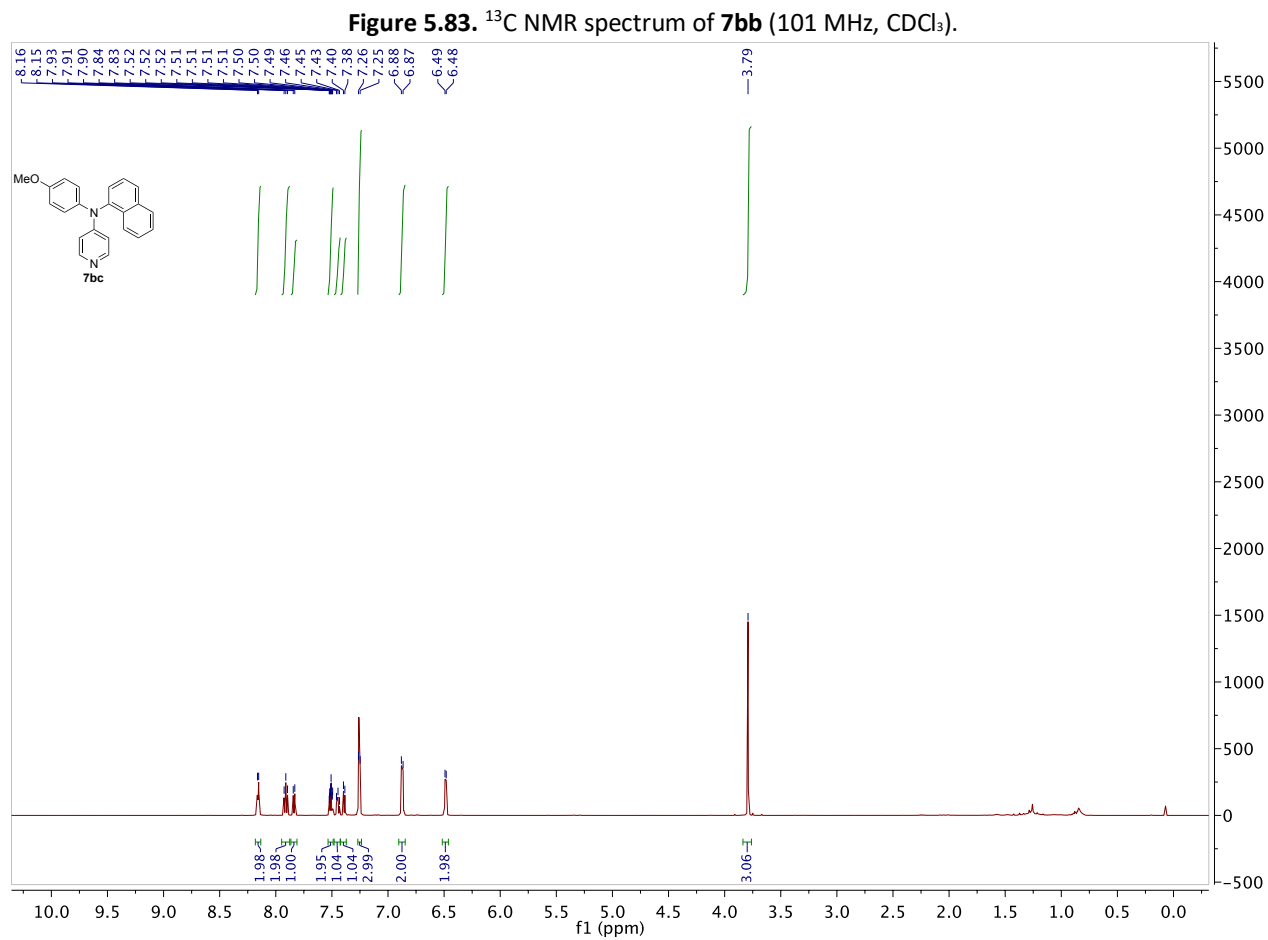
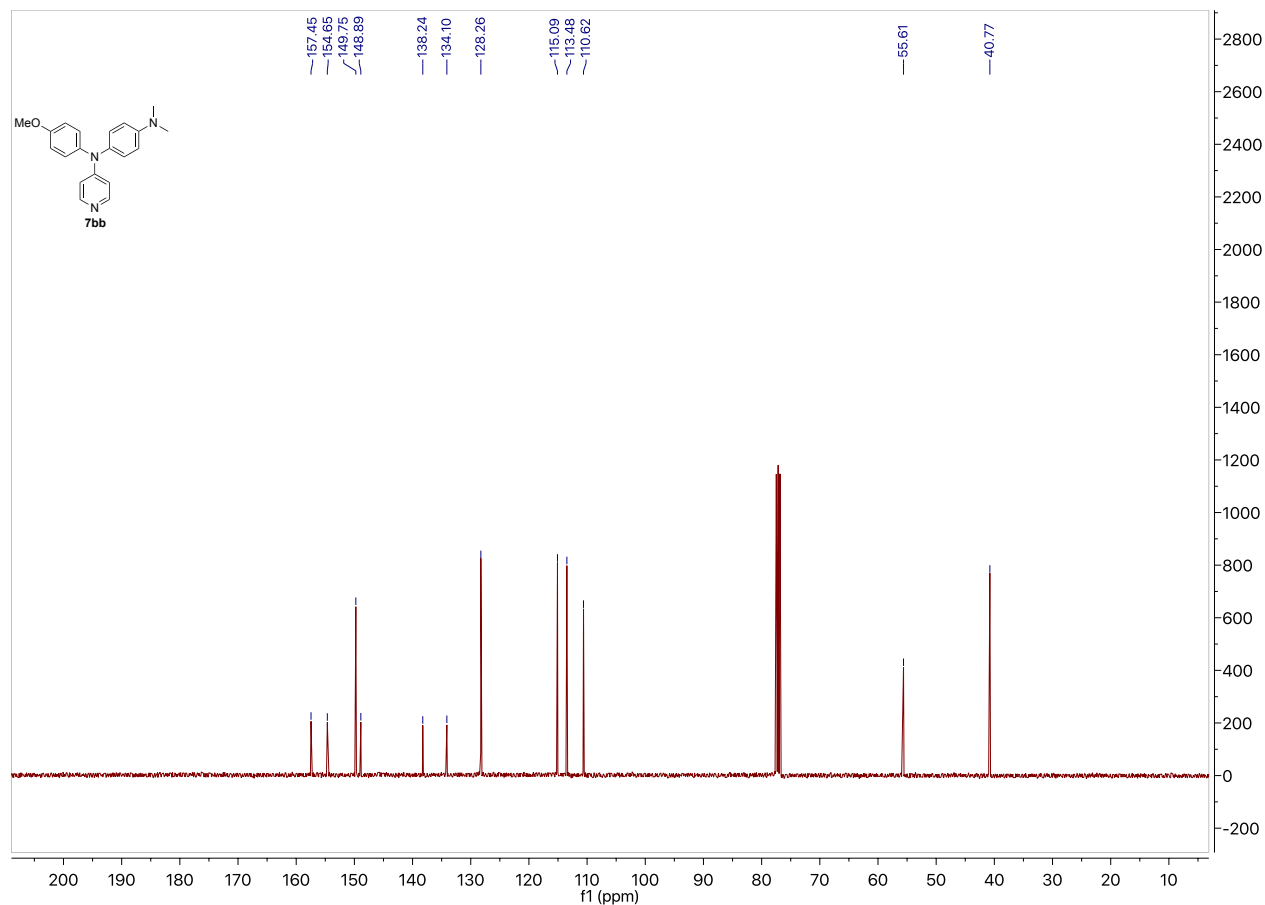
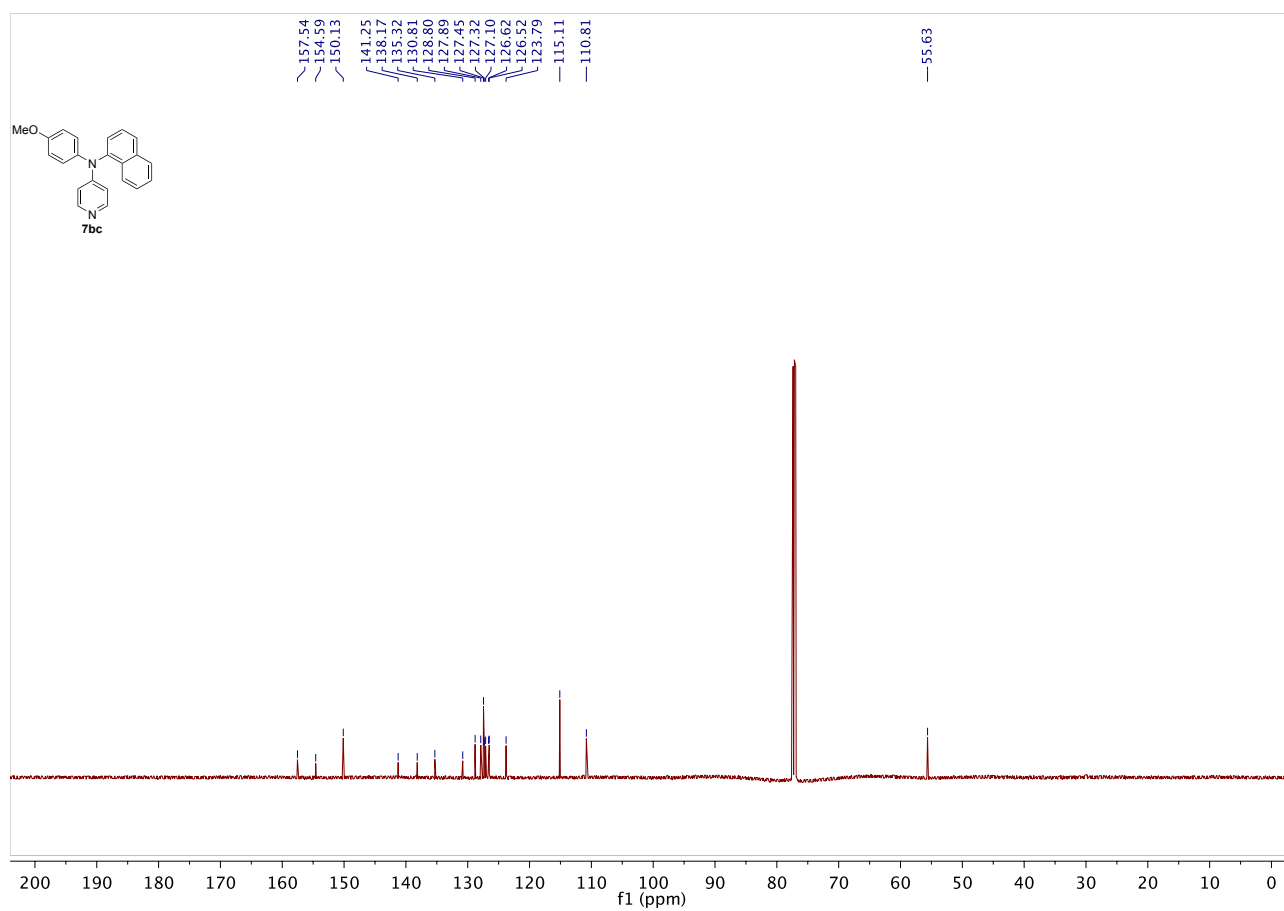
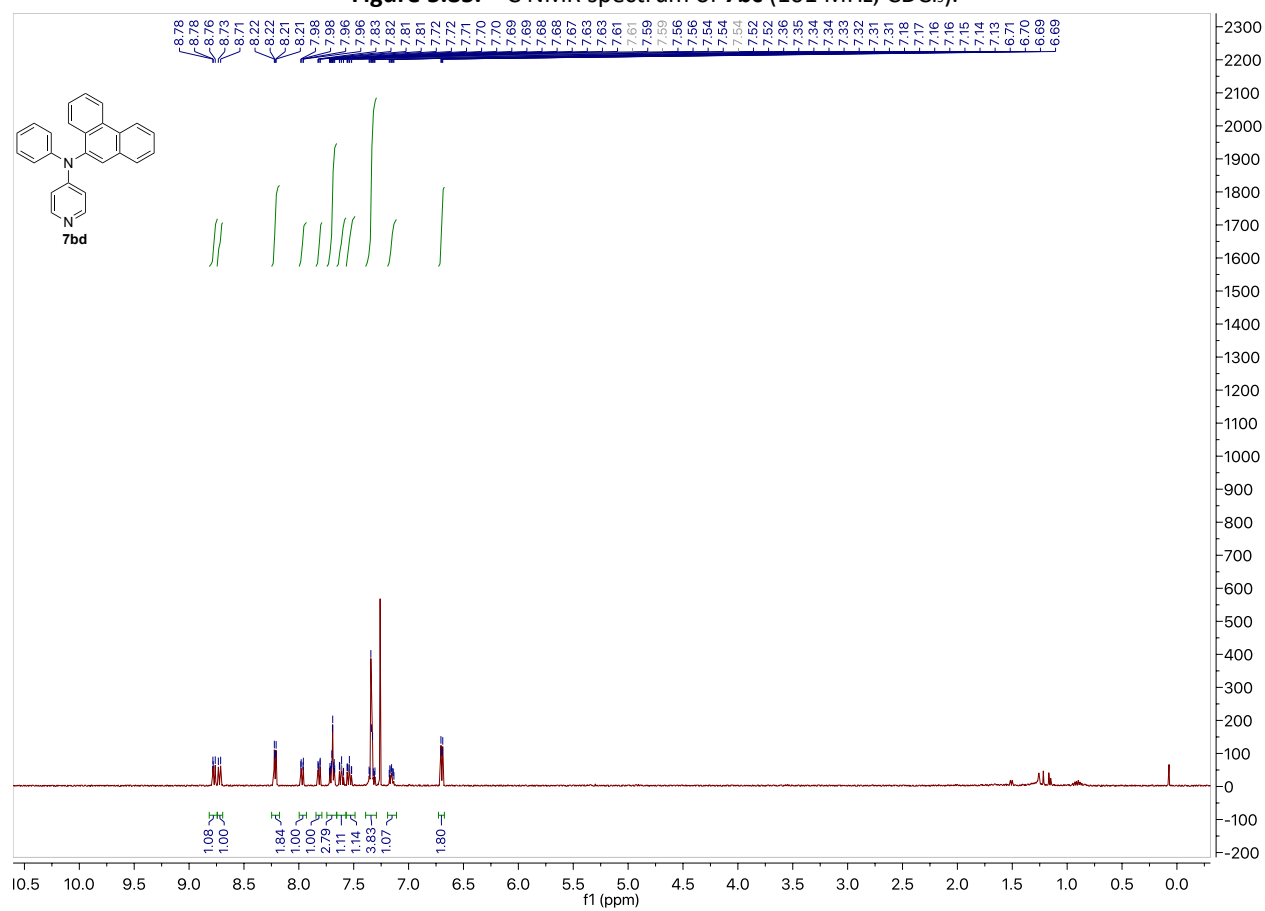


Figure 5.80. ¹H NMR spectrum of **7ba** (400 MHz, CDCl₃).

Figure 5.81. ¹³C NMR spectrum of **7ba** (101 MHz, CDCl₃).Figure 5.82. ¹H NMR spectrum of **7bb** (400 MHz, CDCl₃).

Annulated Pyridine Bases



Figure 5.85. ^{13}C NMR spectrum of **7bc** (101 MHz, CDCl_3).Figure 5.86. ^1H NMR spectrum of **7bd** (400 MHz, CDCl_3).

Annulated Pyridine Bases

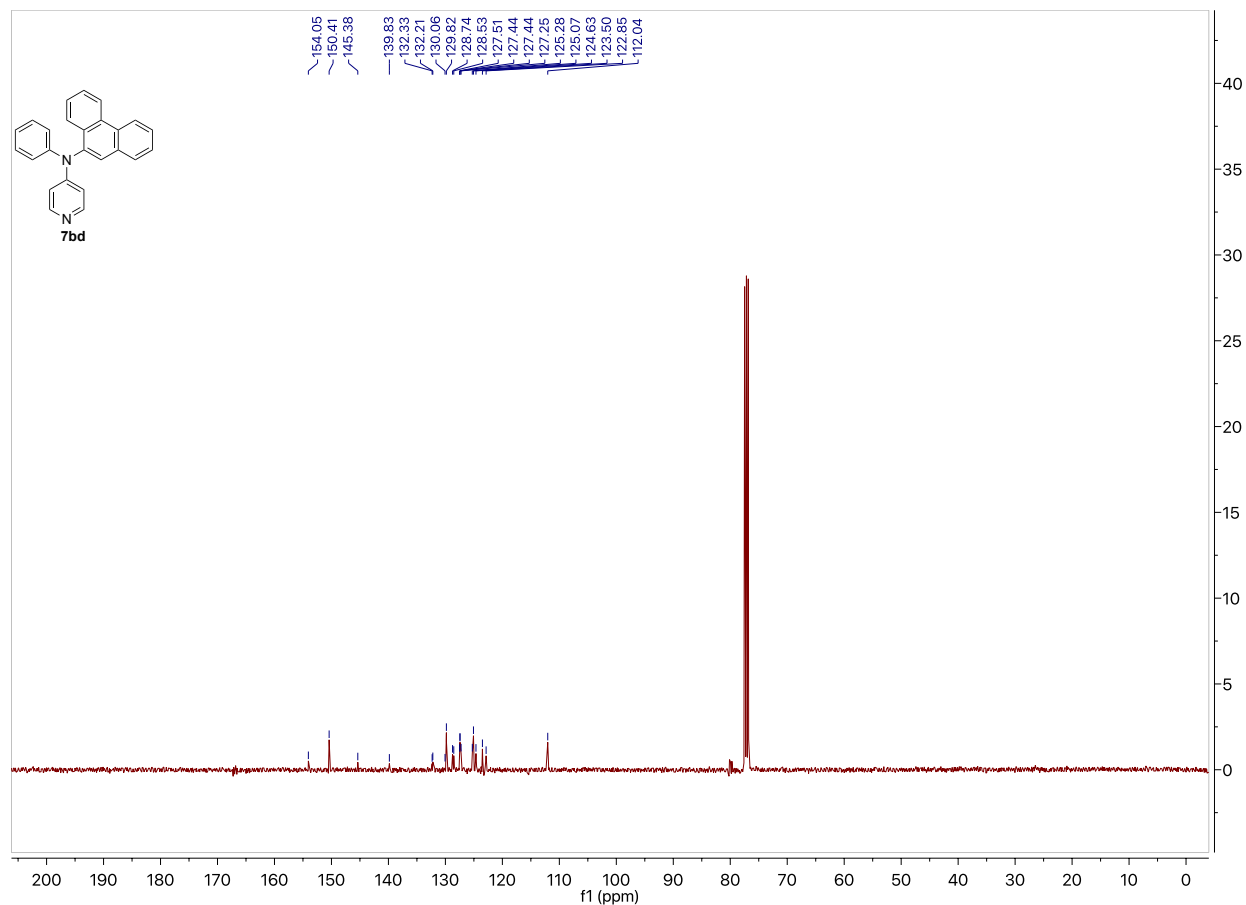


Figure 5.87. ¹³C NMR spectrum of **7bd** (101 MHz, CDCl₃).

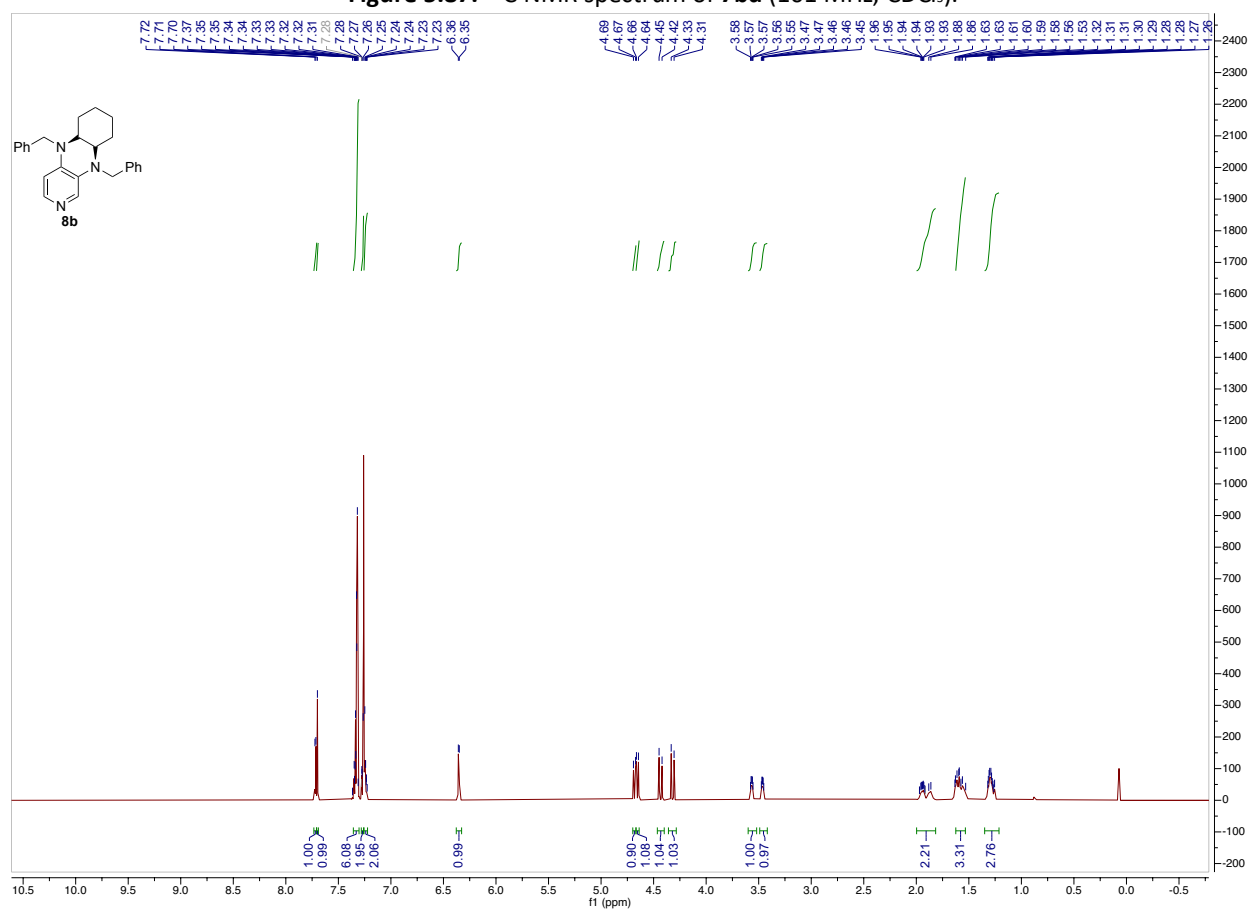


Figure 5.88. ¹H NMR spectrum of **8b** (400 MHz, CDCl₃).

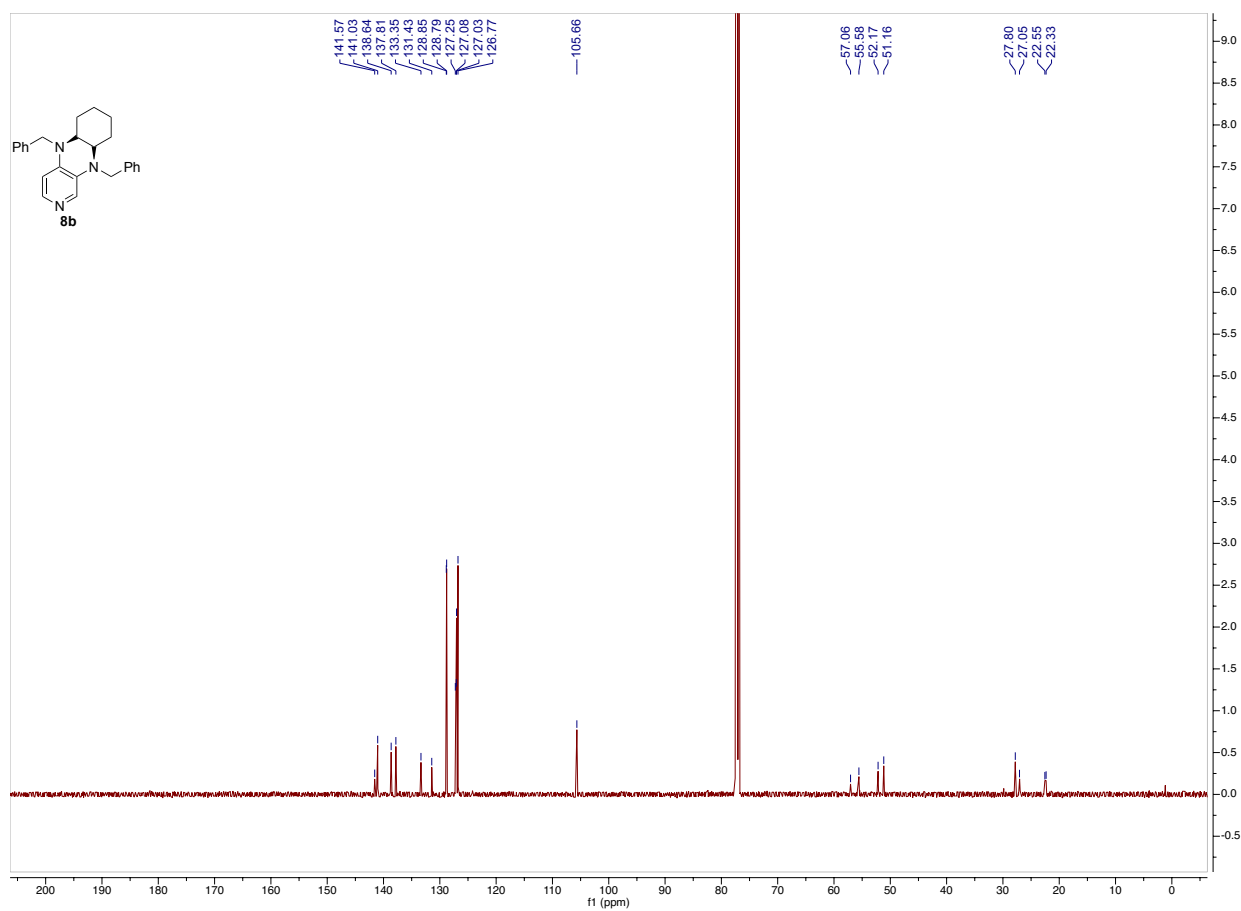


Figure 5.89. ^{13}C NMR spectrum of **8b** (101 MHz, CDCl_3).

5.1.4.5 X-Ray Data

In the following X-ray structures of **25c** (2110005), **27c** (2110006), **4p** (2110007) are listed (in the brackets the deposition number of the CCDC database is shown).

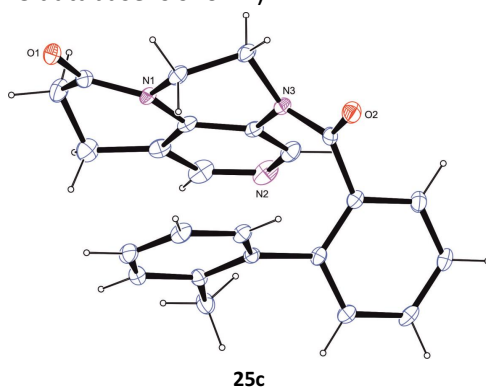


Figure 5.90. Crystal structure of **25c**. The figures have been drawn at the 50% ellipsoid probability level.^[26]

Table 5.12. Crystallographic data of **25c**. The structure has been refined as a 2-component perfect inversion twin.

net formula	C ₂₄ H ₂₁ N ₃ O ₂	absorption correction	Multi-Scan
<i>Mr</i> /g mol ⁻¹	383.44	transmission factor range	0.93–1.00
crystal size/mm	0.090 x 0.060 x 0.050	refls. measured	30939
<i>T</i> /K	103.(2)	<i>R</i> _{int}	0.0675
radiation	MoKα	mean σ(I)/I	0.0413
diffractometer	'Bruker D8 Venture TXS'	θ range	2.777–26.370
crystal system	orthorhombic	observed refls.	3531
space group	'P 21 21 21'	<i>x</i> , <i>y</i> (weighting scheme)	0.0352, 1.2015
<i>a</i> /Å	8.4800(5)	hydrogen refinement	constr
<i>b</i> /Å	14.6197(7)	Flack parameter	0.5
<i>c</i> /Å	14.8795(8)	refls in refinement	3759
α/°	90	parameters	263
β/°	90	restraints	0
γ/°	90	<i>R</i> (<i>F</i> _{obs})	0.0432
<i>V</i> /Å ³	1844.69(17)	<i>R</i> <i>w</i> (<i>F</i> ²)	0.1070
<i>Z</i>	4	<i>S</i>	1.036
calc. density/g cm ⁻³	1.381	shift/error _{max}	0.001
μ/mm ⁻¹	0.090	max electron density/e Å ⁻³	0.261
		min electron density/e Å ⁻³	-0.226

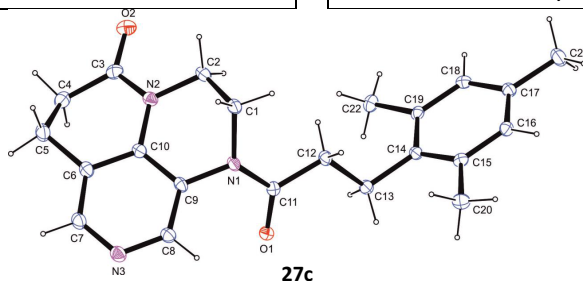


Figure 5.91. Crystal structure of **27c**. The figures have been drawn at the 50% ellipsoid probability level.^[26]

Table 5.13. Crystallographic data of **27c**. The structure has been refined as a 2-component perfect inversion twin.

net formula	C ₂₂ H ₂₅ N ₃ O ₂	absorption correction	Multi-Scan
<i>Mr</i> /g mol ⁻¹	363.45	transmission factor range	0.97–1.00
crystal size/mm	0.030 × 0.020 × 0.020	refls. measured	35146
<i>T</i> /K	106.(2)	<i>R</i> _{int}	0.0505
radiation	MoKα	mean σ(I)/I	0.0243

diffractometer	'Bruker D8 Venture TXS'	θ range	3.030–27.103
crystal system	orthorhombic	observed refls.	3722
space group	'P c a 21'	x, y (weighting scheme)	0.0455, 0.5431
$a/\text{\AA}$	15.2512(4)	hydrogen refinement	constr
$b/\text{\AA}$	8.5443(2)	Flack parameter	0.5
$c/\text{\AA}$	14.2394(4)	refls in refinement	4087
$\alpha/^\circ$	90	parameters	247
$\beta/^\circ$	90	restraints	1
$\gamma/^\circ$	90	$R(F_{obs})$	0.0340
$V/\text{\AA}^3$	1855.55(8)	$Rw(F^2)$	0.0940
Z	4	S	1.067
calc. density/ g cm^{-3}	1.301	shift/error _{max}	0.001
μ/mm^{-1}	0.085	max electron density/ e \AA^{-3}	0.146
		min electron density/ e \AA^{-3}	-0.182

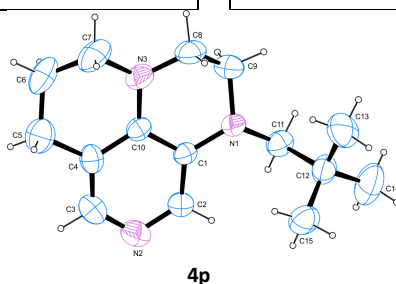


Figure 5.92. Crystal structure of **4p**. The figures have been drawn at the 50% ellipsoid probability level.^[26]

Table 5.14. Crystallographic data of **4p**. Refined as perfect inversion twin. There are two formula units in the asymmetric unit. Both show disorder of one C atom. Split models have been applied with anisotropic refinement. The ratio of site occupation factors refined to about 0.75/0.25. One of the two molecules is shown above containing the main disordered part.

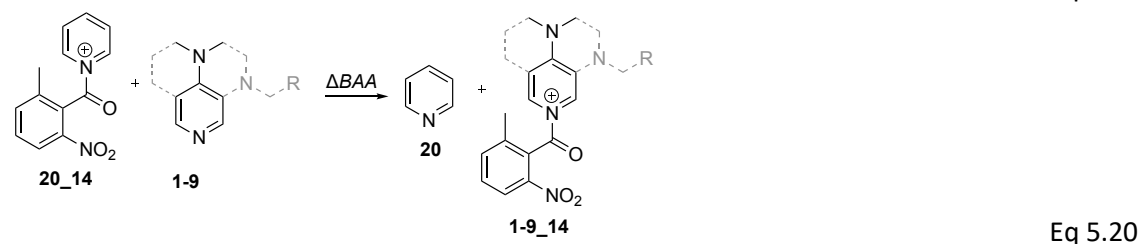
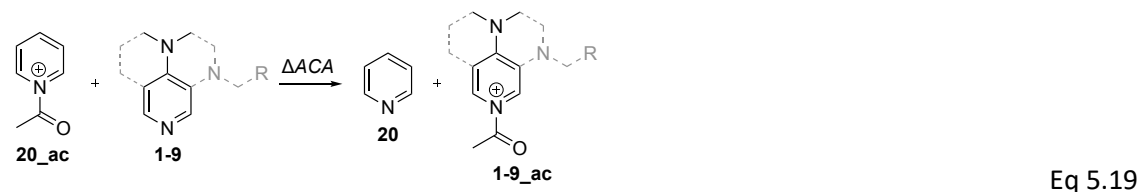
net formula	$\text{C}_{15}\text{H}_{23}\text{N}_3$	absorption correction	Multi-Scan
$M_r/\text{g mol}^{-1}$	245.36	transmission factor range	0.94–1.00
crystal size/mm	0.080 x 0.060 x 0.020	refls. measured	29839
T/K	296.(2)	R_{int}	0.0492
radiation	MoK α	mean $\sigma(I)/I$	0.0345
diffractometer	'Bruker D8 Venture TXS'	θ range	2.599–25.350
crystal system	orthorhombic	observed refls.	3660
space group	'P n a 21'	x, y (weighting scheme)	0.0765, 0.5844
$a/\text{\AA}$	15.6722(8)	hydrogen refinement	constr
$b/\text{\AA}$	9.5856(4)	Flack parameter	0.5
$c/\text{\AA}$	18.8142(9)	refls in refinement	5076
$\alpha/^\circ$	90	parameters	351
$\beta/^\circ$	90	restraints	3
$\gamma/^\circ$	90	$R(F_{obs})$	0.0523
$V/\text{\AA}^3$	2826.4(2)	$Rw(F^2)$	0.1487
Z	8	S	1.050
calc. density/ g cm^{-3}	1.153	shift/error _{max}	0.001
μ/mm^{-1}	0.070	max electron density/ e \AA^{-3}	0.227
		min electron density/ e \AA^{-3}	-0.185

5.2 Computational Study

General information. All geometry optimizations and vibrational frequency calculations have been performed using the B3LYP-D3 hybrid functional^[27] in combination with the 6-31+G(d) basis set.^[28] Solvent effects for chloroform have been taken into account with the SMD continuum solvation model.^[29] This combination has recently been found to perform well for the description of charge-separated intermediates.^[30] Thermochemical corrections to 298.15 K have been calculated for all minima from unscaled vibrational frequencies obtained at this same level. Solvation energies have been obtained as the difference between the energies computed at B3LYP-D3/6-31+G(d) in solution and in gas phase. For the elucidation of the intermediat **INT1**, the thermochemical corrections of optimized structures have been combined with single point energies calculated at the DLPNO-CCSD(T)/def2-TZVPP//B3LYP-D3/6-31+G(d) level.^[31] Solvation energies have been added to the energy computed at DLPNO-CCSD(T)/def2-TZVPP//SMD(CHCl₃)/B3LYP-D3/6-31+G(d) level to yield free energies G_{298} at 298.15 K. Free energies in solution have been corrected to a reference state of 1 mol l⁻¹ at 298.15 K through addition of $RT\ln(24.46) = +7.925$ kJ mol⁻¹ to the free energies. All calculations have been performed with Gaussian 09^[32] and ORCA version 4.0.^[33] Conformational search was performed with Maestro.^[34]

5.2.1 Cation Affinities Values

Based on previous studies of the Zipse group^[1,30a,35] and already assumed in Chapters 3 and 4 we hypothesized that catalysts **1-9** act as Lewis rather than Brönsted bases. One method to describe the Lewis basicity and activity of organocatalysts, is the determination of acetyl cation affinities value (ΔACA , Table 5.15).^[22b,36] Thereby the difference in reaction enthalpy is calculated of the acyl transfer from pyridine **20_ac** to the more Lewis basic organocatalysts **1-9** forming acetylpyridinium cations **1-9_ac** according to equation 5.19. Also benzoic anhydride affinity values (ΔBAA , Table 5.16) according to equation 5.20 were determined, whereby instead of the acyl transfer the transfer of the here studied 2-methyl-6-nitro benzoate were computed.



Scheme 5.16. Model of acetyl cation affinity (ΔACA , Eq. 5.19) and benzoic affinity number (ΔBAA , Eq. 5.20)

In this study the ΔACA were determined out of more catalysts than we experimentally synthesized and explored. Figure 5.93 shows the structure of all catalysts **1-9** which were explored by DFT-methods in this chapter.

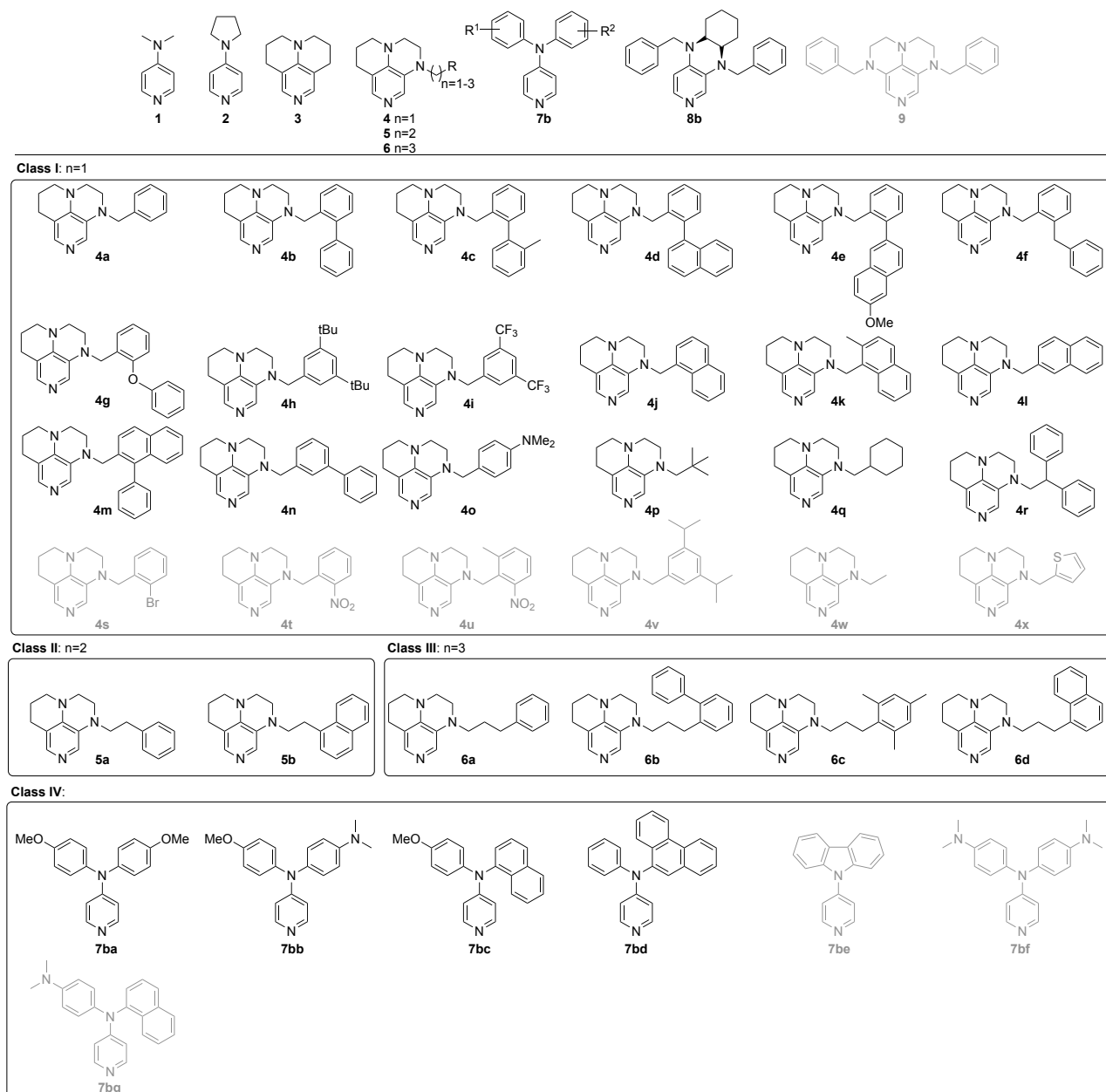
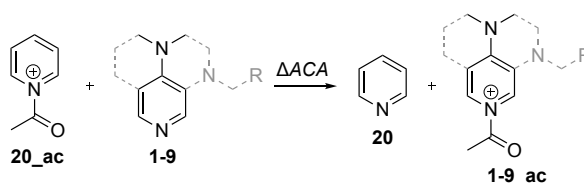


Figure 5.93. Structures of catalysts used in the quantum chemical analysis of the affinity values ΔACA . The black highlighted catalysts were synthesized, used in turnover-limited competition studies and were computed with DFT-models. The grey highlighted catalysts were only computed with DFT-models.

Table 5.15. Total energies, enthalpies, and free energies for catalysts **1-9** (in Hartree). The SMD(CHCl₃)/B3LYP-D3/6-31+G(d) level of theory has been used to calculate the cationic affinity number based on acetyl. Conformational search of catalysts **4c-e** is based on the best 5 conformers of **4b**, **4m** is based on the best 10 conformers of **4b**, **4g** is based on the best 15 conformers of **4f**, **4i** is based on the best 15 conformers of **4h**, **5b** is based on the best 5 conformers of **5a**, **6c** is based on the best 10 conformers of **6a** and **6d** is based on the best 5 conformers of **6a**. (Note that the filenames are used in our calculations and do not follow any guide.)



Catalyst	Filename	E_{tot} SMD/B3LYP-D3/ 6-31+G(d)	H_{298} SMD/B3LYP-D3/ 6-31+G(d)	G_{298} SMD/B3LYP-D3/ 6-31+G(d)	ΔACA
20	cat_001.log	-248.3105322	-248.2133405	-248.2459755	0
20_ac	cat_002.log	-401.3988257	-401.2474645	-401.2883245	

Annelated Pyridine Bases

1	DMAP_1_2.log	-382.2995489	-382.1243915	-382.1671115	-57.9
1_ac	dmap_ac_1.log	-535.4106351	-535.1805795	-535.2307315	
2	ppy_1	-459.7357421	-459.5231405	-459.5677125	-63.1
2_ac	ppy_ac_1	-612.8486385	-612.5813125	-612.6336005	
3	TCAP_1.log	-537.1790988	-536.9291045	-536.9755585	-75.0
	TCAP_2.log	-537.1786144	-536.9286495	-536.9750885	
3_ac	TCAP_ac_2.log	-690.2967017	-689.9917895	-690.0455805	
	TCAP_ac_1.log	-690.2959049	-689.9904955	-690.0445575	
4a	R1_5	-823.5991141	-823.2453426	-823.3063836	-81.5
	R1_4	-823.5988017	-823.2451282	-823.3063712	
4a_ac	R1_ac_6	-976.7192175	-976.3105110	-976.3789670	
	R1_ac_2	-976.7186426	-976.3095921	-976.3777831	
4b	R1_Ph2Ph_6	-1054.6785317	-1054.2390812	-1054.3101252	-85.4
	R1_Ph2Ph_14	-1054.6782515	-1054.2391050	-1054.3104740	
4b_ac	R1_Ph2Ph_ac_10	-1207.8001445	-1207.3057520	-1207.3839050	
	R1_Ph2Ph_ac_30	-1207.8000262	-1207.3055257	-1207.3852147	
4c	R1_Ph2Tol_6b.com	-1094.0006262	-1093.5319357	-1093.6069007	-85.3
	R1_Ph2Tol_25.com	-1093.9995051	-1093.5309886	-1093.6068436	
4c_ac	R1_Ph2Tol_ac_10b.com	-1247.1220155	-1246.5993880	-1246.6784700	
	R1_Ph2Tol_ac_30b.com	-1247.1217624	-1246.5975049	-1246.6780229	
4d	R1_Ph1Np_6.com	-1208.3394277	-1207.8505922	-1207.9272952	-87.6
	R1_Ph1Np_6b.com	-1208.3383912	-1207.8493837	-1207.9257867	
4d_ac	R1_1Np_ac_30b.com	-1361.4619357	-1360.9178592	-1361.0019372	
	R1_1Np_ac_10b.com	-1361.4616989	-1360.9180634	-1361.0032114	
4e	R1_Ph2NpOMe_14b.com	-1322.8703820	-1322.3462255	-1321.9070605	-93.6
	R1_Ph2NpOMe_6b.com	-1322.8702104	-1322.3463659	-1321.9075959	
4e_ac	R1_Ph2NpOMe_ac_30.com	-1475.9950185	-1475.4156820	-1474.9275140	
	R1_Ph2NpOMe_ac_34.com	-1475.9948593	-1475.4161248	-1474.9288938	
4f	R1_X1_7	-1093.9973858	-1093.5279263	-1093.1353303	-85.4
	R1_X1_5	-1093.9972650	-1093.5279495	-1093.1367225	
4f_ac	R1_X1_ac_59	-1247.1192187	-1246.5944422	-1246.1540902	
	R1_X1_ac_21	-1247.1192064	-1246.5946089	-1246.1536349	
4g	R1_O1_7.com	-1129.8957182	-1129.4514027	-1129.5239667	-82.2
	R1_O1_60.com	-1129.8946915	-1129.4505750	-1129.5250660	
4g_ac	R1_O1_ac_59.com	-1283.0163831	-1282.5168006	-1282.5993726	
	R1_O1_ac_68.com	-1283.0162296	-1282.5168401	-1282.5999761	
4h	R1_tbu2_18	-1138.1524214	-1137.5615599	-1137.0565539	-83.8
	R1_tbu2_14	-1138.1523190	-1137.5614555	-1137.0558075	
4h_ac	R1_tbu2_ac_7	-1291.2734743	-1290.6275088	-1290.0744148	
	R1_tbu2_ac_2	-1291.2732267	-1290.6275892	-1290.0769432	
4i	R1_CF_47	-1497.7282715	-1497.3587540	-1497.4398440	-72.6
	R1_CF_43	-1497.7282371	-1497.3588256	-1497.4403046	
4i_ac	R1_CFac_17	-1650.8454156	-1650.4205831	-1650.5069801	
	R1_CFac_7	-1650.8450999	-1650.4206064	-1650.5075234	
4j	r1_1np_3	-977.2570620	-977.2540435	-977.2540435	-80.3
	r1_1np_13	-977.2567737	-977.2537552	-977.2537552	
4j_ac	r1_1np_ac_22	-1130.3766590	-1129.9183575	-1129.9931115	
	r1_1np_ac_1	-1130.3762386	-1129.9175391	-1129.9915161	
4k	R1_1Np2Me_16	-1016.5763156	-1016.1434291	-1016.2137991	-80.8
	R1_1Np2Me_11	-1016.5759383	-1016.1428468	-1016.2127468	
4k_ac	R1_1Np2Me_ac_4	-1169.6963239	-1169.2083324	-1169.2863304	
	R1_1Np2Me_ac_3	-1169.6956368	-1169.2078893	-1169.2861283	
4l	R1_2Np_10	-977.2584799	-976.8551614	-976.9222534	-81.4
	R1_2Np_32	-977.2577676	-976.8548081	-976.9224501	
4l_ac	R1_2Np_ac_11	-1130.3783580	-1129.9201045	-1129.9943575	
	R1_2Np_ac_12	-1130.3781469	-1129.9202734	-1129.9951224	

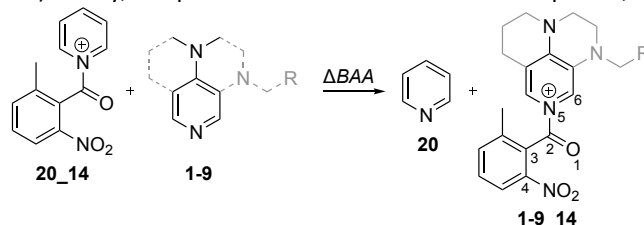
4m	R1_2Np1Ph_6.com	-1208.3348387	-1207.8459132	-1207.9229982	-87.8
	R1_2Np1Ph_14.com	-1208.3346017	-1207.8457612	-1207.9231352	
4m_ac	R1_2Np1Ph_ac_19.com	-1361.4573269	-1360.9134904	-1360.9984964	
	R1_2Np1Ph_ac_18.com	-1361.4562937	-1360.9123272	-1360.9959782	
4n	r1_ph3ph_19	-1054.6817696	-1054.2421951	-1054.3145041	-80.3
	r1_ph3ph_1	-1054.6810159	-1054.2417054	-1054.3147004	
4n_ac	R1_Ph3Ph_ac_20	-1207.8012537	-1207.3067062	-1207.3875242	
	R1_Ph3Ph_ac_19	-1207.8011231	-1207.3069156	-1207.3879586	
4o	R1_PhNMe2_8	-957.5802924	-957.1488819	-957.2199549	-87.6
	R1_PhNMe2_3	-957.5800666	-957.1488061	-957.2196101	
4o_ac	R1_PhNMe2_ac_1	-1110.7024395	-1110.2161860	-1110.2943580	
	R1_PhNMe2_ac_2	-1110.7023686	-1110.2163821	-1110.2949721	
4p	T1_1.log	-749.7991649	-749.4125885	-749.4729145	-81.6
	T1_6.log	-749.7979551	-749.4113505	-749.4717815	
4p_ac	T1_ac_5.log	-902.9192003	-902.4777878	-902.5463478	
	T1_ac_1.log	-902.9188642	-902.4774497	-902.5460777	
4q	R1_cyhex_4	-827.2313369	-826.8062604	-826.8698264	-79.5
	R1_cyhex_13	-827.2307500	-826.8055805	-826.8688275	
4q_ac	R1_cyhex_ac_5	-980.3507709	-979.8706744	-979.9426694	
	R1_cyhex_ac_35	-980.3504656	-979.8698001	-979.9403521	
4r	R1_isoPh_1	-1093.9938017	-1093.5241052	-1093.6002342	-79.6
	R1_isoPh_13	-1093.9936856	-1093.5241451	-1093.6010281	
4r_ac	R1_isoPh_ac_1	-1247.1132700	-1246.5882675	-1246.6699635	
	R1_isoPh_ac_11	-1247.1132536	-1246.5886031	-1246.6711691	
4s	R1_PhBr_8	-3394.7362786	-3394.3908081	-3394.4566701	-84.3
	R1_PhBr_10	-3394.7354462	-3394.3895077	-3394.4538457	
4s_ac	R1_PhBr_ac_21	-3547.8573911	-3547.4570446	-3547.5300456	
	R1_PhBr_ac_19	-3547.8572843	-3547.4567328	-3547.5264048	
4t	R1_Ph2NO2_20	-1028.1148408	-1027.7560363	-1027.8219493	-78.9
	R1_Ph2NO2_13	-1028.1139549	-1027.7551074	-1027.8212184	
4t_ac	R1_Ph2NO2_ac_37	-1181.2345045	-1180.8202110	-1180.8927560	
	R1_Ph2NO2_ac_3	-1181.2339007	-1180.8198932	-1180.8933712	
4u	R1_PhMeNO2_17	-1067.4357426	-1067.0474301	-1067.1154501	-79.8
	R1_PhMeNO2_11	-1067.4345495	-1067.0463710	-1067.1156670	
4u_ac	R1_PhMeNO2_ac_34	-1220.5554412	-1220.1119297	-1220.1867597	
	R1_PhMeNO2_ac_3	-1220.5550694	-1220.1114589	-1220.1860149	
4v	cat_34	-1059.5177881	-1058.9858436	-1059.0659136	-84.8
	cat_26	-1059.5177072	-1058.9859267	-1059.0677867	
4v_ac	cat_ac_4	-1212.6389201	-1212.0523496	-1212.1400666	
	cat_ac_5	-1212.6387883	-1212.0519278	-1212.1395088	
4w	R1_et_11	-631.8425235	-631.5448870	-631.5975530	-78.8
	R1_et_1	-631.8425235	-631.5448870	-631.5975540	
4w_ac	R1_et_ac_26	-784.9619645	-784.6090320	-784.6694500	
	R1_et_ac_3	-784.9619645	-784.6090320	-784.6694500	
4x	R1_Tp_3	-1144.3490600	-1144.0293765	-1144.0906285	-80.9
	R1_Tp_4	-1144.3488718	-1144.0290973	-1144.0900923	
4x_ac	R1_Tp_ac_19	-1297.4690853	-1297.0943098	-1297.1627408	
	R1_Tp_ac_17	-1297.4687167	-1297.0939942	-1297.1631112	
5a	R2_4	-862.9201963	-862.5363058	-862.6002528	-81.6
	R2_7	-862.9200890	-862.5361615	-862.5999055	
5a_ac	R2_ac_11	-1016.0404819	-1015.6014104	-1015.6717564	
	R2_ac_2	-1016.0403426	-1015.6015071	-1015.6724391	
5b	R2_Np_4.com	-1016.5788634	-1016.1452839	-1016.2137239	-83.8
	R2_Np_7.com	-1016.5786139	-1016.1448254	-1016.2136644	
5b_ac	R2_Np_ac_11.com	-1169.7003094	-1169.2113139	-1169.2868509	
	R2_Np_ac_6b.com	-1169.6991077	-1169.2100862	-1169.2849272	

Annelated Pyridine Bases

6a	R3_12	-902.2381770	-901.8243285	-901.8918155	-85.2
	R3_5	-902.2379161	-901.8241826	-901.8924836	
6a_ac	R3_ac_1	-1055.3597639	-1054.8908884	-1054.9650854	
	R3_ac_4	-1055.3595428	-1054.8901983	-1054.9644593	
6b	8b_6	-1133.3196930	-1132.8203245	-1132.8980225	-85.3
	8b_33	-1133.3198679	-1132.8198064	-1132.8954244	
6b_ac	8b_ac_74	-1286.4418495	-1285.8869230	-1285.9701650	
	8b_ac_81	-1286.4416828	-1285.8868953	-1285.9703983	
6c	R3_m_12.com	-1020.1998484	-1019.6974949	-1019.7748089	-87.0
	R3_m_34.com	-1020.1994351	-1019.6969276	-1019.7721526	
6c_ac	R3_m_ac_68.com	-1173.3224794	-1172.7647529	-1172.8451719	
	R3_m_ac_1.com	-1173.3222976	-1172.7645031	-1172.8500111	
6d	R3_np_28.com	-1055.8955579	-1055.4318874	-1055.5035144	-91.0
	R3_np_5.com	-1055.8955059	-1055.4319494	-1055.5054584	
6d_ac	R3_np_ac_1b.com	-1209.0193462	-1208.5007157	-1208.5790147	
	R3_np_ac_68b.com	-1209.0191381	-1208.5004836	-1208.5791156	
7ba^a	cat_ome_1_4	-994.8808400	-994.5246575	-994.5946125	-55.6
	cat_ome_1_1	-994.8808163	-994.5243028	-994.5939218	
7ba_ac^a	cat_ome_ac_4	-1147.9908842	-1147.5797957	-1147.6564767	
	cat_ome_ac_1	-1147.9907550	-1147.5799535	-1147.6578335	
7bb^a	cat_ome_nme2_2	-1014.3314048	-1013.9326193	-1014.0068313	-61.4
	cat_ome_nme2_4	-1014.3312913	-1013.9325888	-1014.0072428	
7bb_ac^a	cat_ome_nme2_ac_4	-1167.4436485	-1166.9898330	-1167.0718670	
	cat_ome_nme2_ac_2	-1167.4434486	-1166.9901361	-1167.0727001	
7bc^a	cat_ome_naph_1	-1034.0080950	-1033.6373865	-1033.7083705	-53.9
	cat_ome_naph_2	-1034.0079741	-1033.6372576	-1033.7086106	
7bc_ac^a	cat_ome_naph_ac_3	-1187.1170916	-1186.6918631	-1186.7691651	
	cat_ome_naph_ac_1	-1187.1170197	-1186.6920262	-1186.7710032	
7bd^a	cat_anth_1	-1073.1375415	-1072.7524650	-1072.8239260	-48.5
	cat_anth_2	-1073.1369740	-1072.7516165	-1072.8219615	
7bd_ac^a	cat_anth_ac_1	-1226.2452470	-1225.8050275	-1225.8820625	
	cat_anth_ac_2	-1226.2451068	-1225.8050643	-1225.8825333	
7be^a	cat_carb_1	-764.6338832	-764.3703927	-764.4247777	-11.5
7be_ac^a	cat_carb_ac_1	-917.7261784	-917.4089019	-917.4713889	
7bf^a	cat_nme2_1	-1033.7819454	-1033.3406359	-1033.4181879	-68.2
	cat_nme2_3	-1033.7818538	-1033.3405093	-1033.4178953	
7bf_ac^a	cat_nme2_ac_2	-1186.8964755	-1186.3999580	-1186.4841070	
	cat_nme2_ac_3	-1186.8962330	-1186.4007315	-1186.4870595	
7bg	nme2_1np_1	-1053.4585871	-1053.0455985	-1053.1203875	-58.5
	nme2_1np_4	-1053.4580102	-1053.0448835	-1053.1184495	
7bg_ac	nme2_1np_ac_3	-1206.5699612	-1206.1020015	-1206.1844585	
	nme2_1np_ac_6	-1206.5698183	-1206.1019935	-1206.1837935	
8b	H1_63	-1133.3082214	-1132.8088709	-1132.8861959	-71.1
	H1_1	-1133.3078777	-1132.8085212	-1132.8850162	
8b_ac	H1_ac_44	-1286.4245120	-1285.8700695	-1285.9544025	
	H1_ac_34	-1286.4243015	-1285.8699910	-1285.9553650	
9	SR1_29	-1110.0185848	-1109.5610153	-1109.6379843	-84.1
	SR1_20	-1110.0185847	-1109.5610152	-1109.6379842	
9_ac	SR1_ac_1	-1263.1394131	-1262.6268336	-1262.7090776	
	SR1_ac_2	-1263.1393034	-1262.6271649	-1262.7105719	

^aComputational results for **7b(a-f)** were done by A. Mateos Calbet^[5] under the supervision of S. Mayr. The herein reported computational data are fully reanalysed.

Table 5.16. Total energies, enthalpies, and free energies for catalysts **1-9** (in Hartree). The SMD(CHCl₃)/B3LYP-D3/6-31+G(d) level of theory has been used to calculate the cationic affinity number based on **14**. The conformational search is based on the previously calculated acylated catalyst structures. For these, the conformers with the lowest total energy and lowest enthalpy were taken. A phenyl group was placed instead of the methyl group of the acetyl. The dihedral angle $\theta_A(O1-C2-C3-C4)$ was changed to 90°. In a second step the dihedral angle $\theta_B(O1-C2-N5-C6)$ was changed about 180°. If there was a collapsing of the side chain with the benzoic part the dihedral angle θ_B was varied until there was no more collapsing. (In the case of **6d** these changes were not possible, the optimization of the conformers results in the previously optimized conformers) Finally, the position of the substituents was replaced, too.



Catalyst	Filename	E_{tot}	H_{298}	G_{298}	ΔBAA
		SMD/B3LYP-D3/ 6-31+G(d)	SMD/B3LYP-D3/ 6-31+G(d)	SMD/B3LYP-D3/ 6-31+G(d)	
Pyridin	cat_001.log	-248.3105322	-248.2133405	-248.2459755	
	pyr_3o_2	-836.9831792	-836.7417057	-836.7417057	
	pyr_3o_1	-836.9829706	-836.7412311	-836.7412311	
1	DMAP_1_2.log	-382.2995489	-382.1243915	-382.1671115	-58.3
1_14	dmap_3o_2	-970.9952880	-970.6749055	-970.7435345	
	dmap_3o_1	-970.9952612	-970.6749797	-970.7434837	
2	ppy_1	-459.7357421	-459.5231405	-459.5677125	-63.4
2_14	ppy_3o_3	-1048.4332775	-1048.0756350	-1048.1462110	
	ppy_3o_2	-1048.4332770	-1048.0753285	-1048.1455465	
3	TCAP_1.log	-537.1790988	-536.9291045	-536.9755585	-76.9
3_14	5_14_2	-1125.8819378	-1125.4866003	-1125.5578193	
	5_14_22	-1125.8819254	-1125.4867559	-1125.5593919	
4a	R1_5	-823.5991141	-823.2453426	-823.3063836	-95.3
4a_14	R1_3o_b	-1412.3088084	-1411.8100219	-1411.8952699	
	R1_3o_a	-1412.3077592	-1411.8092747	-1411.8961827	
4b	R1_Ph2Ph_6	-1054.6785317	-1054.2390812	-1054.3101252	-101.2
4b_14	R1_Ph2Ph_3o_c.com	-1643.3903835	-1642.8059730	-1642.9008880	
	R1_Ph2Ph_3o_d.com	-1643.3894073	-1642.8043608	-1642.8992618	
	R1_Ph2Ph_3o_e.com	-1643.3894073	-1642.8043608	-1642.8992618	
4c	R1_Ph2Tol_6b.com	-1094.0006262	-1093.5319357	-1093.6069007	-101.5
4c_14	R1_Ph2Tol_3o_10b_c.com	-1682.7131089	-1682.0989514	-1682.1954894	
	R1_Ph2Tol_3o_10b_d.com	-1682.7120435	-1682.0972840	-1682.1931850	
4d	R1_Ph1Np_6.com	-1208.3394277	-1207.8505922	-1207.9272952	-106.0
4d_14	R1_Ph1Np_3o_10b_c.com	-1797.0535386	-1796.4193131	-1796.5182991	
	R1_Ph1Np_3o_10b_d.com	-1797.0517479	-1796.4172914	-1796.5174734	
	R1_Ph1Np_3o_10b_e.com	-1797.0517479	-1796.4172914	-1796.5174734	
4e	R1_Ph2NpOMe_14b.com	-1322.8703820	-1322.3462255	-1321.9070605	-96.6
4e_14	R1_Ph2NpOMe_3o_30af.com	-1911.5810268	-1910.9111253	-1911.0169413	
	R1_Ph2NpOMe_3o_30ab.com	-1911.5807022	-1910.9113857	-1911.0186317	
4f	R1_X1_7	-1093.9973858	-1093.5279263	-1093.1353303	-103.5
4f_14	R1_X1_3o_59_c.com	-1682.7106586	-1682.0957011	-1682.1925761	
	R1_X1_3o_59_d.com	-1682.7090056	-1682.0937181	-1682.1898911	
4g	R1_O1_7.com	-1129.8956793	-1129.4513408	-1129.0825948	-98.4
4g_14	R1_O1_3o_68_a.com	-1718.6069921	-1718.0171936	-1718.1141466	
	R1_O1_3o_59d.com	-1718.6069920	-1718.0171905	-1718.1140265	
4h	R1_tbu2_18	-1138.1524214	-1137.5615599	-1137.0565539	-98.8
4h_14	R1_tbu2_3o_2d.com	-1726.8635680	-1726.1275595	-1726.2342515	
	R1_tbu2_3o_7c.com	-1726.8629353	-1726.1271318	-1726.2329788	
4i	R1_CF_43	-1497.7282371	-1497.3588256	-1497.4403046	-91.4
4i_14	R1_CF3o_17d.com	-2086.4370030	-2085.9219975	-2086.0236305	
	R1_CF3o_7_b.com	-2086.4370029	-2085.9219994	-2086.0236274	

Annelated Pyridine Bases

4j	r1_1np_3	-977.2570620	-976.8536395	-976.9204225	-83.7
4j_14	r1_1np_3o_d.com	-1565.9628651	-1565.4139026	-1565.5046946	
	r1_1np_3o_c.com	-1565.9626920	-1565.4137645	-1565.5046525	
4k	R1_1Np2Me_16	-1016.5763156	-1016.1434291	-1016.2137991	-84.7
4k_14	R1_1Np2Me_3o_c.com	-1605.2824444	-1604.7040559	-1604.7977069	
	R1_1Np2Me_3o_d.com	-1605.2824260	-1604.7040605	-1604.7986375	
4l	R1_2Np_10	-977.2584799	-976.8551614	-976.9222534	-100.5
4l_14	R1_2Np_3o_11b.com	-1565.9702084	-1565.4218029	-1565.5109509	
	R1_2Np_3o_12b.com	-1565.9695303	-1565.4210008	-1565.5112558	
4m	R1_2Np1Ph_6.com	-1208.3348387	-1207.8459132	-1207.9229982	-94.6
4m_14	R1_2Np1Ph_3o_19d	-1797.0443418	-1796.4102953	-1796.5118653	
	R1_2Np1Ph_3o_19b.com	-1797.0443215	-1796.4099430	-1796.5112260	
4n	r1_ph3ph_19	-1054.6817696	-1054.2421951	-1054.3145041	-99.2
4n_14	R1_Ph3Ph_3o_19b.com	-1643.3934191	-1642.8083516	-1642.9067696	
	R1_Ph3Ph_3o_19a.com	-1643.3926164	-1642.8075149	-1642.9038549	
4o	R1_PhNMe2_8	-957.5802924	-957.1488819	-957.2199549	-105.8
4o_14	R1_PhNMe2_3o_1b.com	-1546.2941262	-1545.7175587	-1545.8102127	
	R1_PhNMe2_3o_2b.com	-1546.2941262	-1545.7175587	-1545.8102137	
4p	T1_1.log	-749.7991649	-749.4125885	-749.4729145	-88.5
4p_14	T1_3o_5c	-1338.5069102	-1337.9746687	-1338.0589047	
	T1_3o_5d	-1338.5062268	-1337.9740873	-1338.0599443	
4q	R1_cyhex_4	-827.2313369	-826.8062604	-826.8698264	-92.6
4q_14	R1_cyhex_3o_5d_b	-1415.9407188	-1415.3698553	-1415.4561753	
	R1_cyhex_3o_5d_a	-1415.9407062	-1415.3698837	-1415.4568337	
4r	R1_isoPh_13	-1093.9936856	-1093.5241451	-1093.6010281	-92.5
4r_14	R1_isoPh_3o_30a.com	-1682.7033731	-1682.0877596	-1682.1873956	
	R1_isoPh_3o_30b.com	-1682.7021576	-1682.0868051	-1682.1865041	
5a	R2_4	-862.9201963	-862.5363058	-862.6002528	-89.5
5a_14	R2_3o_11b.com	-1451.6280582	-1451.0987667	-1451.1850487	
	R2_3o_11a.com	-1451.6279912	-1451.0987207	-1451.1847387	
5b	R2_Np_4.com	-1016.5788634	-1016.1452839	-1016.2137239	-88.5
5b_14	R2_Np_3o_11d	-1605.2864573	-1604.7073698	-1604.8008158	
	R2_Np_3o_11a	-1605.2863159	-1604.7071264	-1604.7989764	
6a	R3_12	-902.2381770	-901.8243285	-901.8918155	-93.0
6a_14	R3_68_3o_c	-1490.9476898	-1490.3881033	-1489.9209713	
	R3_68_3o_b	-1490.9466389	-1490.3876084	-1489.9226674	
6b	8b_6	-1133.3196930	-1132.8203245	-1132.8980225	-96.2
6b_ac	8b_3o_74_d.com	-1722.0301432	-1721.3853197	-1721.4852897	
	8b_3o_74_a.com	-1722.0301426	-1721.3853181	-1721.4852911	
6c	R3_m_12.com	-1020.1998484	-1019.6974949	-1019.7748089	-92.5
6c_14	R3_m_ac_68d	-1608.9095585	-1608.2610660	-1608.3588660	
	R3_m_ac_68b.log	-1608.9093478	-1608.2611043	-1608.3587713	
6d	R3_np_28.com	-1055.8955579	-1055.4318874	-1055.5035144	-93.1
6d_14	R3_np_30_1bb.com	-1644.6047786	-1643.9957181	-1644.0927531	
	R3_np_30_1d	-1644.6047574	-1643.9956169	-1644.0923849	
7ba	cat_ome_1_4	-994.8808400	-994.5246575	-994.5946125	-56.7
7ba_14	cat_ome_ac_1_14b.com	-1583.5758920	-1583.0746255	-1583.1697365	
	3a_4a.com	-1583.5758849	-1583.0741294	-1583.1681054	
7bb	cat_ome_nme2_2	-1014.3314048	-1013.9326193	-1014.0068313	-63.2
7bb_14	3b_4a.com	-1603.0287959	-1602.4845914	-1602.5826824	
	3b_4c.com	-1603.0287225	-1602.4850540	-1602.5851490	
7bc	cat_ome_naph_1	-1034.0080950	-1033.6373865	-1033.7083705	-55.2
7bc_14	3c_3c.com	-1622.7023972	-1622.1863907	-1622.2807147	
	3c_3b.com	-1622.7019930	-1622.1867605	-1622.2821065	
7bd	cat_anth_1	-1073.1375415	-1072.7524650	-1072.8239260	-49.8
7bd_14	3d_1a.com	-1661.8302635	-1661.2996830	-1661.3933330	

	3d_2b_a.com_d	-1661.8301549	-1661.2998154	-1661.3933414	
8	H1_63	-1133.3082214	-1132.8088709	-1132.8861959	-85.8
8_14	H1_3o_44b.com	-1722.0149796	-1721.3699291	-1721.4723611	
	H1_3o_88b.com	-1722.0149795	-1721.3699290	-1721.4723630	
9	SR1_29	-1110.0185848	-1109.5610153	-1109.6379843	-99.9
9_14	SR1_3o_1a.com	-1698.7300434	-1698.1274389	-1698.2267329	
	SR_14_1c	-1698.7299063	-1698.1274428	-1698.2270918	

In Figures 5.94 to 5.98 the ΔACA and ΔBAA values are illustrated according to the type of catalysts. For 3,4-aminopyridine catalysts **4** (Figure 5.95) the affinity values range between $\Delta ACA = -79 - 88 \text{ kJ mol}^{-1}$ excluding **4e** and **4i**. **4i** is the lowest Lewis base of this 3,4-aminopyridine class I with $\Delta ACA = -72.6 \text{ kJ mol}^{-1}$, whereby on the other side **4e** with $\Delta ACA = -93.6 \text{ kJ mol}^{-1}$ is the catalyst with the highest Lewis basicity. The CF_3 -groups in *meta*-position are deactivating, because of their -I - effect. This sequence is changing when calculating the ΔBAA values. In general, all affinities values of ΔBAA are shifted to higher Lewis basicities, but not for all catalysts in the same manner. Now **4d** with $\Delta BAA = -106.0 \text{ kJ mol}^{-1}$ and **4o** with $\Delta BAA = -105.8 \text{ kJ mol}^{-1}$ are the catalysts with the highest affinity value, whereby **4j** with $\Delta BAA = -83.7 \text{ kJ mol}^{-1}$ and **4k** with $\Delta BAA = -84.7 \text{ kJ mol}^{-1}$ are the catalysts with the lowest affinity numbers. It can be highlighted that for **4i** the ΔBAA is 18.8 kJ mol^{-1} higher than the ΔACA . We assumed, that these changes of the affinity numbers are based on NCI between the CF_3 group and the NO_2 group which do not exist in the ΔACA (see Table 5.17). Plotting ΔACA vs. ΔBAA two groups are visible in Figure 5.94a. **4e,m** and **i** (red dots) are statistical exceptions in comparison to the further **4** (blue dots). In the case of the blue dots the affinity numbers of **4** are increasing similarly from ΔACA to ΔBAA , whereby in the case of **4i** the affinity value is significantly higher and for **4m** and **4e** computing ΔACA or ΔBAA is equal because no significant changes were found. Looking at the optimized structures of **4e,m** again (Table 5.17), the NCI are similar for ΔACA and ΔBAA , in contrast to the further catalysts motifs of **4**. Comparing the different kinds of 3,4-diaminopyridine catalysts **4a**, **5a**, **6a**, **8b** and **9** ($R = \text{Ph}$) according their Lewis basicity (Figure 5.96), we find out that for ΔACA **6a** ($-85.2 \text{ kJ mol}^{-1}$) is the strongest Lewis base in this group. **9** is with $\Delta ACA = -84.1 \text{ kJ mol}^{-1}$ on the second place. **4a** and **5a** are similar in their basicity to $\Delta ACA = -81.5 \text{ kJ mol}^{-1}$ and is followed by **8b** with $\Delta ACA = -71.1 \text{ kJ mol}^{-1}$. When the transfer group is changed again, an increase in affinity arises. A big step of about $-17.1 \text{ kJ mol}^{-1}$ in affinity catalyst **8b** is determined between ΔACA vs. ΔBAA . Also, for **4a** the ΔBAA value is $-13.8 \text{ kJ mol}^{-1}$ higher. The increase in affinity does not follow any trend which gets visible by plotting ΔACA vs. ΔBAA (Figure 5.94b, $R^2 = 0.57$). How the Lewis basicity is changed by varying the length of the CH_2 linker, is shown in Figure 5.97. ΔACA values are very similar in this group ($\Delta ACA = -82 - -87 \text{ kJ mol}^{-1}$), only **6d** fall out of line with $\Delta ACA = -91.0 \text{ kJ mol}^{-1}$. Computing the ΔBAA **4j** doesn't change much. The further catalysts are influenced more by changing the acyl transfer group. Plotting the ΔACA vs. ΔBAA for **4a**, **5a** and **6a** ($R = \text{Ph}$, Figure 5.94c, blue) no correlation was found. In contrast, when plotting ΔACA vs. ΔBAA for **4j**, **5b** and **6d** ($R = 1\text{-Np}$, Figure 5.94c, red) a dependency is visible with $R^2 = 0.96$. Finally, we were exploring the affinity values for the 4-aminopyridine catalysts **1-3** and **7b** (Figure 5.98). **7be** ($R = \text{carbazole}$) has a $\Delta ACA = -11.5 \text{ kJ mol}^{-1}$ and, consequently, is a very weak Lewis base compared to pyridine. Catalysts with a big aryl group have a lower (**7bc,7bd**) or equal Lewis basicity than DMAP (**1**, $\Delta ACA = -57.9 \text{ kJ mol}^{-1}$). Also **7ba** has a similar affinity value as **1**. Only adding NMe_2 as strong activation group increases the Lewis basicity (**7bb**: $\Delta ACA = -61.4 \text{ kJ mol}^{-1}$ and **7bf**: $\Delta ACA = -68.2 \text{ kJ mol}^{-1}$) but does not achieve the affinity of TCAP (**3**, $\Delta ACA = -75.0 \text{ kJ mol}^{-1}$). Only small changes in affinity were achieved by determining ΔBAA , which is confirmed by plotting ΔACA vs. ΔBAA (Figure 5.94d, $R^2 = 0.99$). In this class of catalysts neither the acetyl group nor the 2-methyl-6-nitro benzoate should be able to interact with a part of the catalysts, so no change in affinity is achieved.

Annelated Pyridine Bases

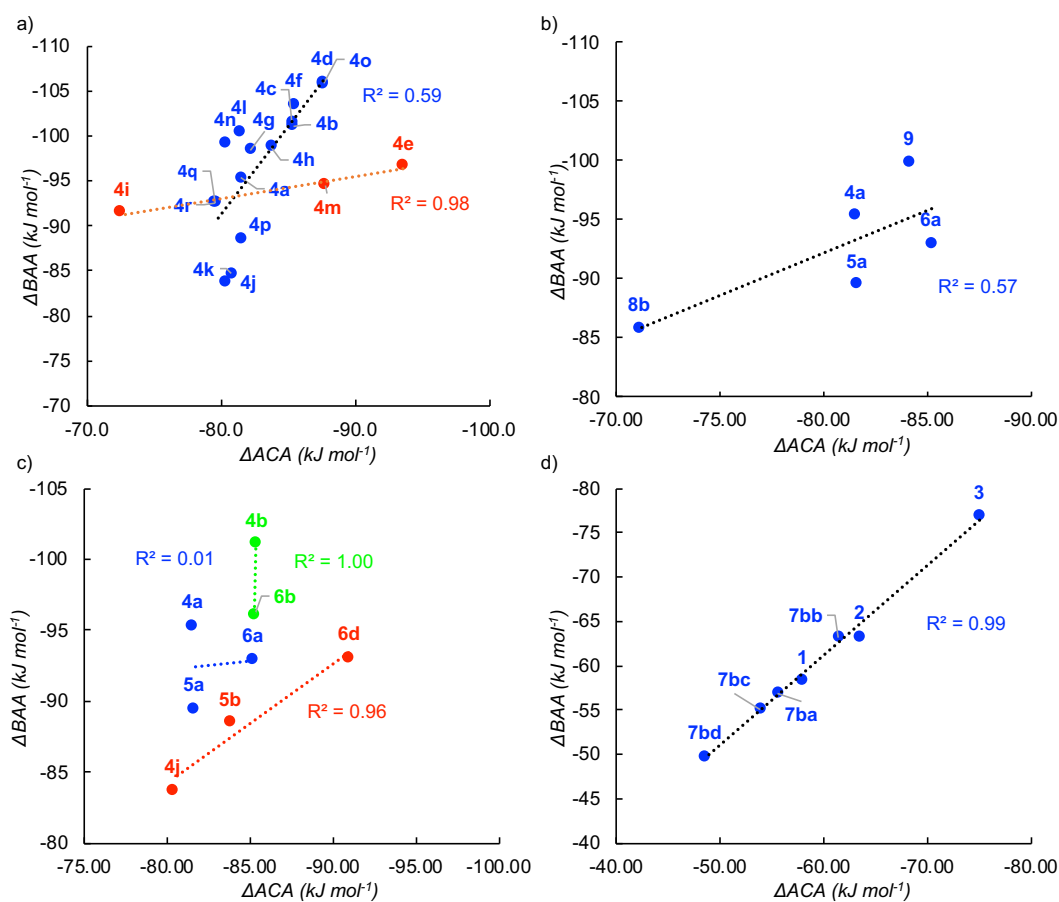


Figure 5.94. Plot of ΔACA (kJ mol^{-1}) vs. ΔBAA (kJ mol^{-1}) for a) catalysts **4a-r**, b) 3,4-diaminopyridine based catalysts **4a**, **5a**, **6a** and **8b** ($R=\text{Ph}$), c) 3,4-diaminopyridine based catalysts **4-6** with CH_2 -linker $n = 1-3$ and d) 4-aminopyridine based catalyst **1**, **2**, **3** and **7ba-bd**.

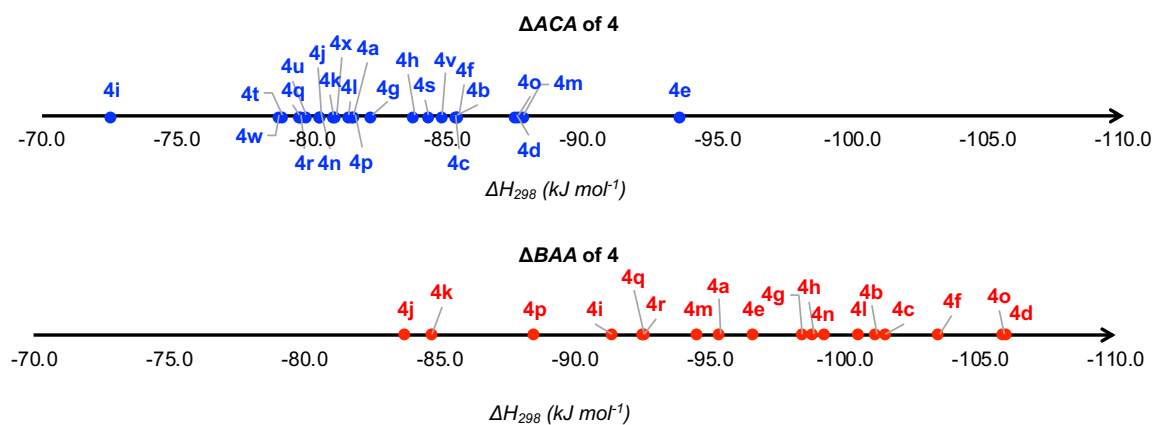


Figure 5.95. Lewis basicity values of catalyst **4** for a) acetyl cationic affinity (ΔACA) and b) benzoic anhydride affinity (ΔBAA).

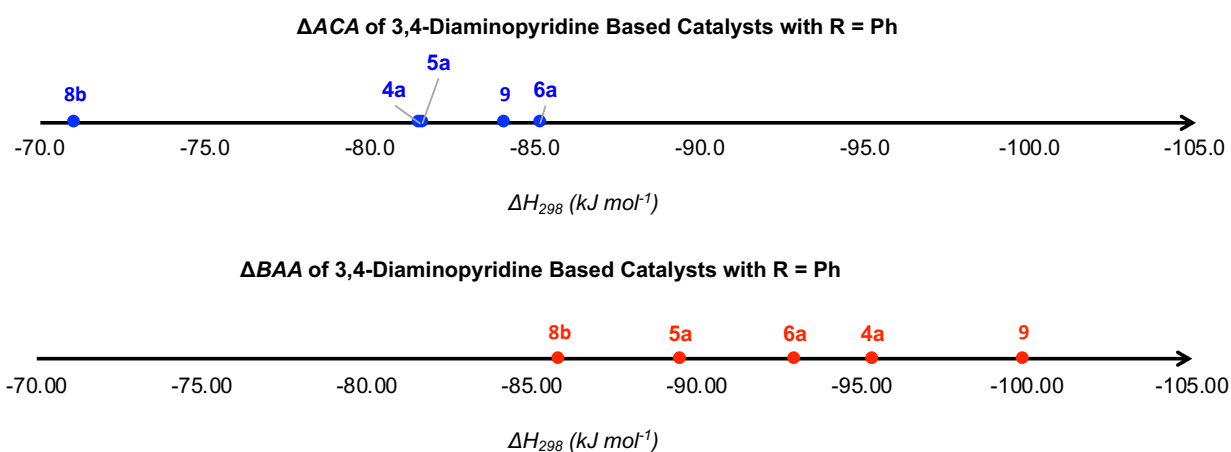


Figure 5.96. Lewis basicity of 3,4-diaminopyridine based catalysts **3-6**, **8b** and **9** with R = Ph for a) acetyl cationic affinity (Δ ACA) and b) benzoic anhydride affinity (Δ BAA).

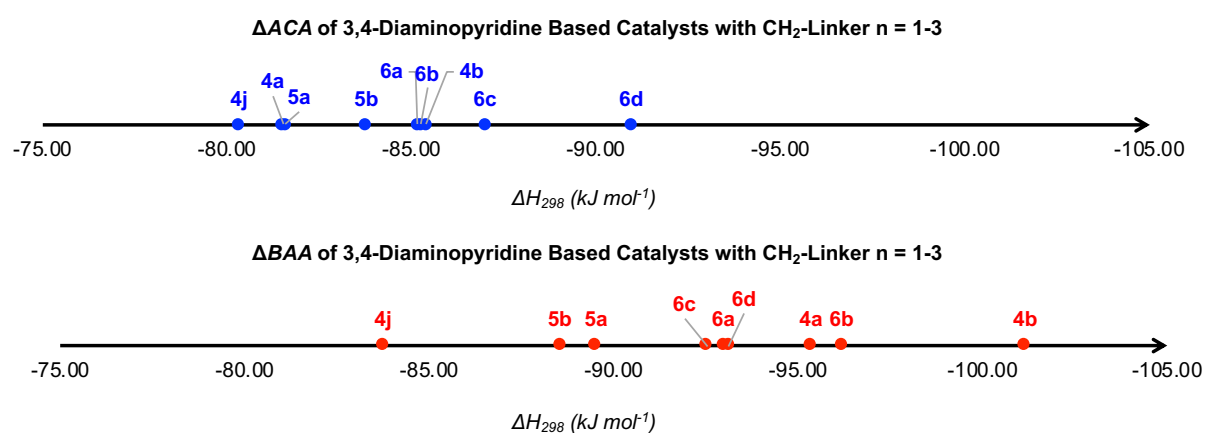


Figure 5.97. Lewis basicity of 3,4-diaminopyridine based catalysts **4-6** with CH₂-linker n = 1-3 for a) acetyl cationic affinity (Δ ACA) and b) benzoic anhydride affinity (Δ BAA).

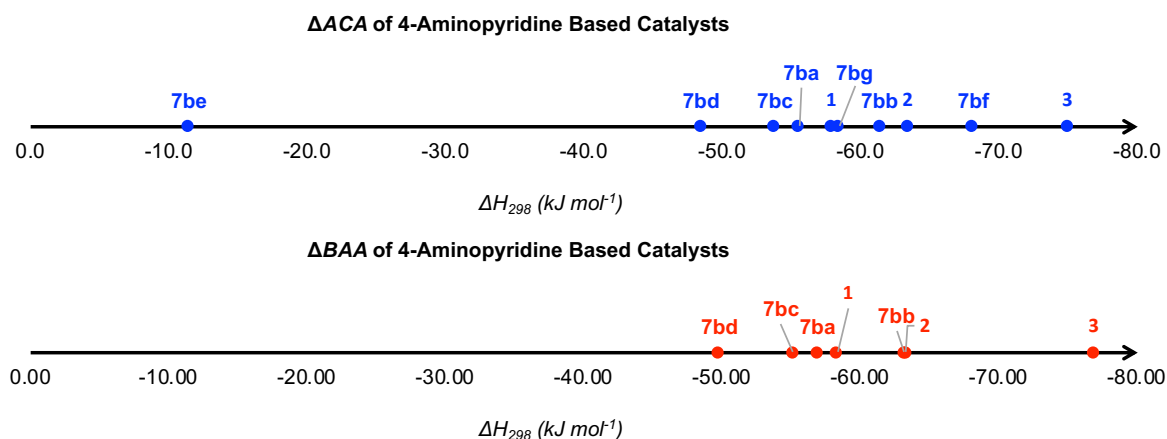


Figure 5.98. Lewis basicity of 4-aminopyridine based catalyst **1**, **2**, **3** and **7b** for a) acetyl cationic affinity (Δ ACA) and b) benzoic anhydride affinity (Δ BAA).

In how far the size effects between the side group of the catalyst and the *N*-aminopyridinium surface of the catalysts shown in Table 5.17 is influencing the Lewis basicity of the catalysts was an important point of our study. It is clearly visible that catalysts **1-3** and **7b** are not able to form NCI with the acyltransfer group. This is different for catalysts **4-6** and **8b** because here the aromatic part of the side chain interacts either with the aminopyridinium surface or with the acyltransfer group like shown in Figure 5.99. High affinity values are achieved if strong cation- π interactions or sandwich conformations are possible (**4e**, **4m**). Short CH₃- π interactions could determine a high Lewis base (**6d**, $r = 354$ pm).^[37] It is of particular relevance that most of the catalysts **4** building NCI between the *N*-aminopyridinium face and aromatic face of the side chain,

perform better than **3** in the competition experiments between **10** vs. **11** (k_{rel}). We may conclude at this point that on the one hand electronic effects (+/- I) and on the other hand attractive Van der Waals forces can influence the Lewis basicity in either direction. However, the lowest selectivity k_{rel} was achieved when the *N*-cation was stabilized by cation- π interactions.

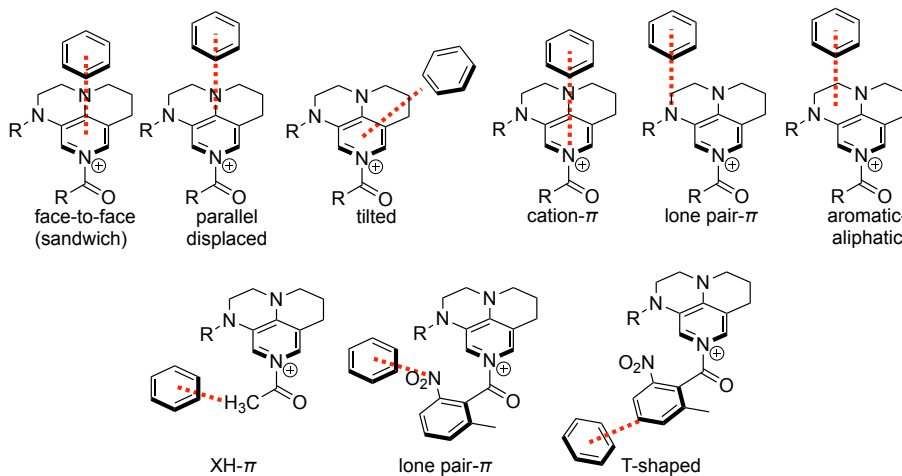


Figure 5.99. Stacking interactions between pyridinium surface, surface of the substituent (here simplified as benzene ring) and acyl group.^[38]

Strong π - π stacking interactions were found by quant chemical analysis for **4e**. We wondered if we were able to detect some proton-proton interactions in a NOESY NMR spectrum of **4e**, caused by the overlapping of the 2-Np substituent and the pyridinium surface. In Figure 5.100, only a section of the NOESY NMR spectrum of **4e** is shown. Indeed, we see some proton-proton interactions in the NOESY spectrum. For example, the protons of CH_2 -14 are interacting with the proton of Ar-6 and also with Ar-22. More interesting is the proton-proton interaction which is visible between the proton integrals of CH_2 -12/13 and Ar-29, which suggests an overlapping of the 2-Np substituent and the pyridinium surface.

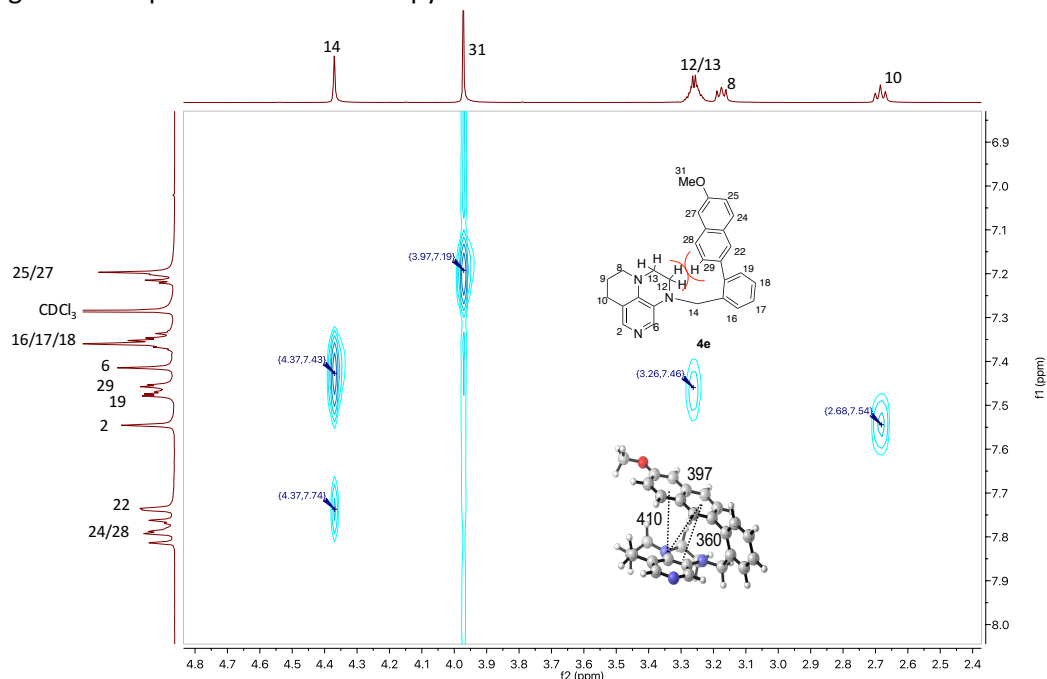
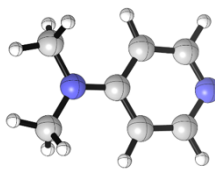
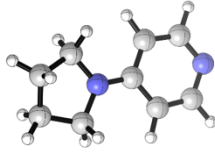
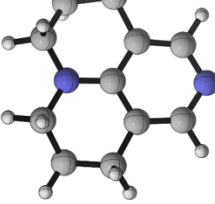
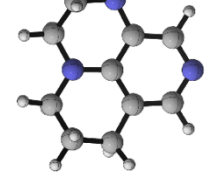
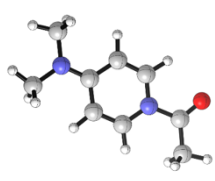
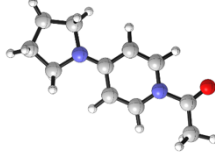
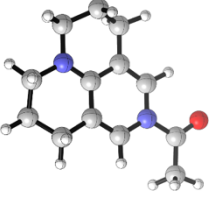
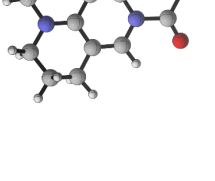
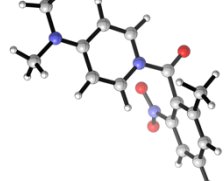
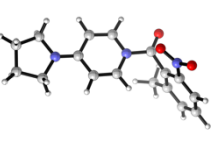
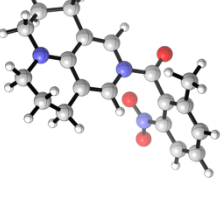
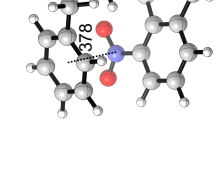
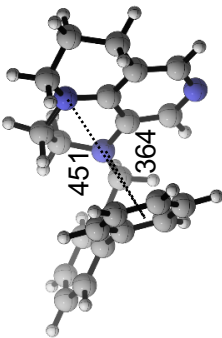
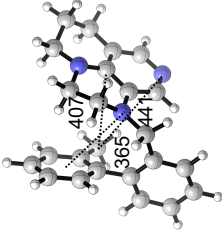
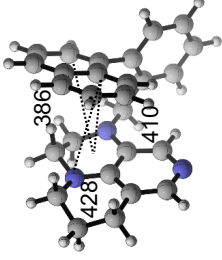
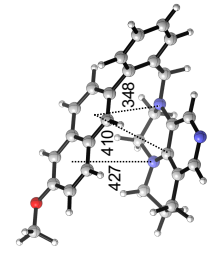
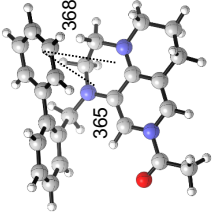
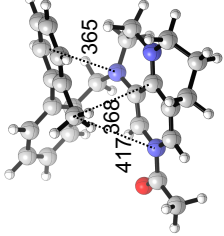
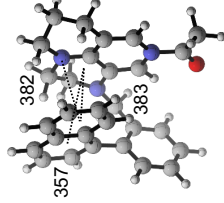
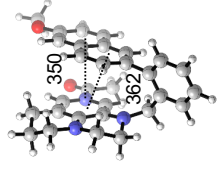
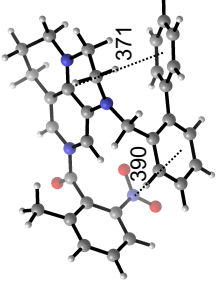
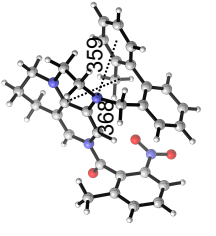
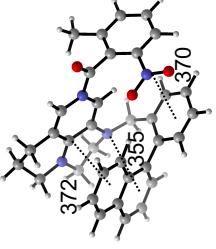
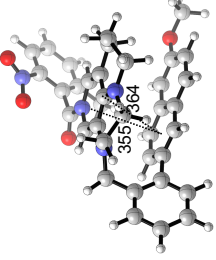
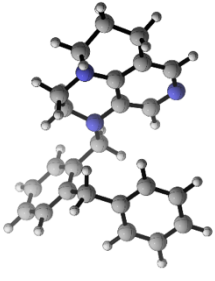
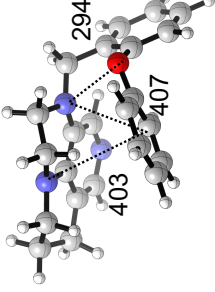
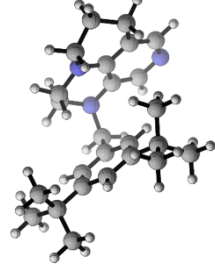
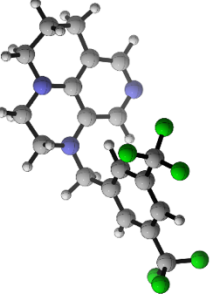
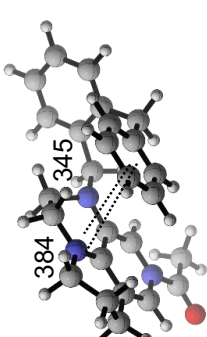
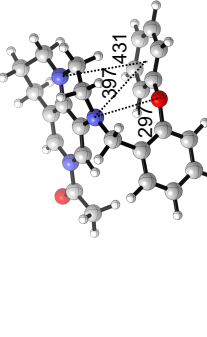
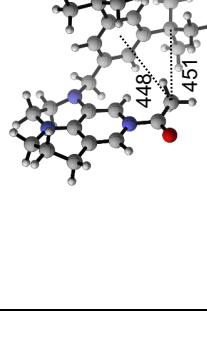
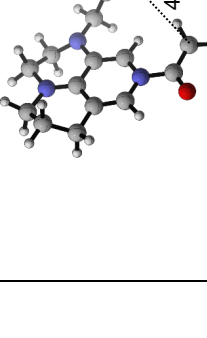
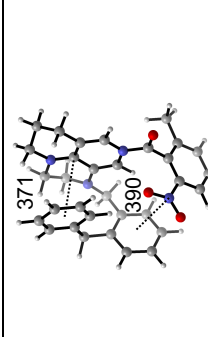
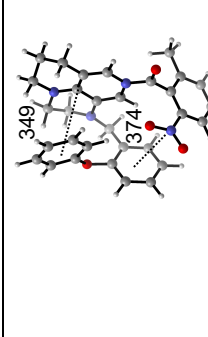
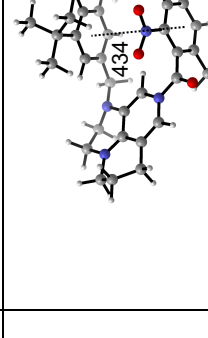
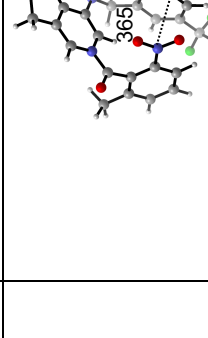
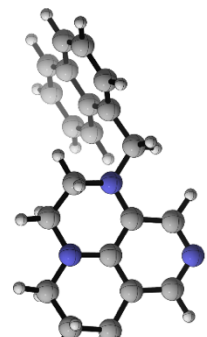
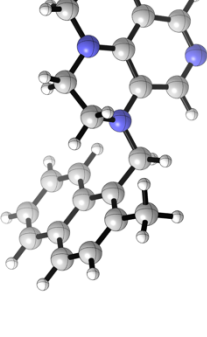
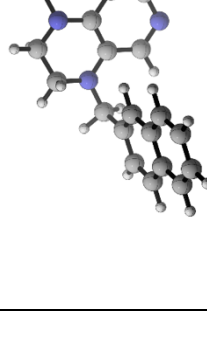
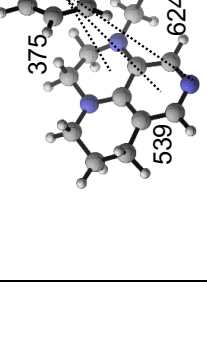
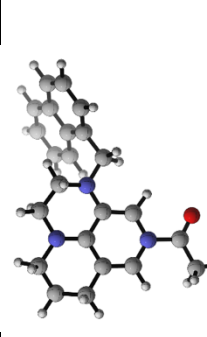
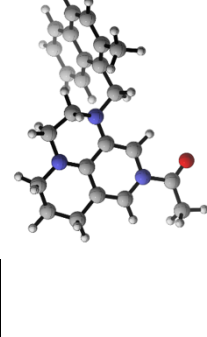
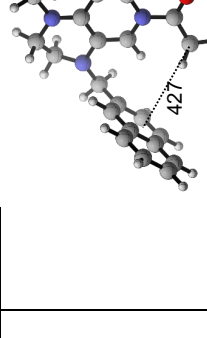
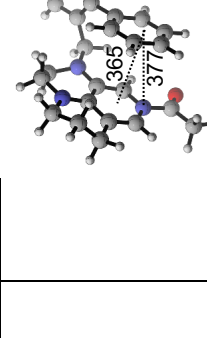


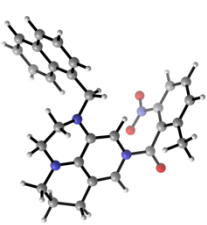
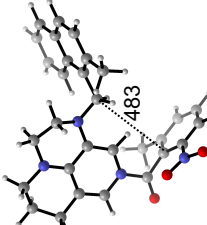
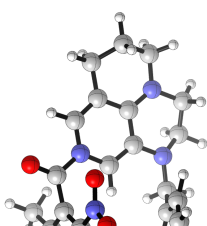
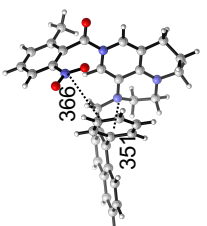
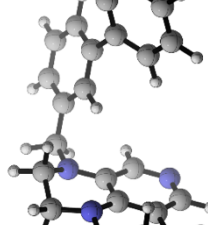
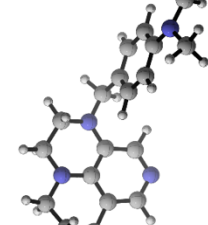
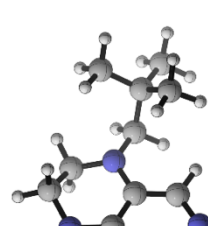
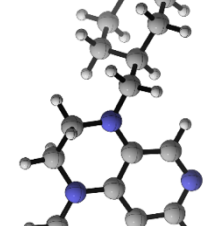
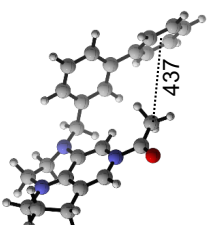
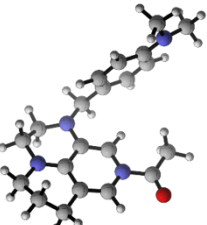
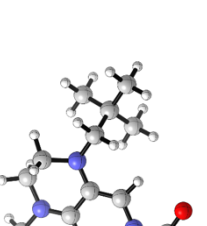
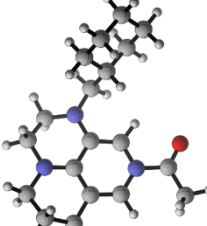
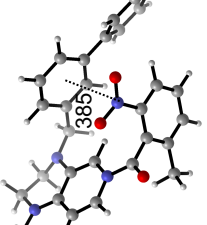
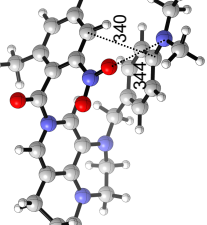
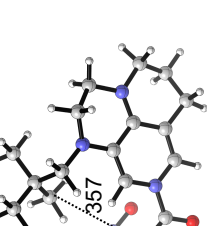
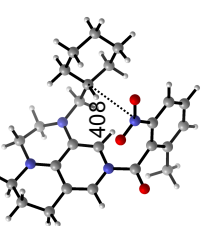
Figure 5.100. NOESY NMR spectrum of **4e**.

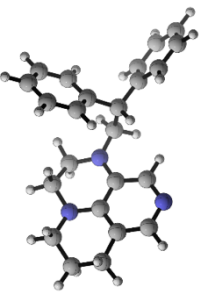
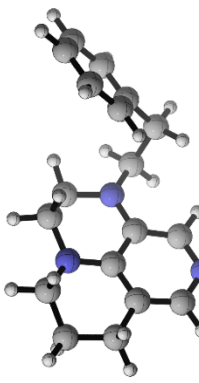
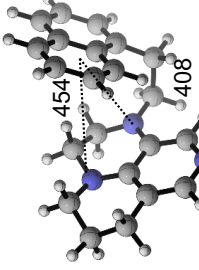
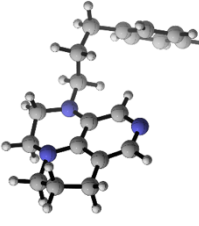
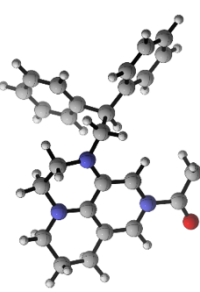
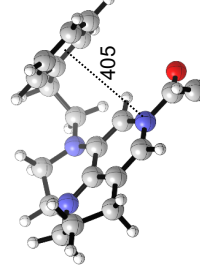
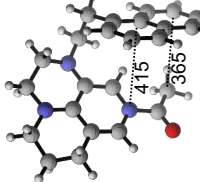
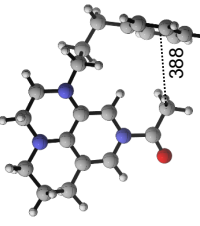
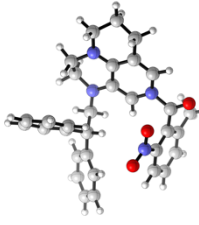
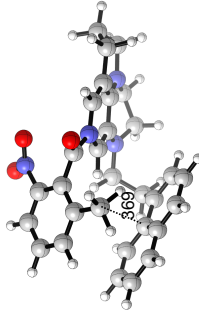
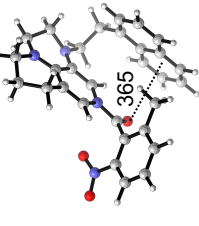
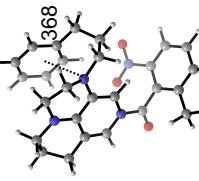
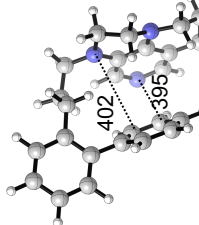
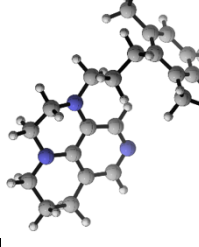
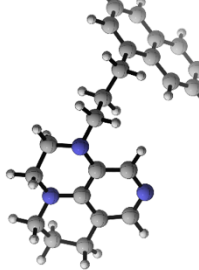
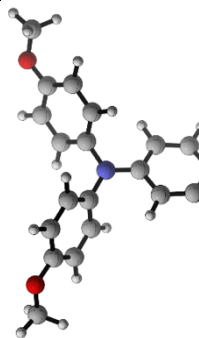
Table 5.17. Structures of optimized catalysts **1-8** and acylated catalysts **1-8_ac** and **1-8_14**. The corresponding distances between side group -aminopyridol surface or side group -acetyl are given in pm.^[39]

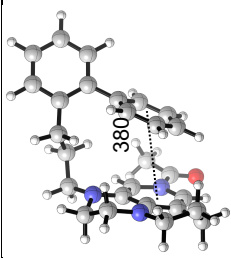
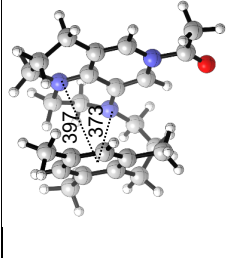
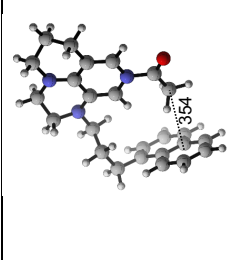
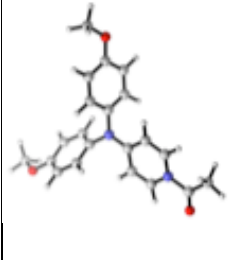
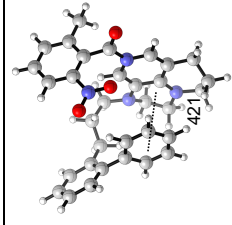
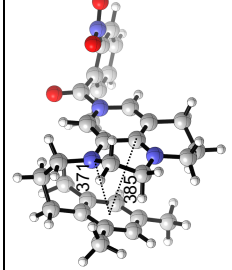
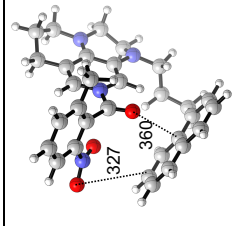
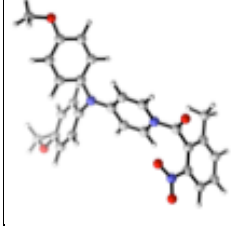
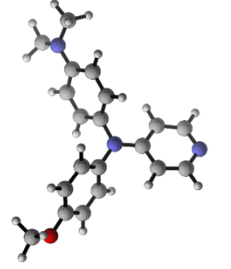
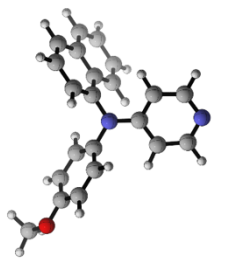
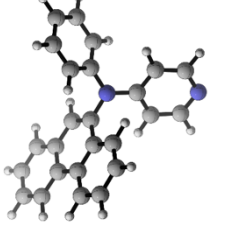
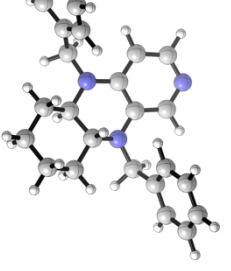
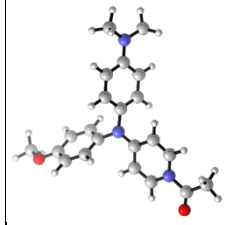
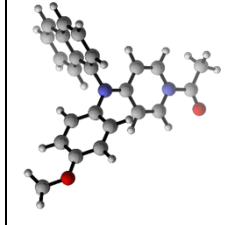
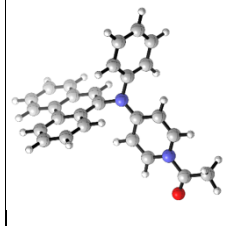
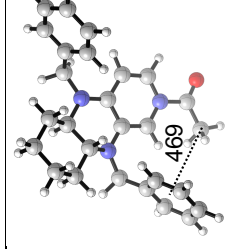
k_{rel}	ΔACA ($kJ mol^{-1}$)	ΔBAA ($kJ mol^{-1}$)	k_{rel}	ΔACA ($kJ mol^{-1}$)	ΔBAA ($kJ mol^{-1}$)	k_{rel}	ΔACA ($kJ mol^{-1}$)	ΔBAA ($kJ mol^{-1}$)	k_{rel}	ΔACA ($kJ mol^{-1}$)	ΔBAA ($kJ mol^{-1}$)
											
	1		2	3		4a					
											
	1_ac		2_ac	3_ac		4a_ac					
											
	1_14		2_14	3_14		4a_14					
1.42	-57.9	-58.3	1.23	-63.4	-63.4	0.68	-75.0	-76.9	0.78	-81.5	-95.3

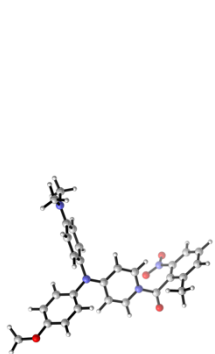
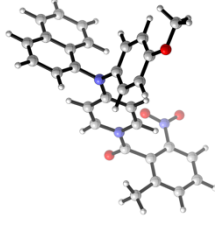
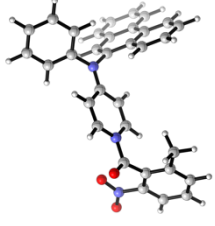
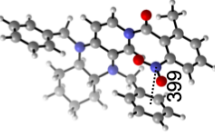
			
4b	4c	4d	4e
			
4b_ac	4c_ac	4d_ac	4e_ac
			
4b_14	4c_14	4d_14	4e_14
0.65	0.63	0.63	0.57
-85.4	-85.3	-87.6	-93.6
-101.2	-101.5	-106.0	-96.6
			
4f	4g	4h	4i

			
4f_ac	4g_ac	4h_ac	4i_ac
			
4f_14	4g_14	4h_14	4i_14
0.67	0.68	0.69	0.67
-85.4	-82.2	-83.8	-72.6
-103.5	-98.4	-98.8	-91.4
			
4j	4k	4l	4m
			
4j_ac	4k_ac	4l_ac	4m_ac

			
4j_14	4k_14	4l_14	4m_14
0.75	0.77	0.78	0.63
-80.3	-80.8	-81.4	-87.8
-83.7	-84.7	-100.5	-94.6
			
4n	4o	4p	4q
			
4n_ac	4o_ac	4p_ac	4q_ac
			
4n_14	4o_14	4p_14	4q_14
0.77	0.77	0.80	0.90
-80.3	-87.6	-81.6	-79.5
-99.2	-105.8	-88.5	-92.6

			
4r	5a	5b	6a
			
4r_ac	5a_ac	5b_ac	6a_ac
			
4r_14	5a_14	5b_14	6a_14
0.89	0.78	0.76	0.84
-79.6	-81.6	-83.8	-85.2
-92.5	-89.5	-88.5	-91.6
			
6b	6c	6d	7ba
402	395	415	368
395	405	365	388

			
6b_ac	6c_ac	6d_ac	7ba_ac
			
6b_14	6c_14	6d_14	7ba_14
0.81	0.81	0.79	0.72
-85.3	-87.0	-91.0	-55.6
-96.2	-92.5	-93.1	-56.7
			
7bb	7bc	7bd	8b
			
7bb_ac	7bc_ac	7bd_ac	8b

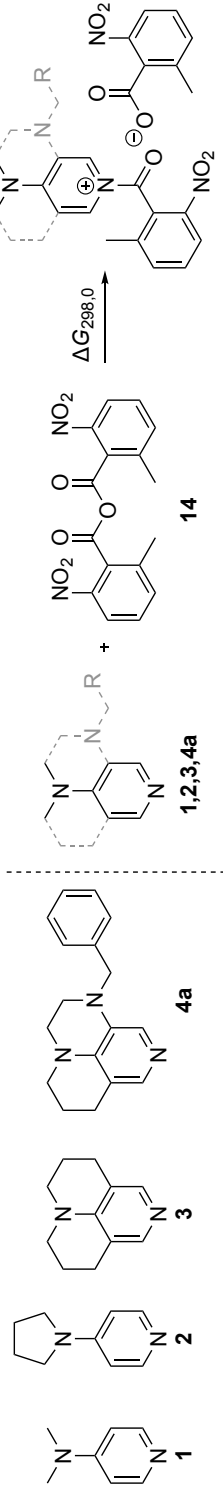
				7bb_14			8b_14				
				0.82	-61.4	-63.2	0.86	-53.9	-55.2	0.94	-48.5

5.2.2 Computational Data of INT1

The first step in the catalytic cycle is the nucleophilic attack of the catalyst on acid anhydride **14** to form the acylpyridinium intermediate **INT1**. Afterwards, 1,2-diol **16** was included to perform the acyl transfer step by undergoing **TS2**, which is the rate determining step. In this step the alcohol is nucleophilic attacking the carboxylic center, before the C-N bond is cleavage to obtain monoester **17/18** and recycled catalyst.^[1] Computing the complete mechanism is related with much time and high computing costs. For this reason, we decided to compute only the acylpyridinium intermediate **INT1**. To ensure that the Lewis bases **1-4** are able to act as active catalysts, it is important that the formed **INT1** is not too stable in terms of Gibbs free energy. In this case, a lot of free energy is needed to pass through **TS2**. For DMAP as **INT1** a free energy of $\Delta G_{298} = +20.6 \text{ kJ mol}^{-1}$ was obtained, whereby **INT1** of PPY is located at $\Delta G_{298} = +12.5 \text{ kJ mol}^{-1}$. For the more Lewis basic catalyst TCAP, the **INT1** is placed 12.3 kJ mol^{-1} more stable with $\Delta G_{298} = +8.3 \text{ kJ mol}^{-1}$. Again 11 kJ mol^{-1} lower with $\Delta G_{298} = -2.7 \text{ kJ mol}^{-1}$ for **4a** was found, which means that for the *N*-acylpyridinium intermediate with **4a** the intermediate is somewhat too stable. **4a** was chosen to compute the **INT1** with catalyst **4** as a model system with $R = \text{Ph}$, because of less conformers. Furthermore, it seems that **INT1** with the stronger Lewis base catalysts **3**, **4** and acylation reagent **14** is energetically at the same level as the starting material. These findings are agreeing with the experimental impressions, e.g. change of color, shifts of proton peaks in $^1\text{H NMR}$, during the experimental measurements.

Table 5.18. Total energies and free energies for **1-3**, **4a**, **14** and **INT1-1**, **INT1-2**, **INT1-3** and **INT1-4a** (in Hartree). Molar free energies in solution at 298.15 K ($G_{298,\text{sol}}$) have been calculated at the SMD(CHCl₃)/DLPNO-CCSD(T)/def2-TZVPP//SMD(CHCl₃)/B3LYP-D3/6-31+G(d) level and corrected for a solution standard state of 1 M through addition of +7.925 kJ mol⁻¹ (0.00301848 Hartree). The SMD(CHCl₃)/B3LYP-D3/6-31+G(d) level of theory has been used to optimize the geometries and calculate solute thermal corrections and solvation energies.

Note that the filenames are used in our calculations and do not follow any guide. The conformational search of **INT1-3** was based on findings of **INT1** in previous study.^[1] The conformational search of **INT1-1** on the findings of **INT1-2** on the findings of **INT1-1**. The conformational search of **INT1-4a** is based on the conformers of int1_tcap_18.com and int1_tcap_28.com (lowest total free energy based on SMD(CHCl₃)/B3LYP-D3/6-31+G(d) level of theory) to fix the position of the corresponding acid.



INT1-(1,2,3,4a)

Filename	E_{tot} SMD/B3LYP-D3/ 6-31+G(d)	ΔG_{298} SMD/B3LYP-D3/ 6-31+G(d)	E_{tot} SMD/B3LYP-D3/ 6-31+G(d)	E_{tot} B3LYP-D3/ 6-31+G(d)	E_{tot} SMD/DLPNO-CCSD(T)/ def2-TZVPP	$G_{298,\text{sol}}$ SMD/DLPNO-CCSD(T)/ def2-TZVPP	$\Delta G_{298,\text{sol}}$
14							
ph_me_no2_1_9	-1252.9298177	0.2111220	-1252.9298177	-1252.9010773	-1250.8436912	-1250.6582912	
ph_me_no2_1_1	-1252.9319557	0.2128600	-1252.9319557	-1252.9043871	-1250.8463401	-1250.6580303	
1							
DMAP_1_2.log	-382.2995489	0.1294189	-382.2995489	-382.2844247	-381.5732973	-381.4559842	
INT1-1							
int1_DMAP_11.com	-1635.2504472	0.3614810	-1635.2504472	-1635.2026041	-1632.4230744	-1632.1064180	20.6
int1_DMAP_18.com	-1635.2540483	0.3650740	-1635.2540483	-1635.2052346	-1632.4256533	-1632.1063746	20.7
2							
ppy_1	-459.7357421	0.2095831	-459.7357421	-459.7178539	-458.8579618	-458.7078204	
INT1-2							
int1_PPY_2.com	-1712.6913542	0.4002070	-1712.6913542	-1712.6369184	-1709.7101559	-1709.3613662	12.46
int1_PPY_15.com	-1712.6880504	0.3965650	-1712.6880504	-1712.6388418	-1709.7102879	-1709.3599130	16.27
3							
TCAP_1	-537.1790988	0.2005210	-537.1790988	-537.1599188	-536.1519420	-535.9675826	
TCAP_2	-537.1786144	0.2005070	-537.1786144	-537.1591846	-536.1505485	-535.9664528	
INT1-3							

int1_tcap_18.com	-1790.1388331	0.4364970	-1790.1388331	-1790.0846844	-1787.0080887	-1786.6227219	8.3
int1_tcap_1.com1	-1790.1358371	0.4349430	-1790.1358371	-1790.0887002	-1787.0112311	-1786.6204066	14.4
4a							
R1_12	-823.5976102	0.2886080	-823.5976102	-823.5665543	-822.0199485	-821.7593779	
R1_5	-823.5991141	0.2897120	-823.5991141	-823.5699842	-822.0222908	-821.7586902	
INT1-4a							
int1_r1_7	-2076.5617545	0.5235880	-2076.5621622	-2076.5036156	-2072.8867385	-2072.4186786	-2.7
int1_r1_17b	-2076.5635602	0.5264830	-2076.5637861	-2076.5117610	-2072.8958825	-2072.4184061	-1.9

Table 5.19. Total energies and enthalpy for **1-3, 4a, 14** and **INT1-1, INT1-2, INT1-3** and **INT1-4a** (in Hartree). Molar free energies in solution at 298.15 K ($G_{298,\text{sol}}$) have been calculated at the SMD(CHCl₃)/DLPNO-CCSD(T)/def2-TZVPP//SMD(CHCl₃)/B3LYP-D3/6-31+G(d) level and corrected for a solution standard state of 1 M through addition of +7.925 kJ mol⁻¹ (0.00301848 Hartree). The SMD(CHCl₃)/B3LYP-D3/6-31+G(d) level of theory has been used to optimize the geometries and calculate solute thermal corrections and solvation energies. Note that the filenames are used in our calculations and do not follow any guide. The conformational search was based on findings of **INT1** in previous study.^[1] The conformational search of **INT1-1** on the findings of **INT1-3**. The conformational search of **INT1-2** on the findings of **INT1-1**. The conformational search of **INT1-4a** is based on the conformers of int1_tcap_18.com and int1_tcap_28.com (lowest total free energy based on SMD(CHCl₃)/B3LYP-D3/6-31+G(d) level of theory) to fix the position of the corresponding acid

Filename	E_{tot} SMD/B3LYP-D3/ 6-31+G(d)	ΔH_{298} SMD/B3LYP-D3/ 6-31+G(d)	E_{tot} SMD/B3LYP-D3/ 6-31+G(d)	E_{tot} B3LYP-D3/ 6-31+G(d)	E_{tot} SMD/DLPNO-CCSD(T)/ def2-TZVPP	$H_{298,\text{sol}}$ SMD/DLPNO-CCSD(T)/ def2-TZVPP	$\Delta H_{298,\text{sol}}$
14							
ph_me_no2_1_9	-1252.9298177	-1252.6416657	-1252.9298177	-1252.9010773	-1250.8436912	-1250.5812612	
ph_me_no2_1_1	-1252.9319557	-1252.6436087	-1252.9319557	-1252.9043871	-1250.8463401	-1250.5825433	
1							
DMAP_1_2.log	-382.2995489	0.1721389	-382.2995489	-382.2844247	-381.5732973	-381.4132642	
INT1-1							
int1_DMAP_11.com	-1635.2504472	0.4631420	-1635.2504472	-1635.2026041	-1632.4230744	-1632.0047570	-23.4
int1_DMAP_18.com	-1635.2540483	0.4635990	-1635.2540483	-1635.2052346	-1632.4256533	-1632.0078496	-31.5
2							
ppy_1	-459.7357421	0.1650111	-459.7357421	-459.7178539	-458.8579618	-458.6632484	
INT1-2							
int1_PPY_2.com	-1712.6913542	0.5009020	-1712.6913542	-1712.6369184	-1709.7101559	-1709.2606712	-38.93
int1_PPY_15.com	-1712.6880504	0.5006660	-1712.6880504	-1712.6388418	-1709.7102879	-1709.2558120	-26.17
3							
TCAP_1	-537.1790988	0.2469760	-537.1790988	-537.1599188	-536.1519420	-535.9211276	

TCAP_2	-537.1786144	0.2469460	-537.1786144	-537.1591846	-536.1505485	-535.9200138	
INT1-3							
int1_tcap_18.com	-1790.1388331	0.5386500	-1790.1388331	-1790.0846844	-1787.0080887	-1786.5205689	-44.2
int1_tcap_1.com1	-1790.1358371	0.5386720	-1790.1358371	-1790.0887002	-1787.0112311	-1786.5166776	-34.0
4a							
R1_12	-823.5976102	0.3505700	-823.5976102	-823.5665543	-822.0199485	-821.6974159	
R1_5	-823.5991141	0.3507530	-823.5991141	-823.5699842	-822.0222908	-821.6976492	
INT1-4a							
int1_r1_7	-2076.5617545	0.6421660	-2076.5621622	-2076.5036156	-2072.8867385	-2072.3001006	-52.1
int1_r1_17b	-2076.5635602	0.6423120	-2076.5637861	-2076.5117610	-2072.8958825	-2072.3025771	-58.6

The main conformational search of **INT1-4a** is based on the conformers of int1_tcap_18.com (int1_r1_5-14, Figure 5.101 blue dots) and int1_tcap_28.com (int1_r1_16-25, Figure 5.101 red crosses, lowest total free energy based on SMD(CHCl₃)/B3LYP-D3/6-31+G(d) level of theory) to fix the position of the corresponding acid. int1_r1_1-4 has a further position of the corresponding acid based on previous studies (Figure 5.101 green triangles).^[1] Afterwards the side chain was connected on position 3 and the Ph group was turned around the three possible places. Finally, the substituents R1-4 were arranged, so that 24 conformer groups are exited.

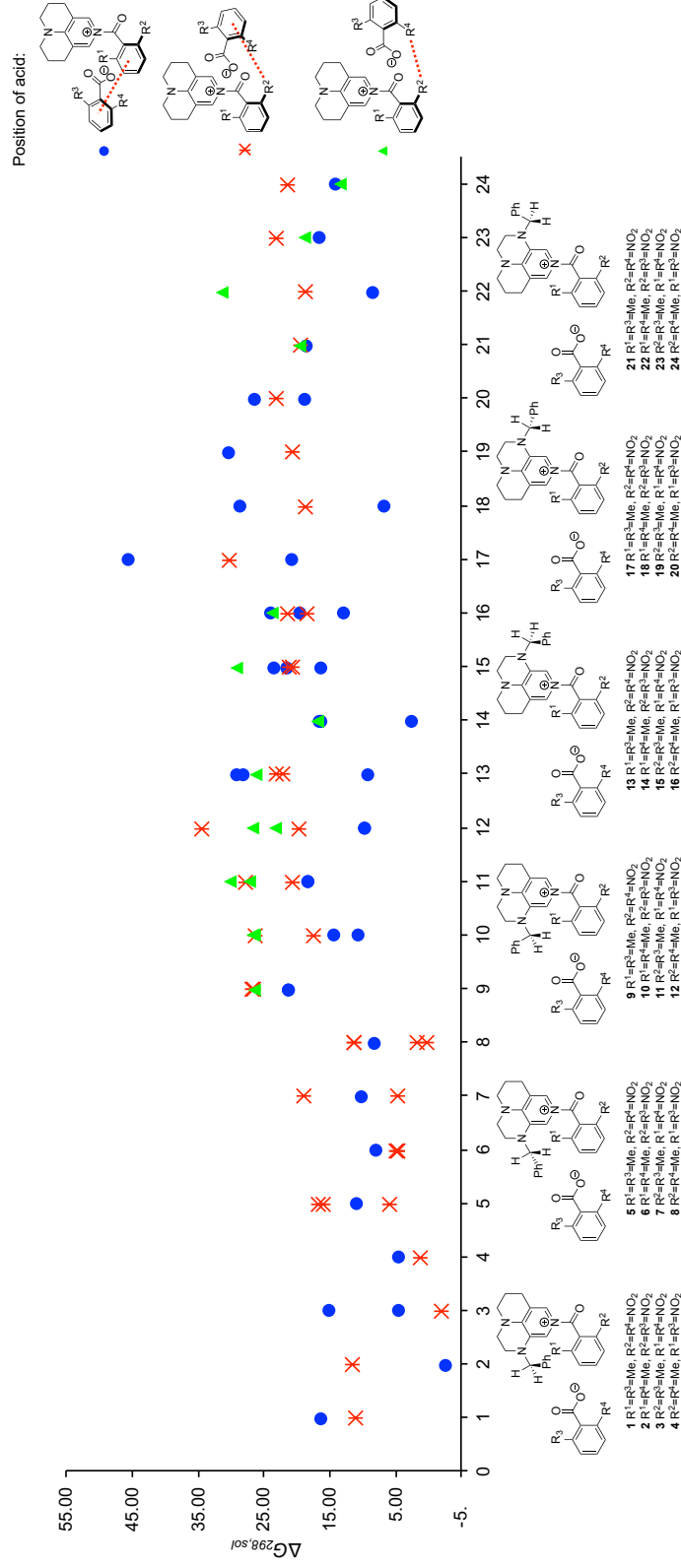


Figure 5.101. Relative Gibbs free energy at the SMD(CHCl₃)/DLPNO-CCSD(T)/def2-TZVP//SMD(CHCl₃)/B3LYP-D3/6-31+G(d) level of theory for **INT1-4a**.

5.3 References

- [1] S. Mayr, M. Marin-Luna, H. Zipse, *J. Org. Chem* **2021**, *86*, 3456-3489.
- [2] S. Mayr, H. Zipse, *Chem. Eur. J.* **2021**, *27*, 18084-18092.
- [3] H. B. Kagan, J. C. Fiaud, *Top. Stereochem.* **1988**, *18*, 249-330.
- [4] S. Hoops, S. Sahle, R. Gauges, C. Lee, J. Pahle, N. Simus, M. Singhal, L. Xu, P. Mendes, U. Kummer, *Bioinformatics* **2006**, *22*, 3067-3074.
- [5] A. Mateos Calbet, *Aromatische Wechselwirkungen und induktiver Effekt in der chemoselektiven Acylierung von Alkoholen*, Research report, LMU München (Munich), **2019**.
- [6] E. Kattinig, M. Albert, *Org. Lett.* **2004**, *6*, 945-948.
- [7] R. Tandon, T. Unzner, T. A. Nigst, N. De Rycke, P. Mayer, B. Wendt, O. R. P. David, H. Zipse, *Chem. Eur. J.* **2013**, *19*, 6435-6442.
- [8] Y. Liu, J. Wang, T. Li, Z. Zhao, W. Pang, *Tetrahedron* **2019**, *75*, 130540.
- [9] D. N. Korolev, N. A. Bumagin, *Tetrahedron Lett.* **2005**, *46*, 5751-5754.
- [10] F. Krätzschmar, M. Kaßel, D. Delony, A. Breder, *Chem. Eur. J.* **2015**, *21*, 7030-7034.
- [11] R. Yu, X. Chen, S. F. Martin, Z. Wang, *Org. Lett.* **2017**, *19*, 1808-1811.
- [12] J.-J. Pi, X.-Y. Lu, J.-H. Liu, X. Lu, B. Xiao, Y. Fu, N. Guimond, *J. Org. Chem.* **2018**, *83*, 5791-5800.
- [13] S. R. Smith, C. Fallan, J. E. Taylor, R. McLennan, D. S. B. Daniels, L. C. Morrill, A. M. Z. Slawin, A. D. Smith, *Chem. Eur. J.* **2015**, *21*, 10530-10536.
- [14] A. Matviitsuk, M. D. Greenhalgh, J. E. Taylor, X. B. Nguyen, D. B. Cordes, A. M. Z. Slawin, D. W. Lupton, A. D. Smith, *Org. Lett.* **2020**, *22*, 335-339.
- [15] A. Costa, C. Nájera, J. M. Sansano, *J. Org. Chem.* **2002**, *67*, 5216-5225.
- [16] V. Magrioti, A. Nikolaou, A. Smyrniotou, I. Shah, V. Constantinou-Kokotou, E. A. Dennis, G. Kokotos, *Bioorg. Med. Chem.* **2013**, *21*, 5823-5829.
- [17] K. D. Reichl, N. L. Dunn, N. J. Fastuca, A. T. Radosevich, *J. Am. Chem. Soc.* **2015**, *137*, 5292-5295.
- [18] W. Liu, W. Ren, J. Li, Y. Shi, W. Chang, Y. Shi, *Org. Lett.* **2017**, *19*, 1748-1751.
- [19] A. Takallou, A. Habibi, A. Z. Halimehjani, S. Balalaie, *J. Organomet. Chem.* **2019**, *888*, 24-28.
- [20] D. Leow, Y.-H. Chen, T.-H. Hung, Y. Su, Y.-Z. Lin, *Eur. J. Org. Chem.* **2014**, *2014*, 7347-7352.
- [21] H. Yan, Z.-F. Li, Z.-F. Guo, Z.-L. Lu, F. Wang, L.-Z. Wu, *Bioorg. Med. Chem.* **2012**, *20*, 801-808.
- [22] a) I. Held, S. Xu, H. Zipse, *Synthesis* **2007**, *2007*, 1185-1196; b) E. Larionov, F. Achrainger, J. Humin, H. Zipse, *ChemCatChem* **2012**, *4*, 559-566.
- [23] D. Weng, Y. Shi, J. Zheng, C. Xu, *Org. Electron* **2016**, *34*, 139-145.
- [24] R. J. Key, A. K. Vannucci, *Organometallics* **2018**, *37*, 1468-1472.
- [25] Q. Shen, T. Ogata, J. F. Hartwig, *J. Am. Chem. Soc.* **2008**, *130*, 6586-6596.
- [26] L. Farrugia, *J. Appl. Crystallogr.* **2012**, *45*, 849-854.
- [27] a) A. D. Becke, *J. Chem. Phys.* **1993**, *98*, 5648-5652; b) C. Lee, W. Yang, R. G. Parr, *Phys. Rev. B* **1988**, *37*, 785-789; c) S. Grimme, *J. Chem. Phys.* **2006**, *124*, 034108.
- [28] G. W. Spitznagel, T. Clark, J. Chandrasekhar, P. V. R. Schleyer, *J. Comput. Chem.* **1982**, *3*, 363-371.
- [29] A. V. Marenich, C. J. Cramer, D. G. Truhlar, *J. Phys. Chem. B* **2009**, *113*, 6378-6396.
- [30] a) M. Marin-Luna, P. Patschinski, H. Zipse, *Chem. Eur. J.* **2018**, *24*, 15052-15058; b) M. Marin-Luna, B. Pölloth, F. Zott, H. Zipse, *Chem. Sci.* **2018**, *9*, 6509-6515.
- [31] a) C. Riplinger, F. Neese, *J. Chem. Phys.* **2013**, *138*, 034106; b) C. Riplinger, B. Sandhoefer, A. Hansen, F. Neese, *J. Chem. Phys.* **2013**, *139*, 134101; c) F. Weigend, R. Ahlrichs, *Phys. Chem. Chem. Phys.* **2005**, *7*, 3297-3305; d) L. A. Curtiss, P. C. Redfern, K. Raghavachari, V. Rassolov, J. A. Pople, *J. Chem. Phys.* **1999**, *110*, 4703-4709.
- [32] Gaussian 09, R. D.01, M. J. Frisch, G. W. Trucks, H. B. Schlegel, G. E. Scuseria, M. A. Robb, J. R. Cheeseman, G. Scalmani, V. Barone, B. Mennucci, G. A. Petersson, H. Nakatsuji, M. Caricato, X. Li, H. P. Hratchian, A. F. Izmaylov, J. Bloino, G. Zheng, J. L. Sonnenberg, M. Hada, M. Ehara, K. Toyota, R. Fukuda, J. Hasegawa, M. Ishida, T. Nakajima, Y. Honda, O. Kitao, H. Nakai, T. Vreven, J. A. Montgomery Jr., J. E. Peralta, F. Ogliaro, M. Bearpark, J. J. Heyd, E. Brothers, K. N. Kudin, V. N. Staroverov, R. Kobayashi, J. Normand, K. Raghavachari, A. Rendell, J. C. Burant, S. S. Iyengar, J. Tomasi, M. Cossi, N. Rega, J. M. Millam, M. Klene, J. E. Knox, J. B. Cross, V. Bakken, C. Adamo, J. Jaramillo, R. Gomperts, R. E. Stratmann, O. Yazyev, A. J. Austin, R. Cammi, C. Pomelli, J. W. Ochterski, R. L. Martin, K. Morokuma, V. G. Zakrzewski, G. A. Voth, P. Salvador, J. J. Dannenberg, S. Dapprich, A. D. Daniels, Ö. Farkas, J. B. Foresman, J. V. Ortiz, J. Cioslowski, D. J. Fox, Gaussian, Inc., W. CT, **2010**.

- [33] F. Neese, *Wiley Interdiscip. Rev. Comput. Mol. Sci.* **2012**, *2*, 73-78.
- [34] *Schrödinger Release 2019-2: Jaguar*, Schrödinger, LLC, New York, NY, **2019**.
- [35] E. Larionov, M. Mahesh, A. C. Spivey, Y. Wei, H. Zipse, *J. Am. Chem. Soc.* **2012**, *134*, 9390-9399.
- [36] a) C. Lindner, R. Tandon, B. Maryasin, E. Larionov, H. Zipse, *Beilstein J. Org. Chem.* **2012**, *8*, 1406-1442; b) I. Held, E. Larionov, C. Bozler, F. Wagner, H. Zipse, *Synthesis* **2009**, *2009*, 2267-2277; c) Y. Wei, T. Singer, H. Mayr, G. N. Sastry, H. Zipse, *J. Comput. Chem.* **2008**, *29*, 291-297; d) Y. Wei, G. N. Sastry, H. Zipse, *J. Am. Chem. Soc.* **2008**, *130*, 3473-3477; e) I. Held, A. Villinger, H. Zipse, *Synthesis* **2005**, *2005*, 1425-1430.
- [37] a) C. R. Kennedy, S. Lin, E. N. Jacobsen, *Angew. Chem. Int. Ed.* **2016**, *55*, 12596-12624; b) J. P. Gallivan, D. A. Dougherty, *J. Am. Chem. Soc.* **2000**, *122*, 870-874; c) O. Takahashi, Y. Kohno, M. Nishio, *Chem. Rev.* **2010**, *110*, 6049-6076.
- [38] a) A. J. Neel, M. J. Hilton, M. S. Sigman, F. D. Toste, *Nature* **2017**, *543*, 637-646; b) J. w. Hwang, P. Li, K. D. Shimizu, *Org. Biomol. Chem.* **2017**, *15*, 1554-1564; c) R. K. Raju, J. W. G. Bloom, Y. An, S. E. Wheeler, *ChemPhysChem* **2011**, *12*, 3116-3130.
- [39] CYLVIEW: CYLview,1.0b;Legault, C. Y., Université de Sherbrooke, **2009** (<http://www.cylview.org>); 3D-Pictures were generated with the CYLview program.

Chapter 6. Conclusion

Until today selective esterification reactions are a hot topic in organic chemistry.^[1] Especially in natural product chemistry or pharmaceutical systems, diols are a main component and it is extraordinary interesting, to protect these functional groups in a site selective way.^[2] One way to perform selective protection reactions is the organocatalyzed acylation with activated carboxylic acid derivatives, like acid chlorides or acid anhydrides.^[1c,3] Pyridine based Lewis base catalysts are one of the first choices for acylation reactions with these reagents.^[4] Although in the last years the crucial role of non-covalent interactions (NCI) in organocatalyzed reactions was further explored,^[5] there are only few kinetic studies in which NCI are considered to accelerate the conversion of single functional groups in a regioselective way. In this study, the influence of size effects of substrate alcohols, reagents and DMAP-based catalysts were studied in selective acylation reactions of 1,2-diols. The main objective was to acylate selectively the less reactive secondary alcohol in the presence of the (intrinsically) more reactive primary alcohol.^[6]

To inhibit attractive intramolecular hydrogen bond interactions between the two OH-groups in the 1,2-diol by influencing the reaction rates, a separated aromatic ethanol system (**A/B**) was chosen. Ethanol alcohol **A/B** should reflect the structure motif of 1,2-diol **C**. By comparing the two alcohols owing to the same size of aromatic rings in a so-called turnover-limited competition experiment (Figure 6.1, Chapter 2 and 3) statements about their relative acylation rates are feasible. Investigations about different acylation reagents (acid chlorides, acid cyanides or acid anhydrides), size of substrate and Lewis base catalysis illustrate that the size of all three reaction components are influencing the acylation of primary and secondary alcohols.

In Chapter 3 an inversion of selectivity from primary **B** to secondary ethanol **A** was detected, depending on the size of the aromatic ring of the substrate and the steric bulk of the acid anhydride derivative. Visualized by a quantum chemical study of the reaction pathway, a stacked triple “sandwich” conformation between the aromatic ring of the alcohol (green), the pyridinium ring of the catalyst (red) and the bulky substituent of the anhydride reagent (blue) were obtained for the rate-determining transition state (Figure 6.1, Chapter 2 and 3). Accelerating the acylation of both alcohols by increasing the size of the alcohols pointed to strengthened attractive London dispersion interactions. Since in the TS for the secondary alcohol the two aromatic faces are able to stack in a more convenient way, the acceleration depending on the size of the alcohol is stronger pronounced than for the primary alcohol. Finally, the acylation of secondary alcohol is more preferred than the primary alcohol. For an inverted selectivity, a 2,6-disubstituted benzoic anhydride carrying at least one Me group or 2-substituted 1-naphthoic anhydride has to be used as acylation reagent. Inverted selectivity means, that the preference for acylation of secondary alcohol is higher than for the primary alcohol. Finally, it was a success to favour the acylation of secondary pyrene alcohol of around 2.3 times stronger in comparison to the primary pyrene alcohol.

To mimic better the hydroxyl groups of 1,2-diol **C**, the corresponding propanols (**D/E**) were studied, whereby the Me group of the propanol should mimic the second OH-group of the 1,2-diol (Scheme 6.1, Chapter 4). Only small changes in comparison to the ethanol system were observed. However, this picture is changing when a 1,2-diol system **C** is employed as alcohol system. First of all, 1,2-diol systems, in contrast to separated alcohol systems, are a more multifaceted reaction system which includes first acylation of the hydroxyl groups in the diol **C** to two monoesters, a second acylation of the monoesters to the diesters and a migration acyl transfer between the two monoesters. Finally, six rate constants are influencing each other during the acylation. Several kinetic studies and subsequently numerical simulations of the reaction kinetics reveal a good overview about the acylation of a 1,2-diol system **C**. Large differences in selectivity and reactivity between first- and second acylation were obtained. In both cases the size of the 1,2-diol plays the major part again. In the first acylation of 1,2-diol, with increasing size of the alcohol side chain from phenyl to 2-naphthyl, the effective rates are increased. These findings guide again to size effects between the aromatic side chain of the diol and the catalysts face in the suggested triple “sandwich” TS.

Conclusion

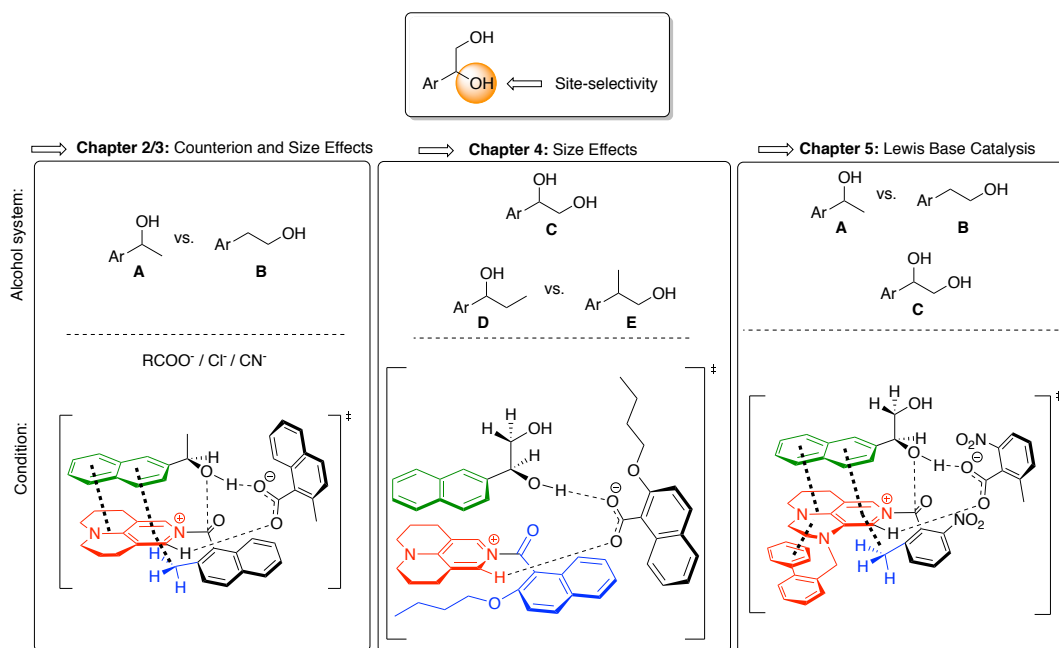


Figure 6.1. Graphical overview of studied selective acylation reactions and the driving non-covalent stacking forces in the corresponding systems.

Using bulky 2-substituted 1-naphthoic anhydrides, the acylation of the secondary OH group and the (intrinsically) more reactive primary OH group of the 2-naphthyl-1,2-ethanediol are preferred in the same manner. In the second acylation of the monoesters to the diesters, size effects and differential hinderance are found to be more pronounced. Here for the bulkiest 2-substituted 1-naphthoic anhydride a selectivity with $k_{rel} = 0.18$ was found, suggesting that the preference for acylation of secondary alcohol is five times higher than for the primary alcohol. In contrast to the separated ethanol system, the first acylation of a 1,2-diol also depends on the reaction conditions. Selectivity changes by temperature effects demonstrate, that at lower temperature acylation of the secondary OH-group is preferred, whereby at in only loosely organized system at higher temperature the primary OH-group is privileged. The polarity of the solvents defined by Reichardt's solvent parameter $E_T(30)^{[7]}$ affect the selectivity of the first acylation, too. In dipolar non-hydrogenbonding donor solvents the preference in the acylation of secondary OH-group is larger than in apolar non-hydrogenbonding donor solvents. Furthermore, the attractive intramolecular H-bond forces of a second OH-group in the system to the additional OH group was determined in an absolute kinetic study by comparing the effective acylation rates of first- and second acylation for primary and secondary OH groups in the system. For the primary alcohols, the first acylation is up to 30 times faster than the second acylation. In contrast, for the secondary alcohols, the first acylation is only up to 7 times faster than the second acylation. Both cases reflect results with 1-naphthoic anhydride derivatives. Furthermore, a strong decrease in absolute reaction rate was determined for the bulky anhydrides in comparison to benzoic anhydride, whereby the effective rate constants for acylation of the secondary alcohols are less affected than the effective rate constants for acylation of the primary alcohols. Strong repulsive effects are suggested during the formation of the predicted triple "sandwich" conformation of the rate-determining TS, which increase the intrinsic reaction barrier. Surprisingly, the repulsive effects are affecting the primary alcohols more than the secondary alcohols. Focusing on the second acylation of the monoesters to the diester, for the secondary alcohol still "triple-sandwich" conformation for the rate-determining TS is assumed. However, this "triple-sandwich" structural characteristic is missing in the TS of the primary alcohol, where the naphthyl side chain of the monoester is orientated towards that of the carboxylate counter ion.

Finally, the impact of Lewis basicity of the catalysts on the selective acylation of 1,2-ethanediol was examined. Via acetyl cation affinity analysis, it was demonstrated that the Lewis basicity of the DMAP-based catalysts could be enhanced by installing dispersion-energy donor (DED) substituents. The substituents are folded over the pyridinium face of the modified DMAP-motif. Driving forces are attractive intramolecular π -

π stacking interactions between aromatic faces of the substituent and the pyridinium face of the modified DMAP-motif. How the size, the spatial configuration and the Lewis basicity of the catalyst impact the selectivity was first tested with the 2-naphthyl ethanol system (**A/B**) acylated with 2-methyl-6-nitrobenzoic anhydride. Planar and large catalyst surfaces have a stronger preference for catalysing the acylation of secondary ethanol **A**, whereby smaller catalysts like DMAP or PPY or not planar catalysts are catalysing stronger the acylation of primary ethanol **B**. The reasons are cation- π stacking interactions of the flat and large face of the catalyst with the aromatic face of the secondary alcohol. Strengthening these size effects with an intramolecularly stacked substituent in the catalyst, the secondary alcohol **B** is preferred slightly more. With these results in mind, the catalytic potential in the selective acylation of the 1,2-ethanediol **C** was analysed. Unexpectedly the weaker and smaller Lewis base catalysts like DMAP and PPY have the same catalytic potential in the acylation of **C** than the stronger Lewis base catalyst TCAP. Indeed, the strongest tricyclic Lewis base catalysts developed here are less catalytically active because of differential size hindrance. Focussing on the selectivity, the acylation of secondary OH-group is preferred when the planar size of the catalyst is increasing, based on stronger stacking interactions. Analysed by computational methods, the *N*-acylpyridinium cation intermediate (formed by the activation of catalysts with acid anhydride) of strong Lewis base catalysts form intermediates, which are more stable in their Gibbs free energy terms than the separated starting materials. Thus, the reduced catalytic potential of strong Lewis bases could be justified. Only Lewis base catalysts with a similar cation affinity than commercially available TCAP and larger π -surface are showing a slightly better catalytic potential in the acylation of 1,2-diols.

In conclusion, we demonstrated how size effects are changing the selective acylation of alcohols with variable reactivity. Non-covalent interactions are stabilizing the transition states via a triple sandwich motif which results in an acceleration of reaction rates. Using non-covalent interactions like London dispersion forces in the field of protection group chemistry thus points to new opportunities to the selective installation of functional groups in natural products or drugs.

Conclusion

6.1 References

- [1] a) G. Sartori, R. Ballini, F. Bigi, G. Bosica, R. Maggi, P. Righi, *Chem. Rev.* **2004**, *104*, 199-250; b) S. Yoganathan, S. J. Miller, *J. Med. Chem.* **2015**, *58*, 2367-2377; c) N. A. Afagh, A. K. Yudin, *Angew. Chem. Int. Ed.* **2010**, *49*, 262-310; d) O. Robles, D. Romo, *Nat. Prod. Rep.* **2014**, *31*, 318-334; e) K. C. Nicolaou, J. S. Chen, *Classics in Total Synthesis III*, Wiley-VCH, Weinheim, **2011**.
- [2] a) G. Zong, E. Barber, H. Aljewari, J. Zhou, Z. Hu, Y. Du, W. Q. Shi, *J. Org. Chem.* **2015**, *80*, 9279-9291; b) M. Koshimizu, M. Nagatomo, M. Inoue, *Angew. Chem. Int. Ed.* **2016**, *55*, 2493-2497; c) C. A. Lewis, S. J. Miller, *Angew. Chem. Int. Ed.* **2006**, *45*, 5616-5619.
- [3] a) M. Nahmany, A. Melman, *Org. Biomol. Chem.* **2004**, *2*, 1563-1572; b) A. H. Haines, *Adv. Carbohydr. Chem. Biochem.* **1976**, *33*, 11-109; c) E. Kattnig, M. Albert, *Org. Lett.* **2004**, *6*, 945-948; d) E. Guibe-Jampel, G. Le Corre, M. Wakselman, *Tetrahedron Lett.* **1979**, *20*, 1157-1160.
- [4] a) G. Höfle, W. Steglich, H. Vorbrüggen, *Angew. Chem. Int. Ed.* **1978**, *17*, 569-583; b) W. Steglich, G. Höfle, *Angew. Chem. Int. Ed.* **1969**, *8*, 981-981; c) S. E. Denmark, G. L. Beutner, *Angew. Chem. Int. Ed.* **2008**, *47*, 1560-1638.
- [5] a) R. P. Wurz, *Chem. Rev.* **2007**, *107*, 5570-5595; b) C. E. Müller, P. R. Schreiner, *Angew. Chem. Int. Ed.* **2011**, *50*, 6012-6042.
- [6] C. B. Fischer, S. Xu, H. Zipse, *Chem. Eur. J.* **2006**, *12*, 5779-5784.
- [7] C. Reichardt, *Solvents and Solvent Effects in Organic Chemistry*, Wiley-VCH, Weinheim, **2003**.

Abbreviation

Ac	acetyl	NMR	nuclear magnetic resonanz spectroscopy
ACA	acetyl cationic affinity	NOESY	nuclear overhauser enhancement spectroscopy
Ar	hroamtic	Np	naphthyl
B3LYP	Hybrid DFT method with Becke's three parameter exchange functional and Lee-Yang-Parr's correlation functional	O	oxygen
BAA	benzoic anhydride affinity	OBu	buthoxy
Br	brom	OEt	1thoxy
calcd	calculated	OH	hydroxyl
CCDC	Cambridge Cyristallographic data Centre	OHex	hexanoyloxy
CCSD(T)	coupled cluster theory with single, double and perturbative triple excitations	OMe	methoxy
Chem	chemoselectivity	PG	protection group
Cl	chlor	Ph	phenyl
Conv.	conversion	PPY	4-pyrrolidinpyridin
CyHex	cyclohexane	Prop	propanol
DABCO	1,4-Diazabicyclo[2.2.2]octane	Py	pyrene
DBN	1,5-diazabicyclo[4.3.0]non-5-en	QTAIM	quantum theory of atom in molecules
DCC	dicyclohexylcarbodiimid	R	rest
DEAD	diethylazodicarboxylate	RMSD	root-mean-square deviation
DED	dispersion energy donor	rt	room temperature
DFT	desinty functional theory	s	selectivity
DIPEA	diisopropylethylamin	SAPT	symmetry-adapted perturbation theory
DLPNO	domain based local pair natural orbital	St. dev	standard deviation
DMAP	4-dimethylaminopyridin	T	temperature
DMF	dimethylformaid	TCAP	9-azajulolidine
DMSO	dimethoxy sulfoxide	TFT	trifluorotoluene
ee	enatioselectivity	THF	tetrahydrofuran
EI	electronic ionization	TLC	thin-layer chromatography
eq	equivalent	Tol	toluene
ESI	electrospray Ionisation	Tp	thiophene
Et ₃ N	triethylamin	TS	transition state
EtOAc	ethyacetate	TsCl	tosylchloride
EtOH	ethanol	UV/VIS	ultraviolet ad Visual light
F	fluoro	VdW	Van der Waals
H	hydrogen	WH	Wheeler and Houk's model
HRMS	high resolution mass spectrometry		
HS	Hunter and Sander's electrostatic model		
INT	Intermediate		
iPr	iso-propyl		
IR	infrared		
LD	london dispersion		
m. p.	melting point		
Me	methyl		
MeCN	acetonitrile		
MeOH	methanol		
Mes	mesitylene		
MTBE	methyl- <i>t</i> -butyl ether		
NBO	natural bond orbital		
NBS	<i>N</i> -bromosuccinimid		
NCI	non-covalent interactions		